GEOLOGICAL SURVEY OF CANADA
COMMISSION GÉOLOGIQUE DU CANADA

PAPER
ÉTUDE 82-1A

CURRENT RESEARCH PART A

RECHERCHES EN COURS PARTIE A

Canada

1982

Notice to Librarians and Indexers

The Geological Survey's thrice-yearly *Current Research* series contains many reports comparable in scope and subject matter to those appearing in scientific journals and other serials. All contributions to the Scientific and Technical Report section of *Current Research* include an abstract and bibliographic citation. It is hoped that these will assist you in cataloguing and indexing these reports and that this will result in a still wider dissemination of the results of the Geological Survey's research activities.

Avis aux bibliothécaires et préparateurs d'index

La série Recherches en cours *de la Commission géologique paraît trois fois par année; elle contient plusieurs rapports dont la portée et la nature sont comparable à ceux qui paraissent dans les revues scientifiques et autres périodiques. Tous les articles publiés dans la section des rapports scientifiques et techniques de la publication* Recherches en cours *sont accompagnés d'un résumé et d'une bibliographie, ce qui vous permettra, nous l'espérons, de cataloguer et d'indexer ces rapports, d'où une meilleure diffusion des résultats de recherche de la Commission géologique.*

Technical editing and compilation
Rédaction et compilation techniques
R.G. Blackadar
H. Dumych
P.J. Griffin
L. Machan
W.C. Morgan
E.R.W. Neale

Production editing and layout
Préparation et mise en page
Leona R. Mahoney
Mike Kiel
Debby Busby

Typed and checked by
Dactylographie et vérification
Betty Birtch
Susan Gagnon
Janet Gilliland
Shirley Kostiew
Janet Legere
Sharon Parnham

GEOLOGICAL SURVEY
PAPER 82-1A

COMMISSION GÉOLOGIQUE
ÉTUDE 82-1A

CURRENT RESEARCH
PART A

RECHERCHES EN COURS
PARTIE A

1982

Available in Canada through

authorized bookstore agents
and other bookstores

or by mail from

Canadian Government Publishing Centre
Supply and Services Canada
Hull, Québec, Canada K1A 0S9

and from

Geological Survey of Canada
601 Booth Street
Ottawa, Canada K1A 0E8

A deposit copy of this publication is also available
for reference in public libraries across Canada

Cat. No. M44-82/1AE Canada: $10.00
ISBN 0-660-11005-9 Other countries: $12.00

Price subject to change without notice

Introduction

In January 1958 the Geological Survey issued a 23-page informal report summarizing the field work undertaken by its staff during the 1957 field season. In the following four years similar reports were issued, each being somewhat larger than its predecessor. The results of the 1961 field season were released as Paper 62-30 – "Summary of Research: Office and Laboratory 1961" – and being published in the Paper series of the Survey were brought to the attention of a much wider audience. Not all of the Survey's work derives from field studies, and a second part, released in the summer and comprising mainly reports resulting from office and laboratory studies, was started in 1963. Succeeding years have seen the evolution of these reports from a collection of brief, summary reports to a series that includes many papers comparable in scope and quality to those appearing in the principal scientific journals. This development is most visible in the sheer bulk of the recent versions of the report and to assist in making the volumes more manageable for the reader and more flexible for the contributor, it was decided in 1975 to publish the Report of Activities series in three parts.

In 1977 the title was changed to "Current Research" to better describe the range of reports included in the volumes. The value of this series whereby results of on-going studies are made available expeditiously to the user is attested to by the responses received to user questionnaires and by informed comments received by the senior management of the Geological Survey.

This volume, Geological Survey of Canada Paper 82-1, Part A, marks the 20th anniversary of this series of collections of brief reports. The format has evolved considerably during this time and no doubt will evolve in the future. Comments from our readers are always welcome and such comments will help us produce a product of most use to the widest possible audience.

La Commission géologique publiait en 1958 un rapport officieux de 23 pages dans lequel étaient résumés les travaux entrepris sur le terrain par son personnel au cours de la saison de 1957. D'autres rapports semblables ont été publiés au cours des quatre années suivantes, chacun étant plus étoffé que le précédent. Les résultats de la saison de 1961 ont été divulgués dans l'Étude 62-30 – "Summary of Research: Office and Laboratory, 1961"; le fait de paraître dans cette série de la Commission leur a permis d'être plus largement diffusés. Tous les travaux de la Commission ne résultent pas d'études sur le terrain; la diffusion d'une deuxième partie, publiée en été, et qui comprend les principaux rapports résultant d'études effectuées dans les bureaux et les laboratoires, a débuté en 1963. Au cours des années, ces rapports, qui n'étaient au début qu'un recueil de rapports résumés ont été intégrés pour former une série de documents dont l'envergure et la qualité sont comparables à celles de ceux qui paraissent dans les principales publications scientifiques. On constate cette évolution surtout d'après le volume élevé des versions récentes du rapport; pour rendre sont format plus pratique pour le lecteur et plus souple pour le contributeur, il a été décidé en 1975 de publier la série des Rapports d'activités en trois parties.

En 1977, le titre est devenu "Recherches en cours" pour mieux refléter la gamme des sujets traités dans les volumes. La valeur de cette série, qui repose sur la rapidité avec laquelle les résultats des études en cours sont communiqués aux utilisateurs se vérifie par les réponses données dans les questionnaires remplis par les utilisateurs et par les observations réfléchies reçues par la haute direction de la Commission géologique.

Ce volume, soit l'Étude 82-1, partie A, de la Commission géologique du Canada, marque le vingtième anniversaire de cette série de recueils de rapports. Leur présentation a évolué considérablement au cours de cette période et nul doute qu'elle évoluera également à l'avenir. Les observations formulées par nos lecteurs sont toujours appréciées car elles nous permettront de fournir un produit qui pourra servir au plus grand auditoire possible.

R.G. Blackadar
Chief Scientific Editor/Rédacteur scientifique en chef

Separates

A limited number of separates of the papers that appear in this volume are available by direct request to the individual authors. The addresses of the Geological Survey of Canada offices follow:

601 Booth Street,
OTTAWA, Ontario
K1A 0E8

Institute of Sedimentary and Petroleum Geology,
3303-33rd Street N.W.,
CALGARY, Alberta
T2L 2A7

Cordilleran Geology Division
100 West Pender Street,
VANCOUVER, B.C.
V6B 1R8

Atlantic Geoscience Centre,
Bedford Institute of Oceanography,
P.O. Box 1006,
DARTMOUTH, N.S.
B2Y 4A2

When no location accompanies an author's name in the title of a paper, the Ottawa address should be used.

Tirés à part

On peut obtenir un nombre limité de "tirés à part" des articles qui paraissent dans cette publication en s'adressant directement à chaque auteur. Les adresses des différents bureaux de la Commission géologique du Canada sont les suivantes:

601, rue Booth
OTTAWA, Ontario
K1A 0E8

Institut de géologie sédimentaire et pétrolière
3303-33rd, St. N.W.,
CALGARY, Alberta
T2L 2A7

Division de la géologie de la Cordillère
100 West Pender Street
VANCOUVER, Colombie-Britannique
V6B 1R8

Centre géoscientifique de l'Atlantique
Institut océanographique de Bedford
B.P. 1006
DARTMOUTH, Nouvelle-Ecosse
B2Y 4A2

Lorsque l'adresse de l'auteur ne figure pas sous le titre d'un document, on doit alors utiliser l'adresse d'Ottawa.

SCIENTIFIC AND TECHNICAL REPORTS
RAPPORTS SCIENTIFIQUES ET TECHNIQUES

ECONOMIC GEOLOGY/GÉOLOGIE ÉCONOMIQUE

GEOCHRONOLOGY/GÉOCHRONOLOGIE

GEOPHYSICS/GÉOPHYSIQUE

MINERALOGY/MINÉRALOGIE

PALEONTOLOGY/PALÉONTOLOGIE

PETROLOGY/PÉTROLOGIE

QUATERNARY GEOLOGY/GÉOLOGIE DU QUATERNAIRE

Inventory Mapping and Stratigraphic Studies/Inventaire cartographique et stratigraphique

Precambrian Shield/Bouclier précambrien ✓

GENERAL/GÉNÉRAL

SCIENTIFIC AND TECHNICAL NOTES
NOTES SCIENTIFIQUES ET TECHNIQUES

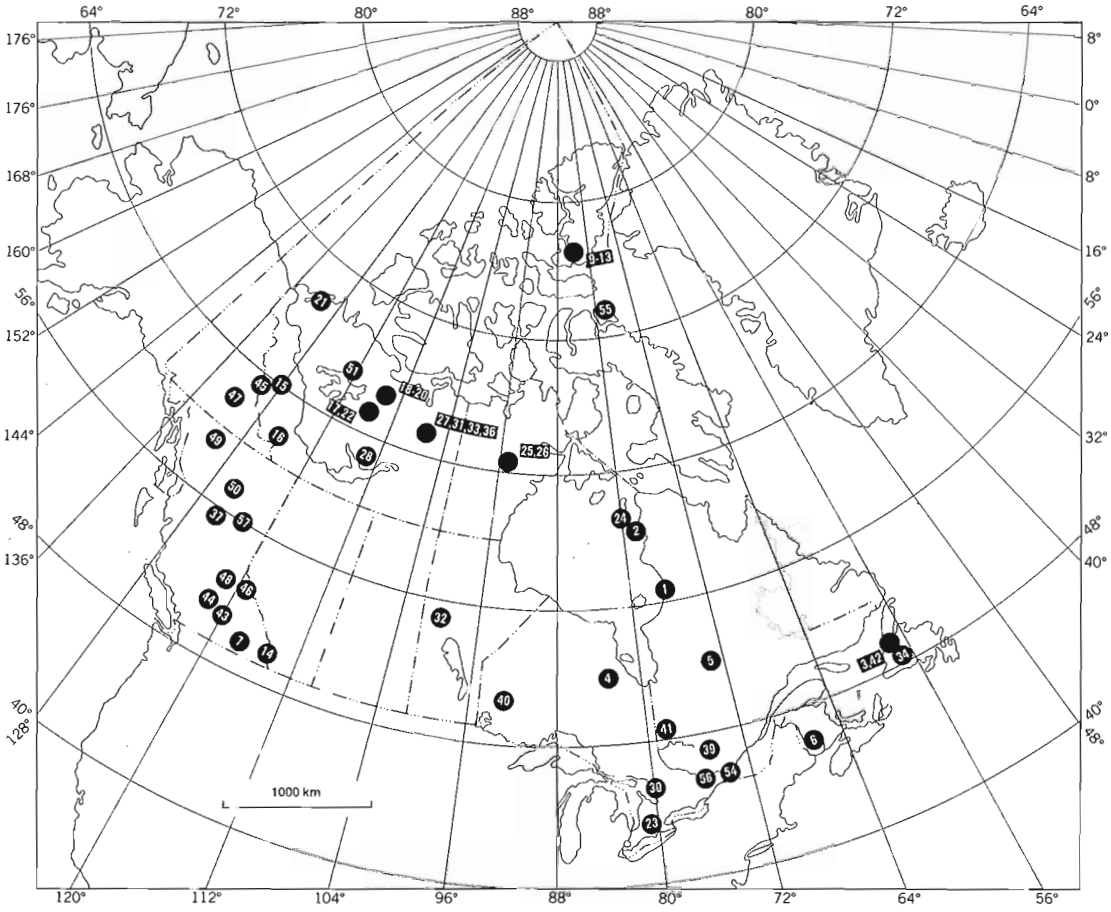

Numbers on index map refer to Scientific and Technical Reports in this volume

SCIENTIFIC AND TECHNICAL REPORTS

RAPPORTS SCIENTIFIQUES ET TECHNIQUES

1. THE STRUCTURE OF THE RICHMOND GULF GRABEN AND THE GEOLOGICAL ENVIRONMENTS OF LEAD-ZINC MINERALIZATION AND OF IRON-MANGANESE FORMATION IN THE NASTAPOKA GROUP, RICHMOND GULF AREA, NEW QUEBEC – NORTHWEST TERRITORIES

Project 770027

F.W. Chandler
Precambrian Geology Division

Chandler, F.W., The structure of the Richmond Gulf Graben and the geological environments of lead-zinc mineralization and of iron-manganese formation in the Nastapoka Group, Richmond Gulf area, New Quebec – Northwest Territories; in Current Research, Part A, Geological Survey of Canada, Paper 82-1A, p. 1-10, 1982.

Abstract

The Richmond Gulf Graben is a complexly-faulted, symmetrical, east-striking structure. Both north and south margins are downfaulted towards the axis, by several normal, listric, faults. Paleocurrents and sedimentary facies in sediments (Richmond Gulf Group) in the previously unstudied southern margin of the graben bear no relation to the faulting. Thus, as previously thought, these rocks predate the faulting. Mafic dykes and sills and downwarp of the Richmond Gulf Group sediments are all most prominent in the axial part of the graben.

The overlying unfaulted Nastapoka Group in the Richmond Gulf region consists of a lower carbonate sequence overlain by a clastic sequence. The carbonates show evidence of shallow marine deposition with emergence. Lead-zinc mineralization is confined to a unit with abundant stromatolite growth. The clastic sequence, of shallow marine origin, contains granular, possibly oolitic, cherty oxide-silicate iron formation and manganese carbonate. The iron formation is correlated, according to one tectonic model, with the onset of subduction in the Belcher Islands. Other evidence suggests a connection with spreading-related volcanism. Also the underlying Richmond Gulf Group contains abundant evidence of an oxygenated atmosphere.

Introduction

This report is a preliminary account of studies carried out during August 1981, mainly around the southern part of Richmond Gulf (Fig. 1.1). Mapping and sedimentary studies on the Richmond Gulf Group were undertaken south of the Gulf to clarify the structural evolution of the south margin of the Richmond Gulf Graben (see Chandler and Schwarz, 1980). Sections were measured across the overlying Nastapoka Group both on the mainland and on Belanger Island, one of the Nastapoka Islands (Fig. 1.2) to further understanding of the tectonic and sedimentary setting of contained iron formation and lead-zinc mineralization.

Previous work in the area is listed by Chandler and Schwarz (1980). The stratigraphic nomenclature of these authors is used in this report. Unstinting logistical support was given to the writer by A. Ciesielski of the Geological Survey of Canada and his crew who helped the writer map the southern exposure of the Richmond Gulf Group. G. Gross provided valuable discussion on iron formation geology.

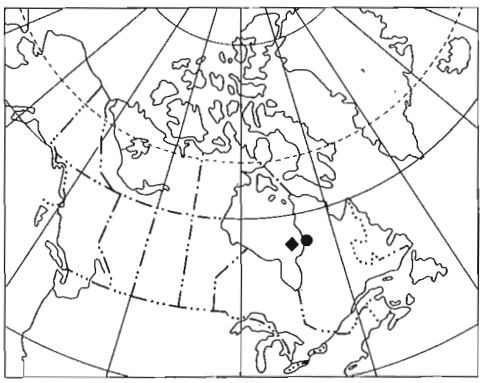

● *Richmond Gulf*
◆ *Belcher Islands*

Figure 1.1. *Index map.*

Structural Geology

The Richmond Gulf Graben was interpreted by Chandler and Schwarz (1980) to be a failed arm related to continental rifting to the west of the Belcher Islands. According to their model, Aphebian arkosic sediments, the Richmond Gulf Group that fill the graben were transported from the west and northwest, from a thermal dome that preceded the rifting. Paleocurrent patterns unrelated to the graben, absence of conglomerates near graben-margin faults, and extensive faulting and drag folding of the group adjacent to the faults indicate development of the graben after deposition of the arkoses. The Richmond Gulf Group is overlain unconformably on the coast of Hudson Bay by carbonate and quartzite, the lower part of the Nastapoka Group which is essentially unfaulted and probably represents miogeoclinal sedimentation following the rifting.

The above model was developed from work extending only 10 km to the south of Richmond Gulf. During August 1981, sedimentary facies and paleocurrents and structural data were recorded farther south to test the hypothesis and check the as yet unproved symmetry of the graben. Also, to assess deeper crustal structure, a gravity survey across the graben was carried out by S. Fogarasi of the Gravity and Geodynamics Division of the Earth Physics Branch using two north-south lines, one along the Hudson Bay coast, the other 25 km inland.

The field data show that granitic conglomerates do not occur in the Richmond Gulf Group adjacent to the faults on the margin of the graben's granitic south side, and that fluvial paleocurrents follow the pattern found farther north, indicating flow to the southeast and east, unrelated to the marginal faults.

Figure 1.2 shows that south of Richmond Gulf the graben is bordered by at least three major faults that all downthrow the Richmond Gulf Group to the north. Strata, at some distance from the faults on their downthrown sides, dip to the southwest reflecting the effect of east-trending normal faults on a generally westward regional dip. But adjacent to the faults the strata are dragged, in some cases strongly, to give small local west-plunging synclines immediately to the north of the faults (Fig. 1.3). At the northern limit of the graben the Richmond Gulf Group can be seen in outcrop to be faulted out against the granite basement by a southeast striking fault (Fig. 1.2, 1.4) which does not displace the overlying Nastapoka Group. There granitic basement rises to the north in steps by means of south-facing cliffs one or two hundred metres high. Two of these cliffs represent the upthrown sides of major faults. At the south limit of outcrop of the Richmond Gulf Group where exposure is not good, the group is faulted out against the granitic basement in a manner probably similar to that at the northern limit (Fig. 1.5). From the data discussed above and from previous work (Chandler, 1979; Chandler and Schwarz, 1980) it seems that the Richmond Gulf Graben is a symmetrical structure.

The gravity survey, mentioned above, showed an east-west positive anomaly that lies, as measured by the distribution of the downthrown sediments, approximately in

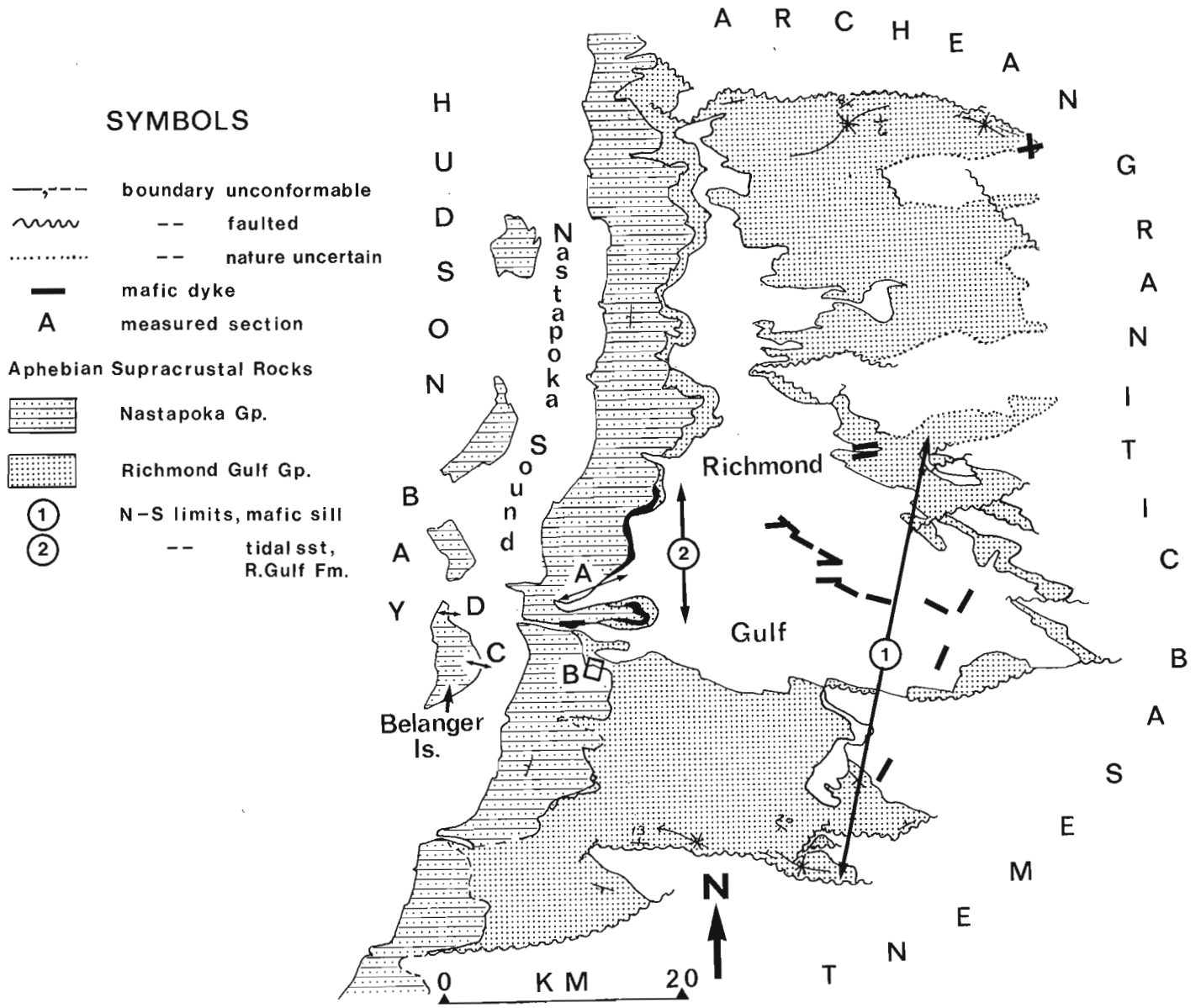

Figure 1.2. Location of sections and of some features of structural significance, Richmond Gulf. Measured sections shown in Figures 1.7 and 1.8.

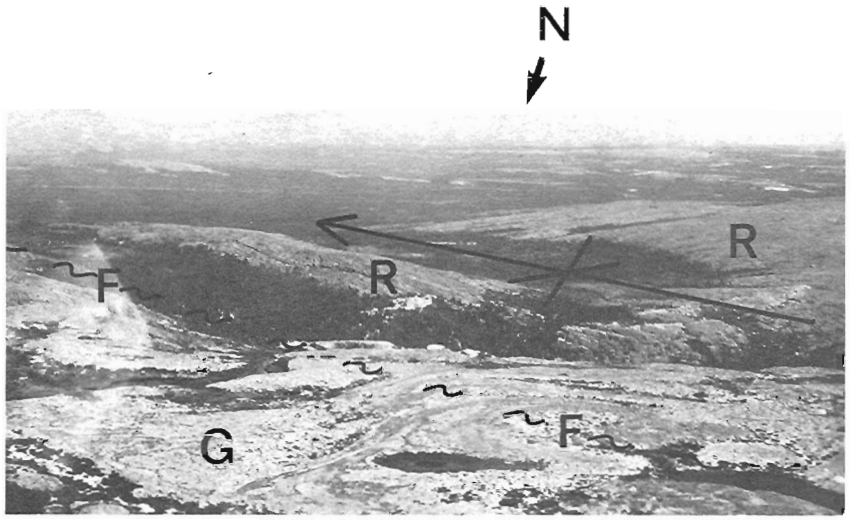

Figure 1.3. West-plunging syncline in Richmond Gulf Group (R) caused by downthrow on fault (F) against Archean basement (G), south margin, Richmond Gulf Graben. Cliffs in distance are Nastapoka Group carbonates overlain by basalt flows (N). Syncline is the western of two shown in lower part of Figure 1.2. GSC 203265-E

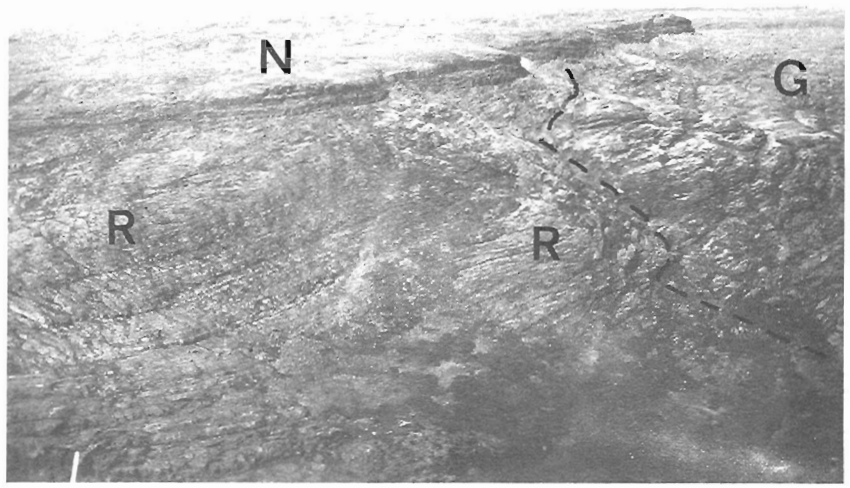

Figure 1.4. Arkose of Richmond Gulf Group (R) downfaulted against Archean granitic basement (G), north margin, Richmond Gulf Graben, looking northwest to 100 m cliff. Note that unconformably overlying Nastapoka Group (N) is not disturbed by the fault. GSC 203265-B

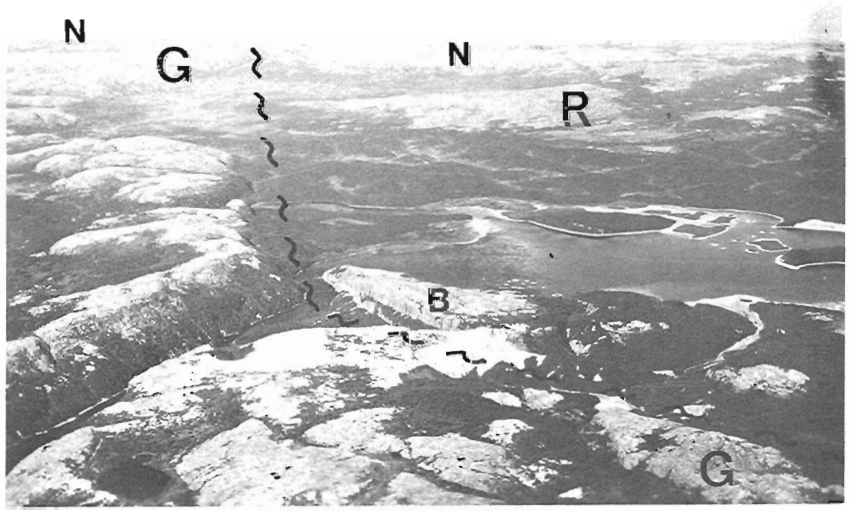

Figure 1.5. Southern boundary of Richmond Gulf Group arkoses (R) and basalt (B) of the Persillon Formation downthrown to north against Archean granitic basement (G). The unfaulted Nastapoka Group (N) rims Hudson Bay. GSC 203265-C

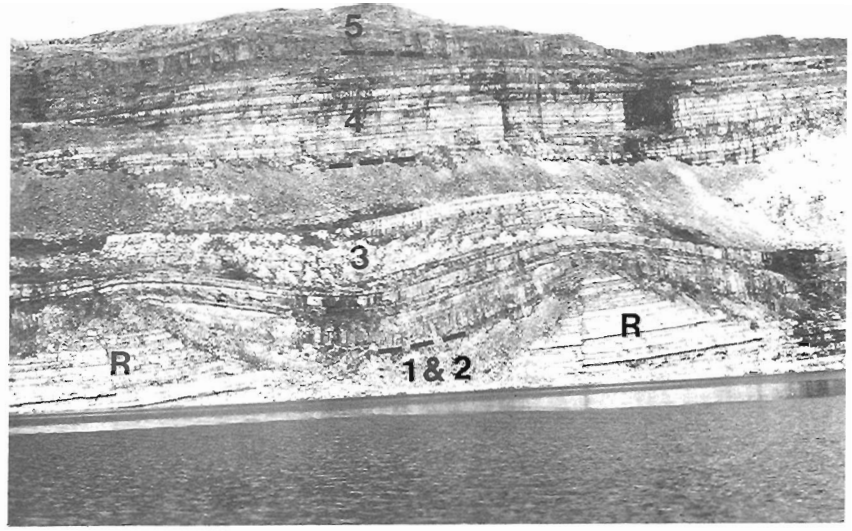

Figure 1.6. Nastapoka Group unconformably overlying Richmond Gulf Group tidal member (R), Section A, Figure 1.2. Subdivisions of the Nastapoka Group are units 1 to 5 as discussed in Figure 1.7. Cliff is 300 m high. GSC 203264-X

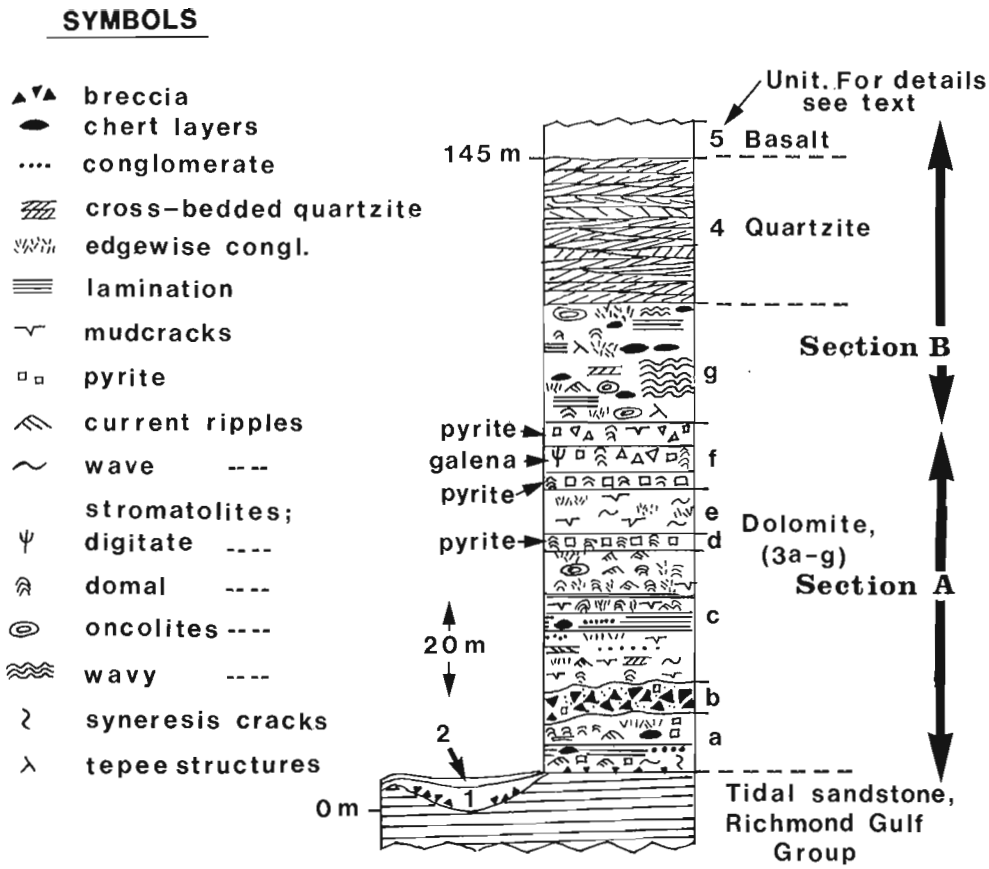

Figure 1.7. *The Nastapoka Group, upper part, Richmond Gulf. Location of Sections A, B on Figure 1.2.*

the centre of the graben. Figure 1.2 shows three features that might be important in interpreting the anomaly and are centred approximately on the trace of the anomaly: first, the concentration of mafic dykes cutting the Richmond Gulf Group, but not the Nastapoka Group; second, mafic sills within the Richmond Gulf Group, restricted to the central part of its outcrop area; third, the tidal sandstone member locally present at the top of the Richmond Gulf Group (Fig. 1.6). This unit is truncated against the unconformity at the top of the group; therefore it was probably once more widespread. Its presence over the anomaly suggests that maximum downwarp in the graben occurred there. These features are consistent with a focus of rifting and upwelling of mafic igneous material on the site of the anomaly.

The Nastapoka Group

At the latitude of Belanger Island (Fig. 1.2), the Nastapoka Group consists of an upper and a lower part separated by the waters of Nastapoka Sound which cover approximately 500 m of section. On the mainland the group consists of a southward thickening sequence of stromatolitic dolomite and quartz arenite capped by basalt flows (Fig. 1.7). These rocks outcrop on cliffs on the east side of a cuesta up to 420 m high that separates Richmond Gulf from Nastapoka Sound. On the Nastapoka Islands to the west of Nastapoka Sound the upper part of the group consists of clastic rocks with iron formation (Fig. 1.8). These rocks have been described by the Geological Survey of Canada in several reports dating from the turn of the century.

The Nastapoka Group at Richmond Gulf

At the north limit of the gulf the group is represented by a few metres of grey sandstone overlying the Archean basement. Thickening southward for 80 km and composed essentially of carbonate, it mainly overlies feldspathic sandstone of the Richmond Gulf Group in the Richmond Gulf Graben (see Chandler and Schwarz, 1980). Southward, across the graben it again overlies the granitic basement (Fig. 1.2), having thickened to about 150 m. Several sections of this carbonate-quartzite sequence have been examined. A composite section from the cliffs at the southwest corner of the gulf (Fig. 1.7) is presented as a preliminary account of the sequence.

The Nastapoka Group overlies the Richmond Gulf Group with gentle angular unconformity whose surface has a relief generally measured only in metres but which locally forms rugged topography (Fig. 1.6). At section A, beneath the unconformity a sandstone-siltstone member is conformable on the dominantly fluvial Qingaaluk Formation of the Richmond Gulf Group. Well developed herringbone crossbeds indicate a tidal marine mode of deposition. The preservation of this unit only in this region (Fig. 1.2) may indicate that the maximum downwarp in the graben is recorded here. At section A a metre or so of sandstone-cobble conglomerate (Fig. 1.9), that thickens to 3-4 m on the flanks of depressions, lies on the unconformity surface.

The basal unit of the Nastapoka Group, above the conglomerate, is composed of a chain of coarsening upward lenticular bodies (unit 1, Fig. 1.7), up to 16 m thick, each one draped in the bottom of a depression (Fig. 1.6). At the base

the unit is composed of parallel – laminated to bedded black mudstone and fine-grained sandstone including massive pebble conglomerates up to 20 cm thick underlain by dragfolds indicating downslope movement. Bedding scale increases upward to about 0.5 m at the top of the unit where beds are strongly slumped. Sedimentary structures in the unit include massive and laminated beds, ball and pillow horizons, and current ripples. Some beds display massive bases and laminated upper parts, and are capped by several millimetres of black mudstone. This unit was probably deposited by local resedimentation. The succeeding unit 2, again disposed in lenses in the depressions on the unconformity surface, has a maximum thickness of 6m. It is quite unlike the underlying unit 1, being a well crossbedded fine- to coarse-grained quartz arenite. Beds range from 30-100 cm in thickness and are formed of crossbeds terminating in ripples. Pyritic stylolites are present. The unit was probably deposited by sand wave and dune migration.

At the base of the carbonates, unit 3a is composed of 4 m of clastics overlain by 8 m of carbonate. The clastics contain fine grained wave rippled sandstone and black siltstone with syneresis cracks and carbonate pebble breccia. In the succeeding 2 m of laminated dolomite, the laminae are truncated, probably by current scour. Laminite pebble breccia layers, one 70 cm thick, and grit layers are present. The upper 6 m of the laminated dolomite contains pyrite crystals up to 1 cm across, tabular black chert and 2-10 cm thick laminite breccia zones as well as poorly preserved ripples and laminae.

Unit 3b is 4 m of massive chert breccia, with interstitial pyritic quartz arenite. Though the units above and below are broadly conformable, unit 3b overlies unit 3a on an irregular erosion surface with a relief of up to 3 m, and the uppermost 1 m of unit 3a is brecciated. This unit, interpreted as a solution breccia, also occurs at the same stratigraphic level 30 km to the south.

The chert breccia is succeeded on a gently undulating surface (15 cm) by 25 m of dolomite, unit 3c, divisible into six subunits. Subunit 1 is 4 m of laminated pyritic dolomite with laminite and carbonate-chert breccia zones up to 10 cm thick. Low domal stromatolites, the lowest in the section, are draped by laminae of alternating fine grained quartz arenite and mudcracked mudstone. Subunit 2 is 2 m of quartz arenite with current and wave ripples up to 5 cm high, carbonate-pebble beds up to 8 cm thick, and mudcracks in the finer grained parts of the quartzite. Subunit 3 is 3.5 m of white crossbedded quartz arenite, including carbonate- and chert-pebble conglomerate in a quartz arenite matrix, and grey rippled siltstone. Subunit 4 is 4.5 m of parallel- and wrinkle-laminated dolomite with carbonate grit layers up to 8 cm thick and isolated domal stromatolites up to 4 cm high. Subunit 5, 5 m thick, consists of alternating beds of dolomite, crowded with stromatolites and about 60 cm thick, and beds of grey mudstone about 15 cm thick. The stromatolites are buns and spherical domes up to 1.5 m across separated by pockets of edgewise laminite breccia (Fig. 1.10). The mudstone layers contain rippled carbonate draped by mudcracked mudstone. Subunit 6 is 6 m of mud-free well-laminated pale grey dolomite, again containing stromatolite spheres and buns separated by edgewise laminite breccia. Black chert layers, about 5 per cent of the rock and up to 8 cm thick, and carbonate grit layers are present.

The lower of two abundantly pyritic zones (3d) is a 3 m thick, heavily limonite-stained, cavernous bed containing pyrite nodules and a central 1 m thick layer crowded with stromatolites similar to those in the underlying unit. Unit 3e is 10 m of flaggy cream coloured dolomite, that is chert, pyrite and stromatolite-free. Features include wave ripples, edgewise laminite breccias up to 3 cm thick, and mudcracked, rippled dolomite.

The tripartite upper pyritic zone (3f) is 13 m thick. The lower and upper parts, 3 and 5 m thick respectively are very similar to unit 3d. The central part (5 m) is markedly cavernous and limonite-stained and contains pyrite bodies up to 50 cm long (Fig. 1.11). It is abundantly stromatolitic and contains disoriented blocks of the same material. Nearly all stromatolites are similar to those seen lower in the section. Delicate digitate stromatolites are present in this zone (Fig. 1.12) and were recorded at this level in several other sections. Only in one section was a similar form of stromatolite found at another level. This stromatolite may be of significance because it is in the central part of this upper pyritic zone that galena-sphalerite mineralization is found. Earlier literature (Stevenson, 1968; Bell, 1879, p. 15c) records the presence of lead mineralization in these carbonates from the head of Manitounuk Sound to the opening of Richmond Gulf. Gangue minerals include euhedral dolomite and quartz crystals lining vugs. In the upper pyritic part of unit 3f where iron staining and brecciation are less, pyrite and quartz were seen to lie preferentially within large stromatolites.

Unit 3g and succeeding parts of the carbonate-quartzite section of the Nastapoka Group were studied in section B (Fig. 1.2). Unit 3g is a pyrite-free grey, laminated dolomite containing edgewise laminite breccia and oncolites. The lowest 3 m contains isolated stromatolite buns and tepee structures. The succeeding 9 m is dominated by close-packed wavy stromatolites superficially like in-phase climbing ripples in vertical section, and is a useful marker zone. Rare crossbedded and rippled quartz arenite lenses up to 15 cm thick in the upper part of unit 3g presage sedimentation of quartzite. The next 11 m of carbonate is parallel and crinkly laminated and marked by (5-10%) of pale grey chert layers. Isolated stromatolite buns and clubs, some pyrite nodules 1 cm across, edgewise laminite breccia, and a few oncolites

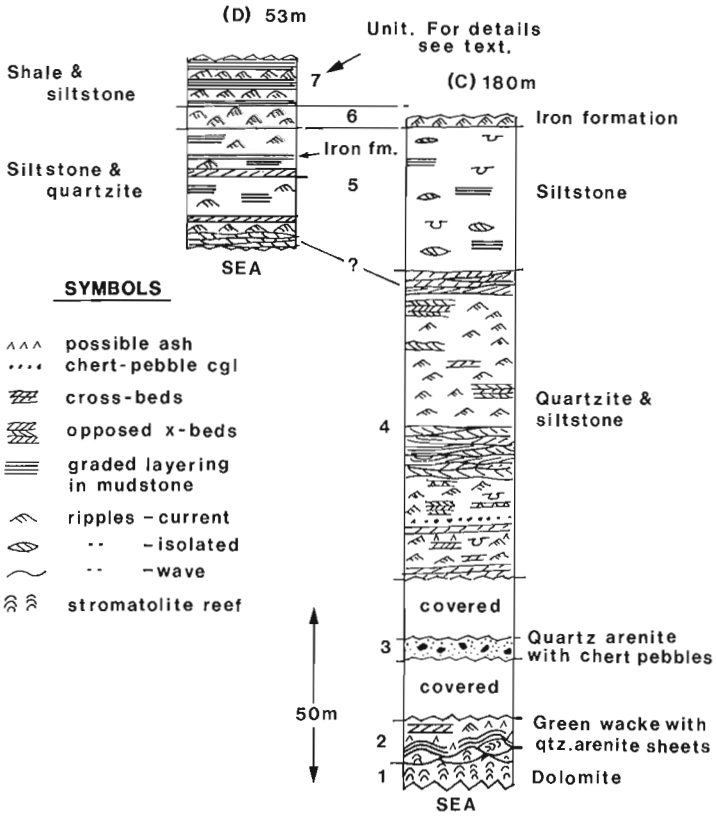

Figure 1.8. The Nastapoka Group, upper part, Belanger Island. Locations of Sections C, D on Figure 1.2.

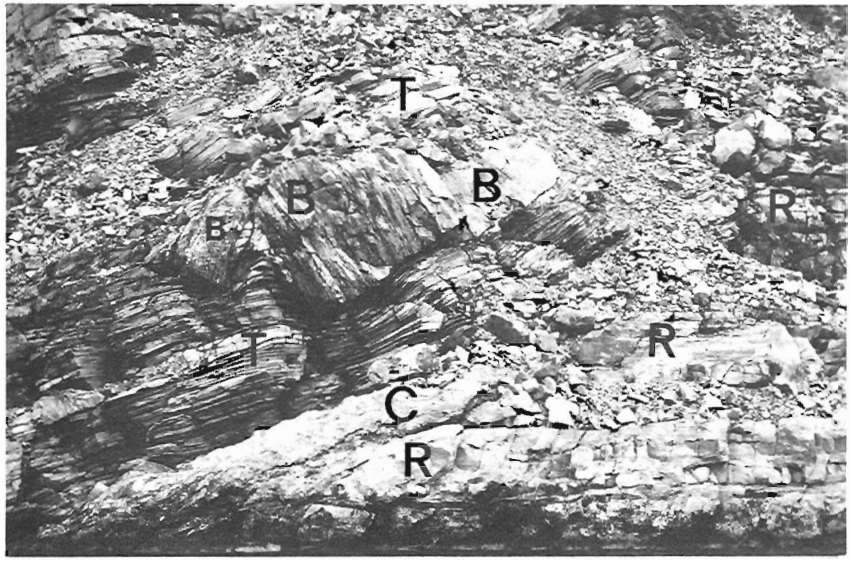

Figure 1.9. *Detail of unconformity (Fig. 1.6), with Nastapoka Group thin bedded turbidites (T) overlying tidal sandstone of Richmond Gulf Group (R). 1 m of sandstone conglomerate (C) overlies unconformity. Blocks of tidal sandstone (B) now lodged in turbidites tumbled down steep slope of unconformity during Aphebian time. GSC 203265-G*

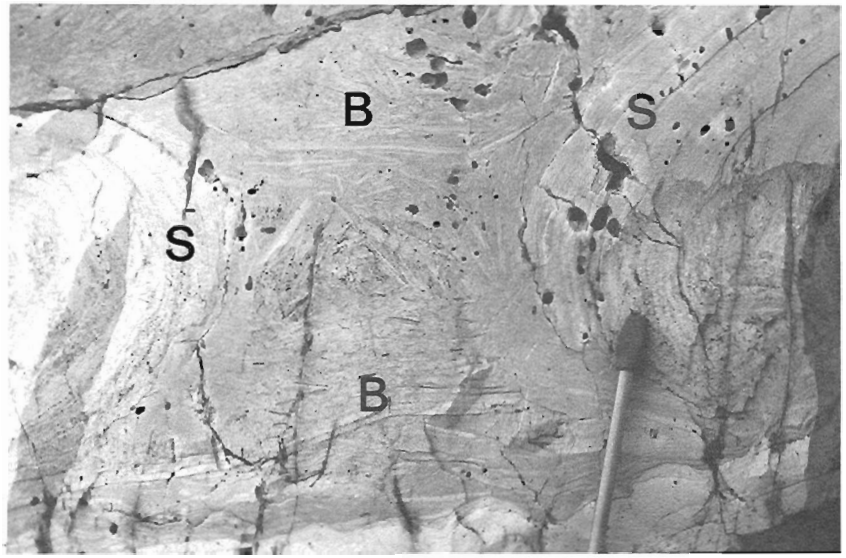

Figure 1.10. *Vertical section of spherical stromatolites (S) with intervening laminite breccia (B); subunit 5, unit 3c of Nastapoka Group in Figure 1.7. GSC 203264-V*

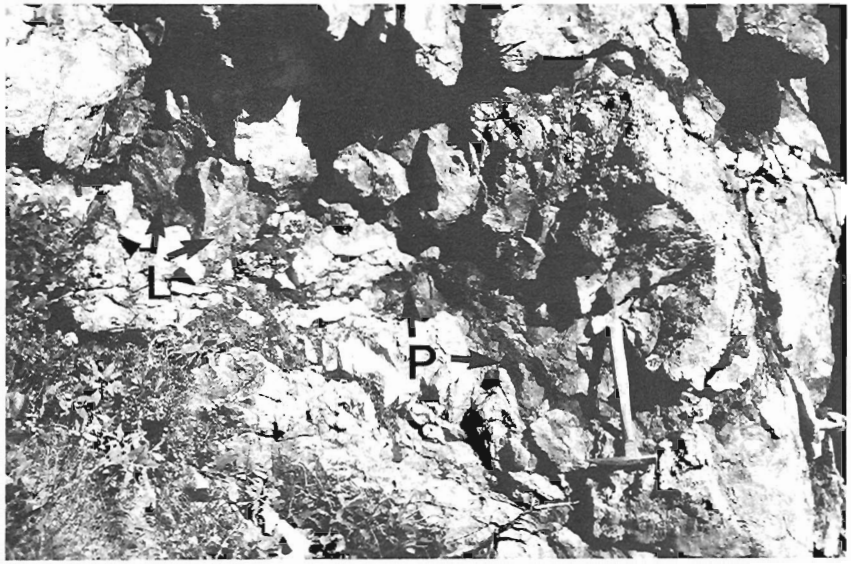

Figure 1.11. *Cavernous, brecciated appearance of lead-zinc-bearing zone; Unit 3f of Nastapoka Group in Figure 1.7. Limonate stains (L) and pyrite bodies (P) are characteristic. GSC 203265-A*

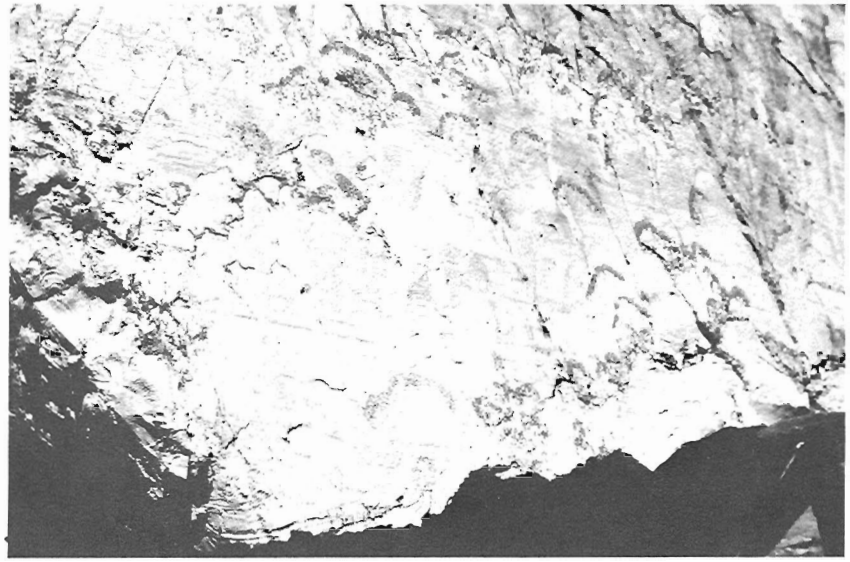

Figure 1.12. *Vertical section of digitate branched stromatolites of lead-zinc-bearing zone; unit 3f, Nastapoka Group, Figure 1.7. Photograph represents vertical distance of about 1 m. GSC 203264-W*

are present. The top of this 11 m thick subunit contains a 35 cm long oncolite and several 25 cm thick 2-3 m long lenses of edgewise laminite breccia supporting stromatolite growth.

Carbonate sedimentation is terminated by unit 4, which begins as 3 m of dolomite-cemented crossbedded quartzite that leads up to 24 m of white weathering quartzite. This unit is mainly planar-crossbedded on a scale of 10-15 cm. Paleocurrents seem to have come from the west and few wave ripples are rare. The quartzite is succeeded by basalt flows with spiracles 2.5 cm long and 4 mm across in the basal 30 cm. The basalt unit (5) dips gently westward beneath Nastapoka Sound. The top of the unit was not seen.

A preliminary environmental analysis of the carbonates of the Nastapoka Group rests on the sedimentary structures in the carbonates. Edgewise laminite conglomerate, pebble conglomerates, oncolites and truncated laminae all point to vigorous current activity. Oolites, seen elsewhere, indicate very shallow water, and mudcracks indicate emergence. These structures are common in modern and ancient carbonates of tidal and subtidal environments (Eriksson, 1977; Ginsberg, 1975).

Nastapoka Group, Belanger Island

The bulk of the formation, from the basal dolomite to the iron formation, was measured in cliffs on the east side of Belanger Island (section C, Fig. 1.2). The part immediately including the iron formation was again measured at the northern tip of Belanger Island where better exposed (section D, Fig. 1.2).

Section C, commences at sea level with 10 m of dolomite, (unit 1 of Fig. 1.8). This dolomite is crammed with stromatolites. The upper surface of the unit is moulded into northeast-trending ridges (Fig. 1.13).

Thickening of stromatolite laminae on the outer sides of the ridges is evidence that the ridges are the exhumed, current-moulded topography of a reef. Between the ridges lie isolated patches of coarse grained quartz arenite with dolomite and chert pebbles, some pebbles apparently replaced by pyrite. One 5 cm-long oncolite was also seen. In the hollows between the ridges are disoriented blocks of dolomite similar to that of the ridges. Except for a gentle westward dip no signs of post-depositional disturbance are visible. This carbonate unit was swept by rigorous currents.

The dolomite is draped abruptly by unit 2, 12 m of green fine grained generally featureless wacke, that has a well developed conchoidal fracture. The basal 10 cm is pyritic and the lowest two metres is normally size-graded in units up to 2 cm thick (Fig. 1.13). Other sedimentary structures in the unit are quartz-arenite-filled syneresis cracks and a few poorly preserved ripples. Prominent within unit 2 are several per cent of quartz arenite sheets up to 60 cm thick, many of which are strongly slumped and composed of plutonic quartz grains. Sedimentary features of the arenite bodies range from 45 cm-thick planar crossbeds, through a 25 cm-thick trough-crossbedded unit with a scoured base and lenticular bodies representing isolated sand waves, to beds 8 cm thick or less composed entirely of current ripples.

Unit 1 is interpreted as a stromatolite reef, washed by vigorous, possibly tidal currents. Stromatolitic growth may have been terminated by burial in muddy debris deposited from either suspension or turbidity currents. The distinctive green colour of unit 2, quartz shards seen in thin section, and the presence of thin massive units of similar material higher in the section suggest that it may contain volcanic ash. The quartz arenite bodies within the unit may represent incursions of continent-derived debris washed in during re-establishment of traction current transport.

Unit 3, isolated from unit 2 by a 17 m covered interval, is 6 m thick. It is a contorted but otherwise structureless grey quartzite containing scattered grey chert pebbles, some up to 25 cm long. After a second covered interval of 17 m unit 4, comprising 87 m of coarse- and fine-grained quartzite and siltstone, divided into subunits of crossbedded quartzite and rippled fine grained quartzite and siltstone, follows (Fig. 1.14). Opposed crossbedding (Fig. 1.15) occurs at several levels through the unit. In the lower part some quartzites have dolomite matrix or contain abundant chert pebbles. Syneresis cracks are present in the finer grained material. Two green, parallel sided massive wacke units, 9 and 13 cm thick, may be volcanic ash layers. Crossbeds up to 80 cm thick are present in thicker beds. The finer grained material of the unit contains abundant ripples both of wave and current type. Wavy and lenticular bedding are common as is flaggy parting. Subordinate thin crossbedded to rippled quartzite beds are present. This unit was deposited in a tidally influenced low-energy traction regime.

The succeeding unit 5 was studied in sections C and D (Fig. 1.2) as was the overlying iron formation. In the former section it is 25 m thick and in the latter it is 30 m thick. In both sections it is a very dark weathering upward-fining dark grey-green texturally immature siltstone-argillite with widely spaced parallel partings. Crossbedded sandstone is rare. One 2 m thick crossbedded unit contains rounded and angular quartz grains, carbonate oolites and abundant diagenetic chlorite. In the lower part of unit 5, one horizon of flute marks indicates transport to the east. At several horizons north-trending irregular assymetric linear wrinkles, reminiscent of incipiently slumped ripples, mark the tops of sand beds. These may indicate westward slumping. Ball and pillow structures in layers up to 4 cm thick were also noted in the unit. Ripples in some exposures are isolated. In others they mark the bases of several 5 cm-thick fine grained sand- to silt beds that terminate with dark green mudstone. Faintly discernible lamination from a sub-millimetre to a 3 cm scale is present through the unit. This lamination commonly has bases of fine- to medium-grained sand and fines upward to terminate as dark green mud against the pale grey-green sand at the base of the succeeding laminae.

Unit 6, a 7 m-thick iron formation is heavily iron-stained and lichen covered. At its base lies a 60 cm unit composed of granules with syneresis cracks, now largely rhodochrosite. It may originally have been an iron oxide oolite. The succeeding iron formation is grey, granular and rippled in outcrop and the ripples are draped by laminae less than 1 cm thick that are rich in magnetite. In thin section the grains are composed of chert with sheaves of a stilpnomelane-like mineral and are coated with iron oxide. The intergranular cement is chert.

The highest unit, no. 7 in section D (Fig. 1.2), is 14 m thick, heavily iron-stained and nonmagnetic. It consists of a coarsening upward sequence of black fissile shale with subordinate parallel-bedded pyritic siltstone. The siltstone beds contain current ripples and some, less than 5 cm thick, can be traced over 200 m. Towards the top of the sequence 15 cm thick sandstone beds contain wave- and current-ripples. The unit is overlain by overburden.

The sequence on Belanger Island records the swamping of a shallow marine carbonate regime by fine grained clastics, some possibly of volcanic origin. Periodic re-establishment of traction currents, some tidal in origin, others possible storm generated, could have deposited the arenites including the iron formation in the sequence. Chert-pebble-rich thin quartzite beds may be storm lag deposits. The rippled and graded fine grained clastics could be turbidite deposited but a more likely mechanism is redeposition by weak currents after suspension during storms. The parallel bedded siltstone in unit 7 could be turbidite

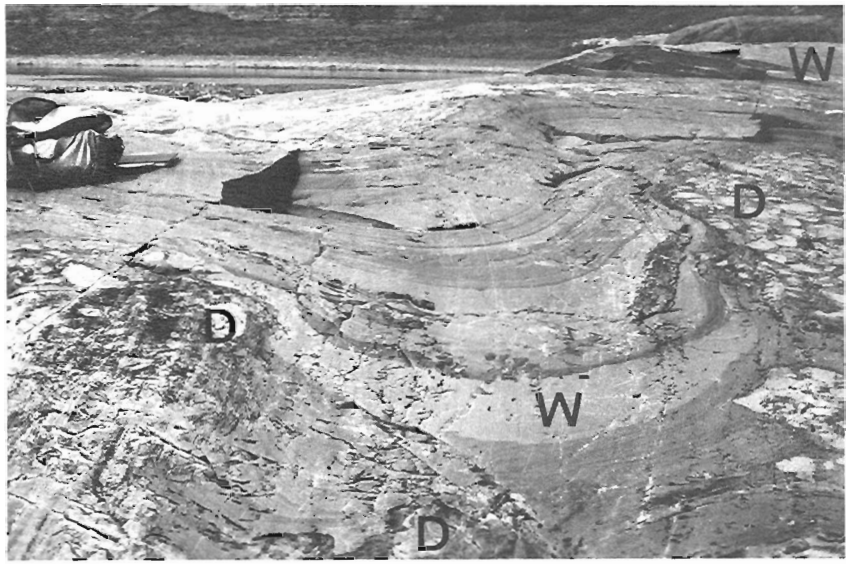

Figure 1.13. Nastapoka Group at base of section C (Fig. 1.8), Belanger Island. Stromatolitic dolomite (D) of unit 1 is moulded into ridges and overlain by laminated green wacke of unit 2 (W). GSC 203264-Y

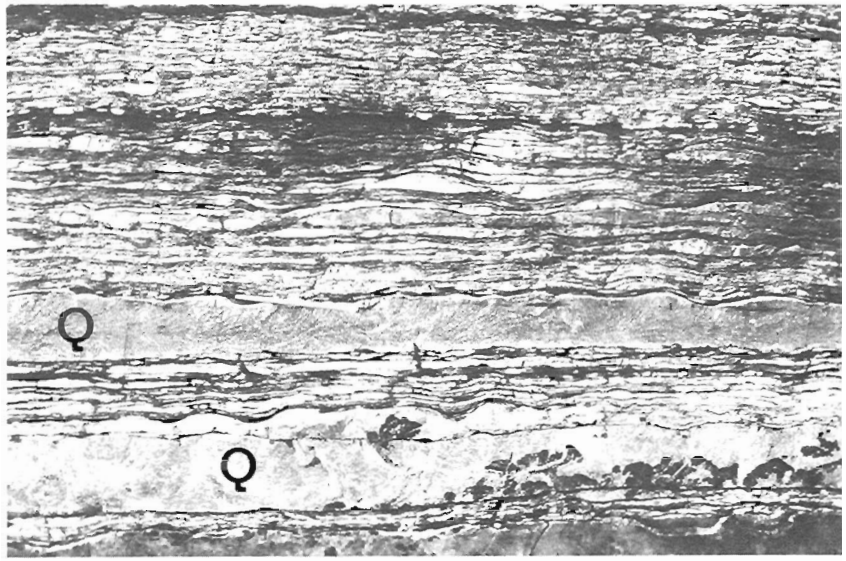

Figure 1.14. Rippled quartzite beds (Q) in lenticular and wavy-bedded siltstone to fine grained sandstone; unit 4 of Figure 1.8, Nastapoka Group, Belanger Island. GSC 203264-Z

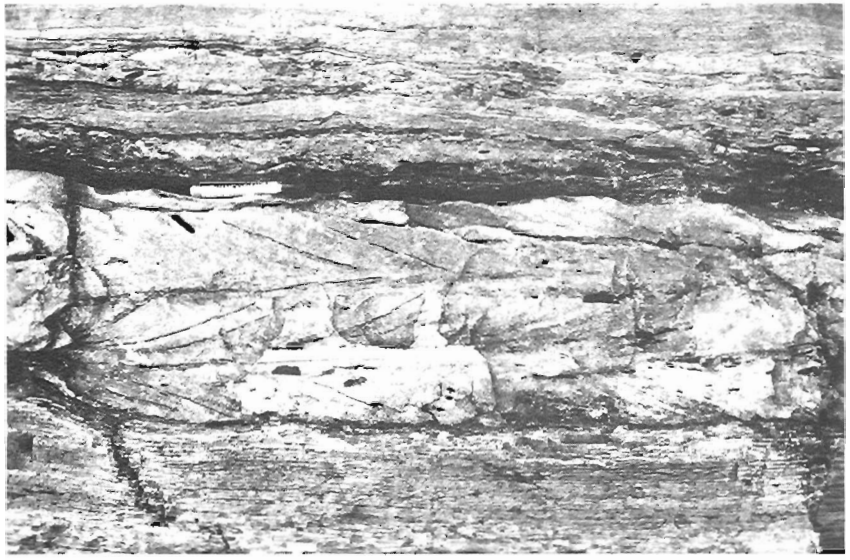

Figure 1.15. Opposed crossbedding in quartzite; Unit 4, Figure 1.8, Nastapoka Group, Belanger Island. Foresets picked out in ink. GSC 203265-D

Figure 1.16. Spheroidally weathered basalt boulder (pencil shows scale) in red volcanic conglomerate at base of Qingaaluk Formation. White stripes are calcite separating exfoliated basalt layers. GSC 203265-F

deposited, but symmetrical ripples indicate sedimentation above wave base. These features are consistent with a tidally influenced marine shelf.

Speculations on Mineralization

Mineralization associated with the Nastapoka Group includes strata-bound lead-zinc, copper and iron-manganese formation. Abundant pyrite development in the carbonates in section A (Fig. 1.7) is correlated with a high concentration of stromatolites. The lead-zinc mineralization lies within the centre of such a zone where the concentration of stromatolites and pyrite is high. The association of this mineralization almost exclusively with a branched columnar stromatolite may have significance. Mudcracks several metres above and below the lead-zinc zone may be evidence for an intertidal deposition of the host carbonate.

The abundant stromatolite growth in distinct horizons probably provided an organic substrate for sulphate-reducing bacteria to contribute to sulphide generation at distinct stratigraphic levels. The existence of highly mobile sulphur-bearing solutions is suggested by pyritization of varied rock types beneath the unconformity at the base of the Nastapoka Group. They include the basement granite as well as basalt and sandstones of the Richmond Gulf Group. In the latter case a continuous bleached zone up to 200 m thick is developed, from which iron-titanium oxide heavy minerals are leached and in which pyrite, chalcopyrite and bornite are deposited.

The genesis of Precambrian iron formations has a vast literature and is largely beyond the scope of this report. Field data, however, allow comment on two important aspects of the matter, the roles of (a), volcanism and (b), oxygenation of the atmosphere. Granular iron-mangenese formation on Belanger Island is composed of a mixture of silicate, oxide and carbonate phases. It occurs as rippled arenite in finer grained clastics in a tidal marine clastic succession, possibly on a marine shelf. Concentric structures in some of the granules suggest derivation from oolites. Quartz arenite beds in the finer grained clastics contain rounded grains with strained extinction patterns consistent with derivation from the Archean gneiss terrain to the east, but many quartz grains in the poorly sorted fine grained clastics are extremely angular and have clear sharp extinction. A possible source rock is felsic to intermediate tuff. A likely source rock has yet to be found, for the broadly correlative Flaherty Formation of volcanics on the Belcher Islands, though containing a large amount of tuff, is basaltic (Leggett, 1974). Jackson (in Dimroth et al., 1970) correlated the iron formation of Belanger Island with the Kipalu iron formation of the Belcher Islands. He recorded tuff among the lithologies of the underlying Mukpollo Formation, presumably correlative with that of Belanger Island, so it seems that explosive volcanism was present nearby during the deposition of these iron formations.

Amongst the Aphebian rocks of east Hudson Bay, basalts are present at several stratigraphic levels. They include the Eskimo Formation of the Belcher Islands (Stirbys, 1975) and its probable correlative (unit 5 of Fig. 1.7) as well as at least two units in the pre-Graben Richmond Gulf Group. These volcanics are probably rift-related.

The only iron formation recorded with these volcanics is 1 m with the Eskimo Formation (Dimroth et al., 1970). The main iron formations of eastern Hudson Bay, the up to 120 m thick Kipalu Formation and equivalents occur immediately beneath the Flaherty Formation (that lies somewhat higher in the succession). This unit is regarded by some as the remains of a large volcanic arc, the product of compressive tectonism. Overlying turbidites, the Omarolluk Formation, and molasse, the Loaf Formation, were transported eastward to southward (Bell and Hofmann, 1974; Leggett, 1974; Ricketts and Donaldson, in press). According to Ricketts and Donaldson (op. cit.) the molasse came solely from a cratonic source to the north of the Belcher Islands. From the above it would follow that the Proterozoic iron formations of eastern Hudson Bay occur at the change from extensional to compressive tectonics. A different opinion is that of Baragar and Scoates (1981) who, thinking on a wider scale, related the iron formations of the Circum-Superior Belt to volcanism associated with rifting.

Tectonics apart, the scale of the volcanism and its sedimentary environments might contribute to the development of the iron formation and the manganese mineralization. The Flaherty Formation with which the Kipalu and equivalent iron formation is associated is up to 2 km thick, contains abundant pyroclastics and was deposited in both submarine and subaerial environments (Dimroth et al., 1970; Leggett, 1974). The Eskimo Formation, with 1 m of associated lean iron formation is up to 1 km thick. The volcanic units of the Nastapoka Islands and the mainland are about a tenth of the thickness of the Eskimo Formation and iron formation has not been reported from them. All units except the Flaherty are essentially subaerial flow units (Chandler and Schwarz, 1980; Stirbys, 1975).

Iron, manganese and silica are released hydrothermally from modern ocean-floor spreading ridges (Edmond et al., 1979; Grill et al., 1981). Long distance transport of these elements by ocean currents, perhaps in particulate suspension (Bolger et al., 1978), could explain iron and manganese mineralization such as that of Belanger Island where local evidence of volcanism is tenuous.

The other important aspect is whether or not many of superior-type iron formations were formed more or less synchronously around the world as a result of the rapid development of atmospheric oxygen about 2 Ga ago as suggested by Cloud (1968). This hypothesis has been attacked by Dimroth and Kimberley (1975) who drew attention to stratigraphically lower redbeds in the Labrador Trough.

The Nastapoka Group, containing the granular iron formation on Belanger Island is underlain on the mainland by the Richmond Gulf Group (Chandler and Schwarz, 1980). This group contains fluviatile redbeds at several stratigraphic levels. Further, flows of the terrestrial basalt, the Persillon Formation, have reddened tops and the formation itself possesses an intensely reddened spheroidally weathered (Fig. 1.16) top at least 6 m thick. This reddened horizon is overlain by sandy redbeds at the base of the Qingaaluk Formation 80 m thick.

These data from the Richmond Gulf area support a connection between the genesis of this iron formation and volcanism. The question is raised of whether there may be a connection between significant iron formation and a change in tectonic regime from tensional to compressive. The data do not support the view that clustering of many Proterozoic iron formations at an age of about 2 Ga was caused by a sudden influx of oxygen into the oceans as suggested by Cloud (1968).

References

Baragar, W.R.A. and Scoates, R.F.J.
1981: The Circum-Superior belt: a Proterozoic plate margin?; in Precambrian Plate Tectonics, Developments in Precambrian Geology 4, ed. A. Kroner, p. 297-330.

Bell, Robert
1879: Report on an exploration of the east coast of Hudson's Bay; in Geological Survey of Canada, Report of Progress for 1877-78, p. 1c-37c.

Bell, R.T. and Hofmann, H.J.
1974: Investigations of the Belcher Group (Aphebian), Belcher Islands, N.W.T.; in Geological Association of Canada, Program with abstracts, 3rd circular, p. 8.

Bolger, G.W., Betzer, P.R., and Gordeev, V.V.
1978: Hydrothermally-derived manganese suspended over the Galapagos spreading centre; Deep-Sea Research, v. 25, p. 721-733.

Chandler, F.W.
1979: Geology of the Aphebian supracrustal rocks, Lac Guillauve Delisle, Quebec; Geological Survey of Canada, Open File, 600, two bedrock geological maps, scale 1:50 000.

Chandler, F.W. and Schwarz, E.J.
1980: Tectonics of the Richmond Gulf area, Northern Quebec- a hypothesis; in Current Research, Part C, Geological Survey of Canada, Paper 80-1C, p. 59-68.

Cloud, P.E., Jr.
1968: Atmospheric and hydrospheric evolution on the primitive Earth; Science, v. 160, p. 729-735.

Dimroth, E., Baragar, W.R.A., Bergeron, R., and Jackson, G.D.
1970: The filling of the circum-Ungava geosyncline; in Symposium on Basins and Geosynclines of the Canadian Shield, ed. A.J. Baer, Geological Survey of Canada, Paper 70-40, p. 45-142.

Dimroth E. and Kimberley, M.M.
1975: Precambrian atmospheric oxygen: evidence in the sedimentary distributions of carbon, sulfur, uranium, and iron; Canadian Journal of Earth Sciences, v. 13, p. 1161-1185.

Edmond, J.M., Measures, C., Manguri, B., Grant, B., Sclater, F.R., Collier, R., Hudson, A., Gordon, L.I., and Corliss, J.B.
1979: On the formation of metal-rich deposits at ridge crests; Earth and Planetary Science Letters, v. 46, p. 19-30.

Eriksson, K.A.
1977: Tidal flat and subtidal sedimentation in the 2250 m.y. Malmani Dolomite, Transvaal, South Africa; Sedimentary Geology, v. 18, p. 223-244.

Ginsburg, R.N. (ed.)
1975: Tidal Deposits, a Casebook of Recent Examples and Fossil Counterparts; Springer-Verlag, New York, 428 p.

Grill, E.V., Chase, R.L., MacDonald, R.D., and Murray, J.W.
1981: A hydrothermal deposit from Explorer Ridge in the northeast Pacific Ocean; Earth and Planetary Science Letters, v. 52, p. 142-150.

Leggett, S.R.
1974: A petrographic and stratigraphic study of the Flaherty Formation, Belcher Islands, Northwest Territories; unpublished B.Sc. thesis, Brock Univeristy.

Ricketts, B.D. and Donaldson, J.A.
1981: Sedimentary history of the Belcher Group of Hudson Bay; in Proterozoic Basins of Canada, ed. F.H.A. Campbell, Geological Survey of Canada, Paper 81-10.

Stevenson, I.M.
1968: A Geological reconnaissance of Leaf River map-area, New Quebec and Northwest Territories; Geological Survey of Canada, Memoir 356, 112 p.

Stirbys, A.F.
1975: A petrographical and geochemical study of the Eskimo Formation, Belcher Islands, Northwest Territories; unpublished B.Sc. thesis, Brock University, 72 p.

2. THE CIRCUM-UNGAVA BELT OF EASTERN HUDSON BAY: THE GEOLOGY OF THE OTTAWA ISLANDS AND THE CAPE SMITH REGION

Project 780012

W.R.A. Baragar and M. Piché[1]
Precambrian Geology Division

Baragar, W.R.A. and Piché, M., The Circum-Ungava Belt of eastern Hudson Bay: the geology of the Ottawa Islands and the Cape Smith region; in Current Research, Part A, Geological Survey of Canada, Paper 82-1A, p. 11-15, 1982.

Abstract

Smith Island and the Ottawa Islands in eastern Hudson Bay are composed principally of Aphebian komatiitic lavas subdivisible into high-Mg, medium-Mg, and low-Mg lavas and layered flows, each distinguished by characteristic megascopic features. The lavas can be grouped into mappable stratigraphic units on the basis of their Mg content but show little systematic variation of Mg with stratigraphic level. Rather, the lava types seem to interfinger and repeat. Layered flows are particularly abundant in the high-Mg units. They typically comprise a pillowed base and a differentiated massive top composed of olivine cumulate and olivine impoverished zones. Spinifex-textured flows are a rarer variant of the layered flows and known to occur only on Gilmour, Perley, and House islands of the Ottawa group. The thicker of the layered flows are markedly lensoidal and are interpreted as surface conduits for distribution of large volumes of lava to downstream flow fronts. It is postulated that some of the Mg variation in the sequence might be attributed to olivine sedimentation in transit in such distributors.

Introduction

Continuing the project begun in 1979 of mapping in detail volcanic rocks of the Aphebian Circum-Ungava Belt in eastern Hudson Bay (Fig. 2.1), the authors spent approximately one month at each of Cape Smith and the Ottawa Islands. At Cape Smith the volcanic succession was mapped at a scale of 400 feet = 1 inch along a surveyed line across Smith Island and was sampled for chemical analyses at intervals of about 100 to 150 m. In addition, the eastern half of Smith Island and parts of the adjoining mainland were covered by pace and compass traversing consistent with a mapping scale of 1:50 000. Similarly, on the Ottawa Islands surveyed, control lines were run across the northern part of Eddy Island, Pattee Island, and an unnamed island of the Eddy group, and mapping was extended by less precise methods to Gordon, Perley, and the Water islands group.

Dr. N.T. Arndt of the Max Planck Institute, Mainz, accompanied the party to the Ottawa Islands and undertook detailed studies of some of the layered flows on Gilmour Island (Arndt, 1982).

Acknowledgments

We gratefully acknowledge the able assistance given us in the field by Jacinthe Sabourin and John Lech, who were commonly obliged to work long hours in all too short a season. We are also indebted to the Captain and crew of the Peterhead TOOLUK who were responsible for our safe conduct to, from, and among the Ottawa Islands under weather conditions that were generally far from ideal. Finally, we want to extend very special thanks to personnel of the Environment Canada weather station at Inoucdjouac, especially André Soucy and Marcel Savard, for their splendid hospitality during our brief stays there and for the vital and cheerful radio contact they maintained with us during the summer.

General Geology

The geology at Cape Smith is continuous with that of the Cape Smith-Wakeham Bay Belt where it has been generally defined by the work of Bergeron (1957, 1959), Beall (1959, 1960), Gold (1962), Gélinas (1962), Taylor (1974), Baragar (1974), Schimann (1978), and Francis and Hynes (1979). Although not previously mapped in any detail,

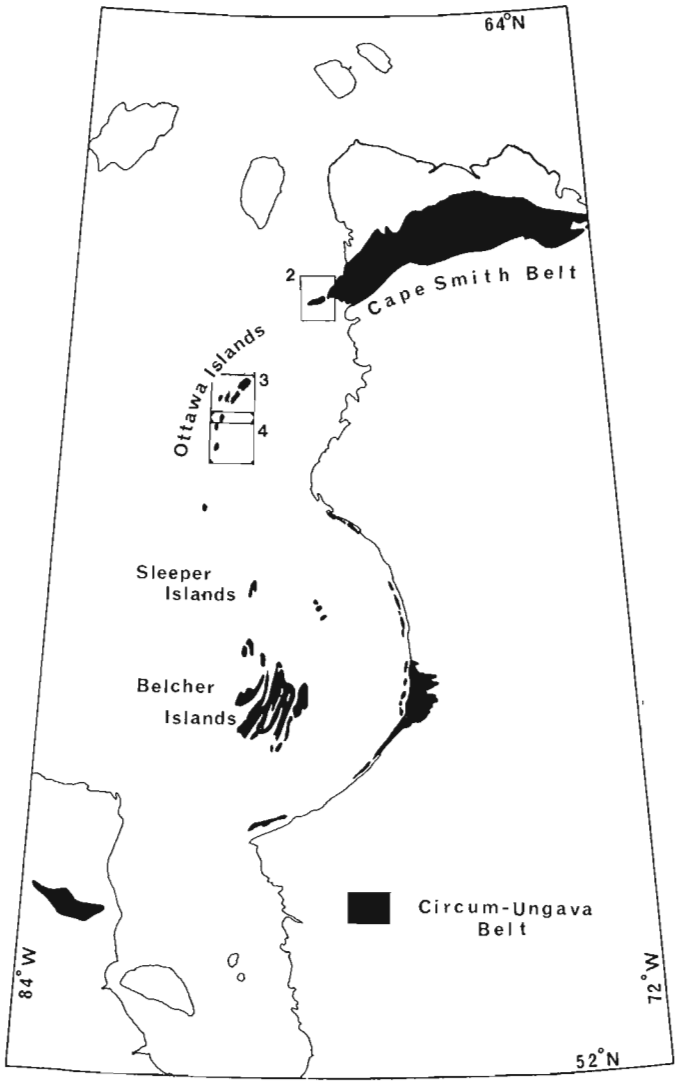

Figure 2.1. Location map showing the areas referred to in the present report in relationship to the Circum-Ungava Belt. Numbers shown are figure numbers.

[1]Département de geologie, Université du Québec à Chicoutimi, Chicoutimi, Québec

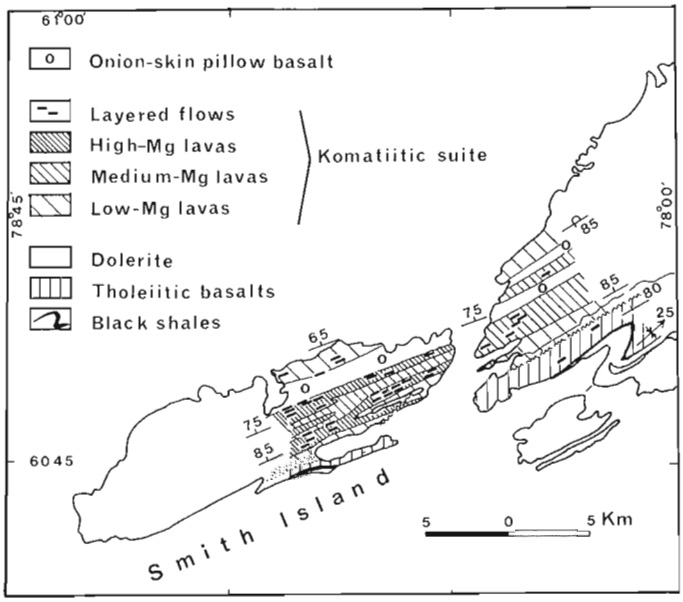

Figure 2.2. Preliminary geological map of parts of Smith Island and the adjoining mainland.

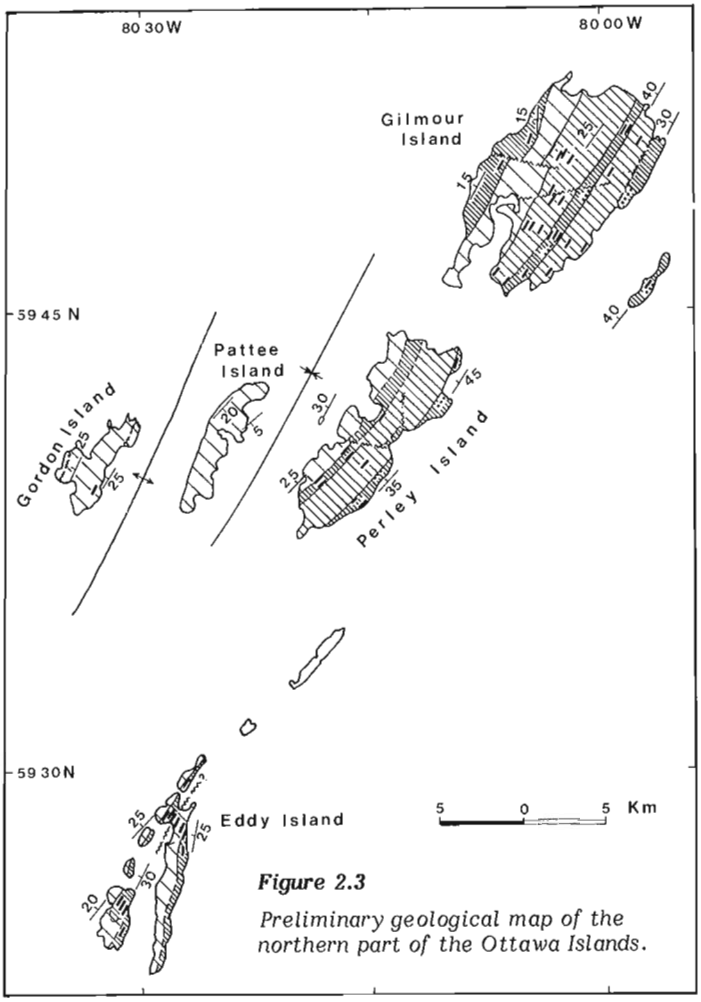

Figure 2.3

Preliminary geological map of the northern part of the Ottawa Islands.

the rocks of Smith Island and the adjoining mainland can be related to those of the main part of the belt by projection along strike. There the stratigraphic sequence can be divided into three groupings: a lower sedimentary succession of mainly shelf-type sediments, a middle division of tholeiitic basalts, and an upper division of komatiitic lavas. In the Cape Smith region the komatiitic suite forms the bulk of the sequence but part of the tholeiitic division may be present at its base. Only the komatiitic suite is present in the Ottawa Islands.

The geology of the Cape Smith region is shown in Figure 2.2. The succession is divided into a number of lithologies. Those forming the komatiite suite will be described in a later section, the others are of less certain affiliation. The assemblage mapped as dolerite, tholeiitic basalt, and black shale along the southern side of the komatiitic sequence is roughly on strike with, and resembles, the tholeiitic sequence in the central part of the belt. The volcanic rocks comprise both pillowed and massive lavas, but are characterized by a higher proportion of thick, massive flows than other parts of the succession and in this respect are similar to the tholeiitic sequence elsewhere in the belt. However, they contain some peridotitic layers (Fig. 2.2) which could be interpreted as a mark of their affinity to the komatiitic suite. Chemical analyses provided by Schwarz and Fujiwara (1977) of samples taken across part of this sequence indicate tholeiitic compositions for all but one high-Mg komatiite. Hence, this lower unit appears to be composed predominantly of tholeiites, with some komatiitic interlayers. These latter were not established definitely as flows and could be intrusives.

Interlayered with the komatiitic suite in the upper part of the succession is a distinctive volcanic rock which was given the name "onion-skin" pillow basalt after its most characteristic feature. Its pillow rims are typically 3 to 5 cm thick and very scaly in appearance, owing to the presence of closely-spaced, concentric layers of what seem to be tiny variolites. The rock has little resemblance to those considered to be part of the komatiitic suite and is tentatively attributed to a separate source.

The succession in the Cape Smith region dips steeply north and faces north. Assuming no repetition by faulting its exposed thickness would exceed 6000 m. Some thrust faulting, however, can probably be assumed. A number of lineaments subparallel to strike can be seen on the air photographs and what is obviously a décollement separates the folded tholeiitic sequence from the unfolded komatiites which overlie it.

The Ottawa Islands can be grouped into 5 subparallel chains of islands, each distributed along its strike direction and probably manifesting successive outcroppings of resistant sequences (Fig. 2.3, 2.4). The chains from east to west are represented by the Waters Island group, Eddy and House islands, Gilmour and Perley islands, Pattee, and Gordon islands respectively. Fold axes separate the three western chains but those on the east dip uniformly westward at shallow angles and are of unknown relationship to one another. They could represent a progressive stratigraphic sequence with rocks of Waters Island at the base and those on the west side of Perley and on Pattee and Gordon at the top. However, it is unlikely to be a continuous sequence. Lineaments, interpretable as faults, are apparent on the air photographs of most of the islands and the sequence on the western limb of the Eddy Island group is sufficiently similar to that of the eastern limb – with which it diverges in strike – that it could be a repetition of the latter. Hence, repetition by faulting is undoubtedly a factor. All the rocks belong to the komatiitic suite. If their distribution does have stratigraphic significance then the most magnesian rocks appear to be in the middle part of the sequence. The least magnesian are probably those of western Perley, Pattee, and Gordon islands at the top of the sequence.

Lithology of the Komatiitic Suite

Subdivision of the komatiitic suite is on the basis of field characteristics but from experience gained from the Gilmour Island studies (Baragar and Lamontagne, 1980) these are interpreted in terms of their magnesian content. Three such divisions are practical – low-Mg, medium-Mg, and high-Mg lavas – although not always easily distinguishable. An additional subdivision is the layered flows, which is so characteristic a feature of komatiitic sequences in general.

Low-Mg lavas (Fig. 2.5)

These commonly occur in thick pillowed flows (± 100 m) with minor massive zones within and generally at the tops of flows. The pillows are thick-rimmed (± 2 cm) and smoothly rounded or very slightly polyhedrally jointed. Multiple drainage cavities in pillows are abundant and many are filled with quartz, as are interpillow spaces. Variolites, commonly present, tend to be large and conspicuous. Probable Mg content is 10-13 per cent.

Medium-Mg lavas (Fig. 2.6)

Typically in thick to moderately thick (30 m+) pillowed flows with massive zones adjoining flow tops, medium-Mg lavas are marked by thick-rimmed (1-2 cm), polyhedrally-jointed pillows. Drainage cavities in pillow centres and interpillow space rarely contain quartz. If variolites are present they tend to be small and inconspicuous. Weathered surfaces are generally brownish. Probable Mg content is 13-16 per cent.

High-Mg lavas (Fig. 2.7)

The flows are generally thin (3 to 50 m) and irregularly pillowed. The pillows are thin-rimmed (± 0.5 cm) and typically form at the base of flows from where they branch up into their interiors. In many cases pillows are incomplete and discontinuous rims project into massive lava. Jointing in the massive upper parts of flows passes upward from coarsely columnar to finely polyhedral near the top. Drainage cavities in pillows tend to be sparse and distorted; quartz filling is absent. Weathered surfaces are brown to orange-brown in colour. Probable Mg content is greater than 16 per cent.

Layered flows (Fig. 2.8)

Various types of layered flows found on Gilmour Island are described by Arndt (1982). The most common type encountered within the komatiitic suite on Smith Island and the Ottawa Islands is that shown in Figure 2.8.

Pillows forming the lower part of the flow are overlain by, or branch up into a grey-weathering massive zone of low, apparent olivine content. This is followed by a coarsely columnar jointed, olivine cumulate zone with a deep orange-brown weathering surface. Upward the olivine-rich zone grades rapidly into massive grey-weathering lava with fine columnar jointing and finally into an aphanitic, polyhedrally jointed, chilled zone at the surface of the flow. The upper massive zone of some flows contains sets of discontinuous veins, commonly 1 to 5 cm thick, subparallel to the flow margins (Fig. 2.8). The substance of the veins appears continuous with that of the host and rarely shows a spinifex-like texture. The proportions of pillowed to massive phases vary greatly; in some flows as much as two thirds of the flow thickness, in others, as little as a single discontinuous pillow layer at the base of the flow. The thickness of the massive zone determines to some degree the extent of differentiation in the layered flows. A typical thickness of 25 to 30 m yields an olivine enriched layer overlain by massive lava similar in appearance to that which forms the pillow lavas at the base. Massive zones in excess of about 50 m thick give rise to the layered flows with an olivine cumulate zone overlain by clinopyroxenite, gabbro, and gabbro pegmatite.

Spinifex-textured flows are an uncommon variant of the layered flows. They are virtually confined to occurrences on Gilmour, Perley, and one newly-found on House Island. The last differs from the spinifex-textured flows on Gilmour and Perley islands described by Baragar and Lamontagne (1980) and Arndt (1982) and warrants separate description.

On the northeastern coast of House Island a sequence of 5 thin flows ranging from 1.5 to 3 m thick all show spinifex texture. The lowermost of the sequence shown in Figure 2.9 is typical. An olivine cumulate zone at the base, enriched in equant olivine, grades abruptly upward into a thin zone of platy olivine with pronounced preferred orientation parallel to flow margins. The olivine plates range from about 0.2 to 2 cm long. This is equivalent to the B_1 zone of Munro Township spinifex-textured flows (Pyke et al., 1973). Upward the flow passes into a blocky spinifex zone in which randomly oriented, platy olivines give the rock a cubic-like breakage surface. The crystal size fines upward and passes into an aphanitic, crackle-jointed flow surface. Thus, in the spinifex zones the platy olivines have not grown downward from a cooling surface as they appear to have done in the Munro Township type of flow. Rather, they appear to have nucleated at many centres within the upper part of the flow and to have grown in random directions.

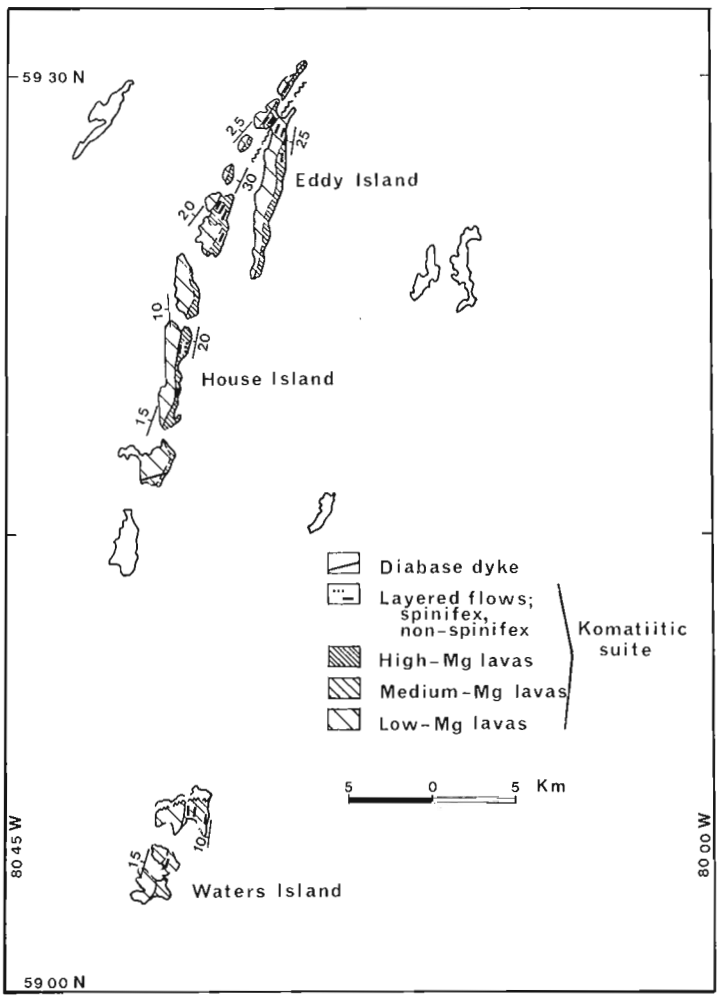

Figure 2.4. Preliminary geological map of the southern part of the Ottawa Islands.

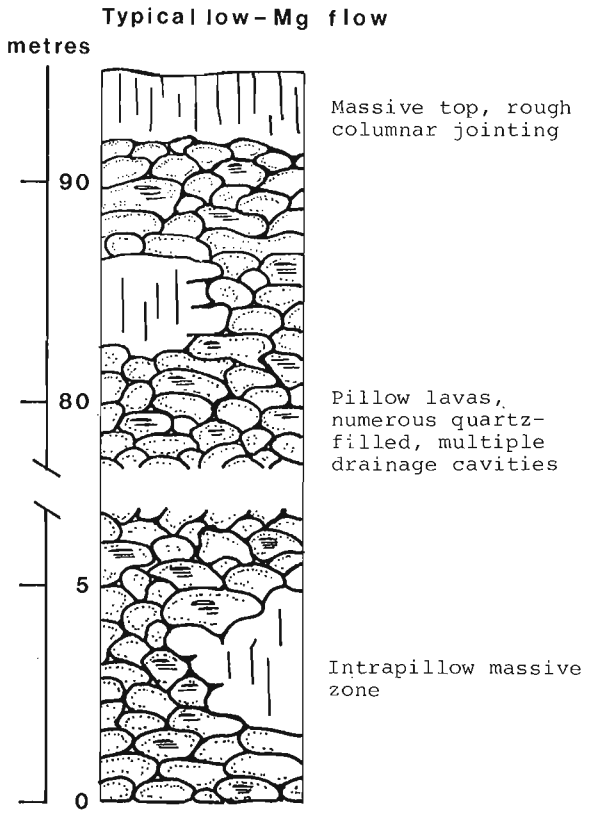

Figure 2.5. Cross-section through a typical low-Mg komatiitic flow characterized by smoothly rounded, thick-rimmed variolitic pillows with abundant quartz-filled drainage cavities. Massive zones are within and at the top of the flow.

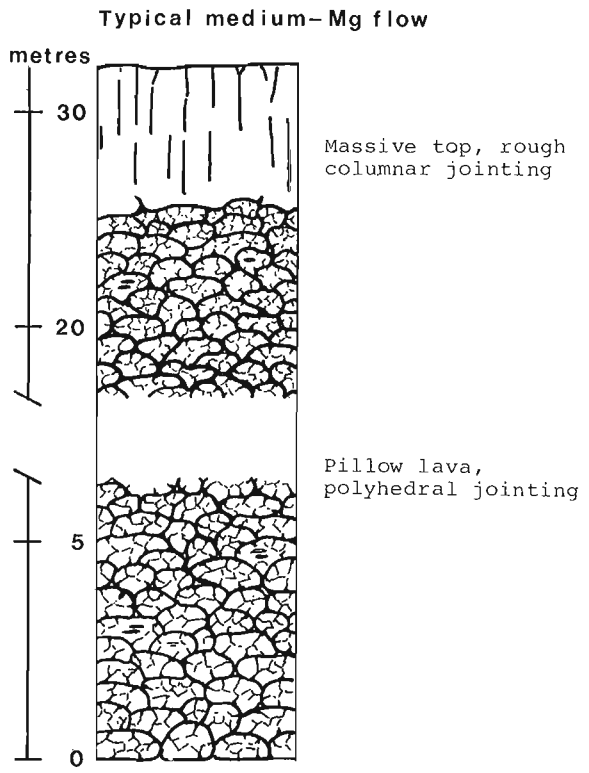

Figure 2.6. Cross-section through a typical medium-Mg komatiitic flow. Note the polyhderally jointed pillows characteristic of this type. Drainage cavities in pillows are less conspicuous than in the low-Mg lavas and rarely contain quartz.

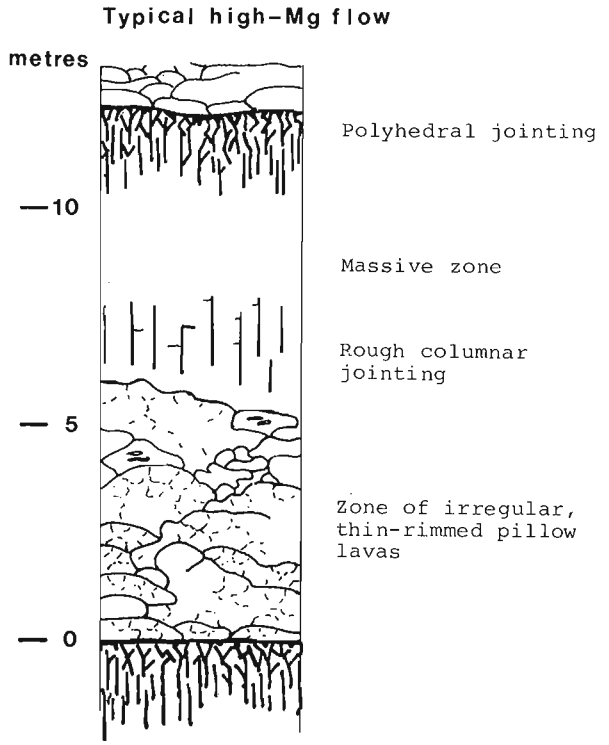

Figure 2.7. Cross-section through a typical high-Mg komatiitic flow. The irregular, thin-rimmed pillows and polyhedral jointing within pillows and at the top of the relatively thin flow are characteristic features.

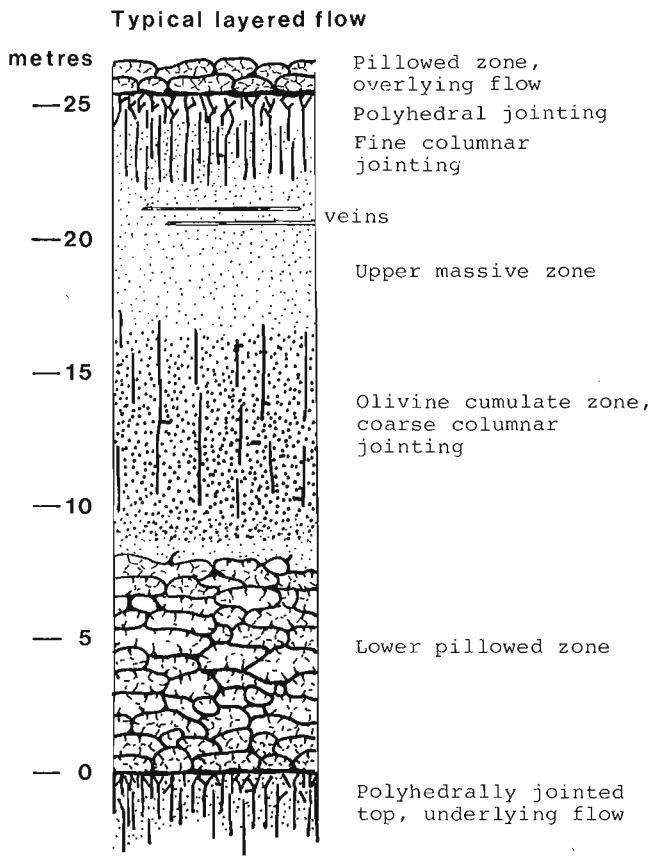

Figure 2.8. Cross-section through a typical layered flow showing the 3 major divisions normally present: a pillowed base, an olivine cumulate layer in the lower part of the massive zone, and an olivine impoverished layer in its upper part.

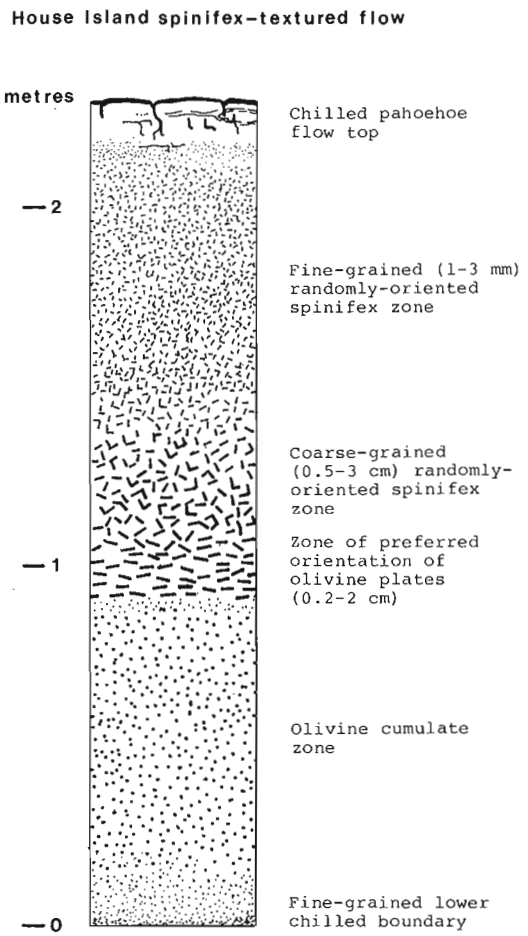

Figure 2.9. *Spinfex-textured flow, House Island; one of a sequence of 5 such flows, all less than 3 m thick.*

Distribution of Komatiitic Lithologies

Komatiites of the various magnesian contents tend to group themselves into discrete stratigraphic units, as shown in Figures 2.2 to 2.4. High-Mg lavas in particular form distinctive belts with considerable continuity along strike. In detail there is much fine interfingering of the various lava types even though one may dominate in any given part of the section. Layered flows are abundant in the high-Mg units but are also present in the other two, although rare in the low-Mg members. Hence, within the komatiitic suite the Mg content of the magmas appears to have been subjected to repeated and commonly short-lived variations.

Discussion

As noted by Arndt (1982), the thicker layered flows are generally lens-shaped, in places to an extreme degree. These can be interpreted as trunk conduits responsible for the distribution of large volumes of magma. Sedimentation of suspended olivine crystals along the distributor could lead to lava flows of greatly varying Mg content at the point of discharage, depending on the rate of flow, the length of conduit, the size of crystals, and the viscosity of the fluid. This mechanism might be responsible for some, or much, of the compositional variation found within the medium- to high-Mg units. However, it could hardly account for the magnesian content of the low-Mg units where layered flows are sparse. In this case the composition of the magma is presumably attributable to a longer-acting mechanism at depth.

References

Arndt, N.T.
1982: Proterozic spinifex-textured basalts of Gilmour Island, Hudson Bay; in Current Research, Geological Survey of Canada Paper 82-1A, Report 24.

Baragar, W.R.A.
1974: Volcanic studies in the Cap Smith-Wakeham Bay Belt, New Quebec; in Report of Activities, Part A, Geological Survey of Canada, Paper 74-1A, p. 155-157.

Baragar, W.R.A. and Lamontagne, C.
1980: The Circum-Ungava Belt in eastern Hudson Bay: The Geology of Sleeper Islands and parts of the Ottawa and Belcher Islands; in Current Research, Part A, Geological Survey of Canada, Paper 80-1A, p. 89-94.

Beall, G.H.
1959: Cross Lake area, New Quebec; Quebec Department of Natural Resources, Preliminary Report 396.

1960: Laflamme Lake area, New Quebec; Quebec Department of Natural Resources, Preliminary Report 435.

Bergeron, R.
1957: Cape Smith-Wakeham Bay Belt, New Quebec; Quebec Department of Natural Resources, Preliminary Report 355.

1959: Povungnituk Range area, New Quebec; Quebec Department of Natural Resources, Preliminary Report 392.

Francis, D.M. and Hynes, A.J.
1979: Komatiite-derived tholeiites in the Proterozoic of New Quebec; Earth and Planetary Science Letters, v. 44, p. 473-481.

Gélinas, L.
1962: Watts Lake area, New Quebec; Quebec Department of Natural Resources, Preliminary Report 471.

Gold, D.P.
1962: Brisebois Lake area, New Quebec; Quebec Department of Natural Resources, Preliminary Report 470.

Pyke, D.R., Naldrett, A.J., and Eckstrand, O.R.
1973: Archean ultramafic flows in Munro Township, Ontario; Geological Society of America Bulletin, v. 84, p. 955-978.

Schimann, K.
1978: Geology of the Wakeham Area eastern end of the Cape Smith Belt, New Quebec; Unpublished Ph.D. thesis, University of Alberta.

Schwarz, E.J. and Fujiwara, Y.
1977: Komatiitic basalts from the Proterozoic Cape Smith Range in northern Quebec, Canada; in Baragar, W.R.A., Coleman, L.C., and Hall, J.M., ed., Volcanic Regimes in Canada; Geological Association of Canada, Special Paper 16, p. 193-201.

Taylor, F.C.
1974: Reconnaissance Geology of a part of the Precambrian Shield, northern Quebec and Northwest Territories; Geological Survey of Canada, Paper 74-21.

3. VOLCANIC AND PLUTONIC ROCKS IN THE RAINY LAKE AREA, NEWFOUNDLAND

Project 730044

J.B. Whalen and K.L. Currie
Precambrian Geology Division

Whalen, J.B. and Currie, K.L., Volcanic and plutonic rocks in the Rainy Lake area, Newfoundland; in Current Research, Part A, Geological Survey of Canada, Paper 82-1A, p. 17-22, 1982.

Abstract

The Rainy Lake region consists of plutonic and volcanic rocks ranging in age from Late Precambrian to Devonian, rather than a Devonian granitic batholith as previously supposed. The oldest rocks appear to be fragments of continental or old orogenic terranes split off during formation of an island arc complex (Rainy Lake complex) in Early Paleozoic time. Rocks younger than the Rainy Lake complex form bimodal suites of volcanic and plutonic rocks probably correlative to the Caradocian Buchans Group and Silurian (?) Springdale Group in the surrounding region. Two bimodal suites younger than the Springdale equivalents contain peralkaline felsic fractions. The felsic portion of all these suites seems to have been repeatedly reactivated by basic intrusion. Physical evidence of magma mixing is ubiquitous, but hybridization was relatively minor.

The discovery of an old island arc complex in this terrane requires major revision of tectonic models of Newfoundland. Relicts of the Iapetus Ocean must lie to the west, presumably in Grand Lake, with the volcanic terranes of central Newfoundland forming a back arc sequence. Persistent igneous activity in the Rainy Lake region may be related to local tensional stresses within a competent block under long-lived compression. The presence of abundant felsic volcanic rocks, locally containing accessory fluorite, suggests that the region may be of some economic interest.

Introduction

Large scale compilations of Appalachian geology (Poole et al., 1970; Williams, 1978) show a Devonian granitic terrane ('Topsails batholith') separating the oceanic and island arc volcanic sequences of central Newfoundland from the autochthonous continental and miogeoclinal terrane of western Newfoundland, with its local cover of ophiolite-bearing allochthons. Reconnaissance mapping (Riley, 1957; Baird, 1959) failed to subdivide the Topsails terrane, although it discovered a variety of plutonic and volcanic rocks. Taylor et al. (1980) subdivided the northern part of the Topsails terrane into peralkaline granite, biotite granite, and biotite-hastingsite granite. We have mapped the Rainy Lake map area (12 A/14) and parts of surrounding map areas at 1:50 000 scale. This work demonstrates that a 'Topsails batholith' does not exist in the sense of the single or composite Devonian batholith postulated by earlier workers. The region contains a petrographically and chronologically diverse suite of igneous rocks suggestive of repeated reactivation and partial melting, followed by interaction of melts derived from various sources. The study of chemical and chronological progression of melting and mixing episodes is continuing. We here discuss field evidence for long-lived bimodal igneous activity and hybridization, and the effect of these data on tectonic models of Newfoundland.

General Geology

The geographical features of the Rainy Lake area are outlined in Figure 3.1. Large parts of this region do not support forest cover, except for a more or less dense growth of stunted spruce ("tuckamore"). Considerable areas of bedrock are exposed on the higher hills, but the degree of exposure is variable, and large tracts are covered by bouldery till. Stoss-and-lee structures and local striations suggest latest ice advance from the northwest.

All rock units mapped by us (Table 3.1), except for a small area of Carboniferous clastic sedimentary rocks east of Grand Lake, are of igneous or plutonic derivation. In the absence of radiometric dating, only relative dating by cross-cutting relations is possible. In Table 3.1 we show the deduced relative ages of the units, with tentative correlations based on regional considerations.

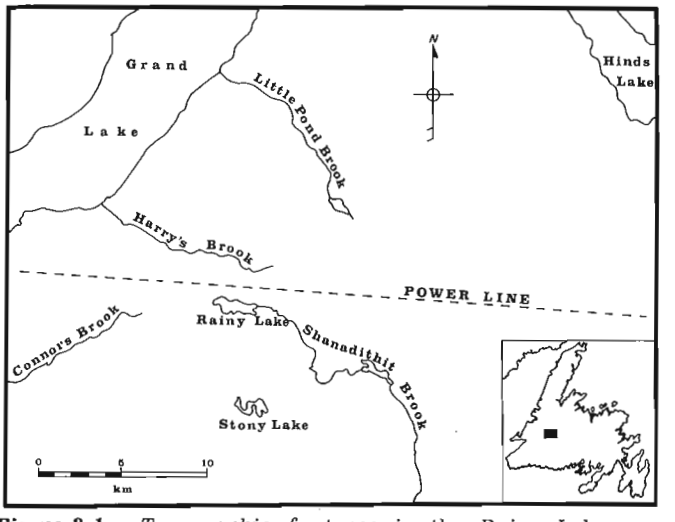

Figure 3.1. *Topographic features in the Rainy Lake map area (12 A/14).*

On the basis of intense alteration, deformation and diversity of dyking, we consider three areas of plutonic rocks to be the oldest rocks exposed in the map area. On the eastern edge of the map sheet south of Hinds Lake and east of Shanadithit Brook, an area of foliated diorite and quartz diorite, pervasively altered to chlorite and epidote and cut by altered mafic dykes, may be continuous with the Hungry Mountain complex (Thurlow, 1981) in the Buchans map area to the east. The Hungry Mountain complex yielded a Rb-Sr isochron date of 660 ± 70 Ma (Bell and Blenkinsop, 1981).

To the south of these exposures of deformed dioritic rocks, two narrow belts containing mafic rocks trend south-southwest, one crossing the lower part of Shanadithit Brook, the other lying in the southeast corner of the map area. These mafic belts, from 0.5 to 1 km in width, consist mainly of basaltic and gabbroic rocks with subordinate diorite. They separate differing granitic units, and exhibit complex

Table 3.1

Rock units in the Rainy Lake map-area

Period	Tentative correlation	Supracrustal units (with unit number)	Plutonic units (with unit number)
Carboniferous	Anguille Group	sandstone, conglomerate (14)	
		--- unconformity ---	
Devonian (?)		basalt, rhyolite (12)	composite dykes, quartz-feldspar porphyry (13) - ? - ? - ? - ? - mafic and felsic syenite, basaltic dykes (11) -- intrusive contact -- biotite and biotite-amphibole granite (10) -- intrusive contact -- amphibole granite, peralkaline in part
		--- unconformity ---	-- intrusive contact --
Silurian (?)	Springdale Group	basalt, rhyolite composite dykes and flows (7)	fine grained red biotite-amphibolite granite (8), mafic dykes
		--- unconformity ---	-- intrusive contact --
Ordovician (?)	Roberts Arm and Buchans groups	pillowed basalt, felsite (5)	fine grained biotite-amphibole granite (6)
			-- intrusive contact --
Ordovician (?) and older			gabbro, diorite (Rainy Lake complex) (4)
			- ? - ? - ? - ? -
Precambrian (?)	Mansfield Head complex		coarse, pink biotite-amphibole granodiorite (3) - ? - ? - ? - ? - mafic screens, blocks, may be equivalent to 1 in part, includes younger material - ? - ? - ? - ? -
	Hungry Mountain complex		diorite, quartz diorite

relations with them. More mafic variants of the granites occur adjacent to, and crosscut, the belts. In some exposures the mafic rocks occur as blocks from a few centimetres across up to 15 m, which are veined and crosscut by granite. In other exposures the mafic rocks clearly intrude a granitic host. We interpret these belts to represent remnant screens of mafic rocks (unit 2), possibly equivalent in part to the Hungry Mountain complex, which have been intruded by younger granites. The belts have also served as foci of intrusion for later mafic dykes.

South of Little Pond Brook, a heavily fractured, epidotized biotite granodiorite contains numerous and diverse dykes. This body (unit 3) is richer in potash feldspar and more altered than the Rainy Lake complex (unit 4) which it resembles in its dyke suite. In a general way it resembles the Mansfield Head granodiorite within the Roberts Arm Group (Bostock et al., 1979), which gave a minimum age on zircon of 594 ± 10 Ma. A possibly correlative body occurs to the north between Hinds and Goose brooks (map sheet 12 H/3).

The Rainy Lake complex (unit 4), an igneous complex ranging from gabbro through diorite to minor granodiorite, outcrops mainly along Harry's Brook and near Rainy Lake. However, a few small outcrops and the anomaly pattern on GSC Aeromagnetic Map 273G suggest that the Rainy Lake complex underlies an extensive tract from Rainy Lake south through the east side of Stony Lake to the southern edge of the map sheet. No contacts between the Rainy Lake complex and presumed older granitoid rocks were observed, but on the basis of degree of alteration, and relation to younger volcanic rocks, the Rainy Lake complex is believed to be younger than units 1 and 3.

The Rainy Lake complex consists of a distinctive gabbro, now mildly saussuritized, which exhibits clots of biotite and amphibole. The gabbro grades to, and is cut by, various mesocratic diorites to leucocratic tonalites. The rocks display intricate crosscutting and gradational relationships, but the more salic members invariably cut the more mafic ones. Although moderately altered and partly

recrystallized, the complex does not show a penetrative fabric. The complex is cut by a multitude of dykes, some of them composite, of younger units.

The western part of the complex contains many basaltic enclaves, and to the north and west the complex passes by gradation and digitation into a westward facing sequence of pillowed mafic lava flows with minor interstitial red chert. The flows are strongly fractured, and altered to chlorite and epidote, but they show no significant penetrative deformation. Although the pillowed sequence cannot be traced along strike, basaltic rocks apparently correlative in degree of fracturing and alteration fringe much of the Rainy Lake complex (unit 5). These rocks contain within them, in their upper part, thick lenticular masses of buff to grey, massive felsite. The association of fractured, epidotized submarine basalt with felsite strongly resembles the Middle Ordovician volcanic sequences of this region, notably the Roberts Arm Group (Bostock, 1978), the Buchans Group (Thurlow, 1981), and the Glover Formation.

The Rainy Lake complex strikingly resembles the Oligocene to Miocene island arc intrusive complexes of New Britain (Whalen and McDougall, 1980). Rocks of this type have recently been investigated in the Papua New Guinea-Solomon Islands region (Mason and McDonald, 1978; Hine and Mason, 1978; Chivas, 1978), in the Aleutian Islands (Kay et al., 1977; Perfit et al., 1980), in the Caribbean region (Kessler et al., 1977) and in the Southern California batholith (Silver and Early, 1977; Taylor and Silver, 1978, Gromet and Silver, 1979; Silver et al., 1979). By analogy to the tectonic setting of these occurrences, the Rainy Lake complex is tentatively interpreted as a segment of a Lower Paleozoic island arc complex.

South of Little Pond Brook, the old granodiorite appears to pass gradationally southward into red, fine grained to granophyric granite with the same degree of fracturing, alteration and epidotization as the basalts connected with the Rainy Lake complex. These granitoid rocks (unit 6) typically appear heterogeneous in hand specimen, though they are monotonously homogeneous on outcrop scale. The grain size varies from less than 1 mm to more than 1 cm over metre distances, although fine grain sizes predominate. The colour index ranges up to 30, compared to indices generally less than 15 for younger granitoid rocks. The major mafic was biotite, now largely chloritized, although relicts of chloritized amphibole occur locally. At the falls on Connors Brook, mafic dykes of at least two ages have been broken up and strewn through the granite, along with inclusions from the Rainy Lake complex. Hybrid dioritic rocks are locally developed around inclusions.

A thick volcanic section younger than the marine basalts of unit 5 outcrops south of Little Pond Brook. One contact, exposed along a brook, and the low degree of fracturing and alteration, suggest that these rocks rest unconformably on the older volcanics. Red rhyolite with little layering or flow banding forms the lowest part of the section, overlain by characteristic basalt flows. Each flow ranges from 5-20 m in thickness, and exhibits strong reddening, and frothy, vesicular flow tops indicative of subaerial extrusion. The upper part of the section consists of brightly coloured red to orange rhyolites with sparse, small phenocrysts. Near the rhyolite-basalt contact, spectacular rhyolite-basalt mixtures occur, including a flow composed of alternating globules of basalt and rhyolite, and composite dykes grading from rhyolite cores to basalt edges. The upper part of the section contains rhyolite breccias of well sized, angular fragments up to 5 cm across in a rhyolitic matrix, and laharic breccias with rhyolite and basalt boulders up to 30 cm across in a chaotic rhyolitic matrix.

Limited areas of similar rhyolitic rocks occur in the southeastern and eastern parts of the map area, where they form narrow screens separating younger intrusive units, but the only other similar section of basaltic and rhyolitic rocks occurs just southwest of Hinds Lake. The basalt-rhyolite sequences closely resemble in lithology, structural style and degree of alteration the volcanic rocks of the ?Silurian Springdale Group. Fragments identical to rocks in the Rainy Lake map area were observed in conglomerates of the Springdale Group 40 km to the north of the mapped area.

The volcanic assemblage is intruded by, and passes gradationally into, red, aplitic to granophyric, amphibole granite (unit 8), thought to be the plutonic equivalent of the rhyolites. This granite is closely associated with rhyolite enclaves and patches, particularly along its margins, and much of the intrusion is fine grained with miarolitic cavities, suggesting high level to subvolcanic intrusion. Fluorite occurs commonly in cavities in the granite and as vuggy fracture fillings in adjacent rhyolite.

Coarse grained, white to pink amphibole granite with prominent quartz grains and a distinctive interstitial habit to the amphibole (unit 9) outcrops over a large area extending from south of Rainy Lake to northeast of Shanadithit Brook. Thin section studies show that the unit varies from biotite-bearing through biotite-absent to alkali-pyroxene-bearing facies which appear to be peralkaline. Mapping northeast of Hinds Lake indicates that megascopically identical granite forms part of the peralkaline granite unit of Taylor et al. (1980). In the southeast corner of the map area, a large body of pink to red, medium grained, equigranular biotite granite is crosscut by syenite (unit 11) from which it is separated by a screen of mafic rocks. In the northwest corner of the map sheet porphyritic red amphibole granite intrudes Springdale-type rhyolites and basalts. The relative age relations of these granite masses to other plutons are unclear, but their freshness, and the available intrusive relations suggest that they are of similar age to the coarse grained amphibole granite.

Southwest of Rainy Lake coarse grained, biotite-dominant potash granite (unit 10) intrudes the amphibole granite. Both units exhibit abundant finer grained to aplitic zones. Within and around the belts of mafic rocks (unit 2) minor fine- to medium-grained amphibole-biotite granitoids intrude the coarse amphibole granites. These phases become more mafic adjacent to the mafic rocks, where they contain abundant, partially disaggregated, fine grained, mafic xenoliths. Field relations suggest they have interacted with basic rocks or magma producing minor volumes of quartz dioritic to granodioritic compositions.

Both the amphibole- and biotite-bearing granites are cut by numerous mafic dykes, including basalt, olivine-phenocrystic basalt, diabase and medium to coarse gabbro (unit 11). Unlike their host rocks, which appear fresh, many of these dykes are perceptibly altered, and on large outcrop surfaces can be seen to be broken up into segments, presumably by movement within a still hot, or reheated, granitic host.

A suite of syenitic rocks ranging from mafic to felsic syenite (unit 12) occurs west of Shanadithit Brook and in the southeastern part of the map sheet. The mafic varieties contain coarse grained euhedral pink feldspar and amphibole, while more felsic varieties are deep orange, medium grained rocks containing minor acicular amphibole and quartz. The syenites intrude biotite granite (unit 10) and correlative dykes cut coarse amphibole granite (unit 9) south of Rainy Lake.

The youngest igneous rocks consist of rhyolite and minor basalt (unit 12), and probably correlative quartz-feldspar porphyry (unit 13) and composite dykes. Rhyolites

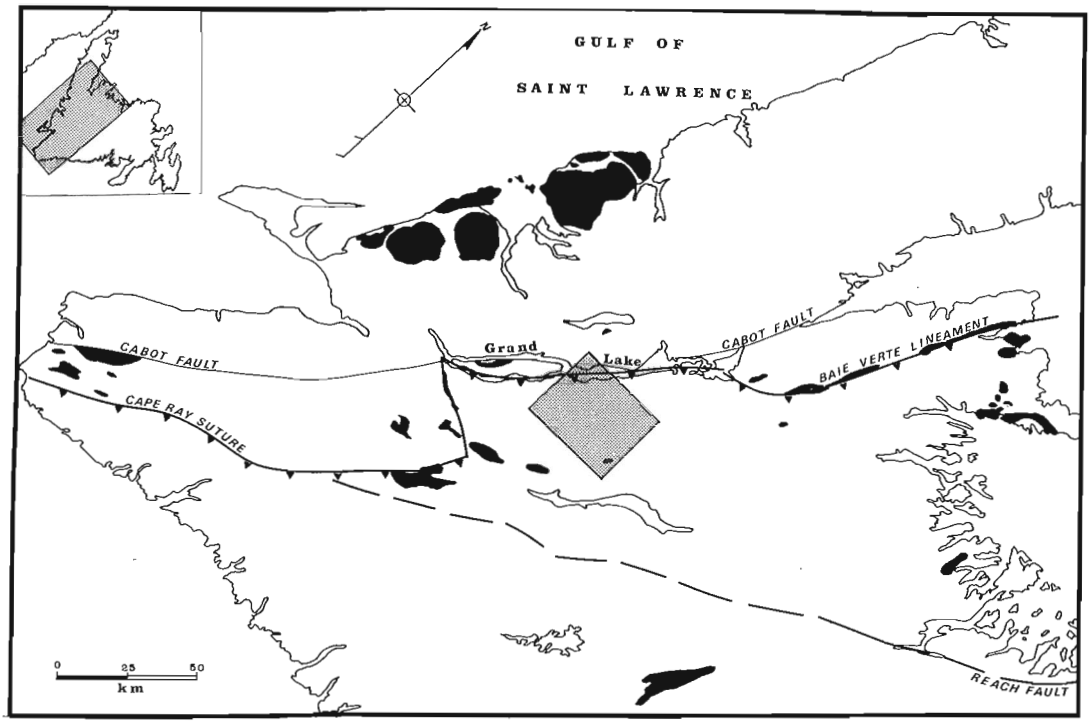

Location of the suture suggested by the geology in the Rainy Lake area, and the work of Williams et al. (1977) and Herd and Dunning (1979).

Suggestion of McKerrow and Cocks (1977).

Ultramafic fragments of ophiolitic affinity.

Location of the Rainy Lake map area. The inset shows the location of the proposed sutures relative to Newfoundland as a whole.

Figure 3.2. *Possible locations of the Iapetus suture in western Newfoundland. The inset shows the location of the proposed sutures relative to Newfoundland as a whole.*

and porphyries contain feldspar phenocrysts up to 1 cm across, commonly brick red, but locally white or lime green. Mafic minerals occur only in the matrix in minor amount. Quartz has the characteristic bipyramidal high temperature form. Very fresh aphanitic basalt occurs interbedded with rhyolite north of Little Pond Brook. The porphyries locally exhibit flow banding and grade to rhyolite, but they form substantial, presumably subvolcanic, plutons north of Little Pond and Shanadithit brooks. Petrographic studies show that some samples contain alkaline pyroxenes and amphiboles, suggesting that the porphyries are, in part at least, peralkaline. Similar porphyry dykes cutting the coarse grained amphibole granite (unit 9) have glassy chilled contacts, suggesting a significant time gap between the emplacement of the two peralkaline units.

Spectacular composite dykes up to 50 m in width cut the porphyry. Aphanitic basalt margins pass gradationally through basaltic zones with potash feldspar phenocrysts, to a zone of globules of basalt up to 5 cm across in an intermediate matrix, to a cental core of rhyolite porphyry.

A thin fringe of Carboniferous clastic sedimentary rocks (unit 14) occurs along the eastern edge of Grand Lake, varying in width from 0 to 2 km. The main rock type is grey-green, coarsely bedded sandstone and grit, with local lenticles of pebble conglomerate. This material appears correlative to the Howley beds of the Cape Anguille Group (Baird, 1959). The sedimentary debris consists mainly of orthoquartzite fragments, many in the form of dreikanters. However several conglomeratic beds up to a metre thick contain small, rounded pebbles of all igneous rock types found on the high plateau to the east. Clearly relief between the basin and the igneous terrane was much less than at present during sedimentary accumulation. Indeed during much of the accumulation, influx from the igenous terrane was negligible.

Structure

Penetrative deformation is relatively rare in the Rainy Lake region, even in rocks which are observably folded. This may reflect deformation of relatively homogeneous rocks, but the general lack of foliation probably reflects an environment relatively sheltered from strong directed stress compared to the surrounding regions of strongly foliated rocks.

Folding can be traced in volcanic rocks on both mesoscopic and macroscopic scales. Volcanic rocks believed to be equivalent to the Springdale Group exhibit two periods of open to tight folding. One set of axial planes trends northwest and dips steeply southwest, while the other trends northeast and dips steeply southeast. The trends and style of deformation are roughly similar to those observed in the Springdale Group south of Springdale.

Much larger northeast-trending folds can be defined by using the basaltic units as markers. A major northeast-trending, north-plunging antiform east of Grand Lake is clearly outlined on the magnetic map by the pronounced positive anomaly over the basalt of unit 5. The Rainy Lake complex appears to occupy the core of this structure, the eastern limb of which is truncated by granitoid plutons.

Although minor faults are commonly observed in outcrop, major faulting appears to be absent, or well disguised, except for the large, steep fault between the igneous rocks and the Carboniferous rocks east of Grand Lake. The exact position of this fault cannot be located due to poor outcrop, but sedimentological and geophysical evidence show that it must have substantial displacement with the west side down-dropped relative to the east side.

Among the intrusive rocks, only the youngest quartz-feldspar porphyry exhibits ovoid to subcircular plutons. Older plutons have been segmented to varying degrees. Together with various supracrustal rocks, older plutonic rocks form screens between younger intrusions. Some older mafic intrusions are preserved only as screens of mixed-up blocks. These screens, minor intrusions, and some major contacts tend to trend north to northeast. We believe this elongation to be a primary, rather than an imposed, feature. Where plutons crosscut, minor shearing and alteration but not foliation are commonly observed in the older pluton.

Interpretation

The Rainy Lake region represents a long-lived centre of igneous activity with negligible accompanying sedimentary accumulation. Tentative correlations suggest that igneous activity persisted through much of Early Paleozoic time. Unlike the volcanic terranes of central Newfoundland, this activity was predominantly acid, possibly involving continental material, although repeated emplacement of basaltic magma as dykes and flows shows that mantle-derived magma must also have been available. The coexistence of acid and basic magma throughout the igneous history is attested by observed magma mixing in volcanic and plutonic rocks of diverse ages, but despite the evidence of physical mixing, only the oldest intrusions contain significant amounts of intermediate compositions.

Loiselle and Wones in an unpublished manuscript (Australian National University, 1981) suggested that peralkaline granites result from repeated remelting of continental granitoid material. Bowden (1974) pointed out that peralkaline granites are occasionally found above active subduction zones, as in southeastern Hokkaido, Japan, and on Major Island, New Zealand, associated with continental fragments. Both ideas may apply to the Rainy Lake region. We assume the Rainy Lake complex to be a remnant of an island arc formed above an east dipping subduction zone. As pointed out by Williams (1979) and Currie et al. (1980), the widespread miogeoclinal deposits of Cambro-Ordovician age in western Newfoundland require an easterly dip for any contemporaneous subduction zone. We assume that a large marginal basin opened behind the island arc, splitting off fragments of the continent lying to the east, in a fashion analogous to modern day Japan, where a subduction zone beneath a continental edge has opened the Japan Sea, leaving fragments of old metamorphic complexes on the Japanese islands. In the case of Newfoundland, the analogue of the Japan Sea would include all of the central mobile belt. The idea that the central mobile belt formed in a back arc basin has been repeatedly advanced on other grounds (see Williams 1979 for summary). We assume the Mansfield Head, Hungry Mountain and Little Pond Brook complexes to be fragments of a continent originally lying to the east of their present position. These fragments provide material to be reworked in the fashion envisaged by Loiselle and Wones (op. cit.), but the model does not explain the remarkably long-lived heat source which repeatedly remelted the raw material. We believe this feature to be related to a peculiarity of the tectonic history.

Implications for Tectonic Models of Newfoundland

According to the now classic plate tectonic model of Newfoundland presented by Bird and Dewey (1970), the geology of the island can be explained by consumption of an Early Paleozoic Iapetus Ocean, bringing together the American craton, and a craton lying to the east of the Iapetus Ocean. Fragments of this eastern continent were left attached to Newfoundland when the Atlantic ocean opened. The model requires that a line of suture marking the vestiges of the Iapetus Ocean must cross Newfoundland roughly in a north-south direction. This line of suture has generally been assumed to lie somewhere in the central mobile belt, but proposed locations of the suture, for example those of McKerrow and Cocks (1977) and Currie et al. (1980), are subject to severe geological objections. The present data suggest that the suture may lie elsewhere.

If there was an active volcanic arc in the Rainy Lake region during Early Ordovician time, as suggested by the Rainy Lake complex, the far-travelled ophiolite allochthons of western Newfoundland (Williams, 1979) can hardly be assumed to have travelled across this active volcanic zone. if the allochthons represent fragments of oceanic crust, their source must lie west of the Rainy Lake complex, presumably in the region of Grand Lake. When combined with the conclusions of Williams et al. (1977) that the most probable root zone for the allochthons lies in the Baie Verte lineament, this suggests a line of suture such as that shown in Figure 3.2. The line of suture south of Grand Lake remains uncertain, but the distribution of the Glover Formation at the south end of Grand Lake, and the large ophiolite complexes in the Annieopsquotch Mountains (Herd and Dunning, 1979) suggest that it must trend eastward at the south end of Grand Lake, leaving the Rainy Lake region as a pronounced salient, before resuming a southwesterly trend toward Port aux Basques.

Ophiolitic fragments have also been mapped to the east of this salient (Dunning, 1981) and east of the central mobile belt (Currie et al., 1980). According to the back arc basin model outlined above, these fragments are slivers of the back arc basin floor emplaced by compressional stresses, and possibly remobilized by later compressive stress. If the old plutonic rocks of the Rainy Lake region represent fragments of continental terranes, they did not give rise to peralkaline granites during the initial tensional conditions associated with formation of the back arc basin. However during subsequent compression associated with closure of the Iapetus Ocean in the Middle Ordovician, and consequent metamorphism under compressive conditions, these fragments probably represented relatively rigid blocks within the surrounding material. Persistent east-west compressive stresses, therefore, should produce relative tension in a north-south direction and possibly open fractures trending roughly east-west. The majority of dykes within the Rainy Lake sheet have roughly this trend. Such fractures can also serve as channels for magmas developed by anatexis of thickened crust (Currie, 1981) or for magmas rising from the mantle into heated crust. According to this model persistent re-appearance of basaltic and granitic magma, with eventual development of peralkaline magma, can be linked to the persistence of tensional stresses generated within a rigid block by uniaxial compression persisting from Ordovician to Carboniferous time.

References

Baird, D.M.
1959: Sandy Lake, west half, Newfoundland; Geological Survey of Canada, Map 47-1959.

Bell, K. and Blenkinsop, J.
1981: A geochronological study of the Buchans area; Newfoundland; in The Buchans Orebodies; Fifty Years of Geology and Mining, edited by E.A. Swanson, D.F. Strong and J.G. Thurlow, Geological Association of Canada Special Paper 22.

Bird, J.M. and Dewey, J.F.
1970: Lithosphere-plate continental margin tectonics and the evolution of the Appalachian orogen; Geological Society of America Bulletin, v. 81, p. 1031-1060.

Bostock, H.H.
1978: The Roberts Arm Group, Newfoundland; Geological notes on a Middle or Upper Ordovician island arc environment; Geological Survey of Canada, Paper 78-15.

Bostock, H.H., Currie, K.L., and Wanless, R.K.
1979: The age of the Roberts Arm Group, north central Newfoundland; Canadian Journal of Earth Sciences, v. 16, p. 599-606.

Bowden, P.
1974: Oversaturated alkaline rocks; in The Alkaline Rocks, edited by H. Sorensen, John Wiley, New York, p. 109-123.

Chivas, A.R.
1978: Porphyry copper mineralization at the Koloula Igneous Complex, Guadalcanal, Solomon Islands; Economic Geology, v. 73, p. 749-760.

Currie, K.L.
1981: Repeated basement reactivation in the northeastern Appalachians; Terra Cognita, v. 1, p. 41.

Currie, K.L., Pickerill, R.K., and Pajari, G.E.
1980: An early Paleozoic plate tectonic model of Newfoundland; Earth and Planetary Science Letters, v. 48, p. 8-14.

Dunning, G.R.
1981: The Annieopsquotch ophiolite belt, southwest Newfoundland; in Current Research, Part B, Geological Survey of Canada, Paper 81-1B, p. 11-15.

Gromet, L.P. and Silver, L.T.
1979: Profile of rare earth element characteristics across the Peninsular Ranges batholith near the international border, southern California U.S.A. and Baja California, Mexico; in Mesozoic Crystalline Rocks, edited by P.L. Abbott and V.R. Todd. Department of Geological Sciences, San Diego State University, p. 133-142.

Herd, R.K. and Dunning, G.R.
1979: Geology of the Puddle Pond map-area, southwestern Newfoundland; in Current Research, Part A, Geological Survey of Canada, Paper 79-1A, p. 305-316.

Hine, R. and Mason, D.R.
1978: Intrusive rocks associated with porphyry copper mineralization, New Britain, Papua New Guinea; Economic Geology, v. 73, p. 749-760.

Kay, S.M., Kay, R.W., and Brueckner, H.
1977: The Finger Bay pluton, Adak, and magmatic evolution of the Aleutian arc; EOS Transactions of the American Geophysical Union, v. 58, p. 532.

Kessler, S.E., Lewis, J.F., Jones, L.M., and Walker, R.L.
1977: Early island arc intrusive activity, Cordillera Central, Dominican Republic; Contributions to Mineralogy and Petrology, v. 65, p. 91-99.

Mason, D.R. and McDonald, J.A.
1978: Intrusive rocks and porphyry copper occurrences in the Papua New Guinea-Solomon Islands region; a reconnaissance study; Economic Geology, v. 78, p. 857-877.

McKerrow, W.S. and Cocks, L.R.M.
1977: The location of the Iapetus Ocean suture in Newfoundland; Canadian Journal of Earth Sciences, v. 14, p. 488-495.

Perfit, M.R., Bruechner, H., Lawrence, J.R., and Kay, R.W.
1980: Trace element and isotope variations in a zoned pluton and associated volcanic rocks, Unalaska Island, Alaska; a model for fractionation in the Aleutian calc-alkaline suite; Contributions to Mineralogy and Petrology, v. 73, p. 69-87.

Poole, W.H., Sanford, B.V., Williams, H., and Kelley, D.G.
1970: Geology of southeastern Canada; in Geology and Economic Minerals of Canada, ed. R.J.W. Douglas, Geological Survey of Canada Economic Geology Report 1, p. 227-304.

Riley, G.C.
1957: Red Indian Lake, west half, Newfoundland; Geological Survey of Canada, Map 8-1957.

Silver, L.T. and Early, T.O.
1977: Rubidium-strontium fractionation domains in the Peninsular Ranges batholith and their implications for magmatic arc evolution; EOS Transactions of the American Geophysical Union, v. 58, p. 53.

Silver, L.T., Taylor, H.P., and Chappell, B.W.
1979: Some petrological, geochemical and geochronological observations of the Peninsular Ranges batholith near the international boundary of the U.S.A. and Mexico; in Mesozoic Crystalline Rocks, ed. P.L. Abbott and V.R. Todd, Department of Geological Sciences, San Diego State University, p. 178-219.

Taylor, H.P. and Silver, L.T.
1978: Oxygen isotope relationships in plutonic igneous rocks of the Peninsular Ranges batholith, southern and Baja California, in Short Papers of the Fourth International Conference of Geochronology and Cosmochronology and Isotope Geology, ed. R.H. Zartman, United States Geological Survey, Open File Report 78-701, p. 423-426.

Taylor, R.P., Strong, D.F., and Kean, B.F.
1980: The Topsails igneous complex; Silurian-Devonian peralkaline magmatism in western Newfoundland. Canadian Journal of Earth Sciences, v. 17, p. 425-439.

Thurlow, J.G.
1981: The Buchanas Group; its stratigraphic and structural setting; in The Buchans Orebodies; Fifty Years of Geology and Mining, ed. E.A. Swanson, D.F. Strong, and J.G. Thurlow, Geological Association of Canada, Special Paper 22.

Williams, H.
1978: Tectonic lithofacies map of the Appalachian orogen; Memorial University of Newfoundland, Map 1.

1979: The Appalachian orogen in Canada; Canadian Journal of Earth Sciences, v. 16, p. 792-807.

Williams, H., Hibbard, J.P., and Bursnall, J.T.
1977: Geologic setting of asbestos-bearing ultramafic rocks along the Baie Verte lineament, Newfoundland; in Report of Activities, Part A, Geological Survey of Canada, Paper 77-1A, p. 351-360.

Whalen, J.B. and McDougall, I.
1980: Geochronology of the Uasilau-Yau Yau porphyry copper prospect, New Britain, Papua New Guinea; Economic Geology, v. 75, p. 566-571.

PROGRESS REPORT ON REGIONAL GEOLOGICAL SYNTHESIS, CENTRAL SUPERIOR PROVINCE

Project 770070

K.D. Card
Precambrian Geology Division

Card, K.D., Progress report on regional geological synthesis, central Superior Province; in Current Research, Part A, Geological Survey of Canada, Paper 82-1A, p. 23-28, 1982.

Abstract

Reconnaissance field investigations indicate that the Kapuskasing Structural Zone can be defined in the area between Kapuskasing and Fraserdale, Ontario, on the basis of structural trends transverse to those of the adjacent Quetico subprovince. North of Hearst and Cochrane, Ontario, the contact between the Quetico and Wabigoon subprovinces is tentatively placed at the southern margins of two small greenstone belts immediately south of the Phanerozoic cover rocks of the James Bay Lowlands. The Quetico-Wabigoon boundary is defined in part by a major northeast-trending fault, and is probably offset by north-northeast faults, some of which may have controlled emplacement of carbonatite-alkalic rock complexes. The Pontiac belt in northwestern Quebec is geologically similar in most respects to the Quetico and the northern part of the English River subprovince, all consisting mainly of metasedimentary rocks and associated migmatitic gneiss and granite. Minor mafic and ultramafic volcanic rocks and a number of late syenitic to dioritic plutons are also present in the Pontiac. Chemical and petrographic studies of felsic plutonic rocks in central Superior Province, combined with field studies of their structural characteristics, permit definition of a number of plutonic suites of various compositions and ages.

Introduction

The reconnaissance field work program in central Superior Province (Card, 1979, 1980, 1981; Card et al., 1980, 1981; Percival, 1981a, b; Lafleur, 1981) continued during 1981. Helicopter-supported investigations were undertaken in the area north of Cochrane, Kapuskasing, and Hearst in northeastern Ontario to examine the rocks and structural relationships of the Quetico and Wabigoon subprovinces and the Kapuskasing Structural Zone. Reconnaissance studies were carried out in the Pontiac belt between Rouyn-Noranda and Belleterre, Quebec, and traverses were made in the Thunder Bay-Armstrong and Rainy Lake-Ear Falls regions of northwestern Ontario to examine the major rock types and structural characteristics of the Wawa, Quetico, Wabigoon, and English River subprovinces. Studies of the chemistry, petrography, and structural characteristics of felsic plutonic rocks in central Superior Province permit distinction of a number of plutonic suites. Current radiometric age studies of these intrusions will be useful in correlating rock units and deformational-metamorphic events in this part of the Shield.

Kapuskasing Structural Zone north of Kapuskasing, Ontario

The Kapuskasing Structural Zone (KSZ) is an elongate, northeast-trending, partly fault-bounded region of high-grade Archean gneiss transverse to the regional east-west structural trends of the adjacent Abitibi, Wawa, and Quetico subprovinces (Bennett et al., 1967; Percival and Coe, 1981; Percival, 1981b). It is characterized by granulite and upper amphibolite facies paragneiss, tonalitic gneiss and anorthosite of Archean age, and by Proterozoic carbonatite-alkalic rock intrusions. It is expressed by positive gravity and aeromagnetic anomalies (Innes, 1960; Gaucher, 1966). Throughout most of its length it can be distinguished from the adjacent lower grade greenstone-granite terranes on the basis of contrasting lithology, metamorphic grade, and structural style and orientation. However, the lithologic and metamorphic contrasts between rocks of the KSZ and upper amphibolite to lower granulite facies gneiss of the Quetico subprovince are not pronounced, and where the KSZ transects the Quetico in the area between Kapuskasing and Fraserdale, Ontario, existing geological data are insufficient to distinguish the two terranes. Outcrops are sparse and are essentially confined to rapids along the major streams.

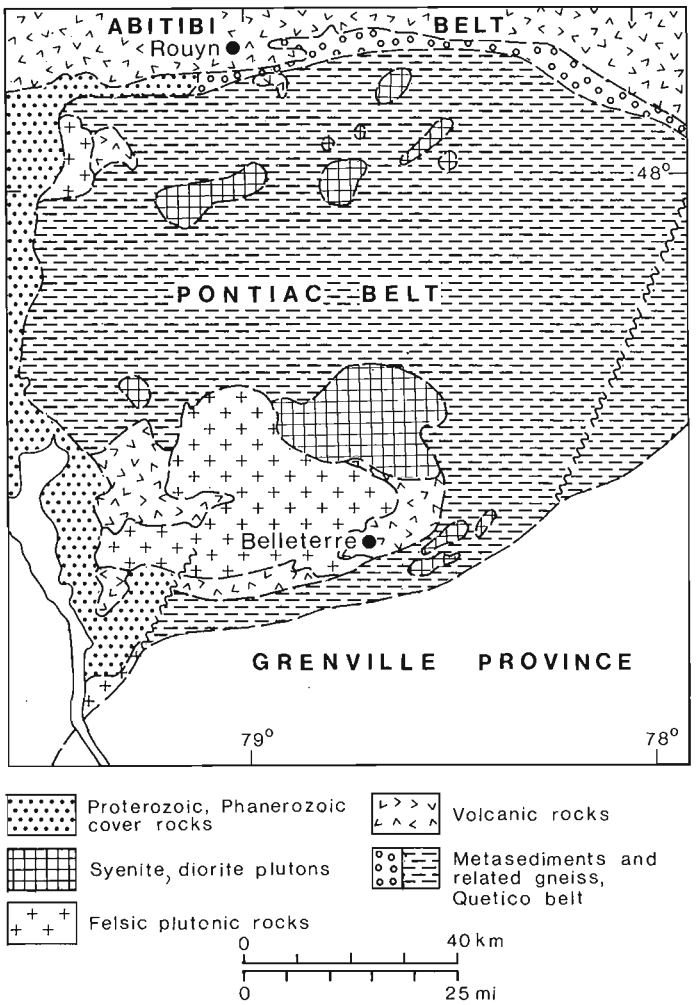

Figure 4.1. *Major geological units and structures in the area north of Cochrane, Kapuskasing, and Hearst, Ontario.*

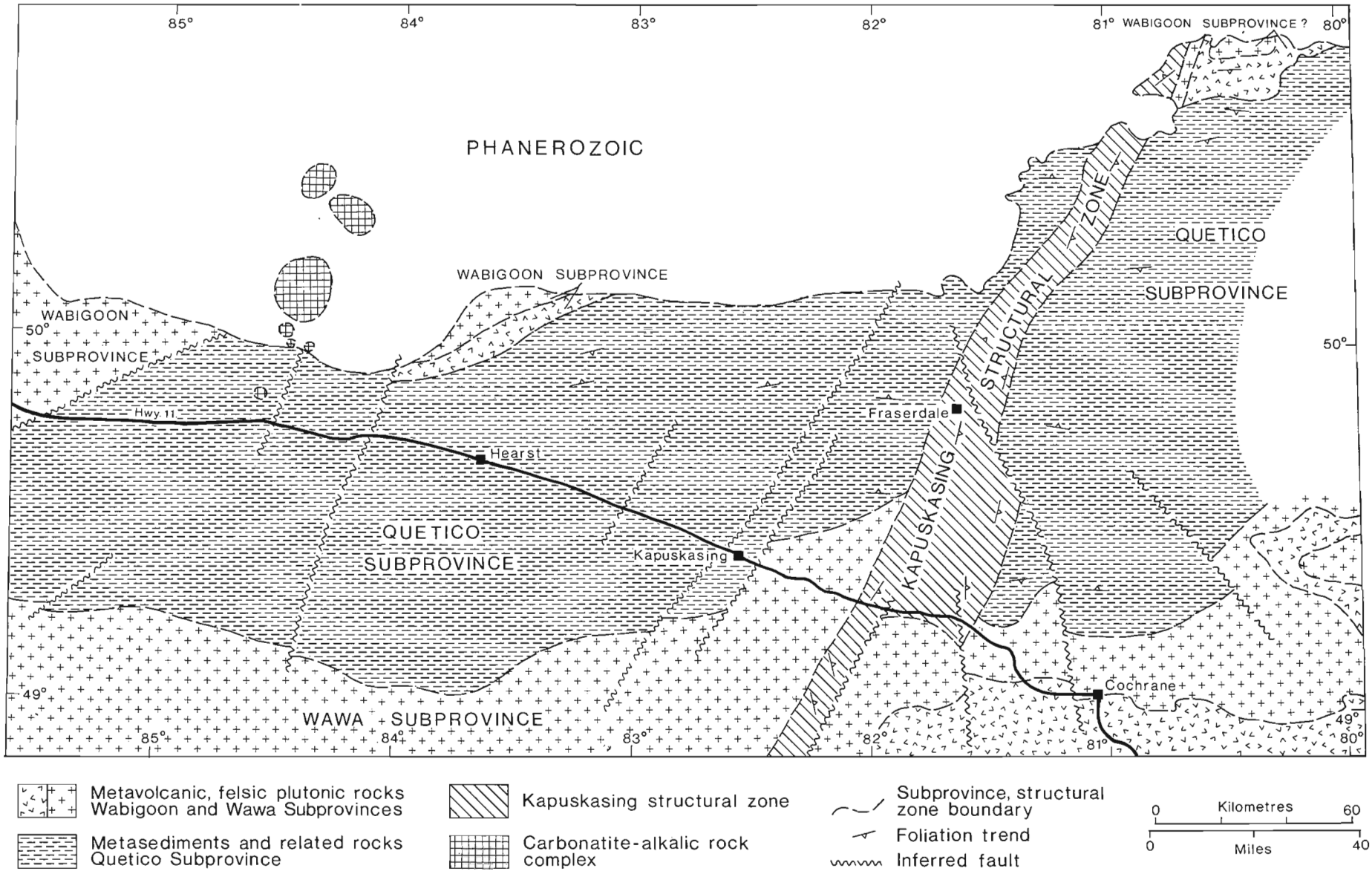

Figure 4.2. *Geology of the western part of the Pontiac belt in the area between Rouyn and Belleterre, Quebec.*

Results of reconnaissance investigations in this area are shown in Figure 4.1. The KSZ can be delineated in the area between Kapuskasing and Fraserdale, mainly on the basis of structural trends. Foliation within the KSZ strikes northeast to north, at high angles to the foliation in the adjacent Quebico gneiss. Cataclastic foliation is prevalent within the KSZ, and mylonite and pseudotachylite zones are present locally. Minor folds with gently plunging axes are abundant. The main rock type of this part of the KSZ is rusty-weathering, greenish, garnetiferous, migmatitic gneiss of probable sedimentary origin. Tonalitic to granitic mobilizate in the form of layers and dykes is present, as are numerous mafic and lamprophyric dykes. Within the KSZ north of Fraserdale the structural characteristics are similar, but here a high proportion of the bedrock consists of dense, mafic gneiss rich in garnet and pyroxene.

Quetico-Wabigoon Boundary

A second problem in the area north of Cochrane and Hearst concerns the eastward extension of the boundary between the Quetico and Wabigoon subprovinces. West of Hearst this boundary is placed at a major fault that separates metasediments and related gneiss of the Quetico subprovince to the south from metavolcanics, felsic plutons, and orthogneiss of the Wabigoon subprovince to the north (Fig. 4.1). The fault contact extends northeastward to the Phanerozoic cover rocks of the James Bay Lowlands. To the east, and immediately south of the Phanerozoic-Precambrian contact, are two metavolcanic belts, one north of Hearst, the other northeast of Fraserdale. These metavolcanic belts could represent local volcanic accumulations within the dominantly metasedimentary sequence of the Quetico subprovince, or conversely, could lie within the southern Wabigoon subprovince.

Reconnaissance investigations of the metavolcanic rocks and enclosing granitoid bodies indicate that the metavolcanic belts lie at the southern margin of the Wabigoon subprovince. The rocks immediately north of the metavolcanic belts are tonalitic and xenolithic orthogneiss and foliated to massive granodiorite, rock types typical of the Wabigoon greenstone-granite terrane. Rocks to the south are typical Quetico migmatitic paragneiss. Consequently, the boundary between the Quetico and Wabigoon subprovinces is tentatively placed at the southern margins of the greenstone belts, as shown in Figure 4.1.

It is possible that the Quetico-Wabigoon boundary northwest of Hearst is offset by northeast-trending faults (Fig. 4.1). These proposed faults are approximately parallel to faults associated with the KSZ to the east and are also subparallel to a major zone of faulting to the west that is considered by R.P. Sage (personal communication, 1981) to control the Prairie Lake, Killala Lake, and Chipman Lake carbonatite-alkalic rock complexes and several diatreme breccia bodies. A number of Proterozoic carbonatite-alkalic rock complexes, as well as several post-Devonian kimberlitic and lamprophyric intrusions, are associated with the KSZ faults north of Fraserdale (Bennett et al., 1967). Several carbonatite-alkalic rock complexes are known in the area north of Hearst and kimberlitic and diatreme intrusions may occur there as well.

Western Pontiac Belt, Quebec

Reconnaissance of the Pontiac belt in the area between Rouyn-Noranda and the Grenville Front south of Belleterre, Quebec, indicates that the geology of the western part of this terrane is generally similar to the eastern part (Card et al., 1981), although there are some differences. Coarse, conglomeratic sediments of the Timiskaming Group and "Granada Formation" form the northern part of the Pontiac belt south of Rouyn-Noranda (Fig. 4.2). According to Goulet (1978), these sediments unconformably overlie volcanics of the Blake River Group north of the Cadillac-Larder Lake Fault and conformably overlie rocks of the Pontiac Group south of this fault. These relationships are explained as a result of repeated uplift north of the fault and subsequent prograding of alluvial and turbidite fans southward.

Mafic and ultramafic volcanics are present within the western Pontiac belt southeast of Rouyn and are correlated by Goulet (1978) with the Blake River Group to the north. Mafic and ultramafic rocks are also present in the Pontiac southwest of Rouyn on the shores of Lake Opasatika (Fig. 4.2). These are mainly massive and layered amphibolite and talc-rich rocks, with minor intermediate to felsic material. They are overlain by typical Pontiac metasediments, and lie east of tonalitic orthogneiss with nearly flat-lying foliation, a rock type distinctly different from the metasedimentary gneiss of the Pontiac.

A number of syenitic plutons are present in the Pontiac belt between Rouyn-Noranda and Belleterre (Fig. 4.2). These bodies range in size from a few hundred metres to about 20 km. Some are simple plutons, consisting either of syenite, quartz syenite, monzonite, or diorite; others are composite intrusions of several of the foregoing rock types. They are typically rich in hornblende and contain numerous amphibolite inclusions. Most are unmetamorphosed and massive, but several display foliation and lineation, possibly the result of magmatic flow. They probably belong to a suite of late- to post-tectonic syenitic intrusions that are common throughout central Superior Province.

Plutonic Suites in Central Superior Province

Chemistry and petrography of felsic plutonic rocks in central Superior Province, coupled with field studies of their structural characteristics, indicate that several major plutonic suites are present. Recognized suites, in approximate order of decreasing age, are:

Tonalite-granodiorite Gneiss Suite

Gneissic rocks of tonalitic to granodioritic composition form large parts of the Abitibi, Wawa, and Wabigoon subprovinces, and are present to lesser extent in the Quetico and Pontiac belts. They are composed mainly of quartz, plagioclase, biotite, hornblende with or without potassic feldspar; the general mineralogical and chemical characteristics of these rocks are shown in Figure 4.3. The orthogneiss typically contains inclusions, layers, and enclaves of mafic amphibolitic and gabbroic rock ranging from a few centimetres to several kilometres in maximum dimension. The xenoliths are recrystallized, massive to foliated, but locally have preserved structures and textures, some of which indicate a metavolcanic origin, whereas others are suggestive of mafic intrusions. Trains of mafic xenoliths and gneiss occur along strike with and at the margins of many greenstone belts; some trains link one greenstone belt with another.

Trondhjemite-quart Diorite Suite

Foliated to massive felsic plutons of trondhjemite, tonalite and quartz diorite are abundant in and around the greenstone belts. Many are relatively small, synvolcanic-type intrusions, but there are also large batholiths formed mainly of these rock types or that include phases of these compositions. Plagioclase (oligoclase-andesine), quartz, hornblende, and biotite are the essential minerals present; the general mineralogical and chemical composition of these rocks are shown in Figure 4.4.

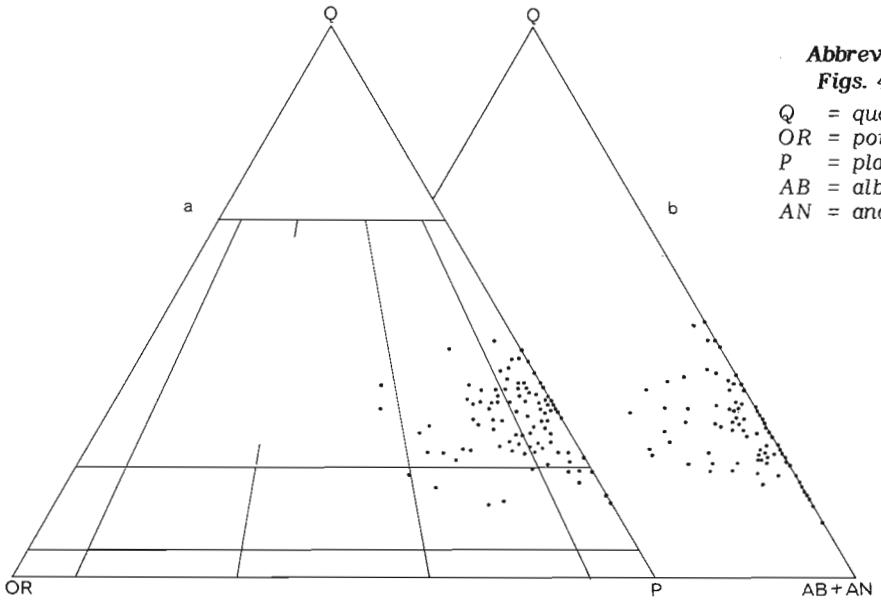

Abbreviations for Figs. 4.3 – 4.8

Q = quartz
OR = potassic feldspar
P = plagioclase
AB = albite
AN = anorthite

Figure 4.3. *Modal (a) and mesonormative (b) plots for rocks of the tonalite-granodiorite gneiss suite, Abitibi, Wawa and Wabigoon subprovinces and Kapuskasing Structural Zone.*

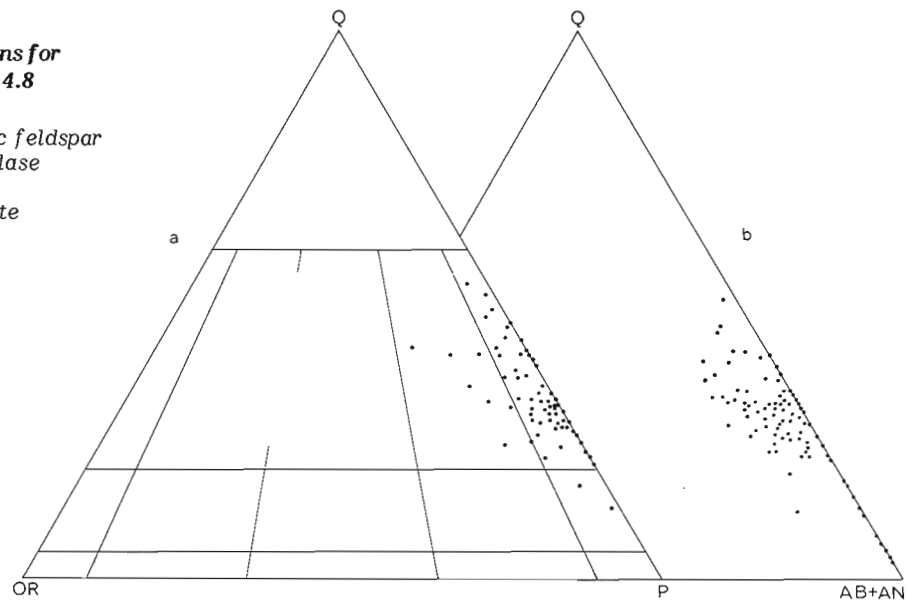

Figure 4.4. *Modal (a) and mesonormative (b) plots for trondhjemite-quartz diorite suite plutons (Eldorado, Round Lake, Rabbit Blanket Lake, and other plutons).*

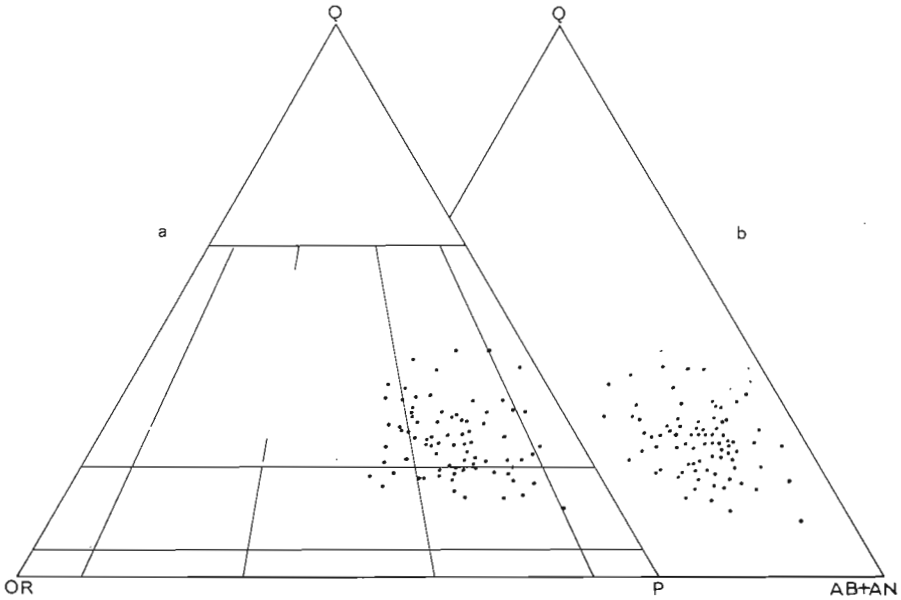

Figure 4.5. *Modal (a) and mesonormative (b) plots for granodiorite suite plutons (Blackstock, Watabeag, Adams, Round Lake, Gargantua Harbour, Gzowski and other plutons).*

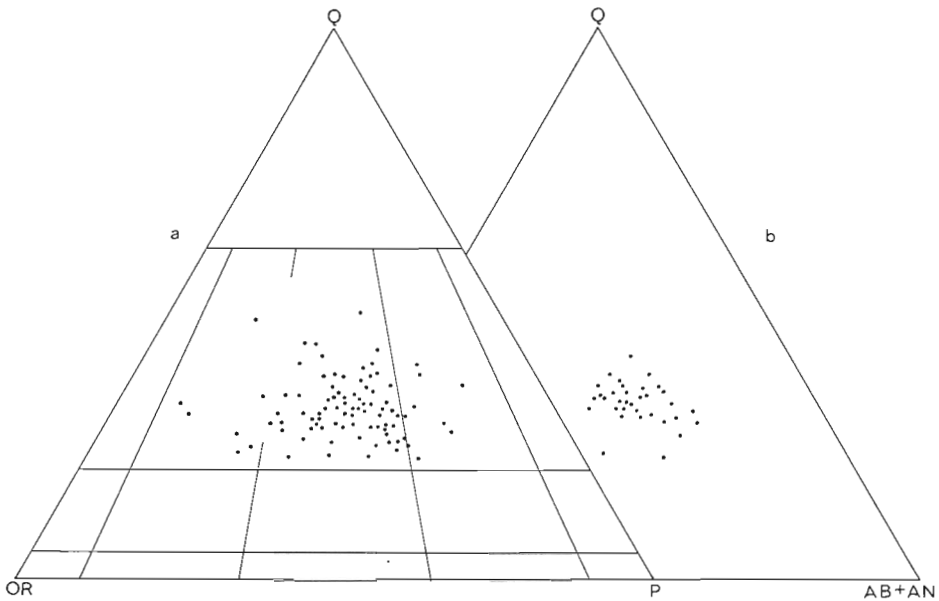

Figure 4.6. *Modal (a) and mesonormative (b) plots for granite suite plutons (Cartier, Mistawak, Rossport, Cutler, Killarney and other plutons).*

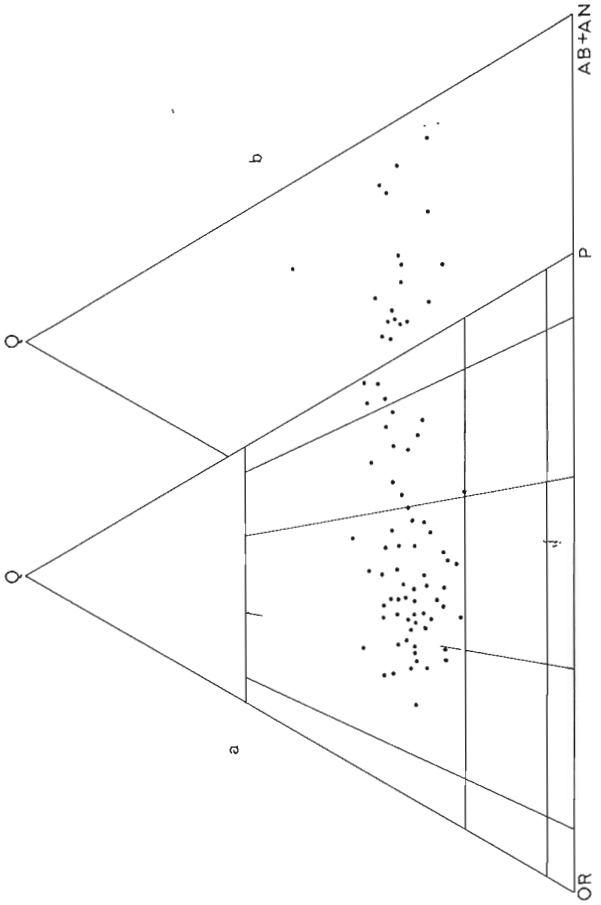

Figure 4.8. Modal (a) and mesonormative (b) plots for anatectic granitoid rocks, Quetico and Pontiac subprovinces.

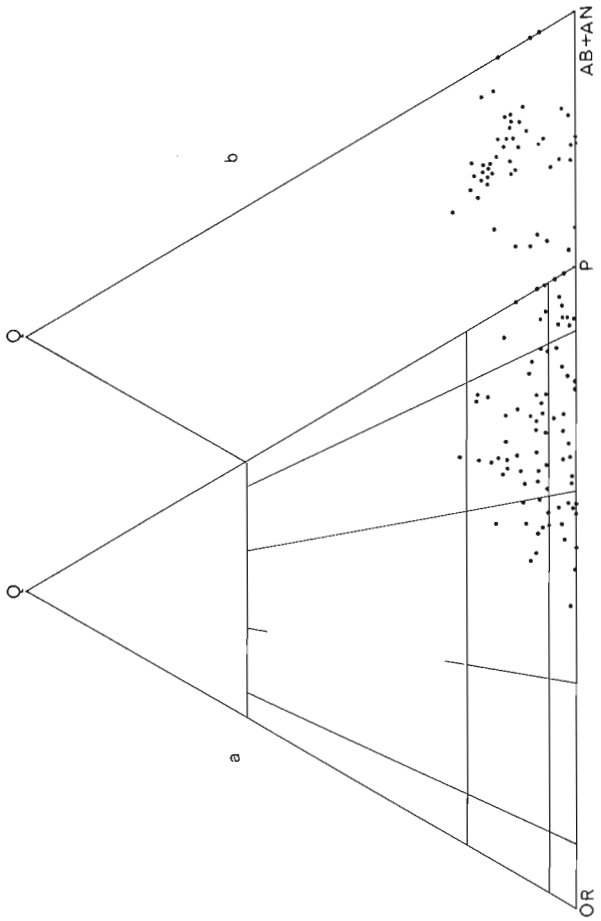

Figure 4.7. Modal (a) and mesonormative (b) plots for syenite-diorite suite plutons (Fallon, Cairo, Otto, East Bull Lake, Deeds Lake, Harcourt Lake, Mishibishu Lake and other plutons).

Granodiorite Suite

Many of the large batholiths of the greenstone-granite terranes consist entirely or largely of granodiorite. These rocks are massive to foliated and consist essentially of quartz, plagioclase, potassic feldspar and biotite with or without hornblende (Fig. 4.5).

Granite Suite

Massive to foliated granite plutons are present throughout central Superior Province. They are mainly B granites (Streckeisen, 1976) or quartz monzonite of some classifications and consist of quartz, plagioclase and potassic feldspar in approximately equal proportions, and biotite (Fig. 4.6). The granite plutons within the greenstone belts are typically small and range from granite to granodiorite in composition. Granites marginal to the greenstone belts or entirely within the gneiss terranes are typically large batholiths, and although dominantly B granites, also contain distinctly potassic phases. Most of the granite plutons are massive, or only weakly foliated, and contain little xenolithic material.

Syenite-diorite Suite

Simple plutons of syenite, quartz syenite, monzonite, monzodiorite, and diorite, and composite bodies consisting of several or all of the foregoing rock types are present throughout central Superior Province. They consist essentially of plagioclase, potassic feldspar, hornblende, and biotite (Fig. 4.7). Many bodies contain 5 to 10 per cent quartz; only a few have nepheline. They are generally massive and nonmetamorphosed; geological relationships indicate that they are the youngest Archean plutonic suite present.

Anatectic granitoid rocks of the Quetico and Pontiac Belts

The Quetico and Pontiac belts, both consisting dominantly of metasediments, also contain abundant layers, veins, sills, and dykes of granite and pegmatite in migmatitic paragneiss as well as granitoid bodies of batholithic dimensions. Many are gneissic to massive diatexite, granitic rocks derived from partial melting of metasediments, and contain abundant metasedimentary xenoliths in various stages of digestion. In addition to quartz, plagioclase, and potassic feldspar, these rocks commonly have muscovite and biotite, with abundant garnet and less common cordierite. They are typically white and display abrupt changes in grain size and texture from fine grained, aplitic through medium grained, hypidiomorphic granular, to coarse, pegmatitic. They range in composition from granite to tonalite although most are granite (Fig. 4.8).

Acknowledgments

The author was capably assisted in the field by David Thomas. Information and field guidance from R. Sutcliffe, F. Breaks, R. Sage, and H. Poulsen, Ontario Geological Survey, and E. Dimroth, Université du Québec à Chicoutimi are gratefully acknowledged.

References

Bennett, G., Brown, D.D., George, P.T., and Leahy, E.J.
1967: Operation Kapuskasing; Ontario Department of Mines, Miscellaneous Paper 10, 98 p.

Card, K.D.
1979: Regional geological synthesis, central Superior Province; in Current Research, Part A, Geological Survey of Canada, Paper 79-1A, p. 87-90.

Card, K.D. (cont.)
1980: Preliminary maps, central Superior Province compilation – Sudbury (41 I), Blind River (41 J), Gogama (41 P), Chapleau (41 O); Geological Survey of Canada, Open File 690.

1981: Preliminary maps, central Superior Province compilation – Sault Ste Marie (41 K), Michipicoten (41 N), Foleyet (42 B), White River (42 C), Schreiber (42 D), Longlac (42 E), Hornepayne (42 F), Kapuskasing (42 G); Geological Survey of Canada, Open File 729.

Card, K.D., Percival, J.A., and Coe, K.
1980: Progress report on regional geological synthesis, central Superior Province; in Current Research, Part A, Geological Survey of Canada, Paper 80-1A, p. 61-68.

Card, K.D., Percival, J.A., Lafleur, J., and Hogarth, D.D.
1981: Progress report on regional geological synthesis, central Superior Province; in Current Research, Part A, Geological Survey of Canada, Paper 81-1A, p. 77-93.

Gaucher, E.H.
1966: Elsas-Kapuskasing-Moosonee magnetic highs; Geological Survey of Canada, Paper 66-1, p. 263-338.

Goulet, N.
1978: Stratigraphy and structural relationships across the Cadillac-Larder Lake Fault, Rouyn-Beauchastel area, Quebec; unpublished Ph.D. thesis, Queen's University, p. 38-90.

Innes, M.J.S.
1960: Gravity and isostasy in Manitoba and northern Ontario; Dominion Observatory, Publication 21, p. 263-338.

Lafleur, J.
1981: Preliminary map, geology of the Round Lake Batholith, Kirkland Lake area, Ontario; Geological Survey of Canada, Open File 752.

Percival, J.A.
1981a: Geological evolution of part of the central Superior Province based on relationships among the Abitibi and Wawa subprovinces and the Kapuskasing Structural Zone; unpublished Ph.D. thesis, Queen's University, 300 p.

1981b: Preliminary map, Geology of the Kapuskasing Structural Zone in the Chapleau-Foleyet area, Ontario; Geological Survey of Canada, Open File 763.

Percival, J.A. and Coe, K.
1981: Parallel evolution of Archaean low- and high-grade terrane: A view based on relationships between the Abitibi, Wawa and Kapuskasing belts; Precambrian Research, v. 14, p. 315-331.

Satterly, J.
1970: Aeromagnetic maps of carbonatite-alkalic complexes in Ontario; Preliminary map p. 452 (revised).

Streckeisen, A.
1976: To each plutonic rock its proper name; Earth-Science Reviews, v. 12, p. 1-33.

5.

EVIDENCE FOR EXTENSIVE ARCHEAN SHALLOW MARINE SEDIMENTATION IN THE CHIBOUGAMAU AREA, QUEBEC

EMR Research Agreement 232-4-81

Erich Dimroth[1], Wulf Muller[1], Paul Archer[1], André Gobeil[2], and Gilles O. Allard[3]
Precambrian Geology Division

Dimroth, E., Muller, W., Archer, P., Gobeil, A., and Allard, G.O., Evidence for extensive Archean shallow marine sedimentation in the Chibougamau area, Quebec; in Current Research, Part A, Geological Survey of Canada, Paper 82-1A, p. 29-36, 1982.

Abstract

A preliminary study has suggested the presence of widespread shallow marine deposits in the Archean of Chibougamau area. The Stella and Hauy formations consist in the east of fluvial braid-fan deposits showing excellent upward-fining fluvial cycles. These interfinger eastward with argillites. Transitional facies show sedimentary structures like clay drapes on foreset beds in sandstone, clay drapes in the troughs of megaripples, that are absent from either fluvial or submarine (turbidite) fan sequences. Four repetitive facies are described that appear to define upward-coarsening littoral cycles. The Blondeau Formation at Lake Barlow and in Richardson township and parts of the Chebistouan Formation in Richardson township also contain features that seem to indicate a shallow marine origin. The fine grained units of these formations consist of shale or argillite, generally with sharply bounded, nongraded, laminae of siltstone and fine grained sandstone. Current ripples and flaser structure have been recognized in the sandstone laminae. Many of the sandstone laminae contain a high proportion (up to 100%) of shale pellets. Intercalated within the shale-argillite sequence are beds of shale-pellet sandstone and conglomerate, produced by reworking of older sediment. Many of these shale-pellet sandsotne and conglomerate beds are graded. It is suggested that these shale-pellet sandstone and conglomerate beds are storm-surge deposits of the deeper shelf.

Introduction

This paper documents the existence, in the Archean of Chibougamau area, of shallow marine sedimentary rocks that appear to have wide lateral extent. This is an important discovery because it suggests a basic difference between the paleogeographic evolution of the internal (Chibougamau-Mattagami) and external (Val d'Or-Timmins) zones of Abitibi orogenic belt. Detailed sedimentological studies in Kirkland Lake and Noranda-Val d'Or areas (Dimroth et al., 1975; Dimroth and Rocheleau, 1979; Rocheleau, 1980) demonstrated deposition of sediments in the external zone of the belt in steep-sloped environments, where fluvial sediments deposited on volcanic islands grade directly in to sediments of a submarine turbidite fan without an intervening shelf. It is known that part of the volcanic sequence erupted in shallow marine environments (Dimroth et al., 1975; Dimroth and Rocheleau, 1979; Lichtblau and Dimroth, 1980; Cousineau, 1980), but shallow marine sediments have not been described from the southern part of Abitibi belt and from its southern foreland (Pontiac belt).

The sequence of Chibougamau-Chapais area (Table 5.1 modified from Allard et al., 1979) is subdivided in the Roy and Opémiska groups. The upper stratigraphic units of this sequence occupy three major synclines, from south to north the Chapais syncline, the Chibougamau syncline and the Wakonichi syncline. Stratigraphic relations of the Roy and Opémiska groups are disputed. In the east part of Chapais syncline (Fig. 5.1), Cimon and Gobeil (1976) showed that the Opémiska Group overlies the Roy Group, the Doré Lake Anorthosite Complex and the Chibougamau Pluton with profound unconformity. Unconformities between the Opémiska and Roy groups at other localities have been described by Norman (1937). On the other hand, conformable transitions may be present at other localities and the contact of the Roy and Opéminska groups is not everywhere traceable with certainty. Such, for example are the relations in the Wakonichi syncline (Caty, 1975, 1977, 1979), where it is not clear which of the map units is part of the Roy Group and which belongs to the Opémiska Group.

For this reason, detailed investigation of the stratigraphy, sedimentology and structure at the contact or transition of the Roy and Opémiska groups might provide the key to a paleogeographic and paleotectonic interpretation of the Chibougamau-Chapais area. Research on this project will continue. Wulf Müller studied sections across the Stella and Hauy formations of the Chapais syncline; Paul Archer logged

Table 5.1

Stratigraphy of Chibougamau area
(modified from Allard et al., 1979)

	South (Chapais Syncline)	North (Wakonichi Syncline)
Opemiska Group	Haüy Fm.	
	Stella Fm.	Chebistouan Fm.
	unconformity	unconformity?
		Bordeleau Fm. (relations to Blondeau and Chebisotuan Fm. unkown)
Roy Group	Blondeau Fm.	Blondeau Fm.
	Filman Fm.	Gilman Fm.
	Wakonichi Fm.	Wakonichi Fm.
	Obatogamau Fm.	

[1] Sciences de la Terre, Université du Québec à Chicoutimi, 930 est, rue Jacques-Cartier, Chicoutimi, Québec, G7H 2B1.

[2] Ministère de l'Energie et des Ressources du Québec, 375, 3e Rue, Chibougamau, Québec.

[3] Department of Geology, University of Georgia, Athens, Georgia 30601, U.S.A.

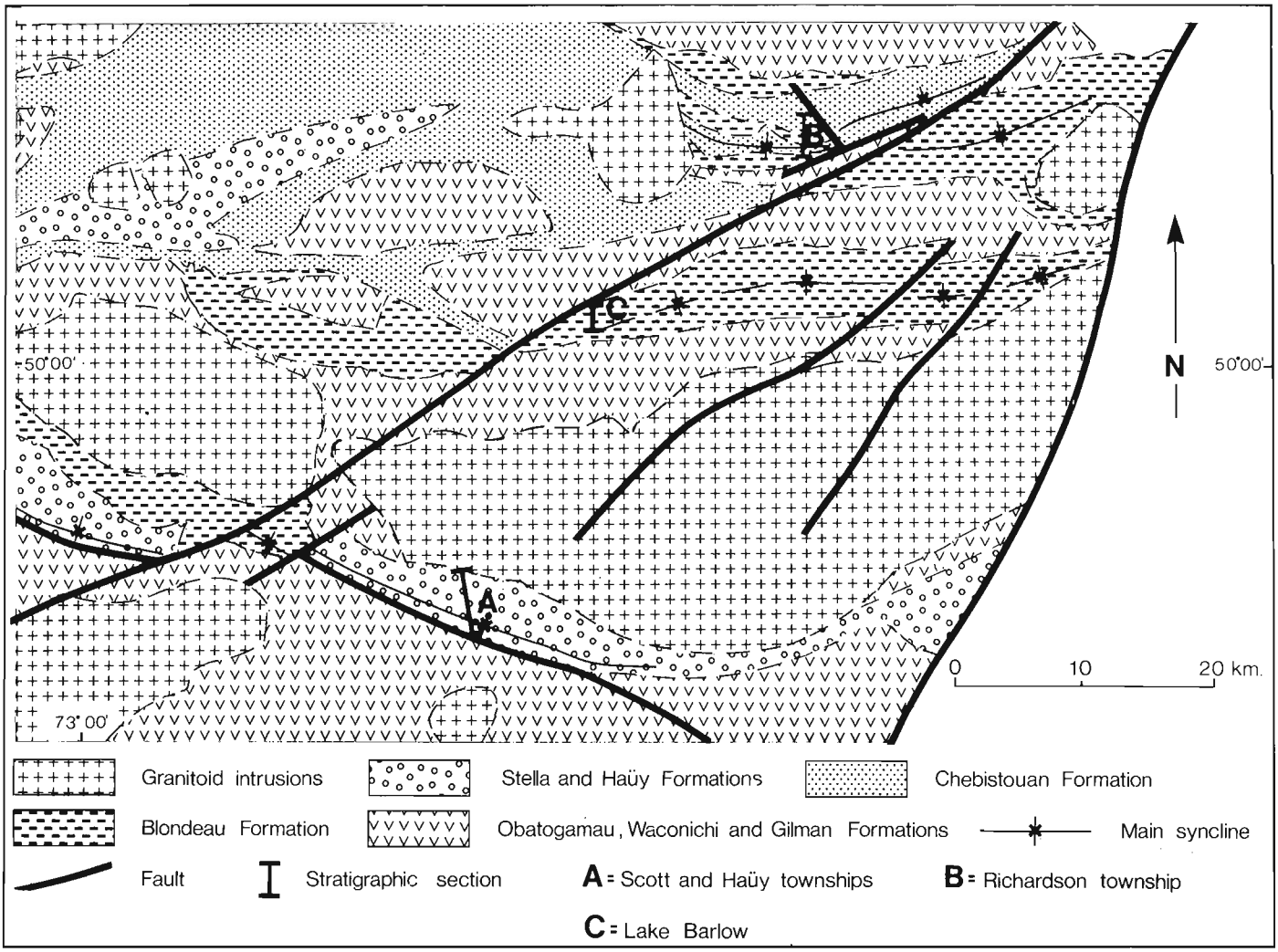

Figure 5.1. Map showing distribution of formations and sections studied.

drill core of the Blondeau Formation in the Chibougamau syncline; André Gobeil and Gilles O. Allard advised us on the regional stratigraphy and geology.

Deltaic and Shallow Marine Sediments in the Stella and Haüy Formations

The Stella and Haüy formations (Cimon and Gobeil, 1976) are a sequence of conglomerate, sandstone, argillite and lava flows overlying the Roy Group, the Doré Lake anorthosite complex, and the Chibougamau Pluton with a profound angular unconformity. The two formations are not clearly defined and are best taken as one unit; vertical and lateral facies changes are pronounced. Laterally, facies changes from a predominating conglomerate-sandstone association in Scott and Haüy townships to a sequence predominantly composed of argillite in Queylus township to the east. Vertical facies changes in Scott and Hauy townships are defined by at least six upward coarsening then fining piedmont fan cycles (Rust, 1979, Fig. 8). The conglomerate of each piedmont fan cycle has its own characteristic pebble association. Sandstones of different cycles also have different compositions. The proportion of volcanic lava flows and of detrital material derived from them increases upward in the sequence, whereas the proportion of fragmental material derived from the Roy Group and from trondhjemitic – syenitic plutonites decreases. Crossbeds indicate predominant transport to the east-northeast and northeast.

In Scott and Haüy townships, the bulk of the formations is composed of fluvial sandstones and conglomerates (Fig. 5.2a). Vertical aggradation deposits of fluvial channels are characteristic of the base of the formation; these channel aggradation deposits alternate with a minor volume of debris-flow deposits. Fluvial upward-fining sequences predominate higher up and their properties change characteristically upward in the stratigraphic sequence (Fig. 5.2).

The deltaic and shallow marine sediments represented in Figure 5.2 form intercalations, up to about 25 m thick, repeated at least four times in the lower part of the piedmont fan sequence. Four facies are present. Facies 1 to 3 form an upward coarsening, gradational sequence; facies 4 contains channels incised into facies 1-3 and laterally grades into facies 3.

Facies 1

Facies 1 (Fig. 5.3) is composed of laminated argillite, siltstone and very fine grained sandstone in that order of abundance. Continuous planar lamination is characteristic. Siltstone and sandstone laminae, however, not uncommonly

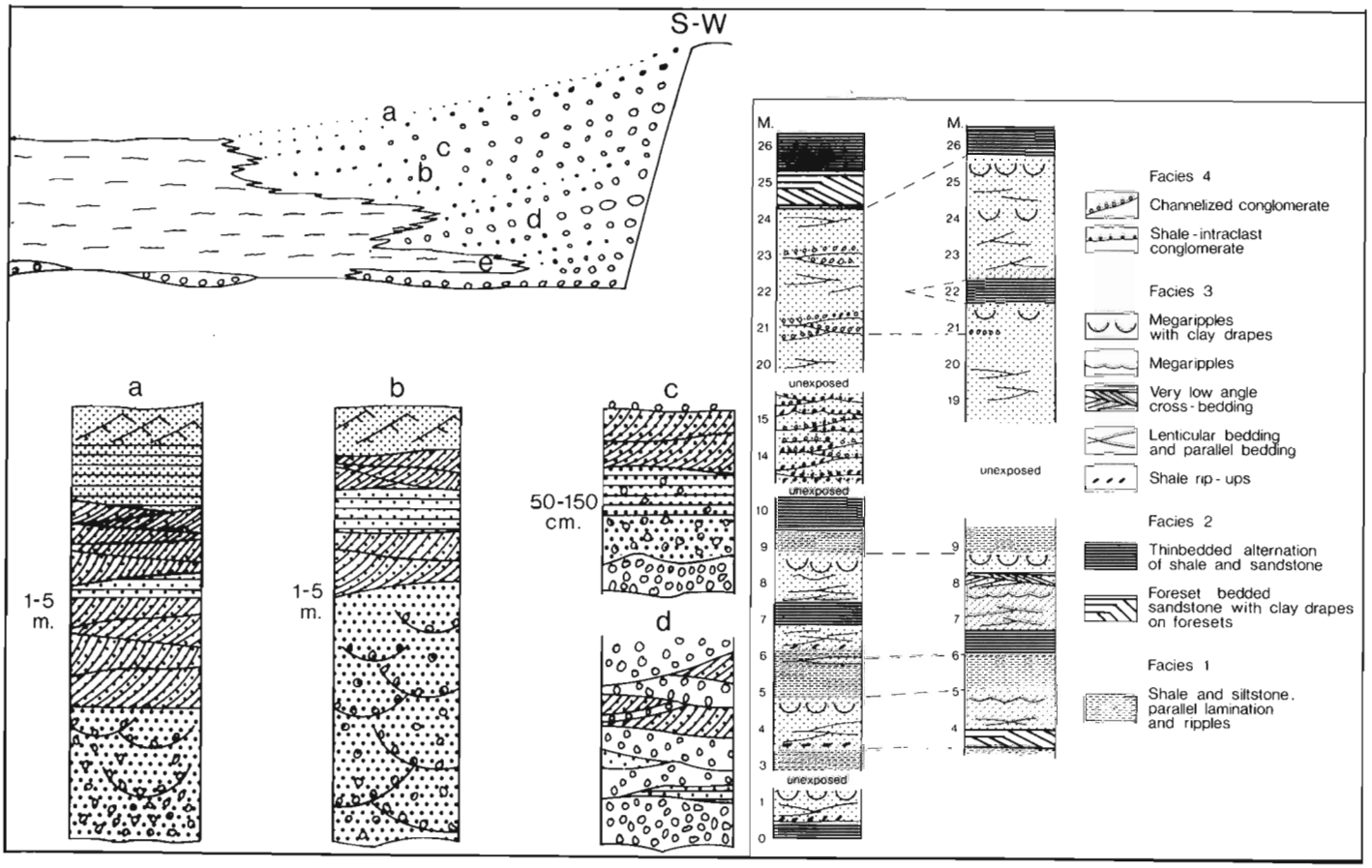

Top: general model – several upward coarsening then fining piedmont fan cycles (vertical and lateral grain size variations schematically shown by size of conglomerate symbols) interdigitate with shoreline and shallow marine sediments (shale symbol) to the east. Location of sections a to e indicated by lettering.

Sections a, b, c: upward fining fluvial cycles at various stratigraphic levels of the fluvial fan. Schematic but based on sections measured bed by bed.

Section d: fluvial vertical channel aggradation deposits at base of fluvial sequence. Schematic but based on section measured bed by bed.

Section e: measured section of littoral facies association. Both sections separated by ca. 20 m, correlated by continuous (base) or discontinuous (top) exposure. See text for detailed descriptions of facies.

Figure 5.2. *Tentative basin model of the Stella and Haüy formations south of Chibougamau.*

occur as lenticular laminae, as laminae showing pinch and swell structures in rhythmic repetition (starved ripples?), and as rippled crossbedded laminae. These traction current structures are particularly common immediately below overlying facies 2 or 3. About 5-20 cm thick interbeds of coarse grained sandstone with parallel lamination define a variant (facies 1a). Where these sandstone beds thin out, they show foreset lamination at a very small angle (< 5°).

Facies 2

Facies 2 (Fig. 5.4) is composed of beds of medium- to coarse-grained sandstone 3 mm to 20 cm thick, alternating with clay films and argillite laminae 1 mm to 5 cm thick. Characteristic of the sandstone beds is their lateral continuity, the absence of erosional bases, the absence of traction structures (parallel or cross lamination) and their sharp boundary against overlying argillite laminae. About one third to one half of the sandstone beds show graded bedding, the others do not show grain size variations recognizable with a hand lens.

A variant of facies 2 (facies 2a) contains interbeds of coarse grained sandstone, 5-20 cm thick with parallel lamination. Foreset bedded sandstone-shale complexes also occur in facies 2a (Fig. 5.5); these consist of foresets and topsets of alternating massive sandstone and argillite.

Facies 3

Facies 3 is an upward coarsening sandstone unit, 50 cm to several metres thick, and characterized by a vertical variation of sedimentary structures in four divisions. This vertical structure sequence may be repeated or interrupted.

The lowermost division of facies 3 is composed of coarse to very coarse grained sandstone in long-lenticular beds 5-20 cm thick, separated by films or laminae of fine grained sandstone or argillite. Beds show erosional bases and, at the base, contain rip-up clasts of argillite and/or very fine grained sandstone (Fig. 5.6). Some beds show graded bedding whereas no grain size variation is detectable in others. Traction current structures are absent.

5.3

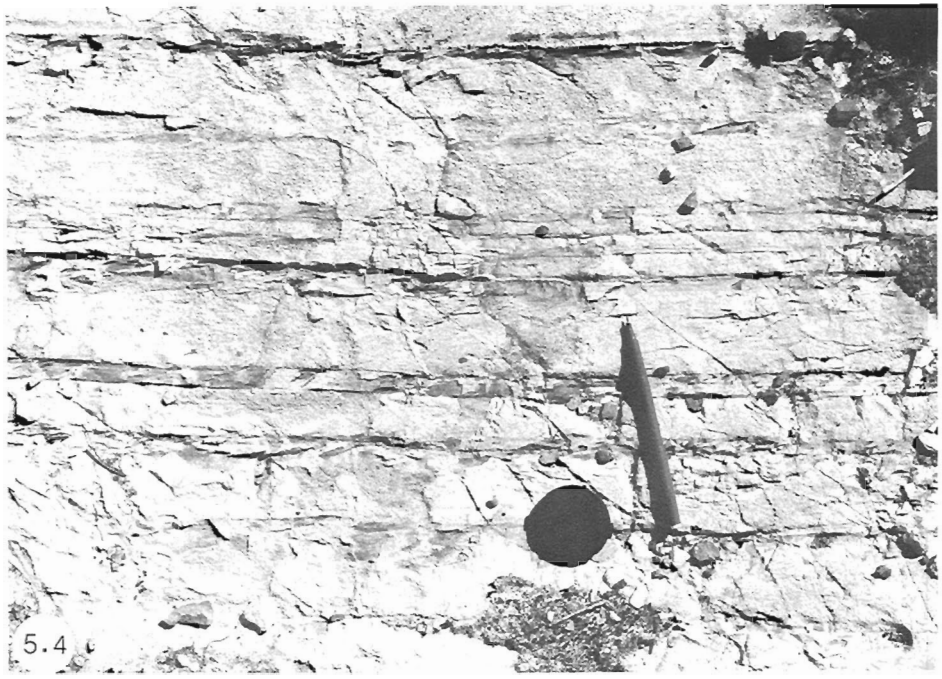

5.4

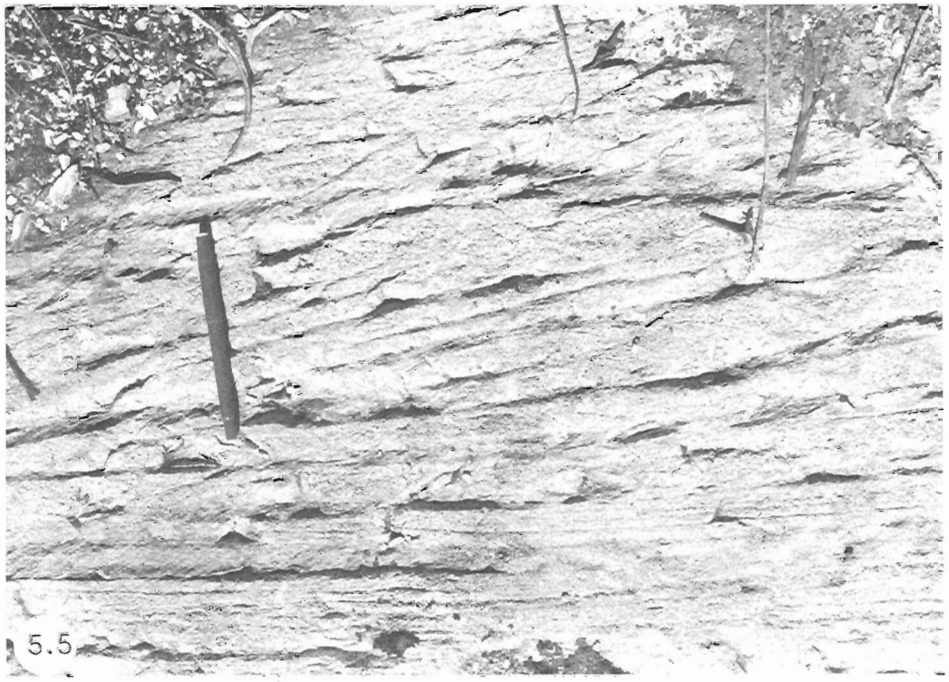

5.5

5.6

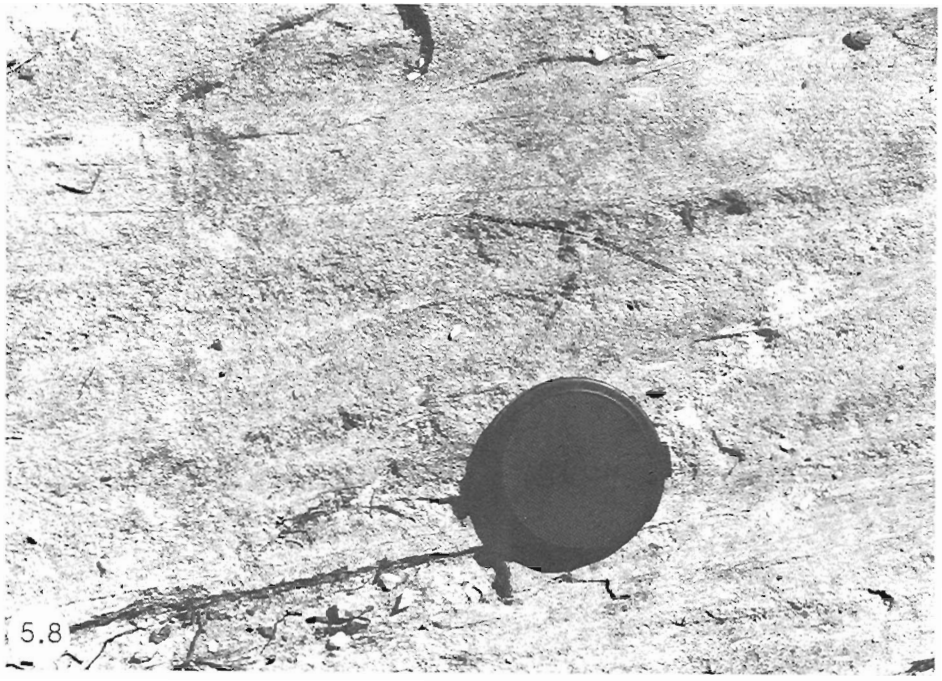

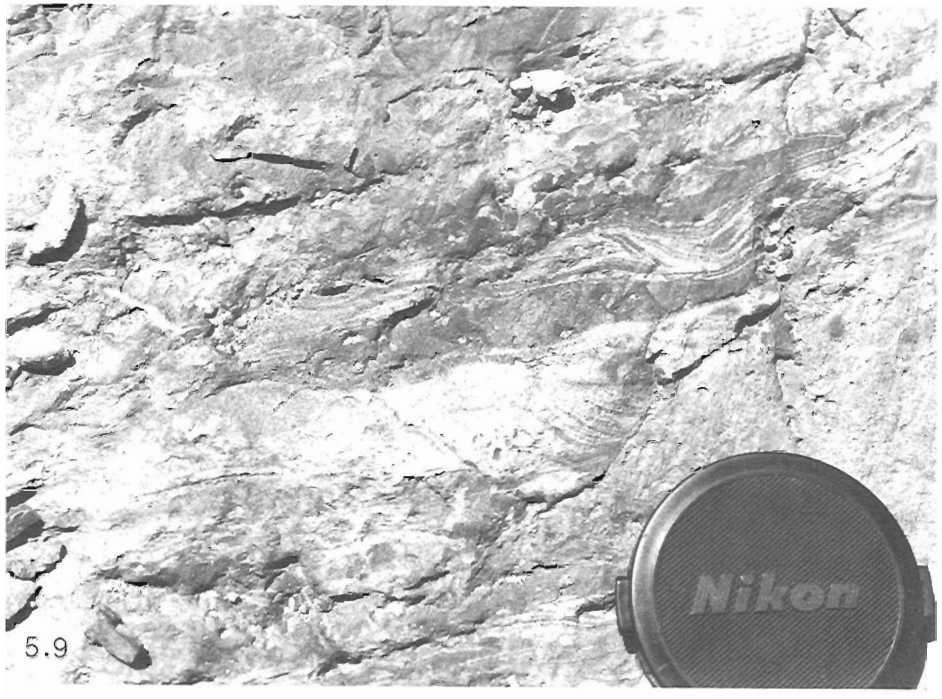

Figure 5.3. *Facies 1 of littoral deposits in Stella Formation.*

Figure 5.4. *Facies 2 of littoral deposits in Stella Formation.*

Figure 5.5. *Foreset-bedded sandstone-argillite complex in facies 2. Note argillite drapes on sandstone foresets.*

Figure 5.6. *Rip-up clasts of argillite and fine grained sandstone in facies 3.*

Figure 5.7. *Discontinuous trough-shaped clay drapes in coarse grained sandstones, interpreted as clay drapes on megaripples. Facies 3, Stella Formation.*

Figure 5.8. *Low-angle planar crossbedding in granule conglomerate of facies 3, Stella Formation.*

Figure 5.9. *Ripple crosslamination in nongraded siltstone of shale-siltstone facies, Blondeau Formation. Note black pits in siltstone indicating high proportion of shale pellets. Richardson township.*

The second division, 30-50 cm thick is composed of lenticular beds, without traction structures, of coarse to very coarse grained sandstone, alternating with laminae of fine grained sandstone. Division 3 contains megaripples about 5 cm high and 30 cm in wavelength defined by laminae of fine grained sandstone and by rhythmic, trough shaped structures of the same dimension, emphasized by argillite films (Fig. 5.7). These structures are interpreted as small trough crossbeds and as wave megaripples, not uncommonly with clay films deposited on their troughs. Division 4 is composed of very coarse grained sandstone and granule conglomerate in low-angle (< 5°) planar crossbeds (Fig. 5.8).

A variant of facies 3 (facies 3a) contains 5-20 cm thick interbeds of coarse grained sandstone with parallel lamination in divisions 1 or 2.

Facies 4

Facies 4 is a conglomerate-sandstone association in beds 5-30 cm thick. Conglomerate and sandstone generally show massive bedding. Conglomerate is channelized into sandstone. This facies grades laterally into facies 2 and 3 over a distance of about 20 m. Where channels are incised into facies 1, the conglomerate and sandstone contain a very high proportion of argillite intraclasts. In general, facies 1, 2, and 3 succeed one another in vertical section, whereas facies 4 is incised into any of the three.

Discussion

Argillites and fine grained sandstones occur intercalated between fluvial deposits in two settings, namely as overbank deposits and as lacustrine or deltaic deposits. Fluvial overbank deposits form the top of fluvial upward-fining cycles, whereas the facies described above form an upward-coarsening sequence into which conglomerates are channelized. This upward coarsening sequence of facies 1 to 3 is similar to the facies of wave-dominated deltas (Miall, 1979) and of the shoreface and foreshore of barrier island systems (Reinson, 1979). Facies 1 is interpreted as shallow marine, and comprises very fine grained suspension deposits (argillite and siltstone with millimetre size parallel lamination) partly reworked by bottom currents (siltstone and very fine grained sandstone with lenticular and ripple cross lamination).

Facies 2 is interpreted as sediment of the deeper shoreface below normal wave base. Absence of erosional bases of beds and of traction structures suggests that all sediments are suspension deposits, sandstone beds either deposited from suspensions generated at the shoreline during storms or from suspensions generated by river floods. Such deposits are common on the deeper shoreface (Reinson, 1979).

Facies 3 represents a foreshore-beach complex. Division 1 is interpreted as sediment of the breaker zone because beds show strong bottom erosion (argillite rip-ups). Divisions 2 and 3 represent the even and rough bottom zones of the foreshore, and the low angle cross stratification of division 4 is interpreted as beach cross-stratification. Clay drapes over wave-megaripples, and laminae of fine grained sandstone are interpreted as sediment settled from suspension during tranquil periods.

Facies 4 is interpreted as channel deposits in distributary delta channels. Facies 1a, 2a, and 3a are interpreted as fluvially influenced: sandstone with parallel laminations was deposited by bottom traction during river floods, and the foreset-bedded sandstone-argillite complexes formed by lateral aggradation of sand banks just below wave base.

The significance of graded bedding in this facies requires special consideration. Graded beds in this facies lack any kind of traction structures; they are sharply overlain by argillite laminae and, thus, the graded-bedded sand and the overlying argillite belong to different sedimentation units. In our view, such graded sandstone beds, although suspension deposits, are not turbidites.

Blondeau and Chebistouan Formations in Southwest Richardson Township

The southwest quarter of Richardson township was mapped by Caty (1975), and the units described here are units 6A, 6B, 6C, and 6D of that quarter township. The stratigraphy and stratigraphic nomenclature of this zone are in a state of flux (see Caty, 1975, 1977, 1979). At present, we consider units 6A and 6B of Caty (1975) to represent the Blondeau Formation, and units 6C and 6D to represent the Chebistouan Formation.

Unit 6A

This unit is composed of mafic lava flows and intercalated carbonaceous and pyritiferous siliceous shale and subordinate siltstone as in unit 6B.

Unit 6B

Unit 6B is composed of three facies, namely a shale facies, a shale-siltstone facies, and a conglomerate facies. The first facies is composed of siliceous shale rich in organic matter and commonly containing much nodular (and, less commonly, laminated) pyrite. Units of this shale are several metres to decametres thick. Primary sedimentary structures are poorly preserved because this is the least competent unit of the region; however submillimetre to millimetre parallel laminae can be recognized.

This facies grades into the shale-siltstone facies. Laminated shale-siltstone and fine- to medium-grained sandstone form the bulk of the unit. Shale is graphitic and pyritiferous, although less so than in the shale facies. Siltstone and sandstone laminae 1 mm to 3 cm thick are intercalated with the shale. They show parallel, long lenticular, lenticular and ripple cross-lamination (Fig. 5.9). Graded bedding is rare, and shale is abruptly draped over the sandstone laminae. Convolute lamination and small-scale slumps are present.

Intercalated between this background sediment are sandstone and pebble conglomerate beds 5-30 cm thick. Their bed thickness increases with the grain size. The beds consist of sand, granule, and pebble sized shale intraclasts virtually to the exclusion of all other components (Fig. 5.10). The beds have erosional bases; about 75 per cent of the beds show graded bedding (Fig. 5.10), the others do not show grain size gradation. All bed types are overlain by shale with sharp contact and gradation of the sandstone at the top of beds into siltstone and shale is absent. Many beds show a massive base followed by parallel laminations, others show graded bedding without internal structure.

The conglomerate facies is composed of well rounded pebbles of plagioclase-phyric volcanic rocks set in a matrix of quartz-poor sandstone containing many sand-size shale intraclasts. This facies is rare, and poor exposure has not permitted the recognition of its sedimentary structures.

Unit 6C

Unit 6C is mainly composed of argillite and siltstone. At one locality, an angular unconformity is exposed between units 6B and 6C, but the content and sedimentary structures of both units are so similar that we suspect the unconformity to be a local erosional discordance. Three facies are

recognized, namely a shale-siltstone facies identical to the shale-siltstone facies of unit 6B, a predominating argillite-siltstone facies, and a conglomerate facies. The argillite-siltstone facies is coarser grained than the shale-siltstone facies of unit 6B but has the same sedimentary structures. Intercalated intraclast sandstones and conglomerates are present but contain a fairly large proportion of volcanic rock fragments.

The conglomerate facies is poorly exposed. Where exposed it consists of individual conglomerate beds and of packets, up to 10 m thick, of conglomerate that alternates with the predominating argillite-siltstone facies. Conglomerate is composed of well-rounded fragments of volcanic rock, a high proportion of which are plagioclase-phyric. Intraclasts of argillite and shale are present. Sandstone is plagioclase-rich and quartz-poor. Conglomerate beds are 20-100 cm thick, generally show well defined graded bedding, and grade upwards into sandstone, with graded bedding and parallel lamination. Argillite or shale is sharply draped over these graded beds.

Unit 6D

This unit locally grades into unit 6C by alternation on a 10 m scale of the Unit 6C argillite-siltstone facies and a massive-bedded conglomerate-sandstone facies. Higher up, only massive-bedded conglomerate and sandstone are exposed.

The argillite-siltstone facies is identical to the argillite-siltstone facies of unit 6C, and has the same sedimentary structures as the shale-siltstone facies of unit 6B.

Figure 5.10. *Shale intraclast sandstone with graded bedding in Blondeau Formation. Note composition exclusively of reworked material and intercalation between a shale-siltstone sequence from which graded bedding is absent. Richardson township.*

Very good exposure of the massive-bedded conglomerate-sandstone facies is not present. This conglomerate is composed of well rounded cobbles and pebbles of volcanic rock fragments; the proportion of plagioclase-phyric fragments appears to decrease upwards. Some tonalite fragments are present. Intraclasts of argillite are present where the conglomerate overlies the argillite-siltstone facies.

Conglomerate beds range from one pebble thickness to about 50 cm thick. Each bed has an erosional base; beds lack graded bedding or any kind of internal stratification. Amalgamation of conglomerate beds is very common. Sandstone interbeds are lenticular. Many are scoured into the underlying conglomerate, and none seem to grade into the underlying conglomerate. Many sandstone beds contain isolated pebbles. Erosion surfaces, parallel bedding and crossbedding are common. None of the sandstone beds shows graded bedding.

North of Chebistouan river, the conglomerate contains about 50 per cent of coarse grained lencocratic tonalite fragments, and the sandstone contains some (perhaps 10-20%) quartz. We suspect that this tonalite-rich conglomerate is higher stratigraphically than the conglomerates composed mainly of volcanic rock fragments.

Small scale folding makes it difficult to reconstruct the exact thickness of the sequence. We estimate that units 6B and 6C each have a thickness of less than 150 m.

The similarity of sedimentary structures in units 6B and 6C, the similarity of the pebble association in the conglomerates of both units, absence of unconformity on a map scale (see Caty 1975, 1977) and the fact that units 6B and 6C contain the same schistosities, suggest that the exposed unconformity is local and erosional. Thus, we believe that both units form part of one essentially concordant sequence. Units 6C and 6D also form part of a concordant sequence as follows from the alternation of argillite and conglomerate of the two units. For these reasons, we interprete units 6B to 6D as an essentially concordant, upward-coarsening, stratigraphic sequence.

Upward coarsening sequences of shale, argillite, sandstone and conglomerate form in turbidite fans, and in prograding shelf and littoral deposits. However, the sequence described above does not resemble sediments of turbidite fans as described by Walker (1979b), since turbidites make up only small part of the sequence and are mainly composed of reworked sediment. On the other hand, for reasons discussed below, units 6B and 6C resemble sediments of storm-dominated deeper shelf areas, in particular the sediments described by Goldring and Bridges, (1973) and by Brenchley et al. (1979) and to a less degree those described by Walker (1979a).

In our view, parallel lamination of shales and argillites in units 6B and 6C is best interpreted by settling of the sediment from dilute suspension. Thin laminae of siltstone and very fine grained sandstone show structures (lenticular and flaser bedding, ripple cross-lamination) indicating transport by bottom traction. Many of these beds have erosional bases, and contain shale pellets. These laminae thus indicate intense reworking of earlier sediment and the absence of graded bedding indicates that reworking is not due to turbidity currents.

Erosional bases, graded bedding and parallel laminations at the top of beds suggest that the intercalated sandstone beds are turbidites. However, many of the sandstone beds are exclusively composed of shale intraclasts which suggests a local derivation by reworking of shale. Similar sharp-based sheet sandstones with graded bedding, intercalated between shales, have been interpreted as storm-surge deposits by Goldring and Bridges (1973), by Brenchley et al. (1979), and by Walker (1979a). Such an interpretation is particularly

attractive for these beds because they consist mainly or exclusively of reworked material derived from the shale within which they occur.

Of course, the polymict conglomerate beds of unit 6C do not have this origin. These beds have the graded-stratified structure sequence of coarse grained turbidites described by Walker (1979a). The stratified, nongraded, sandstone-conglomerate facies of unit 6D do not show the structures of turbidite-associated conglomerates and tentatively is interpreted as fluvial. In summary, it appears to us that units 6B and 6C probably have been deposited in offshore environments at or slightly below storm wave base. The sharp-based sheet sandstones and conglomerates with shale intraclasts are interpreted as storm-surge deposits. The rare graded-stratified polymict conglomerates of unit 6C may represent delta-front or shore-slope turbidites and the conglomerate-sandstone facies of unit 6D is tentatively interpreted as fluvial.

Blondeau Formation at Lake Barlow

The Blondeau Formation of Chibougamau syncline was studied in a stratigraphic drillhole by the Quebec Department of Energy and Resources at Lake Barlow. A few outcrops in northwest Roy township and at Lake Barlow were also studied. Most of the formation consists of shale, siltstone and very fine grained sandstone, much of which is silicified. Sandstone beds 5 to 100 cm thick and a few pyroclastic flows are intercalated between these sediments and comprise but a few per cent of the thickness of the formation. Characteristic bedding structures in the shale, siltstone and very fine grained sandstone are parallel lamination, flaser lamination, and ripple cross lamination. Erosion surfaces at the base of laminae occur here and there. Much of the fine grained sandstone, contains abundant shale pellets and some of the shale is pelleted. Graded bedding is not characteristic. Synsedimentary deformation structures (small-scale slumps and convoluted bedding) occur. These sedimentary structures suggest deposition by settling from diluted suspensions, followed by intense reworking of the sediment by bottom currents. In particular, the abundance of shale pellets is indicative of reworking by fairly strong currents.

The intercalated sandstone beds exhibit the same properties (abundant shale pellets, sharp bases, common graded bedding, presence or absence of lamination at the top of beds) as the sheet sandstones in Richardson township. Like the latter we consider these sediments as probable storm-surge deposits.

Conclusions

We have presented evidence that suggests deposition of substantial sediment volumes within a wide district surrounding the Chibougamau area in a shallow marine environment. The relations of these deposits to fluvial sediments and shoreline sediments on the one hand, to turbidites on the other, remain to be established.

The absence of convincing evidence for tidal influence in any of these sediments is noteworthy. In particular, we never observed herringbone crossbedding, although crossbeds in the sequences are multidirectional and suggest complex current patterns. It appears therefore that these rocks were deposited in microtidal environments, with tidal amplitudes less than 1 m. Such microtidal environments are common on oceanic islands, but not on extensive shelf areas.

References

Allard, G.O., Caty, J.L., Chown, E.H., Cimon, J., Gobeil, A., and Baker, D.
1979: Stratigraphie et métallogénie de la région de Chibougamau; Geological Association of Canada/Mineralogical Association of Canada, Excursion B-1, Université Laval, Québec.

Brenchley, P.J., Newall, G., and Stranistreet, I.G.
1979: A storm surge origin for sandstone beds in an epicontinental platform sequence, Ordovician, Norway; Sedimentary Geology, v. 22, p. 185-217.

Caty, J.L.
1975: Géologie de la demie ouest du Canton de Richardson; Ministère des Richesses Naturelles, Québec, DP-342.

1977: Géologie de la demie est du Canton de Richardson; Ministère des Richesses Naturelles, Québec, DPV-447.

1979: Géologie de la demie ouest du Canton de Bignell. Ministère des Richesses Naturelles, Québec.

Cimon, J. and Gobeil, A.
1976: The Stella Formation: its implications for the genesis and relative age of the mineralization of the Chibougamau Mining camp; Bulletin of Institute of Mining and Metallurgy, v. 69, No. 767, p. 96.

Cousineau, P.
1980: Stratigraphie des andésites d'Amulet près de la mine Norbec, Rouyn-Noranda; Mémoire de maîtrise, Université du Québec à Chicoutimi.

Dimroth, E., Gélinas, L., Provost, G., Rocheleau, M., and Tassé, N.
1975: Sedimentology and volcanology of Rouyn-Noranda area; Guidebook. Ministère des Richesses Naturelles, Québec (bureau du géologue-résident, Noranda).

Dimroth, E. and Rocheleau, M.
1979: Volcanology and sedimentology of Rouyn-Noranda area; Geological Association of Canada/Mineralogical Association of Canada, Québec, 1979, Excursion A1, Université Laval, Québec.

Goldring, R. and Bridges, P.
1973: Sublittoral sheet sandstones, Journal Sedimentary Petrology, v. 43, p. 736-747.

Lichtblau, A.P. and Dimroth, E.
1980: Stratigraphy and facies at the south margin of the Archean Noranda Caldera; in Current Research; Part A, Geological Survey of Canada, Paper 80-1A, p. 69-76.

Miall, A.D.
1979: Deltas. In R.G. Walker, ed., Facies models; Geoscience Canada Reprint Series 1, p. 43-56.

Norman, G.W.H.
1937: East half Opemiska map area, Quebec; Geological Survey of Canada, Paper 37-11.

Reinson, G.E.
1979: Barrier Island Systems; in Facies Models, R.G. Walker, ed., Geoscience Canada Reprint Series 1, p. 57-76.

Rocheleau, M.
1980: Stratigraphie et sédimentologie de l'Archéen dans la région de Rouyn, Abitibi, Québec; Thèse de doctorat, Université de Montréal, 313 p.

Rust, B.R.
1979: Coarse alluvial deposits; in Facies Models, R.G. Walker, ed., Geoscience Canada Reprint Series 1, p. 9-22.

Walker, R.G.
1979a: Shallow marine sands; in Facies Models, R.G. Walker, ed., Geoscience Canada Reprint Series 1, p. 75-90.

1979b: Turbidites and associated coarse clastic deposits; in Facies Models, R.G. Walker, ed., Geoscience Canada Reprint Series 1, p. 91-104.

STRUCTURAL RECONNAISSANCE OF THE GREEN HEAD GROUP SAINT JOHN, NEW BRUNSWICK

Project 730044

Damian Nance[1]
Precambrian Geology Division

Nance, Damian, Structural reconnaissance of the Green Head Group, Saint John, New Brunswick; in Current Research, Part A, Geological Survey of Canada, Paper 82-1A, p. 37-43, 1982.

Abstract

The ?Neohelikian platform carbonates and quartz-rich clastics of the Green Head Group show at least three deformational phases. The earliest (D_1) produced a variable fabric (S_1) that is axial planar to rare mesoscopic F_1 isoclines. Deformation was strongly heterogeneous and strain was principally accommodated by ductile flow in the carbonates which are strongly foliated. The clastics responded by boudinage and the development of a weak muscovite-chlorite or muscovite-biotite S_1 cleavage parallel to the bedding. D_1 probably corresponds to a Taconic phase of partial melting and diapirism in the adjacent ?Aphebian Brookville gneiss but is likely to be a composite fabric with coplanar components as old as the Grenvillian. D_2 produced northeast and southwest plunging folds (F_2) on both a mesoscopic and megascopic scale. These close, upright, flexural-slip structures are coaxial with F_1, but typically lack an axial (S_2) fabric. However, faulting parallel to the axial plane, axial fracture cleavage fans, and incipient axial crenulation cleavage are developed locally. D_3 produced mesoscopic and megascopic folds (F_3) which are similar in appearance to those of F_2 but plunge to the east-southeast and west-northwest. Axial fabrics (S_3) are again only locally developed. Both deformations may have accompanied a retrogression that partially reset Green Head Group zircon ages during the Acadian.

Introduction

The Precambrian Green Head Group of southern New Brunswick has long been studied as part of the Avalon Zone of the Canadian Appalachians. However, due to a complex deformational, metamorphic and magmatic history, the tectonics of the region remain unresolved while the relationship of the Green Head Group to adjacent groups remains unclear or controversial. The following report presents the initial results of a detailed structural re-examination of parts of the Green Head Group and forms one aspect of a current multidisciplinary project (Currie et al., 1981) aimed at resolving the tectonic history of the rocks of the Saint John area.

Acknowledgments

The author gratefully acknowledges financial assistance from the Ohio University Research Council (OURC 9637).

Regional Setting

The broad stratigraphy of the Saint John region has long been described (Hayes and Howell, 1937; Alcock, 1938) and is traditionally considered in terms of five principal units: (1) the Golden Grove suite of plutonic and metamorphic rocks, (2) the Green Head Group, comprising marbles with subordinate siltstones and quartzites, (3) the Coldbrook Group, comprising acid and basic volcanics with minor sediments, (4) the Saint John Group, containing fossiliferous Cambrian to Lower Ordovician (Arenig) shales and sandstones, and (5) Carboniferous and younger conglomerates and sandstones. With the exception of the Golden Grove suite which includes rocks of various ages, this sequence is in chronologic order. A Middle Riphean (Neohelikian) age has been suggested for the Green Head Group (Hofmann, 1974) on the basis of the stromatolite **Archaeozoon acadiense,** while a late Precambrian (Hadrynian) age for the Coldbrook Group is indicated by a 750 ± 80 Ma Rb-Sr isochron obtained by Cormier (1969). The plutonics of the Golden Grove suite include acid and basic rocks of Hadrynian (800-850 Ma), Ordovician (470 Ma) and probably Devonian (335-370 Ma) ages (Olszewski et al., 1980). Currie et al. (1981) attributed much of this plutonic history to repeated partial melting and diapirism of the metamorphic core of the Golden Grove suite known as the Brookville Gneiss (Wardle, 1978). To emphasize this relationship while avoiding temporal connotations they reterm the suite the 'central plutonic core'. Following Williams et al. (1972) they further suggested that the Brookville Gneiss, which appears structurally distinct from other units of the region, represents a crystalline basement to the Green Head Group rather than being its metamorphic equivalent as suggested by Alcock (1938) and Rast et al. (1976). The presence of pre-Green Head Group protolith is supported by a Paleohelikian or Aphebian (1640 Ma) zircon age obtained by Olszewski et al. (1980) from the Brookville Gneiss.

The distribution of major units (Fig. 6.1) is broadly that of an anticlinorium with a core of plutonic and metamorphic rocks successively flanked to the northwest and southeast by the Green Head, Coldbrook and Saint John groups respectively. However, the area has a complex history of deformation with Acadian, Taconic, and probably earlier phases all of which accompanied metamorphic events of various intensity. In addition, the southerly Carboniferous formations have been sliced up and transported northwest along a number of thrusts which constitute the 'Variscan front' of Rast and Grant (1973).

The Green Head Group

Detailed examination of the Green Head Group was conducted in three areas of almost continuous outcrop at Drury Cove, Snowflake Quarry and Howes Lake (Fig. 6.1). All lie on the northwesterly flank of the anticlinorium within the Drury Cove Formation of Wardle (1978) and are unconformably overlain to the north by the Mississippian Kenebecasis Formation. Structural maps of the three areas are presented in Figures 6.2-6.4.

Lithology and Field Relations

The Green Head Group comprises a metamorphosed sequence of platform carbonates and quartz-rich clastics that are cut by numerous mafic dykes of several generations and, in the areas studied, rare felsic dykes that are probably feeders to the Coldbrook Group. The carbonates include

[1] Department of Geology, Ohio University, Athens, Ohio 45701

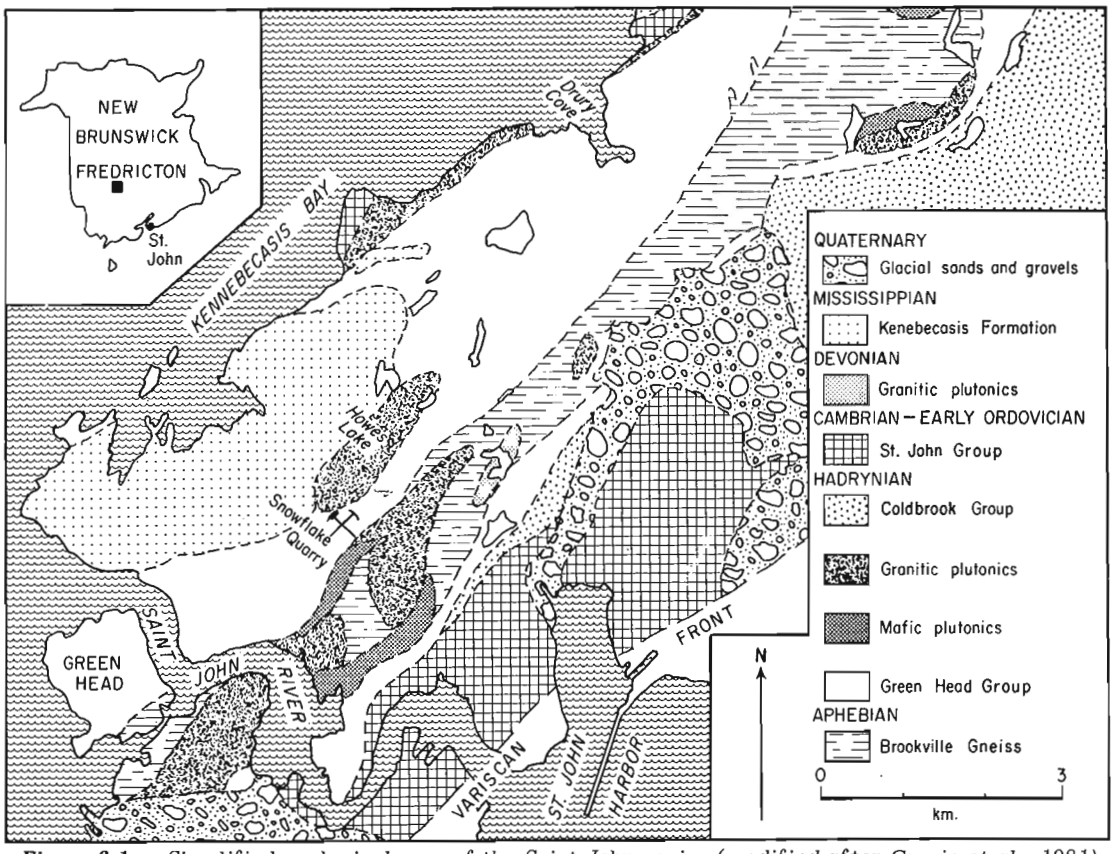

Figure 6.1. *Simplified geological map of the Saint John region (modified after Currie et al., 1981).*

white and grey calcite marbles colour-banded on a centimetre to metre scale and massive, cream-coloured dolomites which form concordant horizons up to 100 m thick. Both carbonates contain occasional, thin phyllite intercalations. The clastics include laminated, grey and green metasiltstones and calc-silicates with less common 1 to 10 m horizons of grey and white quartzite. Clastic horizons range from 5 to 50 m intercalations in marble, to massive, quartz-rich bodies up to 500 m thick. Calc-silicates are typically laminated with marble on a centimetre scale along gradational contacts between marble and more massive, metasiltstone horizons. Clastic horizons, however, show little lateral continuity; laminations are typically boudinaged while more massive horizons are lensoid and enveloped by carbonate colour-banding. Even the thickest units (eg. at Howes Lake) are rarely traceable along strike for distances in excess of 1 km. Contacts between carbonates and clastics may be sharp or gradational, concordant or crosscutting. Discordant contacts are marked by apophyses or dyke-like projections of marble into metasiltstone and diapiric injection of metasiltstone into marble (Fig. 6.5a). Similarly, the calc-silicate laminae of gradational contacts are often highly contorted and boudinaged (Fig. 6.5b). Such relationships clearly indicate that the marbles were highly mobile during deformation and hence their colour-banding may no longer be a reliable guide to bedding. While bedding is widely preserved in the clastics and locally shows indications of grading and soft sediment deformation, the lensoid shape of these horizons and their lack of lateral continuity suggest that they represent megaboudins within the more plastic carbonates. Preservation of small, widely scattered stromatolite occurrences in the marbles may be similarly attributed to slight competency differences. Consequently, past attempts to erect a stratigraphy for the Green Head Group (Leavitt and Hamilton, 1962; Wardle, 1978) may be of dubious validity.

Green Head Group lithologies largely show lower greenschist facies assemblages. Metasiltstones typically comprise quartz-albite-muscovite-actinolite-epidote/clinozoisite ± biotite whereas phyllites contain muscovite/sericite-chlorite-quartz ± biotite. The assemblage calcite-tremolite-epidote-muscovite-quartz ± phlogopite characterizes the calc-silicates while the carbonates are essentially monomineralic with minor amounts of tremolite, muscovite and quartz. Crosscutting mafic dykes are usually low-grade amphibolites with actinolitic hornblende-chlorite-albite-epidote-sericite-quartz ± biotite. In most lithologies, however, there is evidence that the stable assemblage is that of retrograde metamorphism. Biotite is often partially replaced by chlorite in the metasiltstones, relict diopside rimmed by tremolite is common in the calc-silicates/and sericite pseudomorphs of helicitic andalusites occur in some of the phyllites. Wardle (1978) has shown that some of the andalusites and calc-silicate assemblages define thermal aureoles around granitic plutons of the Golden Grove suite. However, many of the higher grade minerals are not spatially related to plutons and may be relicts of an earlier regional metamorphism. Exceptionally steep geothermal gradients, compatible with hot, gneissic diapirism (Currie et al., 1981), are associated with the central plutonic core where sillimanite-bearing assemblages are locally developed in the adjacent Green Head Group.

Structural Geometry

At least three phases of deformation affect all lithologies of the Green Head Group and, on the basis of style, orientation and overprinting, have been placed in the sequential order D_1 to D_3. However, the clastics and carbonates frequently contrast in their response to D_1 deformation, the former behaving in a brittle fashion while being more or less passively carried along in the plastic

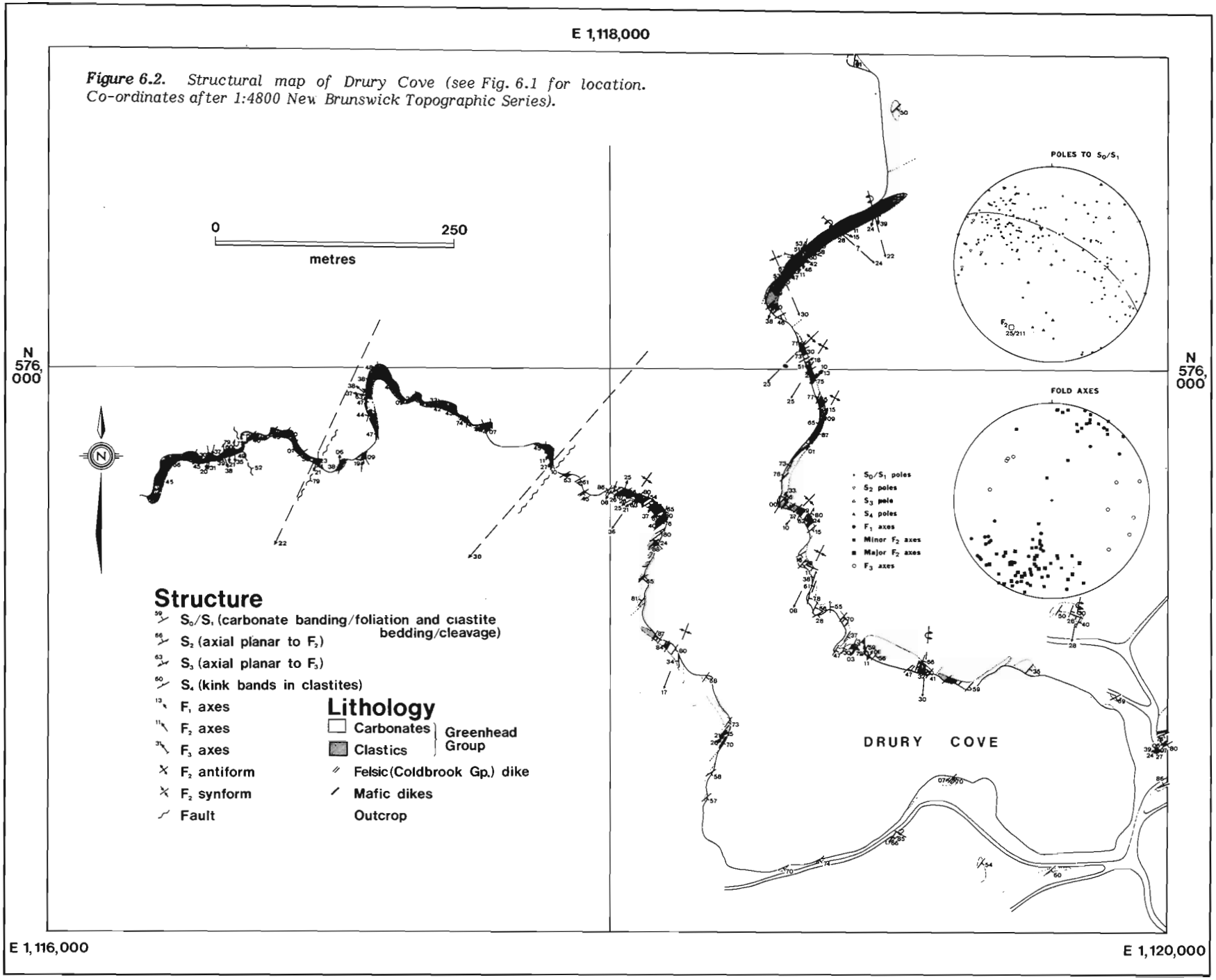

Figure 6.2. *Structural map of Drury Cove (see Fig. 6.1 for location. Co-ordinates after 1:4800 New Brunswick Topographic Series).*

medium of the latter. Furthermore, ductile flow in the carbonates is likely to have occurred on several occasions such that the earliest recognizable deformational fabric may have earlier, coplanar components.

D_1 Structures

The earliest, clearly deformational structures include a marble foliation, or cleavage in the clastics, (S_1) and associated minor folds (F_1).

S_1 is best developed in the marbles where it is defined by a strong, dimensional preferred orientation of coarse calcite grains which commonly parallels the colour-banding. A similar but less well-developed fabric is present in the dolomites. S_1 in the clastic lithologies is a generally weak, bedding (S_0)-parallel fabric defined by a fine grained sericite-chlorite cleavage in the metasiltstones and a stronger phyllitic, muscovite-chlorite cleavage in the more pelitic units. At slightly higher metamorphic grades such as those that exist along the Kenebecasis Bay north of Drury Cove (Fig. 6.2), S_1 is a strong, muscovite-biotite schistosity. In most cases, however, a sharp contrast in the strength of the S_1 fabric occurs across clastic/carbonate boundaries suggesting that much of the D_1 strain was accommodated by heterogeneous ductile flow in the marbles. This is well displayed on the west side of Drury Cove where almost undeformed and widely separated metasiltstone boudins are enveloped by a strong calcite fabric to form prominent 'augen' up to 0.5 m across.

The S_1 fabric is axial planar to a set of rare, tight to isoclinal minor folds (F_1) with similar-style profiles and strongly attenuated limbs. These are most apparent in laminated calc-silicate horizons where they take the form of single, boudinaged isoclinal closures, irregular contortions (Fig. 6.5b) or centimetre-scale, asymmetric structures with consistent senses of rotation. Cleavage is rarely visible in the calc-silicate laminations but in the larger F_1 folds in marble, discordances between calcite fabric and colour-banding may be visible in the fold closures. This, however, is more likely to reflect an earlier period of carbonate ductile flow rather than implying a primary (S_0) origin for the colour bands. The existence of a pre-D_1 deformational event is supported by the helicitic textures of retrogressed andalusites in phyllite that are pretectonic with respect to S_1. F_1 axes generally plunge northeast or southwest at gentle to steep angles (Fig. 6.2, 6.3) but may be locally scattered towards the north and west by megascopic F_3 folding (Fig. 6.4). F_1 folds are notably absent in the clastics and megascopic structures of this generation have not been observed.

D_2 Structures

A second deformation produced numerous folds (F_2) but was only locally a fabric forming event. Mesoscopic F_2 folds are close to tight, upright asymmetric structures and deform both S_1 and S_0. They are most abundant in the clastics where they form flexural slip structures of parallel profile which typically lack an axial fabric (S_2). Nevertheless, intense fracturing parallel to the axial plane is characteristic of the steeper limbs and closures of F_2 folds at Drury Cove while F_2 folded metasiltstone laminae at Howes Lake show weak, S_2 fracture cleavage fans. In the higher grade schists north of Drury Cove (Fig. 6.2) locally intense F_2 crenulation of the S_1 muscovite-biotite fabric has produced a prominent crenulation lineation (L_2) and an incipient S_2 crenulation cleavage. The cleavage dips east at 60-70°. Less common F_2 folds in the carbonates may be parallel or similar and occasionally show a strong, axial planar S_2 calcite fabric which locally overprints S_1 in the hinge zones. F_2 axes are curvilinear and plunge northeast and southwest at gentle to moderate angles (Fig. 6.2, 6.3). Reorientation of plunge towards the south and west at Howes Lake (Fig. 6.4) reflects megascopic F_3 folding. F_2 is thus broadly coaxial with F_1 such that mesoscopic interference patterns produce Type III refolded isoclines (Ramsay, 1967) where the two phases are non-coplanar.

On a regional scale large structures of this generation can be inferred from variations in the attitudes of S_1 and S_0 coupled with systematic changes in mesoscopic F_2 asymmetry. The megascopic F_2 folds are essentially upright, close structures which plunge at a moderate angle southwest and have axial traces in excess of 0.5 km. West of Drury Cove the regional orientation of S_1/S_0 is controlled by two megascopic F_2 folds (Fig. 6.2). Like the minor folds, these structures are associated with intense fracturing and faulting parallel to the steeply east-dipping axial planes which virtually destroy the S_1/S_0 fabric at the fold closures. A series of en-echelon F_2 folds of 100 m wavelength and variable amplitude control the regional orientation of S_1 west of Snowflake Quarry (Fig. 6.3).

D_3 Structures

The prominent L_2 crenulations north of Drury Cove are locally refolded about mesoscopic folds (F_3) that plunge east-southeast (Fig. 6.2). These upright, close to tight folds are parallel structures and preserve the angular relationship of L_2 to F_3 consistent with a flexural slip mechanism. They show no axial fabric. Moderately west-northwest plunging folds of similar appearance occur northwest of Drury Cove (Fig. 6.2) and are considered to be F_3 as their asymmetry is inconsistent with their position within the megascopic F_2 structure. These F_3 folds, however, are associated with an axial fracture cleavage (S_3) that dips steeply southwest. F_3 minor folds can also be recognized at Howes Lake where their symmetry varies systematically about the megascopic F_3 structure discussed below. Elsewhere mesoscopic F_3 folds are not readily distinguishable from those of F_2. West of Snowflake Quarry, for example, F_1 isoclines are refolded about east- and west-plunging axes believed to be F_3 (Fig. 6.3). The younger folds give rise to a second, axial planar calcite fabric (S_3) that dips south at 60°.

The structure of the Howes Lake area is dominated by a megascopic F_3 fold with a near vertical axis and an axial plane that strikes 110°. This major reclined structure lacks an axial fabric but reorients mesoscopic, F_2 S-folds such that they plunge south on the southern limb and west on the northern limb (Fig. 6.4). Associated F_3 minor folds plunge steeply southwest and northeast.

Interference of F_2 and F_3 has not been observed on either a mesoscopic or megascopic scale. However, the basinal structures of the Pokiok area southwest of Snowflake Quarry and the reported curvilinear nature of the megascopic F_2 folds (Wardle, 1978) may reflect superimposed F_3 folding.

Post-D_3 Structures

Late structures include occasional kink bands in the phyllites and widespread fractures with calcitic and chloritic slickensides. Kink band sets dip north and northeast at Drury Cove and southwest and southeast at Snowflake Quarry. Both structural features probably reflect local fault movement.

Timing of Deformation

Although the absolute ages of D_1, D_2 and D_3 are uncertain, they are most reasonably attributed to Paleozoic events. The earliest recognizable deformation (D_1) was a strongly inhomogeneous fabric forming event that produced a gneissic, ductile flow foliation with minor folds in the carbonates but only weak cleavage development and

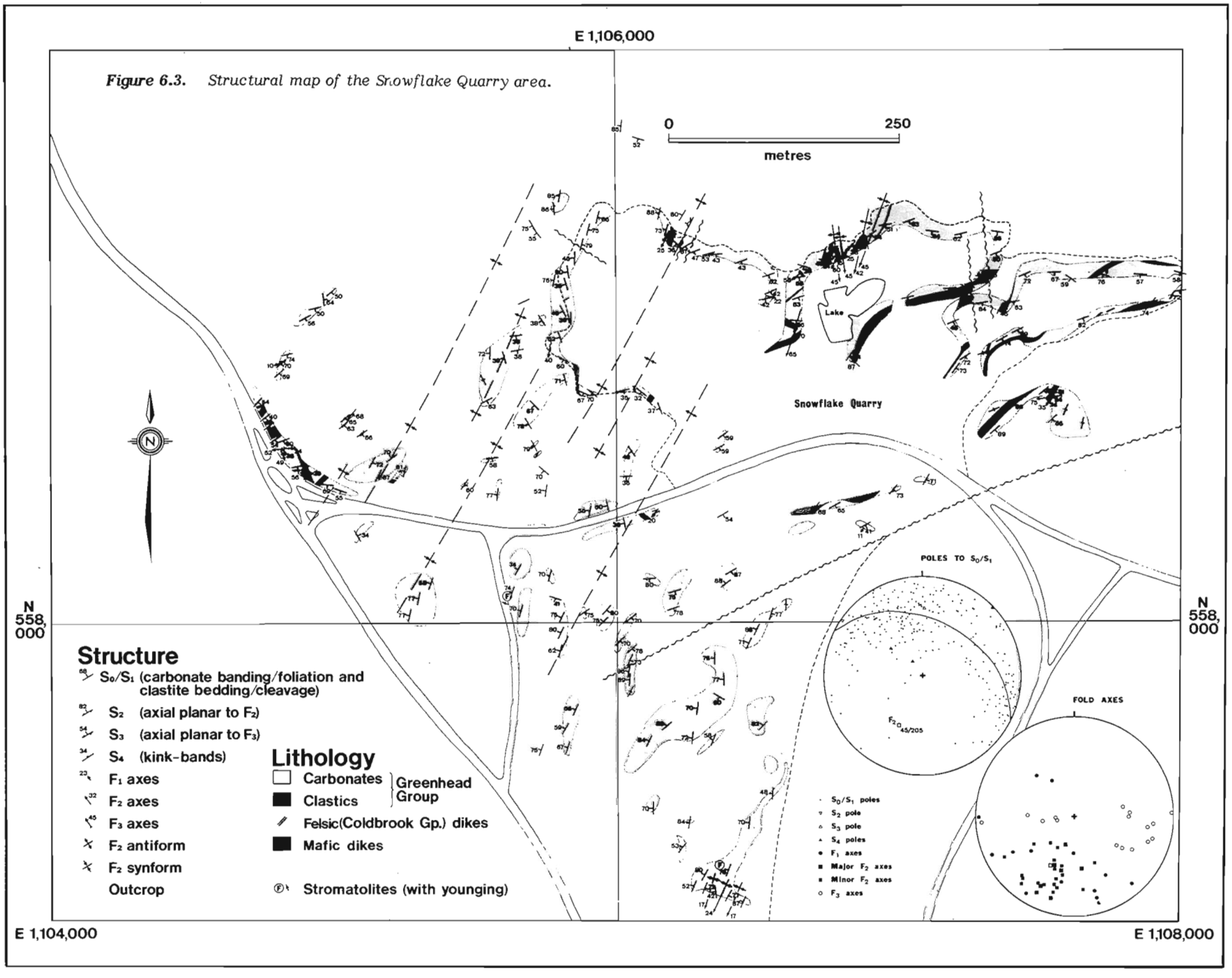

Figure 6.3. *Structural map of the Snowflake Quarry area.*

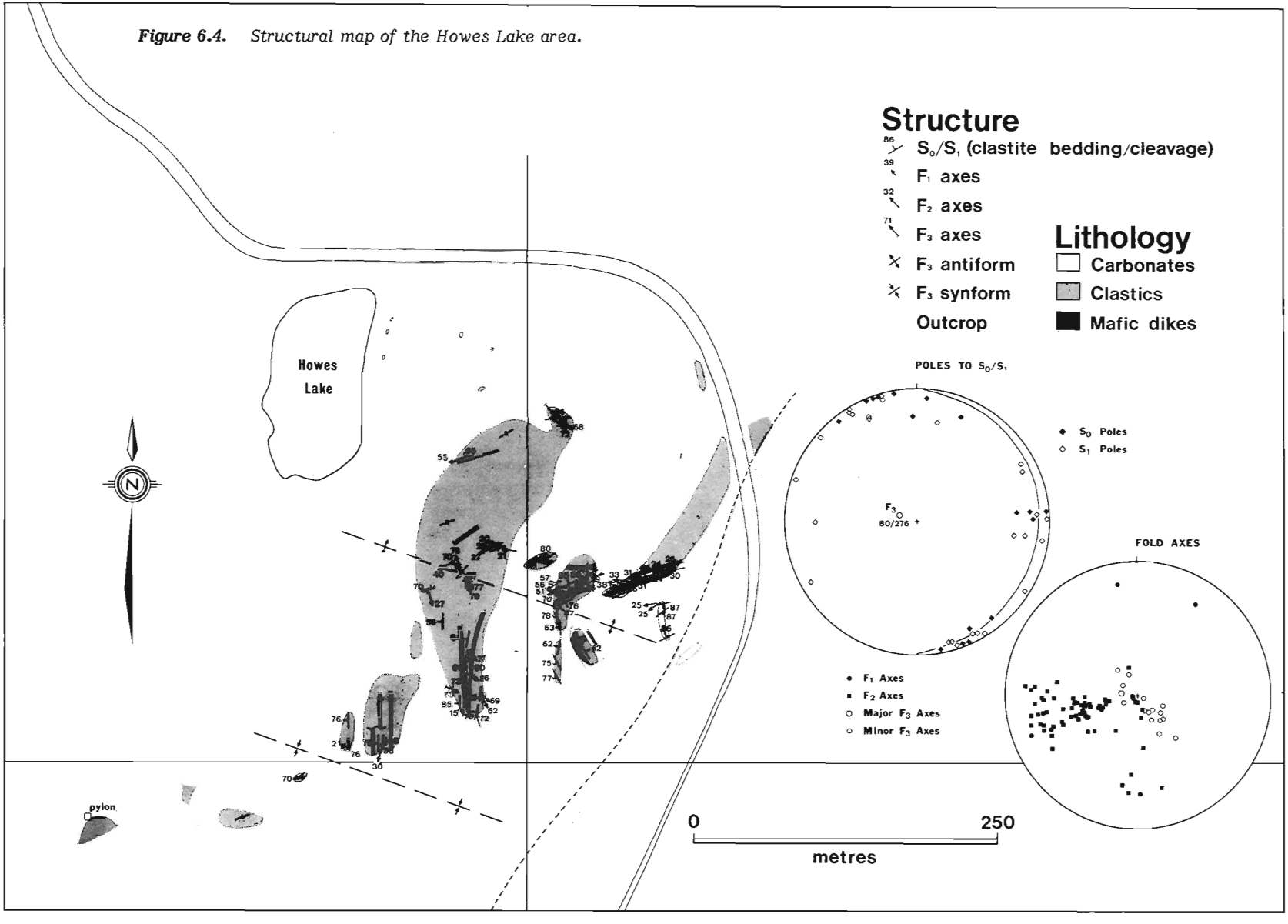

Figure 6.4. Structural map of the Howes Lake area.

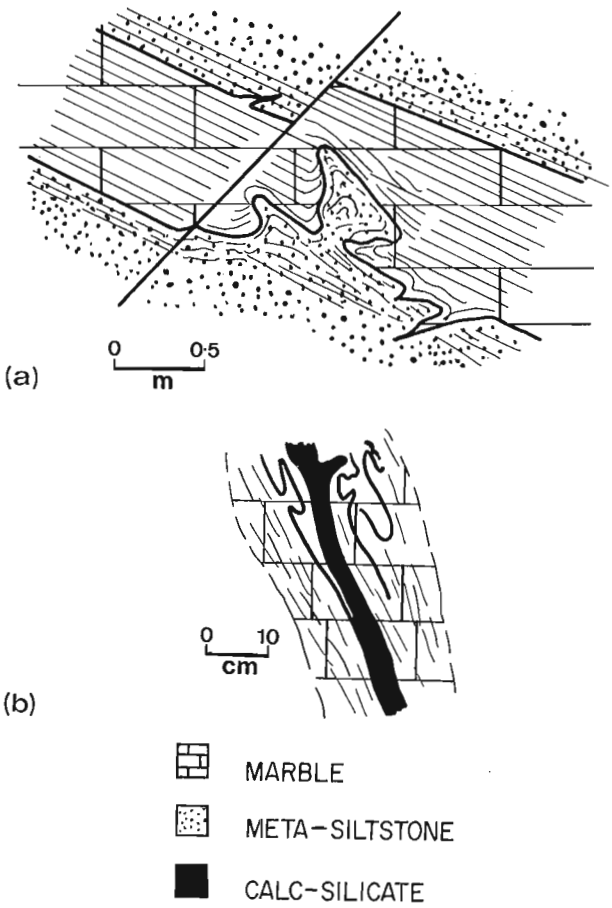

Figure 6.5. *Field sketches of clastic-carbonate contact relationships. (a) Flowed marble/metasiltstone contact, west shore Drury Cove. (b) Contorted and boudinaged calc-silicate laminae, east shore Drury Cove. (Dashed lines parallel S_1).*

boudinage in the clastics. Required temperatures were presumably supplied by partial melting within the central plutonic core as the metamorphic grade of the Green Head Group increases towards the Brookville Gneiss. However, partial melting within the core is thought to have occurred on several occasions (Currie et al., 1981) such that S_1 may be a composite fabric that largely obliterated earlier structures during the last episode of extensive flow. Late Ordovician (470 Ma; Olszewski et al., 1980) pegmatitic sweats in the Brookville Gneiss suggest that the youngest phase of widespread partial melting coincided with the Taconic orogeny. Nevertheless, the scattered occurrence of pretectonic, helicitic andalusite pseudomorphs, some of which appear to be contact metamorphic minerals (Wardle, 1978) around Hadrynian (800-850 Ma; Olszewski et al., 1980) Golden Grove plutons, suggests that the S_1 fabric may have components as old as the Grenvillian. The D_2 and D_3 events, on the other hand, are characterized by lower temperature flexural slip folding and clearly postdate the final period of ductile flow. They are probably late Taconic or Acadian structures and may have accompanied a retrogressive event that partially reset Green Head Group zircon ages at around 350 Ma (Olszewski et al., 1980).

Support for the Paleozoic age of D_1 to D_3 can also be derived from the Saint John Group which, south of the Green Head Group, occupies the core of a major syncline. The axial planar cleavage of this Saint John Syncline is a muscovite-chlorite fabric that broadly parallels S_1 in the Green Head Group. It is not associated with minor structures but is refolded by northeast and southwest plunging folds which are themselves refolded about gently west plunging folds in the Kenebecasis area (Wardle, 1978). This structural sequence is closely analogous to that of the Green Head Group and in the Saint John Group must be entirely post-Arenig.

References

Alcock, F.J.
1938: Geology of the Saint John region, New Brunswick; Geological Survey of Canada, Memoir 216, 65 p.

Cormier, R.F.
1969: Radiometric dating of the Coldbrook Group of southern New Brunswick, Canada; Canadian Journal of Earth Sciences, v. 6, p. 393-398.

Currie, K.L., Nance, R.D., Pajari, G.E., Jr., and Pickerill, R.K.
1981: Some aspects of the pre-Carboniferous geology of Saint John, New Brunswick; in Current Research, Part A, Geological Survey of Canada, Paper 81-1A, p. 23-30.

Hayes, A.O. and Howell, G.G.
1937: Geology of Saint John, New Brunswick; Geological Society of America, Special Paper 5, 146 p.

Hofmann, H.J.
1974: The stromatolite Archaeozoon acadiense from the Proterozoic Greenhead Group of Saint John, New Brunswick; Canadian Journal of Earth Sciences, v. 11, p. 1098-1115.

Leavitt, E.M. and Hamilton, J.B.
1962: Geology of Saint John area; New Brunswick Department of Natural Resources, Mineral Resource Bureau Maps 62-4A and 62-4B.

Olszewski, W.J., Gaudette, H.E., and Poole, W.H.
1980: Rb-Sr whole rock and U-Pb zircon ages from the Green Head Group, New Brunswick; Geological Society of America, Abstracts with Program, v. 12, no. 2, p. 76.

Ramsay, J.G.
1967: Folding and Fracturing of Rocks; McGraw-Hill, New York, 568 p.

Rast, N. and Grant, R.
1973: Transatlantic correlation of the Variscan-Appalachian orogeny; American Journal of Science, v. 273, p. 572-579.

Rast, N., O'Brien, B.H., and Wardle, R.J.
1976: Relationship between Precambrian and Lower Paleozoic rocks of the 'Avalon Platform' in New Brunswick, the northeast Appalachians and the British Isles; Tectonophysics, v. 30, p. 315-338.

Wardle, R.J.
1978: The stratigraphy and tectonics of the Greenhead Group: Its relationship to Hadrynian and Paleozoic rocks, southern New Brunswick; Ph.D. thesis, University of New Brunswick, Fredricton, New Brunswick.

Williams, H., Kennedy, M.J., and Neale, E.R.W.
1972: The Appalachian structural province; in Variations in Tectonic Styles in Canada, R.A. Price and R.J.W. Douglas, ed., Geological Association of Canada, Special Paper 11, p. 181-261.

7.

PRELIMINARY RESULTS ON THE STRATIGRAPHY, STRUCTURE, AND METAMORPHISM OF CENTRAL KOOTENAY ARC ROCKS, SOUTHEASTERN BRITISH COLUMBIA

Project 790030

Alain D. Leclair[1]
Cordilleran Geology Division

Leclair, Alain D., Preliminary results on the stratigraphy, structure, and metamorphism of central Kootenay Arc rocks, southeastern British Columbia; in Current Research, Part A, Geological Survey of Canada, Paper 82-1A, p. 45-49, 1982.

Abstract

West of Kootenay Lake stratigraphic units of the upper Purcell Supergroup, the Windermere Supergroup and the Lower Cambrian are exposed in a moderate to steep westerly facing homocline. To the north, the upper part of the stratigraphic succession is truncated by a thrust (?) fault which juxtaposes a sequence of undivided Paleozoic rocks against the Monk Formation. An eastward increase in metamorphic grade from greenschist to amphibolite facies is defined by the regional metamorphic zones of biotite, garnet, staurolite, kyanite and sillimanite. Field mapping in the study area has revealed evidence of a major fault along Kootenay Lake, involving the apparent right-lateral displacement of the upper Purcell sequence and the Windermere Supergroup.

Introduction

This study has been undertaken as part of a 1:250 000 scale mapping program in Nelson (82 F, east half) map area (Project 790030, J.E. Reesor) to examine in detail complex stratigraphic, structural, and metamorphic problems west of Kootenay Lake. Detailed field investigations in the west central section of the map area revealed the presence of part of the Purcell Supergroup, the complete Windermere Supergroup and some of the Lower Paleozoic stratigraphic succession. The preliminary results of 2 months of geological mapping, at a scale of 1:25 000, in the western half of the Boswell map area (Fig. 7.1) are presented in Figure 7.2.

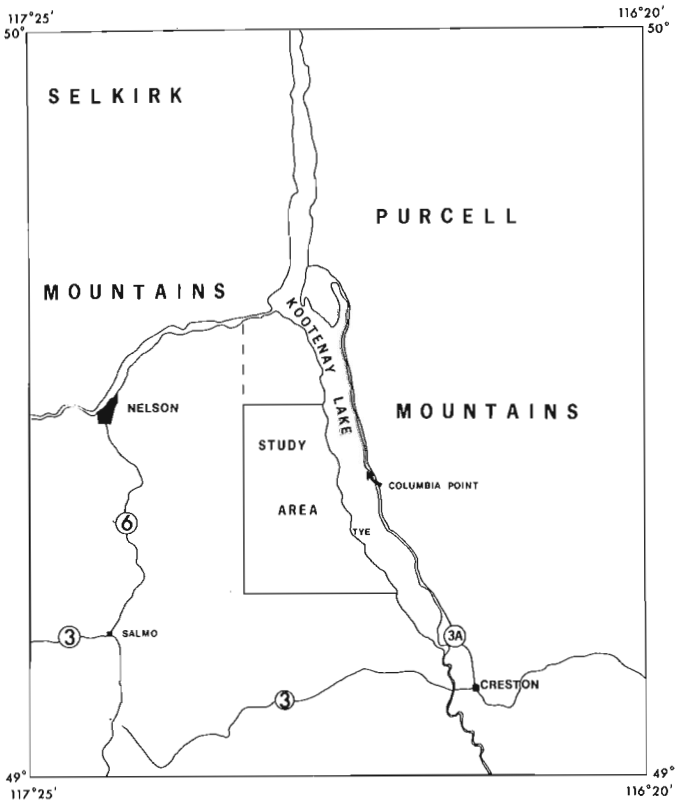

Figure 7.1. *Location map.*

The Windermere Supergroup, which comprises the Toby Formation, the Irene Formation, the Monk Formation and the Three Sisters Formation, forms a north trending belt of variable width extending across the study area. To the east, it unconformably overlies upper strata of the Purcell Supergroup and grades into Lower Cambrian Quartzite Range Formation to the west. An assemblage of "undivided Paleozoic rocks" (Little, 1960) is in contact with the Monk Formation, in the northern part of the area, where the Three Sisters and Quartzite Range formations are absent. In the eastern and southern part of the map area, rocks of the upper Purcell and Windermere supergroups are intruded by the Bayonne Batholith and the Wall Stock of Cretaceous and Jurassic age, respectively (Archibald et al., 1977).

Stratigraphy

Upper Purcell Supergroup

In the eastern half of the study area, a sequence of upper Purcell rocks, possibly correlative with the Dutch Creek Formation, is intruded by the Bayonne Batholith and unconformably overlain by the Toby Formation. The sequence consists mainly of a thick monotonous section of interbedded light grey to grey psammite and dark semipelite with minor pelitic schists and a discontinuous upper unit of white quartz-muscovite schist and white quartzite with several orange to buff dolomite bands. The lower section is characterized by beds of 1 to 20 cm thick.

Windermere Supergroup

The Toby Formation is an easily recognized conglomeratic unit lying with angular unconformity on the upper part of the Purcell sequence. It consists of polymict conglomerate with a micaceous or sandy matrix. Pebbles, cobbles and boulders in the conglomerate are mainly quartzite and dolomite and locally greenstone. The similarity of these clasts to rocks of the underlying Purcell sequence suggests that most of the coarse detritus in the Toby Formation was eroded from the upper part of the Purcell Supergroup (Glover and Price, 1976). The majority of the clasts of the Toby Formation are characteristically oblate ellipsoids flattened in the plane of the foliation but, in areas of intense deformation, dolomite clasts are hardly recognizable.

The Irene Volcanic Formation consists of fine grained, dark bluish green mafic tuff and massive to schistose greenstone with minor intercalations of light grey phyllite. Hornblende porphyroblasts, up to 5 cm long, and minor

[1] Department of Geological Sciences, Queen's University, Kingston, Ontario

Figure 7.2

Geological map of the western half of the Boswell map area.

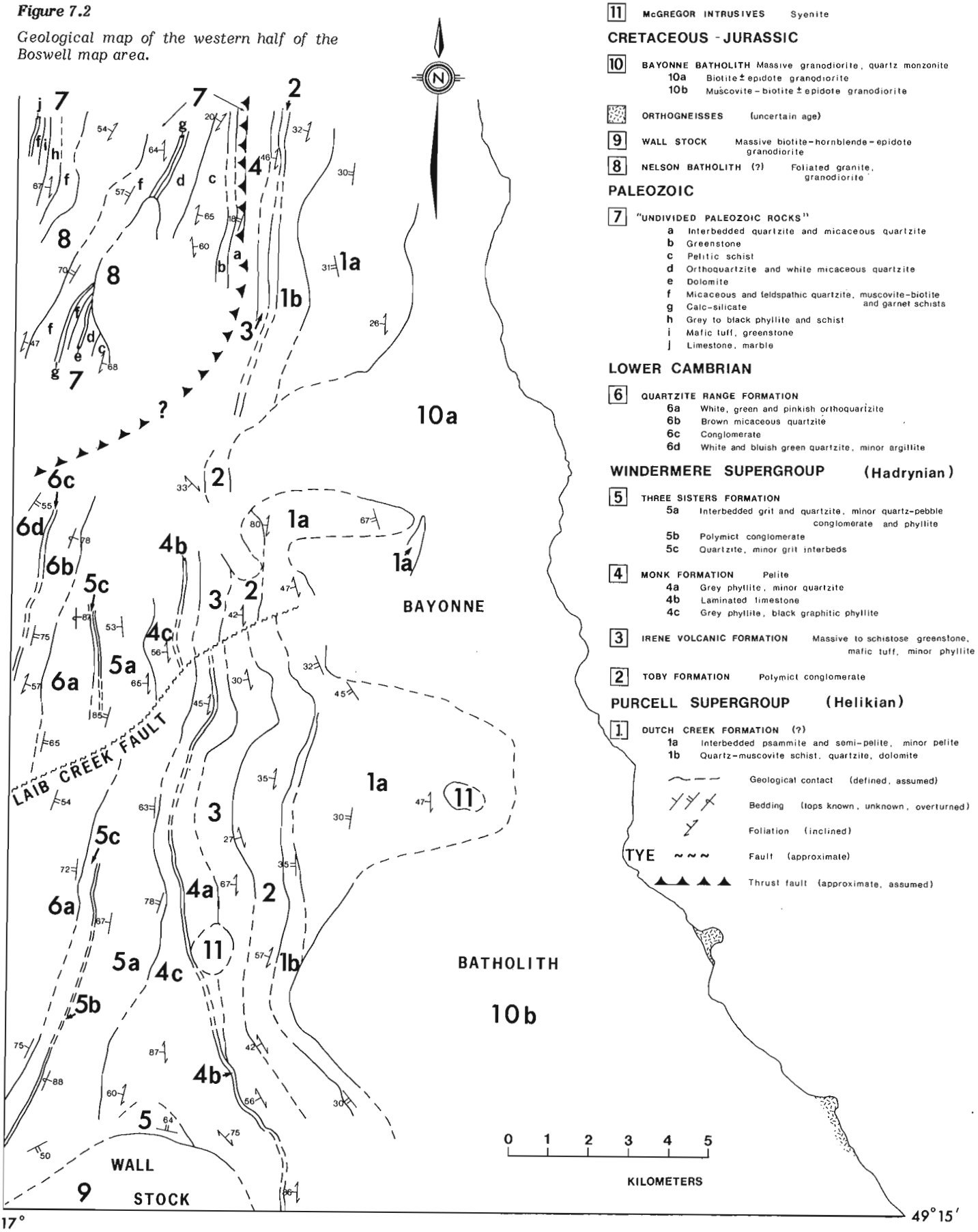

amounts of pyrite are present throughout the section. The base of the volcanic pile is intercalated with rocks of the Toby Formation, suggesting that the final stages of deposition of conglomerate and the initiation of volcanism are overlapping events. A discontinuous and thin buff-coloured-dolomite horizon is present locally near the upper part of the formation. The underlying Toby Formation and the Purcell sequence contain numerous amphibolite sills and dykes which could represent feeders to the volcanic pile of the Irene Volcanic Formation (Glover and Price, 1976).

The Monk Formation was divided into three main units. A lower sequence of very fine grained phyllite of various shades of grey, with minor grey to black quartzite beds, 10 to 25 cm thick, overlies conformably the Irene Volcanic Formation in the central part of the area. Above this is a grey to dark grey laminated limestone unit which forms a diagnostic marker horizon approximately 25 to 60 metres thick. The upper part of the Monk Formation consists of bluish to greenish grey phyllite and black graphitic phyllite with sporadic beds of grit. Towards the south, the lower unit disappeared as a result of westerly directed thrusting of the Irene Volcanic Formation over the Monk Formation, and the upper unit is considerably thickened due to folding. A rusty weathering quartz-muscovite-biotite schist with some quartzite interbeds represents the higher metamorphic grade equivalent of the Monk Formation in the northern part of the map area.

The Three Sisters Formation consists predominantly of grits interbedded with light grey crossbedded quartzite (Fig. 7.3A) and minor quartz-pebble conglomerates. The grits form thick, green to grey, massive beds composed of blue quartz and white feldspar fragments in a siliceous matrix. The base of the formation is intercalated with green and black phyllite and contains, at one locality just south of the Laib Creek fault, a narrow band of intraformational conglomerate composed of pebbles and cobbles of grey phyllite and quartzite. Near the top of the formation a distinctive unit, approximately 15 m thick, of polymict conglomerate is composed of deformed clasts of grit, quartzite, shale and greenstone (Fig. 7.3B). The upper unit of the Three Sisters Formation contains a relatively higher proportion of green to light grey quartzite than grit.

Lower Cambrian

Based on fossil occurrences near the top of the Quartzite Range Formation, Little (1960, 1965) placed the Precambrian-Cambrian boundary at the contact between the base of this formation and the Three Sisters Formation. In the study area this contact coincides with the disappearance of grits and the first appearance of orthoquartzites.

That part of the Quartzite Range Formation exposed near the western edge of the map area has been tentatively subdivided into four units. The basal unit consists of massive to well bedded white, green and pink orthoquartzites with abundant crossbedding and some ripple marks. Beds vary in thickness between 5 cm and 1 m and their surfaces typically weather a rusty colour. This unit grades into a grey to light brown micaceous quartzite which is capped by a band of micaceous conglomerate containing clasts of green and white quartzite. White and bluish green quartzite with minor argillite represent the highest unit of the Quartzite Range Formation exposed in the map area.

Undivided Paleozoic

In the northwest part of the map area an assemblage of rocks that differs greatly lithologically and structurally from the Quartzite Range Formation and the Three Sisters Formation overlies the Monk Formation. The assemblage appears to be the extension of a unit mapped by Little (1960, 1964) and Fyles and Hewlett (1959) as "undivided Paleozoic rocks" in the adjacent Nelson (west half) map area. Little is known at this stage about the age of these rocks and their possible stratigraphic counterparts. However, a consistent internal lithological sequence, which is outlined in the adjoining sketch map, was mapped by the writer.

The sequence contains thinly interbedded grey to light grey quartzite and micaceous quartzite, feldspathic quartzite, thinly bedded orthoquartzite, pelitic and semi-pelitic schists, greenstone, mafic tuff, amphibolite and bands of calc-silicate, orange to buff dolomite and limestone. These rocks are intruded by weakly to strongly foliated granitic plutons which generally differ in texture and composition from the Bayonne Batholith.

Bayonne Batholith

Intrusive rocks of the Bayonne Batholith, which cover a large portion of the study area along Kootenay Lake, consist of massive, medium- to coarse-grained granodiorite and quartz monzonite. They contain biotite and locally epidote. In the southern exposures of the batholith, muscovite-biotite granodiorite is the dominant rock type. Numerous pegmatite dykes, some of which contain pink garnet, occur throughout the batholith and in adjacent country rocks. They are especially abundant near Tye where large inclusions of migmatite are also present.

Two thin bands of granitic orthogneiss (Fig. 7.3C) are exposed along the lakeshore south of Tye. These gneisses are very similar in composition to rocks of the Bayonne Batholith and presumably represent a deeper structural level of the batholith.

Wall Stock

In the southwest corner of the area the north end of the Wall Stock, which truncates the upper part of the Windermere stratigraphic succession, is composed of a uniform, massive, medium grained granodiorite. Unlike the Bayonne Batholith, it contains hornblende as well as biotite and epidote.

McGregor Intrusives

The McGregor intrusives, first described by Rice (1941), are massive, fine- to coarse-grained syenite and porphyritic syenite plutons. Two of these small isolated plutons occur in the map area; one is emplaced in the upper Purcell sequence and the other truncates the contact between the Irene Volcanic Formation and the Monk Formation.

Metamorphism

The regional metamorphic grade increases from greenschist to amphibolite facies roughly from west to east across the map area. It is better defined in the northern part of the area where pelitic and calc-silicate units are common. A series of regional metamorphic zones characterized by biotite, garnet, staurolite, kyanite and sillimanite approximately parallel the dominant structural trend. Kyanite and garnet porphyroblasts up to 5 cm long and 2 cm across, respectively, are common (Fig. 7.3D, E).

In the southwest corner of the map area, the emplacement of the Wall Stock in pelites of the Monk Formation has produced a narrow contact aureole.

Structure

The study area is structurally located within that central part of the Kootenay Arc where the dominant trend, as outlined by stratigraphic units, is roughly north-northeast.


A

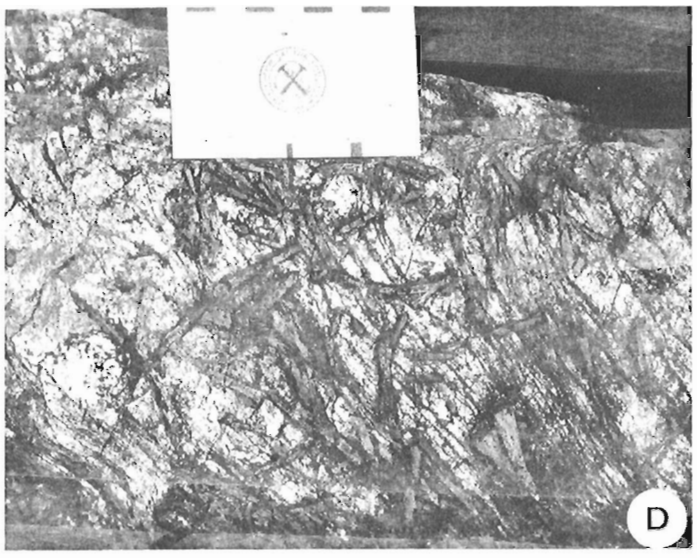
D


B

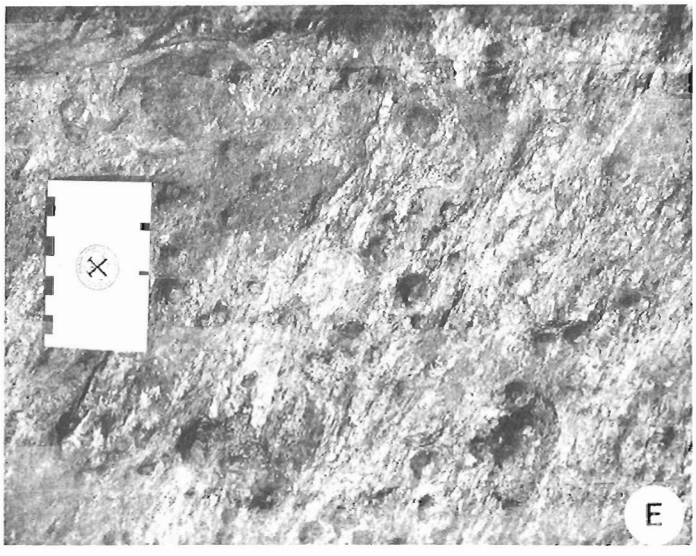
E

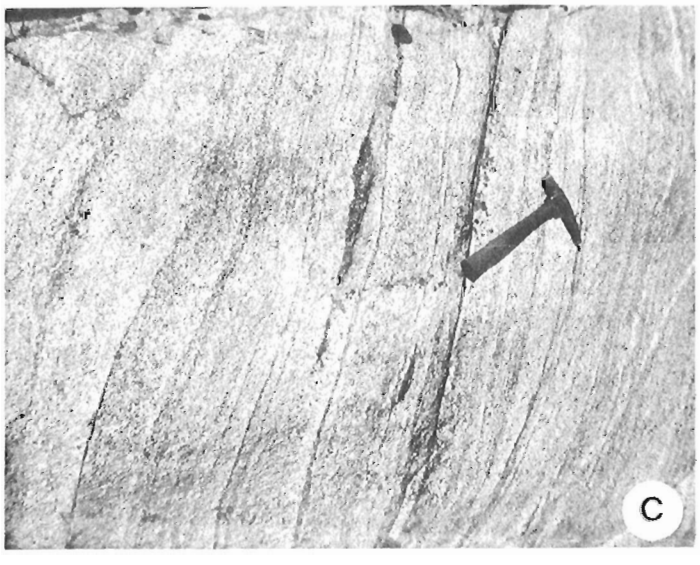
C


F

Figure 7.3

A. Interbedded grits and quartzite of the Three Sisters Formation. Grits are com osed of bluish quartz and whitish feldspar fragments. GSC 202942-N
B. Polymict conglomerate near the top of the Three Sisters Formation. GSC 202942-O
C. Gneissic layering in two-mica granite, on the shore of Kootenay Lake, south of Tye. GSC 202942-J
D. Kyanite porphyroblasts in a thin micaceous band of the Quartzite Range Formation. GSC 202942-L
E. Garnet and staurolite porphyroblasts in a pelitic schist unit of the undivided Paleozoic sequence. GSC 202942-K
F. West-dipping isoclinal folds in thinly interbedded psammite and semipelite of the upper Purcell Supergroup. GSC 202942-M

The main structural element of the area is a well developed penetrative foliation which is more or less coplanar with bedding. Its development is accompanied by the flattening of clasts of the various conglomerate units and appears to be associated with a set of west dipping tight to isoclinal mesoscopic folds with subhorizontal axes (Fig. 7.3F). A local crenulation cleavage superimposed on the foliation is parallel to the axial planes of many gentle minor folds.

The stratigraphic succession comprising the upper Purcell, the Windermere Supergroup and the Lower Cambrian forms a moderate to steep westerly facing homocline which at high structural levels becomes progressively overturned to the west. Primary sedimentary structures as well as bedding-cleavage relationships in the Three Sisters and Quartzite Range formations indicate that the stratigraphic sequence is inverted near the western edge of the map area. To the north, the upper part of the Windermere Supergroup and the Lower Cambrian are apparently truncated by a thrust (?) fault juxtaposing the sequence of undivided Paleozoic rocks against the Monk Formation.

The Purcell Trench, which is a prominent north-south lineament about 650 km long, extending from Pend d'Oreille in Idaho to the Rocky Mountain Trench, parallels the east edge of the study area along Kootenay Lake. Since the reconnaissance mapping by Rice (1941) in Nelson East Half map area, the stratigraphic units of the area have been considered continuous across the segment of the trench occupied by the lake. The results of this study suggest that at least this part of the trench corresponds to a major fault which offsets the upper Purcell sequence and the lower Windermere Supergroup. The best evidence for this fault is the apparent right-lateral displacement of the Toby Formation which outcrops at Columbia Point on the east shore of Kootenay Lake (compare Fig. 7.1 and 7.2).

Acknowledgments

The helpful advice of J.E. Reesor of the Geological Survey of Canada and the enthusiastic assistance in the field of Joerg Beekmann, Tony Fogarassy and Lyndon Hanson of the University of British Columbia is greatly appreciated. R.B. Campbell, H. Helmstaedt and J.E. Reesor revised the report and suggested improvements.

References

Archibald, D., Glover, J.K., and Farrar, E.
1977: K-Ar ages from the Bayonne Batholith and some nearby plutons, southeastern British Columbia, and their geological implications; Geological Association of Canada, Program with Abstracts, v. 2, p. 5.

Fyles, J.T. and Hewlett, C.G.
1959: Stratigraphy and structure of the Salmo lead-zinc area; British Columbia Department of Mines, Bulletin 41, 162 p.

Glover, J.K. and Price, R.A.
1976: Stratigraphy and structure of the Windermere Supergroup, southern Kootenay Arc, British Columbia; in Report of Activities, Part B, Geological Survey of Canada, Paper 76-1B, p. 21-23.

Little, H.W.
1960: Nelson map area, west half, British Columbia; Geological Survey of Canada, Memoir 308, 205 p.

1964: Geology of Ymir, British Columbia; Geological Survey of Canada Map 1144A.

1965: Geology of Salmo, British Columbia; Geological Survey of Canada Map 1145A.

Rice, H.M.A.
1941: Nelson map area, east half, British Columbia; Geological Survey of Canada, Memoir 228, 86 p.

8.

AN INTERACTIVE PROGRAM FOR ESTIMATING THE PARAMETERS OF MAGNETIC ANOMALY SOURCES

Project 780023

D.J. Teskey
Resource Geophysics and Geochemistry Division

Teskey, D.J., An interactive program for estimating the parameters of magnetic anomaly sources; in Current Research, Part A, Geological Survey of Canada, Paper 82-1A, p. 51-53, 1982.

Abstract

An interactive computer program for estimating the best-fit solution of the magnetization and geometric parameters of causative magnetic bodies using a Tektronix compatible terminal is now available. The required input parameters and options are requested sequentially during operation so that little advance experience or familiarity is required. An example of the use of the qualitative interpretation technique is presented utilizing an aeromagnetic profile across the Lomonosov Ridge.

Introduction

A number of quantitative interpretation computer programs for performing fits of magnetic anomalies are available (McGrath and Hood, 1973; Wells, 1979). However the first of these was developed primarily for batch use and the second is valid only for bodies of great strike extent (approximately four times the depth of burial) and does not include automated convergence procedures. Therefore a totally interactive program for use with a Tektronix type interactive terminal connected to a computer with adequate storage (70 K octal) capability and which could be used by geoscientists with little background in computing was developed. The particular features of this program are:

1. A 'best-fit' value of magnetization is calculated automatically for each source configuration.
2. Source geometries which have arbitrarily complex cross-sections can be represented.
3. A generating function is used which is applicable across the central profile of bodies which have finite strike extent, but are symmetrical through a vertical plane containing the profile. This model can also be used as a first approximation in cases where this symmetry is not present.
4. The position of points, outlining the cross-section of the causative bodies can be modified directly, or a nonlinear routine can be used to translate or rotate groups of points.

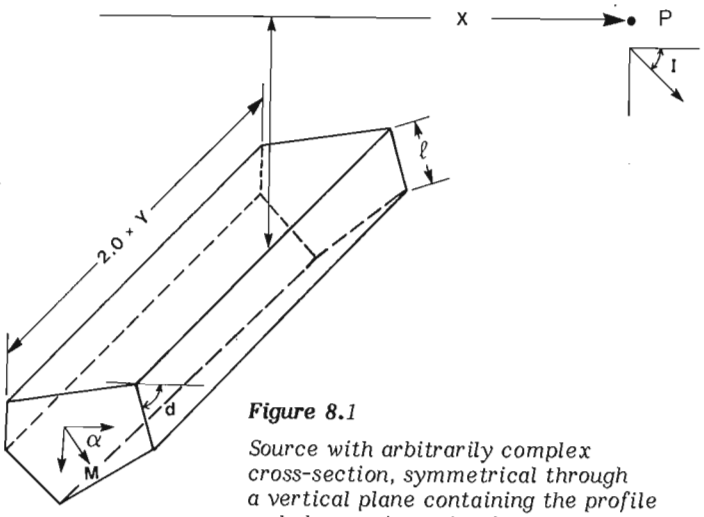

Figure 8.1

Source with arbitrarily complex cross-section, symmetrical through a vertical plane containing the profile and observation point P. The magnetic field is calculated as that due to the sum of the individual surfaces.

Generating Function

The formula for the vertical component of the total magnetic field ΔT at a point above the central profile across a 'pole sheet' at arbitrary dip (d) is given by:

$$\Delta T = M\left[\frac{1}{2}\sin d\left(\ell n\,\frac{A - Y}{A + Y} - \ell n\,\frac{B - Y}{B + Y}\right) + \cos d\left(\tan^{-1}\frac{Y(\ell + h\sin d - x\cos d)}{A(x\sin d + h\cos d)} - \tan^{-1}\frac{Y(h\sin d - x\cos d)}{B(x\sin d + h\cos d)}\right)\right] \quad (1)$$

where $A = \sqrt{(x - \ell\cos d)^2 + (h + \ell\sin d)^2 + Y^2}$

$B = \sqrt{x^2 + h^2 + Y^2}$

$Y =$ 0.5 x strike extent

$M =$ pole strength (normal component of magnetization) (modified from Grant and West, 1965, p. 273-274)

The total field at any inclination can be calculated as only the relative angle (I - d) is important (Fig. 8.1). The field due to a source which is assumed to be symmetrical across a plane which contains the profile, can be calculated as the sum of that due to pole-sheets forming the surface of the source and with the pole strength on a given sheet proportional to the normal component of the magnetization vector to that sheet.

More than one body can be represented and a given sheet may form part of the boundary of a number of sources. Since the anomaly due to a given body is proportional to the magnetization strength of that body, the 'best fit' magnetization strength can be easily calculated and is done each time the anomaly is generated. An additive constant representing the earth's field and that due to deeper sources is also calculated automatically.

Interactive Fitting Program

A flow chart for the interactive fitting program is shown in Figure 8.2. Prior to running the program, the data points must be stored on a file, as the number of data points, followed by the values. The program starts by reading the

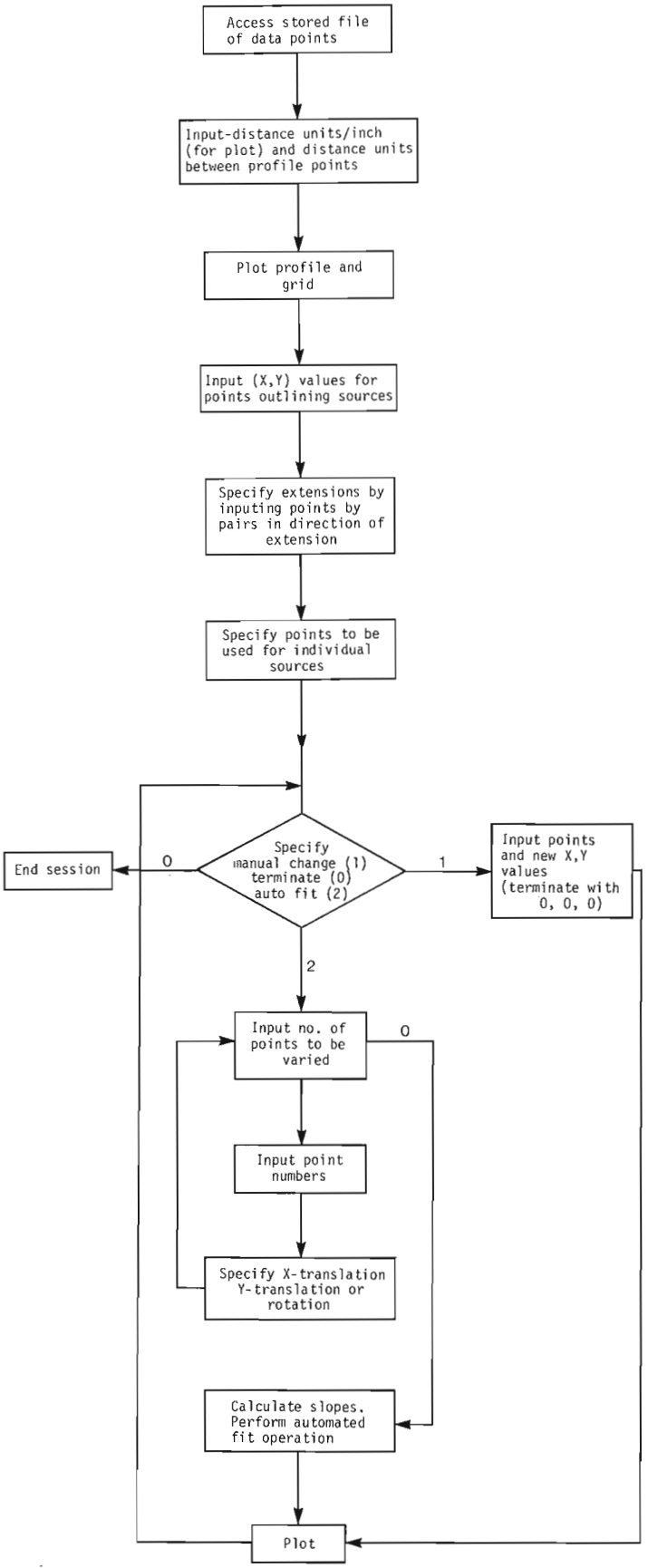

Figure 8.2. *Flow chart for interactive fitting program.*

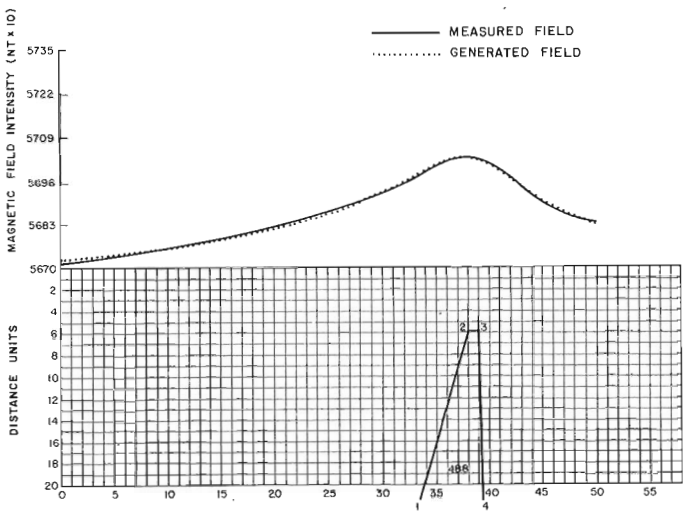

Figure 8.3. *Calculated fit for an aeromagnetic profile across the Lomonosov Ridge.*

data values and proceeds sequentially by requesting further information or options from the user. After receiving basic information, such as the scale (number of length units/inch) and the distance between profile points, the profile is plotted on the top half of the screen, with a square grid in length units on the lower half (Fig. 8.3). The user can then input the points, representing the cross-section of the magnetic sources, in any order, terminating with a zero entry. In the next step, selected sides can be extended by feeding in the two points in the order of the desired extension. This feature is used when it is necessary to represent a source with great depth extent. Finally the individual bodies are defined by inputing the number of points, the approximate strike extent (as estimated from the contour map), and a code to designate whether an open or closed source body is to be used, that is, whether the bottom surface will be considered during anomaly generation. The points that define the outline of each body are then specified in a clockwise direction. A point can, of course, be used in more than one body.

The program now proceeds in an iterative fashion with the operator deciding whether to modify points, enter an automated routine, plot, or terminate the session. These operations can be continued until the user decides that he has obtained the best fit possible and thus that the original hypothesis is possible or not. During the automated fit, the user first specifies the group of points to be varied, followed by an option for X translation, Y translation or rotation (rotation is about the first point entered). This process is continued until all desired movement modes for each group of points has been specified. The program then calculates the changes (slopes) in the 'sum-of-squares' difference between the generated and observed profile for each of the above specified movements. Movement then takes place along the maximum gradient in the least squares surface until a minimum in that direction is reached. The slopes are then recalculated and a new direction established. This process is continued until a minimum in the 'least squares' surface is reached or a specified number of iterations have been exceeded. After plotting the new fit the operator again chooses the appropriate action until an adequate fit has been achieved. This will, of course, usually be a matter of judgment.

Example

In 1980 and 1981, a set of parallel aeromagnetic profiles were flown over the Lomonosov Ridge near the North Pole as part of the Lorex project. The data were collected by the Convair 580 aircraft of the National Aeronautical Establishment, equipped with three rubidium vapour high resolution magnetometers (Hood and Bower, 1980). One particular profile from this set extending from 88°48'N, 164°42'W to 88°57'N, 164°06'E, a distance of 17 km was used as input to the modelling program (the actual profile extended farther north but was terminated to minimize interference from neighbouring anomalies). The result of the computer fit achieved with the described program is shown in Figure 8.3. The distance unit used corresponds to four seconds of aircraft travel which is approximately 340 m. Thus the source appears to be an intrusive body at a depth of approximately 2040 m below the aircraft or 1740 m below sea level. Bathymetric data indicate the depth to bottom at this point to be approximately 1750 ± 50 m.

In general it would be possible to fit the anomaly with a smoother source at shallower depth (clearly unlikely in this case).

Conclusions

This interactive fitting program can be used by persons with little computer experience as a simple technique for evaluating hypotheses concerning the sources of magnetic anomalies. Bodies with arbitrarily complex cross-sections can be represented and easily modified. The efficiency of the program will depend greatly on the experience of the user in postulating geologically reasonable geometries. Copies and demonstrations of the program can be obtained from the author.

References

Hood, P.J. and Bower, M.E.
1980: Aeromagnetic reconnaissance: Lorex Project (Abstract); American Geophysical Union Meeting, Toronto, May 22-27, 1980, EOS, v. 60 (17), p. 277.

Grant, F. and West, G.
1965: Interpretation Theory in Applied Geophysics; McGraw-Hill, New York.

McGrath, P.H. and Hood, P.J.
1973: An automatic least-squares multimodel method for magnetic interpretation; Geophysics, v. 38, p. 349-358.

Wells, I.
1979: A computer program to create two dimensional gravity and/or magnetic models; Geological Survey of Canada, Open File 597.

9.

PRELIMINARY STRUCTURE SECTIONS, SOUTHERN ELLESMERE ISLAND, DISTRICT OF FRANKLIN

Project 790042

Andrew V. Okulitch
Institute of Sedimentary and Petroleum Geology, Calgary

Okulitch, Andrew V., Preliminary structure sections, southern Ellesmere Island, District of Franklin; in Current Research, Part A, Geological Survey of Canada, Paper 82-1A, p. 55-62, 1982.

Abstract

Structures in southern Ellesmere Island were generated during two main episodes, the Ellesmerian and Eurekan orogenies. Tight folds and reverse faults, affected by detachment on Ordovician evaporitic horizons formed prior to Carboniferous times. The intensity of deformation is indicated by the profound structural relief on Carboniferous and Late Cretaceous unconformities. Post-mid-Eocene, pre-Miocene Eurekan deformation accentuated these structures and cut them along thrust faults. Tectonic transport during both orogenies was directed cratonward. Estimates of crustal shortening within the constructed sections range from 25 to 50%. The fold belt and Arctic Platform were affected by several episodes of post-Devonian (possibly post-Eurekan) block faulting some possibly related to Eurekan tectonism. Graben structures may be related to major rifting east and south of Ellesmere Island.

Introduction

During field operations in 1980 and 1981 (Okulitch and Mayr, 1982) mapping of structures and strata on the Arctic Platform and in the Central Ellesmere Fold Belt (Fig. 9.1) allowed provisional construction of cross-sections that illustrate deformation during the Devonian-Mississippian Ellesmerian Orogeny and the Tertiary Eurekan Orogeny. Examination of mesoscopic and macroscopic structural features (e.g. Fig. 9.3) suggested analogues of structural style that were applied to observed attitudes and distribution of rock units to create the cross-sections with their inferred subsurface features. The current state of mapping and the common concealment of essential relationships beneath unconformably overlying strata of Carboniferous, Tertiary and Quaternary ages require that these sections be viewed as working hypotheses which will undoubtedly be extensively revised.

Salient observations and problems illustrated by these sections are: the profound structural relief beneath the Tertiary unconformity, the complex structures above the unconformity in the Eureka Sound Formation and the marked contrast between the considerably foreshortened belt west and east of Vendom Fiord and the extensional regime of the platform in southernmost Ellesmere Island (Fig. 9.1).

Troll Bay to Vendom Fiord Section (Fig. 9.2)

A tranverse section with up to 900 m (3000 ft) relief is available along the sides of Troll Bay. In this region, observable structures are eastward-overturned folds and eastward-directed thrust faults. Figure 9.3 shows similar features on a smaller scale. Considerable shortening is indicated and appears to be the predominant result of deformation. The numerous normal faults shown by Kerr and Thorsteinsson (1972) are therefore of minor displacement or are high angle reverse faults which flatten at depth. Similar features have been noted by McGill (1974) to the southeast. The greatest deformation occurs above evaporitic horizons of the Ordovician Baumann Fiord Formation, although in the few places where subjacent units (O_{CB}) are exposed, prominent folds are evident as well. Presumably additional zones of detachment lie deeper in the section, perhaps near the top of the crystalline basement.

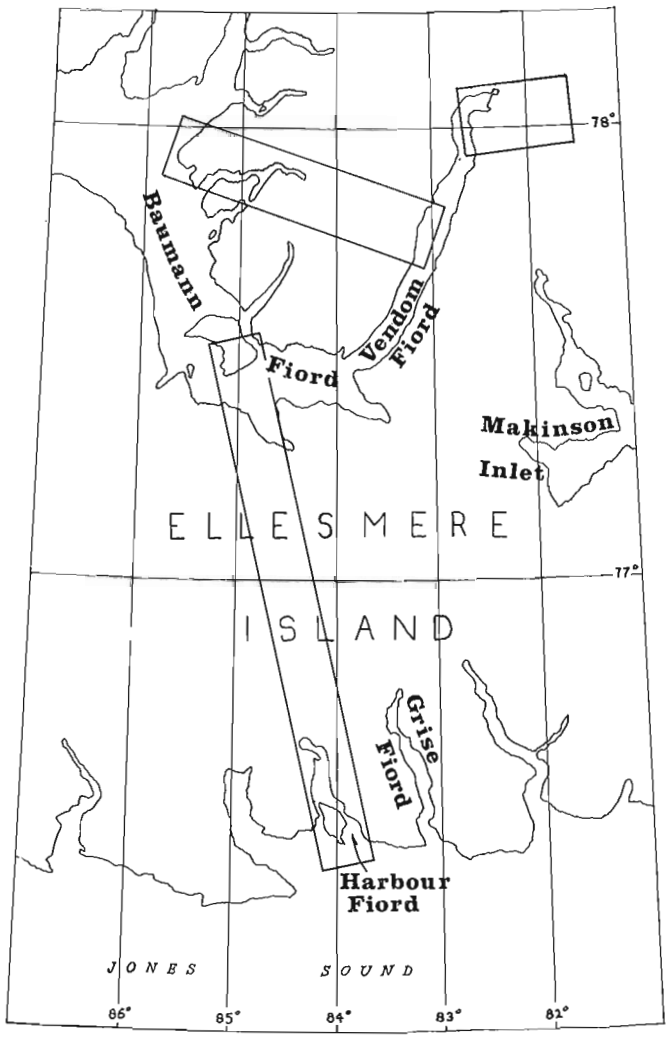

Figure 9.1. Index map of southern Ellesmere Island showing location of strip maps.

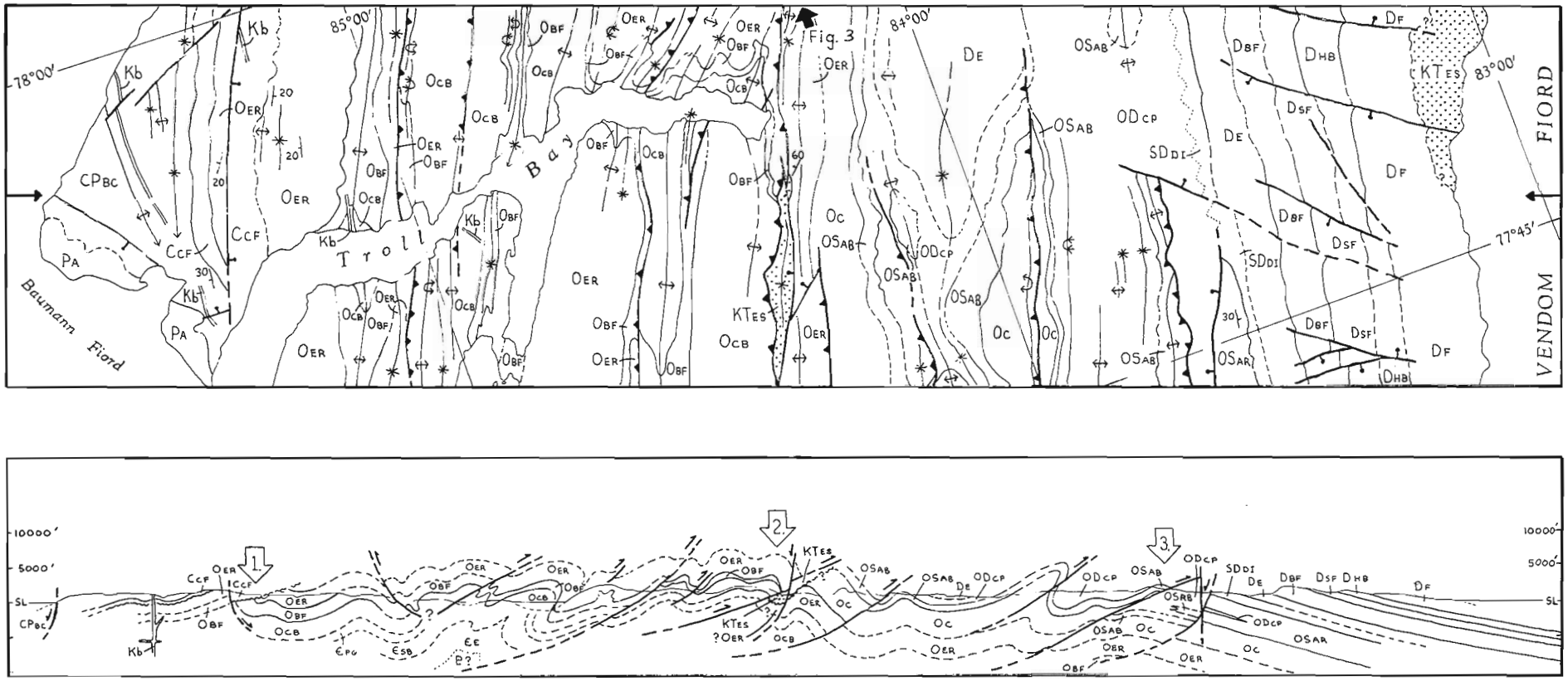

Figure 9.2. *Troll Bay to Vendom Fiord strip map and section. Data from Kerr and Thorsteinsson (1972) and unpublished mapping by Okulitch and Thorsteinsson. Unit thicknesses from Kerr (1967a, b, 1976, and Mayr, 1974). Areas 1, 2 and 3 (arrows) described in text. See Table 9.1 for explanation of symbols. Scale 1:364,000. Vertical scale = horizontal scale.*

Figure 9.3. *Thin bedded evaporitic shale and limestone of the Cornwallis Group, Bay Fiord Formation. Such features as tight, disharmonic folds and blind thrust faults (bottom centre) are believed typical of all scales of deformation in the area. Location on Figure 9.2. View is northward. Height of cliff about 100 m.*

Table 9.1

KT_{ES}	Eureka Sound Formation		S_{CS}	Cape Storm Formation	
Kb	basalt dyke		OD_{CP}	Cape Phillips Formation	
P_A	Assistance Formation		OS_{AR}	Allen Bay and Read Bay Formations undivided. May include S_{CS}, S_D and D_{GF} east of Vendom Fiord only	
CP_{BC}	Belcher Channel Formation				
C_{CF}	Canyon Fiord Formation		OS_{RB}	Read Bay Formation	
D_{HG}	Hell Gate Formation		OS_{AB}	Allen Bay Formation	
D_F	Fram Formation	Okse Bay Group	O_C	Cornwallis Group	
D_{HB}	Hecla Bay Formation		O_{ER}	Eleanor River Formation	
D_{SF}	Strathcona Fiord Formation		O_{BF}	Baumann Fiord Formation	
D_{SF_B}	Bird Fiord tongue within Strathcona Fiord Formation (eastern part of south limb of Schei Syncline only)		O_{BB}	Blanley Bay Formation	facies equivalents
			O_{CB}	Copes Bay Formation. May include O_{CC} and $\mathfrak{E}O_{CF}$	
D_{BI}	Bird Fiord Formation				
D_{BF}	Blue Fiord Formation (include Bird Fiord east and west of Vendom Fiord)		O_{CC}	Cape Clay Formation	
			$\mathfrak{E}O_{CF}$	Cass Fiord Formation	
D_E	Eids Formation. Unnamed transitional beds between the Goose Fiord and Blue Fiord formations are provisionally included		$\mathfrak{E}_{PG}$	Parrish Glacier Formation	
			$\mathfrak{E}_{SB}$	Scoresby Bay	
D_{VF}	Vendom Fiord Formation		$\mathfrak{E}_E$	Ellesmere Group	
D_{GF}	Goose Fiord Formation		$\underline{P}$?	Possible late Proterozoic strata	
SD_{BI}	Possible equivalents to the Barlow Inlet Formation		$\underline{P}b$	Diabase dykes	
			$\bar{A}gn$	Gneiss, granitoid rocks; minor schist, diabase	
SD_{DI}	Devon Island Formation				
S_D	Douro Formation				

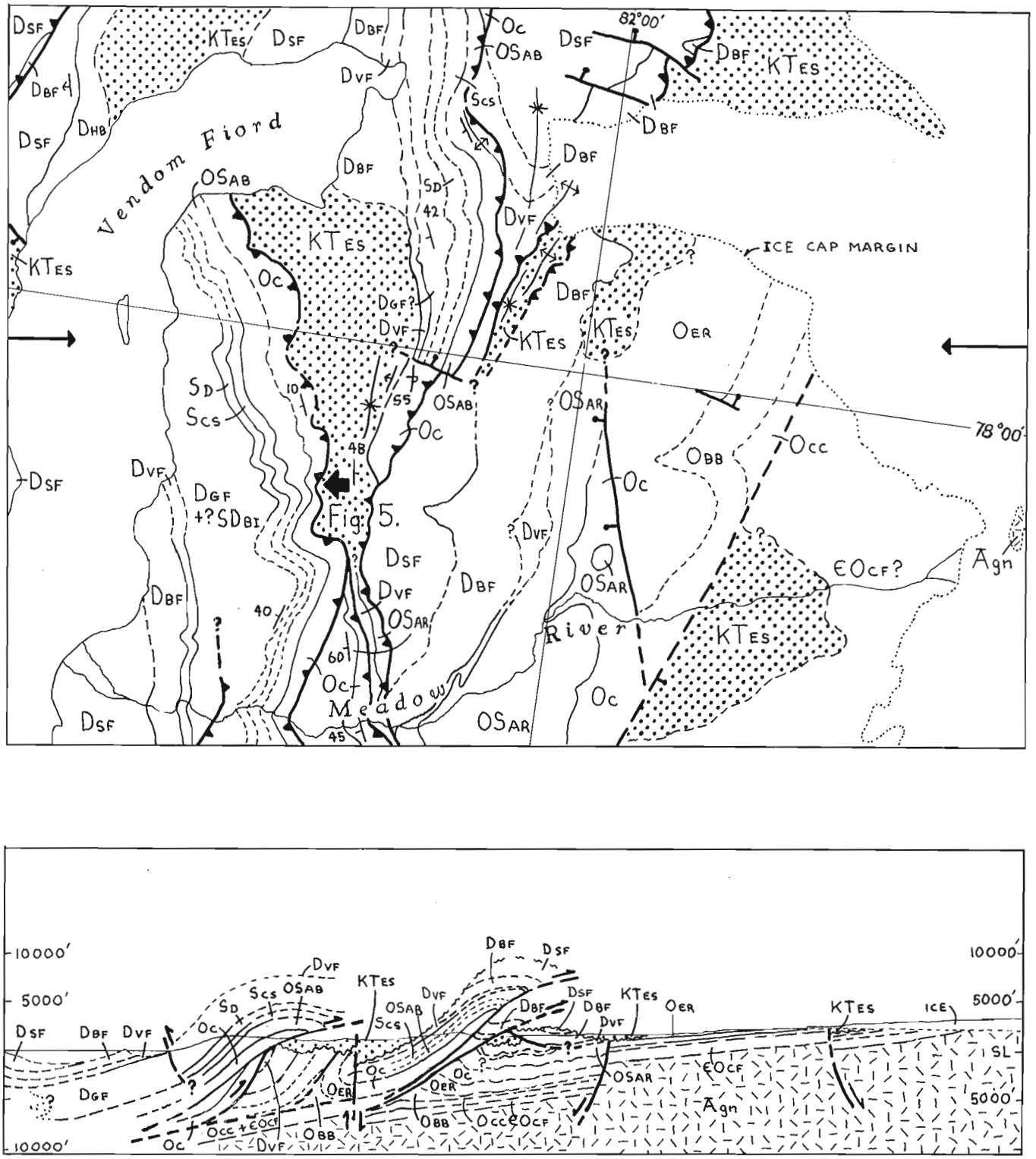

Figure 9.4. *Vendom Fiord and Meadow River strip map and section. Data from Thorsteinsson, Kerr and Tozer (1972) and unpublished mapping by Kerr, Okulitch and Thorsteinsson. Unit thicknesses from Kerr (1967a, b, 1976). See Table 9.1 for explanation of symbols. Scale 1:174,000. Vertical scale = horizontal scale.*

Times of deformation are constrained by data in only a few areas. To the west (area 1), gently folded Carboniferous Canyon Fiord sediments lie with up to 90° discordance over tightly folded Ordovician Eleanor River carbonates. South of the head of Troll Bay (area 2), the Cretaceous to Tertiary Eureka Sound Formation is apparently overthrust by Ordovician carbonates and evaporites. Eureka Sound sediments are gently folded. Although the fault in area 2 places Ordovician upon Tertiary rocks, to the north the Eleanor River Formation is overthrust by itself, suggesting that displacement on this fault may not be extreme.

The fact that Tertiary strata rest on a variety of highly folded units and the likelihood that Tertiary thrusts must cut such structures, renders construction of balanced sections and estimates of crustal shortening imprecise. However the absence of coarse clastic rocks in exposed parts of the Eureka Sound Formation argues against its deposition in local, fault-bounded basins in this area. Therefore, attainment of more complete understanding of structures in this blanketing formation holds the promise of more precise reconstruction of the configuration of Paleozoic features.

Intensity of deformation is apparently reduced to the east of Troll Bay. This is either a lateral variation, or more likely, a vertical one as the zones of detachment in evaporitic units (Baumann Fiord Formation and basal Cornwallis Group) are left behind the thick overlying car-bonates of the upper Cornwallis Group and Allen Bay Formation.

Area 3 contains the easternmost major structure west of Vendom Fiord. It appears to be a major thrust (unless it has beheaded an earlier formed anticline) which carries Allen Bay carbonates perhaps as much as 3 km over shales of the Siluro-Devonian Devon Island Formation. Its trace coincides with a marked facies change (Mayr, 1974) in the Allen Bay-Read Bay formations which may influence the locus of the fault. The rapidity of the facies change may in part be a product of telescoping of diverse successions. Eastward from this thrust sheet is a homoclinal succession which forms the west limb of the Vendom Syncline (McGill, 1974). This feature, similar to the Schei Syncline to the south (Fig. 9.6) but trending about 80° to it, is a distinct structure, unrelated to the latter.

Simplistic measurement of structures proposed along this section, without regard for effects of disharmonic folding and thickening of parts of the succession, provides an estimate of 25% shortening for both Ellesmerian and Eurekan deformation.

Vendom Fiord and Meadow River Section (Fig. 9.4)

The area near and east of the head of Vendom Fiord is of lower relief and less well exposed than that near Troll Bay, however, good exposures with nearly 600 m (2000 ft) of relief are available along parts of the Meadow River. Structures are complex in the western half of the section, the predominant type being easterly-directed thrust faults that place Ordovician to Devonian carbonates on the Eureka Sound Formation (Fig. 9.5).

Several features suggest the presence of structures formed prior to thrusting; some of these also preceded deposition of the Eureka Sound Formation. Just south of the line of section, northeast of the location of Figure 9.5, Eureka Sound clastic sediments rest apparently unconformably on an overturned succession of Cornwallis Group carbonates (Thumb Mountain and Bay Fiord formations). Immediately to the north, across a north-side-down normal fault, the clastic rocks lie on the Devonian Vendom Fiord and Blue Fiord formations which are part of a succession forming the west limb of an anticline cored by the Cornwallis Group. South of the location of Figure 9.5, north of the Meadow River, the Cornwallis Group is thrust upon the Vendom Fiord Formation. This upper panel and the thrust are cut down-section by a major Tertiary thrust fault. One of several possible interpretations is illustrated: an eastern Tertiary thrust cuts and carries an overturned fold set of possible Ellesmerian age. The west limb of the western anticline is faulted, and it and the fault are cut by a second (western) Tertiary thrust. It is possible that this second thrust (Fig. 9.5) dips more gently than shown. In such a case it would behead the anticline above it and cut up-section through Devonian strata below Vendom Fiord. This thrust carries the Vendom Syncline and all structures shown in Figure 9.2. Considerable disharmony is postulated at the level of the Blanley Bay (= Baumann Fiord) Formation in keeping with observed structures at Troll Bay. Tertiary thrusts are also shown as rooted at this level although they may well extend to the crystalline basement.

The eastern half of the section is very poorly exposed and additional structural complexities may be present. However gentle dips and known stratigraphic thicknesses limit possible alternatives.

Total shortening is 50%, as shown on the section between the Vendom Syncline and the westernmost platformal normal fault (at about 78°00'N, 82°00'W). Given the obvious difficulties attendant to construction of the section, such a figure must be considered speculative and even if correct, unlikely to apply to the whole fold belt.

Figure 9.5.

Gently dipping Ordovician carbonates of the Cornwallis Group and Allen Bay Formation thrust over sediments of the Cretaceous to Tertiary Eureka Sound Formation. Trace of the thrust fault lies between the lowest cliff forming unit and the dark, soft weathering gullies and slopes, horizontally across the entire photograph. Total relief visible is about 600 m (2000 ft). View is westward.

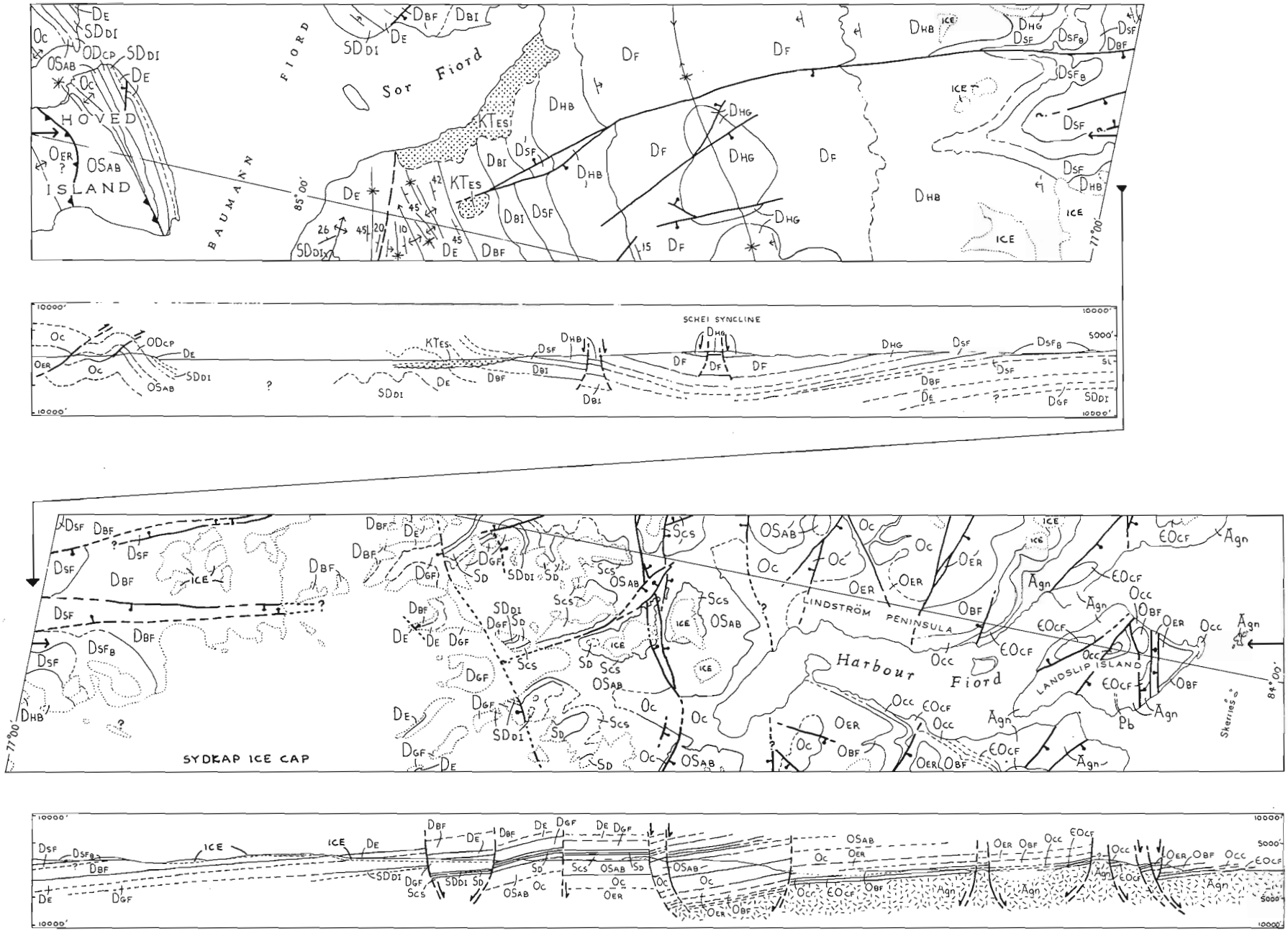

Figure 9.6. Baumann Fiord to Harbour Fiord strip map and section. Data from Kerr and Thorsteinsson (1972), Christie (1962) and unpublished mapping by Christie, Mayr, Okulitch and Thorsteinsson. Unit thicknesses from Mayr (1982) and Packard and Mayr (1982). See Table 9.1 for explanation of symbols. Scale 1:380,000. Vertical scale = horizontal scale.

Figure 9.7

Folded sediments of the Eureka Sound Formation east of Sor Fiord south of the head of Stenkull Fiord. Fold axes and minor faults trend north-northwest, athwart the easterly trend of gentle folds in unconformably underlying Devonian clastic rocks of the Okse Bay Group. View to the north-northwest across Stenkull Fiord (middle distance) and Baumann Fiord (upper left). Local relief is about 150 m (500 ft).

Baumann Fiord to Harbour Fiord Section (Fig. 9.6)

The northern part of the section bordering Baumann Fiord contains tightly folded and thrust faulted Paleozoic strata. Structures trend northeast to east and may represent Ellesmerian structures that have not suffered much accentuation and rotation by northerly trending Tertiary features. Some of the variation in trend may be original, resulting from the interaction of a deforming sedi-mentary wedge with an arcuate cratonic margin. The rapid diminution of intensity of folding at the level of the Blue Fiord Formation may result from disharmonic folding and detachment within the Eids shales. The Schei Syncline is the last surface expression of folding; all units on the south limb of the syncline are planar.

The broad, block-faulted platform of southern Ellesmere Island occupies most of this section. No single pre-dominant sense of motion took place on the east-west faults except near the south coast where substantial south-side-down displacement is present, possibly related to formation of the Jones Sound Graben during the Eurekan Rifting Episode (Kerr, 1977).

Preceding this extensional episode and likely of late Mesozoic to Early Tertiary age (but known only to be post-Devonian in the study area) is another which formed several narrow north-northwest trending grabens with 1-3 km displacement (Strathcona Fiord against Goose Fiord to Allen Bay formations) and many associated normal faults. The relationship of these structures to compressional features to the north is uncertain. Tertiary compressional structures appear to die away southward (cf. Balkwill and Bustin, 1978, Fig. 1) and extensional faults in this section appear to lose displacement northward. If they are contemporaneous, such relationships support hypotheses proposed by Kerr (1980). On Devon Island the predominant episode of normal faulting is late Paleogene (Thorsteinsson, personal communication, 1981).

Structures in Tertiary strata east of the strip map area (Fig. 9.7) are anomalous in that they trend north-northwest and have no reflection in underlying Devonian strata. The tight to open folds and minor thrust faults that have been observed may therefore be related to presently cryptic faulting which, given the nature of the structures in the Eureka Sound Formation, must be presumed to be compressional in origin. Although contacts between this formation and older rocks have commonly been designated as normal faults (McGill, 1974, Fig. 4; R. Thorsteinsson, personal communications, 1980, 1981 re unpublished mapping, Vendom Fiord map area), few are exposed and some may in fact be reverse or thrust faults. The relationships of such hypothetical structures to those of the platform and the adjacent fold belt will form one of the key facets of future studies.

Summary

Data available from the three areas described indicate substantial folding and faulting during post-Silurian to pre-Carboniferous time (Ellesmerian Orogeny) followed by additional folding but predominantly overthrusting during post-mid-Eocene time (Eurekan Orogeny). The presence of Carboniferous and Tertiary clastic sediments on upright and, rarely, overturned strata of Ordovician to Devonian ages supports the interpretation that Ellesmerian structures represent considerable crustal shortening. Involvement of crystalline basement in these structures is uncertain. Eurekan folds, reverse faults and thrusts that emplaced Paleozoic strata above Late Cretaceous to Eocene clastic rocks are further evidence of compression. Tightening and reorientation of Ellesmerian folds and reactivation of faults likely occurred before new thrust faults propagated. Estimates of crustal shortening in the limited areas studied range from 25% to 50%.

The timing of extensional tectonism in these areas is not well constrained. Some normal faulting likely affected the crystalline basement prior to the Paleozoic (cf. Fig. 9.6, west of Landslip Island). Other normal faults may pre-date deposition of the Eureka Sound Formation (eg. Fig. 9.4 near 78°00'N, 82°00'W). Still others bound Eureka Sound strata (eg. Fig. 9.4, upper Meadow River) but do not appear to be contemporaneous with deposition. All are subject to reactivation, hence the times of their initiation are unknown. The numerous intersecting fault sets in southern Ellesmere Island are post-Devonian in age and their tectonic inter-relations with other structures in the region are not presently demonstrable.

References

Balkwill, H.R. and Bustin, R.M.
1978: Late Phanerozoic structures, Canadian Arctic Archipelago; Palaeogeography, Palaeoclimatology, Palaeoecology, v. 30, p. 219-227.

Christie, R.L.
1962: Geology, Alexandra Fiord, Ellesmere Island, District of Franklin; Geological Survey of Canada, Map 9-1962.

Kerr, J.W.
1967a: Vendom Fiord Formation – a new red-bed unit of probable early Middle Devonian (Eifelian) age, Ellesmere Island, Arctic Canada; Geological Survey of Canada, Paper 67-43.

1967b: Stratigraphy of central and eastern Ellesmere Island, Arctic Canada; Geological Survey of Canada, Paper 67-27, Parts I and II.

1976: Stratigraphy of central and eastern Ellesmere Island, Part III, Upper Ordovician (Richmondian), Silurian and Devonian; Geological Survey of Canada, Bulletin 260.

1977: Cornwallis Fold Belt and the mechanism of basement uplift; Canadian Journal of Earth Sciences, v. 14, p. 1374-1401.

1980: Evolution of the Canadian Arctic Islands: a transition between the Atlantic and Arctic oceans; in The Ocean Basins and Margins, v. 5, The Arctic Ocean; ed. A.E.M. Nairn, M. Churkin, Jr. and F.G. Stehli, p. 105-199.

Kerr, J.W. and Thorsteinsson, R.
1972: Baumann Fiord; Geological Survey of Canada, Map 1312 A.

Mayr, U.
1974: Lithologies and depositional environments of the Allen Bay-Read Bay formations (Ordovician-Silurian) on Svendsen Peninsula, central Ellesmere Island; in Proceedings of the Symposium on the Geology of the Canadian Arctic, ed., J.D. Aitken and D.F. Glass; Geological Association of Canada and Canadian Society of Petroleum Geologists, p. 143-157.

1982: Lithostratigraphy (Ordovician to Devonian) of the Grise Fiord area, Ellesmere Island, N.W.T.; in Current Research, Part A, Geological Survey of Canada, Paper 82-1A, report 10.

McGill, P.C.
1974: The stratigraphy and structure of the Vendom Fiord area; Bulletin of Canadian Petroleum Geologists, v. 22, p. 361-386.

Okulitch, A.V. and Mayr, U.
1982: Stratigraphic and structural studies, southern Ellesmere Island, N.W.T.; in Current Research, Part A, Geological Survey of Canada, Paper 82-1A, note.

Packard, J. and Mayr, U.
1982: Cambrian and Ordovician stratigraphy of southern Ellesmere Island, N.W.T.; in Current Research, Part A, Geological Survey of Canada, Paper 82-1A, report 11.

Thorsteinsson, R., Kerr, J.W. and Tozer, E.T.
1972: Strathcona Fiord; Geological Survey of Canada, Map 1307 A.

10.

LITHOSTRATIGRAPHY (ORDOVICIAN TO DEVONIAN) OF THE GRISE FIORD AREA, ELLESMERE ISLAND, DISTRICT OF FRANKLIN

Project 810016

Ulrich Mayr
Institute of Sedimentary and Petroleum Geology, Calgary

Mayr, Ulrich, Lithostratigraphy (Ordovician to Devonian) of the Grise Fiord area, Ellesmere Island, District of Franklin; in Current Research, Part A, Geological Survey of Canada, Paper 82-1A, p. 63-66, 1982.

Abstract

A continuous section from the base of the Thumb Mountain Formation to the top of the Blue Fiord Formation was measured. Formations, thicknesses, and main lithologies in ascending order are:

Thumb Mountain Formation, 308.5 m, massive, dolomitic limestone;

Irene Bay Formation, 40.5 m, argillaceous, nodular limestone;

Allen Bay Formation, 788.5 m, massive limestone and dolomite;

Cape Storm Formation, 225.5 m, silty dolomite;

Douro Formation, 97.3 m, nodular limestone;

Devon Island Formation, 116.0 m, interbedded calcareous shale and argillaceous limestone;

Goose Fiord Formation, 710.5 m, variable dolomite;

Unnamed unit, 248.0 m, variable dolomite;

Blue Fiord Formation, 726.0 m, carbonates with bird's-eye texture.

Introduction

During the summer of 1981 (see Okulitch and Mayr, 1982) a continuous section ranging from the Thumb Mountain to the Blue Fiord Formation (Fig. 10.1) was compiled in the area northwest of the head of Grise Fiord (Fig. 10.2). These rocks are situated in north and northwest dipping fault-blocks which form the southern flank of the Schei Syncline. Formation identifications are based primarily on lithological characteristics. Paleontological collections are under examination, thus no firm age assignments can be made. The Thumb Mountain Formation and the lower member of the Allen Bay Formation are of Ordovician age; the Silurian/Devonian boundary may fall in the highest part of the Devon Island or the lower part of the Goose Fiord Formation.

Thumb Mountain Formation

The Thumb Mountain Formation is a resistant unit, about 300 m thick. Most of it consists of thick bedded, uniform lime mudstone with labyrinthic dolomitic mottles. At the base, about 20 m of thin- and medium-bedded dolomite are present, whereas the uppermost part of the formation consists of nodular lime mudstone. Upper and lower contacts of the formation are sharp and conformable.

Irene Bay Formation

The Irene Bay Formation is about 40 m thick and weathers recessively. The lower part consists of nodular skeletal wackestone or lime mudstone with dolomitic-argillaceous partings. The upper part comprises thick bedded lime mudstone, less argillaceous than the lower part. The Irene Bay Formation is moderately fossiliferous. The upper boundary is gradational.

Allen Bay Formation

The Allen Bay Formation is a cliff-forming unit that consists of three members. The lower member is about 145 m thick and consists of massive limestone with labyrinthine mottling. This lithology is similar to that of the Thumb Mountain Formation. A middle member of dolomite, some 500 m thick, overlies the lower member with a sharp contact. Dark brown, slightly mottled dolomite in thick beds dominate the lower and upper parts of the middle member, whereas dolomite breccia is characteristic of the middle part. In the upper part of the member interbeds of various types of grey, light weathering dolomite give that part of the member a distinct, striped appearance when viewed from a distance.

The upper member, a limestone unit, overlies the middle member with a sharp contact. Maximum observed thickness is close to 100 m. Algal laminae, flat pebble conglomerate, ooids, and oncolites were noted. The member is a discontinuous unit and, in many localities, the Cape Storm Formation rests directly on the dark brown dolomite of the middle Allen Bay Formation. On the Boothia Uplift a disconformity at the base of the Cape Storm Formation has been reported by Kerr (1977); presumably a similar hiatus is present in the Grise Fiord area.

Cape Storm Formation

The Cape Storm Formation, mainly of dolomite, is about 225 m thick. Most of the dolomite is silty and thin bedded. Ripple crosslaminae, shrinkage cracks and fine laminae are common. Interbeds of thick bedded, patterned dolomite are also present, and some beds of stromatolites or abundant gastropods were noted. The uppermost 40-50 m of the Cape Storm dolomites are interbedded with the limestone of the Douro Formation. The formation boundary is placed above the highest, thin and planar bedded dolomite or limestone.

Douro Formation

The Douro Formation, about 100 m thick, consists of uniform, nodular, dolomitic limestone. Minor shaly beds are present in the lower part of the formation. **Atrypella**-type brachiopods are abundant. The upper boundary of the formation appears to be sharp, but exposure is poor at the contact.

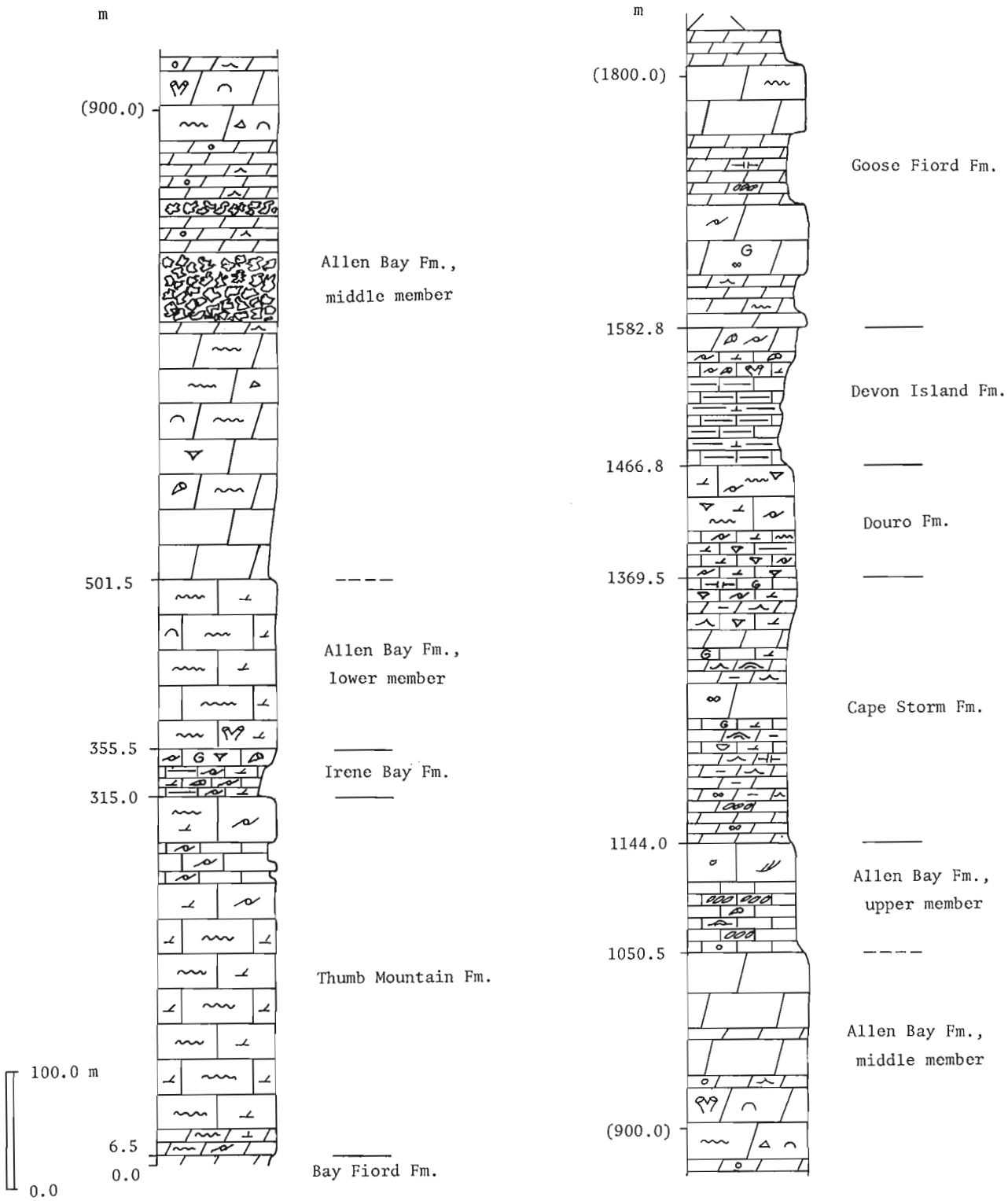

Figure 10.1. *Graphical log of Thumb Mountain to Blue Fiord Formation.*

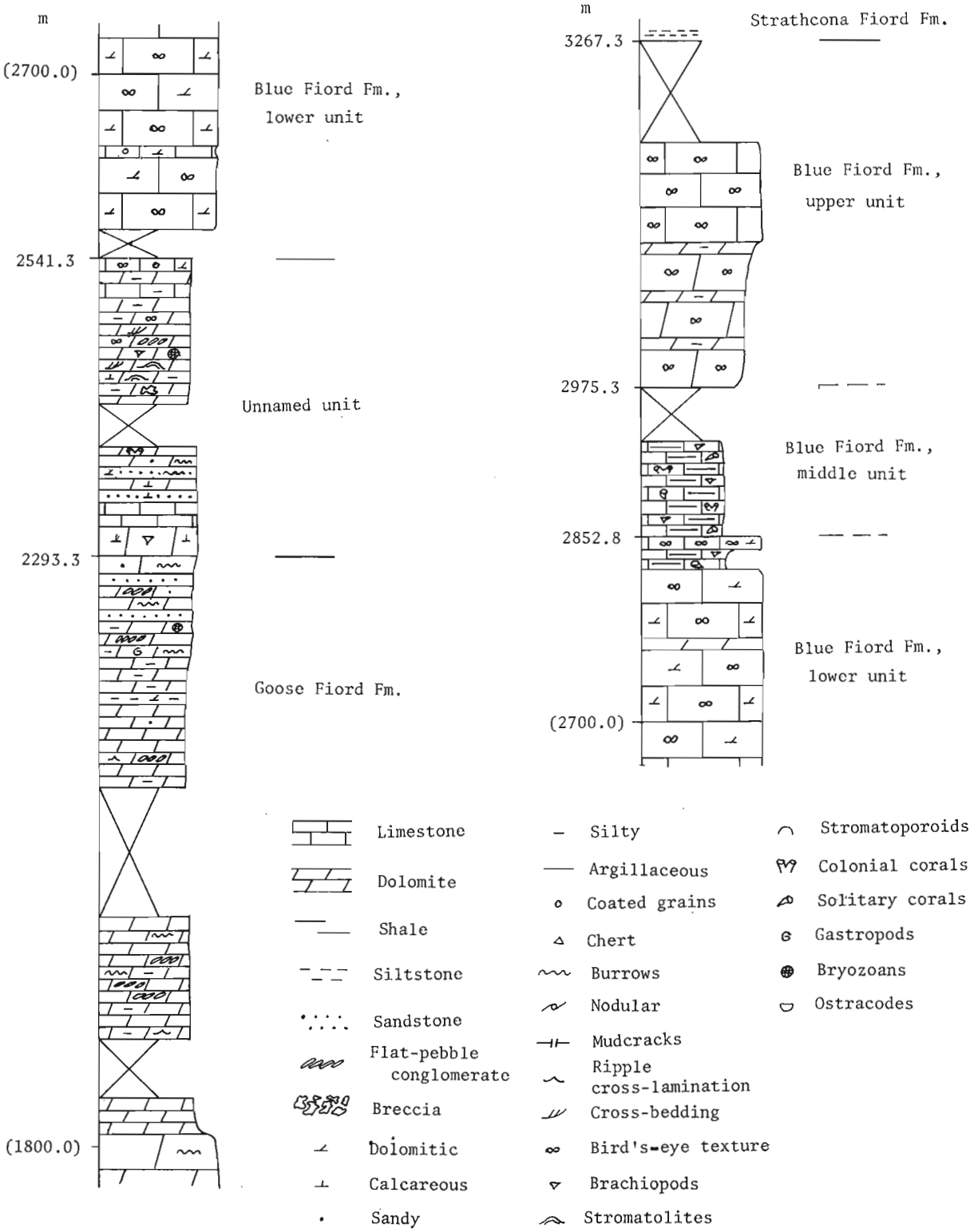
m
(2700.0)
Blue Fiord Fm., lower unit
2541.3
Unnamed unit
2293.3
Goose Fiord Fm.
(1800.0)
m
3267.3
Strathcona Fiord Fm.
Blue Fiord Fm., upper unit
2975.3
Blue Fiord Fm., middle unit
2852.8
Blue Fiord Fm., lower unit
(2700.0)
Limestone
Dolomite
Shale
Siltstone
Sandstone
Flat-pebble conglomerate
Breccia
Dolomitic
Calcareous
Sandy
Silty
Argillaceous
Coated grains
Chert
Burrows
Nodular
Mudcracks
Ripple cross-lamination
Cross-bedding
Bird's-eye texture
Brachiopods
Stromatolites
Stromatoporoids
Colonial corals
Solitary corals
Gastropods
Bryozoans
Ostracodes

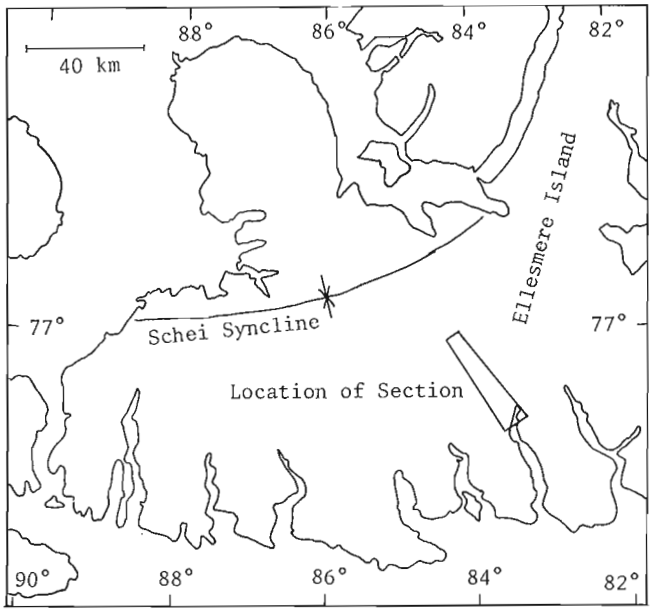

Figure 10.2. *Index map of southern Ellesmere Island.*

Devon Island Formation

Maximum measured thickness of the Devon Island Formation is 116 m. The lower two thirds of the formation consist of thin bedded, argillaceous limestone interbedded with calcareous shale. These lithologies grade upward into nodular limestone similar to that of the Douro Formation. The limestone in turn grades upward into brown, mottled dolomite. The limestone and the dolomite contain abundant corals; though in the latter the fossils have been leached and are now replaced by calcite filled vugs. The thickness of the upper dolomite is variable, also in some localities the Devon Island Formation is only several tens of metres thick or appears to be totally absent. These local variations in thickness imply a disconformable contact with the overlying Goose Fiord Formation.

Goose Fiord Formation

The Goose Fiord Formation, which is almost entirely dolomite, is about 710 m thick and overlies the Devon Island Formation with a sharp contact. Whereas three resistant ledges mark the lower part of the formation, the upper part has a uniform morphological expression. The lowest ledge is of variable thickness (12 m in Fig. 10.1) and consists of vuggy, coarsely crystalline, biostromal dolomite. This dolomite interfingers laterally with rocks of the overlying recessive unit, which are thin- and medium-bedded silty dolomite. The two higher ledges are each about 50 m thick and consist of medium- to thick-bedded dolomite that appears burrowed. The intervening beds comprise medium- to thin-bedded dolomite with flat-pebble conglomerate.

The upper part of the Goose Fiord Formation consists of thin- and medium-bedded, light coloured silty dolomite with flat-pebble conglomerate, ripple crosslamination and planar lamination. Several intervals of sandstone and sandy dolomite are also present.

Unnamed unit

The Goose Fiord Formation is overlain by a unit, as yet unassigned, which may be part of either the Goose Fiord or the Blue Fiord Formation. The regional extent and correlation of this unit are insufficiently known at present.

The unit is about 250 m thick and overlies the Goose Fiord Formation with a sharp contact. The lower part consists of dark coloured, fossiliferous dolomite, which is interbedded with calcareous and dolomitic sandstone. The upper part of the unit is formed by thin- to medium-bedded, silty dolomite interbedded with bird's-eye dolomite. The contact with the overlying Blue Fiord Formation is sharp.

Blue Fiord Formation

The Blue Fiord Formation is over 700 m thick and at least three informal units can be distinguished. The lower unit is about 300 m thick and consists of resistant bird's-eye limestone.

The middle unit is dark coloured, recessive, thin bedded, argillaceous limestone. Brachiopods and corals are abundant in this 120 m thick unit.

The upper unit consists mostly of bird's-eye carbonates. In the lower part bird's-eye dolomite is interbedded with silty, laminated dolomite and minor limestone. The upper part consists of resistant bird's-eye limestone similar to that in the lower part of the Blue Fiord Formation. Total thickness of the upper unit is about 290 m. The Blue Fiord Formation appears to be overlain abruptly by Strathcona Fiord Formation, but the actual contact was not examined.

References

Kerr, J.W.
1977: Cornwallis Fold Belt and the mechanism of basement uplift; Canadian Journal of Earth Sciences, v. 14, p. 1374-1401.

Okulitch, A.V. and Mayr, U.
1982: Stratigraphic and structural studies, southern Ellesmere Island, N.W.T.; in Current Research, Part A, Geological Survey of Canada, Paper 82-1A, note.

CAMBRIAN AND ORDOVICIAN STRATIGRAPHY OF SOUTHERN ELLESMERE ISLAND, DISTRICT OF FRANKLIN

Project 810016

J. Packard[1] and Ulrich Mayr
Institute of Sedimentary and Petroleum Geology, Calgary

Packard, J. and Mayr, Ulrich, Cambrian and Ordovician stratigraphy of southern Ellesmere Island, District of Franklin; in Current Research, Part A, Geological Survey of Canada, Paper 82-1A, p. 67-74, 1982.

Abstract

The Lower Paleozoic stratigraphic succession within the Arctic Platform geological province on southern Ellesmere Island includes 1500 m of predominantly carbonate strata, up to the base of the Thumb Mountain Formation. Composite sections from Makinson Inlet and Grise Fiord are easily correlated, particularly from the upper Cass Fjord Formation to the Baumann Fiord Formation, with several individual marker beds traceable between study areas.

Regionally the southern Ellesmere Island succession can be closely equated to the Lower Paleozoic sequence exposed on Bache Peninsula, 300 km to the north.

Introduction

Detailed stratigraphic studies of a Lower to Mid Paleozoic, predominantly shallow carbonate shelf sequence on southern Ellesmere Island were completed during the 1981 field season (see Okulitch and Mayr, 1982). This paper describes the basal 1500 m of the sequence, commencing at the Precambrian-Phanerozoic unconformity and including formations ranging in age from ?Early Cambrian to Middle Ordovician.

A total of 15 stratigraphic sections were measured; all but one are within two principal study areas, Makinson Inlet and Grise Fiord (Fig. 11.1). A single section was examined at Fram Fiord. This report is a summary of the Lower Paleozoic lithostratigraphy of the two principal study areas, and a tentative correlation between them. At present, only limited biostratigraphic data are available, and thus age assignments are primarily those extrapolated from similar, reliably dated lithostratigraphic sequences elsewhere in the Franklinian Basin or Arctic Platform. Oblique views of sections are shown in Figure 11.2 and characteristic lithotypes are shown in Figure 11.3.

Stratigraphy

Pre-Cass Fjord Sequence

The pre-Cass Fjord sequence within the study area is marked by variation in thickness and lithology. Differences in lithostratigraphy between sections may be due in part to marine encroachment over an original basement topography of considerable relief, in addition to a complex tectonic history resulting in differential preservation of Proterozoic and Cambrian sequences of various ages.

Makinson Inlet. At Makinson Inlet, the pre-Cass Fjord sequence is separated from the crystalline basement by an unconformity and is overlain disconformably by the Cass Fjord Formation.

Above the basal unconformity are at least 5 metres of buff orange to reddish brown weathering, poorly sorted, trough crossbedded coarse grained arkose with polymictic conglomerate phases. These in turn, are overlain by 20 metres of buff weathering, moderately sorted, medium- to coarse-grained quartz arenite in thick bedded units with large planar cross-sets, grading upwards into green-grey weathering, bimodal quartz arenite in thin to medium beds intercalated with thin beds of ?glauconitic siltstone. In vertical section the sandstone is commonly seen to be pervasively penetrated by vertical tubes 3-7 mm in diameter. The presence of paired and often linked burrow openings on bedding planes, as well as rarely preserved spreiten structures between paired tubes, suggest that the trace fossil is the ichnogenus **Diplocraterion.**

Conformably and gradationally overlying this interval is a 45 m thick, partially exposed sequence of thick bedded to massive, medium brown to buff weathering, aphanitic to medium crystalline dolostone. The basal 10 m contain abundant quartz silt. The rock becomes more calcareous towards the top, and granule-sized allochems (chiefly intraclasts) become increasingly distinguishable from the matrix. Stylolitic contacts between beds are common.

Fram Fiord. A relatively thick (215 m+) pre-Cass Fjord succession is present in the vicinity of Fram Fiord. Just above the unconformity is a 25 m siliciclastic sequence composed of planar and trough crossbedded, dusky red to variegated purple and buff, medium grained, poorly sorted arkose with granule and pebble conglomerate lenses. This grades upwards into medium grained, buff quartz arenite with low angle cross-sets and plane laminae which is in turn capped by recessive green-grey weathering dolomitic quartz siltstone.

Conformably overlying the siliciclastic sequence are approximately 155 m of carbonate, predominantly massive, ledge-forming, fine- to medium-grained crystalline dolostone. The lower 25 m and the upper 20 m are composed of buff weathering, massive, weakly laminated dolosiltite. The middle 110 m consist of dark brown, grey weathering, massive, in part mottled, fine- to medium-crystalline dolostone. Two recessive, thin, planar bedded, dolomitic calcisiltite units occur between 127 and 138 m, and between 147 and 155 m above the base of the section. The latter interval yielded fragmentary, and as yet unidentified, trilobite remains. The upper 40 m show an overall gradual increase in quartz sand impurities, culminating in a 10 m+ unit of massive quartz pebble conglomerate.

Age and Correlation. The possible age range of the pre-Cass Fjord rocks is Late Proterozoic to Middle Cambrian. Correlation of the sequences at Fram Fiord, Makinson Inlet and Bache Peninsula is at present uncertain.

Cass Fjord Formation

The Cass Fjord Formation was named by Poulsen (1927) for a 400 m+ thick sequence in NW Greenland of coarse limestone conglomerate alternating with thin bedded impure

[1] Department of Geology, University of Ottawa, Ottawa, Ontario, K1N 6N5

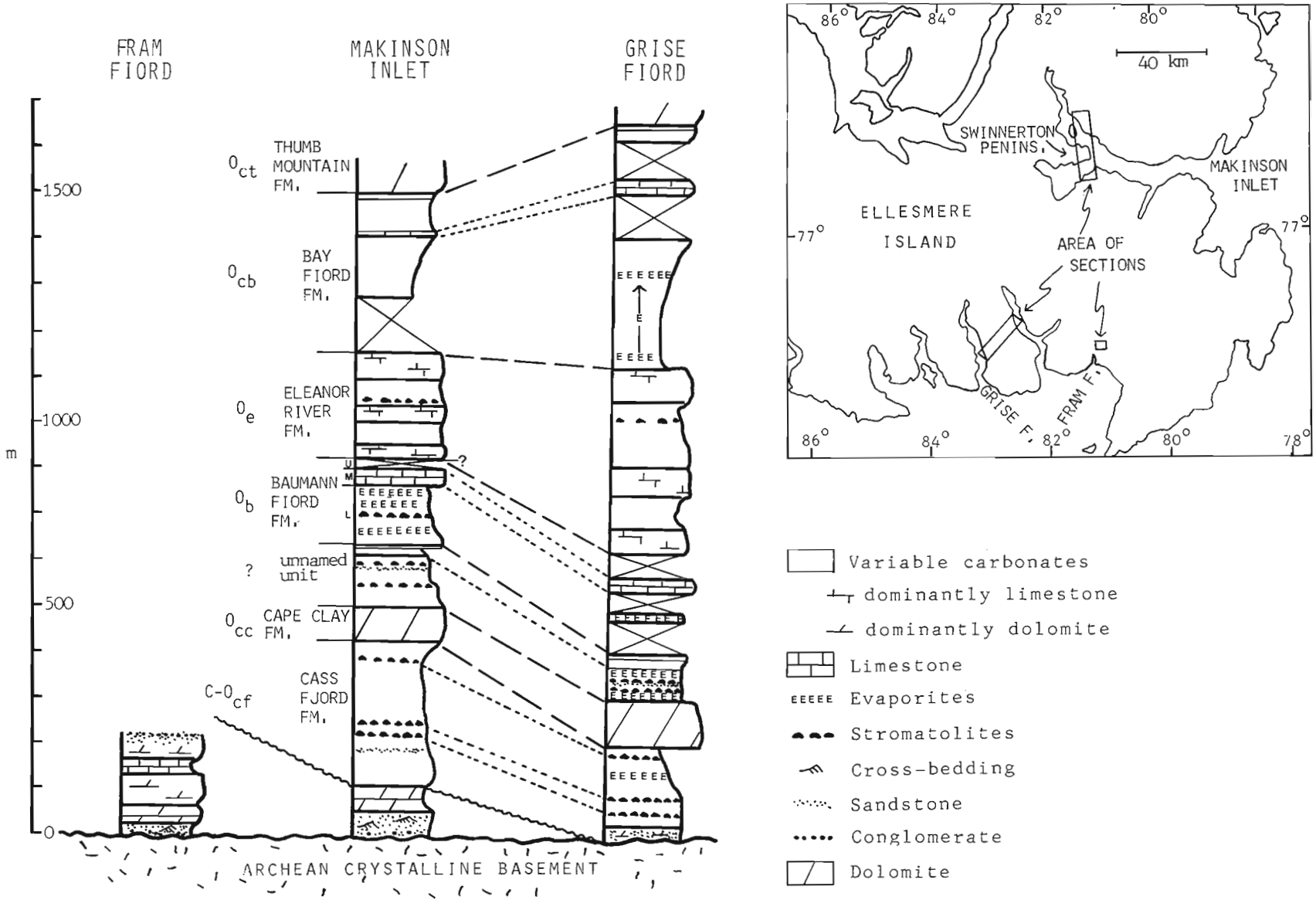

Figure 11.1. *Location of sections and correlation diagram of composite stratigraphic sections.*

grey limestone. On southern Ellesmere Island the Cass Fjord Formation is generally recessive and ranges in thickness from 170-338 m.

Makinson Inlet. The Cass Fjord Formation in the Makinson Inlet area can be subdivided into several distinctive, successive lithological packages. The base of the Cass Fjord is marked by a 0.2 m unit of rusty weathering, quartz pebble conglomerate, overlain by 8 m of interbedded massive, banded dolosiltite, dolomitic rubbly argillaceous limestone, and minor flat pebble conglomerate. The succeeding 15 m consist of thin, planar to slightly wavy bedded, unfossiliferous, argillaceous lime mudstone. Above the limestone is a 96 m interval of interbedded flat pebble conglomerate, massive dolosiltite, distinctive purple, grey and buff banded, massive dolosiltite, and wavy bedded, argillaceous, calcareous dolosiltite. Common structures within this interval include desiccation polygons, small channel infills, flaser bedding, and ripple crosslamination. A pronounced ledge forming, 4 m thick unit of massive, well sorted, medium grained quartz arenite occurs two thirds of the way up this interval.

Overlying the aforementioned interval a 50 m sequence characterized by four 1-2 m thick stromatolite boundstone units interbedded with massive dolosiltite and flat pebble conglomerate. One hundred and twenty metres above the stromatolite interval, there is a marked increase in quartz silt and sand impurities within a succession of lithologies otherwise similar to that found in the lower Cass Fjord beneath the stromatolites.

The upper 42 m of the formation consists of a simple alternation between thin bedded units of flat pebble conglomerate and rubbly argillaceous dolomitic limestone. The uppermost 6 m is ledge-forming, thick bedded, structureless, dark orange-brown, mottled, dolomitic carbonates capped by a veneer of thin bedded, green weathering, dolosiltite.

From a distance, the basal 120 m of the Cass Fjord Formation have an overall purple-red cast, and the upper 218 m a more subdued grey-green colouration.

Grise Fiord. In general, the rocks assigned to the Cass Fjord Formation in the Grise Fiord area can be subdivided into a) a basal 'atypical' sequence consisting of 50 m of light coloured, dolomitic, fine to coarse siliciclastics with basement-derived detritus, and b) an upper 120 m of typical dark carbonates.

The principal rock types in the lower sequence at Grise Fiord include 1-2 m units of interbedded dolosiltite and fine- to medium-grained arkosic to subarkosic sandstone. These units are commonly separated by thin, green-grey weathering shaly intervals (fissile dololutite). Less common are scattered, thin horizons of flat pebble conglomerate and massive, weakly banded dololutite. Convolute and contorted laminations are common; these dewatering structures are suggestive of rapid deposition. Large lithoclasts (up to 20 mm long) of crystalline basement rock are common in conglomerate lenses in the basal 10 m. They also occur up to 35 m above the unconformity as free floating clasts in a fine sand matrix. The clasts are free-floating in a fine sand matrix. Poorly preserved ripple crosslaminae occur, but bedding is represented principally by planar and/or contorted laminae.

The upper sequence begins with a lower, 45 m interval dominated by four major stromatolitic boundstone units. This is overlain by 110 m of interbedded quartz silt-rich flat pebble conglomerate, laminated dolosiltite, and massive, weakly banded dololutite with minor evaporite (satin spar gypsum). The uppermost beds show a reduction in the number of lithological variants, and consist of alternating thin units of flat pebble conglomerate and argillaceous, laminated dolosiltite. The highest beds and the upper contact of the Cass Fjord Formation were not examined at this locality.

Age and Correlation. The Cass Fjord Formation ranges from Middle Cambrian to Lower Ordovician (Christie et al., 1981).

There is a striking similarity between the upper 218 m of the Cass Fjord at Makinson Inlet, and the upper sequence at Grise Fiord. Not only are the general lithological successions and the unit thicknesses similar, but there appears to be a one to one correlation between principal stromatolite boundstone units. The only stratigraphic dissimilarity between the two areas in the upper part of the formation, is the presence of evaporite beds in the Grise Fiord area. The basal 50 m of the Cass Fjord at Grise Fiord have no lithological equivalent in the lower 119 m of the formation at Makinson Inlet.

Cape Clay Formation

In both study areas the Cape Clay Formation is a resistant, ledge-forming, readily mappable unit of massive- to thick-bedded calcareous dolostone. It conformably overlies the Cass Fjord Formation.

No section containing both upper and lower contacts was examined and thus the calculation of total thickness for the formation is based in part on graphic methods. The 65 m figure obtained for the Makinson Inlet area is considered a minimum, whereas the 135 m thickness for the Grise Fiord section is considered a maximum.

Although essentially homogeneous, the Cape Clay Formation shows minor vertical and lateral lithological variations. The abundance of chert nodules, the degree of porosity (2-20%), the pervasiveness of labyrinthine mottling, and the weathering colour, all exhibit various degrees of development. At Makinson Inlet, the basal contact of the Cape Clay is placed at the first occurrence of massive, unmottled, brown weathering, medium crystalline dolostone, following the last unit of flat pebble conglomerate in the underlying Cass Fjord. The upper contact is structurally conformable but abrupt, showing a change from rusty brown weathering, pyritiferous, resistant and massive, medium crystalline dolostone with minor chert nodules, to a recessive, medium buff and grey mottled, wavy banded, blocky weathering, medium crystalline dolostone with 20% chert nodules. From a distance, a very subtle light-dark banding can be discerned in the upper 20 m of the formation.

At Grise Fiord the lower contact is conformable and gradational, showing a progressive loss upwards of fabric detail due to increased dolomitization. This is reflected in an apparent phasing out of flat pebble conglomerates in the uppermost part of the Cass Fjord Formation. The beds associated with the uppermost contact of the Cape Clay, are massive, medium brown to brown grey, in part mottled, calcareous dolostone that exhibit a vague packstone texture with ghosts of peloids and/or intraclasts. The uppermost surface of the Cape Clay Formation at Grise Fiord has an irregular topography (relief ± 0.2 m), and the contact itself is abrupt.

Age and Correlation. The Cape Clay Formation has been dated as Early Ordovician (Christie, 1977; Christie et al., 1981). It can be traced over much of the Arctic Platform and remains largely consistent in thickness and lithological composition within its outcrop distribution.

Unnamed Stratigraphic Unit

Between the Cape Clay and Baumann Fiord formations is a largely recessive, thin- to medium-bedded, grey to buff weathering, predominantly carbonate sequence. It attains thicknesses of 158 m in the Makinson Inlet area and 102 m in the Grise Fiord area. In both areas the upper contacts are abrupt and conformable.

In the Makinson Inlet area, the lower 102 m consist of thin- to medium-bedded units of planar calcilutite and calcisiltite mudstone, flat pebble conglomerate, massive weakly banded dolosiltite and rare units of stromatolitic boundstone. There is an overall upward gradational change from dolostone to limestone, but throughout there is consistent medium grey weathering. The upper 55 m are poorly exposed but show a generally similar suite of lithologies, except that most units contain between 10-40% quartz silt and sand impurities. The uppermost 25 m form a prominent resistant ledge composed in part of a massive, nonbedded mottled carbonate with a distinctive clotted texture (cryptalgal?). Similar lithologies have been termed thrombolites (Aitken, 1967; Rubin and Friedman, 1977).

In Grise Fiord a nearly identical, although thinner, lithological sequence is preserved. Indeed several distinctive marker horizons are found in similar stratigraphic positions at both localities. The only significant difference is the presence of evaporites (comprising 13% of total thickness) in the lower 65 m of the Grise Fiord section.

Age and Correlation. The unnamed unit is tentatively assigned an Early Ordovician age, based solely on its stratigraphic position. It can be correlated with the lower part of the 'unnamed Lower Ordovician carbonate beds' of Devon Island (Christie, 1977), and with 'map-unit 6' of Bache Peninsula (Christie, 1967), both of which contain lithological suites similar to those of southern Ellesmere Island, although neither includes evaporite intervals.

Baumann Fiord Formation

The Baumann Fiord Formation was named by Kerr (1967) for a thick, conformable, recessive, predominantly anhydritic formation that occurs in south central Ellesmere Island. Kerr (op. cit.) proposed three members for the formation, a lower anhydritic member, a middle resistant limestone member, and an upper anhydritic limestone member. Sections of the Baumann Fiord Formation situated within the Arctic Platform (Central Stable Region of Kerr, 1968) studied by Mossop (1979), indicate a range of total thickness for the formation on the Platform of between 200 and 275 m. The proportion of each member relative to the middle limestone member ranges as follows: 2.6-6.4 (lower): 1:1.2-1.6 (upper).

The Baumann Fiord Formation is well exposed in the Makinson Inlet area, but is very poorly exposed at Grise Fiord. However in both areas the tripartite division of the formation is well developed and readily recognized. The ratios of the three members at Grise Fiord are 4.2-4.8 :1: 1.2-1.6 with a composite thickness of 206 m. The Baumann Fiord is 184 m thick at Makinson Inlet, with member ratios of 4.3:1:0.7. At Makinson Inlet the Baumann Fiord Formation is conformably overlain by an 8 m thick resistant ledge of thin, planar bedded lime mudstone, and this represents the uppermost exposed beds of the section. The assignment of these beds to the lowermost Eleanor River Formation or to the upper member of the Baumann Fiord Formation is somewhat arbitrary. Its ledge-forming characteristic is more typical of the Eleanor River Formation, but the basal resistant interval of the Eleanor River Formation at Grise Fiord is considerably thicker and truly cliff forming. In addition, the total thickness of the Baumann Fiord Formation and the thickness ratio of the upper member are both quite low values, suggesting that the upper member may be incompletely represented and should include at a minimum the 8 m resistant ledge.

The lower member (60% exposed in the Makinson Inlet section) consists of interbedded evaporite, fissile grey-green dolosiltite, massive buff to light grey dolosiltite, massive-weathering laminate, medium crystalline brown weathering dolostone, minor stromatolitic boundstone units and flat pebble conglomerate. The evaporite intervals make up 44% of exposed strata in the lower member and consist of laminar and 'chicken-wire' anhydrite, as well as the more common in situ or remobilized secondary hydration products (efflorescent and satin-spar gypsum).

The resistant, ledge-forming middle member is nearly completely exposed in both study areas, and shows little variation between sections. Medium- to thick-bedded, dense, dark grey intraclastic and skeletal packstone, and flat pebble conglomerate constitute the principal rock types. Stromatolitic boundstones cap the middle member in both localities.

The recessive upper member is poorly exposed at Makinson Inlet and not exposed at Grise Fiord. Evaporites occur at the base of the member and are gradationally succeeded by massive (gypsiferous?) dolosiltites.

Age and Correlation. The Baumann Fiord Formation is entirely Early Ordovician in age (Mossop, 1979; Mayr et al., 1978).

The Baumann Fiord of the study areas correlates well on a large scale with other published sections of the formation from Ellesmere. Smaller scale cycles, such as those described by Mossop (1979) were not observed in the sections studied.

Eleanor River Formation

The Eleanor River Formation (Thorsteinsson, 1958; Kerr, 1967) outcrops on southern Ellesmere as a thick, resistant, ledge-forming, dark limestone unit, that conformably overlies the Baumann Fiord Formation and is in turn conformably overlain by the Bay Fiord Formation. In the Grise Fiord area, the measured thickness of the Eleanor River Formation is 420 m. At Makinson Inlet a continuous section containing both upper and lower contacts was not found. On Swinnerton Peninsula (Makinson Inlet) a 231 m sequence of the Eleanor River is preserved that contains the upper contact so that the thickness obtained is a minimum. However, for reasons outlined below, it may be considered close to the true thickness in this area.

---

a. View of east side of Grise Fiord; ? – unnamed stratigraphic unit.

b. North side of Makinson Inlet, view towards southeast.

c. Three resistant intervals of the Eleanor River Formation, Grise Fiord.

d. Three resistant intervals of the Eleanor River Formation, Makinson Inlet.

e. Bay Fiord Formation at Grise Fiord (522 m). Arrow indicates position of fossiliferous resistant limestone member.

f. Fram Fiord. Units 1 to 4 are tentatively correlated with the Rensselaer Bay Formation, Cape Leiper Formation, Cape Ingersoll Formation, and the Police Post Formation respectively.

Figure 11.2. *Oblique views of sections (see Figure 11.1 for explanation of symbols).*

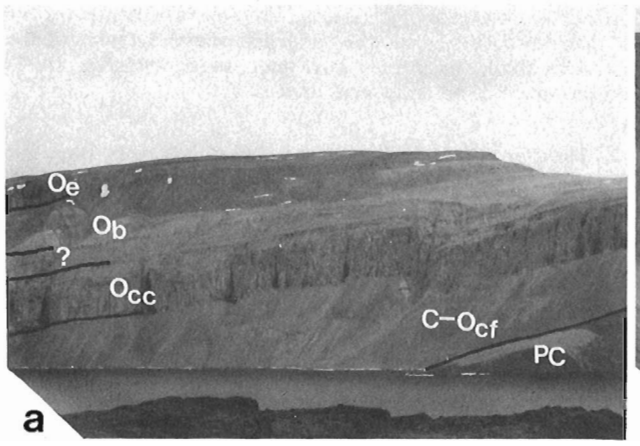
Oe
Ob
?
Occ
C–Ocf
PC
a


Occ
?
Ob
C–Ocf
b

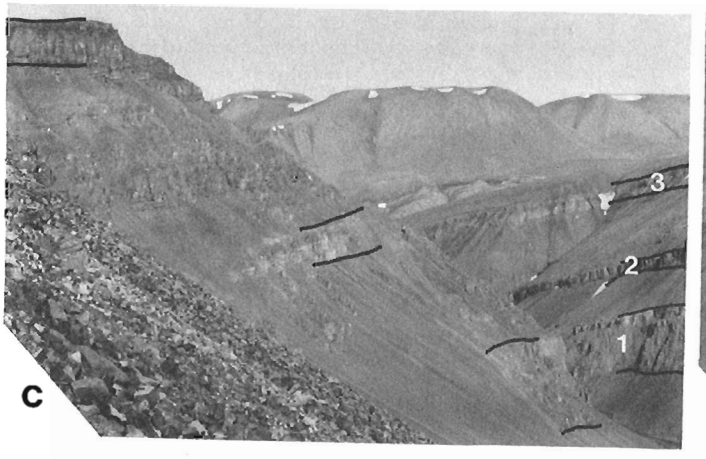
3
2
1
c

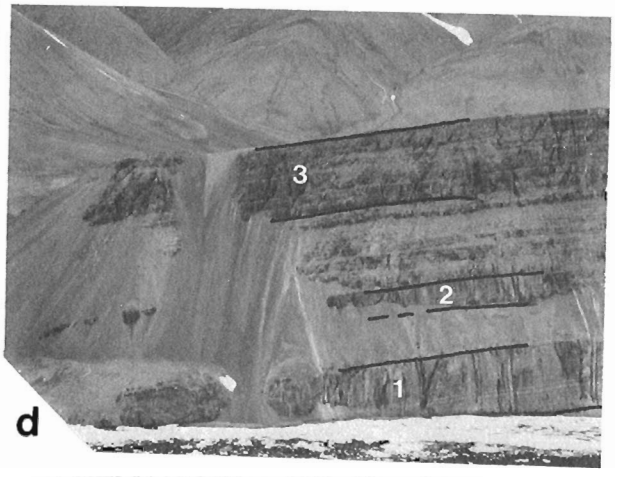
3
2
1
d

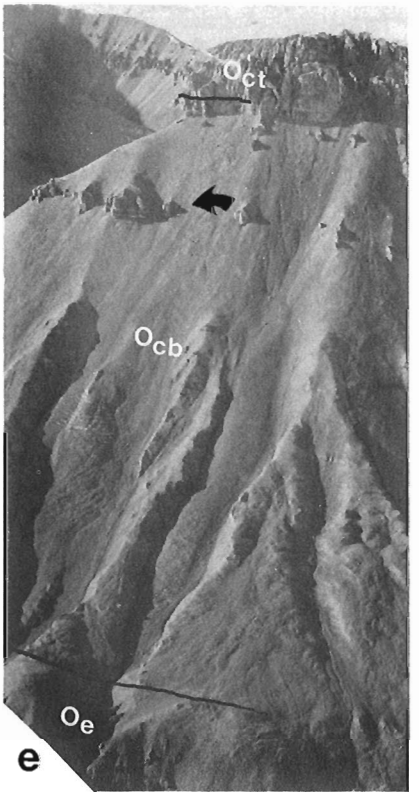
Oct
Ocb
Oe
e

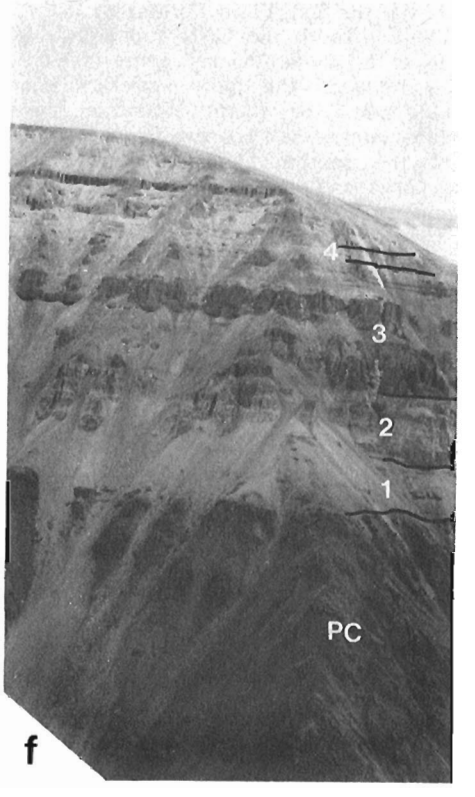
4
3
2
1
PC
f

Less resistant intervals within the Eleanor River Formation contain diverse rock types. Some of these, in approximate order of abundance, are: medium grey, planar, medium bedded, laminated calcisiltite mudstone; fossiliferous, faintly mottled, buff and light grey lime wackestone; massive, weakly banded, buff to orange weathering dolosiltite; flat pebble conglomerate; and stromatolitic boundstone.

Resistant intervals in both study areas form ledges that make up to 52% of the formation's stratigraphic thickness. The ledges consist of dense, nonbedded, poorly fossiliferous, finely crystalline, intraclastic lime packstone to mudstone. This lithology weathers a dark brownish grey that is in places mottled. The sections at Grise Fiord and on Swinnerton Peninsula show a distinctive, five-fold division formed by resistant ledges occurring at the base and the top of the sections, with a third ledge occurring in the middle. The thicknesses of the upper and lower resistant ledges are comparable in the two areas, as are the overall stratigraphic successions. Substantial thickness variation is restricted to the middle divisions of the formation. Thus the Makinson Inlet thickness for the Eleanor River Formation is considered to approach the true formational thickness in this area.

The upper contact in both areas occurs just below the first sustained occurrence of buff-orange weathering dololaminate.

Age and Correlation. Mayr et al. (1978) suggest a late Early to early Middle Ordovician age for the Eleanor River Formation.

This formation is widespread throughout the central Arctic Islands and is typically a thick, resistant, stratigraphic unit composed of fossiliferous, dense limestones.

Bay Fiord Formation

The basal formation of the Cornwallis Group (Thorsteinsson, 1958), the Bay Fiord Formation (Kerr, 1967), outcrops extensively in both the Grise Fiord and Makinson Inlet areas. It is a predominantly recessive unit that conformably lies between the more resistant underlying Eleanor River and overlying Thumb Mountain formations. Although complete thicknesses are available in both study areas, much of the section (64%) lies beneath talus. Fortunately the upper and lower contacts are exposed and measured thicknesses for the Bay Fiord include 348 m for Makinson Inlet and 522 m for Grise Fiord. The upper half of the formation is well exposed in the Makinson Inlet area, and the lower half at Grise Fiord. The differences in principal lithotypes between the two areas may reflect the accident of exposure rather than any real difference in lithology.

Grise Fiord. The basal 250 m consist of argillaceous, weakly laminated, light green to buff-brown weathering dololutite interbedded with evaporite. The wide variety of sulphate salt morphotypes in the section includes secondary gypsum (efflorescent, satin-spar, alabastrine) and anhydrite (nodular 'chicken-wire', laminar). The evaporite units are commonly deformed, show minor 's' and 'z' folds, pinch-and-swell structures, and are associated with outcrop-scale overturned folds and thrust faults.

The upper 270 m are poorly exposed except for one resistant ledge 33 m thick, composed of weakly banded dolosiltite, massive- to thick-bedded mottled carbonate, and fossiliferous lime wackestone.

The upper contact is placed just below the first continuous sequence of massive buff-brown and dark grey mottled dolomitic carbonate, and just above a series of three 0.2-0.4 m thick, light grey-buff to orange, massive, fine- to medium-crystalline dolostone layers.

Makinson Inlet. The basal 120 m of the Bay Fiord Formation are not exposed. The upper 227 m are 72% exposed and consist principally of rubbly weathering, massive to weakly laminated, very dark grey argillaceous dololutite, medium brown, massive, fine- to medium-crystalline dolostone, grey-green weathering, fissile dolosiltite, mottled carbonate, quartzose, weakly laminated dolosiltite, and rare units of solution breccia. Minor efflorescent gypsum occurs as thin crusts on some of the aforementioned rock types, but no discrete evaporite beds are present. A resistant ledge with fossiliferous layers occurs in a stratigraphic position similar to that of a ledge in the Grise Fiord area.

The upper contact with the Thumb Mountain Formation is very similar to that described for the Grise Fiord area, except that only two light coloured dolomitic bands are present.

Age and Correlation. The age of the Bay Fiord Formation is early Middle to late Middle Ordovician on western Ellesmere Island (Mayr et al., 1978). This age is in part corroborated by fossils obtained in the course of this study, from the resistant limestone interval of the Bay Fiord Formation. Disarticulated echinoderm calyx plates, strongly resembling Chazyan age forms illustrated by Sprinkle (1971) and possibly referable to the genus **Palaeocystites**, were recovered 402 m above the base of the formation at Grise Fiord.

Current studies by Thorsteinsson and Mayr indicate that the Bay Fiord Formation on Devon Island can broadly be subdivided into five units. All five are recognized in the Grise Fiord area, suggesting a marked lateral consistency within the formation. Sections of the Bay Fiord Formation from the geosyncline on Ellesmere described by Kerr (1967), indicate only slightly greater thicknesses of the formation towards the geosyncline. The occurrence of evaporite restricted to the basal half of the formation is common to both areas.

---

a. Stromatolitic boundstone unit of the Cass Fjord Formation.

b. Clotted texture in a mottled carbonate. Distinctive fabric (thrombolitic?) of the uppermost unit of the unnamed stratigraphic unit.

c. Massive, rubbly weathering, dark grey (fresh) dololutite, typical of Bay Fiord Formation.

d. Faintly banded, massive, medium grey weathering dolosiltite with preserved isolated ripple crosslaminae.

e. Laminar anhydrite of Baumann Fiord Formation.

f. Satin spar gypsum (ss) of the Bay Fiord Formation.

g. Two units (A&B) of flat pebble conglomerate showing both edgewise and shallow imbricate clast orientations. Arrow points to irregular topography of hardground surface.

h. Bedding plane view of flat pebble conglomerate.

Figure 11.3. *Characteristic lithotypes of Lower Paleozoic succession on southern Ellesmere Island.*

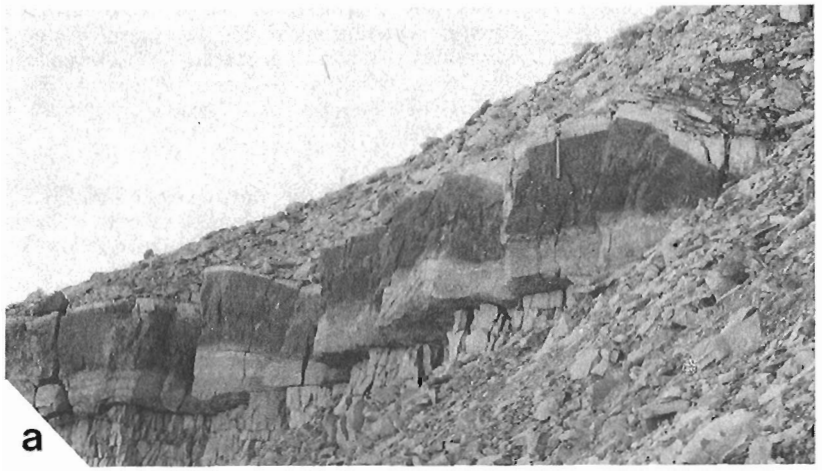
a

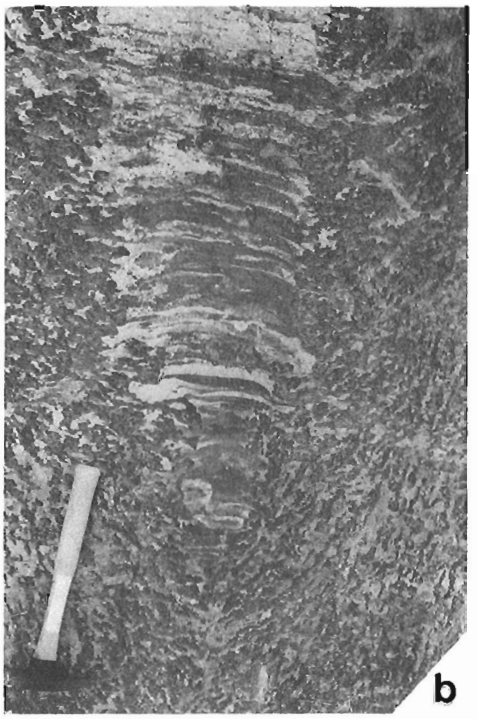
b

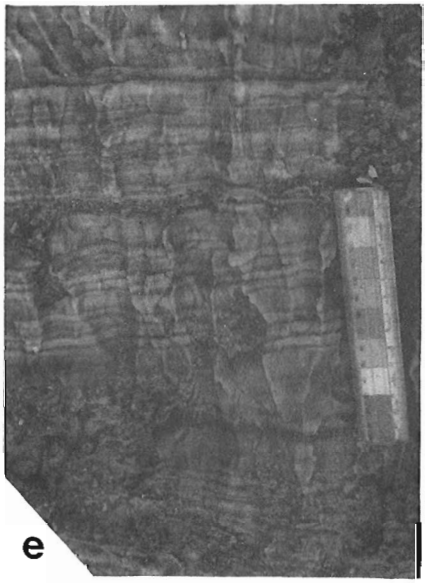
e

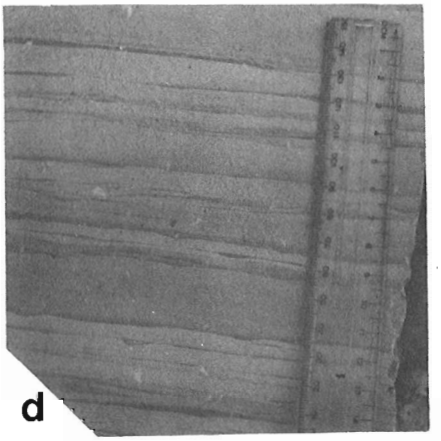
d

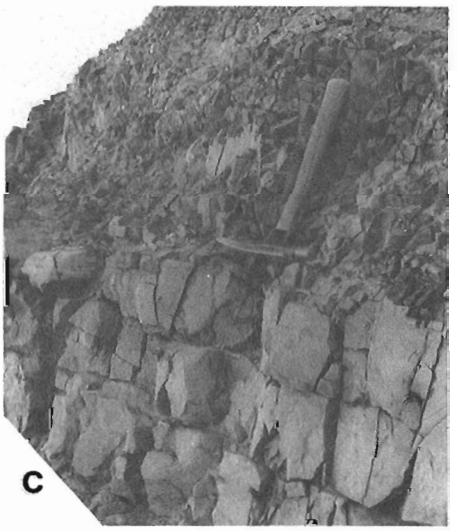
c

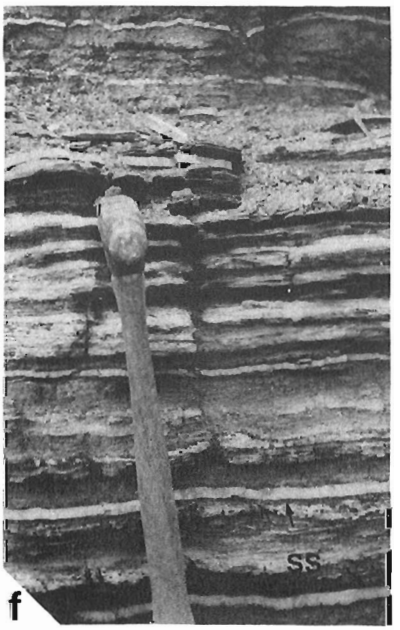
SS
f

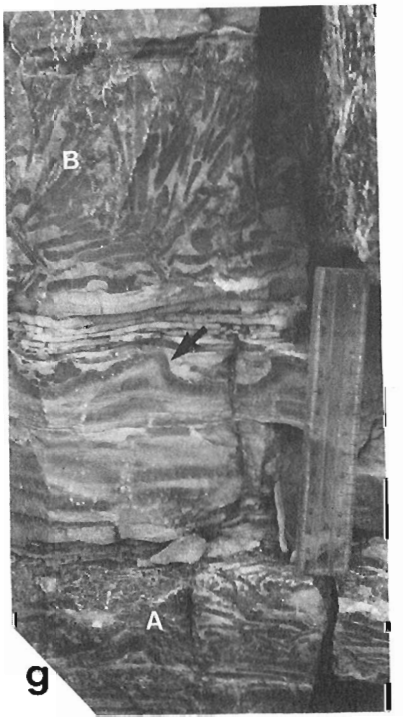
B
A
g

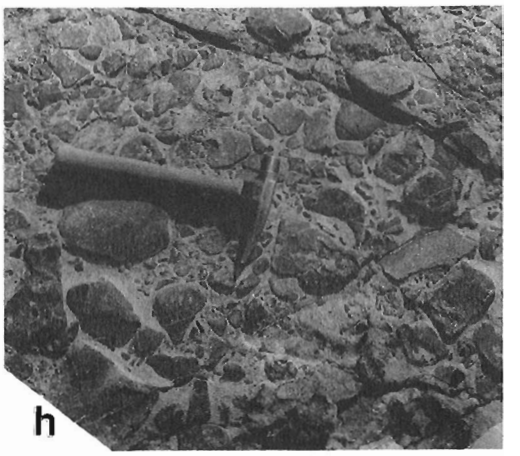
h

References

Aitken, J.D.
1967: Classification and environmental significance of cryptalgal limestones and dolomites, with illustrations from the Cambrian and Ordovician of southwestern Alberta; Journal of Sedimentary Petrology, v. 37, p. 1163-1178.

Christie, R.L.
1967: Bache Peninsula, Ellesmere Island, District of Franklin; Geological Survey of Canada, Memoir 347.

1977: Stratigraphic reconnaissance of lower Paleozoic rocks, eastern Devon Island, Arctic Archipelago; in Report of Activities, Part B, Geological Survey of Canada, Paper 77-1B, p. 217-226.

Christie, R.L., Embry, A.F., and Van Dyck, G.E.
1981: Lexicon of Canadian Stratigraphy, Volume 1, Arctic Archipelago (District of Franklin); Canadian Society of Petroleum Geologists, Calgary.

Kerr, J.W.
1967: New nomenclature for Ordovician rock units of the eastern and southern Queen Elizabeth Islands, Arctic Canada; Bulletin of Canadian Petroleum Geology, v. 15, p. 91-113.

1968: Stratigraphy of central and eastern Ellesmere Island, Arctic Canada, Part II: Ordovician; Geological Survey of Canada, Paper 67-27, part II.

Mayr, U., Uyeno, T.T., and Barnes, C.R.
1978: Subsurface stratigraphy, conodont zonation and organic metamorphism of the Lower Paleozoic succession, Bjorne Peninsula, Ellesmere Island, District of Franklin; in Current Research, Part A, Geological Survey of Canada, Paper 78-1A, p. 393-398.

Mossop, G.D.
1979: The evaporites of the Ordovician Baumann Fiord Formation, Ellesmere Island, Arctic Canada; Geological Survey of Canada, Bulletin 298.

Okulitch, A.V. and Mayr, U.
1982: Stratigraphic and structural studies, southern Ellesmere Island, N.W.T.; in Current Research, Part A, Geological Survey of Canada, Paper 82-1A, note.

Poulsen, C.
1927: The Cambrian, Ozarkian and Canadian faunas of northwest Greenland; Meddelelser om Groenland, v. 70, no. 2, p. 233-343.

Rubin, D.M. and Friedman, G.M.
1977: Intermittently emergent shelf carbonates: An example from the Cambro-Ordovician of eastern New York State; Sedimentary Geology, v. 19, p. 81-106.

Sprinkle, J.
1971: Stratigraphic distribution of echinoderm plates in the Antelope Valley Limestone of Nevada and California; United States Geological Survey, Professional Paper 750-D, p. D89-D98.

Thorsteinsson, R.
1958: Cornwallis and Little Cornwallis islands, District of Franklin, Northwest Territories; Geological Survey of Canada, Memoir 294.

12. PRELIMINARY REPORT ON UPPER ORDOVICIAN TO UPPER SILURIAN CARBONATES BAUMANN FIORD AREA, SOUTHWESTERN ELLESMERE ISLAND, DISTRICT OF FRANKLIN

Project 810016

Jean-Luc Poey[1]
Institute of Sedimentary and Petroleum Geology, Calgary

Poey, Jean-Luc, Preliminary report on Upper Ordovician to Upper Silurian carbonates, Baumann Fiord area, southwestern Ellesmere Island, District of Franklin; in Current Research, Part A, Geological Survey of Canada, Paper 82-1A, p. 75-77, 1982.

Abstract

The Upper Ordovician – Lower Devonian Allen Bay Formation and Read Bay Group are a sequence of partially dolomitized, shallow shelf carbonates, throughout the Arctic Islands. Towards the northwest however, this sequence undergoes a major facies change to basinal shales. This facies boundary tends generally northeast bisecting the area studied at Baumann Fiord, on Ellesmere Island. Two trends can clearly be observed in rocks representing the transitional slope environment. First, slope and shelf margin debris flows become predominantly basinal carbonate mudstone, and eventually calcareous shale northwestward. Second, there is a general upsection trend from shelf and slope facies to basinal carbonates and calcareous shale. A major break occurs at a cherty, fine dolomitic interval, with shelf limestones and dolostones beneath and slope and basinal carbonates above ranging from debris flow breccias to laminated carbonates and calcareous shales. The intervening cherty unit provides a widespread, distinctive lithological marker.

Introduction

From Proterozoic to Late Devonian times the northwestern part of what is today the Canadian Arctic Islands, was the site of a huge NE-trending basinal structure called the Franklinian Geosyncline or Basin. Along its southeast margin is a facies transition from shelf carbonates to basinal mudstones. The area studied in eastern Baumann Fiord (SW Ellesmere Island), and seven sections of Upper Ordovician to Lower Devonian rocks, straddle this facies line. The rocks of interest are undivided shelf carbonates of the Allen Bay – Formation and Read Bay Group and their lateral basinal equivalent, the Cape Phillips Formation. Field work in 1981 (see Okulitch and May, 1982) involved measuring and describing sections, lithological and paleontological sampling, and collection of samples for conodont analysis.

Geological Setting

The Franklinian Geosyncline was a major influence on the depositional history of this area. Shelf carbonates were deposited to the northeast (Trettin, 1979), east (Kerr, 1976), southeast and south (Kerr, 1975; Miall and Kerr, 1980) of the study area. These include the Allen Bay Formation, represented mostly by massive, medium grained, sparsely fossiliferous, somewhat vuggy and petroliferous dolostone, and the overlying Read Bay Group, composed of nodular limestone. However, the sediments and depositional environments are quite distinct and clearly transitional from shelf to basin environments. A gradual northwestward transition from shelf carbonates to slope carbonate turbidites and then to more basinal graptolitic mudstones and shales occurs upsection (Kerr, 1976). The latter represent depositional environments similar to those Davies (1977) interpreted for Upper Paleozoic deepwater carbonates of the Sverdrup Basin. All sections studied in 1981 include rocks representing this slope to basin transition.

Stratigraphy

The Irene Bay Formation underlies the studied sequence, and consists of typically light grey weathering, medium bedded, mottled limestone. Cephalopods, gastropods, crinoids, brachiopods and **Receptaculites** are present, but in general fossils are scarce.

The Allen Bay – Read Bay sequence can be subdivided into five informal units, lettered A to E (Fig. 12.1).

Unit A

Unit A consists of medium bedded, dark grey, light grey weathering, mottled limestone. It is poorly fossiliferous and contains crinoids, brachiopods, gastropods, nautiloids, solitary rugosans, **Receptaculites** and **Pseudogygites.** The unit is between 95 and 150 m thick. The lower part of the unit is similar to the Irene Bay Formation. This together with the fact that the fossil content is also similar would make the Irene Bay Formation and the lowest Allen Bay Formation indistinguishable if it was not for a distinctive, somewhat darker 5 m thick interval at the base of the Allen Bay Formation (Fig. 12.1).

Unit B

This unit consists of massive dolostone and is between 50 and 80 m thick. The dolostone has a very distinctive texture represented by dark brown, petroliferous, very irregular nodules of finely crystalline dolomite in a matrix of light grey, medium crystalline dolomite. Fossils are rare but silicified and include crinoids, brachiopods, solitary rugosans, **Syringopora** sp., **Favosites** sp., **Halysites** sp., and heliolitids. Stylolites are common. The lower contact of unit B is abrupt and is believed to coincide with the Ordovician-Silurian boundary (Thorsteinsson, personal communication, 1981).

Unit C

This unit is 30 to 110 m thick and forms an excellent marker in the area. It consists of dark brown, fine- to medium-crystalline, very petroliferous dolostone, commonly containing chert nodules. Fossils are scarce but include crinoids, brachiopods, **Favosites** sp., nautiloids and gastropods. Unit C forms a major break in the succession; underlying strata representing shelf environments whereas rocks overlying unit C are slope deposits.

Unit D

Overlying the chert-rich unit is a complex series of intercalated debris flows. The varied lithologies occur in repeated cycles with an ideal complete sequence consisting

[1]Department of Geology, University of Ottawa, 770 King Edward Ave, Ottawa, Ontario K1N 6N5

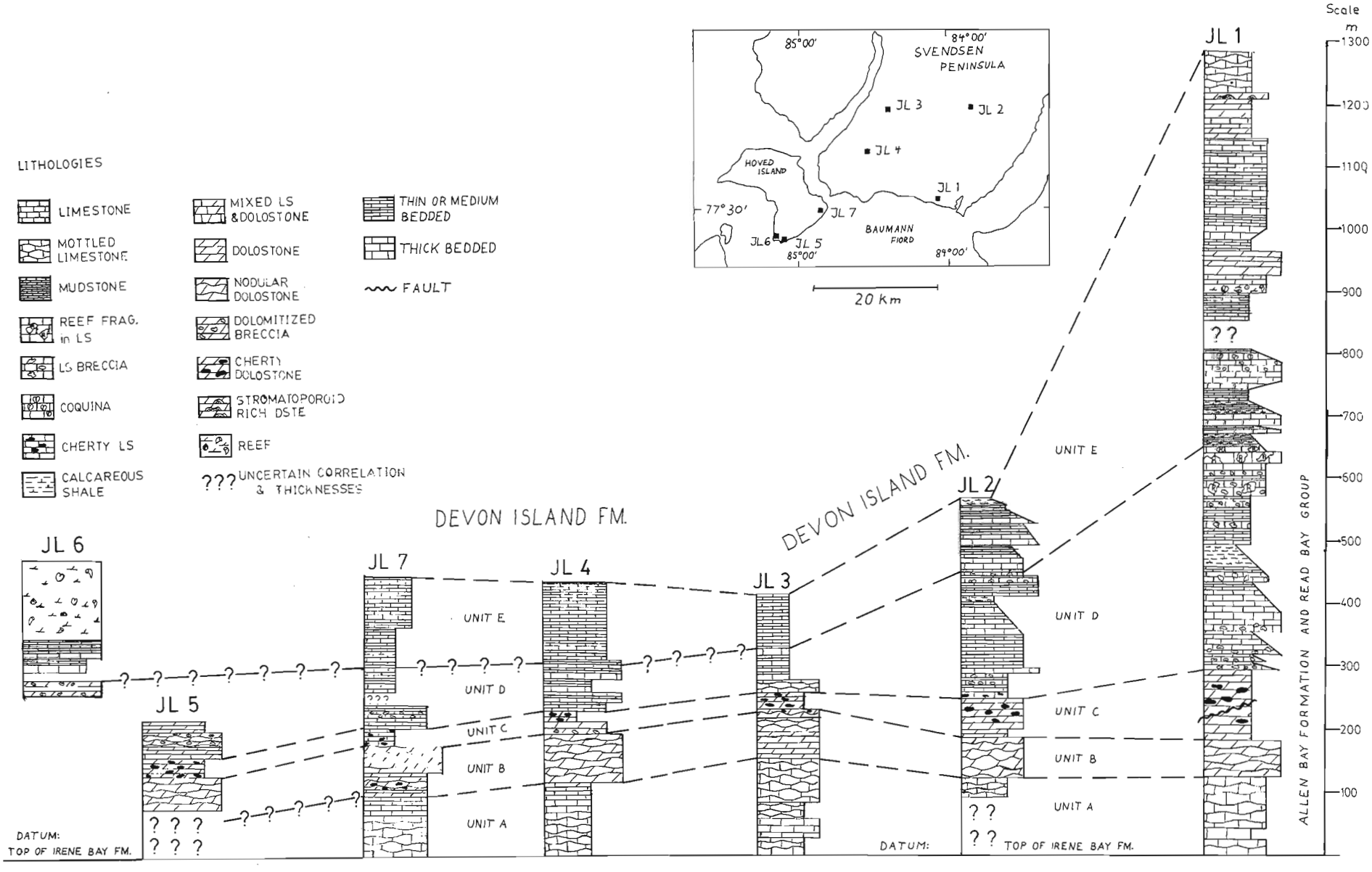

Figure 12.1. *Location of sections and correlation of Ordovician and Silurian carbonates in the Baumann Fiord area.*

of breccias, usually with mudstone clasts, succeeded by grainstones and packstones (crinoidal bioclastics), wackestones, bedded mudstones, laminated mudstones and calcareous shales. However, many of the flows show less complete sequences because of truncation and incomplete depositional cycles. A few beds of pentamerid coquina also occur, as well as olistostromes of huge blocks of reefal material. Unit D is a highly varied, petroliferous sequence which ranges from 75 to 360 metres in thickness.

Unit E

The uppermost unit studied varies from 90 to 625 metres thick. It consists mostly of laminated mudstone with rare breccias and bioclastic rocks. The rocks are a graptolitic facies and may represent distal debris flows.

There are two types of laminated mudstone. One is interbedded with argillaceous partings and contains diverse graptolite assemblages including **Monograptus** sp., **Crytograptus** sp., **Nemagraptus** sp., **Dendograptus** sp., **Retiolites** sp., **Acanthograptus** sp. and **Diplograptus** sp. Other fossils include ostracoderms, brachiopods, cephalopods and trilobites together with trace fossils such as **Planolites** sp., **Skolithos** sp. and trilobite tracks. The second type of mudstone is also laminated, does not contain argillaceous partings but is distinguished by conchoidal fracturing. A reefal section (Fig. 12.1, 3L 6) was measured on Hoved Island and these rocks probably correlate with units D and E. They consist of medium and coarsely crystalline dolostone. Very good intergranular and vuggy porosity is developed. In this reef only the margin has remnants of fossils such as crinoids, solitary and colonial rugosans, **Syringopora** sp., favositids, halysitids and heliolitids. The centre seems to be dolomitized mud.

Interpretation

Tentative interpretation of the Ordovician-Silurian carbonate sequence is as follows: Units A and B apparently represent shelf environments (Kerr, 1976); Unit C is typical of shelf edge and shelf foreslope (Davies, 1977), and Units D and E were deposited on a slope (Davies, 1977; Mayr, 1973).

Conclusion

Research to date shows that the Upper Ordovician to Lower Devonian sequence of carbonates in the study area is a transgressive cycle representing shelf to foreslope to slope, to basinal depositional environments. The basinal character predominates to the northwest. Problems to be resolved by work in 1982-83 include location of the Ordovician-Silurian boundary, precise correlation between sections, interpretation of the apparently complex diagenetic history and determination of the number and extent of the reefal periods, as well as details of depositional environments.

References

Christie, R.L., Embry, A.F., and Van Dyck, G.A.
1981: Lexicon of Canadian Stratigraphy, Volume 1, Arctic Archipelago; Canadian Society of Petroleum Geologists, 123 p.

Davies, G.R.
1977: Turbidites, debris sheets, and truncation structures in Upper Paleozoic deep-water carbonates of the Sverdrup Basin, Arctic Archipelago; Society of Economic Paleontologists & Mineralogists, Special Publication no. 25, p. 221-247.

Kerr, J.W.
1975: Cape Storm Formation – a new Silurian unit in the Canadian Arctic; Bulletin of Canadian Petroleum Geologists, v. 23, no. 1, p. 67-83.

1976: Stratigraphy of central and eastern Ellesmere Island, Arctic Canada, Part III, Upper Ordovician (Richmondian), Silurian and Devonian; Geological Survey of Canada, Bulletin 260, 55 p.

Mayr, U.
1973: Lithologies and depositional environments of the Allen Bay-Read Bay formations (Ordovician-Silurian) on Svendsen Peninsula, central Ellesmere Island; in Proceedings of the Symposium on the Geology of the Canadian Arctic, J.D. Aitken and D.J. Glass, ed., p. 143-158.

Miall, A.D. and Kerr, J.W.
1980: Cambrian to Upper Silurian stratigraphy, Somerset Island and northeastern Boothia Peninsula, District of Franklin, N.W.T.; Geological Survey of Canada, Bulletin 315, 43 p.

Okulitch, A.V. and Mayr, U.
1982: Stratigraphic and structural studies, southern Ellesmere Island, N.W.T.; in Current Research, Part A; Geological Survey of Canada, Paper 82-1A, note.

Trettin, H.P.
1979: Middle Ordovician to Lower Devonian deep water succession at southeastern margin of Hazen Trough, Canon Fiord, Ellesmere Island; Geological Survey of Canada, Bulletin 272, 84 p.

13. SEDIMENTOLOGY OF THE LATE MIDDLE AND UPPER DEVONIAN OKSE BAY GROUP, SOUTHWESTERN ELLESMERE ISLAND: A PROGRESS REPORT

Project 810016

Randy J. Rice[1]
Institute of Sedimentary and Petroleum Geology, Calgary

Rice, Randy, J., Sedimentology of the late Middle and Upper Devonian Okse Bay Group, southwestern Ellesmere Island: a progress report; in Current Research, Part A, Geological Survey of Canada, Paper 82-1A, p. 79-82, 1982.

Abstract

Descriptions and brief preliminary interpretations of five sections measured in three of the five formations of the Okse Bay Group on southwestern Ellesmere Island are presented. The Strathcona Fiord Formation, the lowermost unit, displays a regional and vertical variation in depositional environment from entirely fluvial to paralic. Lower and upper Fram sections on the north limb of the Schei Syncline and a Hell Gate section on the south limb all indicate fluvial depositional environments.

Introduction

A sedimentologic study of the late Middle and Upper Devonian Okse Bay Group was undertaken as part of the regional mapping project on Ellesmere Island initiated by the Geological Survey of Canada (see Okulitch and Mayr, 1982). The study area on Ellesmere Island is shown in Figure 13.1 along with the location of sections measured during the 1981 field season. The Okse Bay Group constitutes the clastic wedge of the Franklinian miogeosyncline in the eastern Arctic Archipelago and cumulatively contains approximately 3000 m of siliclastic sediments (Embry and Klovan, 1976). The stratigraphic framework of the Okse Bay Group has been established through the work of McLaren (1963) and Embry and Klovan (1976).

The Strathcona Fiord, Hecla Bay, Fram, Hell Gate and Nordstrand Point formations are the five constitutent formations of the Okse Bay Group in ascending stratigraphic order.

Strathcona Fiord Formation

Two sections were measured in this formation, S1 and S2 (Fig. 13.1). The first is a basal section representing ~24% of the total formation thickness in that area on the northern limb of the Schei Syncline. The second is a section through the entire formation on the southern limb of the syncline.

Section S1. This section was measured on the eastern side of outer Stenkul Fiord. The Strathcona Fiord Formation at this location is approximately 1168 m thick and weathers dominantly red. It overlies bioclastic limestone, uppermost strata of the Blue Fiord Formation. The Blue Fiord Formation is not present due to a facies transition with the Strathcona Fiord Formation causing the former to pinch out and the latter to increase in thickness (Thorsteinsson and Okulitch, 1981, personal communication). Approximately 886 m of the Strathcona Fiord Formation are poorly exposed to completely covered. Only the lower 283 m were measured.

Lithology. The measured part of the Strathcona Fiord Formation at this location is dominantly a fine- to medium-grained, greyish red weathering, calcareous, quartzose sandstone. The sandstone is occasionally very fine grained, rarely coarse grained and commonly weathers grey, brown grey, yellow-grey and green-grey. Sandstone occurs as either thick homogeneous units or is thinly interbedded with grey-red or grey-brown siltstone or silty shale. Siltstone also occurs separately as thicker horizons. The sandstone and siltstone or silty shale occur together either as thin noncyclic intercalations or as thin fining upward cycles with the siltstone or silty shale as the recessive top part of the cycle. Thin silty shale horizons and lenses infrequently occur in thick sandstone units. Thin (~20 cm) stromatolite beds were found at 104, 160 and 186 m in the section. A wavy laminated white gypsum bed, 0.7 m thick is 94 m above the base of the section. The strata to 17 m below this bed contained white to pink gypsum nodules (7-8 cm) and/or lenses. Gypsum lenses and nodules were also located at 147 and 149 m above the base of the section.

Bioclastic debris was found in silty limestone to limy siltstone or very fine grained sandstone horizons occurring at 165, 169, 181, 186 and 193 m above the base. Hand lens examination indicated that brachiopod fragments dominate the debris.

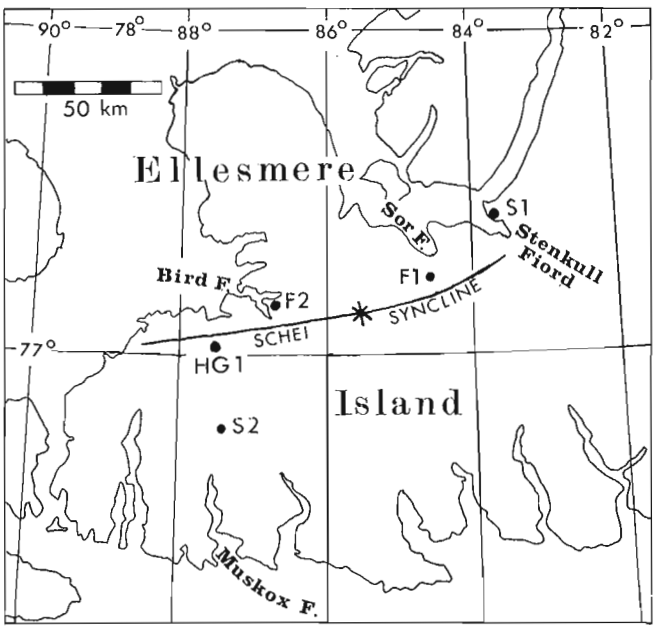

Figure 13.1. *Location of measured sections in the study area on southwestern Ellesmere Island.*

[1]Department of Geology, McMaster University, Hamilton, Ontario, L8S 4M1

Primary and Penecontemporaneous Sedimentary Structures. The dominant primary sedimentary structures are parallel lamination and ripple crosslamination. Climbing ripple drift (type A) occurs three times in the lower half and once in the upper half of the section. Green-grey and greyish red shale rip-up clasts are common constituents of the sandstone. The following primary or penecontemporaneous structures were found only sporadically throughout the section: small and medium scale planar tabular and lenticular crossbeds, oscillation ripples, parting lineation, mud cracks, ball and pillow structure, pseudonodules and contorted laminae.

Fossils and Trace Fossils. **Lingula** is the most common fossil. It occurs in red and grey medium-grained sandstones in the lower half of the section. Small plant impressions occur rarely in association with **Lingula** and whole brachiopods are noted in the bioclastic horizons. Small fish plates were found twice (once in association with root casts and rip-up clasts) within interbedded brown-grey, medium-grained sandstone and siltstone.

Trace fossils are fairly common in the ripple cross-laminated grey-red sandstone throughout the section. Preliminary identification indicates that the following are present: **Conostichus, Skolithos, Planolites, Scalarituba** and **Ophiomorpha.** Root casts, gastropod molds, cephalopod casts and trilobite tracks are rare.

Depositional Environment. A variety of sedimentary environments represented in this section will be defined with more work. The preliminary interpretation is that the depositional setting is paralic, possibly ranging from small tidal flat channels to a nearshore neritic environment.

Section S2. This section in the Strathcona Fiord Formation was measured approximately 15 km NNE of Muskox Fiord. The formation at this locality is 200 m thick contrasting sharply with the 1168 m thickness at Stenkul Fiord. The greatly reduced thickness is due to the presence of the Bird Fiord Formation underlying the Strathcona Fiord Formation in this area and possibly also to the more cratonward position of the Muskox Fiord locality.

Lithology. The dominant lithologies of this section are a grey to red, medium- to fine-grained, noncalcareous to calcareous, micaceous, quartzose sandstone and a greyish red, noncalcareous to calcareous micaceous siltstone or silty shale. As the Hecla Bay contact is approached (above 148 m) the sandstones weather orange grey to grey white and the grain size becomes more variable ranging from very fine to coarse-grained (hand specimen estimate). Locally they have conglomeratic bases, the clasts being green-grey shale with occasional chert pebbles and fish plates. Conglomerates are rare in the red sandstones of the lower part of the section.

Variegated greyish red and grey-white, nodular weathering horizons up to 1.5 m thick were interpreted to be paleosols. These occur throughout the section at the interface of an overlying siltstone and underlying sandstone unit. In many places, the upper zone of the underlying sandstone is mottled grey-white and red indicative of rooting.

Primary and Penecontemporaneous Sedimentary Structures. The dominant primary sedimentary structure in the sandstone throughout this section is ripple crosslamination. Parallel lamination also occurs commonly, either in association with rippling in the same sandstone unit or as the only primary sedimentary structure of the unit. The siltstones are nonstratified or parallel laminated throughout the section. Small and medium scale, planar tabular and lenticular crossbedding occur occasionally at the base of thicker sandstone units. In the lower half of the section red-brown siltstone clasts (2.0 cm maximum) and occasional fish bones occur as lag along the base of the crossbed sets. Planar lenticular crossbeds dominate over planar tabular in the upper half of the section. Occasional mud cracks on the upper surface of a sandstone unit and loading on the bottom surface are also characteristic of the upper half of the section.

Fossils. The only fossils present in this section are fragments of fish bone (3.0 cm maximum) found as lag at the base of crossbed sets in sandstone units.

Depositional Environment. The Strathcona Fiord Formation at this locality is entirely fluvial. Well defined fining upward cycles with a maximum thickness of 8 m occur throughout the lower 75% of the section. An entire cycle contains a basal resistant sandstone, whose upper surface is usually rooted, overlain by a nodular weathering paleosol, in turn overlain by a recessive siltstone interval. The contact with an overlying cycle is usually erosional.

At approximately 110 m above the base a large low angle (< 10°) planar scour occurs possibly representing channel avulsion. Above the scour fining upward cycles are very thin (< 0.5 m) and are not as well defined, consisting of only a resistant sandstone and recessive siltstone.

The beds examined at Muskox Fiord correlate approximately with the unexposed upper part of the section at Stenkul Fiord. Depositional environment in those two examined intervals is distinctly different.

Fram Formation

Sections F1 and F2 were measured in this formation (see Fig. 13.1). The former is a section through the basal and lower middle part of the formation while the latter is through the uppermost part of the formation. Both sections are on the northern limb of the Schei Syncline.

Section F1. This section is located 7.5 km southwest of the head of Sor Fiord. Six hundred and ninety eight metres of an estimated total thickness of 1100 m were measured (total thickness based on visual estimate). The section is of poor quality, however, since approximately 80% is covered interval. Exposures are ridge and nose type outcrops of resistant sandstone. Rare snowmelt cuts in tundra-covered recessive intervals reveal the bedrock as siltstone and/or silty shale.

The resistant ridges are badly cryoturbated. As a result sedimentary structures were commonly observed in displaced sandstone blocks often lying at the base of the outcrop.

Lithology. The resistant ridges of outcrop in this section are dominantly a pale greyish red weathering, slightly calcareous, micaceous, fine- to medium-grained quartzose sandstone. It also weathers grey, brown-grey and green-grey. The fresh surface is usually a pale to medium grey. In the upper half of the section some sandstone is grey-white or greenish white weathering, calcareous, medium- to coarse-grained, loosely cemented and porous.

Conglomerate occurs only as thin horizons (< 0.5 m) at the base of or within the sandstone units of the resistant ridges. Clasts are dominantly red-brown shale with occasional chert and rare fish bone or coal fragments. Maximum clast size is in the upper granule to lower pebble range.

The rare exposures of the siltstone and shale in the recessive, tundra-covered intervals show that the rock is pale red, green or grey and is slightly calcareous. Siltstone and/or shale also occurs in the resistant ridges as thin (< 0.3 m) lenses or horizons in the upper part of sandstone units.

Primary and Penecontemporaneous Sedimentary Structures. The dominant primary sedimentary structures in the sandstone ridges are micro trough crosslamination and parallel lamination. Both are frequently found in the upper part of sandstone units. Other current ripples exposed on depositional surfaces are usually sinuous crested and arranged in an interference pattern. Occasional occurrences of oscillation ripples were also noted. Parting lineation is common on depositional surfaces in thin bedded parts of sandstone units. Sole markings, dominantly prod and groove casts, are common. Crossbedding occurs frequently in the lower part of sandstone units. Low to high angle, small and medium scale, planar tabular and lenticular cross-stratified sets occur more commonly than trough crossbedding which was only rarely noted in the grey-red sandstone of the lower half of the section and the grey-white sandstone of the upper half.

Fossils and Trace Fossils. The only fossils found in this section are unidentifiable plant fragments which are abundant and of varying size, and fish bone fragments usually 2-3 cm in size. Both are found in the lower parts of sandstone units with the latter as clasts in conglomeratic horizons.

The only trace fossils found are occasional small burrows located in rippled tops of sandstone units. Root casts also occur occasionally in the uppermost parts of sandstone units.

Depositional Environment. Sedimentary features of the sandstone and the regular alternation with recessive tundra covered intervals representing siltstone and shale suggest that the section is composed of consecutive fining upward fluvial cycles. The sandstone ridges are interpreted to represent stacked channel sand accumulations of uncertain origin. The recessive siltstone and shale intervals are interpreted as overbank sediments.

The grey-white to greenish white sandstone occurs consistently at the interface of the sandstone and the recessive covered interval above 380 m in the section. The thickness of these sandstones increases from ~0.2 m to ~0.5 m near the top of the section. Although they contain similar features (planar and trough cross strata, shale rip-ups and root casts) they are distinctly different from the normal grey-red sandstone. At present their interpretation is problematic.

Section F2. This section is 420 m thick and is located on the eastern side of the inner part of the southeastern arm of Bird Fiord. It is part of the type section for the Okse Bay Formation as defined by McLaren (1963). It contrasts sharply with F1 in that it is close to 100% exposed.

Lithology. The lithologies present in this section are quartzose sandstone, siltstone and shale. Fine- to medium-grained, micaceous, calcareous, quartzose sandstone is the dominant lithology. The sandstone weathers green-grey, grey, grey-red, orange-white, grey-white and green. No single weathering colour dominates. Grain size in the sandstone ranges from very fine to coarse-grained throughout the section. Some sandstones are noncalcareous, kaolinitic or carbonaceous. The sandstones are platy to blocky, very thin- to thick-bedded, and occur either as homogeneous units or are finely intercalated with siltstone or silty shale.

Siltstone is generally calcareous and weathers green-grey or grey-red. It occurs either as lenses several centimetres thick in thick sandstones units or as thin to very thin beds interstratified with sandstone beds of similar thickness.

Shale weathers grey, green, red or black, is usually friable, and may or may not be calcareous. It is commonly silty and can occur as thick, recessive, highly weathered homogeneous units (maximum measured thickness ~3 m), as thin to very thin beds interstratified with sandstone and/or siltstone beds of comparable thickness or as very thin lenses or thin beds in the upper parts of thicker sandstone units.

Primary and Penecontemporaneous Sedimentary Structures. The dominant primary sedimentary structures are parallel lamination and current ripple crosslamination. These structures occur either in the upper portion of thicker sandstone units overlying a crossbedded or nonstratified lower portion, or individually, or in combination as the sole structure(s) in thin to very thin bedded sandstone and/or siltstone units. Bedding planes occasionally show interference current ripple patterns.

Small to medium scale, planar lenticular and tabular crossbedding is common in the lower parts of thicker sandstone units. Small scale, planar lenticular crossbedding is sporadic in the thin to very thin bedded interstratified sandstone and siltstone units.

Parting lineation, groove and prod marks, and loading are common on the underside of sandstone and siltstone beds. Mud cracks occur occasionally on the upper surface of fine sandstone or siltstone beds in fining upward units.

Fossils and Trace Fossils. The only fossils found in this section were plant fragments and fish bone fragments. The former are commonly found as lag in the basal segments of cross stratified thicker sandstone units whereas the latter can be found either as clasts (1-2 cm) in conglomeratic horizons in the basal parts of thicker sandstone units or on rippled and/or mudcracked upper surfaces of fining upward sandstone units.

Root casts were commonly found on the upper surfaces or underside of fine sandstone beds and often are in association with mud cracks and fish bone fragments. Burrows, 1-2 cm long, are rare in the fine grained uppermost surfaces of sandstone units.

Depositional Environment. As a preliminary interpretation it is suggested that the sediments throughout this section may be placed into one of the following three fluvial styles: (1) channel sand accumulations, (2) proximal overbank sediments, (3) distal overbank sediments. Styles one and two are the most common throughout the section.

Hell Gate Formation

Only one section was measured in the Hell Gate Formation.

Section HG1. The section is 128 m thick and is located ~44 km northeast of the head of Muskox Fiord on the southern limb of the Schei Syncline (see Fig. 13.1). The section represents the lowermost part of the formation in that area.

Lithology. Sandstone and siltstone are the only rock types in this section. The sandstone weathers orange-grey, grey-white, green-grey and purple. It is calcareous and noncalcareous, micaceous and can range from fine to coarse-grained. There is no dominant type. Sandstone occurs in

either thick, lithologically homogeneous units or in interstratified, very thin to thin bedded units of sandstone and siltstone. Siltstone weathers green grey, grey and purple. It is usually calcareous and is found either as the recessive portions of the interstratified sandstone and siltstone units or as thin lenses in the upper parts of thick sandstone units.

Primary and Penecontemporaneous Sedimentary Structures. Current ripple crosslamination and parallel lamination are the dominant structures. They occur together or individually in the resistant sandstone portion of interstratified sandstone and siltstone units. They also occur either as the sole sedimentary structures throughout a thick sandstone unit or in the upper part of such a unit.

Small and medium scale planar crossbedding occur occasionally in the bottom portion of thick sandstone units and less frequently at the base of sandstones in the interstratified sandstone and siltstone units.

Mud cracks were occasionally found on the upper surface of the resistant sandstones in the interstratified intervals. Green-grey siltstone rip-up clasts are common in the basal portion of thick sandstone units and rare at the base of sandstone beds in the interstratified intervals.

Fossils. Unidentifiable plant fragments are abundant throughout the section. They occur as lag in the basal portions of thick sandstone units.

Roots casts are sporadic on the tops of the sandstone beds in the interstratified sandstone and siltstone intervals.

Depositional Environment. A preliminary interpretation is that the sandstones and siltstones of this section were deposited in a fluvial environment similar to that in which the sediments of section F2 were deposited. This is viable because the two sections are in stratigraphic juxtaposition (F2 is in the uppermost portion of the Fram and HG1 is in the lower portion of the Hell Gate Formation). The thicker orange-grey to grey-white sandstone units containing occasional crossbedding, siltstone rip-ups, conglomeratic horizons and large plant fragments as lag, are suggested to be channel sand accumulations. The interstratified sandstone and siltstone intervals that weather green-grey to purple and contained root casts, mud cracks, siltstone rip-ups and occasional conglomeratic or crossbedded horizons may be proximal overbank sediments.

References

Embry, A.F. and Klovan, J.E.
1976: The Middle-Upper Devonian clastic wedge of the Franklinian Geosyncline; Bulletin of Canadian Petroleum Geology, v. 24, p. 485-639.

McLaren, D.J.
1963: Goose Fiord to Bjorne Peninsula; in Geology of the North-Central Part of the Arctic Archipelago, Northwest Territories (Operation Franklin), ed. Y.O. Fortier; Geological Survey of Canada, Memoir 320, p. 310-338.

Okulitch, A.V. and Mayr, U.
1982: Stratigraphic and structural studies, southern Ellesmere Island, N.W.T.; in Current Research, Part A; Geological Survey of Canada, Paper 82-1A, note.

LAHARIC BRECCIAS FROM THE CROWSNEST FORMATION, SOUTHERN ALBERTA

Project 770047

B.D. Ricketts
Institute of Sedimentary and Petroleum Geology, Calgary

Ricketts, B.D., Laharic breccias from the Crowsnest Formation, southern Alberta; in Current Research, Part A, Geological Survey of Canada, Paper 82-1A, p. 83-87, 1982.

Abstract

The coarse, poorly sorted and nonstratified breccias composing the Crowsnest volcanic member are interpreted as lahars. Most of the debris making up these lahars was derived by brecciation of trachytic domes, and not by continuous explosive volcanism as suggested in previous reports. Rainfall was the principal source of water for the lahars.

Introduction

The unusual composition of the Crowsnest volcanic rocks, which contain sanadine trachyte, analcite phonolite and notably, blairmorite, has been documented by several workers including MacKenzie (1914), Pearce (1967, 1970) and Ferguson and Edgar (1978); the latter three authors concentrating on the origin of the analcite and possible differentiation trends within a parent magma. However, despite the fact that the Crowsnest Member consists predominantly of fragmental volcanic debris (volcaniclastics), little attention has been paid to mechanisms of deposition or to the style(s) of volcanic eruption that produced this material. In a preliminary investigation of the mechanisms of deposition I have concentrated on some of the volcanic breccias and sandstones from two outcrops: one on the southern extension of Iron Ridge, and the other within an anticlinal structure along Carbondale River (Fig. 14.1).

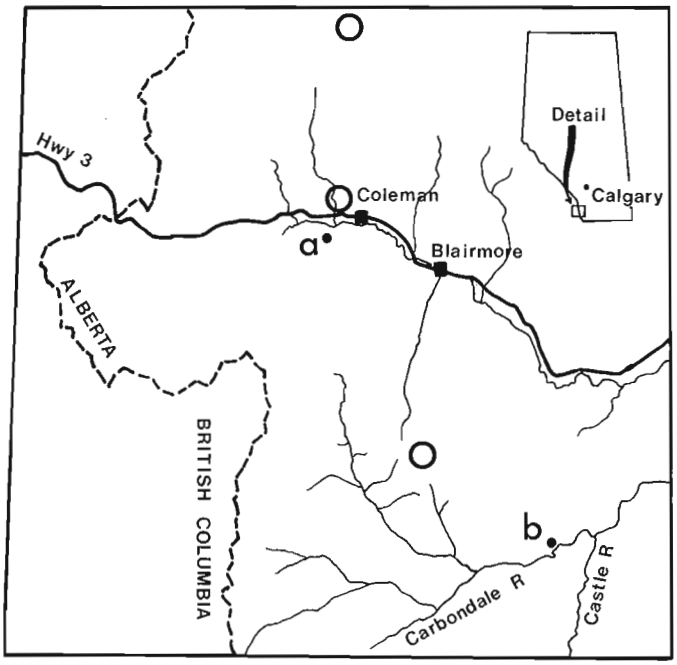

Figure 14.1. *Location of measured sections (a and b) at Coleman and Carbondale River. Large open circles locate the inferred volcanic centres of Pearce (1967, 1970).*

Regional Setting

The Crowsnest Member was formally included in the Lower Cretaceous, nonmarine Mill Creek Formation (upper Blairmore Group) by Mellon (1967). Norris (1964) suggested an Albian age for the volcanic rocks based on the presence of a typical upper Blairmore flora, and a potassium-argon age of 96 Ma obtained from sanidine crystals (Folinsbee et al., 1957). Isopach trends of the volcanics and general lithologic and petrographic descriptions are provided by Norris (1964), Mellon (1967) and Pearce (1970). Exposure of Crowsnest strata is limited to a narrow belt between Highwood River and Mill Creek. The maximum exposed thickness occurs in the Coleman fault plate and is 425 m (Price, 1962), although east and west of this locality the volcanic rocks thin markedly. The principal volcanic lithologies recognized by Pearce (1970) include red trachyte, sanidine-rich trachyte, garnet trachyte, analcite phonolite and blairmorite, and based on the spatial distribution of these rock types Pearce inferred that three main volcanic centres existed during Crowsnest times (Fig. 14.1).

Laharic Breccias

The first suggestion that some of the volcanic breccias might represent lahars was made by Norris (1964, although no criteria were discussed). Volcanic breccias and sandstones from two measured sections through part of the Crowsnest volcanic succession are illustrated in Figure 14.2. The Crowsnest breccia beds range in thickness from 0.5 up to 2.5 m. The most obvious features of the breccias are their extremely poor sorting and lack of internal stratification. In a single bed, clasts range in size from clay, to blocks 60 cm across, and compose a framework that is matrix-supported. The roundness of individual fragments is highly variable, and the composition heterolithic, the most common volcanic components being sanidine and garnet trachytes and only subordinate blairmorite.

Breccias in the Coleman section (Fig. 14.2a) are non-graded, whereas both normal size grading and nongraded types are found in the Carbondale River section (Fig. 14.2b). Bed contacts usually are sharp, with basal scouring apparent in some units. Boulders often project through the upper bed contacts and in places are draped by thin mudstone or volcanic sandstone. Several of the thick breccias were found to be composite units made up of a number of superposed beds; in many cases the only evidence of a depositional break between these beds is a red mudstone veneer, in some places exhibiting small current ripples (Fig. 14.3). The criteria used to identify lahars have been discussed in detail by Fisher (1960), Schmincke (1967) and Crandell (1971), and indeed, all of the textures and sedimentary structures observed in the Crowsnest examples compare favourably with this interpretation.

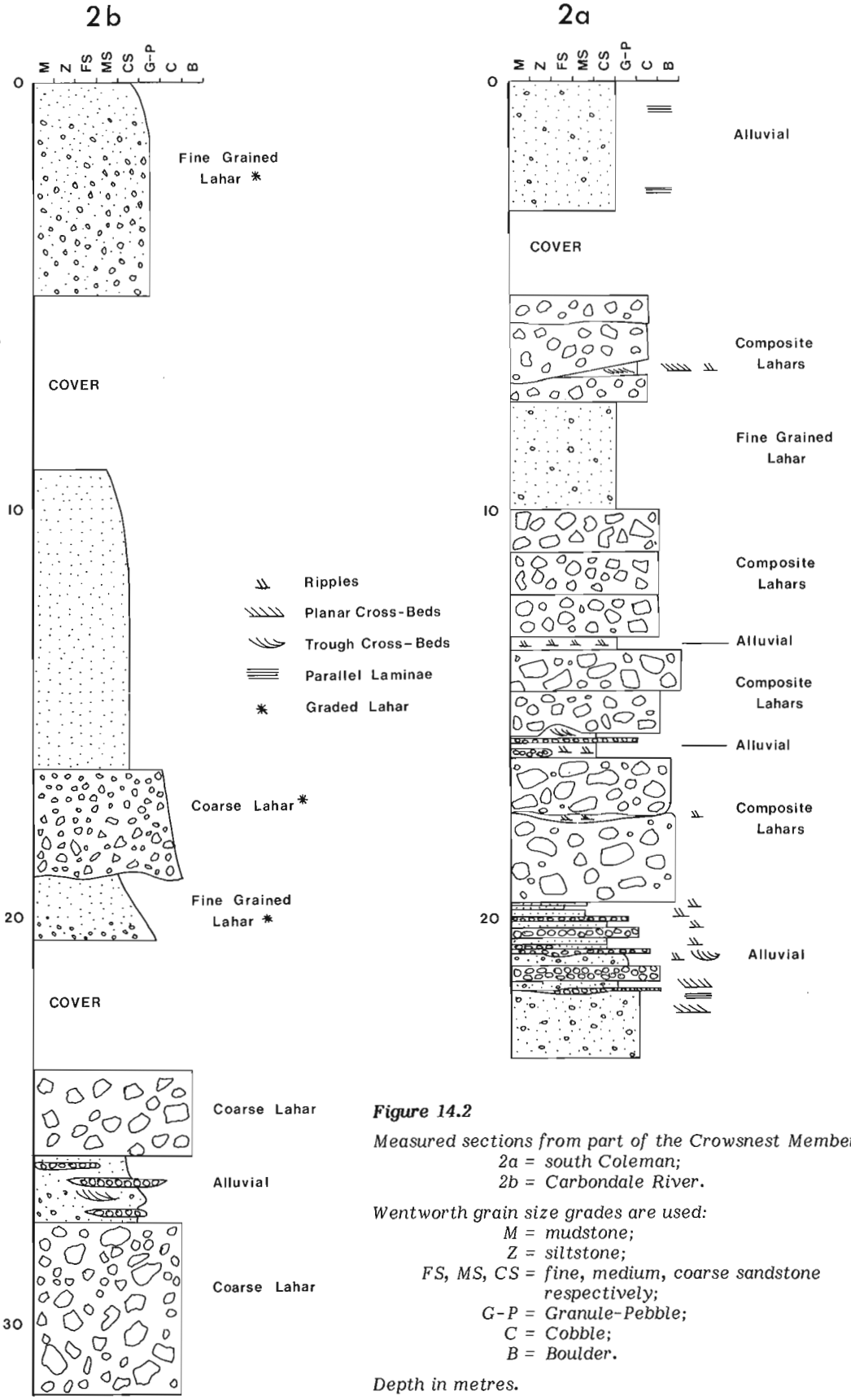

Figure 14.2

Measured sections from part of the Crowsnest Member:
2a = south Coleman;
2b = Carbondale River.

Wentworth grain size grades are used:
M = mudstone;
Z = siltstone;
FS, MS, CS = fine, medium, coarse sandstone respectively;
G-P = Granule-Pebble;
C = Cobble;
B = Boulder.

Depth in metres.

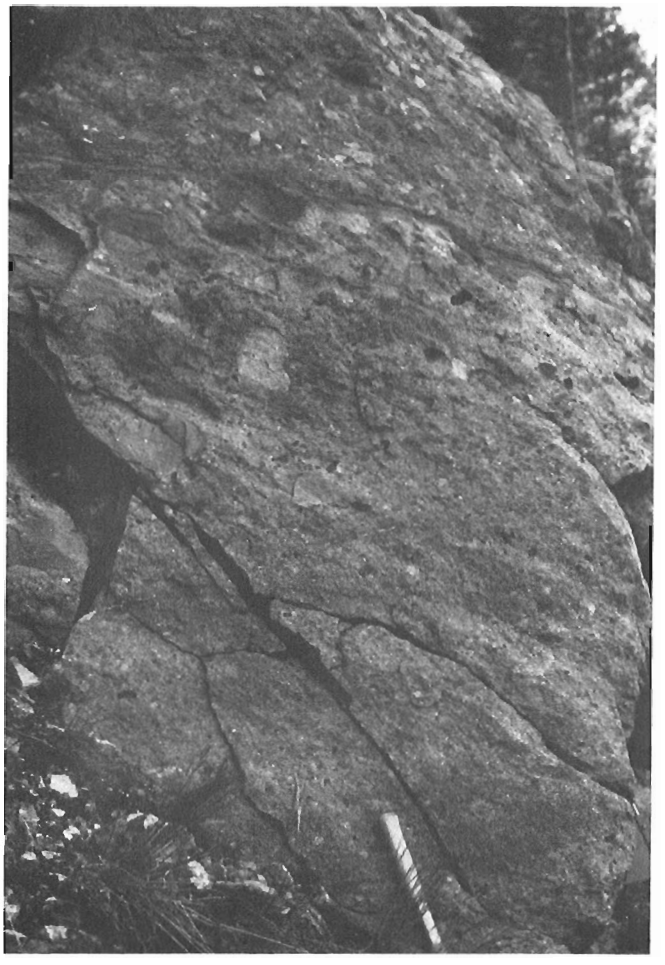

Figure 14.3a. *A section of volcanic breccia consisting of four superposed beds, separated by thin red mudstones. Note the angularity and poor sorting of blocks in the upper breccia. Section 2a.*

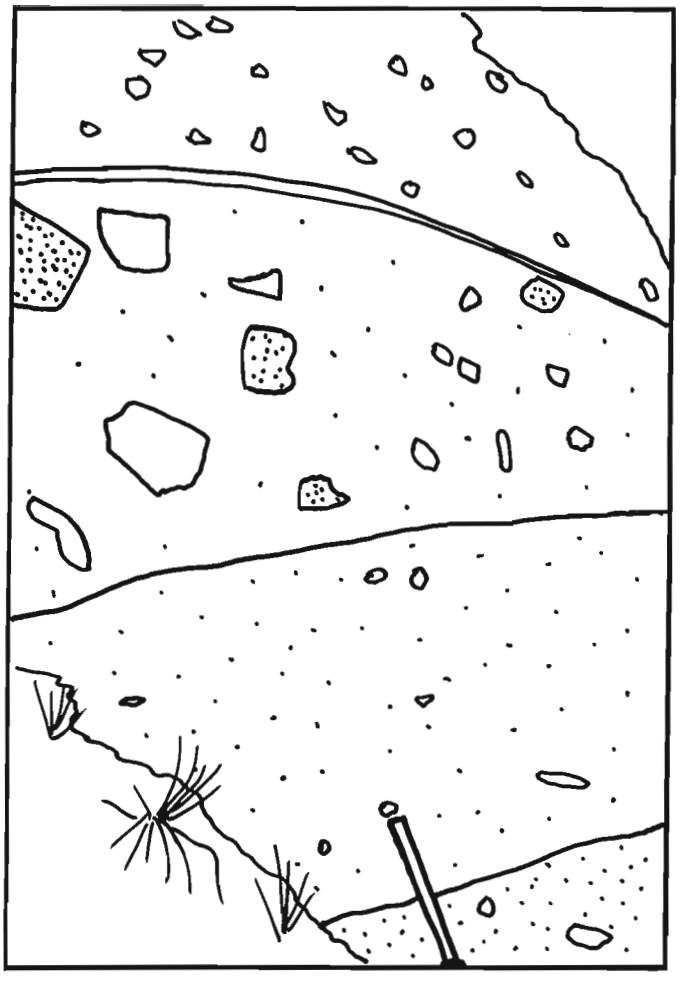

Figure 14.3b. *A sketch of the exposure shown in Figure 14.3a, depicting the four units of volcanic breccia.*

Two alternative interpretations concerning the deposition of the Crowsnest breccias, namely air-fall deposits (pyroclastics), and pyroclastic flows, are discounted for the following reasons:

- air-fall deposits tend to exhibit more pronounced stratification although exceptions do occur close to the source area. Nevertheless, breccias located at a considerable distance from the Crowsnest centres remain unstratified and show features typical of debris flow deposition.
- because pyroclastic flows are a direct result of (explosive) volcanism, deposits tend to be monomict in composition. Also, welded textures, columnar jointing and hydrothermal alteration are common in hot pyroclastic flows; none of these features have been observed in the Crowsnest breccias.

Lateral Variations

Although individual beds cannot be correlated between the two sections, variations in the structure and composition of volcaniclastic rocks at Carbondale River suggest that deposition was more distant from the main source areas when compared with the Coleman section. These variations include: a decrease in maximum clast size in the breccias to about 30 cm; an overall increase in the degree of rounding; an increase in the proportion of fine grained lithologies; and a marked decrease in the amounts of heavy minerals present in the breccias and sandstones i.e. the virtual absence of aegerine and garnet grains in some volcanic sandstones indicates a degree of hydraulic sorting not observed in the more proximal Coleman section. If the locations of volcanic centres suggested by Pearce (1967) are accepted, detritus composing the laharic breccias and volcanic sandstones at Carbondale River has been transported at least 30 km. In addition, graded bedding is relatively common in the Carbondale River lahars and may further reflect a change in the flow mechanism of some of the lahars as distance from the source increased. The coarse, nonsorted and nongraded breccias at Coleman probably represent true debris flows, wherein framework clasts were supported by a cohesive mud/fluid matrix and sediment was deposited by mass emplacement. However, in more turbulent flows framework clasts are held in suspension by fluid turbulence (Middleton and Hampton, 1976); compared to debris flows, turbulent flows posses a lower sediment/fluid ratio and as flow velocities decrease normal size grading of clasts can develop as successively finer material falls out of suspension. Thus it is possible that the graded (turbulent) lahars at Carbondale River are the distal, more dilute equivalents of the nongraded lahars (debris flows) observed at Coleman.

Alluvial Deposits

Lahars in both sections are interbedded or separated by thin mudstones, volcanic sandstones and conglomerates that exhibit evidence of bed-load transport, usually as current ripples, climbing ripples or larger scale crossbeds (Fig. 14.4). Bedded conglomerates are lense shaped, usually associated with trough crossbedded sandstones and probably represent ephemeral stream channels. The conglomerates possess a distinct clast-supported framework (compared to the laharic breccias) and pebbles are moderately rounded. Planar crossbeds in some of the sandstones may be similar to dune or bar structures that develop in braided rivers. Heavy minerals commonly are concentrated along cross-strata.

The lensoidal geometry and relatively restricted occurrence of these deposits indicates short-lived stream flow and reworking of the underlying laharic breccias.

Comment on the Style of Crowsnest Volcanism

In one of the first detailed descriptions of the Crowsnest volcanics, MacKenzie (1914) concluded that eruptions were largely explosive, based on the absence of lava flows or sills, and that there had been many explosive events because of the thin and alternating nature of the bedding. However, as Pearce (1967, 1970) has noted, the Crowsnest volcanic pile probably resulted from degradation of a volcanic terrane in addition to direct volcanic deposition. This is supported by the presence of numerous laharic breccias that represent reworked volcanic debris.

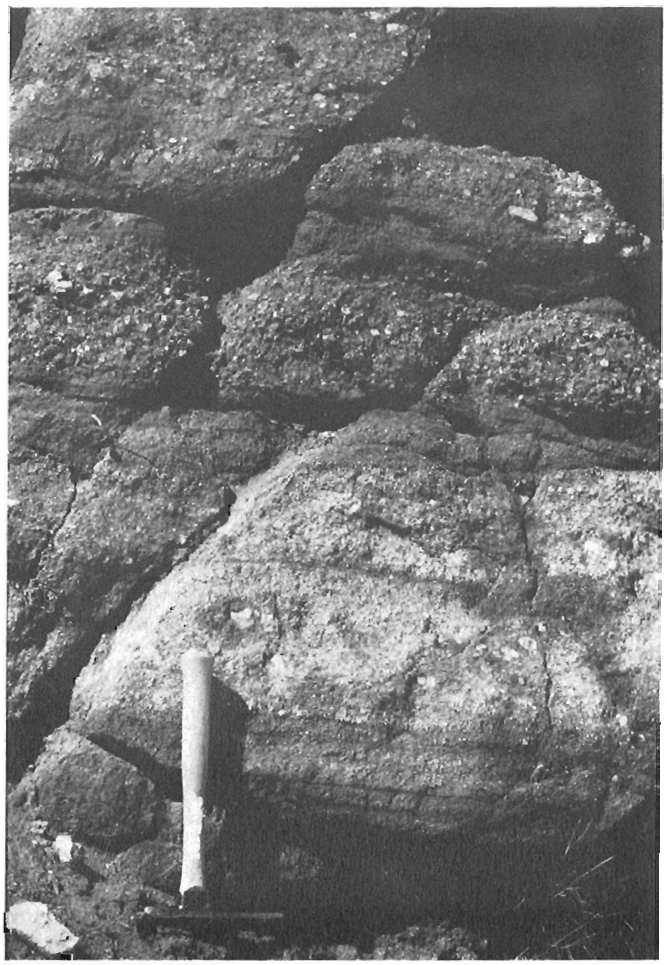

Figure 14.4. *Volcanic sandstone and clast-supported conglomerate with ripples, small planar crossbeds, and parallel laminae. Section 2a.*

Trachytic lavas (the dominant type in the Crowsnest Member) typically are highly viscous, their extrusion usually resulting in volcanic domes or spines and only rarely in lava flows (Hatch et al., 1973, p. 290). Furthermore, the scarcity of vesicular lithologies in the Crowsnest also suggests that these magmas were not highly gas-charged (Pearce, 1967, p. 30, noted one locality only). Therefore, continuous explosive volcanism as the dominant style of eruption, is considered unlikely because of: the paucity of vesicular lithologies; the scarcity of thin, regularly bedded pyroclastics; and the absence of vitric debris which is especially common in phreatic and phreatomagmatic eruptions. Most of the debris composing the laharic breccias resulted from relatively quiet effusion of magma, possibly as volcanic domes.

Shattering of the surface crust of volcanic domes is a characteristic feature and results from cooling and dome expansion (Williams and McBirney, 1979); domes and spines also tend to collapse after growth has ceased (for example the celebrated spine of Mt. Pelee) and consequently there is abundant debris available for reworking or redeposition as lahars. Thus, it is with this analogue that a comparison is made with the Crowsnest volcanics. Relatively mild explosive volcanism also is known to accompany dome formation and, in the case of Mt. Pelee, a nuée ardente preceded extrusion of the magma. Ash deposits (i.e. air-fall) have been reported immediately underlying the Crowsnest Member (MacKenzie, 1914), and also laterally associated with the volcanic rocks, for example at Sheep Creek where they form red-weathering paleosoils and are interstratified with coaly beds. These too likely represent explosive events. However, if explosive eruptions did occur during Crowsnest times they were probably intermittent rather than a continuous explosive phase as suggested by MacKenzie (1914).

The Origin of Water in the Lahars

A lahar is a type of sediment gravity flow (debris flow) consisting of volcanic debris mixed with water and deposited in a subaerial environment. Unlike pyroclastic flows which are directly related to eruptive phenomena, lahars can form during or between periods of eruption, and even after volcanic activity has ceased (Williams and McBirney, 1979). The most important ingredient for lahar formation is an ample supply of water, for which a number of sources have been recorded: rainfall, melting of ice and snow (e.g. Mt. Rainier; Crandell, 1971); discharge of water from crater lakes (as at Ruapehu, New Zealand; O'Shea, 1954); and magmatic water (Lydon, 1968).

Analysis of Cretaceous floras from southwestern Canada indicates an expanding tropical zone until the end of the Albian (Smiley, 1974). More specifically, the Mill Creek flora (upper Blairmore) is dominated by dicotyledons (Mellon, 1967), the proportion of dicotyledons being similar to that found in modern frost-free subtropical climates (Smiley, 1974). Hence the region was subjected to relatively high rainfall and this was the most likely source of water for the Crowsnest lahars (although a magmatic source cannot be ruled out).

Summary

Many of the coarse, poorly sorted and non-stratified breccias composing the Crowsnest volcanics originated as lahars. The Crowsnest lavas (predominantly trachytic) are believed to have been extruded as volcanic domes. The debris making up the lahars probably resulted from brecciation during cooling and expansion of the trachytic

domes, and also from gravitational collapse of the domes. Analysis of the paleoclimate at this time (Albian) suggests that rainfall was the most likely source of water for the debris flows. The proportion of alluvial deposits interbedded with the lahars increases with distance from the principal source areas. Ephemeral braided streams probably developed close to the source.

Acknowledgments

I thank M.P. Cecile and U. Mayr for critically reviewing this manuscript, and Marianne Yuen for her able assistance in the field.

References

Crandell, D.R.
1971: Postglacial lahars from Mount Rainier volcano, Washington; United States Geological Survey, Professional, Paper 677.

Ferguson, L.J. and Edgar, A.D.
1978: The petrogenesis and origin of the analcime in the volcanic rocks of the Crowsnest Formation, Alberta; Canadian Journal of Earth Sciences, v. 15, p. 69-77.

Fisher, R.V.
1960: Criteria for recognition of laharic breccias southern Cascade Mountains, Washington; Geological Society of America, Bulletin, v. 71, p. 127-132.

Folinsbee, R.E., Ritchie, W.D., and Stransberry, G.F.
1957: The Crowsnest volcanics and the Cretaceous geochronology; Seventh Annual Field Conference, Alberta Society of Petroleum Geology, p. 2026.

Hatch, F.H., Wells, A.K., and Wells, M.K.
1973: Petrology of the Igneous Rocks; Hafner Publishing Company, New York, 551 p.

Lydon, P.A.
1968: Geology and lahars of the Tuscan Formation, California; Geological Society of America, Memoir 116, p. 441-475.

MacKenzie, J.D.
1914: The Crowsnest Volcanics; Geological Survey of Canada Museum Bulletin 4, Geological Series No. 20, 37 p.

Mellon, G.B.
1967: Stratigraphy and petrology of the Lower Cretaceous Blairmore and Mannville groups, Alberta foothills and plains; Alberta Research Council, Bulletin 21.

Middleton, G.V. and Hampton, M.A.
1976: Subaqueous sediment transport and deposition by sediment gravity flows; in Marine Sediment Transport and Environmental Management, D.J. Stanley and D.J.P. Swife, ed.; Wiley and Sons, New York, p. 197-218.

Norris, D.K.
1964: The Lower Cretaceous of the southeastern Canadian cordillera; Bulletin of Canadian Petroleum Geology, v. 12, p. 512-535.

O'Shea, B.E.
1954: Ruapehu and the Tangiwai disaster; New Zealand Journal of Science of Technology B 36, p. 174-189.

Pearce, T.H.
1967: The analcite-bearing volcanic rocks of the Crowsnest Formation; Ph.D. thesis, Queen's University, Ontario, 180 p.

1970: The analcite-bearing volcanic rocks of the Crowsnest Formation; Canadian Journal of Earth Sciences, v. 7, p. 46-66.

Price, R.A.
1962: Fernie map-area, east half, Alberta and British Columbia; Geological Survey of Canada, Paper 61-24.

Schmincke, H.
1967: Graded lahars in the type sections of the Ellensberg Formation, south central Washington; Journal of Sedimentary Geology, v. 37, p. 438-448.

Smiley, C.J.
1974: Analysis of crustal relative stability from some late Paleozoic and Mesozoic floral sequences; American Association of Petroleum Geologists, Memoir 23, p. 331-360.

Williams, H. and McBirney, A.R.
1979: 'Volcanology', Freeman, Cooper and Co., 397 p.

15.

PLATEAU OVERTHRUST AND ITS HYDROCARBON POTENTIAL, MACKENZIE MOUNTAINS, NORTHWEST TERRITORIES

Project 770044

M.P. Cecile, D.G. Cook, and L.R. Snowdon
Institute of Sedimentary and Petroleum Geology, Calgary

Cecile, M.P., Cook, D.G., and Snowdon, L.R., Plateau overthrust and its hydrocarbon potential, Mackenzie Mountains, Northwest Territories; in Current Research, Part A, Geological Survey of Canada, Paper 82-1A, p. 89-94, 1982.

Abstract

A structural cross-section through the northern Mackenzie Mountains shows that the hanging wall of the Plateau Thrust has moved as much as 35 km northeastward over Paleozoic carbonates and carbonaceous shales. This overthrusting produces a large (4000 km^2) area with previously unrecognized potential for trapped hydrocarbon deposits. Analyses of surface samples studied to determine the level of organic alteration are ambiguous because of weathering, evaporation loss and low total organic carbon, but indicate alteration is mature to overmature with respect to oil.

Comparison of this section with a second cross-section located in the central Mackenzie Mountains shows the Plateau Thrust achieves shortening on a much higher structural level than a major thrust immediately southeast of the Plateau Thrust. Compensation for the different levels of shortening is noted in the greater shortening, expressed in part by increased numbers of closely spaced folds in strata northeast of the southern thrust, when compared to footwall strata northeast of the Plateau Thrust.

Introduction

The Mackenzie Mountains in the northern Cordillera are generally discounted as a potential hydrocarbon-producing province due primarily to the style of Mackenzie Mountain structure – open folds and zones of complex folding and thrusting (Douglas et al., 1970) – and an erosion level which generally indicates breaching of all major potential reservoir structures (e.g. Aitken and Cook, 1974a). Geological maps of the area, published during the last decade generally substantiate this assessment with one major exception, a large area of Paleozoic carbonates and shales overthrust by Proterozoic strata in the Plateau Thrust Plate. The maximum overthrust width is 35 km covering a total area of 4000 km^2 (Fig. 15.1).

Acknowledgments

This paper arose from discussions with S.P. Gordey on Mackenzie Mountain structure. J.D. Aitken advised us and provided critical data. D.W. Morrow provided samples and information on Devonian carbonates in the area. The manuscript was critically reviewed by J.D. Aitken and A. Okulitch. S.P. Gordey, R.I. Thompson, H. Gabrielse and G.H. Eisbacher offered critical comments and suggestions.

Stratigraphy

The area of the Mackenzie Mountains shown in Figure 15.1 is underlain by a thick succession of unmetamorphosed sedimentary strata ranging in age from Middle Proterozoic (Helikian) to Cretaceous (Table 15.1). The area spans major changes in stratigraphy: the appearance of Lower Cambrian carbonates and quartzites to the southwest and the transition of lower and middle Paleozoic carbonates into basin shales from northeast to southwest. Relevant references, containing stratigraphic descriptions are: Blusson, 1971; Aitken et al., 1973; Gabrielse et al., 1973; Aitken and Cook, 1974a; Fritz (1976), Eisbacher (1978), and Aitken (in press). The Lower Paleozoic 'shale-out' is described by Aitken et al. (1973) and Cecile (1978, in press). Thicknesses shown in Figure 15.2 are from these publications.

Structure of the Overthrust

The Plateau Thrust was first described by Gabrielse et al. (1973, p. 104) as "one of the most important structures in the region", dipping "gently to the southwest and west" and having "a stratigraphic displacement in places of possibly more than 20,000 feet" (6000 m). The Plateau Thrust was extended northwest by Aitken and Cook (1974b, 1975) and is discussed at length in Aitken et al. (in press) who note that there is little displacement on the Plateau Thrust at its northern extremity in the Upper Ramparts River map area. The largest displacement, as interpreted here, is marked by the development of a plateau of flat to gently dipping hanging wall strata associated with the Plateau Thrust Plate in the Sekwi Mountain, Mount Eduni and Wrigley Lake map areas as shown in Figure 15.1. South of the Wrigley Lake map area the northwest-trending Plateau Thrust ends as it swings southwesterly into the Redstone Plateau area (Fig. 15.3).

Figure 15.2 is a cross-section through the central part of the Plateau overthrust* area (A-B Fig. 15.1; from Cecile and Cook, 1981) constructed using geological maps of Blusson (1971); Gabrielse et al. (1973) and Aitken and Cook (1974a) and assuming a thin-skinned style of deformation. Evidence for thin-skinned tectonics is discussed in Aitken et al. (in press). The lowest detachment level, on the northeast, is placed in sub-H1+x strata beneath a large broad box anticline using an excess area method (see Hossack, 1979 for a review of the method initiated by Chamberlin, 1910) and Aitken and Cook, 1974a predicted this detachment on the basis of fold geometry. The presence of box folds and opposing thrust faults across the Mackenzie Mountains suggest a relatively flat detachment allowing shortening to occur through displacement to the northeast or southwest. The second major detachment is placed within the gypsum unit of the Little Dal Group (Aitken et al., in press; cf. Aitken and Cook, 1975), because the gypsum is the lowest stratigraphic unit found along the northeast edge of the Plateau Thrust through the area shown in Figure 15.1.

*Plateau overthrust is the area from hanging wall flexure east to the trace of the Plateau Thrust

A flexure within the Plateau Plate occurs (Fig. 15.2) where bedding changes abruptly from subhorizontal to dipping moderately southwest. We assume:

1. that the Plateau Thrust stays within the same stratigraphic unit westward and accordingly must be flexed with the strata;
2. that the flexure of the thrust marks a step where the thrust has cut up across the Paleozoic carbonate section in the footwall.

Following these assumptions Paleozoic formations can reasonably be interpreted to underlie the entire flat northwestern portion of Plateau Thrust Plate. Stratigraphy is inferred within and beneath the plate by extrapolation of stratigraphic thickness data. The open fold style interpreted beneath the Plateau overthrust is based on the presence of such folding in the footwall south of Redstone River (Fig. 15.1). Projection of Devonian to Mississippian(?) clastics beneath most of the overthrust area is based on the extensive preservation of these strata in the footwall along most of the trace of the Plateau fault. The rest of the section is constructed using stratigraphic thickness data increasing thicknesses westwards on some units and introducing new units that are only found to the southwest. The relationship south of the Ekwi River, showing Proterozoic strata in the immediate footwall, is based on a preliminary map (Aitken and Cook, 1974b). This part of the map, in an area of poor exposures, is now known to be at least partly incorrect and may be grossly in error (J.D. Aitken, personal communication, 1981).

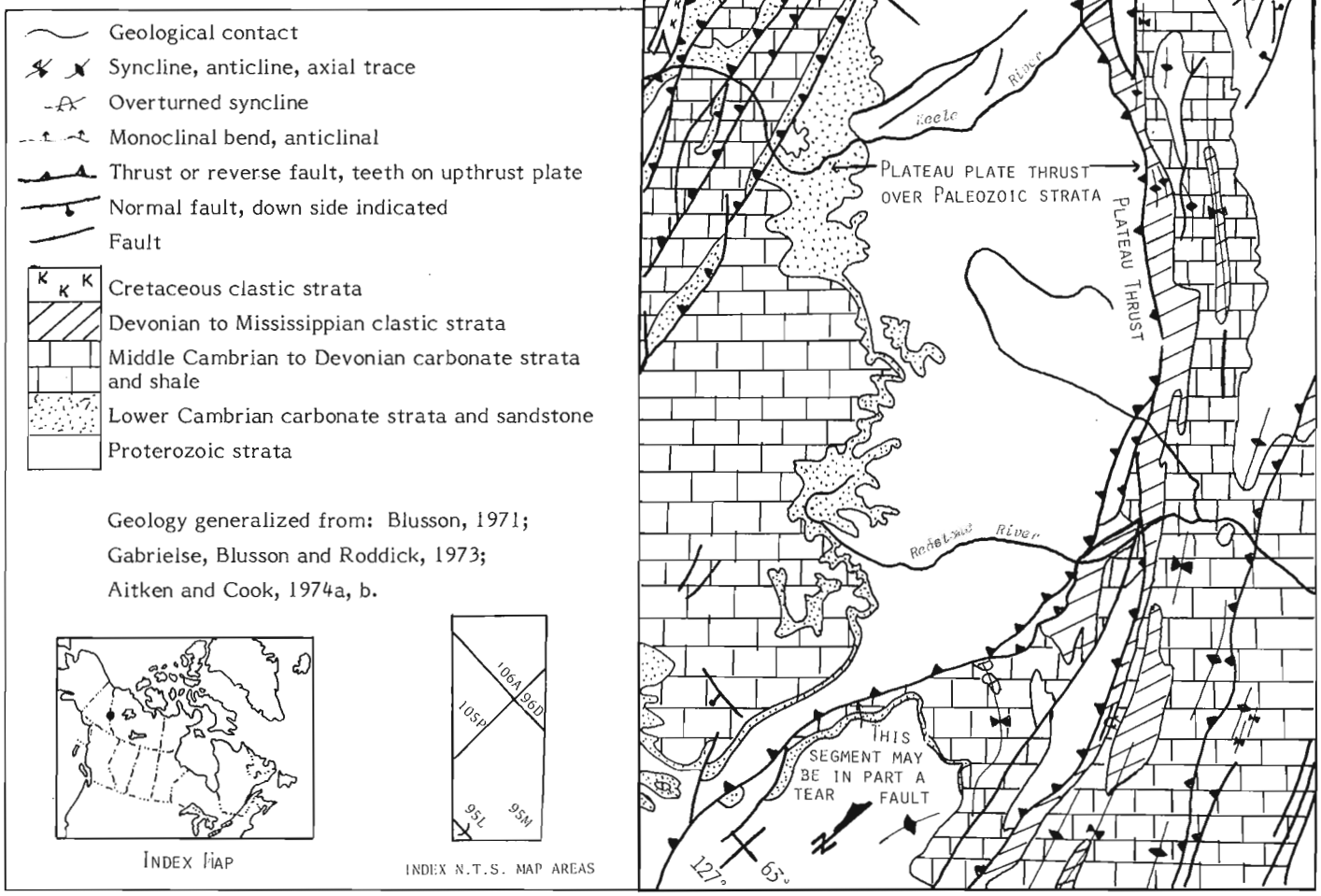

Figure 15.1. Location and generalized geological map along the southern Plateau Overthrust belt.

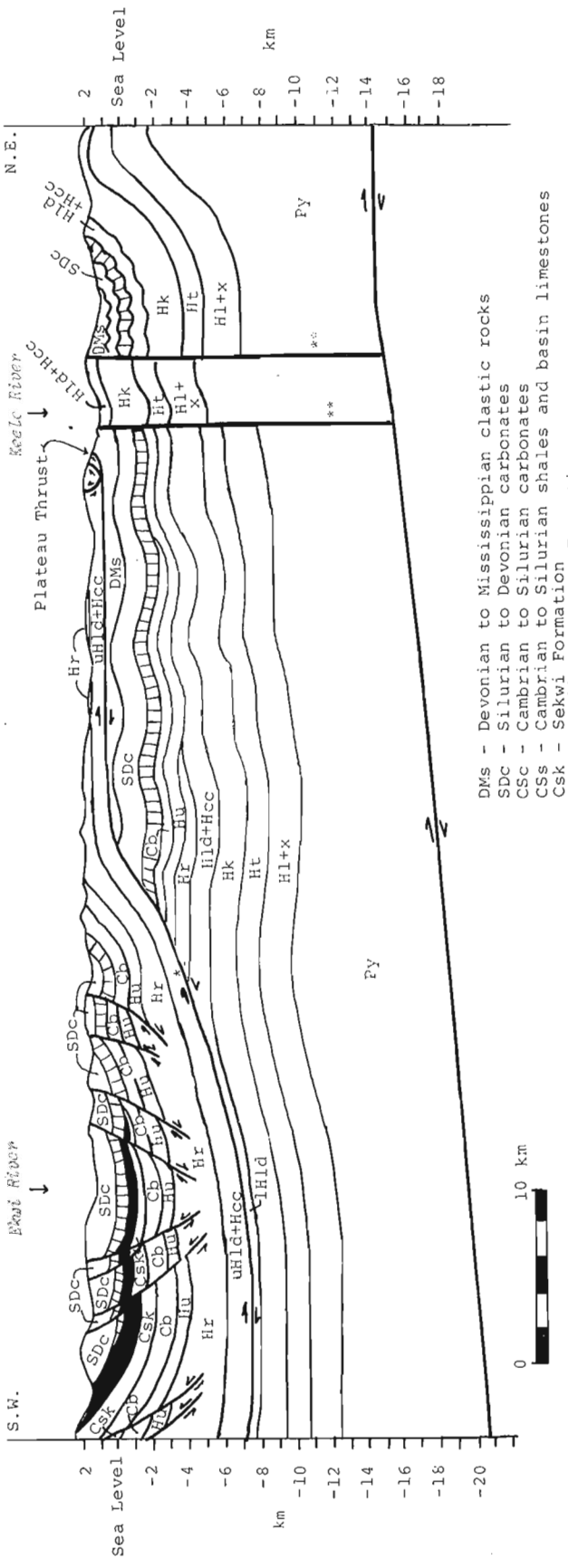

This is part of a regional cross-section by Cecile and Cook (1981) and is based on the geology of Blusson (1971); Gabrielse, Blusson and Roddick (1973); and Aitken and Cook (1974a).

*Little Dal Fm. detachment from J.D. Aitken, pers. comm., 1981 and Aitken and Cook (1975).

**Strike-slip faults?

Figure 15.2. *Geological cross-section A-B. For line of section, see Figure 15.1.*

Aitken et al. (in press) interpret the sub-Plateau Overthrust structure in a completely different fashion. They interpret the Little Dal gypsum as an upper detachment such that the total shortening in the hanging wall would be equalled by folding in the footwall, with the Proterozoic gypsum unit compensating between the two levels of deformation (see Dahlstrom, 1969). That style does not satisfy many of the constraints shown in Figure 15.2, particularly the major jump in the level of dislocation from Proterozoic gypsum to Devonian and Mississippian(?) clastics along the footwall trace of the fault. Nor is there any indication of an abrupt change to high amplitude folds in the footwall which would be required by the upper-detachment model. A cross-section constructed by Gordey (1981b; personal communication, 1981) across the Redstone Plateau (Fig. 15.3) requires substantial change in structural style from the Plateau Overthrust to the Redstone. Using a thin-skinned model, Gordey interpreted shortening on a single deep (sub-Tsezotene) detachment below the Redstone Plateau. Gordey suggested that the Redstone Plate has moved about 45 km eastward and correspondingly that strata deformed in front of the plate were also shortened by about 45 km. Conversely, the Plateau Plate which ends in the Redstone area has been transported on two detachments with an aggregate displacement also of about 50-55 km (35 km of overthrusting and 15-20 km of footwall shortening). To accomplish the same shortening on two detachments to the northwest and on one to the southeast requires compensation through differential movement of the sub-Plateau footwall with respect to strata deformed in front of the Redstone Plateau. This compensation is delineated by a southeast to northwest change in fold styles and by north-northeast trending fault segments (e.g. Gambill Fault, Aitken and Cook, 1974a). In addition, although the Plateau and Redstone plates are continuous southwest of their overthrust areas there must be a steeply-dipping northeasterly trending tear fault between the two plateau areas (see Fig. 15.1, 15.3).

Maturation

To estimate the level of the normal alteration in the area, the content of organic compounds was determined for three outcrop samples (Table 15.2). Total organic carbon, total solvent extract yield, and the proportion of saturates, aromatics, NSO's* and asphaltenes were determined for each sample (Table 15.3). Capillary column gas chromatograms from the saturate fraction and the distribution of n-alkanes and acyclic isoprenoids were noted for the C_{15+} carbon range (Fig. 15.4, for example).

Reliable interpretation of this data is precluded because of weathering and/or storage effects on the samples.

*NSO's = Nitrogen, sulphur and oxygen compounds

Table 15.1

Simplified stratigraphy of area shown in Figure 15.1 and 15.2

MESOZOIC	CRET.	Unnamed shale, sandstone, and conglomerate		
		Unconformity		
	MISS.	IMPERIAL Fm - shale and sandstone		
		HARE INDIAN CANOL Fms. - shale		
		Unconformity?		
PALEOZOIC	DEVONIAN	HUME (Headless, Nahanni) Fm. - limestone and minor shale		
		BEAR ROCK Fm. - dolomite, breccia, minor anhydrite and gypsum	LANDRY - limestone	NATLA- limestone (basin facies)
			ARNICA - dolomite	
			SOMBRE- dolomite	
			CAMSELL - dolomite limestone	
	SILURIAN	DELORME Fm. - dolomite, sandy		
		Unconformity		
		MOUNT KINDLE (Whittaker) Fm. - dolomite, limestone (coral biostromes)	DUO LAKE Fm. - graptolitic shale, minor limestone and dolomite (basin facies)	
		Unconformity		
	ORDOVICIAN	SUNBLOOD Fm. - dolomite, limestone		
		FRANKLIN MOUNTAIN (Broken Skull) dolomite, minor sandstone	RABBITKETTLE Fm. - limestone, siltstone (basin facies)	
		Unconformity		
PROTEROZOIC	CAMBRIAN	ROCKSLIDE Fm. – limestone, siltstone, minor shale, and sandstone.		
		SEKWI Fm. – dolomite, limestone, minor shale, and siltstone.		
		BACKBONE RANGES Fm. – quartzite, minor dolomite, siltstone.		
	HADRYIAN	SHEEPBED Fm. – shale.		
		KEELE Fm. – dolomite and sandstone.		
		*RAPITAN Gp. – shale, diamictite, sandstone.		
		Unconformity		
	HELIKIAN	COPPERCAP Fm. – limestone and laterally dolomite.		
		REDSTONE RIVER Fm. – siltstone, anhydrite, gypsum, and laterally conglomerate.		
		LITTLE DAL Fm. – dolomite, limestone, shale, gypsum (carbonates sandy and silty).		
		KATHERINE Gp. (Tigonankweine Fm.) – quartzite, shale, minor dolomite.		
		TSEZOTENE Fm. – shale, sandstone, dolomite, local limestone.		
		HI – unnamed dolomite with minor chert.		

* Since publication of maps used in Figure 15.2, Eisbacher (1978) has redefined the Rapitan Gp. to include the Keele Fm.

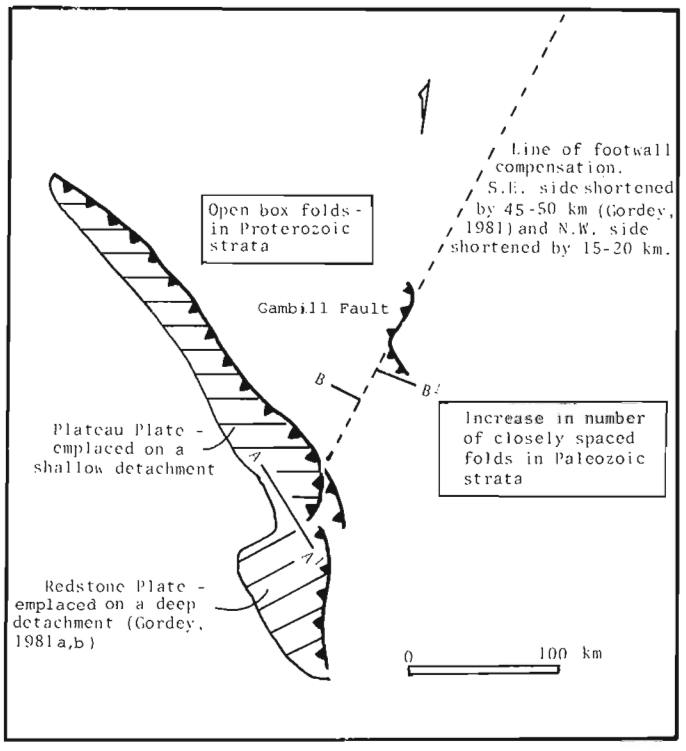

Figure 15.3. *Distribution of the Plateau and Redstone plates. Rocks at point A and A_1 have moved the same distance during deformation A on two major detachments and point A_1 on one detachment. Rocks at points B and B_1 have moved differentially on one deep detachment producing different structural styles on either side of a north-northeast trending line. Map generalized from Douglas (1969).*

Evaporative losses are indicated by the complete lack of n-alkanes and acyclic isoprenoids eluting prior to nC_{16} and the more or less smooth drop off in the concentration of these same compound classes from nC_{20} down to C_{16}. Thus pristane/phytane ratios are clearly lower than they would be in a fresh, unweathered sample. The total organic carbon contents are very low (<0.16%), hence the absolute yields and proportions of the various fractions such as saturates and aromatics are subject to large errors. For example, the total deasphalted extract of sample B weighed 2.5 mg, but when fractionated into saturates, aromatics and NSO's, 1.9 mg, 0.5 mg and 1.0 mg respectively were recovered for a total of 3.4 mg or 136 per cent. This increase in weight is caused by traces of residual solvent or contamination of the sample by alumina fines washing off the chromatography column. Thus saturate/aromatic ratios and per cent hydrocarbons in the extract are not very reliable for these samples.

The pristane/nC_{17} ratio may not be greatly affected by evaporative losses and as such may indicate that these sediments are thermally mature, that is, equivalent to a vitrinite reflectance level of 0.8 per cent or greater. The saturate/aromatic ratio of sample A suggests a higher level of thermal alteration than does the percentage of hydrocarbons and such internal inconsistency indicates an error in the data. The results for samples B and C are somewhat more consistent with the saturate to aromatic ratio and indicative of very high maturity. The per cent hydrocarbons in the extract suggest moderate to high maturity.

Table 15.2

Paleozoic Carbonates - Collected by D.W. Morrow

Sample A, (C-75871) - Arnica Fm. at 105 m above the Bear Rock Fm from 64°01'N and 126°38'W.

Sample B, (C-83595) - Headless Fm. at 23 m above the base of the formation from 63°52'N and 127°13'W.

Sample C, (C-83127) - Bear Rock Fm. at 3 m above the base of the formation from 63°52'N and 127°13'W.

Table 15.3

Organic Analyses

SAMPLE	A	B	C	D*
Organic Carbon (% by wt.)	0.12	0.16	0.09	0.11
Total Extract (mg/g org. carb.)	106.50	32.20	211.30	2585.20
Hydrocarbon Extract (mg/g org. carb.)	36.90	21.10	71.90	2276.80
% HC in extract	34.70	60.00	65.00	88.10
Saturate/aromatic	2.50	3.00	7.30	13.80
Pristane/nC_{17}	0.58	0.64	0.76	-----
Pristane/Phytane	0.42	0.48	0.26	-----

*Sample contaminated with oil-based diamond saw lubricant.

Potential Source Rocks and Reservoir

Potential source rocks for gas generation are Devonian-Mississippian(?) shale (Hare Indian, Canol and Imperial equivalents) and tongues of Road River shale in the footwall of the Plateau Thrust. Potential reservoir rocks are several Cambrian to Devonian carbonate units (Table 15.1). These carbonates are of variable textures (and therefore porosity). Good reservoirs may be abundant sucrose dolostones or Silurian (coralline) and Devonian (amphiporid) biostromes. In general, reservoir potential is good and the porosities and permeabilities of units in regions are untested.

Conclusions

A broad belt, about 4000 km^2 in area in the Mackenzie Mountains, may have potential for hydrocarbon exploration because Paleozoic carbonates and shales can be inferred to underlie the broad flat northeastern part of the Plateau Thrust Plate.

Organic maturity results are equivocal but suggest that the level of thermal alteration is mature to overmature with respect to oil. Source rocks for gas generation are Devonian-Mississippian(?) shales and Road River shale tongues.

Figure 15.4. Saturate fraction gas chromatogram of Sample A.

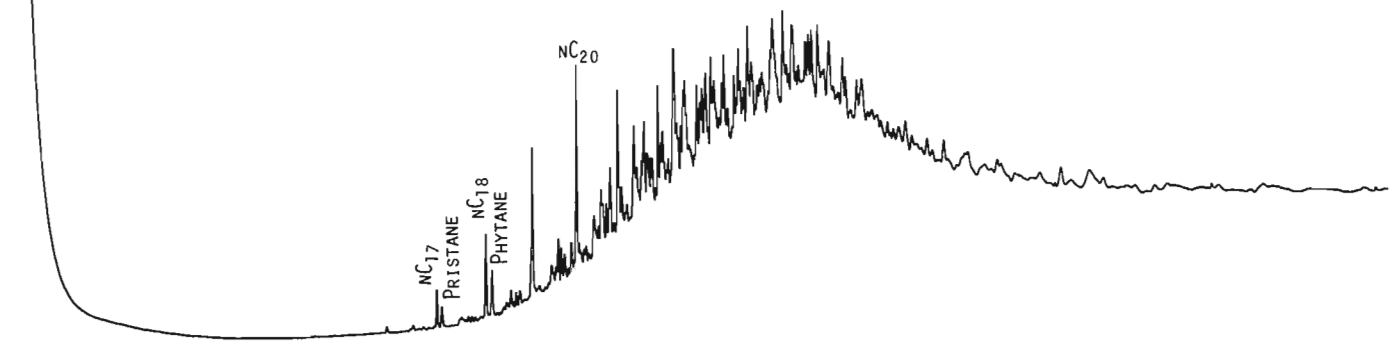

References

Aitken, J.D.
1981: Stratigraphy and sedimentology of the Upper Proterozoic Little Dal Group Mackenzie Mountains, N.W.T.; in ed. F.H.A. Campbell, Proterozoic Basins in Canada; Geological Survey of Canada, Paper 81-10.

Aitken, J.D. and Cook, D.G.
1974a: Carcajou Canyon map-area (96D), District of Mackenzie Northwest Territories; Geological Survey of Canada, Paper 74-13, 28 p.

1974b: Geological maps showing bedrock geology of the northern parts of Mount Eduni and Bonnet Plume Lake map-areas, District of Mackenzie, N.W.T; (106A, B-Scale: 1:125,000); Geological Survey of Canada, Open File 221.

1975: Geology of Upper Ramparts River and Sans Sault Rapids map-areas, District of Mackenzie, N.W.T.; (106G, H-Scale 1:125,000); Geological Survey of Canada, Open File 227.

Aitken, J.D., Cook, D.G., and Yorath, C.J.
Upper Ramparts River (106G) and Sans Sault Rapids (106H) map-areas, District of Mackenzie; Geological Survey of Canada, Memoir 338. (in press)

Aitken, J.D., Macqueen, R.W., and Usher, J.L.
1973: Reconnaissance studies of Proterozoic and Cambrian stratigraphy, lower Mackenzie River area (Operation Norman) District of Mackenzie; Geological Survey of Canada, Paper 73-9, 17 p.

Blusson, S.L.
1971: Sekwi Mountain map-area, Yukon Territory and District of Mackenzie; Geological Survey of Canada, Paper 71-22, 17 p.

Cecile, M.P.
1978: Report on Road River stratigraphy and the Misty Creek Embayment, Bonnet Plume (106B) and surrounding map-areas, Northwest Territories; in Current Research, Part A, Geological Survey of Canada, Paper 78-1A, p. 371-377.

The Lower Paleozoic Misty Creek Embayment, Selwyn Basin, Yukon and Northwest Territories; Geological Survey of Canada, Bulletin 335. (in press)

Cecile, M.P. and Cook, D.G.
1981: Structural cross-section, Northern Selwyn and Mackenzie Mountains; Geological Survey of Canada, Open File 807.

Chamberlin, R.T.
1910: The Appalachian folds of central Pennsylvania; Journal of Geology, v. 18, p. 228-251.

Cook, D.G. and Aitken, J.D.
1978: Twitya Uplift: A pre-Delorme phase of the Mackenzie Arch; in Current Research, Part A, Geological Survey of Canada, Paper 78-1A, p. 383-388.

Dalhstrom, C.D.A.
1960: Concentric folding; in 2nd Annual Field Trip Guide Book; Edmonton Geological Society, p. 82-84.

1969: The Upper detachment in concentric folding; Bulletin of Canadian Petroleum Geology, v 17, p. 326-346.

Douglas, R.J.W.
1969: Geological map of Canada; Geological Survey of Canada, Map 1250 A.

Douglas, R.J.W., Gabrieslse, H., Wheeler, J.O., Stott, D.F., and Belyea, H.R.
1970: Geology of western Canada; in Geology and Economic Minerals of Canada, ed. R.J.W. Douglas, Geological Survey of Canada, Economic Geology, Report 1.

Eisbacher, G.H.
1978: Re-definition and sub-division of the Rapitan Group Mackenzie Mountains; Geological Survey of Canada, Paper 77-35.

Fritz, W.H.
1976: Ten stratigraphic sections from the lower Cambrian Sekwi Formation, Mackenzie Mountains, Northwestern Canada; Geological Survey of Canada, Paper 76-22, 42 p.

Gabrielse, H., Blusson, S.L., and Roddick, J.A.,
1973: Geology of the Flat River, Glacier Lake, and Wrigley Lake map-areas, District of Mackenzie and the Yukon Territory 95E, L, M; Geological Survey of Canada, Memoir 366, 150 p.

Gordey, S.P. (Abs)
1981a: Structure section across south central Mackenzie Mountains, N.W.T.; Geological Association of Canada Abstracts, v. 6, p. A-22.

1981b: Structure section across southcentral Mackenzie Mountains, N.W.T.; Geological Survey of Canada, Open File 809.

Hossack, J.R.
1979: The use of balanced cross-section in the calculation of orogenic contraction: A Review; Journal of the Geological Society of London, v. 136, p. 705-711.

16.

CORRELATIONS BETWEEN THE SUNBLOOD, ESBATAOTTINE AND WHITTAKER FORMATIONS IN THE LOWER PALEOZOIC SEQUENCE OF THE SOUTHERN MACKENZIE MOUNTAINS

Project 750085

D.W. Morrow
Institute of Sedimentary and Petroleum Geology, Calgary

Morrow, D.W., Correlations between the Sunblood, Esbataottine and Whittaker formations in the Lower Paleozoic sequence of the southern Mackenzie Mountains; in Current Research, Part A, Geological Survey of Canada, Paper 82-1A, p. 95-98, 1982.

Abstract

A large part of the Sunblood Formation that is shown on a recent Geological Survey of Canada map of the Virginia Falls map area (95 F) in the region around Sunblood Mountain should be assigned to the Esbataottine and Whittaker formations. Also, the Esbataottine Formation in the Virginia Falls map area was found to correlate stratigraphically with the entire lower member of the Whittaker Formation at its type section on the Whittaker Range in the Root River map area (95 K). Previously the Esbataottine Formation was considered to correlate only with the lower part of the lower member of the Whittaker Formation.

Introduction

During the past decade a divergence has developed between the stratigraphic nomenclature of the Geological Survey of Canada scientists and that of other workers concerning Ordovician rocks of the Southern Mackenzie Mountains. Douglas and Norris (1961, 1976a and 1976b) divided the Ordovician strata of the Virginia Falls (95 F) and Root River (95 F) map areas into two formations; the bright orange weathering Sunblood Formation and the conformably overlying, dull grey weathering Whittaker Formation. Ludvigsen (1975) assigned a part of this sequence to a new formation, the Esbataottine Formation, and he designated a section at Esbataottine Mountain in the northwest part of the Virginia Falls map area (95 F) as its type section (Fig. 16.1).

Douglas and Norris (1960) first restricted the Sunblood Formation (Kingston, 1951) in the Virginia Falls map area to only the bright orange and yellow weathering strata below the dull grey overlying strata that forms the northern dip slopes of both Sunblood and Esbataottine Mountains, which they assigned to an unnamed map unit (Map unit 3, Douglas and Norris, 1960). Ludvigsen (1975) concurred with this subdivision but pointed out that their choice of the upper contact of the Sunblood was about 180 m stratigraphically below the upper contact as originally defined by Kingston (1951). Ludvigsen (1975) assigned 180 m of fossiliferous grey limestone immediately overlying the Sunblood of Douglas and Norris (1960) to a new formation; the Esbataottine Formation, and the remainder of Douglas and Norris's (1960) map unit 3 to the Whittaker and Road River formations. Ludvigsen (1975, 1978) has emphasized that the Esbataottine Formation correlates with the upper part of the Sunblood but also has noted that the upper contact of the Esbataottine with the Whittaker Formation, at the type section of the Whittaker, is placed tentatively at the stratigraphic level where the limestones become slightly thicker bedded and more resistant within rocks that were included previously in the Whittaker Formation.

However, Douglas and Norris (1976a, b) have not included the Esbataottine Formation in their recent final geologic maps of the Virginia Falls and Root River map areas. Instead they have added the lower part of their previous map unit 3 to the Sunblood Formation and have assigned the upper part of map unit 3 to an undivided unit of Ordovician, Silurian and Devonian strata that is structurally continuous with the Road River Formation mapped farther west by Gabrielse et al. (1973).

A part of the month of August (1981) was spent measuring sections of the Sunblood, Esbataottine and Whittaker formations in the Root River and Virginia Falls map area (Fig. 16.1) in an attempt to define more clearly the stratigraphic position of the Esbataottine Formation with respect to the Whittaker and Sunblood formations and also to verify the presence of the Whittaker Formation in the Virginia Falls map area. A Buffalo Airways Bell 206C helicopter stationed at the Cadillac Exploration Limited mine on Prairie Creek in the Virginia Falls map area was provided for logistical support during this time. I particularly wish to acknowledge the help of my field assistant, Martin Teitz, who, during this period, materially aided the progress of this study.

The Type Section of the Whittaker and Esbataottine Formations

The Whittaker Formation at its composite type section near Trench Lake in the Root River map area is divisible into three well defined parts, a lower medium grey fossiliferous and argillaceous limestone, a middle dark brownish grey coralline and cherty dolostone, and an upper light yellowish grey shaly limestone (Fig. 16.1, 16.2). Douglas and Norris (1961) measured thicknesses of 1320 feet (403 m), 860 feet (262 m) and 1890 feet (576 m) for these parts in ascending stratigraphic order for a total thickness of 4070 feet (1241 m). The base of the Whittaker Formation is gradational but well defined both regionally and at the type section at the stratigraphic level where the bright reddish orange and yellow dolostones and limestones of the Sunblood Formation pass upwards abruptly to the dull grey lower part of the Whittaker Formation (Fig. 16.2). A well developed bench also occurs at the top of the Sunblood Formation in the region of the type section on the east flank of the Whittaker Anticline (Fig. 16.2).

The lower part of the type Whittaker Formation, re-examined during this study (Fig. 16.1), is composed of argillaceous thin lumpy to nodularly bedded bioturbated skeletal lime wackestone with an abundant and diverse shallow water fauna including ramose ectoproct bryozoans, brachiopods, trilobites, gastropods and crinoids. Other lithologies present in small amounts include platy yellow and light grey silty lime mudstones, dark grey planar medium bedded coralline lime mudstones and a single prominent orange sandstone bed. This part itself may be subdivided into a recessive, light greyish brown lower division, a middle

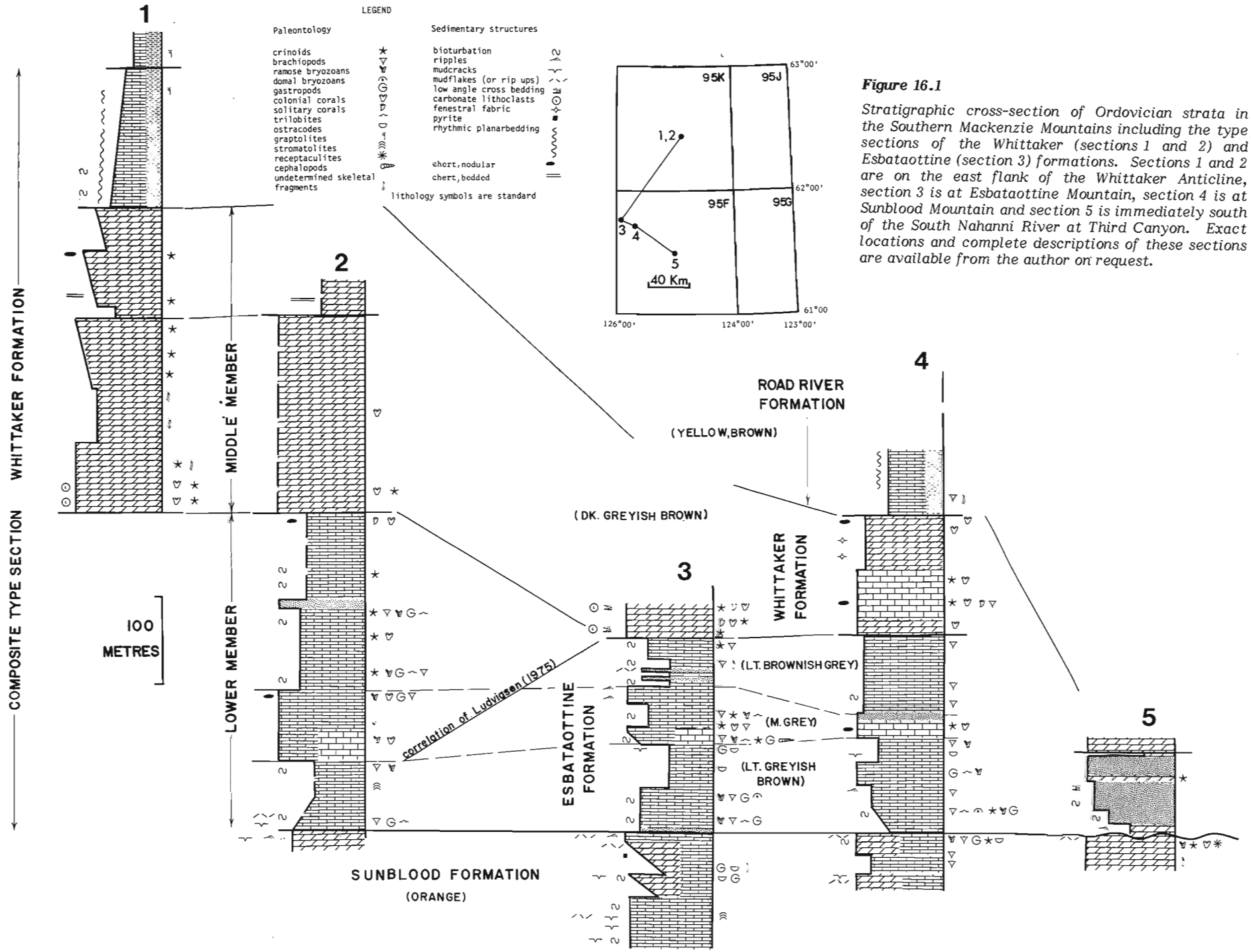

Figure 16.1

Stratigraphic cross-section of Ordovician strata in the Southern Mackenzie Mountains including the type sections of the Whittaker (sections 1 and 2) and Esbataottine (section 3) formations. Sections 1 and 2 are on the east flank of the Whittaker Anticline, section 3 is at Esbataottine Mountain, section 4 is at Sunblood Mountain and section 5 is immediately south of the South Nahanni River at Third Canyon. Exact locations and complete descriptions of these sections are available from the author on request.

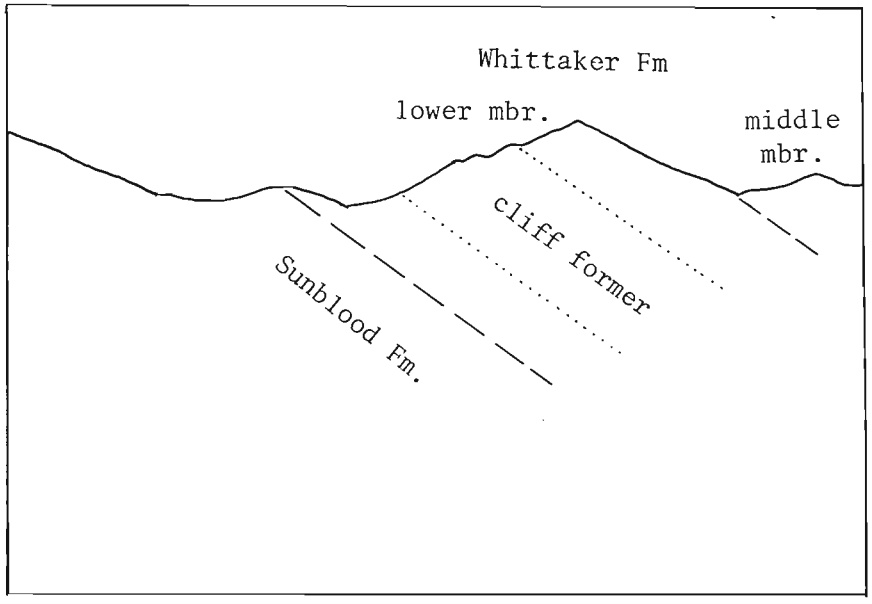

Figure 16.2. *A view of the south side of the Sunblood and Whittaker formations in the ridge immediately north of the Whittaker type section (Section 2). The lower contact of the Whittaker on the Sunblood Formation is well marked as is the contact between the lower and middle members or parts of the Whittaker. There is a resistant cliff-forming subdivision in the middle of the lower part of the Whittaker Formation.*

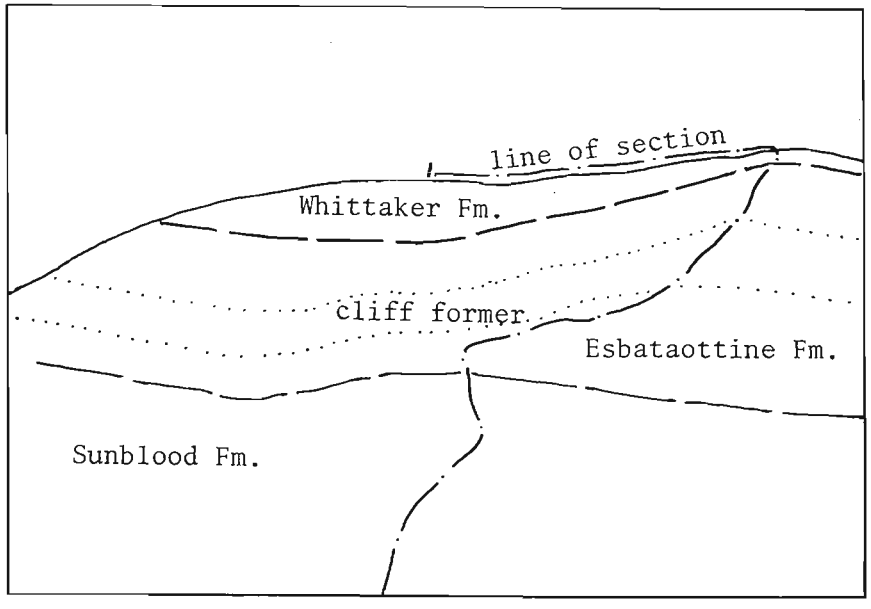

Figure 16.3. *Northward view from Esbataottine Mountain showing the type section of the Esbataottine Formation underlain by the yellowish orange Sunblood Formation and overlain by the Whittaker Formation. Note the tripartite subdivision of the Esbataottine with a middle resistant cliff-forming division.*

resistant cliff-forming chert nodule and coralline limestone division, and an upper recessive light brownish grey division (Fig. 16.1, 16.2). The measured thickness of the lower part of the Whittaker Formation in this study is 372.0 m or slightly less than the 403 m cited by Douglas and Norris (1961).

The middle resistant part of the Whittaker is composed of 349.0 m of cherty and coralline dark brownish grey thin- to medium-bedded dolostone with some intervals of ribbon chert near the top. Also the base of this part is marked by a very resistant light grey unit of skeletal and intraclast (or lithoclast) packstone with abraided crinoid and dolomitized lime mudstone fragments. The upper greyish yellow recessive part is formed of 399.0 m thin planar lime mudstone and shale couplets and platy argillaceous graptolitic lime mudstones. Possibly some of the strata included in the middle part in this study was assigned by Douglas and Norris (1961) to their thick uppermost Whittaker subdivision.

The type section of the Esbataottine Formation at Esbataottine Mountain in the Virginia Falls map area is strikingly similar faunally and lithologically to the lower part of the Whittaker Formation in the Root River map area. The tripartite subdivision of the lower part of the Whittaker is also recognizable in the Esbataottine Formation with a middle resistant coralline cliff former sandwiched between two more recessive subdivisions (Fig. 16.1, 16.3). The thickness of the Esbataottine measured for this study is 223.5 m which is slightly greater than the 190.5 m cited by Ludvigsen (1975). Part of this discrepancy is explained by the choice of an upper contact about 28.0 m higher in the sequence than the upper contact chosen by Ludvigsen (1975). The basal contacts of the two sections are similar and well marked by an orange sandstone bed. Overlying the type Esbataottine is a dip slope sequence of coralline and crinoidal medium planar bedded dolostone and limestone containing some silicified corals tentatively identified as **Bighornia** cf. and **Favosites** sp. Typical Whittaker lithologies of dark greyish brown coralline dolostone are present as thin bands punctuating what is otherwise a medium grey sequence. The base of this sequence is marked by a 1.0 m thick bed of light grey and crossbedded dolomitized crinoidal and lithoclast packstone (or grainstone), and several beds of this type, 1.0 to 3.0 m thick occur higher in the sequence.

Whittaker-Esbataottine Correlations and Regional Development

The correlation by Ludvigsen (1975) of the Esbataottine to the recessive lower subdivision of the lower part of the Whittaker Formation is shown in Figure 1. The close similarity of the lithologies and the subdivisions within both the Esbataottine Formation and the lower part of the Whittaker Formation imply however that these rock sequences are or were part of a single lithostratigraphic unit. This lithostratigraphic correlation is supported by the much closer resemblance of the dolostone sequence overlying the Esbataottine with the middle dolostone part of the type Whittaker Formation. It should be recognized that the Esbataottine Formation is identical lithostratigraphically to the lower part of the Whittaker Formation. The nomenclature of Ludvigsen (1975) for the sequence overlying the Esbataottine including the Whittaker and Road River formations (Fig. 16.1) is preferable to that of Douglas and Norris (1976a) in that the Sunblood Formation should be restricted to the bright orange weathering strata below the dull grey Whittaker-Esbataottine sequence.

The distribution of the Esbataottine Formation (or lower part of the Whittaker) and paleogeographic reconstructions shown by Ludvigsen (1975, p. 692) is consistent with the occurrence of a thin sequence of foreshore buff to orange quartz-arenite sandstones and sandy dolostones resting with a probable unconformity on the Sunblood Formation and underlying Road River platy limestones in Section 5. Orange dolostone pebbles (1-2 cm long) that may have been derived from the underlying Sunblood occur as gravel lags at the bases of some fining-upward (tidal channel?) sequences in these sandstones. This implies that the central region of the Virginia Falls map area was either exposed or receiving very little sediment during deposition of the Esbataottine farther west. The scattered sandstone bodies in the Esbataottine were probably derived in part from the central region of the Virginia Falls map area. The Whittaker Formation that has widespread distribution throughout the Mackenzie Mountains is confined stratigraphically only to the middle and upper parts of the type Whittaker Formation.

Conclusions

1. The nomenclature of Ludvigsen (1975) for the Ordovician strata of the Virginia Falls map area appears to be justified but it should be recognized that the Esbataottine Formation is lithostratigraphically identical to the lower part of the Whittaker Formation at its type section.
2. The fact that the lower part of the Whittaker Formation (or the Esbataottine Formation) is confined to a much smaller area than the overlying middle and upper parts of the Whittaker Formation supports the formal assignment of the lower part of the Whittaker Formation to the Esbataottine Formation. Discussion of this suggestion is deferred to a more authoritative publication in the future.
3. The paleogeographic reconstructions presented by Ludvigsen (1975) are consistent with the data of this study.

References

Douglas, R.J.W. and Norris, D.K.

1960: Virginia Falls and Sibbeston Lake map-areas, Northwest Territories; Geological Survey of Canada, Paper 60-19.

1961: Camsell Bend and Root River map areas, District of Mackenzie, Northwest Territories; Geological Survey of Canada, Paper 61-13.

1976a: Virginia Falls map-area, District of Mackenzie; Geological Survey of Canada, Map 1378A.

1976b: Root River map-area, District of Mackenzie, Geological Survey of Canada, Map 1376A.

Gabrielse, H., Roddick, J.A., and Blusson, S.C.

1973: Geology of Flat River, Glacier Lake, and Wrigley Lake map-areas, District of Mackenzie and Yukon Territory; Geological Survey of Canada, Memoir 366.

Kingston, D.R.

1951: Stratigraphic reconnaissance along Upper South Nahanni River, Northwest Territories, Canada; Bulletin of American Association of Petroleum Geology, v. 35, no. 11, p. 2409-2426.

Ludvigsen, R.

1975: Ordovician formations and faunas, Southern Mackenzie Mountains; Canadian Journal of Earth Sciences, v. 12, no. 4, p. 663-697.

1978: Middle Ordovician trilobite biofacies, Southern Mackenzie Mountains; in Stelck, C.R. and Chatterton, B.D.E. ed., Western and Arctic Canadian Biostratigraphy, Geological Association of Canada, Special Paper 18, p. 1-38.

17.

GEOLOGY OF THE CENTRAL WOPMAY OROGEN (EARLY PROTEROZOIC), BEAR PROVINCE, DISTRICT OF MACKENZIE: REDROCK LAKE AND THE EASTERN PORTION OF CALDER RIVER MAP AREAS

Project 810020

M.R. St-Onge, J.E. King[1], and A.E. Lalonde[2]
Precambrian Geology Division

St-Onge, M.R., King, J.E., and Lalonde, A.E., Geology of the central Wopmay Orogen (Early Proterozoic), Bear Province, District of Mackenzie: Redrock Lake and the eastern portion of Calder River map areas; in Current Research, Part A, Geological Survey of Canada, Paper 82-1A, p. 99-108, 1982.

Abstract

Early Proterozoic and Archean rocks east of the Wopmay Fault Zone, in the Redrock Lake and Calder River map areas, are involved to a greater or lesser degree in one or both collisional orogenies of Wopmay Orogen. The Carousel Massif, an anticline cored by Archean basement, is a disharmonic fold structure in the Asiak fold-thrust belt that formed during the first collision. To the west, the Hepburn Batholith is composed of over 40 discrete plutons in the northern part of the area, each more or less deformed by the first collision event. The orogenic plutons vary in composition from hornblende-diorites to biotite-granites and locally contain abundant partly resorbed supracrustal xenoliths. Intrusive age relationships and the extent of development of a metamorphic fabric indicate at least two periods of emplacement for both granite and tonalite plutons. The association of minor amounts of anorthosite with the hornblende-diorites suggests an evolution from mafic parental liquids for a part of the Hepburn Batholith. West of the batholith the structural style of the Akaitcho Group is dominated by early east-verging recumbent folds at all metamorphic grades investigated, from andalusite-muscovite schists to kyanite-granulites. In the kyanite-granulite terrane a stack of three horizontal to west-dipping thrust nappes show west over east overlap. The present Akaitcho Group map pattern is controlled by a series of faults outlining crustal blocks formed during the second collision event. Emplacement of one of these crustal blocks has juxtaposed rocks containing bathozone 6 and bathozone 3 mineral assemblages. The westernmost Akaitcho Group is characterized by a set of north-south fault blocks marking major breaks in the structural and metamorphic map patterns. Together these blocks constitute the Wopmay Fault Zone.

Introduction

Wopmay Orogen (McGlynn, 1970; Fraser et al., 1972) is the early Proterozoic tectonic-metamorphic belt that flanks the western edge of the Archean Slave craton in the northwestern corner of the Precambrian Canadian Shield. Work in the various tectonic zones of the Wopmay Orogen has, over the years, led to the formulation of the most comprehensive plate tectonic model for the evolution of a Proterozoic orogenic belt (Hoffman, 1980b) so far documented in the literature. This achievement warrants renewed efforts in further mapping and understanding the rocks of Wopmay Orogen.

The present project, begun in 1981, is concerned with resolving the complexities of the internal zone of the orogenic belt south of the Hepburn Lake map sheet, locus of previous studies (Hoffman, 1972, 1973; Hoffman et al., 1978, 1980, 1981; St-Onge and Carmichael, 1979; Easton, 1980, 1981a, b; Hoffman and St-Onge, 1981; St-Onge, 1981). This study focuses on the Proterozoic rocks of the Redrock Lake map area (86 G) west to the Wopmay Fault in the Calder River map area (86 F). The map area thus encompasses foreland fold and thrust style deformation of a platform sequence in the east, a syntectonic plutonic and metamorphic belt in the centre and a zone of thrust nappes, high-pressure rocks and mylonites in the west.

In the course of this project, topical studies are being undertaken as follows: a study of the regional structure and change in style of deformation across the area by J.E. King, under the supervision of H. Helmstaedt (Queen's University), and a study of the syn- to post-tectonic plutons of the internal zone, their petrogenesis and chronology of emplacement by A.E. Lalonde, under the supervision of R.F. Martin (McGill University). Both studies will form the bases of Ph.D. theses.

Systematic 1:100 000 scale mapping of a northern transect across the project map area (Fig. 17.1) was completed in the summer of 1981. The results of the field work show that:

1. The major tectonic, stratigraphic and plutonic units defined in the Hepburn Lake project (Hoffman et al., 1978, 1980; Easton, 1980; Hoffman, 1981) continue and are mappable to the south.
2. The Carousel Massif, an anticline cored by Archean basement (Fraser, 1960, 1974), is a disharmonic fold structure with respect to the deformed and easterly-transported early Proterozoic shelf sequence of the Asiak fold-thrust belt.
3. The Hepburn Batholith is a composite intrusion with plutons that range in composition from hornblende-diorite to biotite-granite. Age relationships show that these plutons do not define a uniform compositional evolution for the batholith. The development of peraluminous compositions appears strongly related, in most plutons, to the presence of pelitic xenoliths.
4. The Akaitcho Group, representing the initial-rift sequence (Hoffman et al., 1978; Easton, 1980, 1981b; Hoffman, 1980b) is involved in east-verging recumbent folds at all grades of metamorphism (from andalusite-muscovite-biotite-plagioclase-quartz to kyanite-biotite-orthoclase-plagioclase-quartz-granitic melt assemblages in pelites; the latter phase is inferred from granitic pods in the metasediment).
5. Crustal block "D" of Hoffman and St-Onge (1981) dominates the map pattern of a significant portion of the western Akaitcho Group in the study area, juxtaposing contrasting metamorphic pressure levels.

[1] Department of Geological Sciences, Queen's University, Kingston, Ontario, K7L 3N6

[2] Department of Geological Sciences, McGill University, Montréal, Québec

6. The kyanite-granulite terrane in the western Akaitcho Group consists of a stack of premetamorphic thrust-nappes characterized by early east-verging recumbent folds and a flat-lying to west-dipping tectonic foliation. These structures are truncated to the west by a prominent north-south trending mylonite zone.
7. The Wopmay Fault Zone (Easton, 1981a), the area between the mylonite zone and the first (fault-bounded) occurrence of Great Bear Batholith rocks (Dumas Group), is dominated by a set of north-south faults that juxtapose various Akaitcho Group units of contrasting metamorphic grade and degree of cataclasis.

Carousel Massif

The Carousel Massif is a unique feature of the Asiak fold-thrust belt, in that the fold structure is cored by Archean basement rocks (Fraser, 1960, 1974) exposed over an east-west width of 6 km at the present erosion level (Fig. 17.2). The Archean of the massif is a homogeneous sheared "b"-granite (Streckeisen, 1976) in which the cataclastic fabric varies in intensity but maintains an average attitude of about 220°/75°W. Locally the granite can be K-feldspar megacrystic and in some localities contains amphibolite boudins up to 50 m long.

On the west side of the anticline a composite lowermost Proterozoic section can be compiled. Where the unconformity is locally exposed a granite-pebble conglomerate of uncertain and likely irregular thickness rests on the Archean granite. The granite pebbles appear identical to the underlying sheared basement granite. Above this, the section is characterized by 4 to 6 m of white orthoquartzite overlain by 260 m of olive-green pelite with 1 to 2 cm thick silty interbeds. The pelite is muscovite-chlorite-plagioclase-quartz-graphite-bearing and is identical in bedding style and lithological aspects to the pelites of the Odjick Formation underlying the Rocknest Formation dolomite in the eastern part of the map area. Overlying this lower clastic section is a 35 m thick mafic member which comprises massive and pillowed basaltic flows, and differentiated sills. This basaltic member is distinctively rich in euhedral plagioclase phenocrysts approximately 1 cm long (Fig. 17.3). The horizon is concordant to the outline of the Archean core (Fig. 17.2), indicating that, up to this stratigraphic level, the Carousel structure is a simple anticline plunging north at 20°, with limbs dipping 15° to 30° west or east (measured in the lower Proterozoic sediments).

Over a covered interval of 400 m, stratigraphically above the mafic member, the style of deformation changes dramatically. Upright, north-plunging chevron-style folds of the overlying Epworth and Recluse groups have a mean wave length of 1 km (Fig. 17.2) with limbs that typically dip 60°. This very tightly folded section is in marked contrast to the open structure of the Carousel Massif anticline. Obviously the amount of east-west shortening is different between that part of the section below the mafic horizon and the section above it. A décollement surface must be present above the mafic horizon near or at the contact with the Odjick pelites. Thus, although the Archean basement and the lower Proterozoic section are involved in some east-west shortening, the Carousel Massif is a disharmonic fold structure with respect to the deformation registered in the overlying Epworth and Recluse groups. The extent to which Carousel Massif is itself allochthonus and whether the décollement surface above the mafic horizon is in fact a sole fault for the thrusting of the overlying strata, should be clear following mapping of the Proterozoic in the northwestern corner of Point Lake map area (86 H).

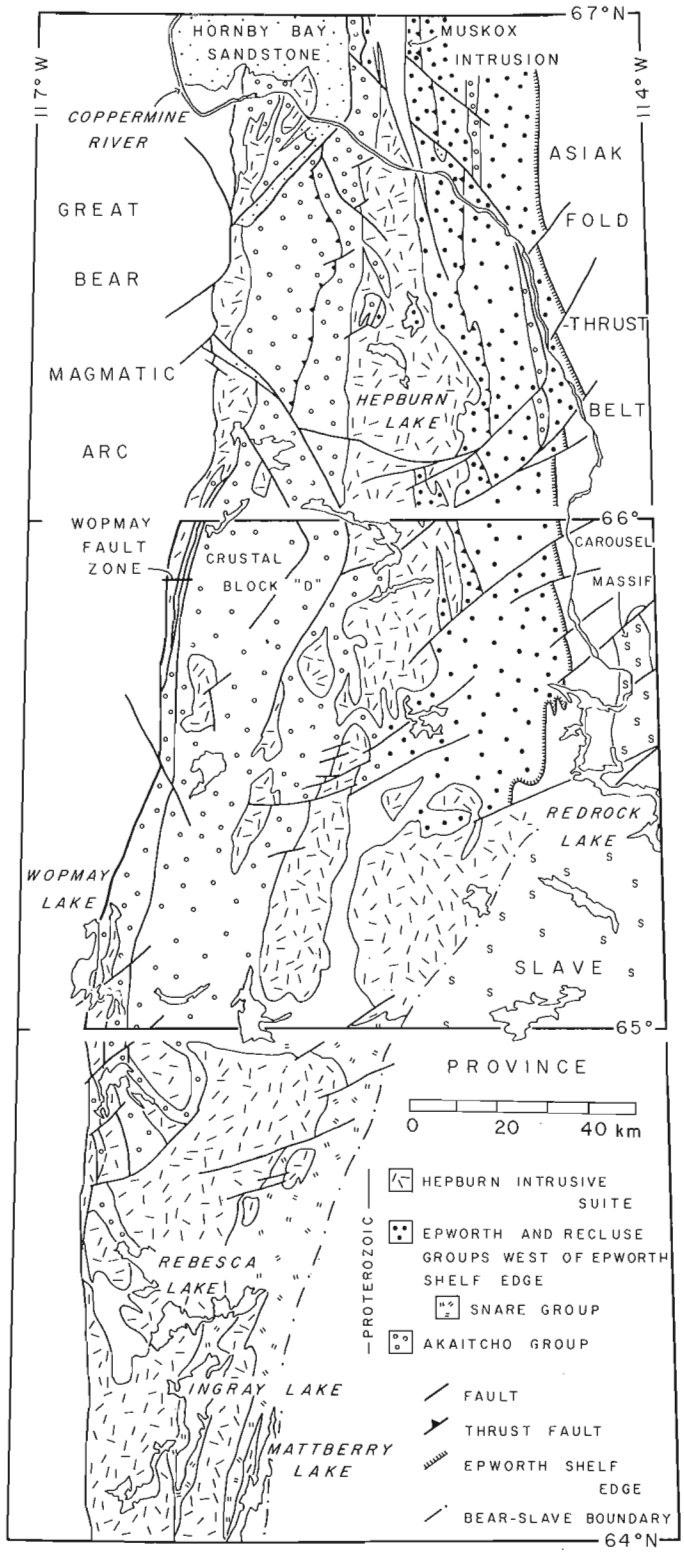

Figure 17.1. Geological map of the Heburn metamorphic-plutonic belt (Zone 3) of Wopmay Orogen showing the location of the project map area. Adapted from Easton (1981a).

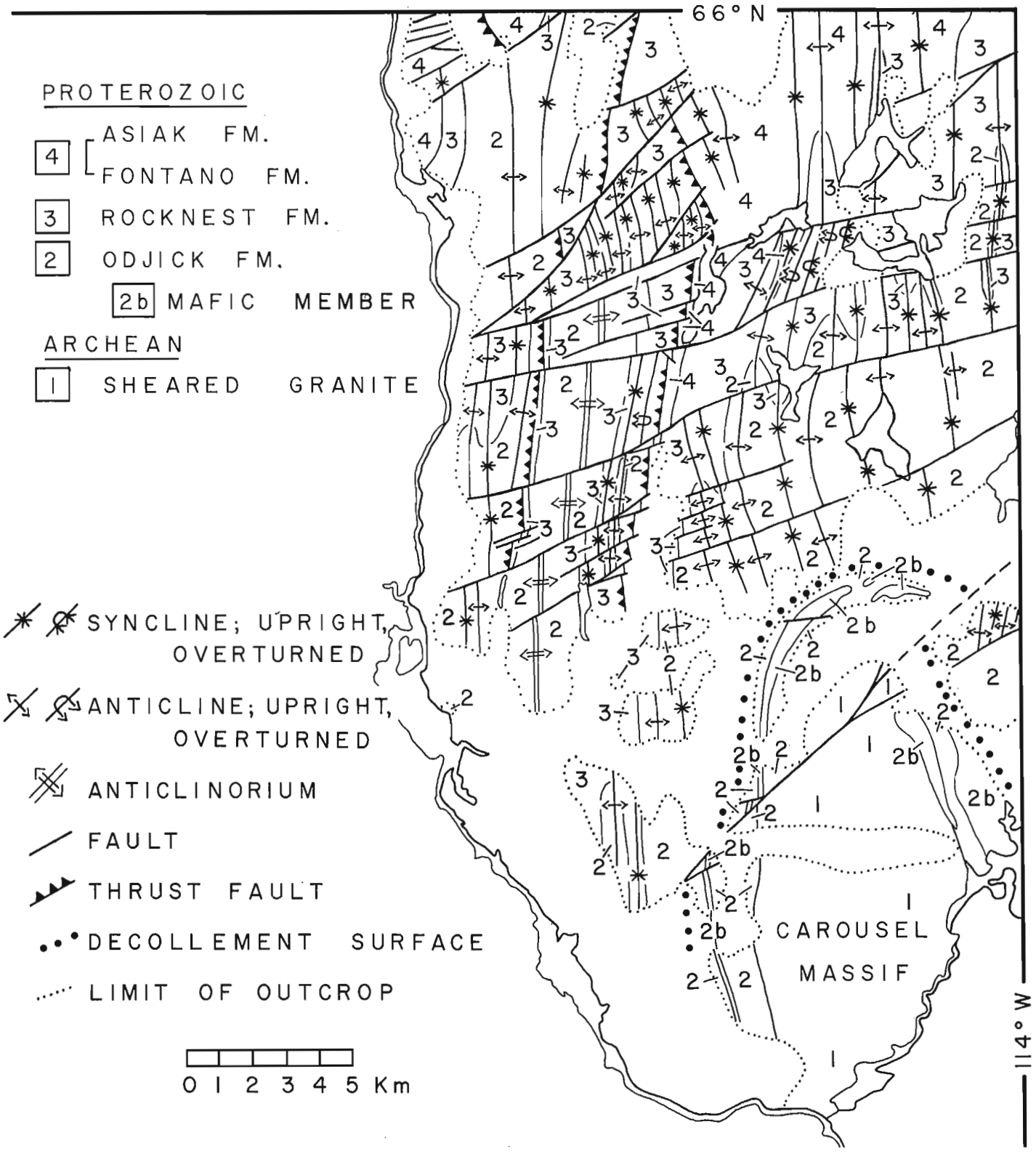

Figure 17.2. *Geological map of the Asiak fold-thrust belt in the northeast corner of the Redrock Lake sheet (86 G). River in figure is the Coppermine River.*

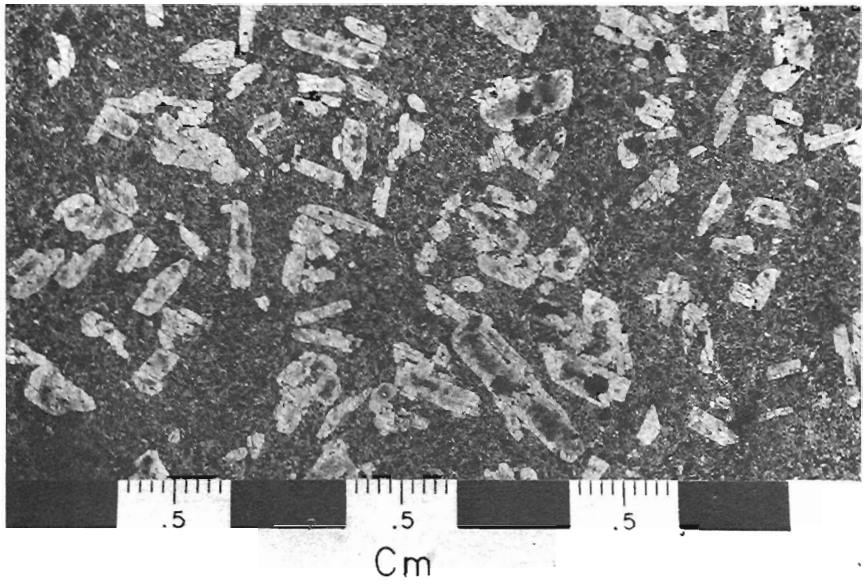

Figure 17.3. Plagioclase-rich basaltic sill on the west side of the Carousel Massif anticline. GSC 203780-E

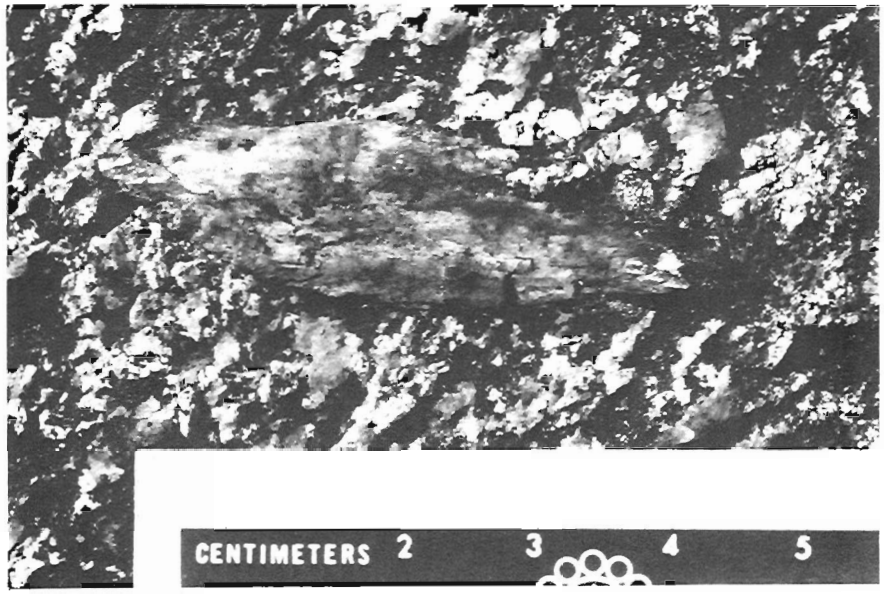

Figure 17.4. Cluster of sillimanite in an eastern granite pluton of the Hepburn Batholith. GSC 203780-F

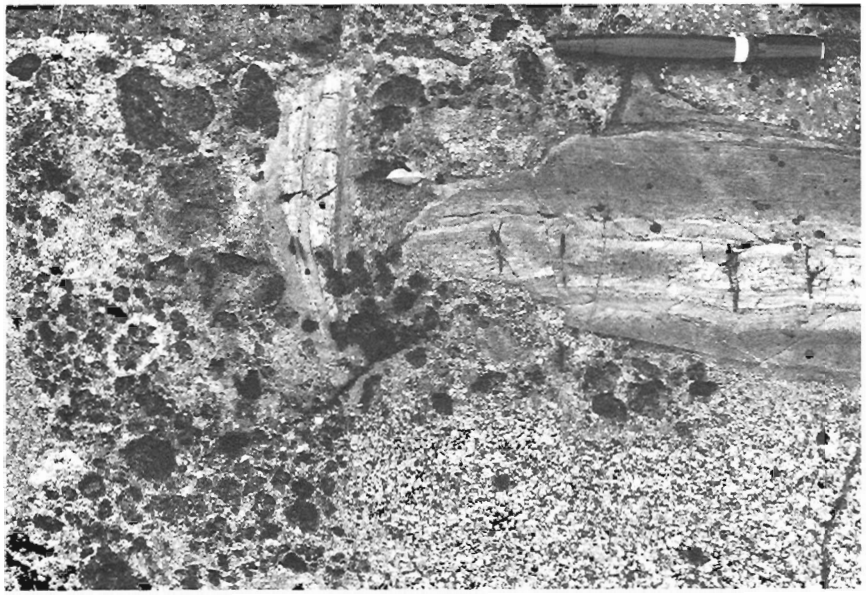

Figure 17.5. Metasedimentary xenoliths and garnets in a Hepburn Batholith tonalite. The garnets form the dark low weathering cluster in the tonalite on the left hand side of the photo. GSC 203780-C

Figure 17.6. K-feldspar megacryst in a Hepburn Batholith granite pluton. Inner core is outlined by inclusion trains of biotite, plagioclase and quartz. GSC 203780-B

Figure 17.7. Early east-verging recumbent folds of gneissic foliation in feldspathic quartzite. Photo taken looking northwest. GSC 203780

Hepburn Batholith

The Hepburn Batholith, as mapped to date in Redrock map area, consists of over 40 discrete plutons distributed along a broad north-south trending zone approximately 25 km wide. Individual plutons are intrusive into earlier units of the batholith and/or high-grade metamorphic equivalents of the Akaitcho or lower Epworth groups. Plutons vary greatly in area from 0.25 km^2 to 65 km^2 and, in a general sense, are petrographically distinct. Zoned plutons have not been observed.

The most abundant rock unit within the batholith is a coarse grained, massive to foliated biotite granite characterized by large K-feldspar megacrysts. This unit forms the larger plutons and accounts for approximately 80 per cent of the batholith in the area mapped. Mineralogically the unit comprises K-feldspar, plagioclase, quartz, biotite or more rarely, hornblende. Common accessory phases include garnet, sillimanite (Fig. 17.4), muscovite and cordierite, reflecting the peraluminous tendencies of these rocks. In outcrop the occurrence of the aluminous phases appears strongly controlled by the presence of metasedimentary xenoliths (Fig. 17.5). The large K-feldspar megacrysts present in this unit are generally subhedral, 4 to 5 cm in length, and commonly display inner cores outlined by inclusion trains of biotite, plagioclase and quartz (Fig. 17.6). Repetitive inner zones, with faces parallel to the actual crystal boundaries, suggest an episodic growth. The central zone of the batholith is occupied by foliated granites with more tabular K-feldspar megacrysts and abundant xenoliths and schlieren of supracrustal rocks. At the edges of the batholith, the granites are massive, have more equant K-feldspar megacrysts, and are particularly free of supracrustal xenoliths. Intrusive age relationships and the development/absence of a metamorphic fabric support at least two periods of emplacement of this unit.

Tonalites occur in the map area but are less abundant than in the Hepburn Lake map area to the north (Hoffman et al., 1980). Petrographically, the tonalites are medium grained, massive or foliated plagioclase, quartz, biotite or biotite-hornblende rocks. They occur as small plutons, 0.25 to 10 km^2 in area, showing variable age relationships to the granites. Late tonalites are massive and commonly have narrow marginal zones with large poikilitic K-feldspars, suggesting an enrichment in potassium by a limited assimilation of K-rich granitic host rocks. Early foliated tonalites occur as small bodies or lenses within the granites and are hosts to numerous granitic pegmatites and aplites.

Hornblende diorites form a suite of over 20 small plutons concentrated along a broad north-south trending zone located in the western half of the Hepburn Batholith. The plutons are massive to very slightly foliated and are emplaced in both the granites and the Akaitcho or Epworth group migmatites. The diorites have biotite and/or hornblende as their ferromagnesian phase and are locally associated with minor amounts of anorthosite, suggesting they evolved from mafic parental liquids.

The close association within the same batholith of mafic, less-evolved rocks such as diorites together with K-rich peraluminous granites, suggests that mechanisms involving mixed magma sources and/or assimilation of pelitic sediments may have been active in the petrogenesis of the Hepburn Batholith.

Akaitcho Group

Stratigraphy

West of the Hepburn Batholith, where at the latitude of present mapping only the initial-rift sequence Akaitcho Group rocks occur, rock types and the style of structural deformation contrast markedly to that of the Epworth and Recluse groups of the east half of the study area. The Akaitcho Group comprises a bimodal volcanic suite (basalt-rhyolite) intercalated with feldspathic quartzites, semipelites and pelites. Dolomites are rare, occurring mainly in the easternmost Akaitcho Group as 1-5 cm beds finely intercalated with quartz-grit-bearing beds of similar widths. A stratigraphic correlation within the Akaitcho Group, however, will require further mapping in both Redrock Lake and Calder River map areas.

In the northern part of the Redrock Lake map area, the Akaitcho Group-Epworth Group transition is obscured by plutons of the Hepburn Batholith. It is hoped that mapping to the south will yield more information on the nature of the contact. To date there is only one reported exposure of the contact northwest of Hepburn Lake (Easton, 1980) where it is conformable.

Early Recumbent Folds

The structural style in the Akaitcho Group of the map area is dominated at all metamorphic grades and pressure-levels, by early east-verging recumbent folds, some of bedding, but mainly of gneissic foliation at meso- to megascopic scales (Fig. 17.7). A well-developed flat to west-dipping tectonic fabric (schistosity at low-grade, gneissic foliation at high-grade) is axial planar to folds of bedding, and is folded about the folds of gneissic foliation. The early recumbent folds occur in rocks ranging in metamorphic grade, as documented in pelitic horizons, from andalusite-muscovite-biotite-plagioclase-quartz to kyanite-biotite-orthoclase-plagioclase-quartz-granitic melt assemblages. Variation in metamorphic pressure levels are from bathozone 3 to bathozone 6 of Carmichael (1978) and are attributed to the dip-slip displacement associated with the

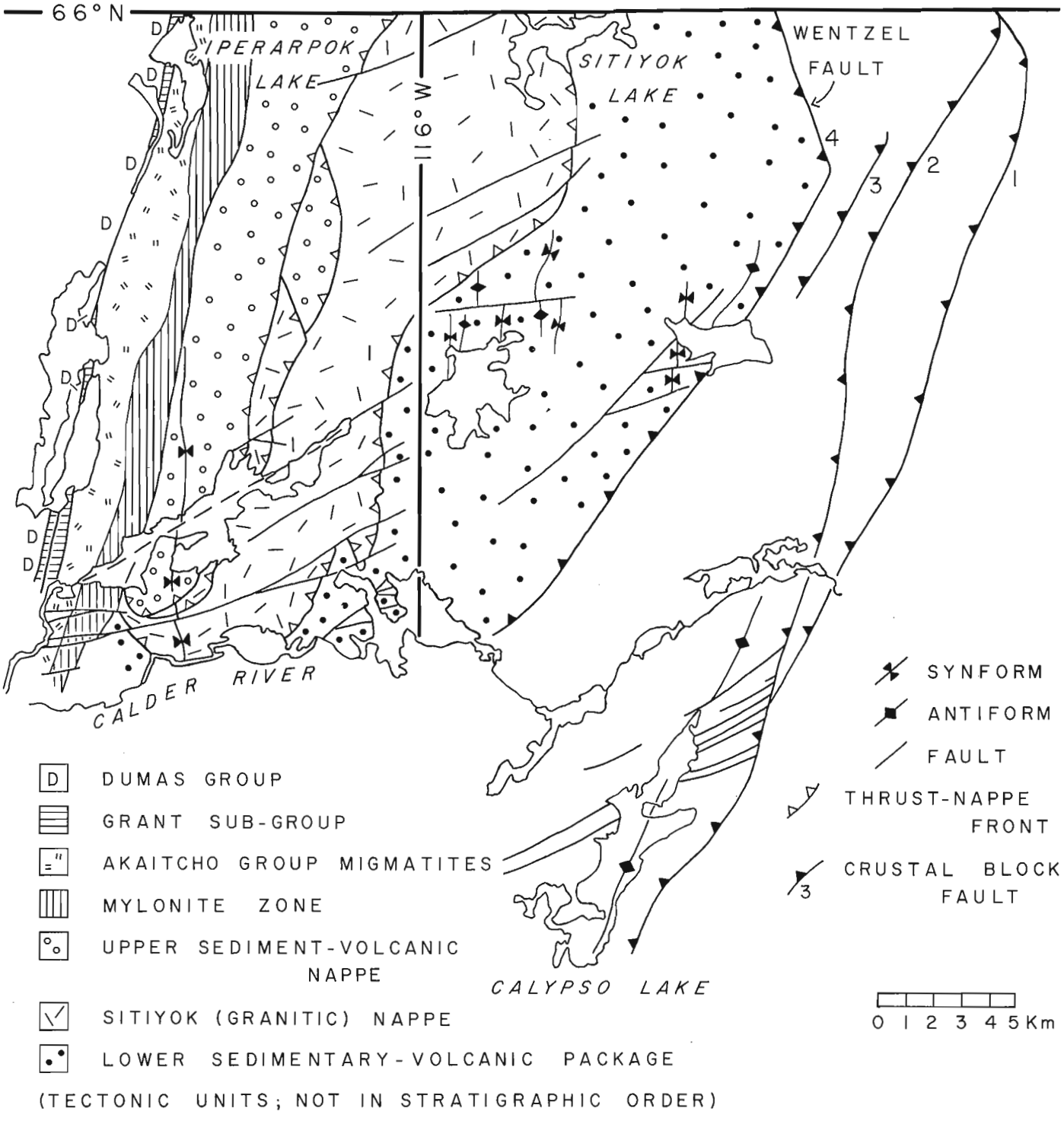

Figure 17.8. *Structural map of the Akaitcho Group in the northwest corner of the Redrock map area and the northeast corner of the Calder River map area.*

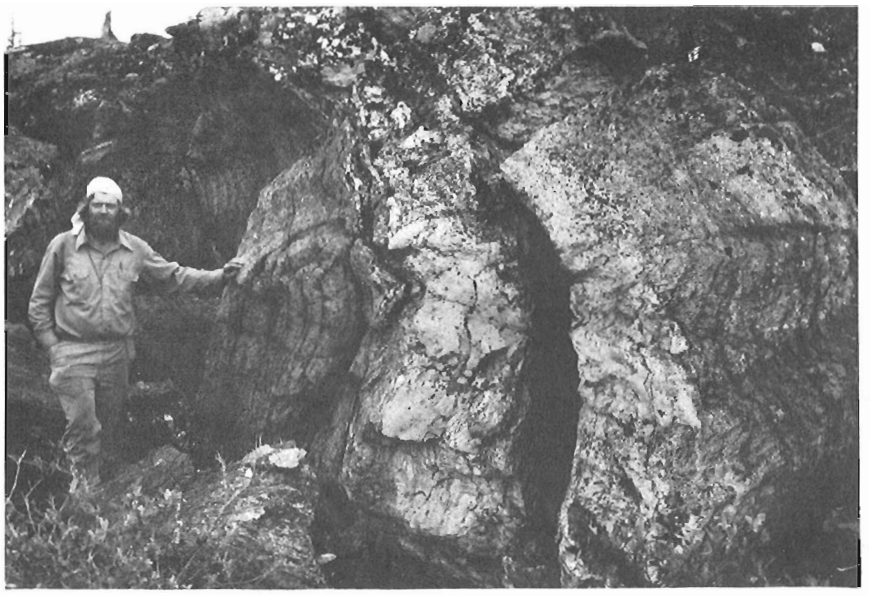

Figure 17.9. *Early recumbent fold hinge in the feldspathic quartzite. Photo taken looking due north. GSC 203870-D*

crustal block "D" of Hoffman and St-Onge (1981) discussed below. The recumbent folding thus occurs over a wide spectrum (and seems independent) of metamorphic P and T; it is an intrinsic characteristic of the Akaitcho Group in contrast to the upright folds of bedding in the Epworth and Recluse groups to the east.

A younger set of structures consisting of broad upright open north-plunging folds of the tectonic fabric, controls the present map pattern (Fig. 17.8). Two megascopic folds of this later set, a broad 7 to 10 km wide synform in the westernmost part of the map area and a 5 km wide antiform centred on Calypso Lake (Fig. 17.8) are structurally truncated; the former by the mylonites of the Wopmay Fault Zone and the latter by one of the fault wedges of crustal block "D".

Thrust-nappes

The Akaitcho Group west of the Wentzel Fault and east of a major mylonite zone (Fig. 17.8) is characterized by the presence of the early east-verging recumbent folds and by a structural stack of at least 2 and possibly 3 thrust-nappes. The lowest (eastern) structural unit is a stratigraphic package consisting of feldspathic quartzite intercalated with garnet-amphibolites. Numerous cliff-or outcrop-scale recumbent fold closures have been mapped (Fig. 17.9), the limbs of which correspond to the regional gneissic foliation dipping 10-40° to the west. Overlying the lower sedimentary-volcanic package is a flat-lying to west-dipping pink cataclasite of "b"-granite composition (Fig. 17.8) in which irregularly-shaped garnet-amphibolite bodies are locally abundant. The fault contact with the underlying structural unit is exposed in several cliff faces. It is near horizontal, parallel to the fabric of the overlying granitic cataclasite and to the gneissic foliation of the underlying strata. The contact itself is a shear zone less than 1 m thick. The nature and attitude of the contact is indicative of a thrust and is interpreted as the lower boundary of an allochthonous thrust-nappe.

The granitic allochthon is in turn overlain to the west by a sedimentary-volcanic package with a stratigraphy distinct from that of the sediments below the granite allochthon; pelites and mafic tuffs are more abundant, whereas feldspathic quartzites are a minor unit. The contact between the granitic cataclasite and the western package is sharp and consists of a narrow shear zone dipping to the west. The transition between the two allochthons occurs over two thrusts, as shown by a structural interleaving of the upper sediment-volcanic package and the granite cataclasite (Fig. 17.8). The stack of horizontal to west-dipping nappes is folded into a broad north-plunging synform of the late fold set in which the thrust contacts can be traced around the fold hinge near the Calder River (Fig. 17.8). The nappe structures are truncated to the west against a prominent 1-3 km wide mylonite zone.

First recognized and mapped by Easton (1981a) as a distinct unit, the granitic allochthon was named the "Sitiyok Complex" and interpreted as basement to the Akaitcho Group. Structural relationships discussed above show that the "Sitiyok Complex" is allochthonous with respect to both underlying and overlying sedimentary-volcanic strata. The regional configuration is undoubtedly that of a thrust-nappe. Whether or not this transported granite cataclasite (Sitiyok Nappe) was once basement to the Akaitcho Group cannot be resolved from the present distribution of units in the field.

Kyanite Granulites

Kyanite-biotite-orthoclase-plagioclase-quartz-granitic melt assemblages are developed in pelites both structurally above and below the Sitiyok Nappe (Fig. 17.10). The mineral assemblage is that of bathozone 6 and infers metamorphic pressures of over 7 kb. In the eastern part of the lower structural unit, the maximum-phase assemblage in the pelites is kyanite-muscovite-biotite-plagioclase-quartz-granitic melt. This assemblage is indicative of a lowering of metamorphic grade eastward, across the kyanite-orthoclase isograd as shown in Figure 17.10. Near the northern sheet boundary similar east-west changes in mineral assemblages occur but with sillimanite as the aluminosilicate phase. A kyanite/sillimanite isograd is present in crustal block "D" as shown on Figure 17.10.

In P-T space, the intersection of the two isograds, the point marked "A" on Figure 17.11, is the basis for the bathograd separating bathozones 5 and 6 (Carmichael, 1978). The intersection of the isograds in the field can be geometrically related to the intersection of univariant reactions on the petrogenetic grid. Thus the trace of the kyanite-orthoclase bathograd can be illustrated (if not rigorously drawn) for the high pressure Akaitcho terrane (Fig. 17.10).

The continuous and regular configuration of the isograds in Figure 17.10 suggests that nappe emplacement preceded the metamorphic culmination. Control using pelitic assemblages is obviously lost in the granite nappe; however, the presence of garnet-amphibolite is indicative of high-pressure metamorphism of the nappe.

Crustal Block "D"

The present map pattern of the western Akaitcho Group is in large part controlled by crustal block "D" of Hoffman and St-Onge (1981). As shown in Figure 17.8 the margin of this block structure is composite with at least four faults (numbered 1 to 4) transecting pre-existing orogenic

structures in the Akaitcho Group. All faults juxtapose contrasting rock units and structural panels. Assemblages in pelites from the different fault blocks provide an estimate of the minimum postmetamorphic dip-slip component of movement for each fault.

Fault 1 (Fig. 17.10) places andalusite-muscovite schists (west side) against sillimanite-orthoclase migmatites of the Hepburn Batholith metamorphic culmination. This culmination is characterized by andalusite at medium grade, on the east side of the batholith. Fault 1 thus juxtaposes contrasting metamorphic temperatures but is not accompanied by any discernible changes in metamorphic pressures. Faults 2 and 3 (Fig. 17.10) have andalusite-muscovite-biotite-plagioclase-quartz assemblages on both sides and thus no distinguishable contrast in metamorphic P-T conditions is produced by the movement on the faults. Fault 4, the inner fault of crustal block "D", juxtaposes blocks with dramatically different pelitic mineral

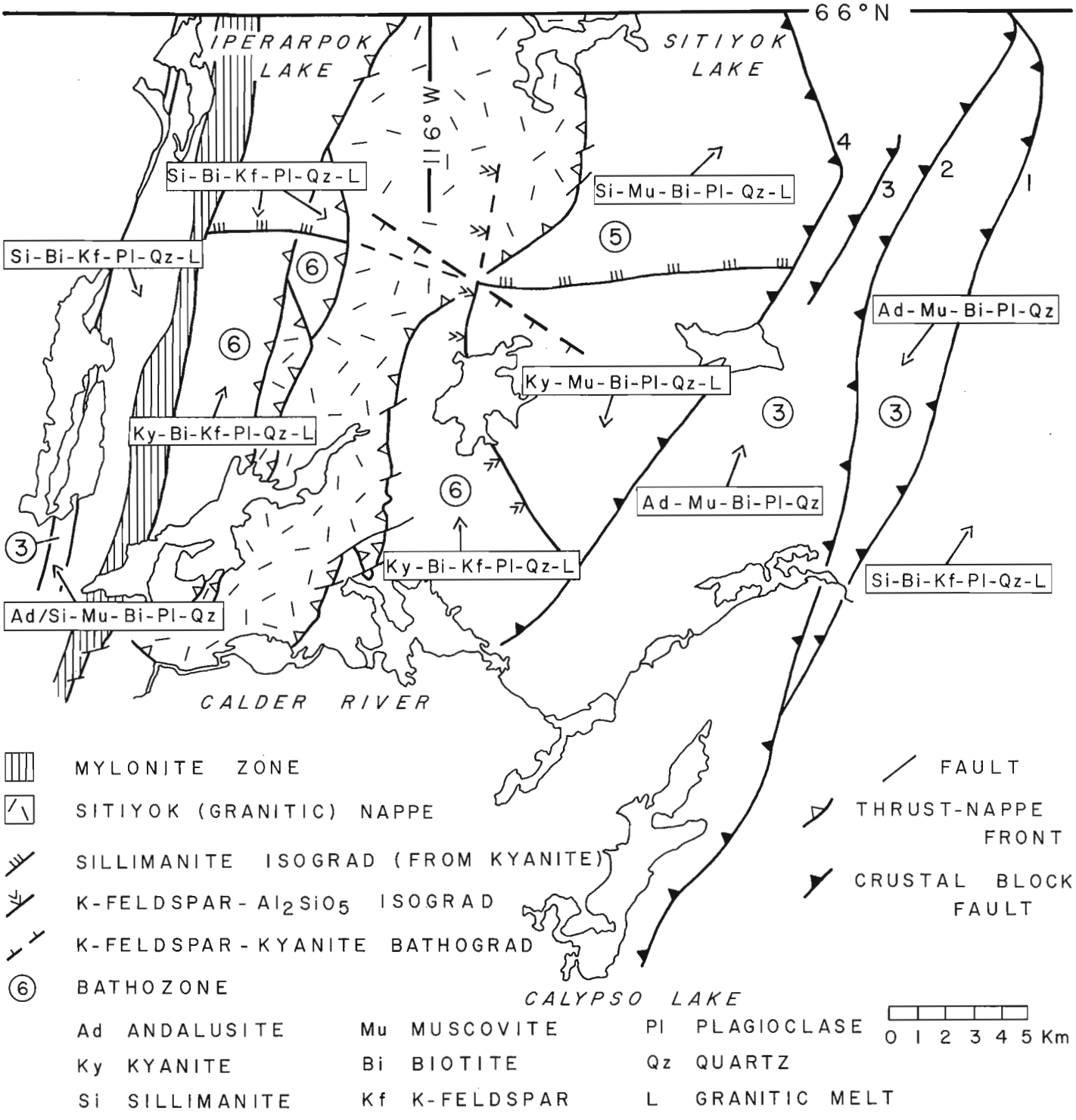

Figure 17.10. Metamorphic map of the Akaitcho Group covering the same area as Figure 17.8.

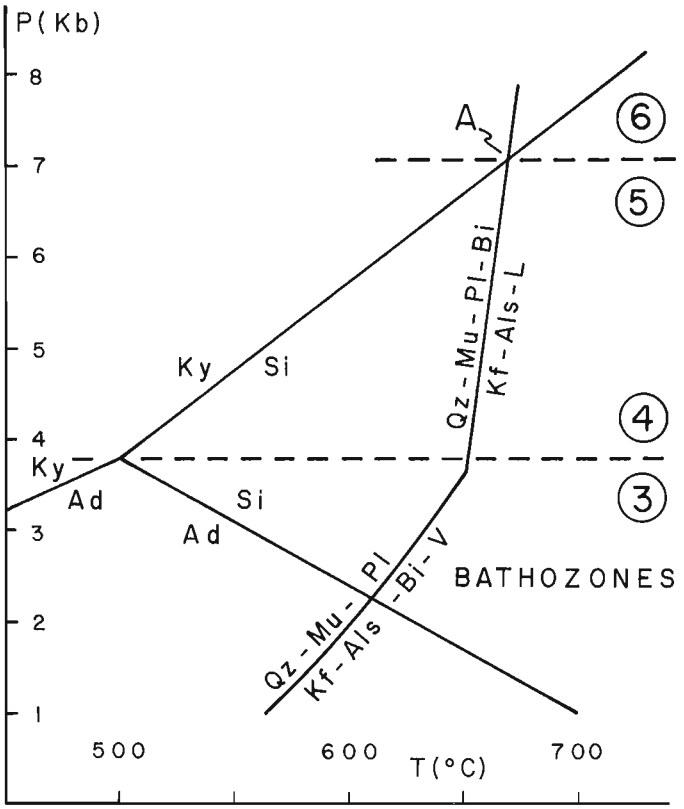

Ky - kyanite	*Mu - muscovite*	*Qz - quartz*
Si - illimanite	*Bi - biotite*	*L - granitic liquid*
Ad - andalusite	*Kf - K-feldspar*	*V - vapour phase*
Als - aluminosilicate	*Pl - plagioclase*	

Figure 17.11. *P-T petrogenetic grid for part of the ideal pelite system SiO_2-Al_2O_3-FeO-MgO-Na_2O-K_2O-H_2O showing the invariant points on which the kyanite-sillimanite and the K-feldspar-kyanite bathograds are based. Adapted from Carmichael (1978).*

assemblages. On the eastern side, the andalusite-muscovite-biotite-plagioclase-quartz-bearing metapelites have an upper pressure limit corresponding to bathozone 3, whereas on the western side, the regionally developed kyanite-biotite-orthoclase-plagioclase-quartz-granitic melt assemblage (kyanite-granulite) is indicative of pressures within bathozone 6. The minimum postmetamorphic displacement on fault 4 is therefore 11 km (Fig. 17.11).

Relative dip-slip movement on all other crustal blocks (including the outer faults of crustal block "D") has always been in the order of 1-2 km when a limit could be established (Hoffman and St-Onge, 1981). Fault 4 is thus unique in the Wopmay Orogen, its documented minimum dip-slip displacement being an order of magnitude greater than all other faults for the other crustal blocks mapped.

Mylonites and the Wopmay Fault Zone

A 1 to 3 km wide zone of mylonites, discrete faults and interleaved variably cataclastic Akaitcho Group rocks defines the east margin of the composite Wopmay Fault Zone (Easton, 1981a). The main planar fabric of the mylonites averages 015°/90°, contains a strong near horizontal mineral elongation lineation and may be locally folded coaxially with the lineation. Within the mylonitic rocks, all the lithologies involved in the nappe structures can be recognized. Over 50 per cent of the mylonite zone is derived from a granitic protolith, the rest of the zone being mylonitized amphibolite and metasediments. The growth of sillimanite parallel to the lineation in the mylonites suggests that at least the late movements in the fault zone occurred at notably high temperatures.

West of the mylonite zone there is a 1 to 2 km wide belt of Akaitcho Group rocks before the first occurrence of Dumas Group units (upper Great Bear stratigraphy). As reported by Easton (1981a), the contact between the Akaitcho and dumas groups is a fault trending north-south from the west shore of Iperarpock Lake (Fig. 17.8). The Akaitcho Group rocks west of the mylonite zone are sillimanite-biotite-orthoclase-plagioclase-quartz-granitic melt-bearing paragneisses, or strongly foliated amphibolites. Minor amounts of very deformed "b"-granite is common in this zone. A strong, near vertical planar tectonic fabric striking 020° is present in the migmatites. This high-grade belt is either in fault contact with the very-low-grade rocks of the Dumas Group or with the low- to medium-grade rocks of the Grant subgroup.

The Grant subgroup (Easton, 1981a) in the northeast corner of the Calder River map area consists of a narrow, 0.5 km wide fault block (Fig. 17.8). Within this fault block metapelites increase in grade to the northeast from biotite slates to andalusite-muscovite schists. These pelites indicate metamorphic pressures of bathozone 3 in marked contrast to the kyanite-granulites of the eastern side of the mylonite. Unfortunately, the migmatites between the mylonite belt and the Grant subgroup are too high-grade to yield useful bathozonal data. Nevertheless, a minimum of 11 km of post-metamorphic dip-slip displacement must be accommodated by either the mylonite zone or the fault between the Grant subgroup and the migmatites or both.

West of the sediments of the Grant subgroup there is in several localities a basalt that is locally pillowed (Easton, 1981a). The basalt is at greenschist facies and is separated from the andalusite-sillimanite pelites to the east by a north-south trending fault. On the west side, across yet another north-south fault, the first outcrops of Dumas Group are marked by either light-coloured felsic tuffs or porphyritic basalts.

Discussion

Two of the more exciting finds of the summer are, firstly, the occurrence of recumbent folds and thrust-nappes in the Akaitcho Group rocks, and secondly, the regional development of kyanite-granulites in the thrust-nappe terrane.

The early set of recumbent folds in the Akaitcho Group invites caution when elaborating a stratigraphy in the initial rift sequence. Only when the scale and intensity of recumbent folding is known and panels of structurally consistent rocks are identified, will it be possible to construct a regional stratigraphy from local data. The recognition of the stack of thrust-nappes in the western Akaitcho Group further emphasizes this point.

The recumbent folds and associated thrust-nappes are of great interest in a study of the tectonic evolution of the Wopmay Orogen as this style of deformation appears to be confined to the Akaitcho Group. Mapping to the south, where the Hepburn Batholith becomes less clustered (Fig. 17.1) should provide insight to the style of structural-stratigraphic transition between the Akaitcho and Epworth groups and to the change from recumbent folds of foliation and bedding to upright folds of bedding.

The occurrence of kyanite-granulites in the Akaitcho Group illustrates dramatically the amount of vertical movement that can be associated with the system of late

northeast- and northwest-trending conjugate transcurrent faults in Wopmay Orogen. These faults have been related to the second of two collisional orogenies by Hoffman (1980a, b) and greatly facilitate the study of structure and metamorphism associated with the first collision (e.g. St-Onge, 1981).

Kyanite-granulites in the Akaitcho Group and andalusite-muscovite schists in the rocks of the Wopmay Fault Zone require a minimum west-side-down postmetamorphic dip-slip displacement of 11 km. A major discontinuity of crustal scale is thus present in the mylonites or along one or more discrete faults of the Wopmay Fault Zone. Could one or the other then be the surface expression of the western edge of underlying autochthonous Archean (Slave) basement?

Acknowledgments

We would like to thank Debbie Lemkow and Pat Pope for their assistance and independent mapping. We are grateful to Herb Helmstaedt and Dugald Carmichael (both of Queen's University) for having spent 2 weeks with us in the high-pressure thrust-nappe terrain of the Akaitcho Group. We are indebted to Mabel Corlett (Queen's University) for her quick X-ray and electron microprobe confirmation of the Akaitcho kyanite. And most of all, this summer would have been impossible without the capable expediting of Win Bowler for DIAND in Yellowknife.

References

Carmichael, D.M.
1978: Metamorphic bathozones and bathograds: a measure of the depth of post-metamorphic uplift and erosion on the regional scale; American Journal of Science, v. 278, p. 763-797.

Easton, R.M.
1980: Stratigraphy and geochemistry of the Akaitcho Group, Hepburn Lake map area, District of Mackenzie. An initial rift succession in Wopmay Orogen (early Proterozoic); in Current Research, Part B, Geological Survey of Canada, Paper 80-1B, p. 47-57.

1981a: Geology of Grant Lake and Four Corners map areas, Wopmay Orogen, District of Mackenzie; in Current Research, Part B, Geological Survey of Canada, Paper 81-1B, p. 83-94.

1981b: Stratigraphy of the Akaitcho Group and the development of an early Proterozoic continental margin, Wopmay Orogen, N.W.T.; in F.H.A. Campbell, ed., Proterozoic Basins in Canada; Geological Survey of Canada, Paper 81-10.

Fraser, J.A.
1960: North-central District of Mackenzie, N.W.T.; Geological Survey of Canada, Map 18-1960.

1974: The Epworth Group, Rocknest Lake area, District of Mackenzie; Geological Survey of Canada, Paper 73-39, 23 p.

Fraser, J.A., Hoffman, P.F., Irvine, T.N., and Mursky, G.
1972: Bear Structural Province; in Variations in Tectonic Styles in Canada; R.A. Price and R.J.W. Douglas, ed., Geological Association of Canada, Special Paper 11, p. 453-503.

Hoffman, P.F.
1972: Cross-section of the Coronation Geosyncline (Aphebian), Tree River to Great Bear Lake, District of Mackenzie; in Report of Activites, Part A, Geological Survey of Canada, Paper 72-1A, p. 119-125.

Hoffman, P.F. (cont.)
1973: Evolution of an early Proterozoic continental margin: The Coronation Geosyncline and associated aulacogen, northwest Canadian Shield; in Evolution of the Precambrian Crust; J. Sutton and B.F. Windley, ed., Philosophical Transactions of the Royal Society of London, Ser. A, v. 273, p. 547-581.

1980a: Conjugate transcurrent faults in north-central Wopmay Orogen (early Proterozoic) and their dip-slip reactivation during post-orogenic extension, Hepburn Lake map area, District of Mackenzie; in Current Research, Part A, Geological Survey of Canada, Paper 80-1A, p. 183-185.

1980b: Wopmay Orogen: A Wilson Cycle of early Proterozoic age in the northwest of the Canadian Shield; in The Continental Crust and its Mineral Deposits; D.W. Strangway, ed., Geological Association of Canada, Special Paper 20, p. 523-549.

1981: Revision of stratigraphic nomenclature, foreland thrust-fold belt of Wopmay Orogen, District of Mackenzie; in Current Research, Part A, Geological Survey of Canada, Paper 81-1A, p. 247-250.

Hoffman, P.F. and St-Onge, M.R.
1981: Contemporaneous thrusting and conjugate transcurrent faulting during the second collision in Wopmay Orogen: Implications for the subsurface structure of post-orogenic outliers; in Current Research, Part A, Geological Survey of Canada, Paper 81-1A, p. 251-257.

Hoffman, P.F., St-Onge, M.R., Carmichael, D.M., and de Bie, I.
1978: Geology of the Coronation Geosyncline (Aphebian), Hepburn Lake Sheet (86 J), Bear Province, District of Mackenzie; in Current Research, Part A, Geological Survey of Canada, Paper 78-1A, p. 147-151.

Hoffman, P.F., St-Onge, M.R., Easton, R.M., Grotzinger, J., and Schulze, D.W.
1980: Syntectonic plutonism in north-central Wopmay Orogen (early Proterozoic), Hepburn Lake map area (86 J), District of Mackenzie; in Current Research, Part A, Geological Survey of Canada, Paper 80-1A, p. 171-177.

Hoffman, P.F., St-Onge, D.A., Easton, R.M., and St-Onge, M.R.
1981: Preliminary geological map of Hepburn Lake, District of Mackenzie; Geological Survey of Canada, Open File 784.

McGlynn, J.C.
1970: Bear Province; in Geology and Economic Minerals of Canada, R.J.W. Douglas, ed., Geological Survey of Canada, Economic Geology Report 1, p. 77-84.

St-Onge, M.R.
1981: "Normal" and "inverted" metamorphic isograds and their relations to syntectonic Proterozoic batholiths in the Wopmay Orogen, Northwest Territories, Canada; Tectonophysics, v. 76, p. 295-316.

St-Onge, M.R. and Carmichael, D.M.
1979: Metamorphic conditions, northern Wopmay Orogen, N.W.T.; Aureole de contact de l'intrusion du Muskox, T.N.O.; Geological Association of Canada, Program with Abstracts, v. 4, p. 81.

Streckeisen, A.
1976: To each plutonic rock its proper name; Earth Science Reviews, v. 12, p. 1-33.

18.

CLOOS NAPPE IN WOPMAY OROGEN: SIGNIFICANCE FOR STRATIGRAPHY AND STRUCTURE OF THE AKAITCHO GROUP, AND IMPLICATIONS FOR OPENING AND CLOSING OF AN EARLY PROTEROZOIC CONTINENTAL MARGIN

Project 810021

P.F. Hoffman and K.S. Pelletier[1]
Precambrian Geology Division

Hoffman, P.F. and Pelletier, K.S., Cloos Nappe in Wopmay Orogen: significance for stratigraphy and structure of the Akaitcho Group and implications for opening and closing of an early Proterozoic continental margin; in Current Research, Part A, Geological Survey of Canada, Paper 82-1A, p. 109-115, 1982.

Abstract

Cloos Nappe is a recumbent, eastward-verging, refolded anticlinorium that exposes thick submarine bimodal volcanics and sediments, stratigraphically beneath the Epworth Group, near the east side of the Hepburn Metamorphic-Plutonic Belt (Zone 3) in the 1.9 Ga Wopmay Orogen. The rocks are correlative with the Akaitcho Group, exposed in the west half of Zone 3, and are interpreted as rift-basin deposits related to crustal stretching prior to break-up along the west margin of the Archean Slave Province. The nappe structures in the Akaitcho Group in Zone 3 may have formed when listric normal faults developed during crustal stretching were rejuvenated as thrusts, re-thickening the crust and shortening the depositional prism, during early stages of the first collision that affects the margin.

Introduction

The Akaitcho Group, which consists of submarine tholeiitic basalt, rhyolite (no intermediate volcanics) and diverse sediments showing rapid facies changes, has been interpreted as a rift-basin assemblage, deposited on stretched continental crust prior to break-up along the west side of the Slave Province (Hoffman et al., 1978; Easton, 1980, 1981c; Hoffman, 1980). These rocks are extensively exposed, at metamorphic grades ranging from greenschist to granulite, in the west half of Zone 3 (Fig. 18.1) in Wopmay Orogen (Hoffman et al., 1981; Easton, 1981a, b; St-Onge et al., 1982).

Similar rocks, most likely correlative with the Akaitcho Group, are exposed in a unique structure known as "Cloos Anticline" (Hoffman et al., 1978), located near the east boundary of Zone 3. This structure, here renamed "Cloos Nappe" (Fig. 18.1), is 130 km in length and from 1.5 to 15 km in width. It plunges to the south, exposing deeper structural and stratigraphic levels at the north end, and revealing a nappe-like internal structure (Fig. 18.2). A high level granite, unlike any other in Zone 3, intrudes the volcano-sedimentary assemblage at the exposed northwest corner of the nappe.

This report summarizes the findings of 1:100,000 scale mapping south of Latitude 67 degrees in 1977-80 (Hoffman et al., 1981) and north of Latitude 67 degrees in 1981. The respective NTS map areas are Hepburn Lake (86 J) and Coppermine (86 O). The report concludes with a tectonic model to account for the nappe-like structural style that seems to characterize the Akaitcho Group (St-Onge et al., 1982). In this model, some implications of the crustal-stretching hypothesis for the collisional deformation of the continental margin (Hoffman, 1980) are considered.

Previous Work

The gross lithological similarity of the Akaitcho Group to typical Archean greenstone belts gave reconnaissance mappers the impression that it was Archean in age (Fraser et al., 1960; Baragar and Donaldson, 1970). However, follow-up work in the southern part of Cloos Nappe prompted Fraser (Fraser and Tremblay, 1969; Fraser, 1974) to correlate it with the Rocknest Formation (Table 18.1) of the early Proterozoic Epworth Group, probably because both contain stromatolitic dolomite. But detailed studies of the Rocknest Formation showed that the western limit of the stromatolitic shelf facies (the "Epworth shelf edge" of Fig. 18.1) lies at least 10 km east of Cloos Nappe at present (i.e. after tectonic shortening) and that the Rocknest Formation generally lacks the quartz-arenaceous beds that are diagnostic of the dolomite in Cloos Nappe. This led Hoffman et al. (1971) to suggest that the rocks in Cloos Nappe might be correlative with the basal Odjick Formation (Table 18.1) of the Epworth Group, a view adopted by Baragar and Donaldson (1973), or that they constitute new formations more-or-less conformable with but beneath the Odjick Formation (Hoffman, 1972). The latter view was re-affirmed by Hoffman et al. (1978), who named the two major stratigraphic units found south of Latitute 67 degrees (Fig. 18.2): the older Vaillant Formation, consisting mainly of

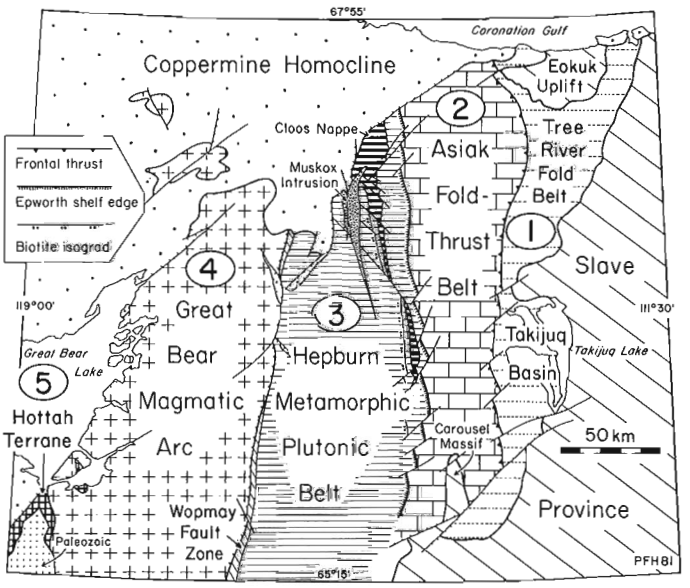

Figure 18.1. Major tectonic elements and location of Cloos Nappe in the north half of Wopmay Orogen. The Epworth shelf edge is located at the shelf-to-slope facies change in the Rocknest Formation and the western limit of crossbedded quartz arenite in the Odjick Formation.

[1] Geology Department, Memorial University, St. John's, Newfoundland. A1B 3X5

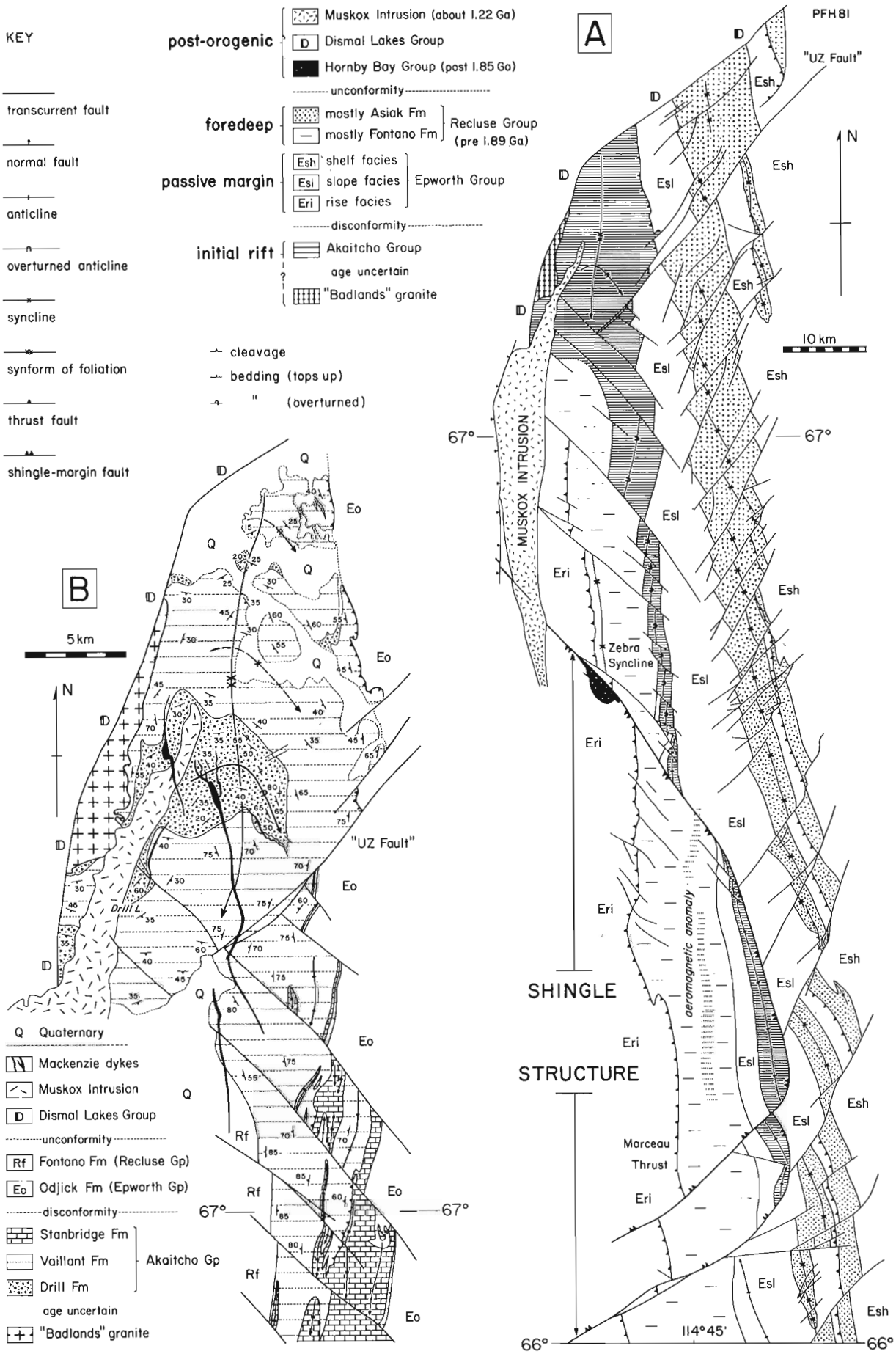

Figure 18.2. Geological maps of Cloos Nappe: A, regional setting; B, north end of the nappe.

Table 18.1

Table of Formations

	WEST SIDE ZONE 3	EAST SIDE ZONE 3	ZONE 2
RECLUSE GROUP		Asiak Fm (Ra) greywacke turbidites, pelite Fontano Fm (Rf) laminated black carbonaceous pelite	Asiak Fm (Ra) greywacke turbidites, minor pelite Fontano Fm (Rf) laminated black carbonaceous pelite Tree River Fm (Rt) quartz arenite, semipelite, minor dolomite
EPWORTH GROUP	Odjick Fm (Eo) quartz arenite turbidites, pelite	Odjick Fm (Eo) quartz arenite turbidites, pelite, minor dolomite	Rocknest Fm (Er) cherty cryptalgal dolomite, dolomitic pelite Odjick Em (Eo) quartz arenite, semipelite, minor dolomite
AKAITCHO GROUP	Tallerk Fm (At) basalt, gabbro, siltstone Aglerok Fm (Aa) pelite, mafic and salic tuff Nassitok Subgp (An) basalt, rhyolite, tuff Zephyr Fm (Az) arkosic turbidites, pelite; intruded by granite-porphyry sills	Stanbridge Fm (As) cherty and quartz-arenaceous dolomite, minor basalt, pelite Vaillant Fm (Av) basalt, mafic tuff, minor rhyolite Drill Fm (Ad) arkosic turbidites, pelite, conglomerate, basalt, rhyolite; intruded by Badlands Granite	Archean granite

submarine metabasalt flows and tuffs, and the younger Stanbridge Formation, composed mainly of cherty and quartz-arenaceous dolomite, in part stromatolitic. They tentatively correlated these rocks with parts of the Akaitcho Group exposed in the west half of Zone 3. There, the Akaitcho Group is also believed to stratigraphically underlie the Odjick Formation (Easton, 1980), although the direct evidence for this is fragmentary to date.

Southern Segment

Cloos Nappe has been segmented by the system of conjugate transcurrent faults related to the terminal collision event in the orogen (Hoffman, 1980; Hoffman and St-Onge, 1981). These faults are distinctly younger than the main folding and thrusting in the belt, which is related to the first collision event to affect the margin (Hoffman, 1980; Hoffman et al., in press). It is convenient to describe three segments of the nappe independently, given that this division is somewhat arbitrary so far as the primary facies are concerned.

The southern segment is that part of the nappe within the "shingle structure" of Figure 18.2A. It appears that the crustal shingle (block "B" of Hoffman and St-Onge, 1981) was thrust 5-8 km eastward during the terminal collision if a 600 gamma aeromagnetic anomaly (GSC Aeromagnetic Maps 8217G, 6997G) is used to locate the nappe at depth beneath the shingle (see Figure 18.2A for location of anomaly). The shingle-margin fault is poorly exposed on the east side of the nappe, which was also the west side of Glacial Lake Coppermine of Quaternary Age (St-Onge, 1980; St-Onge et al., 1981; St-Onge and Guay, 1982).

The internal structure of the nappe is relatively simple – a tightly compressed anticlinorium with an axial plane cleavage that dips steeply west. Where observed, stretching lineations plunge obliquely to the southwest. The anticlinorium is cored by metabasalt, pillowed in part, that is interbedded and overlain by at least 850 m of cherty stromatolitic and crossbedded quartz-arenaceous dolomite.

South of the shingle structure, the metabasalt and dolomite plunge out and the anticlinorium is exposed at the level of the Odjick Formation, which consists of chlorite-grade pelite and semipelite characterized by thin (less than 10 cm) beds of ripple-drift laminated white orthoquartzite and intervals of thinly interbedded dololutite-pelite.

Within the shingle structure, the Odjick pelite west of the nappe becomes devoid of quartzite beds northward. This is partly a facies change but it is also due to an extensional fault, visibly manifested at the Stanbridge/Odjick contact, that removes all but the upper quartzite-free member of the Odjick Formation, based on comparison with the Odjick section east of the shingle structure. The throw on this structure, called "Lupin Fault", increases northward. It is interpreted as a west-side-down normal fault syndepositional with the Fontano Formation (Table 18.1) by Hoffman et al. (1978).

Middle Segment

This segment lies between the shingle structure and the "UZ Fault" (Fig. 18.2). Internally, it is an anticline like the southern segment but becoming wider and M-shaped northward (Fig. 18.3). Its east limb is slightly overturned and, although the contact is poorly exposed, the Stanbridge and Odjick formations appear conformable. There is, however, a distinct break in sedimentation at the contact, which would be equivalent to the so-called "break-up unconformity" (Deighton et al., 1976) of modern continental-margin prisms.

The Stanbridge Formation undergoes a marked change in facies from south to north in this segment. Stromatolitic shallow-water dolomite at the south end passes into spectacular sedimentary breccias, composed of angular blocks of shallow-water dolomite up to 20 m in size, that intertongue at the north end with thin bedded rhythmic dololutite and black carbonaceous shale, locally tuffaceous. The facies change takes place within 40 km along strike and is interpreted as a platform-slope-basin transition. In the transition zone, the northern basinal facies appears at the base of the sequence and shallow-water facies at the top, indicating basinward progradation of the platform. There is no comparable north-south facies change in the Vaillant or Odjick formations.

Along the west side of the nappe, black carbonaceous pelite of the Fontano Formation (Table 18.1) abuts directly against Stanbridge dolomite breccia or Vaillant metabasalt (Fig. 18.2). Hoffman et al. (1978) attributed the absence of Odjick pelite to a northward increase in throw of Lupin Fault. They noted that dolomite blocks derived from Stanbridge Formation occur in Fontano pelite up to 1 km west of Lupin Fault and cited this as evidence for syn-Fontano movement on the fault. Within the nappe, however, most of the breccias appear to be of Stanbridge age, accounting for the absence of blocks derived from the Odjick or Rocknest formations. Alternatively, the continental slope may have been a zone of sedimentary by-pass, or even erosion, during Odjick deposition (Fig. 18.4). This is well illustrated by the Cenozoic of the Atlantic continental margin of the United States (Folger et al., 1979). In this case, Fontano pelite would be deposited directly on and receive debris from the Stanbridge Formation, and Lupin Fault could be a relatively minor structure. A practical difficulty in the field is in distinguishing the black carbonaceous pelites in the Stanbridge and Fontano formations, the more so because similar pelites also occur in the Odjick Formation.

Northern Segment

The segment northwest of the "UZ Fault" is unique (Fig. 18.2B). The normal axial plane foliation has been folded into a broad south plunging synform and the M-shaped anticlinorium as a whole has been refolded. In the plunging core of the anticlinorium, a new formation stratigraphically beneath the Vaillant metabasalt is exposed. It consists of medium- to thick-bedded, feldspathic and sub-feldspathic, granulestone turbidites, intercalated with black carbonaceous pelite and semipelite, and beds of quartz- or locally granite-pebble conglomerate, commonly with outsize dolomite blocks up to 3 m in diameter. Mafic tuffs, flows and sills occur sporadically within the sediments. Small salic flows and crystal-rich rhyolite tuffs, commonly with associated beds of carbonate or jasperite, occur locally within the sediments and, to a lesser extent, within the overlying mafic rocks. The dominantly sedimentary rocks beneath the Vaillant metabasalt are here named "Drill Formation", after Drill Lake (Fig. 18.2B) located on the east margin of the Muskox Intrusion. The base of the formation is not exposed but a distinctive porphyritic metabasalt at the very base of the Vaillant Formation makes the top of the Drill Formation easy to trace around the plunging anticlinal nose in the core of the nappe (Fig. 18.2B).

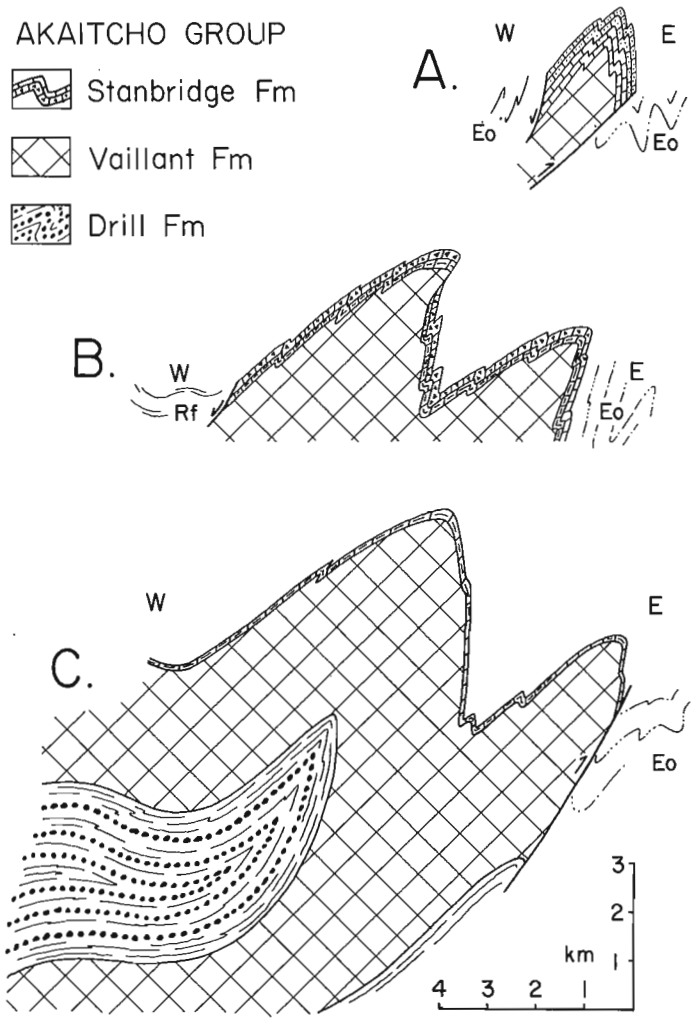

Figure 18.3. Diagramatic structure sections of Cloos Nappe crudely constructed from down-plunge projections: A, southern segment; B, middle segment; C, northern segment. Key to formations: Eo, Odjick Formation; Rf, Fontano Formation.

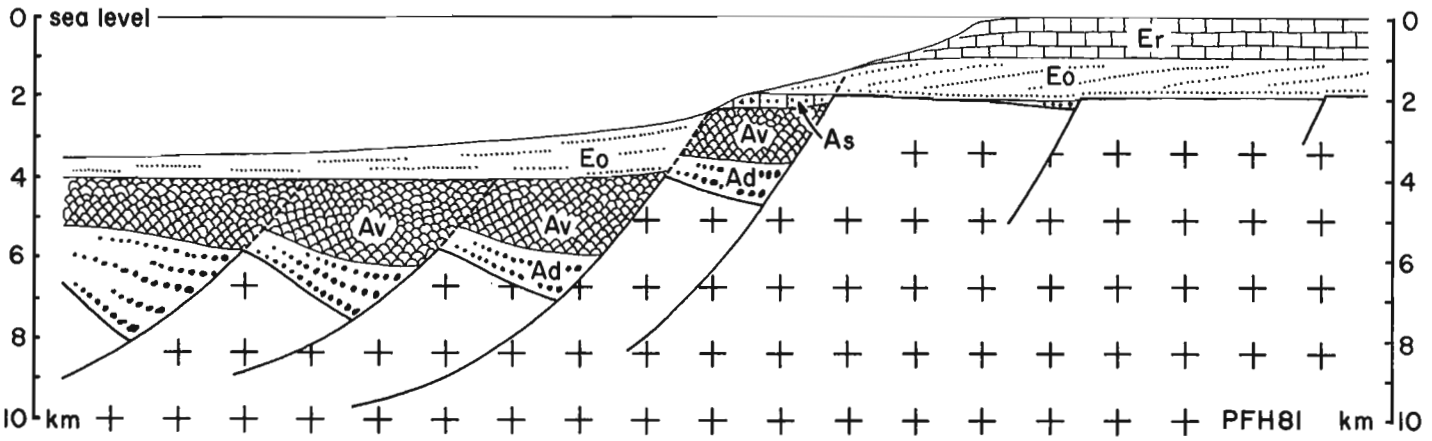

Figure 18.4. Possible configuration of the passive continental margin at the end of the Epworth Group deposition, showing a sedimentary by-pass zone for the Odjick Formation on the lower continental slope. If this margin was subducted, the initial foreland basin deposits (Fontano Formation) would lie directly on the Stanbridge Formation in the by-pass zone. Key to formations: Ad, Drill Formation; Av, Vaillant Formation; As, Stanbridge Formation; Eo, Odjick Formation; Er, Rocknest Formation.

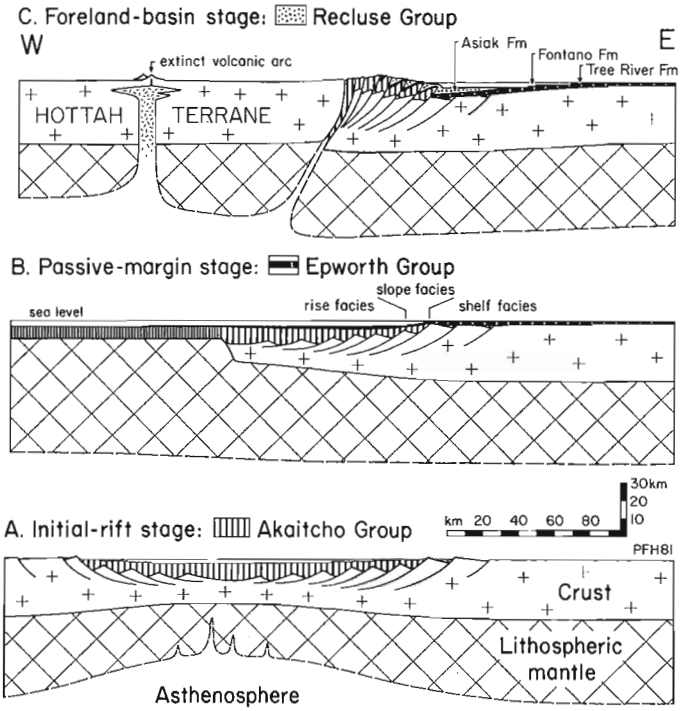

Figure 18.5. Tectonic evolution of the continental margin showing how listric normal faults, resulting from crustal stretching during Stage A, are reactivated as thrusts in Stage C, causing severe shortening and thickening of the depositional prism. In Stage C, deformation of the shelf zone (Zone 2 of the orogen) by the first collision has not yet occurred.

The Stanbridge Formation is absent on the east side of the nappe and there is a structural discordance, probably a thrust that dies out south of "UZ Fault", with the Odjick Formation (Fig. 18.3). The west side of the nappe is intruded by a high level granite, informally named "Badlands Granite" because of the way it weathers due to severe alteration by pre-Dismal Lakes Group (Fig. 18.2) paleoweathering. This granite is unlike any in the Hepburn Intrusive Suite (Hoffman et al., 1980) of Zone 3 in having abundant pegmatite, amphibole (now altered to chlorite) as the dominant mafic, and tourmaline as a prominent accessory. It is mostly a medium-grained, even textured, leucocratic monzogranite (IUGS definition), but there are also zones with K-feldspar megacrysts, zones richer in mafics, and well developed quartz stockworks. The granite has a tectonic foliation but it is highly variable in orientation and intensity. The contact of the granite is extremely sharp and the Akaitcho Group rocks exhibit no obvious metamorphic effect. No granite dykes were observed cutting the Akaitcho Group but a few xenoliths of recognizable mafic tuff were seen well within the granite. The granite contact is highly irregular in detail and clearly truncates bedding in the sediments at the exposed south end of the granite (Fig. 18.2B). Field relations leave little doubt that the granite is intrusive into the Akaitcho Group rocks with which it is in contact.

Samples for zircon chronology were collected from the Badlands Granite, rhyolite tuffs in the Akaitcho Group, and a quartz-bearing crustal tuff discovered in the Odjick Formation east of the northern segment of Cloos Nappe. If dateable, these samples should provide critical age control for the early development of the margin (Fig. 18.5).

Discussion

The findings in the northern segment of Cloos Nappe greatly strengthen the proposed correlation with the Akaitcho Group. The association of submarine arkosic sediments and bimodal volcanics is common to both, the general evolution from clastic sedimentation to basaltic volcanism is similar, and both appear stratigraphically beneath the Odjick Formation.

The nature of the assemblage is quite consistent with the rift-basin model (Easton, 1981c). The rift-basin margin must be located structurally between Cloos Nappe and Carousel Massif (Fig. 18.1), where the Odjick Formation lies directly on the Archean (St-Onge et al., 1982). Therefore, the rift-basin margin coincides at least approximately with the shelf edge of the succeeding Epworth Group (Fig. 18.1), as shown in Figure 18.5.

The nappe-like internal structure revealed in the northern segment fits in with the findings of St-Onge et al. (1982) that early recumbent folds are characteristic of the Akaitcho Group. This implies a great amount of horizontal

shortening. If the basement is similarly shortened, one wonders why it is not extensively exposed in Zone 3. The explanation may be found in a tectonic model proposed by Helwig (1976) for the Alps and recently supported by seismicity in the active Zagros collision zone in Iran (Jackson et al., 1981). In Figure 18.5, the model is adapted to Wopmay Orogen. During initial rifting (Fig. 18.5A), diffuse extension of the lithosphere results in listric normal faulting and block subsidence of the upper crust, and ductile stretching of the lower crust as elegantly demonstrated in the Cenozoic by McKenzie (1978), Montadert et al. (1979), Sclater and Christie (1980), and LePichon and Sibuet (1981). Following continental break-up (Fig. 18.5B), regional subsidence is initiated by thermal contraction and thickening of the lithosphere (Sleep, 1971; Watts and Ryan, 1976; Royden and Keen, 1980), resulting in deposition of the Epworth Group across the passive margin. Early in the first collision event (Fig. 18.5C), the listric normal faults are reactivated as thrusts, thereby rethickening the basement and causing severe shortening of the depositional prism. Because the normal faults were active during Akaitcho Group deposition, they must have exerted a strong control on primary facies and, therefore, it is natural that when they are rejuvenated as thrusts they will juxtapose contrasting facies. This may be why the internal stratigraphy of the Akaitcho Group is considerably different in each of the two main structural slices to the west (Easton, 1980, 1981C) and in Cloos Nappe. This type of crustal deformation would be limited to Zone 3 because the basement to the east was not appreciably stretched to begin with.

Acknowledgments

All pre-Dismal Lakes Group rocks in the southeast quadrant of Coppermine (86 O) and northwest quadrant of Takiyuak Lake (86 I) map areas were mapped in 1981 by a team led by the senior author, Rein Tirrul and John P. Grotzinger. They were capably assisted by Ian de Bie, Robert S. Hildebrand, Wendy Kulp, Karen S. Pelletier, Thomas J. Skulski and Elizabeth Wagner. The authors did most of the mapping in Cloos Nappe. We are grateful to Winnifred Bowler and the Geology Office, Yellowknife, for expediting our field work.

References

Baragar, W.R.A. and Donaldson, J.A.
1970: Coppermine and Dismal Lakes map areas, District of Mackenzie (86 O and N); in Report of Activities, Part A, Geological Survey of Canada, Paper 70-1A, p. 120-124.

1973: Coppermine and Dismal Lakes map areas; Geological Survey of Canada, Paper 71-39, 20 p. and Maps 1337A and 1338A.

Deighton, I., Falvey, D.A. and Taylor, D.J.
1976: Depositional environments and geotectonic framework: southern Australian continental margin; Australia Petroleum Exploration Association Journal, v. 16, p. 25-36.

Easton, R.M.
1980: Stratigraphy and geochemistry of the Akaitcho Group, Hepburn Lake map area, District of Mackenzie: an initial rift succession in Wopmay Orogen; in Current Research, Part B, Geological Survey of Canada, Paper 80-1B, p. 47-57.

1981a: Stratigraphy of a Proterozoic volcanic complex at Tuertok Lake, Wopmay Orogen; in Current Research, Part A, Geological Survey of Canada, Paper 81-1A, p. 305-309.

Easton, R.M. (cont.)
1981b: Geology of Grant Lake and Four Corners Lake areas, Wopmay Orogen, District of Mackenzie; in Current Research, Part B, Geological Survey of Canada, Paper 81-1B, p. 83-94.

1981c: Stratigraphy of the Akaitcho Group and the development of an early Proterozoic continental margin, Wopmay Orogen, N.W.T.; in Proterozoic Basins in Canada, ed. F.H.A. Campbell; Geological Survey of Canada, Paper 81-10.

Folger, D.W., Dillon, W.P., Grow, J.A., Klitgord, K.D., and Schlee, J.S.
1979: Evolution of the Atlantic continental margin of the United States; in Deep Drilling Results in the Atlantic Ocean: Continental Margins and Paleoenvironment, ed. M. Talwani, W. Hay and W.B.F. Ryan; American Geophysical Union, Maurice Ewing Series 3, Washington, p. 87-108.

Fraser, J.A.
1974: The Epworth Group, Rocknest Lake area, District of Mackenzie; Geological Survey of Canada, Paper 73-39, 23 p. and Map 1384A.

Fraser, J.A. and Tremblay, L.P.
1969: Correlation of Proterozoic strata in the northwestern Canadian Shield; Canadian Journal of Earth Sciences, v. 6, p. 1-9.

Fraser, J.A., Craig, B.G., Davison, W.L., Fulton, R.J., Heywood, W.W., and Irvine, T.N.
1960: North-central District of Mackenzie, Northwest Territories; Geological Survey of Canada, Map 18-1960.

Helwig, J.
1976: Shortening of continental crust in orogenic belts and plate tectonics; Nature, v. 260, p. 768-770.

Hoffman, P.F.
1972: Cross-section of the Coronation Geosyncline (Aphebian), Tree River to Great Bear Lake; in Report of Activities, Part A, Geological Survey of Canada, Paper 72-1A, p. 119-125.

1980: Wopmay Orogen: a Wilson cycle of early Proterozoic age in the northwest of the Canadian Shield; in The Continental Crust and Its Mineral Resources, ed. D.W. Strangway; Geological Association of Canada, Special Paper 20, p. 523-549.

1981: Revision of stratigraphic nomenclature, foreland thrustbelt of Wopmay Orogen, District of Mackenzie; in Current Research, Part A, Geological Survey of Canada, Paper 81-1A, p. 247-250.

Hoffman, P.F. and St-Onge, M.R.
1981: Contemporaneous thrusting and conjugate transcurrent faulting during the second collision in Wopmay Orogen: implications for the subsurface structure of post-orogenic outliers; in Current Research, Part A, Geological Survey of Canada, Paper 81-1A, p. 251-257.

Hoffman, P.F., Geiser, P.A., and Gerahian, L.K.
1971: Stratigraphy and structure of the Epworth fold belt, District of Mackenzie; in Report of Activities, Part A, Geological Survey of Canada, Paper 71-1A, p. 135-138.

Hoffman, P.F., St-Onge, M.R., Carmichael, D.M., and de Bie, I.
1978: Geology of the Coronation Geosyncline (Aphebian), Hepburn Lake map area, District of Mackenzie; in Current Research, Part A, Geological Survey of Canada, Paper 78-1A, p. 147-151.

Hoffman, P.F., St-Onge, M.R., Easton, R.M., Grotzinger, J.P., and Schulze, D.E.
1980: Syntectonic plutonism in north-central Wopmay Orogen, Hepburn Lake map area, District of Mackenzie; in Current Research, Part A, Geological Survey of Canada, Paper 80-1A, p. 171-177.

Hoffman, P.F., St-Onge, D.A., Easton, R.M., and St-Onge, M.R.
1981: Preliminary geological map of Hepburn Lake area (86 J), 1:100,000; Geological Survey of Canada, Open File 784.

Hoffman, P.F., Bowring, S.A., Easton, R.M., Hildebrand, R.S., St-Onge, M.R., Tirrul, R., and Van Schmus, W.R.
Magmatic arcs and collision zones in Wopmay Orogen, northwest Canadian Shield; in Proterozoic Symposium, ed. G.L. Medaris, Jr., Geological Society of America, Special Paper. (in press)

Jackson, J.A., Fitch, T.J., and McKenzie, D.P.
1981: Active thrusting and the evolution of the Zagros fold belt; in Thrust and Nappe Tectonics, ed. K.R. McClay and N.J. Price; Geological Society of London, Special Publication 9, Blackwell, London, p. 371-380.

Le Pichon, X. and Sibuet, J-C.
1981: Passive margins: a model of formation; Journal of Geophysical Research, v. 86, p. 3708-3720.

McKenzie, D.P.
1978: Active tectonics of the Alpine-Himalayan belt: the Aegean Sea and surrounding regions; Geophysical Journal of the Royal Astronomical Society, v. 55, p. 217-254.

Montadert, L., Roberts, D.G., de Charpal, O., Roberts, D., Guennoc, P., and Sibuet, J.
1979: Northeast Atlantic passive continental margins: rifting and subsidence processes; in Deep Drilling Results in the Atlantic Ocean: Continental Margins and Paleoenvironment, ed. M. Talwani, W. Hay and W.B.F. Ryan; American Geophysical Union, Maurice Ewing Series 3, Washington, p. 154-186.

Royden, L. and Keen, C.E.
1980: Rifting process and thermal evolution of the continental margin of eastern Canada determined from subsidence curves; Earth and Planetary Science Letters, v. 51, p. 343-361.

Sclater, J.G. and Christie, P.A.F.
1980: Continental stretching: an explanation of the post-mid-Cretaceous subsidence of the central North Sea basin; Journal of Geophysical Research, v. 85, p. 3711-3739.

Sleep, N.H.
1971: Thermal effects of the formation of Atlantic continental margins by continental break-up; Geophysical Journal of the Royal Astronomical Society, v. 24, p. 325-350.

St-Onge, D.A.
1980: Glacial Lake Coppermine, north-central District of Mackenzie, Northwest Territories; Canadian Journal of Earth Sciences, v. 17, p. 1310-1315.

St-Onge, D.A. and Guay, F.
1982: Quaternary geology of the Coppermine River valley between 65°40'N and 66°00'N; in Current Research, Part A, Geological Survey of Canada, Paper 82-1A, report 22.

St-Onge, D.A., Guerts, M.A., Guay, F., Dewez, V., Landriault, F., and Leveille, P.
1981: Aspects of deglaciation of the Coppermine River region, District of Mackenzie; in Current Research, Part A, Geological Survey of Canada, Paper 81-1A, p. 327-331.

St-Onge, M.R., King, J.E., and Lalonde, A.E.
1982: Geology of the central Wopmay Orogen (early Proterozoic), Bear Province, District of Mackenzie: Redrock Lake (86 G) and the eastern portion of Calder River (86 F) map areas; in Current Research, Part A, Geological Survey of Canada, Paper 82-1A, report 17.

Watts, A.B. and Ryan, W.B.F.
1976: Flexure of the lithosphere and continental margin basins; Tectonophysics, v. 36, p. 25-44.

19. A PRELIMINARY ACCOUNT OF THE INTERNAL STRATIGRAPHY OF THE ROCKNEST FORMATION, FORELAND THRUST-FOLD BELT OF WOPMAY OROGEN, DISTRICT OF MACKENZIE

Project 810021

John P. Grotzinger[1]
Precambrian Geology Division

Grotzinger, John, P., A preliminary account of the internal stratigraphy of the Rocknest Formation, foreland thrust-fold belt of Wopmay Orogen, District of Mackenzie; in Current Research, Part A, Geological Survey of Canada, Paper 82-1A, p. 117-118, 1982.

Abstract

Five measured sections of the Rocknest Formation in the northeastern part of the foreland thrust-fold belt of Wopmay Orogen are described. Three of these sections are representative of shelf facies of the Rocknest Formation, one represents the slope facies, and one shows a transition from shelf to slope facies. The Formation is subdivided into five informal members that are correlated over the shelf. The subdivision applies only to the shelf sections.

Introduction

The Rocknest Formation, a carbonate shelf sequence, is part of the early Proterozoic passive continental margin exposed in an area 200 km long and 100 km wide in the foreland thrust-fold belt of Wopmay Orogen (Hoffman, 1980). Generally, the formation consists of cyclically interstratified stromatolitic dolomite and dolomitic shale deposited by the progradation of carbonate tidal flats and lagoons over the ancient Rocknest shelf (Hoffman, 1973, 1975). The Rocknest stratigraphy was first described by Hoffman (1973), who followed up later with more detailed studies of the Rocknest shale-to-dolomite cycles (Hoffman, 1975) and of the Rocknest stromatolites (Hoffman, 1976).

A study of the Rocknest Formation will be the subject of a doctoral dissertation at The Virginia Polytech Institute and State University under the supervision of J. Fred Read. The study is focused on: 1) a detailed stratigraphic and sedimentologic description of the Rocknest Formation, the interpretation of facies, and the reconstruction of environments, and 2) the determination of how the developing early Proterozoic continental margin tectonically influenced the distribution and sequence of Rocknest sediments on the continental shelf and slope.

During the 1981 field season, 18 sections were measured and described in the Hepburn Lake (86 J), Takiyuak Lake (86 I), and Coppermine (86 O) map areas. Sections were selected in the Hepburn Lake map area from the 1:100,000 scale geological map of Hoffman et al. (1981). Geological mapping of the Takiyuak Lake and Coppermine areas is currently in progress at 1:50,000 scale and sections in those areas were chosen as the mapping was completed.

This report provides a preliminary account of the internal stratigraphy of the Rocknest Formation, which is subdivided into five informal members that were mapped at 1:50,000 scale. The descriptions of the members are based solely on information gathered in the field. Figure 19.1 shows the locations of the five measured sections which are correlated in Figure 19.2.

Description of Informal Members

Figure 19.2 shows the stratigraphic interrelationships between the five members and key stromatolite beds. The five members can be correlated over the shelf which includes sections 3, 8 and 9. However, major facies changes occur between the shelf sections and section 17, which represents the shelf slope, and section 18, which represents both shelf and slope. The five members do not extend to sections 17 and 18.

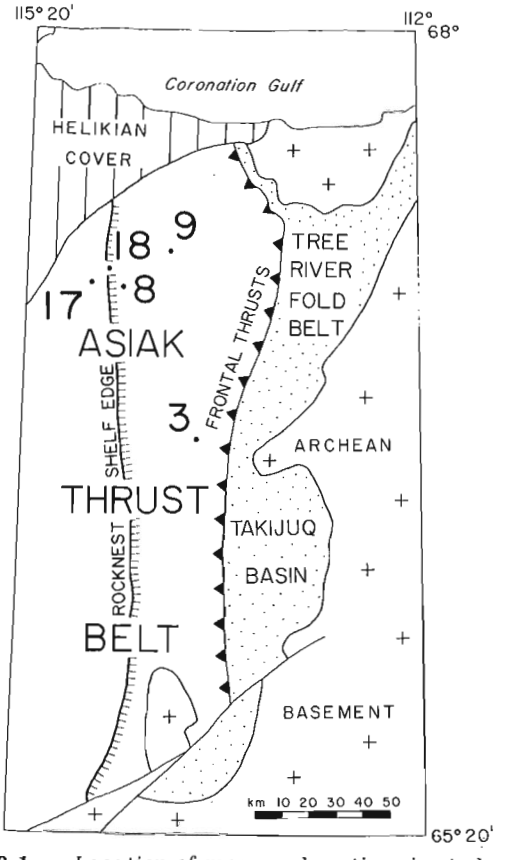

Figure 19.1. *Location of measured sections in study area.*

The base of member 1 is at the base of the Rocknest Formation and is marked by the first metre-thick bed of dolomite above the green and red shales of the Odjick Formation. Generally, this bed contains mounds of columnar, branching, anabariform (Raaben, 1969) stromatolites. The bulk of this member is characterized by cyclic shoaling upward sequences of dolomitic shale-to-stromatolitic dolomite described by Hoffman (1975). In the upper part of the member the tops of cycles are dominated by dark, cherty dolomite containing the tiny, arborescent, tufa-like stromatolite **Lenia** (see Hoffman, 1976, Fig. 5c). The contact with member 2 is sharp.

The base of member 2 is marked by a thick interval of medium grey, resistant weathering dolomite, containing strongly elongate, partially linked columns of **Omachtenia,** that passes upwards into crossbedded intraclastic dolomite.

[1]Department of Geological Sciences, Virginia Polytech Institute and State University, Blacksburg, Virginia 24061

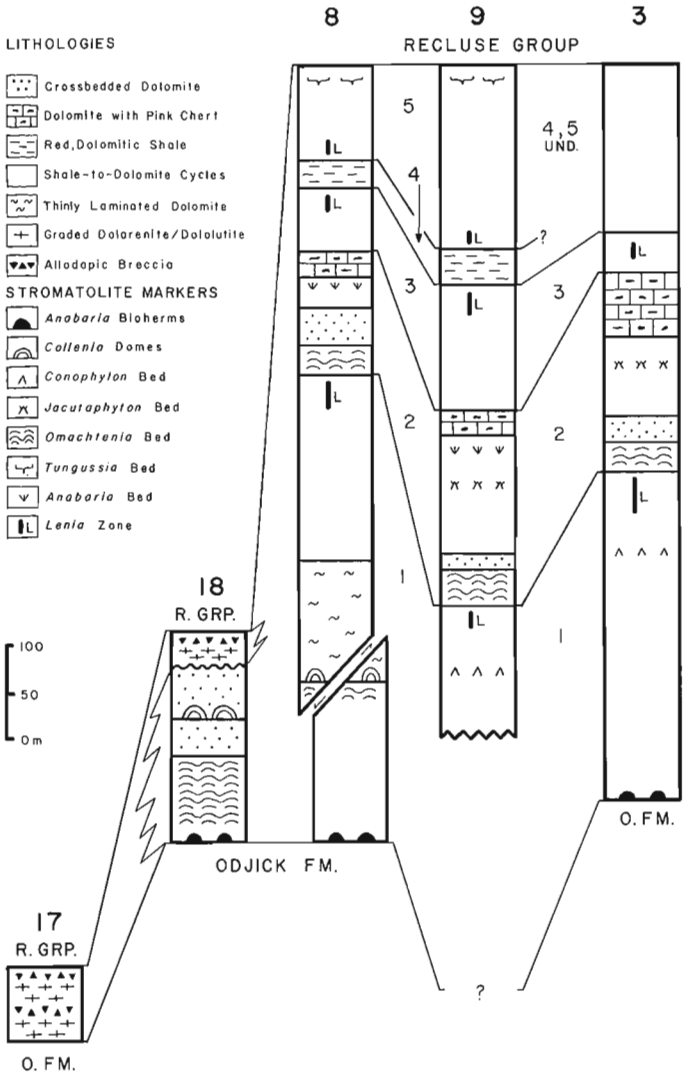

Figure 19.2. *Correlation of five measured sections. Sections are numbered according to the order in which they were measured. Sections 3, 8 and 9 represent the shelf facies of the Rocknest Formation; section 17 represents the slope facies; and section 18 represents both shelf and slope facies. The top of the formation is used as the correlation datum for sections 3, 8 and 9; the base for sections 8 and 18. Section 17 is positioned to give a sense of the paleobathymetry.*

The middle part of the member contains dolomitic shale-to-stromatolitic dolomite cycles that grade up into the upper, recessive weathering part of the member composed of interbedded white and pink dolomite with white and pink chert.

Member 2 is sharply overlain by resistant weathering, interbedded stromatolitic and intraclastic dolomite that composes the lower part of member 3, which, in turn, is overlain by dolomitic shale-to-stromatolitic dolomite cycles. In the upper part of the member, the tops of cycles contain **Lenia** as the dominant stromatolite.

Member 3 is sharply overlain by member 4 which consists entirely of red dolomitic shale with thin intercalations of yellowish dololutite and dolarenite, locally bearing the stromatolite **Stratifera.**

Member 4 is sharply overlain by member 5 which is constructed chiefly of dolomitic shale-to-stromatolitic dolomite cycles in which the upper parts of cycles commonly contain **Lenia** bearing stromatolite beds. The top of the member forms the top of the Rocknest Formation and usually contains beds of columnar, branching, tungussiform stromatolites (see Hoffman, 1976, Fig. 5e). The Rocknest Formation is sharply overlain by black shale, or concretionary black shale, or quartzose siltstones of the Recluse Group.

Because the five members do not carry through to sections 17 and 18, those sections are described below. Section 18 can be subdivided into two intervals. The basal dolomite bed of the lower interval contains mounds of columnar, branching, anabariform stromatolites and is correlated with similar beds in sections 3, 8 and 9. This bed grades up into a thick sequence of **Omachtenia** bearing stromatolitic dolomite that is overlain by crossbedded, intraclastic dolomite containing a bed with large domes of the stromatolite **Collenia.** The domes are filled with cross-bedded, oolitic and intraclastic dolomite. The lower interval is disconformably overlain by the upper interval. The lower part of the upper interval consists of yellowish dololutite and minor dolarenite that occur as graded interbeds which occasionally have been convoluted by penecontemporaneous slumping. These sediments are overlain by allodapic breccia with blocks that range up to 40 m in length.

At section 17, the Rocknest Formation is composed entirely of interstratified allodapic breccia and graded dolarenite/dololutite beds. The breccia clasts, however, are generally less than 20 cm in length, reflecting a more distal, downslope depositional tract. This is the most western (offshore) section of the Rocknest Formation, and beyond this the Odjick Formation is directly overlain by the Recluse Group.

Because the facies changes are very gradual, the five members, as well as particular stromatolite beds, can be correlated over the Rocknest shelf for tens of kilometres. This is before palinspastic reconstruction and it is expected that this figure will be much greater after the tectonic shortening is accounted for.

At present, correlations across the shelf margin, connecting the slope facies with the shelf facies, are not well understood. More sections are needed to document this zone of abrupt facies change.

References

Hoffman, P.F.
1973: Evolution of an early Proterozoic continental margin: the Coronation geosyncline and associated aulacogens of the northwestern Canadian Shield; Philosophical Transactions of the Royal Society of London, Series A, v. 273, p. 547-581.

1975: Shoaling-upward shale-to-dolomite cycles in the Rocknest Formation, Northwest Territories; in Tidal Deposits, ed. R.N. Ginsburg; Springer-Verlag, Heidelberg, p. 257-265.

1976: Environmental diversity of Middle Precambrian stromatolites; in Stromatolites, ed. M.R. Walter; Elsevier, Amsterdam, p. 599-612.

1980: Wopmay Orogen: a Wilson Cycle of early Proterozoic age in the northwest of the Canadian Shield; in The Continental Crust and Its Mineral Resources, ed. D.W. Strangway; Geological Association of Canada, Special Paper 20, p. 523-549.

Hoffman, P.F., St-Onge, D., Easton, R.M., and St-Onge, M.R.
1981: Preliminary geological map of Hepburn Lake area (86 J), 1:100,000; Geological Survey of Canada, Open File 784.

Raaben, M.E.
1969: Columnar stromatolites and late Precambrian stratigraphy; American Journal of Science, v. 267, p. 1-18.

FRONTAL THRUST ZONE OF WOPMAY OROGEN, TAKIJUQ LAKE MAP AREA, DISTRICT OF MACKENZIE

Project 810021

R. Tirrul[1]
Precambrian Geology Division

Tirrul, R., Frontal thrust zone of Wopmay Orogen, Takijuq Lake map area, District of Mackenzie; in Current Research, Part A, Geological Survey of Canada, Paper 82-1A, p. 119-122, 1982.

Abstract

Two down-plunge east-west cross-sections, based on projection of surface structural data, have been drawn in the Asiak fold-thrust belt of Wopmay Orogen. Several features common to younger orogenic forelands are identified. The early Proterozoic sedimentary succession is detached at the basement contact and imbricated along listric thrust faults which climb obliquely through competent units and flatten in incompetent horizons. Several thrusts are folded about axes collinear with the regional thrust trend, and are folded obliquely by a distinctly younger fold generation. Secondary antithetic thrusts are relatively common, and predate local synthetic thrusts.

Introduction

A foreland fold-thrust belt of late Aphebian age makes up that part of Wopmay Orogen onlapping the Archean Slave Craton to the east, and bounded by the Wopmay Fault Zone to the west. It is interpreted as a passive continental margin involved in two early Proterozoic collisions (Hoffman, 1980). West-dipping subduction led to east-directed thrusting and folding of the passive margin during the first collision, and the emplacement of the Hepburn Intrusive Suite. The latter, with its attendant metamorphic aureole, serves as a basis for subdivision of the fold-thrust belt into an internal and external zone (Fig. 20.1). Both zones are cut by a system of conjugate transcurrent faults which date from the second collision.

In this report, certain aspects of the fold-thrust deformation are documented by two structure cross-sections based on mapping in 1981 north of Takijuq Lake (Fig. 20.1).

Stratigraphic Units

The deformed sedimentary succession consists primarily of the Odjick and Rocknest formations (Hoffman, 1981), both 800-900 m thick. North of Takijuq Lake, basal Odjick mudstone rests nonconformably on Archean basement, and forms the most important zone of detachment (Fig. 20.2a), as noted by Hoffman (1973). The mudstone is successively overlain by a 500 m interval dominated by mature quartzite and subfeldspathic arenite, and by an upper mudstone interval which shares a gradational interbedded contact with dolomite of the Rocknest Formation. The Odjick-Rocknest contact is also an important zone of décollement, as indicated by the common occurrence of basal Rocknest on the hanging walls of thrusts.

The Rocknest Formation consists of cyclic cherty stromatolitic dolomite and argillaceous dolomite. Its lithologic variability and characteristic good outcrop make it the most useful formation for resolving fold-thrust geometry. It has been subdivided into three members recognizable everywhere except at the shelf edge, and into five members (Grotzinger, 1982) for selected areas being mapped at 1:50,000 scale. As a result, many minor thrusts have been identified, and some major thrusts have been traced in detail. Although the Rocknest as a whole is a competent formation, several argillaceous horizons within it are commonly the loci of bedding-parallel segments of thrust faults or form fold-detachments. In particular, shaly dolomite of Member 4 and immediately below Member 2 (Grotzinger, 1982) display this behavior.

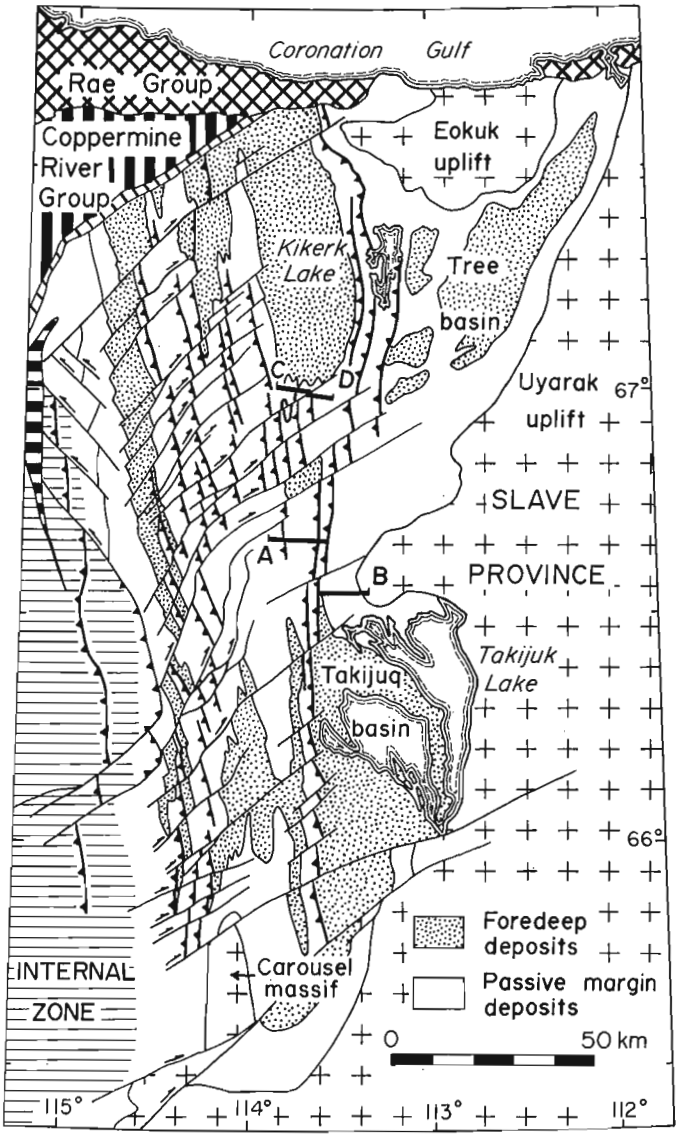

Figure 20.1. East side of Wopmay Orogen, showing the regional setting and major structures of Asiak fold-thrust belt and the locations of the cross-sections of Figure 20.2.

[1]Department of Geological Sciences, University of California at Santa Barbara, CA 93106

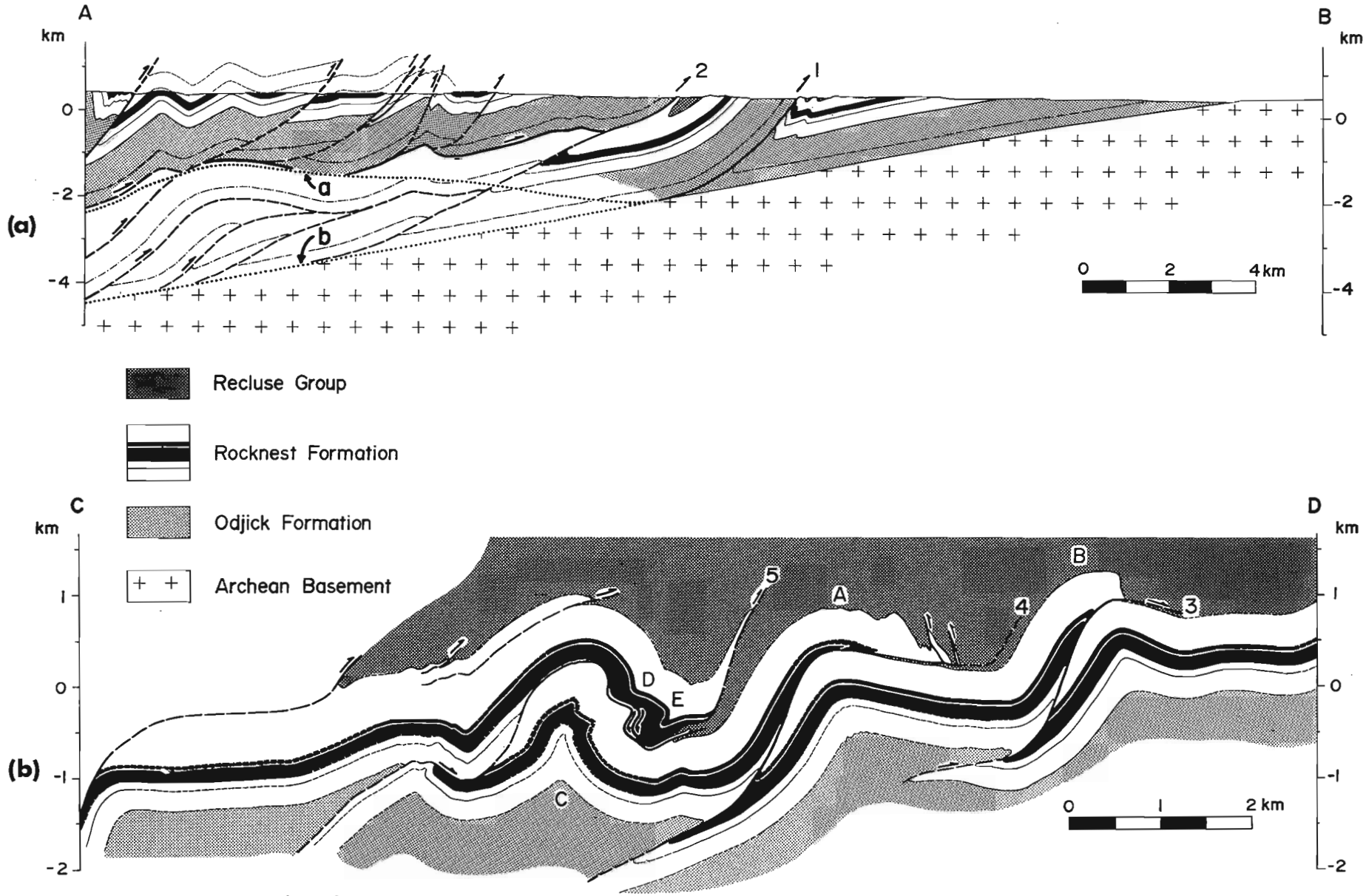

a. Cross-section A-B of the frontal thrust zone. Dotted lines 'a' and 'b' denote different estimates of the depth to basement, beyond the most westerly control point. A possible, but by no means unique, section is constructed for the lower estimate. This solution requires a minimum of 25 km more displacement on thrust 2 than would a section based on the upper basement profile.

b. Cross-section C-D showing folded thrust faults southwest of Kikerk Lake. Because the plunge of these folds is relatively high (12-18°) much use was made of down-plunge construction. Contacts are dashed where down-plunge information is not available. Letters and numbers refer to folds and thrusts discussed in the text.

Figure 20.2

The Rocknest Formation is sharply overlain by terrigenous sedimentary rock of the Recluse Group. A few metres of interbedded quartzite and mudstone (Tree River Formation) is followed by about 50 m of black laminated mudstone (Fontano Formation) and then by a thick succession of interbedded turbidites and mudstone (Asiak Formation). As might be expected, the Fontano Formation is an important fault-gathering zone.

Frontal Thrust Zone

Thrust faults are recognized in the field by duplication or anomalous thickness of known stratigraphic intervals. Where exposed, the thrust surfaces vary considerably in character. Most minor thrusts are sharp, with little disruption of wall rocks. A dominant detachment surface can usually be identified for major faults, but either the hanging wall or footwall or both are strongly deformed. Tight, minor hanging wall folds with axial planes at a small angle to the associated thrust are a recurring feature.

Figure 20.2a is a cross-section of the frontal thrust zone north of Takijuq Lake. In this region, the tectonic plunge is extremely shallow, and topographic relief is low, so that except for the most easterly fault there is little control on subsurface attitudes of thrusts. The listric profile of the frontal thrust determined from hanging wall bedding attitudes and the steep basement slope of the autochthon (about 10° compared with less than 4° for Phanerozoic analogs), as indicated by cover rock dip, are readily apparent. The basement depth west of the point where the frontal thrust flattens is unknown. For the purpose of discussion, two extreme possibilities, 'a' and 'b' are shown. A profile shallower than 'b' is preferred for the following reasons. If the basement slope continues at a relatively steep angle, then a great thickness of imbricated Odjick and Rocknest must be present in the subsurface. Such tectonic stacking is not noted around the nose of Carousel Massif where basement is exposed (St-Onge, 1982). This stacking also requires a large displacement on thrust 2 (a minimum of 30 km for the configuration shown). Although possible, there is no indication from map relations that this is such an important thrust. With the upper basement limit, a balanced cross-section with a minimum of 5-6 km of slip on thrust 2 can be constructed. This requires that the basement is deformed or involved in thrusting, as demanded for other parts of the external zone (Eokuk and Uyarak uplifts, Carousel Massif). An attempt is now being made to estimate basement depth along transects of the thrust belt from a study of magnetic anomalies. This knowledge is critical for the construction of balanced cross-sections and calculations of minimum shortening derived therefrom.

Folded Thrusts

Folded thrust faults, previously recognized in the internal zone (St-Onge, 1981) are now also known from the external zone of the fold-thrust belt. Good examples are exposed at the south end of the synclinorium west of Kikerk Lake (Fig. 20.1). In this area a consistent and relatively steep northerly fold plunge of 12-18° enables the use of down-plunge projections (see Mackin, 1950). Figure 20.2b is a cross-section of the nose of the synclinorium at Rocknest level, constructed by making maximum use of down-plunge views.

Folds with at least three different origins appear on cross-section C-D:

(i) Ramp Folds. Part of the difference in structural form between thrusts 3 and 4 and stratigraphic units in their respective hanging walls at locations B and A is due to the shape of the thrust trajectories. They crosscut the Rocknest abruptly, but become bedding-parallel in the Fontano (base of the Recluse Group). This geometry necessitates an open anticline-syncline pair in the hanging wall.

(ii) Folds Coaxial with Thrusts. At A and B the ramp folds have been modified by folds that involve foot wall rocks as well. Folds of this type have axes collinear with the regional thrust trend. Enough examples are not known to be able to ascertain their general vergence, or whether they are of a different generation than the majority of folds in the belt. The possibility that folds at A, B, and C are ramp folds, or at least modified ramp folds related to 'risers' within the Odjick cannot be eliminated.

(iii) Folds Non-coaxial with Thrusts. A generation of folds with steeply dipping axial planes oriented approximately 30° east of the regional tectonic strike also fold thrusts. Two such folds are shown in oblique section in Figure 20.2b at D and E. Such folds are generally isolated, of small wavelength (less than 500 m) and increase in number to the east. They are probably genetically related to more widespread transecting cleavage with a similar regional orientation. The relationship of these folds to those of the Tree River belt is yet to be determined.

Back Thrusts

Numerous back thrusts have been recognized in the external fold-thrust belt. They are distinguished from folded east-verging thrusts by the asymmetry of associated minor folds and by down-plunge map relations. Some are undoubtedly out-of-syncline thrusts related to fold development, but some have significant stratigraphic separation and are not situated on the limbs of major folds. In particular, an antithetic thrust 40 km west of Kikerk Lake juxtaposes the lowermost beds of the Rocknest Formation against Fontano. Even if the fault has a steep dip, a minimum of 1000 m of throw is required. In three areas where interference of synthetic and antithetic thrusts can be observed, the former displace the latter. This is shown for two minor thrusts on the hanging wall of thrust 4 in Figure 20.2b. This suggests that they developed at the front of the advancing thrust belt in a position analogous to that of back thrusts of the southern Canadian Rocky Mountain Foothills (see Ollerenshaw, 1978) and were subsequently incorporated into it.

Acknowledgments

I. de Bie, J. Grotzinger, R. Hildebrand, P. Hoffman, W. Kulp, K. Peltier, T. Skulski and B. Wagner contributed to the mapping on which this report is based.

References

Grotzinger, J.P.
1982: A preliminary account of the internal stratigraphy of the Rocknest Formation, foreland thrust-fold belt of Wopmay Orogen, District of Mackenzie; in Current Research, Part A, Geological Survey of Canada, Paper 82-1A, report 19.

Hoffman, P.F.
1973: Evolution of an early Proterozoic continental margin: the Coronation geosyncline and associated aulacogens of the northwestern Canadian shield; Philosophical Transactions of the Royal Society of London, Series A, v. 273, p. 547-581.

Hoffman, P.F. (cont.)
1980: Wopmay Orogen: a Wilson Cycle of early Proterozoic age in the northwest of the Canadian Shield; in The Crust of the Earth and Its Mineral Resources, ed. D.W. Strangway; Geological Association of Canada, Special Paper 20, p. 523-549.

1981: Revision of stratigraphic nomenclature, foreland thrust-fold belt of Wopmay Orogen, District of Mackenzie; in Current Research, Part A, Geological Survey of Canada, Paper 81-1A, Report 34.

Mackin, J.H.
1950: The down structure method of viewing geologic maps; Journal of Geology, v. 58, p. 55-72.

Ollerenshaw, N.C.
1978: Geology of Calgary map area, Alberta-British Columbia; Geological Survey of Canada, Map 1457A.

St-Onge, M.R.
1981: 'Normal' and 'inverted' metamorphic isograds and their relation to syntectonic Proterozoic batholiths in the Wopmay Orogen, Northwest Territories, Canada; Tectonophysics, v. 76, p. 295-316.

St-Onge, M.R., King, J.E., and Lalonde, A.E.
1982: Geology of the central Wopmay Orogen (early Proterozoic), Bear Province, District of Mackenzie: Redrock Lake (86 G) and the eastern portion of Calder River (86 F) map areas; in Current Research, Part A, Geological Survey of Canada, Paper 82-1A, report 17.

21.

ACTIVE LAYER GROWTH, ILLISARVIK EXPERIMENTAL DRAINED LAKE SITE, RICHARDS ISLAND, NORTHWEST TERRITORIES

Project 680047

J. Ross Mackay[1]
Terrain Sciences Division

Mackay, J. Ross, Active layer growth, Illisarvik experimental drained lake site, Richards Island, Northwest Territories; in Current Research, Part A, Geological Survey of Canada, Paper 82-1A, p. 123-126, 1982.

Abstract

On 13 August, 1978 a lake (600 by 300 m) located 60 km due west of Tuktoyaktuk, Northwest Territories was artificially drained for experimental research in a region of thick continuous permafrost. Permafrost commenced to grow downwards in the first winter on the exposed lake bottom. Active layer depths have been measured in June and August for the first three summers, viz. 1979, 1980, and 1981. The measurements show no trend towards a thinning of summer thaw depths accompanying downward permafrost growth. The absence of a thinning trend is attributed to the warm subjacent permafrost temperatures whose August minimums are in the -1.5 to -3.0°C range for most of the drained lake bottom. The relatively warm permafrost results from two heat sources – the active layer above and the former sublake-bottom talik, whether frozen or unfrozen, beneath.

In the Tuktoyaktuk and Richards Island region, Northwest Territories, lakes cover from 20 to 40 per cent of the total area. When these lakes drain naturally – a common event – permafrost commences to aggrade downwards on the exposed drained lake bottoms. In 1978, "Illisarvik Lake" (unofficial name), 60 km due west of Tuktoyaktuk, Northwest Territories, was artificially drained in a co-operative research endeavour involving government and universities in order to study permafrost growth under full-scale natural conditions (Mackay, 1981). Illisarvik Lake, prior to drainage, was about 600 m long and 300 m wide. The lake was drained on 13 August 1978. This paper discusses the growth of the active layer from June 1979 to August 1981 – the first three years of active layer growth. In so far as is known, the measurement of active layer growth from year "one" is unique and the data have relevance to disturbance studies.

Active Layer Course

In June 1979 at the commencement of the first summer thaw period an active layer course was established across the long and short axes of the lake and extended a short distance onto the adjacent terrain inland from the former lakeshore (Fig. 21.1). The course followed a north-south grid baseline approximately 045° true (Hunter et al., 1980). Where lake bottom conditions permitted, wooden dowels 1.5 cm in diameter and 1 m long were placed at 25 m intervals. A small cut was made 25 cm from the bottom of each dowel and in August of 1979, 1980, and 1981, each dowel was pushed down to the level of the cut for the purpose of frost heave studies. The depth of the active layer (Table 21.1) was measured with a steel probe, pushed down to refusal. If the active layer was deep and stony, however, it was often difficult to distinguish between the frost table and a stone. Because the ground surface by some dowels was irregular, and strong summer and winter winds have both eroded and deposited some loose organic material which covers about half of the lake bottom, the active layer depths given in Table 21.1 are accurate to no more than several centimetres for shallow depths (e.g. 20 to 50 cm) and to perhaps 10 cm for depths exceeding 100 cm. In 1980 and 1981, the height of the cut, which was flush with the ground surface the preceding August, was measured to study heave and settlement in the top 25 cm of the active layer. The snow depths along the active layer course were also measured in April of 1980 and 1981 (Table 21.2).

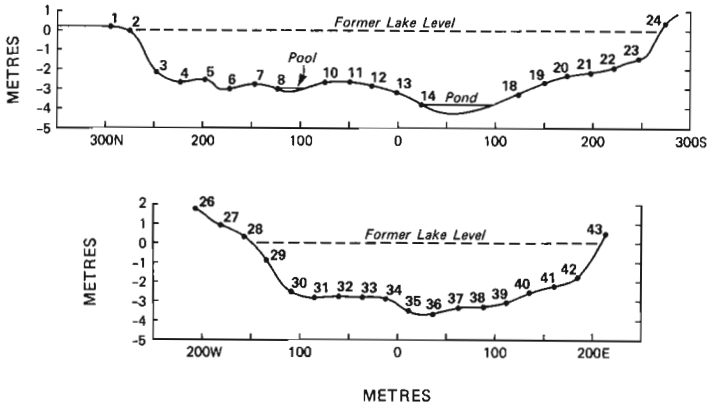

Figure 21.1. Active layer course for the long and short axes of the drained lake bottom along a north-south grid baseline approximately 045° true. The "0" co-ordinate is in the lake centre. Numbers refer to the locations of dowels.

Discussion

Active Layer Depths

It would be natural to assume that the thickness of the active layer would decrease from 1979 to 1981 as permafrost aggraded downwards, but this has not been so. From 1979-1981, the year to year variations in active layer depth (Table 21.1) were, with a few exceptions, similar in magnitude to those at sites with old permafrost and an undisturbed active layer. Most of the exceptions can be explained. First, at the south end of the lake from approximately dowel 20 to 24, strong northeasterly and northwesterly summer and winter winds have blanketed the ground surface with as much as 20 to 30 cm of windblown organic matter. There is therefore little comparability for active layer depths from one year to the next. Second, dowels 41 and 42 are in an area of sands and gravels where, in August 1981, the friction on the probe was so great that it could not be pushed down to the frost table.

[1]Department of Geography, University of British Columbia, Vancouver, B.C. V6T 1W5

Table 21.1

Depth of the Active Layer

Dowel No.	79/06/16 cm	79/06/20 cm	79/08/13 cm	79/08/21 cm	80/06/12 cm	80/08/12 cm	81/06/19 cm	81/08/10 cm	Comment
1	10	12	43	42	14	46	21	57	sedgy polygon
2	19	20	51	40	17	51	24	50	at former lake shore
3	36	37	109	113	30	105	43	108	saturated peat
4	31	31	76	81	28	71	33	72	peaty organic mud
5	22	24	84	87	18	77	38	80	" " "
6	20	21	77	81	22	70	37	72	" " "
7	18	17	60	67	13	51	21	50	" " "
8	19	20	57	69	15	46	23	51	" " "
10	16	14	58	62	16	55	19	46	" " "
11	17	17	61	63	15	59	35	55	" " "
12	14	13	50	53	14	55	21	48	" " "
13	15	15	49	54	16	67	23	74	" " "
14	19	20	63	70	20	60	25	63	" " "
18	14	14	40	41	15	45	20	46	" " "
19	17	16	46	50	14	51	22	48	" " "
20	20	20	68	76	15	52	25	64	windblown peat
21	20	20	73	83	15	66	26	51	" "
22	20	21	88	92	20	77	29	74	" "
23	55	60	149	160	46	122	62	90	" "
24	10	10	64	62	-	-	36	48	" "
26	10	10	38	39	12	39	13	35	hummocky tundra
27	10	10	44	43	09	41	14	44	" "
28	19	24	64	67	16	65	28	57	" "
29	34	37	90	79	29	73	36	70	peaty organic mud
30	19	21	77	83	22	80	24	55	" " "
31	15	17	46	49	20	56	27	54	" " "
32	17	20	41	46	15	58	22	53	" " "
33	16	18	48	52	17	56	21	56	" " "
34	17	19	56	60	13	55	22	57	" " "
35	15	17	45	50	17	51	21	49	" " "
36	20	23	54	60	26	56	24	51	" " "
37	13	14	87	98	24	110+	31	101	peat over sand
38	23	26	69	74	24	66	32	65	peaty organic mud
39	21	23	94	102	17	92	34	95	sandy
40	41	48	137	146	40	141	64	110	"
41	61	73	137	158	61	110	10	63+	"
42	61	66	160	169	60	170+	19	88+	"
43	09	10	59	60	11	50	19	65	tundra

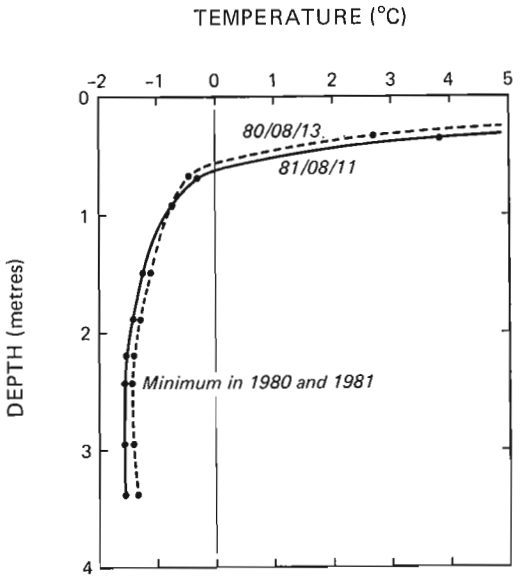

Figure 21.2. *Temperature profiles for a site about 70 m from the former lake shore. See text.*

Table 21.2

	Settlement		Snow depth		
			Pre Drainage[1]	Post Drainage	
Dowel No.	80/08/12 cm	81/08/10 cm	78/04/18 cm	80/04/07 cm	81/04/08 cm
1	1.5	0.0		20	30
2	1.5	0.0		21	30
3	1.0	0.0	30	10	40
4	1.0	1.0		20	25
5	1.5	1.5	15	0	16
6	2.0	2.0		10	37
7	2.0	3.5	21	0	10
8	2.0	2.0		0	20
10	1.0	5.0		0	08
11	1.0	5.0	15	2	10
12	3.5	6.0		10	20
13	2.0	3.0	18	15	25
14	1.0	3.0		07	13
18	3.0	1.0		15	35
19	1.0	1.0	15	12	02
20	-	0.5		02	08
21	1.0	2.0	15	10	30
22	0.0	0.0		20	12
23	-	-	09	35	22
24	-	-		47	15
26	1.0	2.0		15	28
27	0.0	0.0		15	22
28	0.0	1.0		15	30
29	0.0	0.0		45	50
30	2.5	0.0	13	30	27
31	3.5	2.0	09	10	28
32	3.0	1.0		02	25
33	3.0	4.0	09	05	20
34	3.0	2.0		07	28
35	2.0	0.0		15	17
36	0.0	0.0	09	12	22
37	1.0	1.0		14	12
38	2.0	3.0	21	10	15
39	2.0	0.0		10	20
40	0.5	2.0		17	21
41	1.0	0.5	24	25	23
42	0.0	0.5		12	74
43	0.0	0.0		45	55

[1]Snow depth measurements by J.A.M. Hunter, Geological Survey of Canada

Effects of Vegetation and Drainage

The active layer thickness at any given site depends, of course, upon the interaction of a large number of factors including vegetation cover, exposure, drainage, soils, and permafrost temperatures. At Illisarvik, vegetation cover is not yet a factor, because all dowel sites on the lake bottom were bare from 1979 to 1981. On the flattish lake bottom, exposure differences are probably unimportant. The role of drainage is, at present, unknown. When Illisarvik was drained in August 1978, all of the lake bottom was saturated. During the first winter, 1978-1979, ice lenses formed near to the ground surface and a large number of desiccation polygons, about 0.75 m in diameter, formed in the extensive areas of organic muds. The growth of ice lenses just beneath the ground surface and the formation of desiccation crack polygons was at the expense of water withdrawn from depth so that the ground 25 to 50 cm below the surface was, in many areas, unsaturated by late winter. In June 1979 pits were excavated in many places to a depth of at least 0.5 m without the pits becoming quickly flooded with water. The lake bottom continued to dry in July-August 1979 and in the summer of 1980. In 1981, however, July and August were wet months. The groundwater table rose to within 0.3 m or less of the ground surface over much of the lake bottom. Thus the water content of the active layer probably differed little between 1979 and 1981.

Permafrost Temperatures

During the first winter, 1978-1979, the lake bottom was blown nearly clean of snow so there was little in the way of an insulating snow cover. Temperature measurements showed that in nearshore areas, where the predrainage sublake-bottom permafrost was at a shallow depth, such as 4 m, temperatures were below 0°C by March 1979, because of both downward and upward freezing. However, near the lake centre, where permafrost was at a depth of 20 to 30 m prior to lake drainage (Judge et al., 1980), the ground froze to only about 2.25 m by March 1979; to about 3.5 m by March 1980; to about 5 or 6 m by March 1981; and to about 6 or 7 m by August 1981. With such thin permafrost, minimum summer temperatures have tended to remain high. In mid-August 1981, the minimum temperature in the new permafrost at dowel 3 was about -3.1°C at a depth of 5 m; at dowel 4, about -1.7°C at a depth of 3 m; near dowel 6, about -1.4°C at a depth of 2.5 m; near dowel 7, about -1.0°C at a depth of 2.25 m; and in the lake centre (dowels 13, 34 and 35) about -14.°C at a depth of 4.5 m. For example, Figure 21.2 shows temperature profiles at a site 70 m from the old lakeshore where downward and upward aggrading permafrost have merged. Note the similarity of temperatures on 13 August 1980 and 11 August 1981, the "warm" minimum temperatures at a depth of only 2.5 m, and the gradual increase of temperature with depth below 2.5 m. Thus the permafrost beneath the active layer, being "warm" as shown in Figure 21.2, is relatively ineffective in contributing towards a gradually thinning active layer.

Frost Heave

The August 1980 and 1981 heave and subsequent settlement data, as measured from the dif-ference between the ground surface and the cuts 25 cm from the bottoms of the dowels, are given in Table 21.2. Since the dowels were inserted only to a depth of 25 cm the previous August, the heave/settlement data refer to

differential movement within that depth. In some areas, the heave/settlement data are in error because of removal or addition of material by wind action. In any event, the heave of the lake bottom was not excessive, despite the high water table, and in the range of heave frequently encountered elsewhere at both disturbed and undisturbed sites.

Snow Depths

Predrainage snow depths, where available for 4 April 1978 (unpublished data, J.A.M. Hunter) when the lake was present, and April 1980 and 1981 depths are given in Table 21.2. In April 1978, the snow was underlain by lake ice and in the winter of 1978-1979 the lake bottom was nearly bare. Snow depth measurements in other recently drained lakes suggest that once vegetation becomes established on Illisarvik, there will be much less snow drifting than now, the density will be lower, the mean depth will be greater, and the insulating effect will increase.

Conclusion

The growth of the active layer on the bottom of Illisarvik, an experimentally drained lake, has been measured for the first three summers following drainage. Contrary to what might be anticipated, the active layer depths have shown no decrease in response to the growth of permafrost. The likely reason is that the newly aggrading permafrost is relatively "warm", with minimum temperatures in mid summer, within several metres of the surface, being in the -1.5°C to the -3.0°C range beneath most of the lake bottom. The permafrost is relatively warm in summer because of heat conduction downward from the bare lake bottom and upward from the warmer former sublake-bottom talik, whether frozen or unfrozen, beneath. As the ground is nearly bare, a vegetation cover plays no role; neither does drainage appear important.

References

Hunter, J.A., MacAulay, H.A., Gagne, R.M., Burns, R.A., Harrison, T.E., and Hawkins, J.P.
1980: Hydraulic jet drilling operations at Illisarvik – geological and geophysical logs; Proceedings of a Symposium on Permafrost Geophysics (No. 5), 13 and 14 November 1978; National Research Council Canada, Associate Committee on Geotechnical Research, Technical Memorandum No. 128, p. 5-20.

Judge, A.S., Burgess, M., Allen, V., and Taylor, A.
1980: Thermal studies at Illisarvik prior to lake drainage; Proceedings of a Symposium on Permafrost Geophysics (No. 5), 13 and 14 November 1978: National Research Council Canada, Associate Committee on Geotechnical Research, Technical Memorandum No. 128, p. 26-34.

Mackay, J.R.
1981: An experiment in lake drainage, Richards Island, Northwest Territories: a progress report; in Current Research, Part A, Geological Survey of Canada, Paper 81-1A, p. 63-68.

22.

QUATERNARY GEOLOGY OF UPPER COPPERMINE RIVER VALLEY, DISTRICT OF MACKENZIE

EMR Research Agreement 5-4-81

D.A. St-Onge[1] and F. Guay[1]
Terrain Sciences Division

St-Onge, D.A. and Guay, F., Quaternary geology of upper Coppermine River valley, District of Mackenzie; in Current Research, Part A, Geological Survey of Canada, Paper 82-1A, p. 127-129, 1982.

Abstract

Perched deltas of coarse gravel at an average altitude of approximately 365 m a.s.l. indicate that glacial Lake Coppermine occupied Coppermine River valley as far south as 65°40'N. A deposit of poorly varved silt and sand deformed by large dropstones suggests that, during its maximum extent, the glacial lake occupied Point Lake basin which was a glacier calving bay.

Introduction

This paper, based on field work in the northeast corner of Redrock Lake map area (86 G) between 65°40' and 66°00'N, describes the distribution of unconsolidated deposits associated with the former presence of glacial Lake Coppermine (St-Onge, 1980) within an upstream section of Coppermine valley.

Surficial Materials

Figure 22.1 shows the southern continuation of mapping along Coppermine valley from the Hepburn Lake map area (86 J) (St-Onge et al., 1981; Hoffman et al., 1981). The stratigraphic relationships between glacial, glaciofluvial, and glaciolacustrine sediments are shown in Figure 22.2.

Till deposits of sufficient thickness to mask the bedrock structure are limited to valley bottoms. Till is commonly plastered on hillsides where it has been modified by mass movement processes; however, the deposits are seldom thick enough to mask the structural lineations of underlying bedrock. In low areas till has been fluvially washed, resulting in boulder strewn surfaces. Fluting in till on the east side of Coppermine River indicates an ice-flow direction of 295°-300° which is identical to that reported by Craig (1960).

An extensive deposit of outwash sand and gravel, up to 5 km wide and 25 km long, trends north-south in Coppermine valley. A steep sided, sharp crested esker follows the trend of the outwash deposit and is associated with numerous flat topped hills bordered by flights of collapsed ridges (St-Onge et Geurts, in press).

Deltas of coarse gravel and sand were constructed on both sides of the river valley, but more commonly on the west, during the high level phase of glacial Lake Coppermine. All these perched deltas lie at approximately 365 m a.s.l., and thus their construction is associated with the Kamut Lake outlet phase (St-Onge et al., 1981).

Below the level of the deltas are extensive sand terraces, 10 to 15 m above present river level.

Discussion

Although the presence of deltas confirms the former occupation of this segment of Coppermine valley by a glacial lake, no varved sediments were found. Fine sediments, clay to fine sands, have only been found in a segment of the valley extending from 4 km south of the mouth of White Sandy River to the mouth of Quicksand Creek in Hepburn Lake map area to the north (Fig. 47.1, St-Onge et al., 1981). During the Kamut Lake outlet phase the minimum depth of water in that part of the lake was at least 85 m. But in the segment of the valley shown in Figure 22.1, where the depth of the lake was less than 35 m, fine sediments were not deposited or were later removed by erosion.

The southern limit of glacial Lake Coppermine has not yet been mapped; however, following an invitation by R.M. Easton who was mapping to the south for the Department of Indian and Northern Affairs, a brief study was made of a deposit on the north shore of Point Lake, 60 km farther upstream. Wave erosion has exposed 10 m of poorly laminated fine sand and silt, exhibiting bedding commonly deformed by large dropstones. These poorly developed varves at approximately 365 m elevation are presumed to have been deposited in the upper reaches of glacial Lake Coppermine at a time when active glacier ice was calving icebergs into the lake. This would explain the presence of numerous large dropstones. Obviously more work needs to be done around Point Lake before it can be established whether or not it was a calving bay in the uppermost reaches of glacial Lake Coppermine.

Acknowledgments

We are grateful to Energy, Mines and Resources for funding made available through a research agreement. Dr. B. Padgham, Resident Geologist, Department of Indian and Northern Affairs, Yellowknife, provided essential logistical support. We thank R.M. Easton for telling us of the Point Lake exposure and for accompanying us to the site. Dr. M.R. St-Onge and Dr. P.F. Hoffman, Precambrian Division, were generous with their support in the field and were stimulating in their discussions with the authors.

[1] Department of Geography, University of Ottawa, Ottawa, Ontario K1N 6N5

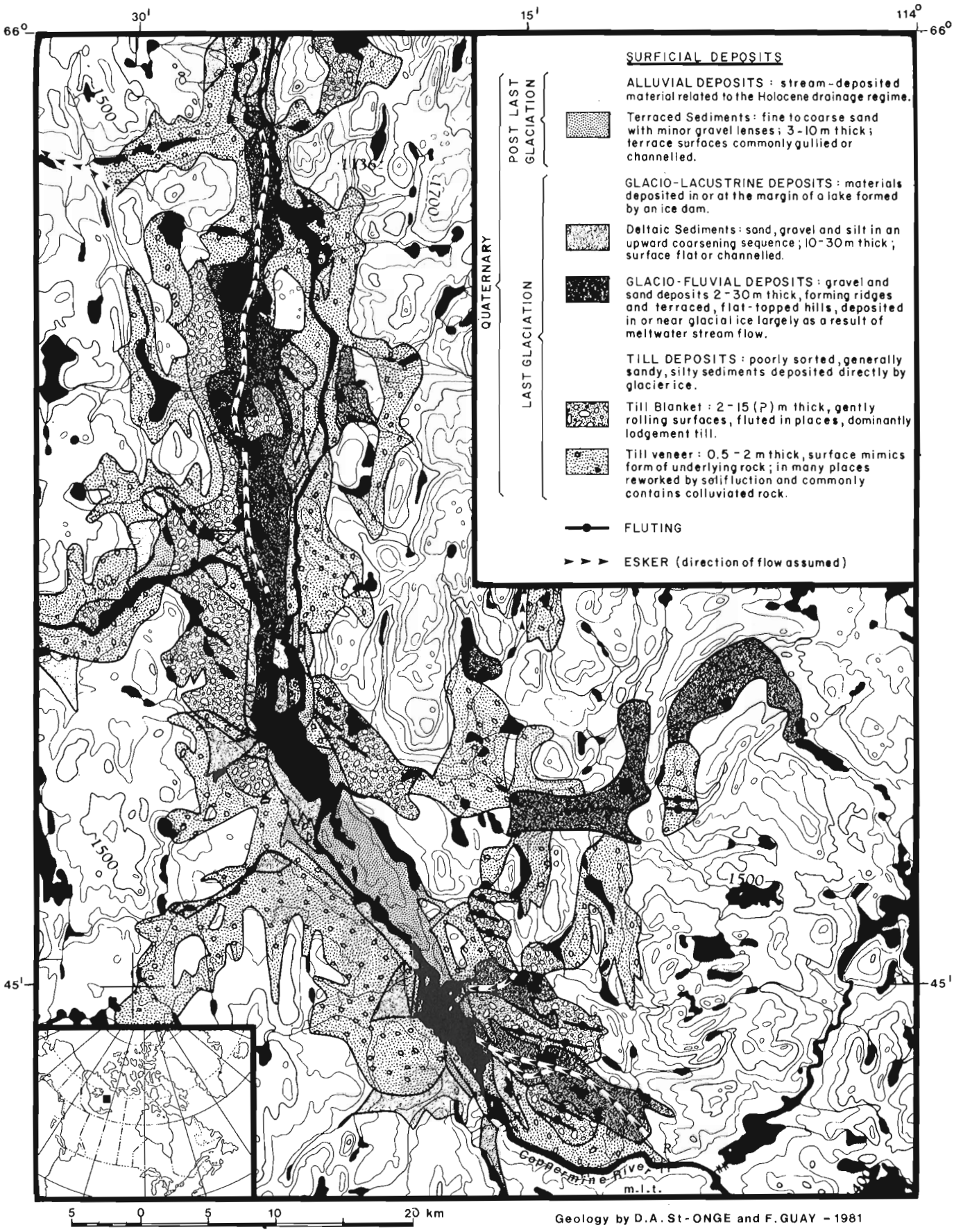

Figure 22.1. *Location map showing surficial deposits of part of the Coppermine River valley.*

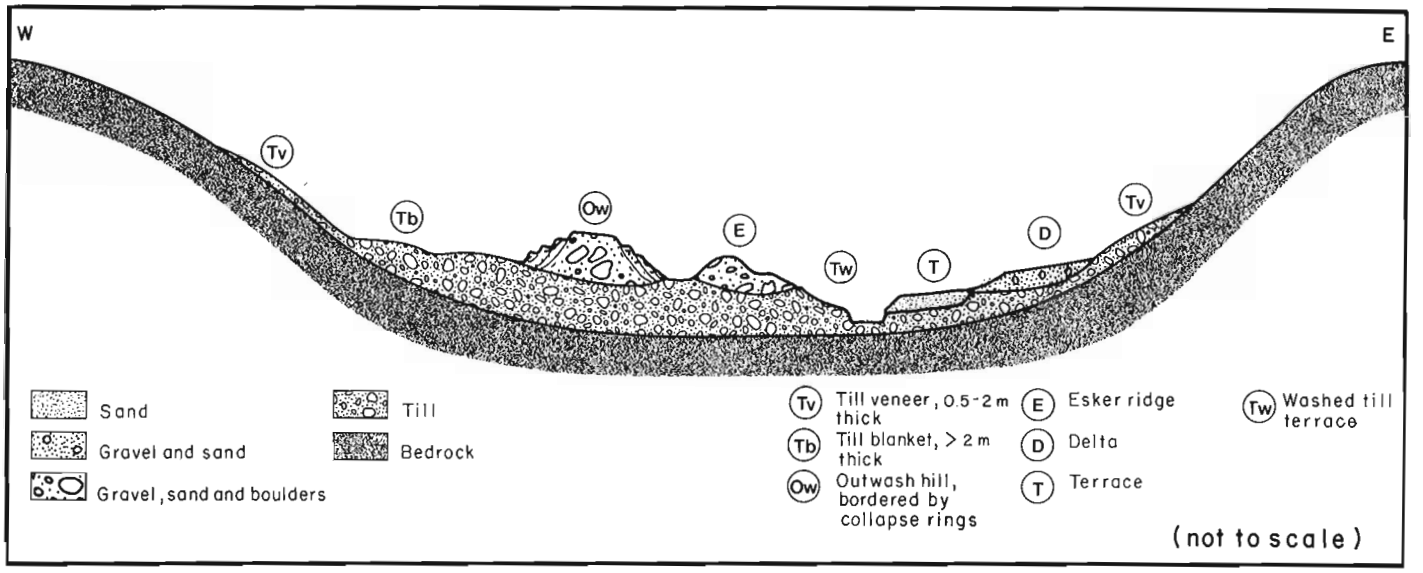

Figure 22.2. *Diagrammatic section across Coppermine River valley.*

References

Craig, B.G.
1960: Surficial geology of north-central District of Mackenzie, Northwest Territories; Geological Survey of Canada, Paper 60-18, 26 p.

Hoffman, P.F., St-Onge, D.A., Easton, R.M., and St-Onge, M.R.
1981: Preliminary geological map of Hepburn Lake, District of Mackenzie (86J); Geological Survey of Canada, Open File 784, scale 1:100 000.

St-Onge, D.A.
1980: Glacial Lake Coppermine, north central District of Mackenzie, Northwest Territories; Canadian Journal of Earth Sciences, v. 17, no. 9, p. 1310-1315.

St-Onge, D.A., Geurts, M.A., Guay, F., Dewez, V., Landriault, F., and Léveillé, P.
1981: Aspects of the deglaciation of the Coppermine River region, District of Mackenzie; in Current Research, Part A; Geological Survey of Canada, Paper 81-1A, p. 327-331.

St-Onge, D.A. et Geurts, M.A.
Les formes d'effondrement et le mode de déglaciation de la région du Lac Qingaluk, Territoires du Nord-Ouest. Géographie physique et Quaternaire, Numéro spécial pour le congrès de l'INQUA, Moscou 1982. (sous presse)

23.

POLLEN AND PLANT MACROFOSSIL ANALYSES ON LATE QUATERNARY SEDIMENTS AT KITCHENER, ONTARIO

Project 780033

T.W. Anderson
Terrain Sciences Division

Anderson, T.W., Pollen and plant macrofossil analyses on late Quaternary sediments at Kitchener, Ontario; in Current Research, Part A, Geological Survey of Canada, Paper 82-1A, p. 131-136, 1982.

Abstract

Combined pollen and plant macrofossil studies were carried out on an excavated peat-marl sequence at Gage Street bog, Kitchener, Ontario. High percentages of ***Picea, Salix, Artemisia,*** *and Cyperaceae pollen, supported by macrofossils of* ***Picea glauca, P. mariana, Salix,*** *and tundra herbs indicate forest-tundra characterized the Kitchener area prior to 12 500 years ago. Pollen and macrofossils of* ***Picea*** *increase while those of* ***Salix*** *and herbs decrease or are absent after about 12 500 years ago implying conditions became more boreal-like and less tundra-like. By about 10 500 years ago, spruce gave way to a mixed forest of* ***Pinus, Abies, Betula,*** *and other hardwoods confirmed in part by macrofossils of these taxa. Seeds of* ***Pinus strobus*** *and* ***P. resinosa*** *at the pine pollen maximum provide positive evidence that white and red pine grew close to the site between 7000 and 9000 years ago. A pollen succession from pine to hemlock and deciduous hardwoods took place shortly after 8000 years ago.*

Introduction

This study is part of a larger multidisciplinary study of a peat-covered marl deposit at Kitchener, Ontario. The peat bog was excavated with a backhoe down to unconsolidated sand and gravel at the base which made it possible to collect large bulk samples and samples for pollen analysis at regular intervals in the peat and marl. Sufficient sediment material is a prerequisite to undertaking such a study. The bulk samples were distributed to various laboratories to extract fossil insects, ostracodes, molluscs, plant macrofossils and to carry out studies on carbon and oxygen isotopes and radiocarbon dating.

Some of the major findings based on the pollen and plant macrofossil changes, excluding aquatics but including some bryophytes, are reported here. A study combining both pollen and plant macrofossils provides for a more complete paleoenvironmental analysis than can an analysis of either alone (Birks and Birks, 1980). To date, there have been only a few studies of this kind on the late Quaternary from southern Ontario and most of these involve only a short interval or a particular event during this time period. For example, Terasmae and Matthews (1980) reported on pollen and plant macrofossil occurrences in a late-glacial peat and pond sediment exposure near Brampton, Ontario and Anderson (1979; in Karrow et al., 1975) carried out a pollen and plant macrofossil study of glacial Lake Algonquin and early post-Algonquin-aged sediments in the Kincardine and Alliston regions of Ontario. Pertinent pollen records alone are those by McAndrews (1981), Mott and Farley-Gill (1978), and Sreenivasa (1968, 1973).

The excavated peat-marl sequence (henceforth referred to as the Gage Street bog site) thus offered a rare opportunity for postglacial lake sediments (marl) to be studied both micro- and macroscopically. A detailed study of the fossil insects was carried out by Schwert (1978).

Location and Characteristics of the Site

Gage Street bog is one of several bog and swamp deposits which lie within the outskirts of the Kitchener-Waterloo area (Fig. 23.1), occupying one of many depressions in the Waterloo kame moraine (Karrow, 1971). The moraine is capped by a silty clay till which has been interpreted by Karrow (1974) to have been deposited during the Port Bruce Stadial, but he did not rule out a Nissouri Stadial age as well.

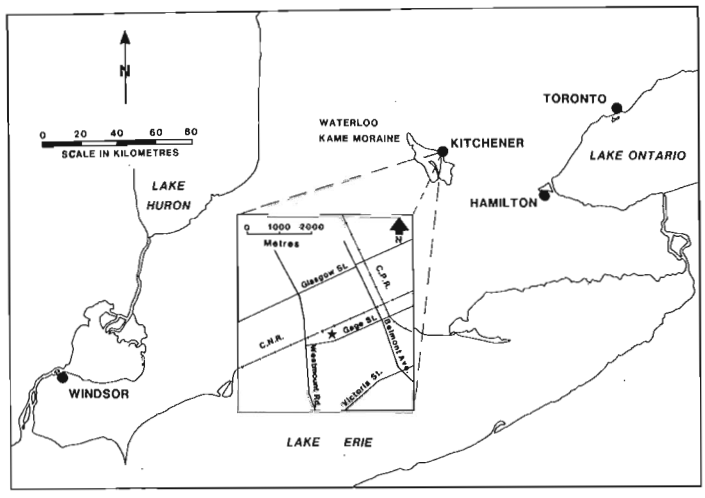

Figure 23.1. *Map showing location of Gage Street bog (indicated by a star).*

The site, therefore, dates to at least 14 000 years B.P., the age of the last glacial advance over this part of southern Ontario (Dreimanis, 1977). Relief is generally high (up to 400 m); the region is underlain by predominantly dolomitic and limestone bedrock of Silurian age.

The vegetation of the area falls within but close to the southern edge of the Great Lakes-St. Lawrence Forest Region of Rowe (1977). A transitional expression is evident as northern hardwoods and evergreens infringe upon the deciduous elements of the Deciduous Forest to the south. The regional climax forest is an **Acer saccharum-Fagus grandifolia** association which forms mixed stands on well drained sites. Up until the bog succumbed to urban expansion, it supported a stand of **Thuja occidentalis** with interspersed **Prunus serotina, Acer negundo, Populus deltoides, P. balsamifera,** and **Tilia americana** (Schwert, 1978).

Coarse sand and gravel presumed to represent outwash material derived from the kame moraine were the deepest sediments sampled at the site. The sand and gravel give way to marly clay which in turn grades into marl. The marl is pinkish banded near the base, otherwise massive and greyish, and rich in ostracode and mollusc shells and plant macrofossils. The contact with the overlying woody peat is sharp indicating that the marl may be truncated.

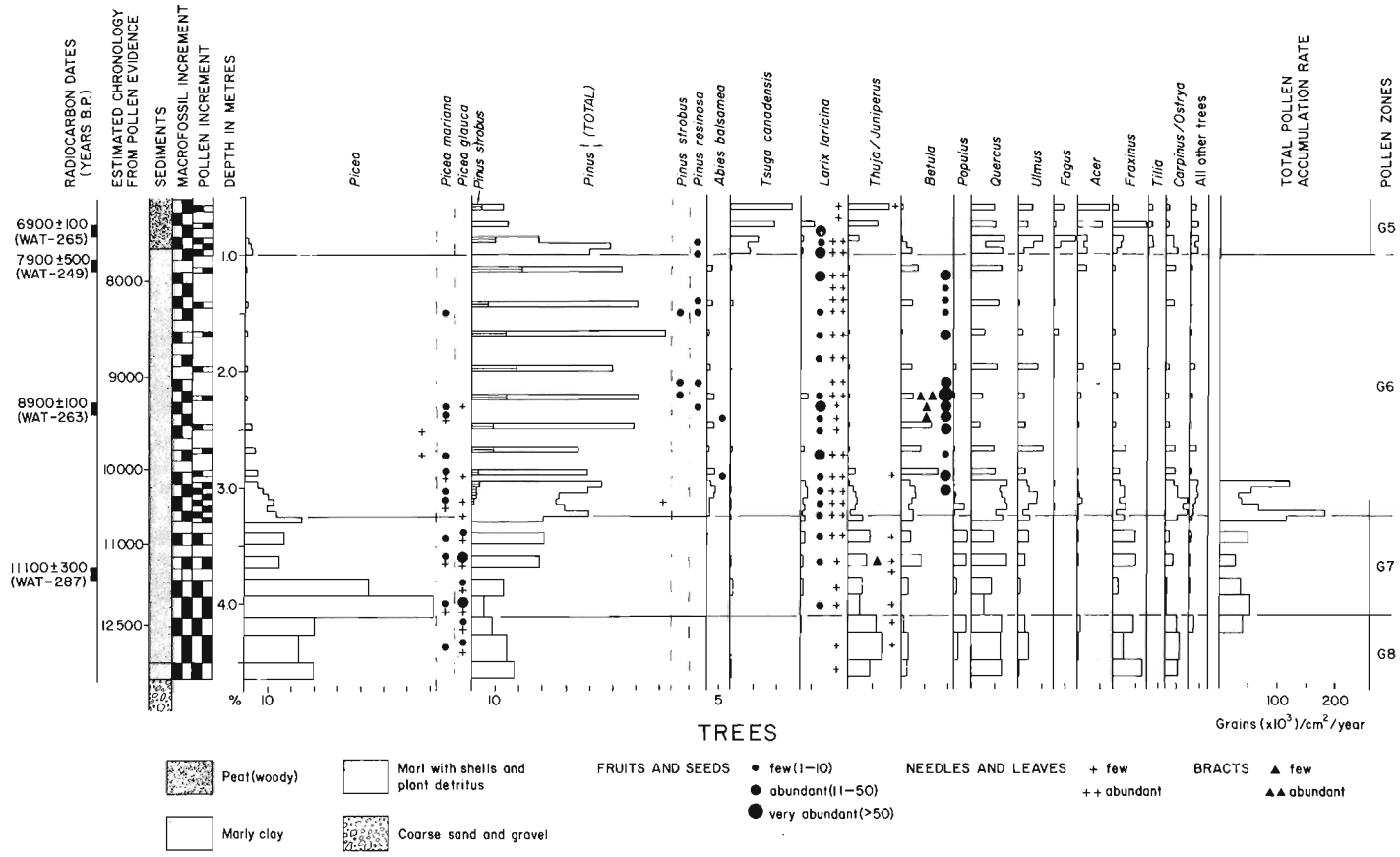

Figure 23.2. *Diagram showing tree pollen percentages and plant macrofossil occurrences, Gage Street bog.*

Radiocarbon dates on the sediments range from 20 000 years B.P. at the base to 6900 years B.P. on the peat. Problems encountered in dating various fractions of the basal marl are discussed by Schwert (1978). Because different pretreatment techniques were used on the marl and because there is so much variability amongst the dates, none of the basal dates can be accepted as reliable. One other date (7800 ± 300 years, WAT-298) higher up in the marl does not fall into place possibly because there was insufficient organic material or because of humate contamination (Schwert, 1978). The remaining four dates are in sequence and fit the chronology based on pollen evidence (see Fig. 23.2). The lowermost inferred age of 12 500 years at 4.2 m is based on pollen correlation with the pollen record at Maplehurst Lake, 40 km to the south-southwest (Mott and Farley-Gill, 1978).

Methods

Samples for pollen and bulk samples (up to 63 kg wet sediment) for plant macrofossil analysis were collected continuously at 5 and 10 cm increments, respectively, down to 3.3 m. Below 3.3 m pollen samples were obtained from the bulk samples and the sampling interval was expanded appreciably because of the danger that the walls of the excavation might collapse.

Pollen was extracted using the standard KOH procedure for peat, HCl and KOH for marl, and HCl and HF digestion for marly clay followed by acetolysis (Faegri and Iversen, 1975). Relative percentages were calculated on the basis of a minimum pollen sum of 200 arboreal, shrub, and herb taxa, excluding aquatics. **Eucalyptus** pollen was added to obtain pollen influx estimates for the interval 2.5 to 4.2 m.

The bulk samples were soaked in water and washed through a 52 mesh (300 μm) sieve to concentrate the organic debris as well as plant macrofossils. Two fractions of the concentrate were examined under a low power binocular microscope – a floatant fraction derived from previous treatments using kerosene to extract fossil insects, and the non-floatant residue. Additional sediment from the lowermost samples was washed through a 100 mesh (149 μm) sieve in an effort to concentrate more plant macrofossil material.

Palynostratigraphy and Inferred Vegetation

The pollen stratigraphy (Fig. 23.2, 23.3) is divided into four assemblage zones numbered in sequence (and prefixed "G" for Gage Street) from top to bottom as at Maplehurst Lake (Mott and Farley-Gill, 1978), one of the better dated pollen sequences in southwestern Ontario. Relative abundances of fossil fruits, seeds, leaves, needles, and bracts are diagrammatically illustrated inside the pollen profiles. Some taxa profiles are based only on pollen representation; others, like the aquatics, are based on occurrences of plant macrofossils.

Pollen Assemblage Zone G8

This lowermost zone is designated the **Salix-Artemisia**-Cyperaceae assemblage zone on the basis of high percentages of these taxa. **Picea** and **Juniperus-thuja** reach maxima of about 30 and 20 per cent, respectively. The relatively high percentages of **Pinus, Quercus, Ulmus, Fraxinus nigra** type, and **Carpinus-Ostrya** are typical of other late-glacial spectra from southern Ontario (McAndrews, 1981; Mott and Farley-Gill, 1978; Karrow et al., 1975; Sreenivasa, 1968, 1973). Substantial amounts of herb pollen of the composites, chenopods, heaths, Urticaceae, **Thalictrum, Shepherdia canadensis**, and **Vitis riparia** are present.

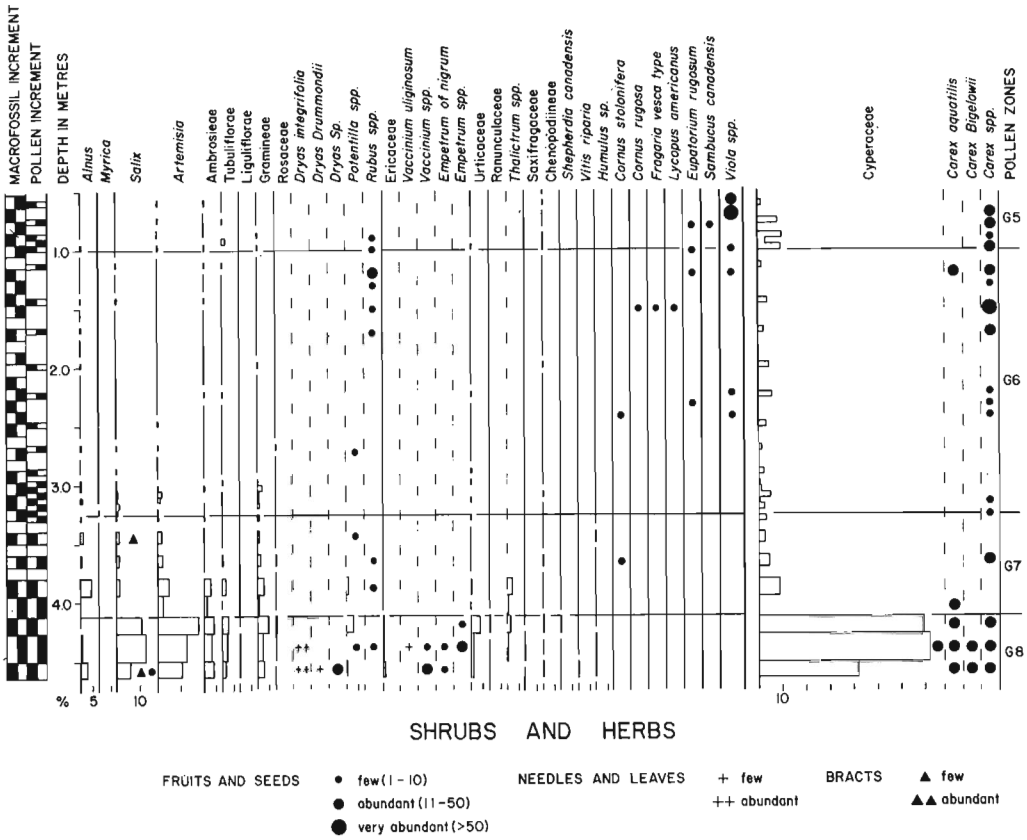

Figure 23.3. Diagram of shrub and herb pollen percentages and plant macrofossils, Gage Street bog.

The high percentages of **Salix** and herb pollen in this zone imply that tundra or forest-tundra vegetation prevailed at this early stage. With the exception of **Artemisia,** maximum percentages of **Salix,** Cyperaceae, and other herbs are characteristic of tundra regions today (Webb and McAndrews, 1976; Davis and Webb, 1975). The pollen spectra are supported by seeds and bracts of **Salix,** by achenes of several **Carex** species (notably the tundra meadow sedge, **C. Bigelowii),** and by macrofossil remains of **Dryas integrifolia, D. Drummondii, Vaccinium uliginosum, Empetrum** cf. **nigrum,** and **Selaginella Selaginoides. Salix, Dryas,** and **Vaccinium uliginosum** are the dominant taxa of the **Dryas** Heath and **Dryas** Fell-field zones in interior Alaska (Glaser, 1981) and of arctic herbmats which characterize the inner fiords of eastern Ellesmere Island (personal observation). Seeds and needles of **Picea mariana** and **P. glauca** provide evidence, however, that groves of spruce trees possibly grew nearby. It is interesting to note the presence of twigs of **Thuja occidentalis** and **Larix laricina** even at this early stage. The relatively high values of **Pinus** and thermophilous hardwoods are taken to represent exotic pollen derived from long-distance transport.

Pollen Assemblage Zone G7

Picea pollen increases to a maximum of over 80 per cent and remains high throughout this zone – the **Picea** assemblage zone. The high percentages of **Salix, Artemisia,** and Cyperaceae of the underlying zone decline to minimal amounts. **Pinus, Juniperus-Thuja, Betula, Populus, Quercus, Ulmus,** and **Fraxinus nigra** type remain high or show increasing trends towards the top. Total pollen influx shows a slight increase at the G8/G7 boundary and at the top of the zone reflecting the trends of spruce and pine. Seeds and needles of **Picea mariana, P. glauca,** and **Larix laricina** and twigs of **Thuja occidentalis** are common, but macrofossil remains of shrubs and herbs are extremely low or absent.

The abrupt increase in **Picea** pollen and decrease in **Salix, Artemisia,** and Cyperaceae indicates that tundra or forest-tundra was replaced by spruce. This is corroborated by significant declines in numbers or the near absence of shrub and herbaceous macrofossils and increases in numbers of seeds and needles of **Picea mariana** and **P. glauca** across the G8/G7 boundary. Mott and Farley-Gill (1978) interpreted a similar replacement of tundra or forest-tundra by spruce at or shortly after 12 500 years ago at Maplehurst Lake as "spruce woodland" vegetation. Whether or not there was a closed spruce forest or tundra-like openings in association with spruce (woodland) at this time is difficult to ascertain. Bryophytes such as **Meesia triquetra,** a common element of rich fens, wet-sedge meadows, and streamsides, and **Tomenthypnum nitens,** which often forms a conspicious but minor component of the higher hummocky sedge-moss meadows (J. Janssens, personal communication, 1979-80), were extracted from below the 3.5 m level. The presence of these sedge-moss meadow indicators at the base of this zone and their disappearance half-way up more than likely signifies an increase with time in the proportion of spruce trees versus tundra-like openings. **Cornus stolonifera,** a common understory component of the forests of eastern North America, apparently formed part of the shrub vegetation as fruits of this species appear mid-way up in the zone.

Pollen Assemblage Zone G6

The high **Picea** values of zone G7 are replaced by maximum percentages and influx rates of **Pinus** in this zone – the **Pinus** assemblage zone. **Abies balsamea, Betula, Quercus, Ulmus, Acer, Fraxinus nigra** type, and **Carpinus-Ostrya** increase to about 10 per cent maximum at the beginning of the zone on the percentage diagram (Fig. 23.2). Plotted as influx (Fig. 23.4), however, these taxa increase, then

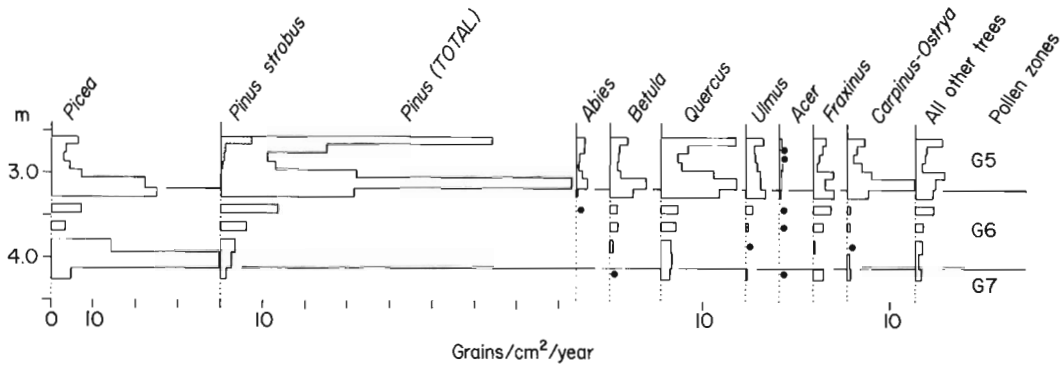

Figure 23.4. *Influx diagram for the interval 2.5 to 4.5 m (the black circles denote less than 250 grains/cm²/year).*

decrease, and increase again, as does **Pinus** and to some extent **Picea** as well. The high **Pinus** percentages mask all other taxa throughout most of the zone.

Spruce gave way to a pine-dominated mixed forest in this zone. This was a regional vegetative event which took place after about 10 500 years ago (Karrow et al., 1975; Mott and Farley-Gill, 1978). Noticeable increases in influx of **Abies, Betula, Quercus, Ulmus, Acer, Fraxinus,** and **Carpinus-Ostrya** at the base of this zone indicate that these taxa formed part of the upland mixed forest at this time. **Pinus banksiana** presumably contributed most to the first peak in the **Pinus** influx curve while **Pinus strobus** appears for the first time and, with **P. resinosa,** contributed most towards the second increase. The gradual replacement of **Pinus banksiana** presumably created openings in the upland forest which may have allowed **Abies** and the hardwoods to compete rather successfully. The low pollen influx values of all taxa prior to the rise in **Pinus strobus** reflect this competitive ability of **Abies** and the hardwoods, the result of which would have been a net decrease in the availability and influx of **Pinus banksiana** pollen.

Seeds of both white and red pine **(Pinus strobus** and **P. resinosa)** occur throughout the **Pinus** pollen maximum, i.e. where pine reaches values of 60 per cent and greater. This is the first known occurrence of fossil seeds of white and red pine in Holocene sediments east of Minnesota. Fossil needles of white pine have been reported from early Holocene sediments in Pennsylvania (Watts, 1979) and New Hampshire (Davis et al., 1980) and wood, needles, and cones of white pine were recovered from a mid-Holocene peat exposure in Quebec (Terasmae and Anderson, 1970). The presence of these seeds demonstrates beyond doubt that both white and red pine grew close to the Gage Street site between about 7000 and 9000 years ago. **Picea mariana, P. glauca, Abies balsamea, Larix laricina, Rubus** spp., **Cornus stolonifera, C. rugosa, Fragaria vesca, Lycopus americanus,** and **Eupatorium rugosum** were prominent elements of the mixed forest at this time as macrofossil remains of these taxa occur well up in the pine pollen maximum.

Pollen Assemblage Zone G5

The high **Pinus** percentages give way to increases in **Tsuga** and the hardwoods in this, the **Tsuga-Acer-Fagus** assemblage zone. **Tsuga** increases abruptly from less than 1 per cent to about 30 per cent in this zone. **Juniperus-Thuja, Ulmus, Fagus, Acer, Fraxinus,** and **Tilia** also show significant increases from the previous zone.

The decline in pine and corresponding rise in hemlock and the hardwoods represent another regional vegetative event which took place between 6900 and 7900 years ago but is more accurately dated at 7600 years B.P. at Kincardine (Karrow et al., 1975) and Belleville, Ontario (Terasmae, 1980). A hemlock-beech-maple association replaced red and white pine as the dominant forest of the uplands at this time. **Quercus, Ulmus,** and **Fraxinus** also became prominent, but **Betula** played a minor role.

Discussion and Conclusions

The pollen stratigraphy of the Gage Street site is similar to that of other pollen-analyzed sites from southern Ontario, but here it is supported by plant macrofossil evidence. Plant macrofossils provide convincing fossil evidence that a particular species or assemblage of species grew at or close to the sampling site; they have certain limitations, however, particularly with respect to reconstructing upland vegetation (Birks and Birks, 1980). The majority of the plant macrofossils recovered at the Gage Street site are representatives of the local aquatic and wetland vegetation. Nevertheless, there are occurrences of diagnostic tree, shrub, and herb plant macrofossils which support the regional upland pollen interpretation.

For example, spruce and herb pollen, substantiated by plant macrofossils of **Picea mariana, P. glauca,** and of herbs presently found in arctic and alpine environments **(Dryas integrifolia, D. Drummondii, Vaccinium uliginosum, Empetrum** cf. **nigrum, Carex aquatilis, C. Bigelowii,** and one or more species of **Salix),** indicate the initial vegetation in the Kitchener area was more forest-tundra-like than tundra following retreat of late Wisconsin ice. Similar mixed assemblages of spruce and herbs occur at other sites in southern Ontario, but there are slight differences in the interpretations of these assemblages. Terasmae and Matthews (1980) suggested that leaves of **Dryas integrifolia** and **Salix herbacea** in association with spruce and herb pollen are indicative of dwarf-shrub tundra but they did not entirely rule out the possibility that spruce trees may have been growing nearby at the time. Low pollen influx estimates in the basal sediments at Maplehurst Lake were interpreted by Mott and Farley-Gill (1978) as forest-tundra or "woodland". McAndrews (1981) similarily inferred a pollen assemblage of spruce and herbs supported by frequent occurrences of spruce needles in the oldest zones at Pond Mills Pond and Edward Lake, Ontario, as forest-tundra.

Forest-tundra was replaced by a spruce-dominated vegetation at the Gage Street site shortly after 12 500 years B.P. Although the vegetation may not have resembled a closed spruce forest, the macrofossil data, or lack of it, indicate there was less of a tundra influence and more of a boreal influence at this time.

Spruce played a prominent role in the upland vegetation at other sites in southern Ontario at this time and later. An abundance of cones identified as **Picea glauca** as well as spruce needles and twigs were extracted from pond sediments at Brampton where a radiocarbon date of 12 320 ± 360 years

B.P. (BGS-551) was obtained on the cones (Terasmae and Matthews, 1980). However, spruce seeds and needles occur in association with plant macrofossils and pollen of **Shepherdia canadensis, Dryas Drummondii, Arctostaphylos uva-ursi, Elaeagnus commutata, Potentilla anserina,** and **Selaginella Selaginoides** in 11 300 ± 140 (GSC-1374) year-old sediments at Kincardine (Anderson, 1979) and 10 500 ± 150 and 10 600 ± 160 (GSC-1126, -1127) year-old sediments at Eighteen Mile River (Karrow et al., 1975). All these species presently have low arctic, arctic-alpine, and widespread boreal distributions as does a fossil coleoptera assemblage also reported from Eighteen Mile River (Ashworth, 1977). The mixed-boreal-forest-tundra assemblage is consistent with a "spruce woodland" interpretation at Maplehurst Lake (Mott and Farley-Gill, 1978), based on low pollen influx rates up to 10 500 years B.P.

Studies involving large quantities of sediment such as this sometimes reveal plant taxa unrecognized before on a macroscopic basis but normally recorded by pollen. Macroscopic remains also make it possible to carry out precise identifications which are not always possible with pollen. For example, plant macrofossils of the Ericaceae, Empetraceae, and Cyperaceae allowed identifications even to species level which is usually not attempted on pollen of these taxa. Specific identifications were especially helpful within the Cyperaceae in that seeds of the aquatic sedge, **Carex aquatilis,** were readily distinguished from seeds of the tundra-meadow sedge, **Carex Bigelowii. Juniperus** and **Thuja** pollen, likewise, are indistinguishable from one another but these genera can be separated macroscopically. **Thuja occidentalis** twigs with well preserved leaves were identified at several levels in the Gage Street marl sequence; however, occurrences of these twigs as early as 12 500 years ago in association with forest-tundra elements is perplexing. Equally perplexing is the presence of **Larix laricina** needles in the lowermost sediments where its pollen is absent.

Seeds of **Abies balsamea, Betula populifolia, Pinus strobus,** and **P. resinosa** provide positive evidence that these tree species formed part of the flora in the vicinity of the site between 10 000 and 9000 years ago and possibly later. Until now, **Abies** has been inferred purely on the basis of a minor peak in pollen at or shortly after the transition from spruce to pine in most pollen diagrams from southern Ontario; seeds of this species now substantiate this inference. While white pine can be identified with certainty from both pollen and plant macrofossils, precise identification of red pine can only be made on the basis of the macrofossils. Seeds of white and red pine confirm the presence of these tree species in the vicinity of the site up until about 7000 years ago.

It would be most useful to have macrofossil data of hemlock and of some of the other hardwoods to complement the pollen records. Hemlock macrofossils, however, are uncommon in Holocene sediments but have been recorded in Pennsylvania (Watts, 1979) and New Hampshire (Davis et al., 1980). More combined pollen and macrofossil analyses are required in order to resolve the presence of certain plant taxa throughout the Holocene.

Acknowledgments

This study was carried out in association with insect studies by D.P. Schwert, University of North Dakota, and I acknowledge him for providing the sediment samples. I am grateful to J.A. Janssens, formerly of the University of Alberta, now at the Limnological Research Center, University of Minnesota, for kindly identifying the fossil bryophytes and providing paleoecological interpretations. W. Blake, Jr. and R.J. Mott provided helpful comments on the manuscript.

References

Anderson, T.W.
1979: Stratigraphy, age, and environment of a Lake Algonquin embayment site at Kincardine, Ontario; in Current Research, Part B, Geological Survey of Canada, Paper 79-1B, p. 147-152.

Ashworth, A.C.
1977: A late Wisconsinan Coleopterous assemblage from southern Ontario and its environmental significance; Canadian Journal of Earth Sciences, v. 14, p. 1625-1634.

Birks, H.J.B. and Birks, H.H.
1980: Quaternary Palaeoecology; Edward Arnold, London, 289 p.

Davis, M.B., Spear, R.W., and Shane, L.C.K.
1980: Holocene climate of New England; Quaternary Research, v. 14, p. 240-250.

Davis, R.B. and Webb, T., III
1975: The contemporary distribution of pollen in eastern North America: a comparison with vegetation; Quaternary Research, v. 5, p. 395-434.

Dreimanis, A.
1977: Late Wisconsin glacial retreat in the Great Lakes region, North America; Annals of the New York Academy of Science, v. 288, p. 70-89.

Faegri, K. and Iversen, J.
1975: Textbook of Pollen Analysis; 3rd ed. Hafner Press, New York, N.Y., 295 p.

Glaser, P.H.
1981: Transport and deposition of leaves and seeds on tundra: a late-glacial analog; Arctic and Alpine Research, v. 13, p. 173-182.

Karrow, P.F.
1971: Quaternary geology of the Stratford-Conestogo area, Ontario; Geological Survey of Canada, Paper 70-34, 11 p.

1974: Till stratigraphy in parts of southwestern Ontario; Geological Society of America Bulletin, v. 85, p. 761-768.

Karrow, P.F., Anderson, T.W., Clarke, A.H., Delorme, L.D., and Sreenivasa, M.R.
1975: Stratigraphy, paleontology, and age of Lake Algonquin sediments in southwestern Ontario, Canada; Quaternary Research, v. 5, p. 49-87.

McAndrews, J.H.
1981: Late Quaternary climate of Ontario: temperature trends from the fossil pollen record; in Quaternary Paleoclimate, ed. W.C. Mahaney, p. 319-333, Geo Abstracts, Norwich, England.

Mott, R.J. and Farley-Gill, L.D.
1978: A late-Quaternary pollen profile from Woodstock, Ontario; Canadian Journal of Earth Sciences, v. 15, p. 1101-1111.

Rowe, J.C.
1977: Forest regions of Canada; Department of Fisheries and the Environment, Canadian Forestry Service, Publication 1300 (1972), 172 p.

Schwert, D.P.
1978: Paleoentomological anlayses of two postglacial sites in eastern North America; unpublished Ph.D. thesis, University of Waterloo, Ontario.

Sreenivasa, B.A.
1968: A late-glacial and postglacial pollen diagram from the Waterloo Moraine, Waterloo county, Ontario; unpublished M.Sc. thesis, University of Waterloo, Ontario.

1973: Paleoecological studies of Sunfish Lake and its environs; unpublished Ph.D. thesis, University of Waterloo, Ontario.

Terasmae, J.
1980: Some problems of late Wisconsin history and geochronology in southeastern Ontario; Canadian Journal of Earth Sciences, v. 17, p. 361-381.

Terasmae, J. and Anderson, T.W.
1970: Hypsithermal range extension of white pine (**Pinus strobus** L.) in Quebec, Canada; Canadian Journal of Earth Sciences, v. 7, p. 406-413.

Terasmae, J. and Matthews, H.L.
1980: Late Wisconsin white spruce (**Picea glauca** (Moench) Voss) at Brampton, Ontario; Canadian Journal of Earth Sciences, v. 17, p. 1087-1095.

Watts, W.A.
1979: Late Quaternary vegetation of central Appalachia and the New Jersey coastal plain; Ecological Monographs, v. 49, p. 427-469.

Webb, T., III and McAndrews, J.H.
1976: Corresponding patterns of contemporary pollen and vegetation in central North America; Geological Society of America, Memoir 145, p. 267-299.

PROTEROZOIC SPINIFEX-TEXTURED BASALTS OF GILMOUR ISLAND, HUDSON BAY

Project 780012

Nicholas T. Arndt[1]
Precambrian Geology Division

Arndt, Nicholas T., Proterozoic spinifex-textured basalts of Gilmour Island, Hudson Bay; in Current Research, Part A, Geological Survey of Canada, Paper 82-1A, p. 137-142, 1982.

Abstract

Many lava flows in the Proterozoic volcanic succession on Gilmour Island, Hudson Bay, have komatiitic basaltic compositions and are layered with mafic upper parts and ultramafic, cumulate lower parts. In some flows, the upper layers show a regular progression of textural types, from olivine spinifex at the top, to pyroxene spinifex near the base. These flows have an elongate lens shape. When they erupted, the tops of the lenses appear to have protruded well above the level of the surrounding lavas. The shapes of these flows, and the internal arrangement of olivine crystals, suggest that spinifex texture formed while lava was still moving within the flows.

In other layered flows, spinifex texture develops only sporadically in veins, and still others have gabbroic-textured upper parts and no spinifex texture at all. The presence or absence of spinifex texture could not be related in any simple way to any distinctive petrological or morphological features of the flows.

Introduction

Lava flows with ultramafic compositions and well developed olivine spinifex zones were reported by Baragar and Lamontagne (1980) to form part of a Proterozoic volcanic succession on the Ottawa Islands in eastern Hudson Bay. This was the first published report of olivine spinifex-textured komatiites in a Proterozoic succession[2]. Although subsequent chemical analyses showed that most magnesian liquids were probably of komatiitic basalt rather than komatiite compositions (maximum MgO contents in noncumulate rocks are about 15%), the flows seemed interesting enough to warrant further investigation.

Two weeks were spent mapping and sampling selected flows on Gilmour Island. Emphasis was placed on units with ultramafic lower layers. Not all of these had spinifex-textured sections. The aim was to concentrate initially on the petrology and morphology of the flows and to compare them with Archean spinifex-textured komatiites. It was hoped that the study would contribute to our understanding of the conditions under which the flows erupted and crystallized, and would explain why spinifex texture develops in some flows and in some regions but not in others.

The work was carried out in conjunction with W.R.A. Baragar's field party who continued their geological investigations of other islands in the Ottawa Island group. For a description of the regional geology the reader is referred to Baragar and Lamontagne (1980) and Baragar (1982).

Descriptions of Lava Flows

To illustrate the range of mafic-ultramafic lava flows found on Gilmour Island, three types are described. The first has well developed spinifex and cumulate layers, the second has only sporadic development of spinifex texture and limited olivine settling, and the third, a gabbro-peridotite flow, has no spinifex whatsoever.

Spinifex-Textured Flows

Vertical Zonation. This type of flow was illustrated and briefly described by Baragar and Lamontagne (1980). Closer study showed that the upper spinifex zone contained a regular variation of textural type. Various aspects of these textures and layering differ from features of typical Archean komatiites. The units are, from top to base (Fig. 24.1):

a) a flow top, 1-3 m thick, polyhedrally jointed in its upper 50-100 cm, and columnar jointed below. The uppermost lava is aphanitic or olivine porphyritic (the rocks are metamorphosed to greenschist facies, and primary mineralogy is generally inferred from the mineral habits of secondary phases). Fine olivine spinifex texture first develops about 1 m below the top of the flow.

b) Olivine spinifex texture is present in the interval from 1 to 4 m from the flow top. Olivine crystals have a skeletal plate habit and are randomly oriented. Grain length increases from less than 5 mm at the top to as large as 2 cm at the base of this zone, although the grains are invariably very thin, never exceeding 0.5 mm in thickness. The proportion of olivine is low (10-20%).

c) A 'string beef' pyroxene spinifex layer (Arndt et al., 1977), made up of long thin pyroxene needles oriented perpendicular to strike, normally underlies the olivine spinifex layer. In some flows this layer is absent, but in others it is repeated two or three times. The needles, which probably had pigeonite cores and augite margins, lie in a matrix of stubbier, smaller augite grains and minor plagioclase. Unusually long (up to 5 cm) olivine wafers may lie parallel to the pyroxene needles.

d) Below 'string beef' spinifex, or intervening between layers, the rock has a texture made up of pyroxene needles arranged in sheaves, in which the needles splay out in a downwards direction.

e) The lowermost rock in the upper part of the flow consists of randomly oriented pyroxene needles 1 to 20 mm in length, in an augite-plagioclase matrix.

f) At the top of the cumulate part of the flow is a layer dominated by coarse, elongate hopper to plate olivine crystals. These are randomly oriented at the top of the layer, but rapidly acquire a preferred orientation parallel to strike. This layer corresponds to the B_1 zone of Archean komatiites, but is far thicker (50-80 cm) and contains much coarser olivine crystals (up to 2 cm in length).

g) The rest of the olivine cumulate layer contains 50% equant solid olivine grains in a matrix of acicular pyroxene and devitrified glass. The rock usually has a foliation parallel to flow contacts and commonly is columnar-jointed. The olivine content diminishes in the lower 1-2 m to form a basal marginal zone, and the lowermost 2-5 cm is a chilled aphanitic lava.

---

[1] Max-Planck-Institut für Chemie, Postfach 3060, D-6500 Mainz, F.R. Germany
[2] Francis and Hynes (in press) have since reported olivine spinifex texture in a single komatiitic basalt flow from the Cape Smith belt

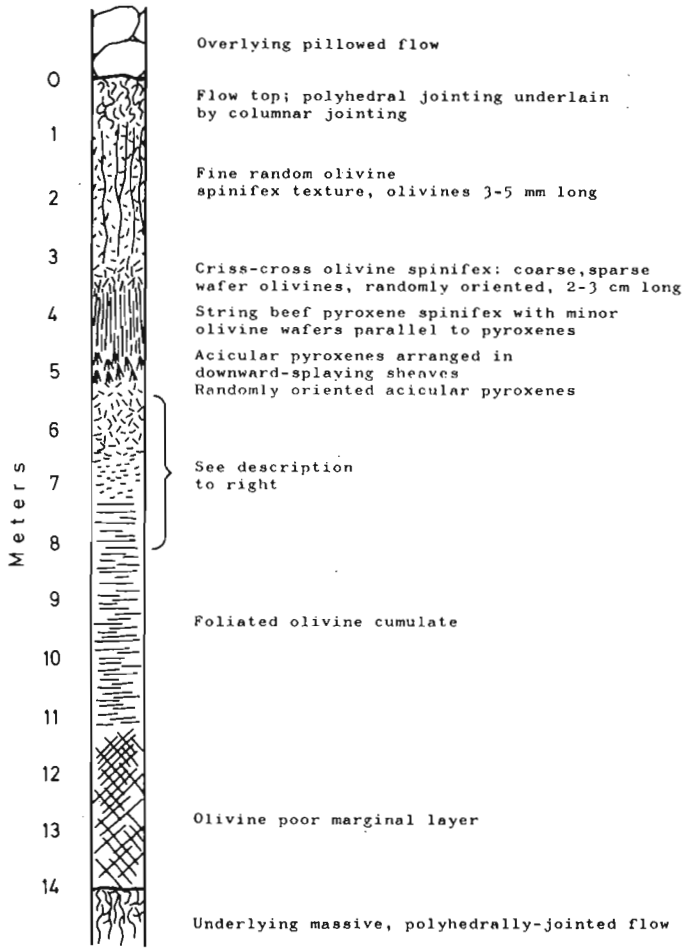

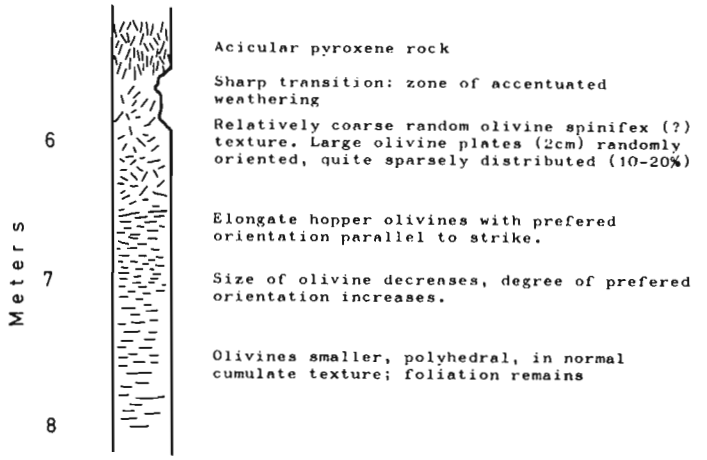

Figure 24.1. *Diagrammatic cross-sections through a flow with well developed spinifex and cumulate layers.*

The above sequence differs from that in Archean komatiites in the following ways: the polyhedrally jointed cap is thicker (1-3 m, cf. 5-10 cm in Archean flows); the B_1 layer is far thicker and better developed; columnar jointing is more pronounced; and the flows themselves are thicker (12-16 m cf. 0.5 to 4 m in typical Archean examples).

Lateral Variations. Although some flows end abruptly after 100-200 m, at faults or in the type of termination described below, many can be traced along strike for several kilometres. Along this length, the flows for the most part maintain a very constant thickness (usually varying less than 1 m from the mean of 12-14 m), and show little variation in the proportion of spinifex-textured to cumulate layers nor in the proportions of the different types of spinifex-textures. One flow grades from a layered unit with well developed spinifex-texture, to a unit in which olivine settling is less pronounced and spinifex texture is only sporadically developed.

Along each flow, however there are intervals in which the flow becomes thinner and the spinifex-cumulate layering disappears. The intervals without spinifex texture vary from 20 to 200 m long and are separated by spinifex-textured intervals 60-300 m long. Thus, spinifex-textured lava constitutes only about 50 to 70 per cent of total measured flow lengths (Fig. 24.2).

The ends of spinifex-textured parts of a flow are illustrated in Figures 24.2 and 24.3. The polyhedrally-jointed top of the flow rapidly arches down, and in this interval the orientation of columnar jointing and spinifex needles rotates to maintain a direction perpendicular to the cooling surface. The lower cumulate layer continues a farther 5-10 m, but within it polyhedral jointing and fine spinifex texture develop. After 10 m the distinction between upper and lower sections of the flow is lost. Finally, the flow grades into pillow lava. These flow terminations are symmetrical; i.e. the one at the other end of the spinifex interval would be the mirror image of the one shown in Figure 24.2. Thus, they probably represent the sides of highly elongate, flat-topped lenses of komatiitic lava within which the direction of lava movement was at a high angle to present strike.

Normally the attitude of the lower flow contact does not change as the overlying lava grades from spinifex-textured to pillow lava. This indicates that the floor on which the flows were erupted was level. In one case, however, a 2 m high mound in the floor coincides with, and may have influenced, the disappearance of spinifex-cumulate layering.

The thickness of polyhedrally jointed or pillowed flow sections is generally 1-3 m less than that of the spinifex-textured parts of the flows. The tops of these spinifex texture intervals would therefore have stood well above the level of the surrounding lavas. One can imagine that as these flows erupted, they consisted of elongate lenses of highly mafic liquid fully enclosed in strong, elastic skins of chilled lava (Fig. 24.2, 24.3).

Flows with Limited Olivine Settling and Sporadic Development of Spinifex Texture

This type of flow does not have a sharp demarcation between the layer of settled olivine and on overlying layer of spinifex or aphanitic lava; rather there is a gradual increase

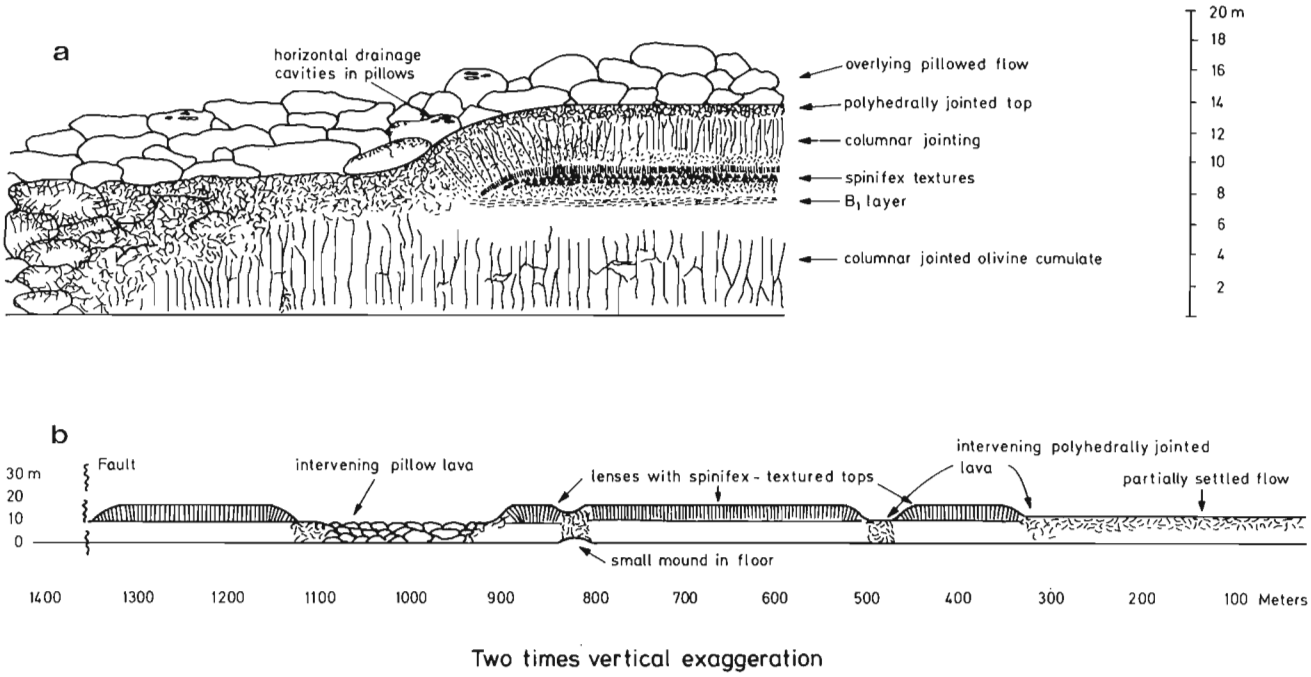

Figure 24.2. *(a) Sketch of the termination of the spinifex-textured portion of a flow; (b) Sketch of a measured interval along a spinifex-textured flow.*

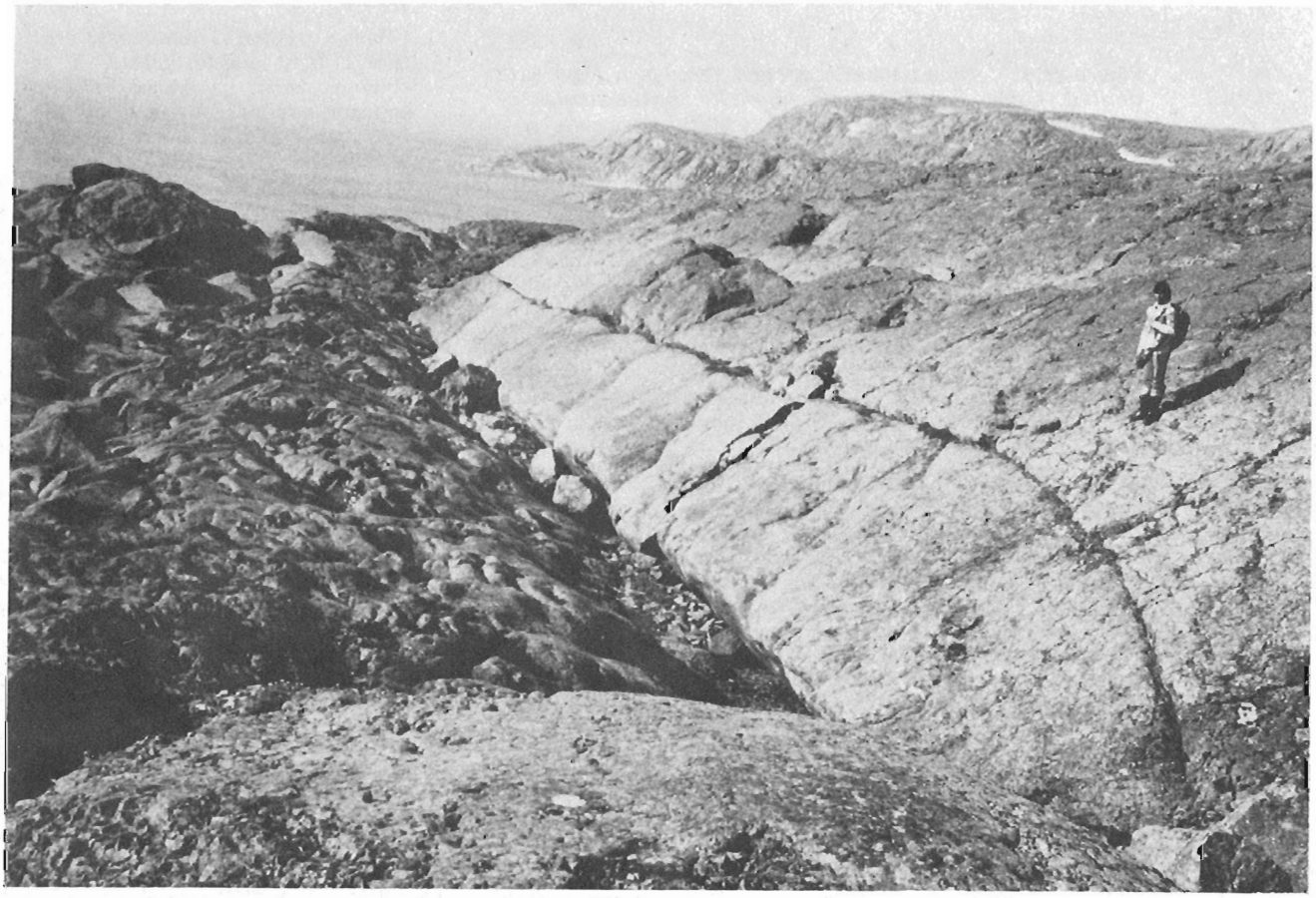

Figure 24.3. *Photograph of the termination of a spinifex-textured flow. The flow dips steeply to the right and faces in the same direction. The spinifex-textured upper part and the overlying pillowed flow are well exposed on the smooth rock face. The lower cumulate portion forms poorer outcrop on the left of the picture. Note the pronounced downward curvature of the flow top. In the foreground is polyhedrally jointed lava along strike from the cumulate layer.*

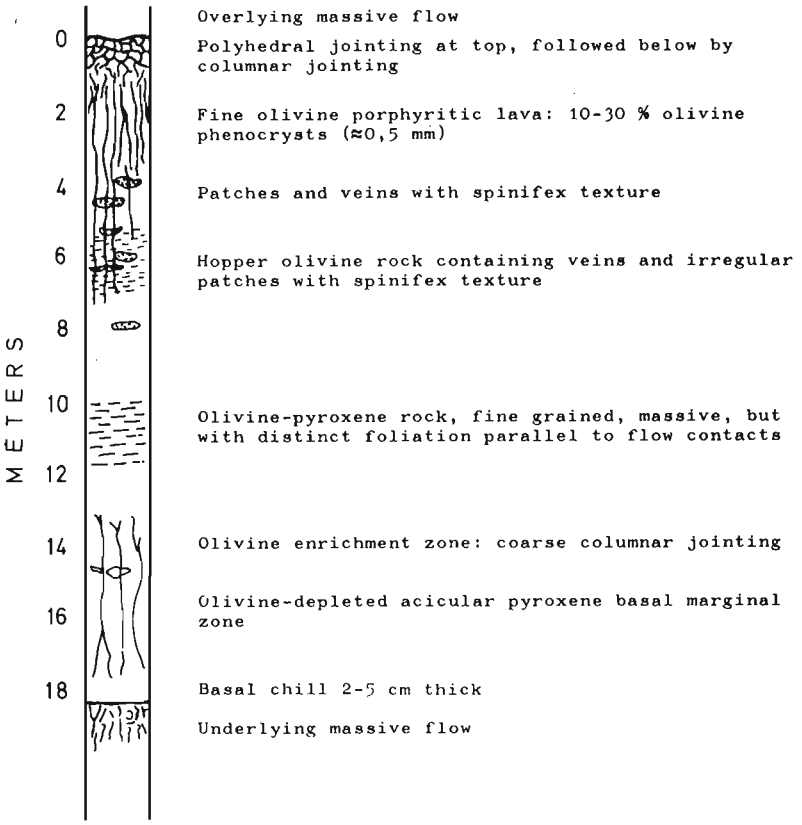

Figure 24.4. *Diagrammatic section through a flow with limited olivine settling and sporadic development of spinifex texture.*

in the abundance of solid equant olivine grains towards the base of the flow (Fig. 24.4). A maximum olivine content is reached in the 3-4 m thick columnar-jointed layer that overlies the olivine depleted basal layer.

The upper 2-5 m of this type of flow is composed of polyhedrally or columnar jointed, fine grained olivine porphyritic lava. From 5 to 7 m the lava is rich in large (0.5 to 2 cm) hopper olivine grains oriented parallel to flow contacts, and below this, the lava is fine grained and massive, or has a foliation manifested in closely-spaced fine joints oriented parallel to the flow contacts.

In the interval from 3 to 8 m from the flow top, spinifex texture develops in lenses, veins and irregular blobs. Some of the veins and lenses have a concave-upwards crescent shape, and are oriented parallel to flow contacts. The contacts between spinifex-textured rock and the host lava, which may contain fine solid olivine phenocrysts or coarser hopper olivines, are abrupt but are not marked by obvious discontinuities of a type that would indicate intrusion of the vein material. Instead, the matrix between the olivine grains is continuous, and at the contact there is only a change in the habit of the olivine grains, from the platey spinifex grains to the hopper or polyhedral grains of the host lava. The nature of the contacts suggests that the spinifex texture formed in isolated nucleus-free volumes of liquid, at a stage in the cooling history of the flow when the hopper olivines were mobile and suspended, though relatively closely packed, in an olivine-normative liquid.

The dimensions of this type of flow are similar to those of the spinifex flows on Gilmour Island (12-20 m thick) and although they can be traced considerable distances along strike, they too give way at irregular intervals to spinifex-free, polyhedrally-jointed lava, and to pillow lavas.

Layered Olivine-Cumulate-Pyroxenite-Gabbro Flows

An example of this flow type was illustrated and briefly described by Baragar and Lamontagne (1980). Although most are far thicker than normal flows (up to a maximum of about 100 m) other examples have more modest dimensions comparable to those of the spinifex flows (about 20 m thick).

Within a typical example the following units are developed (from top to base, Fig. 24.5).

a) Flow top breccia (1-2 m thick) containing subangular to plastically-deformed amoeboid clasts of fine grained, olivine-porphyritic lava (less than 1 cm to 20 cm in maximum dimension), lying in a palagonite-hyaloclastite matrix. In some places purplish weathering, fine ferruginous cherty material forms part of the matrix.

b) Massive to columnar-jointed mafic lava (20-40 m thick), grading from fine olivine porphyry, layered in places, to medium grained gabbro. In the interval from 17-20 m the rock is more mafic than most of this layer and contains up to 5 per cent coarse (1-3 mm) skeletal, leucoxene grains.

c) Clinopyroxenite (1-2 m thick) made up of fine (1 mm) augite grains, 5 per cent orthopyroxene. Minor plagioclase appears towards the top of the layer. Both upper and lower contacts are sharp. Within the pyroxenitic layer and in the immediately overlying gabbro occur bulbous to podiform veins and patches of a rock with a texture that resembles spinifex. The rock contains radiating clusters of elongate tabular to highly acicular grains of plagioclase and lesser amounts of acicular pyroxene. The plagioclase grains may reach 3 cm long, although they average about 5 mm.

d) Olivine cumulate (40-60 m thick). Most of this layer is dominated by polyhedral olivine grains which average 0.5 to 1 mm in size. In the upper 20 m, augite forms large (2-4 mm) oikocrysts. In the remainder of the layer the augites are smaller, prismatic and form part of the matrix which presumably is composed of plagioclase and pyroxene. In the 10-15 cm thick basal pyroxenite layer, the olivine content decreases to less than 10 per cent.

The uppermost 50-100 cm of the olivine-rich layer contains about 50 per cent of coarse (up to 7 mm in length) delicate skeletal hopper olivine grains. The contact between this rock and overlying pyroxenite is marked by prominent flame structures and load clasts. "Flames" of deformed skeletal olivine rock penetrate up to 60 cm into overlying pyroxenite.

Underlying most flows are pillows with a composition and texture very similar to that of the fine grained margin of the layered flow. The frequent association of highly mafic pillows and layered flows may indicate that both are products of the same extrusive event (see Baragar, 1982).

The thicker layered gabbro-peridotite units are not continuous along strike; rather they terminate after 100 to 800 m, a distance of only 3-10 times their thickness. Normally in cross-section the flows are lens-shaped: both upper and lower layers are thickest in the centre of the lens, and coverage towards much thinner ends where the coarser

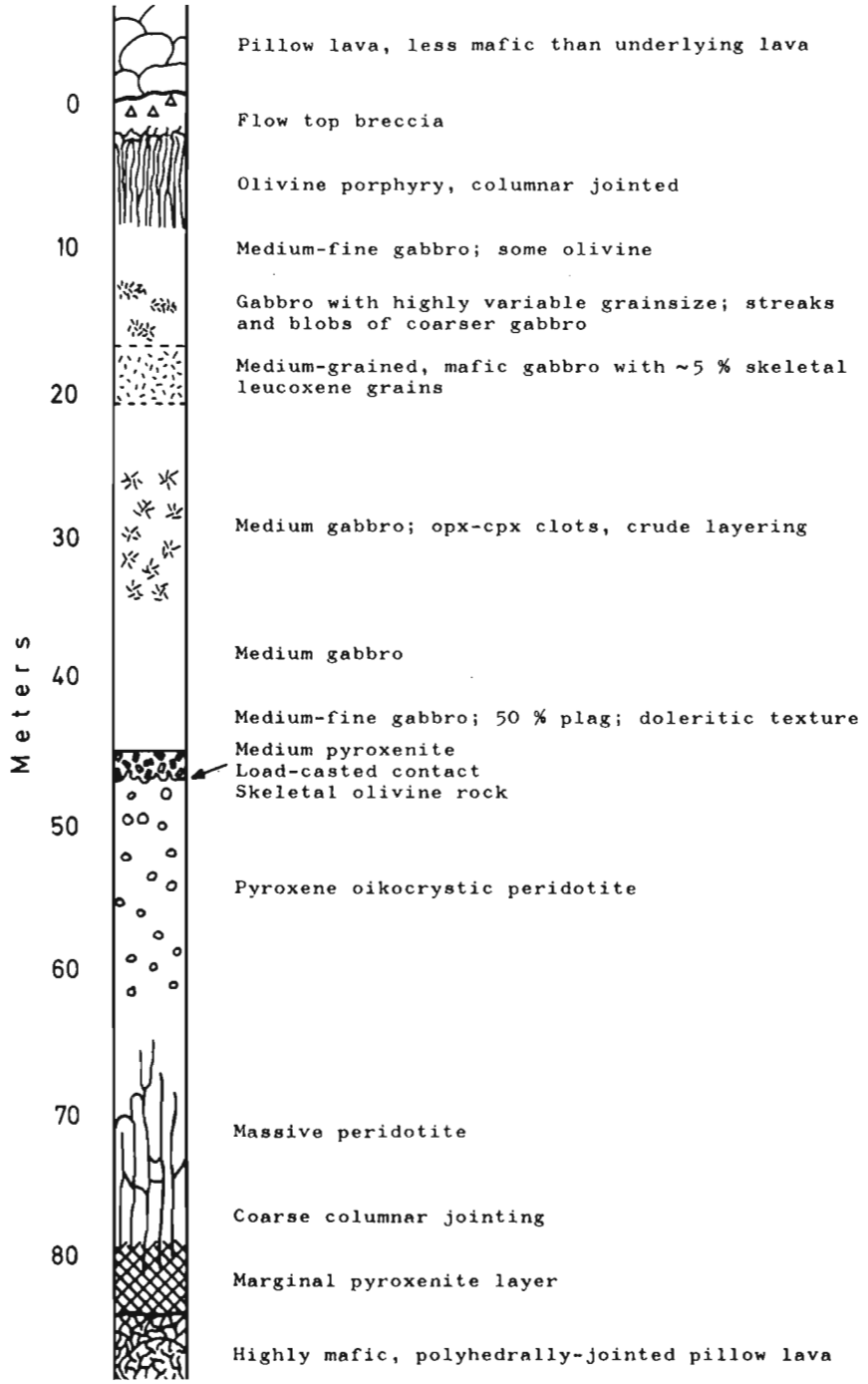

Figure 24.5. *Diagrammatic section through a thick gabbro-peridotite flow.*

gabbros and peridotites grade into fine grained, polyhedrally-jointed or pillowed olivine porphyries. Most of the lenses appear to lie in depressions in the underlying pillow lavas, but their tops project well above the level of the valley sides. Other units have more or less level floors but steeply domed roofs. The lower olivine cumulate parts of the lenses a.e themselves composed of a number of smaller lenses, each 3-30 m thick and 10-100 m long, and each with its own set of large columnar joints. No textural changes such as chilling or reductions in olivine content was observed at the contacts between these internal lenses.

Discussion

The speculations that follow are preliminary and may have to be modified on the basis of petrographic and geochemical investigations that will be carried out in the coming year.

The Formation of Spinifex Texture

There are several models for the formation of the spinifex-textured and cumulate portions of komatiite flows. Pyke et al. (1974) and Arndt et al. (1977) proposed a model in which olivine phenocrysts settled to the lower part of the flow forming the cumulate layer, leaving an upper layer in which spinifex texture developed by crystal growth downward from the chilled flow top. Lajoie and Gélinas (1978) envisaged a rather different sequence. They proposed on the basis of textures such as crossbedding in the cumulate olivine layers and normal and reverse grading in the B_1 zone, that the spinifex layer develops first, narrowing the conduit through which lava continues to move, developing turbulence and leading to the observed 'sedimentary' structures in the accumulating lower olivine rich layer. Donaldson (in press) proposed that olivine crystallized simultaneously throughout the flow. According to this model some olivine may have originated as transported phenocrysts and settled downwards, but throughout each unit the olivine habit reflects the cooling regime in the interval in which it is found; viz, fine and skeletal olivine grains in the flow top, coarse skeletal plates in spinifex, hopper grains in the B_1 layer and polyhedral grains in the lower B zone.

Various features of the Ottawa Islands flows suggest that they form under dynamic conditions closer to those envisaged by Gélinas and Lajoie (1978) or Donaldson (in press), than to the static conditions envisaged by Pyke et al. (1974) and Arndt et al. (1977). The variations in crystal habit and mineralogical compositions accurately reflect the differences in cooling rate expected in a cooling flow, and the orientation of the large elongate hopper olivines of the B_1 layer strongly suggests that lava continued to flow even after the formation of the spinifex layer. More significant, though, is the shape of the lava flows, and particularly the manner in which the upper spinifex layers in the spinifex lenses (Fig. 24.2) stick up above the level of the surrounding lavas. To maintain a volume of lava enclosed within an elastic skin of chilled material but above the level of the surrounding lavas must have required a considerable hydraulic head of lava within each lens. Most probably lava flowed through these lenses, from the sources of eruption to the active flow front, and it is under these conditions that the spinifex texture formed.

The komatiitic lava flows of Munro Township and of many other Archean areas show few of the features that indicate active movement of lava during spinifex growth. This may indicate that these flows did indeed crystallize under more static conditions, or it may simply indicate that the flowage features are not preserved in the more ultramafic and less viscous Archean lavas.

The lenses and veins with olivine spinifex texture in the upper parts of partially settled flows may have formed in a different way. In these flows, for a reason that is unclear at the moment, the olivine phenocrysts did not settle effectively but remained distributed throughout the flow. Their presence provided abundant nucleation sites and prevented the formation of spinifex texture. However, at a stage in the cooling history when the lava contained maybe 50 per cent solid olivine grains suspended in a silicate liquid matrix, volumes of crystal-free liquid developed, perhaps as a result of shearing caused by fluctuations in the rate of flow of lava in the underlying more mobile portions of the flow. Within these volumes of nucleus-free liquid in the rapidly cooling upper parts of the flow, spinifex texture would grow from the still olivine normative liquid.

The lenses of acicular plagioclase rock within layered gabbro-peridodite flows may have still another origin. Their plagioclase-rich mineralogy, which indicates formation from a liquid of more evolved composition, and their occurrence within the pyroxenite layer deep within the lava flows suggests that they may have formed in a manner similar to pegmatites. They may represent portions of the last remaining liquid which migrated upwards into fractures in the largely solid flow, and their acicular mineral habits and overall texture may have more to do with a high concentration of volatiles than to rapid cooling.

No answer can be given to the question of why spinifex texture develops so well in some flows but only sporadically or not at all in others. No significant differences in lava composition could be deduced from field observations, and neither could differences in the dimensions of the flows, nor in the local eruptive environment of spinifex bearing and spinifex free flows, be found. The layered gabbro-peridotite flows appeared identical in all these aspects to flows with well developed spinifex layers. The answer may come during subsequent petrographic and geochemical studies, or it may be related to indeterminate features such as the length of the time interval before a particular lava flow is covered by a second, insulating lava flow.

Shape of the Lava Flows

The most remarkable aspect about the shape of the lava flows is the manner in which the tops of spinifex textured and the layered gabbro-peridotite flows stick up above the level of the surrounding lavas. The lava would have had a very low viscosity, and the steep sides of the flows could not have persisted unless this liquid was fully enclosed in a strong skin of chilled lava. In the case of the largest dome-shaped flows the strength of this skin must have been considerable.

As mentioned before, the elevated tops of these flows must have been maintained by the hydraulic head of lava as it moved from source to active flow front. The intervening intervals of polyhedrally jointed or pillow lava between spinifex lenses (Fig. 24.2), may represent stagnant areas at the flow front formed at an early stage of eruptions. They would have remained as immobile buttresses during subsequent flowage. The doming of the upper parts of the larger gabbro-peridotite flows may be caused by the injection into the flow of numerous pulses of lava. The present manifestation of these pulses would be the internal lenses in the lower parts of the flows (Fig. 24.4).

Acknowledgments

I wish to thank Bob Baragar for his kind cooperation and assistance throughout the project. I also thank Peter Inukpuk who acted as field assistant and polar bear guard. The Geological Survey of Canada and the Max-Planck-Institut für Chemie in Mainz provided logistic and financial support. Lina Echeverria reviewed an early draft of the paper.

References

Arndt, N.T., Naldrett, A.J. and Pyke, D.R.
1977: Komatiitic and iron-rich tholeiitic lavas of Munro Township, northeast Ontario; Journal of Petrology, v. 18, p. 319-369.

Baragar, W.R.A. and Lamontagne, C.G.
1980: The Circum-Ungava Belt in eastern Hudson Bay: the geology of the Sleeper Islands and parts of the Ottawa and Belcher Islands; in Current Research, Part A, Geological Survey of Canada, Paper 80-1A, p. 89-94.

Baragar, W.R.A. and Piché, M.
1982: The Circum-Ungava Belt of eastern Hudson Bay: The geology of the Ottawa Islands and Cape Smith region; in Current Research, Part A, Geological Survey of Canada, Paper 82-1A, report 2.

Donaldson, C.H.
Spinifex-textured komatiites: a review of textures, mineral compositions and layering; in Komatiites, N.T. Arndt and E.G. Nisbet, ed. Allen and Unwin. (in press)

Francis, D.M., Hynes, A.J., Ludden, J.N., and Bedard, J.
Crystal fractionation and partial melting in the petrogenesis of a Proterozoic high-MgO volcanic suite, Ungava, Quebec; Contributions to Mineralogy and Petrology. (in press)

Lajoie, J. and Gélinas, L.
1978: Emplacement of Archean peridotitic komatiites in La Motte Township, Quebec; Canadian Journal of Earth Sciences, v. 15, p. 672-677.

25.

GEOLOGY OF BAKER LAKE MAP AREA, DISTRICT OF KEEWATIN: A PROGRESS REPORT

Project 800008

Mikkel Schau, F. Tremblay[1] and A. Christopher[2]
Precambrian Geology Division

Schau, Mikkel, Tremblay, F., and Christopher, A., Geology of Baker Lake map area, District of Keewatin: a progress report; in Current Research, Part A, Geological Survey of Canada, Paper 82-1A, p. 143-150, 1982.

Abstract

In the north of the Baker Lake map area the Archean(?) Ketyet River group and the Quoich River gneiss complex have been intruded by the Tehek Lake plutonic complex. Subsequently, the Akutuak River gneiss complex has been tectonically emplaced onto the above complexes. In the south of the map area the Archean Kramanituar complex has been tectonically emplaced onto the Archean Ingilik Point gneiss complex. The east-west trending Chesterfield Fault Zone separates the northern and southern part of map area. Although the zone has undergone considerable strain, as shown by mylonites, transcurrent movement has probably not been great. Accompanying uplift, mafic stocks and dykes, and quartz syenites have been intruded, and subsequently the Dubawnt Group has been deposited. The region has been cut by the west-northwest-trending Baker Lake Cataclasite Zone. Late granite stocks have been intruded north of the fault zones. A Mackenzie dyke has been the latest igneous event in the area.

Introduction

The geology of the east half of the Baker Lake map area was mapped at a scale of 1:250 000 and selected regions in the west half were re-examined in the 1980 field season.

The area is divided into twelve map units (Fig. 25.1). These are described below and topics of special interest are appended.

Geological Units: An Extended Legend

Unit 1 (informally the Ketyet River group)

The Ketyet River group extends from Whitehills Lake eastward to the Ketyet River and thence northeastward towards the northeast corner of the map area.

The group consists of metasedimentary rocks, including white quartzites (1a), siltstones, wackes, phyllites, mica schists, polymictic paraconglomerates, calc-silicate bearing carbonates, iron formations and thin greenstone layers (Heywood and Schau, 1981; Nadeau, 1981). The quartzites extend northeastward in a sinuous band that is conformable with metasediments and gneisses. Paraconglomerates contain stretched granitoid and quartz pebbles set in a dark biotite-bearing matrix. Conglomerate becomes more flattened to the northeast. Black sulphidic units associated with the quartzites locally carry small amounts of galena with pyrrhotite.

Greenstone layers consist of rare volcanogenic sediments and volcanic units such as those described by Nadeau (1981) north of Whitehills Lake. Sills and dykes of fine grained greenstone cut quartzites and volcanic rocks, as is well shown north of Whitehills Lake.

Stratigraphic sequences are difficult to determine since fold patterns have not yet been resolved. Folds have shallow-dipping axial planes. Minor folds indicate several phases of folding and more than one fold axis. Sections suggest that there is probably more than one quartzite unit (Table 25.1).

The metamorphic grade of the Ketyet River group is generally middle amphibolite. The quartzites commonly carry sillimanites although south of Whitehills Lake chloritoid-staurolite assemblages occur in the quartzites. The associated metasediments change from biotite-muscovite-chlorite-phyllites and biotite schists to biotite paragneisses in a northeasterly direction.

The age of the Ketyet River group is uncertain. It is probably the oldest unit in the region. A few dykes of granitic composition similar to the structurally overlying Akutuak River Gneiss Complex cut the Ketyet River Group, suggesting that the group is older than the gneiss complex. It is cut by the Tehek Lake plutonic complex and is the precursor to part of the Quoich River Gneiss Complex.

Extension of the quartzites to the northeast allows one to speculate that they project along strike to join with the Archean Prince Albert Group (Schau, 1977, in press). These two groups share similar lithologies and structural trends. An Archean age assignment is therefore suggested although these sediments have been previously assigned to the early Proterozoic (Wright, 1967).

Unit 2 (informally the Quoich River gneiss complex)

The Quoich River gneiss complex underlies northeast portions of the map area. The complex consists of layered, medium grained, biotite-bearing gneisses with layers of varying thickness, colour and composition, and is generally

Table 25.1

Selected Lithologic Sequences of the Ketyet River group

Northeast of Whitehills	Quoich River
Quartzite	Biotite metasiltstone
Quartzose schist	Paraconglomerate
Quartz-rich garnetiferous biotite schist	Biotite metasiltstone
Feldspathic schist	Quartzite (thin)
Laminated metasediments of light green felsic and dark green amphibole layers	Iron formation and biotite schist
Muscovite schist with local chromian muscovite and tourmaline	Feldspathic biotite schist
Iron formation (silicate facies)	Quartzite (thick)
Quartzite	
Grey feldspathic schist	
Quartzite (thick)	

[1]Département de géologie, Université du Québec à Chicoutimi, Chicoutimi, Québec.
[2]Department of Geology, McMaster University, Hamilton, Ontario.

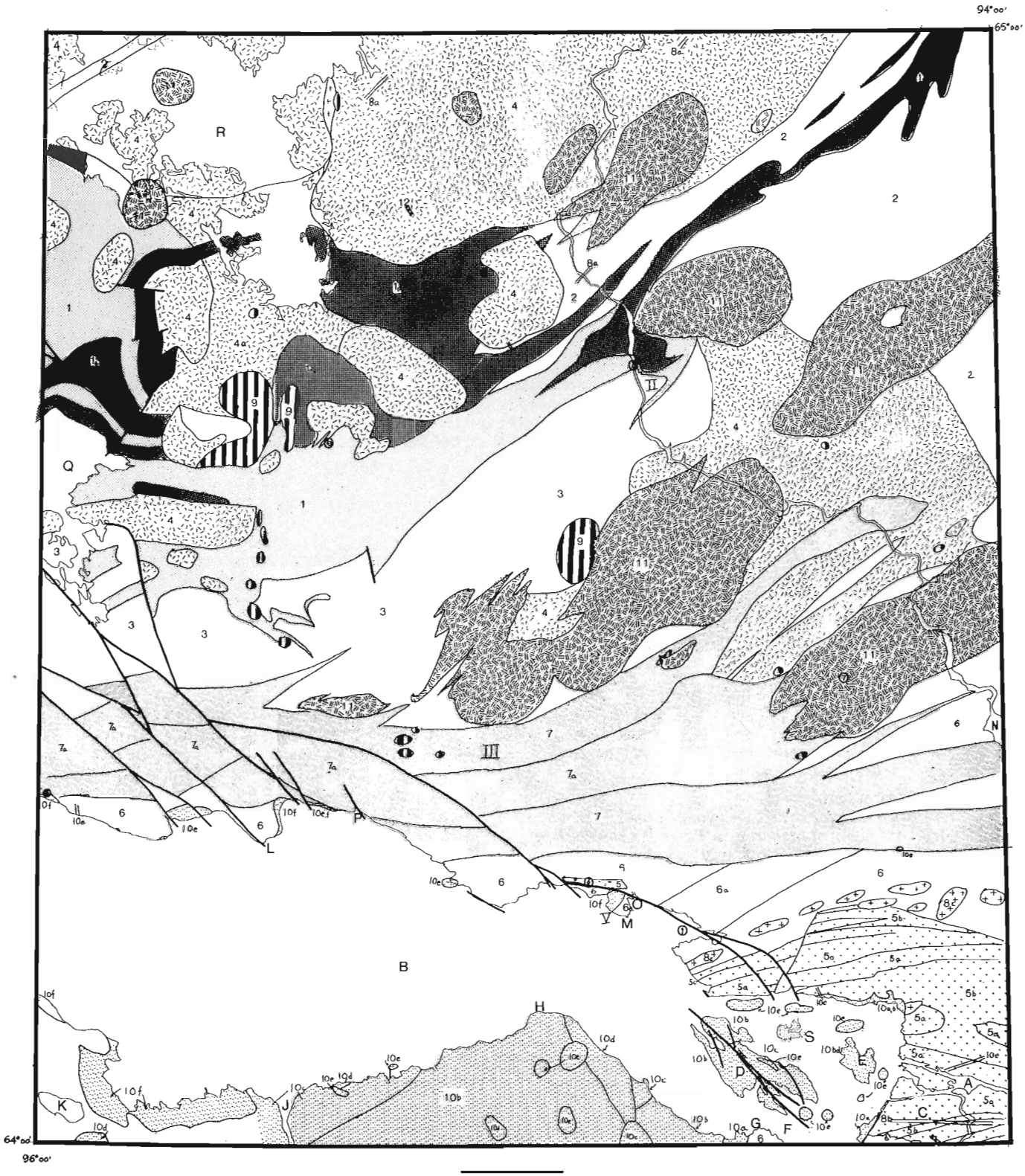

A - Chesterfield Inlet	F - South Channel	K - Gull Lake	P - Akutuak River
B - Baker Lake	G - Severn Point	L - Ingilik Point	Q - Whitehills Lake
C - Bowell Islands	H - Lofthouse Point	M - Jigging Point	R - Tehek Lake
D - Christopher Island	I - Clearwater River	N - Quoich River	S - Red Point
E - Rio Island	J - Kazan River	O - Ketyet River	

Figure 25.1. *Sketch map of the Baker Lake map area. Numbers correspond to units described in expanded legend (see text) letters to place names mentioned in text and roman letters to localities of sketch maps (Fig. 25.2-25.5). Circled numbers are mineral localities. Compilation is based on field work this season, Heywood and Schau (1981), Schau and Ashton (1980), manuscript maps from Wright (1967), and personal communications of Fraser and Heywood (1981).*

mapped as grey granodioritic gneisses. Near the Ketyet River group quartzite, thin garnetiferous and amphibolite layers occur within the grey gneisses. These layers are parallel to the quartzites. The gneisses are interdigitated with Ketyet River Group metasediments and apparently are, in part, high grade equivalents of them. They form inclusions in the Tehek plutonic complex.

Unit 3 (informally the Akutuak River gneiss complex)

The Akutuak River gneiss complex underlies the central portion of the map area. The complex consists of variably foliated and sheared grey quartz diorite to biotite granodiorite (Heywood and Schau, 1981). The foliation is generally shallow dipping.

The northern contact is partly a set of shallow reverse faults bringing plutonic rocks of the complex to rest upon the Ketyet River Group. A sketch map showing this thrust relationship is shown as Figure 36.2 in Heywood and Schau (1981). The eastern border is intruded by the Tehek Lake plutonic complex. Southern parts of the complex are cut by the Chesterfield Fault Zone.

Legend for Figure 25.1

	Unit 12	Mackenzie Diabase
	Unit 11	Late Granite
	Unit 10	Dubawnt Group
		10f, Thelon sandstones 10e, Martell Syenite and dykes 10d, Christopher Island volcanic rocks 10c, Red Point mudstone 10b, Kazan arkose 10a, South Channel
	Unit 9	Quartz Syenite Stocks
	Unit 8	Mafic Stocks and Dykes
		8c, Metagabbro stocks 8b, EW metadiabase dykes (Bowell Islands basic dyke swarm) 8a, NE metadiabase
	Unit 7	Chesterfield Fault Zone
		7a, Augen gneiss
6	Unit 6	Ingilik Point Gneiss Complex
		6a, Porphyritic granite
	Unit 5	Kramanituar High Grade Complex
		5c, Marker horizons of plagioclasite 5b, Anorthositic suite 5a, Granulite suite
	Unit 4	Tehek Lake Plutonic Complex
		4a, Complex mixture of 1 and 4
3	Unit 3	Akutuak River Gneiss Complex
2	Unit 2	Quoich River Gneiss Complex
	Unit 1	Ketyet River Group
		1a, Quartzites of KRG

NOTE: All names, except for units 10, 12, are informal. Dykes are schematic.

Faults of Baker Lake Cataclasite Zone

Geological contacts schematic; includes concordant, intrusive and fault contacts

The metamorphic grade of the complex indicates that shearing retrogressed mineral assemblages to be those typical of upper greenschist-lowermost amphibolite facies. Chlorite, white mica, actinolitic amphibole, epidote, and strained, often blue quartz, and common constituents in the rocks of the sheared and thrusted northern boundary.

The Quoich River gneiss complex and the Akutuak River gneiss complex are separated from each other by the Tehek Lake plutonic complex. Their relative age is unknown but the Akutuak River gneiss complex seems to be structurally emplaced onto the Ketyet River group that nearby is interdigitated with the Quoich River gneiss complex. The tectonic emplacement of the group may also postdate the Tehek Lake plutonic complex, as shown by the reverse fault border along the north side of a stock exposed southeast of Whitehills Lake, although the formation of plutonic rocks of the Akutuak River gneiss complex would predate the Tehek Lake plutonic complex.

Unit 4 (informally the Tehek Lake plutonic complex)

The Tehek Lake plutonic complex underlies substantial parts of the map area north of the Chesterfield Fault Zone.

The complex consists of an orange to pink weathering, pink to white, porphyritic to seriate, biotite-rich, granite in which potash feldspar megacrysts are recrystallized and the biotite flakes outline a foliation. Accessory magnetite and sphene are irregularly distributed; muscovite (and rarely garnet) becomes an important accessory mineral near contacts with quartzite. Border zones are crowded with inclusions or consist of granite sills and/or biotite pegmatite emplaced in the metasediments (Nadeau, 1981; Heywood and Schau, 1981). This mixed unit is labelled as unit 4a in Figure 25.1.

The Tehek Lake plutonic complex cuts the Ketyet River group, the Quoich River gneiss complex, and the Akutuak River gneiss complex. It is cut by northeast-trending metadiabase dykes, quartz syenite stocks and late granite.

Unit 5 (informally the Kramanituar complex)

The Kramanituar complex underlies the southeast corner of the map area. One small outlier lies to the northwest of Jigging Point.

The complex is composed of a suite of granulites (unit 5a) and a suite of anorthositic rocks (unit 5b) (Schau and Hulbert, 1977; Schau and Ashton, 1979, 1980; Schau, 1980b). The granulites range from granitoid to ultramafic compositions and the anorthositic rocks range from anorthosite to iron-rich diorites. The rocks are extremely flattened and individual units (unit 5c) only metres thick can be traced for tens of kilometres along the east-west strike.

The main part of the complex is intruded to the south by a white weathering granodiorite and cut by east-west faults. The northern boundary is determined by a variety of faults, some with shallow dips, most steep. The outlier is a thin sliver that is bounded by mylonitic rocks. Along the south side mylonitic granodiorite dips shallowly under the outlier.

The maximum metamorphism of the complex occurred under medium pressures and high temperatures of the granulite facies, as indicated by various mineral assemblages such as clinopyroxene-orthopyroxene-garnet-hornblende-plagioclase-quartz-opaques, sapphirine-enstatite-garnet-phlogopite and quartz-perthite-sillimanite-kyanite-garnet-graphite.

The age of the complex is at least 2573 Ma (U-Pb, zircon; Schau, 1980a). It is cut in the map area by gabbro stocks, small granitic stocks, east-west metadiabase dykes, and is unconformably overlain by the Dubawnt Group.

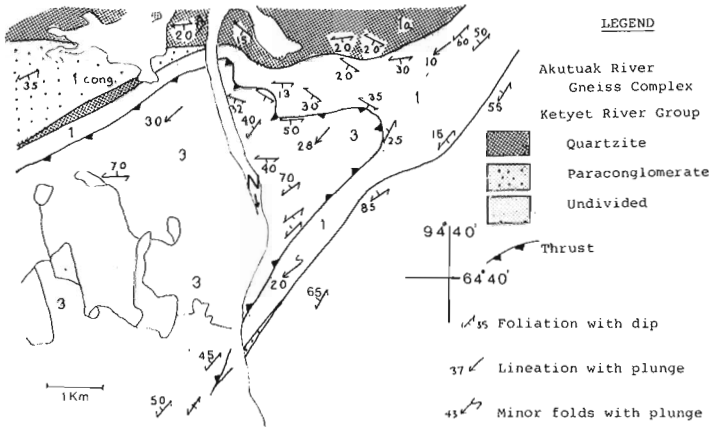

Figure 25.2. *Sketch map of folded shallow reverse fault with sheared Akutuak River gneiss appearing above and below folded rocks of Ketyet River group. Note thick sequence of paraconglomerates which occur only as a thin extremely flattened unit at end of southern tongue. Also note that quartzites are not folded concordantly with the gneiss sheet. Region labelled as Po is pyrrhotite-rich and gives anomalous magnetic ground readings. This unit apparently carries galena on either side of river in this vicinity (Roscoe, personal communication, 1981).*

Unit 6 (informally the Ingilik Point gneiss complex

The Ingilik Point gneiss complex is found along the north shore of Baker Lake and is bounded to the north by the Chesterfield Fault Zone and to the south by the Kramanituar high grade complex.

The complex is composed of white to grey weathering, grey, foliated, locally porphyritic granodiorite to gneissic granodiorite with granitoid or amphibolitic inclusions and septa. The gneisses are cut by variously deformed gabbro stocks, mafic dykes, and pink weathering, pink to grey foliated, locally porphyritic or augened granites (unit 6a). Planar structures in the complex generally dip moderately to the south and locally, open subhorizontal east-west trending folds can be mapped. To the north the complex is cut by plutonic units of the Chesterfield Fault Zone. It is cut by lamprophyre dykes and Martell Syenite stocks, and is unconformably overlain by sediments of the Dubawnt Group.

The layered gneissic septa locally resemble the Akutuak River gneiss complex and the porphyritic granite locally resembles the Tehek Lake plutonic complex. An age of 2675 Ma has been obtained (U-Pb, zircon) for gneissic rocks from this complex (Schau, 1980a).

Unit 7 (the Chesterfield Fault Zone)

The east-west trending Chesterfield Fault Zone underlies a zone 7 to 20 km wide. It is characterized by steeply-dipping easterly or east-northeasterly-striking sheared or foliated granitoid rocks with local development of mylonite zones. One unit near the northern edge is a sparsely porphyritic biotite granodiorite which is flattened. It is succeeded to the south by a megacrystic granite (unit 7a) which contains variable amounts of biotite, hornblende, garnet and quartz. At some localities the feldspars are augened; elsewhere fabrics are massive but generally the granite is foliated. The foliation is locally folded and the augen themselves may be bent. Unit 7a may be folded on a kilometre scale. Mylonite and narrow ultramylonite zones occur within augen gneisses and related flattened granitoid rocks (e.g. Fig. 36.3, Heywood and Schau, 1981).

The northern contact of the fault zone is jagged. Foliations change along strike from east to east-northeast-trending and become less pronounced. Within the zone the east-northeast trends locally cut the east-west trends. Elsewhere, one or the other foliation is developed. There is abundant evidence, such as minor folds with different orientations and folded foliated metagabbro dykes which were emplaced along an earlier foliation, that the zone has endured several episodes of movement.

For example, east of the map area (in 56 C/4) the Chesterfield Fault Zone is apparently cut by a plutonic complex which has yielded an Rb-Sr errorchron of 2400-2500 Ma. Movement along this part of the zone may be latest Archean in age. On the other hand, mafic stocks (unit 8c) were deformed in the zone about 1900 Ma, indicating that the late local movement occurred just prior to the deposition of Dubawnt Group.

Unit 8 (mafic stocks and dykes)

Unit 8 consists of mafic dyke sets and stocks. In the north, northeast-trending metadiabase dykes (unit 8a), tens of metres wide, cut Tehek Lake plutonic complex.

On the Bowell Islands, east-trending metadiabase dykes (unit 8b), metres thick, form a swarm (Bowell Islands basic dyke swarm) parallel to the eastward projection of Baker Lake. The dykes cut across the Kramanituar complex and associated faults and are unconformably overlain by the Dubawnt Group.

Metagabbro stocks are emplaced in the Ingilik Point gneiss complex and in the Kramanituar complex. The Dubawnt Group rests unconformably upon one such stock.

Unit 9 (quartz syenite stocks)

Unit 9 consists of small, massive, locally hornblende-bearing, biotite-rich, syenite or quartz syenite stocks. They vary in grain size and colour index ranging from mesocratic and medium grained to melanocratic and coarse grained. The stocks are heterogeneous and show pronounced changes in mineralogy and grain size over short distances.

The syenites are intruded into sheared and foliated granites and gneisses and they cut reverse faults. They are invaded by pegmatites and apophyses of late massive orange-weathering granite. They may be correlated with similar rocks from the Amer Lake region dated at 1849 Ma (U-Pb, zircon, Heywood and Schau, 1981) or they may be a variant of the Martell Syenite of the Dubawnt Group.

Unit 10 (Dubawnt Group)

The Dubawnt Group underlies the area south of Baker Lake and also occurs as small outliers along the north shore of the lake. The Dubawnt Group has been subdivided into a number of formations (Donaldson, 1965; Blake, 1980).

There are nomenclatural problems regarding the assignment of rocks to formations within the Dubawnt Group. Although lithologies are distinct and the terrestrial model of deposition with intermittent volcanism is generally agreed upon, the difficulty centres on where to draw formational boundaries. Some volcanogenic arkoses and mudstones assigned to the Kazan Formation by Donaldson (1965) were reassigned to the Christopher Island Formation by Blake (1980). The mudstones are here informally referred to as the Red Point mudstones in an effort to reduce the confusion. Volcanogenic rocks of Christopher Island Formation exposed south of Lofthouse Point appear to underlie Kazan arkose, although outcrops are sufficiently scarce that faults can be drawn to eliminate this apparent anomaly. Similarly, lenses of conglomerate resembling South Channel conglomerate occur within the Kazan arkoses on Rio Island, for example.

The units used in Figure 25.1 are South Channel conglomerate (unit 10a), Kazan arkose (unit 10b) and Red Point mudstones (unit 10c), Christopher Island volcanic rocks (unit 10d), Martell Syenite (unit 10e) and Thelon sandstones (unit 10f).

Unit 10a South Channel Conglomerates: In the map area the South Channel conglomerates are basal conglomerates that occur in the northeast corner of Baker Lake, on the west coast of Bowell Island, west of Severn Point, and on a small peninsula of Christopher Island.

It is a poorly sorted, closely packed, polymictic conglomerate with subangular, boulder to pebble sized clasts of granulites, anorthosites, granitoid gneisses, granites, and quartz veins set in medium arkosic matrix. Descriptions of the unit are available in Donaldson (1965, 1967), Macey (1973), Schau and Hulbert (1977), Blake (1980), Miller (1980). It rests unconformably on the basement and is cut by igneous rocks of the Christopher Island volcanics. It grades into the Kazan arkose.

Unit 10b Kazan Arkoses: In the map area pink arkoses of the Kazan underlie the area between the Kazan and Clearwater rivers south of the lake, and in small outliers in the northeast corner of Baker Lake.

The arkose is mainly pink, medium grained, moderately sorted, well indurated, well-bedded and shows granitic clasts, crossbedding, and ripple marks, and local conglomerate lenses with granitic clasts. The unit is described in the publications previously cited for the South Channel conglomerates.

The Kazan arkose grades into the Red Point mudstone near the mouth of the Clearwater River, and is cut by Martell Syenites, lamprophyre dykes and diatremes of the Christopher Island volcanics.

Unit 10c Red Point Mudstone: Red Point mudstone is best displayed on Red Point on an unnamed island north of Christopher Island and on Christopher Island, but it occurs south of the lake as well. This is a new informal unit. The mudstone is very fine grained, deep red to maroon, poorly bedded unit with thin lenticles of volcanogenic sandstones. The outcrop pattern on Christopher Island indicates the mudstone occupies the core of southwest plunging anticline.

The mudstone overlie the Kazan arkoses, are intruded by the Martell Syenites and lamprophyres and diatremes of the Christopher Island volcanics. They may contain lenses of volcanogenic arenites and/or tuffs assignable to the Chrisopher Island volcanics.

Unit 10d Christopher Island volcanics: In the map area Christopher Island volcanics occur in irregular patches on Rio Island, Christopher Island, near Lofthouse Point, and south of Gull Lake.

The Christopher Island volcanics consist of mafic trachyte flows and volcanic fragmental units including vent breccias, lahars, airfall tuffs, and locally, rhyolite cumulo-domes.

The petrology and petrochemistry of the Christopher Island volcanics has been discussed by Blake (1980). On Rio Island the transition from Martell Syenite to volcanic breccia (a pyroclastic debris flow?) was seen to be interbedded with pink feldspathic sandstones. Apparently at least one Martell Syenite laccolith was a magma chamber for a small Christopher Island volcano. Diatremes are common and probably in part represent phreatomagmatic eruptions. The Christopher Island volcanics overlie, interfinger, or are interbedded with Red Point mudstone and possibly Kazan arkose. They are cut by or grade into Martell syenite.

Unit 10e Martell Syenites and related(?) mafic dykes: Martell Syenites form small stocks in the southern part of the map area. They are generally laccolithic when emplaced in sediments and often only the lower intrusive contact can be seen. They form stocks with irregular form when emplaced in the basement. They consist of medium grained porphyritic rocks with phenocrysts of biotite, K-feldspar or pyroxene set in feldspathic matrix.

The Martell Syenites may possibly be correlated with the quartz syenites (unit 8). This possibility can be tested by comparing the concentrations of trace elements such as Ba and Cr in the two intrusive suites.

Some lamprophyre dykes strike into Martell Syenites and may be directly linked with the syenites. Other lamprophyres and feldspar pyroxene porphyry dykes do not resemble the syenites and presumably belong to separate swarms. Feldspar pyroxene dykes are emplaced along the northern shore of Baker Lake.

Unit 10f Thelon Sandstone: The Thelon sandstone underlies the southwest part of the map area and small outliers occur as far north and east as Jigging Point.

The Thelon sandstone in the area is a series of red to beige conglomerates with white quartz cobbles and well-bedded, poorly sorted beige to mauve sandstones in which quartz is the main clastic component. The matrix is rich in kaolin. It also contains detrital hematite cobbles and Cecile (1973) has reported the presence of a matrix mineral resembling goyazite. The unit has been described by Cecile (1973) as well as Donaldson (1967).

On Jigging Point a basal conglomerate and sandstones are seen to rest unconformably on a granite (unit 6a) which has undergone argillitic alteration of feldspars and a change in colour from pink to beige up to a hundred metres below the unconformity. Beneath the unconformity north of Ingilik Point sheared rocks of the Ingilik Point gneiss complex are deep red due to hematite staining (Heywood and Schau, 1981, Fig. 36.5).

Unit 11 (late granite)

Unit 11 is found mainly in the eastern part of the map area. It consists of an orange-weathering, medium to fine grained biotite granite which is massive and jointed and which weathers to form blocky terrains. The unit carries magnetite, accessory sphene, and allanite. The contacts of unit 11 are irregular; shallow dipping granite dykes increase in abundance towards the stocks and related biotite pegmatites are widely dispersed.

Unit 11 cuts all units north of and including the Chesterfield Fault Zone, except unit 12, with which it is not in contact.

Unit 12 ("Mackenzie Swarm" Diabase)

Northwest-trending, fresh, brown-weathering diabase dykes a few metres thick have been attributed to the Mackenzie swarm because of their lithology, freshness and structural trend. They are seen on Bowell Island, Christopher Island and in the northern part of the area west of Quoich River. They do not have a characteristic magnetic signature, perhaps since they are much narrower than the dykes in neighbouring regions.

Special Topics

Low-angle Faults

The northern edge of the Akutauak River gneiss complex is locally a shallow-dipping reverse fault. It is well displayed in both the east and west half of the area. A sketch map of an area in the west half (Fig. 36.2, Heywood and Schau, 1981) and the sketch map from east of Quoich River (Fig. 25.2) both show relatively flat-lying, gently folded sheets of gneissic granodiorite resting upon folded rocks of the Ketyet River group. It is assumed that the sheets travelled northwestward onto the Ketyet River group. The sheets can be considered thrusts.

The timing of this low-angle faulting is difficult to establish. The fault slices are cut by quartz syenite stocks. The flat foliation of the Akutuak gneiss complex postdates the Tehek Lake plutonic complex but is cut by the Chesterfield Fault Zone whose movements range in age from late Archean to Middle Proterozoic.

Mylonites at Curves in the Chesterfield Fault Zone

Thin mylonite belts are developed in the Chesterfield Fault Zone. A sketch map of a spectacular outcrop was shown last year (Fig. 36.3 in Heywood and Schau, 1981). Upon tracing this mylonite zone it became apparent that this zone is curved and that the mylonite is widest and nearly aphanitic at the bend (Fig. 25.3).

Baker Lake Cataclasite Zone

A west-northwest-trending zone, several tens of kilometres across, in which northwest- and west-trending steep faults with dextral separation and a curved trace have been developed, crosses the map area from Severn Point to just south of Whitehills Lake. Gouge and cataclasites are well displayed in many outcrops of the faults and the faults are generally extensively hematitized.

The gross movement of the fault zone, based on separation, would appear to be dextral. A few subhorizontal slickensides support this. The fault blocks may have been rotated with respect to each other as well. Paleomagnetic data (Park et al., 1973) suggest that magnetic fabric in the Dubawnt Group on either side is rotated with respect to each other (Fig. 25.4). This hypothesis, which needs additional testing, does not specify which side is the least rotated. Steep dips, up to 50°, in the Thelon sandstone also suggest that rotation may have occurred (Fig. 25.4).

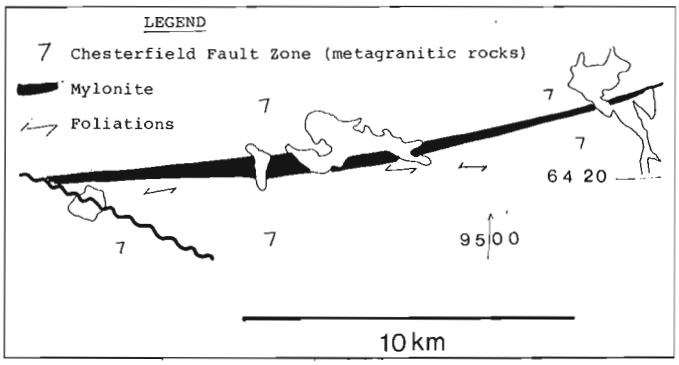

Figure 25.3. Sketch map showing bent zone of mylonite development cut by a strand of the Baker Lake cataclasite zone to the west. Note the increased thickness at bend. Figure 36.3 of Heywood and Schau (1981) is of the area west of large central lake showing best development of zone.

The age of the cataclasite zone postdates the Thelon sandstone and predates the emplacement of a Mackenzie dyke.

Correlations and Speculations

1. The Ketyet River group is probably equivalent with the "Woodburn Group" (Ashton, 1981, 1982) and both are probably equivalent to the Archean Prince Albert Group (Schau, 1977, in press).
2. The thrusts in the Baker Lake map area are part of a regional pattern of northwest transport.
3. The Kramanituar complex outlier rests upon shallow north-dipping mylonite (Fig. 25.5) and the main outcrop also rests in fault contact upon Ingilik Point gneisses. Is it possible that these lower crustal rocks have been elevated to their current position by the same regional compression as mentioned above in point (2).
4. The Chesterfield Fault Zone is a zone of considerable jostling but, since mylonites are curved and some units (biotite-bearing porphyritic granite of Tehek Lake plutonic complex and biotite-bearing porphyritic granite of the Ingilik Point gneiss complex) resemble each other across the fault zone, it is thought that only little transcurrent movement has occurred along it.
5. The Chesterfield Fault Zone was apparently not the fault scarp which supplied the sediments for the Dubawnt Group, as shown by Donaldson's (1965) study of paleocurrents. Since the fault does limit the northward appearance of Dubawnt sedimentary rocks, it probably played some part in the development of the sedimentary basin into which the Dubawnt sedimentary rocks were dumped. The Thelon sandstones were deposited unconformably on rocks of the fault zone, indicating that no topographic feature marked it at this time. This is borne out by the clastic debris in the basal Thelon sandstones which consists largely of quartz pebbles that are not locally derived.

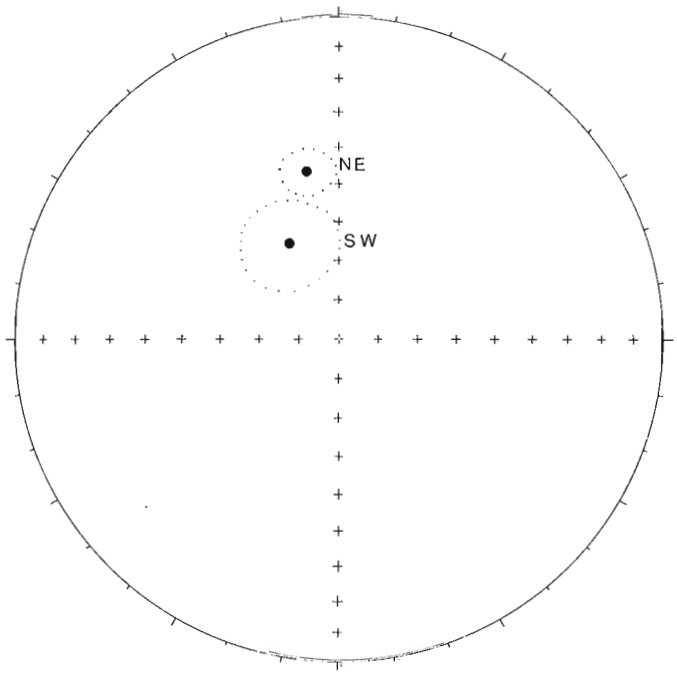

Figure 25.4. Stereogram showing stable remanent declination and inclination and α_{95} of cleaned samples from northeast and southwest of Baker Lake Cataclasite Zone. Data from Park et al. (1973). The original data set had been "corrected" for bedding so that only the fact there is a difference between the two vectors is significant.

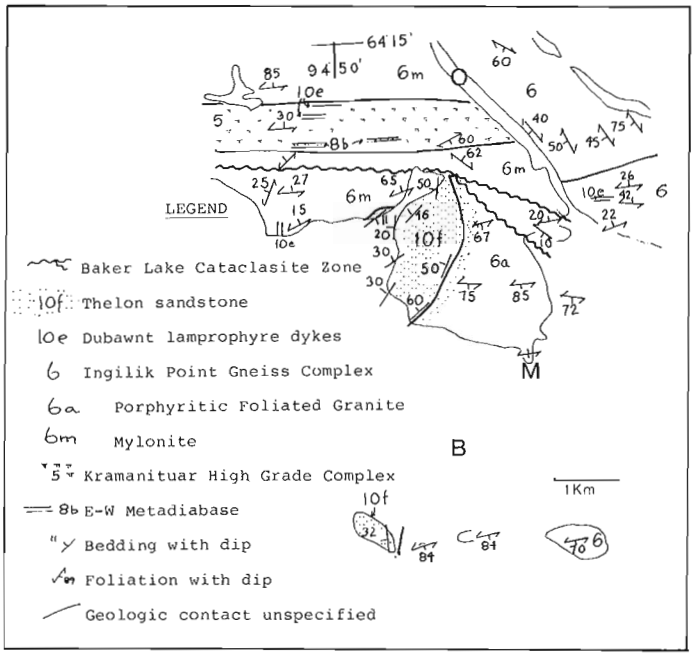

Figure 25.5. *Sketch map shows tilted Thelon sandstone, zone of flat foliations which dip under Kramanituar complex and the Dubawnt dykes which cut the shallow foliations, the high grade complex, and the mylonite zone to the north. The tilting of the Thelon sandstone along a branch of the Baker Lake cataclasite zone is a much younger event than the tectonic emplacement of the Kramanituar complex which predated the Dubawnt Group. Dotted pattern indicates regolith developed in granite of the Ingilik Point gneiss complex beneath the Thelon unconformity.*

6. Alteration of the Dubawnt Group is ubiquitous and is the result of many different processes which have affected the rocks variably. Cecile (1973), Macey (1973), Miller (1980) and Blake (1980) have detailed the changes within the group. The postdepositional changes probably explain the range in radiometric dates reported from the group. It is not yet clear when the various formations of the Dubawnt Group were deposited.

Mineral Occurrences

The southern region contains a number of uranium showings described in detail by Miller (1980). Showings in the southeast corner were discussed by Schau and Hulbert (1977) and Schau and Ashton (1979). Showings in the west half were discussed by Heywood and Schau (1981). Mineral occurrences noted this year (see Fig. 25.1, Table 25.2) include (1) sparse molybdenite in quartz veins with pyrite in foliated granite on a small island southeast of Jigging Point; (2) sparse molybdenite and scheelite in biotite pegmatites in metasediments in the central western portion; (3) pyrrhotite layers in metasediments at the same locality as (2); (4) oxide iron formation west of the Quoich River; and (5) galena in gossans in quartzose metasediments along the Quoich River (Roscoe, personal communication, 1981).

Industrial minerals include soapstone (6) northwest of Jigging Point, potential granite building stone (7), and gravel from the Thelon Formation (8).

Table 25.2

Mineral Localities	(UTMS Zone 15W)	
1. Molybdenite	7119800	419000
2. Molybdenite, scheelite	7170000	384500
3. Pyrrhotite	7170050	384550
4. Iron formation	7186000	402000
5. Galena	7177000	415000
6. Soapstone (occasional pit)	7124500	406500
7. Building stone	4143300	435000
8. Gravel (commercial pit)	7136000	353000

Acknowledgments

The authors thank Brigitte Bilodeau, Cathy Caldwell, Jonathan Phillips, John Robins, juniors; Janien Schwarz, cook; Al King and Michel Plourde, pilots; Seigo Takamuchi and Ken Codd, apprentice engineers, for their efforts this summer. The camp by Ingilik Point was moved in by skidoo and bombardier, and functioned from last snow on June 17 to the first snow on August 29. Break-up on Baker Lake was July 17-19. We also thank our colleagues J.A. Fraser and W.W. Heywood for help with logistics, and W.F. Fahrig and K. Christie for discussions regarding paleomagnetic data.

References

Ashton, K.E.
1981; Preliminary report on Geological Studies of the "Woodburn Lake Group" northwest of Tehek Lake, District of Keewatin; in Current Research, Part A, Geological Survey of Canada, Paper 81-1A, p. 269-274.

1982: Further geological studies of the "Woodburn Lake Group" northwest of Tehek Lake, District of Keewatin; in Current Research, Part A, Geological Survey of Canada, Paper 82-1A, report 26.

Blake, D.H.
1980: Volcanic rocks of the Paleohelikian Dubawnt Group in the Baker Lake Angikuni Lake area, District of Keewatin, N.W.T.; Geological Survey of Canada, Bulletin 309, 39 p.

Cecile, M.P.
1973: Lithofacies Analysis of the Proterozoic Thelon Formation, Northwest Territories (including computer analysis of field data); unpublished M.Sc. thesis, Carleton University, Ottawa, 119 p.

Donaldson, J.A.
1965: The Dubawnt Group, Districts of Keewatin and Mackenzie; Geological Survey of Canada, Paper 64-20.

1967: Two Proterozoic clastic sequences: A sedimentological comparison; Geological Association of Canada, Proceedings, v. 18, p. 33-54.

Heywood, W.W. and Schau, Mikkel
1981: Geology of Baker Lake Region, District of Keewatin; in Current Research, Part A, Geological Survey of Canada, Paper 81-1A, p. 259-264.

Macey, G.
1973: A Sedimentological Comparison of two Proterozoic Redbed successions (The South Channel and Kazan Formations of Baker Lake, N.W.T.) and the Martin Formation at Uranium City, Saskatchewan; unpublished M.Sc. thesis, Carleton University, Ottawa, 176 p.

Miller, A.R.
1980: Uranium Geology of the Eastern Baker Lake Basin, District of Keewatin, Northwest Territories; Geological Survey of Canada, Bulletin 330, 63 p.

Nadeau, L.
1981; The geology of Whitehills Lake map area, District of Keewatin; in Current Research, Part A, Geological Survey of Canada, Paper 81-1A, p. 265-268.

Park, J.K., Irving, E., and Donaldson, J.A.
1973: Paleomagnetism of the Precambrian Dubawnt Group; Geological Society of America Bulletin, v. 84, p. 859-870.

Schau, Mikkel
1977: Komatiites and quartzites in the Archean Prince Albert Group; in Volcanic Regimes in Canada, W.R.A. Baragar, L.S. Coleman and J.M. Hall, ed., Geological Association of Canada, Special Publication 16, p. 341-354.

1980a: Zircon ages from a granulite-anorthosite complex and a layered gneiss complex northeast of Baker Lake, District of Keewatin; in Loveridge, W.D., Rubidium-Strontium and Uranium-Lead Isotopic Age Studies, Report 3; in Current Research, Part C, Geological Survey of Canada, Paper 80-1C, p. 237-238.

Schau, Mikkel (cont.)
1980b: Geological History of Anorthosites and Granulites at the edge of the Armit Lake Block, northern Churchill Structural Province, Canada (abstract); Geological Association of Canada, Abstracts with Program, v. 5, p. 79.

Geology of the Prince Albert Group in parts of Walker Lake and Laughland Lake map areas; Geological Survey of Canada, Bulletin 337. (in press)

Schau, Mikkel and Ashton, K.E.
1979: Granulite and plutonic complexes northeast of Baker Lake, District of Keewatin; in Current Research, Part A, Geological Survey of Canada, Paper 79-1A, p. 311-316.

1980: Geological map of the granulite and anorthosite complex at the southeast end of Baker Lake, 56D1, 56C4, parts of 55M16 and 55N13; Geological Survey of Canada, Open File 712.

Schau, Mikkel and Hulbert, L.
1977: Granulites, anorthosites and cover rocks northeast of Baker Lake, District of Keewatin; in Report of Activites, Geological Survey of Canada, Paper 77-1A, p. 399-407.

Wright, G.M.
1967: Geology of the southeastern Barren Grounds. Parts of the Districts of Mackenzie and Keewatin; Geological Survey of Canada, Memoir 350.

FURTHER GEOLOGICAL STUDIES OF THE 'WOODBURN LAKE GROUP' NORTHWEST OF TEHEK LAKE, DISTRICT OF KEEWATIN

Contract 1147919

K.E. Ashton[1]
Precambrian Geology Division

Ashton, K.E., Further geological studies of the 'Woodburn Lake Group' northwest of Tehek Lake, District of Keewatin; in Current Research, Part A, Geological Survey of Canada, Paper 82-1A, p. 151-157, 1982.

Abstract

In the southeast corner of the Amer Lake map area, the 'Woodburn Lake Group' is exposed in several northeast-trending belts of metavolcanic and metasedimentary rocks. Metamorphosed felsic tuffs and rhyolites exposed in the core of an overturned anticline west of Pipedream Lake are thought to be the oldest metavolcanic rocks within a sequence which passes stratigraphically upwards into komatiites, felsic to intermediate metavolcanic rocks and metasediments including abundant volcaniclastic rocks, banded iron formation and greywacke. Early gabbroic sills and dykelets intrude the metavolcanic sequence.

Several bands of locally conglomeratic quartzite of uncertain age are exposed in the eastern and northwestern parts of the area. The quartzites are generally recrystallized and primary features have been preserved in only a few localities. Crossbedding in the best-preserved quartzites in the northwest corner of the study area indicates that at least part of the sequence has been locally overturned. Isoclinal folds were also observed in the northwestern quartzites.

The supracrustal rocks have been affected by two episodes of granitic intrusion. A foliated, cataclastic granodiorite underlies much of the northern part of the area. It is fault-bounded to the south, but inclusions of mafic rocks and quartzite suggest that it is younger than the supracrustal rocks. Late, massive, coarse grained granites are common throughout the study area. Many of these are characterized by margins containing locally deformed and migmatitic, granitoid and gabbroic intrusive rocks. Several deformed gabbro plutons are spatially associated with the late granites and may be co-magmatic. The age relationships of a few relatively small, undeformed gabbros is unclear. Late biotite porphyry dykes represent the last recognizable igneous activity.

Early isoclinal folds, observed in the metavolcanic rocks plunge northeastward and are overturned to the northwest. Subsequent low-angle faulting is suggested by cataclasis of gently-dipping granitic rocks. Late, southeast-plunging kink folds and high-angle faults have also affected the area.

Most contacts between the quartzites and metavolcanic rocks are characterized by sheared chlorite schists, probably indicating the presence of low-angle faults. However, quartzite pebbles in metasedimentary rocks which appear to pass conformably into the metavolcanic sequence suggest that the quartzites may be the oldest rocks exposed in the study area.

Introduction

Geological mapping of the southeast corner of the Amer Lake map area (66 H/1), 80 km north of Baker Lake, Northwest Territories, was completed during the summer of 1981. The work was carried out under contract with the Geological Survey of Canada and represents the second half of a project designed to systematically map and determine the geological history of an area containing an unusual association of metavolcanic rocks and quartzites. The project was suggested by W.W. Heywood as a follow-up to the reconnaissance-scale mapping of the southern half of the Amer Lake map area in 1978. At that time it was noticed that the metavolcanic sequence had a great deal in common with rocks of the Archean Prince Albert Group which outcrops far to the northeast in the vicinity of Laughland Lake. Although quartzite is also common in the Prince Albert Group, it was thought that the quartzite in the study area was more likely correlative with the Aphebian(?) Hurwitz Group which outcrops southeast of Baker Lake or the Aphebian(?) Amer group which has been described from just north of the study area. The uncertainty in the relative age of the quartzite has been the focal point of this study.

The author's understanding of the geology of the area has benefited greatly from numerous discussions with Mikkel Schau, H. Helmstaedt, W.W. Heywood and I. Annesley. Assistance in the field was ably provided by D. Harding. The author would also like to thank Joan Scottie for very kindly providing the last and only means of leaving the field at the end of the summer, and expediters Liz and Boris Kotelewetz whose patience and hospitality in Baker Lake were greatly appreciated. This report has had the benefit of critical reviews by Mikkel Schau, S. Tella and P. Lee.

General Geology

The geology of the "Woodburn Lake Group" has been briefly described previously (Ashton, 1981). The supracrustal rocks of the "Woodburn Lake Group" can be divided into two major lithological groups – the metavolcanic and related metasedimentary rocks, and the quartzites. The metavolcanic rocks (unit 1) are dominated by felsic to intermediate tuffs, flows and shallow intrusive rocks. Ultramafic rocks (unit 1a), some of which are spinifex-textured and polyhedrally-jointed, are common in the central part of the area (Fig. 26.1). By contrast, mafic metavolcanic rocks are much more restricted in occurrence. Those observed are highly deformed and contain few recognizable primary features. Fine- to medium-grained metagabbroic rocks are locally common as sills and dykelets throughout the metavolcanic rocks.

[1] Department of Geological Sciences, Queen's University, Kingston, Ontario

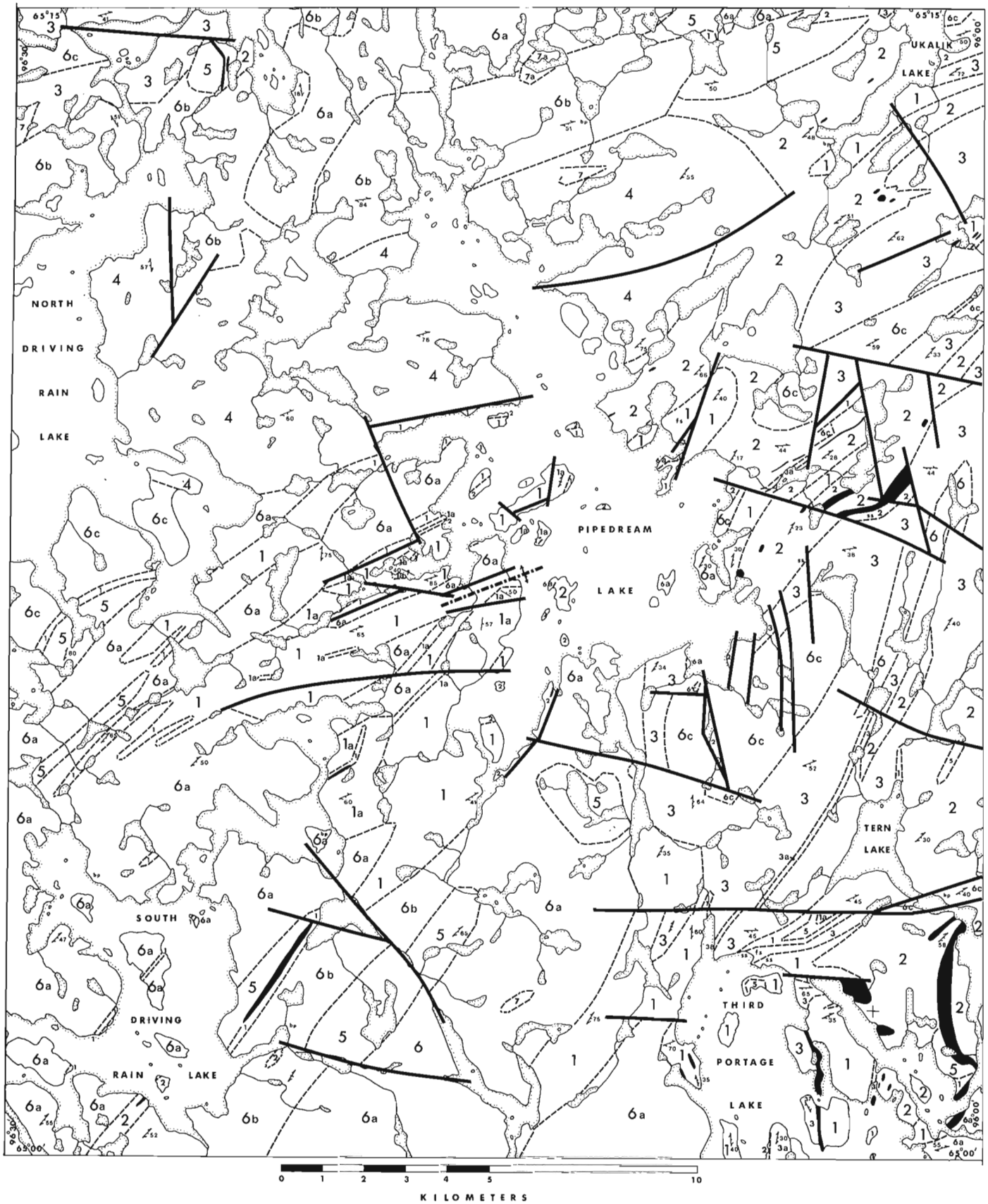

Figure 26.1. *Geological map of the southeast corner of the Amer Lake map area. All lake names which appear on the map are informal and were included only to facilitate discussion of the geology.*

Legend for Figure 26.1

7 "Late" Mafic to Ultramafic Intrusive Rocks: 7a, peridotite

6 Late Granitic Rocks: 6a, massive granite; 6b, granite margins; 6c, cataclastic granite

5 "Early" Mafic Intrusive Rocks

4 Foliated Granodiorite

3 Quartzite: 3a, phyllite

2 Metasedimentary Rocks (iron formation blacked in)

1 Metavolcanic Rocks: 1a, ultramafic rocks

bp Biotite Porphyry

cs Sheared Chlorite schist

fs Cr-Muscovite

—— Lithological Contact

▬ Fault

Anticline

Bedding (horizontal; inclined; overturned)

Schistosity (vertical; inclined)

Metasediments (unit 2) consisting of banded greywackes, chlorite schists, fragmental rocks and chemical precipitates, including iron formation and chert, conformably overlie the metavolcanic rocks. Relatively massive arkosic wackes are spatially associated with the volcanogenic metasediments and are believed to be derived from the volcanic rocks.

Two major bands of quartzite (unit 3) extend from the east-central part of the study area northeast to the boundary with the Woodburn Lake map area to the east (Fig. 26.1). Several smaller bands of similar quartzite are also present on the west shore of Ukalik Lake and north of North Driving Rain Lake. Most of the quartzites are white, fine grained and recrystallized to the extent that rocks exhibiting bedding and other primary features are rare. Outcrop-scale variations in grain size are present, however, and conglomeratic horizons consisting of quartzite pebbles in a quartzite matrix have also been recognized. White micas are ubiquitous in the quartzites, locally forming quartz-white mica schists. Green Cr-muscovite is also common in trace quantities. Black, phyllitic schists occur as thin layers and lenses within both large bands of quartzite.

A large, strongly foliated, cataclastic granodiorite pluton (unit 4) underlies much of the northern half of the area. Its age relationships are uncertain, but inclusions of fine grained mafic rocks and quartzite suggest that the granodiorite postdates the supracrustal rocks.

The last major igneous activity in the area resulted in the intrusion of several granitic plutons (unit 6). The largest of these are commonly rimmed by migmatitic to agmatitic margins containing a range of intermediate intrusive rock types. In some places individual pluton margins and entire 'sheets' of granitic rocks are characterized by strong shearing and cataclasis. By contrast, the cores of these large plutons are generally homogeneous and contain relatively undeformed, coarse grained granites. Many smaller granitic intrusions are common around the central part of Pipedream Lake (Fig. 26.1). The large number of these apparent cupolas, together with the presence of numerous northeast-trending metavolcanic and metagabbroic roof pendants, may suggest that the southwest Pipedream Lake area represents the exposed roof of a large granitic pluton.

Several ages of metagabbroic rocks are thought to be present in the area. Apart from those associated with the volcanic rocks, there are several small plutons which appear to be related to the late granitic rocks. Although some of these have clearly been granitized and therefore predate the late granites, others outcrop as massive, polyphase intrusions which appear to postdate granite emplacement.

Late, undeformed and randomly-oriented biotite porphyry dykes crosscut rocks of the metavolcanic sequence and some late granites.

Numerous low-angle faults and shear zones which trend subparallel to the structural fabric in the region, are recognized by extensive 'sheets' and thin 'slices' of highly sheared granitic rocks, gently-dipping chlorite schists at structural discontinuities and a number of other consistent, small-scale features.

Metavolcanic Rocks

Metavolcanic rocks outcrop in two major northeast-trending belts and as several smaller outliers (Fig. 26.1). Felsic to intermediate tuffs, flows and shallow intrusive rocks appear to be the oldest metavolcanic rocks based on crosscutting relationships displayed by ultramafic dykes associated with younger komatiites. The felsic volcanic rocks are mainly porphyritic rhyolites containing up to 20 per cent blue quartz and/or white feldspar phenocrysts in a massive to locally layered white to pink, aphanitic matrix. Layered, fine grained, grey-green, intermediate tuffs and flows are associated with the rhyolites.

Dark green to rusty-brown, fine grained ultramafic rocks are common in the region around southwest Pipedream Lake (Fig. 26.1). Most are strongly deformed but surprisingly well-preserved komatiites display primary layering, spinifex textures and polyhedral jointing outcrop at several localities. Individual flows are 2-3 m thick and consist of a dark green to brown, spinifex-textured layer and a brown, fine- to medium-grained, massive layer. Within the spinifex-textured zones, the decreasing size of elongate grains towards the top of the flow has been used to establish the stratigraphic top. The few localities at which top determinations can be made have been used to define a tight anticline overturned to the northwest and plunging northeastwards into Pipedream Lake. A dyke of altered ultramafic rocks crosscuts intermediate tuffs near the west shore of Pipedream Lake, further indicating the stratigraphic top within the metavolcanic sequence. Thin sections of the ultramafic rocks show that they mainly consist of tremolite, chlorite and opaque minerals. Serpentine is abundant in the most altered samples.

The komatiites are locally overlain by a sequence passing stratigraphically upwards from felsic metavolcanic rocks to a thin band of layered volcanogenic metasediments and finally into a second sequence of felsic to intermediate metavolcanic rocks.

Mafic metavolcanic rocks are not common in the area and those observed tend to be poorly preserved.

A cursory petrographic study of the metavolcanic rocks indicates that they are made up of various proportions of actinolite, epidote, biotite, chlorite, white mica, carbonate, quartz and feldspar.

Metasedimentary Rocks

The metavolcanic rocks are conformably overlain by a sequence of volcanogenic metasediments including greywacke, felsic mica schists, volcaniclastic rocks and chemical precipitates consisting of oxide facies iron formation and chert. Primary features are only locally preserved. Graded bedding was recognized on wave washed outcrops of banded tuffs and associated metasediments along the southern shore of Pipedream Lake and can be used to show that tops are to the southeast. A relatively undeformed volcanic breccia containing fragments up to 30 cm in a matrix of iron formation and greywacke is also exposed near the southern end of Pipedream Lake.

Iron formation occurs as several bands within thinly-layered volcanogenic metasediments. Typical samples consist of laminated magnetite, chert and chlorite, but grunerite and pyrite are also present in some areas.

Most of the remaining rocks classified as metasedimentary are massive chlorite-quartz-feldspar schists. Although clastic textures can be seen in some samples, it is likely that minor amounts of sheared metavolcanic and granitic rocks have also been included.

Poorly-layered to massive greywacke is common in the belt of predominantly metasedimentary rocks between Pipedream Lake and Ukalik Lake. The greywackes weather orangy brown to green and generally exhibit a good clastic texture. Rounded blue quartz and white feldspar grains are abundant in the fine grained chlorite-white mica matrix.

At the quartzite-metasediment contact south of Ukalik Lake (Fig. 26.1), the greywacke is very sheared and contains thin calcareous horizons and iron formation. The greywacke also contains abundant, flattened quartzite pebbles adjacent to the contact and looks very similar to a wave washed outcrop observed on the shore of Third Portage Lake where quartzite pebbles occur within quartzites and greywackes (Ashton, 1981).

Quartzite

Two wide, northeast-trending bands of quartzite and several smaller outliers were mapped (Fig. 26.1). The quartzite tends to be more resistant than the surrounding rocks and outcrops as high ridges and plateaus. Although most of these rocks have been recrystallized, textures and the original grain size can be recognized in some coarse sands and conglomerates. Pebbles within the quartzite conglomerates are invariably quartzites. The rocks generally weather white but quartzites rich in white mica are buff-coloured. The mica-rich horizons are common and can vary in thickness from a few centimetres to tens of metres. It is not known whether these schists represent clay-rich horizons or zones of late shearing. Green chromian(?) mica is present in trace quantities throughout the quartzites. Kyanite, zircon, tourmaline, feldspar and opaque minerals have also been noted during petrographic examinations.

Bedding has been recognized at very few localities. One good wavewashed outcrop on southeast Pipedream Lake exhibits thin, dark-coloured laminae which define tight, isoclinal folds in bedding. Crossbedding in the less deformed, northwestern quartzite indicates that tops there are to the northwest.

Two structural fabrics are common to most of the quartzites. A strong cleavage defines outcrop topography and is parallel to bands of quartz-white mica schist within the quartzite, major contacts with the supracrustal rocks and the regional fabric. The other fabric is a strong, pervasive mica schistosity. Both fabrics dip gently to moderately to the southeast but the schistosity tends to strike more easterly and dip at slightly steeper angles than the cleavage. Kink folding has affected both fabrics but neither exhibits the tight isoclinal folds characteristic of the bedding on the shore of Pipedream Lake.

A dark grey, phyllitic rock is common at two localities. Within the quartzite in the southeast corner of the area, a thin, continuous band of phyllites has been traced. However, directly south of Ukalik Lake, the phyllite in the northeastern band of quartzite occurs only as discontinuous layers and lenses. A petrographic study of the southern phyllites revealed that they are chloritoid-chlorite-white mica-quartz ± kyanite ± feldspar schists.

Foliated Granodiorite

A large, foliated, cataclastic granodiorite pluton underlies much of the northern portion of the study area but is poorly-exposed in felsenmeer-like topography. The pluton is homogeneous and medium grained with only minor variations in the degree of cataclasis and colour. Fresh rocks are grey but the majority of samples weather red. The granodiorite is believed to postdate the supracrustal rocks since it contains inclusions of fine grained mafic rocks and quartzites. To the north, the granodiorite is intruded by a marginal phase of the late granite. Both rock types are strongly foliated and locally cataclastic there, making it difficult to distinguish between rocks of the two plutons.

Mafic to Ultramafic Intrusive Rocks

Small plutons of gabbroic rocks are common in the area. Most are medium grained, hornblende-plagioclase rocks which have been locally deformed and altered into amphibole-chlorite schists. There appear to be two ages of gabbroic rocks which postdate the early gabbroic sills and dykelets associated with the metavolcanic rocks. One set of gabbroic plutons has clearly been emplaced prior to the intrusion of the late granites. Microcline porphyroblasts are found in many of the 'old' gabbros adjacent to granite contacts and inclusions of fine grained gabbroic rocks are common in the migmatitic to agmatitic margins of some granites. The 'younger' set of gabbros is similar but shows no obvious effects of granite emplacement. Further, they tend to be polyphase with fine grained diabase, medium grained gabbro and gabbroic pegmatite all present in the same pluton. One small ultramafic body outcrops near the northern map boundary. It is also thought to be related to the 'later' intrusive phase.

Late Granitic Rocks

Late granitic rocks occur as several large plutons and numerous small cupolas. The large plutons north and south of Pipedream Lake (Fig. 26.1) are mainly massive, homogeneous, coarse grained granites but are partially rimmed by highly deformed migmatitic rocks. These margins typically contain abundant, fine- to medium-grained mafic inclusions in locally-gneissic granitic to intermediate intrusive rocks. Intrusive relationships between phases are uncommon but those observed consistently indicate that the most felsic phases were emplaced last. By contrast, the pluton cores are generally homogeneous, coarse grained granites distinguished by about 30 per cent blue quartz and only about 3 per cent chloritized biotite. Minor amounts of aplite are common locally but are never extensive enough to be mappable.

The western margin of the southern Pipedream Lake granite is strongly cataclastic, becoming progressively less deformed towards the interior of the pluton. This deformation, coupled with the moderate southeast dip of the underlying volcanogenic metasediments to the west, suggests that the contact is a low-angle fault (Fig. 26.2). The intense deformation associated with this type of faulting might help to explain the relatively sharp transition from nearly massive granite to migmatitic rocks at some pluton margins.

The South Driving Rain Lake pluton is somewhat different from the others in that it contains numerous roof pendants and has many small cupolas associated with it. The lithological similarity of the granites within the three main plutons led to the initial interpretation that all were parts of a large batholith with the South Driving Rain Lake pluton representing the top. However, the recognition of low-angle faulting in the area points out the need for further study before this assumption can be made.

The granitic pluton southeast of Pipedream Lake also appears similar to the others in the few undeformed localities observed. It is clear, however, that it has undergone far more extensive cataclasis than the others, resulting in more widespread deformation. The rocks typically weather red and are much finer grained than the granites previously described. This trend is the same for most of the small bodies of granite in the eastern portion and far northwestern corner of the map area. They consist of predominantly sheared, cataclastic rocks which are locally difficult to recognize as ever having been granitic. As well as entire sheets of these rocks, such as outcrops in the pluton south of Ukalik Lake, there are numerous thin "slices" of cataclasite too small to map. These rocks presumably have been involved in the low-angle faulting and have therefore been used to mark the sites of individual faults (Fig. 26.1).

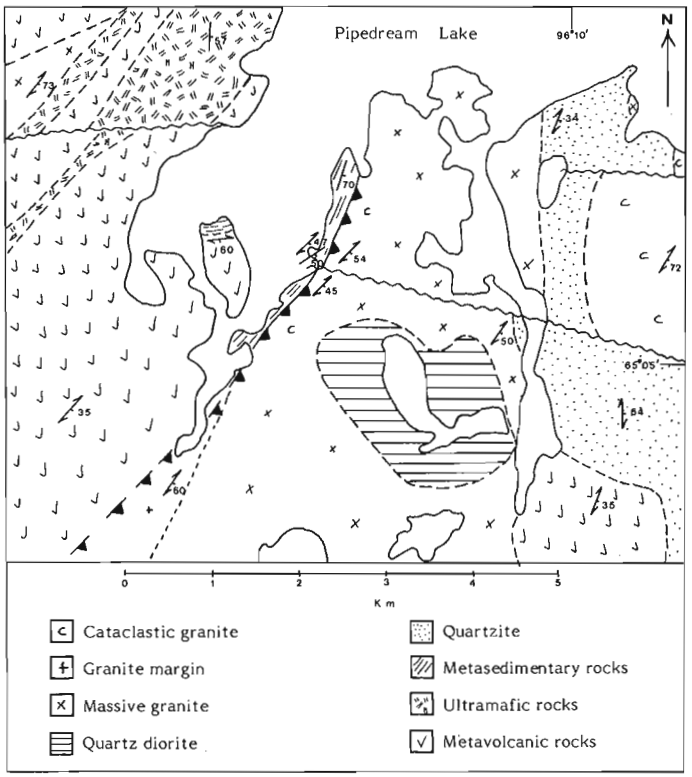

Figure 26.2. Sketch of low-angle fault at southwest end of Pipedream Lake placing granite on top of volcanogenic metasedimentary rocks.

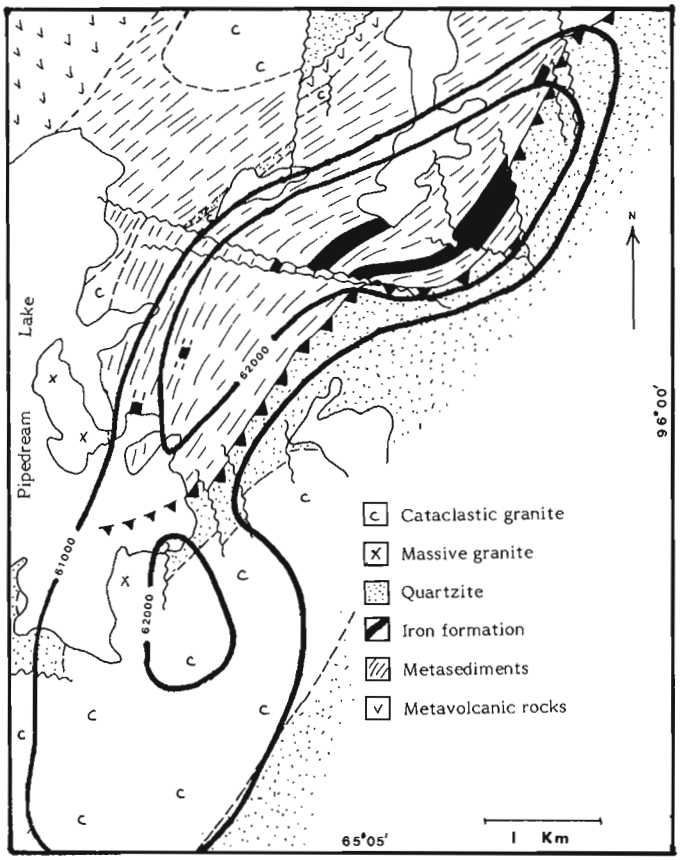

Figure 26.3. Sketch map showing low-angle fault placing granite and quartzite on top of iron formation and metasediments. Note that the thin bands of quartzite and cataclastic granite in the northwestern part of the map also suggest low-angle faulting in that area. Aeromagnetic contours in gammas.

The late granitic rocks are clearly younger than all of the supracrustal rocks. Intrusive relationships are common and the absence of a pervasive structural fabric indicates that the granites may have escaped much of the early deformation and only been involved in the low-angle faulting.

Biotite Porphyry

Subsequent to the emplacement of the granites, a set of biotite porphyry dykes intruded the area. Two dykes were found this year, one trends west-northwest at the southwest end of Ukalik Lake and clearly crosscuts volcanogenic metasediments, and the other trends northeast and intrudes migmatites of the northern granitic pluton north of Pipedream Lake. A thin section from a similar dyke found on the shore of eastern Tern Lake (Ashton, 1981) contains zoned biotite and clinopyroxene phenocrysts in a fine grained matrix of amphibole and feldspar. Late biotite porphyry dykes are relatively common in the Baker Lake area and are thought to be related to the Aphebian(?) Dubawnt Group.

Structure

The dominant structural fabric in the area trends northeast and dips gently to steeply southeast. It appears to be axial planar to an early set of northeast-plunging isoclinal folds. Large-scale fold closures are rare but primary layering in the komatiites appears to define an overturned anticline west of Pipedream Lake (Fig. 26.1). Minor folds are somewhat more common in the iron formation and layered metasediments. Refolded isoclines were observed at one

locality within the iron formation, which may suggest a more complex history, although the "early" fold could be a result of primary slumping.

A set of later structures has been interpreted as indicating that low-angle faulting has played a significant role in the structural history of the area. These include: 1) a number of gently to moderately dipping faults which, in at least one locality at the south end of Pipedream Lake, place granitic rocks on top of volcanogenic metasediments (Fig. 26.2). An aeromagnetic anomaly helps to outline another low-angle fault which places granitic rocks and quartzite structurally above iron formation at the southeast end of Pipedream Lake (Fig. 26.3). At both localities the granitic rocks in the vicinity of the fault zone are severely sheared and cataclastic. 2) Thin bands of gently to moderately dipping chlorite schists, thought to be the sheared equivalents of mafic volcanic rocks, characterize many contacts between metavolcanic rocks and quartzite. 3) Green chromian(?) mica schists mark shear zones at two localities in the study area, in felsic metavolcanic rocks on the east side of Pipedream Lake, and at a quartzite contact north of Third Portage Lake (Fig. 26.1). 4) Large areas adjacent to many of the proposed faults are characterized by relatively gently-dipping strata and near-recumbent isoclinal folds. 5) The eastern part of the study area also contains an extensive set of horizontal, east-northeast-trending crenulations and a strong southeast-plunging stretching lineation. Taken together, these structures appear to be consistent with a model involving low-angle faulting, possibly in the form of northwest-verging thrust faults, and associated large-scale recumbent folding.

Late, southeast-plunging kink folds have also affected the rocks east of Pipedream Lake. These may be related to late faulting which further dissects the area. In the east, an apparently conjugate set of late faults has disrupted the outcrop pattern. One set of faults trends north-northwest with an apparent left-lateral offset, the other trends west-northwest with an apparent right-lateral displacement. The direction and sense of fault movement in the western part of the map area are somewhat more difficult to determine. One set is subparallel to the dominant structural fabric and may be related to the early low-angle faulting. The other set trends northwest and is dominant in the granitic rocks.

Metamorphism

Although a petrographic study has not yet been completed, macroscopic mineral assemblages indicate that the area has undergone greenschist facies metamorphism. Indicator minerals are not common in the thin sections. The assemblage kyanite-chlorite-white mica-quartz is present in some of the quartzites while the phyllitic rocks within the quartzites locally contain chloritoid-chlorite-white mica-quartz. Kyanite and chloritoid coexist in samples from the quartzite-phyllite contact.

Narrow thermal aureoles around the late granites are locally defined by the presence of garnet and abundant biotite in metasedimentary rocks.

Economic Potential

Extensive gossans in ultramafic rocks and associated metasediments are exposed along the western shoreline of Pipedream Lake. Samples collected from these rocks have yet to be analyzed.

Numerous small gossans within felsic metavolcanic rocks suggest that there has been substantial hydrothermal activity in the area. Disseminated pyrite is common in many of the metasedimentary rocks but concentrations are restricted to small quartz veins into which the pyrite has presumably been remobilized. Medium- to coarse-grained pyrite cubes are also common in metasedimentary rocks adjacent to some faults. Traces of chalcopyrite and galena were observed in a northwest-trending fault zone in the northwest corner of the area. Arsenopyrite was found in an east-trending fault zone separating deformed granites and rocks of the metavolcanic sequence (Ashton, 1981).

Thin, discontinuous layers and lenses of conglomeratic quartzite are pyritiferous and locally form small gossans.

Iron formation is abundant in the area but isoclinal folding and late faulting has prevented accurate determinations of its regional extent and thickness. The greatest concentrations are east of Pipedream Lake east of South Driving Rain Lake and of Third Portage Lake (Fig. 26.1).

Glacial Features

Glacial features trend predominantly northwest-southeast and are consistent with the suggestion that the latest movement of ice was northwestwards (Ashton, 1981). A clearly distinct set of east-west oriented glacial striae and grooves were measured but the sense of ice movement was not determined for these features. A large esker transects the area running southeastwards from the northern map boundary to the eastern boundary south of Ukalik Lake.

Age of the Quartzite and Metavolcanic Rocks

The age of the metavolcanic sequence is believed to be Archean based on lithological similarities with the Prince Albert Group and on an unpublished U-Pb date from felsic metavolcanic rocks located a few kilometres north of the study area (W.W. Heywood, personal communication, 1980). The quartzite predates the earliest granitic rocks recognized in the area. Several types of quartzite contacts have been observed, including: 1) fault contacts characterized by cataclastic granites and chlorite schists (Fig. 26.1-26.3). 2) apparent disconformable or unconformable contacts

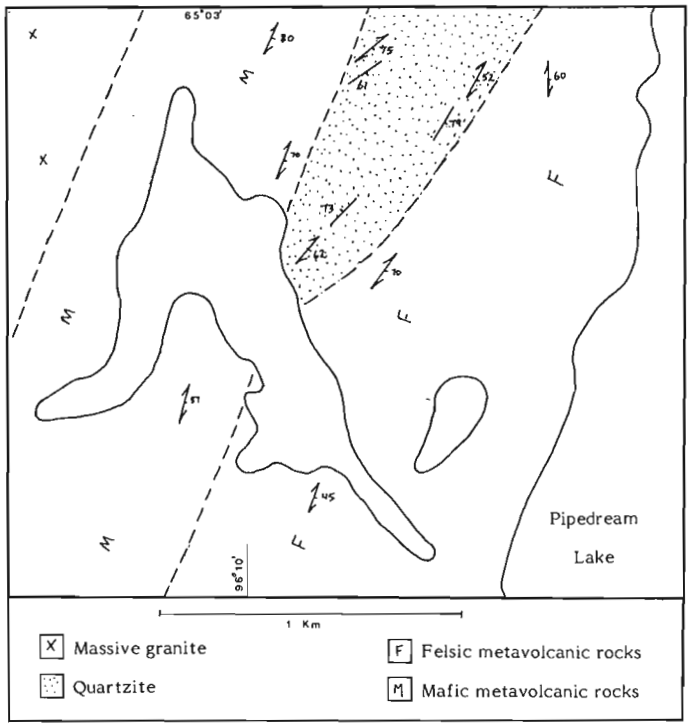

Figure 26.4. Sketch map showing apparent unconformity between quartzite and metavolcanic rocks.

suggesting that the quartzite was deposited prior to the volcanogenic metasediments. 3) an apparent gradation of black phyllites, which are generally restricted to thin layers and lenses within the quartzite, into greywacke across a contact containing quartzite pebbles. 4) an apparent facies change from quartzite to iron formation indicated by the presence of thin bands of magnetite in quartzite. 5) apparent unconformities suggesting that the quartzite postdates the metavolcanic rocks (Fig. 26.4).

Using a model based on widespread thrust faulting in the area, which seems reasonable in view of the structural arguments listed above, the quartzites could be interpreted as klippen tectonically emplaced from some distance away and genetically related to rocks not exposed in this region.

It is also possible that the quartzite is older than the metavolcanic sequence. The conglomerates described earlier which contain quartzite pebbles in a greywacke matrix are difficult to explain unless the quartzite was deposited prior to greywacke deposition. Since the greywacke appears to grade conformably into other metasediments, iron formation and ultimately into metavolcanic rocks at both of the localities at which this type of contact was observed, the apparent conclusion is that the quartzites are the oldest exposed supracrustal rocks.

An alternate possibility is that the quartzites are younger than the metavolcanic rocks. While this theory has been generally favoured in the past (Wright, 1967), very little evidence has been found to support it. Apparently unconformable contacts such as the one depicted in Figure 26.4 do not necessarily imply a younger quartzite since the stratigraphic top is unknown. Further, the quartzite could have been either faulted into place or deposited during a lull in volcanic activity.

References

Ashton, K.E.
1981: Preliminary report on geological studies of the "Woodburn Lake Group" northwest of Tehek Lake, District of Keewatin; in Current Research, Part A, Geological Survey of Canada, Paper 81-1A, p. 269-274.

Wright, G.M.
1967: Geology of the southeastern barren grounds, parts of the Districts of Mackenzie and Keewatin; Geological Survey of Canada, Memoir 350.

27.

FELSIC DOMES AND FLANK DEPOSITS OF THE BACK RIVER VOLCANIC COMPLEX, DISTRICT OF MACKENZIE

Project 740019

M.B. Lambert
Precambrian Geology Division

Lambert, M.B., Felsic domes and flank deposits of the Back River volcanic complex, District of Mackenzie; in Current Research, Part A, Geological Survey of Canada, Paper 82-1A, p. 159-164, 1982.

Abstract

Two of the 23 felsic domes in the Back River cauldron subsidence complex (of Archean age) illustrate a small composite dome, the roots of a dome, and coarse epiclastic deposits derived from the domes. The Crutch Lake dome is a composite body that evolved during two main stages of effusion beginning with the eruption of a rhyolite dome. A dacite dome rose through and largely destroyed the previous dome. Mass wasting produced banks of coarse debris on the flanks of the domes and lahars carried debris for distances of 1500 m off the east side. The rhyolite body at Thlewyco Lake is the root of a dome that rose along the outer ring fracture system and through a succession of greywacke and siltstones. Extensive rhyolite breccias are the products of destruction of this dome and represent debris flows that travelled for 4500 m into the adjacent sedimentary basin.

Introduction

The Back River volcanic complex in the eastern Slave Province is centred about 480 km northeast of Yellowknife, Northwest Territories. The complex is an essentially flat lying succession of volcanics surrounded by more highly deformed metagreywacke-mudstone turbidites. The complex records a history of volcanism that began with the effusion of basaltic and andesitic magma on the seafloor. The volcanic pile gradually emerged and explosive eruptions of voluminous felsic pyroclastics culminated in cauldron subsidence and development of two ring-fracture systems in the southern half of the complex. Rhyolite dykes and domes rose along ring fractures and in shallow seas marginal to the emergent volcanic pile.

Various aspects of the geology of this complex are discussed in greater detail (Baragar, 1975; Henderson, 1975; Lambert, 1976, 1977, 1978; Lambert and Henderson, 1980).

Twenty-three felsic dome-flow complexes occur along the inner and outer ring-fracture systems and form isolated bodies north and west of the ring fractures (Fig. 27.1). Most are composite bodies in which the precise number of intrusive or flow units is not known. Along ring fractures complexes are long and narrow, ranging between 0.5 to 2 km wide and up to 8 km long. Away from ring fractures they tend to be equant. The largest single complex is about 13 km across. Some domes developed entirely in a subaqueous environment, whereas others (the larger complexes) straddle subaqueous and subaerial environments.

This paper documents (1) a small composite dome and its flank deposits (at Crutch Lake), and (2) the roots of a dome and the products of its disintegration (at Thlewyco Lake).

The Crutch Lake Dome

The Crutch Lake Dome (Fig. 27.2) is a composite body that has a roughly oval outline about 2200 m by 1500 m across. The complex comprises (1) remnants of an early rhyolite dome, (2) a dacite dome that intruded the rhyolite dome and makes up about 55 per cent of the present complex, and (3) coarse epiclastic flank deposits. The dome intruded through and effused upon sediments that are mainly shale, argillite, volcanic grits and wackes.

The dome is undeformed in contrast to the surrounding sediments which are folded.

Rhyolite Dome

Remnants of this dome form an irregular margin (100 to 500 m wide) along the north and east sides of the complex, a wedge-shaped body near the west side, and lobes 200 to 300 m across in sediments on the southeast side. If the present distribution of rhyolite indicates the approximate extent of the original body, the ancestral dome may have been an oval-shaped body 2100 by 1000 m across.

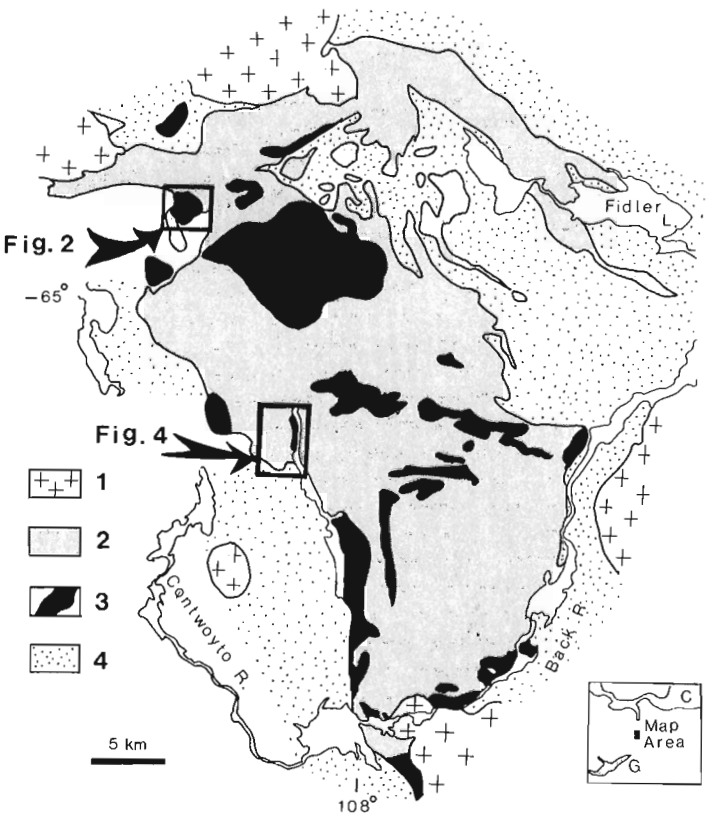

Figure 27.1. *Rhyolite domes in the Back River volcanic complex. 1, plutonic rocks; 2, volcanic suite; 3, rhyolite domes; 4, greywacke-mudstone turbidites of the Yellowknife Supergroup. Index map: C, Coronation Gulf; G, Great Slave Lake.*

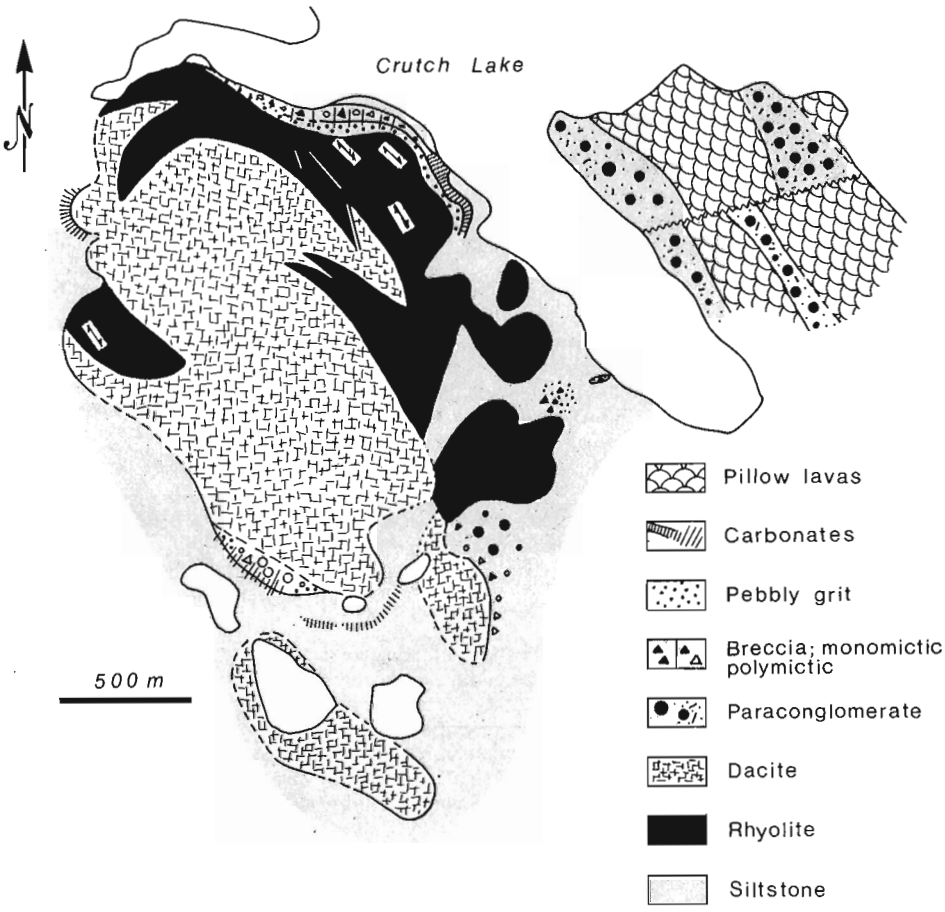

Figure 27.2. *Dome complex at "Crutch" Lake.*

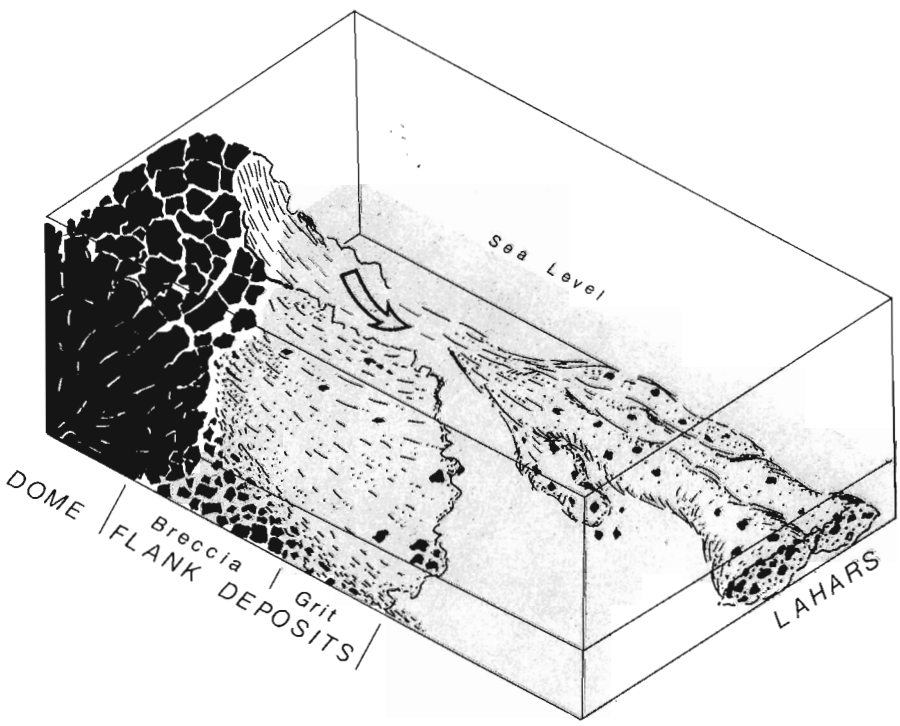

Figure 27.3. *Facies of flank and distal deposits around the east side of the Crutch Lake dome.*

In general, the rhyolite overlies the surrounding sediments. Shallow dipping contacts between the two units contour roughly around the topography on the east side. In some places flank deposits appear to be lying against the dome, whereas in others the transition from brecciated dome to coarse flank breccias appears gradational.

Rhyolite is white weathering, pale- to medium-grey, aphanitic to sparsely porphyritic rock that contains phenocrysts of quartz and feldspar. The rock is unusually porphyritic in the northwestern part of the dome where it contains 15 to 20 per cent phenocrysts as much as 3 mm across.

Shattered and brecciated rhyolite is ubiquitous; massive rhyolite is rare. Most rocks are autoclastic breccias, but some are epiclastic. Autobreccias are monomictic, nonsorted, nonlayered, tightly packed masses of rhyolite clasts. Matrix, where present, is a fine crush of rhyolite. Epiclastic rocks are monolithic rhyolite block- and boulder-grits comprising rounded to subangular clasts (4 to 10 cm) in a matrix of fine- to coarse-rhyolite fragment grit. In one place these breccia contain rare blocks of carbonate. Such units are always massive and unsorted.

Most of the northeastern side of the rhyolite is intensely sheared. Trend of shearing is northwesterly and nearly vertical. Shear planes cut through fragments of the breccia and divide outcrops into masses of lenticles and large slivers. These clasts have preferred orientation which locally gives outcrops a pseudo-layered appearance.

Dacite Dome

The dacite part of the complex includes a roughly oval body 2000 m by 1100 m and a satellite body roughly 1000 m by 300 m off the south end.

Contacts between dacite and rhyolite are generally intrusive. Dacite partly encloses large portions of the rhyolite. In some places both units are brecciated so that at contacts lithology changes gradually from rhyolite-block-laden dacite breccia to rhyolite breccia over a distance of about 10 m.

The dacite lies above the surrounding sediments. The shallow dipping contact between the dome complex and the sediments contours around the topography along the western and southern sides. Thick, stubby wedges of coarse breccia which lie against the dome from which they were derived, are considered structurally as part of the dome-flow complex. These contact relations and the lack of deformation indicate that the dacite dome is not folded.

In contrast to the rhyolite dome, the dacite dome is massive (generally devoid of any layering) and not brecciated, except for autobrecciation along parts of its margin and local shear zones in the northern parts. Dacite is devoid of layering. It forms distinctive smooth, rounded outcrops that have widely spaced, blocky joint patterns defined by three sets of fractures that make high angles with one another.

Dacite forms dark-grey weathering, dark-grey, aphanitic to porphyritic rocks that are very uniform. Plagioclase phenocrysts range from 1 to 2 mm and generally make up less than 1 to 2 per cent of the rock. Inclusions of rhyolite occur throughout the dacite dome. They are rounded, less than 5 cm across, and scattered randomly throughout the rock, commonly in amounts of 1 to 3 per cent. Inclusions are most abundant and largest near contacts with rhyolite where they make up 15 per cent of the rock, and locally they choke the dacite so that the distinction between rhyolite breccia and inclusion-laden dacite is not obvious. In these areas inclusions are pebble to cobble size and occasionally range up to 300 cm across. Xenoliths of carbonate impregnated grit are rare near contact zones.

Flank Deposits

Flank deposits include all epiclastic breccias, coarse volcaniclastic grits and carbonates that lie against or immediately below the edges of the dome complex (Fig. 27.3). These deposits form aprons of debris around the complex that generally extend for distances of less than 200 m from the dome. Generally, flank deposits comprise (1) basal coarse breccias that form the main part of the deposit, (2) fine breccias, pebble grits and wackes that overlie coarse breccia, or form distal lobes of breccia in sediments and (3) carbonate that thoroughly impregnates parts of fine breccias, grits and wackes and the matrix of coarse breccias. The succession lies on slates and siltstones of the surrounding sedimentary succession. Paraconglomerate derived from the dome lies off the southeast flank and on the peninsula 1500 m east of the dome.

The coarse breccias typically form massive, nonsorted, nonbedded deposits. Lithology of clasts in epiclastic breccias reflect the compositions of the immediately adjacent dome. They tend to be dominantly monomictic where the dome is of one lithology (east and west sides of the dome) and polymictic where both phases of the dome are present (near the north and south sides of the dome). Clast sizes vary with location within a particular deposit. The deposit on the southwest side of the dome, for example, is a wedge of boulder conglomerate 200 m wide and 500 m long in which closely packed boulders up to 50 cm across (but generally between 10 to 20 cm) make up 50 per cent of the rock. Clast sizes dwindle laterally toward both ends of the deposit where the rock is a pebbly to bouldery grit. This is a polymictic boulder breccia comprising dominantly dacite boulders and blocks, minor rounded rhyolite boulders (to 20 cm) and rare blocks of brown-weathering carbonate grit to 30 cm across.

Breccia along the north side of the dome is polymictic, but clasts are dominantly white-weathering rhyolite. The angular to subangular clasts generally range from 1 to 10 cm and rarely large (ca. 15 x 100 cm) slabs may be suspended in the finer breccia. Clasts tend to be equant and have no preferred orientation except in sheared zones where orientation is strong. In this area clasts include white rhyolite, grey aphanitic dacite, feldspar phyric dacite and medium-green aphanitic volcanic rock. Matrix is a coarse grit (containing clasts of the same composition as the blocks) that is impregnated with carbonate so that clasts weather in relief.

On the southeast side of the dome some coarse breccias form elongate lobes in shallow troughs radial to the dome.

Pebbly to bouldery grits form the uppermost parts of the epiclastic flank deposits. They lie above and locally beneath the coarse breccias and conglomerates, or directly against the shattered and brecciated dome. Grits are massive, unsorted units (up to 10 m thick), that carry angular to subangular clasts, to crudely bedded units in which well-rounded pebbles and boulders show crude grading or concentrations at the base. Matrix generally is nonlayered, fine- to coarse-rhyolite grit that is impregnated by carbonate. Generally these units are part of a fining-upward sequence so that the upper parts are volcanic wackes or siltstones largely replaced by carbonate.

Carbonate also occurs in arcuate zones in sediments, generally within 100 m of the dome.

Paraconglomerate off the southeast side of the dome contains well-rounded cobbles and boulders to 10 cm (and occasionally up to 30 cm) that are suspended randomly in a coarse rhyolite pebble grit or form boulder-rich horizons that define crude beds up to 20 cm thick.

Paraconglomerate on the peninsula is about 100 m thick. It ranges from fine- to coarse-conglomerate and has minor sandy beds. Deposits comprise subangular to well-rounded boulders and blocks generally less than 10 cm, but occasionally up to 70 cm, suspended in volcanic grit containing high proportions (locally up to 70%) of feldspar crystals. Clasts are dominantly rhyolite but some mafic compositions are also present. Locally the unit displays thick, crudely-graded beds. Andesite pillow lavas overlie the paraconglomerates. This unit is interpreted as a distal part of subaqueous debris flows derived from the flanks of the dome complex. Matrix of the conglomerate may be crystal-rich ash related to explosions that heralded emplacement of the dacite dome.

Underlying Sediments

Flank deposits lie on slates, siltstone and wackes of the surrounding sediments. Sediments immediately beneath dacite along the northwestern side of the dome are black argillite and grits (some impregnated with carbonate) to pebbly grits. Units are thick-bedded, 10 to 60 cm thick, and generally massive. Locally, grits contain rip-up slabs of shale (up to 20 cm long and 2 cm thick) rhyolite fragments and pebbles of quartzite to 2 cm across. In one place the rocks are sedimentary breccias containing angular blocks and slabs of black argillite to 1 m across (ranging from 10 to 60 cm) in carbonate grit matrix.

At least 3 units of slate occur within the northeast part of the rhyolite where the rhyolite is intensely sheared. They range up to 15 m wide and are traceable intermittently for 100 to 200 m. Contacts of these units appear almost vertical and undulate because of numerous small fault offsets. In some places contacts of the slate bodies and slaty cleavage are parallel to shearing in the surrounding rhyolite. Some slate units are clearly sheared pods within the rhyolite breccia. These slates and slaty-siltstones locally contain blocks of rhyolite and rarely carbonate to 20 cm. These bands, which may be only 10 m above the base of the rhyolite in which they occur, could be fault slivers tectonically emplaced by differential movements along shear planes.

Interpretation

The Crutch Lake dome represents two stages of effusion of felsic magma. Initial rhyolite effusions formed an oval-shaped dome-flow complex approximately 1000 m by 2100 m across (at the present level of erosion). Most of the dome was destroyed before or during emplacement of the dacite portion of the complex. Ubiquitous brecciation possibly resulted from a combination of processes: (1) flow

brecciation; (2) explosive shattering and crumbling of the dacite; (3) landsliding; and (4) tectonic shearing after dome emplacement.

The dacite dome rose through the rhyolite dome, probably largely destroying it in the process, grew upwards and spread westward over the surrounding sediments.

The paucity of brecciation in the dacite, the general lack of dacite fragments in breccias and sediments peripheral to the complex, the lack of any other effusive phases, and the fact that the dacite dome composes most of the present complex, suggest that the dacite body represents the last major activity from this centre and the dome was not destroyed by subsequent volcanic activity, as was the rhyolite dome.

Mass wasting from the complex produced banks of talus, deposits of conglomerate and coarse sands (pebble grits). Landsliding and debris flows carried coarse debris into sediments for distances of at least 1500 m from the dome on the east side. Crystal-rich ash settled in shallow water around the dome or was carried to its present location on the peninsula by lahars that issued from tuffaceous flanks of the volcano.

Quartzite pebbles in the grits may represent relicts of quartz sands that formed beaches locally at the edge of a partly emergent rhyolite dome.

That the domes rose in shallow water or possibly subaerial environments is suggested by (1) coarse conglomerates and grits surrounding the dome; (2) quartzite pebbles in wacke adjacent to the dome; and (3) abundant crystal tuffs along the east side (suggesting explosive subaerial or shallow submarine activity).

Carbonate that impregnates flank deposits may have precipitated from late stage fumaroles during the waning stages of volcanism from this eruptive centre.

If the present distribution of rhyolite is taken as the approximate limit of the original domes, the rhyolite was approximately the same size as the dacite dome. Judging from morphology and relative dimensions of domes known amongst recent volcanoes, the Crutch Lake Dome represents a section through the lower 60 m of a dome complex which may have been more than 400 m high (assuming a conservative ratio of diameter to height of 3:1). Both the domes probably had almost equal dimensions and the two of them probably represent an effusion of about 1 km^3 of magma.

Thlewyco Lake Dome

Remnants of a rhyolite dome form a body 2800 m long and 400 m wide that is well exposed in a 45 m cliff at the northwestern end of Thlewyco Lake (Fig. 27.4). Rhyolitic debris derived from the dome is preserved southwest of the dome in north to northwesterly trending folds.

The rhyolite body is massive and nonbrecciated except for locally along its western margin. A blocky joint pattern defines steep elongate columns in the lower part of the cliff face, and gently to moderately plunging, 5 to 6 sided columns on some upper parts of the exposure. Regular joint sets are interpreted as tectonic features, whereas the polygonal joints may be primary columnar joints formed during cooling of the body. The southern 200 m of the rhyolite narrows to a neck-like feature, 150 m wide, that makes steep contacts with sediments on both sides.

The white to pink weathering rhyolite is pale- to medium-grey on fresh surface and contains 2 to 15 per cent albite phenocrysts and 1 per cent quartz phenocrysts (less than 0.5 mm) in an aphanitic matrix. The matrix consists dominantly of albite microlites and quartz. Its grain size (averaging 0.5 to 0.15 mm) is coarser than the microfelsic matrix of many extrusive rhyolite complexes in the map area. Near contacts, the matrix becomes finer grained and the fresh rock becomes dark grey.

At the southeast end of the dome the intrusive nature of the body is indicated by (1) sharp, steep contacts between sediments and rhyolite; (2) lack of brecciation in contact

Figure 27.4. Rhyolite dome and breccias at Thlewyco Lake.

zones (brecciation would be expected at margins of an extrusive dome or lava); (3) chilled margins; and (4) siltstones in contact with rhyolite that are recrystallized to hornfels or siliceous argillite.

Rhyolite fragment breccias, conglomerates and grits extend for 3300 m southwest of the dome. If unfolded, the restored apron of breccia would extend about 4500 m. The unit is thickest in its central part (in the order of 400 m), thins slightly toward the dome and tapers out at the northern and western extremities. Southwest of the dome a massive (nonpillowed) andesite lava flow, 6 to 10 m thick, lies conformably between rhyolite breccia and the underlying siltstones and wackes. Sediments beneath the flow have abundant soft sediment deformation and the lava has incorporated slabs and blocks of the sediment within its basal flow breccia. This flow may be related to the andesite unit northwest of the dome complex upon which the breccias lie. Where the andesite lava is absent, the breccia grades laterally into rhyolite pebble conglomerate, then into coarse pebbly wackes. Near the western side of the breccia unit, a lens of basalt pillow lavas lies between rhyolite breccias and the underlying sediments.

Breccias form massive units in which clasts have strong preferred orientation parallel to axial traces of folds. Characteristically they lack stratification and are not sorted. Composition of fragments is dominantly white-weathering rhyolite, some of which is similar to the exposed dome and some of which is much more abundantly porphyritic than any rhyolite exposed. Breccias become polymictic distally from the dome where they contain fragments of andesite, but rhyolite fragments always dominate. Clasts generally range from angular to rounded and may form open to intact framework. Matrix is a fine breccia or coarse grit composed of clasts identical in composition to the larger clasts.

Near the nose of the southernmost fold, massive breccia grades laterally into interbedded felsic fragment conglomerate and pebbly wackes, then into interbedded pebbly wackes, coarse grits and massive wackes. Bedding becomes increasingly better developed as size and abundance of pebbles decreases and the proportion of wackes increases. Wackes vary from thick massive beds to graded and cross-stratified units. They carry subrounded to subangular rhyolite and andesite pebbles, generally less than 4 cm but some are up to 10 cm, that are suspended in massive beds, entrained to define crude cross-stratification or concentrated at the bottom of beds.

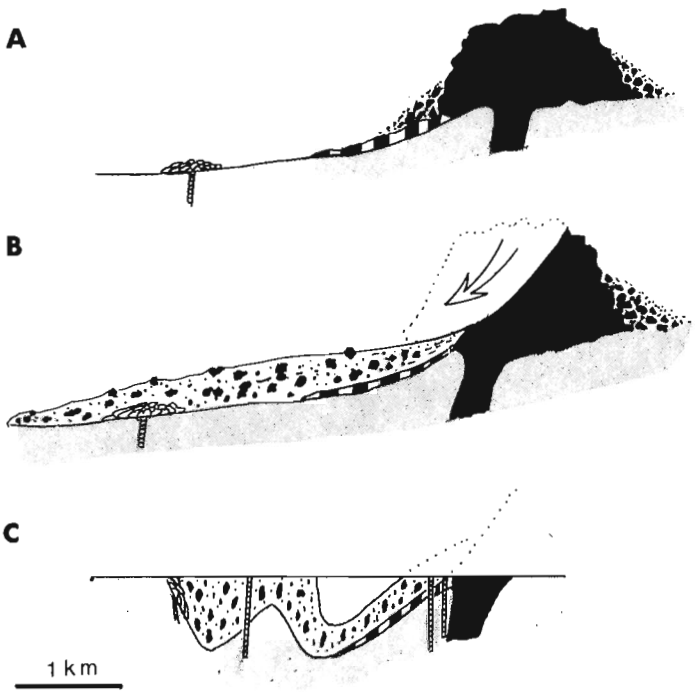

Figure 27.5. Evolution of the rhyolite dome and flank deposits at north end of Thlewyco Lake. Patterns as for Figure 27.4.

Section A-B (Fig. 27.4) shows internal stratigraphy through a section of the breccia that is about 800 m from the dome. This section contains lower, middle and upper units of felsic breccia (90 to 170 m thick), each overlain conformably by units 20 to 40 m thick of coarse wackes, pebbly wackes, or grits. The lower and middle breccias may represent more than one depositional unit. The lower 100 m of the lower breccia unit is a coarse, unsorted breccia containing angular to rounded boulders and blocks of abundantly porphyritic rhyolite in a gritty sand matrix. Clasts, that generally range up to 15 to 20 cm and rarely to 50 cm across, are not touching. Near the 100 m level, however, clasts are less than 10 cm across and are closely packed. The remaining upper 70 m of the unit is a massive conglomerate containing pebble size clasts. In spite of the crude upward grading of clasts, all parts of the unit are unsorted and not stratified.

The lower breccia unit is overlain conformably by 40 m of massive to poorly stratified coarse wacke and 10 m of massive andesite.

The middle breccia unit is a rhyolite boulder breccia similar to the basal part of the lower breccia except for the upper 80 m which is a polymictic breccia containing rhyolite (dominantly) and feldspar-phyric andesite clasts. The subangular to subrounded blocks (up to 20 cm) form a framework that locally makes up 75 per cent of the rock. This breccia grades upward into massive pebbly wacke that divides this breccia from the upper breccia unit.

The upper breccia, which contains blocks and boulders to 30 cm, grades at its top into pebbly grit containing clasts smaller than 2 cm. In some places the wackes form thick beds (1 to 3 m) that alternate with crossbedded pebbly wackes.

In one place on the southwestern side of the dome clastic rocks may be crystal-lithic lapilli tuffs rather than epiclastic rocks. These massive but well-sorted rocks comprise closely packed fragments of quartz-albite phyric rhyolite and plagioclase crystals and very little fine matrix. The subrounded to angular clasts have strong preferred orientation. Plagioclase crystals, both as phenocrysts in rock fragments and as single crystals make up 30 to 45 per cent of the rock.

Rocks interpreted as talus deposits are massive, unsorted coarse breccias containing 80 per cent closely packed angular and rounded blocks that range up to 60 cm. These rocks occur within 400 m of the dome.

Interpretation

The dome rose through a greywacke-siltstone succession along the margin of the main volcanic complex (A, Fig. 27.5). Elongate form and location of the present dome suggest that it rose along linear fractures related to the outer ring fracture system of the caldera complex. Massive andesite lavas effused on soft sediments near the eruption site and basalt lava erupted to form a mound of pillow lavas in the sedimentary basin about 3 km west of the fissure of impending felsic volcanism.

Felsic volcanism began with explosive (possibly phreatomagmatic) eruption in which phenocryst-rich magma exploded to form crystal-lithic tuffs. As the dome rose it shed aprons of coarse detritus along its flanks. The dome was

destroyed probably by massive landsliding (and possibly by violent explosions) which produced extensive debris flows into the sedimentary basins to the west (B, Fig. 27.5). Debris flows incorporated material from andesite lavas that were adjacent to the dome and lining the sedimentary basin. Regional deformation rotated and deformed clasts in the breccias so that they became oriented along axial planes of folds. The present level of erosion exposes the roots of the rhyolite dome and the voluminous breccias that represent its destruction (C, Fig. 27.5). The bulk of the original dome that grew on the surface is no longer exposed.

References

Baragar, W.R.A.
1975: Miscellaneous data from volcanic belts at Yellowknife, Wolverine Lake and James River, N.W.T.; in Report of Activities, Part A, Geological Survey of Canada, Paper 75-1A, p. 281-286.

Henderson, J.B.
1975: Sedimentological Studies in the Yellowknife Supergroup in the Slave Structural Province; in Report of Activities, Part A, Geological Survey of Canada, Paper 75-1, p. 325-330.

Lambert, M.B.
1976: The Back River Volcanic Complex, District of Mackenzie; in Report of Activities, Part A, Geological Survey of Canada, Paper 76-1A, p. 363-367.

1977: The southwestern margin of the Back River Volcanic Complex, District of Mackenzie; in Report of Activities, Part A, Geological Survey of Canada, Paper 77-1A, p. 179-180.

1978: The Back River Complex – a cauldron subsidence structure of Archean age; in Current Research, Part A, Geological Survey of Canada, Paper 78-1A, p. 153-158.

Lambert, M.B. and Henderson, J.B.
1980: A uranium-lead age of zircons from volcanics and sediments of the Back River Volcanic Complex, Eastern Slave Province, District of Mackenzie; in Loveridge, W.D., Rubidium-strontium and uranium-lead isotopic age studies, Report 3; in Current Research, Part C, Geological Survey of Canada, Paper 80-1C, p. 239-242.

28.

SYNVOLCANIC INTRUSIONS IN THE CAMERON RIVER VOLCANIC BELT, DISTRICT OF MACKENZIE

Project 730040

M.B. Lambert
Precambrian Geology Division

Lambert, M.B., Synvolcanic intrusions in the Cameron River volcanic belt, District of Mackenzie; in Current Research, Part A, Geological Survey of Canada, Paper 82-1A, p. 165-167, 1982.

Abstract

Swarms of amphibolite dykes and sills, that form up to 35 per cent of the Cameron River volcanic belt, intrude the granitic basement but not sediments that are adjacent to or overlie the volcanics. They are an integral part of the volcanic stratigraphy. The dykes mark extensive linear fracture systems, along the margins of a fault bound basin, that were the conduits along which magma rose and fed lavas at the surface. As magma shifted progressively to fractures farther from the edge of the basin, lavas effused at the surface and the volcanic pile spread laterally from east to west. The present volcanic belt reflects the width of the original belt, not its thickness. Regional deformation deformed the belt against the granitic block which bound the basin on its eastern side.

Introduction

Swarms of amphibolite dykes and sills make up significant proportions of the Cameron River and Beaulieu River volcanic belts of Archean age in the southern Slave Province of the Northwest Territories. The intrusions, because they are restricted to the volcanic belts and adjacent granitic terrane, but do not intrude overlying and adjacent sediments of the Burwash Formation, are regarded as feeders for the lavas. The intrusions were emplaced while the belts were developing and thus not only do they play fundamental roles in the growth of the belts but they form an integral part of the volcanic stratigraphy.

This report documents dyke swarms in the Cameron River volcanic belt between Webb Lake and Cameron River.

The Cameron River volcanic belt is a northerly trending strip of volcanic rocks, 80 km long, that marks the boundary between a basin of sedimentary rocks of the Yellowknife Supergroup to the west and granitic terrane to the east. The belt contains a succession of volcanic rocks metamorphosed to amphibolite grade that comprise 97 per cent basaltic to andesitic compositions (pillow lavas, breccias, mafic intrusions, and minor volcaniclastic and 3 per cent rhyolitic to dacitic compositions (domes, flows, and breccias). Various aspects of stratigraphy, structure and regional relationships of this belt are discussed by Baragar (1966), Henderson (1976), Henderson et al. (1973) and Lambert (1974, 1977). The belt is a homoclinal succession overturned to the northwest that has been deformed against granitic terrane to the east. Deformation by folding is local and of minor consequence.

The eastern side of the belt is irregular where it lies unconformably against or makes fault contact with granitic rocks of the Sleepy Dragon Metamorphic Complex. The relief of the contact is about 2000 m. In contrast, the western side of the belt is generally smooth and gently undulating, where it is overlain conformably by greywacke turbidites and mudstones of the Burwash Formation.

Amphibolite Intrusions

Dyke swarms in the central part of the southern half of the Cameron River Belt and in adjacent Sleepy Dragon Complex are shown in Figure 28.1. In this area intrusions make up 20 to 35 per cent of the volcanic belt. Between Webb and Paterson lakes, the greatest concentration of dykes is along or near the eastern margin of the belt and in the adjacent granitic terrane, whereas in others the distribution is more or less even across the belt.

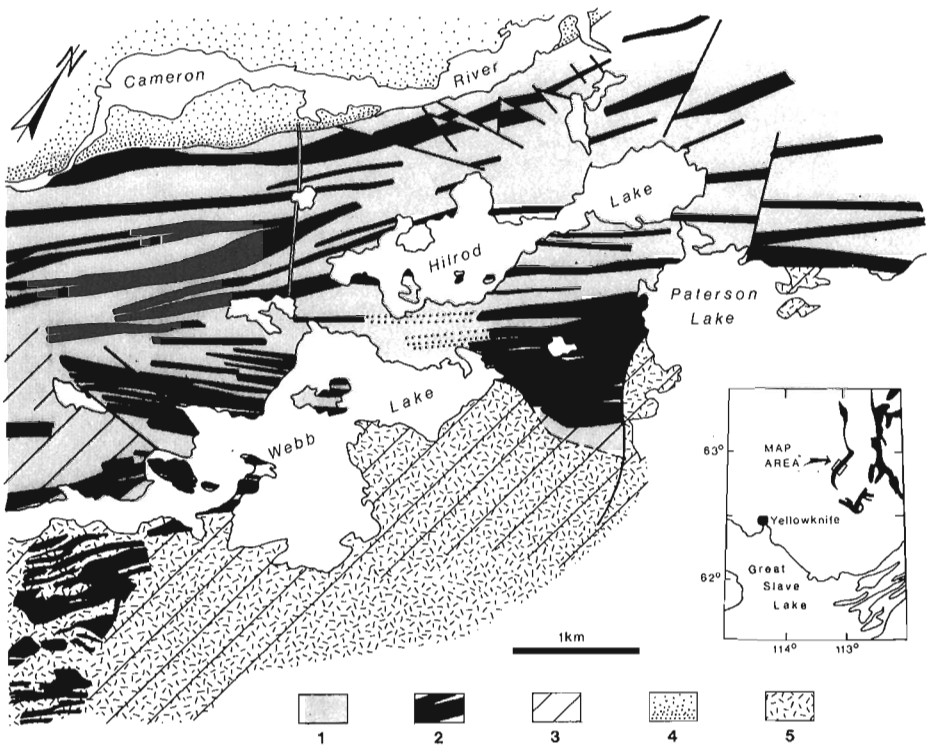

Figure 28.1. Amphibolite dyke swarm(2) in the Cameron River volcanic belt(1) and in the Sleepy Dragon Metamorphic Complex(5). 3, dyke swarm, not mapped in detail; 4, Burwash Formation, greywacke-mudstone turbidites.

These vertical to steeply dipping intrusions are almost parallel to the general trend of the volcanic belt, internal stratigraphy and trend of flattening of pillow lavas. Dykes in the granitic terrane have less regular trends than in the volcanic belt but still have crude northeasterly orientations. The swarm extends up to 3 km into the granites east of Webb Lake.

Thickness of dykes varies from a few tens of centimetres to 200 m; most are between 20 and 100 m. Some large intrusions that have been traced for 6 km pinch and swell and occasionally split into two or more thinner units that surround lenses of pillow lava.

Figure 28.2. Palinspastic reconstruction of dykes and sills (black) in the Cameron River volcanic belt and in the Sleepy Dragon Metamorphic Complex, based on the present density of intrusions between Webb Lake and Cameron River.

Contact Relations

Intrusions generally conform to the trend of stratigraphy within the volcanic belts, but locally they cut across it. Some large dykes and sills have intruded along contacts between units and some have split units longitudinally.

The intrusive nature of these bodies is indicated by: (1) contacts that cut across pillows; (2) sharp, regular contacts that lack surface structures typical of lava flows; (3) relict contact metamorphic aureoles defined by coarsening of grain size of amphibolite pillow lavas adjacent to contacts with dykes; (4) zonal textural variations ranging from coarse grained, gabbroic-textured centres to fine grained or aphanitic margins; and (5) inclusions of fine grained amphibolite in margins.

The large intrusion along the western side of the belt shows clear intrusive relations with pillow lavas where it is thick, but near the northeastern end, where it thins, the contact between massive amphibolite and pillows is gradational. Massive dyke "buds" into pillows having the same texture as the dyke. These areas document the transition where dykes have surfaced and effused as lavas. Such transitions are common but present only locally along the length of some dykes. Where deformation in pillow lavas is mild sharp crosscutting and minutely irregular dyke contacts may be seen. Contact relations are difficult to establish in areas of intense deformation. Dykes within granitic terrane east of Webb Lake are essentially undeformed and make sharp intrusive contacts with the granitic host.

Internal Structures

Most dykes are massive throughout, except for a diffuse layering defined by gradual fining of grain size towards contacts. Some coarse grained dykes have pronounced, steeply plunging mineral streaking defined by preferred orientation of coarse hornblende and in some places by felsic constituents. In at least some cases the mineral streaking is approximately parallel to the margin of the dyke. Sheared dykes are schistose and locally genissic where they include granitic material.

Margins of some thick intrusions have diffuse layering defined by continuous to streaky segregations of plagioclase ranging from 0.2 cm to 10 cm wide. Generally, the layered amphibolites are fine- to medium-grained but some coarse grained parts are also layered. Massive interiors of intrusions commonly have a blocky, square to rectangular pattern of joints.

Lithology

Mafic intrusions within the volcanic belt are homogeneous massive amphibolites that weather dull brown, rusty brown, grey-green to buff-green, and dark grey. Weathered surfaces accentuate relict gabbroic and diabasic textures. Dykes typically have medium- to coarse-grained centres that grade into dark grey (almost black), fine grained to aphanitic margins (relict selvages). Commonly dykes that have intruded other dykes lack fine grained margins and are medium grained throughout. Dykes that presumably have been spread apart longitudinally by later dykes show a succession of margins with "one-way" chilling.

Amphibolite intrusions within the volcanic belts are completely recrystallized rocks. The typical metamorphic assemblage is hornblende(actinolite)-plagioclase-quartz ± epidote and calcite. Amphibole is typically poikiloblastic, blue-green hornblende that encloses irregular minute grains of crystalloblastic plagioclase and quartz, and in some cases, calcite and epidote. In some medium grained rocks of slightly lower metamorphic grade, where actinolite rimmed with blue-green hornblende dominate, amphibole appears to have replaced pyroxene, grain for grain, and thus preserves the original gabbroic texture. Plagioclase in most rocks is recrystallized or polygonized to a fine irregular crystalloblastic aggregate. Relicts of primary plagioclase are aggregates whose outlines define elongate to stubby lath forms. In some cases twin units are still distinguishable. In porphyritic rocks plagioclase phenocrysts are not recrystallized or only partly polygonized on margins.

Dykes within the granitic terrane in contrast to those in the adjacent volcanic belt are less intensely recrystallized, fine grained rocks. They preserve ophitic textures in which plagioclase forms euhedral to anhedral laths that are clear, unaltered, and not polygonized. Cores of plagioclase phenocrysts range up to bytownite (An_{85}) and thin margins may have normal to oscillatory zoning. Mafic minerals are completely recrystallized to blue-green hornblende.

Dykes invariably contain swarms of felsic inclusions where they have intruded granitic rocks. East of Webb Lake granitic xenoliths vary from angular equant blocks, irregular slivers and large screens to rounded, elongate amoeboid blobs and lensoid schlieren. Elongate inclusions have preferred orientation parallel to dyke contacts. Inclusions range from a few centimetres to 10 m across. Rounded and irregular

inclusions that have diffuse margins (10 to 15 mm wide) appear to have reacted with the host dyke rock and to have deformed in a softened state. Broad areas of mixed amphibolite and granite occur along some contact zones.

Effect of Intrusion on Structure and Stratigraphy

Dykes and sills, because of their great thickness and lateral extent, have had the following effects on local stratigraphy: they (1) offset thin units so that stratigraphic correlation is not obvious; (2) produce apparent displacement of thin units that could be misinterpreted as fault displacements; (3) form apparent multiplicity of units by splitting off parts of untis or splitting units laterally and separating the parts by as much as 100 m; (4) create apparent interfingering of units; and (5) spread units within a formation so that they appear much thicker than they really are.

Removal of sills (graphically) from the volcanic belt generally facilitates stratigraphic correlation in the volcanic succession. However, although removal of sills is necessary for logical correlation within the eastern parts of the belt, the equivalent thickness of these lower sills must be replaced to facilitate correlation within the western parts. Hence, dykes and sills in the eastern part of the belt must have been emplaced before the western parts were deposited. The penecontemporaneous emplacement of pillow lavas and intrusions is further suggested by (1) areas where sills and pillow lavas have the same distinctive lithologies; (2) sills or dykes that locally pass into pillowed lavas; and (3) the restriction of intrusions to the volcanic belt and their absence in overlying and adjacent sediments. Thus the intrusions are an integral part of the volcanic stratigraphy.

Discussion

The Cameron River volcanic belt represents voluminous eruption of mafic magma that accumulated along the margin of a subaqueous fault-bound basin in Archean sialic crust (Henderson, 1981; Lambert, 1977). Extensive linear fracture systems at the margins of major fault blocks were the conduits along which magma rose and fed lavas at the surface (Fig. 28.2). The first intrusions and effusions occurred along the edge of the basins where fracturing was most intense. As the pile grew, magma eventually congealed in the first-used fractures, sealed them off, then shifted to fractures progressively farther from the edge of the basin. With each effusion the volcanic succession gradually spread laterally away from the granitic fault scarp. During each new eruption dykes intruded the preceding lavas. Some intruded laterally (i.e. sills) before emerging as pillow lavas.

Although pillows face westward in almost all cases, probably the succession never was a vertically-stacked pile of lavas. The present surface of erosion exposes a view of the volcanic pile perpendicular to the general flow direction so that we now see an agglomeration of onlapping lavas that accumulated successively from east to west. Hence, the present belt reflects the width of the original belt, not its thickness.

The dykes originally were steeply dipping in northerly or northeasterly trends. During regional deformation the succession was deformed against the bounding granitic block so that in plan view sills, dykes and volcanic stratigraphy now have similar trends.

The Cameron River and Beaulieu River volcanic belts all lie within 5 km of the margin of fault-bound basins. Perhaps the width of belts reflects the extent of fracturing in the underlying granitic basement that is related to these major faults.

References

Baragar, W.R.A.
1966: Geochemistry of the Yellowknife Volcanic Rocks; Canadian Journal of Earth Sciences, v. 3, p. 9-30.

Henderson, J.B.
1976: Yellowknife and Hearne Lake map-areas, District of Mackenzie, Northwest Territories; Geological Survey of Canada, Open file 353.

1981: Archean basin evolution in the Slave Province, Canada; in Precambrian Plate Tectonics, A. Kröner, ed., Elsevier Scientific Publishing Company, Amsterdam.

Henderson, J.B., Lambert, M.B., and Peeling, G.
1973: Yellowknife and Hearne Lake map-areas, District of Mackenzie; in Report of Activities, April to October, 1972, Geological Survey of Canada, Paper 73-1, part A, p. 148-151.

Lambert, M.B.
1974: Archean volcanic studies in the Slave-Bear Province; in Report of Activities, April to October, 1973, Geological Survey of Canada, Paper 74-1A, p. 177-179.

1977: Anatomy of a Greenstone Belt, Slave Province, Northwest Territories; Geological Association of Canada, Special Paper 16, p. 331-340.

29. A PETROGENETIC GRID FOR CALCIUM AND ALKALI-DEFICIENT BULK COMPOSITIONS

Project 750008

J.A. Percival, D.M. Carmichael[1], and H. Helmstaedt[1]
Precambrian Geology Division

Percival, J.A., Carmichael, D.M., and Helmstaedt, H., A petrogenetic grid for calcium and alkali-deficient bulk compositions; in Current Research, Part A, Geological Survey of Canada, Paper 82-1A, p. 169-173, 1982.

Abstract

Based on the composition of minerals in two low-variance assemblages from potassium-poor mafic gneiss, P-T slopes have been estimated for possible univariant curves in the model system SiO_2-Al_2O_3-FeO-MgO-H_2O. The result is a petrogenetic grid involving garnet (G), aluminosilicate (A), staurolite (S), cordierite (C), orthopyroxene (Op), anthophyllite (At), gedrite (Ge), cummingtonite (Cm), chlorite (Ch), and quartz (Q).

The crest of the orthoamphibole solvus, tentatively estimated to be at ∿600°C, separates At-Ge pairs at lower grade from assemblages with hypersolvus orthoamphibole at higher grade. Reactions involving orthopyroxene are consistent with published analyses of Op-Ge pairs which indicate that gedrite is an internal phase in the G-A-Op triangle.

Introduction

Cordierite- and orthoamphibole-bearing rocks are formed by metamorphism of rocks which are enriched in Al_2O_3, FeO and MgO, and depleted in CaO, Na_2O and K_2O. Low-potassium pelites occur in many metamorphic belts and may owe their unusual composition to erosion of potassium-deficient source rocks. Cordierite-orthoamphibole assemblages may also result from partial melting of pelites which leads to removal from the host of K_2O and Na_2O by the melt phase (Grant, 1968). Altered volcanic rocks with a low CaO content may develop cordierite-orthoamphibole assemblages in the amphibolite facies.

Mineral assemblages that develop in potassium-poor rocks during metamorphism are sensitive indicators of metamorphic grade (e.g. Robinson and Jaffe, 1969) of particular value in areas where muscovite-bearing pelitic rocks are absent. Therefore, various petrogenetic grids showing the relationships between assemblages have been developed. Unfortunately, the effects of progressive metamorphism cannot be studied in one metamorphic zonation because of the restricted occurrence of appropriate bulk composition in most metamorphic terranes. This note presents a grid which accommodates assemblages from widely spaced localities at metamorphic grades ranging from greenschist (chlorite zone) to granulite facies (orthopyroxene zone) in terms of a petrogenetic grid.

A large portion of the grid is based on mineral assemblages observed in a potassium-poor mafic gneiss in the kyanite-sillimanite-muscovite zone of regional metamorphism (Percival, 1978) from Hackett River, N.W.T. Common assemblages are G-C-Ge-B-Pl-Q-I(ilmenite), G-Ge-Cm-B-Pl-Q-I and C-Ge-B-Pl-Q-I. Orthoamphiboles with Al(IV) content between ∿0.8 and ∿1.1 have 010 exsolution lamellae, inferred to be anthophyllite in gedrite. Two rare assemblages: (1) Si(sillimanite)-S-C-Ge-Ch-B-Q-I-M(magnetite), and (2) G-S-C-Ge-Cm-B-Pl-Q-I, would be invariant in the model system SiO_2-Al_2O_3-FeO-MgO-K_2O-H_2O in the presence of an aqueous vapour phase. In both specimens, staurolite occurs as armoured relicts in garnet, cordierite or plagioclase, and in (1), sillimanite occurs as minute fibrolite inclusions in cordierite.

An invariant point corresponding to assemblage (1) was included in Korikovskii's (1970) comprehensive P-μH_2O grid involving aluminosilicate, garnet, staurolite, cordierite, gedrite, hypersthene, chlorite, chloritoid and quartz (point 5, Fig. 29.2). Also present on Korikovskii's grid are points 4, 6 and 8 (Fig. 29.2). Point 6, involving aluminosilicate, garnet,

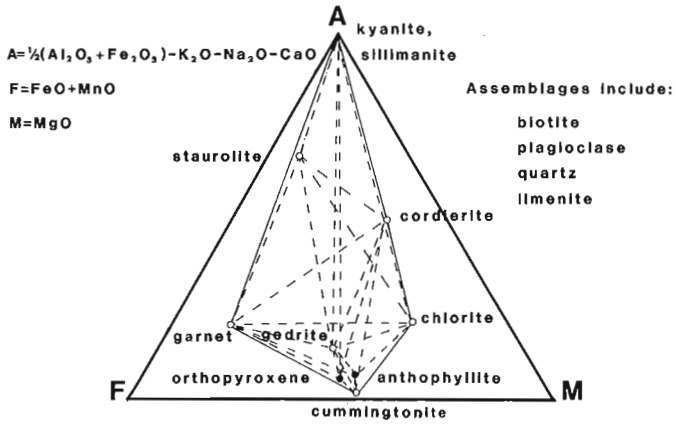

Figure 29.1. *AFM projection of measured (circle) and idealized (dot) mineral compositions (see Table 29.1).*

staurolite, cordierite, gedrite and quartz had previously been documented by Robinson and Jaffe (1969). Point 4 was subsequently independently established on field evidence by Trzcienski (1971; see also Carmichael et al., 1978). Recently Spear (1978a) introduced anthophyllite and cummingtonite into the P-μH_2O grid.

The purposes of this contribution are: (1) to calculate the P-T slopes of univariant curves by Robinson and Jaffe's (1969) method, based on measured mineral compositions; (2) to locate the approximate crest of the orthoamphibole solvus on the P-T grid and to examine its effect on reactions involving two orthoamphiboles; and (3) to examine reactions involving orthopyroxene.

Approach

Analyses of minerals in specimens (1) and (2) (Table 29.1; Fig. 29.1) were obtained on the ARL-AMX microprobe at Queen's University, set up and supervised by Dr. P.L. Roeder. The two sets of staurolite, cordierite and gedrite analyses were averaged for the subsequent treatment. The composition of the orthopyroxene which would coexist with gedrite, garnet and cordierite at higher grade, was estimated from distribution coefficients calculated from mineral analyses reported by Savolahti (1966) and Grant (1978). The anthophyllite composition in Table 29.1 was calculated from gedrite-anthophyllite Fe-Mg distribution coefficients provided by Stout (1972).

Department of Geological Sciences, Queen's University, Kingston, Ontario. K7L 3N6

Figure 29.2. *P–T petrogenetic grid for calcium, alkali-deficient bulk compositions. Slope of univariant curves estimated by Clausius-Clapeyron equation, except those above tonalite solidus (schematic) and those of point 1 (schematic after Spear (1978a)). "Distance" between invariant points is arbitrary. The orthoamphibole solvus may have a positive dP/dT slope as inferred by Crowley and Spear (1981).*

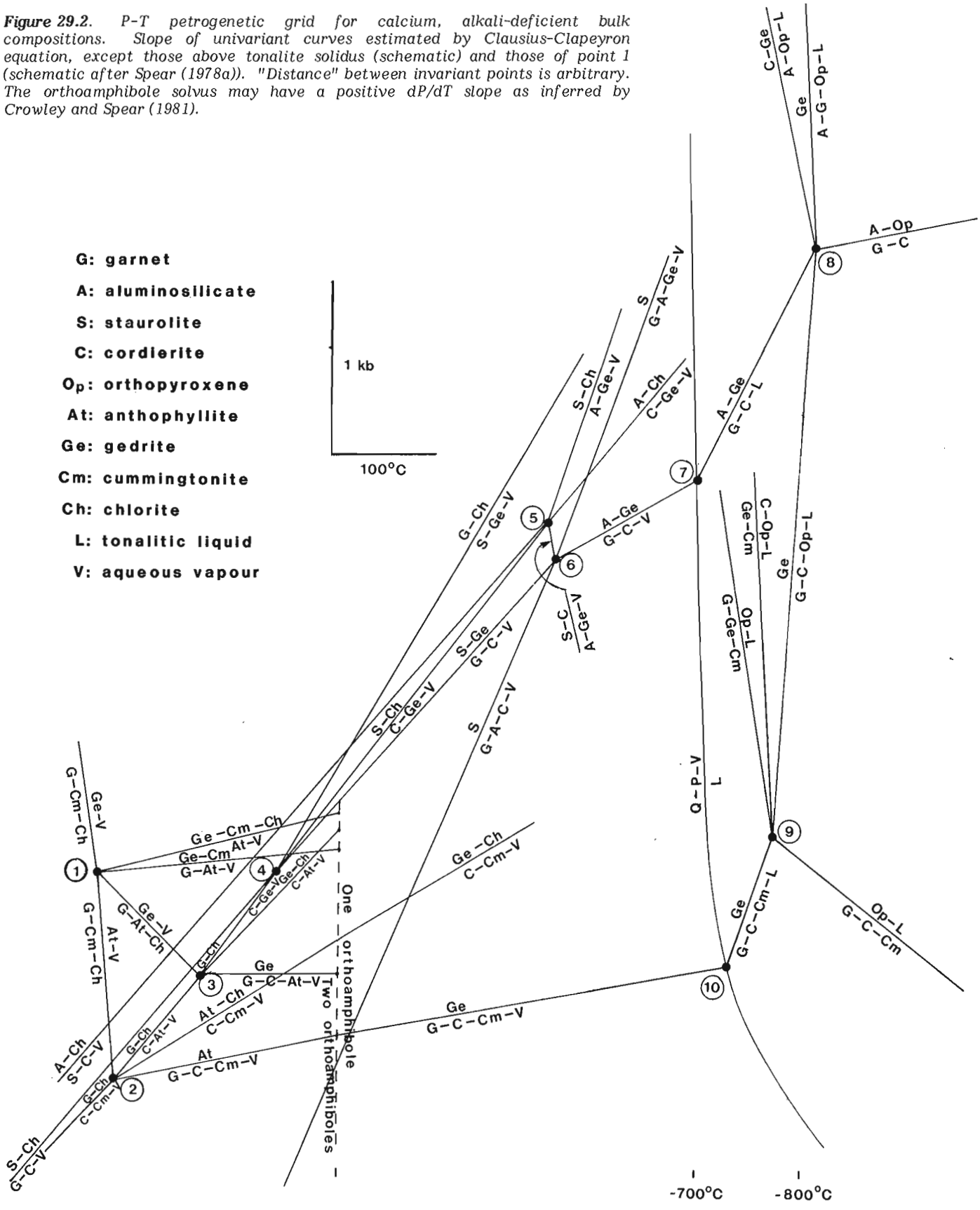

Table 29.1

Microprobe analyses (1-9) of minerals in two mafic gneisses from Hackett River

	1	2	3	4	5	6	7	8	9	10	11
SiO_2	28.08	49.28	45.85	26.47	38.05	27.75	48.46	43.92	53.15		
TiO_2	0.63	0.12	0.18	0.04	0.00	0.60	0.02	0.22	0.02		
Al_2O_3	52.68	32.99	12.75	22.40	21.33	52.29	32.58	14.30	2.24		
[a]FeO	13.12	5.69	22.83	17.51	32.71	13.79	6.43	23.72	25.27		
MnO	0.15	0.09	0.87	0.20	1.70	0.04	0.01	0.32	0.40		
MgO	2.81	10.02	14.87	20.52	4.26	3.18	9.00	13.05	16.48		
CaO	0.05	0.04	0.29	0.00	3.26	0.02	0.02	0.48	0.35		
Na_2O	0.26	0.52	1.81	0.33	0.01	0.38	0.70	1.63	0.44		
K_2O	0.00	0.00	0.02	0.05	0.00	0.02	0.00	0.03	0.01		
Total	97.88	98.85	99.61	87.56	101.46	[c]98.84	97.29	97.67	98.42		
Si	7.782	5.000	6.658	5.34	2.992	7.678	5.01	6.523	7.801	1.842	7.53
Ti	0.130	0.007	0.020	0.006	0.00	0.124	0.002	0.025	0.002		
Al(IV)		3.943	1.342	2.66			3.971	1.477	0.199	0.132	0.47
Al (VI)	17.210		0.84	2.675	1.977	17.051		1.026	0.188	0.132	0.47
[b]Fe^{3+}					0.049						
Fe^{2+}	3.038	0.482	2.772	2.967	2.102	3.189	0.556	2.873	3.101	0.921	3.040
Mn	0.034	0.007	0.107	0.035	0.113	0.008	0.001	0.04	0.05		
Mg	1.158	1.514	3.217	6.198	0.499	1.309	1.386	2.888	3.604	0.947	3.460
Ca	0.015	0.004	0.045	0.00	0.275	0.000	0.005	0.076	0.055		
Na	0.057	0.101	0.509	0.132	0.001	0.211	0.140	0.469	0.125		
K	0.000	0.00	0.004	0.014	0.000	0.000	0.000	0.006	0.002		
(O)	(46)	(18)	(23)	(16)	(12)	(46)	(18)	(23)	(23)	(6)	(23)

a) Total iron as FeO.

b) Fe^{3+} calculated stoichiometrically.

c) Total includes 0.51 wt% ZnO.

Specimen 1 No. 1: staurolite (inclusions in cordierite);
2: cordierite;
3: gedrite;
4: chlorite (assemblage also includes biotite, sillimanite (as inclusions in cordierite), quartz and ilmenite).

Specimen 2 No. 5: garnet;
6: staurolite (inclusions in garnet);
7: cordierite;
8: gedrite;
9: cummingtonite (assemblage also includes quartz, plagioclase (An_{50}), chlorite (secondary), biotite, and ilmenite);
10: orthopyroxene composition that would be in equilibrium with gedrite (3-8 average) (estimated from gedrite-orthopyroxene distribution coefficients from Savolahti (1966) and consistent with those of Grant (1978);
11: anthophyllite composition that would be in equilibrium with gedrite (3-8) (estimated from anthophyllite-gedrite distribution coefficients from Stout (1972)).

Based on the mineral composition data, the $Mg/(Mg+Fe^{2+})$ ratio of minerals increases in the following sequence: garnet, staurolite, gedrite, orthopyroxene, anthophyllite, cummingtonite, chlorite, cordierite (Fig. 29.1). A compilation of natural assemblage data suggests that incompatible mineral pairs are A-Cm, A-At, S-Cm, S-At, S-Op and Op-Ch.

The mineral compositions in Table 29.1, in addition to aluminosilicate, were used to deduce univariant reactions radiating from eight univariant points in the model system. Although mineral compositions (particularly $Mg/(Mg+Fe^{2+})$) vary with changing metamorphic grade, it was necessary to assume constant compositions for the purpose of balancing the reactions. Albite, anorthite, quartz and ilmenite were used in an attempt to balance reactions in the natural system, but these phases are omitted for clarity from Figure 29.2.

Hornblende, rather than biotite, is present with orthoamphibole in many areas (e.g. Stout, 1972; Spear, 1978a). This represents a bulk compositional difference which may alter the phase relations to some extent.

After balancing possible univariant reactions, the P-T slopes of the curves were calculated by the Clausius-Clapeyron equation. Values of ΔS_r were calculated by Robinson and Jaffe's (1969) method of assuming ΔS_r = 544 $dJ \cdot deg^{-1}$ per mole of H_2O released, plus 80 $dJ \cdot deg^{-1}$ per mole of Al changing from VI to IV co-ordination. Molar volumes of all phases were taken from Helgeson et al. (1978). The water content of cordierite was estimated at 1.5(OH) per formula unit (600°C, 5 kb cf. Holdaway and Lee, 1977).

The calculated slopes are plotted on Figure 29.2, along with a schematic tonalite minimum-melt curve, separating a vapour-phase present area of the grid from a vapour-phase absent region. The slopes of reactions above the solidus have been schematically steepened to take account of the low ΔV_r of anatectic reactions relative to the analogous dehydration reactions.

Results

The topology of invariant point 1 is taken from Spear (1978a). The slopes shown on Figure 29.2 are schematic after Spear because those calculated in this study are not compatible with Schreinemakers' analysis. This probably results from inadequate thermochemical data; the effect of aluminum content on the molar volume of orthoamphibole was not considered. Spear (1978a,b) inferred that this point is stable because it accounts for stable gedrite-anthophyllite-cummingtonite assemblages.

Points 2, 3 and 4 (Fig. 29.2) have the same topology as those of Spear's (1978a) grid, but the curves which intersect in low-μH_2O invariant points on the Spear grid terminate at vanishing points as they intersect the orthoamphibole solvus on the present grid.[1] The crest of the solvus is implicit at lower μH_2O (higher temperature) on the Spear grid. The critical assemblage required to support Spear's interpretation is cordierite-cummingtonite-gedrite-anthophyllite.

The P-T conditions of the crest of the orthoamphibole solvus are not well established. Hypersolvus orthoamphibole is reported from the sillimanite zone of the "Amphibole Hill" area (Robinson and Jaffe, 1969). Anthophyllite-gedrite pairs from Telemark, Norway are also from the sillimanite zone (Stout, 1972), where staurolite occurs rarely as inclusions in plagioclase. Exsolution lamellae in orthoamphibole from Hackett River suggest hypersolvus conditions. Here, garnet-biotite and garnet-cordierite thermometry (Holdaway and Lee, 1977) suggest temperatures of ∽600°C (Percival, 1978). Associated pelites with staurolite-quartz also have sillimanite and cordierite but no garnet (Percival, 1978, 1979), suggesting that the samples come from the low-grade side of the $S + Q \rightleftharpoons G + A + C$ boundary. Robinson and Tracy (1979) reported coexisting anthophyllite and gedrite from the orthopyroxene zone of central Massachusetts but indicated that Ti and Fe^{3+} might have stabilized gedrite. Subsolvus pairs reported by Spear (1978b) apparently equilibrated at ∽480°C (Bottinga and Javoy (1973) magnetite-quartz oxygen isotope calibration). The crest of the solvus is thus tentatively placed at ∽600°C.

The tonalite solidus is located on the grid at ∽700°C based on Kilinc's (1979) experimental determination of the quartz diorite solidus. Thus mineral assemblages including quartz and plagioclase would have coexisted with a tonalitic melt at temperatures above ∽700°C.

The topology of point 8 is modified from Korikovskii (1970) to be consistent with the phase compositions of Figure 29.1. Orthopyroxene-gedrite analyses by Savolahti (1966) and Grant (1978) indicate that gedrite has a lower $Mg/Mg+Fe^{2+}$ ratio than coexisting orthopyroxene, indicating that gedrite occurs within the G-A-Op triangle on the AFM diagram.

Orthopyroxene may first appear at the expense of assemblages containing cummingtonite (Fig. 29.2, point 9). Based on analyses of a cummingtonite-orthopyroxene pair, Robinson and Tracy (1979) postulated a continuous reaction, cummingtonite $\rightleftharpoons$ orthopyroxene + quartz + H_2O. Possible discontinuous reactions involving cummingtonite and orthopyroxene are included in Figure 29.2. Experiments on orthopyroxene stability at $X_{H_2O} = 1$ suggest minimum temperatures of ∽780-800°C (Hoffer and Grant, 1980; Clemens and Wall, 1981; Spear, 1981).

References

Bottinga, Y. and Javoy, M.
1973: Comments on oxygen isotope geothermometry; Earth and Planetary Science Letters, v. 20, p. 250-265.

Carmichael, D.M., Moore, J.M., Jr., and Skippen, G.B.
1978: Isograds around the Hastings metamorphic "low"; in Geological Society of America/Geological Association of Canada/Mineralogical Association of Canada, Toronto 1978, Field Trips Guidebook, p. 325-346.

Clemens, J.D. and Wall, V.J.
1981: Origin and crystallization of some peraluminous (S-type) granitic magmas; Canadian Mineralogist, v. 79, p. 111-132.

Crowley, P.D. and Spear, F.S.
1981: The orthoamphibole solvus: P,T,X(Fe-Mg) relations (abstract); Geological Society of America, Abstracts with Programs, v. 13, p. 435.

Grant, J.A.
1968: Partial melting of common rocks as a possible source of cordierite-anthophyllite assemblages; American Journal of Science, v. 266, p. 908-931.

[1] The portrayal of a solvus on the grid is not strictly valid because of the stipulation of constant mineral composition required to balance reactions. The inclusion of the orthoamphibole solvus requires that the aluminum contents of coexisting anthophyllite and gedrite vary continuously with temperature (Robinson et al., 1971; Spear, 1979). The slopes of the reactions involving anthophyllite and gedrite could thus also vary with temperature. Nevertheless, a schematic representation of the solvus is included because it does occur in nature.

Grant, J.A. (cont.)
1978: Orthoamphibole and orthopyroxene relations in high grade metamorphism of pelitic rocks (abstract); Geological Society of America/Geological Association of Canada/Mineralogical Association of Canada, Abstracts with Programs, v. 3, p. 411.

Helgeson, H.C., Delaney, J.M., Nesbitt, H.W., and Bird, D.K.
1978: Summary and critique of the thermodynamic properties of rock-forming minerals; American Journal of Science, v. 278A, 229 p.

Hoffer, E. and Grant, J.A.
1980: Experimental investigation of the formation of cordierite-orthopyroxene parageneses in pelitic rocks; Contributions to Mineralogy and Petrology, v. 73, p. 15-22.

Holdaway, M.J. and Lee, S.M.
1977: Fe-Mg cordierite stability in high grade pelitic rocks based on experimental, theoretical and natural observations; Contributions to Mineralogy and Petrology, v. 63, p. 175-198.

Kilinc, I.A.
1979: Melting relations in the quartz diorite-H_2O and quartz diorite-H_2O-CO_2 systems; Neues Jahrbuch für Mineralogie, Monatshefte 1979-2, p. 62-72.

Korikovskii, S.P.
1970: The influence of depth on the parageneses of K_2O-undersaturated alumina-rich metapelites; Contributions to Physico-chemical Petrology, v. 2, p. 59-87, Nauka Press, Moscow (in Russian) (translation available in library of the Geological Survey of Canada, Ottawa).

Percival, J.A.
1978: Stratigraphy, structure and metamorphism of the Hackett River gneiss dome, District of Mackenzie, N.W.T.; unpublished M.Sc. thesis, Queen's University, Kingston, Ontario.

1979: Kyanite-bearing rocks from the Hackett River area, N.W.T.: implications for Archean geothermal gradients; Contributions to Mineralogy and Petrology, v. 69, p. 177-184.

Robinson, P. and Jaffe, H.W.
1969: Chemographic exploration of amphibole assemblages from central Massachusetts and southwestern New Hampshire; Mineralogical Society of America, Special Paper 2, p. 251-274.

Robinson, P. and Tracy, R.J.
1979: Gedrite-cordierite, gedrite-orthopyroxene, and cummingtonite-orthopyroxene assemblages from ferromagnesian gneiss, sillimanite – K-feldspar zone, central Massachusetts (abstract); Geological Society of America, Abstracts with Programs, v. 11, p. 504.

Robinson, P., Ross, M., and Jaffe, H.W.
1971: Compositional field of the anthophyllite-gedrite series, gedrite-hornblende comparisons, and the anthophyllite-gedrite solvus; American Mineralogist, v. 56, p. 1005-1041.

Savolahti, A.
1966: On rocks containing garnet, hypersthene, cordierite and gedrite in the Kiuruvesi region, Finland. Part 1: Juurikkajarvi; Societe Geologique de Finland, Comptes Rendues, v. 38, p. 343-386.

Spear, F.S.
1978a: Petrogenetic grid for amphibolites from the Post Pond and Amonoosuc volcanics; Carnegie Institution of Washington, Yearbook, v. 77, p. 805-808.

1978b: The reaction: anthophyllite + garnet = hornblende + cummingtonite + gedrite from the Post Pond volcanics, Vermont (abstract); Geological Association of Canada/Geological Society of America, Abstracts with Program, v. 3, p. 496.

1979: The anthophyllite-gedrite miscibility gap: data from the Post Pond volcanics, Vermont (abstract); Geological Society of America, Abstracts with Program, v. 11, p. 521-522.

1981: An experimental study of hornblende stability and compositional variability in amphibolite; American Journal of Science, v. 281, p. 697-734.

Stout, J.H.
1972: Phase petrology and mineral chemistry of coexisting amphiboles from Telemark, Norway; Journal of Petrology, v. 13, p. 99-145.

Trzcienski, W.E.
1971: Staurolite and garnet parageneses and related metamorphic reactions in metapelites from the Whetstone Lake area, southeastern Ontario; unpublished Ph.D. thesis, McGill University, Montreal, Quebec.

30. **A TECTONO-METAMORPHIC FRAMEWORK FOR PART OF THE GRENVILLE PROVINCE, PARRY SOUND REGION, ONTARIO**

Project 760061

A. Davidson, N.G. Culshaw[1], and L. Nadeau[2]
Precambrian Geology Division

Davidson, A., Culshaw, N.G., and Nadeau, L., A tectono-metamorphic framework for part of the Grenville Province, Parry Sound region, Ontario; in Current Research, Part A, Geological Survey of Canada, Paper 82-1A, p. 175-190, 1982.

Abstract

Continuing field work in southwestern Grenville Province between the Grenville Front Tectonic Zone and the Central Metasedimentary Belt has revealed a network of continuous zones of various kinds of tectonite, along which predominantly northwest-directed movement has taken place. Tectonite zones outline domains and subdomains of distinctive character, and tend to truncate lithology, structure and metamorphism on one side. Domains with relatively high pressure granulite facies metamorphism, and eclogite-like rocks and sapphirine-bearing assemblages in tectonic inclusions suggest that tectonism occurred at deep crustal level. Sense of movement indicates emplacement of allochthonous crustal segments by northwest-directed ductile shear and thrusting, with maximum displacement along the tectonite zones. Such a mechanism is compatible with a Himalaya-type model for development of a thickened crust, and has implications concerning equation of rocks and orogenic events on opposing sides of the Grenville Front Tectonic Zone.

Introduction

Previous reconnaissance mapping in the Grenville Province, Ontario, in the region between the Central Metasedimentary Belt and Georgian Bay (Davidson and Morgan, 1981) established several distinctive domains, based on differences in lithologic assemblages, structural style and grade of metamorphism. It was suggested that zones of highly tectonized rock found at or near the margins of Parry Sound Domain and within Muskoka Domain may be the loci of deep crustal thrusting.

During the 1981 field season, work was concentrated in Britt, Parry Sound and Muskoka domains (op. cit., Fig. 41.2) in order to clarify geologic relationships and continuity within these domains, and particularly to study their boundary regions in more detail. Positions of some parts of these boundaries have been revised slightly (Fig. 30.1; compare op. cit., Fig. 41.3). Significant new discoveries, from northwest to southeast, include: a zone of intensely mylonitized rock developed in granitoid rocks at the northwest edge of Britt Domain, adjacent to the Grenville Front Tectonic Zone (Lumbers, 1978); continuation of megascopically folded plutons northeastward in Britt Domain; identification of a curvilinear zone of highly flattened rocks within Britt Domain, in which a tectonic nodule of mafic rock, possibly meta-eclogite, containing sapphirine and kyanite was found; continuation of inward-dipping, spectacular mylonite and related rocks along the west side, around the north end and part way along the east side of Parry Sound Domain; tectonite zones within Muskoka Domain that have remarkably continuous tectonic stratigraphy, are of more than one age, and can be used to divide this domain into several distinctly different subdomains; an older tectonite within one of these subdomains that contains thin sheets of highly flattened anorthositic gneiss, several kilometres long, with associated lenses of eclogite-like rocks (garnet pyroxenite) and metabasite containing sapphirine; the fact that older subdomains in Muskoka Domain underlie Parry Sound Domain at their mutual boundaries, and younger ones, including the Moon River Structure (Schwerdtner and Waddington, 1978), overlie both the older subdomains and Parry Sound Domain. Further details are outlined below.

The authors were ably assisted by P. Maenz, C. Pappas and D. Emerson, and acknowledge stimulating discussions in the field with J.M. Moore, J. Wood, W.M. Schwerdtner and C. Mawer. They are much indebted to W.J. Logan and D.J. Villard, Ontario Ministry of Natural Resources, Huntsville, for their co-operative assistance during the field season. L. Nadeau is currently studying mylonitic rocks developed from anorthositic gabbro at Parry Sound as his M.Sc. thesis topic at Carleton University, Ottawa.

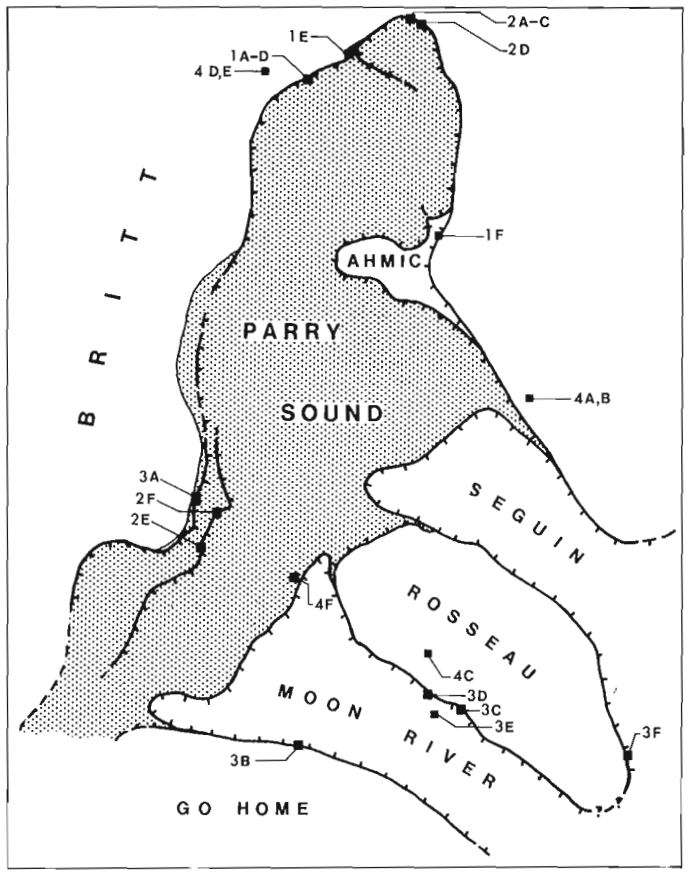

Figure 30.1. *Generalized map of structural subdivisions in the Parry Sound region. Main tectonite zones are shown as heavy lines with direction of dip indicated. Locations of all photographs in Plates 30.1 to 30.4 are given.*

[1] Université d'Ottawa, Ottawa

[2] Carleton University, Ottawa

Britt Domain

Reconnaissance mapping during the 1980 field season (Davidson and Morgan, 1981) enabled characterization of Britt Domain as a complex of highly deformed gneiss and migmatite of both supracrustal (predominantly sedimentary) and plutonic origins that has been subsequently intruded by a suite of younger plutons, followed by further migmatization and deformation. The predominant structural pattern is outlined by the younger plutonic rocks, now sheet-like masses that have been thrown into large scale folds whose axes plunge mainly gently to the southeast. It was stated that these folds become more open to the northeast (op. cit., p. 291). Mapping during 1981 has provided more comprehensive information on the gross internal structure of Britt Domain, and on the nature of its boundaries with the Grenville Front Tectonic Zone to the northwest and with Parry Sound Domain to the southeast.

Several sheets of younger deformed plutonic rocks are characterized by distinctive rocks or rock assemblages. This enables a regional 'stratigraphy' to be recognized and used in tracing units around the major folds. Thus from northwest to southeast the following 'succession' (up structural section) is apparent in the region close to Georgian Bay (plutonic rock nomenclature follows Streckeisen (1976); see Fig. 30.2):

i) pink to brown, K-feldspar megacrystic, clinopyroxene and/or hornblende quartz monzonite to granite orthogneiss;

ii) grey to dark grey garnet-hornblende-plagioclase orthogneiss derived from gabbro and/or diorite, with local plagioclase-rich (anorthositic) phases, and locally associated with small, lenticular masses of pink to light grey, fine, equigranular granitoid orthogneiss;

iii) grey hornblende-biotite granodiorite to tonalite orthogneiss;

iv) predominantly rose-pink, equigranular hornblende syenite to quartz syenite orthogneiss, with or without garnet, that has a characteristic buff to greenish-yellow clinopyroxene-bearing northwest border phase, and contains an internal unit of hornblende-plagioclase-garnet-scapolite orthogneiss of gabbro-diorite-anorthosite affinity;

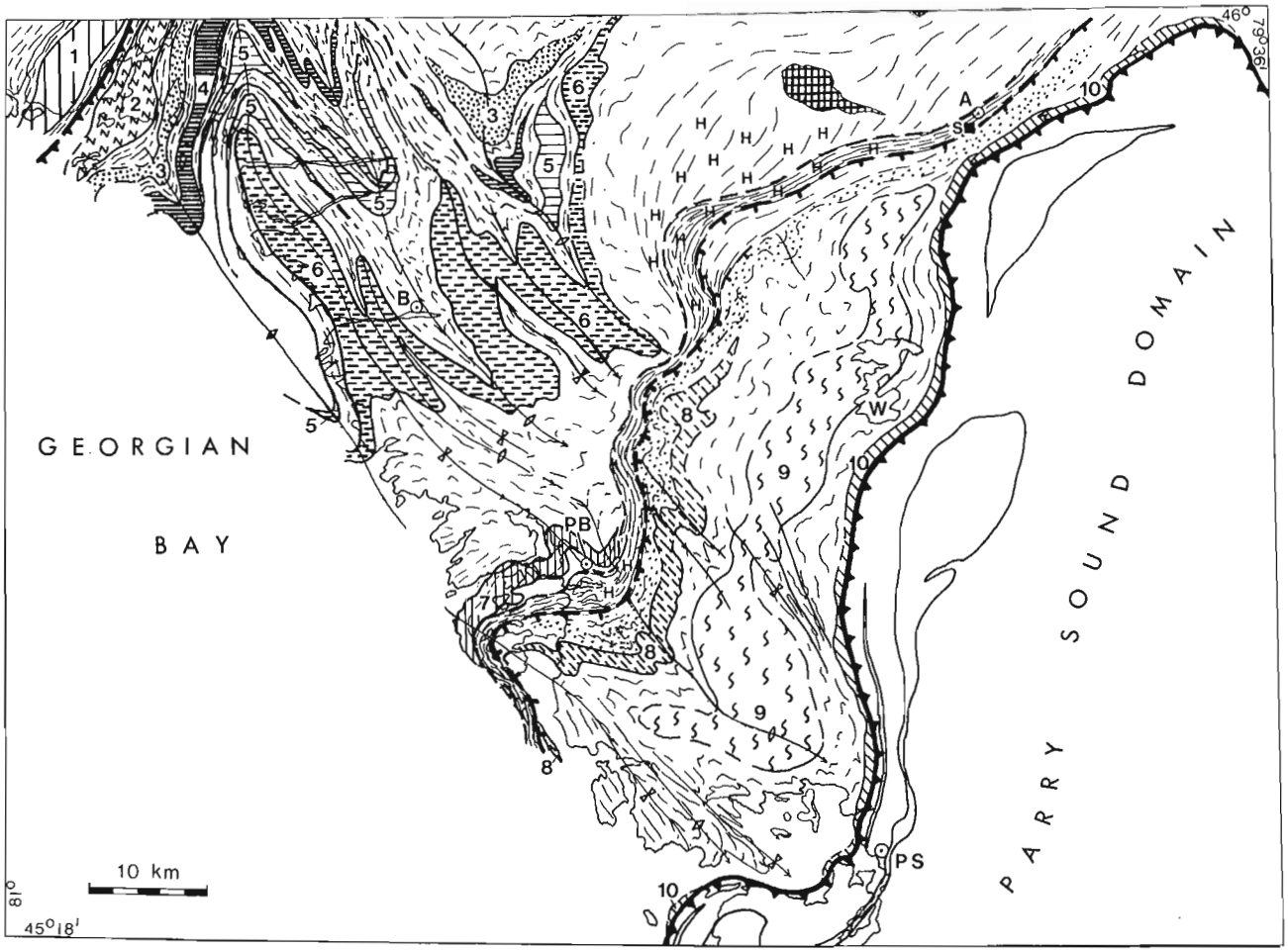

Figure 30.2. Distribution in Britt Domain of folded metaplutonic units (numbered), semipelitic and pelitic gneiss (stippled) and zone of highly tectonized rocks (close-spaced lines). H is hypersthene, S is sapphirine-bearing 'meta-eclogite' nodule in tectonite zone. See text for description of numbered units. Cross-hatched unit is Caribou Lake Gabbro. A – Arnstein, B – Britt, PB – Pointe-au-Baril, W – Wahwashkesh Lake, PS – Parry Sound.

v) two to three narrow and extensive sheets of grey biotite granodiorite orthogneiss, with rare hornblende and garnet and containing large, pink, polycrystalline K-feldspar megacrysts;

vi) a large unit, the Britt Pluton, of remarkably uniform hornblende-garnet-biotite granitoid orthogneiss, commonly streaked with self-generated migmatite sweats, whose composition straddles the quartz monzodiorite-granodiorite field boundary; where least deformed it contains K-feldspar megacrysts with single crystal cores, and it has a characteristic xenolith-rich border phase;

vii) grey, locally megacrystic (white plagioclase) biotite-hornblende quartz diorite to tonalite orthogneiss;

viii) a complex unit, the Shawanaga Pluton, of dioritic, tonalitic, granitic and garnet-rich syenitic orthogneiss;

ix) grey to pink, highly migmatitic and deformed biotite granitoid orthogneiss, with hornblende in the darker phases; composition ranges from granodiorite to granite; may be relatively old;

x) narrow plutons of pink, predominantly granitic orthogneiss, confined to the immediate margin of Parry Sound Domain.

To the east, variations in this succession are due to 'tailing out' of one or more plutonic units. Thus, east of Highway 69, an extensive unit of grey tonalitic to granodioritic orthogneiss (iii) is adjacent to the Britt Pluton (vi) where the metasyenitic and granitic plutons (iv and v) tail out to the northeast. Southwest of Pointe-au-Baril thin sheets of pink, K-feldspar megacrystic biotite granite orthogneiss make their appearance on either side of grey tonalitic orthogneiss (vii), but peter out northeastward, as does (vii). Most of the region between the eastern limit of the Britt Pluton and Arnstein (Fig. 30.2) is underlain by a highly complex series of metaplutonic units, including some charnockite; the Caribou Lake Gabbro is a younger intrusion.

Most of these plutonic units are separated from one another by country rock units of variable map width, ranging from narrow though continuous slivers to bands of gneiss several kilometres wide. The country rocks, too, show a crude compositional zonation from northwest to southeast. Thus, an assemblage of predominantly semipelitic gneiss (hornblende-biotite-plagioclase-quartz with red garnet) with quartzitic and pelitic interlayers (carrying sillimanite and/or kyanite, biotite, graphite, pyrite and characteristically violet-pink garnet, and lacking hornblende) has been traced from the Georgian Bay coast southwest of Pointe-au-Baril northeastward to beyond Arnstein (stippled unit in Fig. 30.2). This unit separates regions in which the country rock gneisses are derived mainly from quartzofeldspathic sedimentary rock and includes the pink, leucocratic, granular gneiss referred to as meta-arkose (Davidson and Morgan, 1981, p. 291-292).

Coinciding approximately with the semipelitic gneiss unit mentioned above is a zone of highly flattened rocks, best described by the terms mylonite and straight gneiss. Most of these gneisses are very fine and even grained and display thin layering of remarkable continuity. They appear to have been derived from both para- and orthogneisses, though commonly their protolith is indeterminate. This zone has a sinuous map trace, rather more so than the margin of Parry Sound Domain to the southeast (Fig. 30.2). As this zone is approached from the northwest, the degree of flattening gradually increases and metamorphic grade rises, judging from at first the intermittent and subsequently common occurrence of hypersthene. The southeast edge of this zone, on the other hand, is relatively abrupt, mylonitic gneiss giving over a few hundred metres to migmatitic gneiss at amphibolite grade. Within the most highly flattened part of this zone, pods and lenses of mafic rock are common. One of these, just south of Arnstein, has a core of light bluish green rock, studded with red-brown garnets, containing the unusual polymetamorphic mineral assemblage garnet-clinopyroxene-hypersthene-Al-amphibole-kyanite-quartz-plagioclase with small knots of sapphirine-corundum-spinel. This rock is tentatively identified as meta-eclogite, and is described more fully in another section of this report.

The northwest margin of Britt Domain is marked close to the Georgian Bay coast by a relatively abrupt increase in northeast-directed penetrative deformation, against which the northwest structures of Britt Domain abut. This is the margin of the Grenville Front Tectonic Zone, and is characterized by extreme flattening or elongation of quartz grains in granitoid rocks, and general reduction in grain size. These rocks are quartzofeldspathic granulites in the classic structural sense, although the term mylonite could also be applied to most of them. Similar rocks continue across strike to the northwest, where hypersthene-bearing gneiss, near Tyson Lake, has been reported (Frarey and Cannon, 1969, p. 3).

Parry Sound Domain

Traverses within the northern part of Parry Sound Domain served little purpose other than to emphasize i) the dominance of relatively mafic rocks, ii) the prevalence of granulite or retrograde granulite facies metamorphism in the central and eastern parts, and iii) the small scale and unpredictable continuity of mappable units. The mafic gneisses are particularly confusing to map, as they change insensibly from uniform rocks of probable plutonic parentage to well layered though commonly highly contorted gneiss. This problem was recognized in Lount Township by Satterly, who stated (1956, p. 15) that he "...found it difficult to identify and separate the members of (the plutonic rocks) from the amphibolite of the paragneiss-amphibolite group. Therefore basic intrusives and their metamorphic equivalents may be much more widespread than the geological map would suggest". Narrow layers of marble were found in many places, and can be used to trace out the regional structure (Fig. 30.3). They are almost invariably breccias of tectonic type, containing fragments, some highly contorted, of disaggregated silicate layers. Quartzite and Al-silicate-bearing gneiss are present locally, but are even more subordinate to the mafic rocks than are the marble breccias. Quartzofeldspathic gneiss and granitoid rocks are also of rare occurrence. Nowhere in Parry Sound Domain have preserved features such as pillows, clasts or phenocrysts been found to support the interpretation that the dominant mafic and intermediate gneisses were derived from volcanic rocks. Potential primary volcanic features invariably turn out to be of tectonic origin.

Overall, a dominantly northerly structure is apparent within Parry Sound Domain, although much deflected around ovoid masses of metadiorite and metatonalite (enderbite). Structural trends are parallel to the western edge of the domain, but are markedly truncated along the east and southeast sides (Fig. 30.3). Internally, careful mapping at a detailed scale must be undertaken before the confused pattern of this enigmatic terrane can be properly understood.

Definitions of Tectonite Terminology

Many references will be made in this paper to the term 'tectonite zone' and to various tectonic rock types occurring in these zones, considered to be of fundamental importance to the geological interpretation of this part of the Grenville Province. Before processing further, therefore, these terms and their usage are defined and discussed below, and various features of these rocks are illustrated in Plates 30.1-30.3.

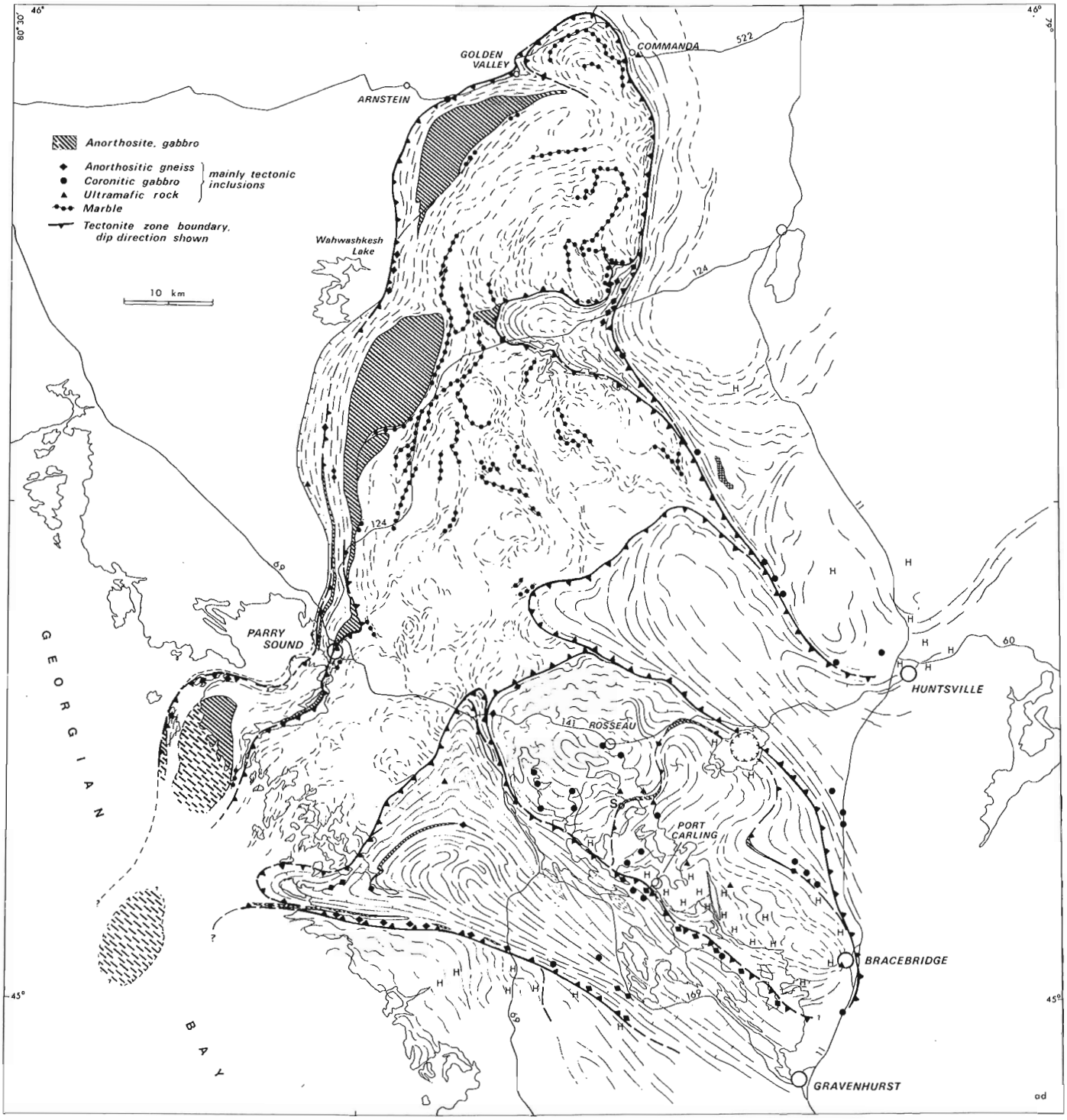

Figure 30.3. Structural trend map showing distribution and features of tectonite zones around Parry Sound and within Muskoka domains. Directions of dip are indicated. H is hypersthene occurrence in Go Home and Rosseau subdomains, S is sapphirine locality in metabasite lens in older tectonite zone.

It is emphasized at the outset that a large proportion of the rocks in this whole region are, in fact, tectonites, to the extent that most of their textural and structural features are the effects of tectonism. For example, primary internal features in metasedimentary gneisses are almost entirely lacking. Compositional layering nearly everywhere can be shown to have been severely transposed, locally so much so that enveloping surfaces cannot be traced; even if they can, it is not certain whether they represent bedding or an earlier transposed layering. All the plutonic rocks show a marked degree of recrystallization in all but the most 'structurally protected' parts of plutons, so that only deformed and attenuated relict igneous texture is preserved. Exceptions are parts of some anorthositic masses in Parry Sound Domain and in gabbroic bodies generally; the apparently greater resistance to deformation by recrystallization of their component minerals explains why these rocks in particular are preserved as tectonic blocks.

Increasing tectonic degradation of recognizable orthogneiss derived from plutonic rock leads to development of highly planar, uniformly fine grained rocks that, on their own, offer no ready clue concerning protolith. In the field, such rocks can easily be mistaken for metasedimentary gneiss, especially where a tectonic layering has formed. On the other hand, some kinds of metasedimentary gneiss have gone through the same process, producing the same kind of tectonite. An example of this is given by semipelitic gneiss in the vicinity of Pointe-au-Baril. In its best preserved state, this gneiss carries feldspar porphyroblasts, but where increasingly intensely tectonized it grades through flattened augen gneiss to uniformly fine grained gneiss. In this case, local, thin interlayers of rusty weathering pelitic gneiss, identified by its content of pale violet-pink garnet, sillimanite and/or kyanite, pyrite and graphite, provide the required evidence for origin. Much of this type of tectonite can be attributed to shear flattening, commonly accompanied by shear folding, at various scales, that appears to be late in the structural scene.

Tectonite Zones

The term 'tectonite zone' is applied to continuous and mappable zones in which rocks layered at various scales collectively display combinations of the following features that are ascribed to tectonism:

- Evidence for reduction of grain size where a progenitor can be deduced (Plates 30.1A, B, E, F, 30.2 A, E, F).
- Single and aggregate mineral flattening or extension (Plate 30.2 A, D-F).
- Sigmoidal augen (feldspars, rarely garnet and hornblende) (Plate 30.2E, F).
- Various sized block, lenses and boudin-like masses, commonly isolated and usually mafic or anorthositic, unlike the enclosing material, and exhibiting discordant or rotated internal structure (Plates 30.1B, D, 30.3A-E).
- Straight foliation and remarkably continuous small scale layering (Plates 30.1E, 30.2A, E, 30.3A, B, D, F).
- Sheath folds, particularly in fine grained layered rocks (Plate 30.1E).
- Lobate, bulbous or detached folds (Plates 30.1B, 30.2B, C).
- Complex mesoscopic folds reminiscent of viscous flow (Plates 30.1B, C, 30.2A, C, D, F).
- Internally cut-off structures in gneiss in which there seems to be no reason for ductility contrast (Plate 30.3F).

In many places, rocks with some of these features are of indeterminate parentage, and some are undoubtedly tectonically mixed.

Tectonite zones can be traced continuously for many tens of kilometres along strike, and are relatively narrow with respect to their lengths. Generally from a few to many hundreds of metres thick, they naturally appear wider on maps where their dips are moderate or shallow. The zones are relatively sharply defined on the sides that truncate older structural trends, and are gradational on the opposing sides with parallel structure. In certain segments, adjacent structure is parallel on both sides, but nowhere is it known to be grossly discordant on both sides. Map traces for the most part are gently sinuous, but locally are abruptly though continuously curved. Evidence for truncation of one tectonite zone by another will be discussed later in the paper.

The types of tectonic rock that occur in these zones vary both along and across strike, likely due to a combination of three factors: i) different types of parent rock adjacent to the zones give rise to tectonites of different aspect; ii) transverse gradations may be due to variation in rate of strain, as suggested by the fact that the most highly strained rocks tend to occur at the sides of zones adjacent to truncated older structure; iii) longitudinal variation may be related to the crustal level at which tectonism took place; increase in grain size and development of quartzofeldspathic leucosome may be evidence for this.

Tectonic Rock Types

The term mylonite is applied to predominantly fine grained rock, usually thinly layered and containing mineral augen or porphyroblasts that may or may not show sigmoidal structure. Internal folding may be pronounced (Plates 30.1A, B, 30.2A, E, F). The term mylonite gneiss is used where relicts of the original mineralogy and texture, particularly in metaplutonic rocks, are discernible. Mineral grains have the form of small augen and are surrounded by foliated, comminuted mineral grains (flaser structure). The term protomylonite may be appropriate in some cases. Associated with mylonite around most of the north end and along part of the east side of Parry Sound Domain are tectonites derived from mafic gneiss, amphibolite and gabbroid rocks. These contain numerous rotated mafic blocks in a granular or streaky mylonitic matrix, and have been referred to as mafic block tectonite; the term mafic mélange is also suitable, but only for those parts, perhaps, that lack a pronounced layered structure (Plate 30.2D).

Thin sections of these tectonites show very little residual mineral strain. Although very fine grained, polygonal grain shape is common in the matrix material, particularly in quartz and feldspars. Elongate quartz lenticles, where present, are generally composed of essentially strain-free, end-to-end rectanguloid grains. Mineral growth is apparent as porphyroblasts, particularly of garnet and hornblende. Foliation may be given by oriented new biotite flakes and by matrix hornblende, but many mylonites are granular with a fine sandy texture. The term 'blastomylonite' connotes grain growth, generally equated with increase in grain size rather than with simple and continued recrystallization of fine grains. Because it is considered that the mylonites in this region are not recrystallized mechanically crushed rocks, in other words that they formed below the level of brittle-ductile transition, the term 'blastomylonite' will not be used. Coarser gneissic rocks in the tectonite zones may have formed, at least in part, under conditions favouring enhanced rates of crystallization during

tectonism, not necessarily by late- or post-tectonic grain growth alone. To these rocks the term 'tectonite gneiss' is applied. Tectonite gneisses contain many features of tectonic origin, such as sigmoidal feldspar augen, internal structural truncations and isolated tectonic inclusions (Plate 30.3D, F). They may be relatively homogeneous or have lensoid to continuous compositional layering. Where they contain numerous tectonic inclusions, particularly adjacent to the coherent rocks of Parry Sound Domain, they are referred to as tectonoclastic gneiss (Davidson and Morgan, 1981, Plate 41.1F). All gradations exist between mafic block tectonite and tectonoclastic gneiss, the difference being mainly one of matrix grain size and mylonitic appearance of the former. Similarly there is a gradation between mylonite and tectonite gneiss, with both occurring interleaved in places. An arbitrary grain size limitation seems inappropriate because intermediate rocks show much internal grain size variation, but as a rule tectonite gneiss would be described as fine to medium grained rather than fine to very fine grained.

The term 'straight gneiss' is used to describe rocks of dominantly fine grain that are continuously foliated and generally layered. For the most part they are S-tectonites, with S > L (Plate 30.3B). Layers are normally thin and persistent, but need not be as compositionally pronounced as in Plate 30.1E. Layering is straight or gently undulating, but shear or sheath folds are developed locally. Extremely tight isoclines with pointed crests and straight limbs may be present. Tectonic inclusions are rare, and augen are small and flattened in the foliation plane, although they may be mildly sigmoidal where a mineral lineation is present (mineral streaks on foliation surfaces). Straight gneiss has much in common with uniformly layered, very fine grained mylonite, such as its even granular texture. Polycrystalline quartz plates are locally evident, but more commonly quartz occurs as tiny equant grains that may or may not be dispersed along particular foliae. Both mylonite and tectonite gneiss may grade into straight gneiss, the main differences being, on the one hand, the style of internal folding and augen development, and on the other, less regularity of grain size.

Many units of tectonite gneiss are migmatitic in varying degree. In most, the leucosome is more or less flattened in the plane of layering, except where associated with pressure shadows of tectonic inclusions. Some straight gneiss shows extremely attenuated quartzofeldspathic lenses and is likely an advanced deformation state of tectonite migmatitic gneiss. Migmatization may follow tectonite formation, with irregular leucosome coarser than its host (Plate 30.3E).

Nature of the Parry Sound Domain Boundary

It was stated in last year's report (Davidson and Morgan, 1981) that along the west-northwest side, Parry Sound Domain is limited by the occurrence of narrow but continuous bodies of granitoid orthogneiss, beyond which relatively leucocratic quartzofeldspathic gneiss and migmatite predominate. It was also recognized that zones of mylonite and mylonite gneiss occur parallel to, but generally within and close to the edge of this domain. There is considerable discordance of gross structural trend between Parry Sound and Britt domains, particularly noticeable west of the town of Parry Sound.

Field work in 1981 has demonstrated that the Parry Sound Domain margin is a tectonic one in its entirety from the northern part of its west-northwest side, around the north end, and all along the east and southeast side. The southeast margin, however, is not a single, inward-dipping tectonite zone, but rather a sequence of zones that dip alternately toward and away from Parry Sound Domain, these alternations being directly related to structural subdomains within the adjoining Muskoka Domain to the southeast (Fig. 30.3). Following the Parry Sound Domain boundary clockwise from Wahwashkesh Lake, a zone of highly tectonized rock that affects both Parry Sound mafic and pelitic gneiss and its adjacent granitoid orthogneiss extends north and then northeastward along Highway 522 to Golden Valley, with maximum tectonic modification close to the lithological boundary (Plate 30.1, A-D). Just east of Golden Valley, a major change in orientation of the tectonite zone, from easterly to northerly, coincides with a zone of strongly foliated rocks that penetrates east-southeast into Parry Sound Domain. Continuing clockwise from Golden Valley, a zone of equally intensely tectonized mafic rocks, full of rotated mafic blocks in a highly confused and contorted, dominantly mafic matrix (Plate 30.2, A-D), forms a gently inward-dipping arc defining the northern extremity of Parry Sound Domain. This arcuate segment has a remarkably continuous stratigraphy, consisting of a 'basal' mafic tectonite overlying a deformed granitoid orthogneiss unit, and overlain, in order, by pelitic tectonite gneiss (kyanite-bearing), more mafic gneiss, in part tectonized, marble tectonic breccia, interlayered mafic, intermediate and feldspathic gneiss with quartzite, passing upwards to complexly mixed gneisses in granulite facies. This sequence becomes attenuated along the east margin south of Commanda, the tectonite zone becomes steeper, and the trend of the Parry Sound gneisses becomes nonconformable with the margin. Mafic block tectonite marks this boundary almost as far south as Highway 124, where the scene is complicated by a splitting of the bounding tectonite zone. The main zone continues south and then southeast, diverging and rejoining the edge of Parry Sound Domain, and finally diverging again, from whence it has been traced continuously as far as Huntsville; everywhere along its length it dips moderately west or southwest. Its character changes southward from Highway 124, the dominant tectonite becoming increasingly flattened, very fine grained straight gneiss. In the vicinity of Highway 124, Parry Sound Domain continues to be bounded with marked structural truncation by a relatively narrow tectonite zone that outlines a dome-like region, the Ahmic subdomain, consisting of well layered quartzofeldspathic gneiss, marginally conformable granitoid orthogneiss slivers, and a core of highly migmatitic gneiss that grades eastward to tectonite gneiss. The rock assemblage in Ahmic subdomain closely resembles that in Britt Domain to the west, and it is conceivable that the two are connected beneath Parry Sound Domain.

Structure, lithology and metamorphic facies of Parry Sound Domain are sharply truncated by tectonites along the entire southeast margin. More complex than previously stated (op. cit., p. 294), description of this boundary is best left until the tectonic subdivisions of Muskoka Domain have been outlined.

Plate 30.1

Tectonic features, margin of Parry Sound Domain.
See Figure 30.1 for locations.
Coin in B and C is 1.9 cm diameter.

A – Mylonite with flow folds (GSC 203770-N);

B – Free-floating, internally folded mafic block in mylonite (GSC 203770-S);

C – Apparent interference fold in mylonite, likely formed in one stage by material flow (GSC 203770-C);

D – 'Turbid flow folding' in mylonite (GSC 203770-U);

E – Sheath fold in straight gneiss, with plunge directly away from viewer (GSC 203770-R);

F – Disrupted structure of mylonite developed from pelitic gneiss (GSC 203669-Z).


A

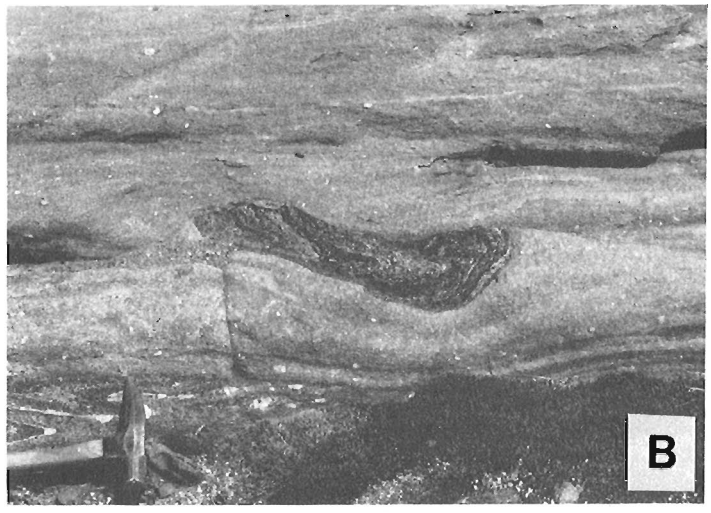
B

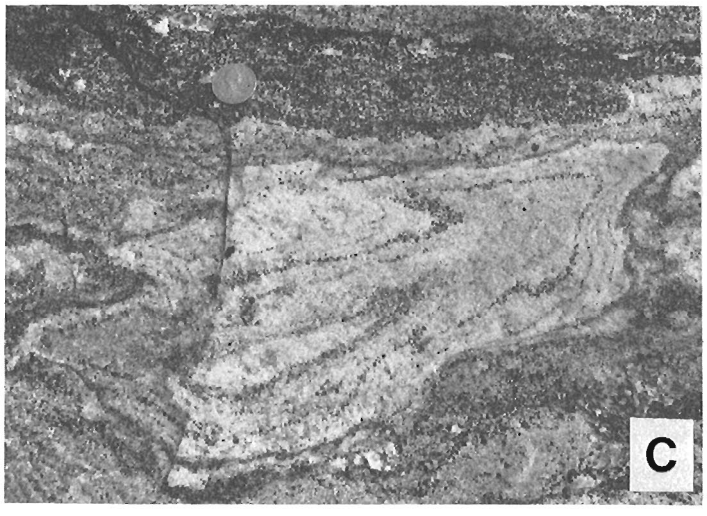
C

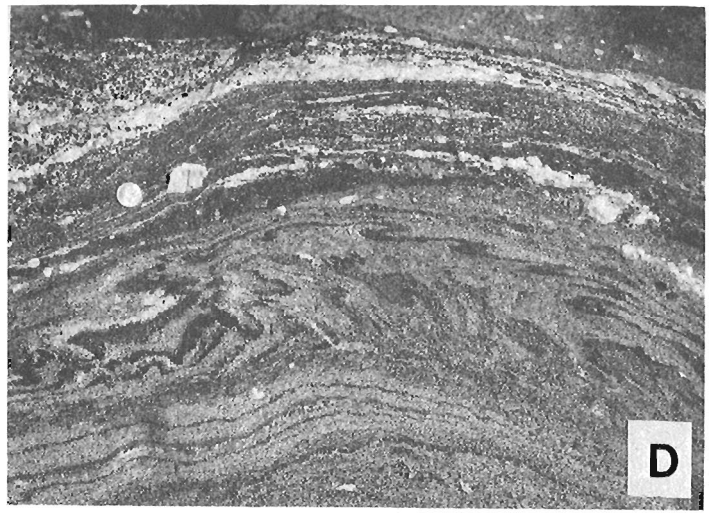
D


E


F

Tectonic Subdivisions Within Muskoka Domain

Muskoka Domain was originally stated (op. cit., p. 294) to be "...characterized by parallel, northwest-trending belts of relatively straight-layered gneiss in amphibolite facies, separated by terranes with less regular structure, higher metamorphic grade and a higher proportion of orthogneiss...". A zone of 'tectonoclastic gneiss' was described as partly bounding the Moon River Structure. Recent work has shown conclusively that not only is the Moon River Structure completely bounded by inward-dipping tectonite gneiss, but that other subdomains within Muskoka Domain are also similarly bounded (Fig. 30.1, 30.3). What is more, these subdomains themselves contain internal tectonite zones (zones of markedly high strain) that are in places truncated by the subdomain boundary tectonite zones. Much further work is needed, but it seems fairly certain that an emerging age hierarchy will enable a considerable history of regional tectonic development to be worked out. The tectonic subdivisions, their mutual relationships and disposition with respect to Parry Sound Domain are described below from southwest to northeast.

Go Home subdomain dips beneath and truncates structure in Parry Sound rocks among the islands off the coast of Georgian Bay. It is in turn overlain, and has its own structure truncated, by the Moon River Structure (subdomain) along a zone of tectonoclastic gneiss with sharp southern and gradational northern boundaries. Associated with this tectonite zone are long, narrow slivers of highly recrystallized and grain-reduced meta-anorthosite that breaks apart to give various sized, isolated clasts in the tectonoclastic gneiss close to its southern boundary. Along its northwest edge, the Moon River Structure is bounded by relatively narrow, branching mylonite and tectonite gneiss zones that dip away from Parry Sound Domain, truncating Parry Sound structure at right angles, and enclosing wedges of Parry Sound rocks in which older structural trend and metamorphism are preserved. The northeast margin of the Moon River Structure is an analogue of its opposite side, marked by a broad, shallowly southwest dipping tectonite zone characterized by numerous mafic blocks and lenses and, extending at least 25 km to the southeast of Port Carling, by slivers and rounded blocks of anorthositic gneiss (Plate 30.3, C). Internally, the Moon River Structure contains a variety of pink and light to dark grey migmatitic gneisses, including many with features highly evocative of tectonic origin. The long, curved sliver of anorthosite gneiss outlining the core of this structure may mark an internal zone of increased strain; anorthositic blocks are present along the line of its south-southeast projection.

Rosseau subdomain, like Go Home subdomain, is domal to the extent that it is bounded by a continuous, outward-dipping tectonite zone. Along its northwest margin it dips beneath Parry Sound Domain, again with marked truncation of Parry Sound lithology, structure and metamorphism. It contains an older tectonite zone, characterized by straight gneiss, that is discontinuously the locus of narrow slivers of anorthositic and mafic gneiss several kilometres long and only a few tens of metres wide in most places. Sapphirine has been identified in mafic tectonite at one locality (S in Fig. 30.3). This internal tectonite zone serves to separate a central and southeastern complex of para- and orthogneiss in granulite facies from predominantly migmatitic rocks containing numerous, scattered coronitic metagabbro and ultramafic blocks.

The Seguin Structure is analogous to the Moon River Structure, being a synformal lobe that overlies all its adjacent domains. It seems likely that these two structures are continuous around the southeast end of Rosseau subdomain, and thus may have once formed a complete carapace over it. By extension, Go Home subdomain and at least part of Algonquin Domain to the northeast may have been similarly covered. What emerges is a pattern of windows of an older terrane seen through a partly eroded, migmatitic gneiss cover whose structural base is marked by a tectonite zone. It is possible that the present disposition is due, at least in part, to subsequent, mild uplift of Go Home and Rosseau subdomains as structural entities, but initial structural analysis of tectonic transport direction, on the basis of the trend of stretching lineations and the sense of twist of sigmoidal mineral augen and rotated tectonic inclusions, is more suggestive of lateral mass transport toward the northwest.

Lineation and Sense of Tectonic Transport

Two complimentary features serve to give a relative sense of tectonic transport in rocks of the tectonite zones: i) sigmoidal augen, generally of feldspar, and ii) apparent sense of twist of foliation or layering in tectonic inclusions. Davidson and Morgan (1981, p. 294) suggested that sigmoidal augen may have been derived from former pegmatite by disaggregation during shearing. However, it seems likely that the subsequent history of individual feldspar clasts so formed is more complex than a simple drawing out of tails of neoblastic feldspar from an original single crystal grain. This may be the starting mechanism, but it may continue until the original grain is entirely comminuted by recrystallization, leaving, perhaps, only a small bulge in a thin seam of fine, granular feldspar. This bulge could cause a perturbation and development of a wave in an otherwise planar flow regime, and could become the site of preferential growth of a single grain. Growth might then continue as shearing feeds back material from the former tail to the nucleation site. The effect of this mechanism would be to reverse the sense of apparent twist, as shown in Figure 30.4A. It would be possible also to start with a seam of granular feldspathic material derived by some other means, equivalent to stage 3 of Figure 30.4A. Alternatively, it would be possible to derive the highly sigmoidal feldspar augen by 'rolling up' the shear tails of a feldspar clast that retained its coherence throughout the process (Fig. 30.4B), probably with late-stage growth. The end-form is the same in all cases, and can be used as a transport direction indicator.

An important and consistent field observation is that the sigmoidal mineral augen give a sense of movement in the direction of the linear element in their host rock, such as elongate quartz plates (Plate 30.2F). When viewed along the lineation direction, feldspar augen give no sense of twist, indicating that the lineations in such rocks are stretching lineations, oriented in the direction of tectonic transport.

Plate 30.2

Tectonic features, margin of Parry Sound Domain.
See Figure 30.1 for locations.
Coin in A and C is 2.4 cm diameter.

A – Augen mylonite (GSC 203770-H);

B – Same with tectonic lens showing lobe folds (GSC 203770-T);

C – Detached lobe folds in mylonite (GSC 203770-D);

D – Mafic block tectonite (GSC 203770-M);

E – Sigmoidal feldspar augen in mylonite developed from metagabbro (GSC 203770-P);

F – Sigmoidal feldspar in mylonite developed from granitoid rock, Mill Lake Quarry, Parry Sound; cut specimen illustrates that axis of rotation is perpendicular to quartz lineation (GSC 203195-K).

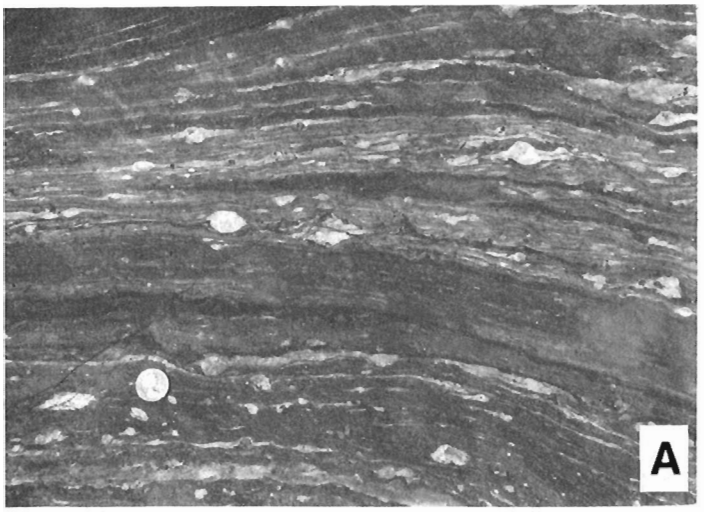
A


B

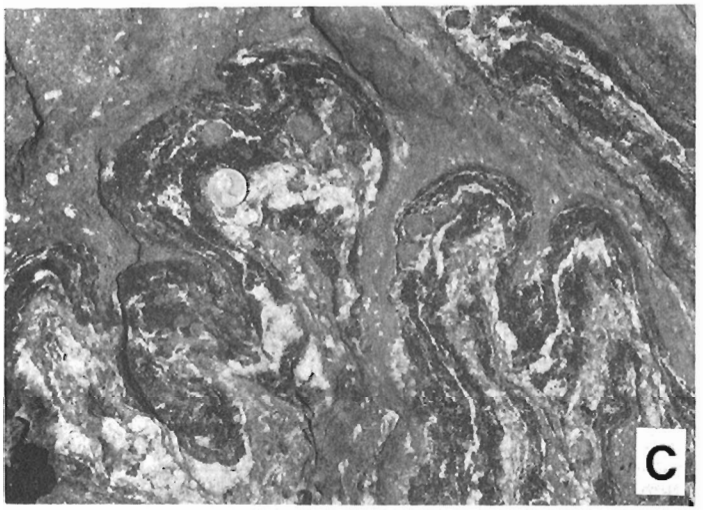
C


D

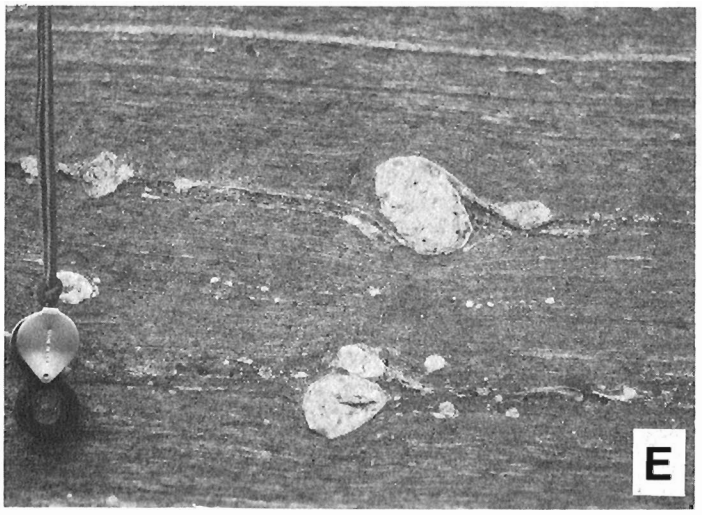
E

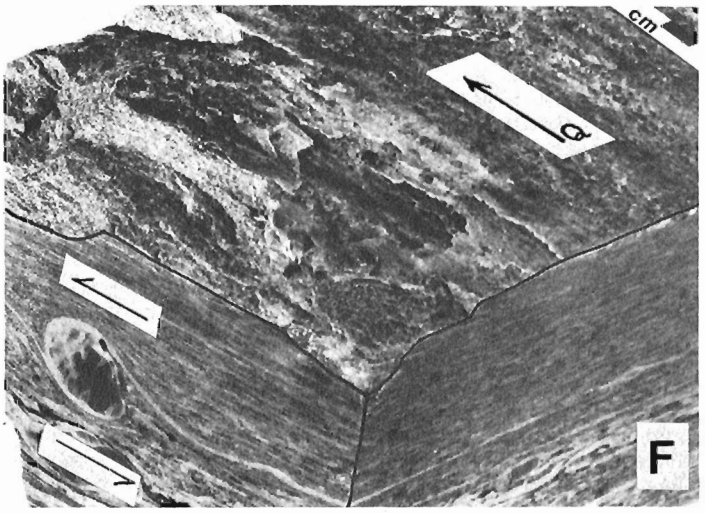
cm
a
F

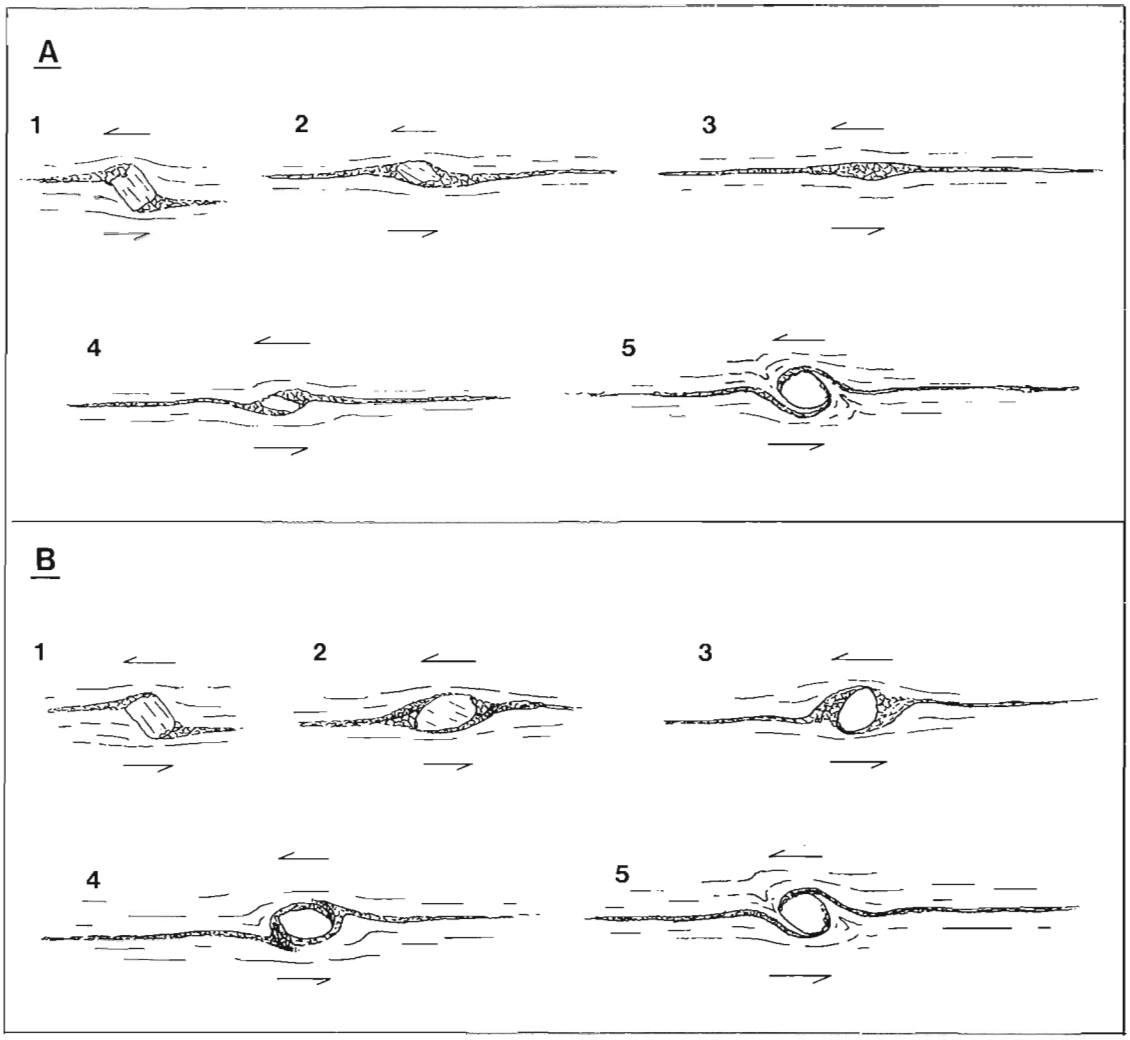

Figure 30.4. *Alternative modes of formation of sigmoidal feldspar augen in tectonites, developed from original porphyroclast: A 1-3, degradation to highly attenuated granular lenticle; 4-5, regrowth of augen during continuing shear; B 1-5, similar, except that porphyroclast retains single crystal core. Starting and end forms are the same in both cases. Note change in apparent sense of rotation.*

It is rare to find tectonic inclusions that give an unequivocal sense of rotation, but they do exist and should be further sought; an example is shown in Plate 30.3B. This and other examples indicate the same sense of movement as do sigmoidal augen in the same rocks.

Preliminary observations of these relationships intimate a dominant sense of transport overriding toward the northwest quadrant in northeast-oriented tectonite zones, as at the westerly edge of Parry Sound Domain. In northwest-oriented zones, as at the margins of the Moon River and Seguin structures, a relative sense of northwest-directed sliding of the overlying subdomains is indicated. A few examples of relatively late shear folds are present in some mylonites and straight gneisses. These fold the stretching lineation and have axes at high angles to the regional lineation direction. Some indicate the same sense of transport as the sigmoidal augen, that is, upper side northwest. By far the majority of stretching lineations plunge moderately or gently to the southeast. Tectonic transport, of whatever magnitude, is therefore dominantly upward toward the northwest, supporting the notion of thrusting.

Plate 30.3

Tectonic inclusions and features of tectonite gneiss.
See Figure 30.1 for locations.
Coin in B and C is 2.4 cm diameter.

A – Isolated boudin-like inclusion of garnet amphibolite in tectonite developed from semipelitic gneiss (GSC 203770-O);

B – Sigmoidal foliation trace in spindle-shaped hornblende-plagioclase gneiss inclusion in uniform straight gneiss containing highly flattened quartz, hornblende porphyroblasts (GSC 203667-C);

C – Disoriented anorthosite gneiss inclusions in tectonite gneiss (GSC 203770-V);

D – Common shape of isolated mafic inclusions in tectonite gneiss (GSC 203669-T);

E – Migmatitic tectonoclastic gneiss with post-tectonic quartzofeldspathic leucosome (GSC 203770-W);

F – Discontinuity in tectonite gneiss; rocks on either side of discordance appear identical and offer no reason for ductility contrast (GSC 203669-Y).

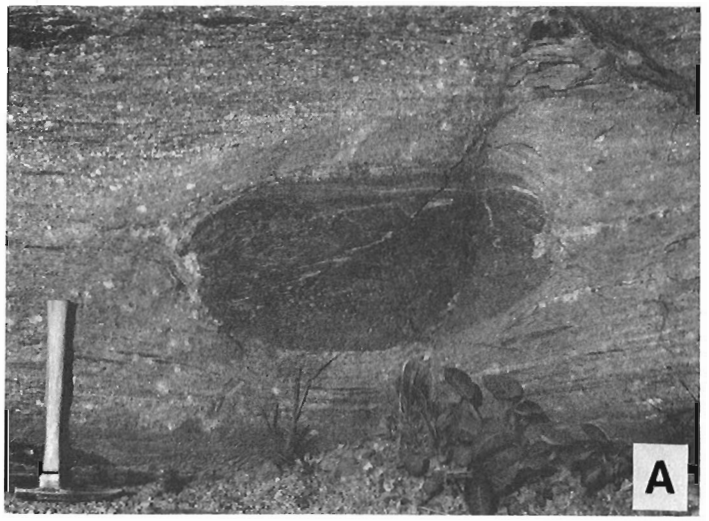
A

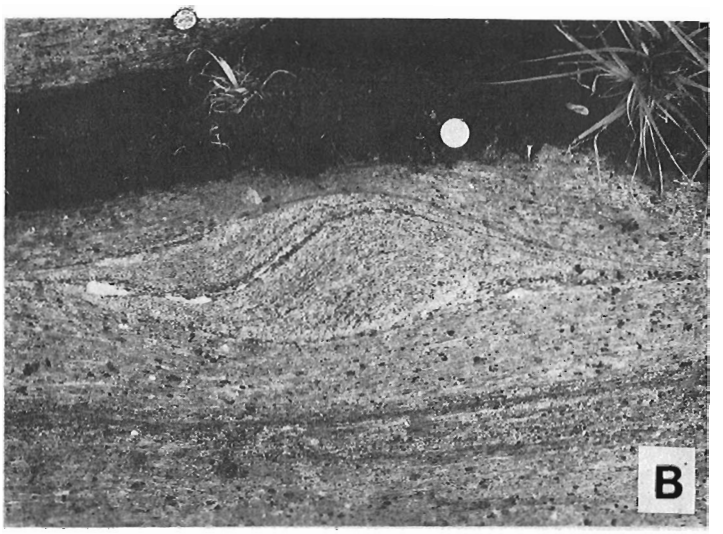
B

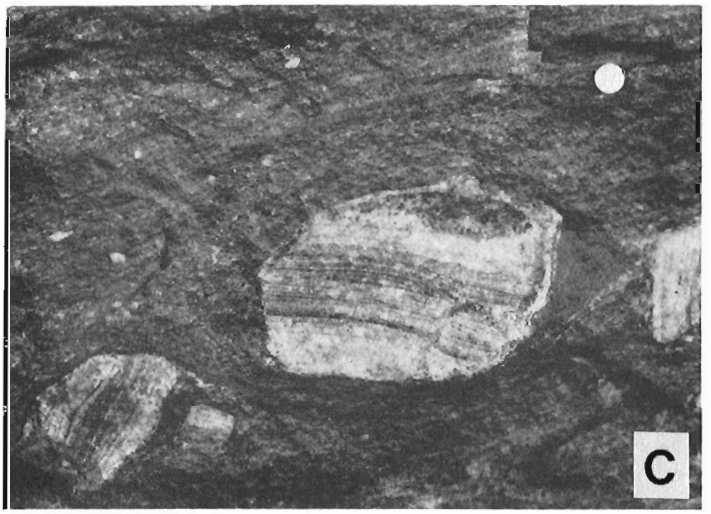
C

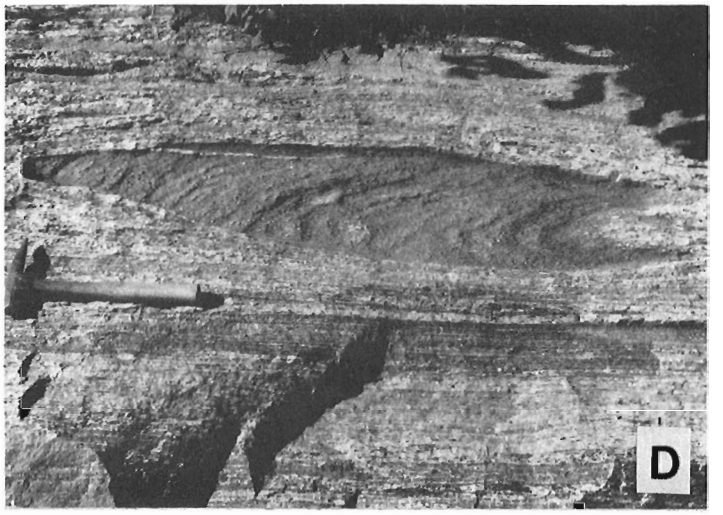
D

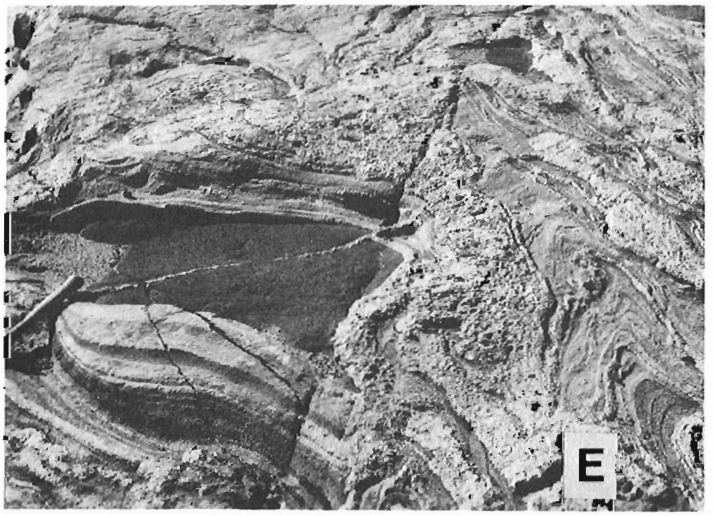
E


F

Metamorphism

As previously outlined (Davidson and Morgan, 1981), middle to upper amphibolite facies dominates in Britt Domain, granulite facies in all but the western part of Parry Sound Domain, and both facies are present in Muskoka Domain. Preliminary field studies near the west side of Algonquin Park suggest that alternating zones of amphibolite facies gneiss and of hypersthene-bearing granulite developed from highly flattened plutonic rocks are characteristic of Kiosk Domain, whereas Algonquin Domain to the south is predominantly in granulite facies. Distribution of metamorphic facies within Muskoka Domain is now known to be related to the subdomains outlined above. Granulite facies is restricted to parts of the domal Go Home and Rosseau subdomains, and is most obvious among metaplutonic rocks, among which olive-green and buff hypersthene-bearing orthogneiss is common. Metamorphism within the Moon River and Seguin structures is at amphibolite grade, although it must be admitted that few rocks with diagnostic assemblages have been found; quartz, two feldspars, biotite and hornblende, with rare clinopyroxene, garnet and epidote, comprise the mineral assemblages in the overwhelming majority of rocks. Small areas of hypersthene-bearing dioritic rock near the margins of the Moon River Structure seem best interpreted as tectonic enclaves of older, higher grade rocks. However, charnockitic rocks occur in the core of the Seguin Structure west and southwest of Huntsville, and where the northeast limb of this structure swings through east to northeast in the vicinity of Huntsville, regional grade changes gradually and apparently progressively from amphibolite to granulite facies.

Coronitic Metagabbro

Of particular interest are the metamorphic mineral assemblages found in mafic rocks that are incorporated as blocks and lenses in the tectonite zones, both within and bordering the various domains and subdomains. One of the commonest types of mafic rock is a distinctive metagabbro that, despite varying degree of metamorphic recrystallization, retains relics of former ophitic texture and, locally, coarse grain size, with plagioclase and augite up to 3 cm. A few relatively large (more than 1 km) bodies of this rock type occur within all domains except Parry Sound Domain. Least altered parts of these masses contain olivine, intimating troctolitic nature. But even in these least altered troctolites, reaction rims (coronas) separate olivine and plagioclase. The coronas are compound, composed of successive rims of orthopyroxene (closest to olivine), clinopyroxene, pale amphibole, and garnet (Plate 30.4, A). The inner part of the garnet rim is commonly microsymplectitic with clinopyroxene and rarely spinel. Primary plagioclase laths are usually fully clouded with fine oriented inclusions, much of which appears to be green spinel. The oriented nature of this fine intergrowth is suggestive of exsolution (Plate 30.4, B). Opaque oxide grains in these rocks also have coronas, generally of brown amphibole and red-brown biotite, surrounded by an outer rim of garnet. Clinopyroxene is not rimmed, and is usually so full of tiny, dark, exsolved inclusions as to render it almost opaque in thin section.

In more advanced stages of corona development, olivine disappears, having been replaced by granular aggregates of orthopyroxene, surrounded by much enlarged and less regular coronas of the same minerals outlined above. Garnet encroaches farther into the original plagioclase laths, and a more sodic, clear plagioclase forms a mosaic between the garnet and amphibole rims; this texture is referred to as a plagioclase moat by McLelland and Whitney (1980a,b), who have admirably illustrated similar textures in metagabbro from the Adirondack region of New York. Continued reorganization, accompanied by hydration, eventually reduces these coronites to garnet amphibolite in which the garnet, encroaching from all sides, has collected at the centres of former plagioclase grains first as strings of crystal and finally as conspicuous single porphyroblasts; pyroxenes are largely or wholly converted to hornblende. Finally, dissolution of the garnet porphyroblasts, leaving pseudomorphs of granular plagioclase, converts these rocks to amphibolite sensu stricto. Where subsequently deformed, these plagioclase spots have been used as local strain gauges (Schwerdtner et al., 1974). The sequence described above shows various modifications, dependent on the amount of strain imposed; in general, it is observed that hydrated coronites are more deformed than nonhydrated ones. Most metagabbro blocks have strained hydrated margins that give rise to smaller amphibolite blocks and lenses in enclosing tectonite gneiss. Internally the amount of hydration and deformation varies from one body to another, but a pattern has not yet been discerned on a regional scale.

Experiment has shown that the reaction between olivine and plagioclase is strongly pressure-dependent, taking place in the neigbourhood of 8 kb (equivalent to a depth of 28 km) (Kushiro and Yoder, 1966; Green and Hibberson, 1970; Whitney and McLelland, 1973). This suggests that these troctolitic gabbros either crystallized originally deep in the crust and cooled at essentially constant pressure, or that they crystallized at pressures lower than that at which their coronas initially formed. If the latter is true, do they reflect increased pressure due to segments of crust emplaced tectonically on top of the rocks that contain them? It should be cautioned, however, that the ubiquitous impurities in the primary plagioclase and other primary mineral composition variations may play an as yet undetermined rôle in the corona forming reactions, possibly allowing them to take place at lower pressure than that determined experimentally.

Plate 30.4

Features of metamorphism.
See Figure 30.1 for locations.

A – Corona between olivine (Ol) and plagioclase (P) in troctolitic gabbro. Successive envelopes are orthopyroxene (Op), clinopyroxene (Cp), amphibole (A) and garnet (Gt).

B – Detail of clouding in plagioclase of A; oriented laths are green spinel and have the appearance of an exsolution texture.

C – Aggregate of sapphirine prisms in calcic plagioclase associated with corundum (Co) and green spinel (Sp); from metabasite lens in Rosseau subdomain tectonite zone.

D – Kyanite (Ky) enclosed in pyropean garnet (Gt) appears to have given rise to sapphirine, corundum and spinel as wormy intergrowth in muscovitic matrix (M) adjacent to plagioclase; rock is possible meta-eclogite from tectonite zone in Britt Domain.

E – 'Exsolved' plagioclase in clinopyroxene in same rock as D.

F – Coarse 'sweat' in mafic granulite, Parry Sound Domain. Fine matrix contains abundant hornblende, but segregation lacks this mineral except as narrow rims on pyroxene. Coin is 1.9 cm diameter. GSC 203669-W

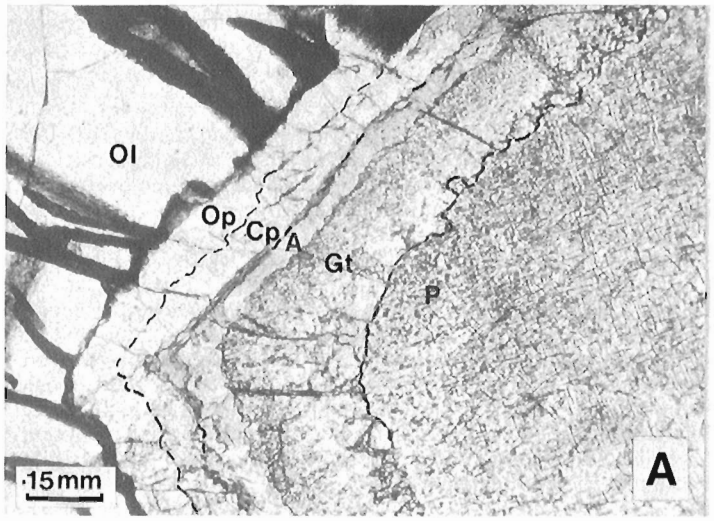
Ol
Op
Cp
A
Gt
P
·15mm
A

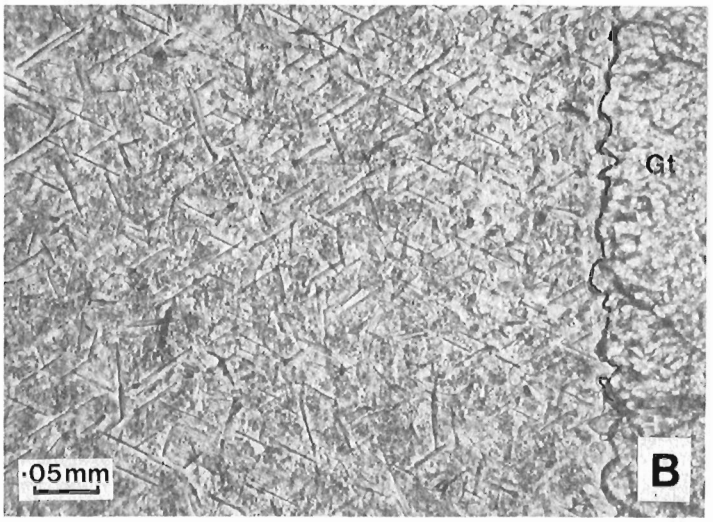
Gt
·05mm
B

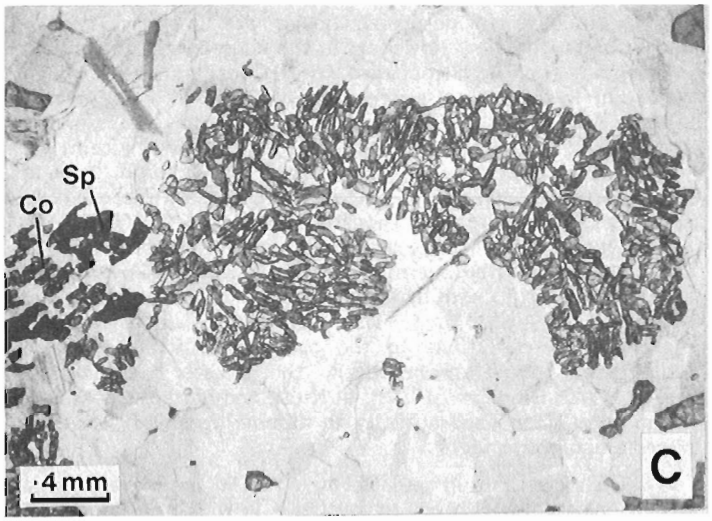
Sp
Co
·4mm
C

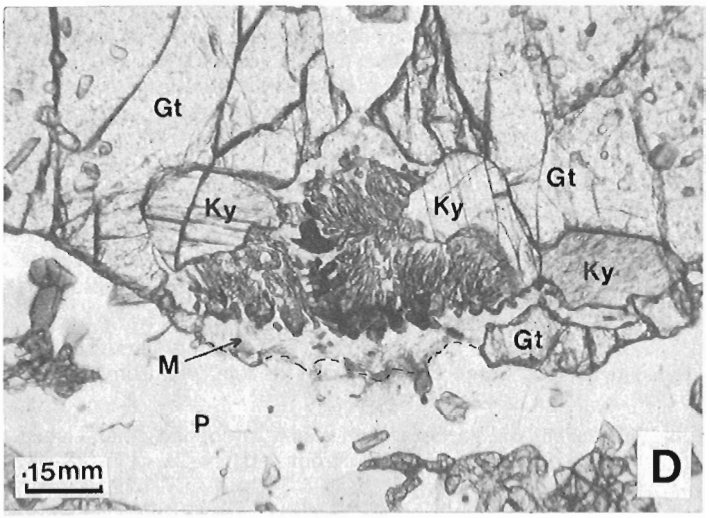
Gt
Ky
Ky
Gt
Ky
Gt
M
P
·15mm
D

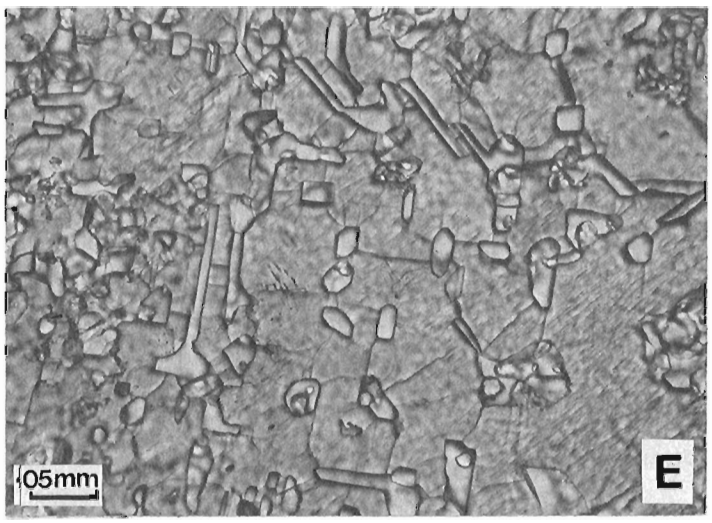
·05mm
E

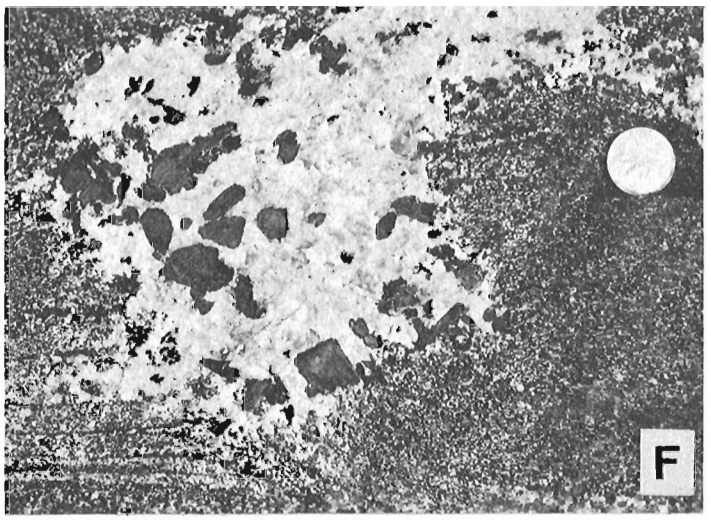
F

Ecologite-like Rocks and the Occurrence of Sapphirine

More important with respect to indication of metamorphic conditions is the occurrence of rocks that have at least some of the attributes of eclogite, again found primarily as blocks within tectonite zones. Some mafic nodules have cores composed chiefly of pale green clinopyroxene studded with brownish red garnets. Most of these blocks exhibit extensive conversion to garnet amphibolite and have foliated amphibolite rims. Also of importance is the discovery of sapphirine in some metabasite masses within tectonite zones. An occurrence is located in the older tectonite zone in Rosseau subdomain (Fig. 30.3). Conspicuous blue patches of sapphirine are scattered throughout a dark, streaky metabasite lens at one of these localities, associated with slivers of highly tectonized anorthositic gneiss. In thin section (Plate 30.4, C) sapphirine is seen to form aggregates of small prisms in calcic plagioclase, and is intimately associated with similar aggregates of corundum and spinel. This rock in addition contains both ortho- and clinopyroxene, garnet, hornblende and minor biotite.

Sapphirine also occurs in a large metabasite nodule near Arnstein, in the high strain part of the broad zone of tectonized rock within Britt Domain (Fig. 30.2). Sapphirine in this rock occurs primarily as small, wormy knots surrounded by a mosaic of metamorphic plagioclase, but in one thin section of an eclogite-like rock from the core of the nodule it is seen to be associated with kyanite that is enclosed in garnet (Plate 30.4, D). Here it is again associated with spinel and corundum, all three occurring in a matrix of fine muscovitic material. Quartz is present in this rock, but not in direct contact with sapphirine. Large early formed grains of clinopyroxene, in part surrounded by secondary pale amphibole, contain oriented plagioclase inclusions (Plate 30.4, E).

Initial results of electron microprobe analyses of mineral phases from the Arnstein nodule are summarized below:

i) Cores of garnets are more pyropean than rims; composition ranges from Gr 14-21, Py 38-58, Al 26-46.

ii) Clinopyroxene with plagioclase inclusions is predominantly diopsidic, Mg/MgFe 0.90, Na_2O and Al_2O_3 contents range up to 1.4 and 8.1 weight per cent respectively; maximum jadeite content is 10.3 mol per cent.

iii) Relics of early orthopyroxene are highly magnesian, with Mg/MgFe 0.82.

iv) Metamorphic pyroxenes are less magnesian and aluminous, Diopsidic clinopyroxene, Mg/MgFe 0.85, Na_2O and Al_2O_3 contents up to 1.4 and 3.4 weight per cent respectively. Orthopyroxene Mg/MgFe 0.68.

v) Metamorphic amphibole is aluminous and magnesian, with composition ranging from pargasite to pargasitic hornblende (Leake, 1978).

vi) Plagioclase is in the range An_{28}-An_{46}. Plagioclase inclusions in clinopyroxene are An_{38}-An_{45}.

vii) Sapphirine is highly aluminous, with considerable substitution of AlAl for (MgFe)Si; Mg/MgFe is 0.81-0.89. Associated spinel has Mg/MgFe 0.55 and contains up to 3 mol per cent gahnite ($ZnAl_2O_4$).

Texturally (Plate 30.4, D) it appears that kyanite enclosed at the margins of garnet grains has given rise to sapphirine and spinel. A balanced reaction between kyanite and garnet can be written: 4Gr + 1Py + 10Ky = 12An + 1Sa + 1Sp, but this does not explain the muscovite material associated with the intergrowth, nor the fact that most garnet-kyanite interfaces show no sign of incipient reaction. Ions released during other metamorphic reactions occurring in the rock must somehow be involved.

The sapphirine-bearing rocks have not yet been analyzed. However, the highly magnesian nature of the contained femic minerals indicates an unusual composition; the presence of considerable Na and Ca (plagioclase) rules out an original ultramafic composition, but a magnesian gabbroic progenitor is possible. Garnet composition is compatible with those found in eclogite nodules of amphibolite and granulite terrains (type C of Smulikowski, 1972). The early clinopyroxene, although somewhat sodic, is not omphacite, however, but if its oriented plagioclase inclusions are interpreted to have been exsolved, its original composition would have been more omphacitic. The term meta-eclogite may thus be applicable. It is likely that more localities of similar rocks will be found within the tectonite zones; hopefully one or more will provide less modified material.

Distribution of Kyanite and Sillimanite

Sillimanite is widespread, though rare, in its occurrence within Britt Domain. However, in the zone containing pelitic gneiss that runs northeastward from Georgian Bay through Arnstein, kyanite is also present. In most of these rocks, sillimanite is texturally stable, with kyanite occurring as corroded relics. In pelitic gneiss and tectonite within the western and northern edges of Parry Sound Domain, kyanite is the dominant stable Al-silicate; K-feldspar is present in some of these rocks, though secondary muscovite is prominent. Within the granulite facies in Parry Sound Domain, however, sillimanite reappears, locally, in apparent stable relationship with hypersthene and quartz (Davidson and Morgan, 1981, p. 293). This assemblage may reflect metamorphic conditions in the order of 900°C at 9.5 kb (equivalent to 33 km depth in the crust) (Hensen and Green, 1973; Davidson, 1979). In Kiosk and Muskoka domains, sillimanite occurs sporadically in assemblages indicative of upper amphibolite facies.

This distribution points to a shift in metamorphic conditions from northwest to southeast in which an important increase in pressure occurs from Britt to Parry Sound domains, decreasing again farther southeast. The distribution of metamorphic facies series is not as simple as the 'transcursive facies series' proposed for the Grenville Province of Ontario by Chesworth (1972). When the distribution of metamorphic variation in each structural domain is known, it will provide a powerful aid in unravelling the tectonic history in this part of the Grenville. Further careful work is needed to demonstrate whether or not sudden changes occur across all the domain boundaries, especially those marked by tectonite zones. However, it can be stated unequivocally that the southeast side of Parry Sound Domain is not only one of abruptly cut off structure but also of metamorphic facies. Features such as two-pyroxene – plagioclase sweats in mafic hornblende-bearing granulites of Parry Sound Domain (Plate 30.4F) simply do not occur southeast of the bounding tectonite zones, except in tectonic slivers.

Summary

Field studies in the southwestern Grenville Province have served, as commonly is the case, to raise more questions than they have answered. A tectonic framework is emerging, however, that is dominated by features suggesting mass transport of crustal material in a northwesterly direction. The types of tectonite produced and the variation in metamorphism outlined above lend credence to the idea that this has all taken place deep within the crust. Movement is

of the same sense that some workers have postulated for the Grenville Front (e.g. Wynne-Edwards, 1972), for the north edge of the Central Metasedimentary Belt (Culshaw and Fyson, 1981) and for the Adirondack region of New York at the opposite side of the Province (e.g. McLelland and Isachsen, 1980; Turner, 1980), where nappe structures have been identified.

Studies in the region east of Georgian Bay suggest that the exposed crust is composed of a number of segments, expressed as distinctive domains and subdomains, that have moved relatively past, over, and perhaps even under one another. Dispositions of tectonite zones that bound these segments suggest that Parry Sound Domain, with its characteristic lithology, structure and metamorphism, lies on top of Britt Domain to the northwest, Algonquin and Kiosk domains and Ahmic subdomain to the east, and Rosseau and Go Home subdomains to the southeast. With the exception of Ahmic subdomain, Britt Domain has little in common with the domains on the opposite side. Deep geophysical studies may help to determine whether or not Parry Sound Domain 'bottoms out' or has a narrowing root separating Britt Domain from the eastern segments. Go Home and Rosseau subdomains have a great deal in common, and are on the whole distinctly different from Moon River and Seguin subdomains. Whether the former have moved downward beneath Parry Sound Domain after its emplacement above Britt Domain, or whether Parry Sound Domain has moved over all of these has yet to be determined. Britt Domain and Rosseau and Go Home subdomains all contain internal tectonite zones. Those in Rosseau and probably also in Go Home subdomains are truncated by the bounding tectonites of Moon River subdomain. If Moon River and Seguin subdomains can be unequivocally connected around the southeast end of Rosseau subdomain, they would together constitute two lobes of a single tectonic unit. These lobes appear as if they had slid past the adjacent segments and abut Parry Sound Domain with overriding sense. Full of migmatitic gneiss at amphibolite grade, they may have been derived from the southeast and emplaced as a single sheet of tectonic cover on the adjacent and intervening segments. Steep structures in their cores suggest that they have keels and are not flat bottomed, but this need not be the case. Whether or not the adjacent older segments have risen subsequent to tectonic cover emplacement has yet to be ascertained.

If this pattern is further substantiated in the regions to the east and northeast, and in particular if the Central Metasedimentary Belt with its relatively low grade metamorphosed sedimentary and volcanic rocks is also bounded on its northwest side by a massive tectonite zone (Davidson and Morgan, 1981, p. 297) with northwest-directed movement sense, then a Himalaya-type model, such as proposed by Dewey and Burke (1973), must be seriously entertained for the Grenville Province. Occurrence of granulite facies terranes with relatively high pressure assemblages, Parry Sound Domain in particular, that are separated from amphibolite facies rocks by tectonite zones, and the presence of eclogite-like rocks and sapphirine-bearing assemblages in metabasite tectonic inclusions in these zones, together suggest that tectonism took place deep in the crust. Certainly some, if not all, segments are allochthonous with respect to one another and to source, and their present disposition may reflect some sort of deep level, tectonic interleaving, with maximum displacement by ductile flow and thrusting primarily along the tectonite zones.

This type of model would necessitate re-assessment of attempts to recognize rock units and orogenic events equivalent to those found beyond the Grenville Front. How much of the Grenville Province is made up of reworked North American craton as opposed to crustal material carried in from elsewhere (e.g. Irving et al., 1972; Seyfert, 1980) is a question whose answer may depend on the identification and interpreted significance of tectonite zones elsewhere in the Province, particularly adjacent to and within the Grenville Front Tectonic Zone. The Huronian may indeed disappear, perhaps within the Grenville Province, not in the manner envisaged by Quirke and Collins (1930), but beneath a pile of slices of some other continental crust!

References

Chesworth, W.
1972: Metamorphic facies series in the Grenville Province of Ontario; Tectonophysics, v. 14, p. 71-78.

Culshaw, N.G. and Fyson, W.K.
1981: Structures associated with ductile thrusting in Grenville gneiss, Bancroft, Ontario; Geological Association of Canada, Annual Meeting 1981, Abstracts, v. 6, P.C. A12.

Davidson, A. and Morgan, W.C.
1981: Preliminary notes on the geology east of Georgian Bay, Grenville Structural Province, Ontario; in Current Research, Part A, Geological Survey of Canada, Paper 81-1A, p. 291-298.

Davidson, L.M.
1979: Nagssugtoqidian granulite facies metamorphism in the Holsteinborg region, West Greenland; Groenlands Geologiske Undersoegelse, Rapport, v. 89, p. 97-108.

Dewey, J.F. and Burke, K.C.A.
1973: Tibetan, Variscan and Precambrian basement reactivation: products of continental collision; Journal of Geology, v. 81, p. 683-692.

Frarey, M.J. and Cannon, R.T.
1969: Notes to accompany a map of the geology of Proterozoic rocks of Lake Panache – Collins Inlet map-areas, Ontario (41I/3, H/14); Geological Survey of Canada, Paper 68-63, 5 p.

Green, D.H. and Hibberson, W.
1970: The instability of plagioclase in peridotite at high pressures; Lithos, v. 3, p. 209-221.

Hensen, B.J. and Green, D.H.
1973: Experimental study of the stability of cordierite and garnet in pelitic compositions at high pressures and temperatures; III. Synthesis of experimental data and geological implications; Contributions to Mineralogy and Petrology, v. 38, p. 151-166.

Irving, E., Park, J.K., and Roy, J.L.
1972: Palaeomagnetism and the origin of the Grenville Front; Nature, v. 236, p. 344-346.

Kushiro, I. and Yoder, H.S., Jr.
1966: Anorthite – forsterite and anorthite – enstatite reactions and their bearing on the basalt-eclogite transformation; Journal of Petrology, v. 7, p. 337-362.

Leake, B.E.
1978: Nomenclature of amphiboles; Canadian Mineralogist, v. 16, p. 501-520.

Lumbers, S.B.
1978: Geology of the Grenville Front Tectonic Zone in Ontario; in Toronto '78, Field Trips Guidebook, ed. A.L. Currie and W.O. Mackasey; Geological Association of Canada, p. 347-361.

McLelland, J.M. and Isachsen, Y.
1980: Structural synthesis of the southern and central Adirondacks: a model for the Adirondacks as a whole and plate-tectonics interpretations: summary; Geological Society of America, Bulletin, Part I, v. 91, p. 68-72.

McLelland, J.M. and Whitney, P.R.
1980a: A generalized garnet-forming reaction for meta-igneous rocks in the Adirondacks; Contributions to Mineralogy and Petrology, v. 72, p. 111-122.

1980b: Compositional controls on spinel clouding and garnet formation in plagioclase of olivine metagabbros, Adirondack Mountains, New York; Contributions to Mineralogy and Petrology, v. 73, p. 243-251.

Quirke, T.T. and Collins, W.H.
1930: The disappearance of the Huronian; Geological Survey of Canada, Memoir 160, 129 p.

Satterly, J.
1956: Geology of Lount Township; Ontario Department of Mines, Annual Report for 1955, v. 64, part 6, 46 p.

Schwerdtner, W.M. and Waddington, D.H.
1978: Structure and lithology of Muskoka – southern Georgian Bay region, central Ontario; in Toronto '78, Field Trips Guidebook, ed. A.L. Currie and W.O. Mackasey; Geological Association of Canada, p. 204-212.

Schwerdtner, W.M., Waddington, D.H., and Stollery, G.
1974: Polycrystalline pseudomorphs as natural gauges of incremental paleostrain; Neues Jahrbuch für Mineralogie (Monatshefte), Heft 3/4, p. 174-182.

Seyfert, C.K.
1980: Paleomagnetic evidence in support of a middle Proterozoic (Helikian) collision between North America and Gondwanaland as a cause of the metamorphism and deformation in the Adirondacks: summary; Geological Society of America, Bulletin, Part I, v. 91, p. 118-120.

Smulikowski, K.
1972: Classification of eclogites and allied rocks; Kristalinikum, v. 9, p. 107-130.

Streckeisen, A.
1976: To each plutonic rock its proper name; Earth-Science Reviews, v. 12, p. 1-33.

Turner, B.B.
1980: Polyphase Precambrian deformation and stratigraphic relations, central and southeastern Adirondack Mountains, New York: a reinterpretation: summary; Geological Society of America, Bulletin, v. 91, p. 72-74.

Whitney, P.R. and McLelland, J.M.
1973: Origin of coronas in metagabbros of the Adirondack Mts., N.Y.; Contributions to Mineralogy and Petrology, v. 39, p. 81-89.

Wynne-Edwards, H.R.
1972: The Grenville Province; in Variations in Tectonic Styles in Canada, ed. R.A. Price and R.J.W. Douglas; Geological Association of Canada, Special Paper No. 11, p. 263-334.

31.

THE HEALEY LAKE MAP AREA AND THE THELON FRONT PROBLEM, DISTRICT OF MACKENZIE

Project 780009

John B. Henderson, Peter H. Thompson, and Donald T. James[1]
Precambrian Geology Division

Henderson, John B., Thompson, Peter H., and James, Donald T., The Healey Lake map area and the Thelon Front problem, District of Mackenzie; in Current Research, Part A, Geological Survey of Canada, Paper 82-1A, p. 191-195, 1982.

Abstract

Completion of 1:250 000 scale mapping in the area has revealed that the change from Slave Province style curvilinear structural pattern in the west to a consistently northerly trend in the east and the low pressure metamorphic gradient increasing from greenschist to granulite grade toward the southeast is Archean in age. Superimposed is an intermediate pressure Proterozoic metamorphism that was accompanied or preceded by cataclastic to mylonitic deformation that is most evident in the north northeasterly trending straight zone in the southeast corner. As this structure is coincident with major geophysical features and, on the basis of its magnetic and geomorphologic expression appears to extend beyond the area to both the Macdonald and Bathurst faults, it is a candidate for any relocation of the position of the Thelon Front.

Introduction

The Healey Lake area, in the eastern Slave Province, contains the change from typical Slave geology with low to intermediate grade metavolcanic and metasedimentary rocks with curvilinear structural trends intruded by massive granitoid rocks to the higher grade gneisses, foliated granitoids and linear structural pattern of the adjacent Queen Maude Block of the Churchill Structural Province. This transition has been termed the Thelon Front (Wright, 1967). The 1981 field season marked the completion of the mapping of the area at 1:250 000 scale. This report is a summary of the 1981 field work which largely constituted the linking of areas mapped during previous field seasons together with a summary of the nature of the Thelon Front at least as represented in the Healey Lake area.

General Geology

Various aspects of the geology of the area have been discussed in previous preliminary reports on the area (Henderson, 1979; Henderson and Thompson, 1980; 1981) and are summarized in the following.

Approximately one third of the Healey Lake area is underlain by Archean supracrustal rocks of the Yellowknife Supergroup (Fig. 31.1). These rocks occur throughout the area and can be followed continuously from the northwest corner where they are least complexly deformed and at the lowest metamorphic grade through to the southeast. As is typical of most of the Slave Province, greywacke-mudstone turbidites and their metamorphosed equivalents constitute the greatest proportion of the supracrustal rocks. Metavolcanic units occur in several distinct centres as well as one linear belt along the east margin of the area. The well preserved, flat lying, low metamorphic grade volcanic complex in the northwest corner has been described in considerable detail by Lambert (1976, 1977a, 1978). Like the other volcanic centres in the area, it is characteristically of more intermediate composition than the typically more mafic Yellowknife volcanics of the southern and western Slave Province.

Northwest of Healey Lake is a block of complexly deformed heterogeneous granitoid gneisses that are thought to be older than the Yellowknife supracrustal rocks. Even more highly deformed equivalents of this unit occur to the southeast of Healey Lake.

Intrusive into the supracrustal rocks and to a lesser extent the basement block are a series of plutonic units that range in composition from granite through granodiorite, tonalite to diorite with the more mafic compositions dominant.

Three sets of post Archean diabase dykes intrude most units.

The rocks of the Healey Lake area have been involved in two phases of metamorphism. The earlier metamorphism, Archean in age, is the typical low pressure type characteristic of the Slave Province (Thompson, 1978). As expressed in the Yellowknife pelitic rocks, the metamorphic gradient increases from greenschist in the northwest to kyanite bearing, sillimanite migmatites and possibly orthopyroxene granulites in the southeast corner. Also increasing in grade to the east the later, intermediate pressure Proterozoic metamorphism is expressed in the metamorphism of two of the Proterozoic dyke sets and the superposition of younger metamorphic mineral assemblages on Archean assemblages.

One of the most striking features of the map area is the change in structural style from the complex locally curvilinear structural pattern characteristic of the Slave Province in the west half of the area to the consistently northerly trend of almost all units in the east half. That the trend of Proterozoic diabase dyke sets metamorphosed during the second metamorphism remains essentially undeflected throughout the area suggests that the northerly linear pattern in the east half is Archean. Later deformation has imposed on the Proterozoic dykes in the east half a weak foliation parallel to the older principal foliation in the rocks they intrude. In the southeast corner of the area a north-northeasterly trending cataclastic 'straight zone' occurs within a belt of Yellowknife supracrustal rocks and has a pronounced geophysical, geomorphologic and as well as geological expression. The straight zone postdates the Archean metamorphism but is involved with the Proterozoic metamorphism. The trend of the zone is distinct from the northerly Archean trend although in detail they tend to merge where they intersect.

1981 Highlights

Completion of the mapping of the area during the 1981 field season has on the whole supported the above summary based on previous seasons work.

[1]Geology Department, Carleton University, Ottawa

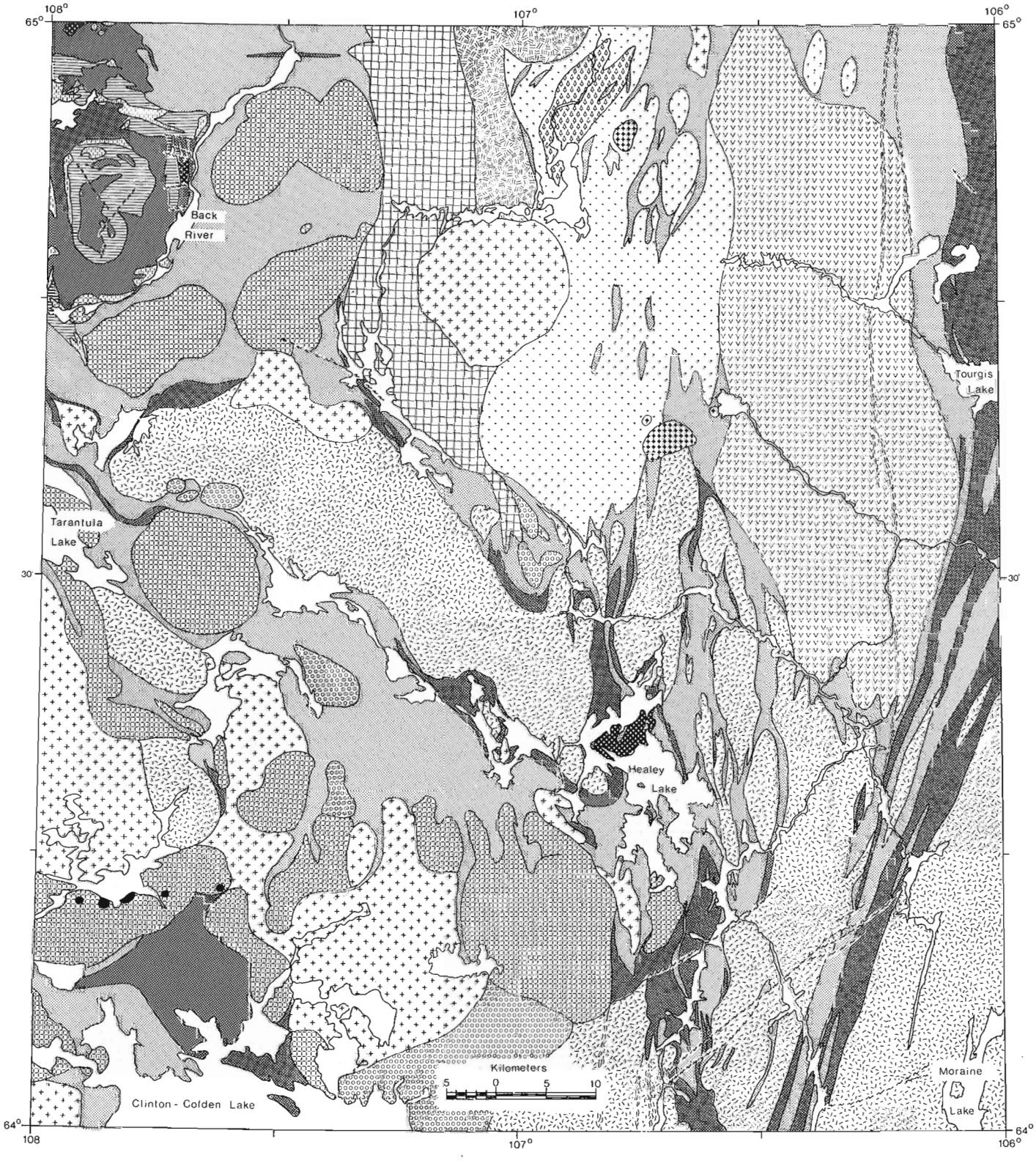

Figure 31.1. *General geology of the Healy Lake area.*

LEGEND

Granite

Pink granite - granodiorite

Granodiorite with many inclusions of msed. locally tonalite, two mica granodiorite

Two mica granodiorite

Augen granodiorite

Quartz tonalite

Tonalite

Diorite - tonalite

Diorite

Ultramafic rocks

Yellowknife Supergroup

Greywacke - mudstone, schist - psammite, migmatite

Rhyolite

Dacite

Dacite - andesite, amphibole gneiss

Andesite - basalt, amphibolite

Undifferentiated massive to gneissic to migmatitic granite to diorite

Shear or mylonite zones

Faults

Outlining the distribution of the Yellowknife Supergroup was completed with the recognition that the belt of metavolcanic and metasedimentary rocks at Tourgis Lake extends into the zone of supracrustal rocks in the straight zone to the south. The steeply dipping straight zone structure apparently continues to the north-northeast beyond the map area on the basis of its aeromagnetic expression but the supracrustal belt and principal foliation assumes a more northerly trend with a moderate easterly dip through Tourgis Lake.

The major unit of metavolcanics north of Clinton-Colden Lake was outlined. As with the other volcanic units in the area it is dominantly of intermediate composition consisting of northwesterly trending volcaniclastic units. Pillowed flows occur in the northwesterly part of the unit.

The block of heterogeneous complexly deformed granitoid gneisses in the central part of the east half of the area that is thought to be basement to the Yellowknife rocks has been completely outlined. Although no unconformities have been recognized, narrow discontinuous metavolcanic units of intermediate composition occur along its margins. In this respect it is similar to the somewhat larger basement block east of Yellowknife in the southern Slave Province (Lambert, 1977b; Henderson, 1981) and the Hanimor complex 100 km to the northwest (Frith and Percival, 1978). Equivalents of this unit are deformed into northerly trending structures at and east of Healey Lake. The dominantly granulite grade granitoid rocks east of the straight zone are also considered to be part of this unit. Remnants of supracrustal rocks unmapped at the scale of Figure 31.1 occur in this unit and may be equivalent to Yellowknife supracrustal rocks to the west. The correlation remains unsure due to the very high metamorphic grade and degree of deformation of these rocks.

Two mica granite granodiorite intrusions are the dominant lithology in the southwest corner of the map area north of Clinton-Colden Lake. Several irregularly shaped bodies occur in a generally northwest-trending zone that conforms to the regional northwesterly structural trend in the east central Slave Province that is evident on small scale maps (McGlynn, 1977). This trend is also apparent in the metasedimentary belt to the north as well as the orientation of the basement block north of it. This northwesterly trend is superimposed by the much more tightly defined northerly directed linear pattern east of 107°.

In addition to the previously described cataclastic straight zone in the southeast part of the area, several other shear zones have been recognized. The largest of these is a north-trending structure 10 km west of Tourgis Lake. The zone is a ductile shear that in the north contains the highly crushed equivalents of migmatized metasediments, garnet amphibolite sills that are strongly and steeply lineated and granitoid sills that are severely mylonitized. Migmatitic metasediments occur on both sides of the structure but the proportion of leucosome is higher to the east and kyanite is absent to the west. This structure continues another 30 km to the north of the area (Frith, 1982). To the south, in the large tonalite body, the exposure is rather poor but there is a consistent topographic expression of the structure and scattered outcrop and felsenmeer blocks in the zone are strongly foliated. It ultimately merges with the north-northeasterly trending straight zone to the south. The inflection contour between the major positive and negative gravity anomalies that is coincident with most of the straight zone (Fig. 31.2; Henderson and Thompson, 1981) swings away from the straight zone where the shear zone joins it and remains essentially coincident with the northerly trending surface trace.

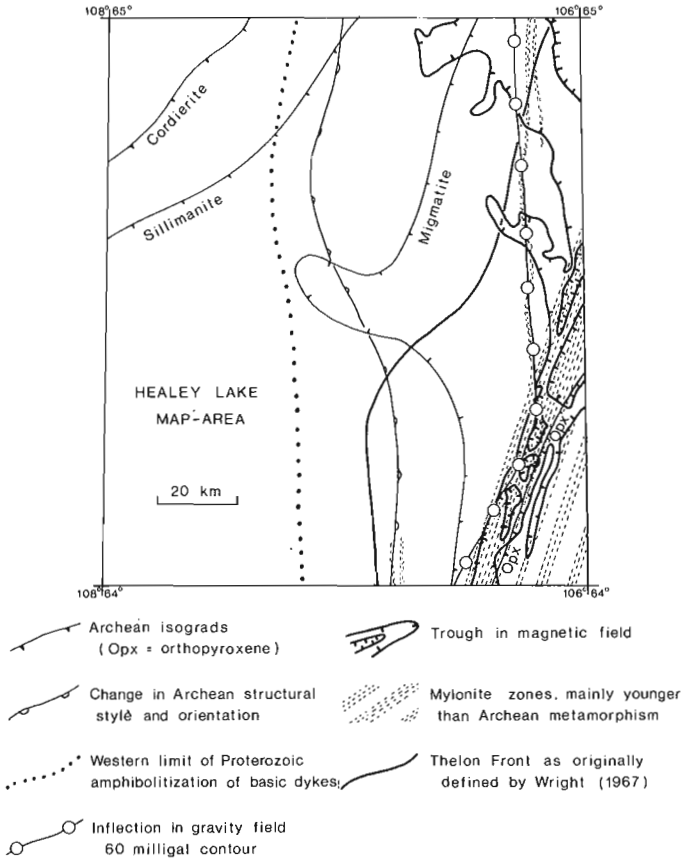

Figure 31.2. *Distribution of various geological and geophysical features with respect to the position of the Thelon Front as originally defined by Wright (1967). The predominant metamorphic gradient and changes in structural style and orientation are Archean. Following the intrusion of Proterozoic diabase dykes, a later phase of metamorphism and some reactivation of the pre-dyke structure occurred. Deformation in major mylonite zones is younger than Archean metamorphism but the same age or older than the later metamorphism. Both a large part of the inflection of the gravity field between major positive and negative gravity anomalies and a prominent trough in the magnetic field are coincident with a major cataclastic straight zone. This feature is considered a good candidate for a revised position of the Thelon Front.*

A series of wide mylonite zones occurs in the eastern part of the granitoid gneisses east of Clinton-Colden Lake and south of Healey Lake. Like the previously discussed structure the trend of these zones is northerly. In the granulite terrane east of the straight zone are a series of relatively narrow shear zones that are parallel to both the major straight zone and the high relief magnetic grain characteristic of this terrane. Another major shear zone has a northwesterly trend and occurs north of the block of granitoid gneiss northwest of Healey Lake and south and partially within the quartz tonalite body to the north. In the northwest this structure is a narrow brittle fault but to the southeast, within the quartz tonalite, it broadens to a ductile shear zone several kilometres wide before disappearing east of 107°.

Several advances have been made regarding the understanding of the complex metamorphic history of the area. Completion of mapping has revealed that the migmatite isograd in the metasediments forms a lobe that projects farther west than previously indicated (Fig. 31.2). In addition, an orthopyroxene isograd has been mapped southeast of the major straight zone. In the granulite terrane the orthopyroxenes are deformed in the shear zones that postdate the Archean metamorphism. This supports the suggestion that the granulite terrane is a continuation of the Archean metamorphic gradient rather than a product of the later Proterozoic metamorphism. While it seems unlikely that the granulite metamorphism is Proterozoic in age, the possibility that the granulites are pre-Yellowknife Supergroup remains.

Preliminary petrographic work has been started to determine the significance of kyanite which occurs in Yellowknife metasedimentary rocks in a narrow zone east of the shear zone west of Tourgis Lake and in lower grade equivalents of these rocks at and east of Healey Lake. In several places field observations and petrography indicate that kyanite formed before or during Archean migmatization. Kyanite in association with chloritoid and staurolite also occurs within Archean andalusite porphyroblasts near Healey Lake as small euhedral grains. Although chloritoid and staurolite are readily attributable to the later metamorphism, textural relations of kyanite are sufficiently ambiguous that nucleation of andalusite on the high pressure polymorph is also a reasonable explanation. On the other hand textures in a kyanite bearing rock from the straight zone imply that the kyanite is younger than mylonitization of the Archean migmatites. The available evidence points to a complex P-T history for this eastern terrane with supracrustal rocks being taken down to depths compatible with the formation of kyanite and brought back to the surface twice.

Two features of possible economic interest were noted this past season. A small gold bearing quartz vein was recognized in metavolcanic rocks north of Healey Lake by Jurate Lukošius in the course of collecting material for a geochemical study of the volcanic rocks (UTM Zone 13 413800 7141400). A single spodumene bearing pegmatite was located in the metasediments east of Clinton-Colden Lake (UTM Zone 13 362100 7101800). This pegmatite is presumably related to the nearby two mica granite and is similar to Li pegmatites associated with two mica granites east of Yellowknife.

The Thelon Front

With the completion of the 1:250 000 scale mapping of the area, a preliminary reassessment of at least that part of the Thelon Front within the map area is in order. On the basis of 1:1 000 000 scale geological reconnaissance across the entire northwestern Precambrian Shield (Wright, 1957; Fraser, 1964), Wright (1967) described the Thelon Front as a feature which marked changes in lithology, metamorphic grade and structural style that reflected the farthest westward extent of the 'Hudsonian orogeny' and was thus the boundary between the Slave and Churchill structural provinces. He described the 700 km long feature as "...gradational, probably over several miles..." but pointed out that "...on the present regional scale it appears as an abrupt, clearly defined feature...".

In the area between the Bathurst and MacDonald faults, which includes the Healey Lake map area, the term Thelon Front was applied to a transition eastward from a terrane where undeformed granitoid plutons intrude medium grade metasedimentary and metavolcanic rocks of the Yellowknife Supergroup to a gneissic terrane with abundant foliated granitoid rocks. The sinuous nature of the transition line as originally defined within the Healey Lake area appears to be related to variations in foliation trend which on the basis of scattered K-Ar mica ages were interpreted as Hudsonian features. Gibb and Thomas (1977) noting the coincidence of

the geological change with the steep gravity gradient in the area suggested the feature is a suture formed during a Proterozoic collision between the Slave Craton and rocks of the Churchill Province.

With the more detailed geological knowledge now available in the Healey Lake area a much more complex scenario is indicated. In Figure 31.2 various metamorphic, structural and geophysical boundaries are compared with the location of the Thelon Front as originally defined. None of the prominent geological or geophysical features of Archean or younger age coincide with the front. As presently defined, the location, age, origin and significance of this feature must be considered open questions.

On the basis of the updated mapping it is evident that Yellowknife Supergroup rocks extend completely across the area to the eastern boundary; the age of the striking structural change across the area is Archean, not Proterozoic, but there is a zone of cataclastics to mylonitization that predates or is synchronous with a Proterozoic metamorphic event. The Proterozoic K-Ar ages may represent cooling ages related to this event.

As previously suggested, the straight zone in the southeast corner of the area is perhaps the best candidate for a single boundary feature if such a line must be selected (Henderson and Thompson, 1981). It would appear to be the most prominent of a series of mylonitic zones with similar trend that continue beyond the map area to the east. It is a prominent feature that corresponds to two geophysical features. On the basis of its magnetic and geomorphological expression it would appear to be a mappable structure beyond the Healey Lake area to at least the Bathurst fault 75 km to the northwest and to the MacDonald fault 100 km to the southwest. The continued updating of mapping in the region of the Thelon Front to the east as well as to the north and south must be completed before the significance and age of this 700 km long tectonic feature as a structural province boundary will be understood.

Acknowledgments

Completion of the Healey Lake area was made possible by the able and enthusiastic assistance of Gaele Card, Mike Bradfield, Jurate Lukošius and Rob Macfie. Tobi Heller of Canwest Aviation Ltd. did a first class job as helicopter pilot. Assistance provided to the party by the Geology Office of the Department of Indian and Northern Affairs at Yellowknife is acknowledged, with special thanks to their excellent expeditor Win Bowler. J.C. McGlynn critically read this report.

References

Fraser, J.A.
1964: Geological notes on northeastern District of Mackenzie, N.W.T.; Geological Survey of Canada, Paper 63-40 (Map 45-1963).

Frith, R.A.
1982: Second preliminary report on the geology of the Beechey Lake – Duggan Lakes map areas, District of Mackenzie, N.W.T.; in Current Research, Part A, Geological Survey of Canada, Paper 82-1A, p. 203-211.

Frith, R.A. and Percival, J.A.
1978: Stratigraphy of the Yellowknife Supergroup in the Mara-Back Rivers area, District of Mackenzie; in Current Research, Part C, Geological Survey of Canada, Paper 78-1C, p. 89-98.

Gibb, R.A. and Thomas, M.D.
1977: The Thelon Front: a cryptic suture in the Canadian Shield?; Tectonophysics, v. 38, p. 211-212.

Henderson, J.B.
1979: Healey Lake map area, District of Mackenzie; in Current Research, Part A, Geological Survey of Canada, Paper 79-1A, p. 400.

1981: Archean basin evolution in the Slave Province, Canada; in Kröner, A. (ed.), Precambrian Plate Tectonics, Elsevier, Amsterdam, p. 213-235.

Henderson, J.B. and Thompson, P.H.
1980: The Healey Lake map area (northern part) and the enigmatic Thelon Front, District of Mackenzie; in Current Research, Part A, Geological Survey of Canada, Paper 80-1A, p. 165-169.

1981: The Healey Lake map area and the enigmatic Thelon Front, District of Mackenzie; in Current Research, Part A, Geological Survey of Canada, Paper 81-1A, p. 175-180.

Lambert, M.B.
1976: The Back River Volcanic Complex, District of Mackenzie; in Report of Activities, Part A, Geological Survey of Canada, Paper 76-1A, p. 363-367.

1977a: The Southwestern margin of the Back River Volcanic Complex, District of Mackenzie; in Report of Activities, Part A, Geological Survey of Canada, Paper 77-1A, p. 179-180.

1977b: Anatomy of a greenstone belt – Slave Province, N.W.T.; in Baragar, W.R.A. et al. (ed.) Volcanic Regimes in Canada; Geological Association of Canada, Special Paper 16.

1978: The Back River Complex – a cauldron subsidence structure of Archean age; in Current Research, Part A, Geological Survey of Canada, Paper 78-1A, p. 153-158.

McGlynn, J.C.
1977: Geology of the Bear-Slave structural provinces; Geological Survey of Canada, Open File 445.

Thompson, P.H.
1978: Archean regional metamorphism in the Slave Structural Province – a new perspective on some old rocks; in Fraser, J.A. and Heywood, W.W., Metamorphism in the Canadian Shield; Geological Survey of Canada, Paper 78-10, p. 85-102.

Wright, G.M.
1957: Geological notes on eastern District of Mackenzie, Northwest Territories; Geological Survey of Canada, Paper 56-10.

1967: Geology of the southeastern barren grounds, parts of the Districts of Mackenzie and Keewatin (Operations Keewatin, Baker, Thelon); Geological Survey of Canada, Memoir 350.

METAMORPHISM IN THE CROWDUCK BAY AREA, MANITOBA

Project 800014

Terence M. Gordon and Quentin Gall[1]
Precambrian Geology Division

Gordon, T.M. and Gall, Q., Metamorphism in the Crowduck Bay area, Manitoba; in Current Research, Part A, Geological Survey of Canada, Paper 82-1A, p. 197-201, 1982.

Abstract

Interbedded greywackes and shales of the Amisk Group are lithologically similar to the File Lake Formation, interpreted as submarine fan deposits. Overlying crossbedded sandstones and conglomerates of the Missi Group have some interbedded siltstone and mudstone. This contrasts with the complete absence of fine material in Missi rocks at Flin Flon, interpreted as alluvial fan deposits. Interbedded with, and overlying Missi sedimentary rocks is a sequence of lavas and fragmental volcanic rocks. A welded ash flow within the sequence indicates subaerial deposition.

Two periods of folding can be recognized. An early thrust fault, deformed during F_1, is postulated to explain the outcrop pattern in the northern part of the area. Highest grade metamorphic conditions were reached during the second period of deformation. Metamorphic grade ranges from garnet-chlorite zone to garnet-biotite-sillimanite zone and is highest in both the northwest and southeast parts of the area. Gold deposits occur in quartz veins that formed following peak metamorphic conditions.

Introduction

The Crowduck Bay area lies on the eastern side of Wekusko Lake near the east end of the Flin Flon-Snow Lake volcanic belt. The area has been mapped by Stockwell (1936), Armstrong (1941), and Frarey (1950) but no further geological studies have been undertaken. The aims of this study are to elucidate the metamorphic regime in the area and link with the more recent work to the west (Froese and Moore, 1980) and to the east (Bailes, 1976). The present note reports on aspects of general geology required as a background for continuing chemical and petrographic investigations (Fig. 32.1). All rocks in the area are metamorphosed but, for the sake of brevity, the prefix "meta" is omitted from lithologic names.

The rocks of the Crowduck Bay area can be assigned to the general stratigraphic framework of the Flin Flon – Snow Lake belt, as outlined by Bailes (1971, 1980).

The oldest rocks are the Amisk Group, which, at its base, consists dominantly of submarine mafic volcanic flows. A larger proportion of intermediate to felsic lavas and fragmental rocks occurs higher in the section. A greywacke-shale turbidite sequence overlies the volcanic rocks.

The Missi Group, lying unconformably above Amisk Group, is composed of polymictic conglomerates and cross-bedded sandstones. In the Crowduck Bay area a series of intermediate to felsic volcanic rocks have also been assigned to the Missi Group (Frarey, 1950).

Syntectonic and late tectonic plutons ranging from gabbro to tonalite in composition have intruded the sedimentary-volcanic package.

Lithology of the Amisk Group

In the map area, volcanic rocks of the Amisk Group consist mainly of mafic pillow lavas with associated mafic dykes and sills. They have been metamorphosed to hornblende schists and amphibolites with a well developed foliation. Although facing directions may be inferred from some outcrops, metamorphism and deformation have obliterated most primary volcanic features. Felsic volcanic breccia occurs within the mafic flows south of Niblock Lake.

Amisk Group sedimentary rocks are interbedded greywackes, siltstones and slates and derived schists and gneisses. They are lithologically similar to the File Lake Formation of Bailes (1980). Along the north shore of Wekusko Lake the rocks are chiefly grey weathering sandstone and siltstone. Graded bedding and scours are common in beds ranging from 10 to 200 cm in thickness. On the shore and islands near Herb Lake townsite the proportion of slate is higher and parallel lamination and flame structures are observed. The absence of recognizable crosslaminated divisions may be due to post-depositional tectonic disruption.

At lowest metamorphic grade the rocks consist of chlorite, plagioclase, white mica, and quartz. North of Wekusko Lake, grade is higher and the rocks are coarser grained with porphyroblasts of garnet, staurolite, and sillimanite. Most primary sedimentary structures are destroyed, although graded bedding can be inferred from the distribution of aluminous minerals.

A 3 m thick unit of dark grey weathering biotite schist with abundant 5 to 10 mm euhedral garnet porphyroblasts is exposed on the east side of Crowduck Bay. Bailes (1980) has noted the similarity of this outcrop to the Corley Lake member of the File Lake Formation.

The preceding observations lead us to assign the sedimentary rocks within the map area and west of the Grass River to the Amisk Group. Bailes (1980) has interpreted similar rocks as part of a subaqueous fan system.

Lithology of Missi Group Sedimentary Rocks

Missi Group rocks occur in several distinct structural blocks within the map area.

South and east of a fault extending from Puella Bay to Roberts Lake is a sequence of crossbedded sandstones, pebbly sandstones and conglomerates. Rare 10 to 50 cm lenses of siltstone have been observed. The grey weathering sandstones commonly exhibit curvilinear crossbeds in 10 to 50 cm sets. Pebbles occur scattered randomly within coarse sand beds and in pebbly sandstone beds, which locally show weak graded bedding. Tabular conglomerate bodies up to 300 m in thickness are polymictic, and poorly sorted with subangular to subrounded clasts up to 50 cm in diameter. Both matrix and framework-supported fabrics were observed. Intermediate and felsic volcanic lithologies form over half the clast population, with quartz, quartzite, and mafic volcanic rocks in subordinate amounts.

[1] Department of Geology, Memorial University of Newfoundland, St. John's, Newfoundland, A1B 3X5

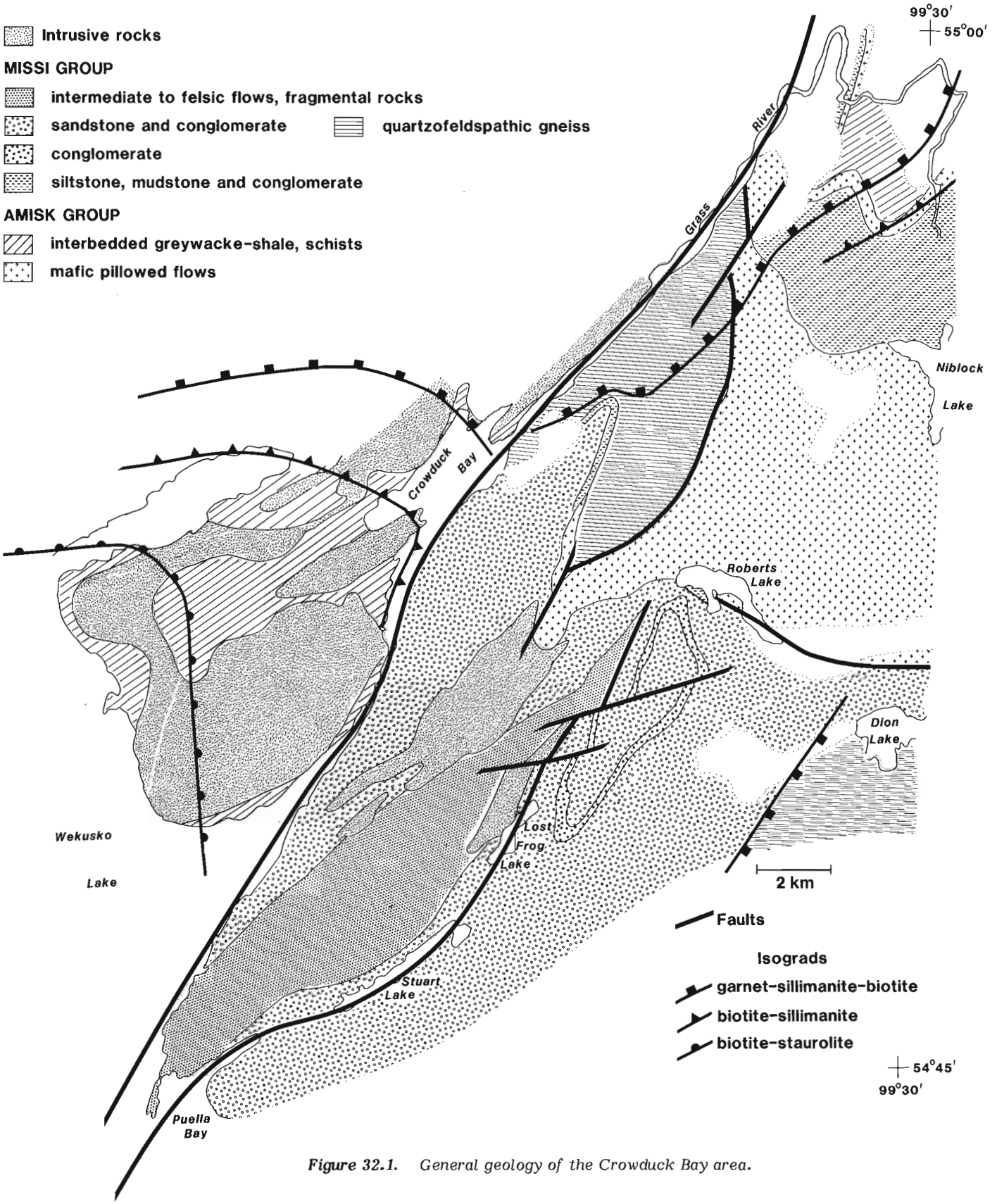

Figure 32.1. General geology of the Crowduck Bay area.

No metamorphic minerals were observed in these rocks at Puella Bay, but to the northeast garnet, staurolite, and hornblende porphyroblasts ocur locally in siltstones and in the matrix of conglomerates. Magnetite is ubiquitous in the sandstones, probably resulting from metamorphism of hematite that is common in lower grade Missi rocks elsewhere in the Flin Flon belt.

Shanks and Bailes (1977) summarize a 2700 m composite section measured within this block. They note the similarity of these rocks to the type Missi strata at Flin Flon.

A second block of Missi metasedimentary rocks occurs northwest of Niblock Lake. Staurolite and garnet bearing siltstone contains 1 to 3 m quartz pebble and sandstone beds as well as thicker beds of poorly sorted polymictic framework-supported conglomerate. Sedimentary structures have generally been obliterated by metamorphic recrystallization, although in places 2-10 cm beds in the siltstone are defined by staurolite concentration. These rocks are assigned to the Missi Group because of the similarity of the conglomerates to Missi rocks elsewhere in the area.

Quartzofeldspathic gneisses lying between the Grass River and Amisk volcanic rocks are also assigned to the Missi Group. These rocks weather in 10 to 100 cm slabs due to a layering defined by slight changes in muscovite and biotite concentration. Amphibolite and metaconglomerate layers occur locally, as do beds with thin magnetite and biotite lamellae. Near the contact with Amisk volcanic rocks, the gneisses are particularly quartz-rich, weather light grey and have preserved crossbedding. Garnet occurs locally and quartz-sillimanite nodules are sometimes abundant. A 10 to 50 m thick unit of staurolite-garnet bearing siltstone lies between the gneisses and sedimentary rocks to the south. Similar gneisses occur south of Dion Lake and are also considered to be of Missi age.

A fifth block of Missi rocks occurs as a tight synform lying between the Grass River and the Puella Bay – Roberts Lake fault. Stockwell (1936) mapped this structure in detail as part of a study of gold deposits in the Herb Lake area. At Herb Lake townsite a medium grey sandstone overlies interbedded greywackes and slates of the Amisk Group. Crossbeds in 10 to 40 cm sets are common as are scattered pebbles and pebble beds. A conglomerate, varying in thickness from 5 to 200 m overlies the sandstones. It is poorly sorted, dominantly clast supported, and polymictic, with felsic to intermediate volcanic clasts more abundant than quartz, mafic volcanic, and granitoid pebbles. Clasts reach 40 cm in maximum dimension. On the southeast limb of the syncline the sedimentary sequence contains less conglomerate. At Lost Frog Lake, along Stuart Creek, and at Puella Bay, minor amounts of thin bedded siltstone and mudstone were observed. The rocks are otherwise similar to those described above.

Garnet porphyroblasts occur sporadically in the sandstones, while hornblende porphyroblasts have been observed in both the matrix of conglomerates and in sandstone beds.

Although these rocks are slightly more mafic and less well sorted than Missi sediments in the southeastern part of the area, their stratigraphic position, sedimentary structures, and clast population lead us to assign them to the Missi Group.

Mukherjee (1974) interpreted Missi rocks at Flin Flon as subaerial alluvial fan deposits. No depositional environment has been deduced for Missi rocks in the Crowduck Bay area. However, the presence of some siltstone and mudstone contrasts with the complete absence of fine material in the type area.

Lithology of Missi Group Volcanic Rocks

Interbedded with, and overlying the conglomerate are a series of felsic volcanic tuffs and breccias. The breccias commonly have angular fragments of a single lithology in a somewhat darker fine grained matrix. One locality, interpreted as a debris flow, consists of angular fragments of rhyolite up to 50 cm in size supported in a matrix of coarse pebbly sand. Matrix pebbles are subrounded, and include volcanic lithologies, quartz, and banded magnetite-quartz iron formation. Tuffs are massive to thin bedded and contain conspicuous 1 to 3 mm quartz and feldspar crystals.

Several bodies of pink weathering quartz-feldspar porphyry lie within the volcaniclastic sequence. This lithology is characterized by inconspicuous 1 mm quartz and feldspar crystals in a very fine grained groundmass. Locally these bodies contain recognizable fragments. In several places clastic rocks overlie porphyry with apparent depositional contacts. Thus, although Stockwell (1936) interpreted all of these bodies as intrusive, we believe they are in part extrusive.

Overlying the felsic volcaniclastic rocks are a series of intermediate flows and fragmental rocks. The flows are generally massive with local patchy development of quartz amygdules. Monolithologic fragmental rocks occurring between some massive flows are thought to be flow breccias, but metamorphism and deformation preclude identification of individual flow units. Polymictic volcaniclastic breccias are most common in the northern part of the syncline. They contain angular fragments up to 20 cm supported in a grained matrix and probably originated as debris flows.

Several fragmental rhyolite units occur within the volcanic succession. Shanks and Bailes (1977) reported flattened shard-like fragments and suggested that these rocks might be welded tuffs. Detailed work in 1981 confirmed their observations. Flattened shards and fragments occur in orientations perpendicular to the regional foliation, indicating that the shapes are not due to tectonic flattening. One 30 m thick fragmental unit has a recognizable 1 m thick nonwelded base and a 3 m thick nonwelded top. Detailed petrographic study is underway to document welded textures in the central zone.

Interbeds of volcaniclastic and sedimentary material at the base of the sequence indicate that initial volcanic activity was contemporaneous with Missi sedimentation. The absence of pillow structures and the presence of welded tuffs suggest accumulation under subaerial conditions.

Chemical sampling, using a scheme similar to that of Cameron et al. (1979) was carried out in order to establish the chemical characteristics of Missi Group volcanic rocks.

Intrusive Rocks

Four ages of intrusion can be recognized in the area. Synvolcanic intrusions include dacite and granite porphyry. They are strongly foliated and mineralogically similar to associated volcanic rocks. Syntectonic tonalite bodies are foliated and have boundaries parallel to the foliation of surrounding rocks. Late tectonic intrusions are chemically complex, contain several intrusive phases and form equant bodies with undeformed central zones. Granitic pegmatites appear to be the youngest intrusive rocks. Field relations, petrography, and chemistry of the intrusive rocks have been reported in detail by Černý et al. (1981).

Structural Geology

The structural history of the Flin Flon-Snow Lake belt has been reviewed by Bailes (1975). Most workers agree that the earliest deformation produced tight to isoclinal

recumbent folds (F_1). A second period of deformation produced north-northeast plunging folds (F_2) which now dominate the structural grain of the region.

In the Crowduck Bay area F_1 has resulted in a foliation defined by a preferred orientation of biotite subparallel to compositional layering. Megascopic F_1 folding can be inferred from opposed primary facing directions in Amisk metasedimentary rocks at the north end of the area and probably accounts for overturned bedding in structures east of Crowduck Bay.

Mesoscopic isoclinal folds have been observed in outcrops of both Amisk and Missi rocks. F_2 folds can be isoclinal and in places are parallel to F_1 axial planes. The age of these mesoscopic folds is thus unclear.

Steeply dipping tight to isoclinal F_2 folds dominate megascopic structures in the area. F_2 folds are particularly well delineated by an Amisk metabasalt unit at the north end of the area and by conglomerate strata northeast of Lost Frog Lake. The F_2 syncline mapped by Stockwell (1936) was named the Herb Lake Syncline by Bell (1980). In axial regions of the folds an F_2 foliation is defined by orientation of biotite. Elongate clasts and mineral segregations define a northeast plunging F_2 lineation.

In the northern part of the area primary facing directions, although rare, indicate that Amisk volcanic rocks lie above both Missi and Amisk sedimentary rocks. One explanation for these relationships is the existence of a thrust fault or faults. Similar field relations to the west caused Froese and Moore (1980) to postulate the McLeod Road thrust fault.

The outcrop pattern of the Amisk volcanic rocks suggests interference of two fold systems, possibly F_1 and F_2. Interpolating the volcanic rocks through areas of no outcrop (Fig. 32.2a) allows the field relationships to be explained by a single folded fault trace. Under this hypothesis, a slice of Amisk metavolcanics, with overlying Missi sediments, has been emplaced above Amisk sediments in the north and Missi sediments in the south (Fig. 32.2b). An assumed, unexposed unconformity separates the two lower sedimentary groups. The truncation of metavolcanic rocks and distribution of staurolite bearing siltstone is explained if it is assumed that the fault trace climbs through the volcanic strata and parallels bedding within the overlying siltstone. Figure 32.2c is a schematic cross-section illustrating the geometry after folding.

Two faults mapped by earlier workers were named by Bell (1980). The Crowduck Bay Fault extends along the Grass River from Wekusko Lake to the north end of the map area. Evidence for this fault includes the prominent foliation in adjacent rocks as well as offset of metamorphic isograds (Gordon, 1981; Shanks and Bailes, 1977).

The Roberts Lake fault extends east from Roberts Lake and offsets map units in the Saw Lake area (Bell, 1980). At Roberts Lake, pillowed mafic volcanic rocks near the fault are silicified and have developed a pervasive foliation.

A third, unnamed fault was recognized by Frarey (1950) as extending southwest from Roberts Lake and truncating the southeast limb of the Herb Lake syncline. On the basis of detailed work, Shanks and Bailes (1977) extended this fault through Stuart Lake. The presence of strongly sheared rocks on the north shore of Puella Bay suggests that this fault extends the full length of the syncline.

Mineral assemblages in pervasively foliated rocks near these faults indicate greenschist facies conditions. This, coupled with the faulted isograds on the Grass River, suggests that faulting occurred after peak metamorphic conditions were reached.

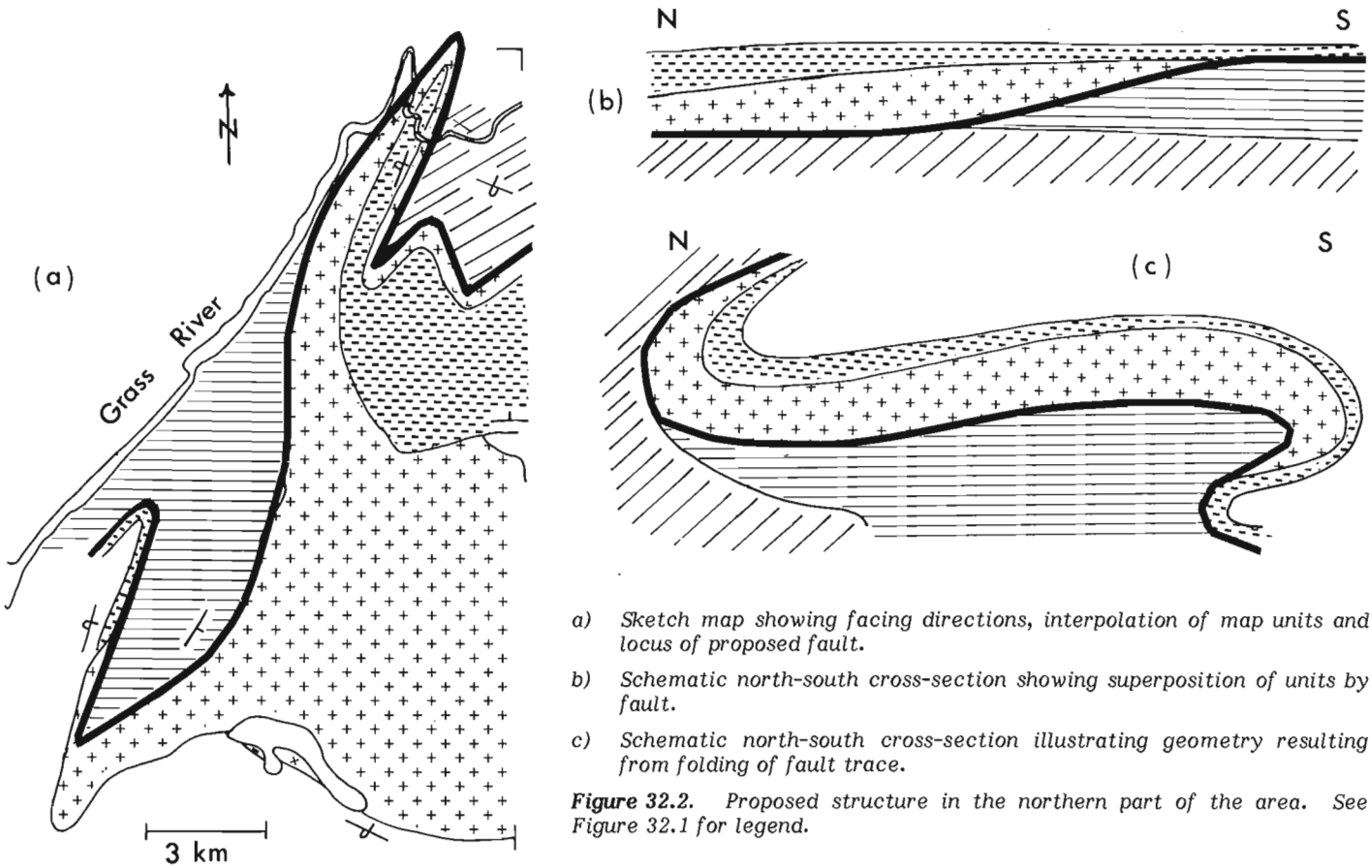

a) Sketch map showing facing directions, interpolation of map units and locus of proposed fault.

b) Schematic north-south cross-section showing superposition of units by fault.

c) Schematic north-south cross-section illustrating geometry resulting from folding of fault trace.

Figure 32.2. *Proposed structure in the northern part of the area. See Figure 32.1 for legend.*

Metamorphism

Froese and Gasparrini (1975) identified several metamorphic isograds in the Snow Lake area based on reactions in muscovite bearing pelitic rocks.

From low to high grade they are:

1. appearance of staurolite coexisting with biotite due to the reaction: chlorite + garnet + muscovite + biotite = staurolite + quartz + H_2O
2. appearance of sillimanite with biotite due to the reaction: chlorite + staurolite + muscovite + quartz = biotite + sillimanite + H_2O
3. disappearance of staurolite and appearance of garnet-sillimanite-biotite assemblages due to the reaction: staurolite + muscovite + quartz = biotite + sillimanite + garnet + H_2O.

Isograds based on field identification of assemblages have been extended into the Crowduck Bay area (Gordon, 1981). Further delineation of metamorphic zones was hampered this year by a paucity of rocks of appropriate compositions.

Siltstones and mudstones on Roberts Lake, Lost Frog Lake, and Stuart Lake contain staurolite-garnet-biotite assemblages. No sillimanite was observed at these localities. Garnet-sillimanite-biotite assemblages were observed both north and south of Dion Lake. Although isograds cannot be drawn with any precision, it can be concluded that the entire central part of the map area is in the staurolite-biotite zone. Grade increases both to the northwest and southeast from this central zone.

Metamorphic minerals are undeformed. On Crowduck Bay, staurolite and sillimanite porphyroblasts lie roughly parallel to the F_2 foliation, but are randomly oriented within the foliation plane. At higher grades, sillimanite-quartz segregations are elongate parallel to F_2. It appears that peak metamorphic conditions were reached during the late stages of F_2 deformation.

West of the map area isograds trend east and metamorphic grade increases from south to north. The change to northeast trends and reversal of gradient in the Crowduck Bay area remains unexplained. No textural evidence was found for a separate episode of metamorphism, and deformation of isograd surfaces is not consistent with the undeformed nature of porphyroblasts. The present configuration of metamorphic zones may be a result of a peculiar heat flow regime or from currently unrecognized faulting.

Mineral Deposits

Gold deposits (Stockwell, 1936) occur in quartz veins within the Missi volcanic sequence. Hydrothermal alteration has produced chlorite-sericite assemblages which have been preserved, indicating that mineralization postdates peak metamorphic conditions.

Lithium bearing pegmatites (Černý et al., 1981) were emplaced following F_2 deformation.

References

Armstrong, J.E.
1941: Wekusko (Herb) Lake, Manitoba; Geological Survey of Canada, Map 665A.

Bailes, A.H.
1971: Preliminary compilation of the geology of the Snow Lake-Flin Flon-Sherridon area, Manitoba; Manitoba Mines Branch, Geological Paper 1/71.

1975: Geology of the Guay-Wimapedi Lakes area; Manitoba Mineral Resources Division, Geological Services Branch, Publication 75-2.

1976: Saw Lake area (Grass River Project); in Report of Field Activities 1976; Manitoba Mineral Resources Division, p. 45-50.

1980: Geology of the File Lake area; Manitoba Mineral Resources Division, Geological Report 78-1.

Bell, C.K.
1980: Geology, Wekusko Lake map area, Manitoba; Geological Survey of Canada, Memoir 384.

Cameron, E.M., Ermanovics, I.F., and Goss, T.I.
1979: Sampling methods and geochemical composition of Archean rocks in southeastern Manitoba, Canada; Precambrian Research, v. 9, p. 35-55.

Černý, P., Trueman, D.L., Ziehlke, D.V., Goad, P.E., and Paul, B.J.
1981: The Cat Lake-Winnipeg River and the Wekusko Lake Pegmatite Fields, Manitoba; Manitoba Mineral Resources Division, Economic Geology Report ER80-1.

Frarey, M.J.
1950: Crowduck Bay, Manitoba; Geological Survey of Canada, Map 987A.

Froese, E. and Gasparrini, E.
1975: Metamorphic zones in Snow Lake area, Manitoba; Canadian Mineralogist, v. 13, p. 162-167.

Froese, E. and Moore, J.M.
1980: Metamorphism in the Snow Lake area, Manitoba; Geological Survey of Canada, Paper 78-27.

Gordon, T.M.
1981: Metamorphism in the Crowduck Bay area, Manitoba; in Current Research, Part A, Geological Survey of Canada, Paper 81-1A, p. 315-316.

Mukherjee, A.C.
1974: Some aspects of sedimentology of the Missi Group and its environment of deposition; Canadian Journal of Earth Sciences, v. 11, p. 1018-1019.

Shanks, R.J. and Bailes, A.H.
1977: "Missi Group" Rocks, Wekusko Lake Area; in Report of Field Activities 1977; Manitoba Mineral Resources Division, p. 83-87.

Stockwell, C.H.
1936: Gold deposits of Herb Lake area, northern Manitoba; Geological Survey of Canada, Memoir 208.

33. SECOND PRELIMINARY REPORT ON THE GEOLOGY OF THE BEECHEY LAKE-DUGGAN LAKES MAP AREAS, DISTRICT OF MACKENZIE

Project 800006

R.A. Frith
Precambrian Geology Division

Frith, R.A., Second preliminary report on the geology of the Beechey Lake-Duggan Lakes map areas, District of Mackenzie; in Current Research, Part A, Geological Survey of Canada, Paper 82-1A, p. 203-211, 1982.

Abstract

The Bathurst Fault System divides the map area in half. The west block is made up principally of metasedimentary rocks of the Beechey Lake Group which are intruded by late Archean granites and granodiorites. They form a metamorphic progression toward the southeast, grading from low grade greenschist facies rocks over a relatively short distance to upper amphibolite facies rocks (or greater). Structures, which are dominantly oriented northwest-southeast become strongly north-northeast – south-southwest toward the southeast where they become parallel to mylonite shear zones.

The Bathurst Fault system, a relatively simple set of sinistral fault planes in the northwest, becomes splayed near the centre of the map area and, degenerates into a series of parallel ductile shear zones, locally characterized by mylonite, ultramylonite, pseudotachylite, and coho-red discoloration.

The east block comprises more highly deformed rocks which consist of migmatites, augen and flasered potash feldspar gneiss, and remnant, little migmatized, elongated zones of paragneiss that resemble and may be equivalent to metasedimentary rocks of the Yellowknife Supergroup. Small areas of granulite facies leucogneiss underlie an aeromagnetically low area in the northeast of the map area.

Mineralization is present along the margins of most of the long narrow andesitic volcanic belts that have been mapped both west and east of the Bathurst Fault system.

Introduction

This report summarizes the findings of the second season's mapping of the Beechey Lake (east half) and Duggan Lake (west half) map areas (Fig. 33.1). The entire area has now been mapped at 1:50 000 with traverses approximately 2 km apart, for final publication at 1:100 000 or 1:250 000 scale. The mapping was almost entirely carried out by foot traverses with helicopter support either from a base camp near the centre of the area or from fly camps supplied from Healey Lake (Henderson et al., 1982).

This report deals primarily with the geology of the region east of the Bathurst Fault and along the Back River, which flows through the southeastern part of the map area. The report complements previous work by Frith (1981) and Tremblay (1971), other simultaneous mapping to the south in the Healey Lake area (Henderson and Thompson, 1980, 1981; Henderson et al., 1982), and the more regional mapping of Wright (1967).

The major aims of geological investigations in this region were: to understand the nature of the transition between the Slave and Churchill Structural provinces known as the Thelon Front (Wright, 1967); to relate the ages of deformation, metamorphism and intrusion of rocks within the Slave to those within the Churchill Province; to determine the movement and style of displacements along the Bathurst Fault system; and to produce a final map and report describing the rocks and their geological history that would assist future geological and mineral exploration activity.

Acknowledgments

The successful completion of the mapping during the 1981 season was due to the excellent work and energy of Raynald Lapointe, Donald James and Jūrata Lukošius and by the assistance of Robert Macfie, Michael Bradfield and Gaele Card. Canwest Aviation of Calgary, with their pilot Tobias Heller, provided excellent service in the field, and Winifred Bowler, through the Resident Geologist's Office in Yellowknife, gave us reliable logistic support. Peter Thompson and John B. Henderson kindly consented to critically read this paper.

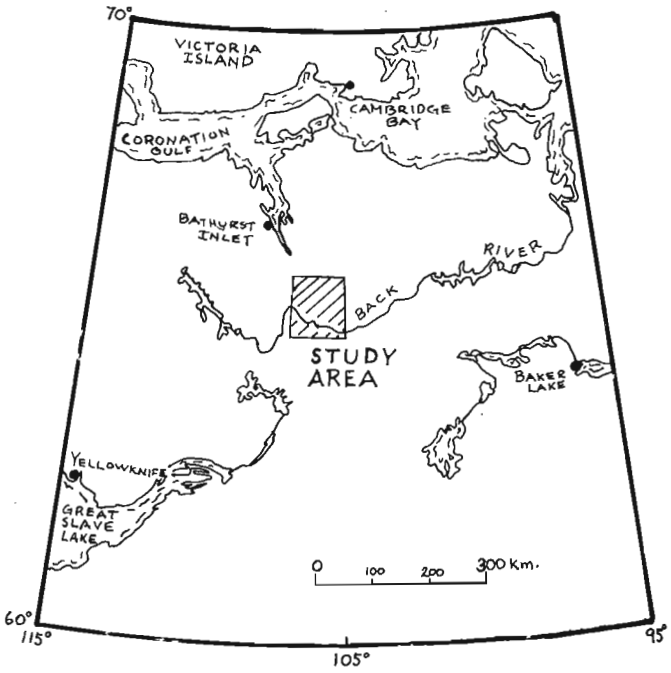

Figure 33.1. *Location of Beechey-Duggan Lakes map areas.*

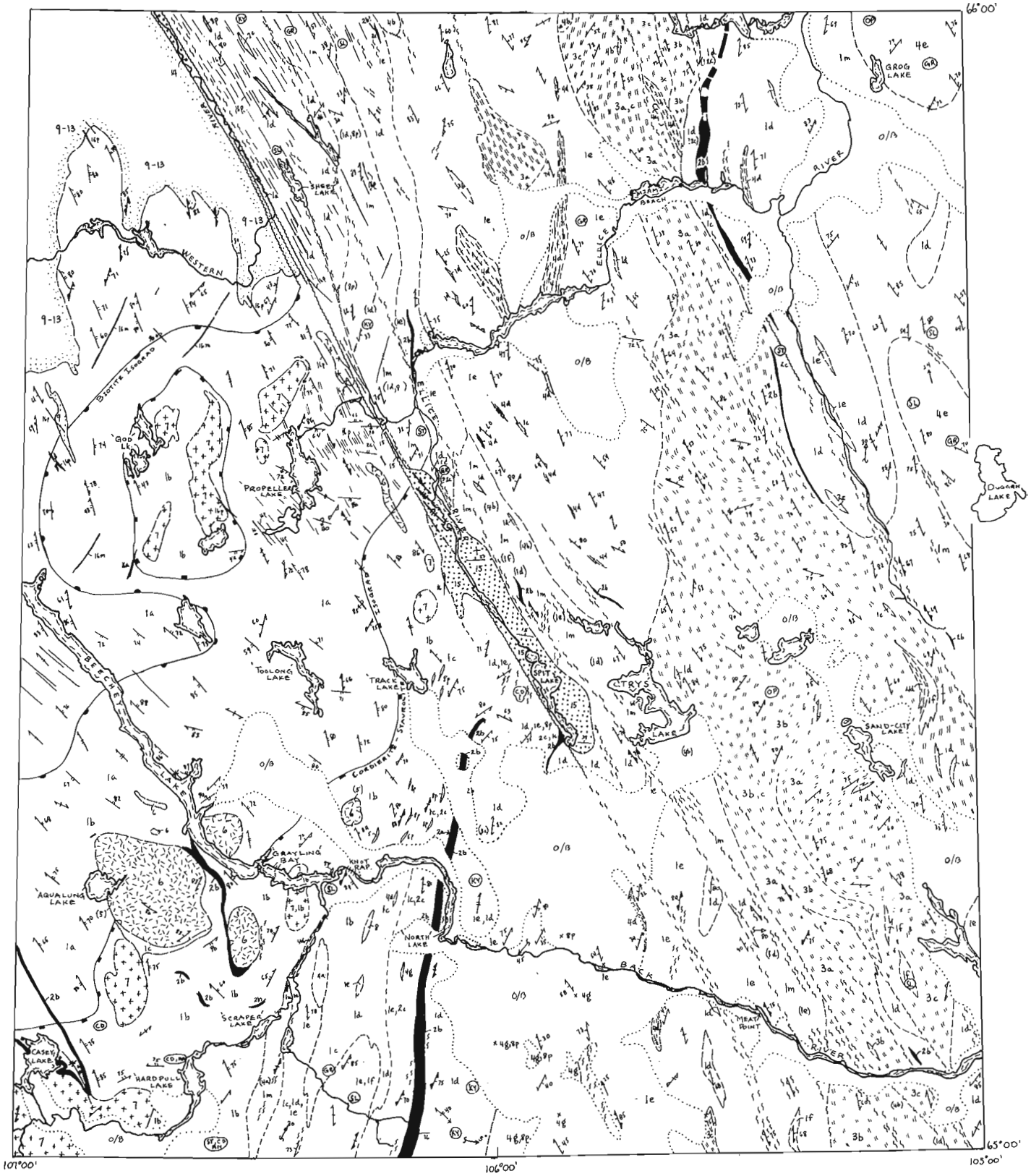

Figure 33.2. *Geological sketch-map of the Beechey-Duggan Lakes map areas, adapted in part from Tremblay (1971).*

Legend for Figure 33.2

16 — Diabase and gabbro dykes and sills and their metamorphosed equivalents: 16p - older suite, metamorphosed, deformed; 16m - Mackenzie dykes; 16a - Malley Diabase

15, 14 — Ellice and Tinney Cove Formations

9, 13 — Goulburn Group - undifferentiated

8 — Pegmatitic muscovite granite; dykes and sills, 8p.

7 — Biotite-muscovite granite

6 — Biotite granodiorite

5 — Biotite and/or hornblende diorite

4 — Gneiss and migmatite of uncertain origin:
4a, granitic composition with biotite, ± muscovite, hornblende
4b, granodioritic composition with biotite, ± hornblende
4d, dioritic composition with hornblende, ± biotite, garnet
4e, leucogneiss of tonalitic or aplitic composition, ± garnet, biotite

3 — Potash feldspar augen or flaser gneiss:
3a, granodioritic composition
3b, dioritic composition
3c, migmatitic in part
3d, containing remnant paragneiss

2 — Volcanic rocks and their metamorphosed equivalents:
2a, felsic to intermediate composition
2b, intermediate to basic composition
2c, volcanogenic paragneiss

1 — Greywacke-mudstones and their metamorphosed equivalents:
1a, biotite and sub-biotite grade
1b, porphyroblastic biotite gneiss and schist, ± cordierite, andalusite, sillimanite, kyanite, staurolite
1c, biotite gneiss or schist with no porphyroblasts, ± 8 or 8p
1d, biotite gneiss with potash feldspar-bearing segregation veining
1e, migmatite with less than 50% resistite
1f, migmatite with less than 25% resistite
1m, undifferentiated paragneiss, paraschist. May be sheared, mylonitized and discoloured to a coho red.

Bedding: tops probable, tops certain, tops unknown, horizontal

Bedding-Foliation: (as above)

Foliation: locally first, second and third

Unit Contacts: probable, assumed

Airphotograph lineaments

Overburden × Isolated outcrop

eg (AN) — AN - andalusite; SL - sillimanite; KY - kyanite; ST - staurolite; GR - garnet; OP - orthopyroxene

eg (1d) — Unit in brackets signify local abundance

Fault - defined, assumed, shear zone

0 5 10 15 Km.

General Geology

Bathurst Fault is a left lateral fault system about 350 km long. The fault system divides the map area into two roughly equal parts (Fig. 33.2) and may be readily identified in the northern half of the area by its deep valley and topographic expression. However, the southern half of the fault system is not as distinctive. The major movement plane changes from a fault with much breccia and relief to a ductile shear zone with little topographic expression. In addition, the major movement plane that extends to Bathurst Inlet becomes splayed in the vicinity of 'Spit' Lake[1] into two or more shear zones. The principal one extends through the east side of 'Trys' Lake.

The mapping of the fault in this area has not resolved the amount of displacement along it. An estimate of left lateral displacement of 32 km (Tremblay, 1971), based on the displacement of Goulburn strata, and 140 km, based on the displacement of bioherms (Campbell and Cecile, 1979) are prone to error due to vertical movements, whereas the 18 km displacement of an aeromagnetic anomaly (Thomas et al., 1976) only measures the displacement of a single offset and is a minimum.

The rocks west of the fault system are deformed, but primary sedimentary features are preserved in the north half where regional metamorphism is of greenschist facies. Toward the southeast the west block becomes progressively more deformed where regional metamorphism is of upper amphibolite or granulite facies grade. The rocks are mostly Beechey Lake Group-Yellowknife Supergroup greywacke-mudstones which prograde in metamorphism and increase in the degree of deformation from bedded sedimentary rocks with primary sedimentary features and easily recognizable isoclinal folding to migmatites and mylonites that are polydeformed. In places the rocks can only be described as tectonites of a certain composition.

East of the Bathurst Fault system, highly deformed but locally recognizable equivalents of the Yellowknife Supergroup are present, along with migmatites and augen gneiss derived from Yellowknife paragneiss. These rocks, together with locally abundant hornblende, melanogneiss and garnetiferous leucogneiss of uncertain origin, make up the bulk of the rock types of the east block. Other rocks include amphibolite gneiss (derived from volcanic rocks), pegmatites and diabase dykes and sills.

In general, the metamorphic grade of the rocks east of the Bathurst Fault is high; kyanite is locally evident in the vicinity of the fault system and orthopyroxene within 20 km of it. However, the east block contains zones of relatively low grade rocks with low proportions of quartzofeldspathic segregations and garnet, staurolite and sillimanite porphyroblasts which overgrow existing fabric.

In Figure 33.2 the extent of the various subunits is not always outlined due to heterogeneity, lack of continuity, or in some places lack of outcrop. This is commonly the case for subunits 1c and 1d, 1e and 1f, 1 e and 1 m and for all the subunits of unit 3.

Greywacke-mudstone and their metamorphosed equivalents (unit 1)

Subunit 1a is the relatively unmetamorphosed part of this unit, made up of bedded greywacke-mudstone of greenschist grade and has been described previously by Frith (1981) as part of the Beechey Lake Group (Frith and Percival, 1978).

Subunit 1b is derived from subunit 1a but is more schistose and commonly contains one or more porphyroblasts of staurolite, cordierite, garnet and an aluminosilicate polymorph of andalusite, sillimanite or kyanite (Frith, 1981).

Subunit 1c is made up of rusty weathering biotite quartz plagioclase gneiss with no porphyroblasts as in subunit 1b, but commonly contains secondary muscovite that postdates an equally common shear foliation. The rocks are cut by abundant quartz veins and quartzofeldspathic and muscovite-bearing pegmatites that are locally sheared. These rocks contain no potash feldspar and may be of similar grade of metamorphism to rocks of subunit 1b. However, deformation has destroyed any porphyroblasts originally present. The rocks of this subunit are metamorphic tectonites, discernible by degree of deformation from more highly deformed rocks of this unit farther to the east. The rocks are not always easily distinguished from metavolcanic paragneiss of unit 2c, which also have no porphyroblasts.

[1] Names given in single quotes are unofficial and are used for convenience only

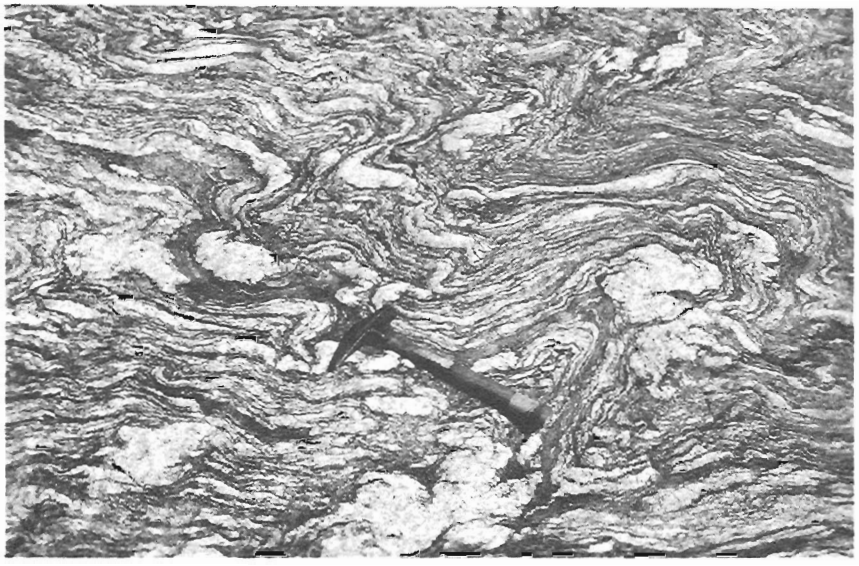

Figure 33.3. *Contorted migmatite of subunit 1e found on the Back River, west of the Bathurst Fault system. GSC 203647-E*

Figure 33.5. *Deformed north-south metadiabase dykes that intrude as a north-south trending swarm. These rocks are highly deformed and locally mylonitized by north-northeast trending shear zones. GSC 203647-F*

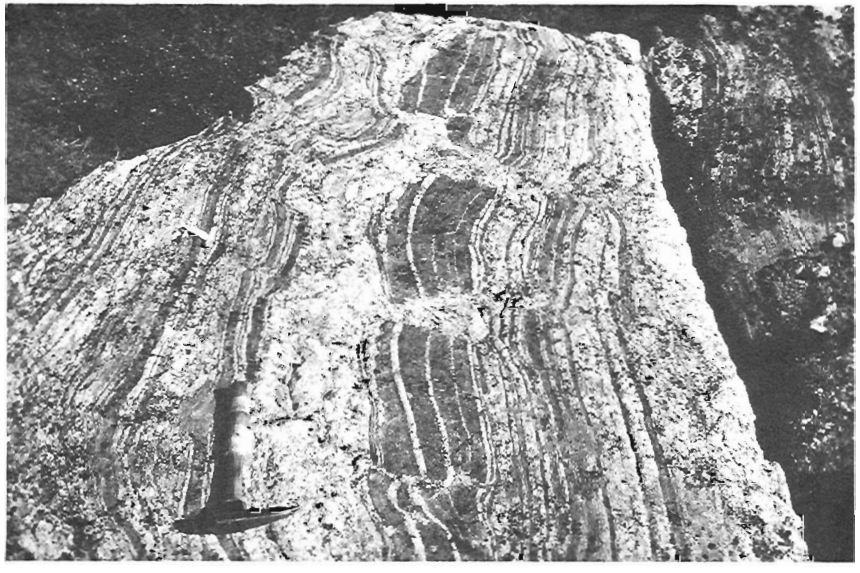

Figure 33.4. *Banded migmatite of subunit 1e found south of the Ellice River, east of the Bathurst Fault system. GSC 203644*

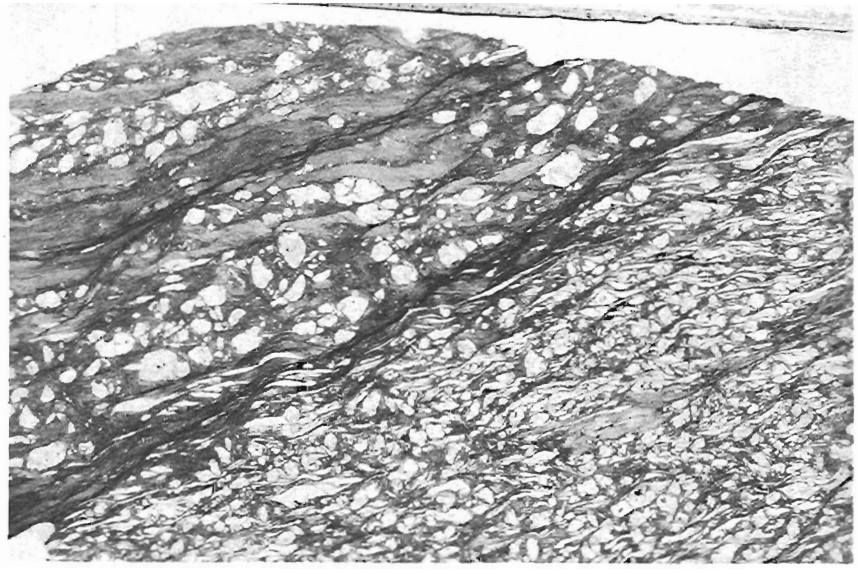

Figure 33.6. *Mylonite formed by the north-northeast trending shear zones found just east of 'Track' Lake. GSC 203716-F*

Subunit 1d comprises granodioritic, rusty coloured, biotite, quartz, plagioclase gneiss with variable (but less than 50 per cent) proportions of leucosome quartz, plagioclase and potash feldspar. The rocks are commonly intruded by muscovite-bearing alaskite, pegmatite, aplite and quartz veins. Hornblende is locally abundant, particularly where diorite (subunit 4d) is common.

The rocks may contain porphyroblasts but these are not prevalent. The most common porphyroblasts are garnet and potash feldspar, which form limited areas of augen gneiss similar to and gradational with the augen gneiss of unit 3. Other porphyroblasts and metamorphic index minerals include staurolite, kyanite or sillimanite.

The subunit is distinguished from subunit 1c by the presence of potash feldspar, from subunit 1e by the proportion of leucosome which is less than half of the rock, and from unit 3 by lack of pervasive potash feldspar porphyroblasts or augen.

Subunits 1e and 1f are migmatites found on both sides of the Bathurst Fault system. They are probably derived from rocks similar to those of subunits 1a to 1d. Where the proportion of leucosome is between 50 and 65 per cent (Fig. 33.3 and 33.4) of the rock, it is designated subunit 1e; where greater than this, as subunit 1f. It was found that migmatitic regions may have a preponderance of one type over the other, but rarely to the exclusion of the other. The restite phase of these rocks is similar to subunit 1d in mineral composition but exotic minerals other than garnet are absent. The leucosome is usually simple, with quartz, plagioclase and potash feldspar, but may contain garnet, tourmaline and muscovite. The migmatites near Back River are intruded by numerous diabase dykes which have been metamorphosed and deformed along with the migmatites, locally leading to heterogeneous, seemingly chaotic patterns (Fig. 33.5). Like subunit 1d, these rocks may contain potash feldspar augen which grade into rocks of unit 3, but are distinguished from them by the lack of pervasive augen development.

Subunit 1m is made up principally of unit 1 rocks that have been highly deformed and not readily divisible into subunits 1c through 1f. The unit may also contain areas of rocks resembling units 3 and 4, which are not mappable at a 1:50 000 scale. Three main areas are shown in Figure 33.2; at 'Scraper' Lake, through 'Trys' Lake and in the northeast and southwest corners of the map area.

The 'Scraper' Lake rocks are sparsely exposed, but where present are heterogeneous, highly sheared granodioritic gneiss and mylonites that have locally been discoloured to a deep coho-salmon pink. Mafic minerals have been retrograded and secondary epidote is common. Parts of the subunit are composed of foliated, but locally massive, coarse grained granites similar to units 7 or 8 and several zones of schist similar to subunit 1c alternate with subunit 1d.

The zone of subunit 1m that runs through 'Trys' Lake extends almost the length of the map area parallel to the Bathurst Fault system. In the north it is composed of abundant coarse grained pegmatite of unit 8p interlayered with subunit 1d paragneiss. From casual observation the pegmatite dominates, but this is probably due to erosional resistance of the pegmatite relative to the paragneiss. Near Ellice River, where kyanite was noted (Fig. 33.2), the rocks are partly metamorphically segregated paragneiss but are intimately interlayered with migmatites of 1e and 1f. In the locality marked by the presence of staurolite, coarse pegmatitic granite of unit 8 is also interlayered with paragneiss. Deformation is extreme along the Fault zone where highly discoloured rocks of granitic and granodioritic composition were converted to mylonites, flinty rocks in general, and possibly pseudotachylites. From Ellice River to 'Trys' Lake intense shearing is pervasive but locally, red granodiorite gneiss (4b), rusty paragneiss (1d) and migmatites (1e, 1f) can be recognized. Southeast of 'Trys' Lake unit 1 is highly sheared and mylonitized, grading to lesser deformed 1e migmatites or granodioritic augen gneiss (unit 3).

Volcanic Rocks and their Metamorphosed Equivalents (unit 2)

Subunit 2b includes intermediate basic volcanic rocks which occur on both sides of the Bathurst Fault system. They were less affected by the effects of thermal and dynamic metamorphism and have generally retained their fine grain size and bulk composition. The least metamorphosed are subcordierite/staurolite grade rocks of the Casey Lake belt (Frith, 1981). The 'Scraper' Lake belt is of slightly higher metamorphic grade and is more highly sheared, but remnant pillowed and brecciated andesites were recognized.

The 'North' Lake volcanic belt is more highly sheared with mylonitic textures noted in places, particularly along the margins. The west margin contains calcium carbonate and either pyrite or pyrrhotite. Remnant pillow-like structures are preserved in some of the central parts of the belt, particularly in the segment mapped north of the Back River.

Within the east block, several small amphibolite masses have been mapped in the highly deformed zone of rocks that parallels the Bathurst Fault system. These are fine grained, hornblende-plagioclase rocks, locally with garnet that, due to their composition (2b), have resisted the migmatization that has affected the rocks of unit 1. However, deformation has stretched them to thin slivers bounded by sheared out migmatites and rusty biotite gneiss. These rocks may be similar to and gradational with the more dioritic rocks of units 3 and 4, and are only separated from them by the degree of migmatization, development of augen texture, and by deformation. Usually deformation is too far advanced to recognize any volcanogenic structures. The 'Miami' Beach belt is a meta-andesitic belt that is highly deformed with gossans occurring along the west margins. The belt is 1.25 km wide to the north, but thins to a few tens of metres towards the southeast, pinching out west of Duggan Lake.

Subunits 2a and 2c are felsic to intermediate volcanics and volcanic paragneiss. These rocks generally occur along the west side of the North Lake belt. Some felsic volcanic rocks have been recognized north of the Back River but they are difficult to separate from units of 1c. They are rusty coloured biotite, plagioclase, quartz gneiss with no porphyroblasts and are intruded by abundant granite-pegmatite bodies.

Similar 2c rocks were found at the sillimanite occurrence northeast of 'Sheet' Lake and along the west margin, and, possibly, the east margin of the 'Miami' Beach belt. These rocks are slate-like, commonly rusty coloured and locally gossanous. They are biotite- and quartz-rich and distinguished from unit 1 rocks by the sparsity of feldspathic segregations. Quartz, however, is common and forms veins parallel and discordant to the foliation.

Potash Feldspar Augen or Flasered Gneiss (unit 3)

The gneiss of this unit is characterized by the presence of augen or flasered development of potash feldspar, and generally, by granodioritic (3a) or dioritic bulk composition (3b). Migmatitic rocks (3c) or those with mobilizate veins or layers less than 50 per cent of the rock are also common and may grade into migmatites of subunit 1f or 1e. On the other hand, migmatitic paragneiss (subunit 1d) may form elongate zones within unit 3 and rocks along their contacts may be alternately augen-bearing and augen-barren. This observation and the intimate border relationships with unit 1 migmatites elsewhere suggests that these rocks may be high grade equivalents of unit 1.

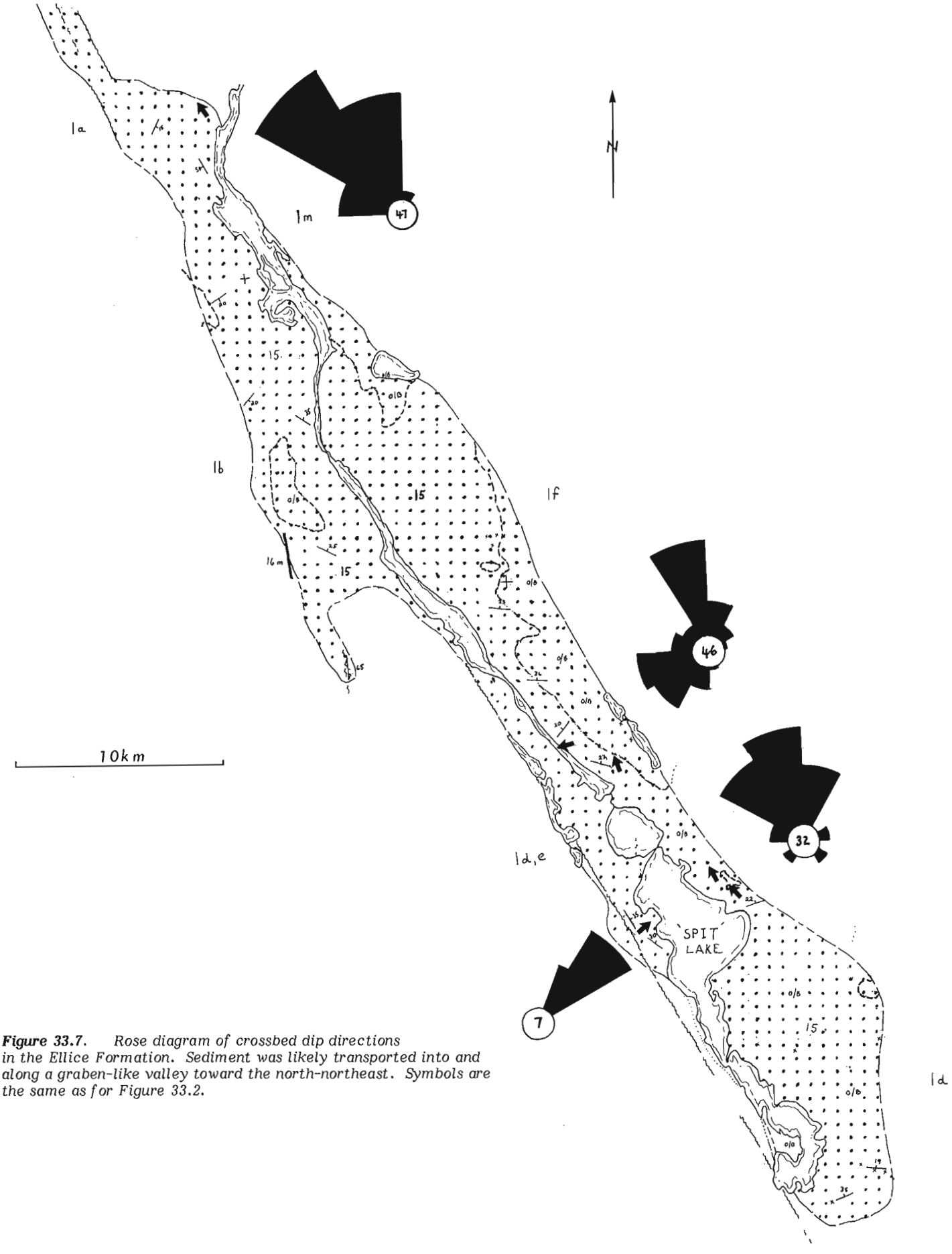

Figure 33.7. *Rose diagram of crossbed dip directions in the Ellice Formation. Sediment was likely transported into and along a graben-like valley toward the north-northeast. Symbols are the same as for Figure 33.2.*

The rocks are simple mineralogically, containing biotite, quartz, plagioclase and potash feldspar. However, there are some localities that contain orthopyroxene, as indicated in an area northwest of 'Sand City' Lake.

Where shearing and mylonitization was intense, the gneiss is discoloured red, as in the sheared rocks of the southeast corner. The augen or flaser development clearly predates the last stages of shearing.

Gneiss and Migmatite of Uncertain Origin (unit 4)

The gneiss and migmatites of this unit are tectonites or high grade metamorphic rocks. They have been divided into four compositional groups which include granitic (4a), granodioritic (4b), dioritic (4d) and tonalitic-aplitic (4e).

Subunits 4a and 4b. Granitic and granodioritic rocks modified by shearing are present in zones which parallel the Bathurst Fault system. They commonly form parts of unit 1m where they are mixed with remnant migmatite, paragneiss and amphibolites.

Subunit 4d. Dioritic gneiss and migmatites have been mapped in the east block where they form diffusely bounded zones of hornblende-bearing gneiss or migmatite. The gneissic rocks may be garnet-bearing and near Back River hornblende and biotite occurs in roughly equal proportions.

Subunit 4e. Leucogneiss of this subunit is made up of tonalitic or aplitic, usually fine grained gneiss containing bluish quartz, plagioclase or potash feldspar, and commonly, garnet. The rocks outcrop in two areas in the northeast corner of the map area. They may contain porphyroblasts of sillimanite and/or garnet. Locally, orthopyroxene is present. The rocks commonly have a 'greasy', dull-grey, overall appearance. Some porphyroblasts of garnet have grown to fist-size. The unit is approximately coincident with an aeromagnetic low.

Granitoid Plutonic Rocks (units 5-7)

Plutonic rocks occur principally in the west block and have been described previously (Frith, 1981). Chemical analyses carried out on these plutons indicate the bulk of the pluton adjacent to 'Aqualung' Lake and the smaller pluton on the north shoreline of Beechey Lake are granodiorites. Some of the marginal phases of the Aqualung pluton and the pluton northwest of 'Propeller' Lake are tonalitic rather than dioritic, as previously suggested. This corroborates earlier views that these plutons are probably equivalent to the Regan Intrusive Suite (Hill and Frith, in prep.). In thin section the rocks show considerable retrograde reactions of biotite, and in some localities, feldspar. This may be due to thermal effects related to Proterozoic deformation as discussed subsequently.

Muscovite Granite and Pegmatite (unit 8)

The rocks of unit 8 are found in areas of high metamorphic grade as small irregularly shaped bodies elongated in a north-south direction parallel to the regional gneissosity of schistosity. They are very coarse grained and made up of muscovite, quartz and plagioclase.

The boundary relationships with hosting paragneiss or paraschist are sharp and along the west margin of the 'North' Lake volcanic belt they have been deformed by north-northeast trending shearing. The unit postdates the Archean regional metamorphism.

In the east block pegmatitic muscovite granite occur in small bodies intimately associated with remnant schistose biotite-bearing paragneiss. They are locally massive and have, because of their irregular distribution, been included within subunit 1m.

Goulburn Group (units 9-13)

No new mapping of the Aphebian Goulburn Group was carried out during 1981. The rocks exposed in this area have been mapped by Tremblay (1971) as resting unconformably on sediments equivalent to the Yellowknife Supergroup. The rocks are made up of conglomerates, quartz sandstone, siltstone, dolomitic sandstone, argillite and siltstone of the Western River Formation and sandstones, conglomerate and argillites of the Burnside River Formation. The rocks are cut by diabase dykes that are both Mackenzie (16m) and pre-Mackenzie (16p).

The rocks are gently folded and contain a fabric related to this folding oriented in a north-south direction. Frith (1981) considered this fabric and the folding to be related to movements of the Bathurst Fault system, as suggested by Campbell and Cecile (1981) after the model by Wilcox et al. (1973). This fabric is probably the same as that cutting the pre-Mackenzie diabase dykes.

Ellice and Tinney Cove formations (units 14 and 15)

The Helikian Ellice Formation consists of sandstone, arkose and conglomerate with some shale and carbonate rocks (Tremblay, 1971). The west margin of the unit is locally sheared, due perhaps to the movements along the Bathurst Fault system. The conglomerates noted in some localities by Tremblay (1971) contain some fragments of red feldspar and red granitoid rock which, during this study, were found along shear zones of the Bathurst Fault system.

Paleocurrent determinations using data from Tremblay (personal communication) and from this study indicate a principal north-northwest direction of transport with northeast and southwest, probably subsidiary transport directions (Fig. 33.7).

The Helikian Tinney Cove Formation occurs between faults along the Western River valley, as mapped by Tremblay (1971). It is made up of rocks similar to the Ellice Formation and are more extensive and better exposed farther northwest in the Bathurst Inlet area (Campbell, 1979).

Diabase and Gabbro Dykes and Sills and Their Metamorphosed Equivalents (unit 16)

Apart from the three sets of dykes described previously by Frith (1981), which include the Malley Diabase (16a), the Mackenzie diabase dykes (16m) and a pre-Mackenzie set of similar trend (16p), there are a few east-west trending dykes in the south-centre of the map area which are retrograded, have a north-south fabric, and contain some deformed quartz veins. In addition, there are significant numbers of north-south trending dykes present in the North Lake-Back River area. These dykes are now garnetiferous amphibolites which have been highly deformed, mylonitized and injected by quartz and quartzofeldspathic veins (Fig. 33.5). Some dykes are as much as 50 m wide. The north-south dykes may be of Archean age, as they are deformed along with the segregations that may be part of an Archean prograde metamorphism in the region. The numerous dykes in the 'Propellor' Lake area form an arcuate northwest pattern that dies out to the northwest and southeast.

Northwest-trending dykes in the 'Sheet' Lake area are very numerous (perhaps more numerous than shown in Fig. 33.2), locally making up 20 per cent of the area and more. The dykes have intruded parallel to the principal Bathurst Fault planes and are usually sheared and amphibolitized. The ages of these dykes are unknown since movements on the fault were probably episodic and long-lived. However, they have no pronounced aeromagnetic signature and are probably pre-Mackenzie (16p).

Structure, Metamorphism and Age Relationships

The age relationships among structure, metamorphism in the Nose Lake (E/2) – Beechey Lake (W/2) map areas (Fyson and Frith, 1979; Frith and Percival, 1978; Frith and Loveridge, in prep.) probably holds true for much of the west block of the present map area. In brief the Yellowknife volcanic and sedimentary rocks were deformed (D_1 and D_2) and metamorphosed regionally before the emplacement of late Archean plutons of 2600-2500 Ma age. The metasedimentary rocks and the late Archean plutons are cut by a northeast cleavage (D_3) and their K-Ar mica systems have been reset by an early Proterozoic thermal event.

In the west block, D_1 through D_3 are observed in the western margin of the map area, but these structures become difficult to recognize anywhere east of 'Grayling' Bay[1] due to the intensity of two additional structures recognized in the earlier stages of this investigation (Frith, 1981).

D_4 Structures. Mapping across the Thelon Front as defined by Wright (1967) revealed parallel north-northeast trending shear zones that extend over a width of at least 35 km. These shear zones parallel and may be of similar age to the Proterozoic 'straight zone' found in the southeast corner of the Healey Lake map area. The latter zone (Henderson and Thompson, 1981) extends 250 km south to the McDonald Fault.

The shear zones and the best mylonitic textures are developed where lithological contrast is greatest, such as along the interface between the granodiorite and host metasediment located between 'Scraper' Lake and 'Grayling' Bay and along the margins of the volcanic belt that extends parallel to 'North' Lake.

Thin section studies of some mylonitic zones, such as that found east of 'Track' Lake (Fig. 33.6), show the most dramatic development in granitic migmatites.

In the vicinity of 'Meat' Point, north-northeast trending mylonitization gives way to north-northwest trending shear zones that form part of the Bathurst Fault system. Within the east block shear zones of similar north-northeast orientation were noted. It is not clear if these are related to D_4.

D_5 Structures (the Bathurst Fault System). The intensity of the shearing in the Bathurst Fault Zones (D_5) is impressive; not only does it extend the length of the map area (and probably beyond) but it occurs as a highly deformed and locally mylonitized zone over a width of 10 km or more. Where lithologies are less competent, as in the rusty biotite gneiss zones of 'Sheet' Lake, the complexity is increased by multiple diabase dyke emplacement.

The most intense shearing occurs between rocks of different rheomorphic properties, usually granitoid rocks and paragneiss or metavolcanic rocks and paragneiss. Along the Ellice River near the staurolite location (Fig. 33.2) the east block near the Ellice Formation contains flinty-crush breccias, ultramylonite zones, and pseudotachylites. These rocks are in the area where fault splays are thought to occur, as seen on air photo lineaments (Fig. 33.2).

Metamorphism

Recent mapping in the west block outlined a kyanite-bearing zone that extends along the east side of the 'North' Lake volcanic belt. This polymorph is present in migmatitic rocks along with garnet and biotite and contrasts with the first appearance of cordierite-andalusite-staurolite at 'Grayling' Bay, a distance of only 20 km. From these end points the estimated path of regional metamorphism using a Holdaway (1971) aluminosilicate grid would have gone from an estimated pressure of $\sim$3.5 kb and temperature of $\sim$500°C to a pressure of $\sim$6.5 kb and temperature of $\sim$700°C, providing the kyanite is produced from a melting reaction. None of these parameters have been sufficiently investigated as yet. This excessive pressure jump would support a dramatic uplift of the region along the many ductile shear zones mapped between these two points.

East of the kyanite occurrences there is a dearth of exotic minerals, as pervasive deformation, migmatization and the development of potash feldspar porphyroblasts take their toll.

In the east block, kyanite and staurolite were recognized in a rusty, slightly migmatized paragneiss zone that extends along the east margin of the Bathurst fault zone from the north limit of the map area to Ellice Formation. The kyanite is euhedral and associated with staurolite and garnet, which appear to be deformed and corroded. These rocks are intruded by coarse muscovite-bearing pegmatite, less deformed and probably younger in age.

Orthopyroxene was noted between 'Trys' and 'Sand City' lakes and in the 'Grog' Lake area. The former is found in fine- to coarse-grained subhedral augen gneiss of granodioritic composition that contains amphibole, alkali-feldspar, orthopyroxene-plagioclase-biotite and magnetite. This is an isolated occurrence and further work is needed to determine if granulite facies rocks are present regionally. In the 'Grog' Lake area the rocks look like granulites, with dull, greasy feldspar, bluish quartz in leucogneiss of tonalitic composition. Orthopyroxene occurs as medium grained, bronze-coloured blasts along with amphibole and possibly biotite. In the region, garnets and large sillimanite porphyroblasts are common, some garnets growing to a diameter of 10 cm.

The 'Thelon' Front

In previous reports concerning the area it was noted that the Thelon Front, as described by Wright (1967) was a structural-metamorphic and lithologic transition, but Frith (1981) noted that none of these parameters were present to properly define the zone as it was noted that structures of Proterozoic age were sporadic and extended 70 km or more into the Slave Province. In addition, the most dramatic metamorphic changes were probably Archean, and lithologies were similar over the same width. However, this rejection was perhaps overzealous. If the concept of a zone and a change of structures are used to delineate provinces, as suggested by Stockwell (1961), then the Thelon Front as delineated by Wright is close to where the zone should be, on the understanding that the north-northeast trending shear zones define the 'Front' where they have realigned or cleaved Archean structures. In this map area a convenient line would be that east of the 'North' Lake volcanic belt and its extension to the first principal movement plane of the Bathurst Fault system. Everything west of this line is deformed only sporadically by the deformation that produced the north-northeast cleavage, whereas east of this line the cleavage is pervasive.

References

Campbell, F.H.A.
1979: Stratigraphy and sedimentation in the Helikian Elu Basin and Hiukitak Platform, Bathurst Inlet-Melville Sound, N.W.T.; Geological Survey of Canada, Paper 79-8.

Campbell, F.H.A. and Cecile, M.P.
1979: The northeastern margin of the Aphebian Kilohigok Basin, Melville Sound, Victoria Island, District of Franklin; in Current Research, Part A, Geological Survey of Canada, Paper 79-1A, p. 91-97.

[1] informal name

Campbell, F.H.A. and Cecile, M.P. (cont.)
1981: Evolution of the early Proterozoic Kilohigok Basin, Bathurst Inlet and Victoria Island, N.W.T.; in Proterozoic Basins of Canada, Geological Survey of Canada, Paper 81-10.

Frith, R.A.
1981: Preliminary account of the Geology of the Beechey Lake-Duggan Lakes map areas, District of Mackenzie; in Current Research, Geological Survey of Canada, Paper 81-1A, p. 333-339.

Frith, R.A. and Loveridge, W.D.
1982: Ages of Yellowknife Supergroup Volcanic Rocks: Granitoid intrusive rocks and regional metamorphism in the northeastern Slave Structural Province; in Current Research, Part A, Geological Survey of Canada, Paper 82-1A, Report 36.

Frith, R.A. and Percival, J.A.
1978: Stratigraphy of the Yellowknife Supergroup in the Mara River area, District of Mackenzie; in Current Research, Part C, Geological Survey of Canada, Paper 78-1C, p. 89-98.

Fyson, W.K. and Frith, R.A.
1979: Regional deformation and emplacement of granitoid plutons in the Hackett River greenstone belt, Slave Province, Northwest Territories; Canadian Journal of Earth Sciences, v. 16, p. 1187-1195.

Henderson, J.B. and Thompson, P.H.
1980: The Healey Lake map area (northern part) and the enigmatic Thelon Front, District of Mackenzie; in Current Research, Part A, Geological Survey of Canada, Paper 80-1A, p. 165-169.

1981: The Healey Lake map area and the enigmatic Thelon Front, District of Mackenzie; in Current Research, Part A, Geological Survey of Canada, Paper 81-1A, p. 175-180.

Henderson, J.B., Thompson, P.H., and James, D.T.
1982: The Healey Lake map area and the Thelon Front problem, District of Mackenzie; in Current Research, Part A, Geological Survey of Canada, Paper 821A, report 31.

Hill, J.D. and Frith, R.A.
Petrology of the Regan Intrusive Suite in the Nose-Beechey Lakes area, District of Mackenzie; Geological Survey of Canada, Paper. (in prep.)

Holdaway, M.J.
1971: Stability of andalusite and the aluminum silica phase diagram; American Journal of Science, v. 271, p. 97-131.

Stockwell, C.H.
1961: Structural Provinces, Orogenies and Time Classification of rocks of the Canadian Precambrian Shield; in Age Determinations by the Geological Survey of Canada, No. 2, compiled by J.A. Lowdon, Geological Survey of Canada, Paper 61-17, p. 108-117.

Thomas, M.D., Gibb, R.A., and Quince, J.R.
1976: New evidence from offset aeromagnetic anomalies for transcurrent faulting associated with the Bathurst and McDonald faults, Northwest Territories; Canadian Journal of Earth Sciences, v. 13, p. 1244-1250.

Tremblay, L.P.
1971: Geology of Beechey Lake map area, District of Mackenzie; Geological Survey of Canada, Memoir 356, 56 p.

Wanless, R.K., Stevens, R.D., Lachance, G.R., and Rimsaite, J.Y.H.
1965: Age determinations and geological studies, Part 1 – Isotopic Ages, Report 5; Geological Survey of Canada, Paper 64-17.

1966: Age determinations and geological studies, K-Ar isotopic ages, Report 6; Geological Survey of Canada, Paper 65-17.

Wilcox, R.E., Harding, T.P., and Seely, D.R.
1973: Basic Wrench Tectonics; American Association of Petroleum Geologists Bulletin, v. 57, p. 74-96.

Wright, G.M.
1967: Geology of the southeastern barren grounds, parts of the Districts of Mackenzie and Keewatin (Operations Keewatin, Baker, Thelon); Geological Survey of Canada, Memoir 350.

34. SEDIMENTOLOGY OF TWO MIDDLE PALEOZOIC TERRESTRIAL SEQUENCES, KING GEORGE IV LAKE AREA, NEWFOUNDLAND, AND SOME COMMENTS ON REGIONAL PALEOCLIMATE

Projects 760027, 770026

F.W. Chandler
Precambrian Geology Division

Chandler, F.W., Sedimentology of two Middle Paleozoic terrestrial sequences, King George IV Lake area, Newfoundland, and some comments on regional paleoclimate, in Current Research, Part A, Geological Survey of Canada, Paper 82-1A, p. 213-219, 1982.

Abstract

A belt of deformed but unmetamorphosed alluvial sedimentary rocks within the King George IV Lake area, southwest Newfoundland, consists of two parts. A redbed sequence containing felsic volcanic flows and pyroclastics was probably deposited under a dry climate. A possibly younger grey sequence, lacking contemporary volcanism may have been deposited by a meandering fluvial system under a humid climate.

Supporting evidence of dry climate of deposition for the redbeds comes from identification of calcrete in the probably correlative Silurian or Devonian Springdale Group. Calcrete is strongly developed in the broadly coeval Cinq Isles Formation. These last two units (if the redbeds at Kings Point are part of the Springdale Group) contain limestone beds that have been previously cited as evidence for marine sedimentation. Pedogenic and dry-climate lacustrine environments should be considered as alternatives for the formation of these limestones.

The redbeds were transported from the southwest and overlie the southwest margin of the Annieopsquotch ophiolite. Therefore at least some of the ophiolite clasts within the redbeds came from sources other than the presently exposed ophiolite. Such sources included large amounts of felsic volcanic rocks as well as mafic volcanic and granitic rocks. The grey sequence rests on weathered granite and contains granitic and mafic and felsic volcanic clasts.

Introduction

The area studied lies along the western margin of the central mobile belt of Newfoundland, a region presumably containing rocks of the Grenville basement, plutonic and volcanic rocks generated during both the Taconic and Acadian orogenies and Siluro-Devonian? deformed but unmetamorphosed sedimentary and volcanic rocks probably related to the Acadian. It is with this last group of rocks that the present report is concerned. Recent mapping covering all or part of these rocks includes that of Riley (1957), DeGrace (1974), Herd and Dunning (1979), Dunning (1981), Dunning and Herd (1980) and Kean and Jayasinghe (1981a,b).

The two sequences discussed below lie mainly within NTS map area 12A/4 and extend northward over the southern boundary of NTS 12A/5. The northerly rocks can be reached by a gravel road, Route 480, that was cut in 1979 and connects the Trans-Canada Highway with the port of Burgeo. Most of the rest of the rocks are best reached by helicopter.

Acknowledgments

The field assistance of G. Dunning and M. Best is greatly appreciated. Valuable technical discussions were had with K.L. Currie and R.K. Herd of the Geological Survey of Canada and with R. Hyde and B. Kean, both of the Newfoundland Department of Mines and Energy. B. Rust of the University of Ottawa critically read the manuscript.

Previous Work

Riley (1957) considered the sediments and volcanics Devonian or earlier, noting their similarity with the nearby Baie du Nord Group which has been mapped as Devonian. DeGrace (1974) disputed Riley's (op. cit.) comparison, instead relating them to the Carboniferous sediments found elsewhere in Newfoundland. Dunning and Herd (1980), describing the new exposures in the roadcuts of the Burgeo Road (Fig. 34.1) likened the sequence to the redbeds of the Springdale and Botwood groups of north and central Newfoundland, though the Silurian age of these two groups rests upon slender evidence.

Kean and Jayasinghe (1981a) divided the sedimentary sequence into three parts; (a) mainly-red rhyolitic flows and pyroclastics with lesser amounts of redbeds; (b) vesicular mafic volcanics and (c) a grey boulder conglomerate with minor sandstones and black argillite beds, the last containing plant fossils tentatively identified as Early Devonian. The writer did not visit the area where the mafic volcanic rocks of Kean and Jayasinghe (op. cit.) are exposed but recognizes the grey and red subdivisions. Also, having visited the new roadcuts where the succession is almost entirely of redbeds he feels that Kean and Jayasinghe have overstressed the volcanic part of the rhyolitic subdivision.

The present study shows that the grey subdivision, here termed the grey sequence, contains two major elements, orthoconglomerates and an interbedded sandstone-mudstone unit. The sandstone is grey and the mudstone, black to dark grey and the two are clearly separated and interbedded in the manner of meandering fluvial cycles. Though volcanic clasts are abundant in this sequence there is no contemporaneous volcanism. The red subdivision, here termed the redbeds, has the following differences from the grey sequence. It contains abundant felsic flows and pyroclastics (Kean and Jayasinghe, 1980). Also there is no clear separation of sandstone and mudstone. For these and other reasons given below it appears that the grey sequence and the redbeds are two separate sequences.

The Redbeds

This sequence is described from three different parts of the area, each of which illustrates different aspects. They are: (a) adjacent to the Annieopsquotch ophiolite (site 21), (b) along the Burgeo Road and (c) several locations to the southwest.

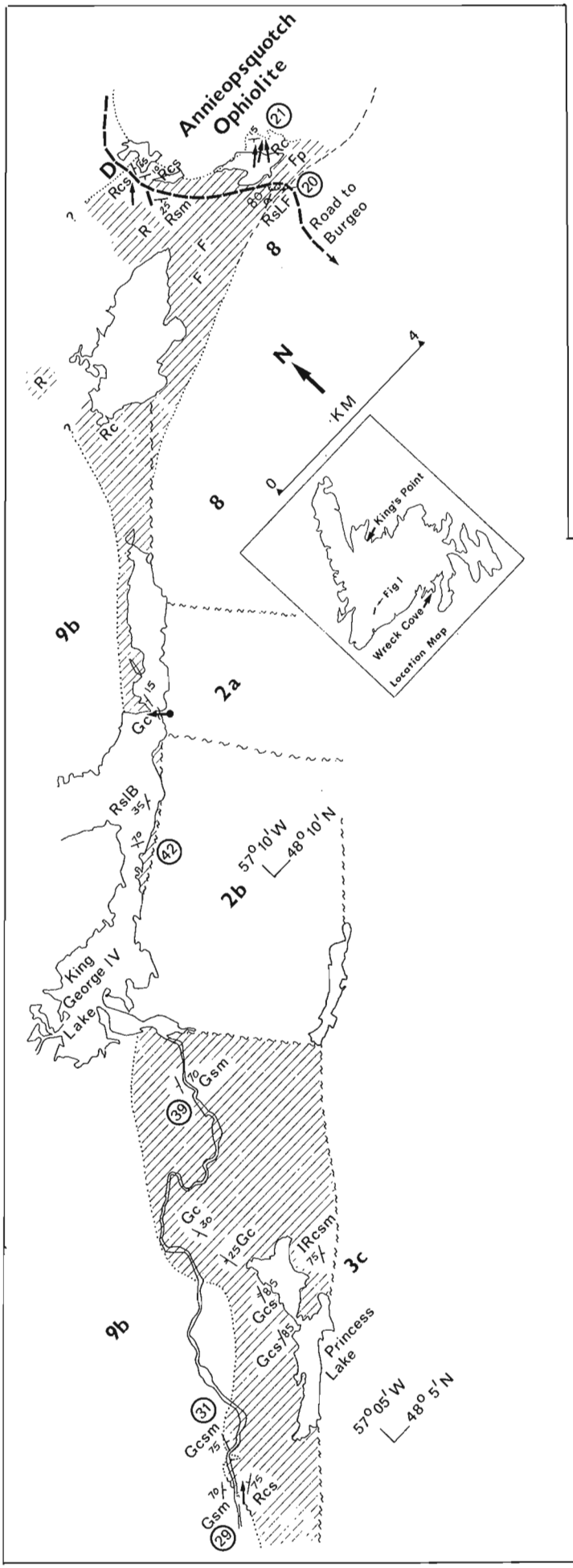

According to Riley (1957) clasts from the Annieopsquotch ophiolite and of diorite (units D and 8, Fig. 34.1) were found in the redbeds. This source relationship is implied by Herd and Dunning (1979) who noted that the redbeds lap northeastward onto the base of the hills formed by the ophiolite. Kean and Jayasinghe (op. cit.) however disagreed, considering that unit 8, a gabbro-diorite was intruded into the redbeds.

At site 21 (Fig. 34.1) on the northeast shore of the lake and on the lower slopes of the hillside to the northeast redbeds dip southwestward off the ophiolite at about 15 degrees. At the unconformity, which is exposed in several places the ophiolite consists of dykes, sheeted on a scale down to 15 cm as well as of pods of diabase and gabbro. (See also Dunning and Herd, 1980, Fig. 35.1). At the sharp contact the ophiolite appears fresh apart from being reddened up to 1 cm away from cracks. Here the redbeds consist of crudely size-stratified pebble to boulder orthoconglomerate and minor paraconglomerate. A few per cent of laminated and trough crossbedded, coarse grained sandstone occurs in beds several centimetres thick. The sandstone beds may be pinched out at curved scour surfaces

Legend

Sedimentary & Volcanic Rocks

R	Redbed sequence
G	Grey Sequence
c	Conglomerate
s	Sandstone
m	Mudstone
F	Felsic volcanics
I	Intermediate
B	Mafic
L	Lahar
p	Pyroclastics

Surrounding geological units*

2a,b	Sheeted dykes,mafic volcanics
3c	Metasediments,paragneiss
8	Gabbro,diorite
9b	Feldsparphyric granite
D	Diorite,granite

Geological boundary,faulted, approximate,assumed

Paleocurrent

(20) Location of outcrops

* Numbers of rock units after Kean and Jayasinghe (1981)

Figure 34.1. Summary data map of the redbed sequence, the grey sedimentary sequence and surrounding units, King George IV Lake area, Newfoundland.

at the bases of conglomerate units. In most outcrops megaclasts are dominantly of ophiolite, locally at the 90-100 per cent level. Again locally, felsic volcanic clasts predominate and rare granitic boulders were found. Roundness of the clasts is varied. Well developed imbrication (Fig. 34.2) in several otherwise massive conglomerate beds indicates sedimentary transport to the northeast (Fig. 34.1) in longitudinal bar bedforms.

The redbeds along the Burgeo Road are finer grained than those overlying the ophiolite. In the northern part of the roadcut they dip gently to the southwest. Toward the south, particularly in the quarry (site 20, Fig. 34.1) they are more disturbed. At the quarry they dip steeply, are overturned and cut by conformable and near-conformable breccia-zones and faults. Also in the quarry are a rhyolite unit and a lahar (Dunning and Herd, 1980). The redbeds along the road appear to fine upward, a trend also seen in some of the larger outcrops, but this opinion should be taken with caution on account of the poor exposure and disturbance of the strata.

The northernmost sedimentary outcrop on the road is a fine grained greenish-pink pebble conglomerate composed of fragments of quartz, pink feldspar and rare altered basaltic and felsic volcanic clasts. Six hundred metres along the road to the north lie outcrops of granite (s.l.) that appear to have digested mafic material. G. Dunning (personal communication) interprets this rock to be a phase of a diorite, ingesting the diorite itself with both cutting the Annieopsquotch ophiolite. Thus this outcrop seems to have been derived mainly from these felsic igneous rocks. Other outcrops in the northern part of the Burgeo Road section but to the south of the above include poorly sorted pebble to cobble conglomerate with crude size-layering, finer grained than the conglomerate overlying the ophiolite, and with imbrication indicating transport to the northeast. Some fine grained pebble conglomerate beds are crossbedded. Calcite cement that may indicate a dry climate during deposition (Glennie, 1970, p. 12) is patchily developed. In these outcrop megaclasts are almost entirely of felsic volcanic composition. Minor crossbedded and horizontally laminated, generally fine grained, sandstone contains mudflake horizons that are evidence of exposure.

In the probably overlying southern part of the Burgeo Road section laminated current-lineated, fine grained sandstone is the main rock type. Waning-current cycles on a scale of 20 cm include flat bedded current-lineated fine grained sandstone with mud chips, overlying a basal scour and succeeded by rippled silt. A second type of cycle, on a 5-8 cm scale, contains climbing ripples overlain by about 0.5 cm of red mud. Within the rarer coarse grained sandstone, cycles include coarse grained, crossbedded or massive sand with mud chips, resting on a scoured base either present as nested sets or passing up through laminated fine grained sand and rippled sand to a mud capping. Rare 5-8 cm thick grit layers in the sandstone sequence show a mixed parentage of felsic volcanics, basalt and granite (s.l.). Other sedimentary features include mudcracks, mud flake layers and mud curls (Fig. 34.3). A noteworthy lack of separation of a clearly defined muddy facies points to ephemeral streams and floods. These characters may be evidence of a dry climate (Glennie, 1970, p. 12).

Contemporaneous felsic volcanism in the redbed sequence is indicated by the large hills, cored by felsic flows and pyroclastics (marked F on Fig. 34.1) that lie on strike to the east and west of the Burgeo Road section (cf. Kean and Jayasinghe, 1981a). At the base of the about 100 m section at the quarry (site 20), lies a 10 m thick weakly flow-banded rhyolite. Its base is faulted against a few metres of red mudstone. The rhyolite is vesiculated around inclusions of red mudstone, suggesting incorporation of damp sediment. Overlying the rhyolite is 10 m of poorly sorted unwelded paraconglomerate with a faulted upper surface and composed of clasts up to boulder size. Two warped 5 cm-thick sand layers 40 cm apart and traceable at least 10 m along strike suggest that the unit was deposited by at least three events. The clasts in the conglomerate are poorly sorted and, depending on place in the unit, can consist of 75-90 per cent of flow-banded, feldsparphyric or rarely vesicular felsic volcanic material. Up to 25 per cent of gabbro and no pumice were recorded. A preliminary test of the natural remanent magnetism of four clasts from one block from the unit showed no consistency of magnetic direction among the clasts (G.N. Freda). These data are consistent with Dunning and Herd's (1980) suggestion that the unit is a lahar.

Redbeds along the southeast shore of King George IV Lake are all sandstone except for an aphanitic grey unfossiliferous limestone of unknown origin about 2 m thick. One 25 cm thick pebble orthoconglomerate bed is predominantly composed of felsic volcanic clasts with lesser amounts of granite, red sandstone and quartz. East of Princess Lake a 204 m section of redbeds and volcanics occur over a partly covered stratigraphic thickness of 320 m. The sequence comprises 60 per cent intermediate to mafic volcanics, 25 per cent cobble felsic volcanic conglomerate, 10 per cent of laminated red fissile siltstone-argillite with one mudcracked layer and minor crossbedded red sandstone. The siltstone-argillite may be an ephemeral-lake deposit.

On the southeast side of the river bed at site 29 (Fig. 34.1) lie 12 m of redbeds that young northwest, a direction opposite to otherwise apparently conformable strata of the grey sequence (see below). The redbeds consist of pebble conglomerate beds upto 1 m thick, grit, sandstone and minor mudstone. Megaclasts are almost entirely of felsic volcanic composition. Prominent among the redbeds is a waning current cycle (Fig. 34.4a, b) that starts with massive pebble conglomerate up to 45 cm thick with pebbles pressed into underlying red mudstone. Pebble imbrication at an inclination of 25 degrees indicates northeastward pebble transport. The conglomerate bed is overlain in turn by crossbedded grit up to 20 cm thick, several centimetres of graded or crossbedded, medium grained sand and about 0.5 cm of dark red mud. No evidence of emergence such as mudcracks was found. These cycles may be the deposits of a braided or laterally uncontained flow.

The Grey Sequence

According to DeGrace (1974), these rocks, on King George IV Lake, overlie the granite 9b (Fig. 34.1) as judged by their attitude and the irregular line of apparent contact with it. The relation between this granite and the grey and red sequences (the unit 7) was not discussed by Kean and Jayasinghe (1981a). Because they believed their unit 8 (Fig. 34.1) to intrude the redbeds, they seemed to imply that the red and grey sequences predate granite 9b. Later Kean and Jayasinghe (1981b) considered the boundary an unconformity.

Granite with pink feldspar phenocrysts (9b) is exposed along the northwest side of the river bed at several places between sites 29 and 31 (Fig. 34.1). The granite is succeeded by a grey-green, limy, fine grained massive rock about 10 m thick, that contains remnant patches of quartz and pink feldspar phenocrysts. This rock, interpreted as a regolith, is succeeded by several beds of grey grit 30-45 cm thick that dip steeply to the southeast off the granite. Grading in the grit indicates tops to the southeast, that is in a direction opposite to that of the redbeds that appear to overlie it on the other side of the river (see above). Interbedded with the grit are black mudstone layers upto 30 cm thick. The grit is overlain by about 15 m of apparently massive grey grit and pebble conglomerate.

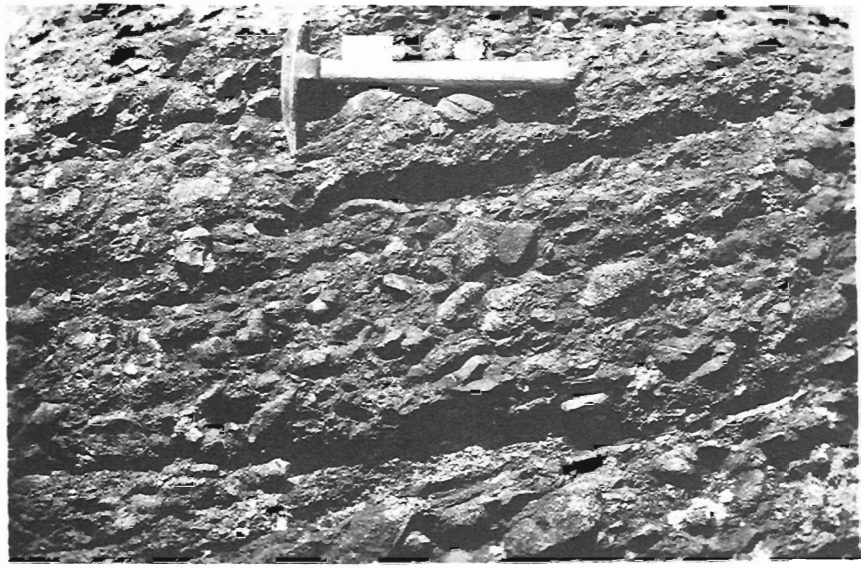

Figure 34.2. *Weakly size-stratified mafic conglomerate overlying ophiolite, site 21, (Fig. 34.1). Imbrication of clasts indicates transport from the southwest (left). GSC 203265-L*

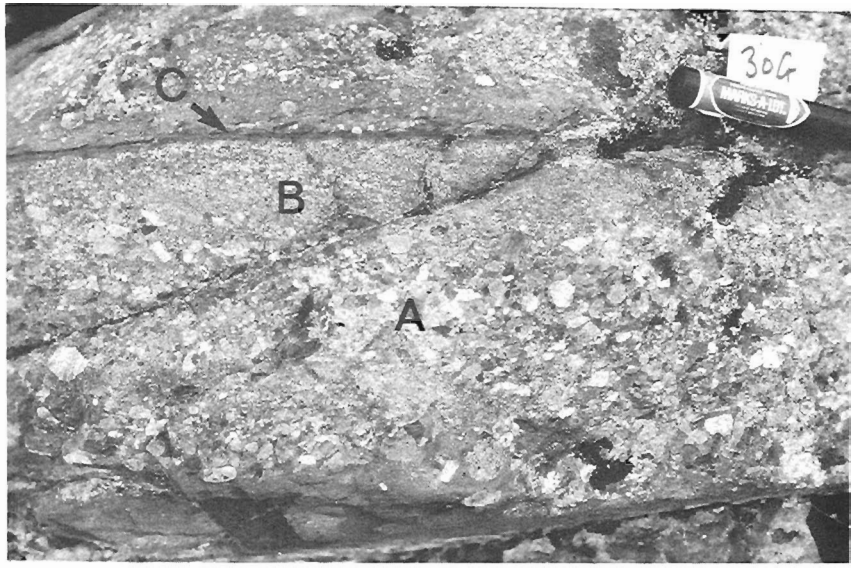

Figure 34.4a. *Flood cycle including massive pebble conglomerate (A) overlain by crossbedded grit (B) and terminated by a thin red mud layer (C). Flow from left. GSC 203265-J*

Figure 34.3. *Mud curls on base of slab of fine-grained red sandstone, outcrop opposite quarry, location 20, (Fig. 34.1), Burgeo Road. GSC 203265-K*

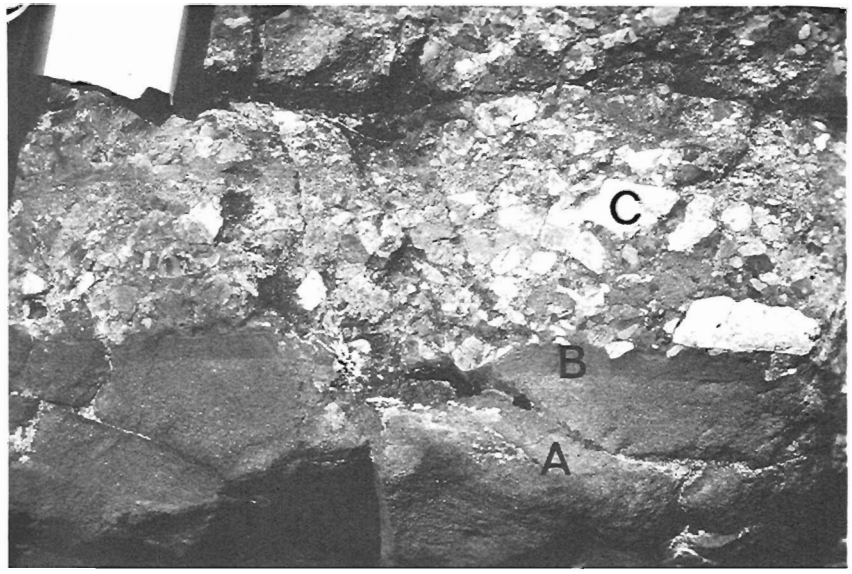

Figure 34.4b. *Contact of two cycles of the type shown in figure 4a. Crossbedded medium grained sand (A) grading up to laminated silt (B) of lower cycle and overlain by conglomerate basal part of overlying cycle (C). Width of photo, 20 cm. GSC 203265-I*

At site 31, 1 km down river, granite with pink feldspar phenocrysts is exposed in the river bed. It is directly overlain, at a sharp boundary by pebble to cobble conglomerate with rounded clasts. The regolith of site 29 is absent here though present at several places between sites 29 and 31. The conglomerate, 75 m thick, is composed of mafic and felsic volcanic and minor granitic clasts. It is crudely stratified and interlayered with laminated and crossbedded pebbly grit. The conglomerate fines upward to at least 40 m of gray arkosic grit with granite fragments interlayered with black mudstone. Thus the grey sequence clearly overlies the granite (9b) and is probably separated from the redbeds at sites 29 and 31 by a fault.

At site 39 granite and conglomerate are not exposed. Instead there is a 60 m section composed entirely of interbedded grey feldspathic sandstone and grit units and black mudstone units (Fig. 34.5). In the lower 45 m the sandstone units are 2-3 m thick and the mudstone 0-1 m thick. In the upper 15 m the sandstones have thinned to 0.5-1 m and the mudstone units have thickened to about 1 m except where nested. The sandstones are crossbedded and have scoured bases above which rounded and angular pebbles of black mudstone or felsic volcanic rock are common. Lack of upward thinning of crossbedding may be due to erosion of intervening mudstone beds which results in nesting of the sandstone beds and incorporation of angular fragments at the bases of the beds (Fig. 34.8).

The Black mudstone beds generally are massive dark grey siltstone to black mudstone. Nesting within the fine grained member is indicated by contacts where graded black mudstone is overlain by dark grey siltstone. Horizontal lamination and ripples are rarely seen and locally cycles 0.1-1 m thick grade up from medium- to coarse-grained sand, through laminated and rippled dark grey sand to black mud. Also within the fine member flat-topped lenticular sand bodies with undulose scoured bases 15 cm thick traceable several metres along strike.

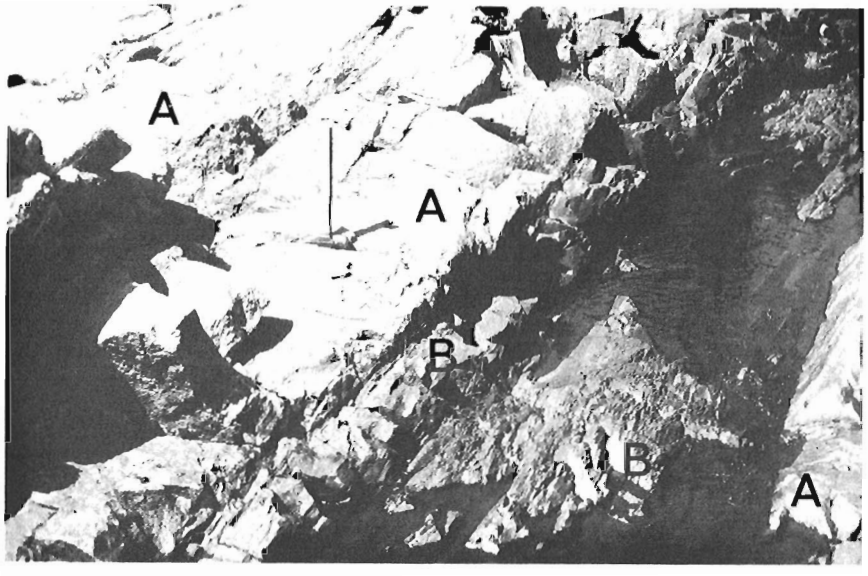

Figure 34.5. *Interbedded grey sandstone (A) and black mudstone (B) of possible meandering fluvial cycles of grey sequence (Site 39, Fig. 34.1). Top is toward left. GSC 203265-N*

The interbedded grey sandstone-black mudstone facies may be of meandering fluvial origin. The grey grits are interpreted as channel sands and the black mudstones as overbank deposits. The sandstone lenses within the fine member may be crevasses splay deposits. A terrestrial interpretation is supported by the identification from the mudstone at site 39 of abundant vascular plant tissue and trilete spores, possibly of Early Devonian (Emsian) age, coupled with the absence of marine palynomorphs (C. McGregor, personal communication, 1981). Development of some attributes of the meandering fluvial style of sedimentation, the paleobotanical data, grey and black colour of the sequence suggest deposition on a vegetated, that is, post-Silurian terrane. These data and what may be a drab regolith on unit 9b suggest terrestrial deposition under a humid climate.

Several outcrops of cobble to boulder orthoconglomerate north and west of Princess Lake and one of pebble conglomerate on King George IV Lake are included in the grey sequence because of their colour. The coarser conglomerates contain well rounded, often highly spherical clasts dominantly of flow-banded and porphyritic felsic volcanics (40-75%) and granite (25-35%). One outcrop contains 25% of mafic volcanics and minor diabase. Small amounts of vein-quartz and red chert-like material are also present. Other features include rare (less than 5%) laminated or trough crossbedded, coarse grained grey sands beds less than 25 cm thick. The matrix of the conglomerates is quartzofeldspathic grit. These conglomerates were deposited by vigorous traction currents.

Figure 34.6. *Two heavily calcreted soil profiles from between major limestone units (see text), Cinq Isles Formation, Wreck Cove. Columnar calcrete (C) developed in red sandstone (S) overlain by discontinuous grey limestone (L) layer (hardpan) produced from advanced calcrete formation. GSC 203265-P*

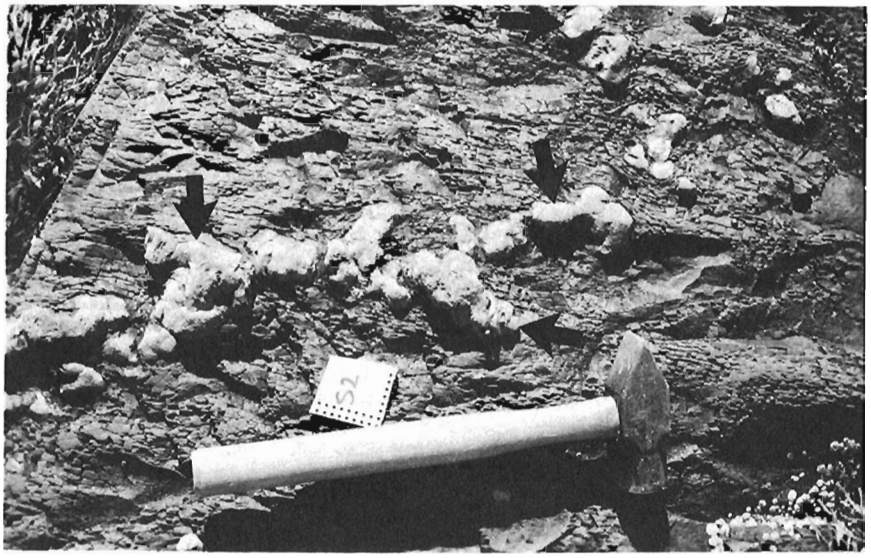

Figure 34.7

Incipient calcrete nodules, arrowed, in red siltstone, Springdale Group (?), King's Point. GSC 203265-O

Figure 34.8. *Contact of two nested sandstone beds, grey fluvial sequence, Site 39 (Fig. 34.1). Contact shown by vertical arrows. Black mudstone clasts from eroded overbank member in base of overlying channel sandstone are shown by inclined arrows. GSC 203265-H*

Discussion

Felsic volcanic rocks are a major source of both the red and the grey sequences, a finding not surprising for the redbeds because of the coeval felsic volcanism. The idea of ophiolite as a source for the redbeds in the northeast is supported by the field relations and by G. Dunning's (personal communication) identification of the clasts. Further he has extracted an Early Ordovician crystallization age (in prep.) from zircons from the Annieopsquotch ophiolite. Unexpectedly, transport of these ophiolite clasts was from the southwest, toward the ophiolite upon which the redbeds are seen to rest. Thus possible source areas include parts of the same ophiolite now buried or removed, units 2a and 2b identified as ophiolite by Dunning (1981) and unit 8. However one should bear in mind that Kean and Jayasinghe (1981) believe unit 8 to intrude the redbeds. Granitic clasts are to be expected in the grey sequence that overlies the granitic unit 9b. Granitic material in the redbeds at the northern end of their exposure on the Burgeo Road raises the possibility that unit 9b is also a source for pebbles in the redbeds.

Sedimentary features of the red sequence mark it as alluvial. The conglomerates may be of alluvial fan or braided fluvial origin. Minor paraconglomerate supports a contribution of the former. The finer grained clastics are not of the meandering fluvial type and were probably deposited either in the braided regime or by flash floods. These characteristics can be explained by either a pre-vegetation (pre-Devonian) age or by a dry climate. Calcite cement in some of the pebble-conglomerate may point to a dry climate (Glennie, 1970, p. 12). The unfossiliferous limestone at King George IV Lake might be climatically significant, for similar limestone is present in the possibly correlative (Dunning and Herd, 1981) but undated Springdale Group at Kings Point (Fig. 34.1, NTS 12H/9, lat. 49°35', long. 56°10'). This latter limestone occurs at the base of a red siltstone unit (playa deposit?) that contains limestone nodules resembling incipient calcrete (Fig. 34.7). The limestone at Kings Point has interbedded chert and contains barite and analcime (X.R.D. analysis by A. Roberts, GSC). This field association and the analcime in the limestone are reminiscent of modern lakes developed on felsic igneous terranes under dry climates for example Lake Magadi (Eugster, 1969) and Lake Chad (Maglione, 1980). Further, in fining-upward cycles alluvial sandstone in the Springdale Group on a nearby outcrop immediately south of Burnt Berry Brook (NTS 12H/8, lat. 49°27'N, long. 56°10'W) limestone pebbles occur in the lag deposit on the basal scour surface and calcrete nodules occur in fine-grained sands at the tops of cycles. Thus there is evidence of deposition of the Springdale Group under a dry climate. So climate rather than a pre-Devonian age might be the cause of the style of sedimentation of the redbeds in the King George IV Lake area if correlation with the Springdale Group is valid. Another caveat applies to the age and correlation of limestones at Kings Point. Neale and Nash (1963) considered them Silurian and part of the Springdale Group. According to Marten (1971) the limestones are more likely of Carboniferous age.

At site 29 (Fig. 34.1) the redbeds and the grey sequence have a similar strike and are separated by about a metre yet they young in opposite directions. Nowhere in the area examined did the writer establish the stratigraphic relation between the two sequences. The difference in sedimentary style, raises the question of how different their ages might be. The redbeds are post-Early Ordovician and the grey sequence might be Early Devonian. The redbeds contain contemporaneous felsic volcanics, yet felsic volcanic material in the grey sequence is present only as abundant clasts. Does this imply that the volcanics of the redbeds are the source of the clasts in the grey sequence? Material has been collected from the redbeds, the grey sequence and from the Springdale Group for fossil extraction and zircon dating. One volcanic unit in the Springdale Group has yielded zircons.

A point of more general interest is the environmental interpretation of the limestones discussed above and others like them. As noted above the limestones lie within alluvial sequences bearing evidences of dry climate. Yet Wessel (1975) has interpreted the limestones at Kings Point to be shallow marine. A similar situation is seen with the Cinq Isles Formation at Wreck Cove, southern Newfoundland (Fig. 34.1, NTS 1M/5, lat. 47°30', long 55°37'). This Devonian or earlier? (Greene and O'Driscoll, 1976) redbed unit is extremely rich in calcrete and contains fine-grained unfossiliferous limestone units upto 12 m thick. Some of the thinner limestones are clearly hardpan derived from advanced calcrete formation (Fig. 34.6). The calcrete has been misinterpreted. For example Widmer (1950) referred to "nodules of limestone in red shales or red sandstone" and interpreted the depositional environment of the formation to be warm marine at the estuarine delta of a large river with greatly fluctuating discharge. Calcutt and Williams (1971) noted "blebs of micrite within shales" and interpreted the formation to have been deposited in a near shore carbonate environment bordering an alluvial fan chain.

The above comments indicate that some carbonates in the Siluro-Devonian? of Newfoundland have been misinterpreted. Correct interpretation of such carbonates, that is whether they be of pedogenic, lacustrine or marine origin is important in regional paleogeography. It is also important in exploration for redbed-associated copper and uranium mineralization, because current models of these forms of mineralization assume a dry climate.

References

Calcutt, M.J. and Williams, H.
1971: The Cinq Isle Formation, Fortune Bay, Southern Newfoundland. Devonian? near shore carbonate redbed environment p. 8-9; in Geological Survey of Canada – Mineralogical Association of Canada, Abstracts, Sudbury, 1971, 80 p.

DeGrace, J.R.
1974: Notes on the geology of the King George IV Lake area, southwest central Newfoundland; in Report of Activities, 1973, Newfoundland Department of Mines and Energy, Mineral Development Division, p. 43-49.

Dunning, G.R.
1981: The Annieopsquotch ophiolite belt, southwest Newfoundland; in Current Research, Part B, Geological Survey of Canada, Paper 81-1B, p. 11-15.

Dunning, G.R. and Herd, R.K.
1980: The Annieopsquotch ophiolite complex southwest Newfoundland, and its regional relationships; in Current Research, Part A, Geological Survey of Canada, Paper 80-1A, p. 227-234.

Eugster, H.P.
1969: Morganic bedded cherts from the Magadi area, Kenya; Contributions to Mineralogy and Petrology, v. 22, p. 1-31.

Glennie, K.W.
1970: Developments in sedimentology; Desert Sedimentary Environments, v. 14, Elsevier, 222 p.

Greene, B.A. and O'Driscoll, L.F.
1976: Gaultois map area; in Report of Activities, 1975, Newfoundland Department of Mines and Energy, p. 56-63.

Herd, R.K. and Dunning, G.R.
1979: Geology of the Puddle Pond, map area, southwestern Newfoundland; in Current Research, Part A, Geological Survey of Canada, Paper 79-1A, p. 305-310.

Kean, B.F. and Jayasinghe, N.R.
1981a: Geology of the King George IV map area, (12A/4), Newfoundland; in Current Research, Department of Mines and Energy, Mineral Development Division, Report 81-1.

1981b: King George IV Lake, Grand Falls District, Newfoundland, NTS 12A/4; Newfoundland Department of Mines and Energy, Mineral Development Division, map.

Maglione, G.
1980: An example of recent continental evaporite sedimentation the Chadian Basin (Africa) p. 1-9, in Evaporite Deposits, illustration and interpretation of some evaporite sequences, Chambre syndicale de la rechérche et de la production du pétrole et du gaz naturel, comité des techniciens, commission exploration, sous-commission laboratories de géologie, Editions Technip, Paris, 266 p.

Marten, B.E.
1971: Stratigraphy of volcanic rocks in the Western Arm area of the central Newfoundland Appalachians; Geological Association of Canada, Proceedings, v. 24, no. 1, p. 73-84.

Neale, E.R.W. and Nash, W.A.
1963: Sandy Lake (East Half), Newfoundland, 12H E1/2; Geological Survey of Canada, Paper 62-28, 40 p.

Riley, G.C.
1957: Red Indian Lake (west half), Newfoundland; Geological Survey of Canada, Map 8-1957.

Wessel, J.M.
1975: Sedimentary petrology of the Springdale and Botwood formations, Central Mobile Belt, Newfoundland, Canada Ph.D. thesis, (unpub.), Massachussets University.

Widmer, K.
1950: The Geology of the Hermitage Bay Area, Newfoundland, Ph.D. thesis (unpub.), Princeton University, 439 p.

GEOMAGNETIC FIELD MODELS: SOME BRIEF PRELIMINARY COMPARISONS

Project 730081

K.G. Shih and Ron Macnab
Atlantic Geoscience Centre, Dartmouth

Shih, K.G. and Macnab, Ron, Geomagnetic field models: some brief preliminary comparisons; in Current Research, Part A, Geological Survey of Canada, Paper 82-1A, p. 221-223, 1982.

Abstract

The derivation of the magnetic anomaly field through application of the standard IGRF magnetic field models has led to serious problems in merging multi-year magnetic data sets collected off the Canadian east coast, on account of inaccuracies in the models' secular variation components. Various models have been proposed as replacements for the current standards, and we have tested three that have been submitted by workers from the U.K. Institute for Geological Sciences; the U.S. National Aeronautical and Space Administration; and the U.S. Geological Survey. Working with selected AGC multi-year data sets, we found that all three candidate models yielded results that were judged to be significantly better than those derived by means of the current standards.

The Problem

The International Geomagnetic Reference Fields for 1965 and 1975 (IGRF 1965 and 1975) have long been the standard magnetic field models used at the Atlantic Geoscience Centre (AGC) to derive marine magnetic anomaly values from total magnetic field measurements.

The data to which this model has been applied consist of numerous sets of total field readings collected during the course of cruises dating back to 1964. The data sets are geographically dispersed over the Canadian east coast offshore, the Arctic, the North and South Atlantic, and the North and South Pacific. They represent densities of areal coverage that range from isolated ship's reconnaissance tracks to closely-spaced systematic surveys. Many of the data sets overlap, as in situations where systematic surveys were carried out in areas previously crossed by reconnaissance tracks, or when certain areas were resurveyed (sometimes after intervals of several years) at closer line spacings.

Not surprisingly, the IGRF models have failed to yield consistent magnetic anomaly values when applied to this diverse collection of data. As pointed out by Dawson and Newitt (1978), there are deficiencies in the secular variation component of the IGRF models, manifested by apparent shifts in the anomaly fields derived from measurements that have been taken over several years. This leads to serious problems in merging multi-year data sets, requiring various 'ad hoc' adjustments to achieve satisfactory integration of the measurements.

Some relief to this situation appears to be at hand, in view of current proposals to replace the IGRF 1965 and 1975 standards with more accurate models. It seemed appropriate to carry out preliminary comparisons by applying some of the candidate models to selected portions of our own data base.

Test Models and Test Data

Three models were investigated: those proposed by workers from the U.K. Institute for Geological Sciences (IGS), the U.S. National Aeronautical and Space Administration (NASA) and the U.S. Geological Survey (USGS). Each was applied to data sets selected from two different geographical areas: the Quiet Magnetic Zone off Nova Scotia, and the northeast corner of the Gulf of St. Lawrence.

Quiet Magnetic Zone Comparison

The Quiet Magnetic Zone (QMZ) is a band of low magnetic relief located over the Northwest Atlantic abyssal plain, and which runs roughly parallel to the continental shelf. Anomalies in the QMZ tend to be highly localized and low in amplitude, with an approximately equal distribution in the positive and negative directions. The mean magnetic anomaly in the zone therefore should tend to be rather small.

The total magnetic field in the QMZ off Nova Scotia has been measured in numerous places during several AGC cruises, but for the purposes of this investigation, we restricted the locality to the one-degree square (ODS)

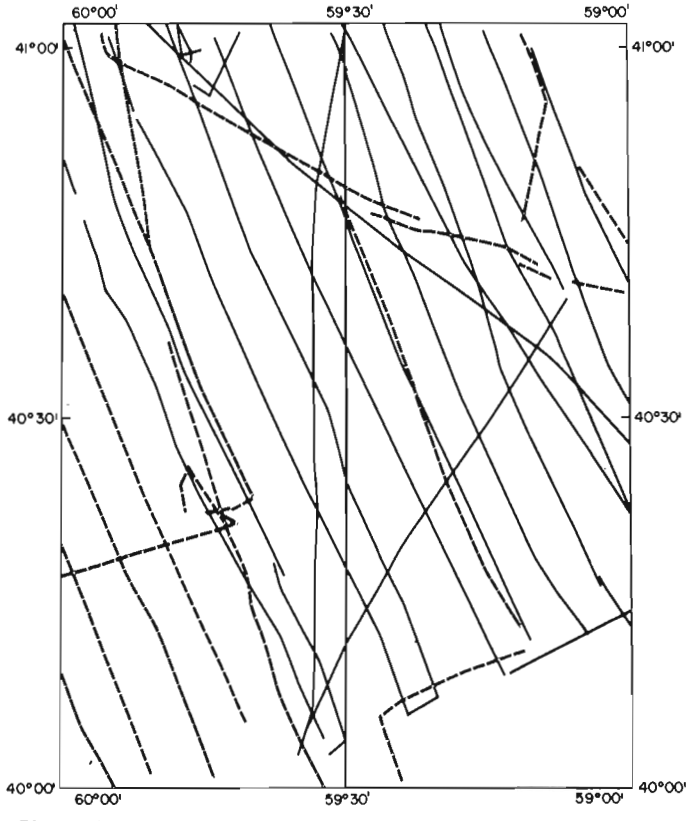

Figure 35.1. *Survey tracks in a one-degree square situated in the Quiet Magnetic Zone (QMZ) in the northwest Atlantic. Solid lines represent 1972 tracks; dashed lines, 1973.*

40°-41°N, 59°-60°W, using data from two systematic survey cruises carried out in 1972 and 1973. Figure 35.1 is a plot of ships' tracks during these two survey cruises, and gives some indication of the density of data. No diurnal corrections were applied to the data.

Applying the IGRF 1965 model to the 1972 and 1973 data sets in the selected ODS, we obtained anomaly fields with mean values of -186 and -218 nanotesla, respectively. Recalling that the mean anomaly field in the QMZ should be near zero, we adjusted the individual anomaly readings in the 1972 and 1973 data sets by their respective means. We then merged the adjusted sets and machine-contoured them to obtain the anomaly field shown in Figure 35.2.

Applying the IGS, NASA, and USGS models to the same data sets, we obtained anomaly fields with near-zero mean values, ranging from -10 to +17 nanotesla. The variations in these mean values could be due in part to the non-uniform distribution of the 1972 and 1973 data throughout the study area, as well as to the lack of diurnal corrections. Even so, we consider that this range of means signifies good agreement between measurements that were taken one year apart.

The anomaly fields derived from the application of the IGS model were merged and machine-contoured to produce Figure 35.3. We feel that the agreement with the adjusted values represented by Figure 35.2 is rather good, considering the nature of the data and the operations that have been carried out on it. The NASA and USGS models produced similar anomaly fields.

Gulf of St. Lawrence Comparison

The northeastern corner of the Gulf of St. Lawrence has been surveyed in considerable detail over a series of closely-spaced east-west tracks. It is also an area commonly traversed by Bedford Institute of Oceanography vessels as they travel to and from more northerly work areas.

It was possible to identify at least four near-coincident segments of ship's tracks in the area, and these are shown in Figure 35.4. The four magnetic profiles along these tracks were augmented with a fifth 'pseudoprofile' made up of readings taken from the east-west survey lines at their points of intersection with one of the transit tracks. Taken together, the profiles represent five sets of what should be nearly identical measurements taken over a ten-year span.

The upper part of Figure 35.5 is a composite plot of these five magnetic profiles after we had applied the IGRF 1965 model to obtain magnetic anomalies. Agreement between profiles is not very good, averaging about 300 nanotesla. Two profiles – 4(1977) and 5(1978) – stand out from the others; this may be due partly to the effects of temporal variations for which we have no corrections, and partly to the fact that the IGRF 1965 model exhibits major deviations in secular variation when applied to data collected after 1975. The IGRF 1975 model, which should be used for data collected in the period 1975-1980, fares worse than the 1965 model when applied to these two profiles; it actually shifts them down by an additional 30 nanotesla.

Figure 35.2. *Computer-drawn magnetic anomaly map from the QMZ, based on data collected along the tracks shown in Figure 35.1. Anomaly values for 1972 and 1973 were derived by means of the IGRF 1965 model, and had to be adjusted by amounts equal to the mean anomalies for both years prior to merging and contouring. Contour interval: 25 nanotesla.*

Figure 35.3. *Computer-drawn magnetic anomaly maps from the QMZ, based on data collected along the tracks shown in Figure 35.1. Anomaly values were derived by means of the IGS model, and required no adjustment prior to merging and contouring. Contour interval: 25 nanotesla.*

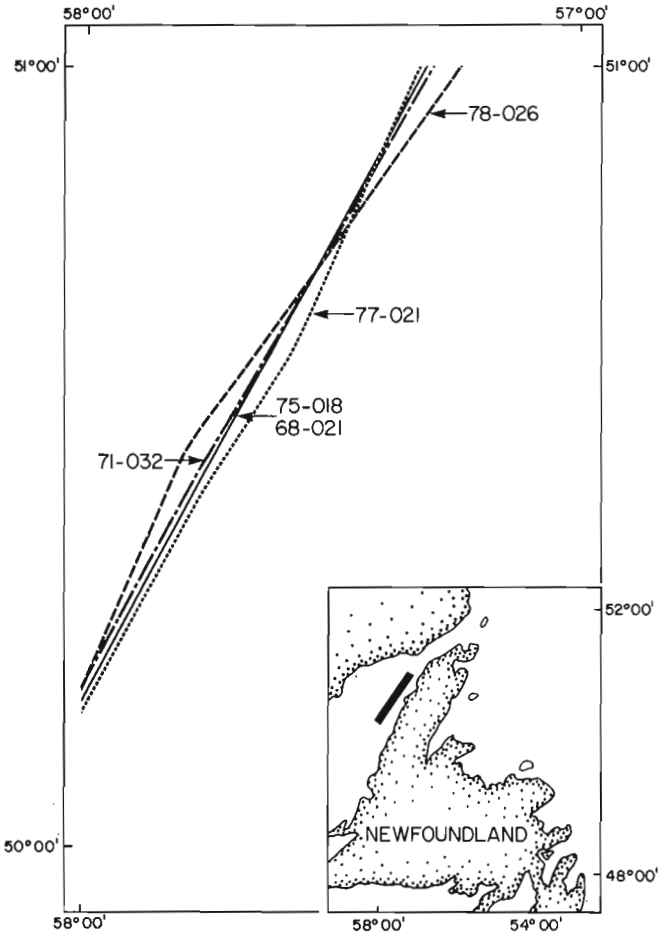

Figure 35.4. *Location of five near-coincident profiles in the Gulf of St. Lawrence. Five-digit labels indicate year and cruise numbers. Four profiles were collected along ship's tracks; 68-021 is a 'pseudo-profile' made up of values taken from closely-spaced east-west survey lines, at points of intersection with the 75-018 ship's track.*

The IGS, NASA, and USGS models were then applied to these same five profiles. The NASA and USGS models gave the best results here, yielding anomaly values that were reasonably consistent over all profiles. The IGS results showed more spread, although it was considerably less than that of the IGRF 1965 results.

The lower part of Figure 35.5 is a composite plot of the magnetic anomaly profiles after application of the NASA model. Agreement between profiles is much improved over the IGRF 1965 composite, staying within 100 nanotesla over most of the range if we disregard the anomalous excursions of profile number 5.

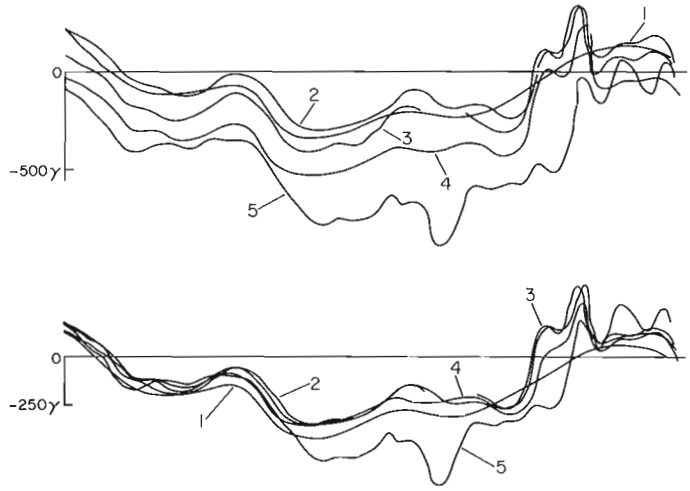

Upper plot: derived with IGRF 1975 model

Lower plot: derived with NASA model

Figure 35.5. *Composite plots of magnetic anomaly profiles along tracks shown in Figure 35.4 Horizontal extent of profiles is approximately 50 nautical miles. North is to the right. Numbers 1 to 5 correspond to data recorded in the years 1968, 1971, 1975, 1977, and 1978, respectively.*

Conclusion

In this preliminary investigation, three new models for the earth's magnetic field were applied to selected multi-year data sets from two different geographical areas. Where year-to-year consistency was of concern, all three models yielded results that were superior to those obtained with the existing IGRF standard. These limited tests lead us to conclude that any one of the three models is probably a significant improvement over the older standard, particularly with respect to the calculation of secular variation.

What we want to do next is to look at the effectiveness of these models in dealing with larger and more numerous data sets that collectively cover a greater area, e.g. the Labrador Sea, and to investigate the effect on computing overhead of the models' increased complexity.

Acknowledgments

Source copies of the subroutines for computing the IGS, NASA, and USGS models were supplied to us by Norm Peddie of the U.S. Geological Survey. The idea for this investigation originated with S.P. Srivastava, who made other contributions through his helpful suggestions.

References

Dawson, E. and Newitt, L.R.
1978: IGRF comparisons; Physics of the Earth and Planetary Interiors, v. 16, p. 1-6.

AGES OF YELLOWKNIFE SUPERGROUP VOLCANIC ROCKS, GRANITOID INTRUSIVE ROCKS AND REGIONAL METAMORPHISM IN THE NORTHEASTERN SLAVE STRUCTURAL PROVINCE

Project 750006

R.A. Frith and W.D. Loveridge
Precambrian Geology Division

Frith, R.A. and Loveridge, W.D., Ages of Yellowknife Supergroup volcanic rocks, granitoid intrusive rocks and regional metamorphism in the northeastern Slave Structural Province; in Current Research, Part A, Geological Survey of Canada, Paper 82-1A, p. 225-237, 1982.

Abstract

Four rubidium-strontium whole rock isotopic studies, two K-Ar muscovite and two U-Pb zircon age determinations were carried out to augment earlier geochronological investigations in the Nose Lake – Beechey Lake map-area, of the northeastern District of Mackenzie. Together the data indicate: (1) a ca. 2670 Ma age for the deposition of the Hackett River Group and Back Group volcanic rocks (of the Yellowknife Supergroup) and emplacement of synvolcanic intrusions; (2) a ca. 2590 Ma age for the late orogenic Regan Intrusive Suite of tonalite-granodiorite and related rocks; (3) Rb-Sr isotopic systems were disturbed during early Proterozoic time.

Introduction

Recent mapping of the Nose Lake – Beechey Lake map area (see Fig. 36.1 and Frith and Hill, 1975) involved the dating of rocks of the Yellowknife Supergroup, the late Archean Regan Intrusive Suite and the late Archean or early Proterozoic metamorphism that affects the area. This paper outlines the results of these studies and complements lead isotopic studies carried out in the Bathurst-Norsemines and Yava massive sulphide deposits and base metal occurrences (R.I. Thorpe, personal communication) and numerous K-Ar mica age determinations conducted as part of earlier reconnaissance and regional studies of this part of the Shield (Wright, 1957; Fraser, 1964; Tremblay, 1971). A total of eight K-Ar determinations, four Rb-Sr isochrons and two U-Pb zircon age determinations have now been carried out in the study area. Sample locations for these studies are shown in Figure 36.2.

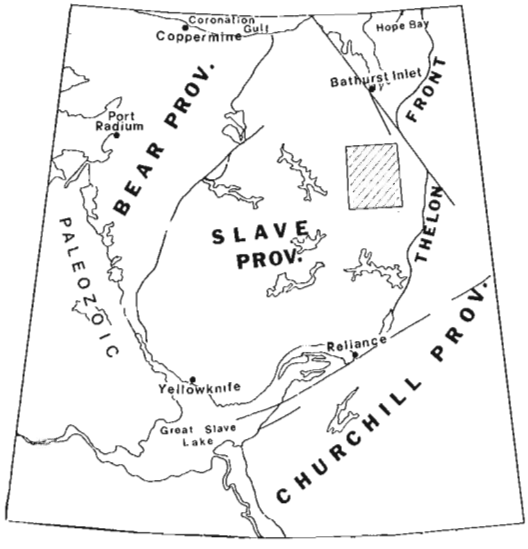

Figure 36.1. *Location map of the Nose Lake – Beechey Lake map area.*

Geological Setting

The rocks of the Nose Lake – Beechey Lake map area have been divided into 12 map units (Frith, in preparation; Fig. 36.2). The oldest, basal, unit consists of migmatite and gneiss that form the core of the Hackett River gneiss dome structure. These rocks, which include the Hackett River granodiorite (dated in this study), form part of the Hanimor granitoid complex (Frith and Percival, 1978). This unit is structurally overlain by the Hackett River Group of volcanic and sedimentary rocks, which in decreasing order of age include: the metasedimentary Siorak Formation, the volcanic Nauna Formation, and the volcano-sedimentary Ignerit Formation. These rocks, along with some undifferentiated metamorphosed equivalents, form a greenstone belt which extends from the northern margin of the map area to the south, where the belt has been folded along the axis of the Malley Rapids anticlinorium (Fig. 36.2).

The Beechey Lake Group of greywacke and mudstone conformably overlies the Hackett River Group and is in turn overlain by and interfingered with volcanic rocks of the Back Group, a caldera succession centred 18 km south of the map area (Lambert, 1978). These three groups of supracrustal rocks form part of the Yellowknife Supergroup which is found throughout the Slave Province.

The basal granitoids and the supracrustal rocks in the western part of the study area were migmatized, deformed and locally intruded by granitoid rocks to form a heterogeneous hybrid rock unit referred to as the Mara River complex. Pegmatites in this unit are mostly undeformed and some are anatectic in origin, as suggested for migmatites in the Hackett River gneiss dome structure (Percival, 1978).

The Regan Intrusive Suite, which covers about 40 per cent of the map area, ranges in composition from quartz diorite to granite. About three quarters of the 70-odd plutons are granodiorite or tonalite in composition. The plutons are mostly anorogenic in the sense of Stockwell (1961) but in detail have been shown to include both syn- and pre-orogenic intrusions (Fyson and Frith, 1979). The suite not only postdates all of the Yellowknife Supergroup supracrustal rocks, but commonly also postdates their deformations and the development of porphyroblasts in them.

Metamorphic highs are centred on two structures: the Hackett River gneiss dome, where kyanite-bearing gneiss of upper amphibolite grade is encountered, and the Malley Rapids anticlinorium, where andesitic metavolcanic rocks have been converted to plagioclase augen gneiss. During the final stages of emplacement the granitic rocks of the Regan Intrusive Suite, have locally pushed up and laterally displaced cordierite-andalusite isograds. On the other hand, more mafic intrusions cut across structures and isograds and show evidence of magmatic differentiation, as in the 'Uist' Lake[1] pluton (Hill and Frith, in preparation).

[1]Informal names are given in single quotes

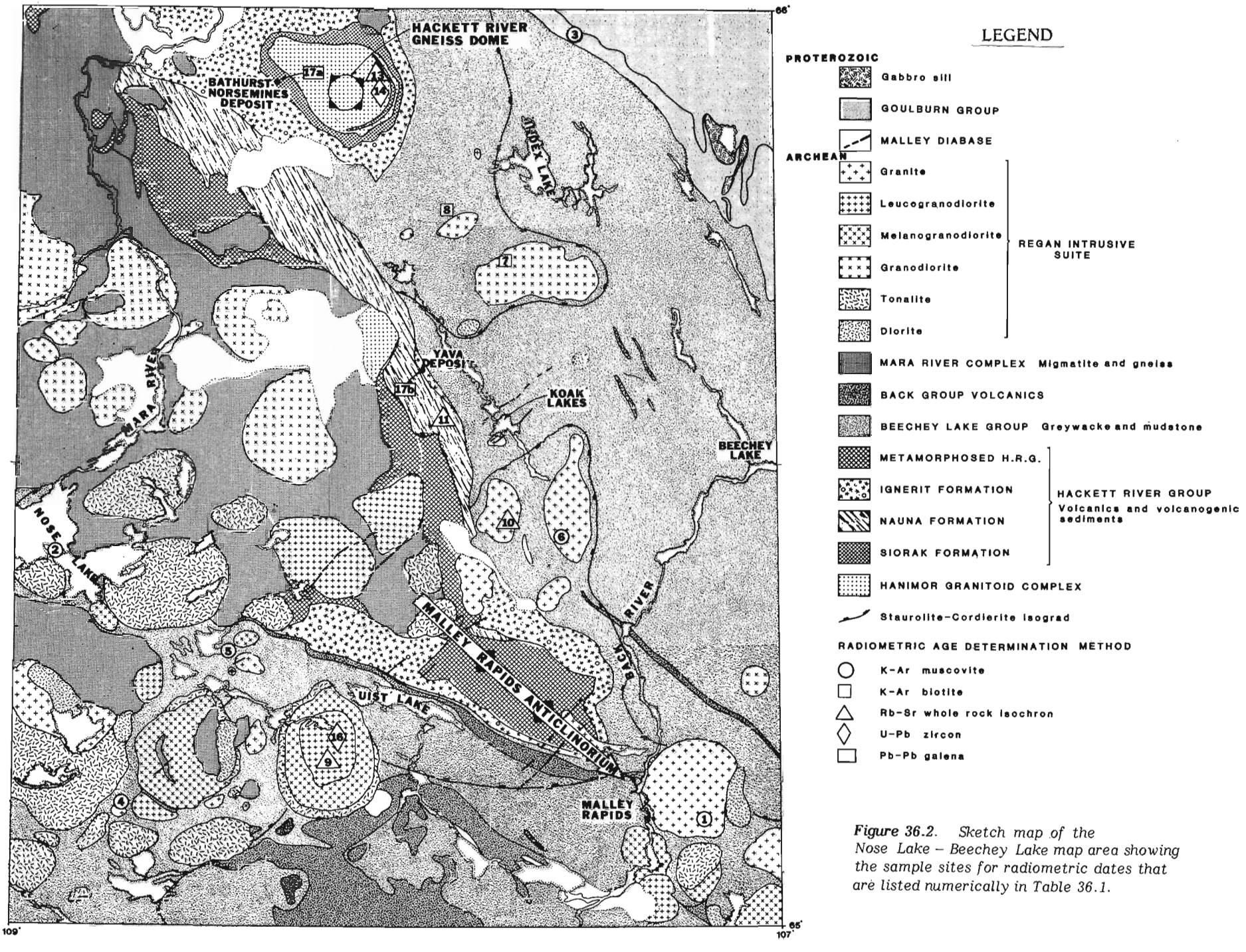

Figure 36.2. Sketch map of the Nose Lake – Beechey Lake map area showing the sample sites for radiometric dates that are listed numerically in Table 36.1.

Three phases of deformation have been determined in the region. The first two most commonly predate the pre-Regan Intrusive Suite but the latter, because it crenulates pegmatites formed in the Beechey Lake Group, is thought to be distinctly postorogenic.

This study reports on isotopic work carried out on rocks of the basal Hanimor granitoid complex (Hackett River granodiorite), the Yellowknife Supergroup (Yava dacite), the Mara River complex and the younger Regan Intrusive Suite ('Uist' Lake granodiorite and 'Koak' Lake granite) and relates the ages and isotopic chemistry to structure, metamorphism and tectonic evolution of this part of the Slave Structural Province.

Geology and Geochronology

Hackett River Area Granodiorite

Rocks in the core of the Hackett River gneiss dome are grey, heterogeneous, biotite- and hornblende- bearing tonalite, trondhjemite or granodiorite gneiss cut by numerous pegmatite dykes of related composition. The rocks have been deformed and involved in the emplacement of the gneiss dome – a relatively late structure that postdates the early deformation (D_1) of the supracrustal rocks. Fyson and Frith (1979) suggest the gneiss dome area was a structurally depressed region during D_1.

Previous reports (Frith et al., 1977; Frith and Hill, 1975; Frith, in preparation) imply that parts of the core gneiss in the Hackett River gneiss dome are pre-Yellowknife Supergroup. The granodiorite, studied in this report, is the only part found to contain zircons, and it forms a somewhat more homogeneous part of the core which may

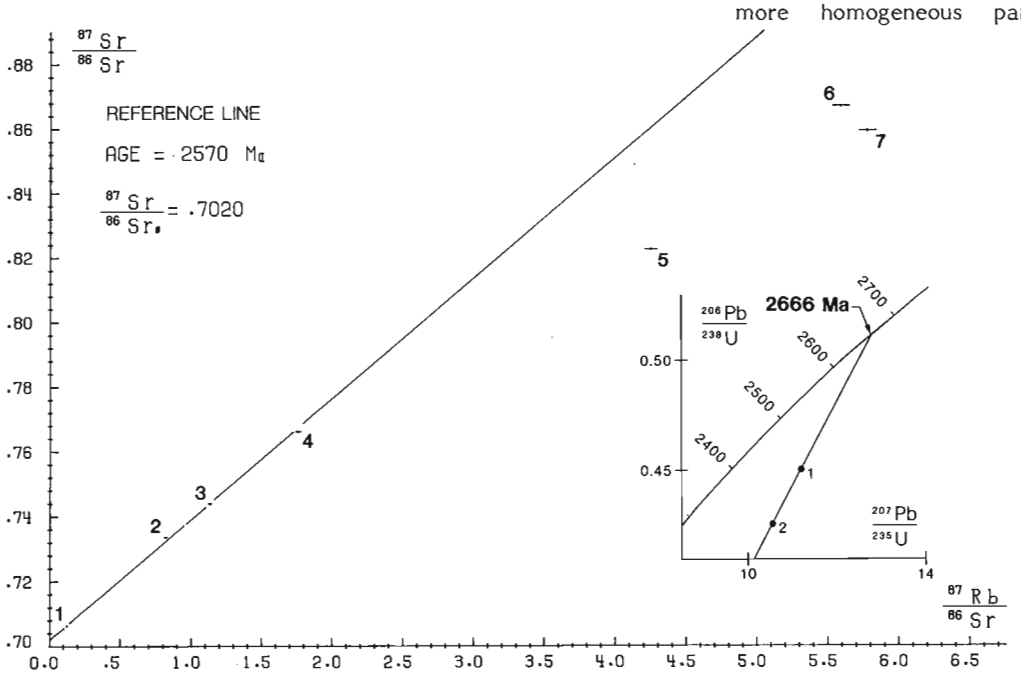

Figure 36.3

Hackett River gneiss dome granodiorite: results of rubidium-strontium studies on whole rock samples plotted for comparison with a 2570 Ma reference line. Concordia diagram (inset) shows the results of uranium-lead analyses on zircon concentrates with a zero intersection.

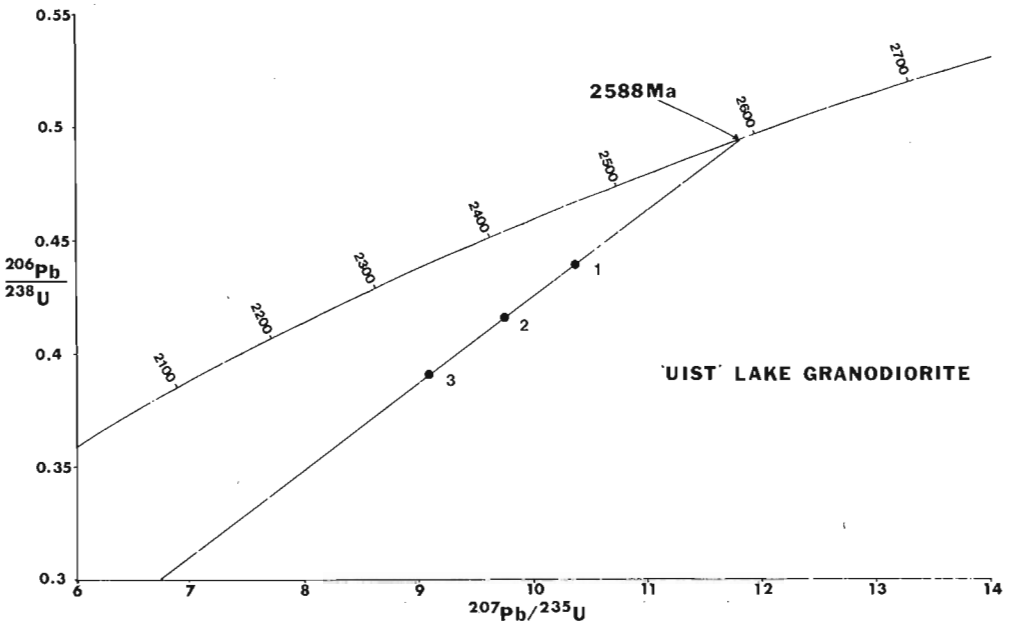

Figure 36.4

Concordia diagram showing the results of analyses on zircon concentrates from the leuco-granodiorite zone of the 'Uist' Lake pluton. The lower chord intersects at zero.

Table 36.1

Radiometric ages of rocks and minerals in the Nose-Beechey Lakes map area and environs

Figure 2 Location No.	Method	Lat.	Long.	Lithology-Location	Age	Ref
1	K-Ar biotite	65°06'	107°12'	Malley Rapids granite (RIS)	1950 ± 105	1
2	" muscovite	65°24'	108°54'	Pegmatite-Nose Lake	2374 ± 54	2
3	" muscovite	65°58'	107°30'	Schist-Western R.Fm.	2380 ± 100	3
4	" muscovite	65°08'	108°44'	Granite-'Lunar' Lake area (RIS)	2455 ± 80	4
5	" muscovite	65°18'	108°19'	Pegmatite-NW of 'Uist' Lake	2484 ± 41	5
6	" muscovite	65°25'	107°33'	'Koak' Lakes granite (RIS)	2535 ± 125	1
7	" biotite	65°45'	107°40'	'Index' Lake granodiorite (RIS)	2380 ± 120	1
8	" biotite	65°47'	107°47'	Schist-Index Lake (BLG)	2475 ± 80	3
*	" biotite	65°08'	106°35'	Thelon Front Area (BLG)	2100	1
*	" biotite	65°22'	106°02'	Thelon Front Area (BLG)	2140 ± 60	3
*	" biotite	65°39'	106°29'	Propeller Lake area (RIS)	2030 ± 60	3
9	Rb-Sr isochron	65°11'	108°10'	'Uist' Lake granodiorite (RIS)	2350 ± 37	5
10	" isochron	65°27'	107°40'	'Koak' Lakes granite (RIS)	2449 ± 30	5
11	" errorchron	65°33'	107°52'	Yava Dacite (HRG)	2499	5
13	" errorchron	65°56'	108°03'	Hackett River area granodiorite	2570	5
14	U-Pb zircon	65°56'	108°03'	Hackett River granodiorite	2666 +20 -28	5
	" zircon	64°44'	107°58'	Felsic volcanics*-(BG)	2670 ± 4	7
	" zircon	64°55'	107°44'	Greywacke (BLG)		
16	" zircon	65°13'	108°10'	'Uist' Lake granodiorite (RIS)	2588 ± 8	5
17a	Pb, secondary isochron	65°55'	108°16'	Sulphides-Bathurst Norsemine (HRG)	2660	8
17b	" " "	65°37'	107°55'	Sulphides-Yava Deposit (HRG)	2660	8

*Located in Beechey Lake, E/2.

1 - Wright, 1960
2 - Frith, 1979
3 - Tremblay, 1965, 1966
4 - Fraser, 1965
5 - This study
6 - Cameron, 1980
7 - Lambert and Henderson, 1980
8 - This study, with data from R. Thorpe, personal communication

RIS - Regan Intrusive Suite;
BLG - Beechey Lake Group
HRG - Hackett River Group
BG - Back Group

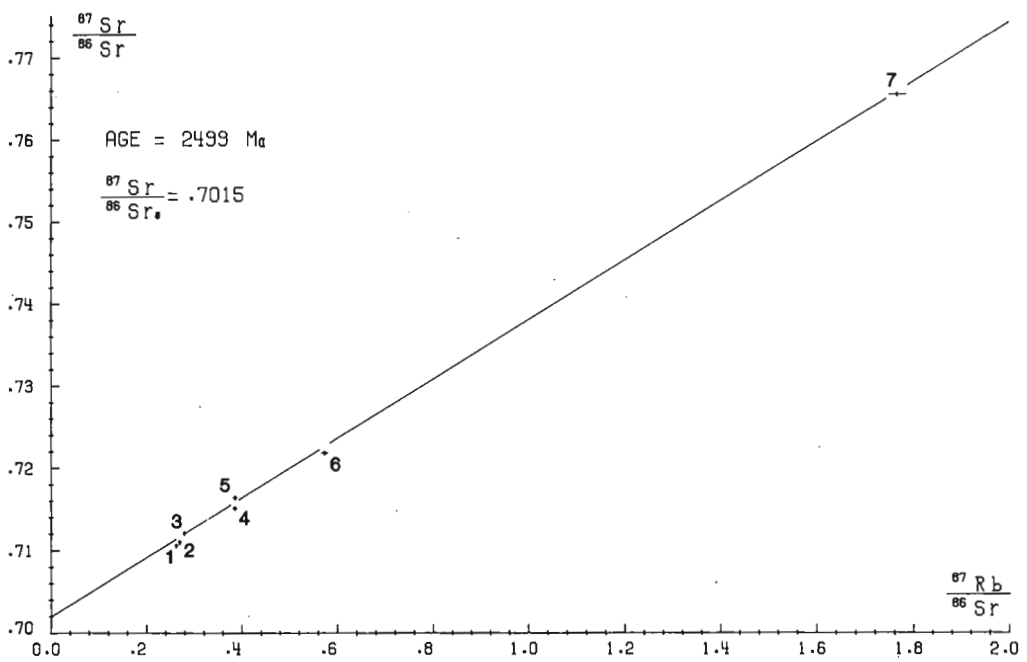

Figure 36.5

Rubidium-strontium whole rock study of massive dacites from an area near the Yava sulphide deposit.

be intrusive and younger than the tonalite and trondhjemite that are also present. However, the contact relationships of the granodiorite with these rocks are too obscure to establish this relationship.

The U-Pb and Rb-Sr age results depicted in Figure 36.3 are not in complete agreement. The zircon age is identical within experimental error to that (2670 ± 4 Ma) obtained for zircons derived from felsic volcanic rocks and volcanogenic greywacke from the Back Group (Lambert and Henderson, 1980) which strongly suggests that the Hackett River area granodiorite was a synvolcanic intrusion. Thus we interpret the U-Pb concordia age of 2666 Ma as the synvolcanic emplacement age of the Hackett River granodiorite.

The Rb-Sr results give younger, presumably re-equilibrated ages, that together do not define an isochron. Although the four lower points are colinear to a reference line of 2570 Ma (Fig. 36.3), the significance of points below this array is not understood.

Yellowknife Supergroup

Previous age determinations of the Yellowknife Supergroup in the Nose Lake – Beechey Lake map area were by K-Ar biotite methods from schists in the 'Index' Lake and areas farther east, which yielded an ages of 2475, 2100, and 2140 Ma.

Other geochronological work includes the previously mentioned U-Pb study of zircons from greywacke and felsic volcanic rocks from the Back River region (Lambert and Henderson, op. cit.) which gave an age of 2670 Ma from a concordia intersection, and which we accept as the age of Back Group volcanism.

In this study rubidium-strontium whole rock analyses of the Yava dacite, which forms part of the Nauna Formation in the Yava deposit area, produced an apparent age of 2499 ± 140 Ma (Fig. 36.5). Since this value is more than 160 Ma younger than that obtained for the Back Group the Rb-Sr isotopic systems were probably disturbed.

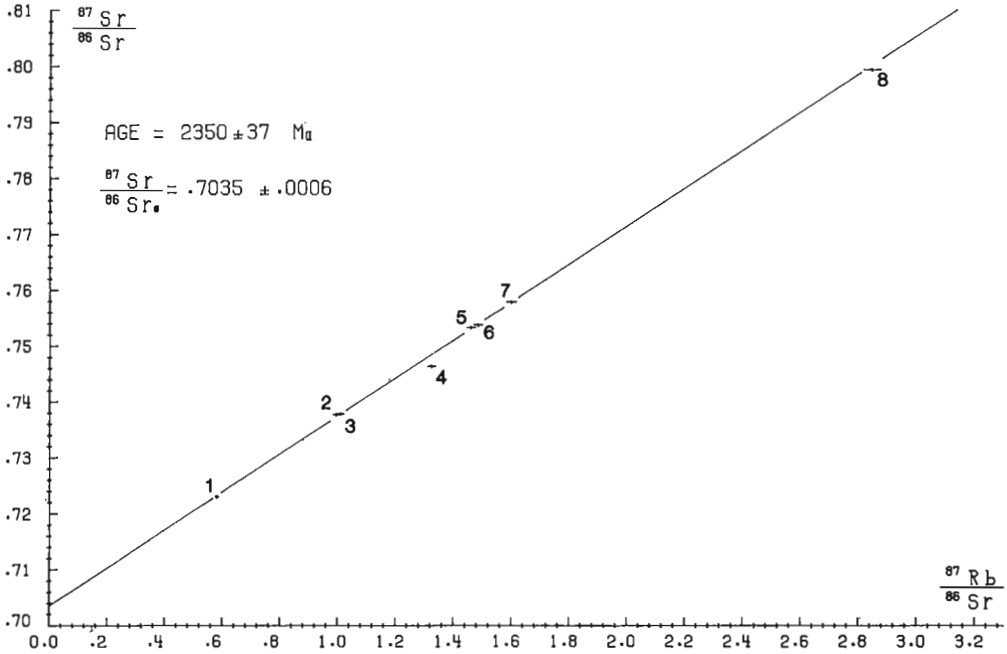

Figure 36.6

Rubidium-strontium whole rock isochron from leucogranodiorite whole rock samples from the 'Uist' Lake pluton.

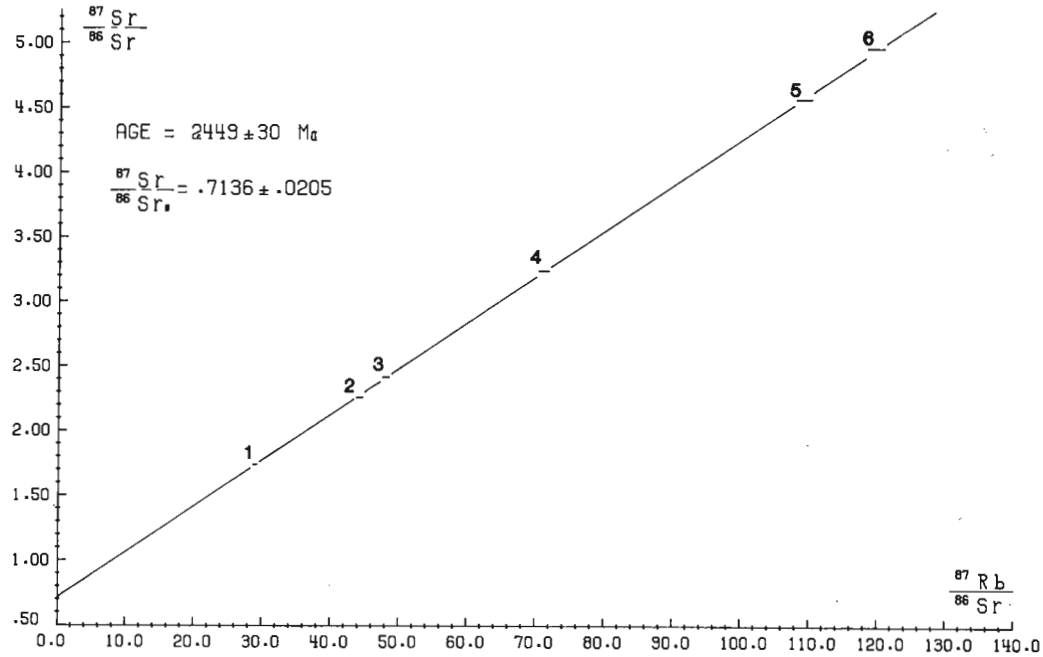

Figure 36.7

Rubidium-strontium whole rock isochron from granite whole rock samples from the 'Koak' lakes granite.

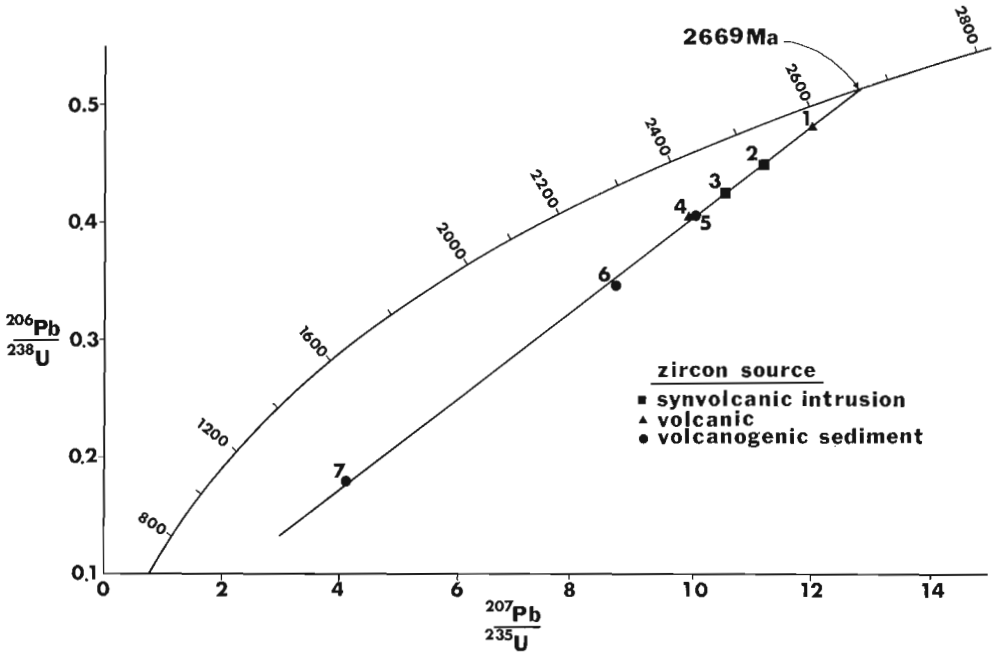

1. *Felsic volcanic rocks, Back River area (Lambert and Henderson, 1980)*
2 and 3. *Synvolcanic granodiorite, this study*
4. *Felsic volcanic rocks, Yellowknife area (Green, 1968)*
5. *Greywacke, Yellowknife area (R.K. Wanless, pers. comm., 1979)*
6. *Greywacke, Yellowknife area (Lambert and Henderson, 1980)*
7. *Greywacke, Yellowknife area (Green, 1968).*

Figure 36.8. *Concordia diagram showing the results of U-Pb analyses on zircons from volcanic, volcanogenic sedi-mentary and syn-volcanic intrusive rocks from several localities in the Slave Province. The regression line intersects the concordia at 2669 and 143 Ma.*

Table 36.2

Analytical data, uranium-lead analyses of zircon fractions, Hackett River granodiorite and 'Uist' Lake pluton

Geological Unit	Hackett River Area Granodiorite		'Uist' Lake Pluton		
Zircon Fraction number	1	2	1	2	3
Fraction size µm	-105+74	-105+74	-105+74	+105	-105+74
Magnetic or non magnetic	nm	mag.	nm	-	mag.
Weight mg	11.92	18.24	3.60	1.43	3.56
Total Pb, ng	422.2	752.2	168.4	75.72	148.0
Pb Blank, %	0.60	0.31	0.89	1.98	0.47
Observed $^{206}Pb/^{204}Pb$	5415	4214	3482	1030	2893
*Abundances (^{206}Pb = 100) ^{204}Pb	0.0057	0.0179	0.0116	0.0601	0.0259
^{207}Pb	18.094	18.188	17.259	17.739	17.212
^{208}Pb	15.297	16.507	16.532	18.322	16.474
Radiogenic Pb, ppm	99.40	105.7	143.9	154.8	156.6
%	99.73	99.16	99.45	97.19	98.76
Uranium, ppm	192.5	215.2	285.5	323.9	351.8
Atomic ratios $^{206}Pb/^{238}U$	0.45058	0.42607	0.43936	0.41616	0.39032
$^{207}Pb/^{235}U$	11.198	10.556	10.369	9.7507	9.0901
$^{207}Pb/^{206}Pb$	0.18024	0.17968	0.17116	0.16992	0.16890
Ages, Ma $^{206}Pb/^{238}U$	2398	2288	2348	2243	2124
$^{207}Pb/^{235}U$	2540	2485	2468	2411	2347
$^{207}Pb/^{206}Pb$	2655	2650	2569	2557	2547

*After subtraction of lead blank

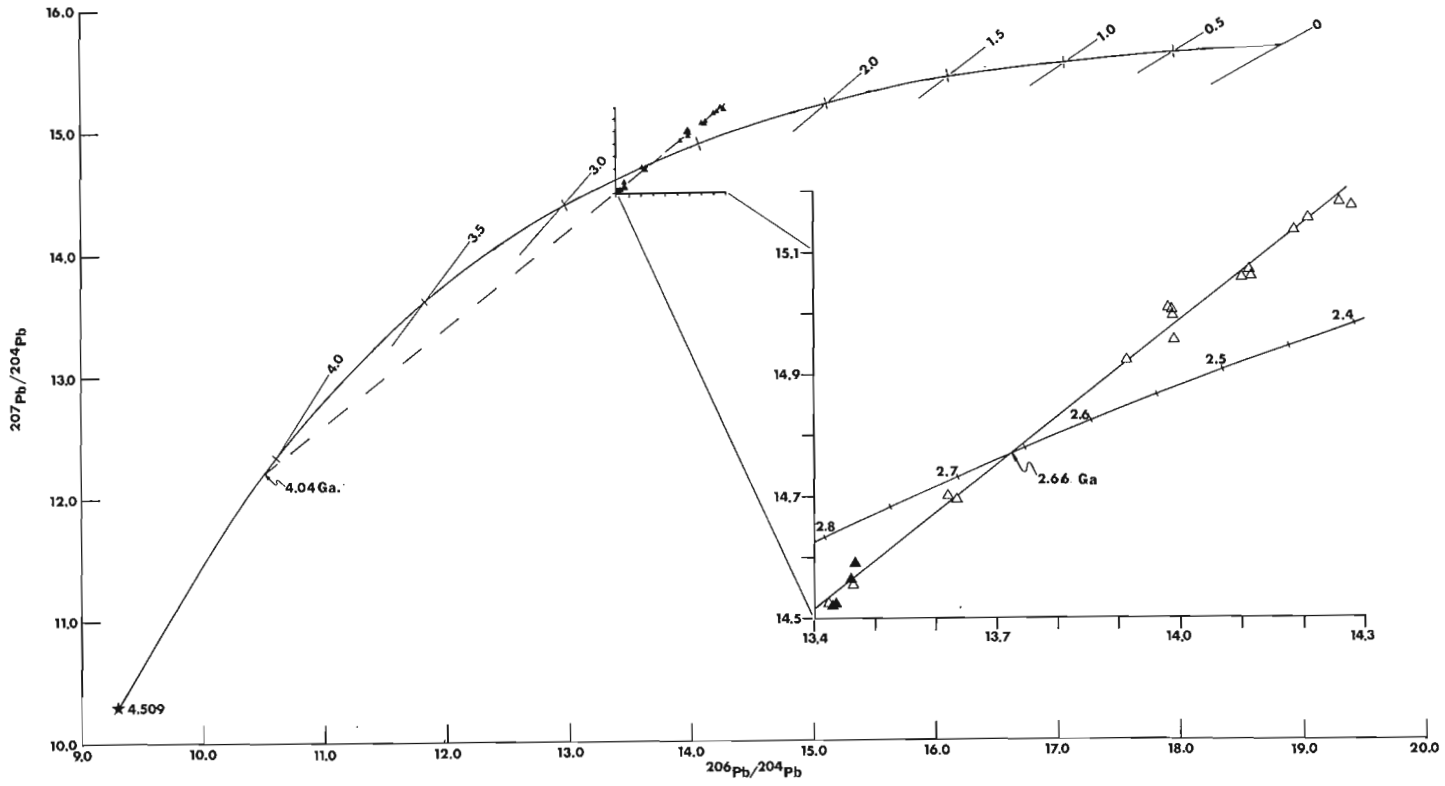

Figure 36.9. *Isotopic composition of galena, stratiform sulphides and vein deposits from Yellowknife Supergroup rocks plotted on lead isotopic growth curve after Cumming and Richards (1975). The inset shows in greater detail the fit of the regression line to the analytical results with the solid triangles indicating the Bathurst-Norsemines and Yava sulphide deposits (Data obtained from R. Thorpe, personal communication, 1979 is listed in Table 36.5).*

Regan Intrusive Suite

The plutons that make up the Regan Intrusive Suite have been studied in detail by Hill (1980) and by Hill and Frith (in press). It was concluded that most of the Suite was consanguineous, formed by fractionation of hornblende and plagioclase from a parental magma with a composition approximated by quartz diorite, similar to the quartz diorite found as inclusions in the margin of some plutons. Possible exceptions to this are the granites, which, on chemical grounds, may be of separate origin. All mineral phases of the plutons were found to be magmatic except for microcline which recrystallized from a higher temperature K-feldspar. The magmatic and fractionated nature of the pluton implies that the more leucocratic phases were younger than the more melanocratic phases. This is borne out by detailed contact relationships, particularly in the case of zoned plutons in which the more leucocratic bodies invariably cut the more mafic ones.

The Regan Intrusive Suite comprises approximately 70 plutons. Granodiorite and tonalite are present in about equal proportions and together make up 70 per cent of the rocks by area, with granite accounting for 26 per cent and diorite 4 per cent. The individual plutons are relatively constant in composition and the chemical compositions of their component phases plot on smooth curves of variation strongly suggesting they are consanguineous. Some plutons are zoned and these appear to be smaller versions of a larger differentiation system that produced individual plutons.

Structures and textures in the Regan plutons indicate they are magmatic in origin and microprobe analyses have shown that hornblende, plagioclase and biotite are primary, whereas microcline is secondary having undergone subsolidus crystalization and local mobilization (Hill and Frith, in prep.). Examination of zircon fractions revealed several oscillatory growth features but no evidence of corroded cores or secondry growth.

Previous geochronological work on plutonic rocks that form part of the Regan Intrusive Suite was restricted to K-Ar determinations on muscovite and biotite (Table 36.1) which gave age values from 1950 Ma for the Index Lake granodiorite to 2535 Ma for the 'Koak' Lake granite. These results are highly divergent for a suite that was initially considered to be more or less contemporaneous with late regional deformation and metamorphism (Frith and Hill, 1975).

The 'Uist' Lake pluton was chosen as the most representative of the Regan Intrusive suite. It is a zoned body grading from marginal tonalite to leuogranodiorite, with granite pegmatite present locally. In addition, the pluton is clearly discordant to structures developed during the second deformational event (D_2) recognized in the region and it cuts across the cordierite-staurolite isograd. Geochronological samples were taken mainly from the leucogranodiorite. The results of U-Pb analyses on zircons from this pluton define a chord which intersects the concordia curve at 2588 ± 8 Ma (Fig. 36.4). This is significantly older than the rubidium-strontium whole rock isochron age of 2350 ± 37 Ma for the same body (Fig. 36.6) and for other plutons of the Regan Intrusive Suite which yield rubidium-strontium isochron ages of 2449 ± 29 Ma ('Koak' Lake granite Fig. 36.7).

On the basis of the morphology of the zircons, which do not show corroded cores or secondary growth structures we interpret the 2588 Ma zircon age as the age of intrusion of the 'Uist' Lake pluton. We believe that most other plutons in

Table 36.3

Analytical data for rubidium-strontium whole rock analyses

Sample	Rb ppm	Sr ppm	$^{87}Sr/^{86}Sr$ spiked	$^{87}Rb/^{86}Sr$
A Hackett River area granodiorite				
1	8.902	217.6	0.7063 ± 0.0004	0.1183 ± 0.0024
2	38.91	138.1	0.7335 ± 0.0004	0.8146 ± 0.0163
3	19.97	51.13	0.7439 ± 0.0004	1.129 ± 0.023
4	77.00	126.6	0.7661 ± 0.0005	1.758 ± 0.035
5	65.18	44.30	0.8224 ± 0.0005	4.254 ± 0.085
6	57.10	29.47	0.8668 ± 0.0005	5.602 ± 0.112
7	79.74	39.83	0.8591 ± 0.0005	5.788 ± 0.116
B Yava dacite dome				
1	14.01	154.5	0.7106 ± 0.0004	0.2622 ± 0.0052
2	13.64	146.4	0.7110 ± 0.0004	0.2694 ± 0.0054
3	13.99	144.9	0.7121 ± 0.0004	0.2791 ± 0.0056
4	15.97	119.9	0.7151 ± 0.0004	0.3851 ± 0.0077
5	27.98	209.9	0.7164 ± 0.0004	0.3854 ± 0.0077
6	18.85	95.11	0.7218 ± 0.0004	0.5730 ± 0.0115
7	41.73	68.26	0.7654 ± 0.0005	1.767 ± 0.035
C 'Uist' Lake granodiorite				
1	106.5	528.7	0.7230 ± 0.0004	0.582 ± 0.012
2	130.0	377.7	0.7377 ± 0.0004	0.995 ± 0.020
3	140.3	401.0	0.7378 ± 0.0004	1.012 ± 0.020
4	153.2	303.4	0.7532 ± 0.0005	1.460 ± 0.029
5	158.7	309.2	0.7537 ± 0.0005	1.484 ± 0.030
6	169.9	307.2	0.7578 ± 0.0005	1.599 ± 0.032
7	175.8	178.5	0.7993 ± 0.0005	2.847 ± 0.057
D 'Koak' Lake granite				
1	243.1	24.37	1.739 ± 0.0010	28.84 ± 0.58
2	240.5	15.78	2.256 ± 0.0014	44.06 ± 0.88
3	228.3	13.76	2.415 ± 0.0014	47.97 ± 0.96
4	242.5	9.863	3.235 ± 0.0019	71.08 ± 1.42
5	290.5	7.699	4.568 ± 0.0027	109.1 ± 2.2
6	252.6	6.105	4.962 ± 0.0030	119.6 ± 2.4

the Regan Intrusive Suite are approximately the same age. If this interpretation is correct then the rubidium-strontium ages determined in this study are too young to be primary and isotopic systems were likely disturbed in some manner.

Rb-Sr isochron studies were also carried out on the 'Koak' Lake granite and an age of 2449 ± 30 Ma was obtained. By itself, the good colinearity would suggest that the body became a closed system shortly after its intrusion which would be compatible with field and geochemical data (Hill and Frith, in press) but since other Rb-Sr systems in the area are of known older age, then an intrusive age of 2449 Ma is in doubt.

Age determinations of Other Rocks

Muscovite from two pegmatites found in the Nose Lake area yielded K-Ar ages of 2374 ± 54 Ma and 2484 ± 41 Ma. The younger value was obtained from pegmatite in the Mara River area, where granitoid gniess, migmatite and pegmatite make up a heterogenous granitoid terrane of high grade regional metamorphism. The older value was obtained from a granite pegmatite found in high grade Beechey Lake Group schists.

Since the pegmatites are found only in regions of high grade regional metamorphism and do not form a conspicuous part of the Regan Intrusive Suite of rocks, Hill and Frith (in preparation) concluded that they were formed during and as a result of regional metamorphism. The above ages probably result from disturbance of isotopic systems.

Table 36.4

Potassium-argon age determination

Muscovite from pegmatite NW of 'Uist' Lake, Location number 5, Figure 2.
Field number T-223A, age 2484 ± 41 Ma
K=8.47%, $^{40}Ar/^{40}K$=0.3105, radiogenic ^{40}Ar=99.2%
Concentrate: Clean, clear, unaltered, very fine grained muscovite with no visible contamination.

Table 36.5

Lead isotopic compositions: galena from massive sulphide deposits and base metal occurrences in the Slave Province (Data supplied by Thorpe, personal communication, 1979)

	Reference	Property	$^{206}Pb/^{204}Pb$	$^{207}Pb/^{204}Pb$	$^{208}Pb/^{204}Pb$	Latitude	Longitude
1.	G.S.C. 1971	'Camp' Lake*	13.430	14.520	33.210	65°55'05"	108°22'00"
2.	G.S.C. 1971	Indian Mtn. L.	13.620	14.700	33.380	63°02'45"	110°56'55"
3.	U.B.C. 1972	Homer L.	14.101	15.058	33.930	62°39'25"	114°17'30"
4.	U.B.C. 1972	Turnback L.	14.209	15.154	33.954	62°44'25"	112°40'35"
5.	U.B.C. 1972	Victory L.	14.279	15.177	33.880	62°39'21"	113°02'28"
6.	Teledyne 1975	Hood River No. 10	13.989	14.955	33.750	66°03'35"	112°45'15"
7.	Teledyne 1975	'Cleaver' L.*	13.436	14.523	33.269	65°55'55"	108°27'40"
8.	Teledyne 1975	Homer L.	13.982	15.008	33.663	62°39'15"	114°17'50"
9.	Teledyne 1975	Ross L.	14.261	15.184	33.946	62°42'55"	113°05'45"
10.	Teledyne 1975	Homer L. (vein)	14.111	15.071	33.921	62°39'15"	114°17'50"
11.	Teledyne 1975	Indian Mtn. L.	13.635	14.697	33.403	63°02'45"	110°56'55"
12.	Teledyne 1975	'Aitch' L.**	13.467	14.591	33.326	65°36'30"	107°56'15"
13.	Teledyne 1974	Homer L.	14.115	15.058	33.929	62°39'15"	114°17'50"
14.	Teledyne 1974	Turnback L.	14.186	15.135	33.782	62°44'25"	112°40'35"
15.	Teledyne 1974	No. 41 deposit	13.987	15.006	33.701	66°02'05"	112°42'30"
16.	G.S.C. 1972	High Lake	13.424	14.526	33.149	67°22'50"	110°51'20"
17.	Teledyne 1977	Izok L.	13.988	14.996	33.710	65°38'00"	112°47'45"
18.	Teledyne 1977	Izok L.	13.912	14.923	33.497	65°38'00"	112°47'45"
19.	Teledyne 1977	'Duck' L.*	13.460	14.564	33.320	65°50'	108°05'35"
20.	Teledyne 1977	High L.	13.463	14.556	33.287	67°22'50"	110°51'20"

* Bathurst Norsemines deposit
** Yava deposit

Discussion

The age of the Yellowknife Supergroup

All zircon data from Yellowknife Supergroup rocks, including volcanic rocks, volcanogenic sedimentary rocks and synvolcanic intrusions have been plotted together in Figure 36.8 where they define a chord that intersects the concordia curve at 2669 +16/-14 Ma. The common age of these rocks from both the southern and the northeastern Slave Province strongly suggests a single pan-Slave volcanic-intrusive episode.

Further evidence for a single pan-Slave event comes from the lead isotopic studies of Thorpe (1972) who reported on galenas from base metal deposits of stratiform and probably related types in the Slave Province. He has kindly provided us with more recent data (Table 36.5; Thorpe personal communication, 1979), from the Camp Lake deposit of Bathurst-Norsemines, from other deposits of the region, and from the Yava deposit. The data form a linear trend which yields a slope of 0.7850 and correlation coefficient 0.9975 when subjected to linear regression.

This linear pattern denotes a secondary isochron which implies that the parent material from which the galena lead was ultimately derived was initially isotopically homogeneous but that subsequent isotopic growth took place in locales of differing U/Pb ratio, terminating in synchronous galena mineralization. The systematics of secondary lead isochrons do not allow a unique determination of either the primary age or the time of mineralization. However one interpretation of this model is shown in Figure 36.9 in which the chord through the data points cuts the model three, continuous lead growth curve of Cumming and Richards (1975) at 4040 and 2660 Ma. We are unable to interpret the 4040 Ma age which is presumably the age of isotopic homogeneity of lead in the parent material, but the 2660 Ma age suggests a time of mineralization close to that of the pan-Slave episode defined by the U-Pb zircon data.

Ages derived from secondary isochron parameters are highly model dependent, but the linearity of the isotopic data provides a strong argument for contemporaneous galena mineralization. If, this event occurred at about 2660 Ma, as suggested, it corroborates the ubiquity of the episode defined by the zircon results and supports the concept of a single pan-Slave orogenic event that resulted in a relatively short-lived break-up of an ancient 3000 Ma tonalitic crust (Frith and Roscoe, 1980) accompanied by simultaneous volcanism, plutonism and sedimentation into graben-like basins similar to the basin models proposed by Henderson and McGlynn (1970) and as discussed recently by Henderson (1981). To satisfy the constraint that the volcanic belts are contemporaneous in age, a fundamental orogenic mechanism must be invoked for the crustal segmentation.

The Age of the Regan Instrusive Suite

The plutons of this suite are late Kenoran intrusions. Studies in this area have shown that plutons within the suite are structureless, except for structures produced during emplacement that were contemporaneous with magmatic

crystallization. However, the rubidium-strontium whole rock age determinations and the bulk of the K-Ar determinations are in conflict with the 2588 Ma age obtained from zircons. If the zircon value is accepted as the age of the Regan Intrusive Suite as a whole, it must be concluded that the Rb-Sr systems were disturbed. The Rb-Sr data for pre-Regan rocks suggests an isotopic re-equilibration between 2570 and 2500 Ma.

The Rb-Sr age determinations from the Regan Intrusions give good values for the mean square of the weighted deviates but low age values of 2350 Ma for the 'Uist' Lake pluton and 2449 Ma for the 'Koak' granite. Although a case may be made for 2449 Ma date being a late metamorphic cooling age, this interpretation can not be used for the 2350 Ma age. We do not understand how these rocks re-equilibrated at this time. The rocks give no indication of later thermal overprint, nor are the rocks overly jointed, discoloured or retrograded. The host rocks, however are strongly deformed by northeast-southwest cleavage, but the age of this structure is only known to be post-intrusive. Further geochronological or geochemical work is needed to explain the isotopic rejuvenation of the 'Uist' Lake pluton.

The Age of Regional Metamorphism

Regional metamorphism in the area ranges from sub-greenschist to upper amphibolite grade. This implies different heating and cooling rates over the study area, rates which are recorded in the mineralogy and isotopic compositions of the various rocks. The earliest effects of the regional metamorphism took place prior to the emplacement of the Regan Intrusive Suite, as porphyroblasts in the Yellowknife Supergroup rocks, particularly cordierite, are typically retrograded. The exception is in the Hackett River gneiss dome where large unpinnitized cordierite porphyroblasts indicate a later high grade metamorphism. The Rb-Sr systems in the granodiorite of the core of the Hackett River gneiss dome have been requilibrated differently at different places within the same body.

The ages younger than 2450 Ma (Table 36.1) were derived from rocks whose isotopic systems were thermally reset by Proterozoic metamorphic events associated with the development of the Thelon Front (Wright, 1957). These age values, are variable, ranging from 2400 to 1950 Ma. Further, more sophisticated geochronological studies are required in the Thelon Front area to determine the age of the Proterozoic structures and the age of locally developed post-deformation muscovite prophyroblasts (Frith, 1982).

Acknowledgments

We thank R.I. Thorpe for providing previously unpublished lead isotopic compositions of galena from base metal deposits in the Slave and for critically reading this manuscript. The paper also benefited from comment and review by R.D. Stevens, J.B. Henderson, and J.C. McGlynn.

References

Cameron, E.M.
1980: Rb-Sr age of the Lineament Lake Granodiorite, District of Mackenzie in Loveridge, W.D., Rubidium-strontium and uranium-lead isotopic age studies, Report 3; in Current Research, Part C, Geological Survey of Canada, Paper 80-1C, p. 223-226.

Cameron, E.M. and Durham, C.C.
1974: Geochemical studies in the eastern Slave Structural Province, 1973; Geological Survey of Canada, Paper 74-27.

Cumming, G.L. and Richards, J.R.
1975: Ore lead isotope ratios in a continuously changing earth; Earth and Planetary Science Letters v. 218, p. 155-171.

Davidson, A.
1979: in Age determinations and geological studies, K-Ar isotopic ages, Report 14; Geological Survey of Canada, Paper 79-2, p. 34-38.

Ewing, T.E.
1979: Two calc-alkaline volcanic trends in the Archean: Trace element evidence; Contributions to Mineralogy and Petrology, v. 48, p. 1-7.

Fraser, J.A.
1964: Geological notes on northeastern District of Mackenzie, Northwest Territories; Geological Survey of Canada, Paper 63-40.

1965: in Age determinations and geological studies, Part 1, Isotopic ages Report 5; Wanless, R.K. et al., Geological Survey of Canada, Paper 64-17 (part 1), p. 56-57.

Frith, R.A.
1979: in Age determinations and geological studies, K-Ar isotopic ages, Report 14; Wanless, R.K., et al., Geological Survey of Canada Paper 79-2, p. 39.

Geology of the Nose-Beechey Lakes map-area (76 G, W/2, 76 F, E/2) District of Mackenzie, Northwest Territories; Geological Survey of Canada, Memoir (in preparation).

Frith, R.A.
1982: Second preliminary report on the geology of the Beechy Lake-Duggan Lake map area, District of Mackenzie, Northwest Territories; in Current Research, Part A, Geological Survey of Canada, Paper 82-1A, report 33.

Frith, R.A. and Hill, J.D.
1975: The geology of the Hackett-Back River greenstone belt – Preliminary Account; in Report of Activities, Geological Survey of Canada, Paper 75-1C, p. 367-370.

1980: Geochemistry and Petrology of the Hackett River Group – an atypical Archean greenstone belt in the northeastern Slave Province (abstract); in Geological Association of Canada, Mineralogical Association of Canada, Joint Annual Meeting, Program with abstracts, v. 5, Halifax 1980, p. 54.

Frith, R.A. and Percival, J.P.
1978: Stratigraphy of the Yellowknife Supergroup in the Mara Rivers Area, District of Mackenzie; in Current Research, Part C, Geological Survey of Canada, Paper 78-1C, p. 89-98.

Frith, R.A. and Roscoe, S.M.
1980: Tectonic setting and sulphide deposits, Hackett River Belt, Slave Province; The Canadian Mining and Metallurgical Bulletin, v. 73, no. 815, p. 143-153.

Frith, Rosaline, Frith, R.A., and Doig, R.
1977: The geochronology of the granitic rocks along the Bear-Slave Structural Province boundary, northwest Canadian Shield; Canadian Journal of Earth Sciences, v. 14, no. 6, p. 1356-1373.

Fyson, W.K. and Frith, R.A.
1979: Regional deformations and emplacement of granitoid plutons in the Hackett River greenstone belt, Slave Province, Northwest Territories, Canadian Journal of Earth Sciences, v. 16, no. 6, p. 1187-1195.

Green, D.C.
1968: Precambrian geology and geochronology of the Yellowknife area, N.W.T.; unpublished Ph.D. thesis, University of Alberta, Edmonton, Alberta.

Henderson, J.B.
1981: Archean Basin Evolution in the Slave Province, Canada; in Precambrian Plate Tectonics, Elsevier, Amsterdam, p. 213-235.

Henderson, J.B. and McGlynn, J.C.
1970: Archean volcanism and sedimentation in the Slave Structural Province in Symposium on Basins and Geosynclines of the Canadian Shield; Geological Survey of Canada, Paper 70-40, p. 31-44.

Hill, J.D.
1980: The structural development and crystallization of the Kenoran granitoid plutons in the Nose Lake – Back River area, Northwest Territories; unpublished Ph.D. thesis, University of Western Ontario, London, Ontario.

Hill, J.D. and Frith, R.A.
Petrology of the Regan Intrusive Suite in the Nose-Beechey Lake area, Northwest Territories Geological Survey of Canada, Paper (in prep.)

Lambert, M.B.
1978: The Back River Volcanic Complex – a cauldron subsidence structure of Archean age; in Current Research, Part A, Geological Survey of Canada, Paper 78-1A, p. 153-157.

Lambert, M.B. and Henderson, J.B.
1980: A uranium-lead age of zircons from volcanics and sediments of the Back River Volcanic Complex, eastern Slave Province, District of Mackenzie; in Loveridge, W.D., Rubidium-strontium and uranium-lead isotopic age studies, Report 3; in Current Research, Part C, Geological Survey of Canada, Paper 80-1C, p. 239-242.

Percival, J.A.
1978: Stratigraphy, structure and metamorphism of the Hackett River Gneiss Dome, District of Mackenzie, N.W.T.; unpublished M.Sc. thesis, Queen's University.

1979: Kyanite-bearing rocks from the Hackett River area, NWT; implications for Archean gradients; Contributions to Mineralogy and Petrology, v. 69, p. 177-184.

Stockwell, C.M.
1961: Structural provinces, orogenies and time classification of rocks of the Canadian Precambrian Shield; in Age determinations by the Geological Survey of Canada, Report 2, Isotopic ages; Geological Survey of Canada, Paper 61-17, p. 108-117.

1972: Revised Precambrian time-scale for the Canadian Shield; Geological Survey of Canada, Paper 75-52, p. 1-4.

Sullivan, R.W. and Loveridge, W.D.
1980: Uranium-lead age determinations on zircon at the Geological Survey of Canada: current procedures in concentrate preparation and analysis; in Loveridge, W.D., Rubidium-strontium and uranium-lead isotopic age studies, Report 3; in Current Research, Part C, Geological Survey of Canada, Paper 80-1C, p. 164.

Thorpe, R.I.
1972: Interpretation of lead isotope data for base metal and gold deposits, Slave Province, Northwest Territories; in Report of Activities, Geological Survey of Canada, Paper 72-1B, p. 72-77.

Tremblay, L.P.
1971: Geology of Beechey Lake map-area, District of Mackenzie, a part of the Western Canadian Precambrian Shield; Geological Survey of Canada, Memoir 365.

1966: Age determinations and geological studies, K-Ar isotopic ages, Report 6; Wanless, R.K., et al.; Geological Survey of Canada, Paper 65-17, p. 31-32.

1965: Age determinations and geological studies, K-Ar isotopic ages, Report 5, Wanless et al., Geological Survey of Canda, Paper 64-17 (part 1), p. 31-32.

Wanless, R.K. and Loveridge, W.D.
1972: Rubidium-strontium isochron age studies, Report 1; Geological Survey of Canada, Paper 72-23.

Wright, G.M.
1957: Geological Notes on the eastern District of Mackenzie, Northwest Territories; Geological Survey of Canada, Paper 56-10.

1960: in Age determinations by the Geological Survey of Canada, Report 1, Isotopic ages; compiled by Lowdon, J.A.; Geological Survey of Canada, Paper 60-17, p. 12-14.

APPENDIX I

Analytical Techniques

1. Uranium-lead age determinations on zircons: Techniques used in the preparation of zircon concentrates for U-Pb analysis are described in Sullivan and Loveridge (1980).

   a. Hackett River granodiorite: A series of 15 whole rock samples weighing 4-8 kg were collected from a relatively massive part of the core zone of the Hackett River gneiss dome over a distance of about 100 m. After crushing, a representative portion of each rock was removed for Rb-Sr isotopic analysis and the remainders were combined for zircon separation. A zircon concentrate was sieved to produce a -105, +74 μ fraction which was separated into relatively magnetic and nonmagnetic subfractions by a Frantz isodynamic separator. These subfractions were not purified by hand picking but impurities were estimated to be less than 5 per cent.

   b. 'Uist' Lake granodiorite: Zircons (Fig. 2, analysis 16) were concentrated from a bulk sample obtained by combining splits of 13 whole rock powders collected for Rb-Sr isotopic analysis. Three zircon fractions approaching 100% purity were obtained by sieving, magnetic separation and hand-picking.

2. Rubidium - strontium whole rock studies: Analytical procedures for rubidium-strontium isotopic analysis of whole rock samples were based on those described by Wanless and Loveridge (1972). Since that time instrumental modifications have resulted in improved accuracy in the measurement of the $^{87}Sr/^{86}Sr$ ratio (to ±0.06 % at the 95% confidence level). For this reason the $^{87}Sr/^{86}Sr$ ratios in this study were determined from spiked Sr analyses only; no unspiked Sr measurements were performed.

   a. Hackett River area granodiorite: Seven samples were analyzed isotopically (Table 36.3a). Of the seven data points only four show a linear trend which is compared in Figure 36.3 with a 2570 Ma reference line with initial $^{87}Sr/^{86}Sr$ of 0.7020. Regression analysis of these points yields an age of 2573 ± 124 Ma and an initial $^{87}Sr/^{86}Sr$ of 0.7021 ± 0.0012 but with a high MSWD of 6.82.

      The scatter of these four points along a 2570 Ma reference line, and the even greater scatter of the remaining three points, suggest that the Rb-Sr system has been open more than once since the time of emplacement (2666 Ma) given by the U-Pb zircon results.

   b. Yava dacite dome: The isotopic compositions of seven whole rock samples are listed in Table 36.3b and depicted in Figure 36.5. Regression analysis yields an age of 2499 ± 140 Ma, initial $^{87}Sr/^{86}Sr$ 0.7015 ± 0.0009 and MSWD of 4.96. This moderately high MSWD also suggests open system behaviour.

   c. 'Uist' Lake granodiorite: The results of isotopic analyses on seven whole rocks are presented in Table 36.3c and depicted in Figure 36.6. The data points show good collinearity and define an isochron of age 2350 ± 37 Ma, intercept 0.7035 ± 0.0006 and MSWD of 0.54. This result is much lower than the U-Pb zircon age of 2588 Ma. (Fig. 36.5).

   d. 'Koak' Lake granite: Isotopic results from six whole rock samples are given in Table 36.3d and plotted as analysis 10 in Figure 36.7. Regression analysis gives an age of 2449 ± 30 Ma, initial $^{87}Sr/^{86}Sr$ 0.7136 ± 0.0205 and a MSWD of 0.41. High rubidium contents (200-300 ppm) and low Sr contents (less than 25 ppm) have produced correspondingly high $^{87}Sr/^{86}Sr$ ratios of 1.7 to 5.0 in the rocks studied. The unusually high initial $^{87}Sr/^{86}Sr$ ratio of 0.7136 may be an artifact of these high $^{87}Sr/^{86}Sr$ ratios; the associated analytical uncertainty of ±0.0205 suggests that it does not differ significantly from 0.7000.

The low MSWD values of 0.54 and 0.41 obtained from the 'Uist' Lake granodiorite and 'Koak' Lake granite regression analyses indicate isotopic homogeneity at the time of closure of the Rb-Sr systems and little if any subsequent disturbance of those systems. Conversely, the relatively high MSWD values of 4.96 obtained from the Yava dacite dome results and 6.82 for the four linear Hackett River area granodiorite points demonstrate open system behaviour since the initial closure of the Rb-Sr systems and/or isotopic heterogeneity at that time.

APPENDIX II

Description of zircon fractions

1. Hackett River area granodiorite: After the initial purification, a -105+74 μm size fraction was separated into relatively more and less magnetic subfractions by use of a Frantz isodynamic separator. Zircon grains in the sub-fractions were morphologically similar, consisting of more than 90% broken grains with 5% impurities made up of sphene and some unidentified platy minerals. The zircons were pale to medium-brown, euhedral to subhedral with rounded terminations. Some crystals were noticeably zoned and many contained inclusions and occasional internal cracks. About half were clear, whereas others were translucent and darker brown. Crystal elongations ranged up to about 2.5:1.

2. 'Uist' Lake Pluton: A coarse (+105 μm) split from the original reasonably pure separate was hand picked to yield a 100% pure fraction of whole and fragmental zircons. The euhedral sharply terminated crystals were a clear brown colour with some bubble-like inclusions and minor black specks. Zoning and chevron growth ring features were evident in many grains as were some internal fractures. Crystals were mostly stubby with 1.5:1 elongation or less.

   The finer fraction (-105 to +74 μ) was separated into more and less magnetic subfractions and the less magnetic was hand-picked to yield 100% pure clear brown euhedral zircons with minor bubble-like inclusions and fine zonal structures. These crystals were also short and stubby but some were elongated (3:1). The more magnetic fraction was hand-picked to give a 100% pure brown euhedral zircon concentrate. These grains were slightly darker, containing dark specks in addition to bubble-like inclusions. The crystals were mostly stubby with elongations less than 2:1. Internal cracks were more evident than in the non magnetic subfraction and fine zoning was observed.

APPENDIX III

Field numbers for age determinations

1. Uranium – Lead:

   a. Hackett River granodiorite – zircons were separated from a composite sample made from 15, 2-5 kg samples (T630, 1-15) obtained within a 100 m square area.

   b. 'Uist' Lake pluton – zircons were obtained from a composite sample made up of 13, 2-5 kg samples obtained over an east-west traverse of the central zone over a distance of 5 km. The following sample numbers were used H-467, H476(1), H 478(3), H 479(4), H 483a, H 483b, H 483c, H 483d, H 486, T343(1), T343(2), T 343c, B 288.

2. Rubidium – Strontium

   The field numbers of whole rock samples used in this study are as follows:

   a. Hackett River granodiorite; 1 = T 630(5); 2 = T 630(9); 3 = T 630(3); 4 = T 630(2); 5 = T 630(12); 6 = T 630(15); 7 = T 630(10)

   b. Yava dacite; 1 = D 83a(2); 2 = D 83a(4); 3 = D 83 a(3); 4 = D 83a(5); 5 = D 83a(6); 6 = D 83a(1); 7 = D 83a(7).

   c. 'Uist' granodiorite; 1 = H 483a; 2 = H 449; 3 = H 479; 4 = T 343d; 5 = H 477; 6 = H 476; 7 = H 483b.

   d. 'Koak' granite; 1 = B 73(4); 2 = B 73(3); 3 = B 73(5); 4 = B 73(2); 5 = T 157 (6); 6 = T 157(1).

37.

CHROMITE OCCURRENCES IN ULTRAMAFIC ROCKS IN THE MITCHELL RANGE, CENTRAL BRITISH COLUMBIA

EMR Research Agreement 203-4-81

Peter J. Whittaker[1]
Economic Geology Division

Whittaker, Peter J., Chromite occurrences in ultramafic rocks in the Mitchell Range, central British Columbia; in Current Research, Part A, Geological Survey of Canada, Paper 82-1A, p. 239-245, 1982.

Abstract

Detailed mapping of a serpentinized and tectonized ultramafic massif in the Mitchell Range, central British Columbia, was undertaken to gain an understanding of the factors controlling the distribution of chromite. Strongly foliated harzburgite and minor dunite underlie much of the map area. Brittle deformation is represented by an extensive breccia zone within the northeastern part of the massif. Gabbro dykes which predate obduction of the ultramafic rocks have been plastically deformed and in places altered to rodingite. Xenoliths of Cache Creek Group metasedimentary carbonate rocks and cherty siltstones, up to 1 square kilometre in area, commonly exhibit grey talc-rich zones at their contacts with serpentinized harzburgite. Fifteen new chromite occurrences were mapped in addition to two that had been described previously. Chromite occurs in layered and nodular forms, and in both cases aggregate and massive chromitite textures were observed. Tectonized harzburgite typically contains accessory chromite (about 1%) and, less commonly, more heavily disseminated layers and nodules (35 to 45% chromite). Deformation of chromitite layers has probably led to formation of nodular chromite. Electron microprobe analyses of chromite in two chromitite samples from different localities indicated average Cr:Fe ratios of 3.8 and 1.7. Silicate, Ni-Fe sulphide and fluid inclusions occur within chromite grains in aggregate chromitite.

Introduction

The Mitchell Range, 240 km northwest of Prince George, British Columbia, is within the Stuart Lake Belt of the Cache Creek Group (Permian). The Cache Creek Group consists predominantly of massive bedded carbonate rocks and minor laminated chert-siltstone and shaly siltstone. The carbonate succession extends 120 km southeast from the Mitchell Range to the Fort St. James area where it attains a thickness of 8 km (Armstrong, 1949). The southeast striking carbonate succession is folded into an open anticline-syncline pair immediately south of the ultramafic rocks. The open folds have east-southeast trending axes suggesting compression from the south-southwest associated with obduction of the Mitchell Range allochthonous rocks. An obduction process has been suggested by Paterson (1977) to account for a serpentinized ultramafic block at Murray Ridge, 120 km to the southeast. Likewise, in the Whitehorse Trough, Yukon, an obducted sequence of rocks includes klippe of predominantly ultramafic rocks belonging to the Anvil Allochthon of the Cache Creek Group (Tempelman-Kluit, 1979). Chromite occurrences in the Mitchell Range were documented by Armstrong (1949). Since then various companies and individuals have shown an interest in both the chromite and nephrite (i.e., "British Columbia jade") that occur in the area.

Mitchell Range Allochthon

General Geology

Allochthonous rocks within the Mitchell Range consist primarily of obducted harzburgite with minor dunite (Fig. 37.1), which are everywhere serpentinized. Sparse pretectonic orthopyroxenite veins and gabbro dykes are deformed and reflect internal deformation presumably developed during obduction. Rodingite dykes are similarly deformed. Layers of chromitite and disseminated chromite within the harzburgite exhibit variable degrees of deformation, as indicated by isoclinal folds and segmented planar layers.

Cache Creek Group rocks form xenoliths which have been rotated during transport of the ultramafic block and are up to 1 km^2 in area (Fig. 37.1). Contacts between harzburgite and xenoliths regularly exhibit a 0.5 m thick, highly fissile zone; a 1-2 cm thick amphibole-rich alteration zone is developed in the harzburgite.

Later, intrusions of metagabbro (Fig. 37.1) and metadiorite dykes may be related to the dioritic-granodioritic rocks of the Mitchell Range Batholith (Armstrong, 1949) which occurs 2.5 km west of the ultramafic body. Clinopyroxene in the dykes is altered to amphibole and primary subophitic and equigranular medium grained textures are preserved.

Structure

The Mitchell Range ultramafic allochthon is bounded by north-northeast and east-trending faults (Fig. 37.1). Rocks of the Cache Creek Group occur to the south and east, Takla Group volcanic rocks (Upper Triassic to Upper Jurassic) outcrop to the north, and the Mitchell Batholith (Upper Jurassic to Lower Cretaceous; Armstrong, 1949) occurs to the west.

Serpentinized harzburgite of the Mitchell Range allochthon exhibits a strongly developed penetrative ductile shear foliation with a north-northeast trend (Fig. 37.2). The dip of the foliation changes from westerly in the western part of the area to easterly in the east. The contour maxima in Figure 37.2 are centered about an east-southeast great circle girdle, indicative of a preferred north-northeast foliation. This foliation reflects a broad antiformal structure. Internal breccia zones in the harzburgite consist of well rounded, randomly oriented, pebble- to cobble-sized fragments set in a finely comminuted serpentinized matrix. The northeast and east central areas of the ultramafic massif are underlain by tectonic breccia (Fig. 37.1) with subangular fragments, predominantly of harzburgite with minor dunite, up to 2 m in size. This coarse tectonic breccia appears to represent the sole of the allochthonous ultramafic rocks.

Tectonized Harzburgite

Tectonized and serpentinized harzburgite forms approximately 90 per cent of the rock exposed in the Mitchell Range allochthon. Harzburgite exhibits a mottled, foliated, weathered surface with pale silvery brown talcose patches.

[1]Department of Geology, Carleton University, Ottawa, Ontario K1S 5B6

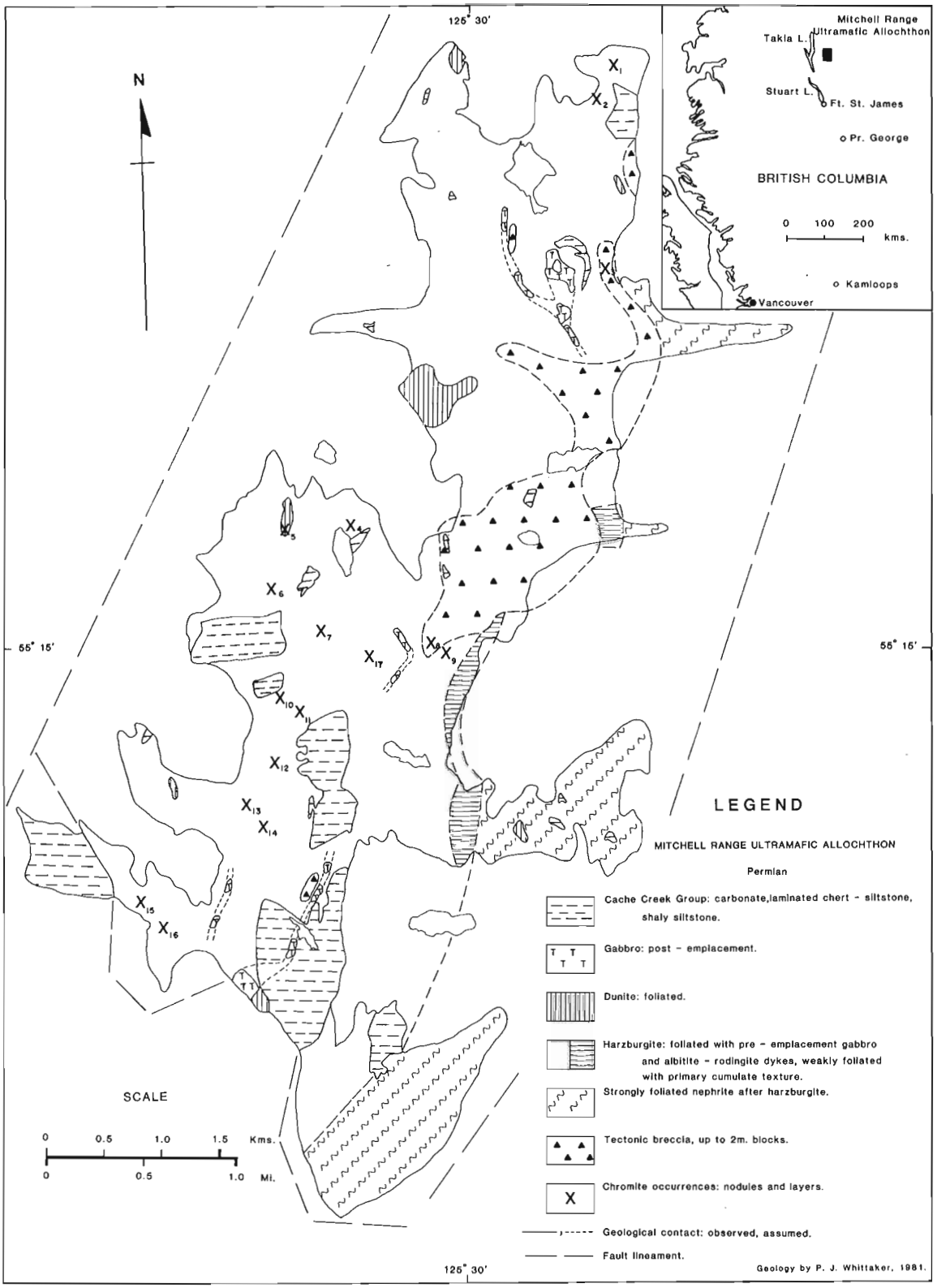

Figure 37.1. *Geology of the Mitchell Range ultramafic allochthon.*

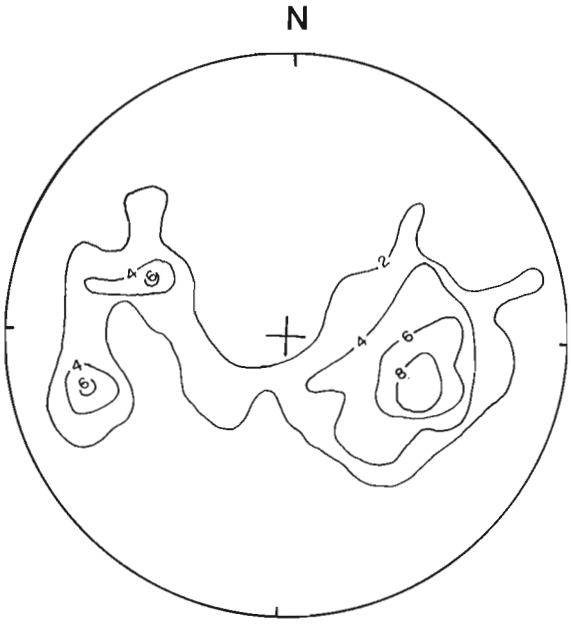

Figure 37.2. *Contoured stereo-projection of poles to foliation planes, Mitchell Range (135 poles). Contour interval at 2% per 1% area.*

On fresh surfaces it is mottled black green to black brown. Talcose patches are 0.5 to 1.5 cm in size, irregular in shape and pseudomorphic after sheared orthopyroxene. Intense shearing has locally resulted in mechanical segregation of orthopyroxene and olivine into 1.0 to 1.5 cm thick discontinuous, granular layers. More extensive shearing has resulted in the development of well rounded augen-like clots, 2-10 cm across, of coarse grained orthopyroxene that has been altered to talc. Orthopyroxene augen are isolated in a fine grained olivine-rich harzburgitic matrix and commonly have length to width ratios of 3:1.

Less intensely foliated harzburgite, in which primary cumulate texture is preserved, outcrops discontinuously in a narrow zone along the east central part of the ultramafic massif. Subhedral orthopyroxene and anhedral olivine range from medium- to coarse-grained. On the northeast ridge very coarse grained harzburgite exhibits primary magmatic, poikilitic texture, defined by orthopyroxene including olivine, both of which are anhedral.

Harzburgite hosts all but one of the observed chromite occurrences of layered and nodular aggregate to massive chromitite. Disseminated chromite occurs throughout the ultramafic rocks, forming an accessory phase, from a trace to 2.0 per cent of the rock.

Dunite

Dunite forms approximately 1 to 2 per cent of the outcrop area and is in contorted irregularly shaped patches reflecting its internal deformation. A planar dunite layer, 15 m long and 30 m thick is one exception. Dunite weathers to a smooth orange-brown surface and is waxy brownish green on fresh surfaces. It consists of fine- to medium-grained anhedral olivine and is strongly foliated so that it exhibits a finely fissile character on weathered surfaces. Chromite constitutes an accessory phase and is fine- to medium-grained and subhedral. With the exception of one chromitite layer (Table 37.1; location X_5), no anomalous concentrations of chromite were observed in dunite.

Pre-Obduction Gabbro

Segmented and deformed gabbro dykes occur predominantly in the central and southwestern parts of the Mitchell Range allochthon. They are fine grained, serpentinized and vary in thickness from 5 cm to 1.5 m. Dyke segments or boudins are up to 3 m long and are openly to isoclinally folded. Associated bone white to pastel shades of brown, green, and pink dyke-like alteration structures are rodingites with very fine grained to aphanitic equigranular texture. Contacts between harzburgite and the alteration "dykes" are sharply defined with a 1 to 3 cm aphanitic black-green selvage.

Post-Obduction Gabbro

North-trending gabbro dykes (Fig. 37.1) up to 15 m thick intrude the harzburgite in the northern, central and southern parts of the massif. The gabbro is fine- to medium-grained with subophitic to equigranular texture and is not serpentinized. Clinopyroxene is altered to amphibole, and the pale green plagioclase is probably saussuritized.

Cache Creek Group

Xenoliths of the Cache Creek Group (Fig. 37.1), the largest of which are about 1 km^2 in area, occur in the southern part of the massif with smaller xenoliths of 10 to 300 m^2 distributed to the north. The xenoliths are of carbonate rocks, siltstone with chert laminae, and shaly siltstone. Carbonate xenoliths are massive bedded and fine grained with equigranular texture. Two to 10 cm, chert nodules in the carbonate blocks are contorted with thin, 1 to 3 mm, quartz veins originating from them. Black siltstone with brecciated grey 0.5 to 2 mm chert laminae is highly contorted.

Chromite Occurrences

Chromite occurrences (Fig. 37.1; Table 37.1) are concentrated in the central and southwestern parts of the Mitchell Range allochthon with some scattered occurrences on the northeast ridge. The Bob and Simpson deposits (Table 37.1; X_3, X_{14}) described by Armstrong (1949) were examined and sampled, and 15 new occurrences are briefly described here.

Chromite occurs in disseminated, layered and nodular forms. Disseminated chromite forms an accessory phase in the ultramafic rocks with heavier disseminations forming layers and nodules. Layered and nodular chromitite (more than 75% chromite) occurs in aggregate and massive forms.

Massive chromitite exhibits a smooth outcrop surface and on fresh surfaces displays coarse hackly fracture and submetallic black-blue lustre. Layers range in thickness from 2 cm (Table 37.1; X_6) to 75 cm (Table 37.1; $X_{8,9}$) and are terminated by joints (Fig. 37.3c) and breccia zones in the host harzburgite. Contacts between chromitite layers and harzburgite are sharp and usually parallel the foliation in adjacent harzburgite.

Chromite in layers of aggregate chromitite and disseminated chromite is fine- to medium-grained. Aggregate chromitite layers (Table 37.1; $X_{16,17}$) contain greater than 75 per cent chromite. They have sharp contacts with harzburgite and internally display a fine- to medium-grained subhedral to anhedral texture. Layers have been plastically deformed into open and isoclinal folds and display pinch and swell structures. Granular trains of chromitite fragments extend from the ends of deformed layers. Brittle deformation has resulted in fragmentation of some layers into angular pieces 2 to 5 cm across which show displacements of 10 to 20 cm.

Table 37.1

Chromite occurrences in the Mitchell Range, British Columbia

Chromite Occurrence	Form	Texture	Trend	Dimensions (cm)	Host Rock
X_1	nodule	a.c.	027	8 x 4	H.
X_2	nodules (4)	a.c.	in loose talus blocks	6 x 3	H.
X_3	nodules (3)	a.c.	145	4 x 3 6 x 4 7 (diameter)	H. H. H.
	schlieren	d.c. (50%)	145/45NE	300 x 15	H.
X_4	nodules (2)	a.c.	010	12 x 3 6 x 4	H. H.
X_5	layers	a.c.	---	30 x 1-3	D.
X_6	layers	a.c.	155/45SW	200 x 2 15 x 1.5	H. H.
	nodules	m.c.	"	30 (diameter) 20 "	H. H.
X_7	nodules	a.c. m.c.	025	50 x 20 40 x 20 10 x 6 50 (diameter) 30 "	H. H. H. H. H.
X_8	layer	m.c.	122/33N	150 x 40	H. (breccia)
X_9	layer	m.c.	151/66NE	200 x 75	H.
X_{10}	nodules	m.c. & a.c.	073	10 x 3 10 x 2 5 x 2 4 x 1 12 (diameter)	H. H. H. H. H.
X_{11}	nodule	d.c. rim on m.c. core	---	130 x 100	H.
X_{12}	nodule	a.c.	121	7 x 3	H.
X_{13}	nodule	a.c.	126	4 x 2	H.
X_{14}	nodules	a.c. & m.c.	012 038 155 ---	50 x 10 40 x 15 40 x 10 8 x 3	H. H. H. H.
X_{15}	nodule	a.c.	---	10 x 4	H.
X_{16}	layers (2)	d.c.	015/V 022/66E	300 x 2-25 100 x 3	H. H.
X_{17}	layer nodules (2)	a.c. a.c.	103/47N ---	25 x 4 5 (diameter) 4 "	H. H. H.

Abbreviations:

a.c. - aggregate chromitite.
d.c. - disseminated chromite.
m.c. - massive chromitite.
H. - harzburgite (serpentinized).
D. - dunite (serpentinized).
cm - centimetres.
X - location of chromite occurrence on Figure 37.1.

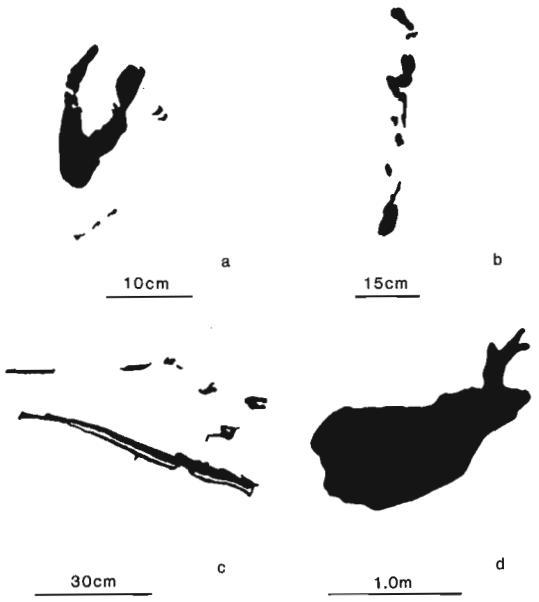

Figure 37.3. *Sketches from photographs of chromite occurrences; (a) deformed nodule, (b) deformed layer with "pull-apart" structure, (c) planar layered couplet with angular truncations, (d) deformed massive chromite nodule.*

Layers containing disseminated chromite, 2 to 25 cm thick, have responded to deformation in ductile fashion, since silicate minerals between chromite grains apparently absorbed most of the strain. Contacts between layers with disseminated chromite and harzburgite are gradational over 2 to 3 mm and are gently undulatory. Pinch and swell structures are present as well as both open and isoclinal folds. Fragments of disseminated chromite layers occur along strike from the ends of unfractured portions of layers and are separated by sheared harzburgite.

Larger, massive chromitite layers (Table 37.1; $X_{8,9}$) contain irregularly shaped patches, 3 to 10 cm across, of coarse grained aggregate chromitite. Aphanitic serpentine forms approximately 10 per cent of these patches and is interstitial to anhedral chromite grains that are about 1 cm in diameter. Contacts between coarse grained patches and massive chromitite are highly irregular.

Disseminated chromite, aggregate chromitite and massive chromitite nodules display fine- to medium-grained subhedral to anhedral textures. Nodules range in diameter from 1 cm to 1.3 m and are rounded to augen-like. Some appear to be thin (0.5 cm) selvages on shear surfaces, whereas more than 75 per cent extend to depths of at least several centimetres. Chromitite nodules exhibit massive, aggregate, and disseminated textures, with brittle fracturing more evident in increasingly massive chromitite. Larger nodules (Table 37.1; $D_{7,10,11,14}$) usually have massive chromitite cores enveloped by discontinuous rims of disseminated chromite. Rims pinch and swell from 0.5 to 5 cm in thickness and are truncated by late joints and small scale faults. Chromite and chromitite textures (massive, aggregate, and disseminated) in layered occurrences are all represented in chromite nodules. The progression from pinch and swell structures to detached segments of chromite layers, some of which are folded (Fig. 37.3a,b), suggests that chromite-chromitite nodules result from the shearing of primary chromite-chromitite layers. Assuming that this is the case, the numerous occurrences of nodules, the largest 1.3 m in size (Fig. 37.3d), and remnant chromitite layers up to 75 cm thick (Table 37.1), indicate extensive primary chromite-chromitite layering. This has since been disrupted and reoriented by ductile shearing during tectonic emplacement of the Mitchell Range allochthon.

Chromite Petrography

Chromite throughout the serpentinizd harzburgite is pale reddish brown to pale amber. Colour varies along fractures and on some grain boundaries where darkening may occur, and the chromite becomes opaque in places. This may represent oxidation of iron in chromite or more iron-rich rims since darker body colour of chromite is correlated to higher iron content. Both disseminated and massive chromite are usually fractured. In reflected light pale white alteration rims are gradational into the enclosed chromite and are possibly ferritchromite. These rims were observed in disseminated grains and along fractures in massive chromitite. Both solid and fluid inclusions occur in chromite, with the former consisting of silicate and sulphide grains. Observations to date indicate that fluid inclusions are predominantly in fine- to medium-grained, subhedral, chromite grains that form aggregate chromitite.

The fluid inclusions are spherical to lensoid and commonly exhibit a thinning or necked appearance (Fig. 37.4a). Isolated fluid inclusions are less common than those occurring in patches or in planar swarms (Whittaker and Watkinson, 1981). The latter may intersect or be subparallel (Fig. 37.4b) and are distinguished from linear inclusion trains as they can be traced through the thickness of the polished section as the focal plane is raised and lowered. Lensoid and tubular fluid inclusions in some cases exhibit shadowed ends and brighter core areas (Fig. 37.4a,b), suggesting that the fluid phase is still present and coexisting with a second fluid or vapour phase. Negative crystal cavities in chromite are euhedral and are paler than the enclosing chromite indicating that, although they were once possibly filled by a fluid or vapour, they are now empty and thus transmit more light.

Solid silicate inclusions, thought to have been olivine or pyroxene, are commonly ovoid in shape and have, in most cases, been serpentinized to lizardite. In reflected light, chromite in contact with some silicate inclusions exhibits a pale white reaction rim, suggestive of post-entrapment equilibration between silicate and chromite.

Solid sulphide inclusions are most abundant in chromite grains forming aggregate chromitite nodules and layers. In massive chromitite layers, sulphide inclusions are present in chromite grains from included patches of fine- to medium-grained aggregate chromitite. In massive chromitite, sulphide occurs as an anhedral, secondary, fracture filling phase. In individual chromite grains, pale yellowish-white and white, possibly primary, sulphide inclusions occur. Two intergrown sulphide phases (Fig. 37.4c,d) are present in contact with enclosing chromite, and no reaction rims are observed.

Sulphides also form inclusion trains (Fig. 37.4c) that have possibly developed along annealed fractures in chromite. Individual inclusions of the train can range from subhedral, possibly filling imperfect negative crystal cavities, to anhedral "blebs".

Energy dispersive spectra (EDS) collected from pale yellowish-white inclusions in chromite indicate they are Ni-Fe sulphides (pentlandite). Arsenic was encountered in one analysis, possibly indicating gersdorffite, while other analyses yielded Ni and S with a trace of Fe, possibly indicating either millerite or heazlewoodite.

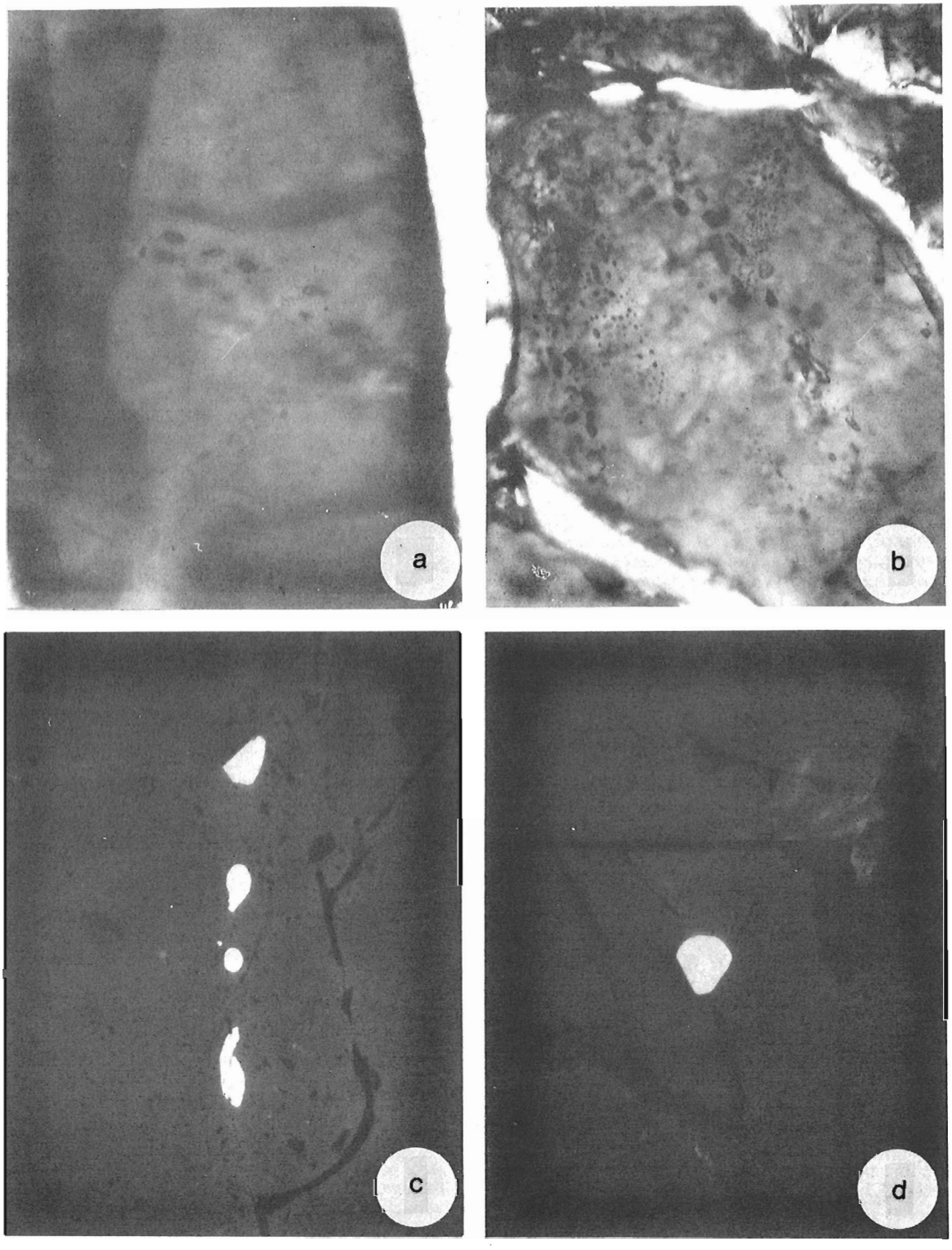

shadowed ends and bright cores indicative of the presence of both fluid and vapour phases;

(b) necked tubular fluid inclusions in intersecting planar swarms, some with bright cores;

(pentlandite) inclusion train;

(d) euhedral Ni-Fe sulphide with irregular and darker exsolution patches, possibly of NiS. Field of view across the width of all photographs is 0.3 mm.

Figure 37.4

Table 37.2

Electron Microprobe Analyses of chromite from the Mitchell Range, British Columbia

Oxide	1	2	3	4	5	6	7	8	9	10
TiO_2	0.13	0.13	0.15	0.13	0.12	0.40	0.38	0.41	0.39	0.39
Al_2O_3	11.87	11.82	11.77	11.59	11.73	22.00	21.26	21.16	21.01	22.33
Cr_2O_3	58.61	58.65	59.12	59.09	58.24	43.20	43.74	43.44	44.70	42.98
FeO_T	15.36	15.39	15.52	15.41	15.74	25.65	25.37	25.53	26.02	25.46
MgO	13.86	13.98	13.83	13.85	13.72	8.61	8.44	8.54	8.30	8.78
MnO	0.47	0.44	0.52	0.54	0.49	0.47	0.47	0.45	0.50	0.48
Total	100.30	100.41	100.89	100.60	100.04	100.33	99.65	99.52	100.92	100.43

Analyses from chromite cores and cores of fragments.

1. to 5. from W81-107, aggregate chromitite nodule.
6. to 10. from W81-157, aggregate chromitite layer.

Chromite Chemistry

Chromite from two samples of aggregate chromitite were analyzed using an electron microprobe (Table 37.2). The reported element concentrations are essentially constant for each sample, but are significantly different for the two samples. The chromite from the aggregate chromitite nodule (locality X_4) has average Cr/Cr + Al and Cr/Fe ratios of 0.83 and 3.80, respectively, whereas the ratios in the aggregate chromitite layer (locality X_6) average 0.67 and 1.70, respectively. The chromite from the chromitite layer may thus be characterized as a high iron type while that from the nodule is a high chromium type. Further analyses are planned to establish whether these compositional distinctions between textural types are consistent throughout the area. The compositions in both samples are within the range observed in chromite from cumulate dunite at Murray Ridge, 120 km to the southeast (Whittaker and Watkinson, 1981).

Summary

Extensive brecciation and penetrative ductile shear foliation within the Mitchell Range allochthon suggest extensive transport of these rocks while in a solid, but perhaps still hot, plastic state. Final movement resulted in brittle (cold) brecciation along the sole thrust plane of the ultramafic massif. Similar emplacement breccias at the soles of allochthonous ultramafic bodies occur in the Table Mountain and St. Anthony Complex ophiolites in Newfoundland (R. Talkington, personal communication, 1981).

Mitchell Range ultramafic rocks are thought to be derived from a low stratigraphic level in the ophiolite succession. This would be a level below the cumulate dunite-layered zone described at Murray Ridge (Whittaker and Watkinson, 1981).

In conclusion detailed mapping of the Mitchell Range allochthon has revealed additional chromite occurrences. Preliminary analyses indicate that both chromium and iron chromite are present in tectonized harzburgite. Additional work on chromite occurrences in other large ultramafic massifs, such as Mount Sydney-Williams and Tsitsutl Mountain to the southwest, is anticipated.

Acknowledgments

The author thanks H. Kukal for capable and cheerful field assistance and R. Talkington and Dr. D.H. Watkinson for helpful discussions. Financial support for field work from the British Columbia Department of Mines and Petroleum Resources and from the Geological Survey of Canada (Grant 203/4/81) to D.H. Watkinson is acknowledged.

References

Armstrong, J.E.
1949: Fort St. James map area, Cassiar and Coast districts, British Columbia; Geological Survey of Canada, Memoir 252, 210 p.

Little, H.W.
1947: The Ultrabasic and Associated Rocks of the Middle River Range, British Columbia; unpublished Ph.D. thesis, University of Toronto.

Paterson, I.A.
1977: The geology and evolution of the Pinchi Fault Zone at Pinchi Lake, central British Columbia; Canadian Journal of Earth Sciences, v. 14, p. 1324-1342.

Tempelman-Kluit, D.J.
1979: Transported cataclasite, ophiolite, and granodiorite in Yukon: evidence of arc-continent collision; Geological Survey of Canada, Paper 79-14, 27 p.

Whittaker, P.J. and Watkinson, D.H.
1981: Chromite in some ultramafic rocks of the Cache Creek Group, British Columbia; in Current Research, Part A, Geological Survey of Canada, Paper 81-1A, p. 349-355.

38.

MODE OF OCCURRENCE OF SECONDARY RADIONUCLIDE-BEARING MINERALS IN NATURAL ARGILLIZED ROCKS: A PRELIMINARY REPORT RELATED TO A BARRIER CLAY IN NUCLEAR WASTE DISPOSAL

Project 770061

J. Rimsaite
Economic Geology Division

Rimsaite, J., Mode of occurrence of secondary radionuclide-bearing minerals in natural argillized rocks: a preliminary report related to a barrier clay in nuclear waste disposal; in Current Research, Part A, Geological Survey of Canada, Paper 82-1A, p. 247-259, 1982.

Abstract

Three processes, that it may be activated by the emplacement of radionuclide-bearing waste are described:

1. *natural decomposition of rock-forming and associated radioactive ore and accessory minerals, such as uraninite, uranothorite, allanite, pyrochlore, apatite, monazite, xenotime, tourmaline, zircon, sulphides and carbonates;*
2. *mobilization, migration and redeposition of U, Th, REE, Zr, radiogenic lead and other elements along fractures;*
3. *neoformation of autunite, torbernite, phosphuranylite, coffinite, boltwoodite, kasolite, uranophane, bayleyite, ruthefordine, liebigite, masuyite, anglesite, wulfenite and complex unidentified U, Th, Pb, REE and Zr compounds in clays and in fractures of hydrated rock-forming minerals.*

The mobilized radionuclides can be fixed by several processes, namely by adsorption, by reacting with other ions, and by entering and capture in the interlayer of swelling mixed-layer clays and hydrated layer silicates.

These observations on the natural behaviour of radioactive and radiogenic materials can be applied in evaluating rock formations and planning preventive measures for the escape of nuclear waste from disposal sites.

Introduction

Steadily increasing consumption and generation of nuclear power creates problems with various types of radionuclide pollution and with management of uranium mill tailings and commercially generated radioactive waste (Fig. 38.1). Uranium mines, stockpiles of uranium ore, mill tailings and uranium extraction plants contain emitters of alpha, beta, and gamma radiation, namely ^{235}U, ^{238}U and ^{232}Th and their daughter products, including radium, radon, bismuth, lead and other isotopes which can become potential hazards to the environment. Damage caused by various types of radiation, accumulation dosages of various radionuclides and protective measures against radiation and radionuclide pollution have been discussed by Fleischer et al. (1975) and in DOE (1979). Considerable care is taken by mining and milling companies and by Provincial Governments to insure safe transportation and disposal of radioactive ore and of alpha-wastes. Some types of high-level nuclear power plant wastes include compactable trash and combustible wastes; concentrated liquids, wet wastes and particulate solids; failed equipment; and noncompactable, noncombustible wastes. These contain the following activation products: ^{55}Fe, ^{58}Co, ^{60}Co, ^{95}Zr in addition to major fission products: ^{3}H, ^{85}Kr, ^{90}Sr, ^{95}Nb, ^{106}Ru, ^{144}Ce, ^{137}Cs; and the actinides ^{237}Np, ^{239}Pu, ^{241}Am and others. Radionuclides released to the atmosphere during the failure of equipment include Sr, Nb, Ru, Te, Cs, Eu, Pu and Cm isotopes. Chemical, radiochemical and thermal properties of fission products at three different periods of time after removal from reactors (120 days, 1 year and 10 years) and examples of accumulation doses of various nuclides in different organs (lungs, kidney, etc.) of persons residing number of years in the vicinity of operating nuclear plants are given in DOE (1979, Tables A-6, A-38, A-39, H-3, I-1 to 12, J-5 and L-29).

Extensive research and symposia related to prevention of radionuclide pollution and planning of temporary and permanent repositories for storage and disposal of nuclear waste are being conducted by many countries (Baeyens et al., 1981; Bonne et al., 1981; Pusch, 1981; Jackson and Lim, 1981; Leech and Pearson, 1981; Langmuir and Riese, 1981; Lamire et al., 1981; and Rimsaite, 1981c,d). Figure 38.1 illustrates schematically a proposed repository for disposal of radionuclide waste in granite, a depth of at least 1 km (IAEA, 1977; DOE, 1979). The repository will protect the biological environment from radionuclide pollution by sealing the waste in rock formations to prevent, or at least delay, migration of radionuclides into the atmosphere, hydrosphere and biosphere. The proposed repository will consist of solidified nuclear waste (embedded in glass), a metal jacket, a clay barrier and a host geological formation (granite, gneiss, clay, salt domes, or ocean floor sediments). It is interesting to point out that nature utilizes similar protective measures to prevent decay and alteration of radioactive grains in some granites: Figure 38.2 shows uraninite enclosed in an inner rare-earth elements (REE)-bearing rim, followed outward by a rim consisting of hydrous silicates, which is analogous to, and serves a similar function to the clay barrier in the proposed repository. It prevents or reduces water flow into the radionuclide source and can absorb or fix radionuclides leached from the source (waste in Fig. 38.1 or radioactive grain in Fig. 38.2).

This paper summarizes and documents the mode of occurrence and behaviour of radioactive and radiogenic materials in natural argillized rocks as discussed by Rimsaite (1981d).

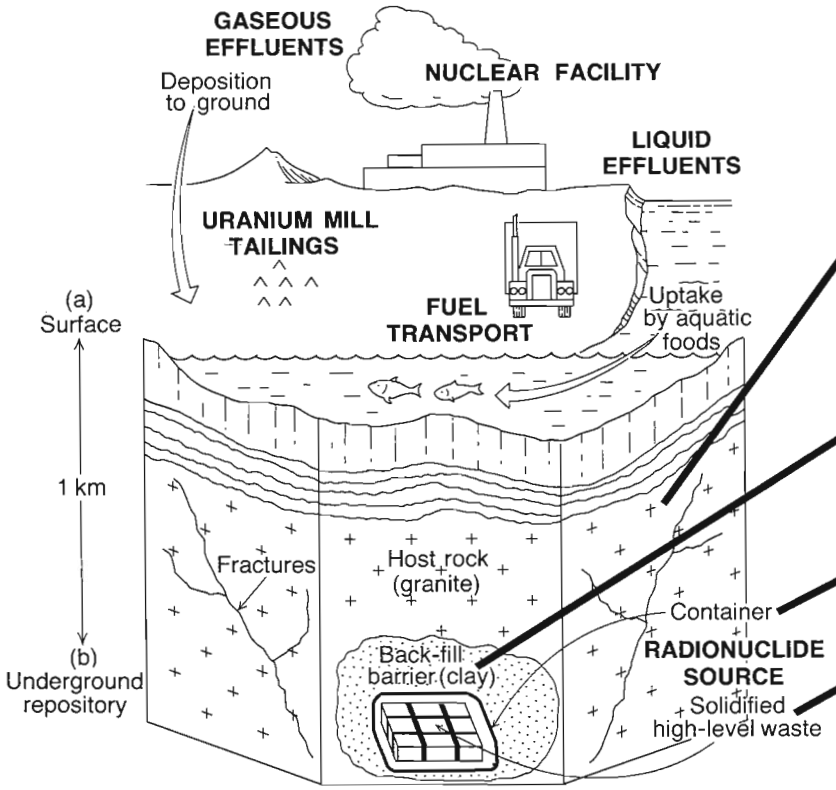

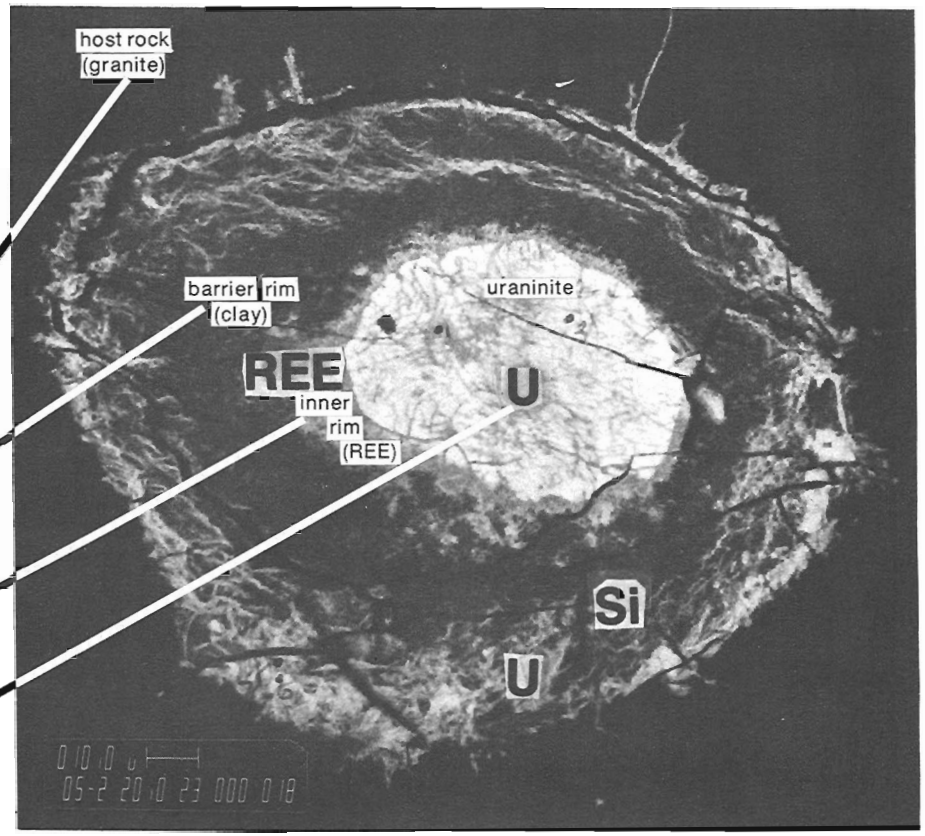

a. *Examples of possible radionuclide pollution sources at the surface include nuclear power plants, uranium mill tailings, liquid effluents and fuel transport. Gaseous effluents sink to the ground. All types of radionuclide waste can eventually contaminate water reservoirs and soil, thus creating pollution hazards to fish, cattle, human population and the whole biosphere.*

b. *The proposed repositories of nuclear waste are designed to protect man and biosphere from radionuclide contamination by placing nuclear waste underground at about 1 km depth. The proposed repository will consist of solidified waste (a possible source of radionuclide contamination), a container, back-fill barrier clay and a host rock, such as granite. The host rock should be free of open fractures.*

Figure 38.1. *Diagrammatic representation of various sources of possible radionuclide pollution and of a proposed radionuclide repository (after DOE, 1979; IAEA, 1977).*

Figure 38.2. *Backscattered electron image (BEI) of uraninite (U) which is surrounded by an inner REE-bearing rim (REE) and an outer (barrier) rim consisting of phyllosilicates (Si) in a granite host. The natural uraninite enclosed in the multiple rim has analogous construction to a proposed radionuclide repository. The rim protects uraninite from alteration and prevents (or delays) migration of uranium into the granite. Some uranium (U, white) precipitates at the periphery of the rim and only small quantities of uraniferous material fills fractures in host granite (in the upper portion of the electron micrograph). GSC 203532-H*

The following aspects, pertaining to mobilization, migration and capture of radionuclides and to hydrothermal alterations of minerals in host rocks, which may be caused by emplaced radionuclide-bearing waste, are discussed:

1. natural decomposition of rock-forming and associated radioactive ore and accessory minerals in and around uranium deposits;
2. mobilization, migration and redeposition of U, Th, REE, Zr, Pb and other elements along fractures;
3. neoformation of secondary uraniferous and Pb-bearing oxides, phosphates, carbonates, silicates, and unidentified compounds;
4. mode of fixation of mobilized radionuclides: (a) by adsorption and dissemination; (b) by reacting with other ions; and (c) by capture in the interlayer of swelling mixed-layer silicates.

Natural Decomposition of Rock-Forming and Associated Radioactive Ore and Accessory Minerals

In an around uranium deposits, granitoid rocks and metasediments are fractured and partly to completely argillized. Some fractures form as a result of radiation damage to mineral structures. Most of the irradiated minerals become amorphous ("metamict") and thus expand and induce strain cracks. Radial and circular fractures form around radioactive grains (Fig. 38.2; Rimsaite, 1967, Plate III, Fig. IX-25; 1980, Fig. 38.1, 38.3). Some fractures and interstices are sealed by metastable secondary radioactive mineral aggregates, hydrated iron oxides, sulphides and/or authigenic clays. Initial alteration of minerals commonly begins at fractures or interstices and proceeds towards the centre of a grain (Fig. 38.6b; Rimsaite, 1981a, Fig. 17.2a and 1981b, Fig. 4.3D).

Plagioclase and ferromagnesian rock-forming minerals are most susceptible to hydration and alter to fine grained phyllosilicates and oxides, such as sericite, illite, chlorite, serpentine, talc, calcite, mixed-layer phyllosilicates, montmorillonite, kaolinite, halloysite, limonite, allophane and amorphous silica (Rimsaite, 1978a, 1979b). Alkali feldspars, perthites and antiperthites alter along "zones of weakness", namely along fractures, twinning planes and around perthitic particles. Sodic feldspars are more susceptible to hydration than potassic feldspars and examples of altered plagioclase associated with fresh microcline can be seen in Figure 38.3 and in illustrations by Rimsaite (1967). Some of the ions released from altered minerals precipitate in fractures of the host (Fig. 38.3b).

Partly argillized rocks consist of resistant remnant minerals, such as quartz, potassium feldspar and some accessory minerals, set in a fine grained clay-like matrix. Such heterogeneous rocks easily crumble into sand (remnant quartz and feldspar) and clay. Figure 38.3 illustrates progressive alteration of feldspars and precipitation of mobilized ions as crusts on the altered surfaces. Small globular aggregates of halloysite (Fig. 38.3h, 38.4E) resemble crinkly and walnut-meat-shaped halloysite aggregates described by Tazaki (1979). Argillized rocks are also fractured (Fig. 38.3g, 38.8a,b) and numerous laboratory experiments have been conducted to study possibilities of reducing rock permeability by sealing fractures with authigenic clay particles. Güven and Lafon (1981) studied argillization of albite using acidic, neutral and basic aqueous solutions and used high resolution analytical spectroscopy, energy dispersive spectra and X-ray diffraction for identification of newly-formed clay particles. The results were as follows: albite fragments treated with acid solutions rapidly dissolved and remnant fragments were 'fur-coated' with kaolinite, boehmite and allophane spherules and needles; in neutral K-bearing aqueous solutions, albite particles dissolved slowly and illite flakes nucleated at the surface of albite fragments; under basic conditions, surfaces of albite particles displayed dissolution pits. The dissolution was markedly incongruent.

Under natural hydrothermal conditions, feldspar grains alter to saussurite, sericite, chlorite and allophane, whereas under weathering conditions at the surface, kaolinite, halloysite and allophane are the major alteration products.

Radioactive ore minerals such as uraninite, uranothorite, pyrochlore and allanite are susceptible to alteration under acidic and alkalic environmental conditions. Most of these minerals are heterogeneous and partly to completely altered. During the initial stage of alteration, they become heterogeneous as a result of differential diffusion of radiogenic lead, uranium, REE and other ions, and the addition of water, silica and other elements, such as iron, calcium and others. At advanced stages of alteration, primary radioactive minerals are replaced by fine grained secondary mineral aggregates, the most common being uranophane, hydrous iron oxides, and phyllosilicates (Rimsaite, 1981c,d).

Accessory minerals that are relatively resistant to hydrothermal alteration and weathering, also alter and ultimately become replaced by clays. Examples of altered and recrystallized tourmaline, zircon, monazite, xenotime and other minerals are given by Rimsaite (1978b, Fig. 6A, G, H, I, 1979a, Fig. 32-2, 1981b, Fig. 4.3, 4.4).

Sulphides are common accessory minerals in radioactive rocks. They display replacement textures and readily alter to oxides under oxidizing environmental conditions (Fig 38.4F, G, 38.6b; Rimsaite, 1981a, Fig. 17.6).

Carbonates are unstable under low pH conditions and can easily be dissolved in CO_2-bearing aqueous solutions, leaving holes and pits. Organic acids also contribute to dissolution/precipitation processes in soils and clays (Halbach et al., 1980).

Alteration of various minerals in radioactive rocks was discussed by Rimsaite (1981c).

Mobilization, Migration and Redeposition of U, Th, REE, Zr, Pb and Other Elements Along Fractures

Radioactive, radiogenic and other ions liberated from primary minerals during their alteration and replacement migrate in aqueous solutions along fractures and interstices. Under favourable environmental conditions, they can precipitate along fractures and on surfaces of altered minerals as crusts and specks (Fig. 38.3b, e, f, 4B, 5-8). Study of materials filling fractures provide information on the behaviour and associations of mobilized radionuclides and other ions.

Silica crusts are the most common; these are frequently stained red by embedded specks of iron oxide (Fig. 38.9d). Multiple crusts of silica coated by globular crusts of coffinite occur in fractures of argillized rocks (Fig. 38.9c; Rimsaite, 1978b, Fig. 7).

Colloform Fe-rich crusts coat and partly replace chalcopyrite, biotite and pyrite, and also form multiple crusts overgrowing uranophane and other U-bearing crusts (Fig. 38.4B, 6b, 8c; Rimsaite, 1979b, Fig. 2C).

Crusts of probably radiogenic galena are common in fractures of molybdenite, on altered accessory minerals and in fractures of argillized radioactive rocks (Fig. 38.4C, 6c, d; Rimsaite, 1978b, Fig. 5C).

Coatings bearing REE are common around uraninite and accessory minerals and in fractures of radioactive rocks (Fig. 38.2; Rimsaite, 1981b).

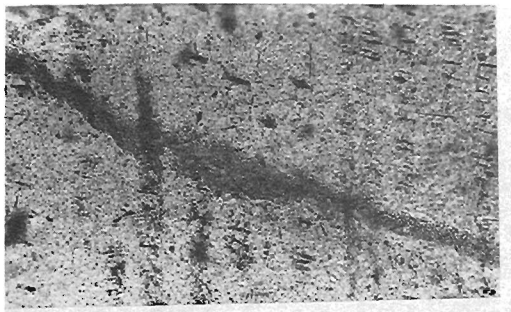

d

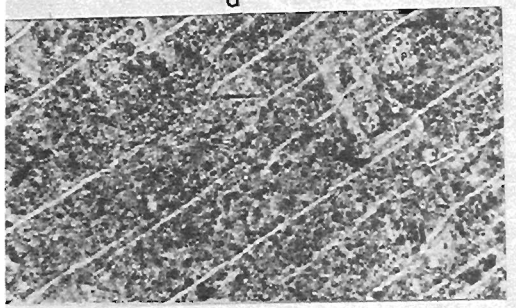

c

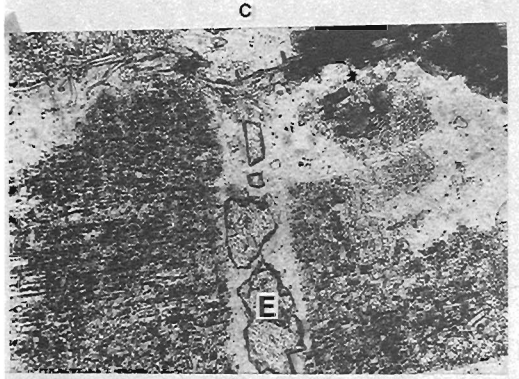

b

a

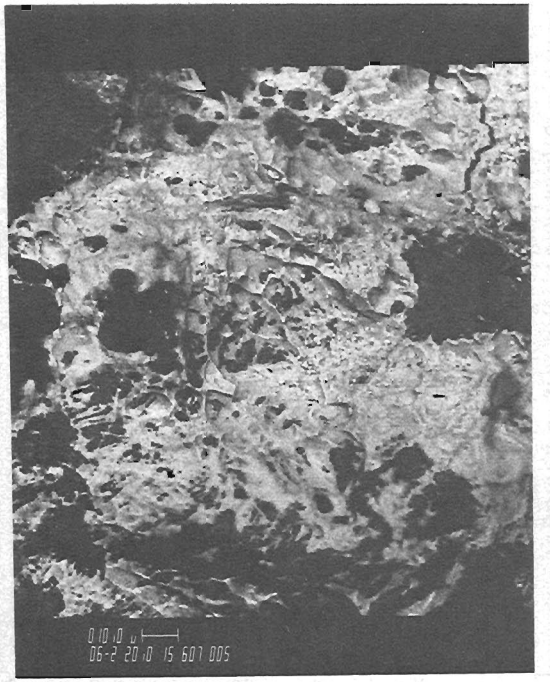

f

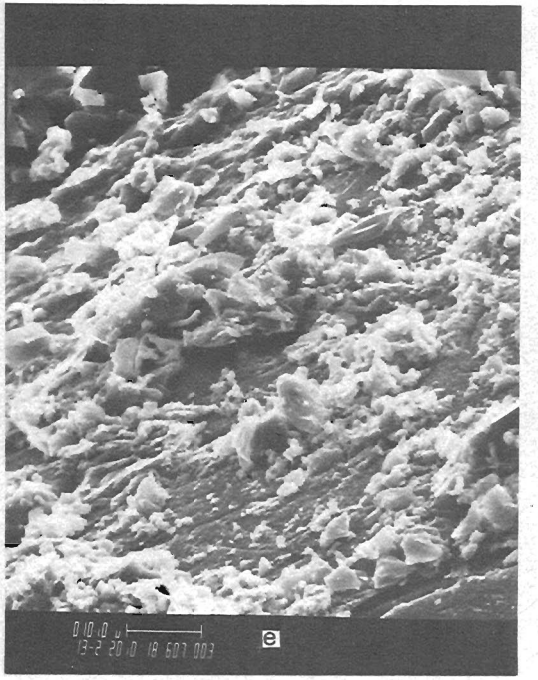

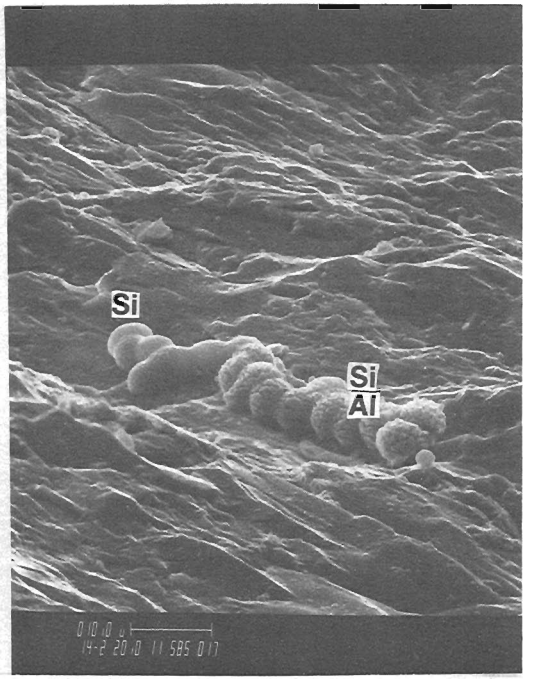

h

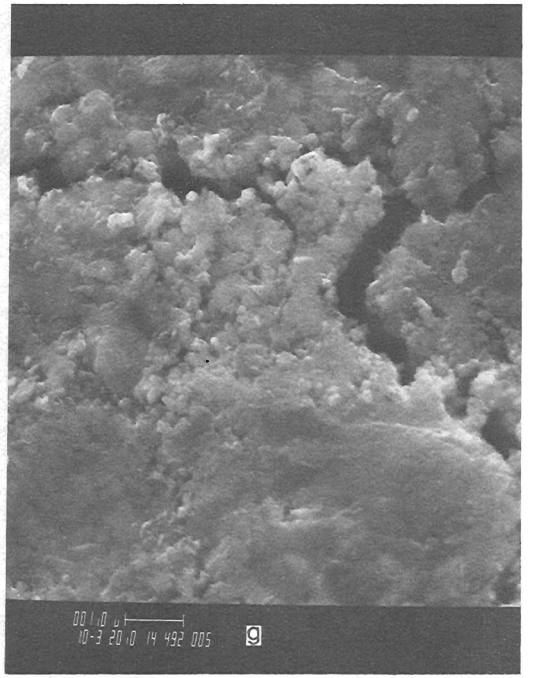

a. *Examples of different susceptibilities to alteration: plagioclase (displaying lamellar albite twinning) has argillized patches, whereas microcline (clear patches displaying albite and pericline twinning) remains fresh.*

b. *Epidote (E) crystallizes in fractures of altered feldspar. Feldspar, epidote and quartz filling fracture are fresh, whereas earlier-crystallized host feldspar is fractured and argillized.*

c. *Altered plagioclase (speckled) with white unaltered bands of potassium feldspar in lamellar antiperthite.*

d. *Alternating altered and unaltered lamellae in plagioclase crystal transected by chlorite-filled fracture.*

e. *BEI of La-, Ce-bearing crusts (white) on surface of an altered titanite.*

f. *BEI of Fe-rich crusts (grey) on microcline.*

g. *Argillized rock transversed by irregular fractures. Fractures increase permeability of the argillized rock.*

h. *Globules of halloysite (Si, Al) and of silica (Si) on surface of an altered grain.*

Figure 38.3. *Different susceptibilities of minerals to alteration results in reduced mechanical strength of the heterogeneous altered rock. Feldspars alter along fractures, along twinning planes and around perthitic particles. (a, b, c, d are photomicrographs (x100); e, f, g, h are electron scanning images) GSC 203755-K*

Fractures filled with coffinite occur in argillized radioactive rocks. Coffinite crusts are embedded in crusts of calcite, quartz, or uraniferous mixed-layer phyllosilicates (Fig. 38.5, 7, Rimsaite, 1978b, Fig. 6).

Lead-bearing kasolite-like and uranophane aggregates and mats, rimmed by narrow bands of white mica fill interstices between feldspar grains and biotite and basal fractures in biotite (Rimsaite, 1981a, Fig. 17.4, 1981b, Fig. 4.3D,E).

Fractures filled with complex unidentified uraniferous Y-, Ti-, Zr-, REE-, and Sr-bearing compounds have been found in fractures of micas. Further listing of complex radioactive materials filling fractures can be found in Rimsaite (1981a, Fig. 17.3A, G, p. 129).

Mineral aggregates filling fractures can be interfingered or tightly intergrown forming dense mats thus clogging the fracture, or they are composed of poorly cemented or loose specks that can easily be removed by percolating aqueous solutions (Fig. 38.8c; Rimsaite, 1981a, Fig. 17.7). Material filling fractures can be remobilized and react with fracture walls (Fig. 38.7).

Mobilized Pb and Mo precipitate in interstices and fractures of argillized rocks as wulfenite (Rimsaite, 1979a).

Other minerals found in fractures of argillized radioactive rocks include gypsum associated with liebigite and other uranium carbonates and barite. Barite may contain notable quantities of radium (IAEA, 1975).

Neoformation of Secondary Uraniferous and Pb-bearing Oxides, Silicates, Phosphates, Carbonates and Unidentified Compounds

In addition to their precipitation as crusts on fractures and in interstices, mobilized radioactive and radiogenic ions precipitate as secondary mineral aggregates of varied and complex chemical composition forming brightly coloured clusters and patches in argillized rocks (Fig. 38.3A, 5, 7, 8d, 9a). According to equilibria diagrams of several U^{4+} and U^{6+} species in aqueous environment, solid quadrivalent uranium compounds can exist over a broad pH range at Eh between + 300 mV and -400 mV whereas solid uranyl-bearing compounds, such as carbonates, can exist only in slightly acidic environment (about pH 6) at positive Eh between + 200 mV and + 600 mV (Halbach et al., 1980, Fig. 3).

In the argillized rocks studied, uranyl-bearing mineral aggregates are more common than minerals containing quadrivalent uranium. Secondary mineral aggregates replace primary minerals and/or crystallize in the vicinity of the source. Lead- and uranyl-bearing hydrous oxides: masuyite, becquerelite, vandendriesscheite, woelsendorfite, associated with hydrous silicates: coffinite, boltwoodite, kasolite, sklodowskite, uranophane and gummite, occur in halloysite-montmorillorite clays surrounding pitchblende deposits. The secondary radioactive mineral aggregates are metastable in a hydrous environment and are partly replaced by montmorillonite and other clays along fractures (Fig. 38.4A, 8d, Rimsaite, 1978a, Fig. 58.4). Kasolite and uranophane aggregates occur also in intergrowths with radiating REE-bearing mineral aggregates (Rimsaite, 1981a, Fig. 17.5, 6, 7).

Uraniferous solutions moving along fractures of argillized rocks can impregnate adjacent parts of the rock and form patches and bands of uraniferous mixed-layer phyllosilicates along fractures (Fig. 38.5, 7). However, in the rocks examined, the uranium content in the mixed-layer clays does not exceed more than 10 per cent of the total uranium present in the argillized rock. Much of the dissolved uranium reacts and forms complex compounds with phosphate radical. Uranyl-bearing phosphates, including autunite, torbernite,

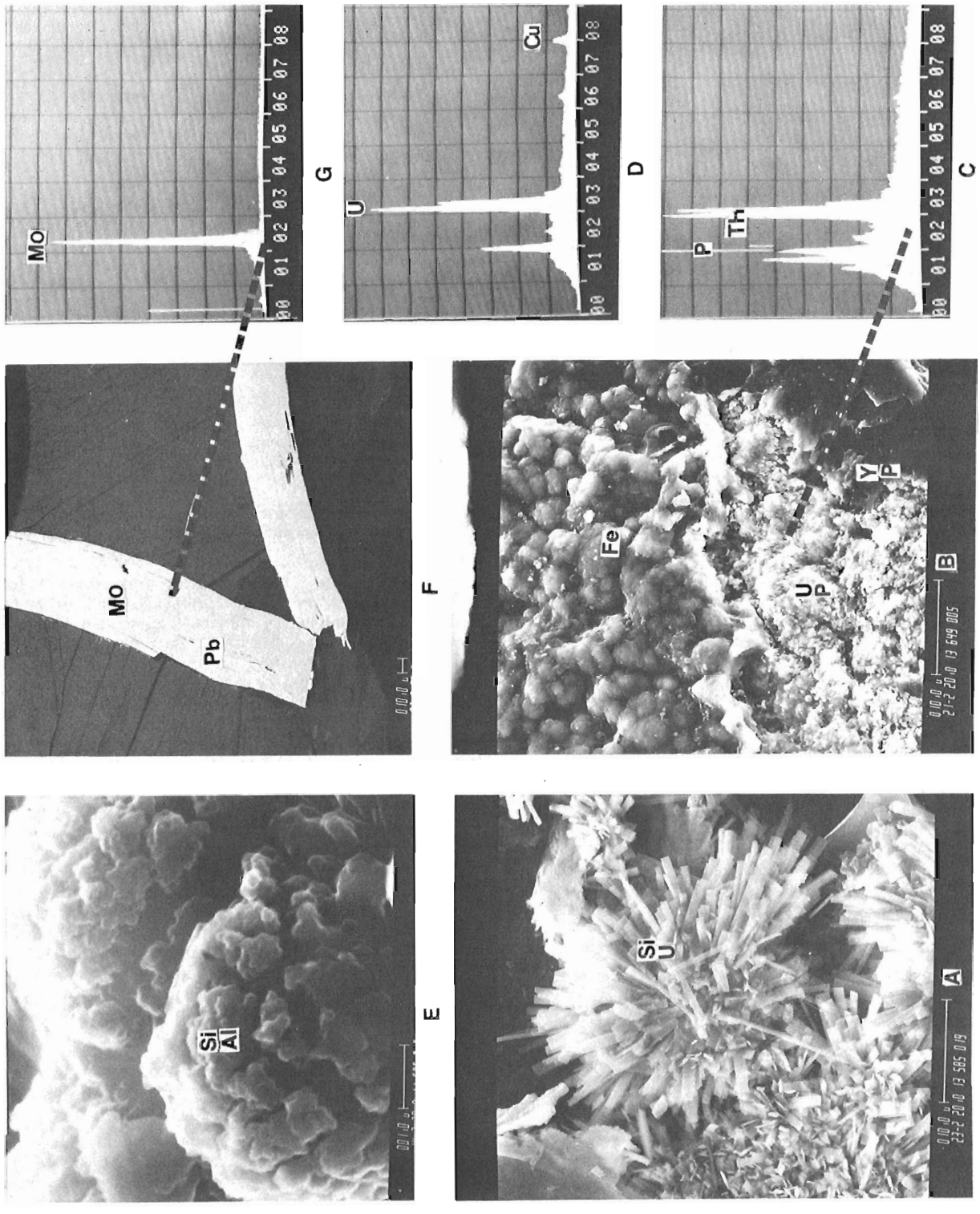
Mo
00 01 02 03 04 05 06 07 08
G
U
Cu
00 01 02 03 04 05 06 07 08
D
P
Th
00 01 02 03 04 05 06 07 08
C
MO
Pb
F
Fe
U
P
Y
P
B
Si
Al
E
Si
U
A

A. *Secondary electron image (SEI) of radiating blades of unidentified uranium silicate (Si, U) in argillized rock.*

B. *SEI of iron-rich crust (Fe) overlying radioactive P-bearing crusts (U, P) on altered xenotime (Y, P).*

C. *ED spectrum (spectrum obtained using an energy dispersive spectrometer) of radioactive P-bearing crust in Figure 38.4B.*

D. *ED spectrum of torbernite adjacent to P-bearing crust in Figure 38.4B.*

E. *Globular halloysite aggregates (Si, Al), enlarged from Figure 38.3h.*

F. *BEI of galena (Pb) that replaces molybdenite (Mo) along fractures.*

G. *ED spectrum of molybdenite.*

Figure 38.4. *Replacement textures. Examples of secondary radioactive and of clay minerals and crusts in altered granitic rocks. GSC 203577-F*

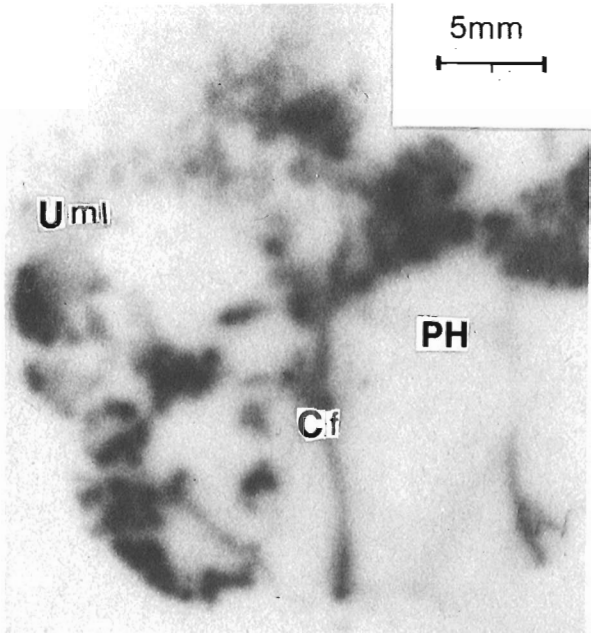

Figure 38.5. *Autoradiograph of a polished thin section of argillized rock that consists of phyllosilicates (PH), weakly-radioactive patches of uraniferous mixed-layer phyllosilicates (grey, Uml) and black U-rich patches and veinlets. Coffinite (Cf) associated with calcite and silica crystallizes in some fractures. GSC 203226-E*

phosphuranylite and sabugalite occur in fractures and interstices of altered biotite, monazite and xenotime (Fig. 38.4D; Rimsaite, 1981a). Unidentified U-, P-bearing globular aggregates occur in surface clays that contain recent organic matter (spores in Fig. 38.9a).

Radiogenic lead is partly fixed with liberated uranium in secondary hydrous oxides, silicates, and phosphates. Some of the mobilized radiogenic lead precipitates as small specks and veinlets of galena in argillized rocks and on surfaces of altered minerals. Lead can also react with sulphate radical and with molybdenum to form anglesite and wulfenite around altered U-bearing grains (Rimsaite, 1981a, Fig. 17.3D, E, F, 4C, 1979a).

Many unidentified secondary mineral aggregates containing Sr, Nb, Ce, Fe, Zr, Th, Ti, U, and P precipitate in fractures of argillized rocks and on surfaces of altered minerals. Some of these resemble hydrous carbonates and phosphates in optical properties, but are too fine grained for positive X-ray identification (Rimsaite, 1981a, p. 127; 1981b). REE-bearing carbonates: bastnaesite, parisite, synchysite, sahamalite, form important REE deposits (Olson et al., 1954; Rose, 1979). Thus, REE reacting with carbonates and phosphates could be an important mechanism to fix some of the major fission products, such as ^{144}Ce and ^{90}Sr which commonly accompanies REE.

Mode of Fixation of Mobilized Radionuclides

In their studies of acid waste liquids from uranium mining and milling, Langmuir and Riese (1981) established a number of environmental conditions for the precipitation of dissolved elements, such as Fe, Ra, Th, Po, U, Co and other ions in clay liners. They found that pH increases as acid waste liquids seep through the clay liners and, with increasing pH, established the following precipitation sequence: ferric oxyhydroxides precipitate near pH 2, followed by Mn and Al oxyhydroxides between pH 3-4; most of ^{226}Ra coprecipitates

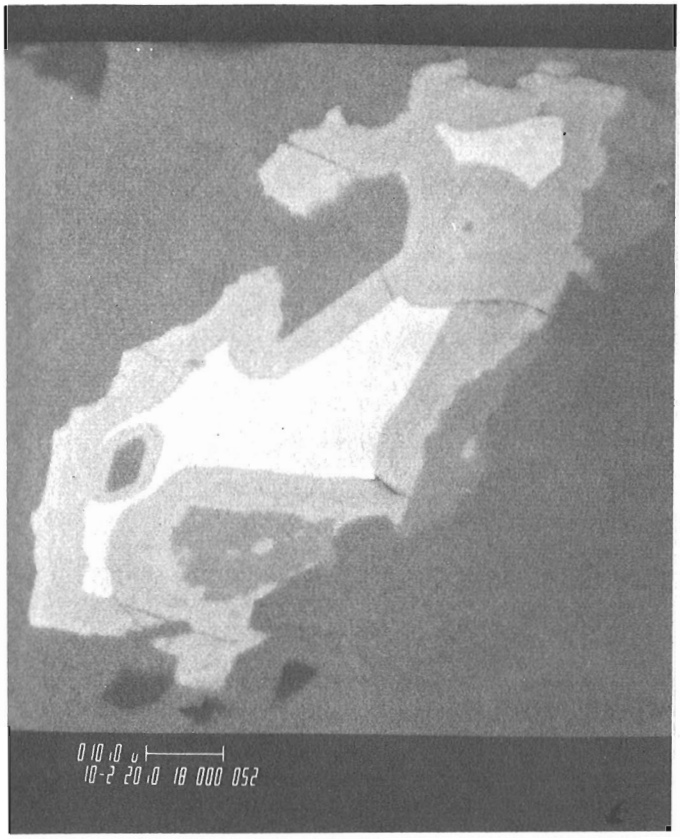
0 10 20 u
10-2 20 10 18 000 052

b

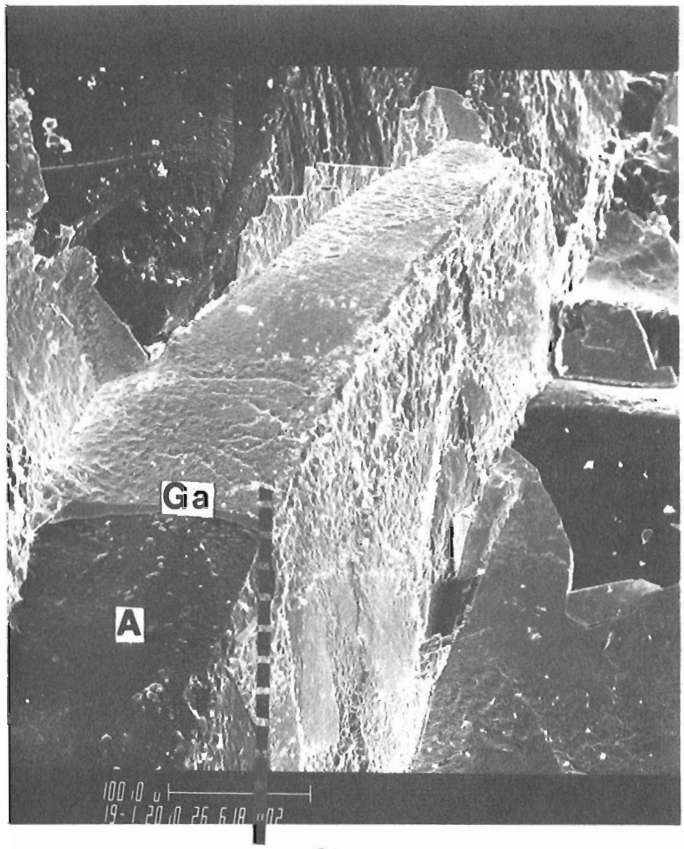
Ga
A
100 10 u
19-1 20 10 26 6 18 002

c

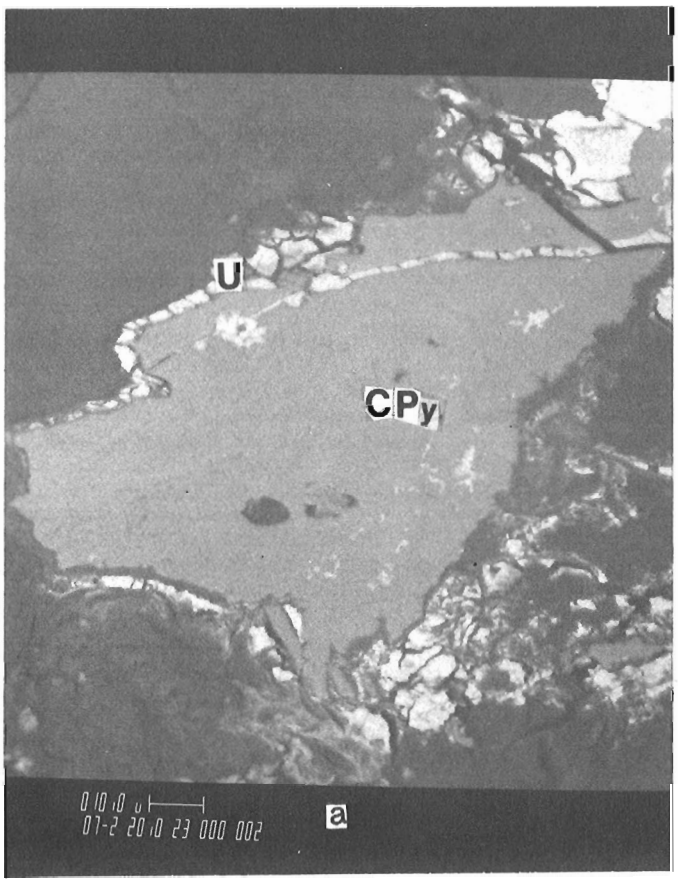
U
CPy
0 10 20 u
07-2 20 10 23 000 002
a

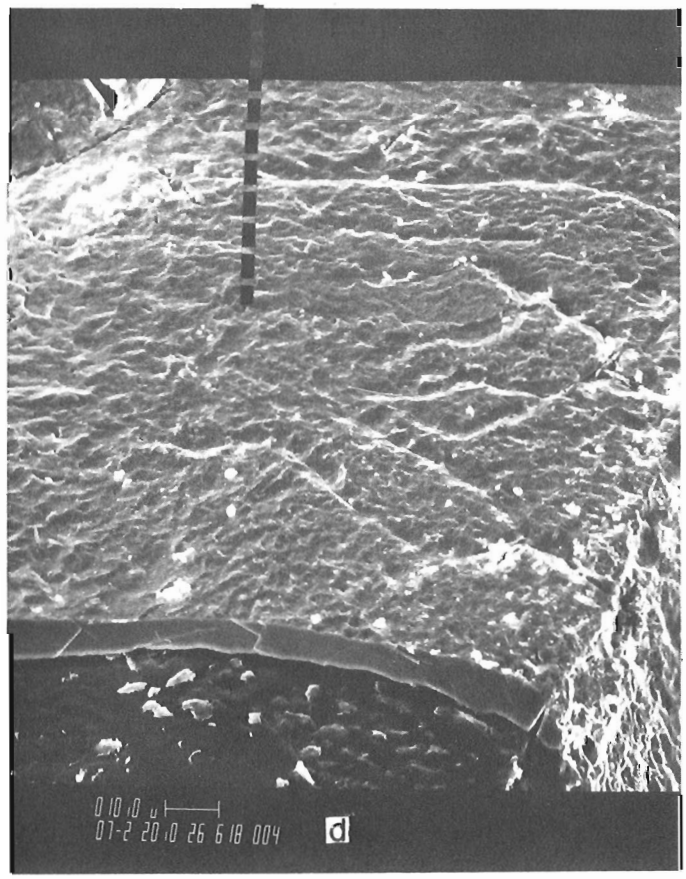
0 10 20 u
07-2 20 10 26 6 18 004
d

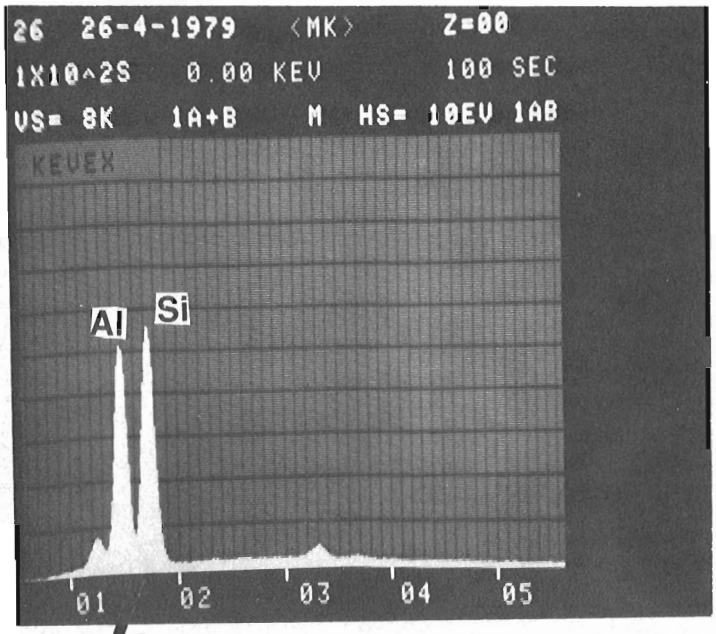

B

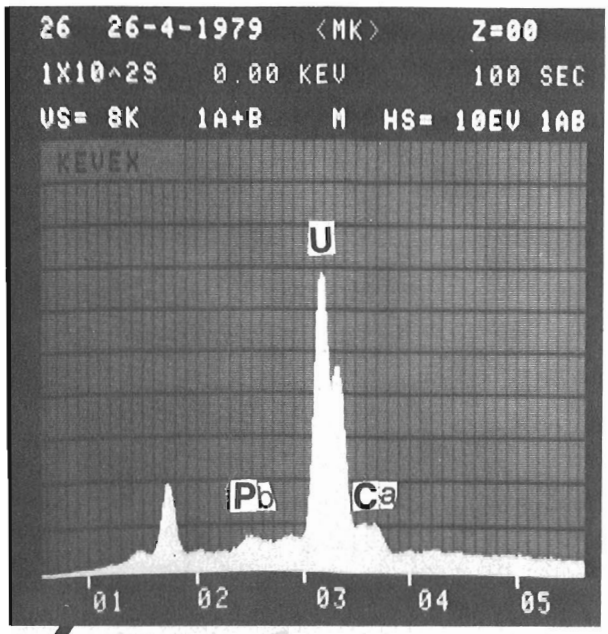

E

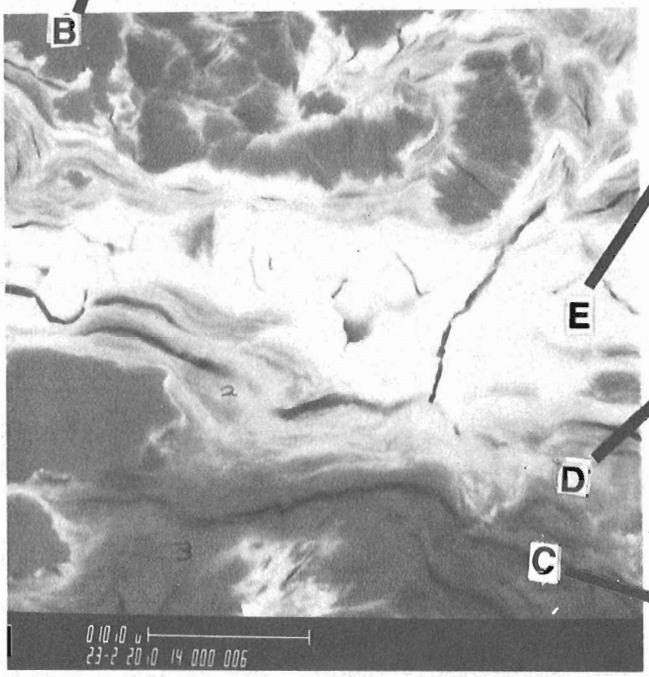

A

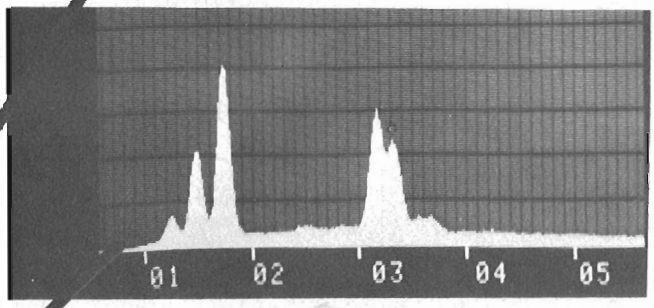

D

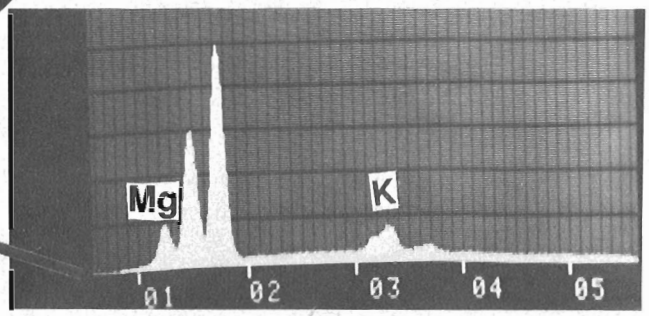

C

Figure 38.6. *(opposite)*

Examples of precipitation and adsorption of radioactive and radiogenic elements and oxidation of sulphides. Crusts on altered minerals. (BEI). GSC 203755-H

a. Uraniferous crusts (white, U) on chalcopyrite fragment (grey, CPy).

b. Calcopyrite (white fragments) corroded and partly replaced by Fe oxide rims (grey).

c. Crusts of galena (Ga) on altered allanite (A).

d. Edge of galena crust on altered and speckled allanite (enlarged from Fig. 38.6c).

Figure 38.7. *(above)*

Migration and redeposition of radionuclides in fractures. Impregnation of argillized rocks adjacent to fractures an fixation of mobilized uranium in mixed-layer phyllosilicates. GSC 203414-P

A. BEI of fracture filled with coffinite (E). The fracture is enclosed in uraniferous phyllosilicates (D) and K-bearing montmorillonite (C) in metasediment altered to halloysite (B).

B. ED spectrum of halloysite (peaks of Al and Si of about equal intensity).

C. ED spectrum of montmorillonite clay adjacent to fracture (peaks of Mg< Al< Si>K>Ca).

D. ED spectrum of uraniferous phyllosilicates (peaks of Mg< Al< Si>U>K>Ca).

E. ED spectrum of coffinite (Prominent peaks of U and Si and traces of Pb and Ca). XRD analyses of glycol-treated and heated mineral concentrates from this specimen are given by Rimsaite (1978a).

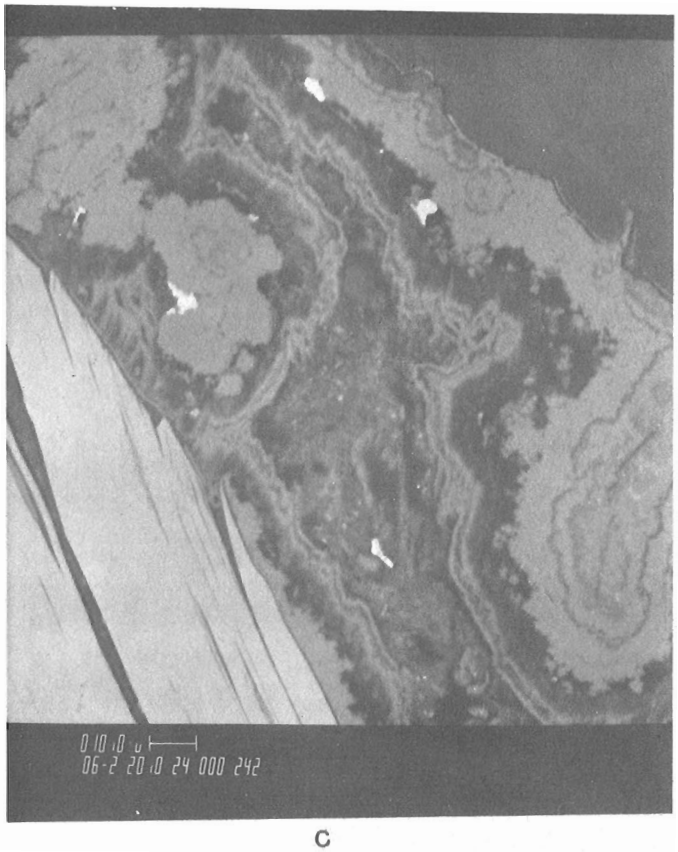
0 10 20 μ
06-2 20 0 24 000 242

c

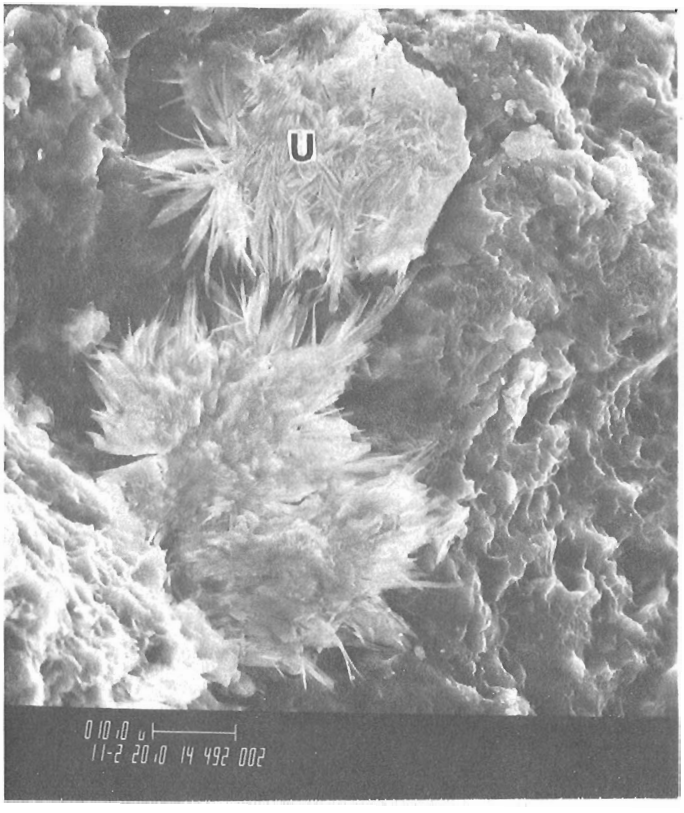
U
0 10 20 μ
11-2 20 0 14 492 002

d

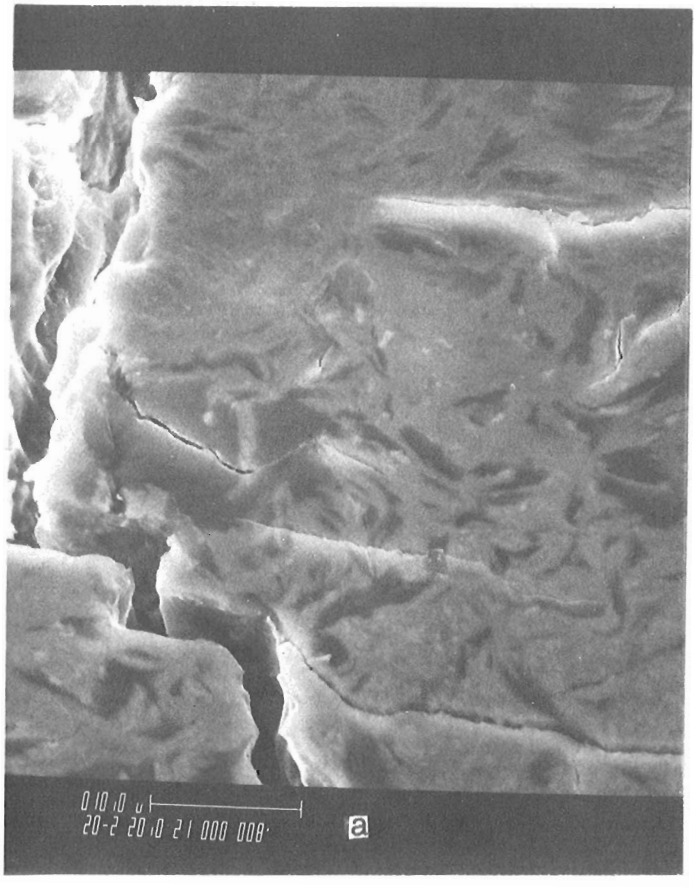
0 10 20 μ
20-2 20 0 21 000 008
a

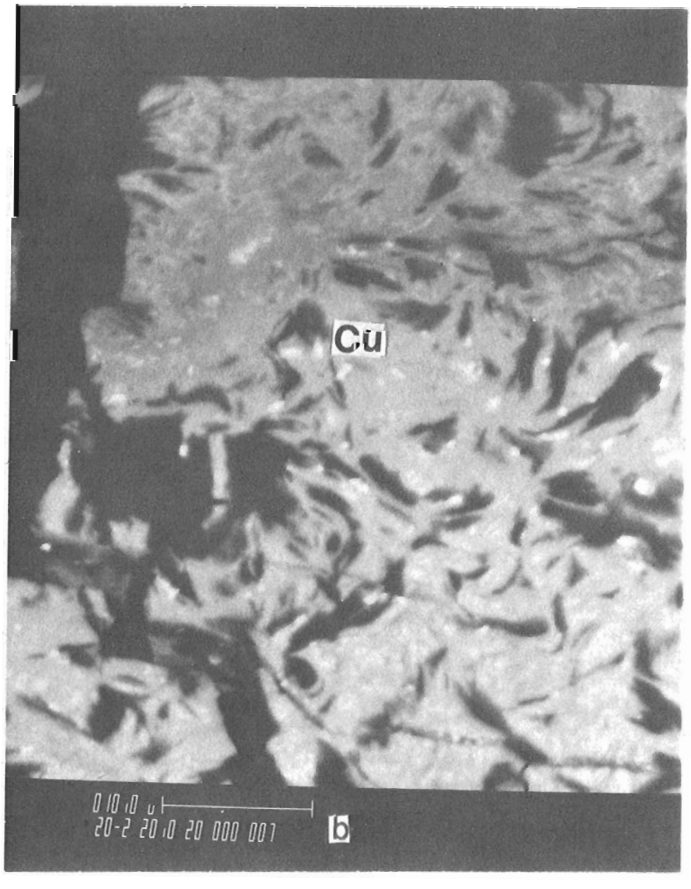
Cu
0 10 20 μ
20-2 20 0 20 000 007
b

a. SEI of a fractured argillized rock.

b. BEI of the same fractured argillized rock as in Figure 38.8a. Here fractures are less prominent, but disseminated copper sulphides (white specks, Cu) can be seen more clearly than on SEI in Figure 38.8a.

c. BEI of biotite fragment (left) that is overgrown by Fe-rich colloform crusts containing disseminated U-rich specks (white).

d. BEI of radiating uranophane aggregates (U) in argillized rocks.

Figure 38.8. *(opposite) Examples of fractured argillized rocks, of secondary radioactive mineral aggregates and of colloform crusts. GSC 203755-F*

with amorphous silica, and ^{210}Pb coprecipitates with sulphate minerals; above pH 3-4, ^{230}Th and ^{238}U are removed from the liquids. They concluded that the neutralizing capacity of clays increases with their calcite content with confirms observations on fixation of various mobilized ions in natural occurrences discussed in the previous sections.

(a) Fixation by Adsorption. In natural argillized rocks, mobilized radionuclide ions are apparently adsorbed on colloform crusts and on surfaces of altered grains, and, with increasing supply of U, Pb and S can grow further as U-bearing and PbS crusts (Fig. 38.6a, c, d, 8a, b c) and as U-bearing crusts on hydrocarbons (Rimsaite, 1978b, Fig. 5).

(b) Fixation by Reaction With Other Ions. In argillized rocks, diverse secondary radioactive compounds form apparently from solutions at the expense of ions mobilized from altered primary minerals: oxides, carbonates, phosphates, sulphides and silicates, described in previous sections. The secondary radionuclide-bearing minerals are metastable under changing natural environmental conditions. They adapt to the environmental changes by dissolution and reprecipitation in crystal forms that are stable in the existing environment (Rimsaite, 1979a). Thus, in a fresh radioactive granite, uraninite is the stable U-mineral, whereas in the altered granite, uraninite alters to hydrous minerals.

(c) Fixation by Capture in the Interlayer of Swelling Mixed-Layer Phyllosilicates. Uraniferous mixed-layer phyllosilicates are relatively rare because they are unstable in natural hydrous environments and ultimately alter to halloysite and montmorillonite clays, whereby uranium is removed by aqueous solutions (Rimsaite 1978a, p. 313). Also with increasing temperature under dehydration conditions, the montmorillonite interlayers that apparently hold uranium collapse and the released uranium is reprecipitated as coffinite or uraninite. Examples of uraniferous phyllosilicates associated with coffinite are given by Rimsaite (1978b).

Summary and Conclusions

On the basis of my studies, I have summarized the mode of occurrence and behaviour of radionuclides in argillized rocks in and around uranium deposits and suggest that the following features pertaining to preventive pollution measures at the proposed repositories of nuclear waste merit special consideration.

Mode of Occurrence. In argillized rocks, radioactive and radiogenic substances and elements similar in their behaviour to major fission products and alpha-wastes, such as daughter products of U, Th, Pb, REE, Bi, Fe, Mo, Nb, Sn, Sr, Zr and others, commonly occur in discrete grains, mineral aggregates and crusts in fractures, voids and interstices. They are metastable and display erratic distribution in argillized rocks. Only a small proportion of these ions is fixed in structure of mixed-layer phyllosilicates.

Secondary Minerals. The above elements form secondary mineral aggregates that belong to the following classes: native metals (Bi in altered pyrochlore); hydrated oxides (Fe, Pb, U, Th); sulphides (Bi, Fe, Mo, Pb, Sn); carbonates (U, REE, Sr); molybdates (Mo, Pb); phosphates (U, REE); silicates (U, Th, Pb, REE, Cs, Sr); and sulphates (Ba, Pb, U).

Changing Environmental Conditions and Migration of Radionuclides. Unlike the controlled environment in laboratory experiments, natural environmental conditions change in space and time. Because of changing pH, Eh and flow rate of aqueous solutions in the natural environment, the above secondary alteration products are metastable. The radionuclides and associated ions can be repeatedly mobilized, transported in aqueous solutions and reprecipitated in the same or other mineralogical forms away from the original site. Mineral associations in fractures suggest that radionuclides migrate along fractures of argillized rocks accompanied by iron, carbonates, sulphides, sulphates and silicates. The distance of transport depends on the hydrologic gradient and on the nature of aqueous solutions and on the physico-chemical environment.

Studies of natural radioactive occurrences suggest that migration rates of radionuclides along fractures in aqueous solutions exceed their migration by diffusion.

Acknowledgments

The author thanks D.A. Walker of the Central Laboratories and Technical Services Division for his assistance with microbeam studies and for providing electron micrographs and energy dispersive spectra. I also thank the staff of the Photographic Services Section of Geological Information Division for preparation of the autoradiograph and for the photographic plates and R.W. Boyle for his constructive criticism of the manuscript.

References

Baeyens, B., Maes, A., and Cremers, A.
1981: Geological storage of radioactive waste: 1. Cesium fixation in Boom clay; Seventh International Clay Conference, 1981, Abstracts, p. 36.

Bonne, A.A., Heremans, R.H., and Henrion, P.N.
1981: Investigations on the Boom clay, a candidate host rock for final disposal of high level solid waste; Seventh International Clay Conference, 1981, Abstracts, p. 49-50.

DOE
1979: Management of Commercially Generated Radioactive Waste; DOE/EIS-0046-D, Volume 2 of 2. United States of America, Department of Energy, Appendices A to T.

Fleischer, R.L., Price, P.B., and Walker, R.M.
1975: Nuclear Tracks in Solids; University of California Press, 605 p.

Guven, N. and Lafon, G.M.
1981: Experimental studies on hydrothermal alteration of albite to clays; Seventh International Clay Conference, 1981, Abstracts, p. 114-115.

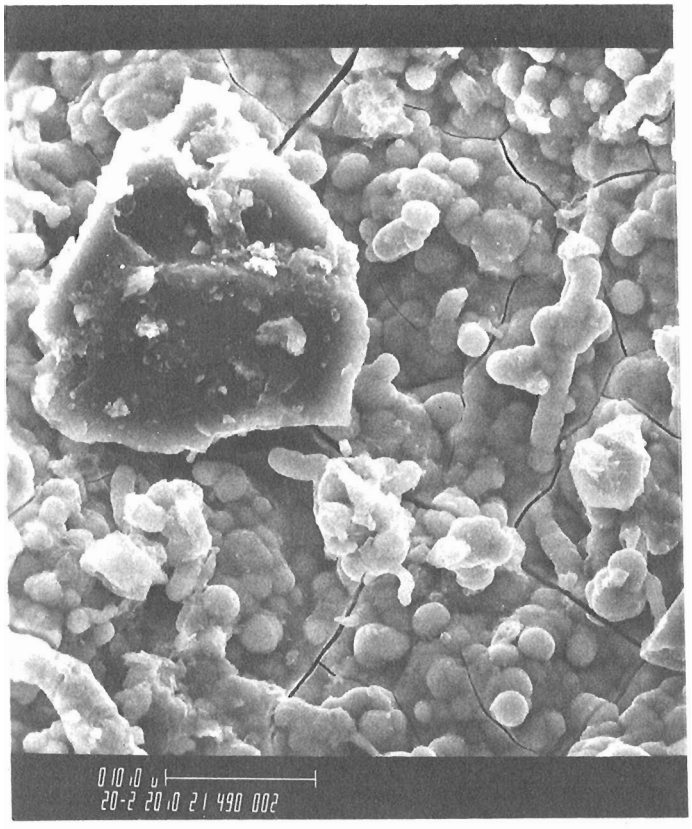
0 10.0 µ
20-2 20.0 21 490 002

c

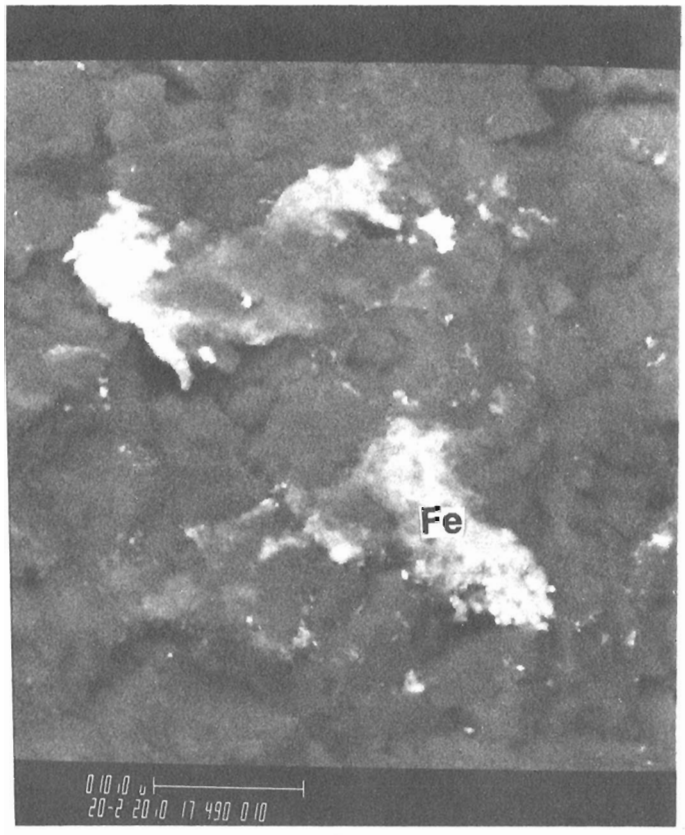
Fe
0 10.0 µ
20-2 20.0 17 490 010

d

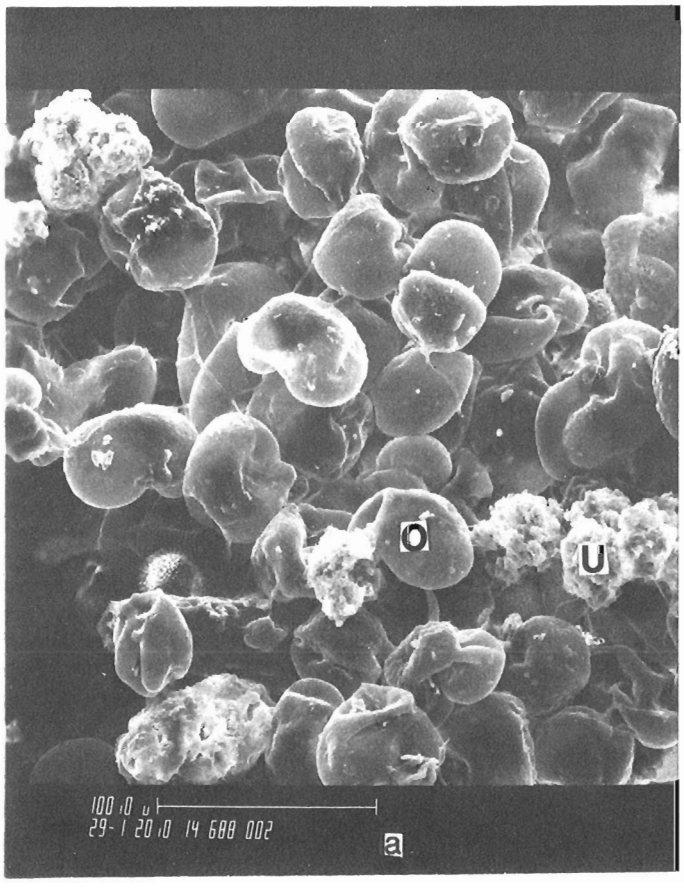
O
U
100.0 µ
29-1 20.0 14 688 002
a

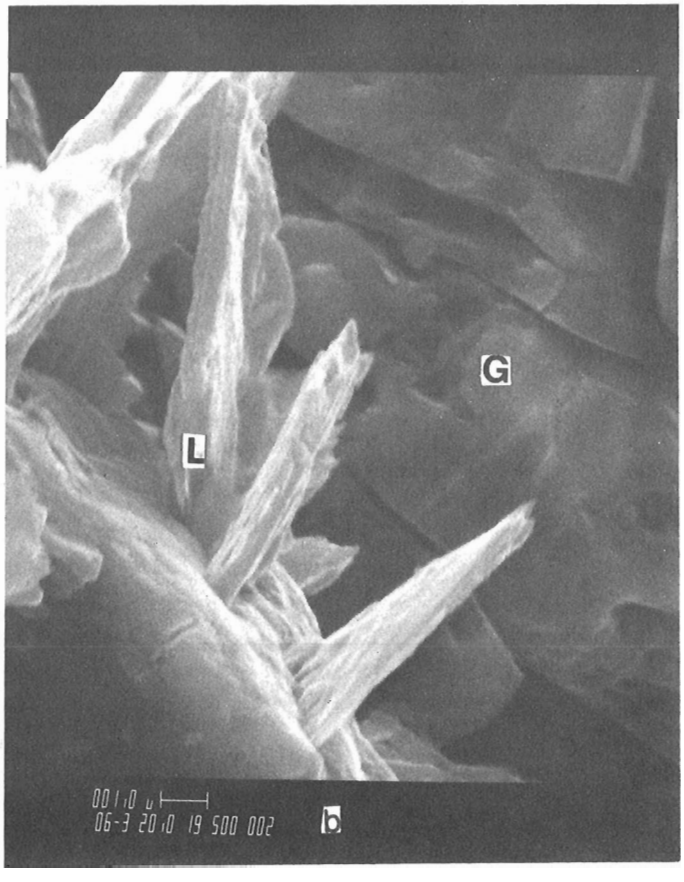
G
L
001.0 µ
06-3 20.0 19 500 002
b

a. *BEI of U-bearing phosphate globules (U) associated with organic matter (spores, O) in a surface soil overlying radioactive rocks.*

b. *BEI of liebigite crystals (L) in a veinlet filled with gypsum (G) in argillized rock overlying pitchblende deposit.*

c. *BEI of globular uranophane coatings on fractures of argillized rocks.*

d. *BEI of red silica crust with disseminated specks of iron oxides (Fe).*

Figure 38.9. *(opposite) Examples of crusts of a U-bearing mineral aggregates associated with recent organic material. GSC 203755-B*

Halbach, P., Borstel, von D., and Gundemann, K.-H.
1980: The uptake of uranium by organic substances in a peat bog environment on a granitic bedrock; Chemical Geology, vol. 29, No. 1/2, p. 117-138.

IAEA
1975: Radon in Uranium Mining; Panel Proceedings Series STI/Pbb/391, International Atomic Energy Agency, Vienna, 175 p.

1977: Site selection factors for repositories of solid high-level and alpha-bearing wastes in geological formations; International Atomic Energy Agency, Vienna, Technical Reports Series No. 177, 62 .

Jackson, M.L. and Lim, C.H.
1981: The role of clay minerals in environmental science; Seventh International Clay Conference, 1981, Abstracts, p. 13-14.

Lamire, R.J., Goodwin, B.W., and Paquette, J.
1981: The behaviour of uranium and plutonium in groundwater to 200°C – implications for geological disposal of nuclear fuel wastes; Geological Association of Canada, Mineralogical Association of Canada, Canadian Geophysical Union, Joint Annual Meeting, 1981, Abstracts, Volume 6, p. A-34.

Langmuir, D. and Riese, A.C.
1981: Geological modelling of radionuclides and chemical species transport in subsurface waters: application to uranium mill tailings; Geological Association of Canada, Mineralogical Association of Canada, Canadian Geophysical Union, Joint Annual Meeting, 1981, Abstracts Volume 6, p. A-34.

Leech, R.W. and Pearson, R.
1981: Hydrogeological research in support of the Canadian nuclear fuel waste management program: the Atikokan, North-West Ontario, research area; Geological Association of Canada, Mineralogical Association of Canada, Canadian Geophysical Union, Joint Annual Meeting, 1981, Abstracts Volume 6, p. A-34.

Olson, J.C., Shawe, D.R., Pray, L.C., and Sharp, W.N.
1954: Rare-earth mineral deposits of the Mountain Pass district, San Bernardino County, California; United States of America, Geological Survey, Professional Paper 261, 58 p.

Pusch, R.
1981: The paths and rate of flow of water through highly compacted bentonite; International Clay Conference, 1981, Abstracts, p. 238-239.

Rimsaite, J.
1967: Optical heterogeneity of feldspars observed in diverse Canadian rocks; Schweizerische Mineralogische and Petrographische Mitteilungen, v. 47/1, p. 61-74.

1978a: Layer silicates and clays in the Rabbit Lake uranium deposit, Saskatchewan; in Current Research, Part A, Geological Survey of Canada, Paper 78-1A, p. 303-315.

1978b: Application of mineralogy to the study of multistage uranium mineralization in remobilized uranium deposits, Saskatchewan; Mineralogical Association of Canada, Short Course in Uranium Deposits, Toronto, Ontario, p. 403-430.

1979a: Petrology of basement rocks at the Rabbit Lake deposit and progressive alteration of pitchblende in an oxidation zone of uranium deposits in Saskatchewan; in Current Research, Part B, Geological Survey of Canada, Paper 79-1B, p. 281-299.

1979b: Natural amorphous materials, their origin and identification procedures; in Development in Sedimentology 27; M.M. Mortland, and V.C. Farmer, ed., International Clay Conference, 1978, p. 567-576.

1980: Mineralogy of radioactive occurrences in the Grenville structural province, Bancroft area, Ontario: a progress report; in Current Research, Part A, Geological Survey of Canada, Paper 80-1A, p. 253-264.

1981a: Petrochemical and mineralogical evolution of radioactive rocks in the Baie-Johan-Beetz area, Québec: a preliminary report; in Current Research, Part A, Geological Survey of Canada, Paper 81-1A, p. 115-131.

1981b: Isotope, scanning electron microscope, and energy dispersive spectrometer studies of heterogeneous zircons from radioactive granites in the Grenville structural province, Quebec and Ontario; in Current Research, Part B, Geological Survey of Canada, Paper 81-1B, p. 25-35.

1981c: Mobilization and migration of uranium and rare-earth elements (REE) in natural environments in relation to site selection factors for repositories of radionuclide wastes; Geological Association of Canada, Mineralogical Association of Canada, Canadian Geophysical Union, Joint Annual Meeting, 1981, Abstracts Volume 6, p. A-49.

1981d: Neoformation of secondary radioactive minerals resulting from natural interaction of primary U, Th, REE minerals, water and host rocks; Seventh International Clay Conference, 1981, p. 245.

Rose, E.R.
1979: Rare-earth prospects in Canada; Canadian Mining Metallurgical Bulletin, v. 72, no. 805, p. 110-116.

Tazaki, K.
1979: Micromorphology of halloysite produced by weathering of plagioclase in volcanic ash; in Development in Sedimentology 27, M.M. Mortland, and V.C. Farmer, ed., International Clay Conference, 1978, p. 415-422.

39.

LITHOLOGICAL AND STRUCTURAL SETTING OF URANIFEROUS PEGMATITES NEAR MEKOOS, MONT-LAURIER, QUEBEC

Project 750058

M. Henderson
Economic Geology Division

Henderson, M., Lithological and structural setting of uraniferous pegmatites near Mekoos, Mont-Laurier, Quebec; in Current Research, Part A, Geological Survey of Canada, Paper 82-1A, p. 261-264, 1982.

Abstract

Lithologies and structural elements were studied to determine the factors controlling the emplacement of uraniferous pegmatites. It is concluded that field evidence confirms the hypothesis of partial melting of metasediments and pre- or synkinematic emplacement of the pegmatite.

Introduction

In order to find out if the occurrence of uraniferous pegmatites of the Mont-Laurier area had structural or stratigraphic control, the lithologies and structural features of the paragneisses and the associated pegmatites near Mekoos (Fig. 39.1) were studied in July 1980.

The dense vegetation and poor rock exposures never permitted the tracing of contacts along strike and only allowed for rock type identification and structural fabric measurements.

The geological map (Fig. 39.2) is an interpretative simplification of the geological and structural data gathered in the field. The rocks are predominently migmatitic. Pegmatites are not shown on the map because their ubiquitous occurrence only confuses the picture. The biotite and garnet-sillimanite paragneisses do not outcrop sufficiently to be mapped separately and are included on the map with the calc-silicate and marble unit with which they are associated.

Previous Work

Tremblay (1974) studied the mineralogy and geochemistry of the radioactive pegmatites of the Mont Laurier area. She determined that all important uranium showings are restricted to the white pegmatites. Her data also indicate that these pegmatites result from partial melting of the paragneisses.

Kish (1977) published a preliminary report and map at 1:20 000 scale covering the Patibre Lake area. In a tentative geological column he assigned the quartz-feldspar-biotite-hornblende gneisses of the Patibre Formation to the pre-Grenville Group and the overlying paragneisses of the La Force Formation to the Grenville Group.

Rimsaite (1978) described the mineralogy of selected specimens from radioactive occurrences in the Grenville Province in Ontario and Quebec. Amongst the specimens studied are gneiss of the Patibre Formation, paragneiss of the La Force Formation, and white pegmatite.

Description of Lithologies

In this report the formational names Patibre Formation and La Force Formation proposed by Kish (1977) are used. On the basis of its more complex deformation, it appears that the migmatitic gneiss of the Patibre Formation is the oldest rock type in the area. The poor exposure and structural complexity did not permit a detailed stratigraphy of the paragneiss succession of the La Force Formation; the order in which its units are described, therefore, has no stratigraphic meaning.

Patibre Formation

Migmatitic gneiss occurs in the southwest corner of the area mapped. It corresponds to Kish's quartz-feldspar-biotite-hornblende gneiss (Patibre Formation). It is pink or buff in hand specimen and fine grained. Microscopic study shows the neosome to be composed of 30% microcline, 30% plagioclase (An_{32}), 30% quartz, with biotite, chlorite, a little sphene and apatite forming the other 10% of the rock. Rimsaite (1978) described the paleosome or melanocratic portion of the migmatite; it consists of green to pale brown hornblende intergrown with partly altered biotite, blue-green

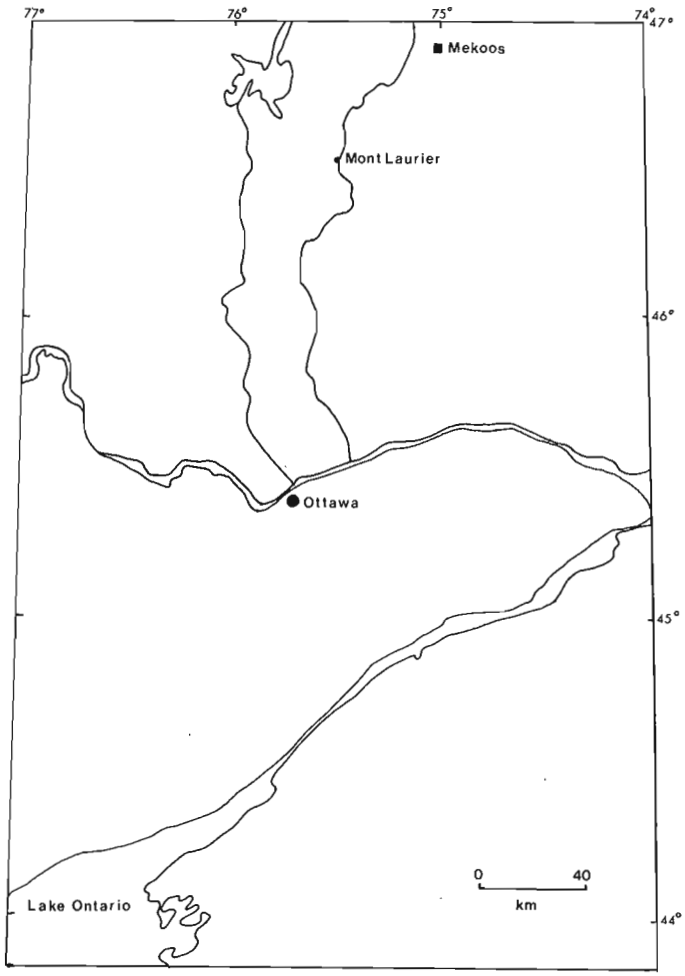

Figure 39.1. *Location of the Mekoos area, Quebec.*

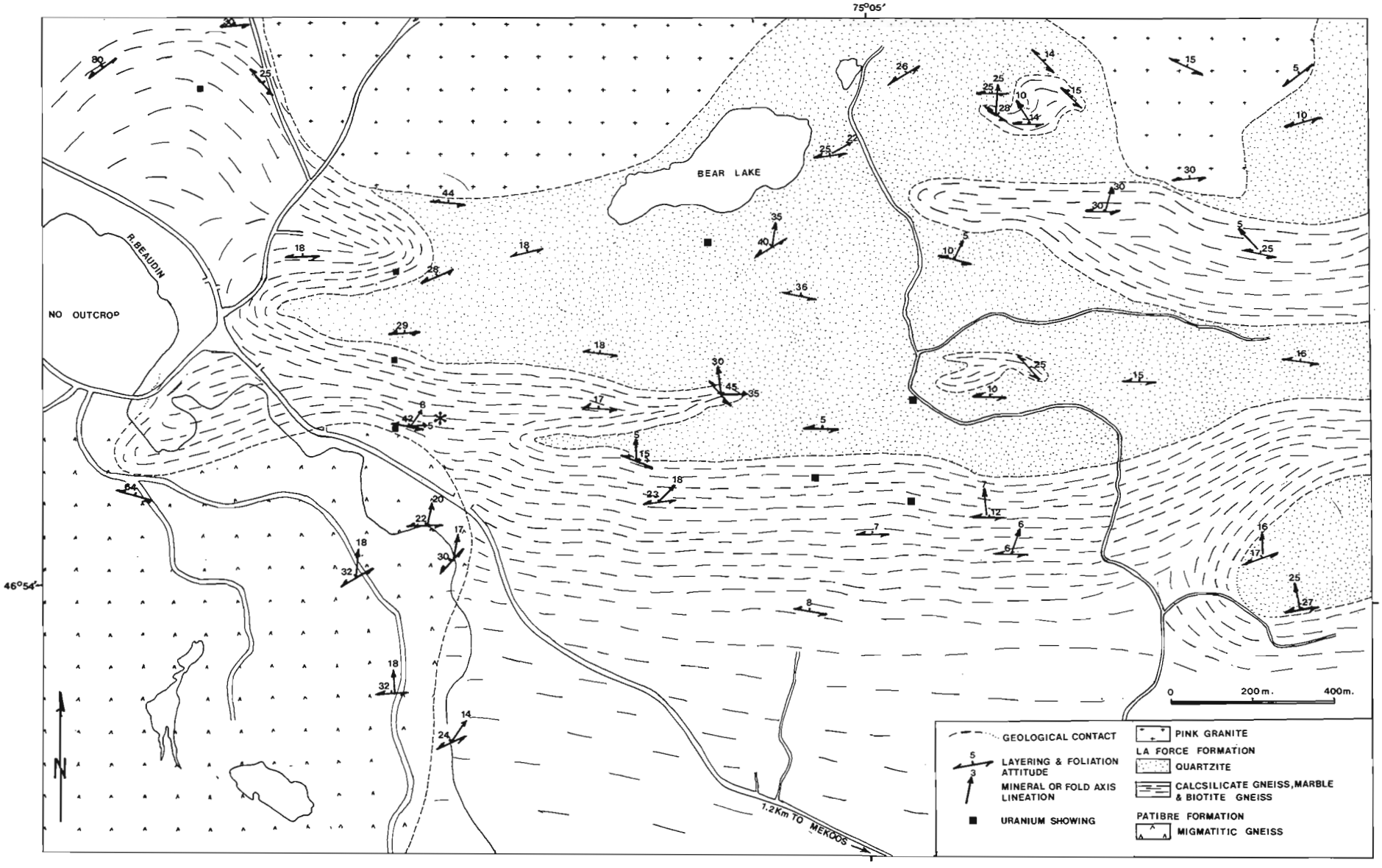

Figure 39.2. *Simplified lithological and structural map of the Mekoos area.*

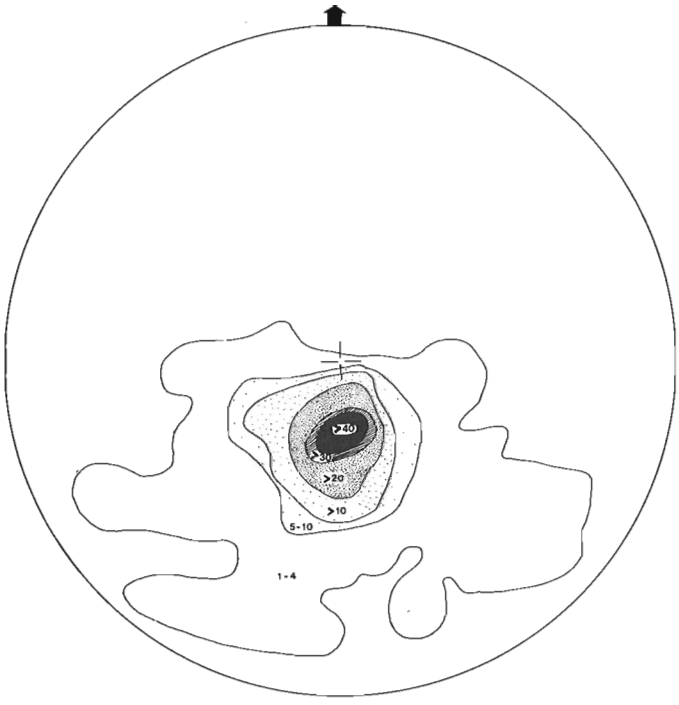

Figure 39.3. Lower hemisphere equal-area projection of 219 poles to foliation planes in the Mekoos area.

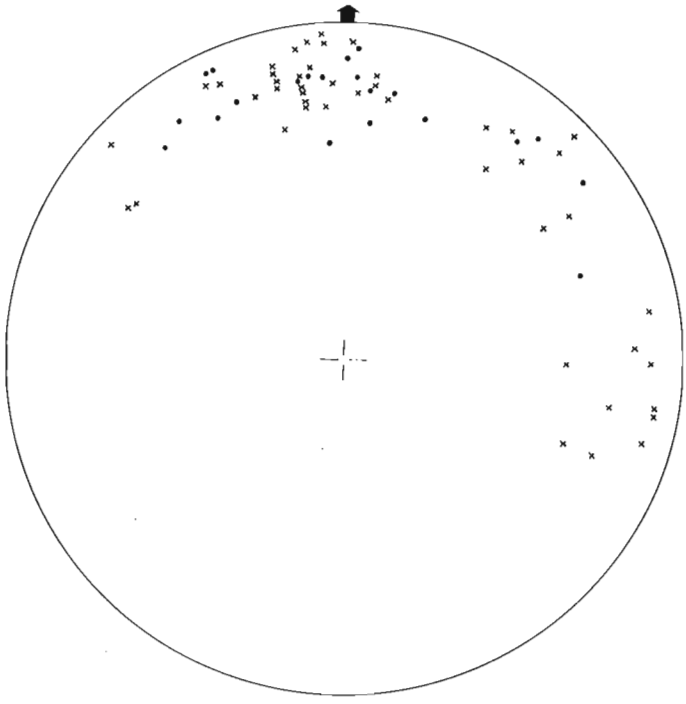

Figure 39.4. Lower hemisphere equal-area projection of 45 fold axes (X) and 20 mineral lineations (dots) from the Mekoos area.

tourmaline and titanite. Those melanocratic minerals are disseminated in fairly fresh, medium grained mosaic of plagioclase, quartz and minor microcline. Accessory minerals are apatite, titanite, rare radioactive allanite and zircon. The migmatite gneiss is intensely deformed in a plastic manner. Its contact with the paragneisses is not visible but it appears to be discordant; the structural elements in both rock types (migmatite and paragneiss) strike east-west while the contact appears north-south. This could be the unconformity separating the Grenville Group from the pre-Grenville rocks as suggested by Kish.

La Force Formation

Calc-silicate gneiss is the most common rock type in the area. Its composition varies greatly, samples contain different minerals in different proportions. Its main components are plagioclase (An_{25} to An_{30}), quartz, diopside, biotite, K-feldspar and scapolite; calcite, sphene, pyrite and graphite are accessory minerals. The quartz content varies from 10 to 30%, diopside forms about 30% and if present scapolite also forms 30%. Feldspar is generally not abundant or is absent except in pegmatitic segregations. The texture of the rock is granular. Its weathered surface is generally rusty.

Marble occurs sporadically throughout the calc-silicate unit and appears to have been remobilized along with the pegmatite with which it commonly is associated. It is mostly formed of coarse pink or buff calcite with a little diopside.

Quartzite is the second most common rock type in the area. It varies from almost pure quartz, often smoky, to feldspathic and/or biotitic quartzite. Biotite shows a preferred orientation and in rare places quartz is strongly rodded.

Biotite paragneiss is a fine grained quartz-rich rock, often migmatized; where it contains graphite and pyrite its weathered surface is rusty and very similar to the surface alteration of the calc-silicate gneiss. In thin section the rock is formed of 30% orthoclase, 30% quartz and 30% plagioclase (An_{30}); sphene biotite and a little chlorite form the other 10%, zircon and apatite are accessory minerals. The texture is granular.

White pegmatite is present throughout the area; it may be concordant or discordant with respect to the various paragneisses. On the basis of geochemical arguments, Tremblay (1974) believed it to result from the partial melting of the paragneisses. The pegmatites are locally completely leucocratic or they contain biotite or diopside depending on the host rock mineralogy. They also contain xenoliths of the latter. Orthoclase forms as much as 65% of the rock, quartz 15% and plagioclase (An_{30}) 15%, a little biotite or diopside, apatite and zircon form the other 5%.

Amphibolite was only observed as thin, discontinuous lenses in the calc-silicate gneiss.

Pink granite observed in the northern part of the map area (Fig. 39.2) intrudes the paragneisses. Its texture ranges from rather coarse grained and massive to pegmatitic in the northwest, to fine grained and faintly foliated in the northeast.

Structural Geology

The structural elements observed in the migmatitic gneiss of the Patibre Formation are foliation and fold axes. In the La Force paragneisses, the foliation is parallel to the lithological layering. The lineations are mineral lineations and include quartz rodding.

The foliation and layering measured strike in a general east-west direction and consistently dip moderately to the north. One outcrop shows in three dimensions an almost vertical layering at the closure of a recumbent fold with an east-west axis (site marked by * in Fig. 39.2). The dips measured elsewhere are thus interpreted as mainly corresponding to the low dips characteristic of limbs of recumbent to gently inclined folds.

The recumbent folds in the La Force Formation are the earliest recognized. The Patibre migmatitic gneiss possibly was affected by previous phase(s) but these are obscured.

The folding along the east-west axis was followed by a pervasive open-style wrinkling along an approximately north-northwest axis, with a strongly developed parallel lineation or rodding in the La Force paragneisses and quartzite.

A plot of poles to foliation planes (Fig. 39.3) indicates a partial distribution about a south-dipping great circle reflecting the open style of the latest period of folding. The concentration of points at about a 20° dip indicates the gently north-dipping limbs resulting from the previous phase of recumbent isoclinal folding.

A plot of lineations (Fig. 39.4) shows a dispersion of points of low to moderate plunge. The small population of fold axes plunging east probably corresponds to axes of the first period of folding. The more scattered group plunging north corresponds to fold axes and mineral lineations related to the second phase.

Conclusion

It can be noted from the rock descriptions that the mafic minerals in the pegmatites are related to the composition of the host rock. It was also noticed that the paragneisses are commonly migmatized. The presence of xenoliths of paragneisses in the white pegmatites was also mentioned. All these observations support the hypothesis (Tremblay, 1974; Kish, 1977) of in situ partial melting of the metasediments of the La Force Formation as the most likely origin of the white pegmatites.

The mapping also confirmed that the white pegmatites are restricted in space to the paragneisses. They were not observed in the Patibre migmatitic gneiss or the more recent pink granites to the north. The radiometric survey carried out concurrently with the geological mapping confirmed that the U anomalies are restricted to the white pegmatite. It was not possible to determine why some pegmatites are radioactive and some are not.

It should also be noted that the white pegmatites are always more or less deformed, sometimes mylonitized and their emplacement may therefore be related to either of the deformations or may be pre-kinematic.

Acknowledgment

I am grateful to Armand Savoie who was working for SOQUEM in the area, for the exchange of ideas and for providing the accurate location of cut lines on the property without which plotting the precise location of outcrops would have been impossible.

References

Kish, J.
1977: Patibre (Axe) Lake area, Preliminary Report; Québec Ministère des Richesses Naturelles DPV-487.

Rimsaite J.
1978: Mineralogy of radioactive occurrences in the Grenville Structural Province: A Preliminary report; in Current Research, Part B, Geological Survey of Canada, Paper 78-1B, p. 49-58.

Tremblay, P.
1974: Mineralogy and geochemistry of the radioactive pegmatites of the Mont-Laurier area, Quebec; unpublished M.Sc. thesis, Queen's University, Kingston.

A COMPARATIVE STUDY OF SULPHUR ISOTOPE DISTRIBUTION OF SULPHIDE FACIES BANDED IRON FORMATIONS AND THE EAST SOUTH C ORE ZONE, DICKENSON GOLD MINE, RED LAKE DISTRICT: A PRELIMINARY REPORT

EMR Research Agreement 213-4-80

M.J. Lavigne[1] and J.H. Crocket[1]
Economic Geology Division

Lavigne, M.J., and Crocket, J.H., A comparative study of sulphur isotope distribution of sulphide facies banded iron formations and the East South C ore zone, Dickenson gold mine, Red Lake district: a preliminary report; in Current Research, Part A, Geological Survey of Canada, Paper 82-1A, p. 265-274, 1982.

Abstract

The Dickenson mine's East South C ore zone is a structurally controlled, auriferous banded sulphide orebody. Geochemical comparison of this zone with sulphide facies banded iron formations and the sulphide poor 30-S.1492 ore zone shows that 1) the major element compositions of the E.S.C. zone and S.F.B.I.F. are similar, and very different from that of the 30-S.1492 zone, 2) the $\delta^{34}S$ values of pyrite in the East South C ore range from 0.82 to 6.21‰ with a mean of 4.1 ± 2 ‰ (one standard deviation), in graphitic sulphide facies banded iron formation from -6.10 to 4.38‰ with a mean of 0.11 ± 3.02 ‰, in carbonaceous sulphide facies banded iron formation from -0.73 to 5.65‰ with a mean 1.96 ± 2.14 ‰, and in the 30-S.1492 ore zone from 7.86 to 8.50 ‰ with a mean of 7.99 ± 0.45 ‰.

Sulphides in the East South C ore zone may have been formed by both volcanogenic and biological processes. Alternatively, they may result from mixture of sulphur from a purely epigenetic hydrothermal system with $\delta^{34}S$ near 8 ‰, as represented by the 30-S.1492 ore zone, with sulphur from sulphides in the sulphide facies banded iron formation.

Introduction

In recent investigations of the East South C ore zone at the Dickenson gold mine, Kusmirski and Crocket (1980), have suggested a possible syngenetic origin for the auriferous banded sulphide horizon. Oxygen isotope investigations by Kerrich et al. (1981) offered some support for this conclusion. However, Rigg and Helmstaedt (1980) proposed an epigenetic origin based on field observation. Pirie (1980) pointed out that because of the sulphide banding in the ore zone, the latter can be interpreted as a sulphide-rich interflow chemical sedimentary rock or alternatively as a highly silicified metavolcanic unit with lenses and stringers of sulphides and quartz veins. He further noted that the East South C ore zone has been severely deformed and that only unequivocal sedimentary textures would prove an exhalative origin. Observations to date by the senior author have failed to reveal any unequivocal primary sedimentary structures and textures. This is not unexpected in a gold camp where the metamorphic grade, at least locally, is amphibolite facies. Due to deformation of the ore zone and host rocks, textural interpretations are likely to be highly subjective. Geochemical data have shed some light on the origin of the ores, but interpretations based on these tend to be complex, and the data permit several hypotheses.

Within this highly deformed volcano-sedimentary complex are pods or domains of rock which have largely escaped deformation and alteration, and in which textures can be interpreted with some confidence. Some of these well preserved pods contain indisputable sulphide facies banded iron formation, exemplified by relatively undeformed, well banded graphitic sulphide facies banded iron formation (Fig. 40.2).

It is the purpose of this study to compare the sulphur isotope distributions, and some compositional characteristics of sulphide facies banded iron formations with those of the East South C ore zone (of questionable origin) and of the less important 30-S.1492 auriferous sulphide horizon.

Field work was undertaken during the summer of 1980. A 350 m crosscut on the 30th level was mapped and sampled in detail to establish stratigraphy (Fig. 40.1). Sections of the ore zone were mapped and sampled on the 30th, 24th and 21st levels. Samples of well-preserved sulphide facies banded iron formation were taken from the 15th and 30th levels. Field work was followed by laboratory studies which are currently in progress.

Description of the East South C Ore Zone

The geological setting of the Dickenson mine has been discussed by Pirie (1980) and MacGeehan and Hodgson (1980) and will not be dealt with in detail here. The East South C ore zone is a linear, siliceous, banded sulphide orebody enclosed by mafic volcanic rocks (Fig. 40.1). Locally the sulphides are massive, but usually they form discontinuous bands less than 1 cm in thickness (Fig. 40.3, 40.4). These bands define the well developed foliation.

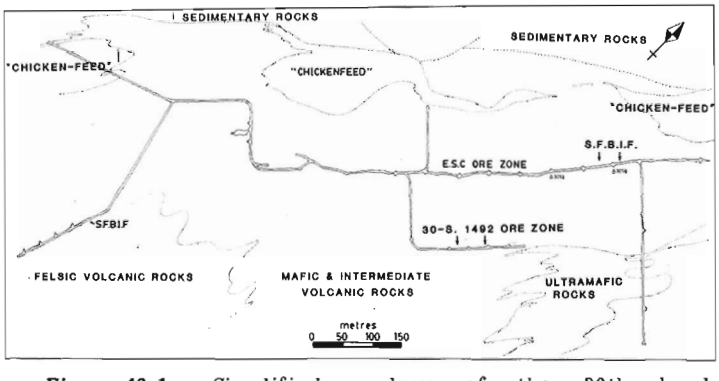

Figure 40.1. *Simplified geology of the 30th level, Dickenson Mine, with sample locations. Note that "chickenfeed" is a mine term for a variety of rocks including ultramafic flows (?) and intrusions, and resedimented volcanic rocks.*

[1]Department of Geology, McMaster University, Hamilton, L8S 4M1

Figure 40.2. *Graphitic sulphide facies banded iron formation, 15th level. Scale is 9 cm long.*

Figure 40.3. *E.S.C. ore zone, 24th level. Sulphides are light grey, host rock is silicified basalt. Note the sulphides along foliation planes.*

Figure 40.4. *Sample from the East South C ore zone. 10.5 cm long.*

Figure 40.5. *Sample (10.5 cm long) of fragmental rock from the East South C ore zone. Note sulphides which are interstitial to silicate clasts.*

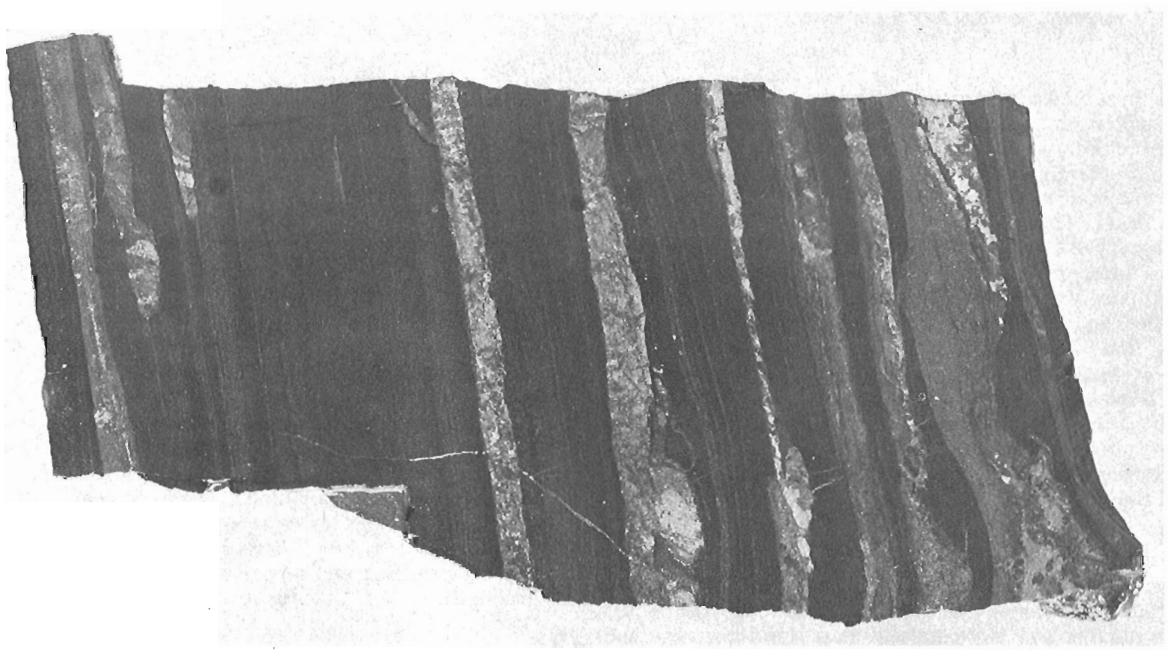

Figure 40.6. *Graphitic sulphide facies banded iron formation. Sample is 9.5 cm long.*

Figure 40.7. *Carbonate sulphide facies banded iron formation. 30 level, 7.5 cm long.*

Figure 40.8. *Carbonate sulphide facies banded iron formation. Note the shard about which bedding has been deformed on the upper left side of the sample. Also note spheroids below the shard. Sample is 8.5 cm long.*

Garnet porphyroblasts commonly preserve an earlier fabric defined by sulphides. Silicate mineralogy is highly variable. Bands range in composition from microcrystalline quartz to muscovite-hornblende-biotite schist. A fragmental texture commonly dominates the ore (Kusmirski and Crocket, 1980; Kusmirski, 1981). It is defined by domains of various silicate minerals separated by a sulphide-rich matrix (Fig. 40.5). This texture was interpreted as volcaniclastic (Kusmirski, 1981), although a purely cataclastic origin also seems possible. Foliation can be traced locally across adjoining domains, transecting the interstitial sulphide. The sulphides can therefore, at least locally, be interpreted as predating the foliation. However, at one location, the 21-12102 stope, the ore clearly transects amygdaloidal pillowed basalts, and pillows have been preserved within the sulphide rich ore. This evidence supports an epigenetic emplacement of the sulphide at the 21-12102 stope site.

Pyrite is the dominant sulphide in the ore zone and occurs as both disseminated grains in the siliceous bands and as massive bands. Pyrrhotite is common in the pyrite bands together with minor chalcopyrite. Arsenopyrite occurs as feathery masses and more locally as prismatic grains less than 0.01 mm in length. Magnetite is associated with iron-bearing silicate minerals.

Sulphide Facies Banded Iron Formations

The units can be grouped into two types: 1) that in which the silicate bands have abundant graphite (Fig. 40.6), and 2) that with both carbonate and sulphide rich bands (Fig. 40.7). Sedimentary structures are well preserved and foliation usually transects bedding obliquely. The sulphide facies banded iron formations occur as interflow sedimentary units 3 to 6 m thick.

The graphitic type consists of continuous pyrite bands interbedded with black graphitic chert (Fig. 40.6). Lithic fragments and disseminated phyllosilicates are found in siliceous bands. Locally iron silicate minerals are predominant in the siliceous bands and are especially well developed in the vicinity of sulphides. Some chert bands are pure, without graphite or detrital components. Pyrite is the most abundant sulphide, with minor pyrrhotite and chalcopyrite. Pyrite, magnetite and rare sphalerite are also disseminated in the chert bands. Arsenopyrite occurs as feathery masses and as prismatic crystals less than 0.01 mm in length.

Figure 40.9. *30-S.1492 ore zone 120 m south of the East South C ore zone, 30 level. Ore zone is light grey and silica-rich. Scale is 9 cm long.*

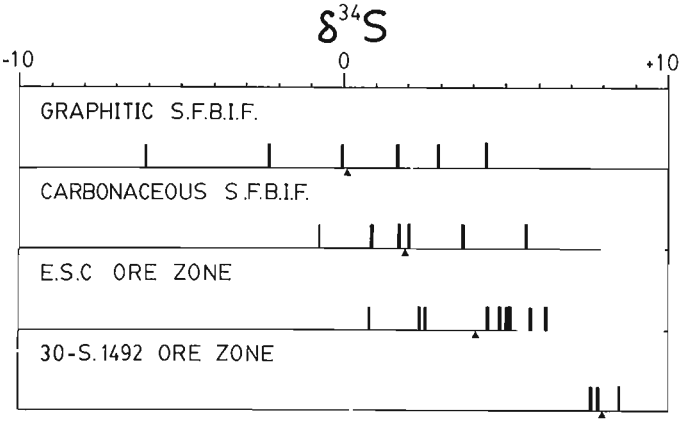

Figure 40.10. *$\delta^{34}S$ distribution in gold-rich units from Dickenson mine. Bars represent individual samples and ▲ is the mean value.*

The sulphide mineralogy is identical in the carbonate type. The chert bands, however, are carbonate-rich and range in composition from pure microcrystalline quartz to pure carbonate. Several bands which have a volcaniclastic component contain shards around which bedding has been deformed (Fig. 40.8). Some bands are dominated by iron silicate minerals and pale biotite. Sample 932 has a clastic band with graded bedding and abundant sphalerite. The clasts are rounded and consist of quartz and plagioclase in a matrix of iron silicate and biotite. One sample has spheroids which are suspected remnants of a micro-organism (Fig. 40.8). Their origin is currently under study.

30-S.1492 Ore Zone

This horizon is approximately 120 m south of the E.S.C. ore zone on the 30th level (Fig. 40.2, 40.9). It contains a mineable grade of gold but is of minor economic significance because of limited lateral extent. This unit is enclosed in pillowed basalt.

In comparison with the East South C ore zone and the sulphide iron formation the 30-S.1492 ore zone is sulphur and base metal poor, and significantly lower in iron. The main metallic mineral is magnetite, which is accompanied by some pyrrhotite, arsenopyrite, ilmenite and traces of chalcopyrite. These minerals occur as disseminated grains in a silicate-carbonate matrix. Well-defined metallic mineral bands, characteristic of the sulphide iron formations, are absent in this unit.

Analytical Methods and Procedures

Major and Trace Element Analyses

Major and trace elements were analyzed by X-ray fluorescence, the major elements and some trace elements (V, Cr, Co, Pb, Cu, Zn and Ni) on powder pellets. Au, As, W and Sb were determined by instrumental neutron activation. S was analyzed with a LECO induction furnace gas analysis system. Reliable loss on ignition data could not be obtained due to the oxidation of Fe^{2+}. Also, carbon analyses by the LECO system were inaccurate due to interference by the high S content of many of the samples; these analyses are still in progress. Consequently, the whole rock data do not include all the volatiles and the analyses are normalized to 99 per cent (Tables 40.1a, b, 2, 4). The relative elemental abundances for an individual sample are correct but the absolute abundances may differ significantly from one sample

Table 40.1a

Major[a] and trace[b] element abundances in the graphitic sulphide facies banded iron formation, 15th Level

Oxide or element	Sample Number 959	960	961	962	963	$\bar{X}$
SiO_2	56.93	57.23	50.33	58.15	73.96	59.32
Al_2O_3	10.91	8.44	6.72	5.90	2.29	6.85
Fe_2O_3	16.24	20.09	25.76	21.65	11.05	18.96
MgO	4.15	2.00	2.53	1.38	5.09	3.03
CaO	2.92	0.96	1.86	0.54	3.45	1.95
Na_2O	0.15	0.12	0.08	0.06	0.05	0.09
K_2O	1.88	1.38	0.42	0.64	0.19	0.90
TiO_2	0.71	0.21	0.24	0.41	0.02	0.32
MnO	0.07	0.02	0.00	0.04	0.26	0.08
P_2O_5	0.08	0.05	0.08	0.05	0.02	0.06
S[c]	9.93	17.00	22.09	15.94	5.22	14.0
Total	103.97	107.50	110.05	106.97	101.61	
Recal-culated S[d]	4.97	8.50	11.05	7.97	2.61	7.02
Final Total	99.00	99.00	99.00	99.00	99.00	
V	105	60	53	49	6	55
Cr	60	34	38	70	22	45
Co	46	57	73	69	24	54
Pb	18	16	3	2	4	8.6
Cu	109	26	27	23	73	52
Zn	393	199	43	22	36	139
Ni	83	53	97	109	28	74
As[e]	92	255	3420	8120	3170	3011
Au	0.019	0.042	2.2	1.6	0.18	0.81
W	19	11	12	15	7.7	13
Sb	210	365	248	155	40	204
Co:Ni	0.55	1.07	0.76	0.64	0.31	
Cu:V	1.04	0.43	0.51	0.47	12.2	

to another as the carbon content of the samples is highly variable. For these reasons a detailed analysis of the whole rock data was not attempted.

Sulphide Separation and Isotopic Analysis

Sulphide mineral separates were obtained from the 100 to 200 mesh fractions of crushed and sieved samples using an efficient graded tube hydrolytic separatory system designed by the senior author. Most sulphide separates were of greater than 99 per cent purity. Separation of pyrrhotite from pyrite was done magnetically. Sulphides from the main East South C ore zone were obtained from whole rock samples, while those from sulphide facies banded iron formations were obtained from individual sulphide-rich bands sawn from the sample. Portions of 10 to 20 mg were used for isotopic analysis.

The sulphur isotope analyses were performed on SO_2 gas in a double collection mass spectrometer using procedures described by Thode et al. (1961), Thode and Rees (1971) and Rees (1978). The $\delta^{34}S$ data are expressed relative to the Canon Diablo troilite standard. The standard deviation of a single determination is ± 0.1 ‰. The isotopic data are presented in Table 40.3 and Figure 40.10.

Discussion

Geochemistry

The salient features of the compositional data are summarized as follows:

1. The sulphide facies banded iron formation have high gold contents by comparison with background levels established by analysis of interflow sedimentary rocks away from the mine environment (Cowan and Crocket, 1980). The Dickenson iron formations are at least 25 times the background level.
2. The sulphide facies banded iron formation and the East South C ore zone show many similar compositional properties. The 30-S.1492 ore zone, however, varies considerably in composition with respect to this group.
3. The sulphide facies banded iron formations and East South C rocks, in addition to carrying high gold content, are rich in base metals, arsenic, iron and sulphur. The 30-S.1492 ore zone, although a gold-rich rock, is in comparison much lower in iron, sulphur and base metals. Other compositional components, such as Co:Ni and Cu:V ratios, differ significantly. These ratios are greater than 0.3 in the iron formations and East South C ore zone and less than 0.3 in the 30-S.1492 ore zone. However, the Co:Ni ratios of samples from the carbonaceous iron formations are less than 3.

Table 40.1b

Major[a] and trace[b] element abundances in the carbonate sulphide facies banded iron formations, 30th Level

Oxide or element	Sample Number 931	932	933	934	935	$\bar{X}$
SiO_2	50.11	46.00	51.05	54.53	53.82	51.10
Al_2O_3	6.68	7.35	8.30	11.49	6.68	8.10
Fe_2O_3	20.31	20.78	14.92	11.60	17.34	17.00
MgO	6.21	6.77	8.20	6.21	6.20	6.72
CaO	6.69	7.21	10.60	7.73	8.52	8.15
Na_2O	0.06	0.06	0.09	0.12	0.15	0.10
K_2O	0.49	0.66	0.62	1.88	0.51	0.83
TiO_2	0.31	0.62	0.28	1.88	0.49	0.72
MnO	0.11	0.14	0.18	0.17	0.17	0.15
P_2O_5	0.05	0.06	0.05	0.16	0.04	0.07
S	15.94	18.71	9.42	6.46	10.13	12.1
Total	106.97	108.36	103.71	102.23	104.07	
Recal-culated S	7.97	9.36	4.71	3.23	5.07	6.07
Final Total	99.00	99.00	99.00	99.00	99.00	
V	83	112	85	341	78	140
Cr	39	352	48	1807	106	470
Co	72	87	38	88	63	70
Pb	46	17	18	25	33	28
Cu	107	79	97	127	201	122
Zn	545	1197	591	501	429	653
Ni	307	275	160	1085	360	437
As	355	380	205	1870	365	635
Au	0.30	0.39	0.17	0.26	0.18	0.26
W	1.1	3.2	1.7	8.0	4.9	3.8
Sb	85	50	26	185	68	83
Co:Ni	0.23	0.31	0.23	0.08	0.17	0.16
Cu:V	1.29	0.71	1.14	0.37	2.58	0.87

Footnotes to Tables 40.1a, b

a) weight %
b) ppm
c) wt. % S, LECO induction
d) S recalculated as the weight % oxygen replaced (Deer et al., 1966)
e) As, Au, W, Sb - INAA

4. The high Al content of the iron formations and of the East South C ore zone suggest that all these rocks are probably mixtures of clastic and chemical components.

Sulphur isotope analysis

The sulphur isotope study was undertaken to compare the isotopic composition of sulphur in the sulphide facies banded iron formation with that in the East South C ore zone. The distribution of sulphur isotopes in the former has been documented by Goodwin et al. (1976). It is argued that such sulphides were precipitated at the seawater-sediment interface and that seawater sulphate was reduced by bacterial activity to produce H_2S, which is the source of sulphur in these deposits. As a result the isotopes were fractionated, producing a ^{32}S enrichment in the sulphides and a wide variation in $\delta^{34}S$ values. If the East South C ore zone has similar $\delta^{34}S$ values to the iron formation, it would support the hypothesis that the sulphur at least was biogenic and that both were syngenetic. However, gold could have been introduced much later by some epigenetic process.

The carbonaceous sulphide facies banded iron formation has a mean $\delta^{34}S$ of 1.96 ± 2.14 ‰ (1 standard deviation) with compositions ranging from -0.73 to 5.65 ‰. The graphitic type has a mean $\delta^{34}S$ value of 0.11 ± 3.82 ‰, with compositions ranging from -6.10 to 4.38 ‰. This difference is significant and must be explained by variations in processes that produced these two types of sulphide facies banded iron formation.

At low temperatures (T less than 50°C) the only mechanism for the reduction of sulphate is bacterial reduction (Rye and Ohmoto, 1974). Harrison and Thode (1958) have shown that fractionation of sulphur isotopes by bacterial activity is controlled by factors such as nutrient provision, sulphate concentration, growth rates and temperature. At higher temperature, as discussed by Ripley and Ohmoto (1977), sulphate may be inorganically reduced to sulphide. A practical mechanism for accomplishing such reduction is the deep circulation of seawater sulphate into hot volcanic piles or rock columns affected by geothermal activity. In such cases the necessary reduction could result

Table 40.2

Major and trace element abundances in the East South C ore zone

Oxide or element	603	609	611	612	$\bar{X}^a$
	Sample Numbers, Location Δ 3058				
SiO_2	50.65	65.85	46.33	51.17	54.93
Al_2O_3	8.72	15.00	5.03	9.90	10.31
Fe_2O_3	23.38	7.85	27.61	13.65	14.07
MgO	6.88	1.61	2.02	7.81	5.94
CaO	3.56	1.49	3.85	11.38	6.59
Na_2O	0.19	0.18	0.08	0.16	0.15
K_2O	1.45	1.41	0.04	1.15	1.54
TiO_2	0.56	0.76	0.14	0.63	0.63
MnO	0.80	0.03	0.03	0.27	0.28
P_2O_5	0.02	0.03	0.05	0.03	0.03
S	5.60	9.57	27.63	5.70	9.10
Total	101.80	103.79	112.82	101.85	
Recal-culated S	2.80	4.79	13.82	2.85	4.54
Final Total	99.00	99.00	99.00	99.00	
V	252	252	72	226	183
Cr	318	337	272	249	258
Co	80	31	110	43	50
Pb	nd	14	5	1	6.7
Cu	111	nd	48	161	75
Zn	694	90	380	196	211
Ni	137	93	158	131	
As	4790	255	2220	4940	
Co:Ni	0.58	0.33	0.70	0.33	
Cu:V	0.44	--	0.66	0.71	
	Sample Numbers, Location Δ 3053				
Oxide or element	868	870	871	872	873
SiO_2	47.69	54.91	60.09	59.64	58.11
Al_2O_3	11.23	11.74	10.86	10.52	9.87
Fe_2O_3	8.84	7.55	7.47	15.91	14.34
MgO	11.71	8.81	7.12	3.11	4.40
CaO	15.32	10.86	7.17	1.93	3.77
Na_2O	0.15	0.10	0.13	0.20	0.19
K_2O	1.52	2.38	1.93	2.08	1.90
TiO_2	0.74	0.85	0.73	0.62	0.61
MnO	0.37	0.24	0.21	0.11	0.19
P_2O_5	0.02	0.11	0.06	0.00	0.01
S	2.83	2.88	6.46	9.74	11.24
Total	100.42	100.44	102.23	103.87	104.62
Recal-culated S	1.42	1.44	3.23	4.87	5.62
Final Total	99.00	99.00	99.00	99.00	99.00
V	326	82	73	98	267
Cr	213	235	212	233	252
Co	29	26	31	51	49
Pb	4	0	17	10	8
Cu	102	96	54	52	37
Zn	69	127	104	117	120
Ni	94	99	105	94	69
As	3160	10200	370	1130	1360
Co:Ni	0.30	0.26	0.29	0.54	0.71
Cu:V	0.31	1.17	0.74	0.53	0.14

Footnote to Table 40.2

a - Averages apply to the nine East South C ore zone samples (ie.-the 600 and 800 series samples)

nd - not detected

Table 40.3

Sulphur isotopic composition, $\delta^{34}S$

Sample Number	$\delta^{34}S$ - pyrite	$\delta^{34}S$ - pyrrhotite
Graphitic sulphide facies banded iron formation 15th level		
959-1*	-2.28	
959-2*	2.96	4.26
959-3*	1.68	1.68
959-4*		3.42
960	-0.05	0.64
962	-6.10	
963	4.38	4.38
	$\bar{X}$ = 0.11	$\bar{X}$ = 2.08
	σ = 3.82	σ = 1.78
Carbonate sulphide facies banded iron formation 30th level		
931-1*	0.40	-0.95
931-2*	-0.73	-0.73
931-3*	0.88	--
932	2.06	1.19
933	1.76	2.18
934	3.69	3.69
935	5.65	--
	$\bar{X}$ = 1.96	$\bar{X}$ = 2.08
	σ = 2.14	σ = 1.95

*subsample from adjacent sulphide bands

Sample Number	$\delta^{34}S$ - pyrite	$\delta^{34}S$ - pyrrhotite
East South ore zone, 30th level		
868[a]	6.21	
870[a]	2.52	2.57
871[a]	2.37	
872[a]	5.01	4.98
873[a]	4.82	5.05
	$\bar{X}$ = 4.19	
	σ = 1.68	
603[b]	5.77	
605[b]	4.43	
611[b]	0.82	1.09
612[b]	5.12	
	$\bar{X}$ = 4.03	
	σ = 2.21	

a) location Δ3053
b) location Δ3058

Sample Number	$\delta^{34}S$ - pyrite	$\delta^{34}S$ - pyrrhotite
30-S.1492 ore zone		
548	8.50	8.25
551	7.62	
553	7.86	7.76
	$\bar{X}$ = 7.99	
	σ = 0.45	

Table 40.4

Major and trace element abundances in the 30-S.1492 ore zone, 30th level

Oxide or element	Sample Number 543	548	551	552	553	$\bar{X}$
SiO_2	57.65	56.41	60.54	69.13	64.33	61.61
Al_2O_3	8.15	9.30	9.31	7.89	8.22	8.57
Fe_2O_3	12.08	8.99	9.25	6.50	8.27	9.02
MgO	8.01	8.53	6.83	6.38	6.84	7.32
CaO	9.68	11.46	7.83	6.53	7.54	8.61
Na_2O	0.46	0.42	0.54	0.47	0.41	0.46
K_2O	1.27	1.67	1.32	0.93	1.35	1.31
TiO_2	0.54	0.56	0.59	0.47	0.49	0.53
MnO	0.36	0.30	0.17	0.21	0.25	0.26
P_2O_5	0.00	0.00	0.00	0.00	0.00	0.00
S	1.58	2.71	5.19	1.00	2.60	2.62
Total	99.79	100.36	101.60	99.50	100.30	
Recal-culated S	0.79	1.36	2.60	0.50	1.30	1.31
Final Total	99.00	99.00	99.00	99.00	99.00	
V	242	230	178	147	180	195
Cr	207	223	209	117	200	191
Co	40	36	46	25	40	37
Pb	8	3	14	20	2	9.6
Cu	48	64	25	48	37	44
Zn	138	148	85	59	20	90
Ni	210	168	327	134	245	217
As	2860	5240	4330	490	5210	3626
Co:Ni	0.19	0.21	0.14	0.18	0.13	
Cu:V	0.19	0.28	0.14	0.32	0.21	

from oxidation of ferrous iron with the magnitude of the isotopic shift depending mainly on temperature. Such processes are considered by Ripley and Ohmoto (1977) to be relevant to massive-sulphide ore deposition at the Raul deposit in Peru, where a wide range of isotopic values and a tendency towards negative $\delta^{34}S$ values are common. This mechanism was proposed in view of the lack of evidence for organic activity in such deposits. It cannot be shown whether this mechanism played an important role in the formation of sulphides in the Red Lake camp. However, the Dickenson setting, with a preponderance of basic volcanic rocks and stratigraphically equivalent volcaniclastic rocks, constitutes an environment where strong geothermal activity was probably an ongoing process during ore deposition. Lacking relevant knowledge of geothermal temperatures and isotopic composition of Archean seawater sulphate, it is difficult to predict the isotopic characteristic of volcanogenic sulphur.

The graphitic sulphide facies banded iron formation provides the most definitive isotopic data. The preponderance of graphitic carbon in this unit is taken as evidence for sedimentation under reducing conditions ideal for the promotion of bacterial sulphate reduction. No other source of sulphur is required to account for the isotopic characteristics of this unit. The sulphur in this iron formation probably formed in a biogenically dominated system, as reflected by a relatively large compositional range with some samples enriched in ^{32}S within the population. The elemental composition of this graphitic iron formation clearly demonstrates that strong gold and moderate base metal enrichment can occur in such reducing sedimentary environments.

The carbonate sulphide facies banded iron formation differs isotopically from the graphitic iron formation in that the isotopic compositions have a significantly narrower range and a mean which is heavier by approximately 2 ‰. The source of sulphur cannot be specified from isotopic characteristics as confidently as in the previous case. A biological source involving a less pronounced isotopic shift, perhaps due to variation in the various critical kinetic actors, is quite feasible, but a volcanogenic sulphur input may also be represented. The main significance of the carbonate iron formation is that it is a sedimentary rock and has a sedimentary sulphur isotopic signature. Again strong base metal and modest gold enrichment characterize this unit.

Sulphur of the East South C ore zone, with a mean $\delta^{34}S$ of 4.1 ± 2.0 ‰, is heavier on average than the graphitic iron formation by 4 ‰ and has a narrower range of isotopic values. In comparison with the carbonate iron formation it is 2 heavier and shows an essentially identical range. The similarity in isotopic characteristics between the ore zone and the carbonate type iron formation suggests that, although not an absolute requirement, both may consist of sulphur of comparable origin.

No isotopic characteristics of the ore zone strongly imply a major presence of biologically generated sulphide. The ore zone represents an environment in which the sulphur sources were similar to those in the carbonate type iron formation, with perhaps a large proportion of volcanogenic or exhalative sulphur.

The degree of deformation represented by the East South C ore zone is significantly higher than that seen in carbonate sulphide facies banded iron formations. The effects of deformation and metamorphism on sulphur isotope composition are poorly known. Schwarcz and Speelman (unpublished data McMaster University) have shown that on a small (outcrop) scale, sulphides tend to become enriched in ^{34}S with increasing metamorphism. This relationship, however, does not hold on a regional scale. However, enrichment in ^{34}S in the ore zone with respect to the isotopic composition of the carbonate type iron formation is possibly the result of local isotopic redistribution due to regional metamorphism.

Alternatively, the sulphur isotopic character of the East South C ore zone could be the result of a mixture of sulphur from two separate sources; sulphur isotope values of the East South C ore zone lie on a mixing path between those of the sulphide facies banded iron formation and the 30-S.1492 ore zone (Fig. 40.10).

Conclusions

The sulphur isotopic character of sulphide facies banded iron formations is influenced by the presence of biological sulphur in the case of graphitic iron formation. Carbonate iron formation has an isotopic signature representative of sedimentary processes but in which the mix of biological and volcanogenic sulphur is uncertain. The sulphur in the East South C ore zone is isotopically similar to that in carbonate iron formation, although somewhat heavier, and a comparable origin is permissible although not required.

Acknowledgments

We would like to thank the Dickenson mine staff for their support, helpful suggestions, and access to the underground. Dr. T. Rees advised on the sulphur isotopic analysis and Mr. Otto Mudrock and Mr. Abdul Kabir helped with the XRF and INAA respectively. Financial assistance was provided by EMR Research Agreement 213-4-80.

References

Cowan, P. and Crocket, J.H.
1980: The gold content of interflow metasedimentary rocks from the Red Lake area, Ontario – A preliminary evaluation; in Current Research, Part B, Geological Survey of Canada, Paper 80-1B, p. 129-133.

Deer, W.A., Howie, R.A., and Zussman, J.
1966: An Introduction to the Rock-forming Minerals; Longman, London, 528 p., p. 515-517.

Goodwin, A.M., Monster, J., and Thode, H.G.
1976: Carbon and sulphur isotope abundances in Archean iron-formations and early Precambrian life; Economic Geology, v. 21, p. 870-891.

Harrison, A.G. and Thode, H.G.
1958: Mechanism of the bacterial reduction of sulphate from isotope fractionation studies; Faraday Society Transactions, v. 54, p. 84-92.

Kerrich, R., Fryer, B.J., Milner, K.J., and Peirce, M.G.
1981: The geochemistry of gold-bearing chemical sediments, Dickenson Mine, Red Lake, Ontario: A reconnaissance study; Canadian Journal of Earth Sciences, v. 18, p. 624-637.

Kusmirski, R.T.M.
1981: Metallogeny of the "East South C" ore zone in the Dickenson mine, Red Lake, Ontario – Evidence for syngenetic gold deposition; unpublished M.Sc. thesis, McMaster University.

Kusmirski, R.T.M. and Crocket, J.H.
1980: Metallogeny of the gold deposits in the Dickenson Mine, Red Lake, northwestern Ontario – A preliminary report; in Current Research, Part B, Geological Survey of Canada, Paper 80-1B, p. 135-144.

MacGeehan, P.J. and Hodgson, C.J.
1980: Relationship of gold mineralization to volcanic and metamorphic features in the area of Campbell and Dickenson Mines, Red Lake District, in Genesis of Archean, Volcanic Hosted Gold deposits, R.G. Roberts, ed.; Ontario Geological Survey, Open File Report 5293, p. 212-242.

Pirie, J.
1980: Regional geological setting of gold mineralization in the Red Lake area, N.W. Ontario; in Genesis of Archean, Volcanic Hosted Gold Deposits, R.G. Roberts, ed.; Ontario Geological Survey, Open File Report 5293, p. 303-358.

Rees, C.E.
1978: Sulphur isotope measurements using SO, and SF; Geochimica et Cosmochimica Acta, v. 42, p. 383-389.

Rigg, D.M. and Helmstaedt, H.
1980: Relations between structures and gold mineralization in the Campbell Red Lake and Dickenson Mines, Red Lake District, Ontario; in Genesis of Archean, Volcanic Hosted Gold Deposits, R.G. Roberts, ed.; Ontario Geological Survey, Open File Report 5293, p. 243-279.

Ripley, E.M. and Ohmoto, H.
1977: Mineralogic, sulfur isotope, and fluid inclusion studies of the stratabound copper deposits at the Raul Mine, Peru; Economic Geology, v. 72, p. 1017-1041.

Rye, R.O. and Ohmoto, H.
1974: Sulfur and carbon isotopes and ore genesis: A review; Economic Geology, v. 69, p. 826-842.

Thode, H.G. and Rees, C.E.
1971: Measurements of sulphur concentrations and the isotopes ratios $^{33}S/^{32}S$, $^{34}S/^{32}S$ and $^{36}S/^{32}S$ in Apollo 12; Earth and Planetary Science Letters, v. 12, No. 4, p. 434-438.

Thode, H.G., Monster, J., and Dunford, H.B.
1961: Sulphur isotope geochemistry; Geochimica et Cosmochimica Acta, v. 25, p. 159-174.

SYNGENETIC DEFORMATION IN MASSIVE SULPHIDES, GALLEN DEPOSIT, NORANDA, QUEBEC

EMR Research Agreement 205-4-81

J.H. McEwen[1] and D.H. Watkinson[1]
Economic Geology Division

McEwen, J.H. and Watkinson, D.H., Syngenetic deformation in massive sulphides, Gallen deposit, Noranda, Quebec; in Current Research, Part A, Geological Survey of Canada, Paper 82-1A, p. 275-280, 1982.

Abstract

Sulphides in the Gallen volcanogenic massive sulphide deposit accumulated on the seafloor within a venting region for metal-rich brines. Sulphide fragments within a sulphide matrix are interpreted to be the result of syngenetic slumping of competent layered sulphide blocks into less competent sulphide material. The venting of hot brines into the accumulating sulphide mound would result in a highly fluidized mass of sulphide grains that was more buoyant than 'colder' less active regions within the mound where sulphides would probably be consolidated into layers. Migration of discharge sites or rhythmic discharging of hot brines could result in the upward movement of fluidized sulphide through semiconsolidated to consolidated layered sulphide. Fragmentation of the layered sulphides and slumpage of these fragments into fluidized sulphide could have produced the observed slumpage textures.

Minor downslope slumpage of the entire sulphide body due to gravitational instability could also explain the slumpage textures.

Introduction

The Gallen zinc deposit (formerly known as the West Macdonald) occurs within felsic volcanic rocks about 8 kilometres northeast of Noranda, Quebec (Fig. 41.1). It consists of two west-northwest trending, dominantly pyritic, massive sulphide lenses. The main lens extends to a depth of 150 m and outcrops over an area measuring 275 by 120 m. The lower and smaller body is located from 275 to 335 m below the surface and is 60 m long and 30 m wide. Total reserves of the two orebodies have been estimated at 8.1 million tonnes grading 3.36 per cent zinc, 0.08 per cent copper, 2.4 grams per tonne silver and 0.06 grams per tonne gold (Oeille, 1949).

Extensive trenching and drilling on the showing throughout the 1930's and 1940's resulted in a five-year underground mining program from 1955 to 1959, operated by Macdonald Mines Ltd. Over that period 27 000 tonnes of zinc, 140 tonnes of copper, 1.6 million grams of silver and 57 000 grams of gold were produced from approximately 900 000 tonnes of ore. Since the early 1970's Noranda Mines Ltd. has been reinvestigating the property. Open pit operations commenced early in 1981 to recover an additional 1.6 million tonnes of ore.

Detailed geological mapping was conducted in 1980 on the main sulphide lens as part of a continuing study. In this paper deformational features observed on surface, previously reported by Roscoe (1965), are described and a model is presented to explain their occurrence.

Geologic Setting

A large domal anticline occurs in volcanic rocks within the Archean Abitibi Greenstone Belt north of Noranda, Quebec (De Rosen-Spence, 1976). The Lake Dufault granodiorite is a composite, crosscutting intrusion located along an eastern extension of this anticline (Fig. 41.1). The granodiorite encloses an elliptical body of felsic rocks, the South Dufault Rhyolite (De Rosen-Spence, 1976), which is the host rock for the Gallen massive sulphide deposit.

The South Dufault Rhyolite is included in the fourth zone of felsic lavas and tuffs comprising the Blake River Group. It consists of plagioclase and amphibole phenocrysts in a fine grained, pale to dark green, mainly chloritic groundmass. Intercalated with this feldspar porphyry unit are felsic tuffs, tuff-breccias and felsic flows.

The main ore lens is enclosed by and locally gradational to a felsic tuff to tuff-breccia rich in sericite and disseminated sulphides. On strike and to the west of the massive sulphides, the felsic material is finer grained and tuffaceous with isolated lapilli. At the northeast contact of the main lens, a unit of tuff-breccia, with fragments up to 30 cm across, has been strongly sericitized and contains abundant disseminated pyrite. Pyrite also occurs as fragments (1-20 cm) and as irregular-shaped veins

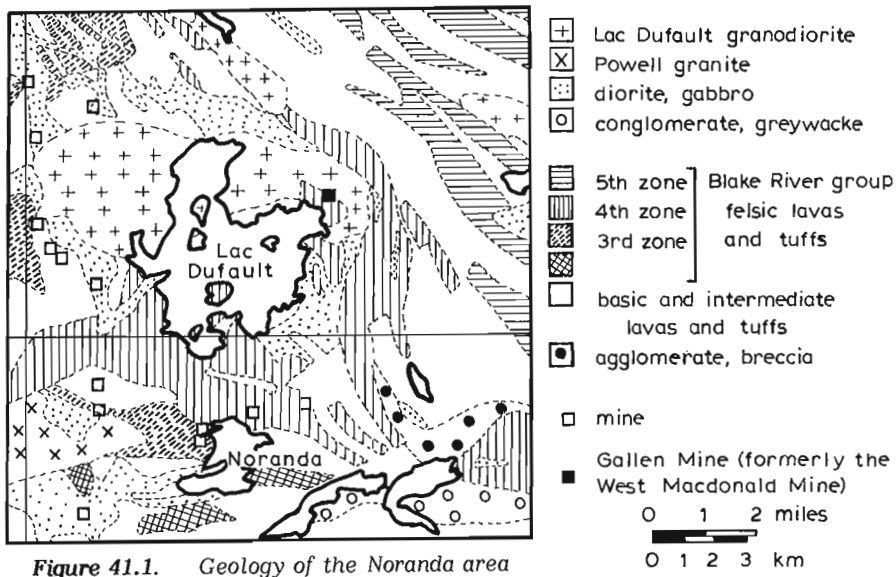

Figure 41.1. *Geology of the Noranda area (after Spence and De Rosen-Spence, 1975).*

[1]Department of Geology, Carleton University, Ottawa K1S 5B6

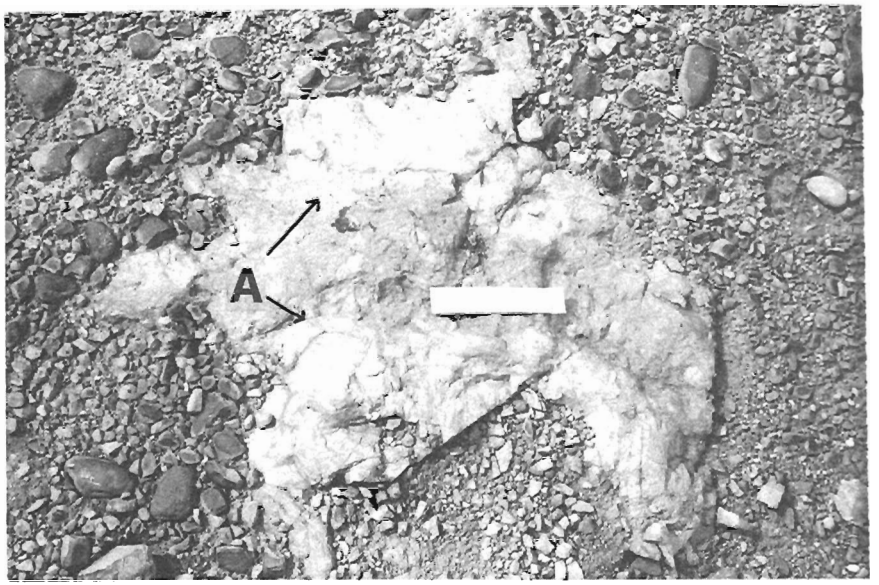

Figure 41.2a. Angular fine grained pyritite fragments (A) set in pyrite matrix (scale – 15 cm).

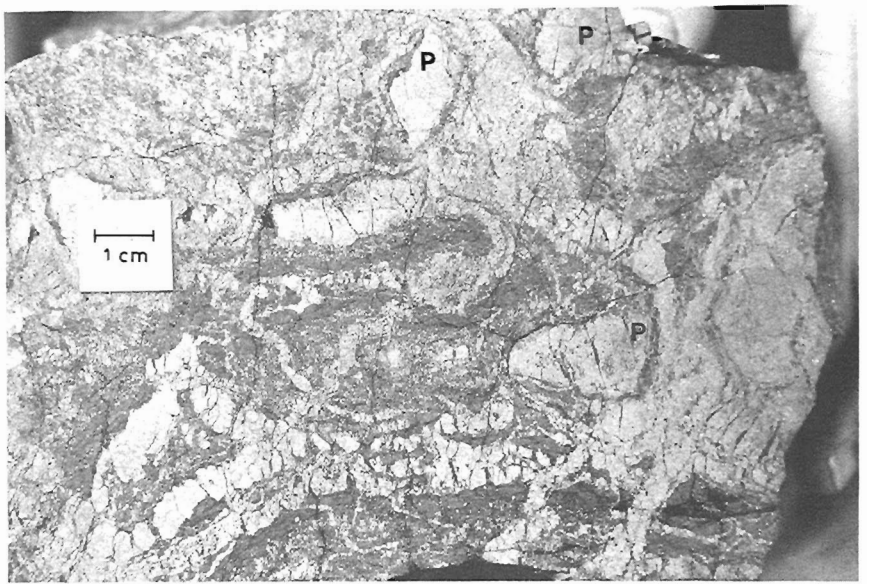

Figure 41.3. Disrupted layers of sulphide with isolated pyritite fragments (P).

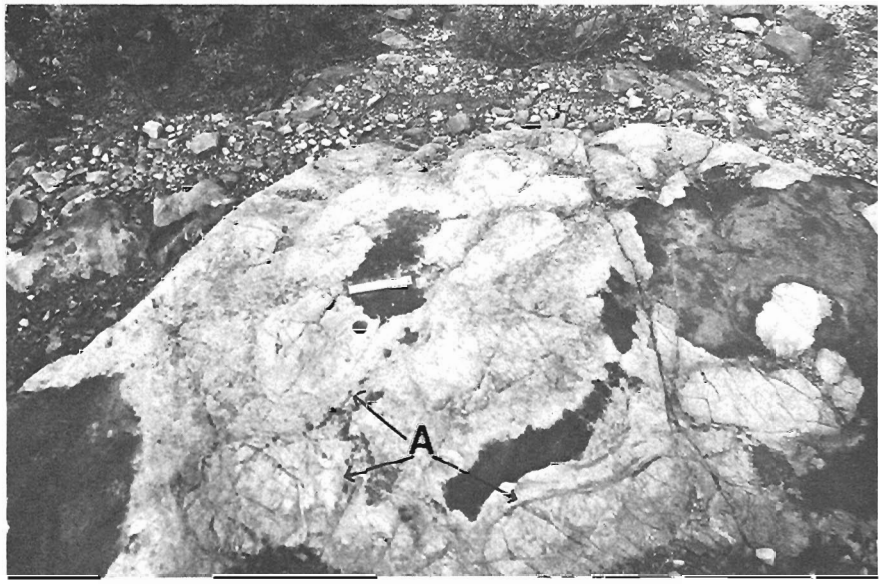

Figure 41.2b. Subrounded pyritite fragments (A) set in pyrite matrix (scale – 15 cm). The thin rusty veneer shows up as dark patches coating massive sulphides.

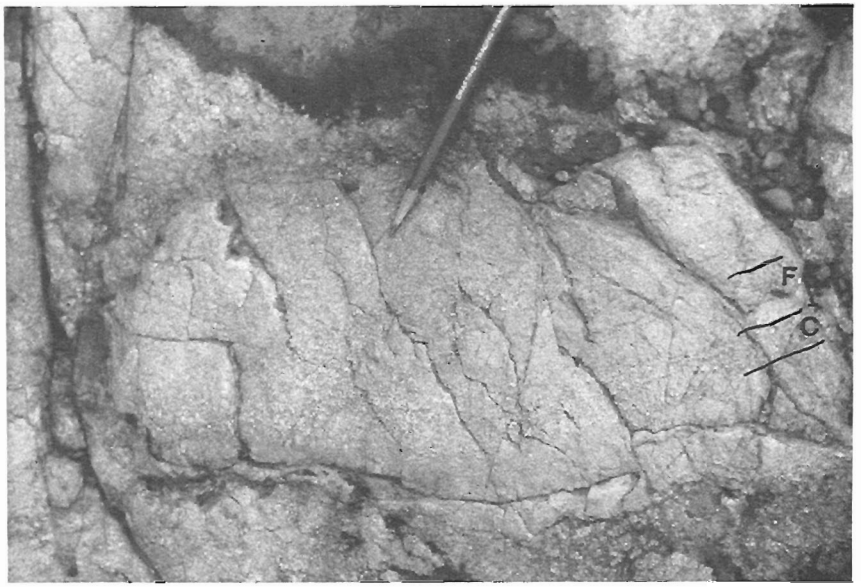

Figure 41.4. Pyritite fragment containing irregular bands defined by pyrite grain size (F – fine; C – coarse).

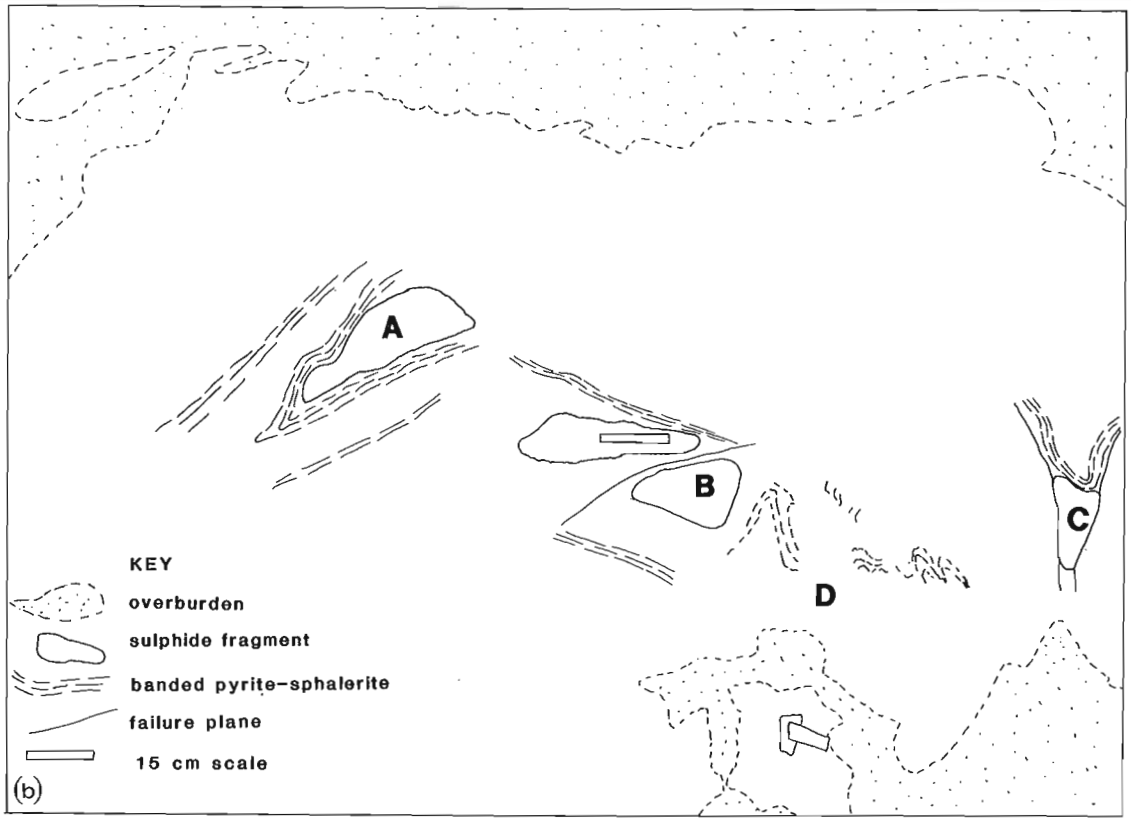

A. *Pyritite fragment has slumped into banded sulphides resulting in 'bedding' sag. An area above and to the right of the fragment contains no banded sulphides which suggests that the general direction of slumpage was down and to the left.*

B. *Movement along a fault plane, probably initiated by fragment slumpage, caused offset in banded sulphides.*

C. *Down-dragging of banded sulphides and matrix into a graben-like structure.*

D. *Distortions in banded sulphides due to slumping.*

Figure 41.5a,b. *Band disruption and slump features observed in outcrop.*

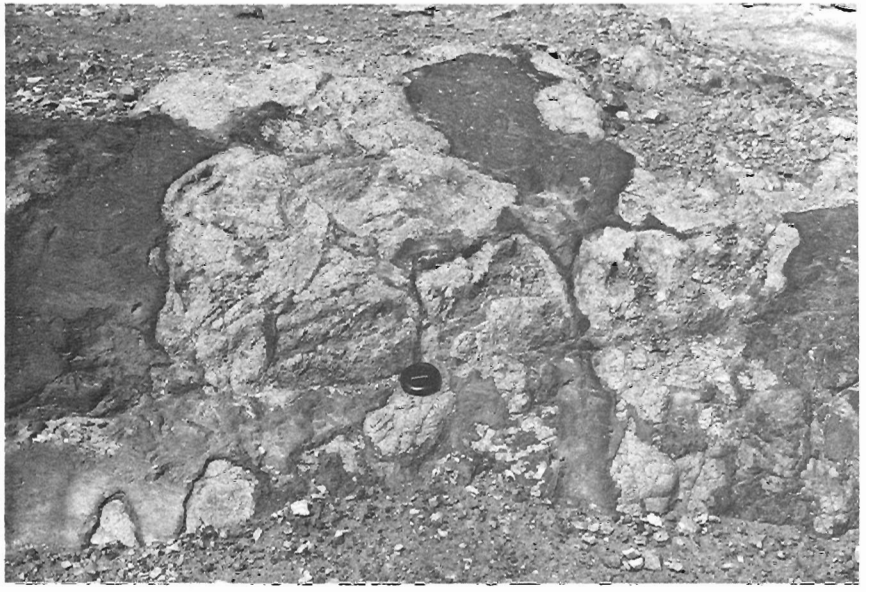

Figure 41.6. Volcaniclastic matrix (dark) to sulphide fragments (light).

Figure 41.8. Pyritite dyke crosscutting and disrupting banded sphalerite.

Figure 41.7. Volcaniclastic unit exhibiting deformed bedding (B).

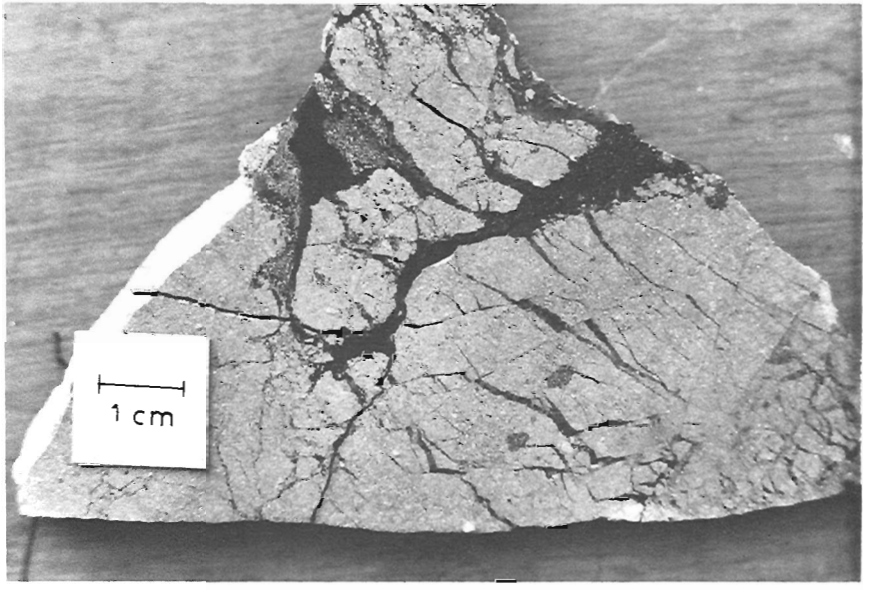

Figure 41.9. Volcaniclastic material filling fractures caused by in-situ brecciation of pyritite.

(2 mm-2 cm thick), forming an interwoven network. Some of the original tuffaceous unit remains as small relatively unaltered islands surrounded by highly altered material. Fractures within the tuff-breccia, probably caused by explosive exhalative activity, have been filled with pyrite, sphalerite and chalcopyrite. The highly altered and fractured nature of the tuff-breccia unit and the abundance of sulphides occurring as disseminations, fragments and fracture fillings indicate that this unit was possibly in a venting region for metal-rich hydrothermal solutions.

Gallen Ore Deposit

The main ore lens, where exposed by overburden stripping, is a massive sulphide body containing approximately 80-100 per cent pyrite, with locally up to 20 per cent sphalerite. The small amount of gangue consists of fine grained quartz, plagioclase, chlorite and sericite. In places, a thin rusty veneer masks the mineralogy and textures. No recrystallization textures due to metamorphism are observed within the sulphides.

Sulphide fragments of many sizes within a dominantly sulphide matrix characterize most of the main ore lens. However, in the southeast corner of the ore lens pyritic material contains relatively few fragments and has fine sphalerite, and laminae can be traced in a discontinuous manner for more than 20 m.

a) Mineralogy and Textures

Pyrite occurs as subhedral to euhedral crystals 1 mm to 5 mm in size and as rare spheroidal growths, and sphalerite as brown to reddish brown, subhedral crystals from less than 1 mm to 5 mm in diameter. Minor irregular patches of galena, up to 3 mm across, have been observed.

Pyritite (Schermerhorn, 1970) is most commonly fragmental, but also forms bands and a major component of the matrix. The pyritite fragments are poorly sorted, angular (Fig. 41.2a) to subrounded (Fig. 41.2b), randomly oriented, and range from less than 1 cm to more than 60 cm in diameter. Individual pyrite grains range from fine to coarse and pyrite fragments are equigranular to inequigranular. Pyritite fragments consisting of equigranular, fine grained pyrite tend to be angular. Commonly, sulphide fragments display 'fragment within fragment' textures. Banded pyrite forms monomineralic layers, several millimetres to 30 cm in thickness, and is found alternating with layers of sphalerite that are 2 mm to 1.5 cm thick. Thin pyritite bands, commonly enclosed in sphalerite, are highly contorted (Fig. 41.3). Larger bands are generally fragmented.

Pyrite, of variable grain size, is also the dominant mineral in the matrix to the fragments. Typically, irregularly shaped, discontinuous bands of equigranular pyrite occur within the matrix as well as within larger sulphide fragments (Fig. 41.4). This gives the matrix a generally contorted appearance. Wispy laminations of sphalerite are also present in the matrix.

Most of the sphalerite occurs in planar to highly contorted, discontinuous laminae and bands that are 2 mm to 1.5 cm thick. Apparent stacking and buckling of these bands has resulted in very irregular localized knots of sphalerite (Fig. 41.5a,b).

Fine grained, probably volcaniclastic material is found within the sulphide lens, predominantly at the northern contact with the felsic tuff-breccia unit. It consists mainly of chlorite, sericite, plagioclase and euhedral pyrite and occurs both as large irregularly shaped fragments within a sulphide matrix and as matrix surrounding sulphide fragments (Fig. 41.6). Locally, well defined bedding occurs in large blocks of the volcaniclastic material (Fig. 41.7).

(b) Deformational Features

Attempted reconstruction of bands of pyrite and interlayered sulphide from neighbouring fragments and evidence of boudinage of layers strongly suggest that the fragmental nature of the main lens of the Gallen deposit was the result of the breakage of continuous sulphide bands. The slumping of the large fragments, derived from thick bands, has contorted and deformed less competent sulphide bands and matrix. Slumpage features observed within the sulphide lens (Fig. 41.5a,b) indicate that the pyrite matrix behaved incompetently and in places was highly mobile (Fig. 41.8).

The volcaniclastic unit within the main ore lens has also undergone deformation. Distinct, highly contorted bedding is present in places in larger fragments of volcaniclastic rock (Fig. 41.7). This bedding is not present in volcaniclastic material forming the matrix to sulphide fragments (Fig. 41.6) and the fillings of fractures in the sulphides (Fig. 41.9). These characteristics suggest that the volcaniclastic unit was, during massive sulphide formation, a water-rich and unconsolidated seafloor mud.

Discussion

Several facts suggest that the main lens of the Gallen deposit is a volcanogenic massive sulphide deposit that formed at the seafloor by the precipitation of sulphides from metal-rich hydrothermal solutions; a) proximity and intimate association of a felsic tuff-breccia unit to massive sulphides, b) fragmentation and alteration of this tuff-breccia by hydrothermal action, c) presence of a volcaniclastic seafloor mud within the massive sulphides and d) rhythmic layering of pyrite and sphalerite, indicative of differential sulphide precipitation from metal-rich brines.

Textures observed in the sulphides are interpreted to be due to slumpage of competent sulphide blocks into less competent sulphide matrix and banded sulphides. The lack of recrystallization textures in the sulphides indicates that metamorphism has not had a great effect, so that the slumping was probably syngenetic. Such downslope slumpage of massive sulphide bodies accounts for many deformation textures observed in other deposits (Kajiwara, 1970; Fisher, 1970; Rickard and Zweifel, 1975; Solomon and Walshe, 1979). The Gallen ore bears a striking resemblance to the 'breccia ore' of the Kuroko deposits, where ore fragments are enclosed in ore matrix. This texture was attributed to downslope movement of massive sulphide lenses by Matsukuma and Horikoshi (1970).

In order to account for the richly fragmented nature of the Gallen ore and for sulphide fragments with 'fragment within fragment' textures, a mechanism of longer duration than an abrupt single collapse of the sulphide mass and with a repetitive nature must have been operative. Two possibilities are suggested: 1) The volume of accumulating sulphide directly overlying the discharge site of hot brines was probably highly fluidized and therefore more buoyant than 'colder' less active volumes. Within this fluidized zone, constant jostling and sifting of sulphide grains as the hot solutions moved upward could have resulted in grain sorting (Henley and Thornley, 1979). This could explain the segregations of pyrite grains as observed in Figure 41.4. In the 'colder' volumes of the sulphide mass, consolidation of sulphides into layers may have occurred contemporaneously. A change in the discharge direction of the brines, perhaps caused by precipitation of sulphides within fractures acting as channelways, could result in the invasion of the 'colder' sections by a hotter, fluidized sulphide mass. This could have led to the fragmentation of the semiconsolidated to consolidated sulphide layers. The sulphide fragments would probably slump into and be engulfed by the fluidized sulphide thereby creating 'breccia ore'. Those fragments derived from

semiconsolidated layers would be rounded by the slumping action. Continuation of this process would produce sulphide fragments exhibiting 'fragment within fragment' textures. 2) A rhythmic or pulsating discharge of the hot solutions could also have occurred. During the waning part of the rhythmic discharge cycle, the loss of fluidizing component within the sulphide mass overlying the discharge site, may have led to the collapse of the fluidized 'hot' volume. Consolidated layered sulphides formed or forming at the boundary of the fluidized channel could break up and the resulting sulphide fragments would follow the collapse of, and become incorporated into, the fluidized sulphide matrix forming the 'breccia ore' texture. If discharge was renewed, further fragmentation of the sulphide breccia would occur.

Continued formation of the sulphide mound most likely led to gravitational instability which, possibly coupled with volcanic tremors, resulted in slope failure and mass slumpage. Failure may have been enhanced by the unconsolidated nature of the underlying volcaniclastic material, some of which probably was incorporated in the sulphide body during slumpage. Although it has not as yet been determined if the sulphide lens and the enclosing felsic material slumped en masse downslope, downslope movement of the sulphide lens relative to the felsic material appears to have occurred. This downslope movement, which probably accounted for some of the fragmentation of layered sulphides, is judged to have been minor due to the interpreted proximity of the venting region and the large sulphide fragment sizes. This is in contrast to a greater downslope movement of granular sulphide as outlined by MacGeehan et al. (1981).

Acknowledgments

We are grateful to Noranda Mines Limited for permission to study the Gallen deposit and, in particular, to Ian Atkinson for his co-operation and assistance throughout the field season. We also thank Drs. J.M. Franklin and R.I. Thorpe for reviewing the manuscripts. The project was financed by E.M.R. research agreement 205-4-81 to D.H. Watkinson.

References

De Rosen-Spence, A.F.
1976: Stratigraphy, development and petrogenesis of the central Noranda volcanic pile, Noranda, Quebec; unpublished Ph.D. thesis, University of Toronto, 166 p.

Fisher, D.F.
1970: Origin of the No. 5 Zone, Horne Mine, Noranda, Quebec; unpublished M.Sc. thesis, University of Western Ontario, London, Ontario, 114 p.

Henley, R.W. and Thornley, P.
1979: Some geothermal aspects of polymetallic massive sulphide formation; Economic Geology, v. 74, p. 1600-1612.

Kajiwara, Y.
1970: Syngenetic features of the Kuroko ore from the Shakanai mines; in Volcanism and Ore Genesis, ed. T. Tatsumi; Tokyo, University of Tokyo Press, p. 197-206.

MacGeehan, P.J., MacLean, W.H., and Bonenfant, A.J.
1981: Exploration significance of the emplacement and genesis of massive sulphides in the Main Zone at the Norita Mine, Matagami, Quebec; Canadian Institute of Mining and Metallurgy, Bulletin, v. 74, no. 828, p. 59-75.

Matsukuma, T. and Horikoshi, E.
1970: Kuroko deposits in Japan, a review; in Volcanism and Ore Genesis, ed. T. Tatsumi; Tokyo, University of Tokyo Press, p. 153-180.

Oeille, A.V.
1949: Noranda Mines Ltd., Internal Report.

Rickard, D.T. and Zweifel, H.
1975: Genesis of Precambrian sulphide ores, Skellefte District, Sweden; Economic Geology, v. 71, p. 672-681.

Roscoe, S.M.
1965: Geochemical and isotopic studies, Noranda and Matagami areas; Canadian Institute of Mining and Metallurgy, Transactions, v. 68, p. 279-285.

Schermerhorn, L.J.G.
1970: The Deposition of Volcanics and Pyritite in the Iberian Pyrite Belt; Mineralium Deposita, v. 5, p. 273-279.

Solomon, M. and Walshe, J.L.
1979: The formation of massive sulphide deposits on the seafloor; Economic Geology, v. 74, p. 797-813.

Spence, C.D. and De Rosen-Spence, A.F.
1975: The place of sulphide mineralization in the volcanic sequence at Noranda, Quebec; Economic Geology, v. 70, p. 90-101.

GEOLOGY OF PASADENA MAP AREA, NEWFOUNDLAND

EMR Research Agreement 218-4-81

Harold Williams[1], R.T. Gillespie[1], and D.A. Knapp[1]
Precambrian Geology Division

Williams, Harold, Gillespie, R.T., and Knapp, D.A., Geology of Pasadena map area, Newfoundland; in Current Research, Part A, Geological Survey of Canada, Paper 82-1A, p. 281-288, 1982.

Abstract

Rocks of the Pasadena map area consist of five contrasting assemblages of mainly Cambrian and Ordovician age, overlain by a Carboniferous cover sequence. Four of the assemblages are allochthonous with respect to the fifth, an underlying carbonate terrane. Allochthonous rocks are mainly clastic sedimentary rocks and ophiolitic suites. Their place of origin and transport can be related to a model involving the evolution and destruction of an ancient continental margin. Southeast facing structures predominate in allochthonous rocks in the central part of the area. These structures are interpreted as superimposed upon conventional westerly transported allochthons. Subhorizontal Carboniferous rocks unconformably overlie older deformed rocks west of Deer Lake. East of Deer Lake, Carboniferous rocks are overturned to the west where overthrust by an ophiolite suite and metamorphic rocks.

Introduction

Mapping of the Pasadena area (12 H/4) began during the summer of 1981 and approximately 60 per cent of the area has been completed in detail suitable for 1:50 000 presentation. This is part of a continuing project in western Newfoundland, which includes the mapping of the Stephenville area (12B), north half (Williams, 1981) and aims to include Lomond area (12 H/5). Within the Pasadena area (Fig. 42.1), H. Williams has mapped parts of the entire area, R.T. Gillespie has concentrated on a broad structural transect from Goose Arm through Old Mans Pond to Hughes Lake as part of an M.Sc. thesis project, and D.A. Knapp has mapped the area east of Deer Lake that includes an ophiolitic complex like that at Glover Island (Knapp, 1980) and elsewhere along the Baie Verte-Brompton Line (Williams and St. Julien, 1981).

The Pasadena area is rugged terrain, that is heavily tree covered except for the highest hills in its central parts and the area of ultramafic rocks at North Arm. A network of private woods roads has greatly facilitated the present mapping. Other parts of the area are accessible by boat from the coast or from Deer Lake. Inland areas are accessible by float plane or helicopter, both of which are available for charter from nearby South Brook.

The geology of the Pasadena area is typical of the west flank of the Appalachian Orogen, but with marked local peculiarities in stratigraphy and structural style. From northwest to southeast, the area provides an uninterrupted corridor from the highly allochthonous ophiolites of the Bay of Islands Complex at North Arm to their possible root zone at Pynns Brook, thus providing an opportunity to study the stratigraphy and structure of the overridden segment of the ancient continental margin of eastern North America.

The Pasadena area was mapped by Baird (1960) as part of the reconnaissance mapping of the Sandy Lake (12 H), west half, area. Westerly parts of the area were included in a more detailed study by Lilly (1963) who subdivided the carbonate sequence and rocks of the Humber Arm Allochthon, although all of the rocks were viewed as autochthonous during these early phases of mapping. Carboniferous rocks of the Deer Lake Basin were studied by Belt (1969) and Popper (1970), and more recently by Hyde (1978, 1979). The mafic-ultramafic rocks of the Pynns Brook area were mapped by geologists of the Asbestos Corporation of Canada during 1979-80 and much of this work is recorded in a M.Sc. thesis by O'Loughlin (1981).

General Geology

Rocks of the Pasadena area are mainly of Cambrian-Ordovician age and include several contrasting lithic assemblages (Fig. 42.1). Crystalline rocks occur in the vicinity of Hughes Lake and these are interpreted as Grenvillian basement of Helikian or earlier age. Carboniferous sedimentary rocks cover an extensive area in the vicinity of Deer Lake.

The Cambrian-Ordovician rocks have been affected by early to middle Paleozoic deformation, which has also affected the crystalline rocks. Carboniferous rocks west of Deer Lake form a subhorizontal cover upon deformed Cambrian-Ordovician rocks. East of Deer Lake, Carboniferous rocks are overturned and deformed, with the Carboniferous structural front roughly coincident with the western contact of structurally emplaced older rocks.

Early Paleozoic rocks of the Pasadena area can be separated into five contrasting assemblages, all partly coeval. The most extensive is a mainly carbonate sequence that is interpreted as essentially autochthonous (map units 1-3)[2]; the other assemblages are all allochthonous with respect to the carbonate terrane. From northwest to southeast these are: the Humber Arm Supergroup (4-8) and Bay of Islands Complex (9-10) of the Humber Arm Allochthon; the Old Mans Pond group[3] (11-13) and small gabbroic bodies (14) of the Old Mans Pond allochthon; the Hughes Lake complex (15) and Pasadena group (16-17) of the Hughes Lake allochthon; and the Pynns Brook complex (18-20) that is also transported. In the account that follows the rocks and structures of each assemblage or allochthon are described separately, followed by a description of Carboniferous rocks and structures, and a brief summary of tectonic history.

Carbonate Sequence

Rocks of the carbonate sequence, best exposed at Goose Arm, can be traced northeastward and eastward across the northern part of the map area. Basal parts of the section are referred to as the Penguin Cove formation (Lilly, 1963) at Goose Arm and the Reluctant Head formation (Lilly, 1963) at Old Mans Pond and northward. The main section of carbonate rocks correlates with the St. George Group (Schuchert and Dunbar, 1934). It is overlain by the Table Head Group (Schuchert and Dunbar, 1934; Klappa et al., 1980), which has been separated only locally during this phase of mapping. At Penguin Arm and southward, the Table Head is overlain by a thin unnamed clastic unit (3).

[1] Department of Geology, Memorial University of Newfoundland, St. John's, Newfoundland, A1B 3X5

[2] Numbers refer to map units of Figure 42.1

[3] All new names informal

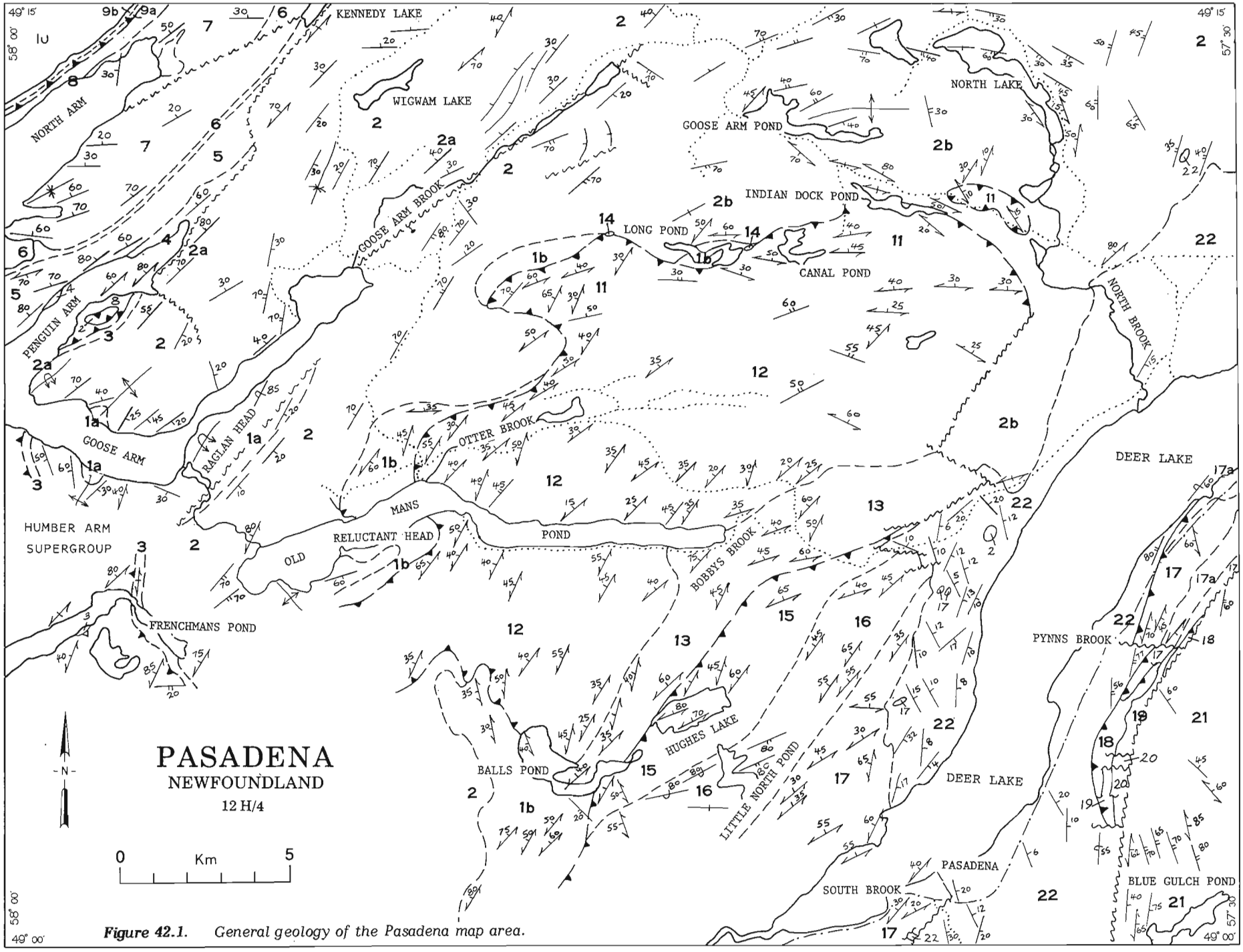

Figure 42.1. General geology of the Pasadena map area.

LEGEND

CARBONIFEROUS

22 DEER LAKE GROUP: buff to reddish pebble to boulder conglomerate, grey and red shale and sandstone

21 ANGUILLE GROUP: thick bedded grey sandstone and black shale, minor conglomerate

HUMBER ARM ALLOCHTHON (4-10)

UPPER CAMBRIAN TO LOWER ORDOVICIAN
BAY OF ISLANDS COMPLEX (9-10)

10 Harzburgite and serpentinized ultramafic rocks

9 Greenschist (9a), black amphibolite and garnetiferous amphibolite (9b)

HUMBER ARM SUPERGROUP (4-8)

8 Chaotic mixture of Irishtown quartzite, Blow Me Down greywacke and Cooks Brook limestone blocks in a black shaly matrix

LOWER ORDOVICIAN

7 BLOW ME DOWN BROOK FORMATION: coarse greywacke, pebble conglomerate, arkosic sandstone, quartz sandstone, minor red shale

6 MIDDLE ARM POINT FORMATION: thin bedded dark grey shale and buff dolomitic siltstone

MIDDLE CAMBRIAN TO LOWER ORDOVICIAN

5 COOKS BROOK FORMATION: thin bedded dark grey shale and light grey platy limestone, coarse limestone breccia units

LOWER TO MIDDLE CAMBRIAN

4 IRISHTOWN FORMATION: dark grey shale and siltstone with thick white quartzite and quartz pebble conglomerate units

CARBONATE TERRANE (1-3)

MIDDLE ORDOVICIAN

3 Grey to green sandstone and shale

UPPER CAMBRIAN TO MIDDLE ORDOVICIAN

2 ST. GEORGE AND TABLE HEAD GROUPS: medium- to thick-bedded limestone and dolomite with thin shale units; 2a, Table Head Group, thick bedded limestone, limestone breccia and minor shale; 2b, recrystallized limestone and marble

LOWER TO MIDDLE CAMBRIAN

1 PENGUIN COVE FORMATION: 1a, thin bedded limestone and shale with quartzites toward base and button algae and oolitic beds at top; RELUCTANT HEAD FORMATION: 1b, thin bedded grey limestone and buff shale, limestone breccia, oolitic limestone at top

UPPER CAMBRIAN OR LOWER ORDOVICIAN
PYNNS BROOKS COMPLEX (18-20)

20 Mafic volcanic rocks, minor conglomerate

19 Mainly altered gabbro

18 Serpentinite and altered ultramafic rocks

HUGHES LAKE ALLOCHTHON (15-17)

CAMBRIAN TO LOWER ORDOVICIAN
PASADENA GROUP (16-17)

17 SOUTH BROOK FORMATION: micaceous quartz-feldspar pelitic to psammitic schists; 17a, tan quartz-muscovite schist, minor marble

16 LITTLE NORTH POND FORMATION: coarse arkosic meta-greywacke, schistose greywacke and phyllitic schist

PRECAMBRIAN? (HELIKIAN?)

15 HUGHES LAKE COMPLEX: mildly foliated to schistose pink granite and granitic gneiss, magnetite-quartz-feldspar gneiss and schist, albite-chlorite schist, amphibolite and metadiabase

OLD MANS POND ALLOCHTHON (11-14)

UPPER CAMBRIAN OR LOWER ORDOVICIAN

14 Metagabbro and serpentinized ultramafic rocks

LOWER CAMBRIAN TO LOWER ORDOVICIAN
OLD MANS POND GROUP (11-13)

13 BOBBYS BROOK FORMATION: thin bedded limestone and shale, limestone breccia

12 OTTER BROOK FORMATION: grey shale and siltstone, phyllite, prominent thick white quartzite units

11 CANAL POND FORMATION: grey to green greywacke, white to pink quartz sandstone, quartzite, pebble conglomerate and grey to purple argillite

Geologic contact (defined, approximate) . . . . . .

Major tectonic contact between contrasting rock groups, teeth on upper plate . . . . . .

High angle fault (approximate, inferred) . . . . . .

Bedding, tops known (upright, overturned) . . . . . .

Bedding, tops unknown (inclined, vertical) . . . . . .

Cleavage, schistosity, foliation (inclined, vertical) . . . . . .

Anticlinal axis (upright, overturned) . . . . . .

Synclinal axis . . . . . .

Trans Canada Highway . . . . . .

Mainly private gravel roads . . . . . .

The Penguin Cove formation is best exposed in two upright to westerly inclined anticlines on opposite sides of Goose Arm. It also occurs in a faulted section between Goose Arm and Old Mans Pond. Total thickness is not more than 200 metres. Basal parts of the section consist of quartzite with thin units of limestone, dolomite and shale. Thin bedded grey shale, buff dolomitic shale and grey limestone are common in central parts of the section, and distinctive oolitic limestone and button algae beds occur at its top. At Goose Arm, the Penguin Cove formation is overlain conformably by medium- to thick-bedded limestones and dolomites of the St. George Group.

The Reluctant Head formation is best exposed at Reluctant Head on the south side of Old Mans Pond. It occurs northward to Long Pond and also west of Balls Pond. South of Balls Pond, it is traceable 30 km southward to Humber Gorge (Lilly, 1963) and far beyond to the south end of Grand Lake (Kennedy, 1981). At Old Mans Pond the section is approximately 200 metres thick and consists of thin bedded, buff, dolomitic shales and grey limestones. Slumped units and breccias consisting of platy limestone clasts in shale are common in some places. The contact between the Reluctant Head formation and overlying St. George Group is well exposed on the woods road north of Old Mans Pond. There, the Reluctant Head contains oolitic limestones at its top and these are overlain conformably by thick bedded limestones and dolomites of the St. George Group.

Both the Penguin Cove and Reluctant Head formations bear the same stratigraphic relationship to overlying beds of the St. George Group, and are thought therefore to be stratigraphic equivalents, at least in part. Their position beneath the St. George Group and lithic similarities to the Forteau Formation (Schuchert and Dunbar, 1934) – especially the thin bedded shales, oolitic beds and button algae horizons – suggest an Early Cambrian age. South of the map area, between Humber Gorge and the south end of Grand Lake, rocks that are physically continuous with the Reluctant Head formation are referred to the Grand Lake Brook Group (Walthier, 1949; Kennedy, 1981).

The St. George Group is well exposed at Goose Arm and northeastward where it is more than a kilometre in stratigraphic thickness. It consists of medium- to thick-bedded grey limestone, buff dolomite and minor shale. In the vicinity of North Lake, Goose Arm Pond and Indian Dock Pond, the rocks are recrystallized and are fine- to medium-grained, dark grey to light grey and white marble (2b).

Upper parts of the carbonate section at Penguin Arm and Goose Arm Brook are thick bedded grey bioturbated limestones typical of the Table Head Group (2a). Other occurrences of Table Head carbonates have been outlined by Lilly (1963) at Raglan Head and southward. Structural complexity and a lack of continuous stratigraphic sections precludes the sharp separation of the St. George and Table Head groups in the map area, especially in the northeast where the rocks are recrystallized and unfossiliferous.

At Penguin Arm the carbonate section is overlain by a thin unit of dark grey shale and sandstone (3), in turn succeeded by chaotic rocks (8) of the Humber Arm Allochthon. More carbonates occur structurally above the chaotic rocks and constitute the Penguin Hills. The Penguin Hills occurrence is interpreted as a carbonate structural sliver near the tectonic base of the Humber Arm Allochthon (Penguin Hills Klippe of Lilly, 1963).

In the western part of the map area, bedding and cleavage of the carbonate rocks trend northeast and the rocks are involved in folds that are upright to westerly inclined and locally overturned to the west, e.g. at Penguin Head and Raglan Head. Farther east at Old Mans Pond, folds in the Reluctant Head formation face east with axial plane cleavage dipping moderately west. This opposing direction of structural polarity is one of the most prominent features of the Pasadena area. In the northern part of the area from Goose Arm Brook to North Lake, bedding, cleavage and fold axes of the carbonate rocks form an arc that is convex northward. This is interpreted as the result of a later open structure about a northerly axis.

Humber Arm Allochthon

The Humber Arm Allochthon in the western part of the area structurally overlies the carbonate terrane, although the contact between the two has been modified by a high angle fault between Penguin Arm and Kennedy Lake. The lower part of the allochthon is composed of sedimentary rocks of the Humber Arm Supergroup (4-8). These are overlain by a higher structural slice of metamorphic (9) and igneous rocks (10) of the Bay of Islands Complex (Cooper, 1936; Smith, 1958; Williams, 1973) at North Arm.

Five sedimentary formations of the Humber Arm Supergroup are represented within the allochthon and these are correlatives of the Summerside, Irishtown, Cooks Brook, Middle Arm Point, and Blow Me Down Brook formations in the type area at Humber Arm (Curling Group of Stevens, 1970). Greywackes of the lowest formation, Summerside, occur in the vicinity of Frenchmans Pond and underlie much of the unmapped southwest portion of the Pasadena area. Between Penguin Arm and North Arm, the rocks of the supergroup form a northwest-facing and northwest-dipping section with the Irishtown shales and quartzites at its base. These are followed northwestward by thin bedded shales, limestones and limestone breccias of the Cooks Brook Formation, followed by thin bedded dark grey to black and buff shales of the Middle Arm Point Formation, in turn followed by thick graded greywacke beds and crossbedded quartz sandstones of the Blow Me Down Brook Formation. The Middle Arm Point Formation is locally slumped and chaotic, with greywacke, quartzite and carbonate blocks in a dark shaly matrix. Similar chaotic rocks (8) occur at North Arm, and are especially prominent along the structural base of the Bay of Islands Complex.

The Bay of Islands Complex consists of a thin dynamothermal aureole of greenschists (9a) and amphibolites (9b) overlain by brown weathering serpentinized ultramafic rocks (10).

No fossils are known within the Humber Arm Supergroup of the Pasadena area and the ages of its formations are assigned by correlation with fossiliferous rocks nearby (Stevens, 1970; Williams, 1973).

At the east side of Kennedy Lake, chaotic shales with greywacke blocks are in sharp vertical contact with deformed and recrystallized limestones. A similar steep contact between grey slates and deformed limestone occurs at the head of Penguin Arm. Both contacts are interpreted as faults because of stratigraphic omission at the top of the autochthon. The contact is also steep at the south side of Goose Arm with possible repetition of Humber Arm clastics and autochthonous carbonates. Structural complications are common all along the east margin of the Humber Arm Allochthon farther south in the Stephenville area (Williams, 1981) and these complications contrast with the clear succession of autochthonous units and sharp structural base of the allochthon along its western margin.

Old Mans Pond Allochthon

The Old Mans Pond allochthon occupies the central portion of the map area, roughly centred at the east end of Old Mans Pond. It is surrounded on all sides by rocks of the carbonate terrane, except at its southeast corner where it is bordered by the Hughes Lake allochthon.

Rocks of the Old Mans Pond allochthon are designated the Old Mans Pond group, which is divisible into three lithic units of formational status, namely the Canal Pond, Otter Brook and Bobbys Brook formations. The Canal Pond formation occupies the northern portion of the allochthon and also occurs in a small outlier between Indian Dock Pond and North Brook. It is an arenaceous unit consisting of grey to green and pink greywackes, grey to white quartzite, quartz pebble conglomerate, and green to purple slates. The Otter Brook formation is the most extensive and underlies the broad central portion of the allochthon. It consists primarily of dark grey slates and siltstones with prominent units of white thick bedded quartzite and quartz pebble conglomerate. Local outcrops of carbonate breccia and thin bedded siltstone and buff dolomite occur along its northwest margin. The Bobbys Brook formation, along the southeast margin of the allochthon, consists of thin bedded grey marble and grey phyllite with local occurrences of oolitic limestone and limestone breccia beds, some of which contain button algae in their matrix. Two small bodies of altered gabbro in the vicinity of Long Pond are also included in the allochthon.

The order of stratigraphic units of the Old Mans Pond group has not been worked out in the field and the boundary between the Canal Pond and Otter Brook formations is little more than a broad gradational zone between mainly arenaceous rocks to the north and argillaceous rocks to the south. In addition, the ages of the units are unknown. However, marked lithic similarities among rocks of the Old Mans Pond group imply correlation with those of the Humber Arm Allochthon. The Canal Pond formation resembles the Summerside Formation at the base of the Humber Arm Supergroup, the Otter Brook formation is virtually identical to the succeeding Irishtown Formation, and the Bobbys Brook resembles the overlying Cooks Brook Formation. Thus the order of stratigraphic units in the Old Mans Pond group is from older to younger from northwest to southeast. Button algae units and local oolitic beds in the Bobbys Brook formation further imply correlation with the Cambrian Penguin Cove and Reluctant Head formations of the carbonate sequence. The Old Mans Pond group is viewed therefore as a proximal equivalent of the Humber Arm Supergroup that shares features with the carbonate sequence to the west and lower units of the Humber Arm Supergroup that lay to the east.

The most prominent structural feature of rocks of the Old Mans Pond allochthon is a pervasive northeast-trending cleavage that dips moderately northwestward across central parts of the allochthon. Farther north at Canal Pond, the cleavage follows the periphery of the allochthon and dips moderately northward. In the vicinity of Old Mans Pond, the cleavage is axial planar to isoclinal folds, and wherever sedimentary features are preserved, cleavage-bedding relationships indicate that the folds face upward and to the southeast. The folds and cleavage are interpreted as first phase deformational effects as no earlier structures or fabrics are present. Later fabrics include a widely spaced weak cleavage that is roughly parallel to the main penetrative cleavage, and an east-dipping crenulation cleavage.

Argillaceous rocks of the central portion of the Old Mans Pond allochthon are mainly phyllites with local incipient porphyroblasts developed on cleavage surfaces. Farther east, its carbonate rocks are recrystallized to marble and interbedded pelitic rocks are glossy grey phyllites.

The Old Mans Pond allochthon has little morphologic expression. Its contact with the carbonate terrane is exposed only along its western margin. Elsewhere the contact is marked by topographic depressions. In the vicinity of Otter Brook, the Reluctant Head formation of the carbonate sequence and the Otter Brook formation of the allochthon are separated by a west-dipping high-angle fault, marked by a narrow zone of intense deformation. Farther north, the contact is interpreted as a fault because of topographic expression and stratigraphic omission. This interpretation is supported by the occurrence of deformed metagabbro bodies at the contact in the vicinity of Long Pond. There is nothing to suggest that these are intrusions and in all likelihood they are of ophiolitic affinity. Similar small mafic-ultramafic bodies occur along a carbonate terrane-metaclastic terrane tectonic contact at the south end of Grand Lake (Kennedy, 1981).

Hughes Lake Allochthon

The Hughes Lake allochthon lies between Hughes Lake and Deer Lake but also includes metamorphic rocks on the east side of Deer Lake at Pynns Brook. The allochthon consists of a basal gneissic complex in the northwest (Hughes Lake complex), overlain by a thick arkosic metagreywacke unit to the southeast (Little North Pond formation), overlain in turn by pelitic and psammitic schists of the South Brook formation. The latter formations (16-17) are collectively referred to as the Pasadena group.

The Hughes Lake complex consists of pink foliated granite, granitic gneiss, magnetite-quartz-feldspar schist, albite-chlorite schist and amphibolite. Its pink gneissic rocks are interpreted as basement and correlated with Grenvillian gneisses of the Long Range Complex to the north of the map area (Baird, 1960). Amphibolites and chloritic schists that form conspicuous melanocratic units in the pink gneisses are interpreted as metamorphosed and deformed mafic dykes. Schists included in the complex may represent Helikian metasedimentary rocks or possibly reworked and retrograded derivatives of original gneisses. Gneissic foliation and schistosities within the complex trend northeast and dip moderately northwest, and are parallel therefore to regional schistosities in the overlying Pasadena group to the southeast as well as to structures in rocks outside of the allochthon.

North of Hughes Lake, coarse grained pink foliated granites of the Hughes Lake complex are in tectonic contact with dark grey phyllites of the Old Mans Pond group. A 15 metre band of pink mylonitic to granular schist at the contact is gradational with gneisses to the southeast and it is in relatively sharp contact with phyllites to the northwest. All fabrics in the contact zone trend northeast and dip moderately northwest.

The Hughes Lake complex is followed to the southeast by a continuous, distinctive, thick (approximately 2 km) sequence of metamorphosed arkosic sandstone, quartz greywacke, pebble conglomerate and pelitic schist of the Little North Pond formation. The clastic rocks form high ridges with little vegetation compared to bounding terrains so that single units can be traced many kilometres without structural complications. Beds are vertical to steeply northwest-dipping and crossbedding in the arkosic beds indicates tops toward the southeast. The actual contact with the Hughes Lake complex to the northwest has not been found but at Little North Pond it is limited to within a few metres and represents a narrow zone of marked lithic contrast. The continuity of the Little North Pond formation, its constant thickness, uniform lithology and consistent southeast-facing stratigraphy all combine to indicate that it is a clastic cover sequence overlying the Hughes Lake complex. Its arkosic sandstones and quartz pebble conglomerates resemble the Bradore Formation (Schuchert and Dunbar, 1934) that overlies Grenvillian basement rocks to the north, although the Little North Pond formation is much thicker and coarser.

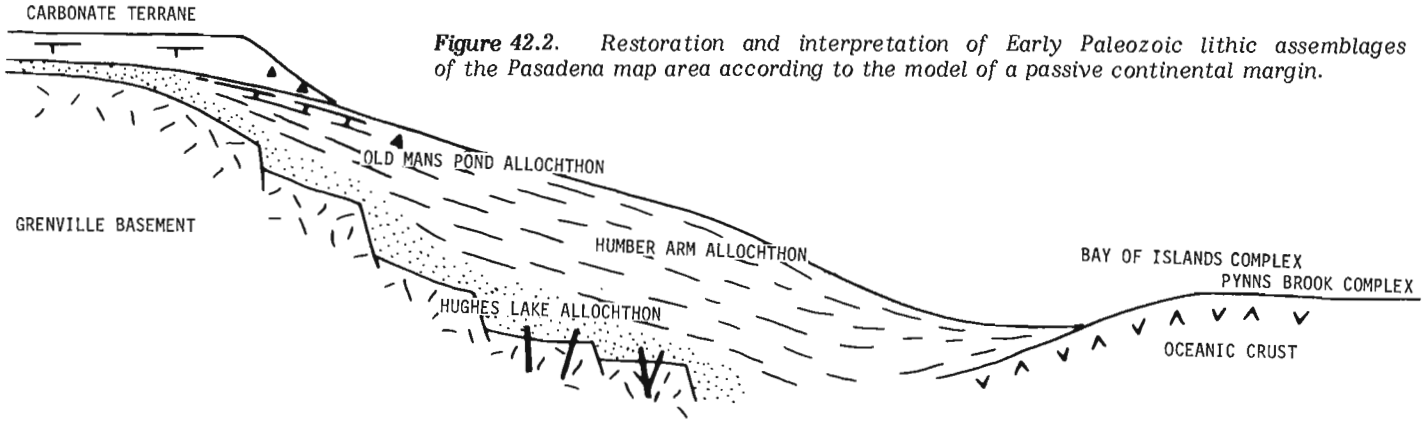

Figure 42.2. *Restoration and interpretation of Early Paleozoic lithic assemblages of the Pasadena map area according to the model of a passive continental margin.*

The South Brook formation lies to the southeast of the Little North Pond formation and is interpreted as stratigraphically younger. Rocks at Pynns Brook on the east side of Deer Lake are inferred to be continuous beneath their Carboniferous cover with similar rocks at South Brook.

The South Brook formation consists of semipelitic and psammitic schists composed of quartz, feldspar, muscovite, biotite and garnet. Quartzitic units, coarse feldspathic units and arkosic metagreywackes are all prominent locally. At Pynns Brook, the rocks are biotite-muscovite-chlorite-quartz-feldspar schists and include more massive tan weathering muscovite-biotite-quartz schists (17a).

Three phases of deformation are recognized in the South Brook formation at its type area. An early schistosity is folded by second phase isoclinal folds containing an axial planar crenulation cleavage. All of these structures are affected by third phase folds with northeast-trending axes and axial planes that dip moderately northwest. An absence of similar structures in the underlying Little North Pond formation reflects the competent nature of its thick clastic units.

The South Brook formation is similar in lithology, metamorphic grade and structural style to rocks of the Fleur de Lys Supergroup to the north at the Baie Verte Peninsula and to the Mount Musgrave Formation (McKillop, 1961) to the south of the map area. Collectively, the Pasadena group is inferred to be of late Precambrian to Early Cambrian age and represents a clastic sequence deposited upon a Grenvillian basement.

Pynns Brook Complex

Mafic and ultramafic rocks located at Pynns Brook and southward are referred to the Pynns Brook complex. The rocks form a discontinuous elongate unit that extends approximately 5 km to the south. It is faulted against Carboniferous rocks to the west and east, and against metaclastic rocks of the South Brook formation to the north.

The Pynns Brook complex consists of metamorphosed and deformed mafic and ultramafic plutonic and volcanic rocks. The western half of the complex consists of serpentinite and talc-carbonate schists derived from ultramafic rocks. These are strongly deformed and well foliated. Coarse grained, light green metagabbro composes much of the western half of the complex and its southern end consists of mafic metavolcanic rocks.

The contact between the Pynns Brook complex and the South Brook formation at Pynns Brook is interpreted as a major southeast-dipping thrust. At the contact, a 5 metre zone of foliated greenschist separates fine grained schists of the South Brook formation from overlying serpentinite. Foliation in both the Pynns Brook complex and the South Brook formation is parallel to foliation in the contact zone.

The order of lithic units from west to east in the Pynns Brook complex suggests it is an east-facing ophiolite sequence. Its structural setting with respect to polydeformed metaclastic rocks to the west and its geographic position with respect to similar ophiolite occurrences to the north at Baie Verte and to the south at Glover Island suggest that the Pynns Brook complex marks the Baie Verte-Brompton Line. Emplacement of the Pynns Brook complex above the South Brook formation probably occurred in the Early to Middle Paleozoic. Its position now is the result of Carboniferous thrusting.

Carboniferous Rocks

The Anguille Group (Hayes and Johnson, 1938; Belt, 1969) outcrops in a number of discontinuous fault-bounded isolated structural blocks, from its type locality in the Anguille Mountains of southwestern Newfoundland to the Conche area of the Great Northern Peninsula. In the map area, the group has been described by Popper (1970) and Hyde (1978, 1979). Maximum thickness is estimated at about 3000 metres (Hyde, 1978).

The Anguille Group consists of thin- to medium-bedded, dark grey, fine- to medium-grained sandstones, dark grey siltstones and black carbonaceous mudstones. Minor pebble conglomerates with carbonate clasts are common locally. Depositional environment is interpreted as a lacustrine delta (Popper, 1970; Hyde, 1978).

The Anguille Group is in fault contact with the Deer Lake Group and older rocks at its western margin. The fault dips steeply to the east and rocks adjacent to it are intensely deformed and foliated.

Spores and plant fossils from the Anguille Group indicate an Early Mississippian, Tournaisian age (Baird, 1960; Belt, 1969).

The Deer Lake Group (Werner, 1956; Belt, 1969) occurs in an elongate northeast-trending basin surrounding Deer Lake. Thickness of the group is estimated at about 600 metres near Deer Lake.

Subhorizontal beds of the Deer Lake Group unconformably overlie deformed rocks along the west side of Deer Lake and locally at Pasadena. Coarse breccias occur at the unconformity and considerable relief on the erosional surface is indicated by inliers of basement rocks exposed through the Carboniferous cover. East of Deer Lake, the Carboniferous rocks are steeply-dipping to overturned where they are overthrust by rocks of the Pynns Brook complex and South Brook formation.

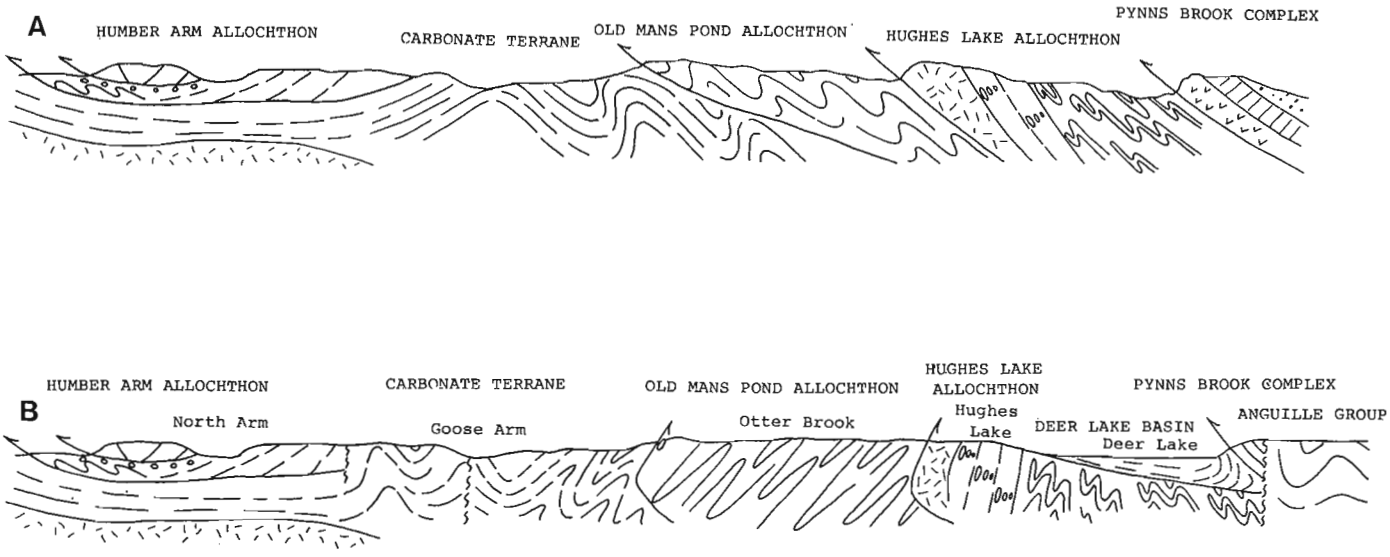

A. Conventional west facing structures related to initial westward transport of allochthonous terranes.

B. Subsequent southeast overturning of initial west directed structures in the Old Mans Pond and Hughes Lake allochthons, followed by Carboniferous deposition and later structures related to final emplacement of the Pynns Brook complex and South Brook formation.

Figure 42.3. *Tectonic development of the Pasadena map area.*

The base of the Deer Lake Group consists of coarse conglomerates and red sandstones that fine upwards into red and grey sandstones, siltstones and shales with oolitic and microcrystalline limestone interbeds. Along the west side of Deer Lake, pink limestone beds up to 20 cm thick occur locally among the red sandstones and conglomerates.

Lower portions of the Deer Lake Group are interpreted as alluvial in origin, while finer grained clastics and limestones in upper portions are interpreted as deposits of a mixed fluvial and lacustrine environment (Belt, 1969; Hyde, 1979).

Spores from the Deer Lake Group indicate a Late Mississippian, Viséan or slightly older age (R.S. Hyde, personal communication, 1981).

Tectonic Evolution

Rocks along the west flank of the Appalachian Orogen fit well with the model of an evolving continental margin that was destroyed by the obduction of oceanic crust and the tectonic transport of slope/rise sediments westward across the continental shelf. According to this model, the carbonate sequence of the map area represents an ancient continental shelf, sedimentary rocks of the Humber Arm and other allochthons represent slope/rise deposits, and ophiolitic complexes represent a sampling of oceanic crust. The distribution of the various rock groups before transport is depicted in Figure 42.2.

The following account is one possible scenario for the tectonic development of the area (Fig. 42.3). The Humber Arm Allochthon was assembled from east to west during the Early to Middle Ordovician (Stevens, 1970). The dynamothermal aureole of the Bay of Islands Complex relates to first displacement of the oceanic crust. Mélange formation accompanied the later assembly of sedimentary parts of the allochthon, and the assembled package was emplaced upon the relatively undeformed rocks of the carbonate bank. Polyphase deformation and metamorphism of the Hughes Lake complex and Pasadena group followed the emplacement of the Humber Arm Allochthon. This phase of tectonic activity that began in the Ordovician (Williams, 1977) may have continued well into the Middle Paleozoic. Assembly and emplacement of the Old Mans Pond, Hughes Lake and Pynns Brook allochthons may have begun as early as Middle Ordovician or as late as Devonian. Folds within the rocks of these allochthons, as well as folds in underlying nearby parts of the carbonate sequence, faced westward at the time of initial emplacement (Fig. 42.3, A). After emplacement, rocks and structures of the Old Mans Pond and Hughes Lake allochthons, as well as easterly parts of the carbonate sequence at Reluctant Head, were overturned to the east (Fig. 42.3, B). This phase of structural development preceded the deposition of Carboniferous cover rocks. After deposition of the Deer Lake Group, the local area to the east of Deer Lake was affected by thrusting that emplaced the Pynns Brook complex and South Brook formation, and this phase of thrusting caused westward overturning of Carboniferous strata at the thrust front (Fig. 42.3, B).

Economic Geology

Sphalerite and galena occur in rocks of the carbonate sequence in the Goose Arm area and northeastwards. The mineralization is localized mainly in lower parts of the St. George Group (Lilly, 1963).

Surface mapping and shallow drilling by Asbestos Corporation have failed to uncover significant quantities of asbestos in ultramafic rocks of the Pynns Brook complex. This ophiolite occurrence is of economic interest because of its position at the Baie Verte-Brompton Line, a well known locus of asbestos deposits elsewhere in Newfoundland and the Quebec Eastern Townships.

Molybdenite has been reported from Burnt Island, near South Brook of Deer Lake (Fogwill, 1965).

Recent interest in the general area centres on uranium discoveries in Carboniferous rocks of the Deer Lake Basin. Most prospecting to date has taken place immediately northeast of the map area.

Acknowledgments

The authors acknowledge the cheerful field assistance of Alex Pittman and the many favours provided by G.R. Dunning and his GSC party stationed at Pasadena. We extend special thanks to Viking Helicopters, Newfoundland Limited, for their excellent field support, and for providing 5 hours of free flying time as a scholarship to one of us (RTG). Permission to use Bowaters woods roads and their living and dining facilities at Old Mans Pond is also very much appreciated.

References

Baird, D.M.
1960: Sandy Lake (west half), Newfoundland; Geological Survey of Canada, Map 47-1959.

Belt, E.S.
1969: Newfoundland Carboniferous stratigraphy and its relation to the Maritimes and Ireland; in North Atlantic Geology and Continental Drift, ed. M. Kay, American Association of Petroleum Geologists, Memoir 12, p. 734-753.

Cooper, J.R.
1936: Geology of the southern half of the Bay of Islands Igneous Complex; Newfoundland Department of Natural Resources, Geology Section Bulletin 4, 62 p.

Fogwill, W.D.
1965: Mines and mineral occurrences map of the Island of Newfoundland; Department of Mines, Agriculture and Resources, Mineral Resources Division, Information Circular No. 11.

Hayes, A.O. and Johnson, H.
1938: Geology of the Bay of St. George Carboniferous area; Geological Survey of Newfoundland, Bulletin 12, p. 42-65.

Hyde, R.S.
1978: Stratigraphic subdivision and mapping of the Lower Mississippian Anguille Group, Deer Lake-White Bay area, Newfoundland; in Report of Activities for 1977, Mineral Development Division, Newfoundland Department of Mines and Energy, Report 78-1, p. 116-123.

1979: Geology of portions of the Carboniferous Deer Lake Basin, western Newfoundland; in Report of Activities for 1978, Mineral Development Division, Newfoundland Department of Mines and Energy, Report 79-1, p. 11-17.

Kennedy, D.P.
1981: Geology of the Corner Brook Lake area, Newfoundland; unpublished M.Sc. thesis, Memorial University of Newfoundland.

Klappa, C.F., Opalinski, P.R., and James, N.P.
1980: Ordovician Table Head Group of western Newfoundland: a revised stratigraphy; Canadian Journal of Earth Sciences, v. 17, p. 1007-1019.

Knapp, D.A.
1980: The stratigraphy, structure and metamorphism of central Glover Island, western Newfoundland; in Current Research, Part B, Geological Survey of Canada, Paper 80-1B, p. 89-96.

Lilly, H.D.
1963: Geology of Hughes Brook-Goose Arm area, west Newfoundland; Memorial University of Newfoundland, Geology Report No. 2, 123 p.

McKillop, J.H.
1961: Geology of the Corner Brook area, Newfoundland, with emphasis on the carbonate deposits; unpublished M.Sc. thesis, Memorial University of Newfoundland.

O'Loughlin, J.P.
1981: Geology of the Deer Lake ophiolite complex, Newfoundland; unpublished M.Sc. thesis, Acadia University, Nova Scotia.

Popper, G.H.P.
1970: Paleobasin analysis and structure of the Anguille Group, west-central Newfoundland; unpublished Ph.D. thesis, Lehigh University, Bethlehem, Pennsylvania, 215 p.

Schuchert, C. and Dunbar, C.O.
1934: Stratigraphy of western Newfoundland; Geological Society of America, Memoir 1, 123 p.

Smith, C.H.
1958: Bay of Islands Igneous Complex, western Newfoundland; Geological Survey of Canada, Memoir 290, 132 p.

Stevens, R.K.
1970: Cambro-Ordovician flysch sedimentation and tectonics in west Newfoundland and their possible bearing on a Proto-Atlantic Ocean; in Flysch Sedimentology in North America, ed. J. Lajoie, Geological Association of Canada, Special Paper No. 7, p. 165-177.

Walthier, T.N.
1949: Geology and mineral deposits of the area between Corner Brook and Stephenville, western Newfoundland; Newfoundland Geological Survey, Bulletin 35, Part 1, 63 p.

Werner, H.J.
1956: Geology of the Humber Valley region, western Newfoundland; unpublished report to Claybar Uranium (Newkirk) and Oil, Ltd., Toronto, 98 p.

Williams, Harold
1973: Bay of Island map area, Newfoundland; Geological Survey of Canada, Paper 72-34, 7 p.

1977: Ophiolitic mélange and its significance in the Fleur de Lys Supergroup, northern Appalachians; Canadian Journal of Earth Sciences, v. 14, p. 987-1003.

1981: Geology of the Stephenville map area, north half, Newfoundland; Geological Survey of Canada, Open File 726.

Williams, Harold and St. Julien, Pierre
1981: The Baie Verte-Brompton Line: Early Paleozoic continent-ocean interface in the Canadian Appalachians; Geological Association of Canada, Special Paper.

STRUCTURAL STYLE IN THE PREMIER RANGE, CARIBOO MOUNTAINS, SOUTHERN BRITISH COLUMBIA: PRELIMINARY RESULTS

EMR Contract 23254-1-0220

Donald C. Murphy[1] and J. Murray Journeay[2]
Cordilleran Geology Division

Murphy, Donald C. and Journeay, J. Murray, Structural style in the Premier Range, Cariboo Mountains, southern British Columbia: preliminary results; in Current Research, Part A, Geological Survey of Canada, Paper 82-1A, p. 289-292, 1982.

Abstract

In the Premier Range, complexly deformed, low to high grade metamorphosed turbiditic sandstones of the Proterozoic (?) Kaza Group have been deformed by four geometrically distinct phases of folding and locally cut by low angle shear zones. Two sets of overturned to recumbent, tight to isoclinal structures were identified: northwest-trending, eastwardly verging F1 structures with first order limb lengths in the order of several kilometres; and coaxial, locally westwardly verging F2 structures with large, but unknown, first order limb lengths. Superimposed in these structures are two, possibly conjugate, sets of crenulations: one northwest-trending set associated with open, regional scale folds and one northeast trending set that locally reverses the plunges of earlier structures, but appears to have no regional manifestations. Low angle shear zones with unknown amounts of offset are present at the northernmost part of the area studied.

Introduction

Structures at the northwestern and southeastern extremities of the southern Cariboo Mountains (Fig. 43.1) exhibit strikingly different styles, reflecting deformation at different structural levels. The southeastern part of the range is underlain by high grade Proterozoic (?) metasediments that are tightly to isoclinally folded and refolded such that early structures are warped into large anticlinoria and synclinoria. In contrast, the unmetamorphosed upper Proterozoic to lower Paleozoic rocks at the northwestern end of the range are unaffected by regional folding; rather, they are faulted along northwest- and northeast-trending high angle surfaces. Separating these two areas is a narrow zone where preliminary data suggest transitional structural geometries (Campbell, 1968, 1973; Campbell et al., 1973).

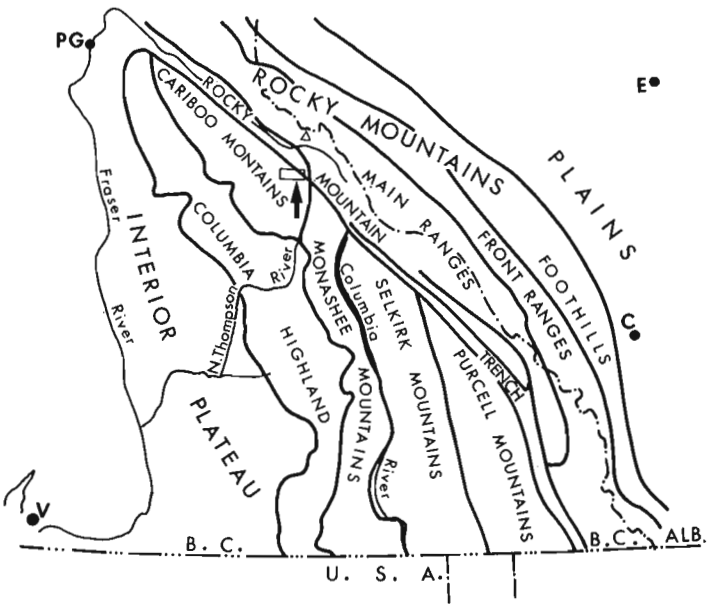

Figure 43.1. Physiographic subdivisions of southern British Columbia (from Campbell, 1973). The location of Figure 43.2 is indicated by the dark arrow.

The juxtaposition of radically different structural styles across a relatively narrow transition zone poses a question that is fundamental to the understanding of the kinematic evolution of orogenic belts: 'How is the strain at lower structural levels accommodated at structurally higher levels?'. A possible answer is that the weakly strained high level strata have been detached from the underlying regionally folded metamorphic rocks; on the other hand, the structural geometry at intermediate structural levels may permit continuous transition from one regime to the other as suggested by Campbell (1973).

In consideration of this question, an investigation of the kinematic evolution of the Cariboo Mountains has been undertaken by the first author (DCM) as a doctoral thesis at Carleton University, under the supervision of Richard L. Brown, whose guidance is most appreciated. The project was initially suggested by R.B. Campbell of the Geological Survey of Canada, whose continuing interest, enthusiasm, and ideas are most gratefully acknowledged.

This report presents the results of the first field season which was spent in the spectacularly folded rocks of the Premier Range, the southernmost range of the Cariboo Mountains.

The Premier Range

Stratigraphy

Located at the southeastern end of the Cariboo Mountains, between 52°30' and 52°50'N, the Premier Range is underlain by regionally folded, low to high grade metasediments of the Proterozoic (?) Kaza Group. The nature of the stratigraphy of the Cariboo Mountains, specifically the Kaza Group, precludes understanding of the structure of the range without some detailed understanding of the sedimentary facies involved.

Kaza Group protoliths consist primarily of coarse feldspathic and locally calcareous sandstones and subordinate conglomerates, sandy and calcareous shales, and limestones. Sedimentary structures are preserved even in rocks containing kyanite and staurolite, enabling one to determine stratigraphic tops and to draw the three following conclusions.

1. Kaza Group sandstones and conglomerates were deposited as turbidites and grain flows.

[1] Department of Geology, Carleton University, Ottawa, Ontario, K1S 5B6

[2] Department of Geology, Queen's University, Kingston, Ontario

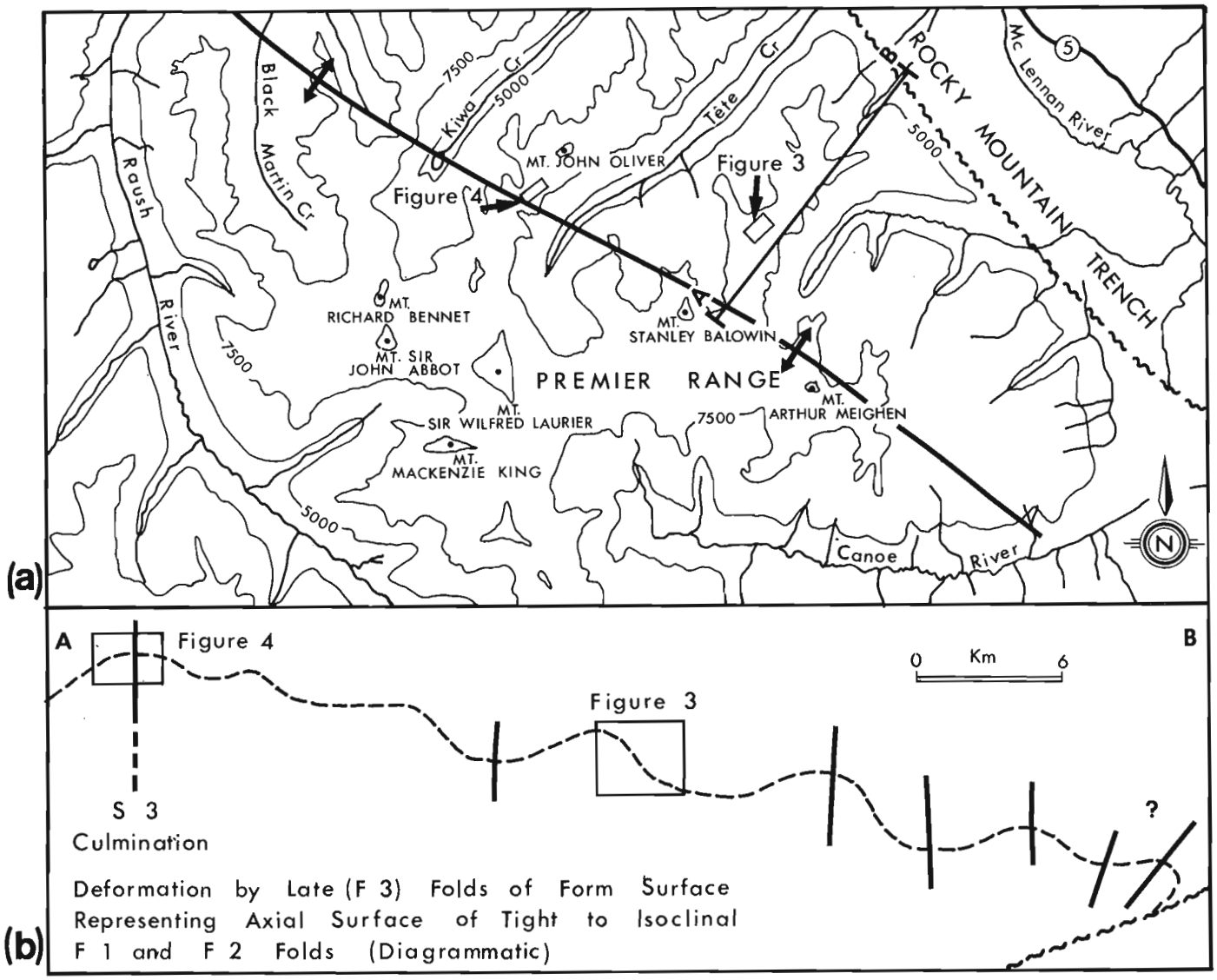

Figure 43.2. *(a): Location map of the Premier Range. Trace of major third phase antiform shown (from Campbell, 1967) as are locations of Figures 43.3 and 43.4. (b): Schematic cross-section illustrating effects of third phase structures.*

Coarse sandstone beds exhibit well developed channels, good to poor, normal and reverse grading, weakly developed distribution grading, and randomly distributed synsedimentary lutite clasts. Crossbeds are rare, occurring in finer, better sorted layers. Sharp, commonly scoured, bases and top transitional to pelitic interbeds are the rule, although beds with both sharp bases and tops have been observed locally. Conglomerates exhibit a well developed segregation of lutite clasts to the tops of beds (as determined from channel incision) suggesting the operation of dispersive forces during flow. Possible "dish" structures have been observed, further supporting a grain flow transport mechanism for Kaza conglomerates.

2. Kaza turbidites and grain flows were deposited in a proximal, channelized setting, possibly as the upper/inner fan facies of an extensive submarine fan complex.

Kaza sandstones exhibit predominance of AE or ACE Bouma sequence beds, high sand/shale ratio, channelized and amalgamated beds, coarse to very coarse grain size and angular grain shape, and lateral transitions from conglomeratic channel facies to thinner, more persistent and finer overbank facies which are all characteristics of a proximal turbidite facies. Due to the structural complexity, only a small thickness of stratigraphy was observed and other facies transitions in more proximal or distal directions were not encountered.

3. The characteristic coarse, commonly angular to euhedral feldspars found in Kaza sandstones may represent the influx of volcanic or plutonic detritus.

Although the feldspars are elongated parallel to F2 fold axes, the angularity that one sees in the XY kinematic plane is somewhat reduced from the pre-deformation condition; thus feldspar clasts were probably very angular at the time of deposition. These sandstones are probably not well-cycled, cratonically derived sediments.

The interbedding of these proximal turbidites with thin, but persistent, marbles and calcareous schists suggest deposition above the carbonate compensation depth.

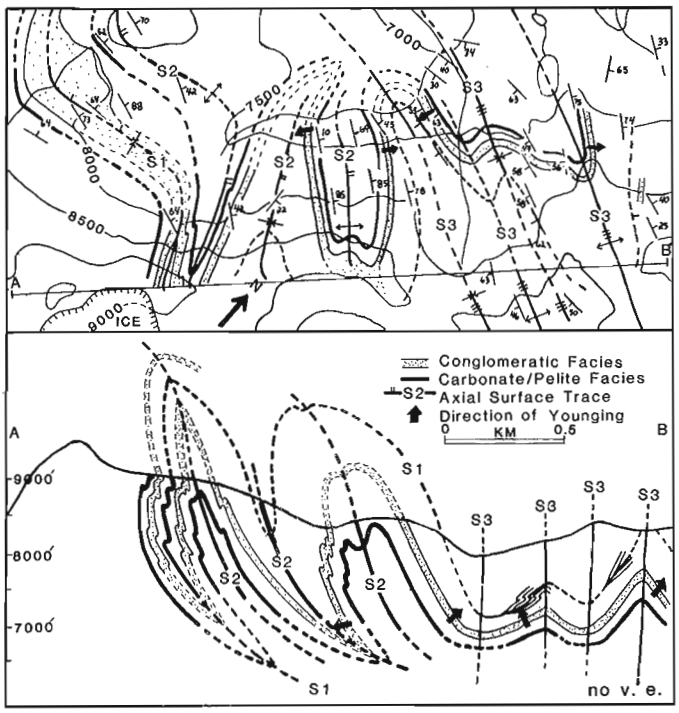

Figure 43.3. Map and cross-section illustrating the interaction of coaxial first and second phase structures on eastern flank of major third phase antiform (Fig. 43.2). The term "facies" is used here (and in Fig. 43.4) to emphasize that conglomeratic deposits are laterally transitional to finer, more thinly bedded, sandstones representative of another turbidite facies. Carbonates, although more persistent, are assumed to have lateral facies equivalents as well.

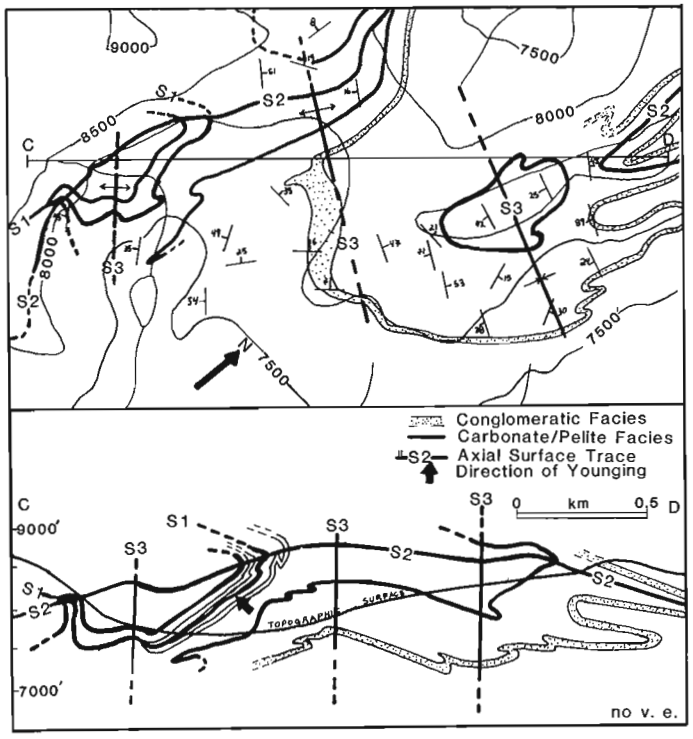

Figure 43.4. Map and cross-section illustrating the interaction of coaxial first and second phase structures in hinge area of major third phase antiform (Fig. 43.2).

Sedimentary structures are lacking, however, so it is not presently possible to determine whether or not the marbles are also turbiditic.

Structural Geometry

Structural analysis of Kaza Group rocks is somewhat complicated by the homogeneous nature and lateral facies variations of Kaza sandstones. However, due to the presence of locally continuous carbonate marker horizons and abundant minor structures four geometrically distinct sets of structures were outlined: two northwest-trending, tight to isoclinal, recumbent fold phases and two, possibly conjugate, sets of crenulations superimposed on the recumbent structures. One crenulation set is coaxial with recumbent structures and is associated with open, regional folds; the other set trends northeast and has no obvious regional manifestations (Fig. 43.3-43.5; Campbell, 1967).

As well, layer-parallel, low angle shear zones with an apparent eastwardly-directed hanging wall motion were encountered in the northwestern part of the area examined.

Recumbent Structures

The earliest structures are strongly attenuated, northwest-trending isoclinal folds with first order limb lengths of several kilometres. First phase structures on all scales are identifiable only when refolded by coaxial, tight to isoclinal second phase folds which have strongly overprinted the earlier structures. The spectacular cliff-face displays of folds in the Premier Range are usually composed of second or third order second phase folds.

Mesoscopic fabric criteria may be used only locally to distinguish first from second phase structures. Second phase axial plane fabric (S2) is usually a crenulation cleavage imposed on an earlier, presumably first phase, foliation (S1); however, complete transposition of early schistosity into second phase axial planes has been observed. In such cases, the resultant foliation is a fine schistosity and therefore indistinguishable from what one might expect a first phase fabric to resemble.

Figures 43.3 and 43.4 depict the relationship between first and second phase structures. The largest first phase structure identified thus far is shown in Figure 43.3. Sedimentary facing criteria on the limbs of this structure require that it be a syncline; unfolding around westwardly verging second phase structures produces a westwardly closing first phase syncline. These data imply eastward vergence of first generation folds.

Early structures were observed in all grades of rock ranging from low grade, garnet-biotite-muscovite zone to higher grade rocks bearing kyanite and staurolite. In the higher grade rocks, coarse staurolite porphyroblasts have overgrown second phase fabrics and have been rotated around third phase axes. Elsewhere, however, tremolite porphyroblasts are strongly aligned in the regional northwest-trending lineation corresponding to second phase fold axes, suggesting growth during F2. Thus, from preliminary results, metamorphism appears to be syn- to post-F2 but pre-F3.

Upright Structures

Fabrics associated with first and second phase structures are overprinted by two sets of late upright structures, one coaxial with the early sets of folds (S3), and the other trending northeast (S4) (Fig. 43.2-43.5). Third phase folds are open, upright warps that culminate in a large antiform that has been traced into an upright anticline in lower grade rocks to the northwest (Campbell et al., 1973). Second order structures east of this culmination verge

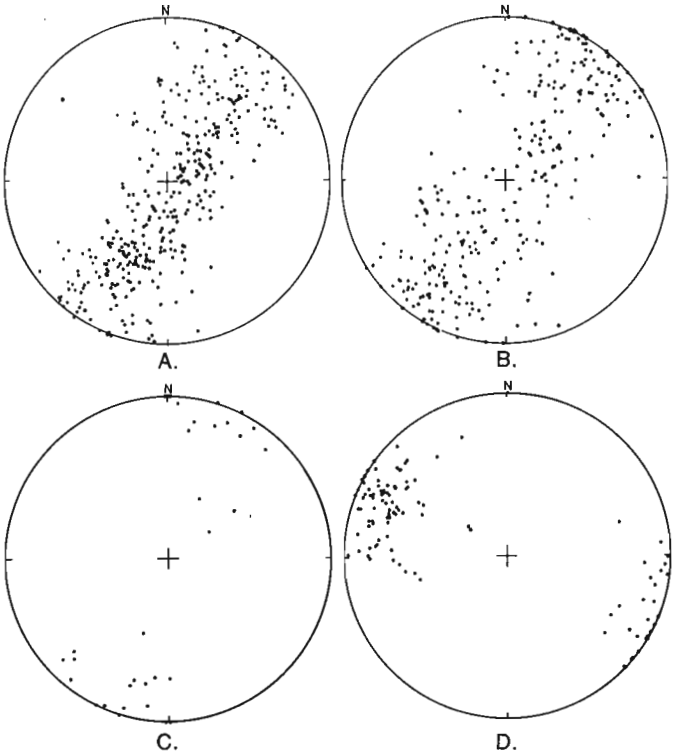

A. Poles to S0 (n=349)

B. Poles to S1 and S2 (Axial surfaces of first and second phase folds, n=363)

C. Poles to S3 (Axial surfaces of northwest-trending high angle crenulations overprinting S1 and S2, n=31)

D. Poles to S4 (Axial surfaces of northeast-trending high angle crenulations overprinting S0, S1, and S2 and possibly conjugate to S3, n=98).

Figure 43.5. *Equal area stereonet compilation of planar fabric element data.*

westward towards the culmination, warping earlier structures as depicted in Figures 43.2 and 43.3. In the culmination itself, early structures are brought into a recumbent position (Fig. 43.2, 43.4). To the east, in the direction of the Rocky Mountain Trench, first and second phase structures are locally oversteepened through the vertical into cleavage fans (Campbell, 1967). This oversteepening may reflect overturning toward the Rocky Mountain Trench of third phase folds but this has yet to be documented (Fig. 43.2).

Upright northwest-trending crenulations which fold both first and second phase fabrics are higher order manifestations of these late folds. Structures intermediate between the regional scale folds and these crenulations have not been observed.

S0, S1, S2, and S3 are all affected by late northeast-trending crenulations that locally reverse the plunges of earlier fold axes but no not seem to be related to more regional folds. S3 and S4 may represent a conjugate set in that poles to S3 and S4 do not fall into point maxima but form diffuse clusters about the axial surface of the other, possibly conjugate, set (Fig. 43.5). In outcrops where both sets of crenulations may be observed, it is rarely possible to determine an order of superposition, further suggesting a conjugate relationship.

Larger third and fourth phase crenulations may be traced upward into discrete faults with minor but documentable normal or reverse offsets. Northwest and northeast-trending faults with substantial offsets are characteristic of the northwestern end of the range (Campbell, et al., 1973).

Low Angle Shear Zones

Low angle, layer-parallel, shear zones were observed in the northernmost area thus far studied. The zones are a few metres thick and are confined to thin bedded pelitic/semipelitic material in a predominantly sandstone interval. Local alteration has been observed.

The internal fabrics associated with the shear zones consist of commonly slickensided, anastamosing foliations and crenulations with distinctly curviplanar axial surfaces. The geometry of these internal fabrics suggests eastward transport of hanging wall with respect to footwall in all cases observed.

The amount of offset along these zones and, therefore, contribution to the regional deformation, cannot as yet be assessed.

Conclusions

1. Characteristics of Kaza sandstones and conglomerates suggest deposition, as turbidites and grain flows, in proximal, inner fan portions of an extensive subsea fan.
2. Composition and angularity of clasts imply that Kaza sediments are not well-cycled cratonically derived sediments. Volcanic or plutonic provenance is suggested.
3. Four geometrically distinct sets of structures have been imposed on the rocks of the Kaza Group in the Premier Range: two phases of recumbent, tight to isoclinal, northwest-trending folds and two, possibly conjugate, sets of upright crenulations, which have been superimposed on the recumbent structures.
4. Low angle, layer-parallel, shear zones are found in the northernmost part of the area examined. The geometry of internal mesoscopic fabrics suggest eastwardly directed motions of the hanging wall. The contribution of these shear zones to the regional deformation and their relationship to the transition to lower structural levels is as yet unknown.

References

Campbell, R.B.
1968: Canoe River, British Columbia; Geological Survey of Canada, Map 15-1967.

1973: Structural cross-section and tectonic model of the southeastern Canadian Cordillera; Canadian Journal of Earth Sciences, v. 10, p. 1607-1620.

Campbell, R.B., Mountjoy, E.W., and Young, F.G.
1973: Geology of McBride map area, British Columbia; Geological Survey of Canada, Paper 72-35, 104 p.

GEOLOGY OF ASHCROFT MAP AREA, SOUTHWESTERN BRITISH COLUMBIA

Project 800029

J.W.H. Monger
Cordilleran Geology Division, Vancouver

Monger, J.W.H., Geology of Ashcroft map area, southwestern British Columbia; in Current Research, Part A, Geological Survey of Canada, Paper 82-1A, p. 293-297, 1982.

Abstract

Ashcroft map area straddles parts of the Intermontane Belt and Coast Plutonic Complex. The different pre-Cretaceous histories of these provinces suggest that they were independent of one another until Early Cretaceous time. The Intermontane Belt was founded on a Late Triassic arc: subduction complex (Nicola: Cache Creek groups) and uplifted by mid-Jurassic time. The eastern Coast Plutonic Complex was founded in part on Triassic to mid-Jurassic oceanic crust, (Bridge River Group) and was uplifted in mid-Cretaceous time. By late Early Cretaceous time the provinces appear to have been linked, for continental volcanics (Spences Bridge Group) of the Intermontane Belt interfinger westwards with marine and nonmarine clastics (Jackass Mountain Group). Structures possibly related to mid-Cretaceous uplift appear to be north-northwest trending, northeast-verging thrust and (?) strike-slip faults in the eastern margin of the Coast Mountains. These structures are offset by about 100 km on the right-lateral strike-slip Fraser Fault system which involves Eocene rocks, and has been linked genetically to pervasive normal faulting of Eocene age in the Intermontane Belt.

Introduction

Field mapping in eastern, northern and western parts of Ashcroft map area (92 I), which is bounded by 50° and 51°N and 120° and 122°W, continues the study initiated in 1980 (Monger, 1981) and follows earlier 1 inch to 4 mile mapping by Cockfield (1948) and Duffell and McTaggart (1952).

The map area spans the western part of the Intermontane Belt and the eastern part of the Coast Plutonic Complex with its southeastern extension, the Cascade Mountains (Fig. 44.1). Within the Intermontane Belt stratified rocks range in age from Mississippian to Neogene and are largely unmetamorphosed or low grade metamorphic except near the predominantly Jurassic granitic plutons. In the Coast Plutonic Complex, the rocks are predominantly Cretaceous granite, with stratified rocks mainly forming septa and ranging in age from Middle Triassic to Neogene, and grading from unmetamorphosed to regional amphibolite grade. Correspondingly, the structural relief is relatively gentle in the Intermontane Belt in comparison with that in the Coast Plutonic Complex. Upper Triassic rocks, although cut by granitic strata and overlain by younger units, extend across two thirds of the map area, from its eastern margin almost to the western limit of the Intermontane Belt, which is delineated by the Pasayten fault. By contrast, within the Coast Plutonic Complex and Cascade Mountains, Upper Triassic and (?) older to Tertiary stratigraphic units form only narrow, structurally bounded strips.

Geological History

Until Early Cretaceous time, terranes now in the Coast Plutonic Complex-Cascade Mountains and Intermontane Belt may have been essentially independent of one another, because no pre-Cretaceous units are common to both and they appear to have had different early histories (Fig. 44.2). the Intermontane Belt appears to be founded on a Late Triassic subduction complex – arc – back arc (?) association (Cache Creek – Nicola – Harper Ranch groups, respectively), above which is an Early to Middle Jurassic marine and nonmarine clastic sequence (Ashcroft Formation and equivalent), succeeded by a regional Late Jurassic hiatus. All these rocks are cut by predominantly Jurassic intrusions, which range in composition from (mainly) granitic rock to ultramafic. By contrast, the foundation of part of the western province is possibly Middle Triassic and (?) Permian to Jurassic oceanic crust (Hozameen, Bridge River Group) upon which were deposited marine clastic rocks (Ladner, Lillooet and Dewdney Creek groups). By late Early Cretaceous time, the two provinces appear to have been linked stratigraphically, for continental volcanic rocks of the Intermontane Belt (Spences Bridge Group) interfinger westwards with marine and nonmarine clastics of the Coast-Cascade province (Jackass Mountain Group). Most of the granitic rocks in the Coast Plutonic Complex appear to have been intruded subsequently, in mid-Cretaceous to earliest Tertiary time. All younger rock units are continental and range from mid-Cretaceous clastics and volcanics (Pasayten Group and equivalents; Kingsvale Group), through Eocene volcanics and clastics (Kamloops Group), to Miocene and younger volcanics and clastics ('plateau', 'valley' basalt).

Structure

There are two sets of dominant structures in the map area, one early Tertiary and one probably pre-Tertiary but post- mid-Cretaceous. In the Intermontane Belt, pervasive normal faults, with trends ranging from northwest to northerly, are at least in part contemporaneous with extrusion of Eocene continental volcanics (Ewing, 1981), and may be linked genetically with the right-lateral, strike-slip Fraser fault system (Price, 1979). In the map area the latter slices acutely across the eastern part of the Coast Plutonic Complex and Cascade Mountains, offsetting mid-Cretaceous and older rock units by distances ranging from 70 to 130 km and involving Eocene strata. The older structures, in the Coast Plutonic Complex and Cascade Mountains, include the Yalakom and Pasayten faults and related structures. These, in part, form the boundaries of rock units as young as mid-Cretaceous and have been interpreted both as strike-slip faults (Tipper, 1968; Davis et al., 1978) and as thrust faults (Misch, 1966; Coates, 1974). Southwest dipping thrust faults in the Coast Plutonic Complex southwest of Lillooet (Fig. 44.1), locally superpose Triassic rocks on Lower Cretaceous strata cut by granitic rocks. The faults are conformable with regional penetrative foliation in this area and their traces parallel the Yalakom fault. Their presence raises the question as to whether all major faults bounding rock units on the east side of the Coast and Cascade Mountains are steepened, modified thrust faults, in which case the Intermontane Belt acted as a foreland to Cretaceous

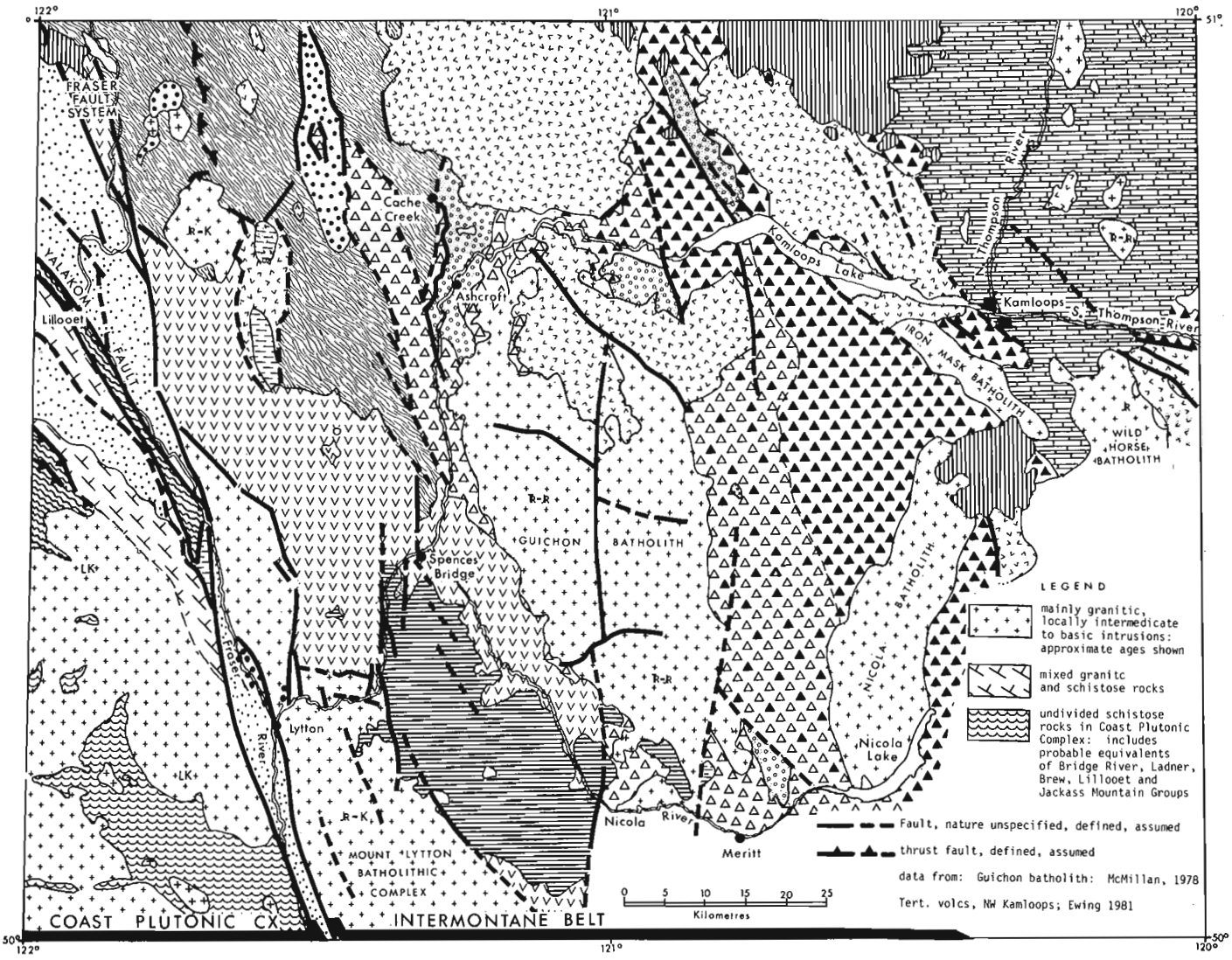

Figure 44.1. *Geological sketch map of Ashcroft map area. Legend for stratified rocks in Figure 44.2.*

thrusting. Still older structures, in units such as the Cache Creek Group, are probably so modified by the late Mesozoic-early Tertiary deformation that their original nature and orientation remain uncertain.

Some rock units of Ashcroft map area: new details

Harper Ranch Group

The Harper Ranch Group (Smith, 1979; W.R. Danner, personal communication), which is also known as the Thompson assemblage (Okulitch, 1979) and Cache Creek Group (Cockfield, 1948), comprises a heterogenous sequence of argillite, sandstone, conglomerate, chert, volcanic flows and clastics, and prominent lenses of carbonate. From the latter come fossils that range in age from Mississippian to Late Permian (Cockfield, 1948; Sada and Danner, 1974, 1976; W.R. Danner, personal communication). However, new evidence is emerging that much of the matrix enclosing the limestones may be Triassic. Smith (1979), who studied the area northwest of Kamloops, which comprises mainly clastic rocks, collected Middle and Upper Triassic conodonts and concluded that rocks called Cache Creek Group near Kamloops contain two sequences: an older one containing the Paleozoic limestones which he referred to as Harper Ranch Group, and a younger one with Triassic fossils which he correlated with the Nicola Group to the west. During field work in 1981, the writer was unable to differentiate much of the matrix enclosing the Paleozoic limestones from Smith's clastic section or from parts of the Nicola Group to the west. Furthermore, extensive areas of augite porphyry flows and breccias interbedded with Harper Ranch argillites and coarser clastics, in areas where Paleozoic limestones are present, superficially resemble rocks of the Nicola Group. Argillite and chert, in sections containing late Paleozoic carbonates, yielded Upper Triassic conodonts (M.L. Orchard, personal communication) and, at one locality, Permian radiolaria (D.L. Jones, personal communication). From this, the writer concludes that the Harper Ranch Group represents either deposits in a long-lived, mainly sedimentary, basin, that are in part a facies equivalent of the Nicola Group and in part older, with at least some upper Paleozoic carbonate olistoliths; or comprises two complexly imbricated sequences, one of late Paleozoic age and one of Triassic age. The writer favours the former, because in places within the section there are channel deposits containing chert pebble

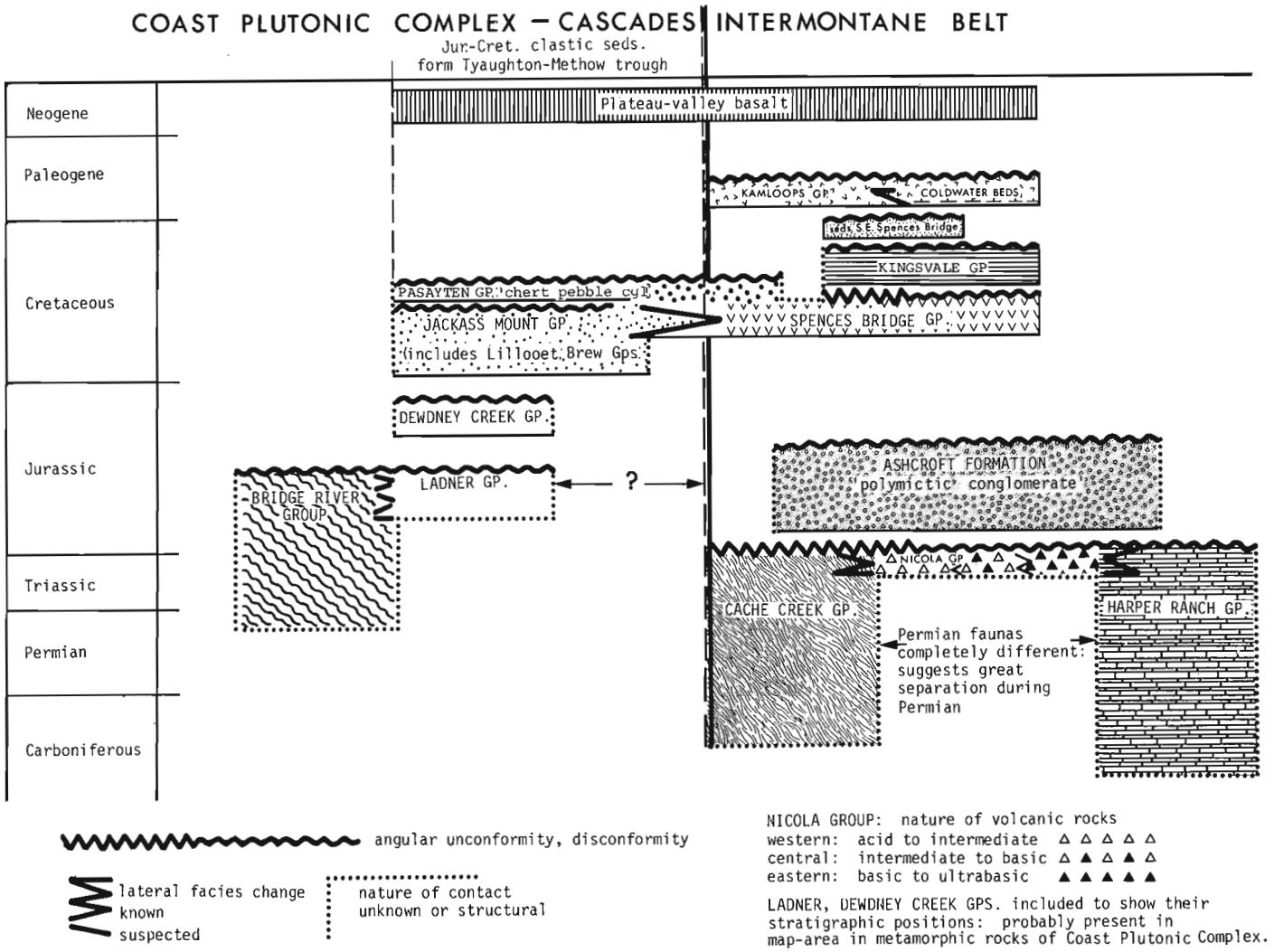

Figure 44.2. *Correlation chart of major stratigraphic units in Ashcroft map area. Note units linking two (or more) different older units, within the Intermontane Belt in the Upper Triassic and between the Intermontane Belt and Coast Plutonic Complex in the Lower Cretaceous.*

conglomerates and, locally, clasts of carbonate, some of which contain Lower Permian fossils, indicating that there was erosion and redeposition during Harper Ranch time.

Nicola Group

Various workers (for example, Morrison, 1980) have subdivided the Nicola Group into belts of different composition but similar, mainly Norian, age. Westernmost are acid to intermediate mainly volcaniclastic rocks, with local carbonates. The writer confirmed in the field with W.J. McMillan that volcanic rocks in contact with and intermixed with the eastern belt of the Cache Creek Group (Monger, 1981; Shannon, 1981) are lithologically similar to acid to intermediate volcanics of the Nicola Group exposed northeast of Ashcroft, in the Promontory Hills and north of Merritt. These rocks grade eastward into a broad belt of mainly intermediate volcanics that extend eastward as far as Kamloops Lake, the Meadow Creek area east of Logan Lake and along Nicola Lake. This belt consists of characteristically red, locally green volcaniclastic rock, typically with fine grained feldspar porphyry clasts. Pillowed and massive flows, laminated red sandstone and volcanic conglomerate are present locally. Carbonate clasts are a very characteristic component of the predominantly volcanic conglomerate and breccia and limestone locally forms large lenses interbedded with the volcanics. The easternmost rocks are mainly green, locally red and green volcanic breccias featuring augite porphyry and augite feldspar porphyry clasts and interbedded with laminated argillites and siltstones. This succession contains little carbonate, but lithologically it appears to be identical with some rocks included in the Harper Ranch Group. Known fossils are Late Norian, slightly younger than fossils in the Nicola Group to the west. A possible variant of this belt includes those tuffs, augite porphyry, "picrite porphry" and picrite tuff, exposed near Copper Creek on the north side of Kamloops Lake and in Watching Creek, northwest of Kamloops, which were mapped as Cretaceous or Tertiary by Cockfield (1948). The Copper Creek rocks lie on trend with the early Mesozoic Iron Mask batholith and may be extrusive equivalents of some phases of it.

Ashcroft Formation: Polymictic Conglomerate

The Ashcroft Formation comprises shale, siltstone and sandstone with locally prominent conglomerate and rare carbonate horizons (Duffell and McTaggart, 1952; Travers, 1978). Polymictic conglomerate exposed north of Kamloops Lake, previously thought to be Cretaceous or Tertiary (Cockfield, 1948; Monger, 1981) is now correlated with the Ashcroft Formation. It locally contains 5 to 10 per cent quartzite clasts, whose only known source is the Proterozoic and Lower Paleozoic strata exposed east of the map area in the Omineca Crystalline Belt. This unit in places lies disconformably but elsewhere with angular unconformity on the Nicola Group, and in its eastern exposures appears to be entirely nonmarine.

Bridge River Group and Associated Rocks in the Coast Plutonic Complex

The Bridge River Group, composed of radiolarian chert, argillite, basalt, minor limestone and associated alpine-type ultramafic rocks, ranges in age from Middle Triassic to Middle Jurassic (Roddick and Hutchison, 1973; Monger, 1977). It extends from Pemberton map area (92 J) southwestwards into Ashcroft map area and forms septa in the predominantly granitic Coast Plutonic Complex. Commonly it is metamorphosed into a distinctive assemblage of siliceous schist (metachert), phyllite, chlorite actinolite schist and talc, and complexly imbricated with other metamorphosed units. The last include Bridge River rocks of higher metamorphic grade laced with granitic and pegmatitic syn- and post-deformational intrusions, as well as calcareous phyllite with local calcareous breccia horizons, correlated with the Upper Triassic Cadwallader Group to the northwest, and greywacke, siltstone and phyllite possibly equivalent to the Lower and Middle Jurassic Ladner Group to the southeast, in Hope map area (92 H), and/or the Lower Cretaceous Lillooet Group near Lillooet.

About 13 km south-southeast of Lillooet, Bridge River rocks lie above a fault surface that dips southwestwards at 50°, above granite that intrudes fossiliferous Lower Cretaceous strata (Brew Group of Duffell and McTaggart, 1952), suggesting that there the Bridge River Group is thrust northwestwards over younger rocks. The plane of the fault is conformable with the penetrative foliation in the upper plate, indicating the two are related. Its trace is parallel with the traces of other faults in the region, including the Yalakom Fault, opening the possibility that all these faults are steepened thrusts. The southern extension of the Yalakom Fault is probably the Hozameen Fault, offset across the right-lateral Fraser Fault system. South of the International Boundary, Misch (1966) showed the extension of the Hozameen fault as a thrust, and most of the major faults in Manning Park were shown by Coates (1974) as thrust faults. Possible thrust faults near Lillooet may be merely the northern extension of the well-documented system near the International Boundary.

Mount Lytton Batholithic Complex

A great variety of rock types occurs within the elongate, north-northwest trending plutonic belt which forms the western part of the Intermontane Belt at these latitudes. Its northern part is known as the Mount Lytton batholith and its southern part as the Eagle granodiorite. The youngest rocks are massive, locally foliated granodiorite, which cuts strongly altered diorite and gabbro as well as foliated amphibolite. The latter, together with quartzofeldspathic rocks that in places are banded with amphibolite, appear to be the oldest rocks in the northern part of the complex. Any of these rock types may be foliated, with foliation ranging from irregular flaser structure in the granodiorite to fine grained, locally mylonitic, layering in the amphibolite and quartzofeldspathic rock. The trends of the foliations commonly are north-northwesterly and are truncated by the Fraser fault system. Speculatively they could be related to the thrust faults in the eastern margin of the Coast Plutonic Complex.

Spences Bridge Group

The late Early Cretaceous (Middle to Upper Albian; W.S. Hopkins, personal communication). Spences Bridge Group is a continental volcanic and sedimentary succession that lies largely east of, and on, the Mount Lytton complex, and thus belongs to the Intermontane Belt. By contrast, the Aptian-Albian Jackass Mountain Group is a marine to nonmarine sedimentary succession, confined to the Tyaughton-Methow trough, west of the Mount Lytton batholith complex. During field work in 1981, rocks of identical lithology to the Spences Bridge Group were found interlayered with Jackass Mountain rocks, 5 km east of Boston Bar. Similarly, Karen Kleinspehn (personal communication) observed that conglomerate in the Spences Bridge Group, exposed on the Thompson River 13 km northeast of Lytton (and east of the Mount Lytton Complex), is similar in composition and nature to many Jackass Mountain conglomerates. This leads to the conclusion that the Jackass Mountain and Spences Bridge groups are (partial?) facies equivalents and interfinger across the Mount Lytton batholithic complex.

Kingsvale Group

Monger (1981) suggested that the Kingsvale and Spences Bridge groups formed a single stratigraphic package, on the basis of their apparently conformable relationships. New and more detailed studies tend to contradict this. Devlin (1981) studied the relationship between the Spences Bridge Group in its type area at Spences Bridge with the Kingsvale Group and concluded that an unconformity separated them. There the Kingsvale, mainly red basaltic flows, is unconformably overlain by Upper Cretaceous (probably post Cenomanian-pre-Tertiary; G.E. Rouse, in Devlin, 1981) coal-bearing sediments. East of Lytton, and south of the Thompson River, the Kingsvale Group lies on deeply weathered, rotten, red-stained granodiorite of the Mount Lytton complex. To the northwest, 4 km across the Thompson River, a thick succession of Spences Bridge Group sedimentary and volcanic rocks, stratigraphically overlies the Mount Lytton complex, although the contact is much faulted. This suggests an interval of erosion following Spences Bridge deposition and prior to Kingsvale deposition, or an extremely rough topography, which confined the Spences Bridge Group to valleys where it was overlapped by the Kingsvale volcanics.

Acknowledgments

During the summer, the writer received advice and assistance from a number of visitors in the field. W.J. McMillan, British Columbia Ministry of Energy, Mines and Petroleum Resources, who mapped the Guichon batholith and surrounding strata (McMillan, 1974, 1976, 1978), and who will be a joint author of the final maps, examined parts of the Nicola Group and contiguous rocks with the writer. Karen L. Kleinspehn, Princeton University looked at the type area of the Spences Bridge Group, in connection with her studies on the sedimentation and tectonics of Jackass Mountain Group and equivalent strata in the Tyaughton-Methow trough. W.S. Hopkins, Geological Survey of Canada, Calgary collection Cretaceous plant fossils.

References

Coates, J.A.
1974: Geology of the Manning Park area, British Columbia; Geological Survey of Canada, Bulletin 238, 117 p.

Cockfield, W.E.
1948: Geology and mineral deposits of Nicola map-area, British Columbia; Geological Survey of Canada, Memoir 249, 164 p.

Davis, G.A., Monger, J.W.H., and Burchfiel, B.C.
1978: Mesozoic construction of the Cordilleran 'collage', central British Columbia to central California; in Mesozoic Paleogeography of the Western United States, D.G. Howell and K.A. McDougall, ed., Society of Economic Paleontologists and Mineralogists, Pacific Coast Paleogeography Symposium 2, p. 1-32.

Devlin, B.D.
1981: The relationships between the Cretaceous Spences Bridge and Kingsvale Groups in south central British Coumbia; University of British Columbia, unpublished B.Sc. thesis, 57 p.

Duffell, S. and McTaggart, K.C.
1952: Ashcroft map-area, British Columbia; Geological Survey of Canada, Memoir 262, 122 p.

Ewing, T.
1981: Geology and tectonic setting of the Kamloops Group, south central British Columbia; University of British Columbia, unpublished Ph.D. thesis, 225 p.

McMillan, W.J.
1974: Stratigraphic section from the Jurassic Ashcroft Formation and Triassic Nicola Group contiguous to the Guichon Creek batholith; British Columbia Department of Mines and Petroleum Resources; Geological Field Work, p. 27-34.

1976: Geology and genesis of the Highland valley ore deposits and the Guichon Creek batholith; Canadian Institute of Mining Metallurgy, Special Volume 15, p. 85-104.

1978: Geology of the Guichon Creek Batholith and Highland valley porphyry copper district, British Columbia; British Columbia Ministry of Mines and Petroleum Resources, Preliminary Map 30.

Misch, P.
1966: Tectonic evolution of the Northern Cascades in Washington State; Canadian Institute of Mining and Metallurgy, Special Volume 8, p. 101-148.

Monger, J.W.H.
1977: Upper Paleozoic rocks of the western Canadian Cordillera and their bearing on Cordilleran evolution; Canadian Journal of Earth Sciences, v. 14, p. 1832-1859.

1981: Geology of Parts of western Ashcroft map area southwestern British Columbia; in Current Research, Part A, Geological Survey of Canada, Paper 81-1A, p. 185-189.

Morrison, G.W.
1980: Stratigraphic control of Cu-Fe skarn ore distribution and genesis at Craigmont, British Columbia; Canadian Mining and Metallurgical Bulletin, v. 73, no. 820, p. 109-123.

Okulitch, A.V.
1979: Geology, Mineral Occurrences; Thompson-Shuswap Okanagan region; Geological Survey of Canada, Open File 637.

Price, R.A.
1979: Intracontinental ductile crustal spreading linking Fraser River and northern Rocky Mountain trench transform fault zones, south central British Columbia and northwest Washington; Geological Society of America, Abstracts with Programs., v. 11, no. 7, p. 499.

Roddick, J.A. and Hutchison, W.W.
1973: Pemberton (east half) map-area, British Columbia; Geological Survey of Canada, Paper 73-17.

Sada, K. and Danner, W.R.
1974: Early and Middle Pennsylvanian fusulinids from southern British Columbia and northwestern Washington, U.S.A.; Transactions proceedings of the Geological Society of Japan, N.S., No. 93, p. 249-265.

1976: *Pseudo-Schwagerina* from Harper Ranch area near Kamloops, British Columbia, Canada; Hiroshima University, Commemoration Volume on the founding of the Faculty of Integrated Arts and Sciences, p. 213-228.

Shannon, K.R.
1981: The Cache Creek Group and contiguous rocks near Cache Creek, British Columbia; in Current Research, Part A, Geological Survey of Canada, Paper 81-1A, p. 217-221.

Smith, R.B.
1979: Geology of the Harper Ranch Group (Carboniferous-Permian) and Nicola Group (Upper Triassic), northeast of Kamloops, British Columbia; University of British Columbia, unpublished M.Sc. Thesis, 211 p.

Tipper, H.W.
1968: Mesozoic and Cenozoic geology of the northeast part of Mount Waddington map-area (92N), Coast District, British Columbia; Geological Survey of Canada, Paper 68-32, 103 p.

Travers, W.B.
1978: Overturned Nicola Group and Ashcroft strata and their relation to the Cache Creek Group, southwestern Intermontane Belt, British Columbia; Canadian Journal of Earth Sciences, v. 15, p. 99-116.

45. GEOLOGY OF THE MACTUNG PLUTON IN NIDDERY LAKE MAP AREA AND SOME OF THE PLUTONS IN NAHANNI MAP AREA, YUKON TERRITORY AND DISTRICT OF MACKENZIE

Project 790044

R.G. Anderson
Cordilleran Geology Division, Vancouver

Anderson, R.G., Geology of the Mactung pluton in Niddery Lake map area and some of the plutons in Nahanni map area, Yukon Territory and District of Mackenzie; in Current Research, Part A, Geological Survey of Canada, Paper 82-1A, p. 299-304, 1982.

Abstract

Two major plutonic suites were distinguished on the basis of lithology, inclusion abundance, structure and intrusive style in the study areas. A megacrystic suite consists of small, composite, inclusion-free, alkali feldspar megacryst- and biotite-bearing granite and quartz monzonite plutons (Mactung, Mount Wilson and Pelly River plutons). The suite without megacrysts consists of a larger, homogeneous, hornblende- and biotite-bearing granodiorite and quartz monzodiorite pluton with relatively abundant inclusions (South Nahanni River pluton). Few characteristics distinguish members of the megacrystic suite associated with tungsten-bearing skarns from those devoid of tungsten.

Introduction

Granitic plutons in the Nahanni map area (105 I) and southeastern corner of Niddery Lake map area (105 O) (Fig. 45.1) are being studied as part of a Visiting Postdoctoral Fellowship with the Economic Division of the Geological Survey of Canada. These plutons are spatially and temporally associated with important skarn-type tungsten deposits (Dawson and Dick, 1978; Dick, 1979, 1980) and they are the last major, posttectonic geological event in these areas (Gabrielse and Reesor, 1974). Granitic plutons and their country rocks in the southeastern Selwyn Basin have been sampled in regional geochemical studies and mapped on a reconnaissance scale by several workers (e.g. Blusson, 1968, 1971, 1974; Garrett, 1971a, b, 1972 a, b; Gabrielse et al., 1973; Harris, 1977; Archibald et al., 1978; Gordey, 1981; Godwin et al., 1980). The purpose of this study is to establish the lithological and petrological characteristics of these plutons and their relation to skarn-type mineralization. During the 1981 field season, three weeks were spent mapping parts of the Mactung, Mount Wilson, Pelly River and South Nahanni River plutons (Fig. 45.1). Field work was carried out by means of helicopter-supported flycamps. Granitoid rock names are consistent with the classification of Streckeisen (1973). Comparison of the nature and style of plutonism in these areas with that in the Intermontane Belt may show the utility of the I- and S-type granitoid classification of Chappell and White (1974) in the Canadian Cordillera.

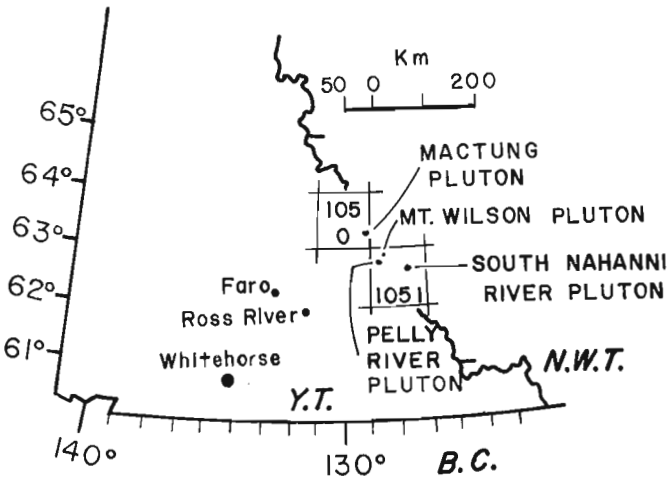

Figure 45.1. Location of Nahanni and Niddery Lake map areas and the plutons described in this report.

Geology of the Plutons

Mactung Pluton

The Mactung pluton is oval-shaped and easterly elongated, underlying an area of 2.9 km^2 that straddles the Yukon-Northwest Territories border (Fig. 45.2a). It is a massive, composite pluton comprising three moderately heterogeneous phases. The equigranular phase is commonly, although not invariably found at the contact with pelitic hornfels and is a sparingly megacrystic biotite granite. Garnet is a rare, scattered but significant accessory mineral and at one locality muscovite occurs with garnet in an equigranular granite apophysis in the country rocks. Along the eastern margin of the pluton, a mafic, equigranular biotite granodiorite forms a marginal subphase.

The megacrystic phase is the most extensive. It comprises common, coarse grained, euhedral to subhedral alkali feldspar megacrysts set in a finer grained, biotite granite matrix which is lithologically similar to the equigranular phase but lacks garnets. The abundance, size and crystalline form of the alkali feldspar megacrysts increase towards the east central part of the phase. An areally insignificant, megacrystic, mafic, biotite-rich subphase is clearly intruded by the more common, felsic, megacrystic subphase in the south-central part of the pluton.

An aplitic or fine grained phase occurs within the northeastern part of the equigranular phase and caps the ridge-forming part of the Mactung Pluton. It consists of phenocrysts of ± biotite ± quartz ± alkali feldspar in an aplitic groundmass or of a fine grained equivalent of the equigranular or megacrystic phases.

Interphase intrusive relations are difficult to determine because of the similarity in lithologies involved and heavily lichen-covered exposures but external intrusive relations are clear (Fig. 45.3a). In the eastern Mactung pluton, the equigranular phase gradationally changes to the megacrystic phase over several tens of metres. Alkali feldspar, which is subhedral to anhedral and equigranular in the equigranular phase, increases in size and euhedralism to form a seriate-textured rock near the gradational contact between equigranular and megacrystic phases (Fig. 45.2). Along the eastern margin, the mafic subphase of the equigranular phase clearly intrudes the megacrystic phase. The larger bodies of

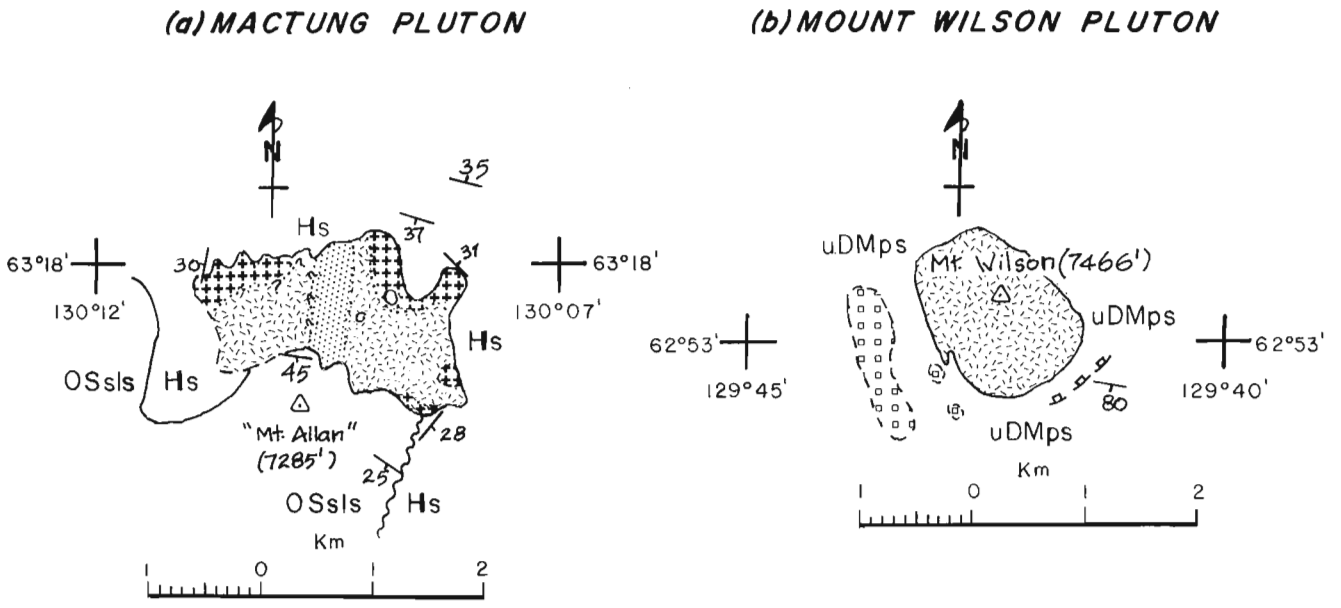

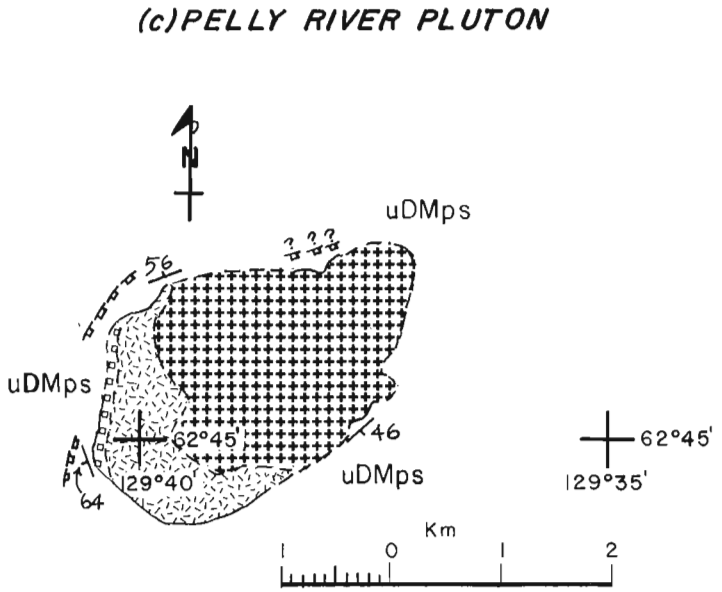

LEGEND

MID-CRETACEOUS

fine-grained biotite quartz syenite and aplite

equigranular biotite granite, minor biotite granodiorite (Mactung pluton); equigranular biotite quartz monzonite (Pelly River pluton)

"porphyritic" biotite-alkali feldspar quartz syenite and granite

megacrystic biotite granite, quartz syenite and quartz monzonite

DEVONIAN AND MISSISSIPIAN

uDMps — *brown to black weathering phyllite, argillite, shale, and hornfelsed equivalents (see Gordey, 1981)*

ORDOVICIAN AND SILURIAN

OSsls — *shale, limestone, minor dolostone and hornfelsed equivalents (see Blusson, 1974; Harris, 1977)*

HADRYNIAN

Hs — *phyllite, minor dolomite and wavy bedded limey siltstone and hornfelsed equivalents (see Blusson, 1974)*

contact: defined, approximate, gradational, inferred

approximate position of andalusite-in isograd

30 *bedding or compositional layering*

fault

Figure 45.2. *Preliminary geological maps of –*

(a) Mactung pluton;

(b) Mount Wilson pluton;

(c) Pelly River pluton.

Border between the Yukon and Northwest Territories in the Mactung and Pelly River plutons is omitted for clarity. Contributions to country rock geology from Blusson (1974), Harris (1977) and Gordey (1981).

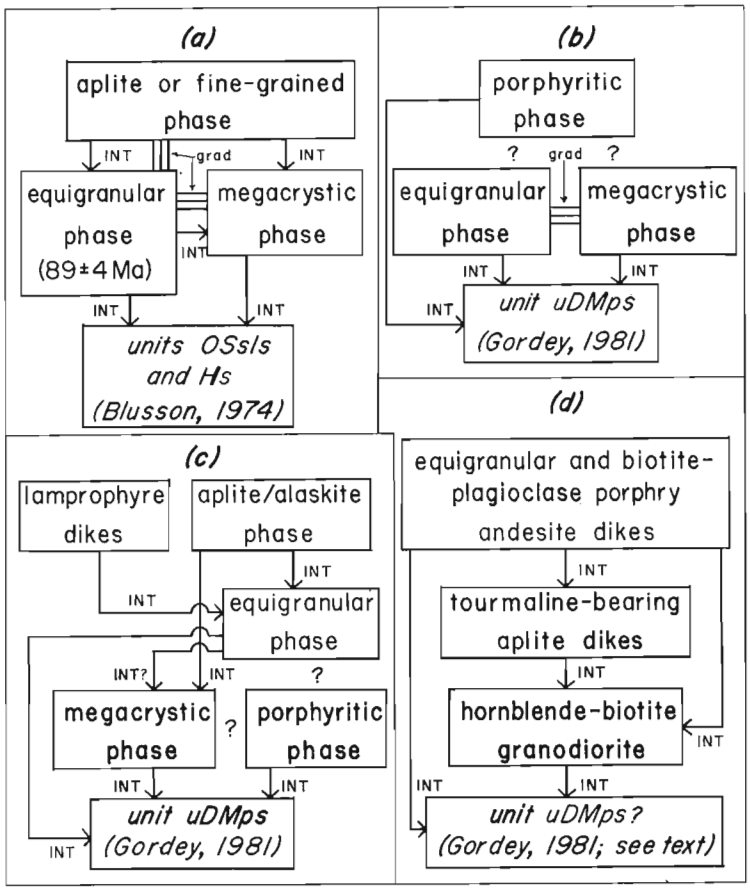

Figure 45.3. *External and interphase intrusive relations for:*

(a) Mactung pluton;

(b) Mount Wilson pluton;

(c) Pelly River pluton;

(d) South Nahanni River pluton.

"INT" refer to intrusive contacts between phases

"grad" refers to gradational contacts.

the aplitic or fine grained phase are also gradational with the equigranular and megacrystic phases but scattered aplite and alaskitic dykes clearly intrude the other phases elsewhere.

The Mactung pluton clearly intrudes, includes and metamorphoses Proterozoic and Ordovician-Silurian rocks (units Hs and OSsls of Blusson, 1974). Apophyses and stockworks occur near the contacts and are rarely chilled; hornfelsed sedimentary and fine grained, biotite-rich mafic inclusions in the granitic rocks appear restricted to within a few tens of metres of the contact. The sediments are metamorphosed to biotite ± andalusite ± cordierite ± feldspar ± quartz assemblages, and the slaty cleavage developed in the sediments away from the contact is obliterated in the hornfelsed rocks. Compositional layering in the hornfels is locally folded but generally dips moderately and radially away from the pluton. Tourmaline-quartz veins intrude equigranular and megacrystic phases and the hornfelsed country rock.

Mount Wilson Pluton

The slightly elongate Mount Wilson pluton comprising sparingly megacrystic (equigranular phase) to slightly megacrystic (megacrystic phase), massive medium grained biotite granite underlies an area of 2.1 km^2 at Mount Wilson in northwestern Nahanni map area (Fig. 45.2b). The equigranular variety is more common at the contact. The megacrystic variety contains 5-10 per cent medium- to coarse-grained megacrysts. A satellitic, southeasterly elongate, massive, porphyritic (alkali feldspar megacrystic-bearing) biotite granite intrusion occurs along the southwestern flank of Mount Wilson (Fig. 45.2b). Although lithologically similar to the megacrystic phase of the main pluton, its groundmass is finer grained. Several varieties of biotite-rich, mafic inclusions compose up to 5 per cent of some outcrops and are most common at the top of the ridge and centre of the pluton.

The equigranular phase grades into the megacrystic phase within a few tens of metres of the contact; the intrusive relations between the "porphyritic" phase and the other phases of the pluton are not known (Fig. 45.3b). Dark brown weathering, hornfelsed, well-cleaved, black shale (unit uDMps of Grodey, 1981) contains fine- to medium-grained andalusite porphyroblasts within 300 m of the contact.

Pelly River Pluton

The Pelly River pluton is a small (5.4 km^2), round body which straddles the Yukon-Northwest Territories border in northwestern Nahanni map area (Fig. 45.2c).

Four phases are recognized in the Pelly River pluton. Equigranular to sparingly megacrystic, massive or rarely foliated or lineated (near contacts), medium grained, hypidiomorphic biotite quartz monzodiorite forms a minor phase gradational with a megacrystic phase in the west and forms a discrete, extensive phase in the east. Mafic inclusions are sparse (1-2 per cent), oval-shaped, and up to 0.5 m long. In a few places inclusions contain smaller inclusions. A megacrystic phase underlies much of the western third of the pluton and is a massive or locally foliated medium- to coarse-grained hypidiomorphic biotite granite or quartz syenite which contains 5-15 per cent, large (up to 4 cm x 2 cm), euhedral to subhedral alkali feldspar megacrysts. Alkali feldspars are only crudely aligned with the local, moderate biotite foliation. Rare, rounded or oval, mafic inclusions persist in the foliated megacrystic phase some distance from the country rock contact. A "porphyritic" phase, consisting of

plagioclase or alkali feldspar ± quartz ± biotite phenocrysts set in an equigranular, fine- to medium grained allotriomorphic to hypidiomorphic groundmass, forms anastamosing dykes in the country rock and is the contact phase along the western margin of the pluton. A minor aplitic or alaskitic phase, locally containing tourmaline spots, is commonly developed near or at the contacts between the equigranular and megacrystic phases. Rare, greenish brown, equigranular, biotite-rich lamprophyre dykes intrude the equigranular phase. Tourmaline-quartz veins in the granitoid rocks are also scarse.

Intrapluton and external intrusive relations for the Pelly River pluton are summarized in Figure 45.3c. Slightly porphyritic, quartz monzodiorite dykes intrude the megacrystic phase near its contact with the equigranular phase; if these dykes are associated with the intrusion of the equigranular phase then the intrusive relations as shown in Figure 45.3c are established. Near some contacts, however, the equigranular phase increases in megacryst content towards the contact and the two lithologies form a sharp, uninformative intrusive contact with no obvious chill effects in either phase. Contacts between the "porphyritic" phase and the megacrystic or equigranular phases are not well exposed and the intrusive relations are unknown. As described earlier, aplite or alaskite and lamprophyre dykes clearly intrude the equigranular and megacrystic phases. The megacrystic, equigranular and "porphyritic" phases intrude, rarely include and metamorphose the phyllite, argillite and minor chert and cherty argillite of the uDMps ("black clastic") unit of Gordey (1981). In the phyllite, along the western and northern margins of the pluton, the approximate location of the andalusite-in isograd is established. Lineated and foliated mylonitic rock occurs along part of the northwestern margin. Mylonitization was clearly contemporaneous with intrusion of parts of the pluton since inclusion-bearing apophyses are mylonitized with the country rock and the contact phase is moderately to intensely foliated or lineated. Rarely preserved bedding or compositional layering in the hornfelsed country rock dips away from the plutonic contact.

South Nahanni River Pluton

The South Nahanni River pluton, underlies an area of 37.5 km^2 in north-central Nahanni map area. The pluton is a round body of homogeneous, massive to faintly foliated or lineated (near contacts), equigranular, medium grained, inclusion-bearing, hypidiomorphic hornblende-biotite granodiorite or quartz monzodiorite. Its outline is given in Gordey (1981). It differs from other plutons studied, in its homogeneity (lack of major constituent phases), abundance of inclusions and presence of hornblende as an important secondary mafic. Mafic inclusions are widespread, commonly form 1-5 per cent of the rock (up to 40 per cent near hornfels contacts), are biotite-rich and polymicitic (but rarely exhibit clear metasedimentary characteristics, 'i.e.', calc-silicate, compositionally layered or rusty hornfels inclusions are rare. They are rounded and up to 2 m long. Northerly trending, greenish grey, anastamosing, aphanitic to porphyritic (plagioclase and (or) biotite phenocrysts) andesite and irregular aplite dykes are common throughout the pluton. Tourmaline patches occur in a few aplite dykes.

Intrapluton and external intrusive relations are given in Figure 45.3d. In addition to the intrapluton intrusive relations described above, locally the aplite dykes are intruded by the greenish grey porphyry dykes. The South Nahanni River pluton intrudes: rusty, tough, thinly compositionally layered (locally crossbedded) quartzose hornfels; rare, thin bedded black chert with buff, oval carbonate nodules; rare platy calc-silicate; and distinctive, black, deformed, coralline limestone which is observed in felsenmeer near one contact and as talus blocks, but not in outcrop, near several other contacts. Commonly the medium grained granodiorite is not chilled against the contact. Assignment of the hornfels according to the stratigraphy of Gordey (1981) is uncertain but may include units uDMps ("black clastic") and OS1 (Road River). All contacts are steeply outward dipping or vertical in outcrop but in some vertical exposures 200-500 m in relief, they are irregular and more gently dipping with increasing elevation. The granitic rock is commonly medium grained and equigranular at contacts; chilled margins are rare. The porphyritic dykes form the obvious anastamosing apophyses which penetrate hundreds of metres into the hornfels. Compositional layering in the hornfels dips moderately to steeply and radially off the pluton.

Age

The plutons in the Niddery Lake and Nahanni map area were mapped as Cretaceous by Blusson (1974), and Gordey (1981). Archibald et al. (1978) and Godwin et al. (1980) have summarized the available K-Ar and Rb-Sr dates for plutons in the southeastern Selwyn Basin (Fig. 45.4). Some dates are discredited because no estimate for atmospheric argon contamination was made during the determination and the dates are probably too old (e.g. the 96 Ma date from the Itsi Range, Sheldon Lake map area (105 J; Baadsgaard et al., 1961) and the 110 Ma date from the Pyramid Mountain stock in the Flat River map area (95 E; Leech et al., 1963, p. 58) or are misquoted from the original source, e.g. the Mactung ("Cirque Lake") pluton (cf. Wanless et al., 1974, p. 26 and Harris, 1977, p. 28; the incorrect 89 Ma date from Harris (1977) was then changed to 91 Ma consistent with the new decay constants by Godwin et al. (1980)) and the Hole-in-the-Wall batholith in the Flat River map area (cf. Gabrielse, 1967, p. 286 and Douglas, 1970). Godwin et al. (1980) concluded that an important period of posttectonic granitic intrusion occurred between 89 and 96 Ma in the southeastern Selwyn Basin. Isotopic studies are underway on samples collected from plutons mapped in the 1981 field season.

Conclusions

Posttectonic granitic plutonism in part of the southeastern Selwyn Basin comprises two suites: a composite, inclusion-free, alkali feldspar megacryst- and biotite-bearing granite and quartz monzonite suite (the Mactung, Mount Wilson and Pelly River plutons); and a homogeneous, inclusion-rich, hornblende- and biotite-bearing granodiorite and quartz monzodiorite suite (South Nahanni River pluton). There is little difference in lithology or intrusive style amongst members of the megacrystic suite which include plutons associated with and devoid of tungsten skarn mineralization. In view of the restricted scope of the present fieldwork and the complex petrogenesis of garnet in granitic rocks (see Clarke, 1981), it is not yet known whether visible accessory garnet is a useful exploration guide for plutons associated with skarn mineralization. In some cases, correlations of hornfelsed country rock with undisturbed stratigraphy is imperfectly known; nevertheless the geological setting of the country rock may be more important than the type of granitic plutonism in localization of economic skarn deposits (e.g. Dick, 1980, p. 429).

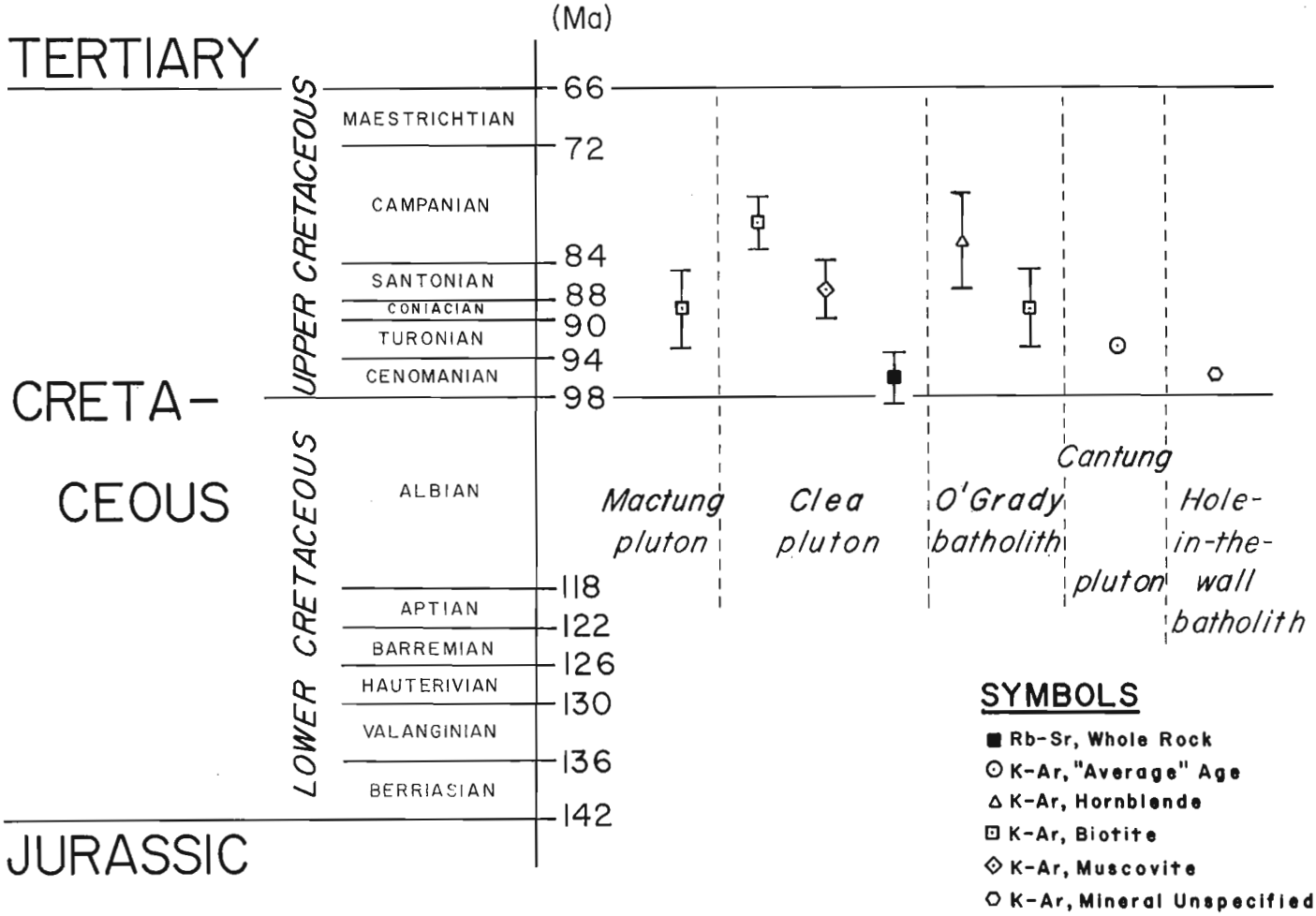

Figure 45.4. *Compilation of isotopic ages from granitic plutons in southeastern Selwyn Basin (Mactung pluton: 89 ± 4 Ma (K-Ar, Bi); Wanless et al., 1974, p. 26; Clea pluton: 80.0 ± 2.7 Ma (K-Ar, Bi), 87.0 ± 3.0 Ma (K-Ar Muscov.), and 96.2 ± 2.7 Ma (Rb-Sr, Whole Rock); Godwin et al., 1980, p. 92; O'Grady Batholith: 82 ± 5 Ma (K-Ar, Hb), 89 ± 4 Ma (K-Ar, Bi); Wanless et al., 1970, p. 37; Cantung plutons: 93 Ma (average K-Ar age, Archibald et al., 1978, p. 1207; Hole-in-the-Wall Batholith, 96 Ma (K-Ar; Gabrielse, 1967)) and Armstrong's (1978) time scale. All dates are consistent with the new decay constants reported by Steiger and Jäger (1977).*

References

Archibald, D.E., Clark, A.H., Farrar, E., and Zaw, U Khin
1978: Potassium-argon ages of intrusion and scheelite mineralization, Cantung, Tungsten, Northwest Territories; Canadian Journal of Earth Sciences, v. 15, p. 1205-1207.

Armstrong, R.L.
1978: Pre-Cenozoic Phanerozoic time scale--Computer file of critical dates and consequences of new and in-progress decay-constant revisions; in Contributions to the Geological Time Scale, G.V. Cohee, M.F. Glaessner and H.D. Hedberg, ed., American Association of Petroleum Geologists, Studies in Geology, no. 6, p. 73-91.

Baadsgaard, H., Folinsbee, R.E., and Lipson, J.
1961: Potassium-argon dates from Cordilleran granites; Geological Society of America Bulletin, v. 72, p. 689-702.

Blusson, S.L.
1968: Geology and tungsten deposits near the headwaters of Flat River, Yukon Territory and southwestern District of Mackenzie, Canada, Geological Survey of Canada, Paper 67-22, 77 p.

1971: Sekwi Mountain map-area, Yukon Territory and District of Mackenzie; Geological Survey of Canada, Paper 71-22, 17 p.

1974: Geology, Operation Stewart (northern Selwyn Basin) Yukon and District of Mackenzie, N.W.T. (106 A, B, C; 105 N, O); Geological Survey of Canada, Open File 205.

Clarke, D.B.
1981: The mineralogy of peraluminous granites: a review; Canadian Mineralogist, v. 19, p. 3-17.

Chappell, B.W. and White, A.J.R.
1974: Two contrasting granite types; Pacific Geology, v. 8, p. 173-174.

Dawson, K.M. and Dick, L.A.
1978: Regional metallogeny of the northern Cordillera: tungsten and base metal-bearing skarns in southeastern Yukon and southwestern Mackenzie; in Current Research, Part A, Geological Survey of Canada, Paper 78-1A, p. 287-292.

Dick, L.A.
1979: Tungsten and base metal skarn in the northern Cordillera; in Current Research, Part A, Geological Survey of Canada, Paper 79-1A, p. 259-266.

1980: A comparative study of the geology, mineralogy and conditions of formation of contact metasomatic mineral deposits in the northeastern Canadian Cordillera; unpublished Ph.D. thesis, Queen's University, 471 p.

Douglas, R.J.W. (editor)
1970: Geology and Economic Minerals of Canada; Geological Survey of Canada, Economic Geology Report 1, Isotopic Age Map 1256A.

Gabrielse, H.
1967: Tectonic evolution of the northern Cordillera; Canadian Journal of Earth Sciences, v. 4, p. 271-298.

Gabrielse, H., Blusson, S.L., and Roddick, J.A.
1973: Flat River, Glacier Lake and Wrigley Lake map-areas, District of Mackenzie and Yukon Territory; Geological Survey of Canada, Memoir 366, 261 p.

Gabrielse, H. and Reesor, J.E.
1974: The nature and setting of granitic plutons in the central and eastern parts of the Canadian Cordillera; Pacific Geology, v. 8, p. 109-138.

Garrett, R.G.
1971a: Molybdenum, tungsten and uranium in acid plutonic rocks as a guide to regional exploration, S.E. Yukon; Canadian Mining Journal, v. 92, no. 4, p. 37-40.

1971b: Molybdenum and tungsten in some acid plutonic rocks of southeast Yukon Territory; Geological Survey of Canada, Open File 51, 5 p.

1972a: Regional geochemical study of Cretaceous acidic rocks in the northern Canadian Cordillera as a tool for broad mineral exploration; in Geochemical Exploration 1972, M.L. Jones, ed., Institute of Mining and Metallurgy, London, p. 203-219.

Garrett, R.G. (cont.)
1972b: Regional geochemical census of plutonic rocks in eastern Yukon Territory (95 E, L, parts of 105 H, J); in Report of Activities, Part A, Geological Survey of Canada, Paper 72-1A, p. 71-72.

Godwin, C.I., Armstrong, R.L., and Tompson, K.M.
1980: K-Ar and Rb-Sr dating and the genesis of tungsten at the Clea tungsten skarn property, Selwyn Mountains, Yukon Territory; Canadian Institute of Mining Metallurgy, Bulletin, v. 73, no. 821, p. 90-93.

Gordey, S.P.
1981: Geology of Nahanni map area, Yukon Territory and District of Mackenzie; Geological Survey of Canada, Open File 780.

Harris, F.R.
1977: Geology of the Macmillan tungsten deposit; in Mineral Industry Report, 1976, Yukon Territory, Department of Indian and Northern Affairs, p. 20-32.

Leech, G.B., Lowdon, J.A., Stockwell, C.H., and Wanless, R.K.
1963: Age determinations and geological studies; Geological Survey of Canada, Paper 63-17, p. 51-53, 58.

Steiger, R.H. and Jäger, E.
1977: Subcommission on geochronology: Convention on the use of decay constants in geo- and cosmochronology; Earth and Planetary Science Letters, v. 36, p. 359-362.

Streckeisen, A.L.
1973: Classification of plutonic rocks; Geotimes, v. 18, no. 10, p. 26-30.

Wanless, R.K., Stevens, R.D., Lachance, G.R., and Delabio, R.N.
1970: Age determinations and geological studies; Geological Survey of Canada, Paper 69-2A, p. 37.

1974: Age determinations and geological studies; Geological Survey of Canada, Paper 74-2, p. 26.

HADRYNIAN HORSETHIEF CREEK GROUP/KAZA GROUP CORRELATIONS IN THE SOUTHERN CARIBOO MOUNTAINS, BRITISH COLUMBIA

EMR Research Agreement 119-4-81

Jennifer Pell[1] and P.S. Simony[1]
Cordilleran Geology Division, Vancouver

Pell, Jennifer and Simony, P.S., Hadrynian Horsethief Creek Group/Kaza Group correlations in the southern Cariboo Mountains, British Columbia; in Current Research, Part A, Geological Survey of Canada, Paper 82-1A, p. 305-308, 1982.

Abstract

The clastic metasedimentary rocks of the Hadrynian Kaza Group stratigraphically overlie most of the Hadrynian Horsethief Creek Group in the southern Cariboo Mountains of eastern British Columbia. The lower units of the Kaza Group are equivalent to the Upper Clastic division of the Horsethief Creek Group which, in turn, can be traced through the Monashee and Selkirk mountains to the northern Purcell Mountains near Rogers Pass. The Kaza Group strata are disposed in broad, nearly upright, compound, phase-two synforms, which are superimposed on the upper limb of a major phase-one south-southwest verging fold nappe, outlined by the Middle Marble division of the Horsethief Creek Group. No major phase-one folds appear to have developed higher in the pile. The style of phase-two folds is controlled by rock type, metamorphic grade and depth within the pile, such that phase-two folds are progressively tighter and more complex as one proceeds eastward and downward.

Introduction

During the summer of 1981, Hadrynian metasedimentary rocks of the southern Cariboo Mountains were mapped at a scale of 1:12 000, between the upper reaches of the North Thompson River in the north, and Thunder River in the south (NTS-83 D). Pell and Simony (1981) showed that Horsethief Creek Group rocks can be traced from the northern Purcells into the southern Cariboo Mountains, and that there, they plunge northwestward under the Hadrynian Kaza and overlying Cariboo groups. In 1981, the Kaza-Horsethief Creek contact zone was investigated in detail.

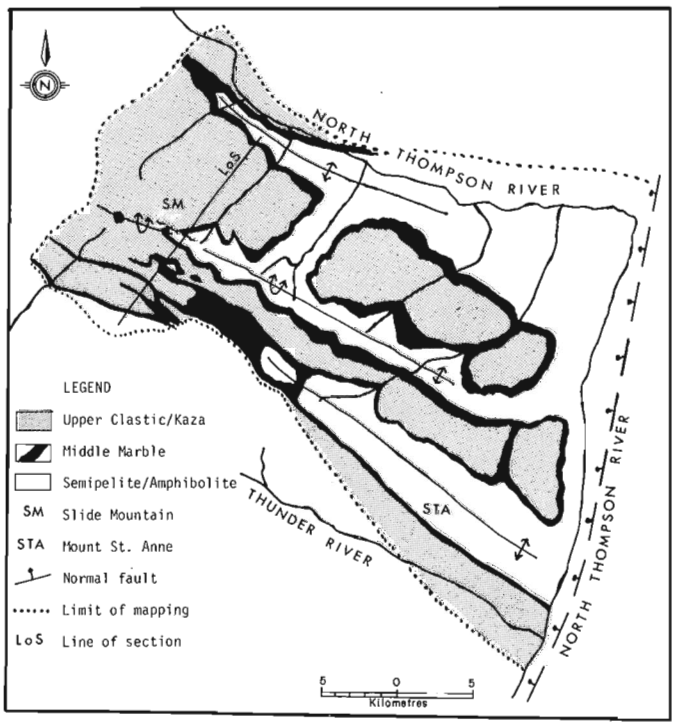

Figure 46.1. *Geology of the southern Cariboo Mountains, British Columbia.*

Garnet-grade rocks form a belt some 10 km wide south of the North Thompson River. That belt is flanked by staurolite – kyanite-grade rocks to the north of the river, and the grade also increases south-southwestward through the staurolite and staurolite-kyanite zones into the sillimanite zone, as the Thunder River is approached. In the broad garnet zone, as well as in the adjacent staurolite zones, sedimentary structures are well preserved, and stratigraphic tops were determined in almost every outcrop. Migmatitic leucosome and pegmatitic bodies occur in the Kaza Group metasediments only within the sillimanite zone. Weakly foliated dykes and sheets of biotite-muscovite granite, 10-50 m thick, are present at widely scattered localities.

Stratigraphy

Three mappable stratigraphic units exist within the study area (Fig. 46.1, 46.2). The lowermost unit is characterized by platy semipelite and amphibolite layers, and is hence termed the Semipelite/Amphibolite division. A full description of this unit was given by Pell and Simony (1981). Within this unit there is a general decrease in the percentage of amphibolites as it is traced to the north and west. The base of the Semipelite/Amphibolite is not exposed within the study area and, therefore, an accurate estimate of thickness is not possible, but it must be in excess of 500 m and possibly up to 1000 m.

Overlying the Semipelite/Amphibolite, is the Middle Marble division. It consists of a basal and an upper carbonate zone, which may each be as much as 100-200 m thick, or as little as 20 m. Massive, grey, thick bedded, pure marbles are always present. In addition, there may be varying thicknesses of massive buff sandy marbles, dolomitic marbles, thin bedded grey marbles with thin rusty pelite interlayers, thicker rusty pelite zones, and pebbly marbles or calcareous grits. Between the two marbles is a clastic zone which can vary from 5-100 m thick. It consists of pelite, psammite, gritty psammite, grits, calcareous garnet psammites, and thin brown sandy carbonate lenses. The drastic changes of thickness within this unit may, in part, be enhanced by tectonism, with a certain amount of thinning on fold limbs, and thickening in hinges, but for the most part, it is due to primary sedimentary variation. The carbonate zones within the Middle Marble division may consist of a single, massive

[1]Department of Geology, University of Calgary

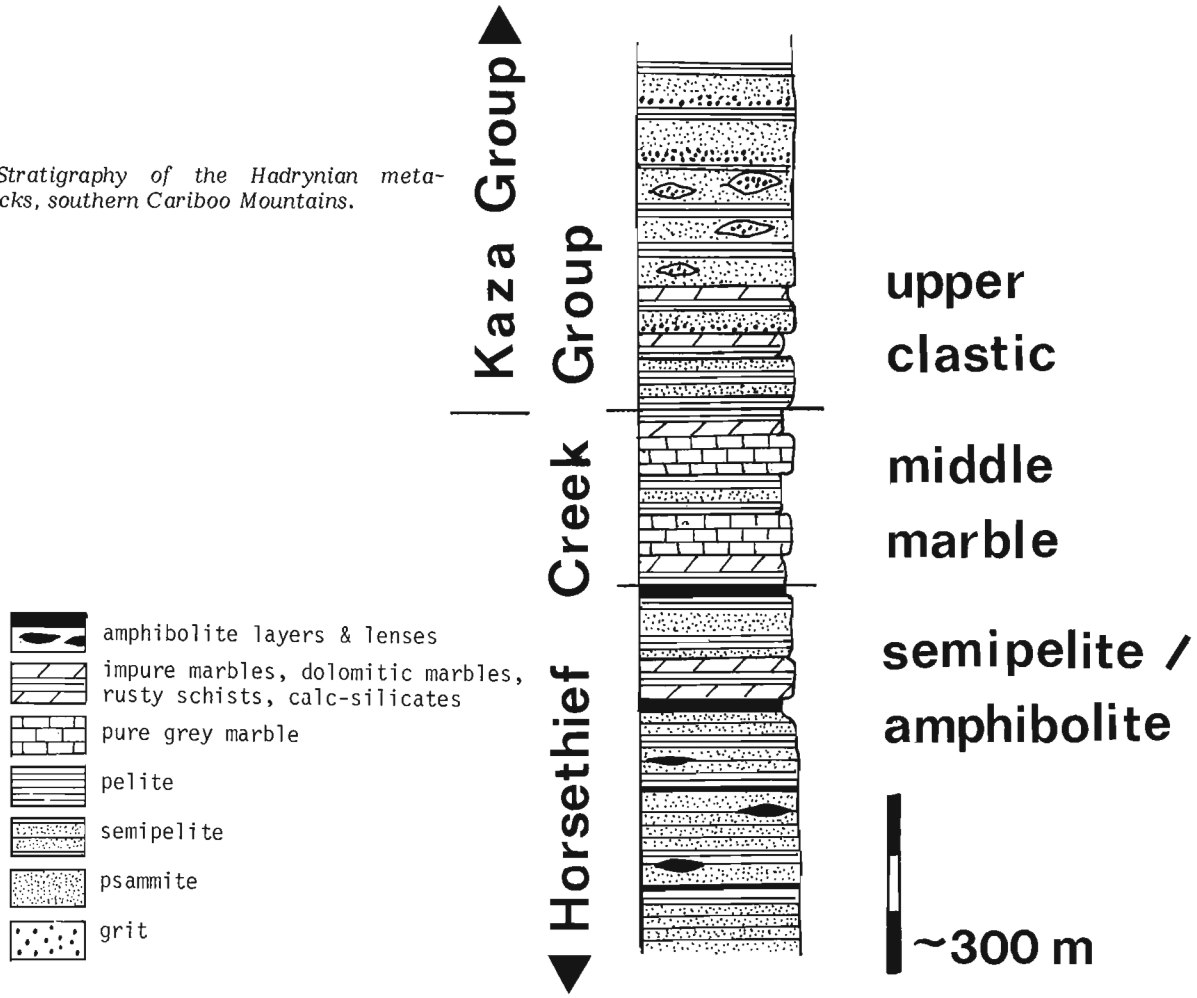

Figure 46.2. Stratigraphy of the Hadrynian metasedimentary rocks, southern Cariboo Mountains.

grey marble bed, or multiple pure grey marbles with some or all of the lithologies described present. This variation is probably due to slight facies changes between on- and off-reef sediments, as suggested by Poulton (1973) for an equivalent stratigraphic horizon in the northern Purcells.

The uppermost stratigraphic horizon, termed the Upper Clastic division, may be broken into four subdivisions, all of which may not be present in every section.

The basal unit consists of thin bedded, alternating psammite or gritty psammite and aluminous pelite layers. Beds average 0.3 m thick. Distinct graded bedding is rarely seen. Some quartzite layers or minor grit lenses may also be present. Hornblende garnet calc-silicate lenses are common in the psammites. This unit is present in almost all sections, and averages 150-1000 m thick.

In many localities, the basal unit is overlain by an impure carbonate horizon, 10-20 m thick. It is generally composed of buff, sandy marbles. In places pure grey marbles occur in this position.

A succession consisting of grit/pelite/carbonate cycles is developed above the impure carbonate in the northern portion of the map area, and can be up to 500 m thick. The individual cycles consist of coarse, graded grits and psammites, often with erosive bases and minor pelite, overlain by thick, dominantly pelite and silty pelite zones, which are in turn overlain by thin sandy carbonates. Each cycle can be 30-50 m thick.

The upper and most widely developed subdivision, the top of which is not exposed within the map area, must have a thickness greater than 2000 m. It consists of thick, dominantly psammitic zones, alternating with pelitic horizons. In the psammitic zones, grit lenses (channels) and more continuous grit beds are common. The individual coarse beds often grade upwards to a fine grained pelite and are topped with a laminated sequence of thin bedded silts and shales. Coarse grit and psammite beds are commonly in excess of one metre thick. The thin alternating silt and shale layers are on the centimetre scale. Flame structures and other loading features are common at the base of coarse beds. In the more pelitic horizons, thin psammitic and grit beds may be present locally. Throughout this subdivision, hornblende garnet calc-silicate lenses occasionally occur in the psammitic beds. Sulphides, mainly pyrite and pyrrhotite, with traces of chalcopyrite and sphalerite, form thin layers as well as disseminations throughout this zone.

Correlations

The lower part of the Kaza Group, as mapped to the west by Campbell (1968) is clearly the same as the Upper Clastic division of the Horsethief Creek Group. The Kaza Group stratigraphically overlies the Middle Marble division of the Horsethief Creek Group in the Cariboo Mountains. The strata which overlie the Middle Marble in the Monashee, Selkirk and Purcell mountains (Brown et al., 1978; Poulton and Simony, 1980) are therefore correlatives of the lower

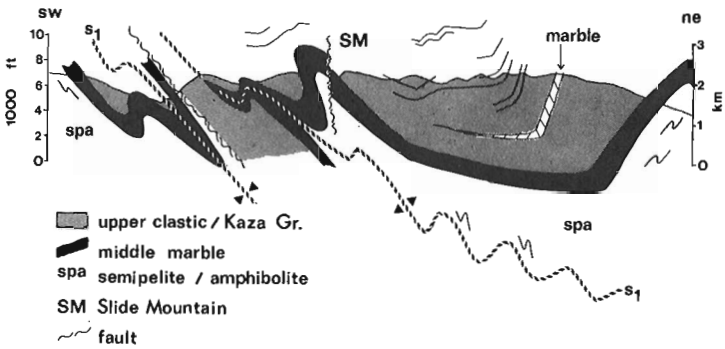

Figure 46.3. Schematic cross-section. See Figure 46.1 for line of section. Horizontal = vertical scale.

portion of the Kaza Group in the Cariboo Mountains. The lower two assemblages of the eastern facies of the Upper Pelitic member, which overlie the Middle Marble in the northern Selkirk Mountains (Brown et al., 1978), and the lower two units of the Upper Clastic division at Rogers Pass (Poulton and Simony, 1980) closely resemble the succession of a lower dominantly pelitic subdivision capped by impure carbonate beds and an upper grit-dominated subdivision of the Kaza/Upper Clastic division in the Cariboo Mountains.

Information from the Canoe River Sheet (Campbell, 1968) indicated that the Kaza Group lying between the Middle Marble and the Isaac Formation of the Cariboo Group is some 5000 m thick. Of this, the lower 3500 m are described here.

In recent years, the Kaza, Cariboo succession has been correlated with the Horsethief Creek Group (Gabrielse, 1972; Young et al., 1973; Brown et al., 1978; Poulton and Simony, 1980). The stratigraphic relationships described above, now show that these correlations cannot be right. The Hadrynian Miette Group of the southern Canadian Rocky Mountains has been correlated with both the Kaza, Cariboo succession of the Cariboo Mountains (Campbell et al., 1973) and the Horsethief Creek Group of the Purcell Mountains (Poulton and Simony, 1980). These correlations now require review and refinement.

Structure

The major mappable structures within the study area are a series of second generation (F_2) antiforms and synforms, with an average shallow northwest axial plunge. Throughout the map area the F_2 folds are characterized by an axial planar crenulation cleavage superimposed upon an earlier S_1 foliation. In the south and east, near Thunder River (Fig. 46.1), where metamorphism reaches sillimanite grade, S_2 is a penetrative strain-slip cleavage. The metamorphic peak postdates the D_2 deformation, as demonstrated by minerals such as garnet, staurolite and kyanite which contain crenulated inclusion trails.

In the vicinity of Slide Mountain (SM in Fig. 46.1, 46.3) the structure is dominated by a large upright F_2 box-type synform, referred to herein as the Slide Mountain Synform. This synform is outlined by the Middle Marble division, and exposes a great thickness of Kaza/Upper Clastic lithologies, in which chevron style mesoscopic folds have developed. On the southwest flank of the Slide Mountain Synform megascopic F_2 folds are overturned to the southwest, and the asymmetry of these folds suggests a major anticlinorium in this direction. On the northeast limb of the synform F_2 vergence is to the northeast. This change in vergence represents a major fan axis, already recognized by Campbell (1968).

In the eastern portion of the map area, near Mount St. Anne (STA in Fig. 46.1), two main megascopic F_2 antiform/synform pairs were mapped (Pell and Simony, 1981). These folds are upright, with complex hinge zones and fanned axial planes. Parasitic folds are very tight.

The structural differences between the eastern and western portions of the map area are a result of various factors. Firstly, on this scale, the major folds are conical, even though the mesoscopic folds may be cylindrical. Major structures such as the Mount St. Anne Antiform diminish and become virtually unidentifiable, while others such as the Slide Mountain Synform increase in importance due to this conicity. The actual differences in fold style from the eastern to the western section are a result of ductility variations between the packages, as influenced by lithology, metamorphic grade, and structural level. In the southeast a package of carbonates, incompetent thin bedded pelites, semipelites and amphibolites of the Semipelite/Amphibolite division were deformed, while to the northwest thickly bedded, much more competent grits and psammites of the Kaza/Upper Clastic division were less deformed, and control the fold style (Fig. 46.3). Where metamorphic grade is greatest (in the southeast) the rock units also behave in a more ductile manner. Also, the eastern part of the area represents a slightly deeper structural level, as the F_2 axial plunge is to the northwest. The increased confining pressure in this zone adds to an increased ductility of the rock, and thus leads to the tightness of folding.

Throughout most of the mapped area, the exposed succession, which outlines the major second generation folds, is entirely on the upright limb of an early recumbent isocline, as confirmed by abundant graded-bedding tops in the Kaza. The bedding/cleavage relationships, observable over a large area at low metamorphic grade, are such that S_1 is steeper north-dipping than bedding, and suggest a southwest vergence for F_1. At high metamorphic grade bedding and the S_1 cleavage are essentially parallel. South of Slide Mountain, a southwest verging F_1 anticline/syncline pair have been mapped (Fig. 46.3) with hinges within the Middle Marble. These folds cause zones of overturned bedding defined by graded-bedding tops, and a reversal in the bedding/S_1 cleavage relationships. A mylonite zone in the Middle Marble, along the northeast limb of the F_1 syncline separates it from the anticline. It is most likely that these folds are relatively minor folds on the upright limb of a much larger structure, the hinge of which would outcrop farther to the southwest.

Numerous postmetamorphic normal faults occur throughout the area. These result in minor offsets in the stratigraphy, but with the exception of the North Thompson River Fault (Fig. 46.1) none have major throws (Pell and Simony, 1981). Some of the faults mapped may be overturned thrusts associated with the F_2 folds. A possible example of this is the fault which offsets the Middle Marble in the overturned antiform to the southwest of the Slide Mountain Synform (Fig. 46.1, 46.3).

Conclusions

Clastic metasedimentary rocks of the Kaza Group conformably overlie the Middle Marble division of the Horsethief Creek Group in the Cariboo Mountains. The Middle Marble and other divisions of the Horsethief Creek Group can be traced continuously from the northern Purcells to the Cariboo Mountains and therefore, the Kaza Group and overlying Cariboo Group represent a northwestward thickening clastic wedge which lies above the northwestward thickening wedge of the Horsethief Creek Group. The Upper Clastic division-Upper Pelite member of Brown et al. (1978) – in the Purcell, Selkirk, and Monashee Mountains represents

the thin edge of the Kaza wedge. Clearly, earlier correlations, which equate formations of the Cariboo Group with the Middle Marble and lower divisions of the Horsethief Creek Group, are incorrect.

In the map area, the Kaza Group lies on the upright limb of a large south-southwest verging fold nappe. This major structure, the axial plane of which must lie in the subsurface, must be the uppermost nappe in a package such as described in the Mica Creek area (Simony et al., 1980; Raeside, 1981). A complete upright stratigraphic section through the Kaza and into the virtually unmetamorphosed Cariboo Group (Isaac, Cunningham, Yankee Belle and Yanks Peak formations) is traceable from this area, through the Quesnel Lake (Campbell, 1963) and into the McBride Map Sheet (Campbell et al., 1973). This enormous, upright stratigraphic package limits the possibility of an overlying nappe.

Large phase-two folds are superimposed upon the phase-one structure. These may be traced northwestward into the McBride Map Area (Campbell et al., 1973). The Slide Mountain Synform is on strike with the Isaac Lake Synclinorium, and the major anticlinorium, suggested by phase-two fold asymmetry on the southwest limb of the Slide Mountain Synform, corresponds with the Lanezi Arch. Within this anticlinorium true Horsethief Creek Group sediments should be exposed at least as far westwards as the Azure River area of the Canoe River Sheet (Campbell, 1968).

The phase-two folds, which started to form before the metamorphic climax, exhibit variations in style. These are influenced by a combination of lithology, metamorphic grade, and tectonic level (confining pressure). The broad box-like form of the Slide Mountain Synform, as seen in Figure 46.3, is typical of the higher levels in the garnet zone.

References

Brown, R.L., Tippett, C.R., and Lane, L.S.
1978: Stratigraphy, facies changes, and correlations in the northern Selkirk Mountains, southern Canadian Cordillera; Canadian Journal of Earth Sciences, v. 15, p. 1129-1140.

Campbell, R.B.
1963: Quesnel Lake (east half) British Columbia; Geological Survey of Canada, Map 1-1963.

Campbell, R.B. (cont.)
1968: Canoe River, British Columbia; Geological Survey of Canada, Map 15-1967.

Campbell, R.B., Mountjoy, E.W., and Young, F.G.
1973: Geology of McBride Map-Area, British Columbia; Geological Survey of Canada, Paper 72-35, 104 p.

Gabrielse, H.
1972: Younger Precambrian of the Canadian Cordillera; American Journal of Science, v. 272, p. 521-536.

Pell, J. and Simony, P.
1981: Stratigraphy, structure, and metamorphism in the southern Cariboo Mountains, British Columbia; in Current Research, Part A, Geological Survey of Canada, Paper 81-1A, p. 227-230.

Poulton, T.P.
1973: Upper Proterozoic "Limestone Unit", northern Dogtooth Mountains, British Columbia; Canadian Journal of Earth Sciences, v. 10, p. 292-305.

Poulton, T.P. and Simony, P.S.
1980: Stratigraphy, sedimentology, and regional correlation of the Horsethief Creek Group (Hadrynian, late Precambrian) in the northern Purcell and Selkirk Mountains, British Columbia; Canadian Journal of Earth Sciences, v. 17, p. 1708-1724.

Raeside, R.P.
1981: Early Columbian nappe folding, Mica Creek, B.C.; Geological Association of Canada, Abstracts 6, p. A-48.

Simony, P.S., Ghent, E.D., Craw, D., Mitchell, W., and Robbins, D.B.
1980: Structural and metamorphic evolution of the northeast flank of the Shuswap Complex, southern Canoe River area, British Columbia; Geological Society of America, Memoir 153, p. 445-462.

Young, F.G., Campbell, R.B., and Poulton, T.P.
1973: The Windermere Supergroup of the southeastern Canadian Cordillera; Proceedings, Belt Symposium, University of Idaho and Idaho Bureau of Mines and Geology, p. 181-203.

GEOLOGY, CHEMISTRY, AND GEOCHRONOMETRY OF THE CRETACEOUS SOUTH FORK VOLCANICS, YUKON TERRITORY

Project 790007

D.H. Wood[1] and R.L. Armstrong[1]
Cordilleran Geology Division

Wood, D.H. and Armstrong, R.L., Geology, chemistry, and geochronometry of the Cretaceous South Fork Volcanics, Yukon Territory; in Current Research, Part A, Geological Survey of Canada, Paper 82-1A, p. 309-316, 1982.

Abstract

The South Fork Volcanics are mafic, calcic, and potassic calc-alkaline andesite and dacite ash flow tuffs and minor associated basaltic andesite flows. They are nearly flat lying in most areas, but basaltic units dip 30 to 50° and ash flow units dip 10 to 15° near Tay and Orchie lakes.

The volcanic rocks unconformably overlie Paleozoic and Mesozoic sedimentary rocks which are folded about northwest trending axes and intruded by a biotite quartz monzonite pluton, which gives a biotite K-Ar date of 104 ± 4 Ma. The top few metres of this pluton are intensely weathered. A whole-rock-mineral isochron for the pluton gives a Rb-Sr isochron date of 89.2 ± 1.9 Ma with an initial $^{87}Sr/^{86}Sr$ ratio of 0.7278 ± 0.0001. The younger date from the isochron is believed to be caused by low grade metamorphism or incipient weathering of the biotite.

Potassium-argon dating indicates the South Fork Volcanics were erupted between 94.4 ± 3.3 and 102 ± 4 Ma ago. A rubidium-strontium whole-rock isochron date of 135.5 ± 9.8 Ma with an initial $^{87}Sr/^{86}Sr$ ratio of 0.7160 ± 0.0002 for the volcanics is believed to be caused by contamination with radiogenic crustal strontium which is greater for more silicic samples. A whole-rock-mineral Rb-Sr isochron for one volcanic sample gave a date of 84.2 ± 1.7 Ma with an initial strontium ratio of 0.7170 ± 0.0001. The young age here is also likely caused by low grade metamorphism or incipient weathering of the biotite.

Introduction

The South Fork Volcanics are an extensive, relatively undeformed suite of intermediate volcanic rocks in south-central Yukon northeast of the Tintina Trench, extending in a 180 km belt across Tay River (105 K) and Sheldon Lake (105 J) map areas. Their age provides an upper limit for the age of deformation of folded and faulted Paleozoic and Triassic strata of outer Selwyn Basin, which they overlie with angular unconformity. Despite their areal extent and significance in being the only extensively preserved volcanics related to widespread mid-Cretaceous plutonism (85-105 Ma) in the Omineca Belt, they have received little systematic study in terms of setting, chemistry, or age.

The South Fork Volcanics were first mentioned by McConnell (1902) who noted that the rocks south of the South Macmillan River were andesite. Keele (1910) noted the presence of andesite tuffs south of the South Macmillan River as well as north of Orchie Lake (in the general vicinity of the areas shown on Fig. 47.1, 47.2). Roddick and Green (1961) described the South Fork Volcanics (their unit 14) of the Tay River (105 K) and Sheldon Lake (105 J) map areas as "grey and dark grey andesite, dacite, and basalt, commonly massive and porphyritic; minor pyroclastic material", and assigned them a Tertiary age on the basis of proximity to Paleocene terrestrial sedimentary rocks. K-Ar dates for the South Fork Volcanics (Green, 1962; Roddick, 1966) showed them to be older than first presumed. GSC K-Ar date 61-43, from unit III of this paper, was 100 Ma, which is very close to the date reported here (102 ± 4 Ma). GSC K-Ar date 61-44, probably from unit E of this paper, was 117 Ma, however its reliability is uncertain since radiogenic argon was reported as 100 per cent. GSC K-Ar date 65-44, also probably from unit E of this paper, was 86 ± 6 Ma, and was interpreted by Roddick (1966) to have been reset by the intrusion of the Anvil Batholith which has about the same age.

Two areas underlain by the South Fork Volcanics in westernmost Sheldon Lake map area were examined during this study; the Orchie Lake area, between Orchie and Tay

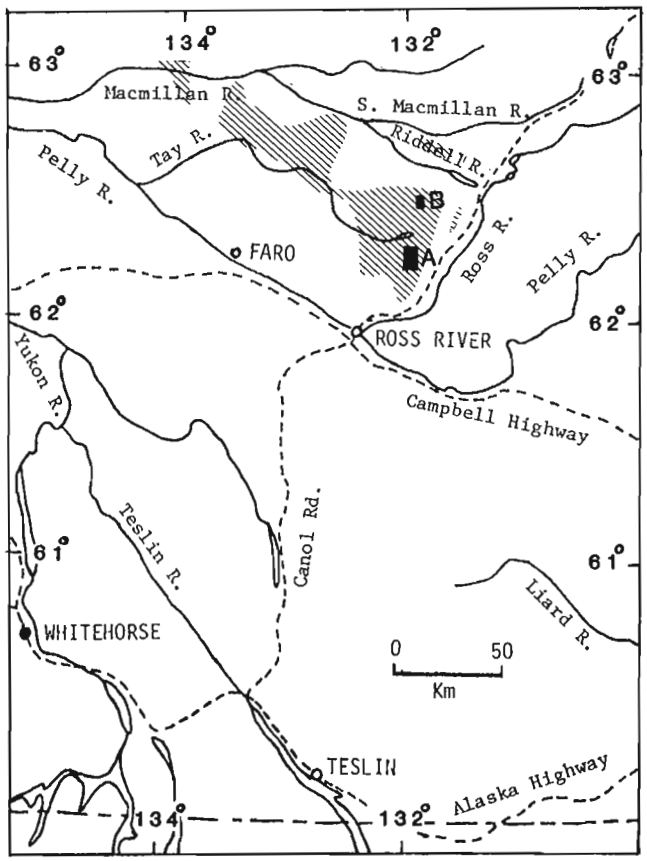

Figure 47.1. Location of Orchie Lake (A) and Riddell River (B) areas. Cross-hatched area is the approximate extent of the South Fork Volcanics.

[1] Department of Geological Sciences, University of British Columbia, Vancouver, B.C., V6T 2B4

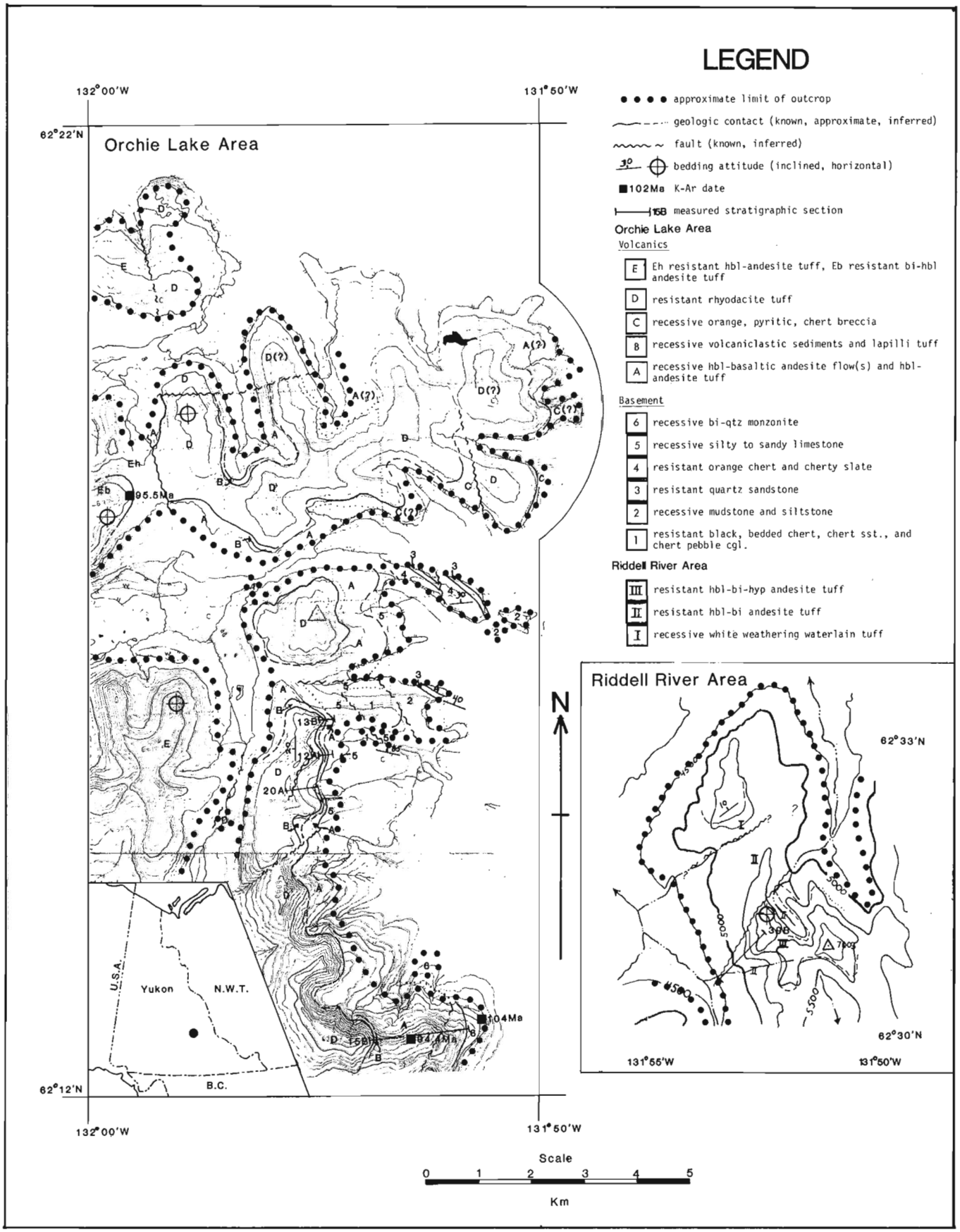

Figure 47.2. *Geologic map of Orchie Lake and Riddell River areas.*

Table 47.1

Major element chemistry and cation normative mineral compositions

	Samples						
	13B1	15B318	20A350	33A	33B	39B	43D
Oxides							
SiO2	58.99	63.04	71.64	68.18	70.24	66.17	67.17
Al2O3	14.51	14.62	12.83	14.22	13.59	13.33	14.59
Fe2O3	7.16	5.99	2.87	4.61	4.15	5.90	3.88
MgO	4.50	3.01	0.82	1.46	1.15	2.22	1.87
CaO	5.43	5.19	2.99	3.76	3.49	4.63	2.95
Na2O	2.29	2.42	2.59	2.50	2.50	1.97	2.41
K2O	1.51	2.40	3.18	2.96	3.30	3.12	4.62
TiO2	0.61	0.55	0.27	0.55	0.51	0.65	0.63
P2O5	0.12	0.13	0.06	0.11	0.10	0.13	0.16
MnO	0.11	0.09	0.05	0.07	0.07	0.09	0.06
H2O	4.32	2.12	2.34	1.16	0.52	1.34	1.21
Minerals							
Qtz	19.63	22.63	36.07	30.48	32.36	28.29	25.62
Or	9.54	14.84	19.75	18.19	20.16	19.32	28.22
Ab	21.88	22.64	24.36	23.25	23.13	18.45	22.27
An	26.63	23.02	14.76	18.66	16.71	19.24	14.05
Opx	18.11	11.55	2.30	5.78	4.12	7.99	5.57
Cpx	1.07	2.44	0.34	----	0.42	3.16	----
Mt	2.27	2.19	1.90	2.20	2.15	2.32	2.27
Il	0.91	0.80	0.40	0.80	0.73	0.95	0.91
Ap	0.27	0.28	0.13	0.24	0.22	0.28	0.35
Cor	----	----	----	----	----	----	0.75

Pressed powder pellets were analyzed by X-ray fluorescence analysis for Si, Al, Fe, Mg, Ca, Na, K, Ti, Mn, and P using the pressed powder method developed by G.C. Brown (1973) and modified by P. Van der Heyden of the University of British Columbia.

Water content was estimated by loss on ignition after heating powder from each sample at 900°C for 12 hours.

Chemical classification was attempted using the procedure of Irvine and Baragar (1971), and cation normative mineral content calculated using a FORTRAN computer program written by G.T. Nixon of the University of British Columbia.

lakes, about 40 km northeast of the settlement of Ross River, Yukon, and the Riddell River area, south of the headwaters of the Riddell River, about 65 km northeast of Ross River (Fig. 47.1, 47.2). Four stratigraphic sections measured in the Orchie Lake area and one section measured in the Riddell River area, as well as detailed petrographic descriptions are reported in Wood (1981).

Orchie Lake Area

Basement Complex

Underlying the South Fork Volcanics are poorly exposed sedimentary rocks of late Paleozoic to Mesozoic age intruded by biotite quartz monzonite. The best exposures of the sedimentary rocks are found along low ridges and in stream gullies in the east-central part of the area.

The oldest rocks exposed are rusty weathering, moderately erosion resistant, black, pyritic, thin-bedded chert, medium-bedded chert sandstone, and massive chert pebble conglomerate, probably equivalent to similar rocks elsewhere in Selwyn Basin of Late Devonian and Mississippian age. Faulted against these Paleozoic rocks, and possibly younger, are recessive, tan-weathering mudstone, siltstone, and very fine grained sandstone which resemble Carboniferous or Permian siltstone found approximately 140 km to the northeast in the Nahanni (105 I) map area (Gordey et al., 1981). Stratigraphically overlying the siltstone are a thin (15-20 m) light grey quartz arenite and orange weathering, orange, and red slate and bedded rusty weathering chert.

The youngest sedimentary rock underlying the volcanics is buff to tan, silty to sandy limestone. Several samples from this unit were examined by M. Orchard (Geological Survey of Canada) who reported conodonts of Late Triassic (Norian) age (**Epigondolella abneptis** and **Epigondolella** cf. **postera**).

At the southern edge of the area are scattered outcrops of light grey, somewhat recessively weathering, biotite quartz monzonite. The top few metres of the pluton are extremely weathered.

South Fork Volcanics

The South Fork Volcanics and related clastic sedimentary rocks within the Orchie Lake area have been divided into 5 laterally extensive units.

Unit A: The lowest volcanic unit in the Orchie Lake area is composed of light greyish green weathering, moderately erosion resistant hornblende-bearing basaltic andesite flow(s) and hornblende andesite ash-flow tuffs. The tuffs are distinguishable from the flows by abundant shale and volcanic lithic clasts. The flows contain 3 to 15% euhedral, 2 to 5 mm long hornblende phenocrysts whereas the tuffs commonly contain fragmented and somewhat smaller hornblende phenocrysts in approximately the same proportions. Both flows and tuffs of unit A contain 20 to 30% plagioclase phenocrysts ranging from An_{60} to An_{75}. Quartz phenocrysts were noted in minor amounts in some specimens. Measured thickness varies from 50 m to more than 600 m.

Unit B: Overlying the basal volcanic unit throughout most of the area are volcaniclastic sandstone, mudstone, conglomerate, lapilli tuff, and a boulder breccia resembling a debris flow. They are recessive and olive-green to dark reddish brown weathering. Where bedding was noted the sediments were either flat lying or dipping gently westward. Measured thickness varies from 30 to 68 m.

Unit C: In the northeastern part of Orchie Lake area, unit D overlies orange weathering, matrix-supported, pyritic chert breccia composed of angular clasts of chert and shale in an orange stained, light coloured, very fine grained siliceous matrix. It is highly fractured and weathers recessively. This unit may be a time equivalent of unit B. Unit C is estimated to have a maximum thickness of over 100 m.

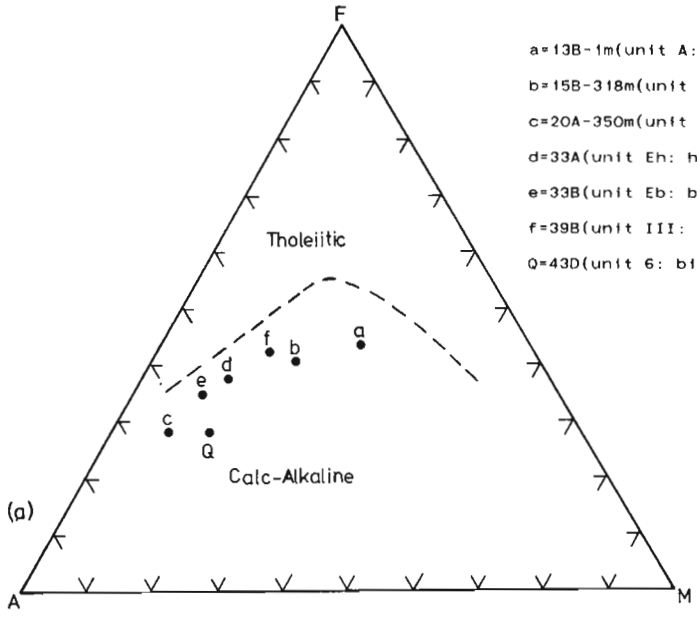

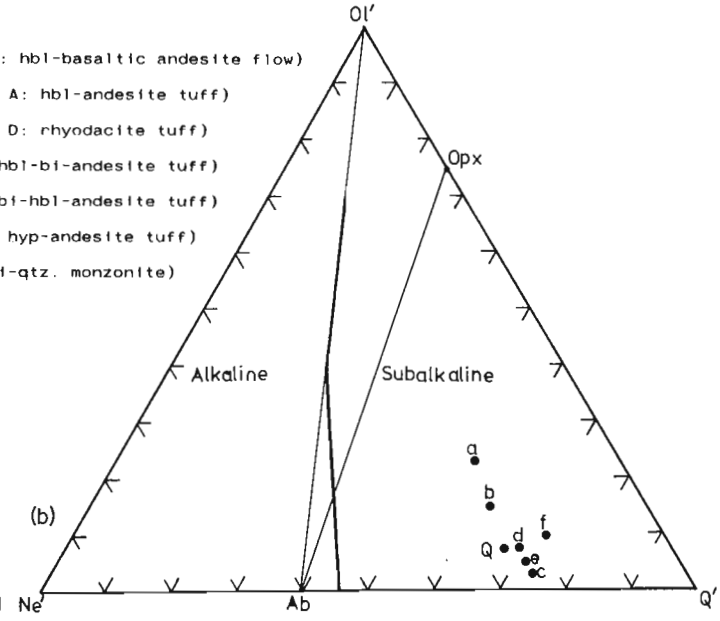

Figure 47.3a. *AFM projection showing a calc-alkaline trend toward alkali enrichment and iron depletion for the South Fork volcanics. Divider after Irvine and Baragar (1971).*

Figure 47.3b. *Ol'-Q'-Ne' projection showing the South Fork Volcanics to be within the subalkaline field. Darker line is the divider suggested by Irvine and Baragar (1971).*

Unit D: Map unit D is composed of welded, massive and bedded, rhyodacite ash flow tuffs with minor flow-banded rhyodacite flows or dykes. Unit D is erosion resistant, cliff forming, and light green to greyish green weathering. Both massive and bedded ash flow tuffs are crystal rich with 10 to 15% alkali feldspar, 7 to 20% smoky quartz, 0 to 12% plagioclase (An_{15}-An_{40}), and minor biotite and hornblende phenocrysts in a light green to greyish pink, welded matrix. Some alkali feldspar crystals are perthitic. Unit D is 400 m thick in central Orchie Lake area, but may be thicker farther north.

Unit E: In the northwest and west part of the area, two similar andesite ash flow tuff units are exposed. Because of chemical and lithological similarities the two rock types are included together as map unit E. Differences between the two, such as the proportion of mafic minerals, warrant some division, however, so they are divided into units Eh (qtz-plag-hbl-bi andesite tuff) and Eb (qtz-plag-bi-hbl andesite tuff).

Unit Eh is dark grey to orange weathering, moderately erosion resistant, and contains unsorted crystal fragments of smoky quartz (20%), plagioclase (20%), hornblende (7%), and biotite (5%) with minor alkali feldspar, pumice lapilli, and lithic clasts in a light greyish green, dusty groundmass. Crystal fragments range in size from 1 to 8 mm. Plagioclase (An_{55}) is mostly homogeneous, but some zoning has been preserved which shows a gradation from approximately An_{45} to An_{60}. In addition to being homogeneous, feldspars have been slightly altered to calcite + sericite, and mafic minerals have been partly chloritized.

Unit Eb abruptly overlies unit Eh and the two are distinguishable by the greater percentage of biotite in unit Eb and by the change in slope caused by the more resistant Eb. Rocks of unit Eb are erosion resistant, blocky, dark grey to rusty-orange weathering, unsorted, crystal-rich, welded andesite ash flow tuffs. Many cliff outcrops display irregularly spaced columnar jointing typical of ash-flow tuffs

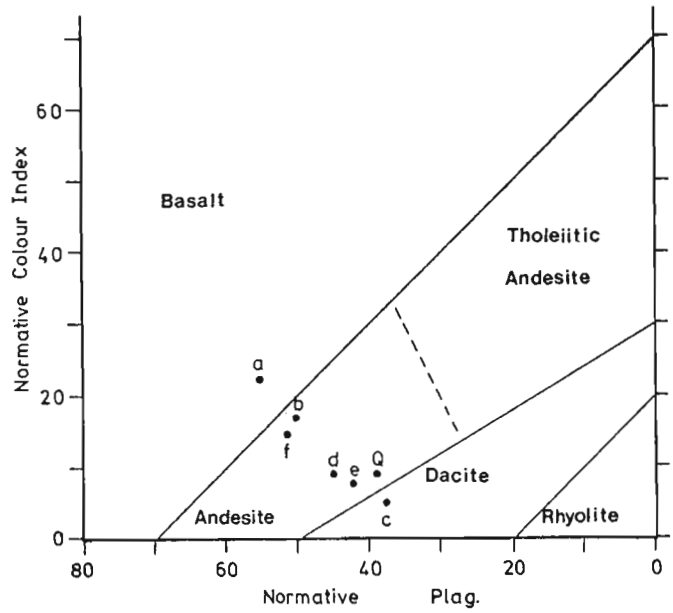

Figure 47.4. *Cation normative colour index vs. cation normative plagioclase diagram for rock classification after Irvine and Baragar (1971). Letters (a-f, Q) are the same as in Figure 47.3.*

(Ross and Smith, 1961). Unit Eb contains fragmented phenocrysts of smoky quartz (15%), plagioclase (15%), biotite (10%), and hornblende (2%). Fragment sizes range from 2 to 7 mm. Plagioclase (An_{52}) is nearly identical to that found in unit Eh. Samples taken from unit Eb show little or no alteration, so that groundmass colour tends to be a little darker than for samples collected from unit Eh.

Table 47.2

K-Ar data for the South Fork Volcanics and underlying biotite quartz monzonite

Sample number	sample Type	Date Obtained	K (weight %)	radiogenic ^{40}Ar ($x10^{-6} cm^3/gm$)	percent of total ^{40}Ar	Location lat	Long
15B-318m	hornblende	94.4 ± 3.3	0.574 ± 0.02	2.162	72.1	62° 13′ 22"N	131° 52′ 36"W
33B	biotite	95.5 ± 3.3	6.64 ± 0.01	25.295	93.7	62° 18′ 13"N	131° 59′ 10"W
39B-6350ft	hornblende	102 ± 4	0.589 ± 0.016	2.402	74.2	62° 30′ 41"N	131° 52′ 38"W
"	biotite	94.9 ± 3.3	4.80 ± 0.02	18.180	93.8	62° 30′ 41"N	131° 52′ 38"W
43D	biotite	104 ± 4	4.97 ± 0.03	20.632	93.5	62° 13′ 29"N	131° 51′ 21"W

K was determined in duplicate by atomic absorption using a Techtron AA4 spectrophotometer and Ar by isotope dilution using an AEI MS-10 mass spectrometer and high purity ^{38}Ar spike.

Errors reported are for one standard deviation.

The decay constants used for K are: $0.581 \times 10^{-10}\ a^{-1}$, $4.962 \times 10^{-10}\ a^{-1}$, and $^{40}K/K = 0.01167$ atom per cent.

Unit E is in fault contact with units A and D. It was not observed in stratigraphic contact with previously described units but is presumed to be younger.

Unit E is distinguishable from unit D by its greater mafic crystal content and more calcic feldspar composition. Units Eh and Eb are flat lying. Unit Eh is estimated to be in excess of 250 m thick and unit Eb more than 200 m.

Riddell River Area

Three units composed of flat lying to gently dipping ash flows and waterlain tuff are present in the Riddell River area. The Paleozoic and Mesozoic sedimentary basement is not exposed.

Volcanic Units

Unit I: The rocks of unit I are white to buff, somewhat recessive weathering, laminated, brown and cream coloured, waterlain tuff. They are fine grained with up to 5 per cent quartz and other crystal fragments. Locally coarse grained lapilli and other ejecta exist within the layering. There are also small convolutions which appear to be a result of soft sediment deformation. When examined closely a slight green or pink colouration was observed on weathered surfaces. Unit I is estimated to be more than 200 m thick.

Unit II: Unit II overlies the waterlain tuff at the northern edge of the area, and is the oldest unit exposed elsewhere. The rocks of unit II are dark greenish grey to orange weathering, erosion resistant, welded, crystal-rich, andesite ash flow tuff. Phenocryst content varies within the unit; phenocrysts are angular fragments of plagioclase (12 to 15% at An_{50}), quartz (10 to 15%), biotite (5 to 10%), and hornblende (0 to 5%) which occur in a fine grained dusty groundmass. Mafic minerals contain abundant zircons in some specimens. The groundmass has devitrified and welding textures were not noted in thin sections. Biotite crystals are deformed around some of the larger crystal fragments; this is interpreted to have been caused by compaction during welding.

Alteration varies from minor to extensive. Plagioclase is altered to sericite + epidote, mafic minerals to chlorite + epidote, and the groundmass is often chloritized. Some specimens show hematite staining. Unit II is 180 m thick where measured.

Unit III. The youngest unit in the Riddell River area is welded, crystal-rich andesite ash flow tuff similar in appearance to unit II. It is dark greenish grey to orange weathering, erosion resistant, and often cliff-forming. Cliff exposures commonly show irregularly spaced large-scale columnar jointing typical of welded tuff (Ross and Smith, 1961).

Phenocrysts are often highly fragmented. They include quartz (15 to 25%), plagioclase (10 to 15% at An_{40}-An_{60}), biotite (7 to 10%), hornblende (5 to 7%), and unique to this unit, hypersthene (4 to 5%). Plagioclase is mostly homogeneous, with slight sericite + epidote alteration, and some faint zoning preserved. Hornblende and biotite crystals are commonly rimmed with chlorite + epidote + ilmenite(?). Hypersthene crystals are nearly completely chloritized. The best preserved hypersthene was found in the cores of some hornblende crystals.

Welding textures are poorly preserved as in unit II but some deformed biotite as well as faint ghosts of flattened pumice lapilli were noted in thin sections. The most characteristic feature that was used in classifying this unit as a welded tuff was the common presence of large-scale columnar jointing observed in cliff outcrops. Unit III is 320 m thick where measured.

Whole Rock Major Element Chemistry

Seven samples were analyzed for major elements; five from the volcanics in Orchie Lake area, one from the volcanics in Riddell River area, and one from the biotite quartz monzonite pluton (unit 6) in Orchie Lake area. Table 47.1 and Figures 47.3 and 47.4 show the results of the chemical analyses and computations.

Table 47.3

Rb-Sr data for the South Fork Volcanics and underlying biotite quartz monzonite

Sample number	sample type	map unit	observed $^{87}Sr/^{86}Sr$	Rb (ppm)	Sr (ppm)	Rb/Sr	Location Lat	Long
13B-1m	whole rock	A	0.7167	51.4	393	0.131	62° 15′ 55"N	131° 54′ 43"W
15B-318m	whole-rock	A	0.7177	92.4	306	0.302	62° 13′ 22"N	131° 52′ 36"W
20A-350m	whole-rock	D	0.7193	145	240	0.603	62° 15′ 34"N	131° 55′ 22"W
33A	whole-rock	Eh	0.7192	122	256	0.477	62° 18′ 18"N	131° 58′ 42"W
33B	whole-rock	Eb	0.7186	125	249	0.504	62° 18′ 13"N	131° 59′ 10"W
"	biotite	"	0.7869	369	18.5	19.98		
"	plagioclase	"	0.7173	24.6	413	0.059		
39B-6350ft	whole-rock	III	0.7181	113	245	0.460	62° 30′ 41"N	131° 52′ 38"W
43D	whole-rock	6	0.7310	198	258	0.766	62° 13′ 29"N	131° 51′ 21"W
"	biotite	"	0.7968	445	23.5	18.9		
"	plagioclase	"	0.7281	50.3	335	0.150		

Rb and Sr concentrations were determined by replicate analysis of the pressed powder pellets using X-ray fluorescence.

USGS rock standards were used for calibration; mass absorption coefficients were obtained from Mo K-alpha Compton scattering measurements.

Rb/Sr ratios have a precision of 2% (1 sigma) and concentrations 5% (1 sigma).

Sr isotopic composition was measured on unspiked samples prepared using standard ion exchange techniques.

The mass spectrometer (60 degree sector, 30 cm radius, solid source) is of U.S. National Bureau of Standards design, modified by H. Faul.

Data acquisition is digitized and automated using a NOVA computer.

Experimental data have been normalized to a $^{86}Sr/^{88}Sr$ ratio of 0.1194 and adjusted so that the NBS standard $SrCO_3$ (SRM987) gives a $^{87}Sr/^{86}Sr$ ratio of 0.71022 ± 2 and the Eimer and Amend Sr ratio of 0.70800 ± 2.

The precision of a single $^{87}Sr/^{86}Sr$ ratio is 0.00013 (1 sigma).

Rb-Sr ages are based on a Rb decay constant of 1.42×10^{-11} a^{-1}.

The regressions were calculated according to the technique of York (1967).

By Irvine and Baragar (1971) classification rules, the South Fork Volcanics are subalkaline, calc-alkaline, and potassium rich. When plotted on the normative colour index versus normative plagioclase diagram (Fig. 47.4), the somewhat peculiar chemistry of the South Fork Volcanics becomes apparent. Sample 13B-1m contains 62.45 per cent silica (Table 47.1), but is classified as a basalt. As a consequence the flows from which this sample was taken are called basaltic andesite in this paper. Analyses of samples 33A and 33B, which contain 69.62 and 71.19 per cent silica (when recalculated as anhydrous and reduced), are classified as andesites. The name rhyodacite is used for sample 20A-350m with 73.85 per cent silica (likewise recalculated) because of the abundance of alkali feldspar in rocks of map unit D from which it came.

The South Fork Volcanics are richer in calcium, iron, and magnesium and lower in alumina and alkalis than most calc-alkaline rocks of similar silica content (Irvine and Baragar, 1971; Jakes and White, 1972; McBirney, 1969; Nockolds, 1954; Ewart, 1979). The alkali/CaO ratio exceeds 1.0 when silica is in excess of approximately 66 per cent; this is higher than for most calc-alkaline rocks. The FeO/MgO ratios average 2.63, which is above the 2.0 dividing line proposed by Jakes and White (1972) to differentiate calc-alkaline island-arc and continental margin volcanics.

Most samples of the South Fork Volcanics contain large amounts of water (Table 47.1) and have undergone lower greenschist facies metamorphism. However, the bulk chemistry apparently has not changed to any great extent. Jolly (1972), working with mafic volcanics, found that under low grade metamorphic conditions, calcium, sodium and

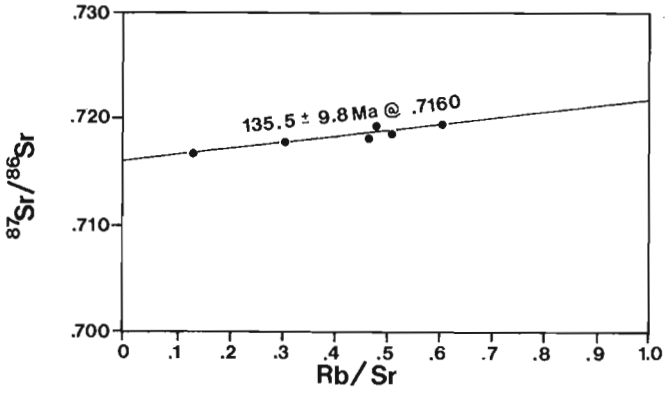

Figure 47.5. Whole-rock Rb-Sr isochron for six samples from the South Fork Volcanics.

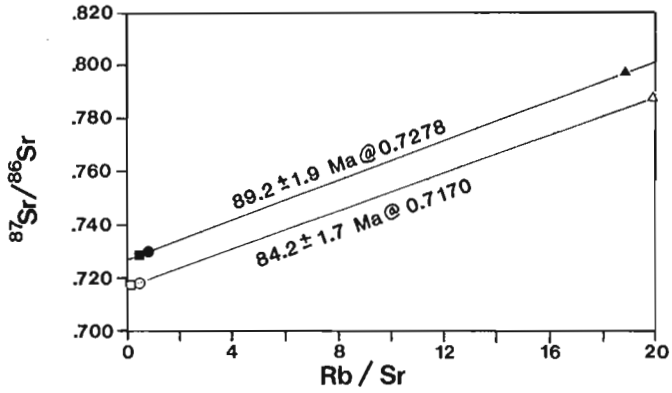

Figure 47.6. Whole-rock – mineral isochrons for sample 43D (solid symbols) and sample 33B (open symbols). Squares are plagioclase analyses, circles are whole-rock analyses, and triangles are biotite analyses.

potassium could become mobile. This may explain the relatively low amounts of alkalis in the South Fork Volcanics, but not the higher than normal calcium content. The chemistry is consistent with the observed primary mineral assemblage, which includes relatively calcic plagioclase, abundant mafic minerals, and abundant quartz.

Mixing of a siliceous crustal melt with a mafic, mantle derived magma may explain the distinctive chemistry of this suite. The tectonic setting, more than 500 km inland from the active subduction zone of the Gulf of Alaska, is unlike that of most modern volcanic fields and may provide additional reasons for the chemical peculiarity of these rocks.

Geochronometry

K-Ar Dating

Five K-Ar dates were obtained from the study areas (Table 47.2), three from Orchie Lake area and two from Riddell River area. Due to lower greenschist facies metamorphism some dates, especially those for biotite, may be reset. However, the biotite date of 95.5 ± 3.3 Ma obtained from the least altered, and probably the youngest ash flow unit in the Orchie Lake area (map unit Eb) is very close to the hornblende date of 94.4 ± 3.3 Ma for the oldest volcanic unit in the same area (map unit A). This suggests that resetting, if any, has been slight or that alteration occurred soon after eruption.

The two dates from the Riddell River area are from biotite and hornblende separates taken from the same sample (sample 39B – 6350 ft). Here the 94.9 ± 3.3 Ma date from the biotite probably represents the time at which this unit (map unit III) underwent metamorphism, and the hornblende date of 102 ± 4 Ma would be close to the time of deposition.

The 104 ± 4 Ma age for sample 43D (biotite quartz monzonite) does not contradict stratigraphic evidence that it was emplaced long enough before the volcanics to allow it to be unroofed and deeply weathered. The lack of shallow emplacement textures such as miarolitic cavities or intergrowth of quartz and alkali feldspar suggest that the pluton was emplaced at a depth of greater than 1 km, and would require several Ma for exposure by erosion.

Rb-Sr Dating

Three isochron dates (see Table 47.3 for Rb-Sr data) were obtained using the Rb-Sr method; a whole-rock isochron (Fig. 47.5) for six volcanic samples, which gives a date of 135.5 ± 9.8 Ma with an initial ratio of 0.7160 ± 0.0002, a whole-rock-mineral isochron (Fig. 47.6) for volcanic sample 33B (map unit Eb) which gives a date of 84.2 ± 1.7 Ma with an initial ratio of 0.7170 ± 0.0001, and a whole-rock-mineral isochron (Fig. 47.6) for sample 43D, from the biotite-quartz monzonite pluton in the Orchie Lake area (map unit 6), which gives a date of 89.2 ± 1.9 Ma with an initial ratio of 0.7278 ± 0.0001.

Although the dates for the volcanic whole-rock and whole-rock-mineral isochrons do not agree, the initial ratios are very close. The initial ratios are accurate in spite of the uncertainty in Rb-Sr whole rock and mineral dates because of the low Rb/Sr ratios of the sample suite.

The high initial ratios for both the volcanics and the pluton have implications concerning the crust beneath the Selwyn Basin. They can be due to: 1) the addition of ^{87}Sr by contamination of the magmas which produced the volcanic rocks and pluton with older and hence ^{87}Sr-enriched crustal rocks, 2) derivation of the primary magmas from partial fusion of lower continental crust (Faure, 1977; Pushkar et al., 1970; Scott et al., 1971), or 3) interaction between mantle-generated magma and ancient subcontinental lithosphere (Brooks et al., 1976).

The initial strontium ratios for the South Fork Volcanics are much higher than for calc-alkaline volcanic rocks of Central America (Pushkar et al., 1970), the Andes (James, 1978), and the southwestern United States (Scott et al., 1971). This indicates that either the source of contamination was older and therefore more enriched in ^{87}Sr or that crustal contamination was greater for the South Fork Volcanics.

The initial ratio for the pluton is also exceptionally high. LeCouter and Tempelman-Kluit (1976) have discussed the gradual northeastward increase of strontium isotope initial ratios across the Yukon Crystalline Terrane, but the highest ratio they observed west of the Tintina Fault was 0.7071. The only initial ratio reported for rocks east of the fault is, like the ones reported here, exceptionally high. Godwin et al. (1980) obtained an initial ratio of 0.7234 for a mid-Cretaceous granitic pluton near the Yukon-Northwest Territories boundary, east of our study area.

The good agreement between individual K-Ar dates (Table 47.2) indicates that they were either all synchronously reset by the same low-grade metamorphic conditions, which does not appear likely, or they closely approximate the age of the volcanic rocks, which is the interpretation we prefer. The isochron dates are then all anomalous. The anomalously old date for the whole-rock isochron is probably caused by the addition of ^{87}Sr through crustal contamination (Faure, 1977). Scott et al. (1971) observed such an increase of ^{87}Sr contamination with increasing silica content in Cenozoic ash flow crystal tuffs of southern Nevada. The young dates for the two whole-rock-mineral isochrons may be a result of removal of ^{87}Sr and/or addition of common Sr by base exchange involving groundwater (Clauer, 1978; Kulp, 1964), either during low-grade burial metamorphism or more recently.

Conclusions

The South Fork Volcanics are areally extensive calc-alkaline ash flow tuffs that appear to have been derived from siliceous but unusually mafic and calcic, and somewhat potassic magmas. They were erupted between approximately 95 and 102 Ma ago during mid-Cretaceous (approximately Albian) time. Some of the rocks show lower greenschist facies metamorphic assemblages, and Rb-Sr mineral dates are reset. Deformation is limited to faulting and tilting. Strontium isotope initial ratios indicate that crustal contamination of the volcanic magmas was extensive. The volcanic whole-rock isochron date has been exaggerated by crustal contamination correlated with silica enrichment.

Acknowledgments

The project was suggested by S.P. Gordey of the Geological Survey of Canada, and undertaken by D.H. Wood as a B.Sc. thesis project at the University of British Columbia. The Geological Survey provided logistical field support. Laboratory costs were covered by a Canadian Natural Sciences and Engineering Research Council operating grant to R.L. Armstrong. J.E. Harakal did the Ar analyses and K. Scott the K analyses. K. Scott also provided assistance with Rb-Sr and Sr analyses.

References

Brooks, C., James, D.E., and Hart, S.R.
1976: Ancient lithosphere: its role in young continental volcanism; Science, v. 193, p. 1086-1094.

Brown, G.C.
1973: New XRF data retrieval techniques and their application to USGS standard rocks; Chemical Geology, v. 11, p. 223-229.

Clauer, N.
1978: Behaviour of strontium and argon isotopes in biotites during a progressive natural weathering; in United States Geological Survey, Open File Report 78-701, p. 68-71.

Ewart, A.
1979: A review of the mineralogy and chemistry of Tertiary-Recent dacitic, latitic, rhyolitic and related rocks; in Trondjemites Dacites and related rocks, F. Barker, ed., Elsevier, Amsterdam, p. 13-121.

Faure, G.
1977: Principles of Isotope Geology; John Wiley and Sons, N.Y., N.Y., 646 p.

Godwin, C.I., Armstrong, R.L., and Tompson, K.M.
1980: Geology, K-Ar, and Rb-Sr dating of the Clea tungsten skarn property, Selwyn Mountains, Yukon Territory; Canadian Mining and Metallurgy Bulletin, v. 73, no. 821, p. 90-93.

Gordey, S.P., Wood, D., and Anderson, R.G.
1981: Stratigraphic framework of southeastern Selwyn Basin, Nahanni Map Area, Yukon Territory and District of Mackenzie; in Current Research, Part A, Geological Survey of Canada, Paper 81-1A, p. 395-398.

Green, L.H.
1962: K-Ar dates for the Tay Formation, Yukon Territory; in Age Determinations and Geological Studies – Report 3, Geological Survey of Canada, Paper 62-17, p. 17.

Irvine, T.N. and Baragar, W.R.A.
1971: A guide to the chemical classification of the common volcanic rocks; Canadian Journal of Earth Sciences, v. 8, p. 523-548.

Jakes, P. and White, A.R.J.
1972: Major and trace element variations in volcanic rocks from orogenic areas; Geological Society of America, Bulletin, v. 83, p. 29-40.

James, D.E.
1978: Origin of high $^{87}Sr/^{86}Sr$ ratios in central Andean calc-alkaline lavas; in United States Geological Survey Open File Report 78-701, p. 199-201.

Jolly, W.T.
1972: Degradation(hydration) – aggradation(dehydration) and low-rank metamorphism of mafic volcanic sequences; in Proceedings of the Twenty-Fourth Session of the International Geological Congress, Section 2, p. 11-18.

Keele, J.
1910: Report on a reconnaissance across the Mackenzie Mountains on the Pelly, Ross, and Gravel rivers, Yukon and Northwest Territories; Canada Department of Mines, Geological Survey Branch, Report 1097, p. 7-50.

Kulp, J.L.
1964: Concordance and discordance between K-Ar and Rb-Sr isotopic ages from micas; in Chemistry of the Earth's Crust, v. 2: Jerusalem, Israel Program for Scientific Translation, p. 592-606.

LeCouter, P.C. and Tempelman-Kluit, D.J.
1976: Rb/Sr ages and a profile of initial Sr^{87}/Sr^{86} ratios for plutonic rocks across the Yukon Crystalline Terrane; Canadian Journal of Earth Sciences, v. 13, p. 319-330.

McBirney, A.R.
1969: Andesitic and rhyolitic volcanism of orogenic belts; in The Earth's Crust and Upper Mantle, P.J. Hart, ed., American Geophysical Union, Monograph 13, p. 501-507.

McConnell, R.G.
1902: The Macmillan River, Yukon District; in Summary Report, Geological Survey of Canada, p. 22-38.

Nockolds, S.R.
1954: Average chemical compositions of some igneous rocks; Geological Society of America, Bulletin, v. 65, p. 1007-1032.

Pushkar, P., McBirney, A.R., and Kudo, A.M.
1970: The isotopic composition of strontium in Central American ignimbrites; Bulletin Vulcanologique, v. 35, p. 265-294.

Roddick, J.A.
1966: K-Ar date for the Tay Formation, Yukon Territory; in Age determinations and geological studies, K-Ar ages, Report 7; Geological Survey of Canada, Paper 66-17, p. 42-43.

Roddick, J.A. and Green, L.H.
1961: Preliminary series maps of Sheldon Lake map area (105J) and Tay River map area (105K); Geological Survey of Canada, Maps 61-12 and 61-13.

Ross, C.S. and Smith, R.L.
1961: Ash-flows: their origin, geologic relations and identification; United States Geological Survey, Professional Paper 366, 81 p.

Scott, R.B., Nesbit, R.W., Dasch, E.J., and Armstrong, R.L.
1971: A strontium isotope evolution model for Cenozoic magma genesis, eastern Great Basin, U.S.A.; Bulletin Volcanologique, v. 35, p. 1-26.

Wood, D.H.
1981: Stratigraphy and geochronology of the Cretaceous South Fork Volcanics, southeastern Yukon Territory; B.Sc. thesis, Unviersity of British Columbia, 56 p.

York, D.
1967: The best isochron; Earth and Planetary Science Letters, v. 2, p. 479-482.

METAMORPHISM AND STRUCTURE OF THREE LADIES MOUNTAIN AREA, CARIBOO MOUNTAINS, BRITISH COLUMBIA

EMR Research Agreement 63-4-81

J.S. Getsinger[1]
Cordilleran Geology Division, Vanvcouver

Getsinger, J.S., Metamorphism and structure of Three Ladies Mountain area, Cariboo Mountains, British Columbia; in Current Research, Part A, Geological Survey of Canada, Paper 82-1A, p. 317-320, 1982.

Abstract

The high grade schists and gneisses of the Snowshoe Formation (Hadrynian) west of the North Arm of Quesnel Lake may be broadly divided into a lower sequence of interlayered micaceous quartzites and quartz-rich schists intruded by quartz dioritic sills and an upper sequence containing aluminous pelites, impure carbonates and amphibolites, and interlayered micaceous quartzites and quartz-mica schists. These are overlain by a clean white marble. Early isoclinal folding was followed by two phases of oppositely-verging, coaxial folding, and later local broad folding. Prograde metamorphism up to sillimanite zone accompanied deformation; recrystallization outlasted major folding. A low angle, postmetamorphic fault superposed younger, low grade marbles and phyllites on older, high grade schists and gneisses, implying major displacement. Structural features demonstrate lateral movement of the hanging wall rocks in the southeast direction.

Introduction

This is a progress report on field research for a Ph.D. degree at the Univeristy of British Columbia. Geologic mapping at a scale of 1:25 000 during the 1980 and 1981 field seasons covered 200 km^2 including Three Ladies Mountain and Mount Stevenson (NTS 93 A). Most of the area was previously mapped by Campbell (1978) as Hadrynian and/or Paleozoic Snowshoe Formation. A preliminary attempt at stratigraphic subdivision of the Snowshoe Formation in this area is made, but no definite correlations are proposed. Four phases of folding were interpreted from minor structures, but not all are clearly exhibited at the map scale. Metamorphic grade is kyanite to sillimanite zone in the Snowshoe Formation, and chlorite to biotite zone in the rocks above the Little River Fault (Fig. 48.1; Klepacki, 1981). This low angle, postmetamorphic fault marks a major difference in metamorphic conditions and may be of regional tectonic significance.

Thanks are given to Dr. H.J. Greenwood of the University of British Columbia for supervision, and to R.B. Campbell and L.C. Struik at the Geological Survey of Canada in Vancouver for their discussion and support.

Stratigraphy

The stratigraphy in the map area has not been positively correlated with any other area of the Cordillera. The high grade metamorphic rocks west of the North Arm of Quesnel Lake, consisting of folded metasediments and various intrusive phases, have been called Snowshoe Formation and assigned a Hadrynian to Paleozoic age by Campbell (1978) and other workers. Fletcher (1972) divided the same rocks into Isaac and Kaza formations on the basis of a similarity to his own field area at Penfold Creek, east of the North Arm of Quesnel Lake. This Snowshoe Formation may share some similarities with the Snowshoe Formation near Wells as mapped by Struik (1981), and resembles parts of the Horsethief Creek Group as mapped by Pell (Pell and Simony, 1981) near Blue River. Fossils and sedimentary structures showing definite facing directions have not been observed. Original bedding is obliterated by cleavage and metamorphism, but some lithologic units are distinguished on the map. Schists presently assigned to the Snowshoe Formation near Maeford Lake are in apparent stratigraphic contact with an overlying, thick, coarsely crystalline white marble mapped as the Cunningham Formation marble, but this identification is debatable (Campbell, 1978; Klepacki, 1981).

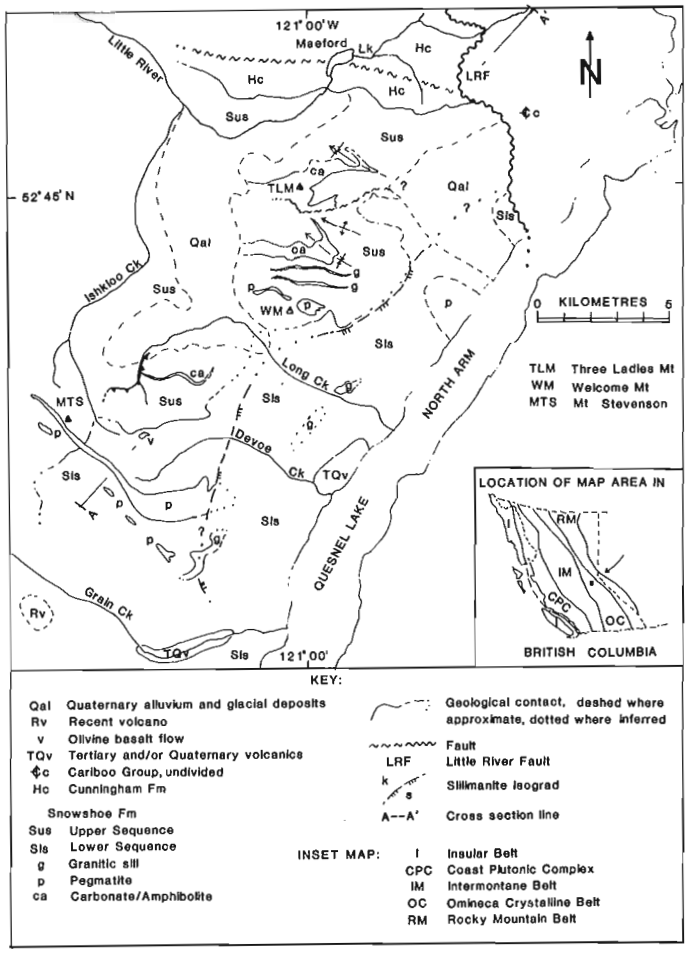

Figure 48.1. *Geology of Three Ladies Mountain/Mount Stevenson area, Cariboo Mountains, B.C. Inset shows location of area and its relation to Cordilleran tectonic belts in British Columbia.*

[1] Department of Geological Sciences, University of British Columbia, Vancouver

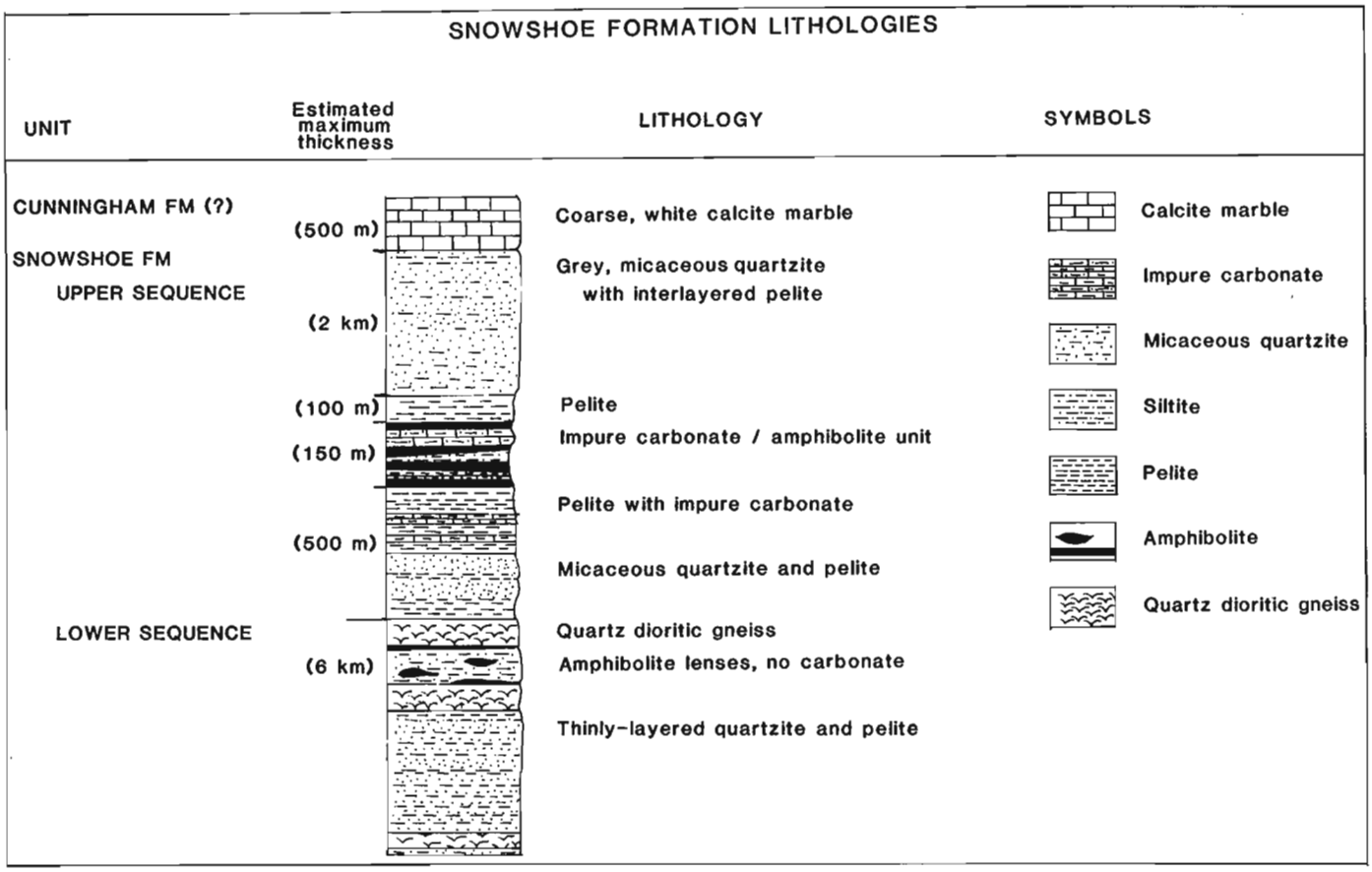

Figure 48.2. *Lithologies of the Snowshoe Formation below the Little River Fault. Thickness not to scale.*

The Snowshoe Formation in the map area may be divided into a lower structural sequence (up to 6 km thick) covering most of the area from Mount Stevenson to the North Arm of Quesnel Lake, and an upper structural sequence best defined in the Three Ladies Mountain area, where it is approximately 3 km thick (Fig. 48.2). Much of the thickness may be due to structural repetition.

The lower sequence consists of interlayered, foliated grey micaceous quartzite, brownish weathering quartz-rich biotite-muscovite schist, and greenish-grey, gneissose quartz dioritic sills, all irregularly intruded by extensive pegmatite. Such rocks outcrop from the western shore of the North Arm of Quesnel Lake south of Gain Creek to Mount Stevenson, and are practically indivisible stratigraphically at the map scale, although some contacts of the intrusive have been mapped over several kilometres. Grain size of the psammitic layers is relatively constant and does not exceed granule size; the expected coarse granule grits and conglomerates characteristic of the Kaza Group are conspicuously lacking. The upper boundary of the lower sequence is arbitrarily chosen at the top of the first continuously mappable hornblende-bearing quartz dioritic sill, which is parallel to other lithologic layers in the section.

The upper sequence, in contrast, contains carbonate and calc-silicate, para-amphibolite, and common staurolite-kyanite schist. It lacks quartz dioritic sills, and is not as extensively intruded by pegmatites. Internal stratigraphy is variable along strike due to discontinuous layering and complex folding. The lowermost subdivision of the upper sequence consists of staurolite-kyanite schist interlayered with whitish, well sorted quartzite, minor marble, and some magnetite-bearing schist. It averages about 500 m thick, but is thickened by leucocratic granodiorite gneiss sills north of Welcome Mountain. Overlying the lower pelite is the most distinctive subdivision of the upper sequence containing a variety of rock types including hornblende amphibolite intercalated with impure marble up to 20 m thick, calc-silicate layers between pelite and carbonate, biotite schist, fine grained, black, graphitic quartz siltite, and green, pyrite-bearing micaceous psammite. Thickness of the unit varies from 10 to 150 m due to folding and repetition. It is generally overlain by another staurolite-kyanite schist with minor magnetite-bearing layers, and a thick section (up to 2 km) of grey, micaceous quartzite interlayered with quartzose, garnetiferous mica schist, which continues up to the base of the Cunningham Formation (?) marble.

The stratigraphy of the low grade marble and phyllite above the Little River Fault has not yet been defined in detail; these metasediments were mapped by Klepacki (1981) as Yankee Belle Formation (upper Hadrynian Cariboo Group).

Metamorphism

The Snowshoe Formation in the map area was regionally metamorphosed in the middle amphibolite facies, whereas the sediments above the extension of the Little River Fault achieved only greenschist to lower amphibolite facies metamorphism. Lack of alumino-silicate minerals and relatively

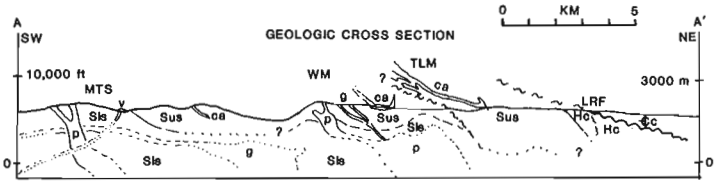

Figure 48.3. *Geologic cross-section from A to A' on map of Figure 48.1. Key is same as for Figure 48.1; vertical equals horizontal scale.*

monotonous compositional layering in the dominant lithology of interlayered quartz-rich mica schist and micaceous quartzite preclude thorough field-mapping of isograds. The more aluminous pelite contains prograde metamorphic index minerals from garnet to sillimanite. Kyanite is common over a large part of the area, both distributed in staurolite-kyanite schist and concentrated in quartz segregations with muscovite. Staurolite appears to be restricted by composition layering and was not observed outside the kyanite zone. Kyanite and sillimanite were not seen in the same rock. Sillimanite is present locally as visible radiating aggregates, but is more widespread as fibrolite in pelitic layers of the lower quartzitic sequence. In the Three Ladies Mountain area, the trace of the isograd corresponding to the first appearance of sillimanite is roughly concordant with the lithologic transition from the lower sequence of quartzites with quartz diorite sills to the upper sequence containing the more aluminous pelite and calc-silicate. This relationship may be fortuitous as previous regional mapping showed that metamorphic isograds crosscut large structures (Campbell, 1971; Campbell, 1978). Prograde metamorphic recrystallization probably outlasted penetrative deformation, although later retrogression and deformation occurred locally. Above the extension of the Little River Fault, the pelite is phyllitic rather than schistose, and contains chlorite and sericite as major minerals. Biotite porphyroblasts occur in a few places near the fault.

Structure

A cross-section of the map area is shown in Figure 48.3.

Folding

The relative sequence of deformational episodes was inferred mainly from observation of minor structures on outcrop scale, rather than map-pattern.

Three phases of penetrative deformation were distinguished in the foliated metasediments. Early isoclinal folding (F1) produced a foliation that was later folded around tight, east-verging, northwest-plunging folds (F2), which in turn were subsequently folded by west-verging, northwest-plunging, tight to normal folds (F3). Pelitic layers display well developed schistosity axial planar to third-phase folds in large hinge zones, whereas quartzitic and calcareous layers have retained dominant first- or second-phase foliation. The east-verging folds are apparently coaxial with the west-verging folds, and where observed in the same outcrop are invariably overprinted by the latter.

A fourth phase of folding is indicated locally throughout the map area by rounded, open to gentle upright folds with shallow northeasterly plunge.

Faulting

No pre-metamorphic faults were identified.

The Little River Fault, mapped by Klepacki (1981) near Maeford Lake, immediately north of the present map area, was traced south into the North Arm of Quesnel Lake. This variably east-dipping fault separates high grade schist and gneiss in the footwall from lower grade metasediments in the hanging wall. The footwall rocks include coarse grained Cunningham Formation (?) marble and the underlying metamorphosed Snowshoe Formation and granitic rocks. The hanging wall rocks, some of which were mapped by Klepacki (1981) as Yankee Belle Formation, consist of a series of 10-15 m thick marble layers intercalated with phyllite and fine grained quartzite. These are mapped as Hadrynian to Cambrian Cariboo Group. Mylonitic textures occur in the marble. Complex fold structures on both sides of the fault are crosscut by the fault. New evidence from minor structures in the Snowshoe Formation (below the projection of the trace of the Little River Fault toward Three Ladies Mountain), such as consistent orientation of slickensides and drag on fault surfaces, indicates that movement in the hanging wall was east-southeast relative to the footwall. This sense of movement strongly suggests that, as the Snowshoe Formation was uplifted, the overlying lower grade rocks slid off to the southeast. Another interpretation is that the hanging wall rocks were thrust over the Snowshoe Formation from the west on a fault that was subsequently tilted to the east by later deformation. Although both interpretations are possible, the first is preferred because of the drag structures associated with the fault and the probable younger-over-older sequence.

Southeast- and northeast-trending high angle faults with small displacements are common.

Igneous Activity

Igneous activity occurred at various intervals in the history of the Snowshoe Formation in the Three Ladies Mountain/Mount Stevenson area.

Quartz dioritic sills, containing biotite, hornblende, and epidote, in the lower micaceous quartzite and pelite of the Snowshoe Formation display well developed foliation and mineral lineation subparallel to that in the adjacent metasediments, and are involved in east-verging, probably second-phase folds. They constitute about a quarter of the lower sequence.

Large areas of pegmatite are exposed from Quesnel Lake up to Mount Stevenson. In many places, pegmatite appears to have intruded as irregular dykes subparallel to axial planes of west-verging, third-phase folds, as well as along other zones of weakness. A crude planar fabric in the larger bodies suggests continuing deformation during crystallization.

Quartz veins averaging about one metre thick are present but not common. Those observed are roughly planar and crosscut earlier structures. Whereas some occur along joint surfaces probably related to the Little River Fault, others are parallel or at a low angle to compositional or metamorphic layering. Nearly vertical northeast-trending veins are most common in the Mount Stevenson area, where rusty alteration zones along their borders are associated with sparse molybdenite, pyrite, and chalcopyrite.

Young olivine basalt flows of limited extent were discovered on the floor of a cirque at 1800 m elevation, 3 km east of Mount Stevenson. Location, association with glacial till, and structures such as pillow breccias suggest eruption beneath alpine glaciers. These previously unmapped lavas may be near the source of similar volcanics that occur directly down-valley at the western shore of the North Arm of Quesnel Lake at Devoe Creek, and may be related to the apparently Recent volcanic cone just south of Grain Creek.

References

Campbell, K.V.
1971: Metamorphic petrology and structural geology of the Crooked Lake area, Cariboo Mountains, British Columbia; unpublished Ph.D. thesis, Univerity of Washington, 192 p.

Campbell, R.B.
1978: Quesnel Lake, British Columbia; Geological Survey of Canada, Open File Map 574.

Fletcher, C.J.N.
1972: Structure and metamorphism of Penfold Creek area, near Quesnel Lake, central British Columbia; unpublished Ph.D. thesis, University of British Columbia, 123 p.

Klepacki, D.W.
1981: The Little River Fault – a low angle boundary fault of the northern Shuswap Complex, Quesnel Lake, British Columbia; in Abstracts, Volume 6, Geological Association of Canada, Mineralogical Association of Canada, and Canadian Geophysical Union, Joint Annual Meeting, p. A-32.

Pell, J. and Simony, P.
1981: Stratigraphy, structure, and metamorphism in the southern Cariboo Mountains, British Columbia; in Current Research, Part A, Geological Survey of Canada, Paper 81-1A, p. 227-230.

Struik, L.C.
1981: Snowshoe Formation, central British Columbia; in Current Research, Part A, Geological Survey of Canada, Paper 81-1A, p. 213-216.

FAULTING AND PLUTONISM IN NORTHWESTERN CRY LAKE AND ADJACENT MAP AREAS, BRITISH COLUMBIA

Project 760016

H. Gabrielse and C.J. Dodds
Cordilleran Geology Division, Vancouver

Gabrielse, H. and Dodds, C.J., Faulting and plutonism in northwestern Cry Lake and adjacent map areas, British Columbia; in Current Research, Part A, Geological Survey of Canada, Paper 82-1A, p. 321-323, 1982.

Abstract

The boundary between the Omineca Crystalline Belt and Intermontane Belt in northwestern Cry Lake and adjacent map areas in northern British Columbia is marked by complex structure and a complicated plutonic history. The oldest set of faults, possibly of mid-Jurassic age, are interpreted as thrust faults placing younger on older strata. The prominent Kutcho and Cassiar fault zones are transcurrent faults with mid-Cretaceous displacements. The youngest faults are easterly trending and may be as young as Tertiary.

The oldest plutons are hornblende diorite to granodiorite of Early Jurassic age. They may be thrust, with Upper Triassic volcanic rocks, over an autochthonous metamorphosed miogeoclinal assemblage. Late Jurassic granodiorite to quartz monzonite intrudes the Early Jurassic suite. The youngest intrusive rocks are mid-Cretaceous quartz monzonites to granites.

Introduction

Northwestern Cry Lake map area (104 I) and adjacent parts of McDame (104 P), Jennings River (104 O) and Dease Lake (104 J) map areas straddle the boundary between the Omineca Crystalline Belt and Intermontane Belt. The boundary is marked by complex structure and a complicated plutonic history. During the 1981 field season studies were directed to determining the nature and relationships of three distinct sets of faults and to resolving the sequence of granitic intrusion.

Stratigraphy

Three stratigraphic assemblages occur in the area and are everywhere separated by faults or intrusions (Fig. 49.1). The presumed oldest rocks comprise strongly foliated micaceous quartzite, garnet-mica schist, crystalline limestone and calc-silicate that are believed to be facies equivalents of miogeoclinal strata underlying areas farther east. Their general lithology suggests an early Paleozoic age.

To the southwest is an extensive terrane of oceanic type strata assigned to the Cache Creek Group of Mississippian to Permian and possibly younger age. Typical lithologies are ribbon chert, shale, limestone, ultramafics, basic volcanics and gabbro.

The youngest assemblage consists of resistant augite andesite porphyry, tuff and minor clastic sedimentary rocks. In northeastern Dease Lake map area these rocks are overlain by clastic strata, including much conglomerate, of Early Jurassic age (H.W. Tipper, personal communication 1981).

Faults

Three distinct sets of faults are recognized. The most prominent is the Kutcho fault which has been traced from southeastern Cry Lake map area (Gabrielse, 1979) into southeastern Jennings River map area. It has a remarkably consistent trend of about 135 degrees and forms a zone as much as 1.5 km wide of strongly cataclastized foliated rocks. These include weakly sheared to mylonitic granitic rocks and metasedimentary strata with extremely planar and consistent foliation. Northwest of Dease River foliations in rocks with trends commonly between 110 and 120 degrees swing into parallelism with the fault zone near its margins. Lineations in and along the Kutcho fault plunge gently and generally range from 0 to 20 degrees to the northwest or southeast. The extreme linearity of the fault and the gently dipping lineations, well seen in the granitic rocks, suggest mainly transcurrent movements.

In southeastern Jennings River map area, east of Cottonwood River, the Kutcho fault zone intersects the more northerly trending Cassiar fault zone. The latter can be traced northerly into the Yukon Territory (Gabrielse, 1969) and is characterized by a major shear zone in which granitic rocks along the western border of the Cassiar batholith have been pervasively sheared and mylonitized over widths of as much as 3 km. The intensity of strain increases towards the western margin of the zone. A strong lineament on trend with the Kutcho fault zone indicates that it probably continues northwest along the headwaters of Parallel Creek. If this is so the Cassiar fault zone may be regarded as a splay off the Kutcho fault zone.

A second set of faults trending generally between 80 and 100 degrees clearly affect sinistral offsets of the Kutcho fault and Jurassic granitic rocks. They are steeply dipping and are typified by strong lineaments and well developed foliation. The foliation has been overprinted on the earlier foliation related to the Kutcho fault. Minor structures suggest upward and eastward movement of rocks on the south sides of the faults.

The third set of faults is represented by the Thibert fault with related splays and faults at the base of Upper Triassic volcanics. Thibert fault is marked by a string of ultramafic bodies, mainly serpentinite, and its trace indicates it dips from steeply south-southwest to nearly vertical. Along the fault the southwest side is structurally high.

Faults at the base of the Upper Triassic volcanic assemblage separate the volcanics from significantly more metamorphosed underlying strata. The volcanics consist of strongly foliated chloritic schist near the faults with decreasing deformation away from the fault. Most foliation dips steeply. The relationship of the volcanics to the underlying more metamorphosed rocks suggests the contacts may be thrust faults that have placed younger on older strata.

Data in the study area are consistent with those obtained farther southeast in Cry Lake map area which show that the earliest recognized structures are thrust faults and related tear faults. They may indicate collision of the

terrane "Stikinia" with ancestral North America with "Stikinia" moving relatively northward. Early, southerly directed movement on the King Salmon Fault probably took place at this time, possibly during the Middle Jurassic (Gabrielse, 1978). Conceivably northerly thrusting of the Upper Triassic volcanic assemblage with its spatially related granitic rocks and of the Cache Creek Group represented coeval deformation in response to the same stress.

The Kutcho and Cassiar fault zones clearly involve mid-Cretaceous granitic rocks and the former truncates a fault at the base of the upper Triassic volcanics. Muscovite generated in the Cassiar fault zone indicates mid-Cretaceous deformation and by analogy it may be assumed that at least some movement on the Kutcho fault took place at the same time. The trends and sense of displacements along Thibert fault and the fault at the base of the Upper Triassic volcanics do not preclude some movement on these faults during the mid-Cretaceous transcurrent faulting along Kutcho fault.

The age of the easterly-trending faults, although clearly post mid-Cretaceous is uncertain. Eocene(?) felsic rocks occur just north of a major easterly-trending fault zone near Four Mile River and may be related to movement along the fault zone. In any event these faults are clearly the youngest developed in the study area.

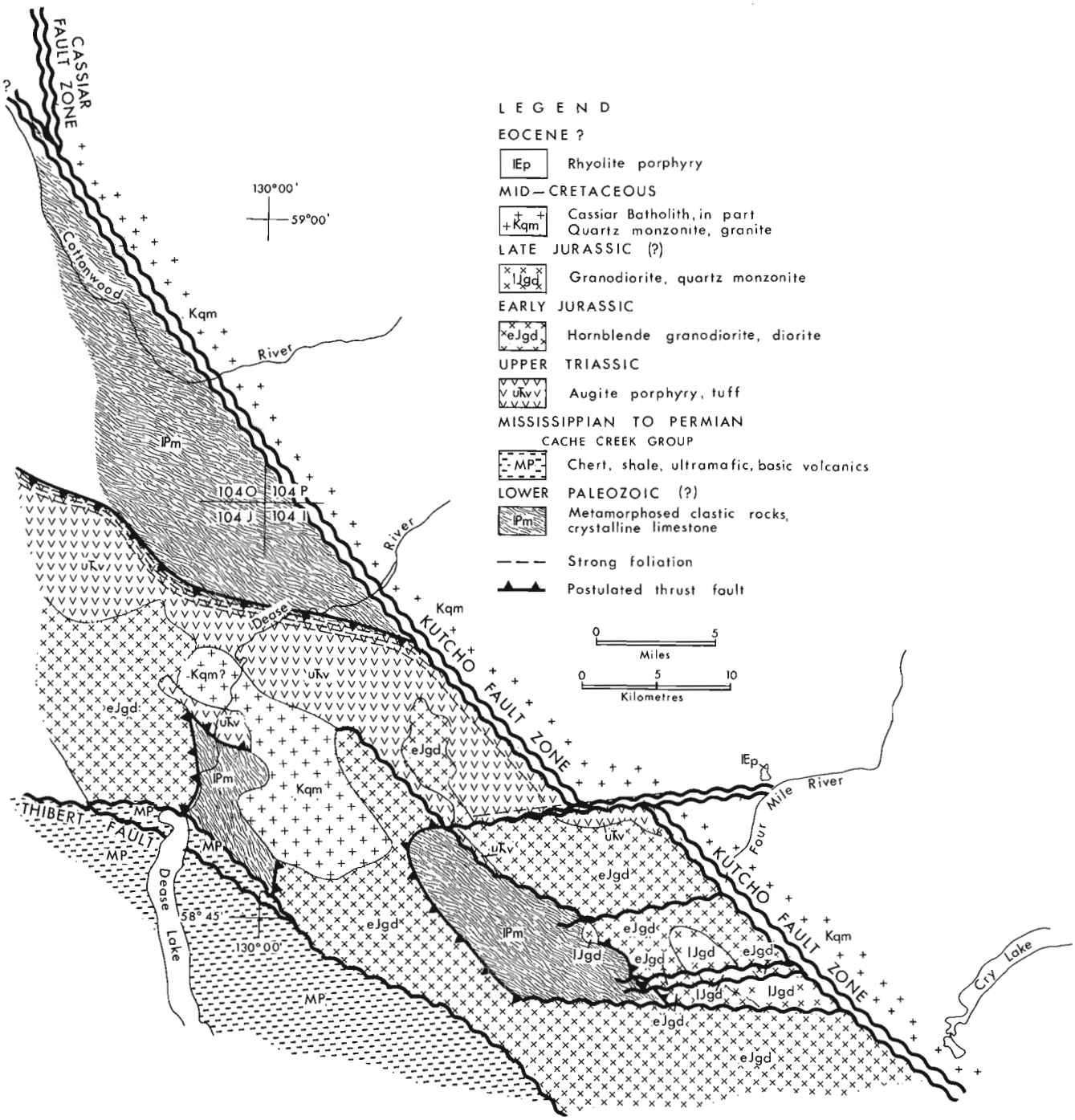

Figure 49.1. Geological map of northwestern Cry Lake (104 I) and adjacent map areas.

Plutons

Four distinctive varieties of granitic rocks have been recognized in the report area. The oldest forms a batholith bounded by Thibert and Kutcho faults. Characteristically it is a medium- to coarse-grained mesocratic granodiorite to quartz diorite with conspicuous crystals of prismatic hornblende as long as 2 cm. The rocks have intruded Upper Triassic volcanic rocks and with the volcanics probably formed in an island arc setting. Similar rocks to the southeast have yielded Early Jurassic K-Ar age dates.

In the southeastern part of the report area even grained biotite hornblende granodiorite to quartz monzonite has intruded the hornblende diorite suite. The granodiorite commonly has small megacrysts of potash feldspar which impart a pink weathering to the rock. Preliminary K-Ar age dates suggest a Late Jurassic age. The rocks may be more widespread than shown in Figure 49.1.

Medium- to coarse-grained, locally coarsely megacrystic quartz monzonite and granite comprise the Cassiar batholith northeast of Kutcho fault and a stock that has intruded all assemblages except the Cache Creek Group northeast of Dease Lake. Numerous K-Ar age dates in the region show that these rocks are mid-Cretaceous.

Just north of the intersection of Four Mile River and an easterly trending fault zone a small area of porphyritic and flow banded felsic rock is exposed in the gorge of a southerly flowing tributary stream. The porphyry is cut by northerly trending basaltic dykes. Presumably the felsic rocks could be as young as Eocene, the youngest age determined in the region on felsic rocks.

References

Gabrielse, H.

1969: Geology of Jennings River map-area, British Columbia; Geological Survey of Canada, Paper 68-55.

1978: Operation Dease; in Current Research, Part A, Geological Survey of Canada, Paper 78-1A, p. 1-4.

1979: Geologial map of Cry Lake map-area; Geological Survey of Canada, Open File Report 610.

1980: Geological map of Dease Lake map-area; Geological Survey of Canada, Open File Report 707.

STRATIGRAPHY, STRUCTURE AND METAMORPHISM IN DESERTERS RANGE, NORTHERN ROCKY MOUNTAINS, BRITISH COLUMBIA

Project 700047

C.A. Evenchick[1]
Cordilleran Geology Division

Evenchick, C.A., Stratigraphy, structure and metamorphism in Deserters Range, northern Rocky Mountains, British Columbia; in Current Research, Part A, Geological Survey of Canada, Paper 82-1A, p. 325-328, 1982.

Abstract

Deserters Range, on the east side of the Northern Rocky Mountain Trench in northern British Columbia is underlain by late Proterozoic and (?) older strata faulted against upper Cretaceous(?) and lower Tertiary rocks along the Trench. The stratigraphic assemblage, more than 2000 m thick, includes amphibolite, schist, quartzite, marble, diamictite, grit and phyllite overlying a basal unit of thick-bedded pure quartzite. The basal quartzite overlies strongly foliated granite gneiss which may be Precambrian basement or a relatively young intrusion. The strata have been deformed into a kinked, east dipping homocline characterized by intense crinkling, boudinage and disharmonic folding. Metamorphic grade increases from lower greenschist in the east to amphibolite in the west where kyanite, staurolite and garnet are present.

Introduction

During the 1981 field season detailed studies on the stratigraphy, structure, and metamorphism were begun in the Deserters and Sifton ranges flanking the Northern Rocky Mountain Trench (NRMT) in northern British Columbia (Fig. 50.1). These ranges are underlain by stratigraphic assemblages of Proterozoic to early Ordovician age whose distinctive lithological, structural, and metamorphic characteristics may provide constraints on estimates of transcurrent displacement along the fault zone within the Northern Rocky Mountain Trench. This report deals only with the Deserters Range.

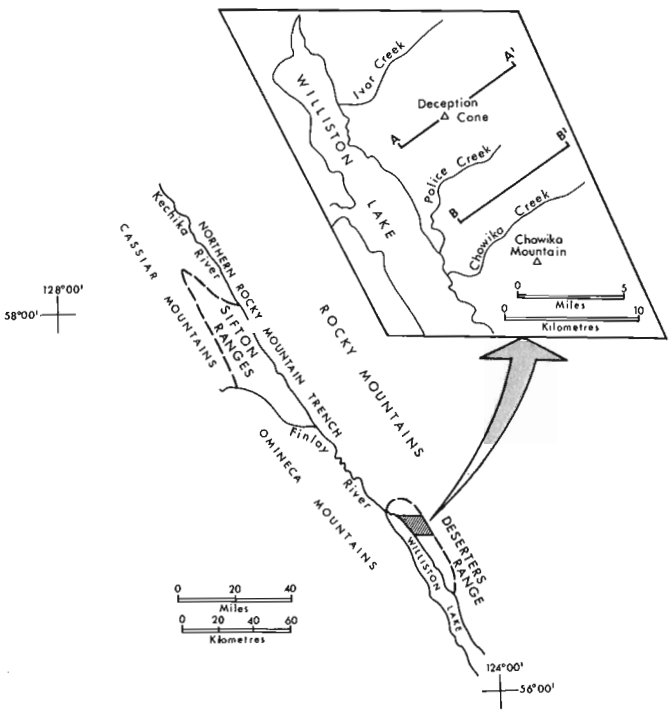

Figure 50.1. Map showing study area and locations of structural cross sections (Fig. 50.4).

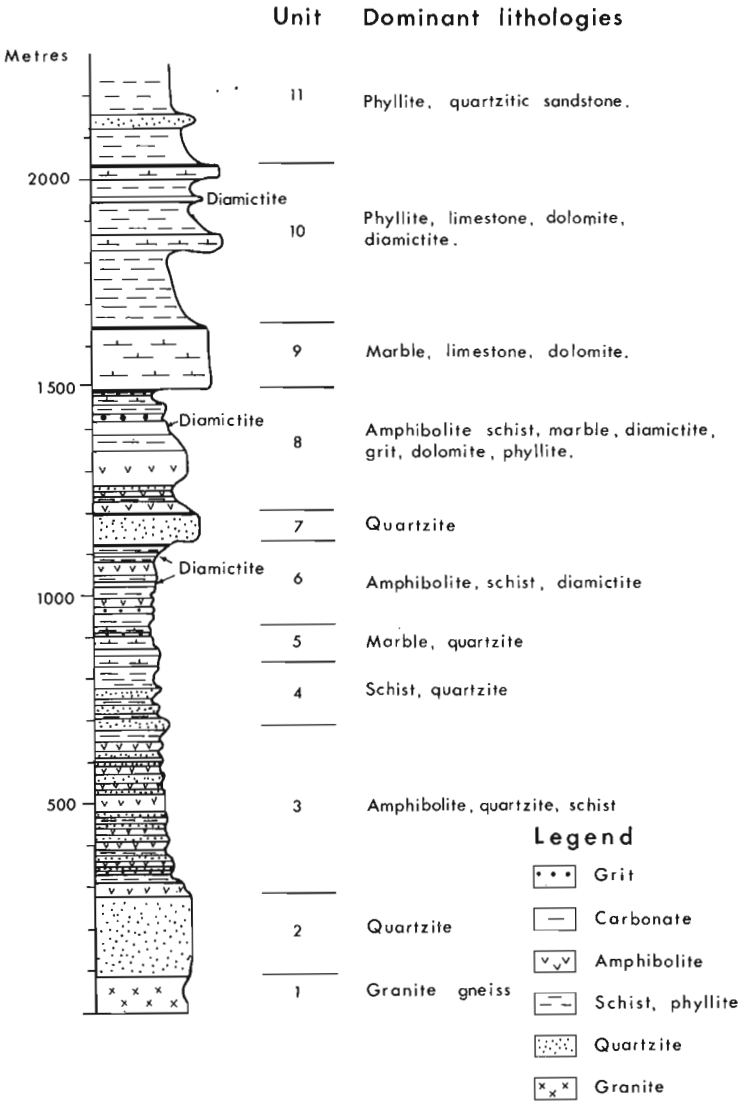

Figure 50.2. Stratigraphic column, Deserters Range.

[1]Department of Geological Sciences, Queen's University, Kingston, Ontario

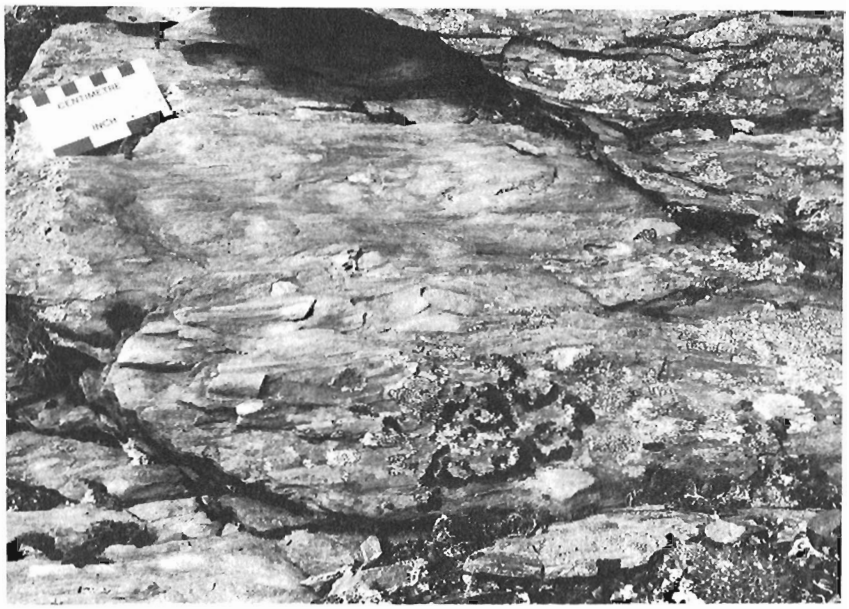

Figure 50.3

Elongated clasts of quartzite in foliation surface; diamictite of unit 8.

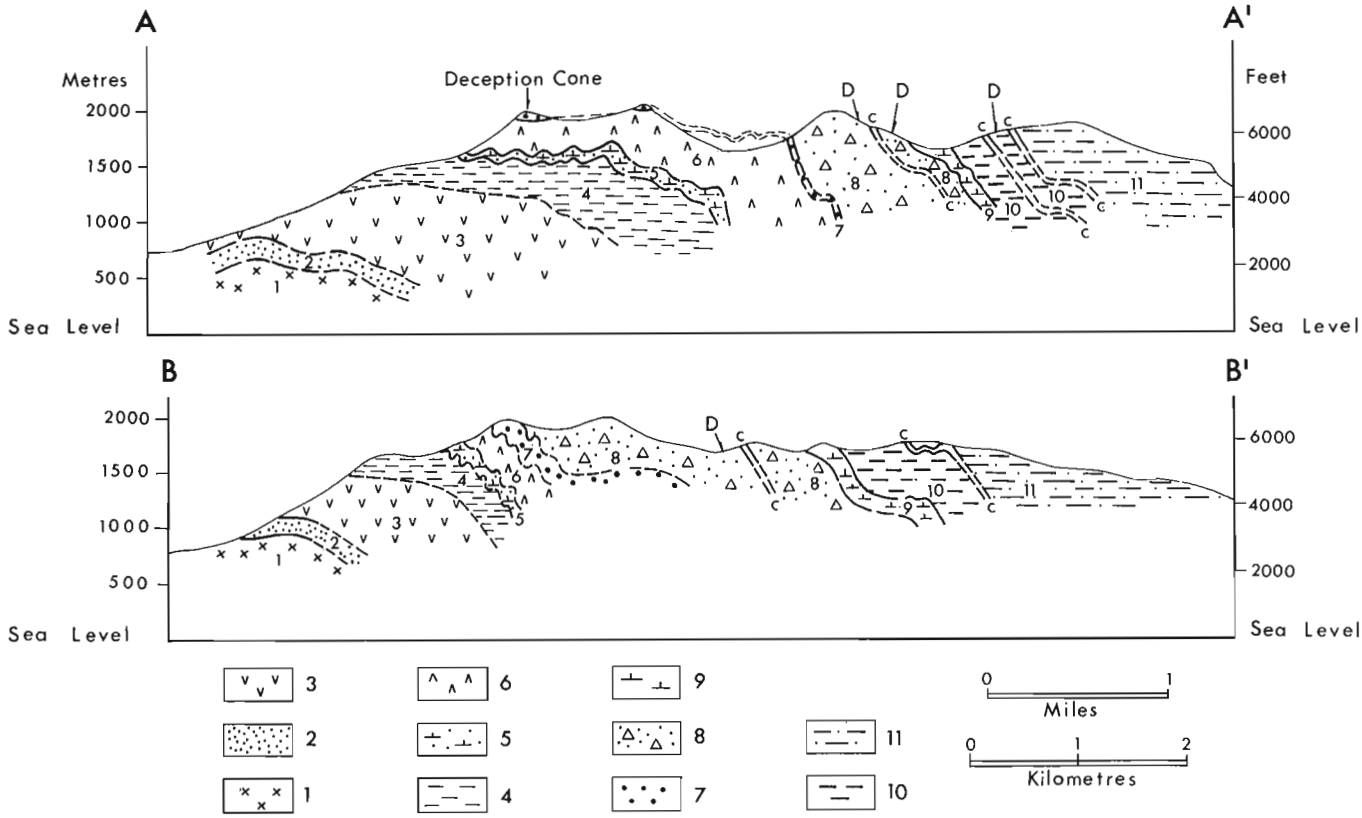

Figure 50.4. *Structural cross-sections, Deserters Range. C, prominent carbonate members, thickness exaggerated; D, diamictite localities. For lithologies see Figure 50.2.*

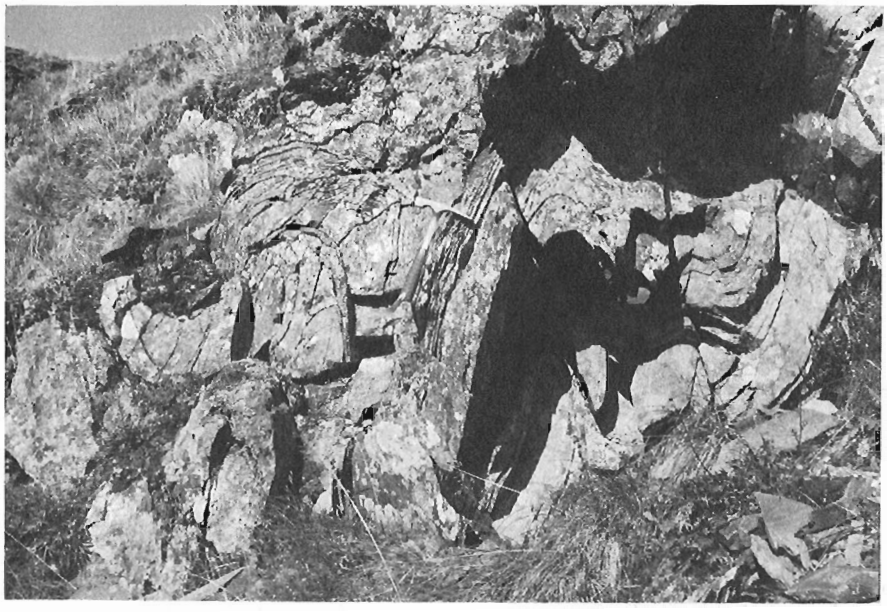

A. Quartzite of unit 7.

B. Calcareous schist of unit 5.

Figure 50.5. *Typical fold styles.*

Stratigraphy

In the study area within the Deserters Range all strata are Proterozoic. The Proterozoic rocks are overlain by Lower Cambrian strata east of the range and fault slices of upper Cretaceous? and lower Tertiary rocks occur along the west flank (Gabrielse, 1975). The exposed stratigraphic assemblage (Fig. 50.2) is more than 2000 m thick but intense deformation of most of the strata precludes accurate measurement. This assemblage, assigned to the Misinchinka Group, has many similarities with upper Proterozoic rocks (Windermere and ?older) in the southern Cordillera.

The oldest stratified rocks are in contact with strongly foliated and locally mylonitized granite gneiss (unit 1) which in places shows well developed crosscutting zones of ultracataclasite ranging from 1 to 40 mm wide. No crosscutting relations of quartzite by granitoid rock have been observed and it is not known whether the granitoid rocks are basement or relatively young intrusions.

Unit 2, Quartzite

Pure, white, vitreous, even-grained, thick-bedded quartzite forms a unit about 200 m thick distinctive in its purity and uniformity. It is the most competent unit in the study area and in many exposures beds are gently and uniformly dipping.

Unit 3, Amphibolite, Quartzite, Schist

Well layered fine- to coarse-grained amphibolite is intercalated with thin-bedded varicoloured pure quartzite and pelitic schist. The amphibolite, which is strongly foliated and occurs in layers 1 to 2 m thick, may represent flows and/or tuffs; no primary structures were observed. Quartzite members also range from 1 to 20 m thick. The unit is at least 400 m thick.

Unit 4, Schist and Quartzite

Pelitic schist, overlying amphibolite of unit 3, is interbedded with flaggy, white to rusty white quartzite. The unit is at least 150 m thick.

Unit 5, Marble and Quartzite

The lower part of this unit comprises a distinctive couplet of thin-bedded white, relatively pure marble approximately 20 m thick overlain by white orthoquartzite that ranges from flaggy to thick bedded and is approximately 15 m thick. The quartzite is overlain by a marble (± actinolite) unit at least 20 m thick, which in the upper part is interbedded with quartzite and amphibolite. The unit is about 80 m thick.

Unit 6, Amphibolite, Schist and Diamictite

Amphibolite and calcareous amphibole chlorite schist are intercalated with pelitic schist. This unit is at least 200 m thick and locally includes quartzite cobble conglomerate (diamictite) and laminated fine grained quartzite. Quartzite clasts are well rounded and range from a few centimetres to more than 15 cm long.

Unit 7, Quartzite

Resistant grey weathering impure quartzite ranges from laminated to thick bedded and is about 70 m thick.

Unit 8, Amphibolite, Schist, Marble, Grit, Dolomite and Phyllite

Medium- to coarse-grained amphibolite is intercalated with calcareous amphibole chlorite schist. Beds of pure marble ranging from 10 to 50 cm thick occur in the middle part of the unit. Quartzite and carbonate pebble to cobble conglomerate in a chlorite phyllite matrix occur in the upper part and are overlain by phyllite and quartzitic grits which in places contain opalescent blue quartz grains. Quartzite clasts are well rounded and are strongly elongate parallel

A. Mullions in quartzite of unit 3.

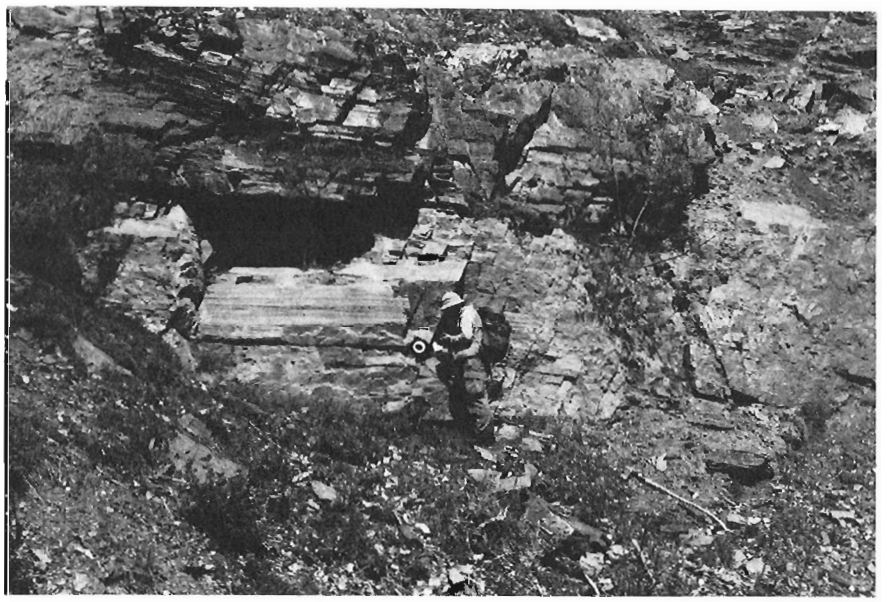

B. Strongly lineated quartzite intercalated with well jointed amphibolite of unit 3.

Figure 50.6

with fold axes (Fig. 50.3). Magnetite chlorite schist locally forms a member 2-3 m thick below the diamictite. The upper part of the unit is thin-bedded sandy dolomite interbedded with phyllite. The unit is at least 300 m thick and could be considerably thicker.

Unit 9, Marble, Limestone and Dolomite

Thin-bedded to massive marble forms one of the most distinctive units in the Deserters Range. Resistant and light grey to cream weathering, the unit is a maximum of 150 m thick. A similar unit is underlain by phyllite, grit, limestone and diamictite in the southeastern part of the Fort Grahame (east half) map area (Gabrielse, 1975).

Unit 10, Phyllite, Limestone, Dolomite, Diamictite

Quartzite and carbonate pebble to cobble conglomerate and phyllite occur between two resistant limestone and dolomite members each 10 to 30 m thick. The upper part of the lower member is well bedded rusty weathering sandy dolomite. The unit is about 400 m thick.

Unit 11, Phyllite and Sandstone

Grey and green phyllite and resistant thick-bedded quartzitic sandstone form the uppermost lithologies of the assemblage in the report area. The unit is several hundred metres thick. East of the report area these rocks are overlain by lower Cambrian strata (Gabrielse, 1975).

Structure

The general structural style (Fig. 50.4) is that of an east dipping, kinked homocline. The well defined kink has a west dipping axial surface and very gentle plunge. On a mesoscopic scale the rocks are intensely folded (Fig. 50.5). Fold styles range from open folds with rounded closures, typical in quartzite members, to tight chevron folds. Boudinage and disharmonic folding between rocks of different competency are characteristic. Boudins of amphibolite in schist or quartzite are particularly common. The lowest quartzite unit (unit 2 and quartzite in unit 3) shows remarkable mullion structure (Fig. 50.6). The long axes of mullions are parallel with the axes of mesoscopic folds.

Metamorphism

The grade of metamorphism increases from lower greenschist in the east to amphibolite facies in the west. Kyanite, staurolite and garnet are present in the highest grade rocks in the westernmost exposures of schist (unit 3) overlying quartzite, (unit 2). Metamorphism was pretectonic and syntectonic as shown by kinked kyanite and well foliated and lineated amphibolite.

Reference

Gabrielse, H.
1975: Geology of Fort Grahame E½ map-area, British Columbia; Geological Survey of Canada, Paper 75-33.

THE NARAKAY VOLCANIC COMPLEX: MAFIC VOLCANISM IN THE HELIKIAN HORNBY BAY GROUP OF DEASE ARM, GREAT BEAR LAKE: A PRELIMINARY REPORT ON DEPOSITIONAL PROCESSES AND TECTONIC SIGNIFICANCE

Gerald M. Ross[1]
Precambrian Geology Division

Ross, G.M, The Narakay volcanic complex: mafic volcanism in the Helikian Hornby Bay Group of Dease Arm, Great Bear Lake: a preliminary report on depositional processes and tectonic significance; in Current Research, Part A, Geological Survey of Canada, Paper 82-1A, p. 329-340, 1982.

Abstract

The Narakay Volcanic Complex is a sequence of mafic pyroclastic rocks within shallow marine strata of the Helikian Hornby Bay Group. Depositional environments of the sedimentary rocks range from shallow shelf (above storm wave base) to supratidal and marginal marine. Fluctuations in relative sea level correspond closely with established trends for Hornby Bay Group strata in the eastern part of the basin. An unconformity near the top of the sequence in the Narakay Volcanic Complex involves juxtaposition of volcanic basement rocks of unknown age and Hornby Bay Group rocks, synsedimentary faulting, and deposition of autochthonous paraconglomerate. This unconformity may correlate with the local unconformity found between the Hornby Bay and Dismal Lakes groups.

Pyroclastic rocks are composed of tuffs and agglomerates deposited on the flanks of maar-like tuff cones. Magma-water interaction was an essential component of the eruptive and depositional processes. Steam explosions generated during magma ascent caused fragmentation of viscous magma and wall rock. Steam- and/or water-saturated eruptive clouds deposited poorly sorted pyroclastic rocks typical of the Narakay Volcanic Complex. The tuff cones were partly preserved in graben-like structures although most underwent some erosion with dispersal of epiclastic debris by storm surge and run-off.

The entire Narakay Volcanic Complex is cut by an east-trending swarm of dykes. The composition of the dyke rock and the pyroclastic fragments is nearly identical, suggesting that they may have been derived from the same magma source. The dyke orientation implies a north-south extensional regime which corresponds with the north-northwest facing geometry of the Dismal Lakes Platform. The dykes record the period of regional tensile stress which occurred at the end of deposition of the Hornby Bay Group and the beginning of deposition of the Dismal Lakes Group.

Introduction

The Narakay Volcanic Complex is exposed on the Narakay Islands, a group of more than 20 rugged islands along the south shore of Dease Arm, Great Bear Lake (Fig. 51.1). These contain the westernmost exposures of the Hornby Bay Group, the basal unit of the Coppermine Homocline. The Narakay Islands also contain the only known volcanic rocks associated with the Hornby Bay Group. In general the islands are composed of a more than 500-m thick, northwest-dipping, homoclinal succession of shallow marine siliciclastics and carbonates which are the deeper water equivalents of Hornby Bay Group strata to the east (Kerans, et al., 1981, Baragar and Donaldson, 1973). Mafic volcanism occurred sporadically throughout deposition of the Hornby Bay Group in this area and deposited pyroclastic tuffs and derivative epiclastic volcaniclastic rocks. The upper part of the succession contains a previously unrecognized unconformity in which autochthonous paraconglomerate rests on both older Hornby Bay Group strata and an igneous basement of unknown age. The entire sequence is cut by a swarm of east-trending dykes of vesicular porphyry.

The only work done on this complex prior to 1980 was the description of two samples of "porphyrite tuff" by A.E. Barlow, who accompanied J.M. Bell in 1899 (Bell, 1901) and a single traverse by J.A. Donaldson in 1969 (J.A. Donaldson, personal communication). During August 1980 and August 1981 the Narakay Islands were mapped at a scale of 1 inch to 500 feet and more than 25 detailed stratigraphic sections were measured. Excellent three dimensional exposure provides insight as to eruptive mechanism and the geometry of resultant deposits. The occurrence of mafic volcanism provides an additional petro-tectonic association important in understanding the tectonic setting and depositional history of the Hornby Bay Group and lower part of the Coppermine Homocline.

Acknowledgments

Field expenses and expediting services were provided by Bill Padgham and the staff of the Department of Indian Affairs and Northern Development office in Yellowknife. Carol Newell, Jeff Chiranzelli, and Don Brown provided cheerful assistance in the field. Maurice Lambert and Paul Hoffman aided in discussion of various aspects of the geology of this area. J.A. Donaldson critically read the manuscript and improved its clarity.

Stratigraphic Setting

The Coppermine Homocline is an unmetamorphosed and undeformed sequence of terrestrial and marine sedimentary rocks and plateau basalts of Paleohelikian to Late Hadrynian age. It rests unconformably on Wopmay Orogen (McGlynn, 1970; Hoffman, 1980), the youngest part of which is 1.85 Ga (Van Schmus and Bowring, 1981). In ascending stratigraphic order the Homocline comprises the Hornby Bay Group, the Dismal Lakes Group, the Coppermine River Group (1.2 Ga, Baragar, 1972) and the Rae Group (Fig. 51.2). The latter three groups form a lithologic sequence which can be traced 300 km east to Bathurst Inlet, whereas no correlative for the Hornby Bay Group has yet been recognized along strike.

The Hornby Bay Group is composed of terrestrial and shallow marine siliciclastics (Unit 8) (nomenclature of Baragar and Donaldson, 1973), marine dolostone (Unit 9) and marginal marine siliciclastics (Unit 10) (Fig. 51.2). It is overlain conformably to locally unconformably by the Dismal Lakes Group. The Hornby Bay Group records deposition in a fluvial environment, followed by transgressive-marine and finally regressive marine (prograding shoreline) environments. Each of these units has been recognized in the Narakay Volcanic Complex, where they are thicker, and were

[1] Research conducted in conjunction with Department of Indian Affairs and Northern Development

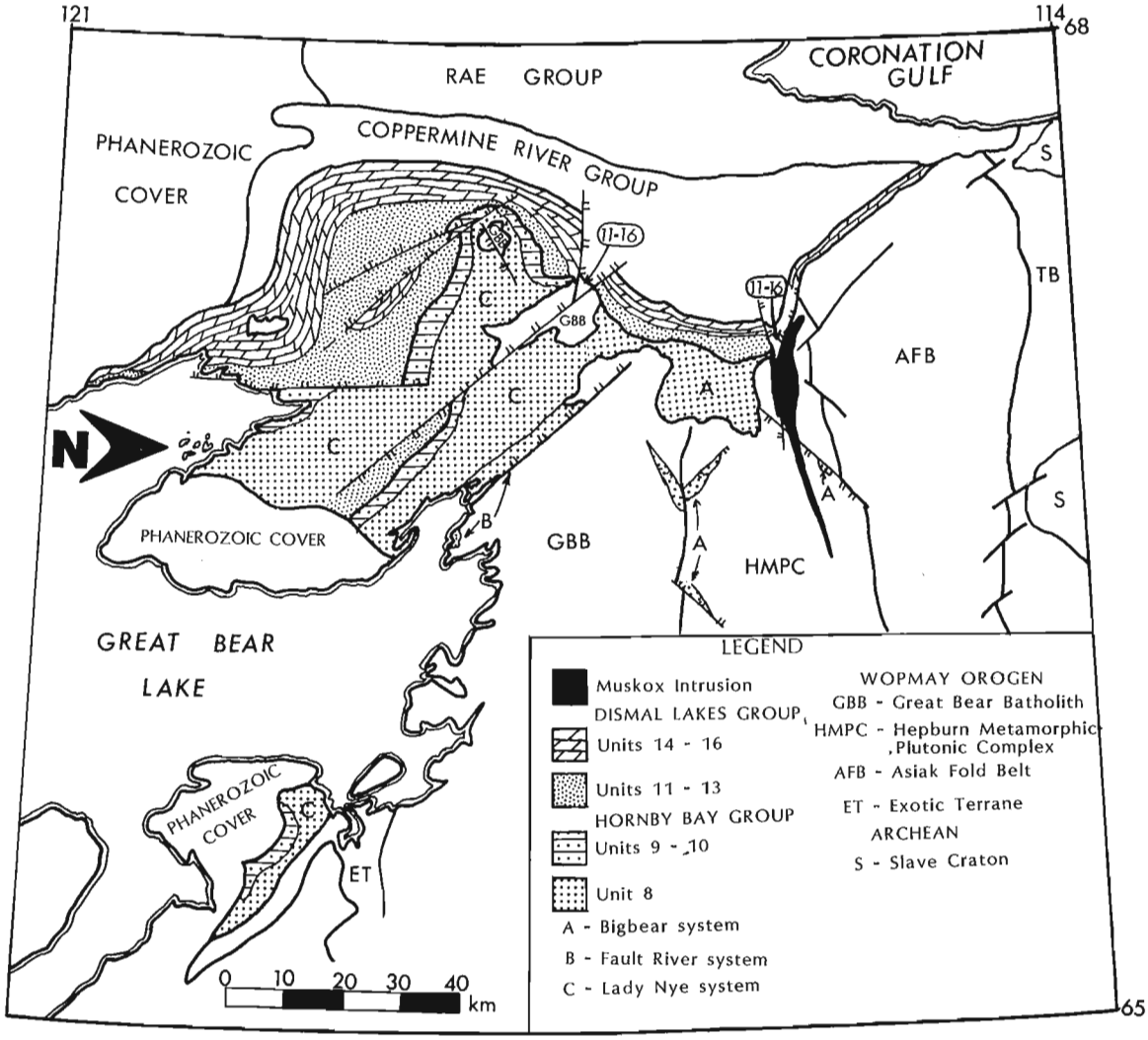

Figure 51.1. *Generalized geologic map of the northwest Canadian Shield showing the main elements of Wopmay Orogen and Coppermine Homocline. "N" marks the location of the Narakay Islands.*

deposited in a deeper water environment. The depositional strike at this time was north-northwest with a west-southwest facing platform. The overlying Dismal Lakes Group was deposited on a north- to northwest-facing platform (Kerans et al., 1981). The change in paleoslope at the end of Hornby Bay Group deposition was accompanied by syndepositional normal faulting (Kerans et al., 1981). The Narakay Volcanic Complex consists of the products of magmatism associated with this extensional event.

Stratigraphic Sequence

Unit 8

This unit is composed of cross-stratified, feldspathic to subfeldspathic quartz arenites intercalated with thin mudstones and sand-streaked mudstones. It is a minimum of 130 m thick, and although the base of the unit is not exposed, it is considered to be gradational with underlying marginal marine siliciclastics on the mainland, 3.2 km to the south (Fig. 51.1). It is gradationally overlain by stromatolitic dolostones of Unit 9A, and pinches out 20 km to the east.

The unit displays an overall upward-fining as the sandstone-shale ratio decreases. Individual sandstone beds are lenticular to tabular, and display low-angle (<10°) cross-stratification, hummocky cross-stratification (cf. Harms, 1975) (Fig. 51.5) and planar lamination. Scour-based sets are commonly amalgamated into cosets with a maximum thickness of 1 m, which decreases up section. Thin black mudstone films bound the cosets towards the base of the unit, but thicken near the top to beds up to 50 cm. They are parallel laminated and contain sand streaks in the form of thin sheets and starved ripples in addition to injection structures (cf. Young, 1969) and, in the uppermost part of the unit, mudcracks.

The arenite beds represent stacked deposits of storm surge origin based on the common occurrence of hummocky cross-stratification and the amalgamated nature of bed sets (cf. Bourgeois, 1980; Hamblin, et al., 1979; Hamblin and Walker, 1979). The intercalated mudstones represent post-storm, "background" sedimentation. The occurrence of starved ripples and sand streaks suggest a tidally influenced subtidal to intertidal setting (cf. Reineck and Singh, 1975).

Unit 9A

This unit records the transition from siliciclastic to carbonate deposition, and is composed of cycles of thin bedded sandstone and desiccated mudstone succeeded by beds of quartzose and stromatolitic dolostone. The thickness of sandstone beds and the overall abundance of siliciclastic detritus decreases stratigraphically as the unit grades into dolostone of Unit 9B. The unit has a minimum thickness of 85 m.

Siliciclastic portions of depositional cycles are composed of hummocky cross-stratified to parallel and ripple crosslaminated quartz arenites interlayered with parallel-laminated mudstone, commonly with mudcracks and/or injection structures. These are overlain by hummocky and low-angle (<10°) cross-stratified calcareous arenite and/or quartzose dolostone that may be succeeded by evenly spaced, compound stromatolite domes. Paleocurrents from the quartzose dolostone and calcareous arenite are bimodal-bipolar along an east-trending axis. The stromatolites are SH-V/LLH (Logan et al., 1964) domes up to 1 m in diameter, and are commonly developed on coarse intraclastic blocks with finer intraclastic debris between domes.

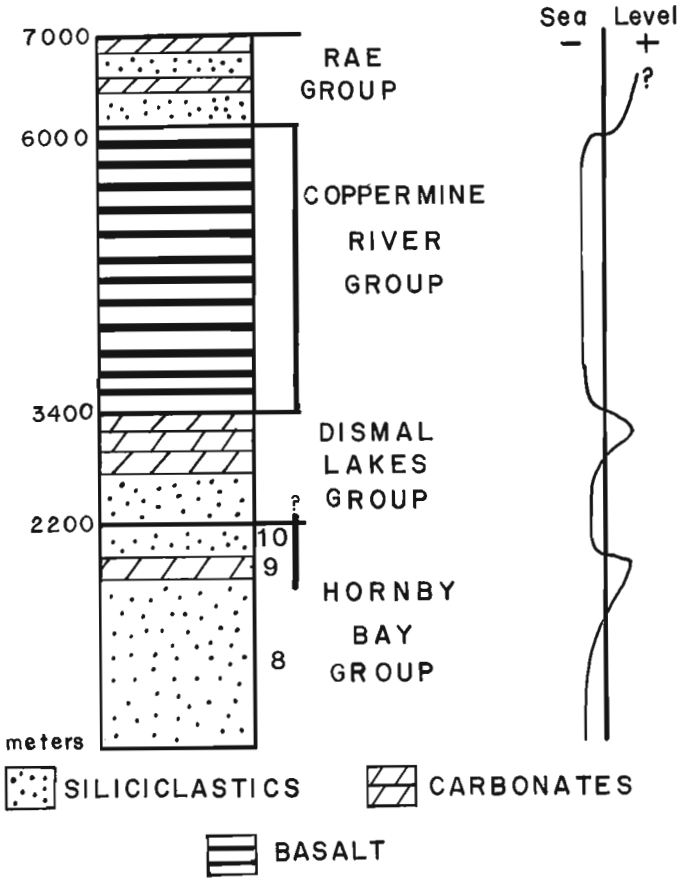

Figure 51.2. *Simplified lithostratigraphic sequence of the Coppermine Homocline. Numbers to the right of the Hornby Bay Group section refer to the main stratigraphic units (see text). Sea level curve shows gross transgressive (+) and regressive (-) trends. Solid vertical bars to the right of the column shows the stratigraphic duration of magmatism. The lower bar represents activity in the Narakay Islands and the upper bar represents the Mackenzie magmatic event (Coppermine River Group plateau basalts, Muskox Intrusion, Mackenzie dykes). From Kerans et al., 1981, Baragar and Donaldson, 1973.*

These cycles represent transgressive pulses during overall platform submergence. The siliciclastic portion of cycles were deposited in a high-energy intertidal sand and mudflat during periods of storm-wave activity followed by normal tidal processes. Gradual deepening led to deposition of quartzose dolostone in a high-energy nearshore setting (cf. Clifton, et al., 1971). The stromatolites formed at the peak of cycles in a high-energy subtidal or intertidal environment.

Unit 9B

This unit, at least 95 m thick, is composed predominantly of dolostone with less than 20 per cent siliciclastic detritus. It is distinguished from overlying and underlying units by distinctive digitate stromatolites and abundance of oolites.

The lower part of the unit is composed of cycles, less than 2 m thick, which contain basal cosets of hummocky cross-stratified calcareous quartz arenite and/or quartzose dolostone, commonly with convolute lamination in the upper parts of cosets. These are overlain by ripple and climbing ripple crosslaminated dolostone which have scoured top surfaces with spaced, compound domal stromatolites. The domes are symmetric to asymmetric along a southwest-trending axis of elongation and are composed of crusts of silicified microdigitate stromatolites.

The upper part of the unit is composed of planar to hummocky and ripple crosslaminated dolostone, amalgmated into scour-based cosets less than 60 cm thick. These are commonly capped by thin sheets of laterally-linked, smooth laminated to microdigitate stromatolites that form low-relief domes on a sharply scoured basal surface. Interbeds of oolitic to intraclastic dolostone (20-40 per cent of the unit) are either massive or display trough crosslamination with strongly unimodal southwest-directed paleocurrents.

The lower part of the unit records cycles of storm surge deposition followed by dewatering and/or high-suspended load deposition. High-energy marine currents scoured the tops of these deposits, which were then populated by the microdigitate stromatolite domes. The microdigitate morphology of the stromatolites also suggests a high-energy subtidal environment of deposition (cf. Tucker, 1977; Hoffman, 1974). High-energy (storm?) currents in a nearshore setting (cf. Clifton et al., 1971) deposited the crosslaminated dolostone in the upper part of the unit. The smooth morphology and common lateral linkage of the associated stromatolites suggest lower energy and rate of sedimentation. Oolitic units represent offshore-directed ebb tidal (or storm surge?) oolite deltas or shoals (cf. Loreau and Purser, 1973).

Unit 10A

This unit is at least 150 m thick and is distinguished by stromatolite morphology and the abundance of lenticular-bedded siliciclastic lithology. The unit is composed predominantly of undulose to lenticular-bedded, parallel to ripple crosslaminated calcareous siltstone (45%) and dololutite (20%). Massive to parallel laminated beds of calcareous, feldspathic quartz arenite occur sporadically (15%) throughout the unit as do intraclastic beds (5%) and scour-based biostromal horizons (15%). The biostromes are composed of SH-V type columnar heads with intraclastic and oolitic detritus or lenticular-bedded siliciclastics in interdomal channels. Columns are composed of smooth to slightly reticulate laminae with common lateral linkage between domes at the top of the horizon. The columns may be up to 1 m in diameter with synoptic relief of 1-2 m and a weak to moderate southwest axial elongation. Several upward-fining, upward-thinning cosets (<2 m thick) of crosslaminated oolitic dolostone also occur and display strong unimodal southwest-directed paleocurrents.

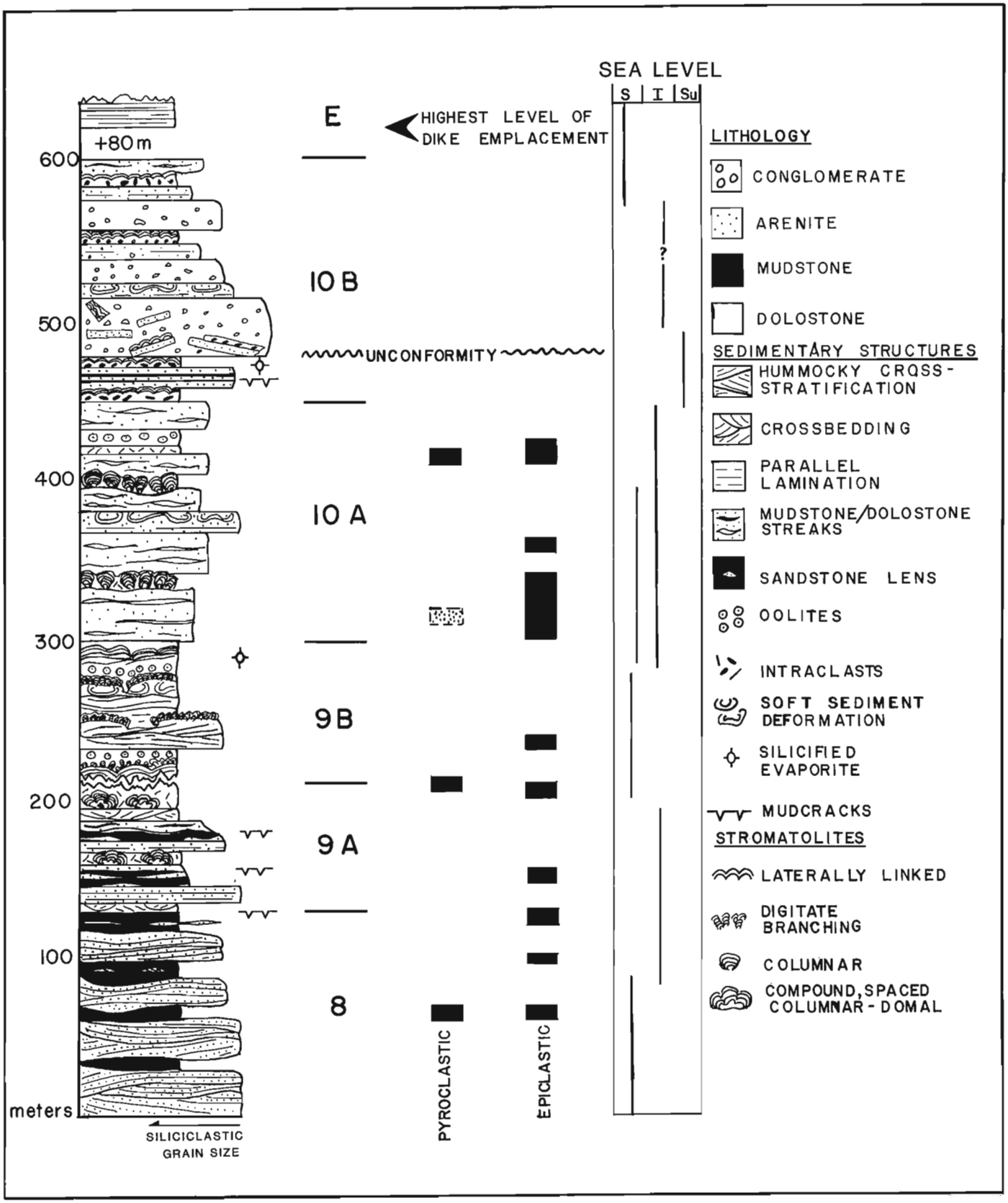

Figure 51.3. Schematic stratigraphic section of sedimentary rocks in the Narakay Islands. Units are discussed separately in the text. Black rectangles to the right of the column indicate periods of pyroclastic and epiclastic deposition of volcaniclastic rocks. Shaded rectangle is pyroclastic event inferred on the basis of the coarse grain size of the epiclastics. Sea level units: S-subtidal, I-intertidal, Su-supratidal. Overlap of lines represents uncertainty in inferred water depths.

The lenticular-bedded siltstone-dolostone facies closely resembles subtidal, wave-generated sequences described by deRaaf et al. (1977) and were deposited in a shallow marine setting with storm deposition of the feldspathic arenites. The stromatolites are very similar to the recent SH-V stromatolites from the intertidal coastal bight of Shark Bay (Logan et al., 1974) and may represent periods of shoaling and scouring of the depositional surface. Oolitic and intraclastic beds were deposited by offshore-directed storm or ebb tidal surges as sheets and patchy shoals.

Unit 10B

This unit is gradational with underlying Unit 10A and is distinguished by the prevalent occurrence of laterally-linked domal stromatolites, the appearance of massive intraclastic granulestones, and relatively pure (noncalcareous) quartz arenites. The stromatolites occur as spaced, compound to individual, low-relief domes with a prominent, southwest axial elongation. Undulose to peaked algal mats, oncolites, and rare silicified, "cauliflower", evaporites (cf. Chown and Elkins, 1974; Milliken, 1979) occur in the uppermost beds below the unconformity. Siliciclastic rocks at the base display lenticular bedding similar to the 10A facies, but beds become more tabular and have parallel lamination up section, where the dololutite gives way to desiccated green mudstone.

The stromatolite morphology suggests an intertidal to shallow subtidal depositional environment which shallowed-up into a supratidal-high intertidal algal mat-oncolite facies (cf. Logan et al., 1974). This coincides with the gradual appearance of the arenites and desiccated mudstones which are probably distal, terrestrially derived sheet flood deposits (cf. McKee et al., 1967).

This unit contains an unconformity which is marked by the abrupt appearance of a locally-derived, calcareous paraconglomerate, and evidence of fault movement before and during deposition of the conglomeratic sequence. The conglomerate, about 100 m thick, is interbedded with typical 10B lithologies at the top, and is overlain conformably by 45 m of 10B dolostones and siliciclastics. Because sedimentary rocks below and above the conglomerate were deposited in the same environment setting, the unconformity probably does not represent a large gap in time.

The conglomeratic rocks form a fining-up sequence of paraconglomerate to arenite that rests unconformably on both Unit 10B and a basement complex. The paraconglomerate, about 30 m thick, is composed exclusively of angular to subround clasts of the immediately underlying and adjacent lithologies (mostly Unit 10B, with local concentrations of basement fragments). The paraconglomerate is massive and unsorted, and is composed of about 30 per cent framework clasts dispersed in a calcareous, clay-rich matrix. Conglomeratic beds gradually become interlayered with beds of massive quartzose litharenite and pebbly arenite. These display normal and reverse grading, soft-sediment deformation caused by dewatering and slumping, and are locally interlayered with intraclastic and stromatolitic dolostone. The sequence grades into interbedded arenite and stromatolitic (LLH) dolostone identical to sedimentary rocks immediately beneath the unconformity.

The basement complex is composed of fresh rhyolite ash tuffs, rhyolite porphyry, flow banded (?) tuff, and a very well layered siliceous rock ("redrock") which may be mylonitic. The basement was deformed prior to deposition, as evidenced by near vertical dips on bedding, and the presence of quartz stockwork and pseudotachylite. A thin zone (<1 m) of hematizaiton and "bleaching" is developed

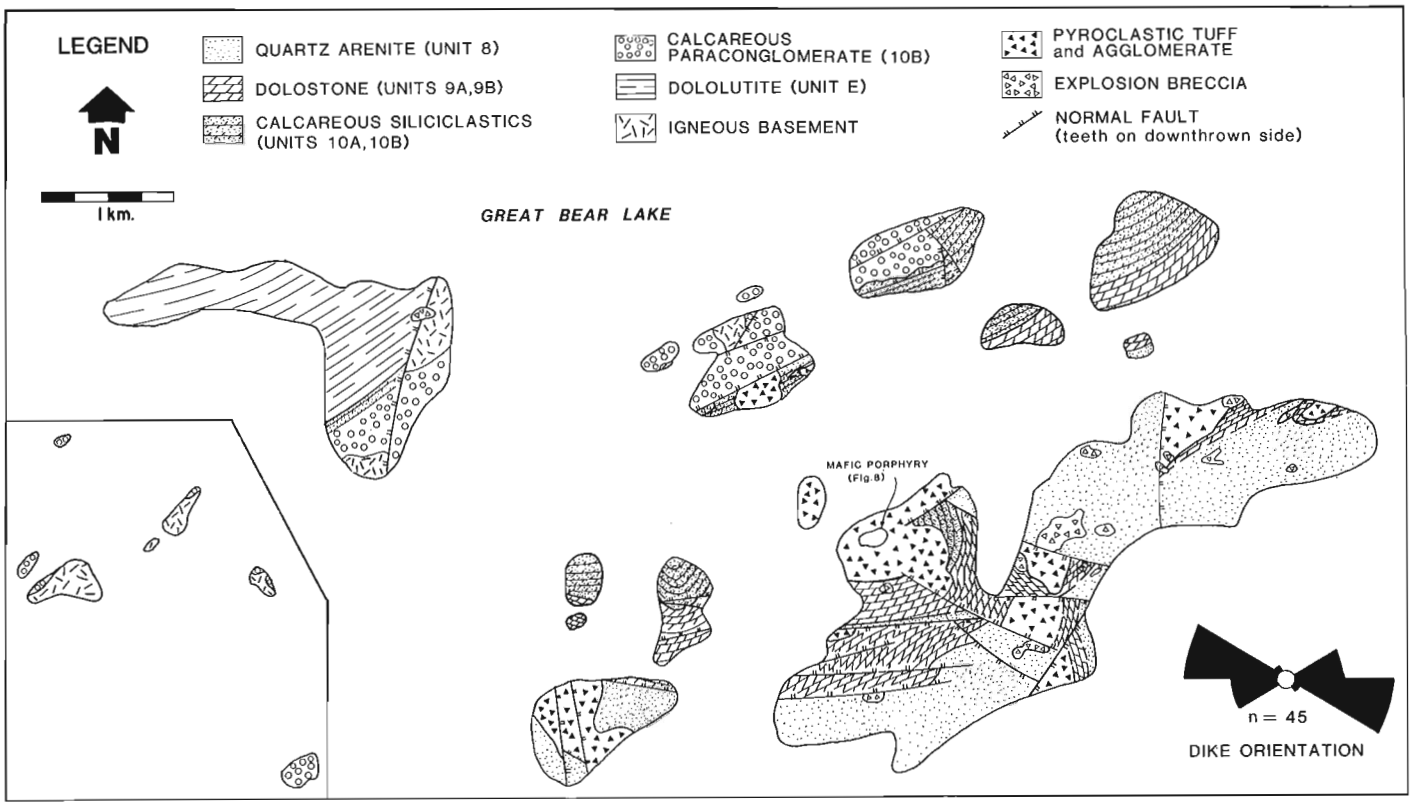

Figure 51.4. *Simplified geologic map of the Narakay Volcanic Complex. Individual dykes and structural data are not plotted for the sake of clarity. The islands that are inset in the lower left are the westernmost Narakay Islands and lie approximately 4 km west of the dogleg-shaped island. The mafic porphyry is illustrated in Figure 51.8.*

Figure 51.5

Hummocky cross-stratified feldspathic quartz arenite of Unit 8. Knife is 7 cm long.

sporadically on top of the basement. The paraconglomerate was deposited on an irregular basement surface and commonly forms the matrix to in situ "jigsaw" breccias of basement at the contact.

The contact with underlying Unit 10B is both depositional and faulted. The paraconglomerate commonly contains large slabs of deformed Unit 10B which display gentle flexure folds, kinking, and brecciation. These slabs (up to 5 m by 5 m by 2 m) are concentrated at the contact and along the downthrown side of the fault. In the best exposure of this relationship, upright slabs of Unit 10B (on the downthrown block) rest on upper Unit 10A and are interbedded in a paraconglomerate matrix which has infiltrated into interstices and buried the slabs. This suggests that the fault was syndepositionally active and that the slabs of Unit 10B sloughed off the fault scarp.

The paraconglomerates and arenites were deposited by mass flow (debris flow) and turbidity currents, respectively. Unfortunately there are no structures suitable for paleocurrent measurement, and the paleoslope is unknown. The appearance of the unconformity marks the culmination of regional uplift and shoaling recorded in the transition from Unit 9B to Unit 10B. Observed relationships in addition to the common occurrence of soft sediment deformation and large deformed slabs of Unit 10B indicate synsedimentary faulting. The mechanism of juxtaposition of basement and Hornby Bay Group rocks is unknown at present. The basement may have been brought up by faulting which requires erosion of more than 1 km of Hornby Bay Group rocks (Fig. 51.2); but no such deposits have been observed.

Unit E

This unit almost 80 m thick, gradationally overlies Unit 10B and is composed of lenticular to parallel-bedded, calcareous quartz siltstone with minor dololutite at the base, that grades upwards into flaggy weathering parallel laminated dololutite. Structures indicative of current movement are rare, as are thin algal mats. The unit apparently was deposited in a quiet-water marine envionment. It represents resubmergence of the platform following shoaling and erosion.

Regional Correlation

The lithostratigraphic sequence in the Narakay Islands records the same relative changes in sea level as Hornby Bay Group rocks to the east (see Kerans et al., 1981) e.g. transgression and deposition of carbonates (Units 8-9B) followed by regression and re-introduction of siliciclastic detritus (Units 10A-B). In the Narakay Islands, Unit 8 is the offshore facies equivalent of marginal marine to fan-delta to fluvial quartz arenites to the east. Unit 9A thins to 10 m, 130 km to the east (Dismal Lakes area, see Fig. 51.1). Unit 9B, with distinctive digitate stromatolites, is a basinwide unit that marks the maximum depth of submergence of the Hornby Bay "platform". In the Narakay Islands it represents the offshore facies of a barrier complex of stromatolite bioherms and oolite shoals developed to the east. Units 10A and 10B correlate with floodplain and distributary delta-marginal marine siliciclastics of Unit 10. The unconformity in this unit may be approximately the same age as the local unconformity at the base of the Dismal Lakes Group (see Kerans et al., 1981) but the units which overlie the unconformity in the Narakay Islands do not have lithologic correlatives in the Dismal Lakes Group. In summary, the Narakay Islands record predominantly shallow-water marine deposition, a conclusion important to understanding the mechanism of eruption, deposition, and geometry of the associated volcaniclastic rocks.

Volcanogenic Units

In the Narakay Volcanic Complex, igneous rocks occur mostly as fragmental volcaniclastic deposits of pyroclastic and epiclastic origin in addition to a single, lopolith-shaped mafic porphyry and a swarm of dykes and associated explosion breccias. The depositional mechanism for

epiclastic and pyroclastic rocks may overlap (suspension deposition and sediment gravity flow) and distinguishing between the two can be difficult. They were differentiated on the basis of clast composition and texture (freshness, roundness, amount of admixed nonvolcanogenic grains), bed geometry, and stratification.

Pyroclastic Deposits

Pyroclastic tuffs and breccias were deposited during Unit 8, late Unit 9A, and Unit 10A sedimentation (Fig. 51.3). They characteristically outcrop as rugged knobs, but no upper contacts have been preserved. Contacts with adjacent sedimentary rocks are steep (70-90 degrees), and the bedding in the sediments is truncated by bedding in the pyroclastic rocks. Massive volcanic breccias at the base of some tuffs crosscuts and "intrudes" adjacent wall rock. No evidence of fault movement (slickensides, tension gashes, etc.) along these contacts was observed, although the country rock adjacent to the pyroclastic rocks commonly displays brecciation, boudinage, and recrystallization, especially in the more calcareous layers. Large blocks of wall rock, up to 3 m wide, are common in the tuffs adjacent to contacts.

Contact relationships suggest pre- and/or syn-eruptive disruption of the country rock. Pre-eruptive doming, commonly observed in recent eruptions (MacDonald, 1972) created tensile stresses which caused boudinage of partly lithified sediments and fractured the lithified units. Syneruptive collapse along these fractures created the steep contacts and disrupted the wall rock. Explosive "stoping" of wall rock during an eruption is evidenced by the incorporation of large blocks of sedimentary rock into the tuffs and locally intrusive contacts. This process may have obscured recognition of fault planes.

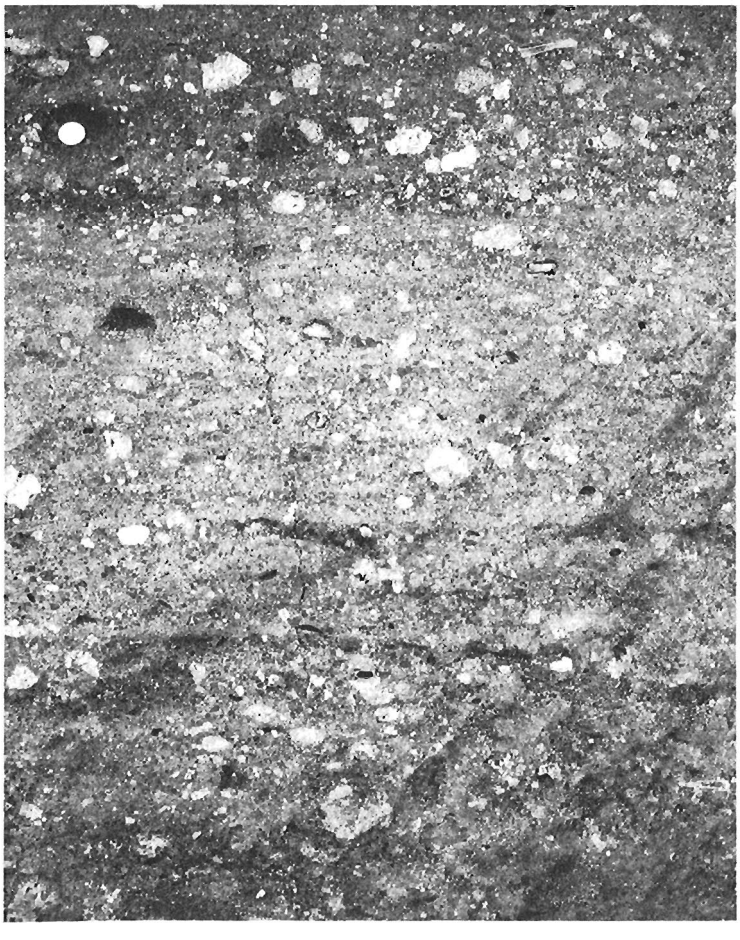

Figure 51.6. *Poorly sorted lapilli tuff displaying crude parallel lamination typical of pyroclastic tuffs. Coin in upper left corner is 25 mm across.*

The pyroclastic rocks occur as parallel, stacked beds of ash, lapilli tuff and agglomerate with poorly developed internal stratification (Fig. 51.6). Beds may have dips as steep as 50 degrees, but 26-30 degrees is the norm. Individual beds range in thickness from 10-200 cm with planar boundaries and constant lateral thickness within outcrops. Internal stratification is defined by sparse, single, grain-thick lamina of evenly sized clasts. Poorly developed normal and reverse grading, and beds of finely laminated ash tuff, also occur. The deposits are poorly sorted and commonly contain about 10 per cent blocks and bombs dispersed in a lapilli tuff matrix. In the laminated ash-rich beds, the coarse blocks have contorted the underlying laminae and formed bomb or impact sag features. Traction current structures are lacking within beds, and contacts between beds are planar and unscoured.

The poorly developed lamination, even bedding, and poorly sorted character of the pyroclastic rocks suggests rapid deposition from suspension or sediment gravity flow. The disorganized, noncyclic bedding sequence tends to favour suspension-dominated deposition. In addition, the pyroclastic rocks closely resemble stratification sequences from recent and Cenozoic tephra cones (cf. MacDonald, 1972, p. 185; Womer et al., 1981; Heiken, 1971). The inferred paleobathymetry of the sedimentary units suggests that water may have been an important component of eruptions. Water- or steam-rich eruptive clouds undergo "ash scavenging" with deposition of poorly sorted, poorly laminated tuffs (cf. Walker, 1981). Plastic deformation of laminae by impact also imply wet rather than dry tephra (Womer, et al., 1981). Such deposits are inferred to represent remnants of tuff cones (as defined by Heliken, 1971) formed by "phreatomagmatic" (hydromagmatic is perhaps a better term as the latter implies groundwater) eruptions and airfall deposition from a water/steam-rich eruption cloud.

On the northwest corner of the largest Narakay Island, a large segment (300 m in diameter) of a tuff cone is preserved (others have been affected by erosion and fault truncation). Bedding in lapilli tuff and agglomerate dips radially in towards a lopolith-shaped body of columnar jointed mafic porphyry (see Fig. 51.7). The axes of the columns are perpendicular to the contact with the tuffs. The tuffs display textures and structures typical of previously described examples. The tuff-mafic porphyry structure is nested topographically within older (penecontemporaneous?) tuffs and Unit 10A sedimentary rocks. This structure is interpreted as the inner portion of a tuff cone – the tuffs and agglomerates were deposited on the inward dipping walls of the cone crater which was later filled by lava which cooled to form the lopolith.

The orientation of bedding in a given outcrop ranges from constant to variable. With the exception of the above example, bedding attitudes are not sufficiently consistent to infer the shape of a cone. Variation in bedding attitude is attributed to slumping and compaction (cf. Lorenz, et al., 1970). Direct evidence of this process is the occurrence, albeit uncommon, of stratiform beds with convolute and deformed lamination and large (up to 30 m by 40 m by 10 m) slabs (intraclsts) of bedded tuff in a lapilli tuff matrix.

Figure 51.7

Cored bombs and blocks of vesicular porphyry in massive agglomerate. Bomb cores are composed of porphyry and lapilli tuff fragments. Matchstick in upper part of photo is 4 cm long.

Grain Shapes

Volcanic rock fragments comprise more than 90 per cent of the pyroclastic deposits with subordinate angular lapilli and blocks of sedimentary wall rock. Clasts of volcanic material (dense to slightly vesicular porphyry and pumice) are equant and are bounded by curviplanar fracture surfaces (although many fragments also display delicate apophyses and re-entrants at grain boundaries). This fragment shape matches the morphology of grains described from hyalotuffs (Honnorez and Kirst, 1975) and basaltic, phreatomagmatic tuffs (Heiken, 1971, 1972). Fragmentation is due to contraction during thermal shock and steam explosions. In view of the lack of fragments in the Narakay Volcanic Complex suggestive of violent vesiculation, much of the pyroclastic activity evidently was the result of interaction between connate fluids and/or seawater with the ascending magma and lava.

Although the morphology of most grains precludes differentiation between subaerial and subaqueous eruption, the presence of bombs and accretionary structures in addition to bomb-sag structures scattered throughout tuff sequeces, indicates that much of the eruptive activity was subaerial.

In agglomeratic beds, fusiform and cored bombs, and slabs of shattered ribbon bombs comprise up to 20 per cent of the bed in addition to angular blocks and lapilli of slightly vesicular to pumiceous porphyry. The cored bombs (Fig. 51.8) are up to 10 cm in diameter. The cores are composed of angular blocks of wall rock, lava, and rarely bedded pyroclastic debris. The cortices are up to 4 cm thick and composed of one or two layers of vesicular lava with vesicles that wrap concentrically around the bomb core. Some bombs have tails, up to 40 cm, composed of lava and agglutinated pyroclastic fragments. Lapilli-size fragments are also coated with lava and are therefore not typical accretionary lapilli (cf. Moore and Peck, 1962; MacDonald, 1972). The occurrence of pyroclastic fragments coated with lava implies a) subaerial extrusive activity and b) sporadic sealing of water from the vent to allow ponding of lava, a requirement necessary to produce the coatings (MacDonald, 1972, p. 128).

Composition

The pyroclastic beds are mostly lithic lapilli tuffs and tuff breccias, although some beds are rich enough in crystal fragments to be considered crystal lithic tuffs. Slightly vesicular mafic porphyry is the most common pyroclast type, pumice is distinctive but subordinate. The matrix of the porphyry may be glassy (now altered to chlorite and white mica) but more commonly it is rich in feldspar microlites which display a hyalopilitic to pilotaxitic and trachytic texture (terminology of Williams et al., 1954). Variable intensity of alteration (see next paragraph) has obscured primary mineralogy, although textures are well preserved. Primary minerals, which are less than 10 per cent, include plagioclase, amphibole, and pyroxene with epidote, magnesian chlorite, sphene, pumpellyite, clinozoisite, white mica, and carbonate as secondary phases.

Most of the pyroclastic fragments are white to tan, but in some examples, fragments only exhibit this colour adjacent to wall rock, whereas away from the contact the fragments become gradually darker (green to black). This corresponds to a change in the degree and nature of secondary mineral growth. Dark fragments contain abundant chlorite and comparatively fresh feldspar with incipient patches of poikilotopic carbonate. In contrast, the white fragments are composed largely of poikilotopic to microcrystalline carbonate, limonite, and white mica. This is interpreted as a syn- to post-eruptive alteration of warm pyroclastic fragments by convected seawater.

Eruptive and Depositional Mechanism

A typical eruptive cycle is outlined below (Fig. 51.9):

1. Pre-eruptive tumescence caused doming and created a tensile stress field. This resulted in boudinage of partly lithified sedimentary rocks and fracture of lithified rock.

2. With the onset of eruption, subsidence in the vent region occurred along normal faults. This caused rotation and foundering of blocks of wall rock. Initial contact between water and ascending magma created violent phreatomagmatic explosions. Brecciation of previously overlying and presently adjacent wall rock formed lapilli to block-size sedimentary rock fragments which were extruded with volcanic fragments, whereas larger blocks remained largely in situ. The magma also underwent brecciation by steam explosion, in addition to fragmentation by thermal shock and contraction.

3. Steam-rich clouds of pyroclastic debris deposited poorly sorted tephra (hyalotuffs) which built up rapidly into subaerial tuff cones. The bedded ejecta began to alter upon interaction with seawater following deposition. When water access to the vent was periodically sealed, lava ponded within the crater. The lopolith in Figure 51.7 resulted from complete solidification of lava which was not removed by subsequent explosions. The depth of explosion that generated the eruptions is unknown; structural truncation and lack of exposure do not allow any single complete cone to be observed.

4. Following the cessation of an eruptive cycle, portions of tuff cones were removed by erosion. This involved runoff, wave, and storm wave destruction of the cone and redistribution as epiclastic deposits on the platform (see following section). Presevation of observed tuff cone material is probably due to its deposition within structural depressions or grabens.

Epiclastic Deposits

Epiclastic volcaniclastic rocks occur sporadically throughout the rock sequence (Fig. 51.3). Some of these were deposited during and after a period of known pyroclastic activity. In other cases, epiclastic rocks cannot be linked to observed pyroclastics which suggest that there may be other vents that are not exposed.

Epiclastic rocks are composed of 30-90 per cent volcanic rock fragments and contain admixed clastic grains of the host unit (e.g. quartz sand in Unit 8, and oolites and intraclasts in dolostone units). The volcanic rock fragments range from comparatively fresh, green clasts to highly altered white and brown clasts. This alteration appears to be pre- or syn-depositional, because epiclastic beds do not display the zonal pattern of alteration observed in the pyroclastic deposits. Grain sizes range from pebble to arenite and display variable amounts of rounding.

The epiclastic rocks occur as scour-based lenticular bodies (2-14 m thick) and as sheets (0.5-4 m thick). In the lenticular, channel-fill deposits, a typical vertical sequence of stratification and grain sizes occur. At the base is a lens of parallel-laminated, granular arenites with granules irregularly concentrated along laminae. This is sharply overlain by graded beds of conglomerate to arenite which infill scour-based trough-like structures. Measurements from bedding surface exposures of trough axes give strong unimodal paleocurrent patterns. The graded beds are overlain by massive, matrix-supported pebbly granulestones and tabular planar to trough crossbedded granular arenites.

Figure 51.8a

Photo of dissected tuff cone (see Fig. 51.4 for location) taken from lake level. Upper dashed white line marks base of columnar jointed porphyry. Dashed line to the left marks zone where bedding in tuffs changes from inward dipping (towards porphyry) to outward dipping.

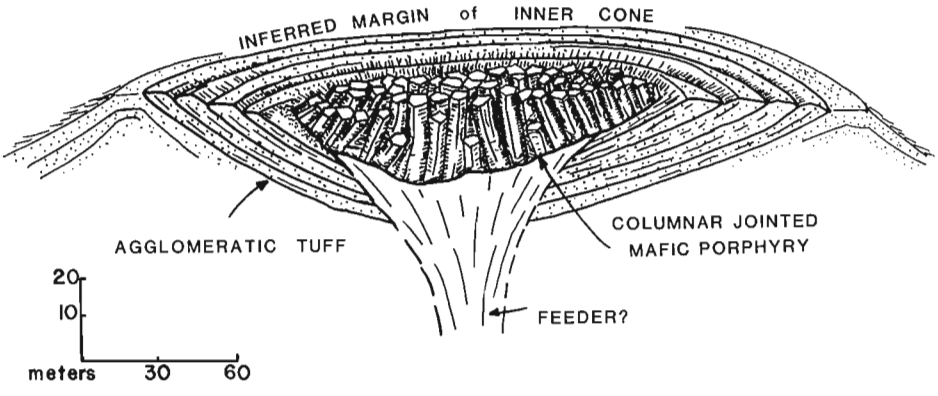

Figure 51.8b

Schematic cross-section of relationships in Figure 51.8a. Inner margin of tuff cone is inferred from changes in dip of bedded tuffs.

Paleocurrents from this horizon show greater dispersal, but still contain a strong component parallel to trends from the graded trough beds. Sheet-like epiclastic units are thinner and finer grained than the lenticular units. They commonly display well developed stacked Bouma cycles (A-D, A-C, A-B, A) (Middleton and Hampton, 1973) and interbedded small-scale scour and fill structures. Both types of epiclastic deposits have scoured tops, some with up to 1 m of relief, which are commony capped by stromatolites.

Volcaniclastic debris was swept off cone flanks by rain, wave spray and storm surge and deposited by turbidity currents and high-bedload traction currents. The difference in grain size and thickness suggest that the sheet-like deposits are more distal than lenticular bodies. Scour surfaces at the base of lenticular units may have formed by storm wave surge that was modified by flow interaction with the topographically positive cone remnant. These channels were filled by high bedload deposits of parallel laminated arenites in the channel thalweg followed by turbidity current deposition of graded beds on a hummocky surface. Final infill is marked by the occurrence of debris flood deposited granulestones and crossbeds formed by migration of marine sand waves and dunes. The sheet-like deposits are thin bedded turbidite deposits with variable amounts of traction deposition by marine currents. The common occurrence of scoured top surfaces with stromatolites suggests that epiclastic deposition took place entirely underwater.

Dykes and Related Breccias

The entire Narakay Volcanic Complex is cut by a swarm of east-trending dykes which are aphanitic to coarsely porphyritic (prismatic phenocrysts up to 1 cm long in a microlitic groundmass with a pilotaxitic texture). The original mineralogy is almost completely replaced by fine grained carbonate and bright green to white mica (illite, phengite(?), celadonite (?)) although relict feldspar may persist in coarser phenocrysts. The dykes are commonly vesicular with coarse spherical to slightly elongate vesicles in the core and smaller spherical vesicles along the chilled outer walls. Contact metamorphic effects in wall rock were not observed.

Dykes are commonly associated with pods of in situ explosion breccias (terminology of Parsons, 1969). The breccias are composed entirely of fragments of immediately adjacent host rock and dyke rock. Dykes can be traced along strike into the breccias, and in several cases, out the other side. The largest outcrop of this breccia is approximately 100 m^2. The breccias are best developed in carbonate rocks where recrystallization-hydrothermal alteration of dolostone has resutled in the formation of coarse (5-10 mm) manganiferous ankerite and/or siderite, massive to prismatic barite, and disseminated (<2 per cent) chalcopyrite.

The explosion breccias were generated when hot magma encountered pockets of connate fluids in the wall rock. Water flashed to steam upon contact with the magma, brecciating wall rock and quenching some of the magma. Hydrothermal fluids and gases generated by magma-water interaction caused recrystallization and alteration of wall rock breccia, and probably contributed to alteration of the dykes.

A second type of explosion breccia is distinguished from the above breccias by an abundance of exotic clasts. These are usually rounded to angular blocks of white, coarse grained quartz arenite, chert, dolostone, and rarely granite. They comprise 30 per cent of the fragments, the remainder being brecciated porphyry similar to the dyke porphyry. The breccias occur as vertical, tabular to podiform bodies with variable orientation, and as subcircular bodies.

The white quartz arenite boulders are lithologically identical to the Cape MacDonnel facies of Unit 8 (Kerans et al., 1981) and the granite clasts may be basement or cobbles from conglomerate. This represents a source area at least 800 m below outcrop level. The breccias formed when magma (dyke porphyry) encountered water at depth. The resultant steam explosion caused some brecciation and aided in ascent of magma/breccia and possibly fracture propagation. Angular blocks of wall rock were rounded during transport up the fracture.

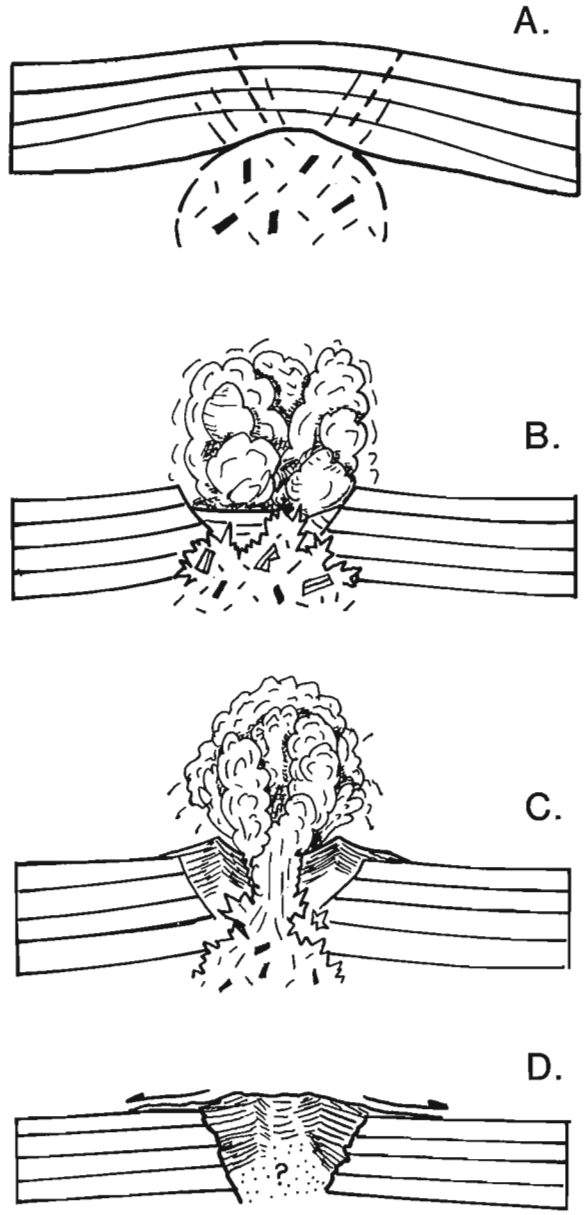

Figure 51.9. *Cartoon of eruptive cycle:*
A. Pre-eruptive doming during ascent of porphyritic mafic magma causes fracturing.
B. Steam explosions occur as magma comes into contact with water. Both wall rock and magma are disrupted by explosions. Gas escape and eruption cause subsidence along fractures formed during A.
C. Continued eruption cause build-up of tuff cone from subaerial air fall.
D. After the eruption ceases, topographically positive parts of the tuff cone are eroded and epiclastic debris is swept into the surrounding shallow marine environment.

Question mark in throat of cone denotes uncertainty in composition plugged conduit. Massive tuff and solidified magma are possibilities.

The texture and composition of the porphyry in the dykes and breccias are very similar to material that forms the pyroclastic fragments. Possibly they are cogenetic and derived from the same magma source. This implies that the magma source (or intruded crust) was stationary during deposition of more than 600 m of sedimentary rock.

The east-trending orientation of the dykes implies emplacement during a north-south extensional regime (cf. Baragar, 1977). The Dismal Lakes Group was deposited on a north-facing platform (Kerans et al., 1981) and it is postulated that the dyke swarm records the period of north-south extension that preceded subsidence and formation of the Dismal Lakes Platform. Although this is the only magmatic product formed during this time, there is evidence of regional extension and normal fault activity (e.g. Teshierpi Fault).

Mineralization and Alteration

No significant mineralization was observed. The most common assemblage is manganiferous ankerite and/or siderite, barite and chalcopyrite developed in and adjacent to explosion breccias associated with dykes. This usually is restricted to the breccia fragments and/or matrix, but a single oolite bed was altered for 200 m along strike. Dark brown to tan dolostone is altered to coarse grained dark brown to purplish carbonate containing needles, vug infills, and massive nodules of barite, and disseminated chalcopyrite. The complex is also cut by thin, randomly oriented veins composed of quartz and siderite without any metallic minerals.

Summary and Implications

The sequence of Hornby Bay Group strata which composes the Narakay Volcanic Complex records deposition in a shallow marine to subaerial setting. Units 8-9B were deposited on a storm-dominated, west-southwest facing transgressive shelf. Unit 10A and 10B mark platform shoaling and reintroduction of terrestrial siliciclastics into the depositional system. Platform shoaling culminated with synsedimentary faulting and formation of an erosional unconformity followed again by submergence. These patterns of relative sea level change are of regional (>100 km) extent. The association of normal faulting and regression is also a regional pattern (see Kerans et al., 1981) and suggests that the sea level change was due to structural behaviour of the crust rather than strictly eustatic changes.

Mafic volcanism occurred sporadically throughout deposition of Hornby Bay Group sedimentary rocks. Doming followed by phreatomagmatic steam explosions led to subsidence via normal faults and explosive stoping of wall rock. Pyroclastic ejecta was generated by steam explosions and thermal quenching. Steam- and/or water-rich eruption clouds deposited poorly sorted and bedded, wet, ash-rich tephra which formed tuff cones. A preponderance of subaerial eruption is indicated by the sporadic occurrence of cored bombs and lapilli, and bomb sag structures. Unconsolidated tephra was swept off the flanks of tuff cones by runoff and storm and normal wave activity. This material was deposited by turbidity currents and high bedload traction carpets. Channel-fill, lenticular deposits formed proximal to the cone with sheet-like deposits in distal regions.

The final phase of igneous activity resulted in the emplacement of a swarm of east-trending dykes and related explosion breccias. The composition of the dykes is similar to volcanic fragments in the pyroclastic deposits, implying derivation from the same magma source. The orientation of the dykes reflects north-south extensional strain, interpreted to have formed during crustal stress imposed before (and to some extent during) deposition of the Dismal Lakes Group.

References

Baragar, W.R.A.
1972: Coppermine River Basalts, District of Mackenzie; in Rubidium – strontium isochron age studies; Report 1, ed. R.K. Wanless, W.D. Loveridge; Geological Survey of Canada Paper 72-23, p. 21-24.

1977: Volcanism of the stable crust; in Volcanic Regimes in Canada, ed. W.R.A. Baragar, L.C. Coleman, and J.M. Hall; Geological Association of Canada Special Paper 16, p. 377-406.

Baragar, W.R.A. and Donaldson, J.A.
1973: Coppermine and Dismal Lakes map areas: Geological Survey of Canada Paper 71-39.

Bell, J.M.
1901: Report on the topography and geology of Great Bear Lake and a chain of lakes and streams thence to Great Slave Lake; Geological Survey of Canada Annual Report, v. XII, pt. C.

Bourgeois, J.
1980: A transgressive shelf sequence exhibiting hummocky stratification: the Cape Sebastian Sandstone (Upper Cretaceous), southwestern Oregon; Journal of Sedimentary Petrology, v. 50, p. 681-702.

Chown, T.M. and Elkins, J.E.
1974: The origin of quartz geodes and cauliflower cherts through silicification of anhydrite nodules; Journal of Sedimentary Petrology, v. 44, p. 885.

Clifton, H.E., Hunter, R.E., and Phillips, R.L.
1971: Depositional structures and processes in the non-barred high-energy nearshore; Journal of Sedimentary Petrology, v. 41, p. 651-670.

Harms, J.C.
1975: Stratification and sequences in prograding shoreline deposits in Harms, J.C., Southard, J.B., Spearing, D.R., and Walker, R.G., ed., Depositional environments as interpreted from primary sedimentary structures and stratification sequences; Society of Economic Paleontologists and Mineralogists Short Course No. 2, p. 81-101.

Hamblin, A.P., Duke, W.L., and Walker, R.G.
1979: Hummocky cross-stratification – indication of storm dominated shallow marine environments; American Association of Petroleum Geologists Bulletin, v. 63, p. 460-461.

Hamblin, A.P. and Walker, R.G.
1979: Storm-dominated shallow marine deposits; the Fernie-Kootenay (Jurassic) transition, southern Rocky Mountains: Canadian Journal of Earth Sciences, v. 16, p. 1673-1690.

Heiken, G.H.
1971: Tuff rings: examples from the Ft. Rock-Christmas Lake valley basin, south-central Oregon; Journal of Geophysical Research, v. 76, p. 5615-5626.

1972: Morphology and petrography of volcanic ashes; Geological Society of America Bulletin, v. 83, p. 1961-1980.

Hoffman, P.F.
1974: Shallow and deepwater stromatolites in a Lower Proterozoic platform-to-basin facies change, Great Slave Lake, Canada; American Association of Petroleum Geologists Bulletin, v. 58, p. 856-867.

Hoffman, P.F. (cont.)
1980: Wopmay Orogen: A Wilson Cycle of Early Proterozoic age in the northwest of the Canadian Shield; in The Continental Crust and its Mineral Deposits, Strangway D.W., ed., Geological Association of Canada Special Paper No. 20, p. 523-549.

Honnorez, J. and Kirst, P.
1975: Submarine basaltic volcanism; morphometric parameters for discriminating hyaloclastites from hyalotuffs: Bulletin Volcanologique, v. 39, ser. 2, p. 1-25.

Kerans, C., Ross, G.M., Donaldson, J.A., and Geldsetzer, H.J.
1981: Tectonism and depositional history of the Helikian Hornby Bay and Dismal Lakes Group, District of Mackenzie; in Proterozoic Basins of Canada, Campbell, F.H.A., ed., Geological Survey of Canada Paper 81-10.

Logan, B.W., Rezak, R., and Ginsburg, R.N.
1964: Classification and environmental significance of algal stromatolites; Journal of Geology, v. 72, p. 68-83.

Logan, B.W., Hoffman, P.F., and Geblin, C.D.
1974: Algal mats, cryptalgal fabrics, and structures, Hamelin Pool, western Australia; Logan, B.W., ed., in Evolution and diagenesis of Quaternary carbonate sequences, Shark Bay, western Australia; American Association of Petroleum Geologists Memoir No. 22, p. 140-194.

Loreau, J.P. and Purser, B.H.
1973: Distribution and ultrastructure of Holocene ooids in the Persian Gulf; The Persian Gulf; in Holocene carbonate sedimentation and diagenesis in a shallow epicontinental sea, Purser, B.H., ed., Springer Verlag, New York, p. 279-328.

Lorenz, V., McBirney, A.R., and Williams, H.
1970: An investigation of volcanic depressions: part III: Maars, tuff-rings, tuff-cones, and diatremes: National Aeronautical and Space Association Progress Report (N.G.R.-38-003-012), Houston, Texas, 198 p.

MacDonald, G.A.
1972: Volcanoes; Prentice-Hall, Englewood Cliffs, New Jersey, 510 p.

McGlynn, J.C.
1970: Bear Province in Geology and Economic Minerals of Canada, Douglas, R.J.W., ed., Geological Survey of Canada Economic Geology Report No. 1, 5th ed., p. 77-84.

McKee, E.D., Cosby, E.J., and Berryhill, H.C., Jr.
1967: Flood deposits, Bijou Creek, Colorado, June 1965: Journal of Sedimentary Petrology, v. 37, p. 829-851.

Middleton, G.V. and Hampton, M.A.
1973: Sediment gravity flows: mechanics of flow and deposition in Turbidites and deep water sedimentation, Middleton G.V., Bouma, A.H., ed.; Pacific Section Society Economic Paleontologists and Mineralogists Short Course, p. 1-38.

Milliken K.L.
1979: The silicified evaporite syndrome: two aspects of silicification history of former evaporite nodules from southern Kentucky and northern Tennessee; Journal of Sedimentary Petrology, v. 49, p. 245-256.

Moore, J.G. and Peck, D.L.
1962: Accretionary lapilli in volcanic rocks of western continental United States; Journal of Geology, v. 70, p. 182-193.

Parsons, W.H.
1969: Criteria for recognition of volcanic breccias: a review: in Igneous and metamorphic petrology, Larsen, L.H., Prinz, M., and Manson, V., ed., Geological Society of America Memoir 115, p. 263-304.

de Raaf, J.F.M., Boersma, J.R., and van Gelder, A.
1977: Wave-generated structures and sequences from a shallow marine succession, Lower Carboniferous, County Cork, Ireland; Sedimentology, v. 24, p. 451-483.

Reineck, H.E. and Singh, I.B.
1975: Depositional Sedimentary Evnironments, Springer Verlag, New York, 439 p.

Tucker, M.E.
1977: Stromatolite biostromes and associated facies in the Late Precambrian Porsanger Dolomite Formation of Finnmark, Arctic Norway: Palaeogeography, Palaeoclimatology, Palaeoecology, v. 21, p. 55-83.

Van Schmus, W.R. and Bowring, S.A.
1980: Chronology of igneous events in the Wopmay Orogen, Northwest Territories, Canada (Abstract): Geological Society of America Abstracts with Program, v. 12, p. 540.

Walker, G.P.L.
1981: Characteristics of two phreatoplinian ashes and their water flushed origin: Journal of Volcanology and Geothermal Research, v. 9, p. 395-407.

Williams, H., Turner, F.J. and Gilbert, C.M.
1954: Petrography: An Introduction to the Study of Rocks in Thin Section, W.H. Freeman and Company, San Francisco, 406 p.

Womer, M.B., Greeley, R., and King, J.S.
1981: The geology of Split Butte: a maar of the south-central Snake River, Idaho: Bulletin Volcanogique, v. 43, p. 453-471.

Young, G.M.
1969: Inorganic origin of corrugated vermiform structures in the Huronian Gordon Lake Formation near Flack Lake, Ontario; Canadian Journal of Earth Sciences, v. 6, p. 795-799.

NOTES ON MINERALOGY OF VARIOUS TYPES OF URANIUM DEPOSITS AND GENETIC IMPLICATIONS

Project 750010

V. Ruzicka and A.L. Littlejohn[1]
Economic Geology Division

Ruzicka, V. and Littlejohn, A.L., Notes on mineralogy of various types of uranium deposits and genetic implications; in Current Research, Part A, Geological Survey of Canada, Paper 82-1A, p. 341-349, 1982.

Abstract

Mineralogical studies on some Canadian uranium deposits revealed some features, which were used for refinement of their conceptual genetic models.

The electron-microprobe studies of the ores from the Elliot Lake quartz-pebble conglomerate deposits indicated that the authigenic uranium-titanium phase ("brannerite") actually consists of a U-Ti-Si compound which was formed by reactions of U and Ti in solutions with the sericitic matrix. Uranium mineralization in deposits spatially related to the pre-Athabasca unconformity formed during the diagenesis of the sedimentary rocks of the Athabasca Group.

Additional minerals were identified in known occurrences: brannerite at the Halo deposit near Bancroft, Ontario; coffinite, acanthite, chlorargyrite and native silver at Box mine, Goldfields, Saskatchewan; coffinite in the Albert Formation, Moncton Basin, New Brunswick; francevillite in the Peribonca Formation, Otish Mountains, Quebec. A new occurrence (Devil's Elbow) containing a U-Ti-Si-Fe phase, was identified near Bancroft, Ontario. The U-Ti aggregates at the Ace-Fay mine, Beaverlodge, Saskatchewan, formed from fluids which carried uranium and titanium simultaneously.

Paragenesis of Brannerite, Elliot Lake, Ontario

A substantial portion of the ore-forming mineral assemblage in the quartz-pebble conglomerate deposits is represented by a uranium-titanium oxide of variable composition, sometimes with calcium, cerium, thorium and iron. The mineral, commonly called brannerite, occurs in the ores in two forms: in allogenic (detrital) grains and as an authigenic uranium-titanium aggregate. Studies on both of these forms are important for interpretation of the ore-forming processes and therefore for establishing a conceptual model simulating formation of the quartz-pebble conglomerate deposits.

Ramdohr (1957, 1958a) used results of his microscopic observations on brannerites from the Canadian and South African deposits as a part of the evidence of the placer origin of these deposits with their subsequent modification by "Pronto-Reaktion" under "pseudohydrothermal" conditions.

According to Ramdohr (1958a, p. 18) the allogenic (detrital, well rounded) brannerite was deposited along with other heavy minerals. That formation of the authigenic brannerite took place at temperatures of at least 225-250°C could be postulated from the presence of coeval valleriite $4(Fe,Cu)\cdot 3(Mg,Al)(OH)_2$. He attributed the elevated temperatures to the great thickness of the overlying sediments, radioactive heating and effects of magmatic intrusions at various times (Ramdohr, 1958b, p. 48). He suspected but did not find evidence for a role of catalysts, such as iron or rare earth elements, in the ore-forming process (Ramdohr, 1958a, p. 17). Roscoe (1969, p. 138) interpreted Ramdohr's statements to mean that "...he (Ramdohr) considered that most of the brannerite is metamorphic in origin... and formed at the expense of uraninite...". Roscoe suggested a diagenetic origin of brannerite in most places rather than a metamorphic origin "...which it may be at Pronto...". Roscoe also stated that "the secondary brannerite was probably formed in two stages, an early stage wherein uranium was extracted from solution and adsorbed by TiO_2, and a later stage wherein much of the uraniferous TiO_2 crystallized to form brannerite".

Our investigations on the Elliot Lake ores from the Quirke II mine using electron-microprobe technique indicate, that the authigenic uranium-titanium phase of the mineralization commonly actually consists of a U-Ti-Si compound containing these elements in various proportions; in addition, traces of Pb and Fe are locally present. It appears, that the U-Ti-Si phases formed by reactions of U and Ti with the sericitic matrix. Both the Ti and U were apparently present in solutions. The U-Ti-Si phases occur either disseminated through the matrix in a mixture with sericite (Fig. 52.1), associated with remobilized pyrite and chalcopyrite, as apparent replacement of sericite (Fig. 52.2), associated with monazite, coffinite and sericite (Fig. 52.3) or as discrete grains. Although the XRD patterns of the discrete grains exhibit an anatase-like structure, the formation of the U-Ti-Si phase did not necessarily take place at the expense of the titanium oxide minerals, since none were observed in the sections.

Deposits Spatially Related to the pre-Athabasca Unconformity

Uranium mineralization spatially related to major Helikian-Aphebian unconformities has been recognized in Canada first in the Churchill geological province. At present about half of Canada's uranium 'Reasonably Assured and Estimated Additional Resources mineable at prices up to $Can 135/kg U' occurs in deposits classified as belonging to this category.

Despite intensive exploration for and extensive studies on this kind of deposits there still remain controversial views on their genesis.

There is no definite evidence of the source. Archean granitic plutons containing above normal clarkes of uranium occur in the vicinity of most deposits (Fig. 52.4). In addition to these plutons Hudsonian felsic intrusive rocks and especially their pegmatitic derivatives are abundant for instance in the source area for the Manitou Falls Formation that surrounds the Key Lake deposits, and which formation might be a source of fluids (e.g. connate waters) supplying uranium to Key Lake deposits. Ray (1977, p. 22), who mapped in the vicinity of the Key Lake deposits, speculated

[1] Central Laboratories and Technical Services Division

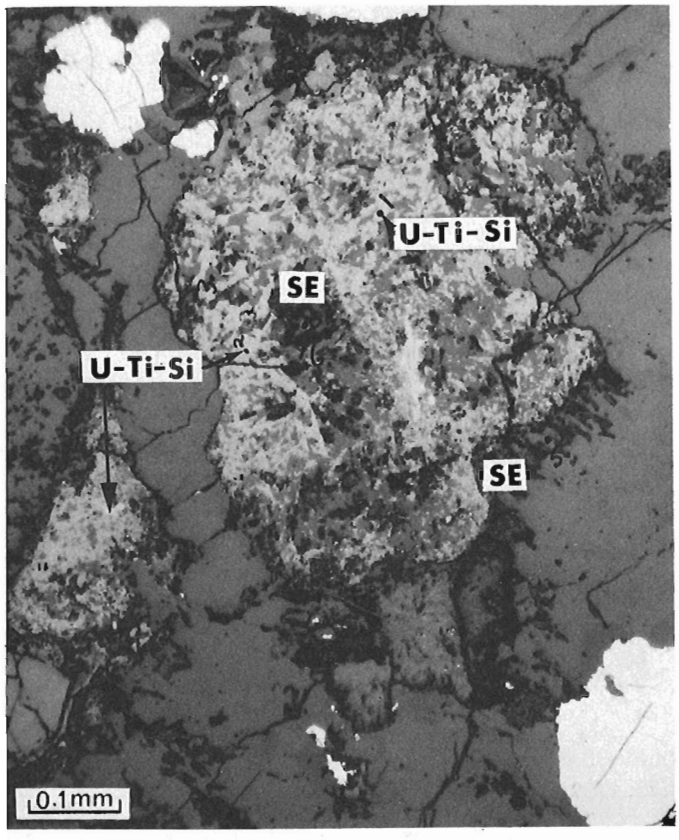

Figure 52.1. U-Ti-Si phase of mineralization associated with sericite(SE); Rio Algom Limited, Quirke II mine, Elliot Lake, Ontario. Reflected plain light.

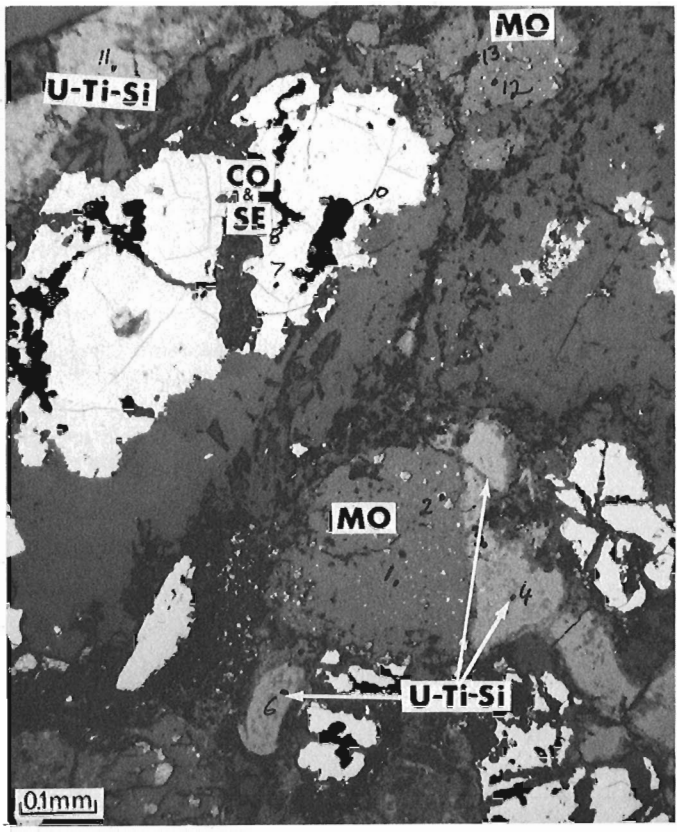

Figure 52.3. U-Ti-Si phase of mineralization in quartz-pebble conglomerate associated with monazite (MO), coffinite (CO) and sericite (SE). Rio Algom Limited, Quirke II mine, Elliot Lake, Ontario. Reflected plain light.

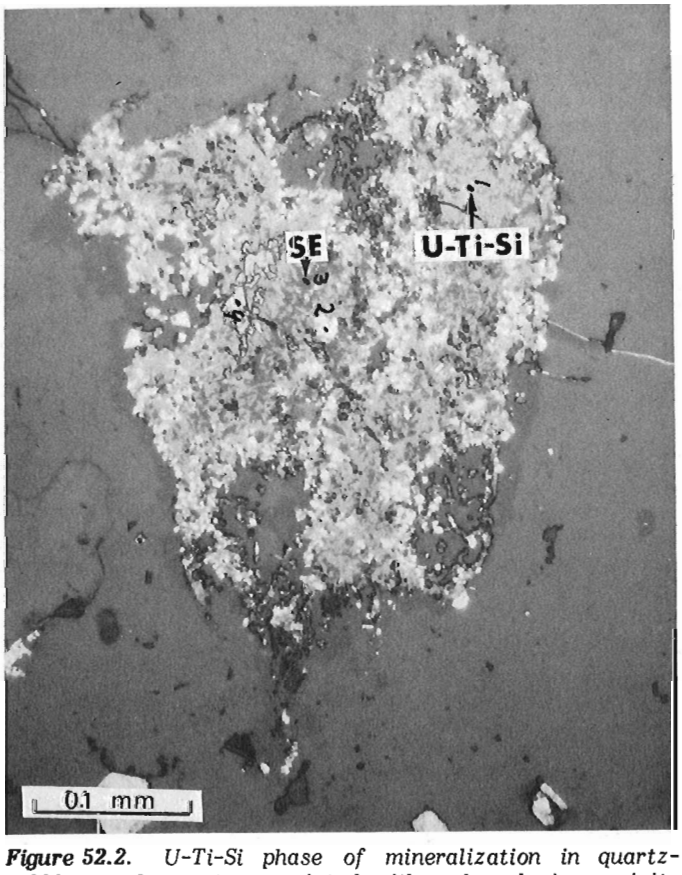

Figure 52.2. U-Ti-Si phase of mineralization in quartz-pebble conglomerate associated with and replacing sericite (SE). Rio Algom Limited, Quirke II mine, Elliot Lake, Ontario. Reflected plain light.

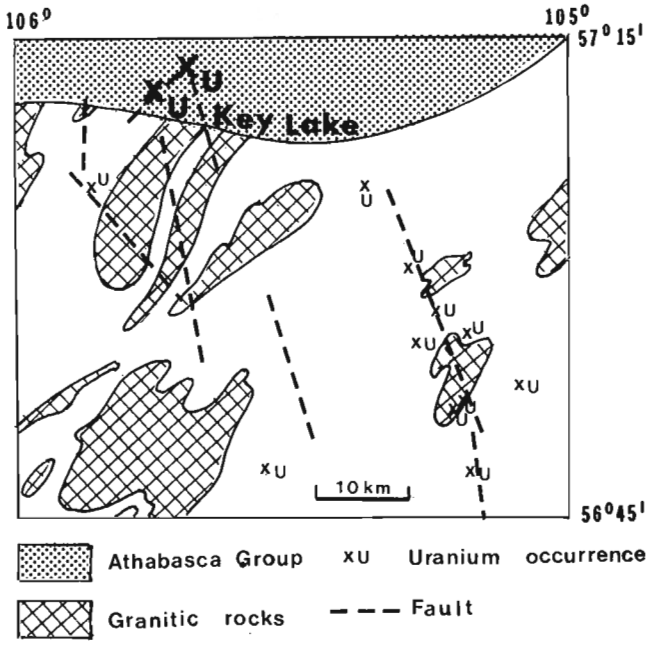

Figure 52.4. Uranium occurrences in the Key Lake area, Saskatchewan (after Ray, 1977). The Key Lake deposits occur in an area where the sedimentary rocks of the Manitou Falls Formation were apparently derived from a source area (to the south and southeast) containing uraniferous granitic rocks. The Archean granitic rocks occur as large plutons shown by cross-ruling; the Hudsonian granitic rocks with associated uraniferous pegmatites are small and shown only as xU.

that "the initial Aphebian sedimentation under anaerobic conditions could have produced suitable conditions for syngenetic uranium concentration within the basal pelites; these may have formed a source for some uranium deposits in northern Saskatchewan". Ramaekers (1981, p. 19) considered the Athabasca Group sedimentary rocks as the "immediate source for the uranium and base metals found in the unconformity deposits at their base...".

Microscope studies of ore samples from the Rabbit Lake, Collins Bay, Eagle Point, Midwest Lake and Maurice Bay deposits in Saskatchewan revealed some genetic features previously identified in additional deposits as listed below.

The uranium mineralization occurs in several phases: (i) as massive pitchblende (first generation) locally surrounded by gersdorffite which also fills fractures in the pitchblende (identified in the Collins Bay 'B' deposit); (ii) as cubic crystalline uranium heptaoxide αU_3O_7 (previously identified at Key Lake and now at the Eagle Point deposit; Fig. 52.5); (iii) as coffinite, which is as a rule younger than the pitchblendes mentioned above (e.g. in the Eagle Point deposit); or is intimately associated with (iv) pitchblende of the second generation (identified in the Maurice Bay deposit; Fig. 52.6); (v) as a complex urano-titanate ("brannerite") with varying amounts of Si, Pb, Fe and Mn (identified in the Rabbit Lake deposit; Fig. 52.7); (vi) in secondary minerals such as uranophane and boltwoodite ($K_2(UO_2)_2(SiO_3)_2(OH)_2 \cdot 5H_2O$) around pitchblende and along fractures and grain boundaries of other minerals (e.g. in the Rabbit Lake and Eagle Point (Fig. 52.8) deposits).

Sulpharsenides and sulphides acted as nuclei for precipitation of uranium mineralization (e.g. Collins Bay 'D' deposit).

Intergrowths of pitchblende and bravoite $(Ni,Fe)S_2$ at Midwest Lake deposit (Fig. 52.9) indicate a simultaneous crystallization and, because of the geothermometric properties of bravoite, also maximal temperature of their crystallization (about 137+6°C; Pechmann and Voultsidis, 1981).

Hoeve et al. (1981) observed two types of alteration controlled by faults. They concluded that the alteration haloes, containing illite and chlorite and associated with mineralization, resulted from basement-Athabasca interaction and are diagnostic of the 1300 Ma unconformity event, whereas the "alteration, marked by intensive kaolinization, may probably be correlated with the late (250 Ma) event of uranium remobilization...". In the second case the surface acidic waters supposedly "percolated down open fault zones, causing conversion of illite and chlorite to kaolinite".

Field observations and some of the above mentioned laboratory observations support the idea that the source of uranium in the unconformity-related deposits were the Archean and Aphebian granitic rocks which supplied the uranium to the Helikian sedimentary rocks, and that the formation of the metallic mineralization in the unconformity-related deposits apparently took place during the diagenetic stage of the sedimentary rocks of the Athabasca Group.

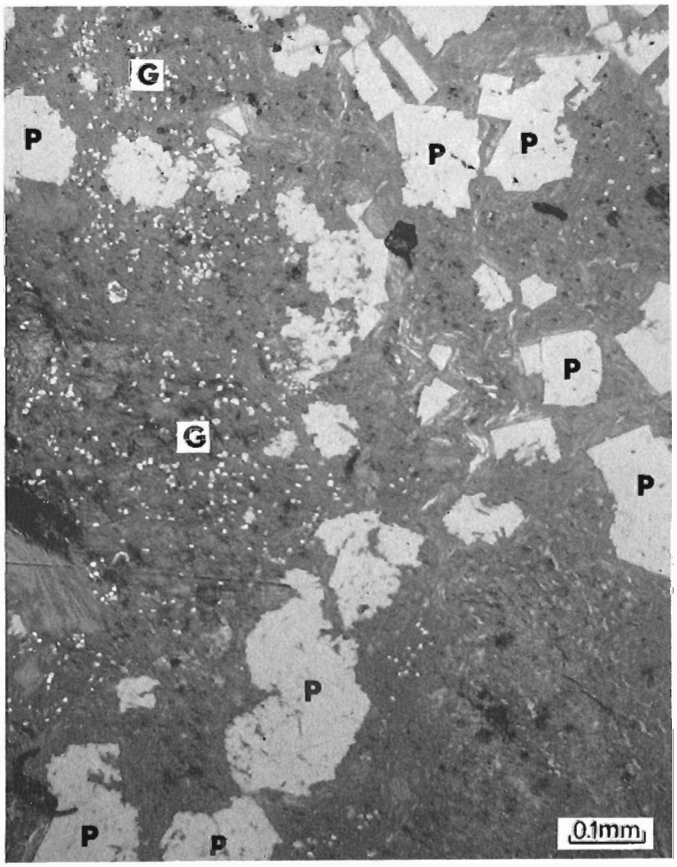

Figure 52.5. *Crystalline pitchblende (P) and specks of galena (G) in ore from Eagle Point deposit, Saskatchewan. Reflected plain light.*

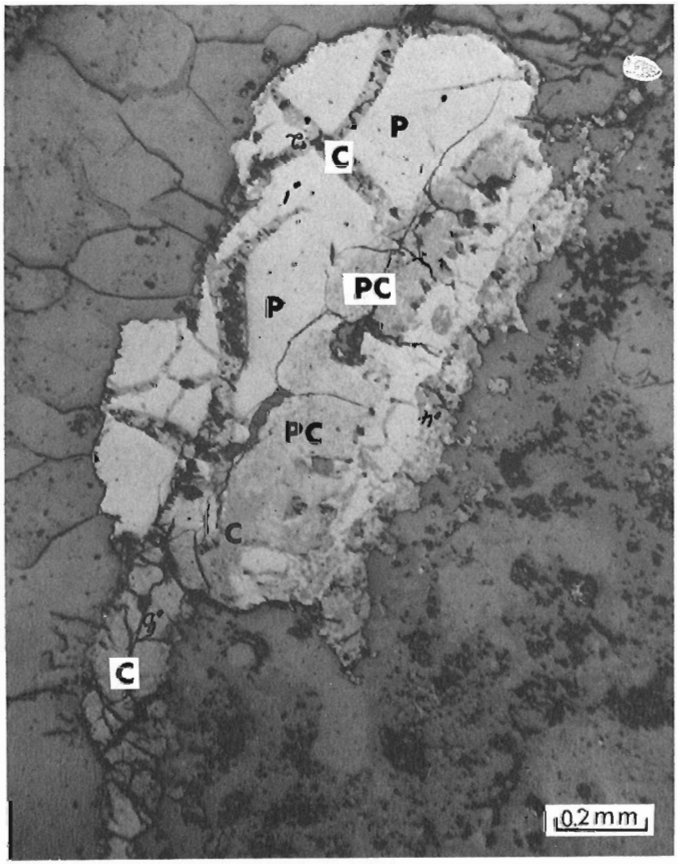

Figure 52.6. *Pitchblende (P), coffinite (C) and mixture of pitchblende and coffinite (PC) in ore from the Maurice Bay deposit, Saskatchewan. Reflected plain light.*

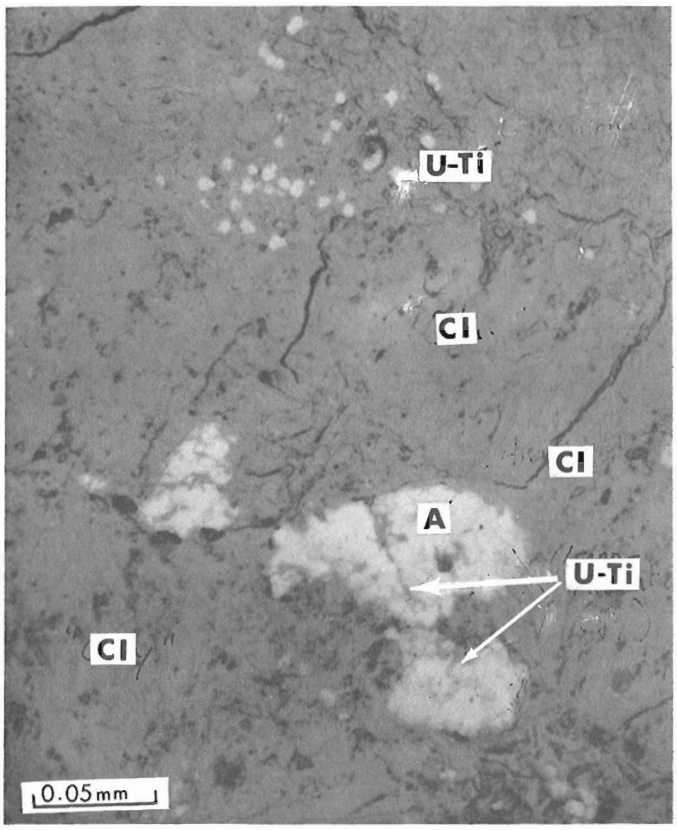

Figure 52.7. *Urano-titanate ("brannerite", U-Ti) and anatase (A) in clay (CL) in ore from the Rabbit Lake deposit, Saskatchewan. Reflected plain light.*

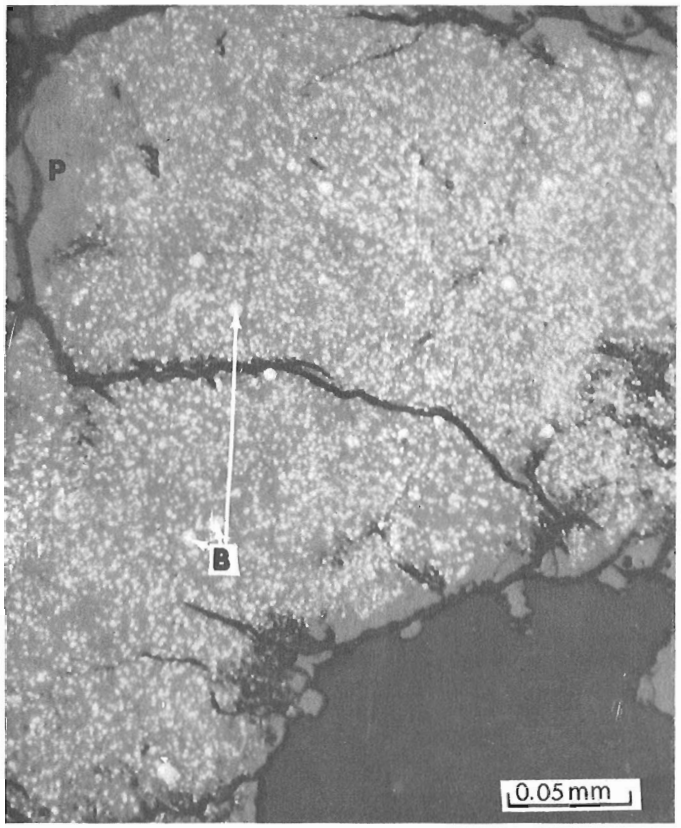

Figure 52.9. *Intergrowth of bravoite (B) and pitchblende (P) in ore from the Midwest Lake deposit, Saskatchewan. Reflected plain light.*

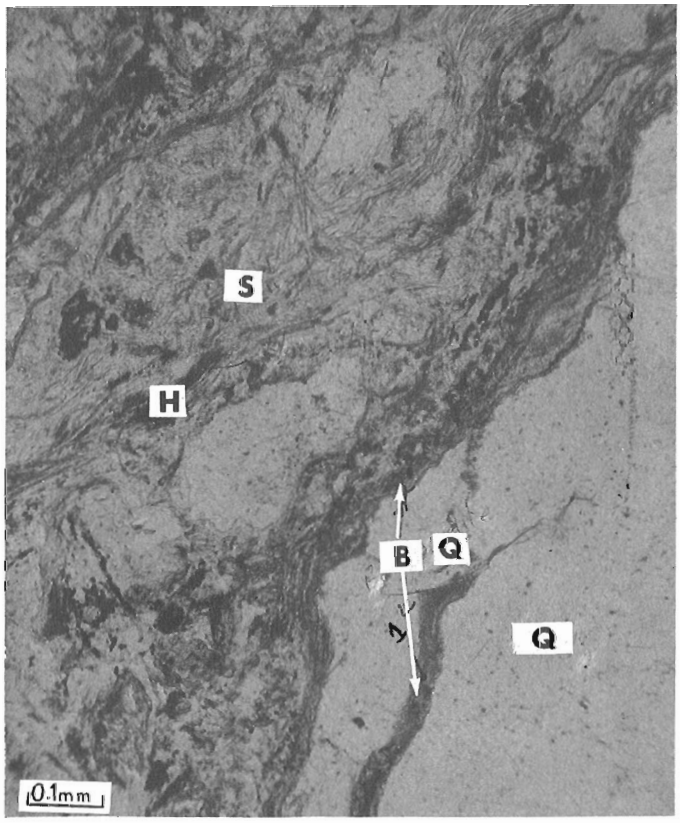

Figure 52.8. *Boltwoodite (B) rimming grains and filling fractures of quartz (Q) and associated with hematite (H) and sericite (S) in ore from Eagle Point deposit, Saskatchewan. Transmitted plain light.*

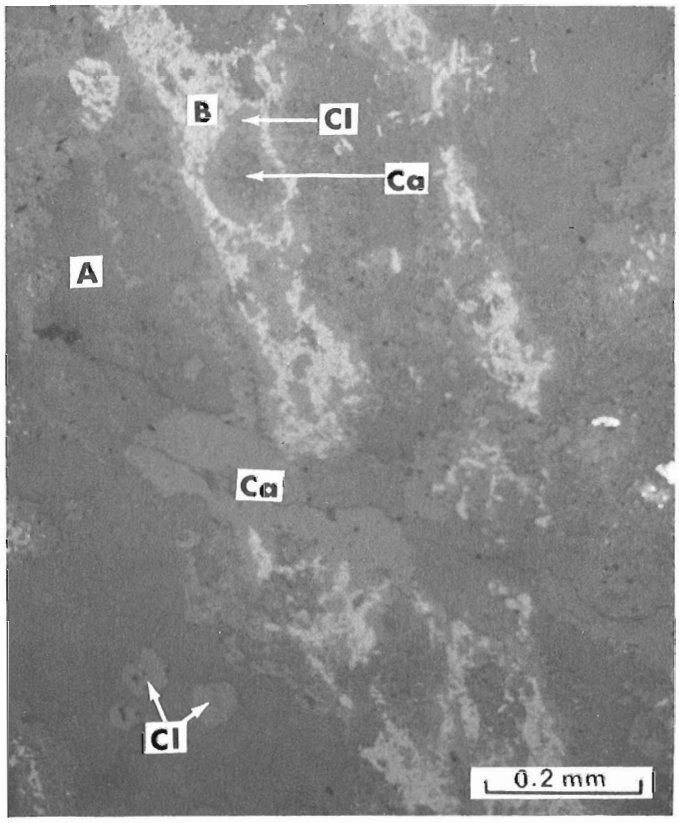

Figure 52.10. *Metasomatic mineral assemblage in ore from the Halo I adit at Wilberforce, Ontario. A = albite, Cl = chlorite, Ca = calcite, B = brannerite. Reflected plain light.*

Brannerite at Halo Deposit, Ontario

Microscope studies on samples of the pegmatite ores from the Halo I adit at Wilberforce, Ontario, revealed numerous inclusions of uraninite in rock-forming minerals such as quartz, feldspar, diopside, plagioclase and titanite. These studies also revealed metasomatic replacement of the rock-forming minerals by albite, chlorite, calcite and brannerite which form fine-grained intergrowths (Fig. 52.10). This is another example of metasomatic modification of the original syngenetic mineralization in the deposits of this type.

New Uranium Occurrence, Bancroft Area

A new occurrence (Devil's Elbow), was discovered by (VR) in 1980 in a roadcut of the highway 500, 19.2 km east of Bancroft, Ontario (45°10'N, 77°38'W). The mineralization is

Figure 52.11. *Devil's Elbow uranium occurrence near Bancroft, Ontario.*

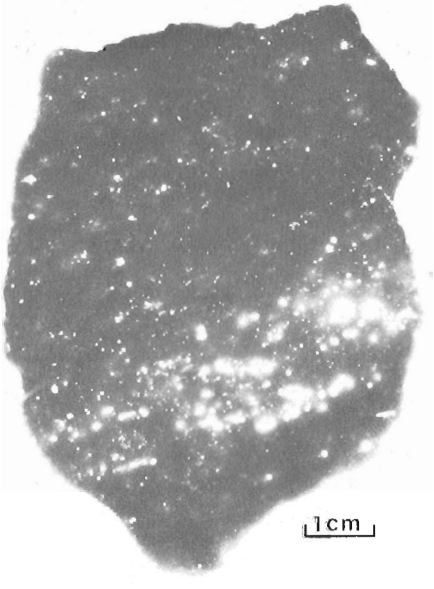

Figure 52.12. *Autoradioluxograph of a sample collected from the Devil's Elbow occurrence near Bancroft, Ontario. Exposure 5 days. Positive image.*

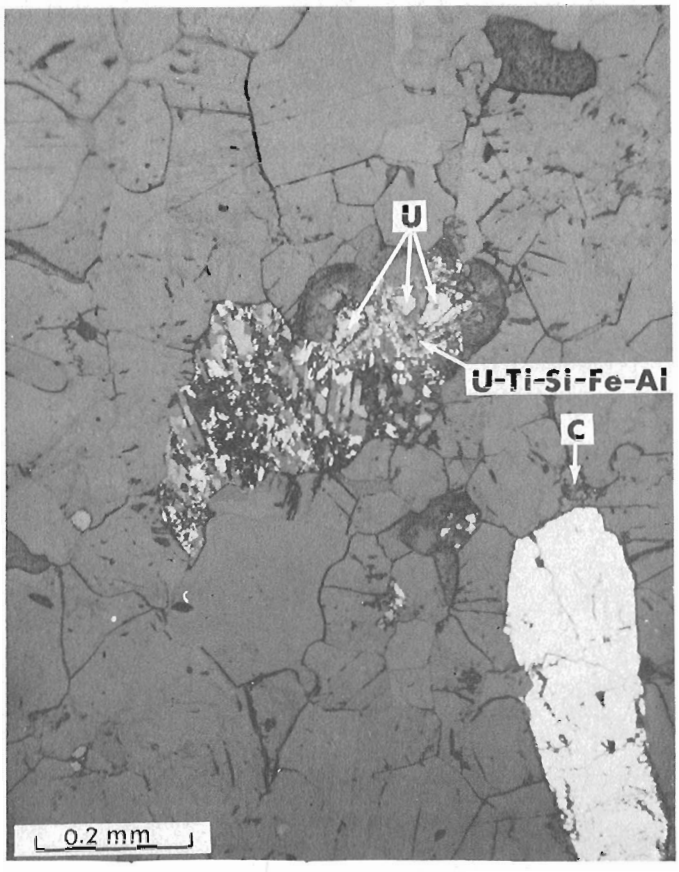

Figure 52.13. *Uraninite (U), coffinite (C) and U-Ti-Si-Fe-Al mineralization of the Devil's Elbow occurrence near Bancroft, Ontario.*

lenticular, up to 0.5 m thick, in a shear zone about 4 m wide striking 090° and dipping 73° to the south in altered biotite gneiss (Fig. 52.11). The uranium mineralization is disseminated (Fig. 52.12) and associated with carbonate veinlets and disseminated pyrite. The shear zone is partly capped by gossan. The main uranium mineral is uraninite, included in titanite and biotite. The titanite has partially broken down to a mixture of titanium oxide, chlorite and quartz. Uranium, apparently derived from the uraninite, reacted with the disintegrated titanite and formed a U-Ti-Si-Fe compound with traces of Pb and Al. Locally it also reacted with silica and formed a coffinite rim on pyrite (Fig. 52.13).

Uranium-silver Mineralization at Box Mine, Saskatchewan

Field and laboratory investigations on the granitic rocks hosting gold mineralization in the Box mine, Goldfields, Saskatchewan (Christie, 1953, p. 77-79 and 92-93; Robinson, 1955, p. 54) led to identification of coffinite in addition to the pitchblende reported by Christie (1953) (Fig. 52.14). The pitchblende veins are probably younger than the gold-sulphide-bearing quartz veins (Robinson, 1955, p. 54). A sample taken from an outcrop of strongly hematitized, carbonatized and fractured granitic rocks (about 200 m east of the shaft) contained mixtures in various proportions of coffinite, pitchblende, native silver, acanthite, chlorargyrite and hematite (Fig. 52.15A,B). The uranium-silver mineralization is epigenetic and is related to a different phase than the gold mineralization.

Millet Brook Occurrence, Nova Scotia

The recently discovered uranium mineralization at Millet Brook, Nova Scotia, is apparently confined to zones of metasomatic alteration in granitic rocks.

Brannerite at Ace-Fay Mine, Beaverlodge, Saskatchewan

The largest known uranium vein deposits in Canada are those in the Beaverlodge area, Saskatchewan, namely the 01-09 orebodies in the Ace-Fay mine of Eldorado Nuclear Limited.

Crystallization of the uranium minerals in the 01-09 orebodies was closely associated with formation of albite, chlorite, calcite and hematite and anatase during alteration of the host rocks. The prevailing uranium minerals are pitchblende, coffinite and U-Ti aggregates ('brannerite').

The U-Ti aggregates (with U and Ti in varying proportions) are invariably associated with chlorite; they locally form small laths or aggregates within pitchblende; they occur in the rockforming minerals, with hematite, chlorite, galena or in a more massive form as fracture filling (Fig. 52.16, 52.17). The ore contains grains (Fig. 52.18) consisting of two phases: one, composed mainly of Ti-U with

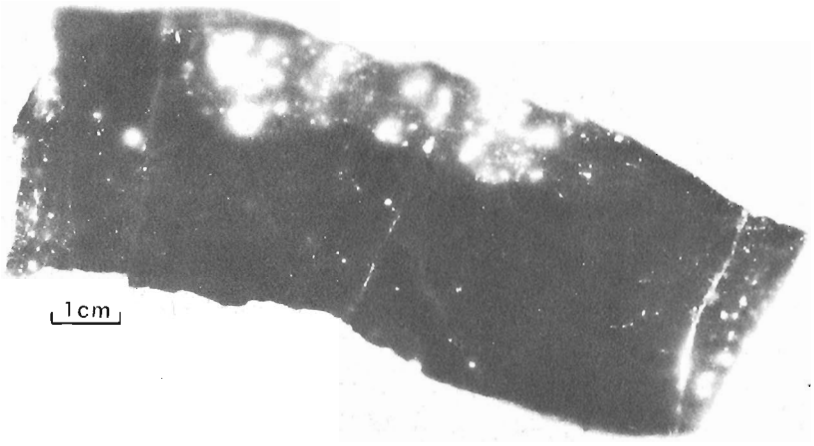

Figure 52.14

Autoradioluxograph of a sample of a hematitized and carbonatized granitic rock from the vicintiy of Box mine, Goldfields, Saskatchewan. Exposure: 5 days. Positive image.

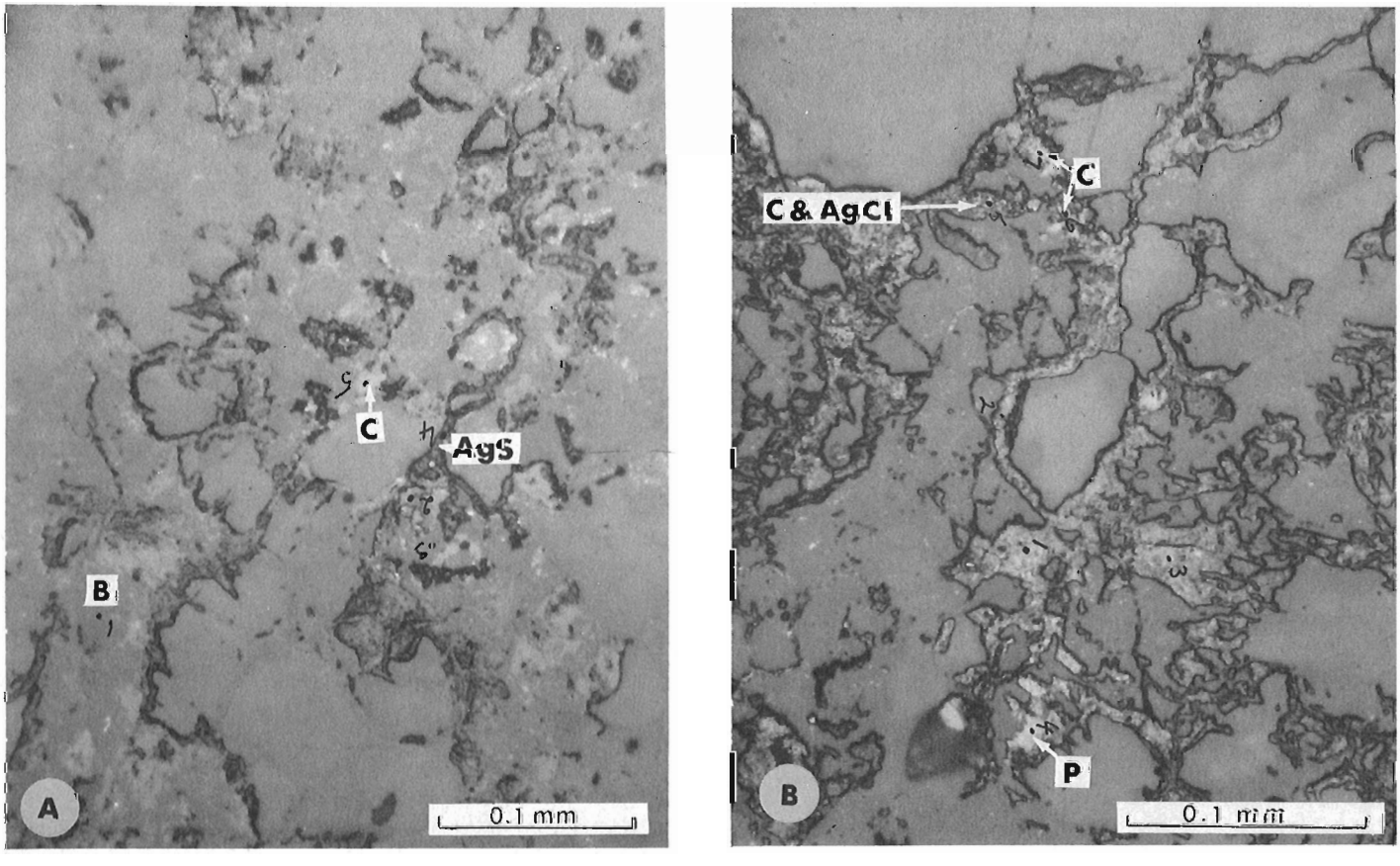

Figure 52.15 A & B. *Uranium and silver mineralization in hematitized and carbonatized granite from the vicinity of Box mine, Goldfields, Saskatchewan. C = coffinite, P = pitchblende, AgS = acanthite, AgCl = chloragyrite, B = biotite. Reflected plain light.*

traces of Fe and Si; the other of U-Si with traces of Ti and Ca. These complex grains always have a rim of the Ti-rich phase suggesting that both titanium and uranium were mobile and were carried in the ore-forming fluids simultaneously. The presence of anatase aggregates with interstitial coffinite within and around chlorite, but without formation of a U-Ti phase supports this.

Coffinite in Albert Formation, Moncton Basin, New Brunswick

The uranium mineralization in sandstone from the Albert Formation, Moncton Basin, was sampled at the Discovery Creek near Lower Millstream, New Brunswick. The uranium minerals (Fig. 52.19) are very small and commonly associated with pyrite. Chemical analysis by probe indicated uranium silicates and the X-ray identification confirmed presence of coffinite. Field observations indicated that the radioactivity increased with increasing amount of bituminous and limey substances in the sandstone. Gross (1957, p. 12-14) investigated radioactive material in a vein of hydrocarbon in the same basin and interpreted the "hydrocarbon as originated from petroleum that was once present in the Albert Formation", and that uranium "may have been leached from the sedimentary rocks by ground water and precipitated by the carbon in the vein". He speculated that another source of uranium might be "some of the rhyolite and porphyritic volcanic rocks in the Kingston Group".

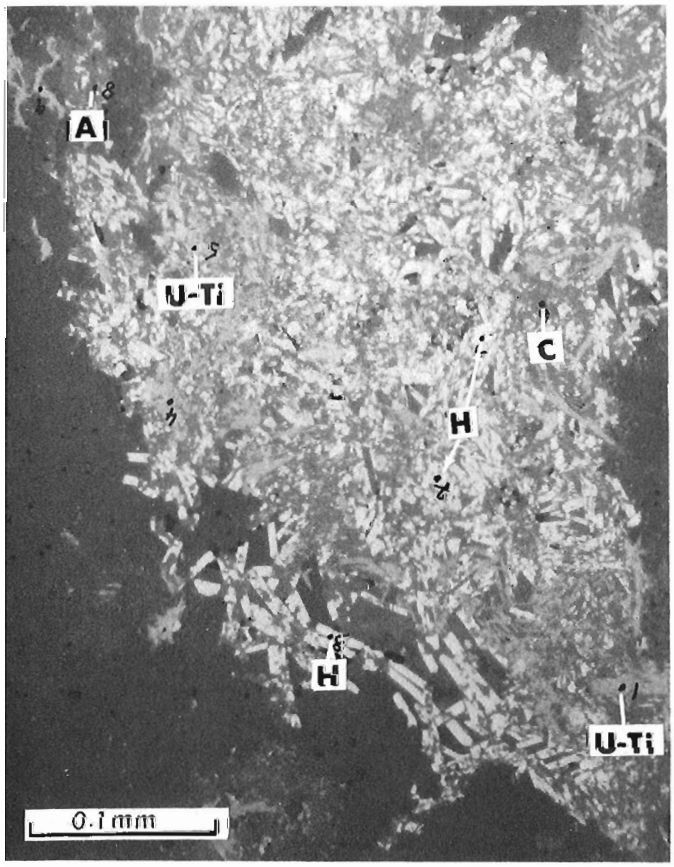

Figure 52.16. *U-Ti aggregates in ore from the 09 orebody, 22nd level, Fay mine of Eldorado Nuclear Limited, Beaverlodge (Uranium City), Saskatchewan; U-Ti = U-Ti aggregate with Ca, Fe and Si; A = albite; C = chlorite, H = hematite. Reflected plain light.*

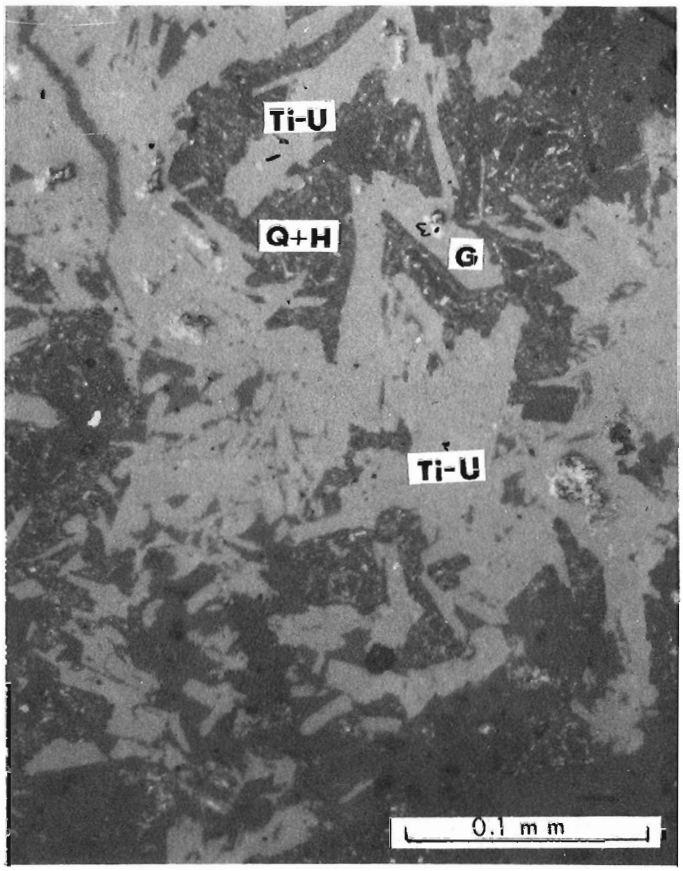

Figure 52.17. *Ti-U aggregate (Ti-U) with minor Fe, Si, Ca and Pb accompanied by galena (G) and quartz-hematite mixture (Q+H) from 09 orebody, Fay mine of Eldorado Nuclear, Beaverlodge, Saskatchewan. Reflected plain light.*

Mineralization in the Peribonca Formation, Otish Mountains, Quebec

Samples of mineralized calc-silicate rocks, consisting mainly of dolomite and some quartz, of the Peribonca Formation from the vicinity of Lac Isabelle, Otish Mountains, Quebec, were collected from boulders derived from an apparently nearby bedrock source.

Uranium minerals are dispersed interstitially to the grains of dolomite and quartz or in cracks in the dolomite (Fig. 52.20). They often contain vanadium. A prominent uranium-vanadium-bearing mineral is francevillite $(Ba,Pb)(UO_2)(VO_4)_2 \cdot 5H_2O$ which also commonly occurs in an amorphous mixture with manganese oxide (Fig. 52.21A). Another U-V compound is an opaque amorphous material consisting of U-V-Si-Pb-Ca in varying proportions; this material is locally replaced by pitchblende, which also occurs in discrete grains (Fig. 52.21B).

A conceptual model for this type of mineralization modified after W.M. Atkins of Pancontinental Mining Canada Limited (personal communication) is: the Peribonca Formation in the Otish Mountains area contains a sequence of sandstone, overlain by dolomite, which is in turn overlain by siltstone. The deposition of the carbonate sequence was followed by an uplift accompanied by the accumulation of uranium minerals and the deposition of siltstone. Connate waters derived from compaction of the siltstone could have introduced uranium and vanadium into the dolomite. This is apparently the reason why the uranium-vanadium mineralization is in the francevillite form.

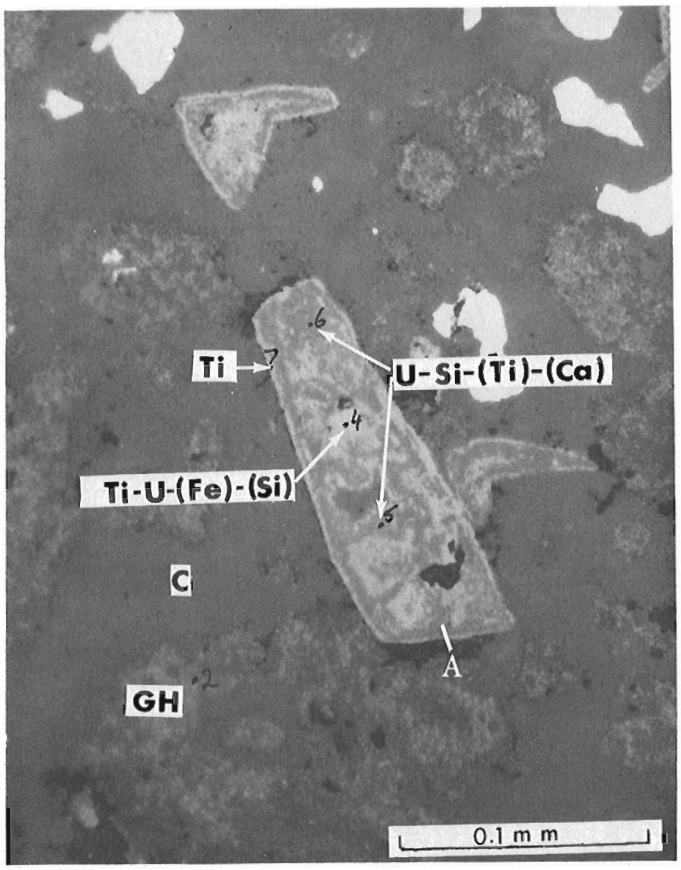

Figure 52.18. *An ore grain (H), composed of two mineralization phases: (a) Ti-U-(Fe)*-(Si) and (b) U-Si-(Ti)-(Ca) and rimmed by Ti; C = calcite, GH = goethite and hematite. Plain reflected light. 09 orebody, Fay mine of Eldorado, Beaverlodge, Sasktachewan.*

**elements in brackets are present in traces.*

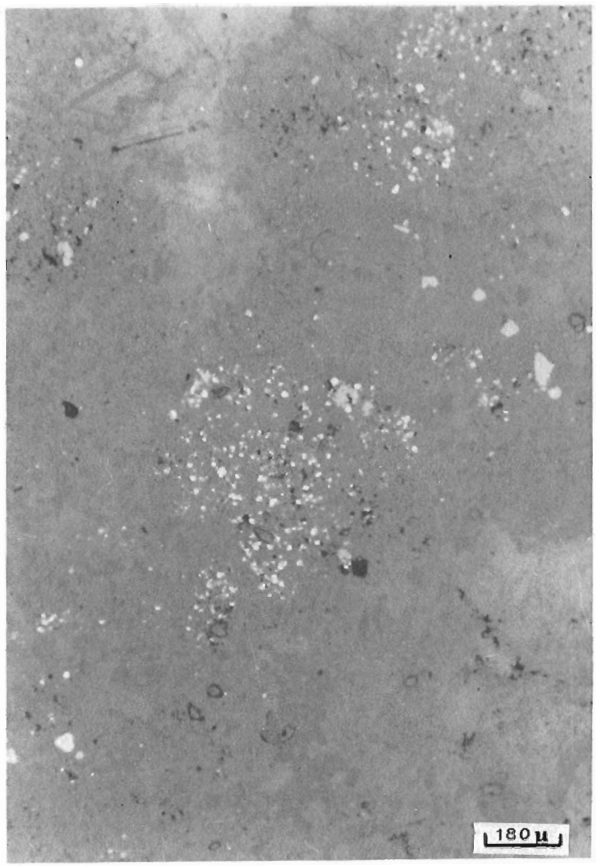

Figure 52.19. *Coffinite (white small specks) in sandstone from Lower Millstream area, New Brunswick. Reflected plain light.*

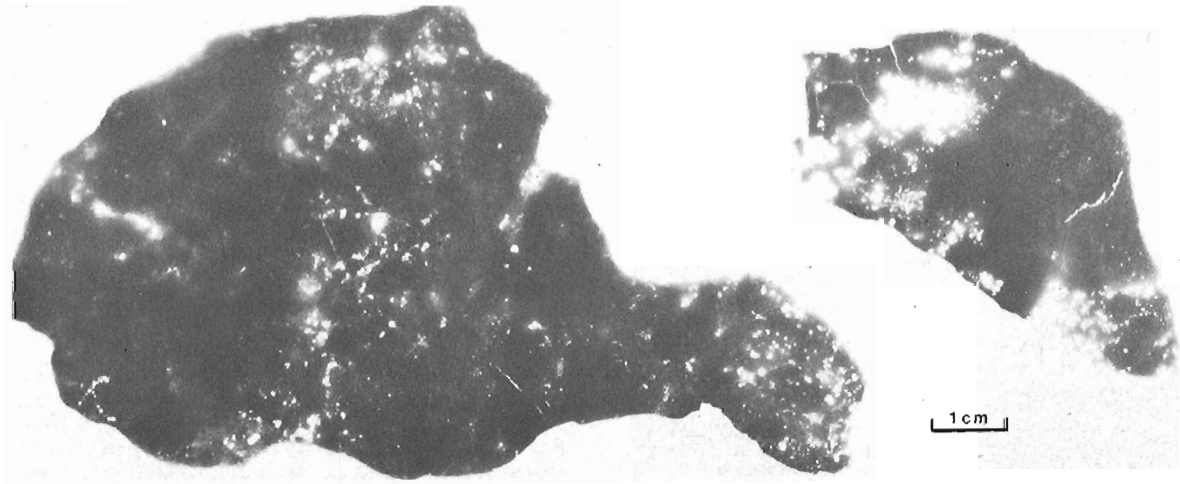

Figure 52.20. *Autoradioluxograph (positive image) of samples of mineralized dolomite of the Peribonca Formation, Otish Mountains, Quebec.*

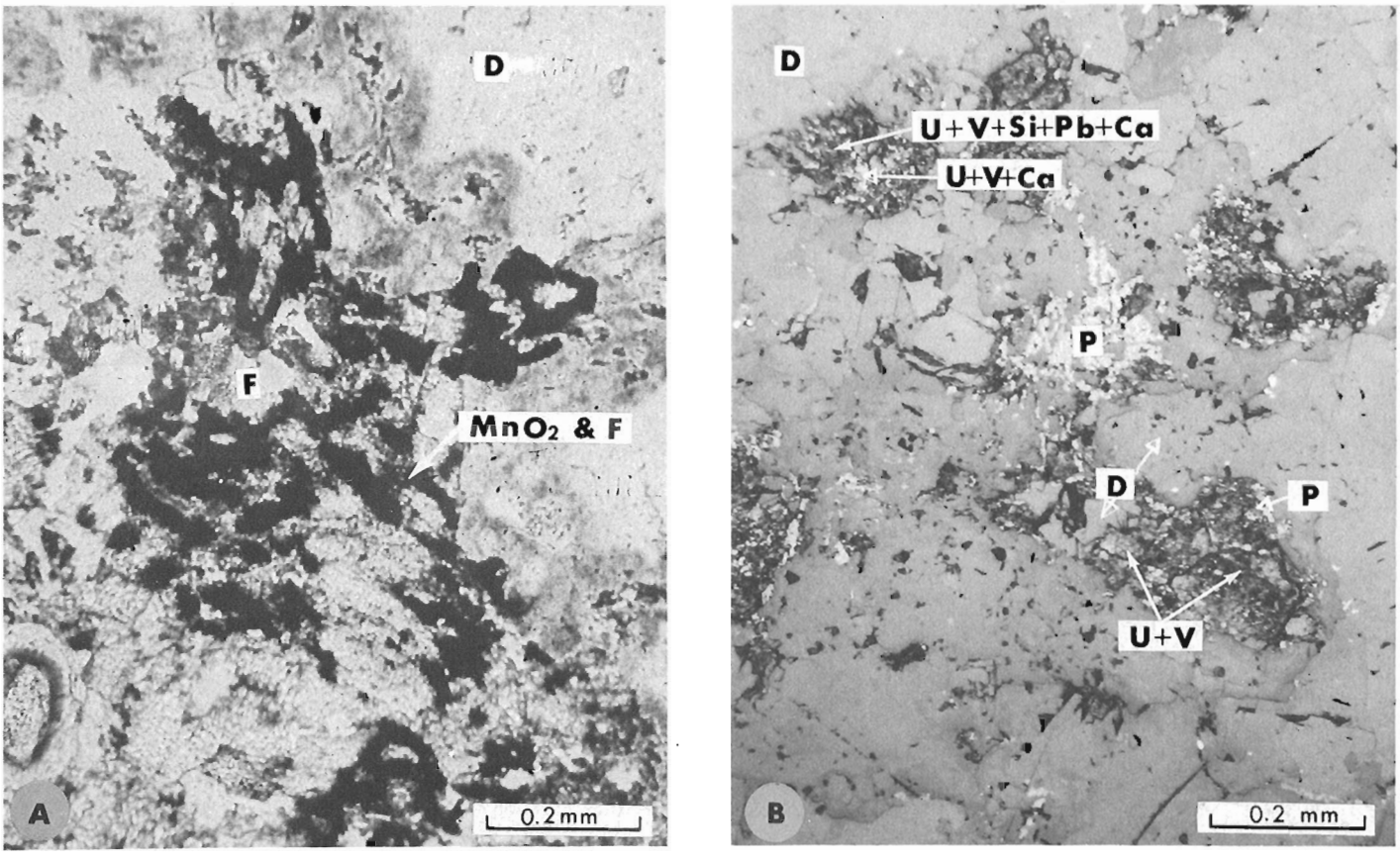

Figure 21 A&B. *Mineralized calc-silicate rock (mainly dolomite) of the Peribonca Formation, Otish Mountains, Quebec. F = francevillite, P = pitchblende, D = dolomite; other compounds, mineralogically unindentified, are designated by chemical symbols.*

Acknowledgments

The authors acknowledge the co-operation of professionals working for companies in areas studied, especially Rio Algom Limited, Gulf Minerals Canada Limited, Uranerz Exploration and Mining Limited, Eldorado Nuclear Limited, Rare Earth Resources Limited, SOQUEM, Pancontinental Mining Limited, Inco Metals Company; and Saskatchewan Geological Survey. The authors acknowledge assistance of J.A. Kerswill in preparation of samples for mineralogical analyses and A.C. Roberts in mineral identification by XRD.

References

Christie, A.M.
1953: Goldfields-Martin Lake map-area, Saskatchewan; Geological Survey of Canada, Memoir 269.

Gross, G.A.
1957: Uranium deposits in Gaspé, New Brunswick, and Nova Scotia; Geological Survey of Canada, Paper 57-2.

Hoeve, J., Rawsthorn, K., and Quirt, D.
1981: Clay minerals as a clue to uranium mineralization in the Athabasca Basin; in "CIM Geology Division Uranium Symposium and Field Tours"; Saskatchewan, September 8-13, 1981, p. 17-18.

Pechmann, E. von and Voultsidis, V.
1981: Further results on the petrography and mineralogy of the Key Lake uranium-nickel orebodies, Saskatchewan, Canada; in "CIM Geology Division Uranium Symposium and Field Tours", Saskatchewan, September 8-13, 1981, p. 14-15.

Ramaekers, P.
1981: Geochemistry of the Athabasca sandstones; implications for uranium genesis; in "CIM Geology Division Uranium Symposium and Field Tours", Saskatchewan, September 8-13, 1981.

Ramdohr, P.
1957: Die "Pronto-Reaktion"; Neues Jahrbuch für Mineralogie, Monatshefte, Jahrgang 1957, v. 10-11, p. 217-222.

1958a: Die Uran- and Goldlagerstätten Witwatersand-Blind River District – Dominion Reef-Sra de Jacobina; Abhandlungen der Deutschen Akademie der Wissenschaften zu Berlin; Klasse fur Chemie, Geologie und Biologie, Jahrgang, No. 3.

1958b: New observations on the ores of the Witwatersrand in South Africa; Geological Society of South Africa, Annexure to volume LX1.

Ray, G.E.
1977: The geology of the Highrock Lake – Key Lake vicinity, Saskatchewan; Saskatchewan Department of Mineral Resources, Report 197.

Robinson, S.C.
1955: Mineralogy of uranium deposits, Goldfields, Saskatchewan; Geological Survey of Canada, Bulletin 31.

Roscoe, S.M.
1969: Huronian rocks and uraniferous conglomerates in the Canadian Shield; Geological Survey of Canada, Paper 68-40, 205 p.

53. COMPILATION TECHNIQUES FOR THE 1:1 MILLION MAGNETIC ANOMALY MAP SERIES

Project 780002

D.J. Teskey, S.D. Dods, and Peter J. Hood
Resource Geophysics and Geochemistry Division

Teskey, D.J., Dods, S.D., and Hood, Peter J., Compilation techniques for the 1:1 million magnetic anomaly map series; in Current Research, Part A, Geological Survey of Canada, Paper 82-1A, p. 351-358, 1982.

Abstract

A program for the production of 1:1 000 000 total field colour aeromagnetic maps using existing data compiled at a scale of 1:50 000 or one inch to one mile has been initiated. Procedures include digitization of existing maps, filing, gridding, subtraction of the International Geomagnetic Reference Field for the year of survey, and levelling at adjacent survey and sheet boundaries. After processing, colour separates are made directly with the Applicon plotter for photography and printing with a range of forty colours. The digital data acquired in this program will be stored in a data base which can be accessed for computer processing and interpretation in conjunction with other data sources.

Introduction

The main end products of the aeromagnetic survey program of the Geological Survey of Canada have been 10 gamma contour maps at a scale of 1:50 000 with the flight lines shown, and composite maps at a scale of 1:250 000 without flight lines to enable users to ascertain the regional trends. Prior to the adoption by Canada of the metric system, these maps were published at the one inch to one mile (1:63 360) and the one inch to four miles (1:253 440) scales. Figure 53.1 shows the extent of such magnetic coverage in Canada to the end of 1981. Because of the recognition that regional trends persist over great distances and that geological provinces commonly have characteristic magnetic patterns, a 1:5 000 000 Magnetic Anomaly Map of Canada was compiled at a 200 gamma interval and the first edition was published in 1967. Two subsequent editions of the map were issued in 1972 and 1977.

It should be pointed out that although the 1:5 million magnetic anomaly map serves a useful purpose because it shows the magnetic patterns across Canada on a reasonably sized sheet, it is felt that there is a requirement for an intermediate series at 1:1 000 000 scale. The main reason for this conclusion is because at the small scale of the 1:5 million map the longer wavelength anomalies will tend to be emphasized. Features which produce anomalies less than about 0.5 mm in width at the map scale cannot be physically drawn on the map; 0.5 mm at the 1:5 000 000 scale represents 2500 metres but only 500 metres at the 1:1 000 000 scale. This means that many important narrow geological features, such as dykes or dyke swarms, will not be portrayed on the resultant end product. Thus the short wavelength cut-off is directly proportional to the scale of the map. Hence the scale and colour contour interval represent the graphical filtering parameters which may be varied to produce various filtering effects on magnetic anomaly maps and inevitably there is a loss of detail in smaller scale maps such as the 1:5 M magnetic anomaly map.

Accordingly, in 1977 an experimental program was initiated to digitally produce coloured 1:1 000 000 residual total field aeromagnetic maps using existing data published by the Geological Survey of Canada at one inch to one mile or 1:50 000 scale. The majority of these data have been determined and compiled on behalf of the Geological Survey by contractors, although in some areas other sources were used if the required specifications were met.

Initially three NTS sheets 64, 74 and 75 were produced under contract by Dataplotting Ltd. of Toronto, with M.T. Holroyd as the technical authority on behalf of the GSC for the contract. These maps, which were plotted using an Applicon colour plotter showed clearly features not readily seen at the 1:250 000 or 1:5 000 000 scales currently available, for example, the north-northeasterly trending dyke swarms which are evident on NP 12/13 (Fig. 53.2).

A program has been initiated to prepare maps of this type for all the areas of Canada with published aeromagnetic coverage using an International Map of the World (IMW) base which is the system adopted by EMR for 1:1 000 000 maps in the National Earth Science Series. An additional objective to be satisfied by the program is the creation of a digital data base that can be used for the production of colour maps at other scales, or for digital processing and interpretation.

Techniques

As part of the original experimental project, a contract was let for the digitization of NTS 65 (IMW NP 13/14) using a contour tracing technique. Procedures developed for the processing of these data will be described below. These procedures will, of course, require some modification for different digitizing techniques or special considerations that will undoubtedly occur in such a large mass of data collected over a long period of time with changing technology and over different terrains. The basic steps, however, will remain the same and it is hoped that procedures described here will form the basis for later development.

The ideal flow chart for processing data of this type is shown in Figure 53.3. For IMW NP 13/14, however, editing of the data was accomplished using the dashed path shown in Figure 53.3 because of difficulties encountered in error detection.

1) Digitization

There are basically three approaches to the digitization of contoured data of this type:

i) Manual digitization of values at even increments of latitude and longitude by overlaying a grid. This technique was used by Dataplotting in the digitization of NTS sheets 64, 74 and 75;

ii) Tracing of selected contours on an electronic digitizer (used by Kenting for NTS 65 (IMW NP 13/14);

iii) Digitization of contour intercepts at flight lines on an electronic digitizer.

In our opinion the third technique produces data in the optimum form for inclusion in a data bank, as it can readily be regridded for processing at any scale. In addition, editing

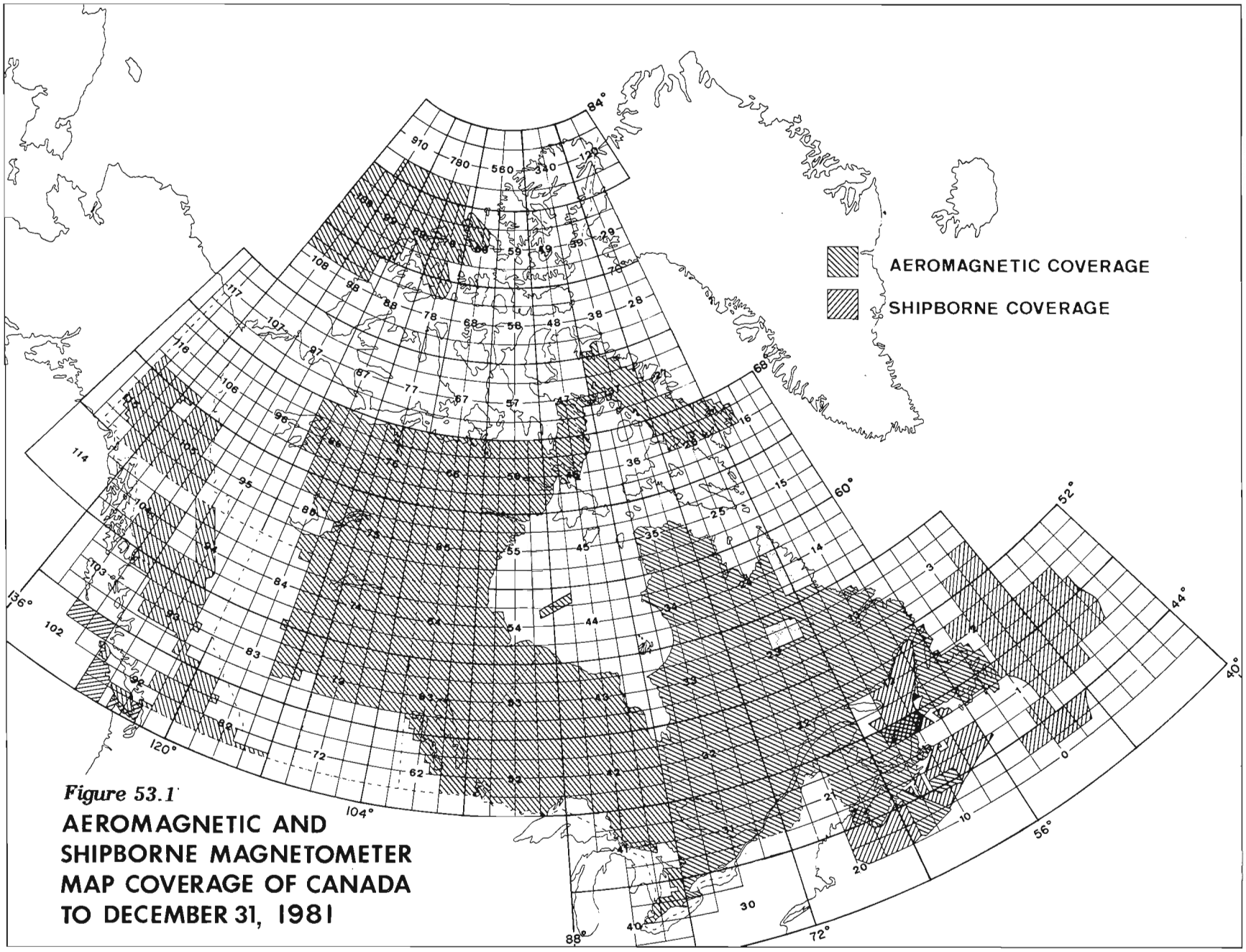

Figure 53.1

AEROMAGNETIC AND SHIPBORNE MAGNETOMETER MAP COVERAGE OF CANADA TO DECEMBER 31, 1981

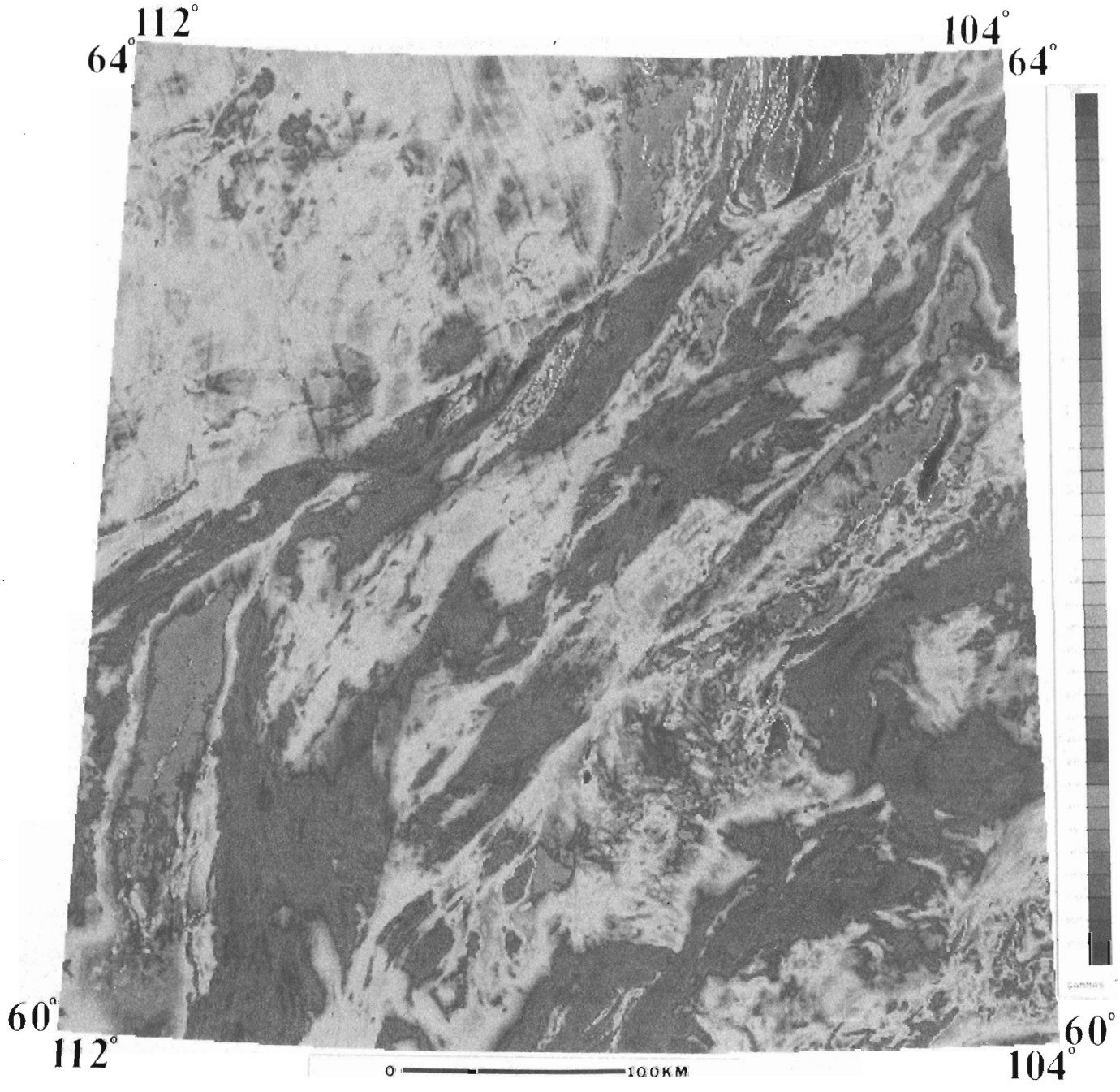

Figure 53.2. *Black and white reproduction of one to one million colour aeromagnetic anomaly map for NTS 75 (IMW NP 12/13). Published in colour as GSC Map 1566A – Lockhart River, Northwest Territories (scale 1:1 000 000).*

can be efficiently carried out using standard techniques for aeromagnetic data. A contract was let for the digitization of IMW sheet NQ 12/13/14 using this technique. The contract specified that points would be digitized at a minimum interval of 1.5 cm (at one inch to one mile) and on the flanks, peaks and troughs of anomalies. It should be noted that this technique is only possible because the flight lines are superimposed on the published contour maps and because of the high quality of the published data.

The digitized data, after editing, are stored by survey area, that is areas flown in a continuous time period and in a compatible manner (Fig. 53.4). These files then become the basic working files for gridding and subtraction of the International Geomagnetic Reference Field (IGRF). Before inclusion in the file the X and Y position of each datum point is converted from arbitrary digitizer units to standard Universal Traverse Mercator (UTM) co-ordinates and then to a Lambert Conformal projection. At this stage, a projection is used which allows all data for the country to be placed in the same reference system with a common origin, thus facilitating the adjustment of different areas required by differences at survey boundaries and at IMW sheet boundaries. Conversion to a standard Lambert projection for each IMW sheet is then done as a final adjustment to the gridded data.

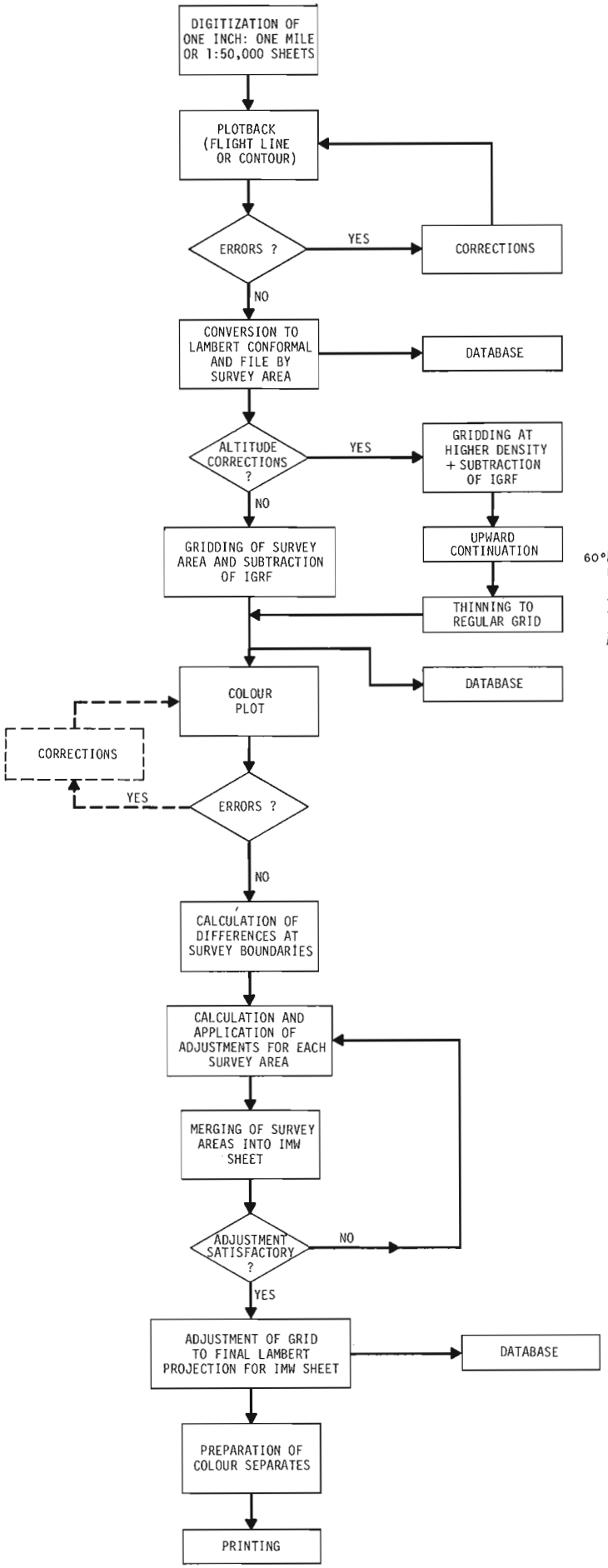

Figure 53.3. Flow chart for compiling one to one million magnetic anomaly maps.

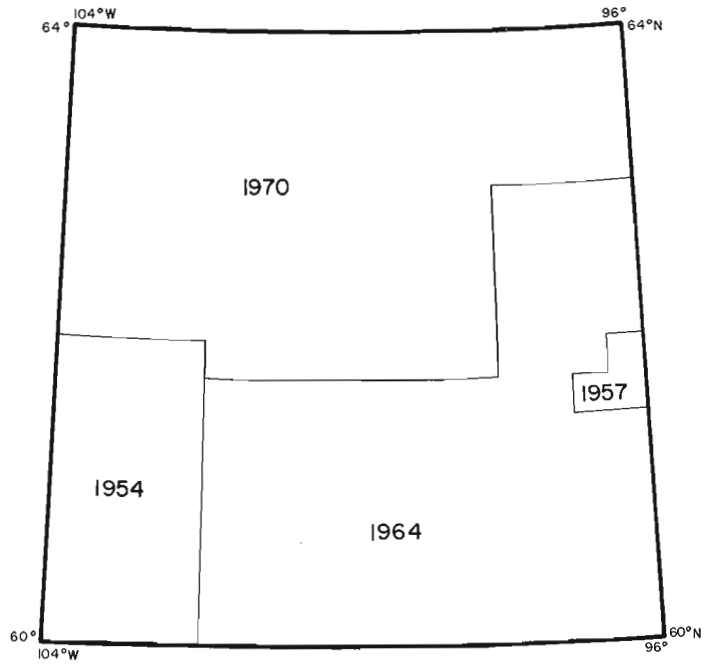

Figure 53.4. Index map of IMW NP 13/14 (NTS 65) showing the average year the various aeromagnetic survey areas were flown.

2) Gridding

Because of the high density of data and the final grid size (812.8 m) which is of the same order as the average flight line spacing (830 m) the actual interpolation technique used in gridding is not critical. In the present case a weighted average of the data points within a small region of each grid point was used, with the weight for each datum point proportional to the inverse of the distance from that point to the grid point.

3) Levelling

Adjustments are required at the survey boundaries due to differences in year of survey and also due to the techniques used by individual companies in processing the survey data. In some of the earlier fluxgate surveys the mean value is arbitrary. Ideally, the adjustments would be done using all of the differences at survey boundaries over a continuously mapped area. However in the present case, only a small amount of this data is available and thus it is necessary to choose a reference survey (1964 area in IMW NP 13/14) and to adjust the adjacent surveys to fit at the common boundaries, continuing this process for surrounding surveys. The actual levelling is done in two stages. First, a simple linear fit was made to the differences along a straight portion of the boundary and applied to the entire survey (i.e. the 1970 area of IMW NP 13/14). If significant differences still exist between adjacent surveys, a quadratic surface is fitted to the differences around the entire boundary, and the surface thus specified subtracted. This second step was not required for any of the component surveys of IMW NP 13/14. Clearly limitations will have to be placed on the amount of curvature allowed, particularly at boundaries for which the adjacent data is not yet available. It is anticipated that there will be some areas, particularly in mountainous terrain, where accurate fits will not be possible without excessive warping and thus some discontinuity will have to be tolerated.

4) Colour Processing and Printing

The Applicon colour plotter produces colours encompassing the visual spectrum by varying the number and pattern of yellow, cyan (blue), and magenta (red) dots in a matrix of

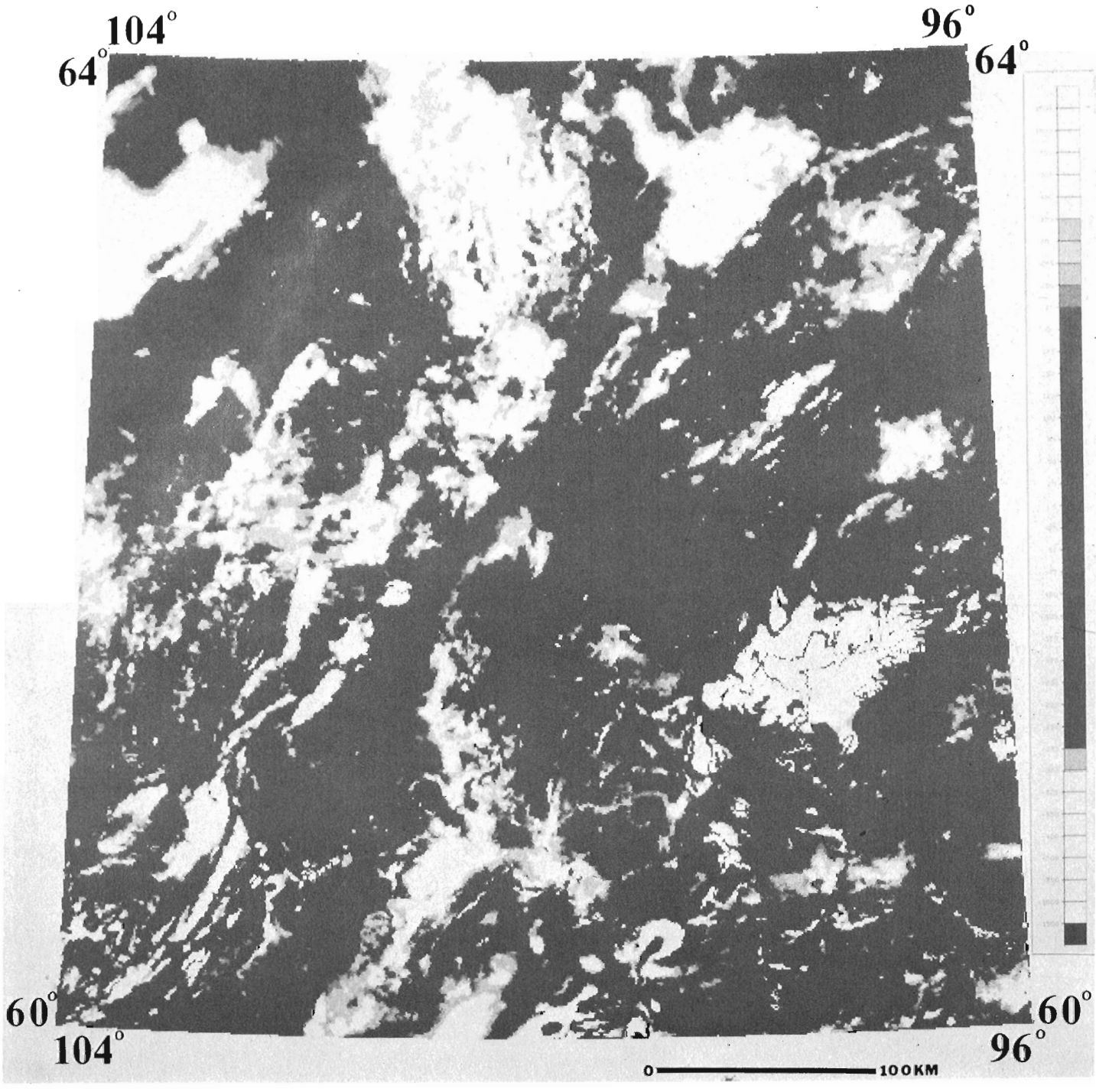

Figure 53.5. *Colour separate (yellow) NP 13/14.*

4 by 4 dots (16 dots). Each dot is 0.2032 mm in size, and the matrix of 16 dots, the colour cell, is 0.8128 mm square. During plotting, a colour is assigned to each colour cell depending on the data value in the corresponding grid cell. To facilitate colour printing, the yellow, cyan and magenta components can be plotted separately (each component is plotted in magenta because of its good photographic reproduction characteristics). Figures 53.5-53.7 show the colour separates that were made for IMW NP 13/14. Each separate and the corresponding topographic map with text is photographed and then dye proofs and printing plates are produced. Four colour printing is performed by a multi-pass process.

The cost of separates, photographic work, dye proof and printing is less than one dollar a copy (1000 copies) and can be performed in approximately one week instead of the usual three to four months required by the manual process. A black and white reproduction of the resultant colour contour map for NP 13/14 is shown in Figure 53.8.

Conclusion

It is felt that the 1:1 000 000 magnetic anomaly map compilation program will greatly enhance the geoscientific data base in Canada and will prove to be of great assistance to the mapping of regional geology. The digital data which

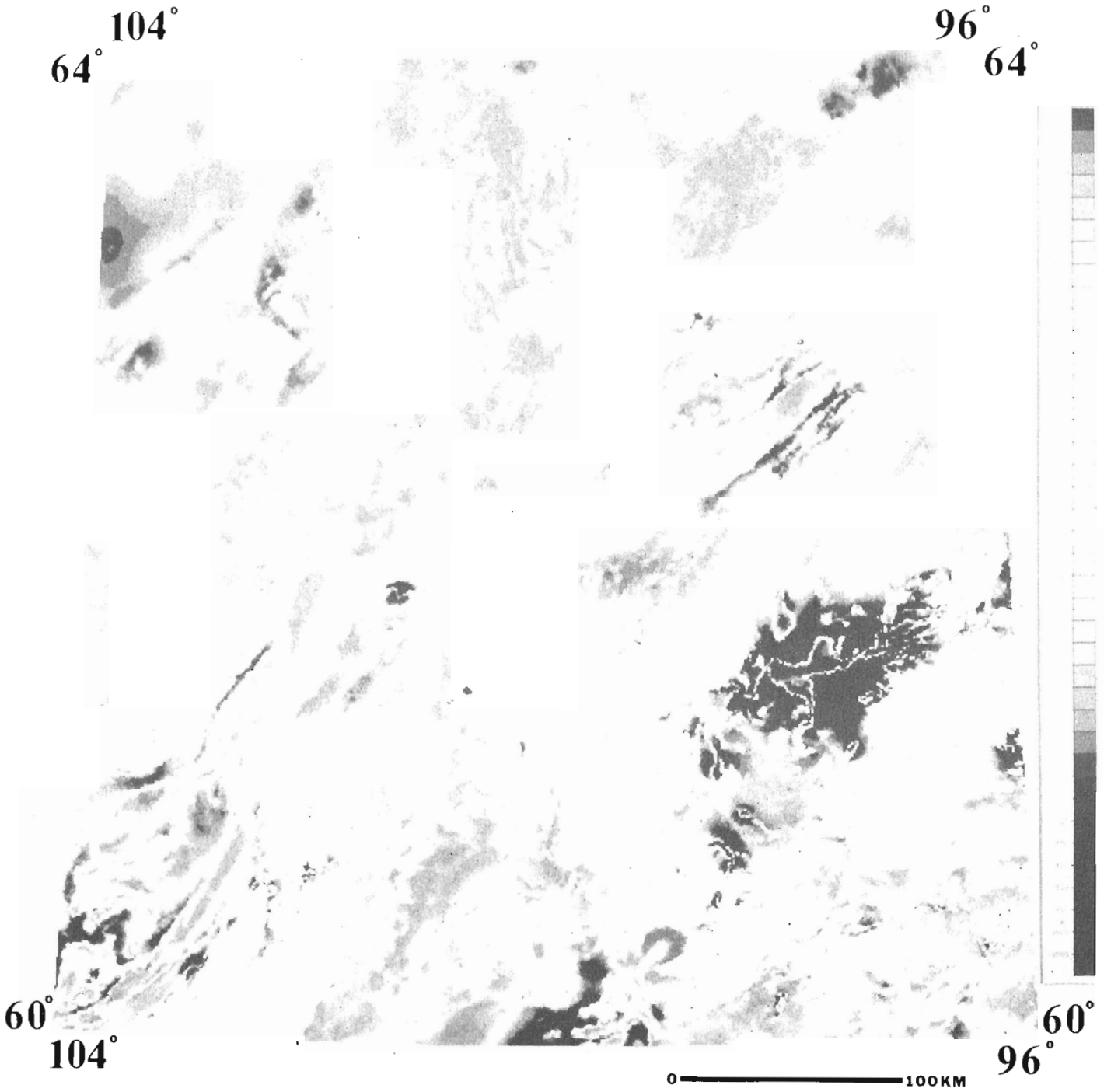

Figure 53.6. *Colour separate (cyan) NP 13/14.*

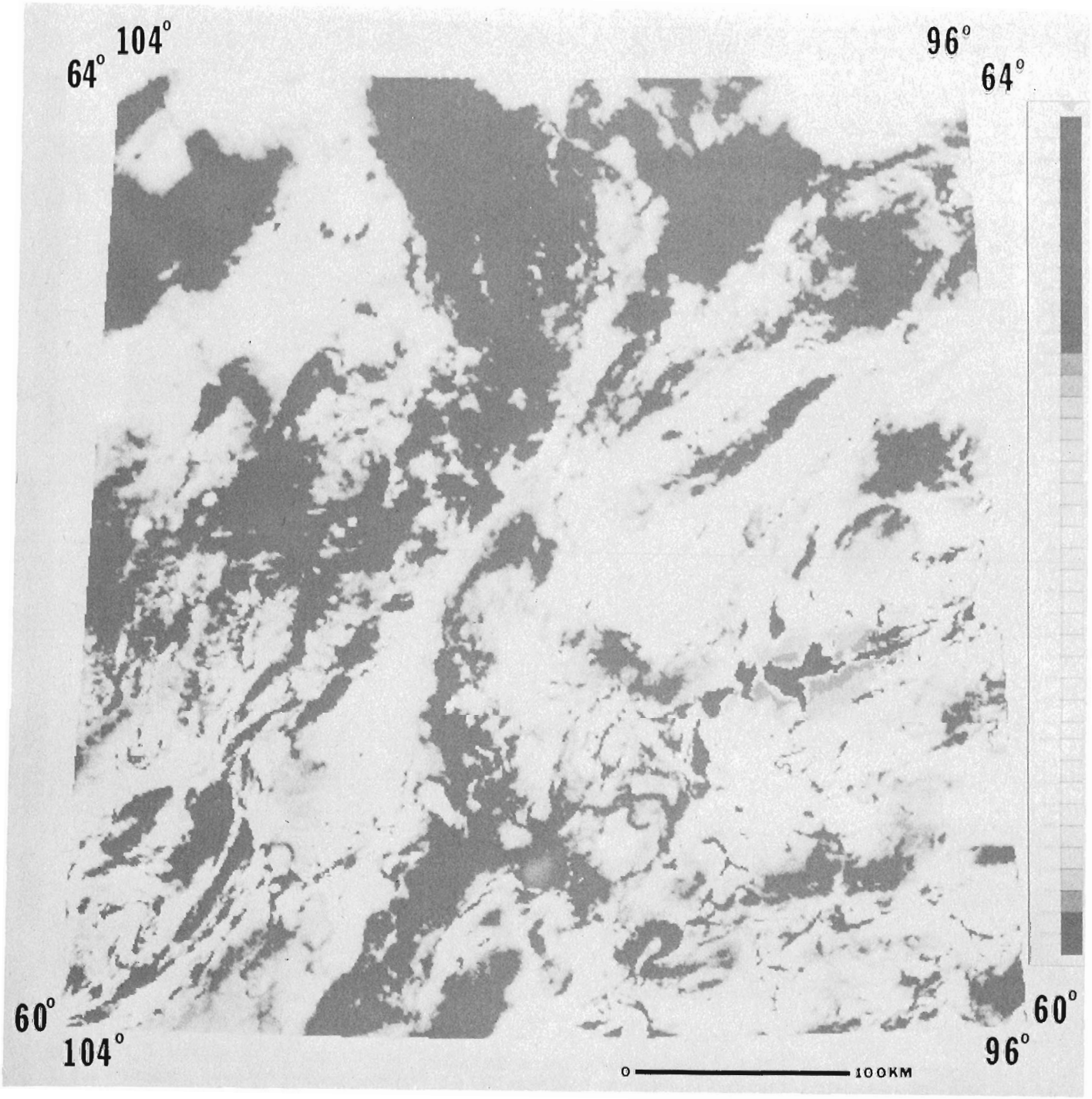

Figure 53.7. Colour separate (magenta) NP 13/14.

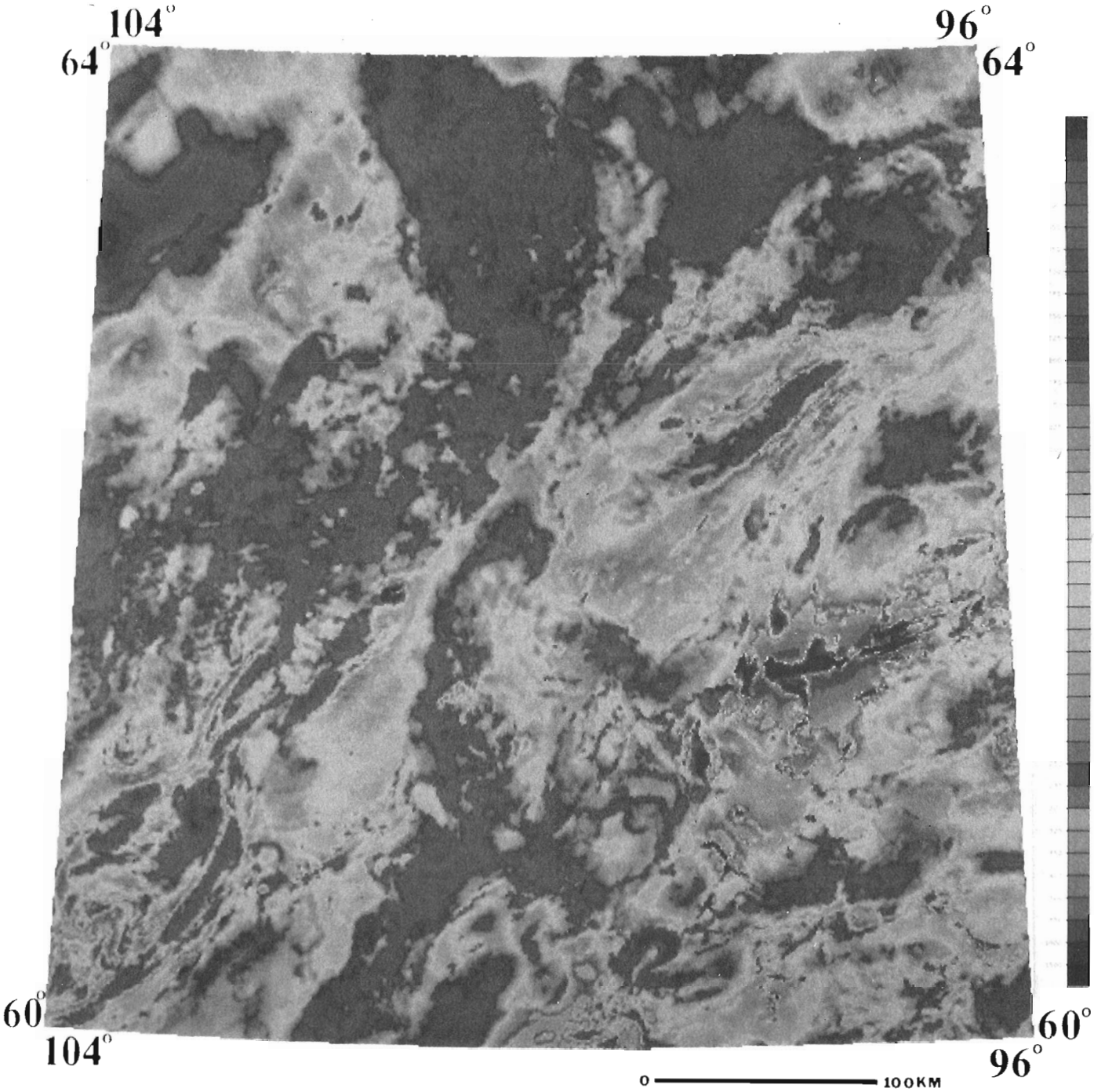

Figure 53.8. Black and white reproduction of one to one million colour aeromagnetic anomaly map for IMW (NP 13/14). Published in colour as GSC Map 1567A – Magnetic Anomaly Map of Dubawnt River, Northwest Territories (scale 1:1 000 000).

will be produced as a byproduct of the program will also be available for computer processing and interpretation at other scales and in conjunction with other data sources.

Acknowledgment

The programs used for subtraction of the IGRF and for co-ordinate conversion were made available by P.H. McGrath.

References

Geological Survey of Canada
1981: Map 1566A, Magnetic Anomaly Map of Lockhart River, Northwest Territories (scale 1:1 000 000).

1981: Map 1567A, Magnetic Anomaly Map of Dubawnt River, Northwest Territories (scale 1:1 000 000).

McGrath, P.H., Hood, P.J., and Darnley, A.G.
1977: Magnetic Anomaly Map of Canada; Geological Survey of Canada, Map 1255A (3rd edition).

RELATIONSHIP OF TEXTURE, COMPOSITION, AND ADSORPTION PROPERTIES TO THE WEATHERING OF MUDROCKS

EMR Research Agreement 13-4-81

R.H. Grice[1], C.S. Kim[1], and G.R. Brown[2]
Terrain Sciences Division

Grice, R.H., Kim, C.S., and Brown, G.R., Relationship of texture, composition, and adsorption properties to the weathering of mudrocks; in Current Research, Part A, Geological Survey of Canada, Paper 82-1A, p. 359-367, 1982.

Abstract

Preliminary observations and analyses of texture, composition, expansion, and adsorption properties, and of weathering behaviour have been made for a small, representative suite of Ordovician mudrocks from the Montreal area. Hand specimens and thin sections indicated interbedded laminae ranging from those of clay-sized to silt-sized grains. Only the fine mudrocks were analyzed: XRF analyses for Si, Al, K, Ti, Fe, Mg, and Ca; XRD analyses for mineralogy; and carbon determinations. The clay mineral content ranged between about 55 and 75%; illite:chlorite ratios and SiO_2:Al_2O_3 ratios were between 3 and 4. Among the variations in other minerals, total calcite content ranged from 0-4%, quartz from 20-30%, and pyrite from 2-10%.

Weathering was assessed qualitatively by the appearance of cracks and of gypsum precipitation during cycles of wetting and drying, and quantitatively by uniaxial strain measurements and by measurements of the amount of water vapour adsorbed. Nitrogen adsorption isotherms have been interpreted to show that the specific accessible areas of the unweathered mudrocks ranged between 6 and 25 $m^2 \cdot g^{-1}$ and that all but one sample are microporous. The exception which appears to be mesoporous is also unusual in that it had the lowest content of Si and the highest of Al, K, Ti, and Fe.

There is a broad interest in a more detailed understanding of the nature, genesis, and weathering of shales and mudstones – principal members of the group of rocks commonly, though not universally, classified as mudrock. Weaver (1980) pointed out that "although the mineralogy of fine-grained sediments is now fairly well understood, there is still relatively little information about their textures". Also, much discussion has centred around the mode of development of fissility (Weaver, 1980, p. 305; Curtis, 1980; Spears, 1980), which is a fundamental characteristic in the evolution and degradation of mudrocks. Olivier (1979a) reported on the influence of mineralogy and moisture redistribution on the weathering behaviour on mudrocks. Lempp (1981) discussed the weatherability of Mesozoic pelitic rocks. The weathering and weakening of mudrocks are of particular interest to engineers in relation to the performance of these rocks as foundation and fill material, in slopes of suspect stability such as in the banks of sections of the St. Lawrence Seaway canals (Olpinski and Christensen, 1981, p. 405), and in the manufacture of bricks and light-weight aggregates. Many classification systems have been evolved by engineers using standard engineering tests; Venter (1980) and Olivier (1979b) are among the most recent innovators, whilst the International Society of Rock Mechanics has an active commission on swelling rocks (Einstein, 1980).

Earlier work (Grice, 1968) suggested that the amount and rate of weathering could be quantified by observing the changes of weight of samples as they are cycled between higher and lower humidity levels. The objectives of the present study, therefore are to define the texture and composition of a limited suite of mudrocks, to determine specific accessible areas of each by nitrogen adsorption, and then to examine the effect of humidity change on water vapour adsorption at normal room temperatures of 20 to 25°C. Samples of different facies of Upper Ordovician mudrock were collected from a shallow section of an active quarry at Laprairie, about 1 km southeast of Montreal and St. Lawrence River, in the general vicinity of some of the shales described by Dean (1962).

A selection of the freshly exposed rock samples were subjected to a single cycle of immersion in water and room drying. This artificial weathering procedure produced several

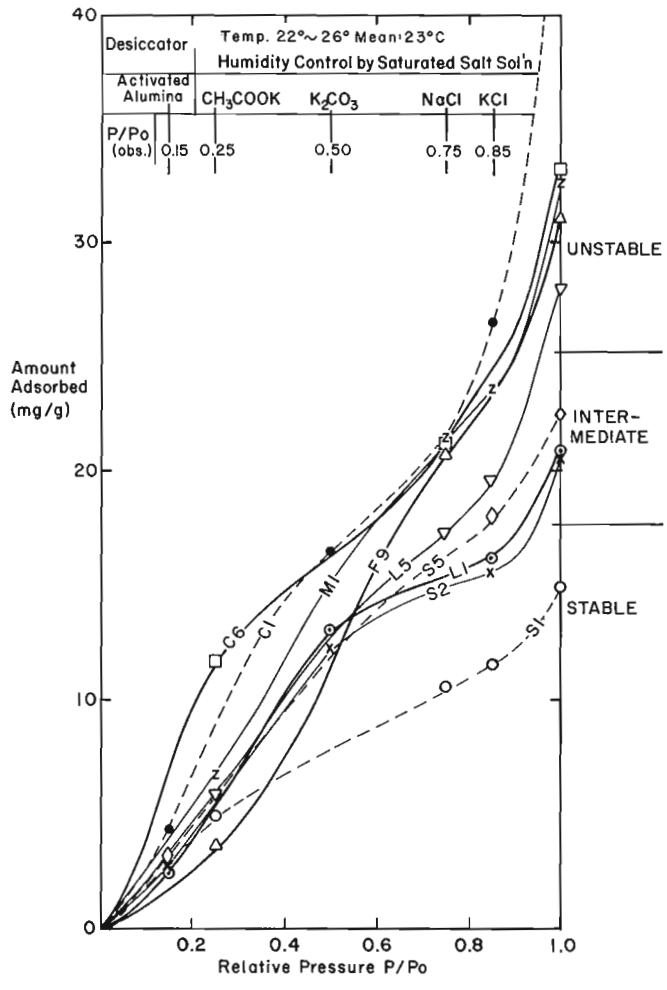

Figure 54.1. *Adsorption isotherms of water vapour on mudrocks (macrosamples, 9-30 g) at room temperature.*

[1] Department of Geological Sciences, McGill University, Montreal, Quebec

[2] Department of Chemistry, McGill University, Montreal, Quebec

Table 54.1

Characteristics of the mudrock facies

	CLAY-RICH MUDROCK	FINE MUDROCK	COARSE MUDROCK	SILT-RICH MUDROCK
	clay shale		mud shale	
Sample No.	C1 - C9	F1 - F9	M1 - M5	S1 - S8
General description	Generally dark grey aphanitic rock	Generally black to dark grey fine grained rock	Generally black coarse mudrocks	Generally grey coarse siltstone
Clay fraction estimated by eye	More than 67% clay size	50-67% clay size	Less than 50% clay size	Less than 20% clay size
Typical lamination	Thin to medium parallel laminae up to 5 mm thick	Thin to medium laminae 2-5 mm thick	Thick laminations commonly greater than 5 mm thick	Laminations and lenses commonly greater than 5 mm thick
HCl Reaction	None	none to slight	slight	moderate to strong
Fracture surface	Smooth flat surface with conchoidal pattern		Hackly and unevenly undulating surface	
Typical observations for examples from each group				
Sample size (cm)	C6-4x3x1	F9-6x3x3	M3-5x4x1.5	S2-4x3x1 (triangular)
After wetting overnight	C6 - very narow bedding joint opening, small fragment fell off edge	F9 - bedding joint and short vertical joint just open	M3 - partially open joint in curved current bedding joint	S2 - less than 1% of sample fell off edges
After drying for 24 hours in room	C6 - bedding joint opened further; disintegration into two major irregular platy fragments; other 20% of sample formed sharp angular fragments from 2x2x0.3 cm to very fine.	F9 - disintegration into four major irregular platy fragments between 4x3x0.3 and 4x0.5x0.3 cm; other 15% of sample mostly sharp fragments smaller than 1x1x0.2 cm	M3 - disintegration into three fragments; less than 2% of sample consists of angular fragments generally less than 1x0.2x0.2 cm	S2 - single continuous bedding joint along microfacies boundary produced platy fragments that detached only when sample was handled.

Note: The L series mudrocks contain closely interbedded laminae of S and C type mudrocks.

degrees of weathering, which were described in terms of the relative proportions of fragments of different sizes (Table 54.1). A more quantitative expression was obtained by subjecting samples to progressively higher levels of humidity and measuring the amounts of water vapour adsorbed.

These adsorption data are summarized in Figure 54.1 and demonstrate a preliminary classification as stable, intermediate, and unstable; this corresponds to degrees of disintegration observed in the samples. The most unstable mudrocks are clay-rich, including such samples as M1 which is predominantly coarse mud but contains thin clay layers. The relative order of stability of the samples differed at various humidity levels. The samples weighed between 9 and 30 g; however, sample size and shape did not appear to be significant, as long as each sample was fairly homogeneous.

Composition of Unaltered Mudrock

The greatly contrasting behaviour of mudrocks sampled from within a few metres of each other confirmed the need for identification of the composition of each subfacies, so thin sections and powder samples were prepared which were representative of the behavioural spectrum. Sample size is a major consideration when dealing with composition as weathering can be expected to occur preferentially in certain zones, and efforts have to be made to separate each component or subfacies from layered and otherwise heterogeneous samples. Indications of the degree of microheterogeneity can be obtained from microprobe studies (Fig. 54.2; Grice, 1975).

The XRD and XRF analyses (Fig. 54.3-54.5) have provided the preliminary ranges of composition and interpretations following procedures of Schultz (1964). The pairs of analyses have been arranged in order of diminishing silica content (Fig. 54.3) regardless of lithologic and stratigraphic sequence. Some parameters have similar or reciprocal trends and others vary erratically. For example, the Fe_2O_3 analyses do not correlate with the amount of pyrite seen in hand specimens and thin sections, therefore sulphur analyses are planned to clarify the situation.

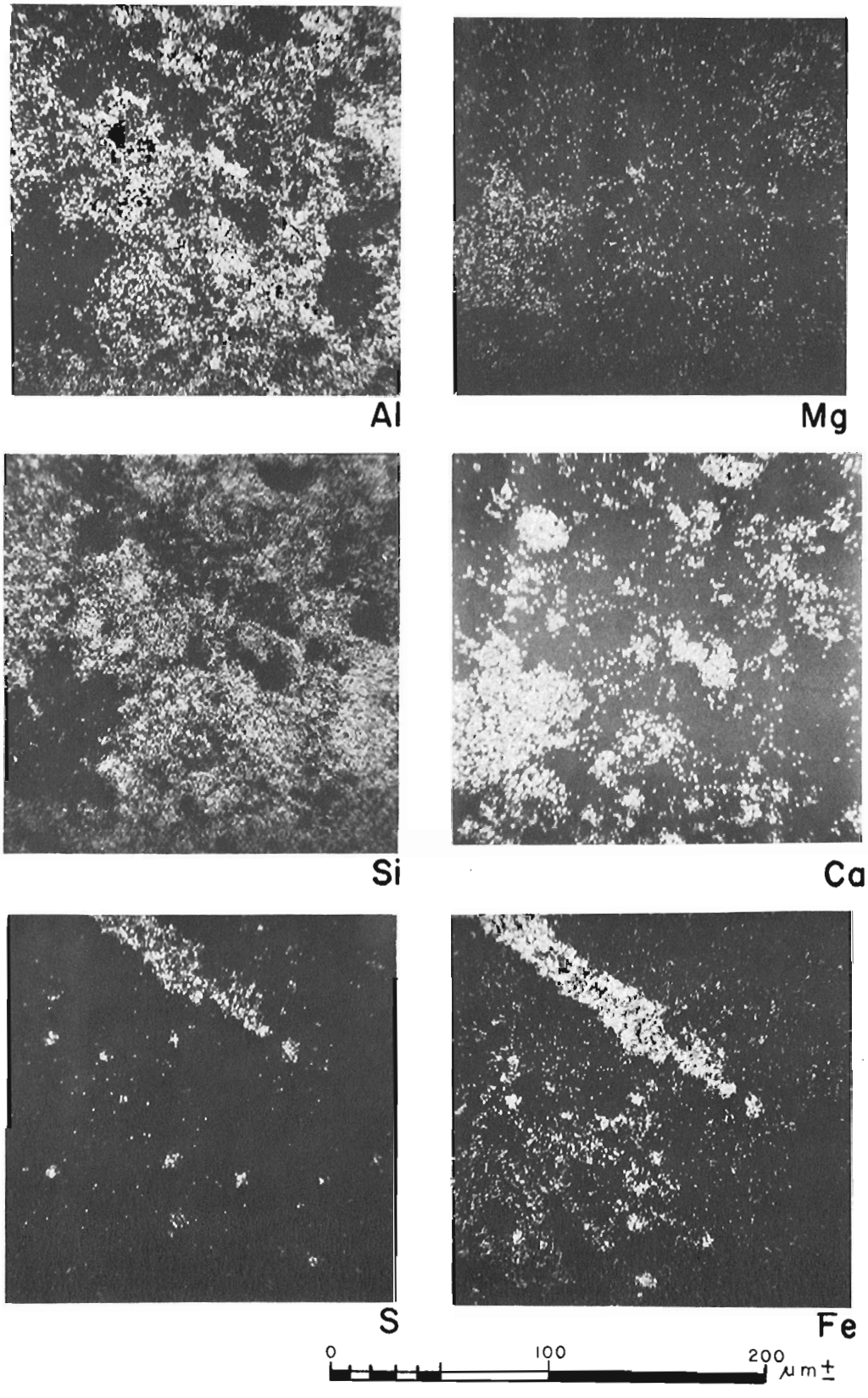

Figure 54.2. *Electron microprobe scan photographs of Al, Mg, Si, Ca, S, and Fe distribution in a mudrock (K distribution was not determined) (from Grice, 1975).*

Textural Analysis

It would be desirable to define mudrock facies by their grain size distributions as well as their compositions. However, many practical problems (Spears, 1980) arise related to recognizing and assessing the significance of diagenetic changes and of degrees of flocculation during sedimentation and to appreciating the effects of the disintegration or disaggregation procedures used preparatory to size analysis. Specific gravity, porosity, and permeability are other relevant parameters, yet their determination by standard methods is likely to provide average values for mixtures of subfacies, each with different weathering characteristics.

Block samples and thin sections have been photographed (e.g. Fig. 54.6, 54.7) and will be examined with the scanning electron microscope.

Crack Development

Figures 54.6 and 54.7 include some details of crack patterns that developed after artificial weathering treatments had been applied. A substantial number of cracks shown in Figure 54.7 are subhorizontal and do not correspond to visible bedding. Some samples were stabilized by impregnation with epoxy resin.

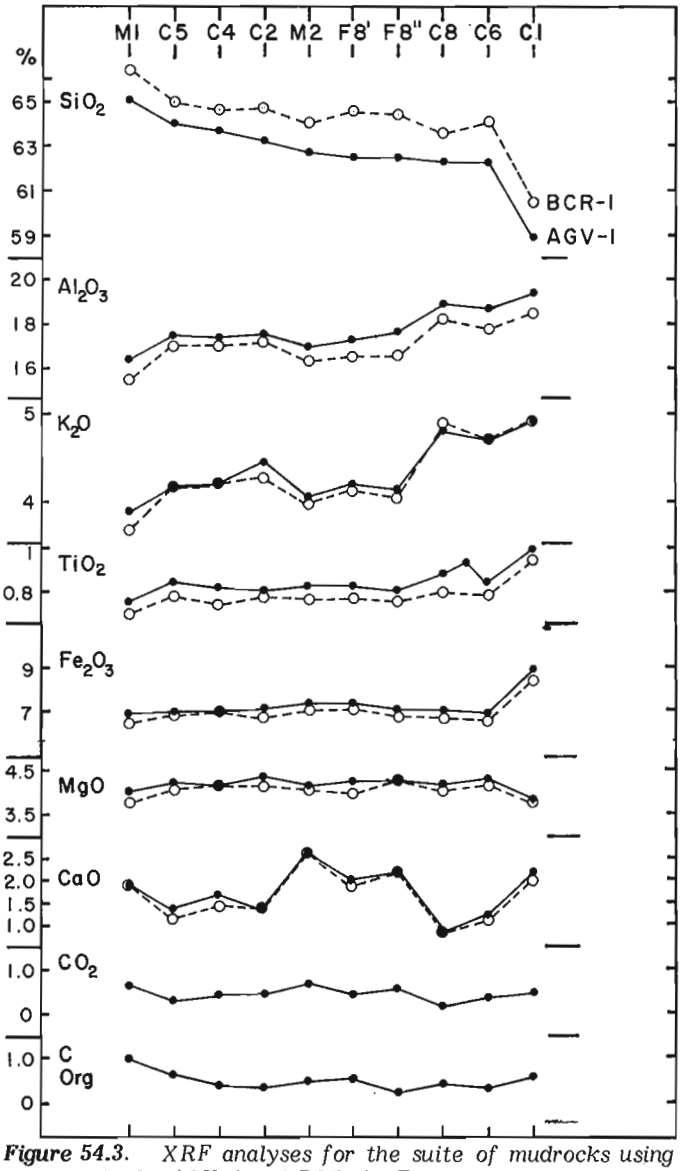

Figure 54.3. XRF analyses for the suite of mudrocks using two standards, AGV-1 and BCR-1. The carbon analyses were by C. Valentin, Institute of Oceanography, McGill University.

Expansion

The amount of expansion of rock samples subjected to an atmosphere saturated with water vapour at room temperature has been monitored with a linear displacement transducer and a continuous recorder. Preliminary expansion data (Fig. 54.8) do not correlate with those for adsorption of water vapour (Fig. 54.1) on 'macrosamples' of similar size (about 50 g); for example, samples M1 and S1 expanded similar amounts, yet the adsorption on M1 as more than 100% greater than on S1.

Accessible Area and Adsorption Isotherms

The degree of weathering is controlled in part by the accessible area comprising the outside surface and the wall surfaces of accessible pores and cracks. Accessible area as well as the general distribution of pore sizes can be determined by the interpretation of adsorption and desorption isotherms obtained with Brunauer, Emmett, and Teller (BET) type gravimetric apparatus such as described by Dollimore et al. (1973). Isotherms of nitrogen and water vapour sorption on a selection of 500 mg samples of mudrocks

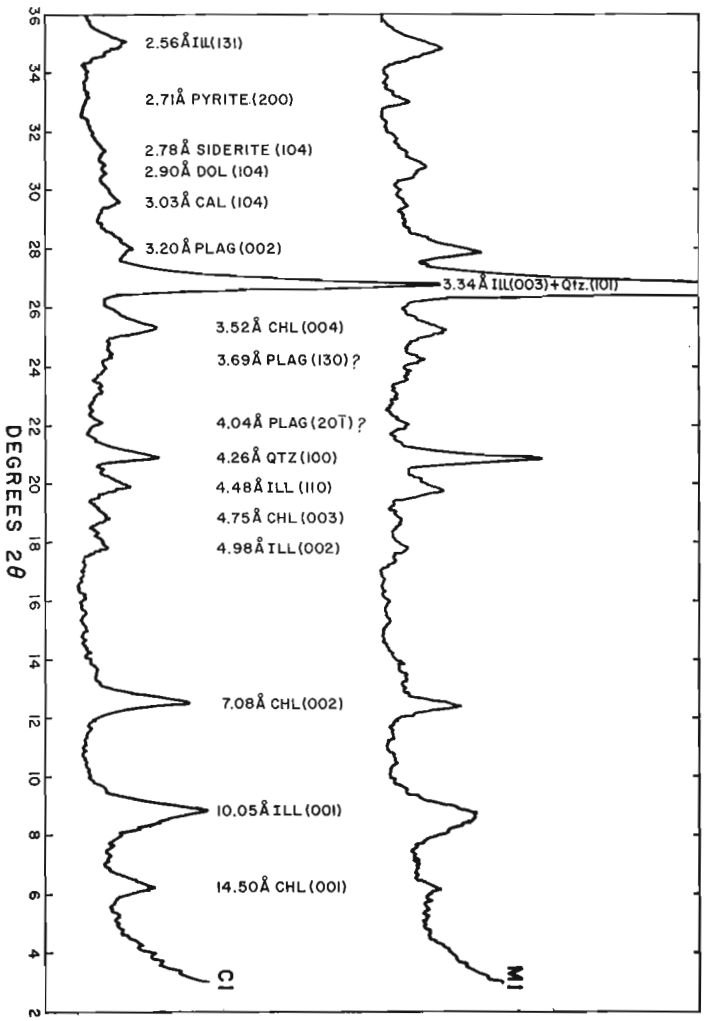

Figure 54.4. X-ray diffractograms for unorientated powder (less than 64 μm (200-mesh) samples, M1 and C1.

are shown in Figures 54.9-54.11. All but one sample have Type I isotherms (Gregg and Sing, 1976) for nitrogen adsorption (Fig. 54.9). These suggest that most samples are microporous, that is, the pores are smaller than 2 nm. The exception, C1, has a sigmoidal isotherm, Type II, indicative of nonporous material, yet if its desorption behaviour with hysteresis (Fig. 54.10) is accepted as valid, then the material of C1 might be mesoporous with its pore sizes between 2 and 50 nm.

A specific accessible area of 10 $m^2 \cdot g^{-1}$ and a BET constant (c) of about 12 were obtained for an Upper Ordovician mudrock also of the Montreal area using volumetric nitrogen adsorption BET methods (Gogo and Grice, 1980). Preliminary interpretation of the new data indicates specific accessible areas of between 6 and 25 $m^2 \cdot g^{-1}$ for different mudrock facies. More readings at low relative pressures are needed to obtain acceptable values of c.

Preliminary adsorption isotherms determined on 500 mg samples in the BET apparatus for water vapour on mudrock have shown some irregularities when the adsorption exceeds about 1% (Fig. 54.11), so that more data collection is required. Nevertheless it does appear that above critical humidities there are rapid increases in the rate of adsorption indicative of the capillary condensation and saturation of pores of various size ranges.

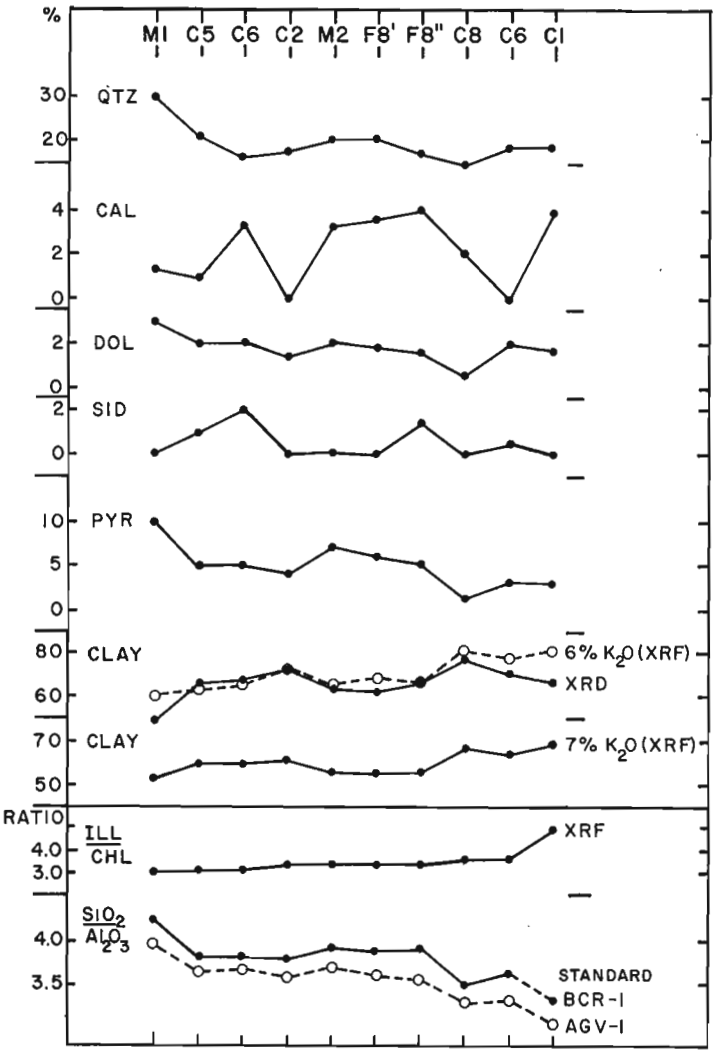

Figure 54.5. XRD and XRF preliminary quantitative interpretation of mineral percentages and of illite-chlorite and silica-alumina ratios.

Experimental Methods

The advantages of the gravimetric BET apparatus include: 1) the use of small samples of about 0.5 g whose composition and texture are more likely to be homogeneous than those of larger samples; 2) the weight changes of samples during adsorption and desorption can be monitored continuously, and 3) humidity levels can be adjusted flexibly from very low values up to near saturation.

Condensation occurs inside the BET apparatus near saturation, that is, when the relative pressure – vapour pressure (p)/saturated vapour pressure (p_0) – is near unity. This problem should be overcome by use of a suction plate apparatus (Penner, 1963; Packard, 1967). Data from this method will complete the upper or saturation end of the isotherms.

Pore Fluids

The pore fluids in the weathering zone are local groundwaters modified considerably by rain water recharge and dissolution of partially weathered minerals on one hand, and by the evaporation of pore water and crystallization of saturated mineral phases on the other. Crystalline precipitation of gypsum (Fig. 54.12) has been observed when saturated rock is air-dried. Pore fluid analyses will be made as well as examinations by the scanning electron microscope of precipitate-coated surfaces.

Summary and Conclusions

1. The general textural and compositional characteristics have been determined for a small suite of Ordovician mudrocks. Textures ranged from clay- to silt-sized with individual laminae thickness of between less than 1 mm and 1 cm. Compositional analyses were made (Fig. 54.3-54.5) only for the fine rocks, including Si, Al, K, Ti, Fe, Mg, and Ca by XRF, mineralogical analysis by XRD, and carbon determinations. Clay mineral content ranged between 55 and 75%; illite:chlorite ratios and SiO_2:Al_2O_3 ratios generally were between 3 and 4. Calcite content was between 0 and 4%, quartz between 20 and 30%, and pyrite between 2 and 10%. (The coarse rocks have not yet been analyzed and XRF analyses for sulphur are planned.)
2. Single-cycle immersion and drying tests of the rock suite have demonstrated different weathering characteristics: considerable disintegration for the clay-rich and coarse mudrocks containing clay-rich laminae and slight disintegration for the siltstones (Table 54.1). More observations, including those of uniaxial expansion and of gypsum precipitation, are required to test correlations.
3. Nitrogen isotherms (Fig. 54.9, 54.10) have been interpreted to show that the specific accessible areas of unweathered mudrocks ranged between 6 and 25 $m^2 \cdot g^{-1}$ and all, but one, are microporous. The exception which appears to be mesoporous is also unusual in that it had the lowest content of Si and the highest of Al, K, Ti, and Fe.
4. The few preliminary data on water vapour adsorption isotherms (Fig. 54.1, 54.11) have general correlation with data from the simple immersion and drying tests, but more detailed work at high humidities is required.
5. The broad range of the nature and behaviour of the suite of mudrocks has now been determined, setting the stage for analyses by SEM and microprobe, for observations of the weathering effects of multiple cycles of humidity changes in the BET apparatus, and for correlation with standard engineering tests.

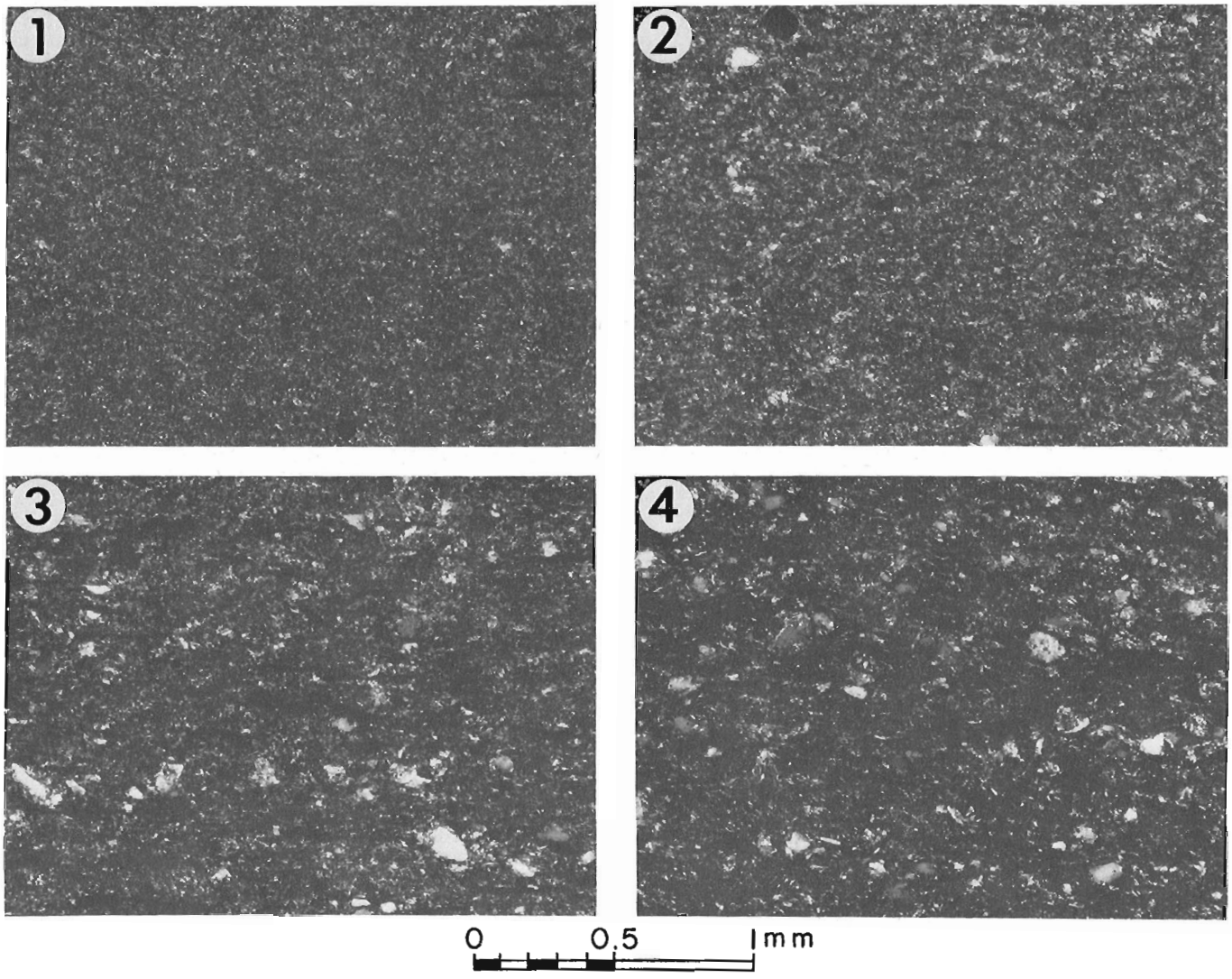
1
2
3
4
0
0.5
1 mm

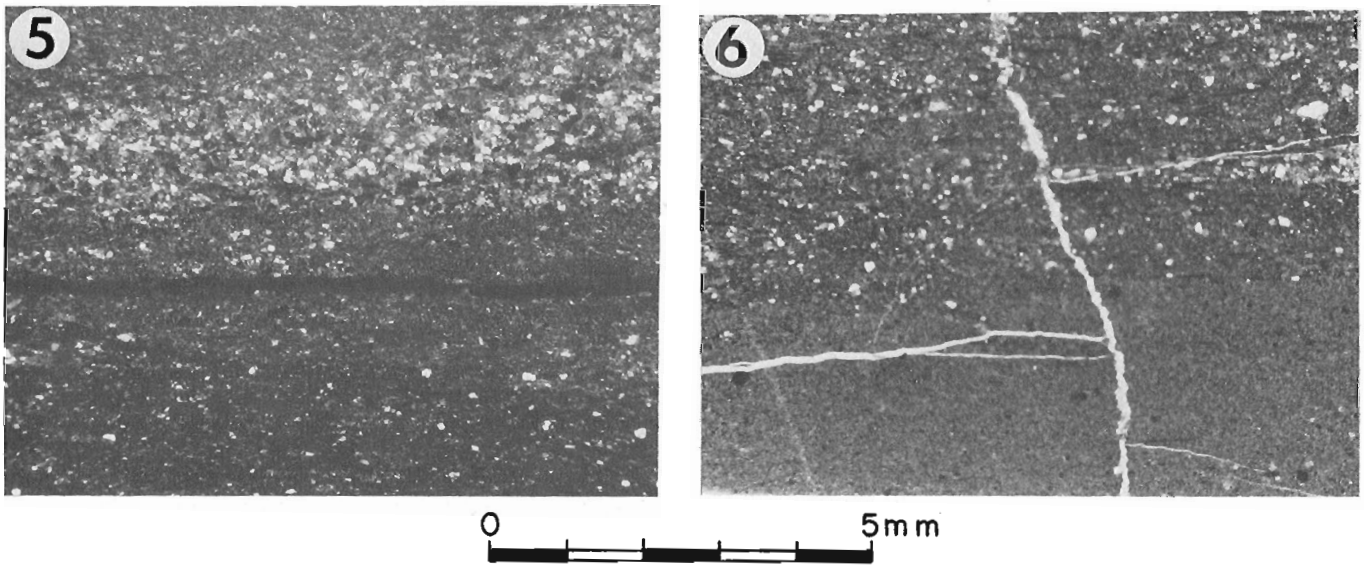
5
6
0
5 mm

Figure 54.6 *(opposite). Photomicrographs of selected samples of mudrocks (crossed nicols):*

1. *Sample C1, typical homogeneous clay shale, abundant pyrite.*
2. *Sample C6, clay shale coarser than C1, silt grains of quartz, carbonate, pyrite; organic streaks parallel to bedding.*
3. *Sample F2, fine grained mudrock, particle size up to 0.15 mm. Organic material, silt grains of quartz and carbonates are oriented parallel to bedding.*
4. *Sample M6, coarse mudrock with quartz and carbonate grains.*
5. *Sample C9, laminated clay shale and mud shale with silt lens in clay shale, bedding joint in clay shale.*
6. *Sample C9, bedding joint terminated at crack passing through clay shale and fine mud shale (polarizer only).*

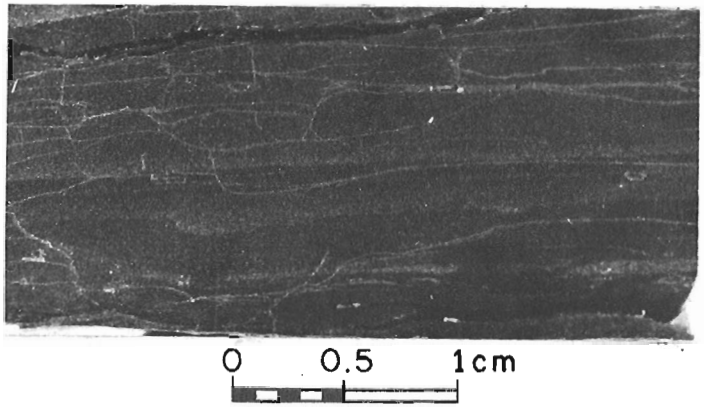

Figure 54.7. *Crack development in mudrock (sample M1).*

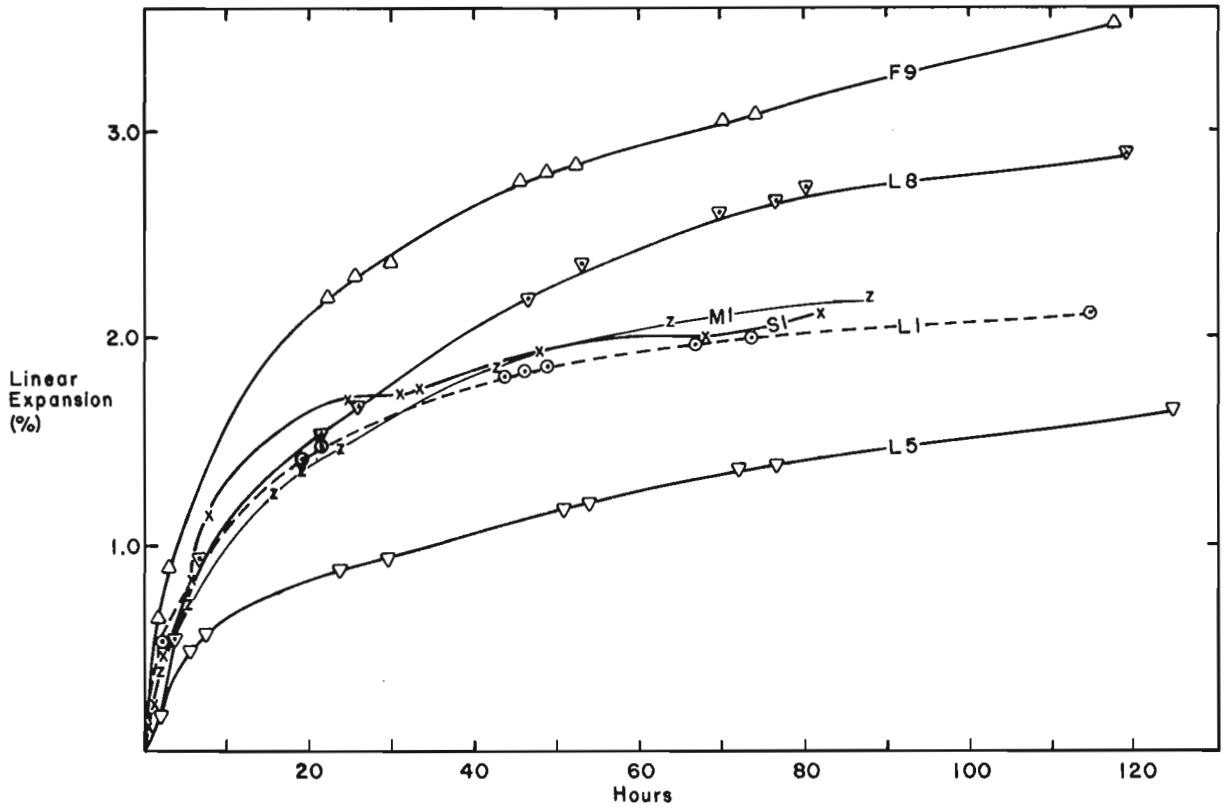

Figure 54.8. *Linear expansion of dry mudrock samples when placed in saturated water vapour at room temperature.*

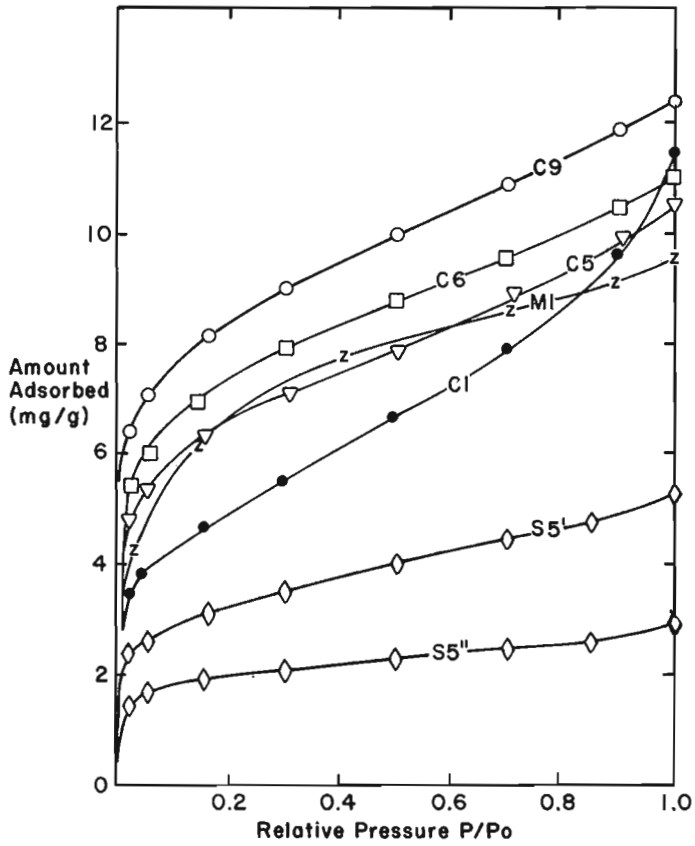

Figure 54.9. *Adsorption isotherms of nitrogen on mudrocks (microsamples of about 500 mg) at 77°K using a gravimetric BET apparatus.*

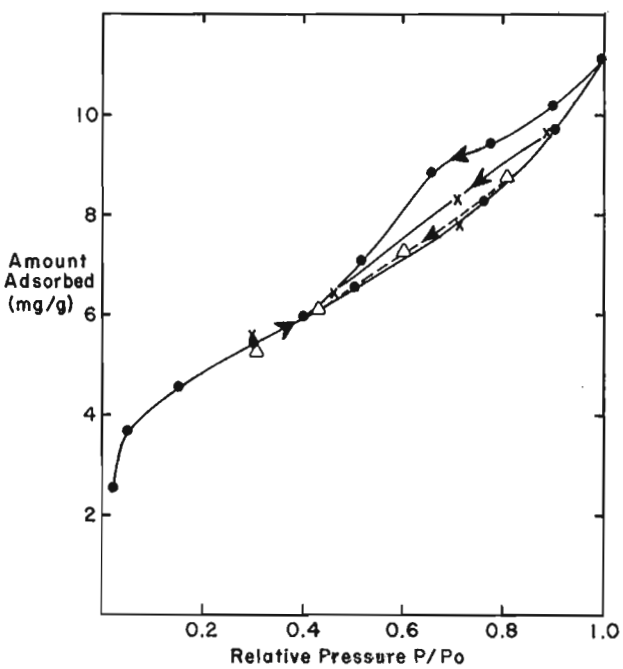

Figure 54.10. *Hysteresis scans for nitrogen adsorption and desorption on mudrock sample C1 at 77°K using a gravimetric BET apparatus.*
1st scan to p/po = 1.0;
2nd scan to p/po = 0.9; and
3rd scan to p/po = 0.8.

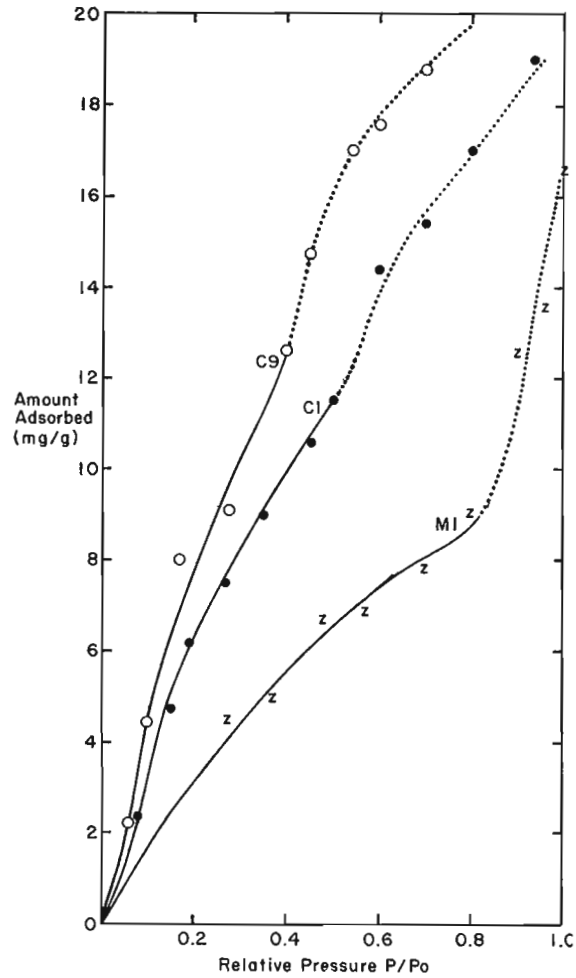

Figure 54.11. *Adsorption isotherms of water vapour on mudrocks (microsamples of about 500 mg) at room temperature using a gravimetric BET apparatus. Portions of curves shown as dotted line need corroboration.*

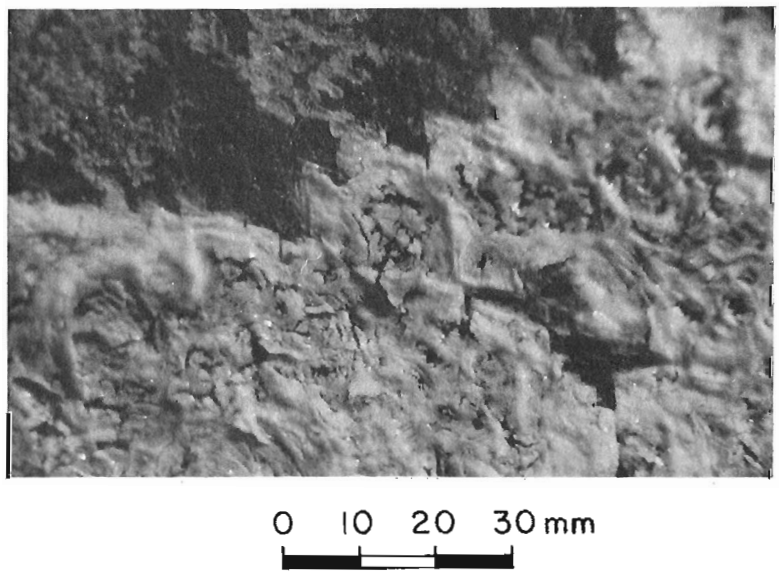

Figure 54.12. *Gypsum precipitation on mudrock (sample F6) exposed overnight to air at room temperature after immersion in water.*

References

Curtis, C.D.
1980: Diagenetic alteration in black shales; Journal of the Geological Society of London, v. 137, p. 189-194.

Dean, R.S.
1962: A study of St. Lawrence lowland shales; unpublished Ph.D. thesis, McGill University, Montreal.

Dollimore, D., Horridge, T.A., and Robinson, R.
1973: A comparison of the water vapor adsorption properties on some related siliceous minerals; in Vacuum Microbalance Techniques; Heydon & Son, London, v. 2, p. 43-59.

Einstein, H.H. (Chairman)
1980: International Society for Rock Mechanics, Commission on Swelling Rock, Work statement and submissions of the North-South American group; Department of Civil Engineering, Massachusetts Institute of Technology, Cambridge, Massachusetts, unpublished.

Gogo, J.O. and Grice, R.H.
1980: Measurement of the specific surface on a problem material: an evaluation test on Utica shale; Proceedings, 7th Regional Conference for Africa on Soil Mechanics and Foundation Engineering, A.A. Balkema, Rotterdam, p. 215-222.

Gregg, S.J. and Sing, K.S.N.
1976: The adsorption of gases on porous solids; in Surface & Colloid Science, ed. E. Maijevic; Wiley, New York, v. 9, p. 231-359.

Grice, R.H.
1968: The effect of temperature-humidity on the disintegration of non-expandable shales; Association of Engineering Geology, Bulletin, v. 5, no. 2, p. 69-77.

1975: Test procedures for the determination of susceptibility of shale to weathering; Engineering Geology, Note 75-14, McGill University, unpublished.

Lempp, Ch.
1981: Weatherability of over consolidated pelitic rocks of the Keuper and Jurassic in Southwestern Germany; Bulletin of the International Association of Engineering Geology, no. 23, p. 101-108.

Olivier, H.J.
1979a: Some aspects of the influence of mineralogy and moisture redistribution on the weathering behaviour on mudrocks; 4th Congress, International Society on Rock Mechanics, Montreux, v. 3, p. 467-474.

1979b: A new engineering geological rock durability classification; in Engineering Geology; Elsevier, London, v. 14, p. 255-279.

Olpinski, K. and Christensen, C.J.
1981: Slope protection along St. Lawrence Seaway canals; Canadian Geotechnical Journal, v. 18, p. 402-419.

Packard, R.O.
1967: Moisture stress in unfired ceramic clay bodies; Journal of the American Ceramic Society, v. 5, no. 5, p. 223-229.

Penner, E.
1963: Suction and its use as a measure of moisture contents and potentials in porous materials; International Symposium on Humidity and Moisture, (ed. P.N. Winn, Jr., Reinhold, New York, p. 245-252.

Schultz, L.G.
1964: Quantitative interpretation on mineralogical composition from X-ray and chemical data for the Pierre shale; United States Geological Survey, Professional Paper 391-C, p. C1-C31.

Spears, D.A.
1980: Towards a classification of shales; Journal of the Geological Society of London, v. 137, p. 125-129.

Venter, J.P.
1980: The engineering properties and road building characteristics of mudrocks with special reference of South Africa; unpublished D.Sc. dissertation, University of Pretoria, Pretoria.

Weaver, C.E.
1980: Fine grained rocks: shales or physilites; in Sedimentary Geology; Elsevier, Amsterdam, v. 27, p. 301-313.

55. GLACIOTECTONIC THRUST PLATES, BYLOT ISLAND, DISTRICT OF FRANKLIN

Project 780018

R.A. Klassen
Terrain Sciences Division

Klassen, R.A., Glaciotectonic thrust plates, Bylot Island, District of Franklin; in Current Research, Part A, Geological Survey of Canada, Paper 82-1A, p. 369-373, 1982.

Abstract

Imbricate glaciotectonic thrust plates composed of outwash sediment were seen on Bylot Island in front of large glaciers. These plates were formed in front of ice during glacier advance and were thrust intact without internal deformation. Outermost plates have not been ice-covered. Sediments were probably frozen at the time of thrusting. A glaciotectonic thrust plate in front of glacier C79 has a maximum radiocarbon age of 120 ± 80 years.

Introduction

Terminal moraines including imbricate glaciotectonic thrust plates composed of outwash sediments were seen near the termini of several large glaciers on Bylot Island (Fig. 55.1). These thrust plates are considered to have been formed by faulting and thrusting of sediments in front of glaciers in response to shear stresses developed either beneath or in front of an advancing glacier. General descriptions of this type of feature are outlined by Embleton and King (1975, p. 446-47) and by Sugden and John (1976, p. 252); in both summaries, however, detailed descriptions of mechanisms of formation are lacking.

Because of good stratigraphic exposure and morphologic definition seen at one site on Bylot Island, a general description of glaciotectonic thrust plates is offered here, along with an inventory of other known occurrences on the island. Observations were made during a study of the Quaternary stratigraphy and glacial history of Bylot Island by the author.

Description of Benches and Related Features

Most observations were made in front of glacier C79*, southwestern Bylot Island (Fig. 55.1), where a large terminal moraine complex extends several kilometres across the valley floor and connects with lateral moraines at the valleysides (Fig. 55.2). Distal to it, the valley is broad and flat, floored by outwash sediments, and crossed by numerous braided stream channels. Thick (2-3 m) deposits of interbedded sand and organic matter occupy much of the valley, particularly at its sides.

The present glacier terminus lies about 1.5 km from the outermost margin of the moraine complex. Comparison of the modern ice margin position with that indicated by 1959 air photographs indicates glacial retreat of about 0.6 km since then. The modern ice surface profile also appears not as steep as that shown by the earlier photographs. Therefore, the outer margin of glacier C79 is retreating.

In front of glacier C79, extending either to or nearly to the outermost edge of the moraine complex, surficial sediment is chiefly till, composed of sand and muddy sand with numerous boulders (Fig. 55.2). The till is derived almost entirely from the crystalline mountainous area where the glaciers originate. It appears of recent origin; clasts within it are angular, little weathered, and without lichen colonization. The till cover extends outwards, ending in a single ridge which is topographically highest within the moraine complex; the ridge crest lies about 30-35 m above the distal outwash plain and 5 m or more above the surrounding glacial deposits. From aircraft, ice was seen beneath till between the till-covered outer ridge and the present ice margin.

Distal to the till-covered ridge, at the outermost edge of the moraine complex, several tilted benches composed of sorted bedded sediments occur (Fig. 55.2, 55.4). These benches are interpreted as glaciotectonic thrust plates. Their outer extent is well defined, and they rise abruptly above the outwash plain. The tops of the benches dip upvalley at low angles (about 2-10°); outer margins dip downvalley at steep angles (about 30°, estimated angle of repose). Up to four separate benches were seen, one stacked on top of another. The thickness of each varies between 5 and 10 m.

Benches consist chiefly of coarse gravel and sandy gravel; bedding within them is defined by 10-30 cm-thick beds of fine sand and pebbly sand. These beds are internally laminated to thin bedded; coarser beds are brightly stained by iron oxides; and organic detritus, including twigs, is common within them. Attitude of the beds within individual benches, where seen, is about parallel with the upper bench surface, dipping towards the glacier margin (Fig. 55.3). Texture and lithology of the benches are similar to those of outwash deposits of the valley floor, but are markedly dissimilar to those of till on their proximal side. A large proportion of the clasts was derived from either Proterozoic or Tertiary rocks, the bedrock units under the valley floor.

At one location, several ridges of outwash sand and gravel 2-4 m high, with segments about 100 m in length, occur distal to the benches (Fig. 55.2, 55.5). Each ridge is nearly symmetrical about a central fissure at its crest. They outline a zig-zag pattern in front of the benches (Fig. 55.2) and appear to be part of a more extensive patterned ground system marked by frost cracks. The ridges decrease in overall height with distance from the bench margin and were not evident beyond about 100-300 m from them.

Elsewhere on Bylot Island tilted benches of sorted coarse sediment are known at glacier margins (Fig. 55.1) but, except for those seen near Tay Bay, are not nearly so well developed. In these other locations, they are seen most commonly close to the fronts of large glaciers, in places directly overlain by modern ice. At all sites, no moraine deposits were seen distal to them and glaciers are considered at, or very near, recent maximum positions.

Age of Features

Twigs from the uppermost bed within the bench closest to the till, and partly covered by it, were determined to be 120 ± 80 ^{14}C years old (GSC-3227) (age corrected for ^{13}C). The date is the maximum age of the most recent advance of glacier C79 on Bylot Island.

*Glacier Atlas of Canada, 1969 Inland Waters Branch, Bylot Island Area 46201

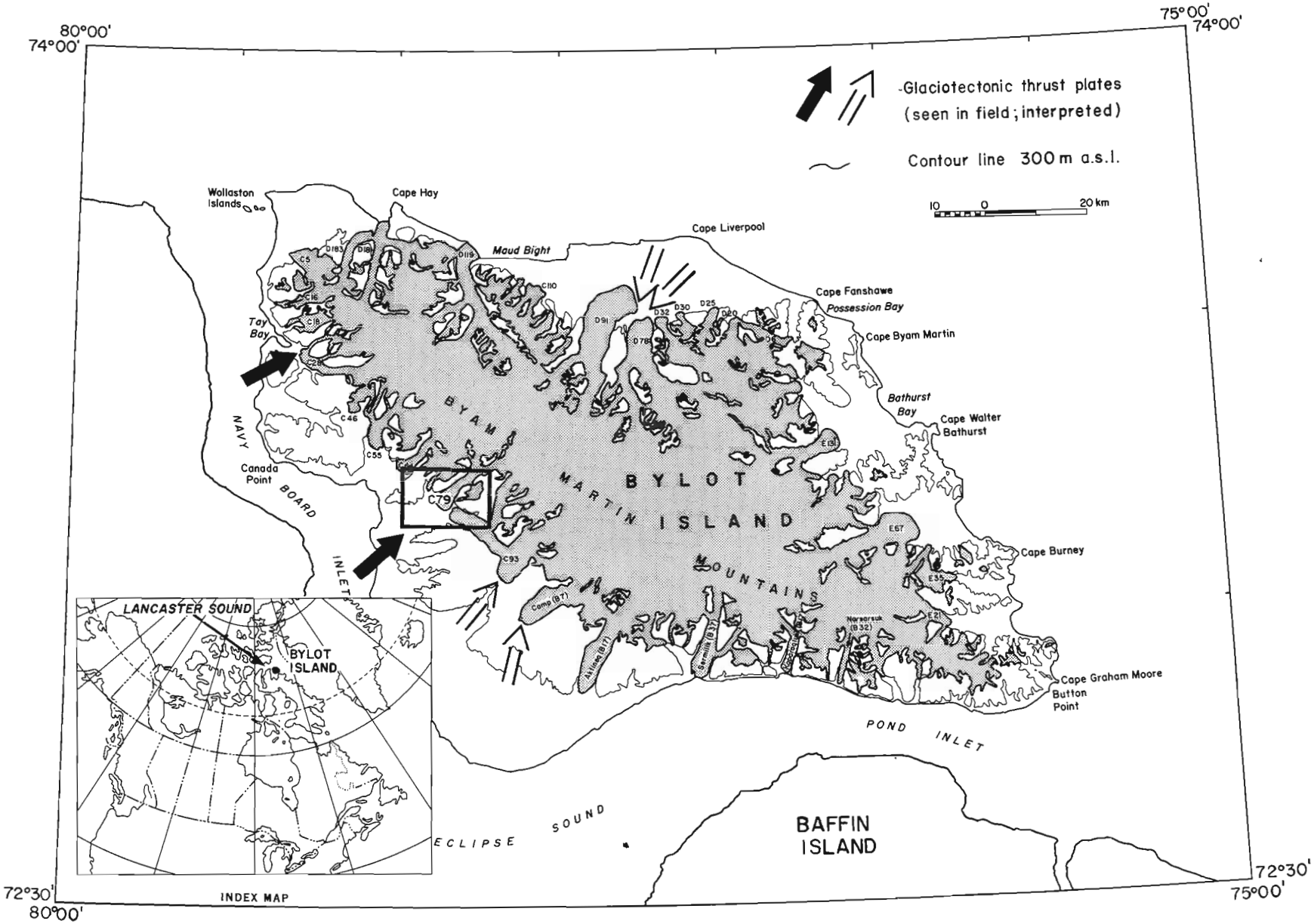

Figure 55.1. Map of Bylot Island, District of Franklin, showing the main site of features described in this report (outlined) and locations of features of inferred similar origin.

Figure 55.2. *Terminal moraine complex in front of glacier C79, Bylot Island. Till occurs up to an outer single ridge (dark arrow); distal to the ridge, deformed plates of outwash sediments form tilted benches (white arrow) interpreted as imbricate glaciotectonic thrust plates. The outer till-covered ridge is cored by outwash sediment. Distal to the thrust plates, fissured ridges occur in a zig-zag pattern that appears to be part of a more extensive patterned ground system. GSC 203639-I*

Figure 55.3. *Organic-bearing beds (indicated by dashed lines) within tilted benches. Three separate benches are evident, a fourth is known to lie beneath the till-covered ridge. The beds could not be traced beneath overlying benches because of slump. GSC 203639-J*

Figure 55.4. *Near view showing relation between outer ridge which is capped by till and tilted benches of outwash sediments. Absence of boulders on the bench surfaces distal to the till-covered ridge is evident and indicates that they formed beyond the glacier front. GSC 203099-P*

Figure 55.5. *Fissured ridges seen in front of tilted benches (cf. Fig. 55.2, 55.4). These ridges, developed in outwash sediments, appear to have formed along frost cracks that are part of a more extensive patterned ground system in front of the moraine complex. GSC 203802*

Origin of Features

The tilted benches of sorted bedded sediments could not have formed as marine or glacial lake deposits in a proglacial setting as drainage in front of glacier C79 could not have been ponded by ice farther downvalley, and marine submergence is not likely by virtue of their elevation (70-80 m a.s.l.) and very young age. The sediments that make up the benches are derived from the valley floor outwash deposits based on close similarity of lithology and texture compared between them. The setting and morphology of the benches suggest that they are glaciotectonic plates, raised above the outwash plain along low-angle thrust faults by glacier movement. Low angle of thrust is suggested by the relatively low upvalley dip of beds within plates and of upper plate surfaces. Separate plates appear to have been thrust downvalley and stacked in an imbricate manner; proximal ones lie on top of more distal ones. These plates appear to have been thrust intact – likely frozen and rigid – because no deformation of internal organic-bearing beds is known, and because separate beds within each bench appear to remain nearly parallel both in stratigraphic section and to the upper bench surface. On that basis, stratigraphy of the original outwash deposit is repeated in each thrust plate. If that interpretation is correct, there is likely more than one buried organic-bearing bed within the original outwash deposit, as up to two separate such beds are known within a single plate.

The outermost thrust plates are not covered by glacial debris and they are consequently considered not ever to have been covered by glacier ice. They formed, then, in front of the glacier margin during advance to a recent maximum. Some plates, however, are known to be till covered, and these must have been overridden by ice either during or subsequent to their formation. The extent of these till-covered plates is not known, but they appear from surface morphology restricted to beneath the outermost till-covered ridge and could form much of that ridge.

The low, fissured ridges that occur in front of the benches also seem related to glacier-induced stresses and may represent an initial stage of bench formation. They could have formed along a pre-existing frost-crack system. Suggestive of this is similarity of ridge outlines to large-scale polygonal patterned ground features seen within the valley floor deposits distal to them. If that is the case, frost-crack polygons may be one control on the size of individual benches and, possibly, their distribution. Modern stream activity has, however, obscured much of the overall frost-crack outline, and its origins are difficult to establish.

The glaciotectonic thrust plates on Bylot Island, as described above, are similar to those occurring in front of Thompson Glacier, Axel Heiberg Island (Robitaille and Greffard, 1962; Kalin, 1971). By airphoto interpretation, Kalin (1971, p. 49) indicated the occurrence of glaciotectonic thrust plates (which he called push moraines) to be widespread on Axel Heiberg and Ellesmere islands. These plates are shown here to occur on Bylot Island and, by inference, may occur generally throughout the eastern arctic region in areas of modern mountain glaciation. In addition, nearly all those inventoried on Axel Heiberg and Ellesmere islands occur within outwash deposits (Kalin, 1971, p. 50), similar to those seen on Bylot Island. This association suggests that coarse grained sorted sediment could represent a medium favourable to the development of glaciotectonic thrust plates.

Acknowledgments

Comments and observations made by Dr. J.L. Tison, University of Brussels, and Dr. W.H. Johnson, University of Illinois, during visits to these deposits are acknowledged to have contributed to this report. Comments on a first draft of this by Dr. R.N.W. DiLabio have proven helpful.

This work forms part of a Quaternary geologic study of the Bylot Island region. Field logistic support was given by Polar Continental Shelf Project (Mr. G. Hobson, Director); that contribution was invaluable.

References

Embleton, C. and King, C.A.M.
1975: Glacial and Periglacial Geomorphology; Edward Arnold (Publishers Ltd.), Great Britain, second edition, Volume 1, 573 p.

Kalin, M.
1971: The active push moraine of the Thompson Glacier; Axel Heiberg Island Research Report, Glaciology No. 4, McGill University, Montreal, 68 p.

Robitaille, B. and Greffard, C.
1962: Notes sur les matéreaux terminaux du Glacier Thompson, Canada Arctique; Geographical Bulletin, No. 17, p. 85-94.

Sugden, D.E. and John, B.S.
1976: Glaciers and Landscape; John Wiley and Sons, New York, 376 p.

SUBBOTTOM PROFILING OF LAKES OF THE CANADIAN SHIELD

Project 800027

R.A. Klassen and W.W. Shilts
Terrain Sciences Division

Klassen R.A. and Shilts, W.W., Subbottom profiling of lakes of the Canadian Shield; in Current Research, Part A, Geological Survey of Canada, Paper 82-1A, p. 375-384, 1982.

Abstract

Subbottom profiling using a portable 3.5 kHz – 200 kHz acoustic profiler has been carried out on 11 lakes in eastern Ontario and Quebec and 2 lakes in the 'Turkey lakes calibrated watershed' north of Sault Ste. Marie. The profiles show significant filling of some lakes with more than 25 m of late-glacial sediment and deformation of sediments by collapse over buried, melting glacier ice. Depressions in, and much of the floor of, most lake basins are covered by an acoustically (3.5 kHz) transparent gyttja-like modern lake sediment up to 5 m thick. Acoustically opaque layers near the base of this sediment in several lakes are interpreted to represent zones of accumulation of gas of unknown origin and composition.

Introduction

A survey of the glacial and postglacial sediment fill in major lake basins of the southeastern part of the Grenville structural province of Ontario and Quebec was begun in June 1981 (Fig. 56.1). Two lakes were also surveyed in the 'Turkey lakes calibrated drainage basin', studied as part of Department of Environment's acid rain program. Although the work completed during the field season was aimed primarily at testing equipment and developing operating procedures, several excellent and illustrative profiles were obtained.

Profiling of selected lake basins was carried out using a Raytheon RTT-1000A-1 'Portable Survey System' with a dual, low-frequency (3.5 and 7.0 kHz) transducer coupled with a high-frequency (200 kHz) transducer. This system was attached to a utility shelf (Shilts et al., 1976) mounted on a 4.5 m **Zodiac** inflatable boat powered by a 15 h.p. outboard motor. The power source for the acoustical signal and transceiver-chart recorder was a standard, heavy-duty, 12-volt automobile battery. Navigation was by 'dead reckoning' between headlands at constant speed of about 4 km/h. Because straightline traverses were difficult to obtain due to the shallow draft of the boat and the drag of the submerged transducer, intersecting traverses were made where possible to cross check profile locations by comparing similar bottom features and configurations. With this system in the 3.5 kHz mode, penetration was achieved through most types of unconsolidated sediment to bedrock. In some lakes more than 25 m of sediment was shown on the acoustical record.

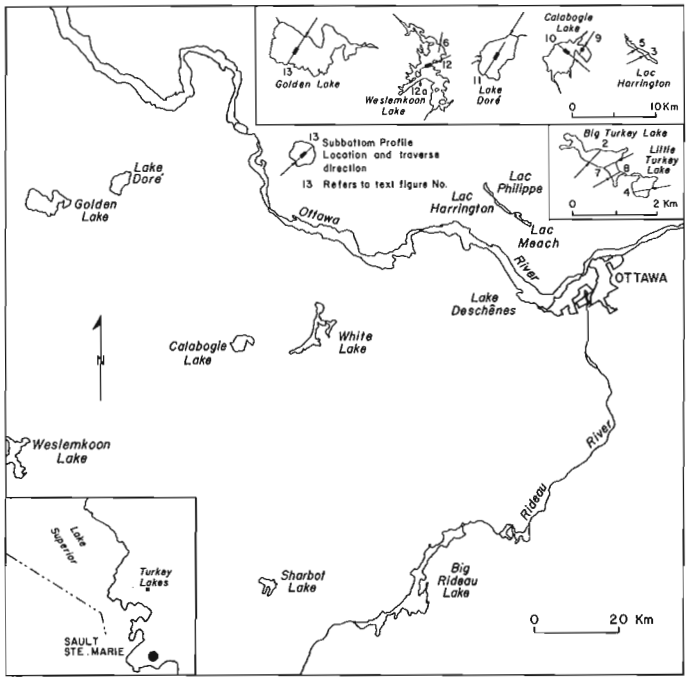

Figure 56.1. *Locations of lakes surveyed. Numbers refer to figure numbers; heavy bars on the profiles refer to that portion of the profile depicted in Figures 56.2-56.13.*

Objectives

The objectives of this survey are threefold:

1. Because there are few deep, natural or man-made exposures of glacial and related sediments on this part of the Canadian Shield, it is thought that subbottom profiling of lakes can yield sections showing sediment facies and stratigraphic relationships that are impossible to observe on land without expensive drilling or seismic studies. Compared to the continuous profiles that can be derived from lakes, land-based studies generally provide a discontinuous record based on stratigraphic data from only one or several points.
2. Because many of the lakes lie in depressions that reflect structural discontinuities, it is thought that if any neotectonic (post- or late-glacial) displacements have occurred, they would most likely be seen along these old zones of weakness. Neotectonic faults have been observed to displace glacial sediments and striated surfaces in Finland (Kujansuu, 1964), and any such bedrock displacement in a lake basin would be relatively easy to detect by noting disruption of sediment structures or bedding. Although continuous subbottom acoustical records are useful in detecting such disruption of unconsolidated sediments, caution must be exercised in deciding first whether the deformation is real and not a seismic artifact, and secondly if it was caused by bedrock movements or by glaciotectonic processes. If neotectonic faulting is detected, it might be dated roughly, if the sedimentation history of the lake is known. This should be of interest to those investigating Precambrian terrane for disposal of radioactive waste because the magnitude and frequency of neotectonic displacement would have important implications in evaluation of the potential for disruption of a radioactive waste repository.

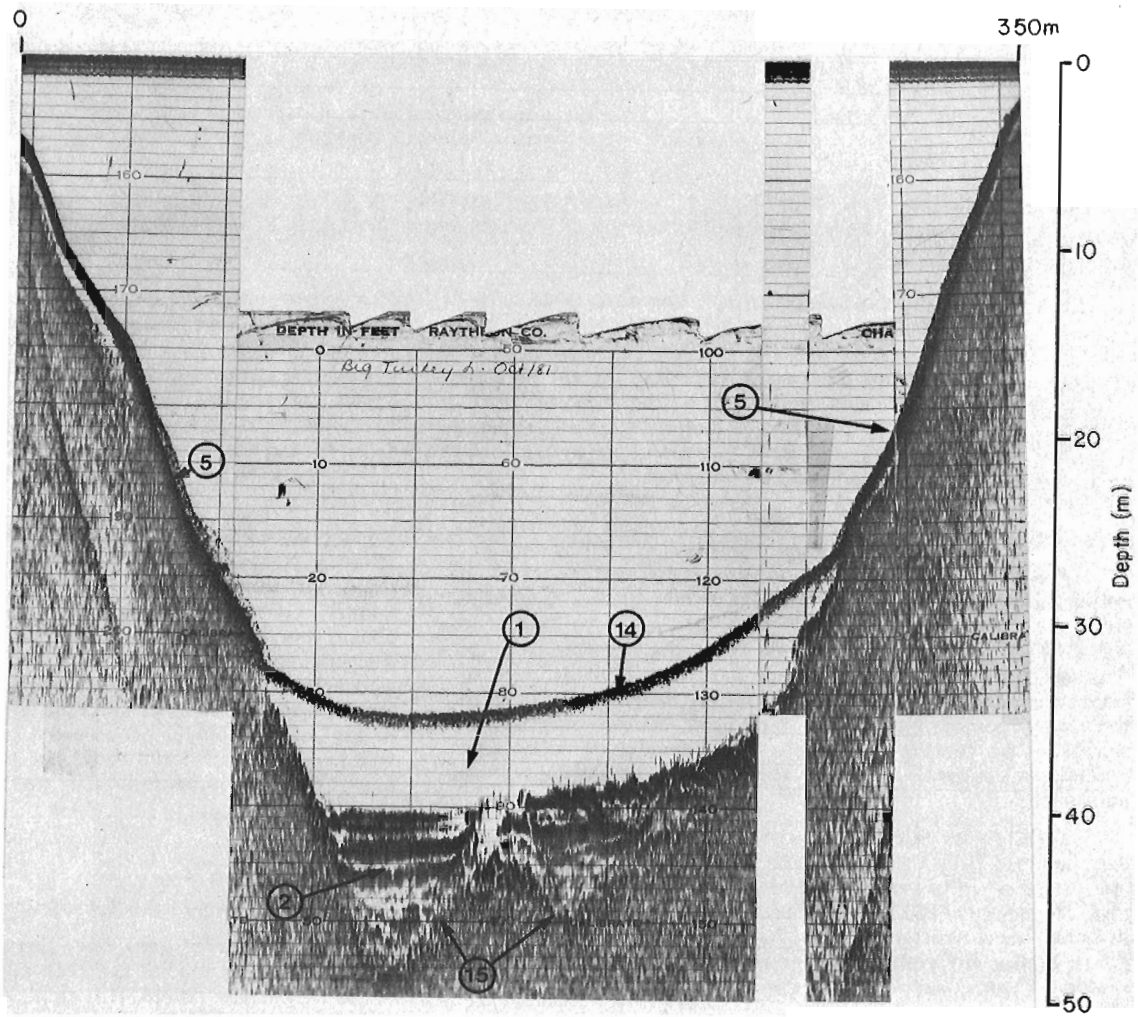

Figure 56.2

Profile across Big Turkey Lake; note clastic glacio-lacustrine(?) fill in bedrock depressions and lack of modern organic lake sediment on steep sides. This lake is one of five in the 'Turkey lakes calibrated drainage basin' which the Department of Environment and associated agencies are studying intensively to quantify the potential effects of acid rain.

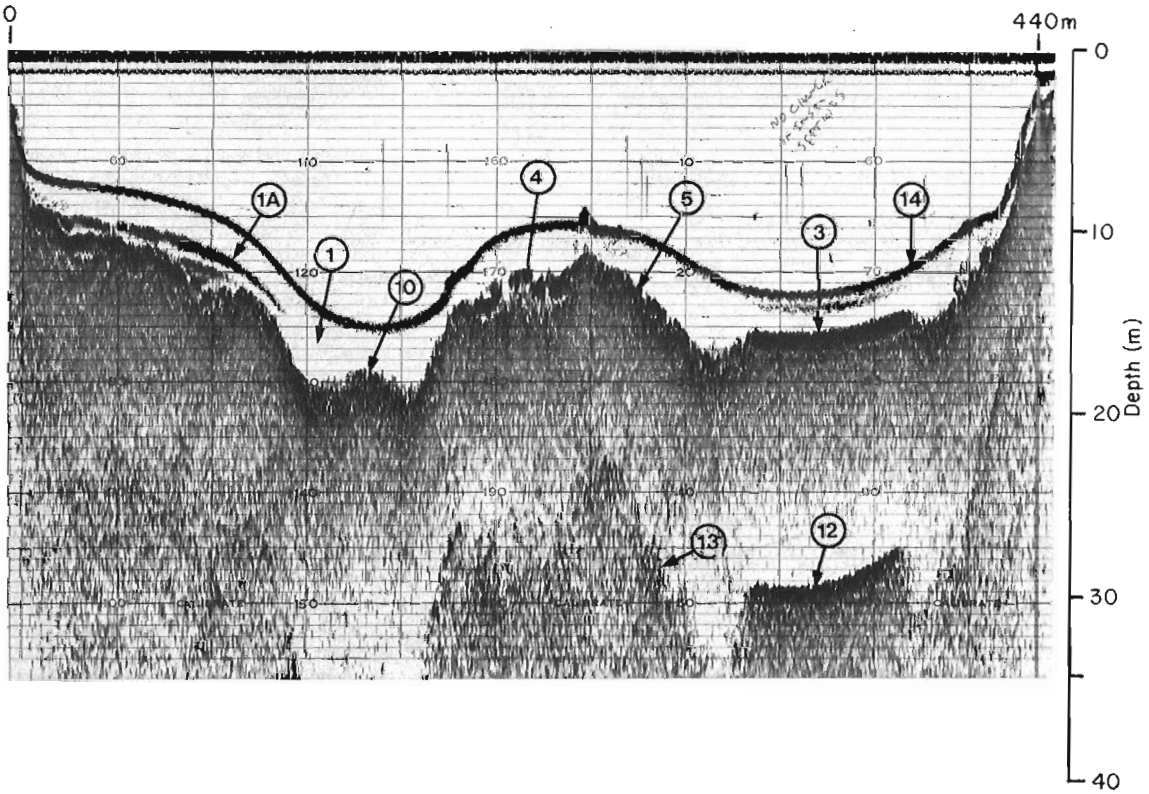

Figure 56.3

Profile across Lac Harrington (Lac Mousseau) in Gatineau Park. Note clastic sediment layer in gyttja. This section illustrates three types of opaque bottom and subbottom reflections: from left to right – 'gas layer'; bedrock surface with typical first multiple; hard sandy or gravelly bottom with typically strong first multiple (raised aspect is presently unexplained).

Table 1

Legend to geological interpretation of acoustical records

This legend has been adopted to simplify comparison of some of the features shown on acoustical profiles reproduced in this paper (Fig. 56.2-56.13). The interpretations are preliminary and have not been confirmed by drilling or sampling. The basis for these interpretations is offered in the text.

1	Lake gel or gyttja; watery, organic modern (postglacial) lake sediment.
1A	Clastic sediment layer in modern, organic sediment.
2	Laminated clastic sediment; proglacial lake sediment or marine sediment.
3	Sand and/or gravel; outwash or other fluvial sediment.
4	Till.
5	Bedrock.
6	Folds; due to collapse over glacier ice blocks.
7	Faults; due to collapse over glacier ice blocks.
8	Zone of attenuation or sediment disruption caused by collapse of part of the sediment pile over melting ice.
9	Anticlinal structures thought to be formed by postdepositional ejection of gas or liquid.
10	Opaque zone in modern lake sediment, thought to be enriched in gas bubbles.
11	Weeds.
12	Multiple (false) reflections of sand-gravel surface.
13	Multiple (false) reflections of bedrock or till surface.
14	200 kHz trace of 'soft bottom', displaced slightly (about 1.5 m) above true position of bottom relative to 3.5 kHz reflections.
15	Till or bedrock surface; approximates shape of basin prior to late glacial sedimentation.
16	Extraneous noise due to rough water.

3. Because the amount and type of sedimentary fill varies widely from lake basin to lake basin, the nature of the sediment-water interface as well as the configuration of flow and chemical modification of groundwater entering the lake and its inflow streams will also vary. The potential for chemical alteration of groundwater entering the lake basin through reactions with soft-sediment aquifers is of paramount importance in studies of the effects of acid rain on drainage systems. Of equal importance for judging how a lake will respond to proton loading is knowledge of the character of the sediment-water interface.

Materials Interpreted from Acoustical Records

Several characteristic acoustical features of the lakes surveyed in 1981 are listed in Table 56.1. These features are interpreted in this paper in light of two principal corroborating lines of investigation: the first is our extensive experience with a 7 kHz system on lakes in the District of Keewatin, the records of which were interpreted by comparing long (>2 m) cores taken by divers, by bottom sampling, and by extensive direct observations of the lake bottoms by diving (Shilts et al., 1976). The second basis for interpretation is our knowledge of properties and distributions of the surficial sediments of the regions surveyed in 1981 as well as knowledge of the Quaternary history of the regions. Most of the structures and sediments interpreted in the acoustical records are visible in pits and other natural or man-made exposures on land. We feel sufficiently confident in our ability to interpret these records that we present a preliminary discussion of many of the most common features of them. From selected profiles, some of the more important features have been identified by means of a numbering system keyed to Table 56.1.

Lake Gel

A gelatinous, organic, water-saturated sediment (gyttja) comprises the bulk of the modern (postglacial) sediment in all lakes profiled. This sediment is by no means ubiquitous, however, and is 0 to 5 m or more thick. Over significant areas of the bottom of many lakes, water is in direct contact with either bedrock or what we tentatively interpret as clastic, inorganic sediment, such as till, glaciofluvial, or glaciolacustrine deposits. Modern organic sediment is particularly rare on slopes (Fig. 56.2). Where glaciolacustrine or marine sediments have filled in irregularities on the glaciated surface, the fill of modern lake sediments may form a relatively thin blanket. Where significant relief remained on the glaciated surface, modern lake sediments have been concentrated in depressions, resulting in pockets of thick (5 m or more) organic sediment fill interspersed with bare bedrock or clastic glacial or glaciolacustrine sediments. Because of the radical differences in composition among the various types of materials that may occur at the sediment-water interface, the influence of sediment type on chemical reactions at the interface may vary significantly from lake to lake and throughout a single lake basin.

Except where it contains a significant proportion of mineral sediment, lake gel is transparent to the 3.5 kHz signal, but its surface forms a prominent reflector for the 200 kHz signal. On the actual profiles, the space between the 200 kHz 'soft bottom' (surface of organic sediment) reflection and the 3.5 kHz 'hard bottom' reflection (surface of clastic sediment) represents the cover of modern, organic lake sediment or lake gel (Fig. 56.2). On these profiles the low frequency reflection has been displaced about 1.5 m downwards from its true position relative to the high frequency reflection due to an internal instrumental offset. The contact between gyttja and underlying clastic sediment is well known in eastern Canada as it commonly marks the base of cores collected for palynological studies. In our experience, the depth of this contact is commonly in the 4 to 5 m range, similar to the thickness of the acoustically transparent zone on these profiles.

In several sections through lake gel, horizontal, partially to completely opaque reflecting surfaces have been observed above the base of the gel. In some cases these layers produce strong multiple reflections (Fig. 56.3) and appear to be composed of sand or gravel (see below). As yet we have no clear explanation of why these seem to be raised as pads within the gel. In other cases (Fig. 56.4) opaque layers produce a more diffuse signal and appear to be similar to a zone that has been noted by R. Gilbert (personal communication, 1981) near the base of modern sediment in lakes of the Kingston, Ontario area. He has interpreted this layer, which was also opaque to his 200 kHz equipment, as a layer of gas bubbles localized near, but not at, the base of the modern sediment. The presence of a gas layer would explain the apparent configuration of the diffuse opaque layer, but leaves intriguing questions both about composition and genesis of the gas and about the cause of its localization near the base of the lake gel blanket.

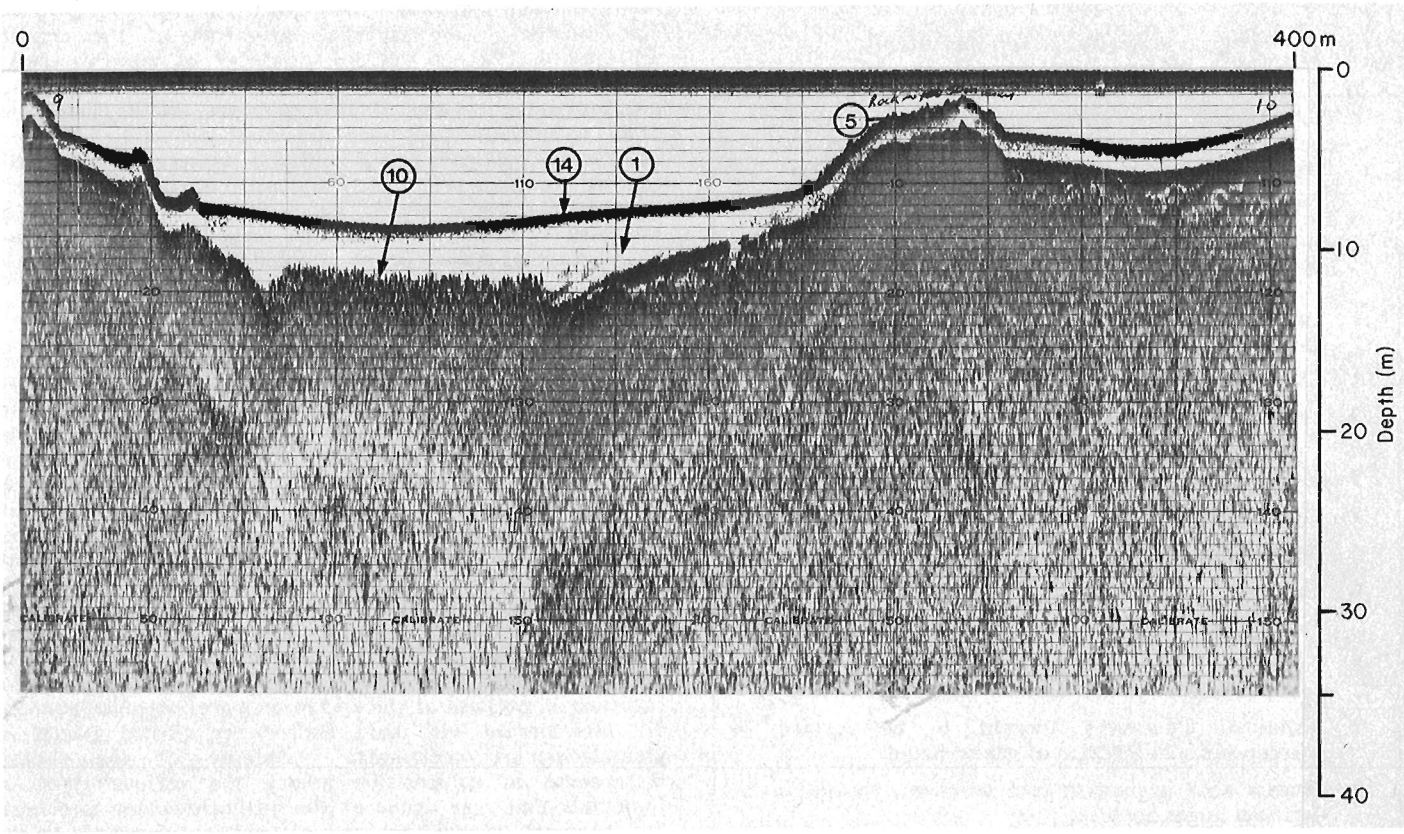

Figure 56.4. *Profile across Little Turkey Lake showing typical occurrence of 'gas layer' and variable thickness of modern sediment (lake gel).*

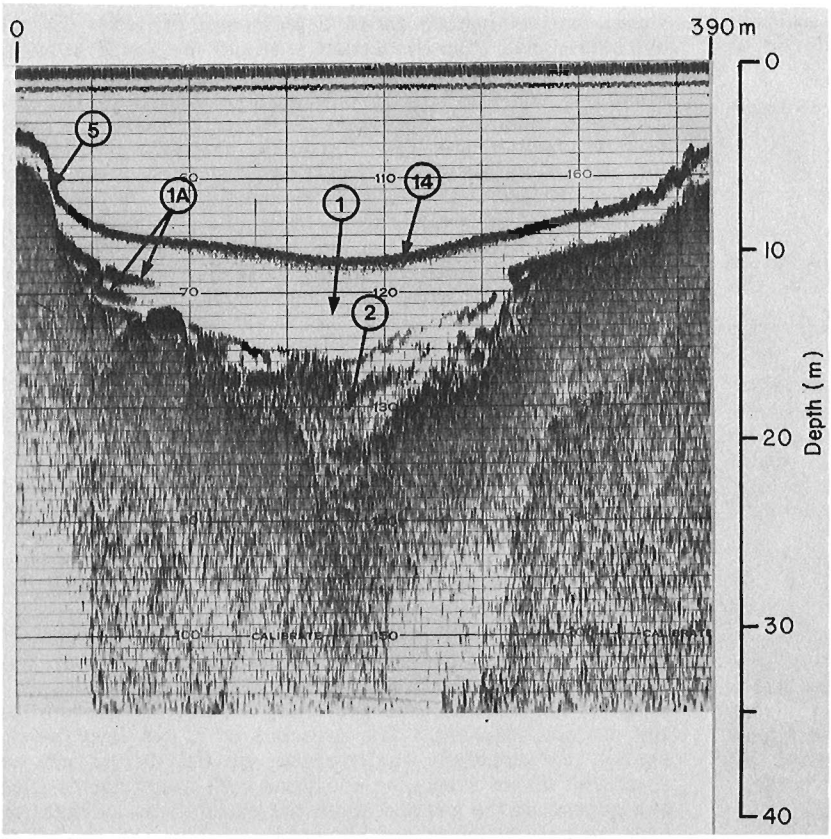

Figure 56.5

Profile across Lac Harrington showing clastic sediment layers in gyttja extending lakeward from the nearshore area.

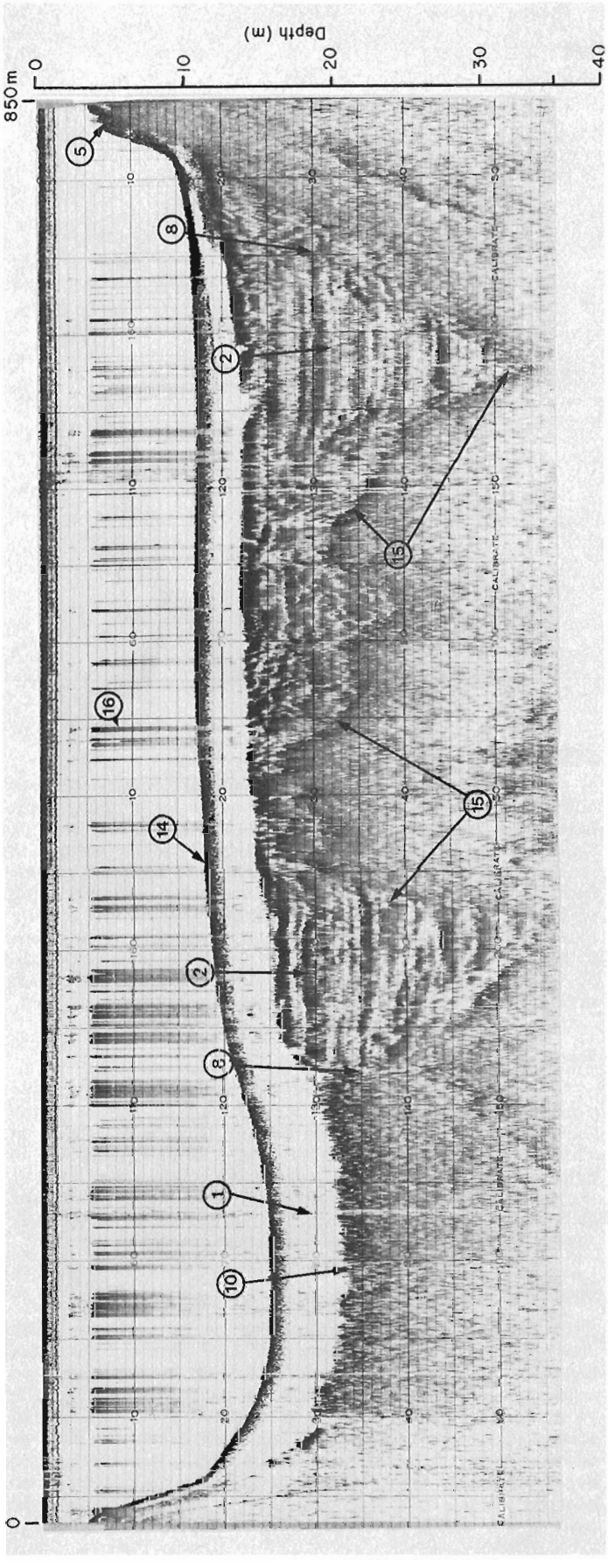

Figure 56.6. *Profile in Weslemkoon Lake showing irregular bedrock bottom filled in by laminated glaciolacustrine(?) sediments. This lake lies entirely within a granite pluton.*

In some lakes, laminations partially opaque to the 3.5 kHz signal were noted within the gel sequence (Fig. 56.5). Because these often extend and fade out lakeward from the shore or mid-lake shoal areas, they are thought to represent thin layers of terrigenous sediment washed offshore from nearshore or shallow areas during exceptional storms, lake ice scouring events, etc.

Laminated Clastic Sediment

In many of the lakes studied, the acoustical record suggests that bedrock or till is covered by thick pockets or blankets of laminated sediment which we interpret to be of either glaciolacustrine or marine origin, depending on altitude of the basin. In most cases, this sediment has effected significant levelling of the till or bedrock surface by filling in depressions (Fig. 56.6). That these sediments were largely deposited in proglacial lakes that were the precursors of the modern lakes is confirmed by the glaciotectonic deformation observed in them. The deformation is thought to have occurred where rapid proglacial sedimentation buried stranded blocks of glacier ice.

The origin of the large-scale laminated structure evident in the profiles through these sediments is not presently known. Where varved or laminated glaciolacustrine sediments were observed on land around some of the basins profiled, the spacing of laminae is much less than the rather coarse 50 cm and greater spacing recorded on the subbottom records. In areas of marine deposition, laminae are rare to absent in the marine silty clay. It is possible that the reflectors in the laminated sequences are thin sand layers deposited during random sedimentation events separated by periods of time greater than the regular, short periodicity represented by varves. Such layers are common in cores through acoustically similar sediment in District of Keewatin.

Till

Till is more difficult to identify on the profiles than are the waterlaid sediments. It is generally interpreted to be present where the acoustical record shows a massive or mottled-appearing unit (Fig. 56.7) between overlying laminated sediments and an underlying opaque reflector, such as bedrock. The relief on the hard lower reflectors (bedrock) is generally jagged in this Precambrian terrane, whereas till surfaces are less so. Small-scale relief, representing boulders, in places can be noted at the contact between till and water or overlying sediments. The mottled appearance of some units, interpreted as till, is thought to be caused by the interference of boulders, sand lenses, or other discontinuities with the 3.5 kHz acoustical signal.

Sand and Gravel

Thick beds of sand and gravel are generally opaque to acoustical signals, and reflect energy so vigorously that the signals commonly bounce back and forth between the bottom and the water surface, creating multiple false reflections (Figs. 56.3, 56.8). Such 'echoing' may form a striking repetitive pattern on records made in shallow water. Some other opaque units, such as the 'gas bubbles' described above, do not generate strong secondary reflections, but seem, rather, to absorb most of the acoustic energy.

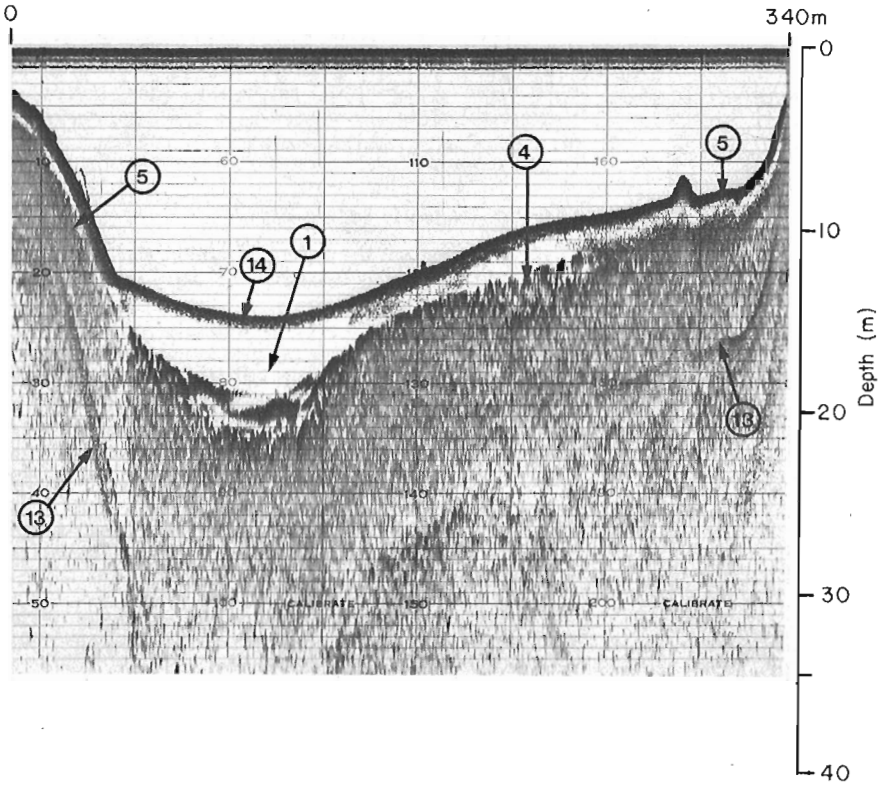

Figure 56.7

Profile across Big Turkey Lake showing pocket of sediment thought to be till. Till on shore is particularly compact, sandy, and stony.

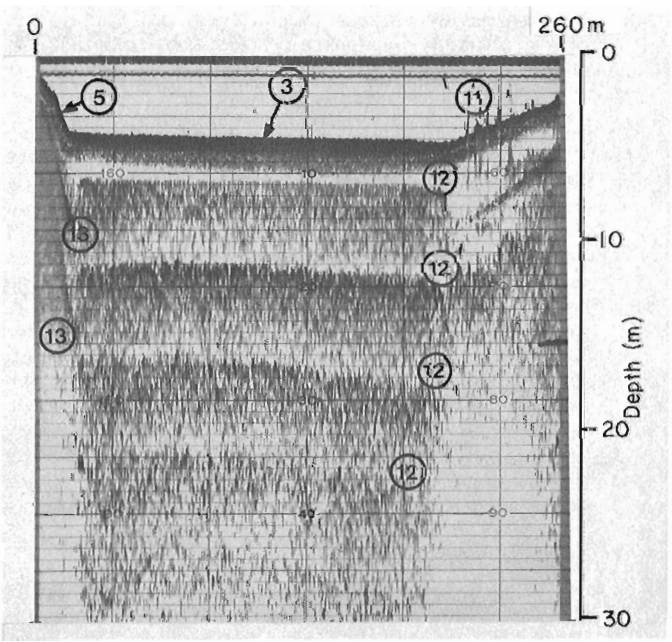

Figure 56.8. *Profile across sandy bottom of bay of inlet stream on Big Turkey Lake. Note strong multiple reflections.*

Bedrock

Around the lakes of the Canadian Shield, bedrock outcrops are common, and the drainage basins of many lakes have little drift cover. Below water level in lakes, bedrock signature can be identified by multiple false reflections in shallow water, similar to those produced by sand and gravel. Bedrock can also be identified by its rough or steeply sloping surfaces, distinctive lack of subbottom reflections, and its location either beneath soft sediment sequences or adjacent to bedrock shores (Figs. 56.2, 56.4, 56.6). In lakes underlain by Paleozoic bedrock, the bedrock surface may be much smoother than that of Precambrian terrane.

Weeds

In shallow water, aquatic weeds produce a distinctive pattern but interfere with the acoustical signal, often preventing penetration of the bottom (Fig. 56.9). Thus, in water depths of less than about 3 m, it is often difficult to obtain useful profile results, particularly when the level of the lakes have been artificially raised by human or beaver damming. In the latter case, submerged forest litter may absorb much of the energy of the acoustical signal.

Structures in Sediments

Deformation of bottom sediments can indicate much about the sedimentation history of lake basins. The most common type of deformation is folding of the laminated sequences, particularly in their basal parts (Fig. 56.10). The type of deformation may have resulted from differential compaction, foundering associated with rapid loading or dewatering, or slumping along basin sides. It is interpreted here, however, to have resulted from the compression exerted by shortening of the beds as they collapsed over melting ice blocks stranded in front of retreating glaciers.

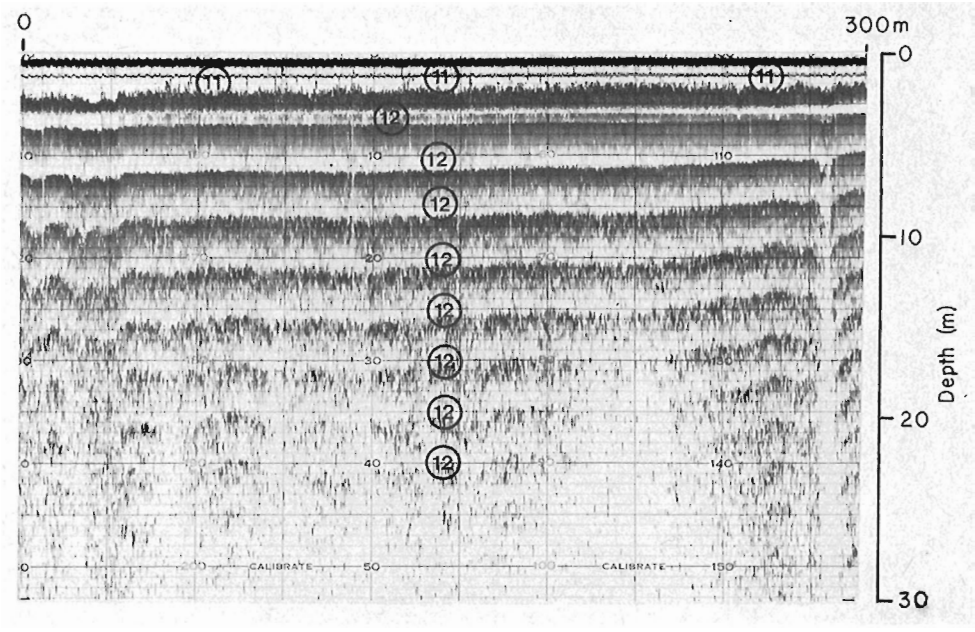

Figure 56.9

Profile across Grassy Bay of Calabogie Lake showing effects of weeds and multiple (false) reflections from sand. This bay was probably created by a 2-3 m rise in lake level as a result of damming.

Shortening is also accompanied by low and high angle reverse faulting (Fig. 56.11) as described by McDonald and Shilts (1975) and by Shilts et al. (1976). Attenuation and disruption of the sediment blanket also may occur in the zone between sediments dropping over melted ice and sediments deposited directly on till or bedrock (Fig. 56.13a,b).

In the profiles examined so far, no evidence of neotectonic movements has been detected, although several traverses have been made across major faults.

In Golden Lake, a number of unusual anticlinal structures occur across one profile (Fig. 56.12). These structures appear to persist through the whole sedimentary column and may reflect gas or fluid injected from below. Paleozoic bedrock, which may underlie this lake, is known to produce methane gas at some places in Ottawa valley. Well developed 'gas layers', similar to those described above occur around these structures.

Discussion and Conclusions

This study has shown that the modern morphology of the lake basins in this part of the Canadian Shield is commonly a result of glacial sedimentation processes, the bulk of the sediment in many basins possibly having been deposited under proglacial conditions that could have existed for no more than a few hundred years after the last glaciers melted from the basins. In Weslemkoon Lake, in particular, sharp bedrock valleys are all but obscured beneath the modern lake floor by up to 25 m of what appears to be glaciolacustrine sediment. The style of deglaciation of the lake basins is also suggested by the deformation of the thick prisms of proglacial sediment. The deformation indicates that many depressions presently occupied by lakes were probably loci of blocks of glacier ice detached from the main glacier mass, stranded, and buried by rapid sedimentation. This is also

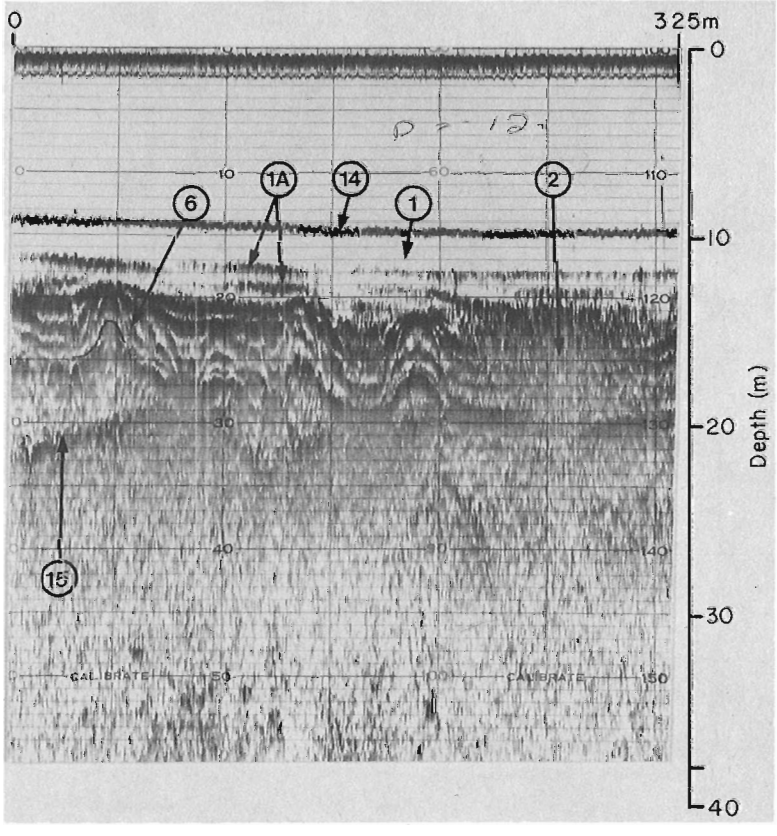

Figure 56.10. *Part of a profile from Calabogie Lake showing tight folding thought to be caused by shortening of the glaciolacustrine sediment blanket due to collapse over melting glacier ice.*

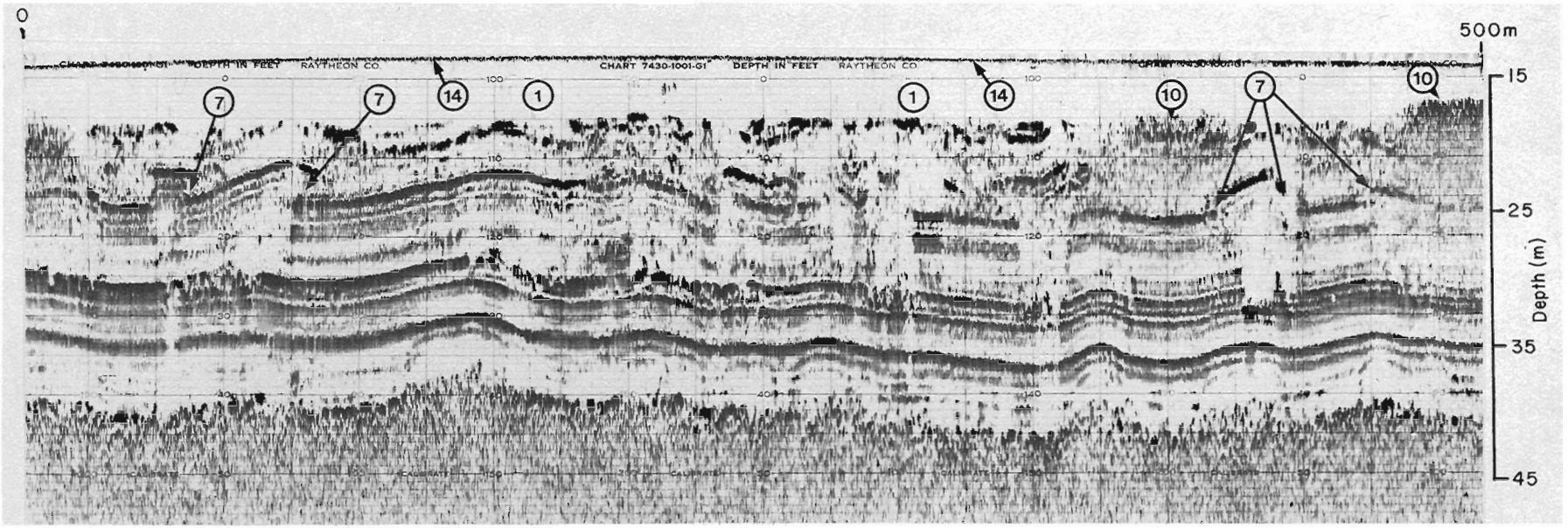

Figure 56.11. *Faults and folding in a portion of a profile across Lake Doré. Disruption was caused by collapse over melting ice. Note 'gas layer' and thick clastic laminated sediment fill in this shallow lake. Lake Doré lies below marine limit and is underlain by Paleozoic limestone.*

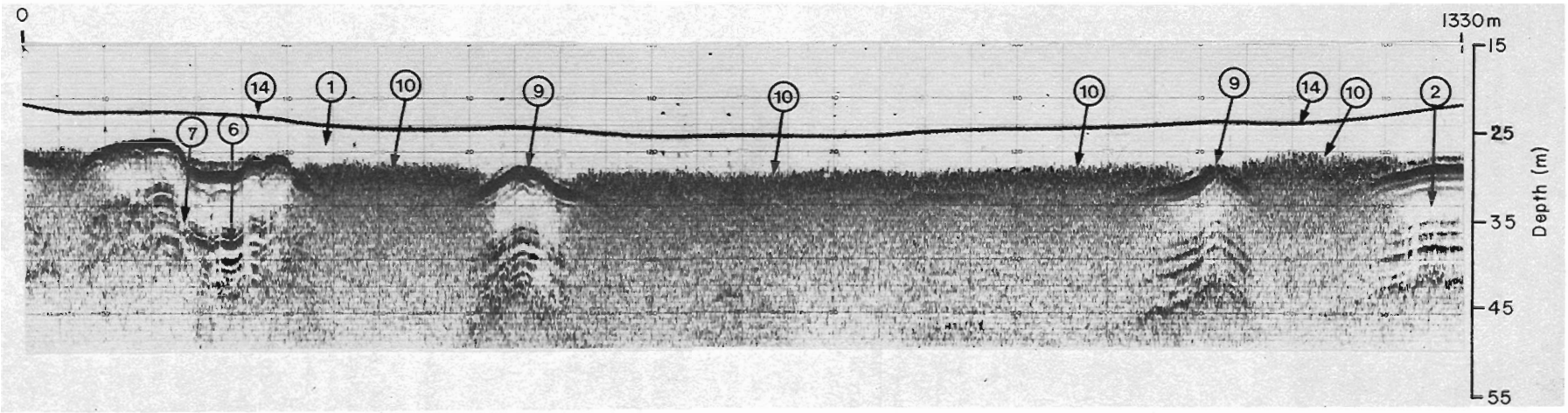

Figure 56.12. *Anticlinal structures thought to be related to upward ejection of gas or liquid in Golden Lake. Note heavy, semi-opaque accumulations of gas(?) near the base of modern sediment.*

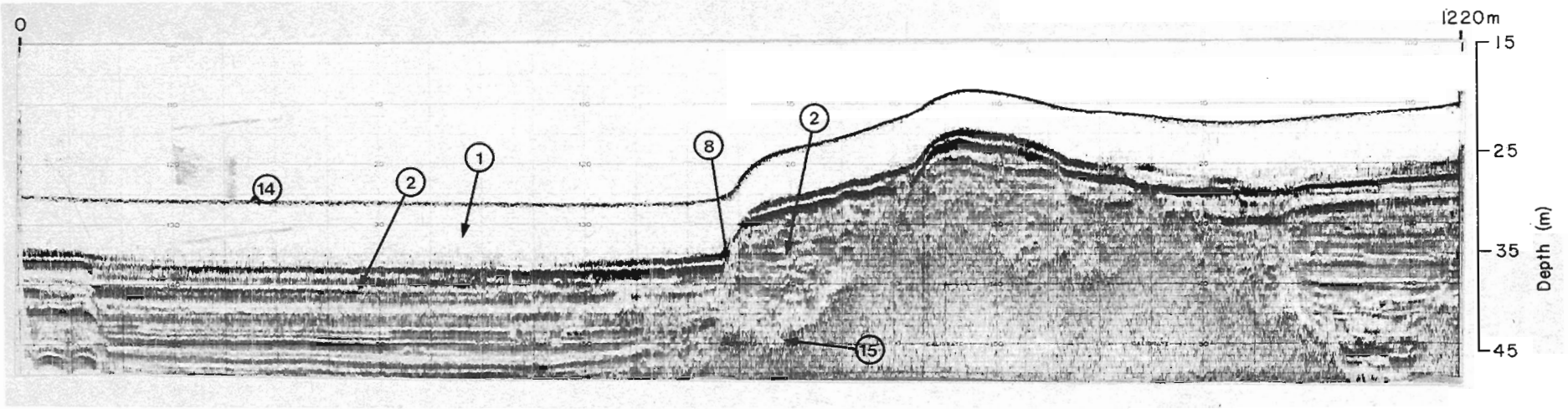

Figure 56.13a. *Graben-like structure caused by collapse over melting ice in Weslemkoon Lake.*

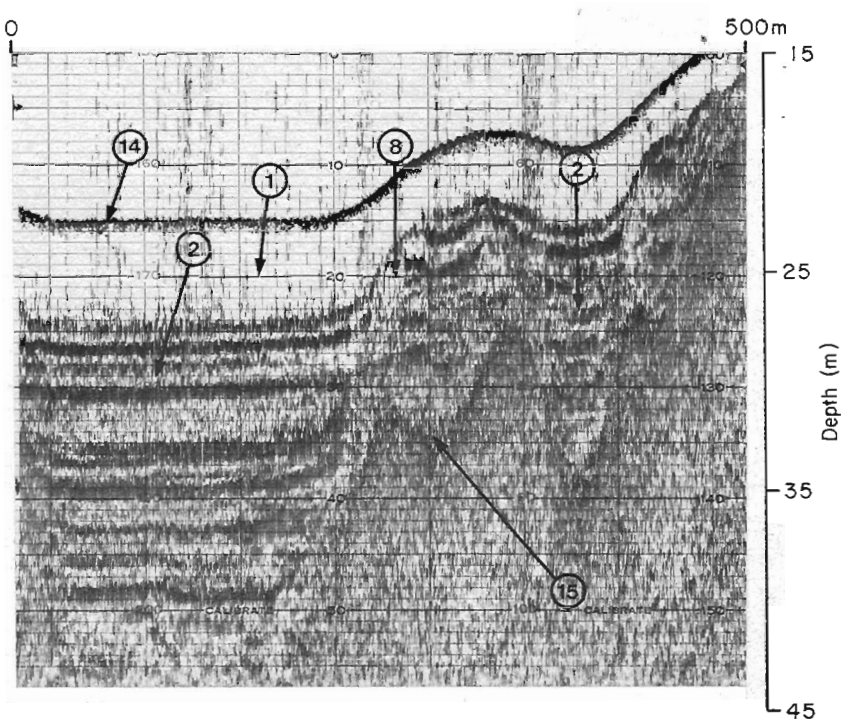

Figure 56.13b. *Differential movement of thick piles of clastic sediment in Weslemkoon Lake, caused by collapse over melting glacier ice. Note disruption, folding, and displacement of marker beds in centre of profile.*

indicated by certain subaerial features, such as fringes of outwash around many lakes, indicating that ice must have provided a temporary platform for free fluvial drainage across what is now a closed basin.

All of the lakes so far examined, including the relatively high altitude Turkey lakes and Weslemkoon Lake, appear to have been part of larger proglacial lakes or, in Ottawa valley, marine systems. It will be interesting to compare these lakes with lakes from higher altitudes in areas where drainage away from the ice front was not blocked and where large systems such as the glacial Great Lakes did not inundate the basins. In such high altitude lakes in the Arctic, proglacial deposition has had much less effect on the basin morphology, and till commonly forms the floor of the lake (J.D. Adshead, personal communication, 1981).

Finally, in regard to our original objectives, we have learned much about stratigraphic relationships and sediment facies distribution related to the last glaciation, but we have not observed any deformation that can be unequivocally attributed to postglacial tectonism. We also believe that significant amounts of apparently fine grained clastic sediment underlie large parts of modern lake basins and in many cases form the sediment-water interface. Both these sediments and till exposed at the sediment-water interface may have compositions that vary significantly from that of the local bedrock. Groundwater flow through the thick prisms of clastic sediment must have important effects on both the physical and chemical aspects of the hydrology of the lakes surveyed. Perhaps this is why Weslemkoon Lake, which lies entirely within a granite batholith, has a relatively high pH, approaching neutrality (Weslemkoon Lake, Ontario Ministry of Natural Resources map, 1973). The thick glacial sediments in Weslemkoon Lake are undoubtedly calcareous, since numerous pieces of glacially transported Paleozoic limestone and Precambrian marble are found in the few exposures of unconsolidated sediment around the shores.

Acknowledgments

Much of the profiling on which this paper is based was carried out by Lorraine Farrell and John Hornbsy, to whom we express our thanks. Co-operation of the National Capital Commission, particularly L. Kingsley and P. Quinn, is gratefully acknowledged. The Turkey lakes survey was carried out in co-operation with Dr. Laura Johnson of the Department of Environment.

References

Kujansuu, R.
1964: Nuorista siirroksista Lapissa (Recent faults in Finnish Lapland); Eripainos geologi-lehdestä, n:o. 3-4, p. 30-36.

McDonald, B.C. and Shilts, W.W.
1975: Interpretation of faults in glaciofluvial sediments; in Glaciofluvial and Glaciolacustrine Sedimentation, ed. A.V. Jopling and B.C. McDonald; Society of Economic Paleontologists and Mineralogists, Special Publication No. 23, p. 123-131.

Shilts, W.W., Dean, W.E., and Klassen, R.A.
1976: Physical, chemical, and stratigraphic aspects of sedimentation in lake basins of the eastern arctic shield; in Report of Activities, Part A, Geological Survey of Canada, Paper 76-1A, p. 245-254.

57.

LATE TRIASSIC (UPPER NORIAN) AND EARLIEST JURASSIC (HETTANGIAN) ROCKS AND AMMONOID FAUNAS, HALFWAY RIVER AND PINE PASS MAP AREAS, BRITISH COLUMBIA

Project 670576

E.T. Tozer
Institute of Sedimentary and Petroleum Geology, Ottawa

Tozer, E.T., Late Triassic (Upper Norian) and earliest Jurassic (Hettangian) rocks and ammonoid faunas, Halfway River and Pine Pass map areas, British Columbia; in Current Research, Part A, Geological Survey of Canada, Paper 82-1A, p. 385-391, 1982.

Abstract

Psiloceras *and other Lower Hettangian ammonites are recorded from northeastern British Columbia for the first time, from a section near Black Bear Ridge in the Peace River valley. New data on the succession of Upper Norian ammonoid and* ***Monotis*** *faunas are also given which show that the age of the Upper Norian strata beneath the Jurassic varies considerably within the vicinity of Peace and Pine rivers. The Hettangian ammonites are in beds that succeed Upper Norian strata (upper part of Cordilleranus Zone). The Hettangian and Upper Norian strata appear to be essentially similar lithologically and the succession provides no certain lithological indication of an interruption in sedimentation. However, the absence of latest Norian faunas (Amoenum and Crickmayi zones) and comparisons with other sections nearby, suggest that at Black Bear Ridge, as elsewhere in the Rocky Mountains and Foothills, the Triassic and Jurassic rocks are separated by an unconformity. At Black Bear Ridge this unconformity is evidently reduced to a paraconformity, the exact position of which is uncertain, despite continuous, perfect exposure of the beds in question.*

Introduction

This paper provides new data on the late Triassic-earliest Jurassic rock and faunal succession recorded in the Pardonet, Bocock and Fernie formations of the Peace River and adjacent Foothills, northeastern British Columbia (NTS 94 B, 93 O). The most novel discovery is that of well preserved Lower Hettangian (earliest Jurassic) ammonites in strata that concordantly follow beds of late (but not latest) Triassic age.

The Peace River valley has been a focal area for geological studies for more than a century, ever since the GSC Expedition of A.R.C. Selwyn in 1875. It may seem surprising that the discovery of Hettangian ammonites was not made before on the well travelled Peace River route. There is an explanation which shows that the earlier investigators were in no way remiss. Until 1967 the Peace River, where it crosses the Foothills, was at a level of about 580 m, flanked by high terraces, above which were hills with fair to indifferent outcrops. At a few places there were also rock exposures at river level, for example at Rapide-qui-ne-parle-pas (Ne-Parle-Pas Rapids). In 1967 Peace River was raised to an elevation of about 670 m where it traverses the Rocky Mountains and Foothills, following completion of the W.A.C. Bennett dam, constructed at Portage Mountain for the generation of hydroelectric power. The resultant body of water is now known as Williston Lake. Since 1967 the old river exposures, as at Ne-Parle-Pas Rapids, have been submerged, but in many places excellent new exposures have developed on the lake shore.

Throughout the area under consideration the beds at the Triassic-Jurassic boundary include relatively incompetent strata which form a topographic notch, or the site of small watercourses, where rock exposures are generally poor or non-existent. Although in the past it has been possible to map the boundary between the Triassic and Jurassic formations with tolerable accuracy (Irish, 1970; Thompson, 1978), good exposures of the sequence at the boundary are rare and none have been described in detail. In 1980 and 1981 I examined many of the new exposures of Triassic rocks at Williston Lake and also sought exposures that would show the relationship between the Triassic and Jurassic formations. The Triassic-Jurassic boundary relationship was found to be exposed at only one place; on the north side of Williston Lake, near Black Bear Ridge.

In order to place the Black Bear Ridge section in perspective some other sections that contribute to our knowledge of the late Triassic-early Jurassic succession from nearby areas are also considered (Fig. 57.1).

Description of Localities

Thicknesses of the stratigraphic units, positions of fossiliferous beds, and suggested correlations of the sections that have a bearing on the age of the Triassic-Jurassic boundary beds are summarized in Figure 57.2. The following notes supplement the figure.

The Triassic rocks discussed below are assigned to the Pardonet and Bocock formations as defined by Gibson (1971). The Jurassic rocks are placed in the Fernie Formation, as assigned by Stott (1967).

The basal Fernie strata in the sections described below are relatively hard and resistant; higher beds are dark, rubbly shales. Some or all of the basal resistant beds have been assigned to the Nordegg Member (Hamilton, 1962; Stott, 1967), which is generally dated as Sinemurian (Frebold, 1969). It would appear, however, that both the lithostratigraphy and biostratigraphy of the basal Fernie in northeastern British Columbia is complicated and not fully understood, particularly as some of the beds formerly regarded as Sinemurian are now known to be Pliensbachian (Frebold, 1970). The discovery of Hettangian ammonites in the Fernie sequence further complicates the picture. D.F. Stott informs me that he is no longer satisfied that all of the basal Fernie rocks of northeastern British Columbia should be assigned to the Nordegg.

Section 1. Pine River (NTS Callazon Creek, 93 O/10E)

This section is on the north side of Pine River at the British Columbia Railway Cut 3 km west of LeMoray. The locality has been visited by many geologists and has been described by Westermann (1962, text fig. 3, p. 750; Ager and Westermann, 1963, p. 601), Tozer (1967, p. 55-57), Westermann and Verma (1967), and Hughes (1967, p. 30-31). The nature of the contact between the Pardonet and Jurassic rocks has also been mentioned (as unconformable) by Gibson (1971, p. 23).

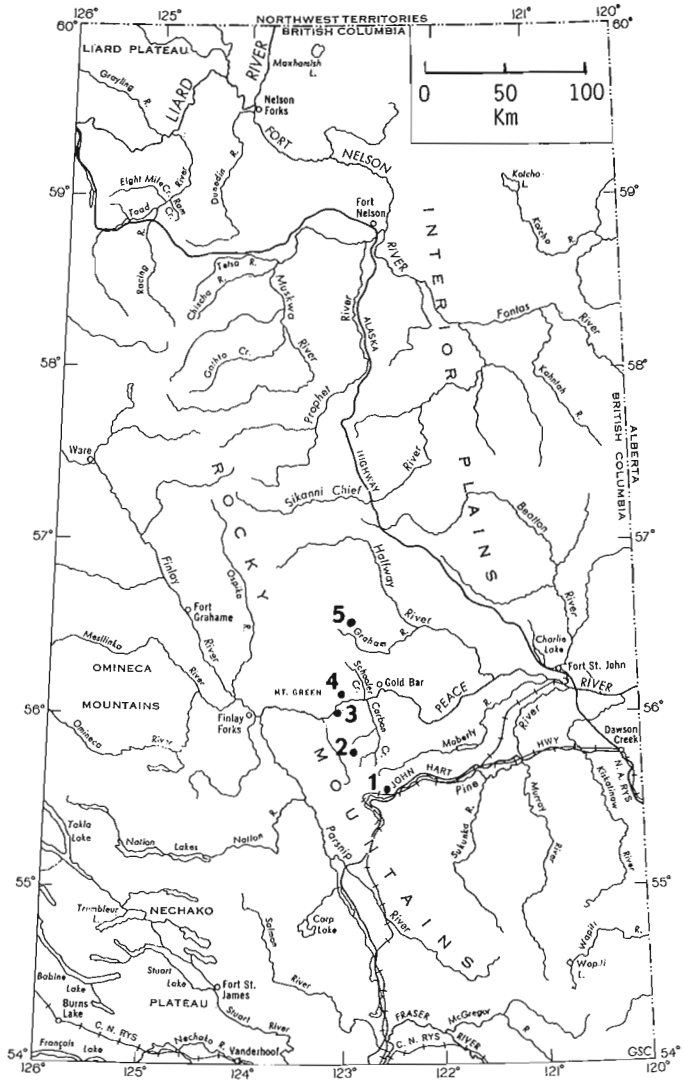

1. *Pine River;*
2. *Eleven Mile Creek;*
3. *Ne-Parle-Pas Rapids;*
4. *Black Bear Ridge;*
5. *Crying Girl Prairie Creek.*

Figure 57.1. *Index map of northeastern British Columbia showing localities described. The map does not show Williston Lake, formed on Peace River in 1967 following completion of the W.A.C. Bennett dam.*

As regards the succession overlying the Upper Norian **Monotis** Beds of the Pardonet Formation, the interpretations of Hughes, Gibson and the writer are essentially the same, namely that the **Monotis** Beds are overlain, in normal stratigraphic sequence, first by about 12 m of hard calcareous siltstone with numerous brachiopods, bivalves and a few poorly preserved ammonites – the "**Pecten** Beds" of Tozer (1967, p. 57) – followed by about 7 m of shale (Section 1, Fig. 57.2). According to Westermann's original interpretation (1962) the "**Pecten** Beds" and overlying shale were believed to be overturned, with the shale at the lower level. A fault was believed to separate the "**Pecten** Beds" from the Pardonet. The visit made by Verma in 1966, recorded in Westermann and Verma (1967) evidently caused Westermann to withdraw his original interpretation. The interpretation given in Westermann and Verma, as far as it goes, is not in conflict with my own and those of Hughes and Gibson.

Visits to this section in 1979, 1980 and 1981 have provided some new data and collections.

The highest **Monotis** Beds, from which collections were made in 1965 (GSC loc. 68311, Tozer, 1967, p. 57), contain **Monotis subcircularis** Gabb[1]. **Monotis ochotica** (Keyserling) has been recorded from about the same level or a little lower (Westermann and Verma, 1967, p. 802). In 1980 a loose block from these upper beds found by M. Orchard provided **Paraguembelites ludingtoni** Tozer associated with **Monotis ochotica** (GSC loc. 97500).

The contact between the **Monotis** Beds and overlying "**Pecten** Beds" is not perfectly exposed but appears perfectly concordant with no more than 1.5 m of strata missing.

The fauna of the "**Pecten** Beds" has not been fully studied.

Ager (in Ager and Westermann 1963, p. 605) has described **Furcirhynchia striata** (Quenstedt) from this locality; Westermann (1962, p. 601) lists:

Cardinia ? aff. **C regularis** Terquem

Gryphaea sp.

Oxytoma cf. **O. inaequivalvis** (Sowerby)

Chlamys n. sp. aff. **C. textorius** (Munster)

Entolium cf. **E. calvum** (Goldfuss)

Most or all of these fossils are duplicated in collections obtained by me (GSC loc. 68310, Tozer, 1967, p. 57).

According to Ager (in Ager and Westermann 1963, p. 605) **Furcirhynchia striata** is Pliensbachian in Europe; he nevertheless interprets the Canadian specimens as Sinemurian. Ager evidently made this interpretation on the assumption that the beds from which they were obtained were firmly dated as Sinemurian by ammonites, although at the time no Jurassic ammonites were known from the Pine River locality. In recent years a few poorly preserved ribbed evolute ammonites have been obtained from the "**Pecten** Beds" (GSC locs. 97522, 97533). Although they prove that the "**Pecten** Beds" are Lower Jurassic, not Triassic, they do not permit a more precise dating.

In 1981 some fragmentary ammonites (GSC loc. 98556) were collected at the contact between the "**Pecten** Beds" and overlying shale. They have not yet been studied but, like those from the "**Pecten** Beds", hold little promise.

Section 2. Eleven Mile Creek (NTS Carbon Creek, 93 O/15W)

This section of the Pardonet and Bocock formations has been described by Gibson (1971, p. 74). The Bocock Formation, a light grey limestone which abruptly overlies the **Monotis** Beds of the Pardonet, is remarkable for its limited geographic extent. Despite its considerable thickness (maximum of 64 m) it is confined to a small area – the foothills between Pine and Peace rivers. The stratigraphic interval in which it would be expected (i.e. the Pardonet-Fernie interval) is exposed in both the Pine and Peace River valleys, but the Bocock Formation is definitely absent. In 1981 the section at Eleven Mile Creek was revisited. New collections were obtained from the Pardonet Formation and the Bocock Formation was sampled for conodonts by M. Orchard.

This section is the type locality for **Lissonites canadensis** Tozer, which occurs near the top of the Pardonet Formation, 1.5 m below the Bocock (GSC loc. 83818; Tozer, 1979, p. 129). In 1981 fossils were collected from two lower levels within the **Monotis** beds of the Pardonet. A loose

[1] The **Monotis** taxonomy employed in this paper is simple but apparently effective. Equivalve specimens are identified as **Monotis subcircularis Gabb;** inequivalve specimens, with a left valve much more convex than the right, as **Monotis ochotica** (Keyserling). The genus **Monotis** is restricted to the Cordilleranus Zone. Monotids from the Middle Norian Columbianus Zone are now assigned to **Eomonotis** Grant-Mackie.

concretion, derived from a bed about 15 m below the Bocock Formation, provided **Paraguembelites ludingtoni** Tozer and **Metasibirites** sp. (GSC loc. 98559). A large block, from about the same level as GSC locality 98559, provided **Rhabdoceras suessi** Hauer (GSC loc. 98558). Associated with ammonoids at localities 83818, 98558 and 98559 is **Monotis ochotica** (Keyserling).

From a level about 23 m below the Bocock, **Monotis subcircularis** Gabb was collected (GSC loc. 98557). The Eleven Mile Creek section thus provides evidence for a succession of three faunas within the **Monotis** Beds: the lower with **Monotis subcircularis;** the middle with **Paraguembelites ludingtoni** and **Rhabdoceras suessi;** the upper with **Lissonites canadensis. Monotis ochotica** characterizes the middle and upper faunas.

The conodonts extracted from the Bocock (GSC loc. C-87549) by M. Orchard (personal communication) comprise a fauna dominated by epigondollelids. Most abundant are specimens identified as **Epigondolella bidentata** Mosher. Orchard reports that **E. bidentata** is characteristically an Upper Norian species although it has also been reported from the latest Middle Norian.

Jurassic strata assigned to the Fernie Formation have been seen above the Bocock Formation but no exact details regarding their age and lithology are available.

Section 3. Ne-Parle-Pas Rapids
(NTS Ne-Parle-Pas Rapids 94 B/3E)

As already mentioned, the section at Ne-Parle-Pas Rapids which exposed the contact between the Pardonet and Fernie formations has been submerged by Williston Lake. The section has been examined by several members of the Geological Survey, starting with A.R.C. Selwyn in 1875, then by F.H. McLearn, in 1937 and 1938, also by the writer, in 1964. The section has been mentioned in several publications (McLearn, 1937, p. 127; McLearn, 1960, p. 6; McLearn and Kindle, 1950, p. 55; Tozer, 1965, p. 222; Tozer, 1967, p. 55) but has never been described fully and in detail. My own collections and those made by McLearn are preserved at the Geological Survey. McLearn's field note books also provide some hitherto unpublished data.

The section exposed at the rapids comprised about 100 m of Pardonet beds; the lower 81 m with **Monotis ochotica** (Keyserling); the upper 19 m characterized by thin beds of black phosphatic nodules, the absence of **Monotis,** and the occurrence of Triassic ammonoids (**Placites polydactylus** (Mojsisovics), **Rhabdoceras suessi** Hauer). This 19 m unit is apparently without any counterpart in other sections of the Pardonet for it represents the only known case of beds with Triassic ammonoids overlying the **Monotis**-bearing strata. For purposes of the discussion that follows the unit is designated as the "**Rhacophyllites** Beds". McLearn collected small specimens of **Rhacophyllites debilis** (Hauer) from near their top (GSC loc. 9776). The **Rhacophyllites** Beds were overlain by 1.5 m of dark siltstone, which was relatively recessive. McLearn found crushed ammonite impressions in this dark siltstone including one ribbed evolute ammonite, 55 mm in diameter (GSC loc. 9775), 1.5 m above GSC loc. 9776 (data from field notebooks, F.H. McLearn). The ammonite is generically indeterminable but it is, without doubt, a Jurassic ammonite, not an Upper Norian ammonoid.

My own field notes, those of McLearn, and my recollections, are that the beds with the Jurassic ammonite followed the harder, but otherwise not dramatically dissimilar Triassic beds with perfect concordance, and with no lithological indication of unconformity.

In 1981 it was found that there are now extensive exposures of the Pardonet Formation on the south side of Williston Lake, extending southwest from the small cove at 55°01'00" N, 123°05'00" W. These beds are exactly on the strike, 1 km to the south, of the beds that were exposed at Ne-Parle-Pas Rapids. The new exposures reveal a substantially greater thickness of Pardonet strata than the old. As at the rapids, the **Monotis** Beds are overlain by the **Rhacophyllites** Beds, 20 m thick at the new exposure. Jurassic rocks were not found, however, Triassic ammonoids (**Placites, Arcestes, Rhacophyllites,** GSC loc. 98500) being present in the uppermost bed of the new section.

Section 4. Near Black Bear Ridge
(NTS Ne-Parle-Pas Rapids 94 B/3E)

This section is on the north side of Williston Lake, opposite Pardonet Hill, at a small cove 3.7 km northeast of the mouth of Nabesche (Ottertail) River (56°05'00" N, 123°02'00" W). The section is on the east limb of the Nabesche syncline (Irish, 1970). Descriptions of the old exposures of Triassic and Jurassic rocks in this vicinity have been provided by Beach and Spivak (1944, p. 3), McLearn and Kindle (1950, p. 61), Irish (1970, p. 141), McLearn (1960, p. 12) and Tozer (1967, p. 59). The Triassic rocks are exposed on a relatively small topographic feature east of Black Bear Ridge as identified on all published topographical and geological maps (e.g. Ne-Parle-Pas Rapids, NTS 94 B/3E). McLearn (1960, p. 12) used the name Black Bear Ridge for the small feature, which is separated from the main ridge by most of which are packed with shells of **Monotis.** The **Monotis** Beds, 27 m thick, have provided ammonoids from two levels. The lower level, 19 m from the top, has **Paraguembelites ludingtoni** Tozer (GSC loc. 98534). The upper level, 1.2 m from the top, has **Placites** sp. associated with poorly preserved small ammonoids, probably **Lissonites canadensis** Tozer (GSC loc. 98545). **Monotis** shells from the uppermost Pardonet Formation are generally packed together and crushed, making specific determination uncertain but the specimens from the two ammonoid beds appear to be **Monotis ochotica** (Keyserling) rather than **M. subcircularis** (Gabb).

The **Monotis** Beds are overlain by 11.5 m of brown siltstone, partly shaly, partly hard and calcareous. The siltstones are much like those interbedded with the coquinoid **Monotis** Beds. About 1 m above the highest **Monotis** bed there is a 20 cm bed of fibrous calcite. Between 7.5 and 9 m above the highest **Monotis** bed, well preserved Jurassic ammonites were collected from 3 beds (GSC localities 98531, 98532, 98533). Study of these ammonites is incomplete. Only those from the lowest bed (GSC loc. 98531) have received detailed attention. The fauna of this bed includes **Psiloceras (Paraphylloceras) calliphyllum** (Neumayr) (Fig. 57.4) associated with one genus of Phylloceratacea; also an ammonite of possible phylogenetic significance sharing characters (degree of involution) of Psiloceratacea with those (suture line) of Phylloceratacea. The occurrence of **P. (P.) calliphyllum** indicates that the ammonites from GSC loc. 98531 are undoubtedly Lower Hettangian, probably as old as any Jurassic ammonites known anywhere in the world.

The age of the 7.5 m of apparently unfossiliferous strata that lie between the **Monotis** Beds and the **Psiloceras** Beds is uncertain. As mentioned below there is good evidence that an unconformity is present within these strata, although the exact position has not been located. Provisionally it is suggested that the fibrous calcite bed represents the Pardonet-Fernie (Triassic-Jurassic) boundary. The unfossiliferous metre of siltstone between the highest **Monotis** bed and the fibrous calcite bed might be an attenuated equivalent of the **Rhacophyllites** Beds of Ne-Parle-Pas Rapids, but there is no evidence to support this correlation. It might, therefore, be considered more appropriate to draw the Pardonet-Fernie boundary immediately above the topmost **Monotis** bed, i.e. 1 m below the bed of fibrous calcite.

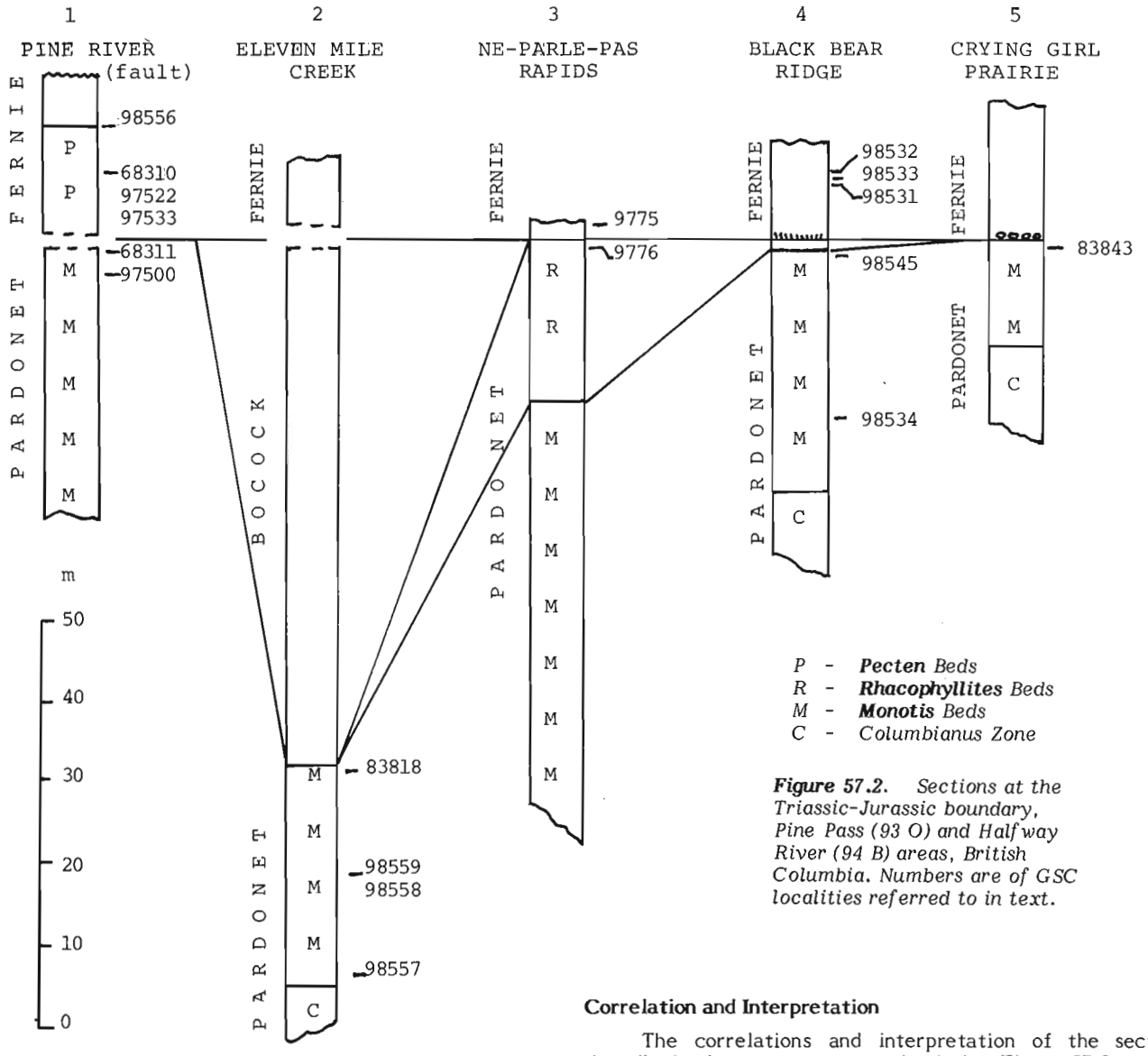

Figure 57.2. Sections at the Triassic-Jurassic boundary, Pine Pass (93 O) and Halfway River (94 B) areas, British Columbia. Numbers are of GSC localities referred to in text.

Section 5. Crying Girl Prairie Creek (NTS Hackney Hills 94 B/7W)

This section exposes much of the Pardonet Formation and about 15 m of overlying Fernie strata. The Triassic rocks have been described by Pelletier (1964, p. 88), Tozer (1967, p. 60), Irish (1970, p. 60) and in most detail by Gibson (1971, p. 66). The Pardonet rocks provide an unusually good sequence of Norian faunas. The Upper Norian **Monotis** Beds at the top of the Pardonet are 12 m thick. The Fernie strata were probably examined by all the authors cited above but no descriptions have been published. In 1969, I observed about 15 m of dark siltstone above the **Monotis** Beds. At the siltstone – **Monotis** Beds contact there are a few centimetres of conglomerate composed of black phosphatic pebbles up to about 4 cm in diameter. **Monotis subcircularis** Gabb was collected from the topmost **Monotis** bed, 5 cm below the base of the conglomerate (GSC loc. 83843). Impressions of evolute ribbed ammonites, like those at Ne-Parle-Pas Rapids, were observed in the overlying siltstones but proved impossible to collect. Although generically indeterminable the field conclusion was that they are Lower Jurassic ammonites, not Triassic ammonoids. The conclusion that the seam of conglomerate represents the Pardonet-Fernie contact (Triassic-Jurassic boundary) thus seems justified.

Correlation and Interpretation

The correlations and interpretation of the sections described above are summarized in Figure 57.3. The chronology for the Upper Norian has been defined and discussed by Tozer (1979, 1980).

The evidence now available indicates that the Upper Norian **Monotis** Beds comprise a succession of at least two biostratigraphic units, the lower characterized by **Paraguembelites ludingtoni,** the upper by **Lissonites canadensis. Monotis subcircularis** Gabb is evidently restricted to the lower part of the **Monotis** succession, **Monotis ochotica** (Keyserling) to the upper. The conclusion that both **Monotis subcircularis** and **M. ochotica** appear in the earliest beds of the Cordilleranus Zone (Tozer, 1980, p. 682) thus appears to be unwarranted. The evidence from Pine Pass nevertheless suggests that the ranges of **M. subcircularis** and **M. ochotica** do overlap and that **M. subcircularis,** at least locally, occurs above **Paraguembelites ludingtoni. Monotis subcircularis,** however, has never been found in the youngest **Monotis** Beds. In terms of the Upper Norian chronology recently proposed (Tozer, 1979), all the **Monotis** Beds are Cordilleranus Zone. The **Paraguembelites ludingtoni** and **Lissonites canadensis** levels probably merit the status of subzones. The faunas of the Pardonet Formation provide no evidence that the Amoenum and Crickmayi zones are represented. It is possible that the **Rhacophyllites** Beds of Ne-Parle-Pas Rapids represent part of this interval but this cannot be established

because the only ammonoids known from the unit range through much or all of the Upper Norian. The Bocock Formation, from its stratigraphic position, is certainly younger than the **Lissonites canadensis** bed and probably younger than the **Rhacophyllites** Beds. The Bocock might therefore represent the Amoenum Zone or the Crickmayi Zone. The Bocock conodonts, as presently known, do not assist in determining the exact age (M. Orchard, personal communication).

Although the age of the Triassic beds immediately below the Fernie cannot be precisely determined in all the sections there are nevertheless enough data to show that younger Upper Norian strata are preserved in some places than in others. This is shown by comparing the age of the highest Pardonet beds between Crying Girl Prairie Creek (locality 5), Black Bear Ridge (locality 4), Ne-Parle-Pas Rapids (locality 3) and Pine Pass (locality 1). At locality 1 and locality 5 the Fernie directly overlies beds relatively low in the Cordilleranus Zone; at locality 4, beds high in the Cordilleranus Zone; at locality 3, beds which may be younger than the Cordilleranus Zone. At Eleven Mile Creek (locality 2), where the Fernie overlies the Bocock Formation, the sub-Fernie rocks are presumably the youngest of all. Incidentally, the fact that the Bocock rests directly on **Monotis** Beds, with no indication of the **Rhacophyllites** Beds in between, suggests an unconformity at the base of the Bocock, a conclusion also reached by Gibson (1971, p. 24) from his study of the nature of the Pardonet-Bocock contact.

The discovery of well preserved Hettangian ammonites at Black Bear Ridge serves to provide an accurate age determination for the Fernie beds at this one locality. As already noted, the Fernie-Pardonet contact is not certainly identified by lithological characters at Black Bear Ridge. This, however, is probably not significant and should not be construed as indicating uninterrupted sedimentation between Triassic and Jurassic time in view of the absence of strata indicated by both biochronology (absence of Amoenum and Crickmayi zones) and the absence of lithostratigraphic units preserved nearby (**Rhacophyllites** Beds and Bocock Formation). The exact age of the basal Fernie strata at localities 1, 2, 3 and 5 is uncertain. Perfect exposure of an undoubted Fernie-Pardonet contact is known only at locality 3; here there is good lithostratigraphic evidence, in the form of a basal Fernie conglomerate, for an interruption in sedimentation.

In 1981, D.F. Stott collected ammonites from Fernie strata which overly the relatively resistant brown siltstones with Hettangian ammonites at Black Bear Ridge. **Peronoceras**, indicating a Toarcian age, has been identified by T.P. Poulton (GSC loc. C-92853). This gives grounds for suggesting that the basal, resistant Fernie beds in Northeastern British Columbia (the Nordegg Member of some authors) are pre-Toarcian. They possibly form a condensed sequence of Hettangian, Sinemurian and Pliensbachian deposits but it is clear that better collections must be obtained before this can be considered established.

It has long been known that the Triassic and Jurassic strata of the Rocky Mountains and Foothills, although structurally concordant, are separated by a low angle unconformity. The broad regional picture has been

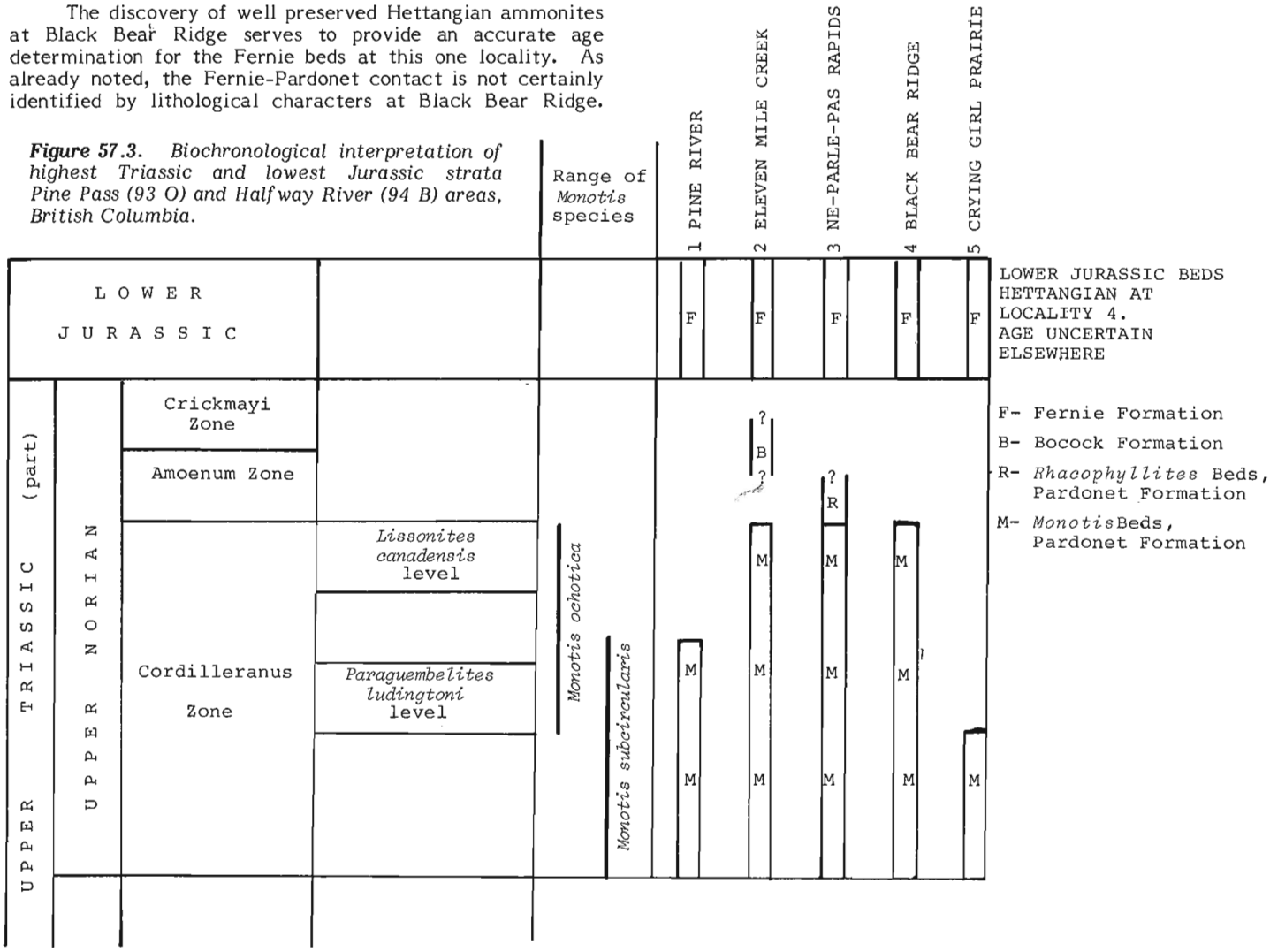

Figure 57.3. *Biochronological interpretation of highest Triassic and lowest Jurassic strata Pine Pass (93 O) and Halfway River (94 B) areas, British Columbia.*

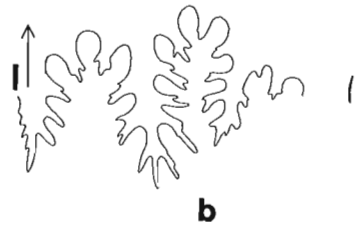

a. side view (X 1). The specimen is preserved in three dimensions to the point marked "X", which probably represents the end of the phragmocone. The venter is rounded. Approximate measurements at "X" are: 70; .26, .20, .54. What appears to be phragmocone is followed by 7/8 of a whorl which is crushed, indicating that the original complete diameter was at least 110 mm.

b. suture line (X 3) at a whorl height of 11 mm. The arrow indicates the mid-line of the venter. The diameter and position of the siphuncle is indicated by the black line.

***Figure 57.4. Psiloceras (Paraphylloceras) calliphyllum** (Neumayr). GSC No. 69149, Fernie Formation, near Black Bear Ridge, Williston Lake, British Columbia. GSC Loc. 98531*

summarized by Springer et al. (1964, Fig. 10-2, p. 139) and by Stott (in Douglas et al., 1970, Fig. VIII-44, p. 465). As shown in these figures the unconformity has its minimum amplitude in the Foothills at about the latitude of Peace River. Towards the north, south and east the Jurassic beds rest on progressively older Triassic strata, eventually, to the south and east, overstepping the Triassic completely, and lying on Paleozoic formations. The discovery of Hettangian beds overlying Upper Norian strata, recorded in this paper, confirms this interpretation and documents a situation in which the amplitude of this unconformity is appreciably reduced. However the unconformity is evidently still present, despite the absence of clear lithological evidence for its presence.

The discovery of Lower Hettangian above Upper Norian rocks in any part of the world provides hope that the elusive, possibly non-existent, situation where marine sedimentation continued without interruption from the Triassic into the Jurassic may have been found. The sequence at Black Bear Ridge, despite the superficial suggestion of continuity, evidently does not fill this role. Looking elsewhere in Canada: the sequence at Tyaughton Creek, western British Columbia, had been thought to possibly provide such a record (Tozer, 1979, p. 128, 1980, p. 849) but this is now uncertain. The specimens identified as Hettangian **Psiloceras** from this locality, which were taken to indicate that Hettangian and latest Triassic (Crickmayi Zone) were in close stratigraphic juxtaposition, are now known to have a lituid internal lobe and can no longer be accepted as representatives of that genus (Guex, 1980, p. 139). The age of the beds that provided these ammonites cannot, at present, be determined. The beds with "**Psiloceras**" (now **Badouxia**) **canadense** Frebold from Tyaughton Creek, formerly interpreted as Hettangian, are now considered to be Lower Sinemurian (Guex and Taylor, 1976; Imlay, 1981, p. 9). The presence of Hettangian in the Tyaughton Creek area is thus unproven. Hettangian has recently been recorded from northern Yukon, but here it is transgressive on Paleozoic (Frebold and Poulton, 1977). From Alaska, Imlay (1981, p. 11, 28) records Hettangian above Upper Norian **Monotis** beds at two localities, with the suggestion that sedimentation was continuous, but in both areas, as at Black Bear Ridge, the presence of Amoenum and Crickmayi Zones is unproven, and continuity thus is unlikely, despite lithological evidence interpreted to the contrary. In North America it would appear that there is only one locality where continuous sedimentation between the Triassic and Jurassic in the marine facies remains a possibility, namely the Gabbs Valley Range in Nevada, where Hettangian follows the Crickmayi Zone (Muller and Ferguson, 1939; Guex, 1980).

Acknowledgments

In 1980 and 1981 I was accompanied in the field by M. Orchard, who sampled the Triassic formations for conodonts. In addition to making his own collections Orchard was of great assistance in the collection of ammonoids and bivalves. In 1981 our field party was visited by D.F. Stott, who also assisted in making collections and gave advice on the outcrops at Black Bear Ridge and elsewhere. I have shown the Hettangian ammonites to J.H. Callomon (London), D.T. Donovan (London), Hans Frebold (Ottawa), Jean Guex (Lausanne), L. Krystyn (Vienna) and David Taylor (Berkeley, Calif.) and I wish to acknowledge the benefits that resulted from discussions provoked by their examination of the specimens.

References

Ager, D.V. and Westermann, G.E.G.
1963: New Mesozoic brachiopods from Canada; Journal of Paleontology, v. 37, p. 595-610.

Beach, H.H. and Spivak, J.
1944: Dunlevy-Portage Mountain Map-area, British Columbia; Geological Survey of Canada, Paper 44-19.

Douglas, R.J.W. (Editor)
1970: Geology and economic minerals of Canada (5th Ed.); Geological Survey of Canada, Economic Geology Report 1.

Frebold, H.
1969: Subdivision and facies of Lower Jurassic rocks in the Southern Canadian Rocky Mountains and Foothills; Proceedings of the Geological Association of Canada, v. 20, p. 76-89.

1970: Pliensbachian ammonoids from British Columbia and southern Yukon; Canadian Journal of Earth Sciences, v. 7, p. 435-456.

Frebold, H. and Poulton, T.P.
1977: Hettangian (Lower Jurassic) rocks and faunas, northern Yukon Territory; Canadian Journal of Earth Sciences, v. 14, p. 89-101.

Gibson, D.W.
1971: Triassic stratigraphy of the Sikanni Chief River-Pine Pass Region, Rocky Mountain Foothills, northeastern British Columbia; Geological Survey of Canada, Paper 70-31.

Guex, J.
1980: Remarques préliminaires sur la distribution stratigraphique des ammonites hettangiennes du New York Canyon (Gabbs Valley Range, Nevada); Bulletin de geologie Lausanne, 1980, no. 250, p. 127-140.

Guex, J. and Taylor, D.
1976: La limite Hettangien-Sinémurien, des Préalpes romandes au Nevada; Eclogae geologicae Helvetiae, v. 69/2, p. 521-526.

Hamilton, W.N.
1962: The Jurassic Fernie Group in northeastern British Columbia; Edmonton Geological Society Fourth Annual Field Trip Guide Book, p. 46-56.

Hughes, J.E.
1967: Geology of the Pine Valley Mount Wabi to Solitude Mountain Northeastern British Columbia; British Columbia Department of Mines and Petroleum Resources, Bulletin 52.

Imlay, R.W.
1981: Early Jurassic ammonites from Alaska; U.S. Geological Survey Professional Paper 1148.

Irish, E.J.W.
1970: Halfway River Map-area, British Columbia; Geological Survey of Canada, Paper 69-1.

McLearn, F.H.
1937: Contributions to the Triassic of Peace River, B.C.; Canadian Field-Naturalist, v. 51, p. 127-131.

1960: Ammonoid faunas of the Upper Triassic Pardonet Formation, Peace River Foothills, British Columbia; Geological Survey of Canada, Memoir 311.

McLearn, F.H. and Kindle, E.D.
1950: Geology of northeastern British Columbia; Geological Survey of Canada, Memoir 259.

Muller, S.W. and Ferguson, H.G.
1939: Mesozoic stratigraphy of the Hawthorne and Tonopah quadrangles, Nevada; Bulletin of the Geological Society of America, v. 50, p. 1573-1624.

Pelletier, B.R.
1964: Triassic stratigraphy of the Rocky Mountain Foothills between Peace and Muskwa Rivers, northeastern British Columbia; Geological Survey of Canada, Paper 63-33.

Springer, G.D., MacDonald, W.D. and Crockford, M.B.B.
1964: Jurassic: in Geological History of Western Canada; Alberta Society of Petroleum Geologists, p. 137-155.

Stott, D.F.
1967: Fernie and Minnes strata north of Peace River, Foothills of northeastern British Columbia; Geological Survey of Canada, Paper 67-19 (Part A).

Thompson, R.I.
1978: Geology of Halfway River Map-area; Geological Survey of Canada, Open File 536.

Tozer, E.T.
1965: Upper Triassic ammonoid zones of the Peace River Foothills, British Columbia, and their bearing on the classification of the Norian Stage; Canadian Journal of Earth Sciences, v. 2, p. 216-226.

1967: A Standard for Triassic time; Geological Survey of Canada, Bulletin 156.

1979: Latest Triassic ammonoid faunas and biochronology, Western Canada; in Current Research, Part B, Geological Survey of Canada, Paper 79-1B, p. 127-135.

1980: Latest Triassic (Upper Norian) ammonoid and **Monotis** faunas and correlations; Rivista Italiana di Paleontologia e Stratigrafia, v. 85, p. 843-876.

Westermann, G.E.G.
1962: Succession and variation of **Monotis** and the associated fauna in the Norian Pine River Bridge Section, British Columbia (Triassic, Pelecypoda); Journal of Paleontology, v. 36, p. 745-792.

Westermann, G.E.G. and Verma, H.
1967: The Norian Pine Ridge Bridge Section, British Columbia, and the Succession of **Monotis**; Journal of Paleontology, v. 41, p. 798-803.

58. HYDRAULIC PERMEABILITY DIFFERENCES BETWEEN GRANITES FROM THE LAC DU BONNET (MANITOBA) AND EYE-DASHWA (ONTARIO) PLUTONS, RELATED TO TEXTURAL EFFECTS

D.C. Kamineni[1] and T.J. Katsube
Resource Geophysics and Geochemistry Division

Kamineni, D.C. and Katsube, T.J., Hydraulic permeability differences between granites from the Lac Du Bonnet (Manitoba) and Eye-Dashwa (Ontario) plutons, related to textural effects; in Current Research, Part A, Geological Survey of Canada, Paper 82-1A, p. 393-401, 1982.

Abstract

The granitic rocks from Whiteshell area (Lac du Bonnet pluton) show considerably higher permeability compared to those from Atikokan area (Eye-Dashwa pluton), particularly, at depth greater than 600 m, although they have similar mineral composition. This difference in permeability may be caused by the difference in texture between the two rock types. The quartz forms an interconnected matrix in the Whiteshell granites, whereas it forms isolated aggregates in the Atikokan granites.

Introduction

The long term safety of disposing of high-level nuclear fuel waste in deep underground caverns in Precambrian crystalline rocks is currently being assessed by the Canadian Radwaste Program (Boulton, 1978; Scott, 1980). In the assessment it is necessary to assume that the nuclear fuel waste will eventually come in contact with groundwater systems and the radionuclides will thus be transported towards the surface of the rockmass. Studies of radionuclide transport in crystalline rocks (Katsube et al., in press) suggest that the pore structure of the rocks plays an important role in controlling the transport rates. Pore structure in crystalline rocks has been studied by a number of investigators (e.g. Brace, 1977; Sprunt and Brace, 1974; Montgomery and Brace, 1975). More recently, pore structure and radionuclide transport studies were carried out by Katsube (1981), Wadden and Katsube (1981) and Katsube and Hume (1981) on granites from selected research areas on the Canadian Shield. These studies provide considerable information on pore structure in crystalline rocks and their effect on radionuclide transport. Although these studies cover a variety of crystalline rock types whose petrography has been thoroughly investigated, there is a lack of information in terms of how pore structure is related to the texture of the rocks.

Matrix permeability (k) is related to some of the pore structure parameters as follows (De Weist, 1965; Katsube et al., in press), if the effect of confining pressure is ignored:

$$k = \frac{d^2}{12}\frac{\phi}{\tau^2} \qquad (1)$$

d = fracture aperture

ϕ = porosity

τ = tortuosity

It has been noted that the matrix permeabilities (k) of similar granites from the Lac du Bonnet batholith, Manitoba, and the Eye-Dashwa lakes pluton, Ontario, show considerable differences. It has also been noted that certain textural variations accompany these differences. Some preliminary results pertaining to the relationship between pore structure and texture are discussed in this paper.

Geological Setting and Petrography

The Lac du Bonnet batholith, Manitoba and Eye-Dashwa lakes pluton, Ontario, are located in the Superior Province of the Canadian Shield and of Kenoran age (2500 Ma, Stockwell, 1964). Core samples from various depths have been collected from boreholes drilled in the Whiteshell and Atikokan research areas.

Various physical properties have been measured (e.g. Katsube, 1981; Annor and Geller, 1979a,b) and a number of petrographic studies (e.g. Kamineni and Dugal, 1981; Chernis, in press) have been carried out on adjoining pieces of core samples. Results of the hydraulic permeability and immersion porosity measurements, and some of the petrographic analysis are used in this study. Additional petrographic analysis of selected samples has also been carried out by the writers.

The principal rock type in both research areas is granite, and all samples selected for this study can be classified under this term, based on the classification of Streckeisen (1976). The samples selected represent two groups of granitic rocks that show differences in terms of texture and mineralogy. In addition, within each group there are some variations that were developed by secondary processes, such as alteration. The altered rocks in both groups display pink colour. Both Whiteshell and Atikokan samples are inequigranular and porphyritic with phenocrysts of potash and plagioclase feldspars. In some Atikokan samples quartz is also present as phenocrysts.

Modal volume per cent of minerals in the selected samples investigated by the writers by petrographic analysis is shown in Table 58.1. The analysis was carried out on two thin sections from each sample cut perpendicular to one another (PG 1 and PG 2 sections are oriented perpendicular and parallel to the core, respectively). About 2000 point counts were made on each thin section.

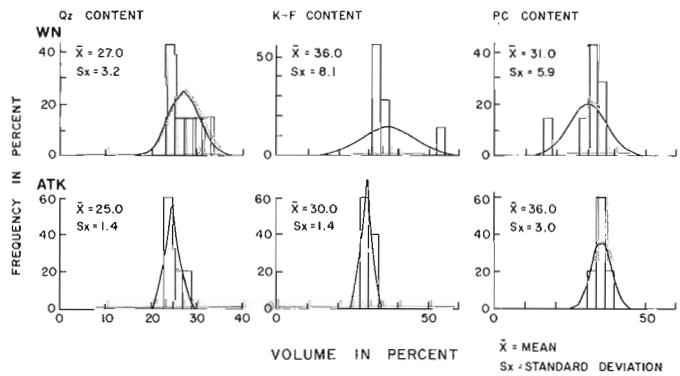

Figure 58.1. *Histograms of the modal volume per cent for the major minerals in samples from Lac du Bonnet (WN) and Eye-Dashwa (ATK) granites.*

[1] Atomic Energy of Canada Limited

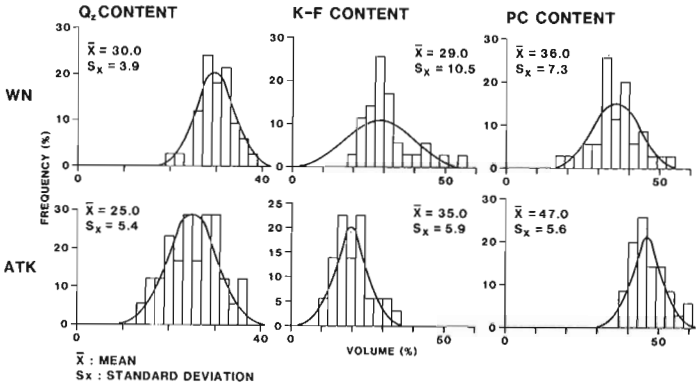

Figure 58.2. Histograms of the modal volume per cent for the major minerals in samples from Lac du Bonnet (WN) and Eye-Dashwa (ATK) granites, based on the study by Chernis (in preparation).

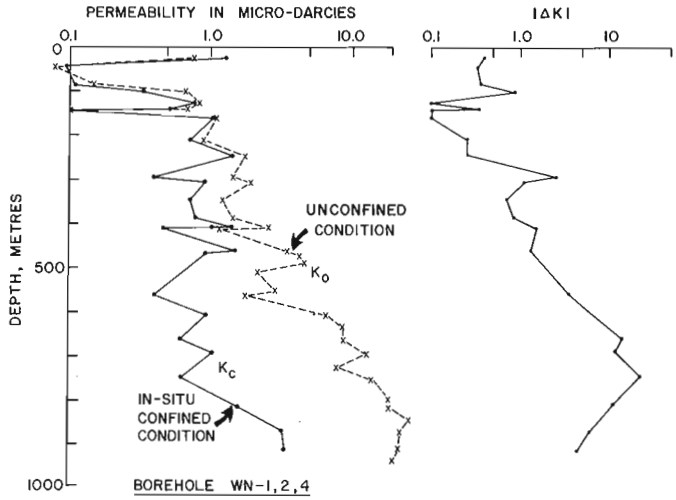

Figure 58.3. Permeability under in situ confining pressure (kc) and unconfined pressure (ko) down a borehole in the Lac du Bonnet batholith (after Katsube, 1981).

Histograms of the modal volume per cent for the major minerals (quartz, potash-feldspar, plagioclase) in the sample sets from Whiteshell and Atikokan are shown in Figure 58.1. This figure shows that the standard deviation for each mineral differs to a certain extent between the two sample sets, but the difference in the mean volume per cent values for each mineral is under 6 per cent. Histograms of a similar study by Chernis (in press) carried out on the same samples (34 samples from WN and 35 from ATK) including selected samples (7 from WN, 5 from ATK) is shown in Figure 58.2. The mean values for quartz is very similar to the writers, but the mean value for potash feldspars and plagioclase differ markedly. An examination of the model volume per cent values produced by Chernis (in preparation) on the same samples as the writers selected samples show similar trends as the mean values illustrated in Figure 58.2. Therefore the slight difference observed between the writers' analysis and that by Chernis (in preparation) is attributed to the difference in the accuracy of the modal analysis: about 2000 point counts for each selected sample and 500-1000 point counts for those shown in Figure 58.2. In conclusion, the granites from both Whiteshell and Atikokan areas show considerable similarities in their major mineral content.

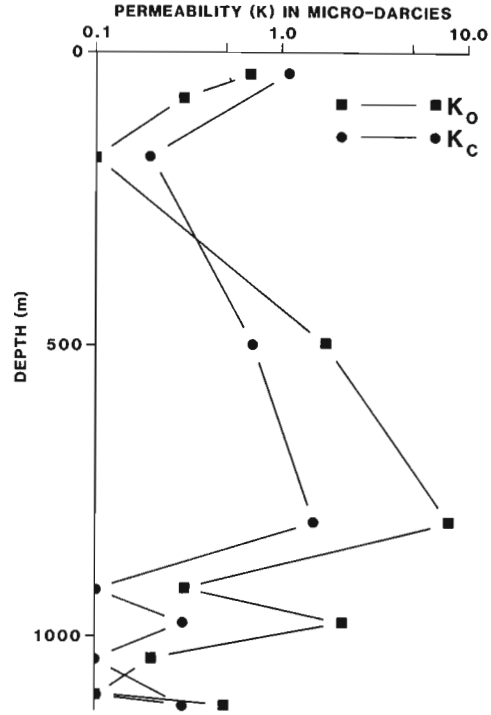

Figure 58.4. Permeability under in situ confining pressure (kc) and unconfined pressure (ko) down borehole ATK-1, in the Eye-Dashwa batholith.

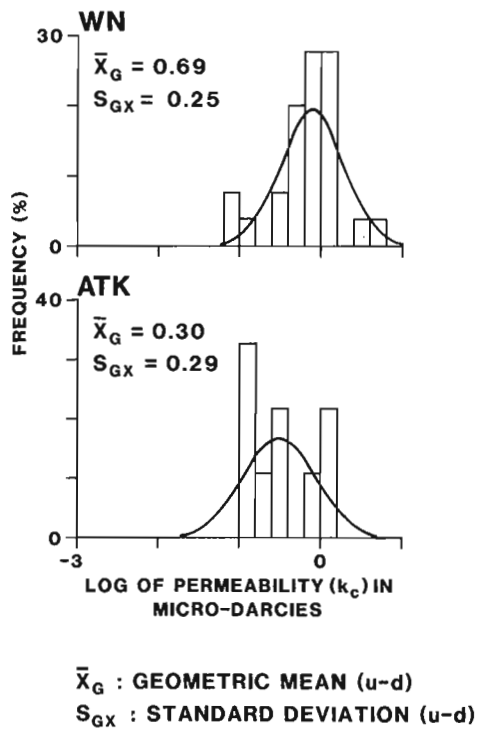

Figure 58.5. Histograms for permeabilities measured under in situ confining pressures (kc) for granites from Lac du Bonnet batholith (WN) and Eye-Dashwa batholith (ATK).

Hydraulic Permeabilities

The hydraulic permeability (k) of these core samples was carried out by Terratek (Cooley et al., 1981). Hydraulic permeability is usually determined by flow rates through a rock sample under a constant hydraulic gradient. However, since the hydraulic permeability for these granites is extremely low (Katsube, 1981), it has been necessary to use the transient method of measurement that was developed by Brace et al. (1968). In this study results on 32 samples from Whiteshell area and 10 samples from Atikokan area were used. Two measurements were made for each sample: one (ko) under a confining pressure of 1.4 MPa and to simulate surface pressure conditions and the other (kc) under a confining pressure equivalent to its in situ condition.

The hydraulic permeabilities with depth for both areas are shown in Figures 58.3 and 58.4. The hydraulic permeability measured under the in situ confining pressure (kc) shows little change with depth for both Whiteshell and Atikokan areas. The hydraulic permeability measured under the constant confining pressure (ko) of 1.4 MPa shows a continuous increase in depth for Whiteshell area, but stays at a generally low level for Atikokan area. The hydraulic permeability histogram for kc for both areas is shown in Figure 58.5. Note how similar the two means (X) and standard deviations (Sx) are for the two areas. The histograms for ko for all samples from both areas are shown in Figure 58.6. The differences seen between the curves of ko versus depth for both areas (Fig. 58.3, 58.4) are reflected in this diagram. The mean value for ko for Whiteshell is 6.3 (log 6.3-0.8) times that for Atikokan. The histogram for ko samples taken only from depth greater than 600 m in both areas is shown in Figure 58.7. This shows that the mean value for ko for these samples from Whiteshell is 20 times that for the mean value for the similar samples from Atikokan.

The distribution for kc shown in Figures 58.3, 58.4 and 58.5 suggest that the in situ hydraulic permeabilities of the rock matrix show little variation with depth and area. This trend coincides very well with those of the rock type and major mineral contents. When rocks are brought to surface from depth, it is known that they expand due to pressure release. This is confirmed by Annor and Geller (1979a,b) for Whiteshell samples. Katsube (1981) indicates that granite rocks from depth in Whiteshell tend to show an increase in pore size for the micropores (poresize: 0.063-2.5 μm) and a forming of new intermediate pores (0.025-0.063 μm). This is related to the increase of ko with depth that is seen in Figure 58.3. It is very interesting that a similar trend for ko for the Atikokan samples cannot be seen (Figure 58.4). Unfortunately, mechanical property data and pore structure studies similar to those produced by Annor and Geller (1979a,b) and Katsube (1981) do not exist for the Atikokan samples. Therefore, it is currently impossible to predict what type of physical changes with pressure release take place, if any, in the pores of the Atikokan samples. However, it is concluded that the difference seen between the trends for ko versus depth for Whiteshell and Atikokan do not coincide with changes in rock types and major mineral contents and thus the reason for this difference must be sought in areas other than major mineral content or rock type. The effect of pressure release could have a significant effect on the long term stability of poreshape, particularly in the vicinity of the subsurface vault for storing the nuclear fuel waste.

Textural Analysis

Quartz, potash feldspar and plagioclase are the essential mineral constituents in granitic rocks. The distribution and arrangement of these minerals can give rise to various textural features. Textures displaying random and

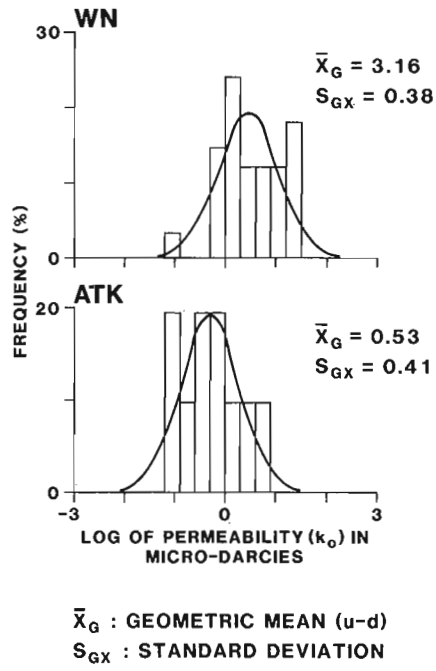

Figure 58.6. *Histograms for permeabilities measured under unconfined pressure (ko) for granites from Lac du Bonnet (WN) and Eye-Dashwa batholith (ATK).*

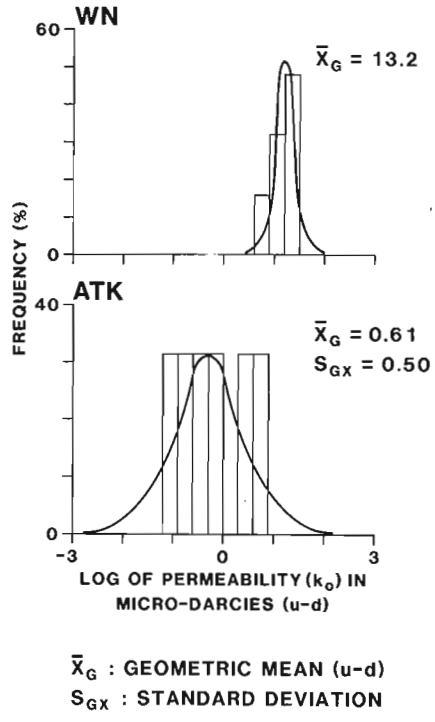

Figure 58.7. *Histograms for permeabilities of granites only from depth greater than 600 m.*

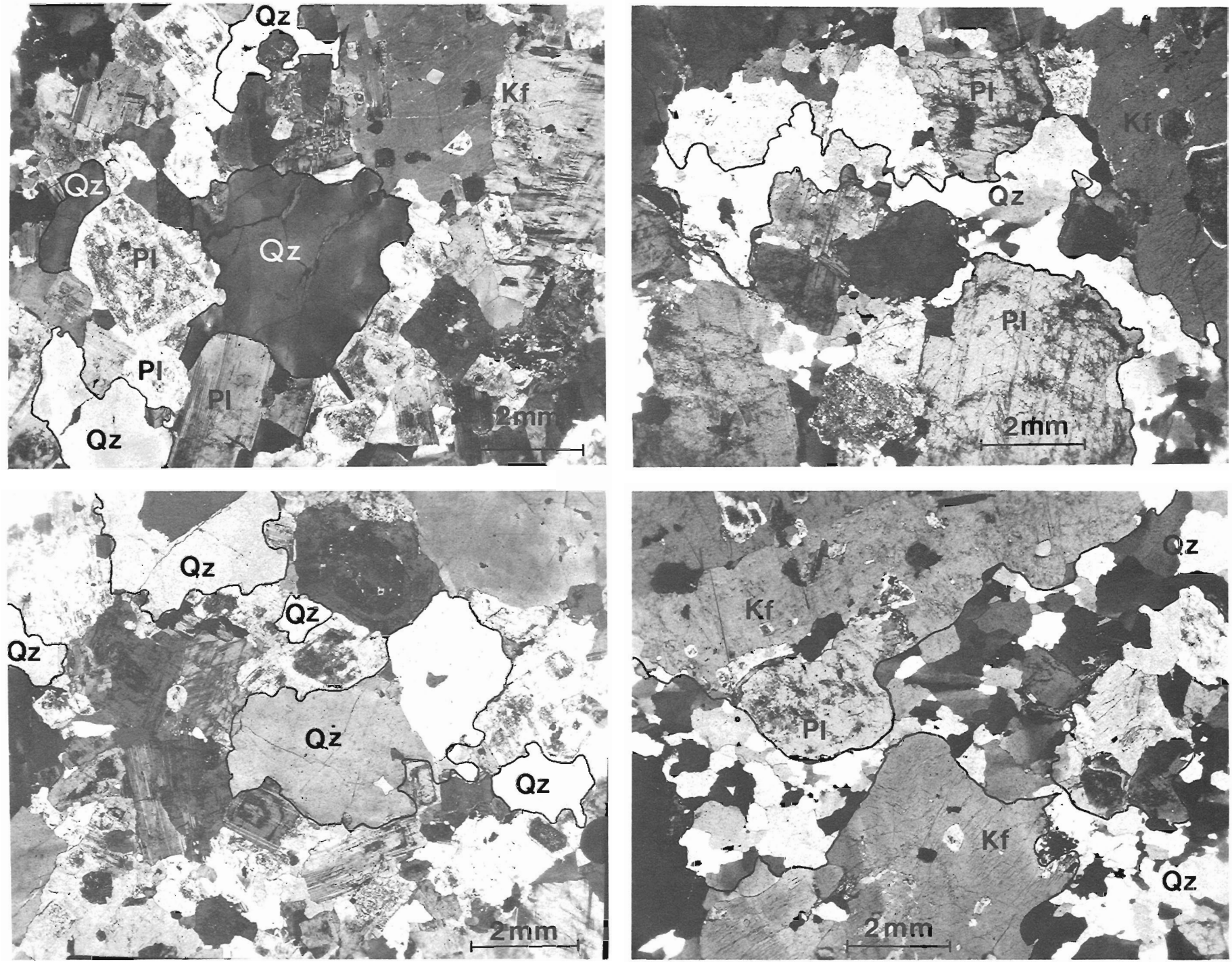

a. Top left WN 138.4 m and top right WN 345 m. Bottom left ATK-79.2 m and bottom right 320.5 m. (GSC 202751-A,E,G)

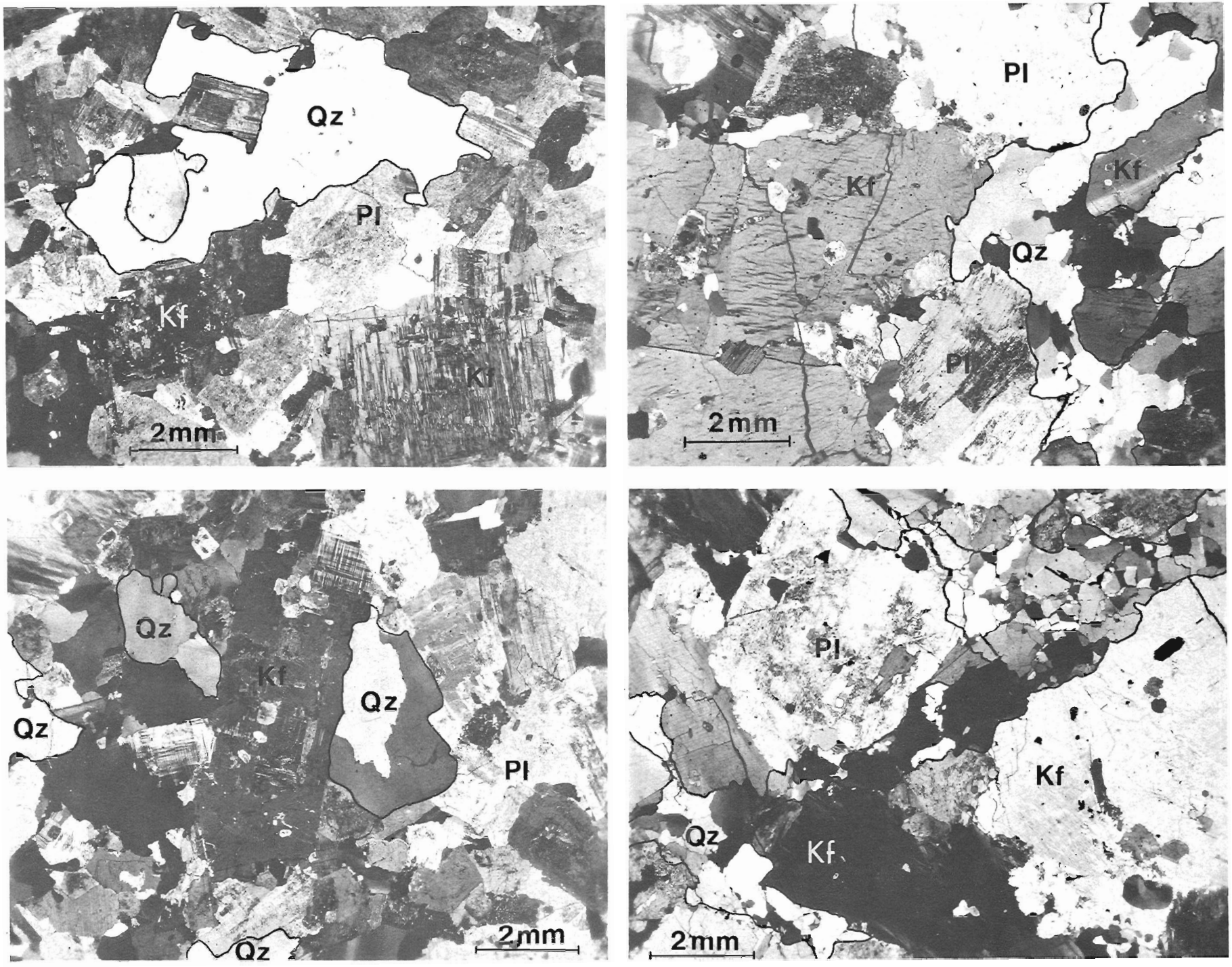

b. Top left WN 692 m and WN 906 m. Bottom left ATK-601 m and WN 923 m. (GSC 202751-D,F,H,I)

Figure 58.8. *Photomicrographs (crossed nicols) of some typical Whiteshell and Atikokan samples on which permeabilities were measured.*

Table 58.1

Modal Analyses (Percentage by Volume)

Sample No.	Quartz	Potash Feldspar	Plagio-clase	Biotite	Horn-blende	Epidote	Chlorite	Muscovite	Sphene	Carbonate	Opaques	Total
WN1 160 PG1	23.4	35.9	32.1	4.8	-	0.5	0.8	1.7	-	-	0.8	100
WN1 160 PG2	25.0	36.7	30.5	4.3	-	0.4	0.8	1.2	-	0.3	0.8	100
WN1 303 PG1	28.3	34.2	32.1	2.1	-	0.4	0.6	1.2	-	0.5	0.6	100
WN1 303 PG2	29.8	32.4	31.5	2.4	-	0.4	0.7	1.5	-	0.5	0.8	100
WN1 384 PG1	24.6	31.7	36.4	3.5	-	0.2	0.8	1.8	-	0.4	0.6	100
WN1 384 PG2	25.8	33.7	34.0	2.6	-	0.3	0.7	1.8	-	0.5	0.7	100
WN1 460 PG1	32.1	32.8	31.0	1.8	-	0.3	0.4	0.9	-	0.2	0.5	100
WN1 460 PG2	33.5	31.0	32.1	2.1	-	0.2	0.5	0.6	-	0.2	0.4	100
WN4 692 PG1	29.5	33.9	30.1	3.6	-	0.5	0.5	1.5	-	-	0.4	100
WN4 692 PG2	30.4	34.7	29.4	2.2	-	0.5	0.6	1.7	-	-	0.5	100
WN4 863 PG1	24.2	54.5	18.5	1.2	-	0.2	0.4	0.8	-	-	0.2	100
WN4 863 PG2	29.2	49.3	19.1	1.0	-	0.2	0.4	0.6	-	-	0.2	100
WN4 906 PG1	26.3	32.3	35.5	4.3	-	0.1	0.3	0.8	-	-	0.4	100
WN4 906 PG2	28.2	35.1	30.2	4.6	-	0.2	0.6	0.7	-	-	0.5	100
ATK1 39 PG1	27.1	28.6	36.5	3.6	0.6	1.0	0.2	0.8	0.5	0.3	0.8	100
ATK1 39 PG2	28.3	27.7	36.0	3.8	0.8	0.9	0.4	0.6	0.4	0.2	0.9	100
ATK1 79 PG1	24.2	29.2	39.8	2.3	0.6	0.8	0.6	1.0	0.7	0.2	0.6	100
ATK1 79 PG2	24.8	31.6	38.4	1.5	0.2	0.5	0.7	0.7	0.6	0.2	0.6	100
ATK1 923 PG1	23.4	31.8	35.9	2.7	0.7	1.9	0.9	1.0	0.6	0.2	0.9	100
ATK1 923 PG2	24.7	31.9	34.0	2.9	0.3	2.5	0.8	1.1	0.6	0.2	0.8	100
ATK1 979 PG1	25.2	31.3	34.6	2.8	2.6	0.8	0.2	0.5	1.0	0.1	0.9	100
ATK1 979 PG2	24.1	33.2	34.7	2.6	2.1	0.9	0.1	0.4	0.9	0.2	0.8	100
ATK1 1120 PG1	24.3	29.6	31.4	-	-	5.9	4.8	2.1	1.5	-	1.0	100
ATK1 1120 PG2	23.8	30.0	32.7	-	-	5.1	4.3	1.8	1.9	-	0.8	100

weak to strong preferred orientation of mineral grains are usually present. The preferred orientation of mineral grains occurs during crystallization (flow fabric) and/or subsequent to solidification (tectonic fabric). Therefore, even though the samples from Whiteshell and Atikokan are of similar rock type and show little differences in mineral composition, texturally they show significant differences.

Results of textural analysis show that the granitic rocks from the two research areas exhibit contrasting textural characteristics. Photomicrographs of five samples from each area taken at different depth are shown in Figure 58.8. In the rocks from Whiteshell area, the feldspar phenocrysts are commonly enveloped by quartz grain aggregates. A detailed sketch of sample WN 4-901 PG 2 is shown in Figure 58.9a. Quartz surrounds feldspars and forms a continuous band defining a weak foliation. It is obvious that the quartz grain aggregates show larger "aspect ratios" compared to the feldspar phenocrysts and form the matrix in the Whiteshell samples. In contrast, the quartz grain aggregates in the Atikokan samples (Fig. 58.8) do not envelop the feldspar phenocrysts and no visible foliation is present. The "aspect ratio" of these aggregates are smaller than those in the Whiteshell rocks and quartz does not form the matrix in the Atikokan samples. A detailed sketch of sample ATK 1-923 PG 2 is shown in Figure 58.9b.

The quartz grains in the samples from Whiteshell area display numerous subgrains and in some sections they show dimensional orientation giving rise to "ribbon structure". The quartz grains enveloping the feldspar phenocrysts and the long axes of the finer quartz matrix and coarse feldspar phenocrysts tend to be parallel to one another. The quartz grains around feldspar phenocrysts appear to have been affected by pressure solution which is indicated by their intrusion into feldspar grains as shown in Figure 58.10. In contrast, the quartz grains in the rocks from Atikokan area contain deformational bands and often show recrystallization features as indicated by development of mosaics of fine quartz grains around larger grains as seen in Figure 58.11. No dimensional orientation of quartz is visible in these samples.

Textural and mineralogical differences due to alteration can also be seen between the Whiteshell and Atikokan granites. However, this subject is complex and will be dealt with in a subsequent paper.

Texture and Permeability Relationship

Regardless of the similarities that exist in rock type and mineral content between the Whiteshell and Atikokan rocks, there is a considerable difference in hydraulic permeability of the rocks from the two areas, and this difference coincides very well with the differences in texture related to quartz. However, the coincidence of these differences provides no proof that the variation in texture related to quartz distribution is the cause of the difference seen in the hydraulic permeability. For example, the results of electron microscope analysis of pores by Chernis (in preparation), where he finds higher porosity in plagioclase compared to quartz, would suggest that the writers should have found higher permeability in the Atikokan rocks compared to the Whiteshell rocks. It is suggested here that the pores in plagioclase may not be interconnective but

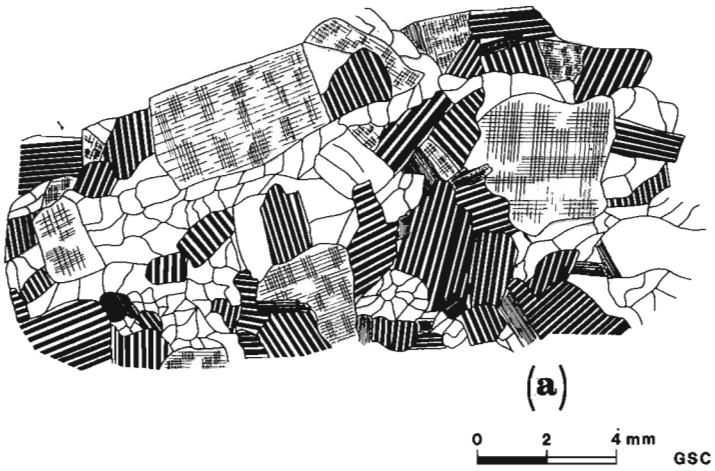

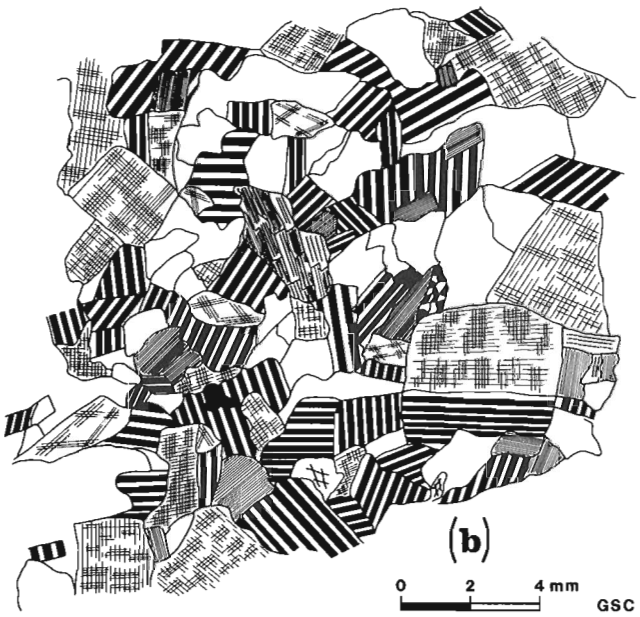

Figure 58.9. *Sketch showing the texture of (a) Lac du Bonnet granite (WN 901 m) and (b) Eye-Dashwa lakes granite (ATK 923 m). Cross hatched grains potash feldspar; twinned grains plagioclase and colourless grains quartz.*

merely storage type without significant contribution towards permeability. On the other hand the small pores in quartz are of interconnective type and thus facilitate permeability. In addition, alteration may be having an effect on the permeability differences.

Contrary to these arguments there are a number of facts that could be supportive of the view that the quartz related texture is the dominant factor in determining the hydraulic permeability of the rocks. For example, Katsube (1981) indicates that the immersion porosity is representative of the connecting pore system. The immersion porosity for the Whiteshell and Atikokan rocks are very similar, as shown in Figure 58.12. In addition, the electron micrographs in the papers by Katsube et al. (in press) and Katsube (1981) suggest that the pores in quartz are less tortuous and less complex as compared to those in plagioclase. This tortuosity and complexity could be the most important factor in determining the hydraulic permeability (see Katsube et al., in press).

Conclusion

The rock samples from Whiteshell and Atikokan research areas are very similar in terms of lithological character and major mineral content. Yet the hydraulic permeability measured at near surface conditions for the samples from the two areas show considerable differences, with the Whiteshell samples showing an average of 6.3 times higher than the Atikokan samples. For rocks taken from depths greater than 600 m, the Whiteshell samples show a hydraulic permeability of as much as 20 times that of the Atikokan samples. This difference coincides very well with the difference seen between the texture related to the distribution of quartz in the samples. The Whiteshell rocks display a quartz matrix with quartz grain aggregates surrounding feldspar phenocrysts. The quartz grains in the Atikokan rocks display isolated aggregates and do not show any continuous features. In other words, quartz does not form a matrix in the Atikokan samples.

Although the rocks with quartz matrix are those that show the higher hydraulic permeability values, it is not known whether the quartz matrix is the only cause for the higher permeability. There are, certain indications however that quartz is the cause, since aggregates of this mineral appear to show less tortuous and less complex pore structure compared to feldspars. Further studies including electron microscope analysis is required on this subject.

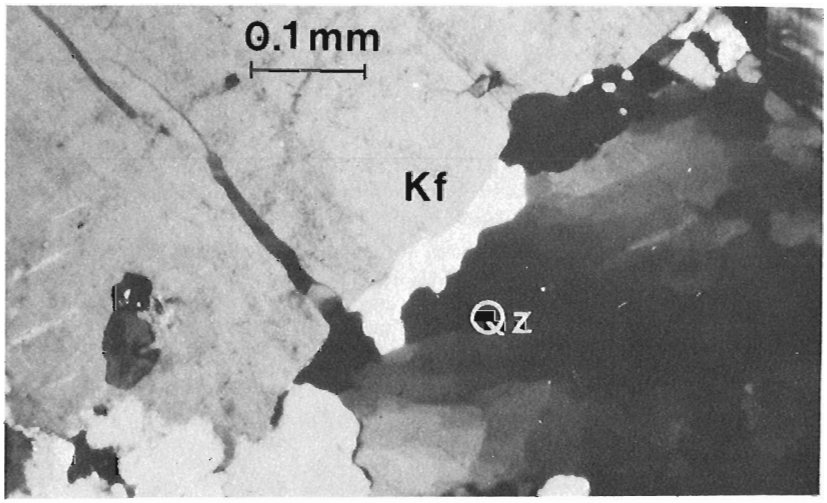

Figure 58.10

Photomicrograph of Lac du Bonnet granite showing inequigranular texture. Note quartz mosaics and intrusion of quartz into feldspar due to pressure solution. (GSC 202671-A)

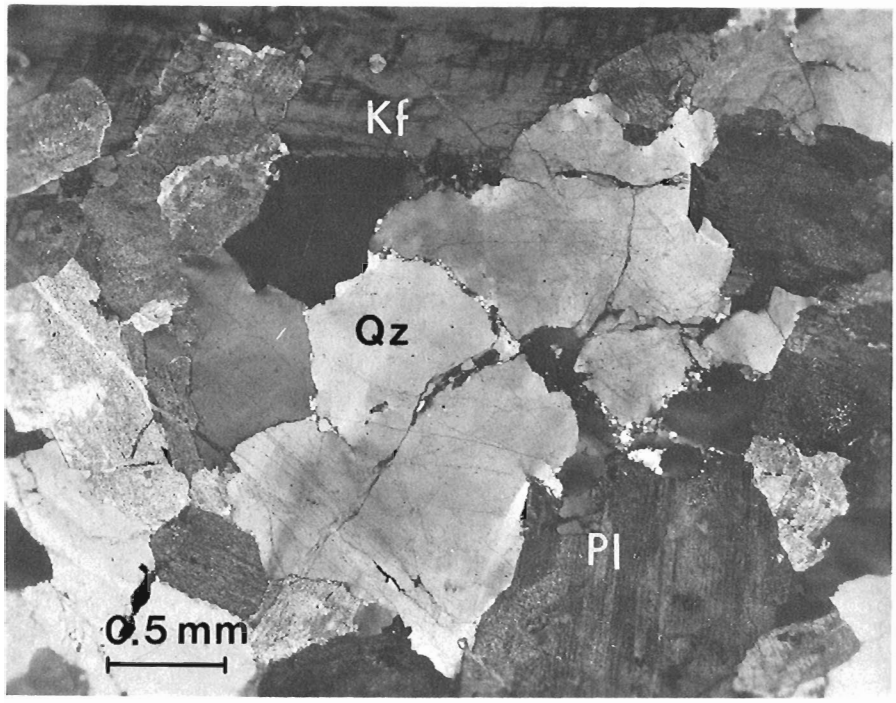

Figure 58.11

Photomicrograph of Atikokan granite. GSC 203555

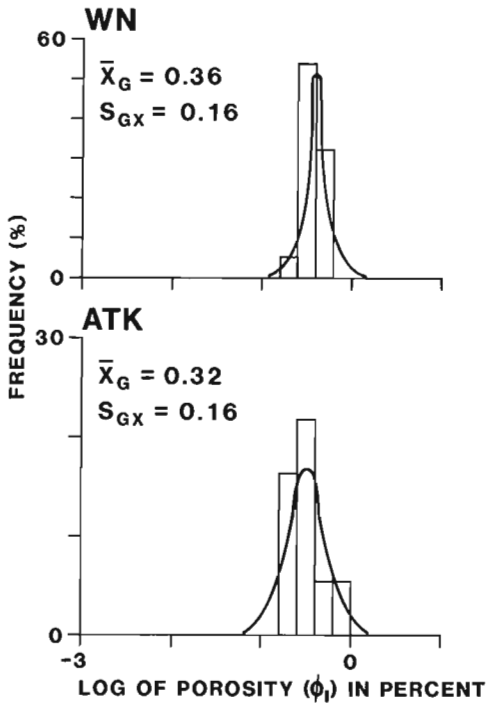

Figure 58.12. *Histograms of immersion porosities of granite samples from Lac du Bonnet (WN) and Eye-Dashwa batholiths.*

Acknowledgments

Miss M. Vladut (summer student, University of Ottawa) is responsible for all the statistical analysis provided in this paper. Grateful thanks are due to B.V. Sanford, K.L. Currie and Dr. W.F. Brace for critical reading and encouragement. Thanks are expressed to G.E. Larocque for his general guidance in the program.

References

Annor, A. and Geller, L.
1979a: Dilatational velocity, Young's modulus, Poisson's ratio, uniaxial compressive strength and Brazilean tensile strength for WN 2 samples; CANMET-Mining Research Laboratories Technical Data 303410-M01/78.

1979b: Dilatational velocity, Young's modulus, Poisson's ratio, and uniaxial compressive strength for WN 1 samples; CANMET-Mining Research Laboratories, Technical Data 303410-M03-78.

Boulton, J. (editor)
1978: Management of Radioactive Fuel Wastes: The Canadian Disposal Program; Atomic Energy of Canada Limited Report, AECL-6374.

Brace, W.F.
1977: Permeability from resistivity and pore shape; Journal of Geophysical Research, v. 82, no. 23, p. 3343-3349.

Brace, W.F., Walsh, J.B., and Frangos, W.T.
1968: Permeability of granite under high pressure; Journal of Geophysical Research, v. 73(6), p. 2225-2236.

Chernis, P.J.
Scanning electron microscope study of the pore structure of a granite sample from Pinawa, Manitoba. (in press)

Cooley, C.H., Paterson, P.E., and Butters, S.W.
1981: Permeability water in granitic rocks in support of Canadian Nuclear Waste Isolation Program; in Katsube and Hume (1981). (in prep.)

De Weist, R.J.M.
1965: Geohydrology, New York, John Wiley and Sons Inc.

Katsube, T.J.
1981: Pore structure and pore parameters that control the radionuclide transport in crystalline rocks. Proceedings of the Technical Program, International Powder and Bulk Solids Handling and Processing. Rosemont Ill. May 12-14, p. 394-409.

Katsube, T.J. and Hume, J.P.
1981: Pore parameters that control the physical retardation of nuclear fuel waste flow. In preparation for publication.

Katsube, T.J., Wadden, M.M., and Chernis, P.J.
Isolation of nuclear waste by the intact rock mass. Submitted for publication in the Canadian Journal of Earth Sciences. (in press)

Kamineni, D.C. and Dugal, J.J.B.
Alteration of the Eye-Dashwa Lakes Pluton, A Preliminary Report and Interpretation; Atomic Energy of Canada Limited, Technical Report.

Montgomery, C.W. and Brace, W.F.
1975: Micropores in plagioclase; Contributions to Mineralogy and Petrology, v. 52, p. 17-28.

Scott, J.S.
1980: EMR program for geological disposal of High-Level Radioactive Wastes; Geological Survey of Canada, Paper 79-10, p. 13-20.

Sprunt, E. and Brace, W.F.
1974: Direct Observation of Microcavities in Crystalline Rocks; International Journal of Rock Mechanics and Mining Science, v. 11(4), p. 139-150.

Stockwell, C.H.
1964: Fourth report on structural provinces, orogenic and tectonic classification of the Canadian Precambrian Shield; Geological Survey of Canada, Paper 64-17, p. 1-21.

Streckeisen, A.
1976: To each plutonic rock its proper name; Earth Science Reviews, v. 12, p. 1-33.

Wadden, M.M. and Katsube, T.J.
1981: Radionuclide diffusion rates in crystalline rocks. Accepted for publication in the Proceedings of the Joint Annual Meeting of GAC-MAC-CGU, May 11-13.

SCIENTIFIC AND TECHNICAL NOTES
NOTES SCIENTIFIQUES ET TECHNIQUES

OGILVIE MOUNTAINS PROJECT, YUKON; PART A: A NEW REGIONAL MAPPING PROGRAM

Project 800022

R.I. Thompson and C.F. Roots[1]
Cordilleran Geology Division, Vancouver

Introduction

The Ogilvie Mountains Project is a long term regional mapping program, initiated in 1981, to provide comprehensive maps accompanied by detailed stratigraphic and structural analyses for Dawson (116 B,C), Larsen Creek (106 D) and Nash Creek (106 C) map areas (Fig. 1).

The stratigraphic theme of this report reflects our 1981 effort to establish a stratigraphic framework for the north-central part of the Dawson map area (116 B,C). Special attention was directed toward the description of volcanic assemblages, preparatory to assessing the role of volcanism during the evolution of the region (see Roots, 1982).

Our results build on the excellent geologic framework provided by Green (1972).

Regional Framework

The Dawson map area contains two stratigraphic assemblages that represent the westward extension of the Selwyn Basin and Mackenzie Platform, respectively (Fig. 1, 2). On the south is a basinal assemblage dominated by clastic and volcanic rocks ranging in age from Late Proterozoic (Windermere Supergroup) to Cretaceous; on the north is a shelf assemblage dominated by shallow water carbonate rocks ranging from the Middle Proterozoic(?) through to the Late Paleozoic. The two assemblages are separated by the Dawson Fault, a northward directed thrust (Fig. 3).

Both assemblages were foreshortened early in the Mesozoic when a complex plutonic-volcanic arc was welded onto the continental margin. Remnants of this arc are represented in the Dawson map area by the Yukon cataclastic terrane south of Tintina Fault (Tempelman-Kluit, 1979). The combination of tight, isoclinal folds and gently south-dipping thrusts demonstrates relative northward transport of the sedimentary veneer along detachments within and/or beneath it. Evidence of earlier periods of tectonic instability is preserved in the stratigraphic record as angular unconformities, massive conglomerate, diamictite, mafic volcanic complexes, and steep north-striking faults.

The shelf assemblage within north-central Dawson map area is exposed in a broad, east-west trending anticlinorium which Green (1972) named 'Coal Creek Dome'. We have continued to use the term for reasons of familiarity, but point out that the 'Dome' resulted from lateral telescoping of shelf strata rather than upward arching of the basement as the term implies.

Stratigraphy

We are confident of the sequence of rock units described below but not of their age. There is no reference to time-stratigraphic boundaries within the shelf assemblage; sparse age data are available for the basin assemblage; and regional correlations are not attempted. The rock units described can be mapped at 1:50 000 scale; Figure 2 illustrates the stratigraphic sequence in both shelf and basin assemblages, and Figure 3 illustrates their areal distribution.

The shelf assemblage contains 12 map units comprising thick carbonates separated by thinner clastic units. The phyllitic shales and fine quartzites of unit 3, the oldest and thickest clastic succession, separates the similar orange weathering carbonates of units 2 and 4. Previously units 2 and 4 had been mapped as the same rock unit (Green, 1972). The orange dolostones of unit 4 undergo a lateral facies change westward to more carbonaceous and recessive dolostones of unit 4a. Unit 5 consists of maroon and black shales with thin beds of conglomerate, diamictite and gritty sandstone. The light grey craggy weathering dolostone of unit 6 is a thick persistent marker separated from younger carbonates by the thin (less than 50 m) recessive siltstone and shale succession of unit 7. Unit 8 consists of carbonaceous dark grey dolostone overlain unconformably by more massive, light grey, cryptalgal laminated dolostone. Unit 9 is a lenticular succession of maroon siltstone and shale overlain by massive pebble and boulder conglomerate composed of dolomite, quartzite and chert clasts. Unit 10 is a thick sequence of mafic volcanic flows, pyroclastics and volcanic debris flows restricted to the area near Mount Harper (Fig. 3; see Roots, 1982). Unit 11 is a massive, oolitic in part, light grey dolostone and unit 12 is a well layered sandy dolostone succession.

The basin assemblage contains 4 main stratigraphic elements: Upper Proterozoic grits, limestone and shale of the Windermere Supergroup (map units Ia, Ib, Ic); Upper Proterozoic – Lower Proterozoic mafic volcanic complexes (map unit II), Ordovician and Silurian siliceous shale, siltstone, chert and limestone of the Road River Formation (map unit III); and pre-Permian chert pebble conglomerate

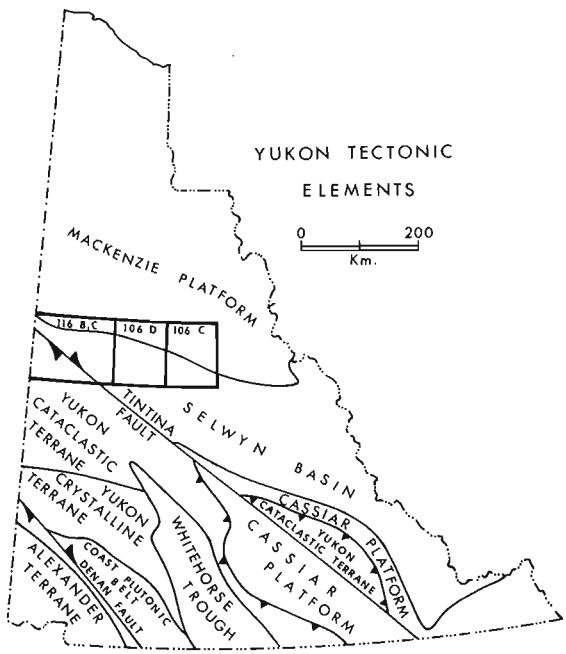

Figure 1. Map of Yukon Territory showing major tectonic elements and location of Dawson (116 B,C), Larsen Creek (106 D) and Nash Creek (106 C) map areas (modified from Tempelman-Kluit, 1979).

From: Scientific and Technical Notes in Current Research, Part A; Geol. Surv. Can., Paper 82-1A.

[1] Department of Geology, Carleton University, Ottawa, Ontario, K1S 5B9

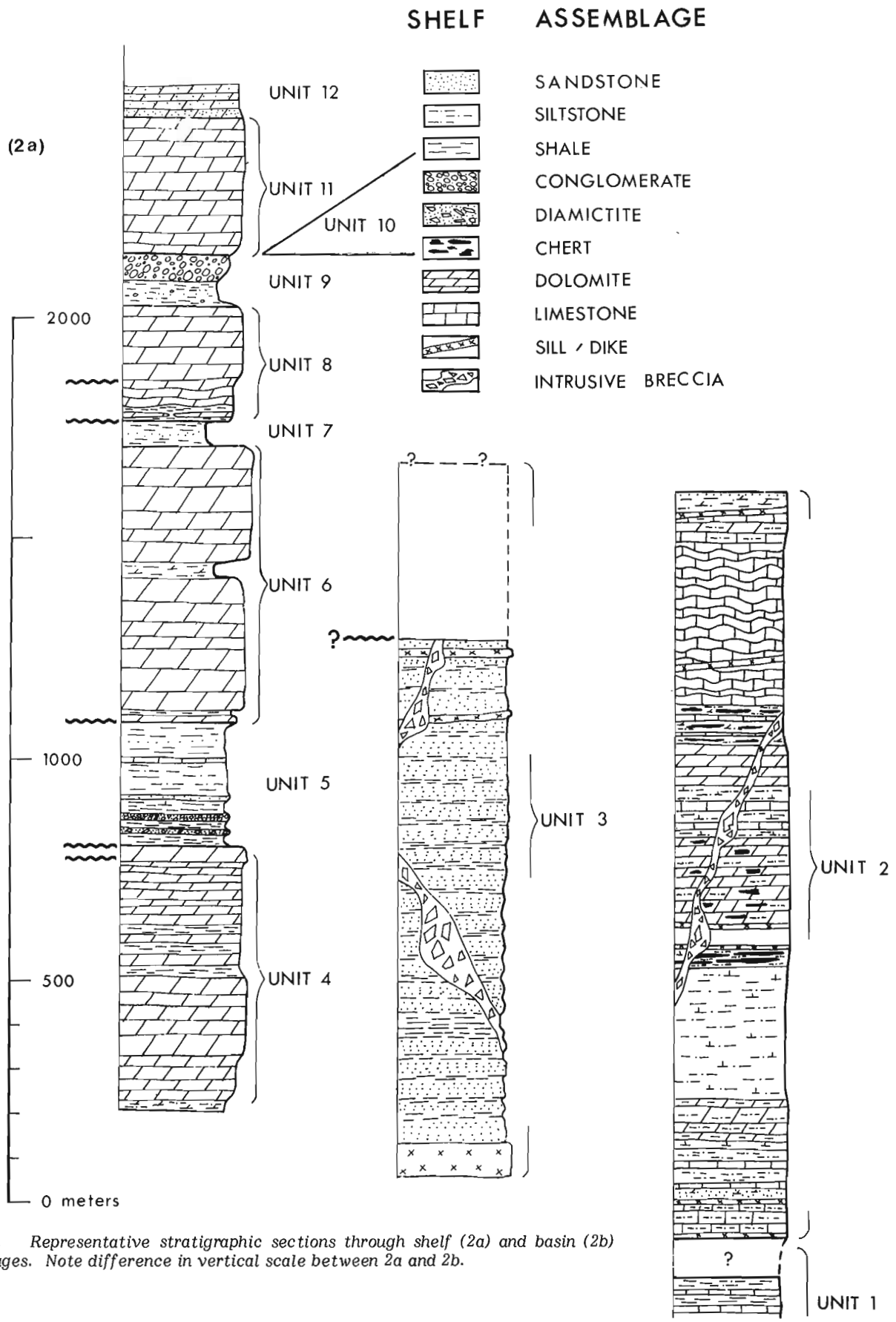

Figure 2. *Representative stratigraphic sections through shelf (2a) and basin (2b) assemblages. Note difference in vertical scale between 2a and 2b.*

BASIN ASSEMBLAGE

(EXCLUDING UNIT II VOLCANICS AND UNITS YOUNGER THAN IV)

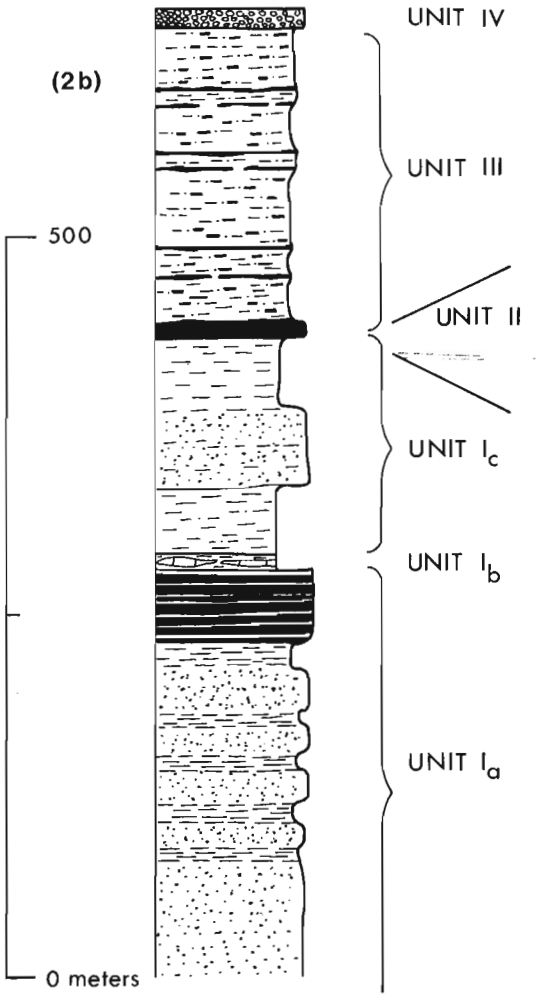

(THICKNESS OF UNIT I_c AND UNIT III APPROXIMATE: SECTION TYPICAL OF SUCCESSION AT NORTH FORK PASS)

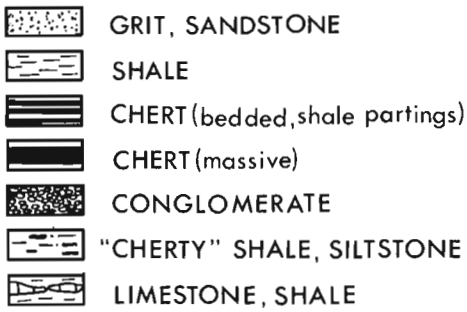

(map unit IV) that probably correlates with the 'Black Clastic Unit' (Gordey, 1978). The overlying Permian and younger rock units are described by Tempelman-Kluit (1970) and Green (1972).

Shelf Assemblage

Unit 1: Unit 1 consists of interbedded dark grey fine crystalline dolomite and black calcareous siltstone; beds are 20 to 70 cm thick. It is recessive, poorly exposed, and has a very restricted areal extent. Total thickness is unknown.

Unit 2: Unit 2 comprises medium to thick bedded orange and pinkish tan weathering limestone, dolomite and siltstone. In section 1 (Fig. 3) it consists of 2 members: 1031 m (± 100 m; base not exposed) of medium to thick bedded, flaggy dolomite, siltstone and siliceous (cherty) shale overlain by 475 m of grey thin wavy banded limestone. Farther south distinction between members is not possible, the wavy banded limestone is orange weathering and contains dolomite beds. The lower contact with unit 1 is sharp with massive light grey unit 2 dolomite against dark recessive ribbed dolomite-siltstone of unit 1; the upper contact is a gradation, 5 to 10 m thick, of orange weathering wavy banded limestone of unit 2 and green phyllite of unit 3. Unit 2 forms the northward verging core of a large anticline within the central part of the Coal Creek Dome, as well as the core of a (fault bounded?) structure on the north flank of the Dome.

Unit 3: Unit 3 is a thick Proterozoic clastic succession. Along the northern flank of the Coal Creek Dome it consists of fine grained, thin to medium bedded quartz sandstone with argillite interbeds; along the southern flank argillite and phyllite are dominant with quartzite and quartzose siltstone subordinate. The conspicuous planar bedding of the quartzites, lack of internal sedimentary features, and sharp bounding contacts suggest they are turbidites.

The thickness of this unit varies: 1800 m are estimated at section 2, and only 300 m near the headwaters of the Fifteenmile River.

Unit 3 is intruded by large heterolithic breccias crosscutting layering and cleavage. The breccias have irregular borders and contain a variety of clast sizes and types - some of which belong to the underlying unit 2.

Correlation with the Wernecke Assemblage (Eisbacher, 1981; Bell and Delaney, 1977) is suggested on the basis of lithologic similarity.

Unit 4: This unit comprises 3 members: two thin light grey weathering dolomite members bound a middle orange weathering dolomite. The middle dolomite is a distinctive map unit along the south flank of the Coal Creek Dome east of Mount Gibben but to the west it undergoes a regional facies change to unit 4a, a recessive colour banded grey laminated dolostone succession.

At stratigraphic section 3 (Fig. 3) the lower member is 129 m thick and consists of planar, laminated light grey microcrystalline dolostone; the middle member is 423 m thick and consists of orange weathering, intricately veined massive dolomite, platy thin-bedded silty dolomite and recessive noncalcareous black shale and siltstone; the upper member comprises 35 m (159 m at section 5 measured 5 km to the west) of thick bedded to massive light grey laminated birdseye dolomite with minor chert silicification.

The lower and middle members are truncated westward from Mount Gibben beneath an unconformity at the base of the upper dolomite member.

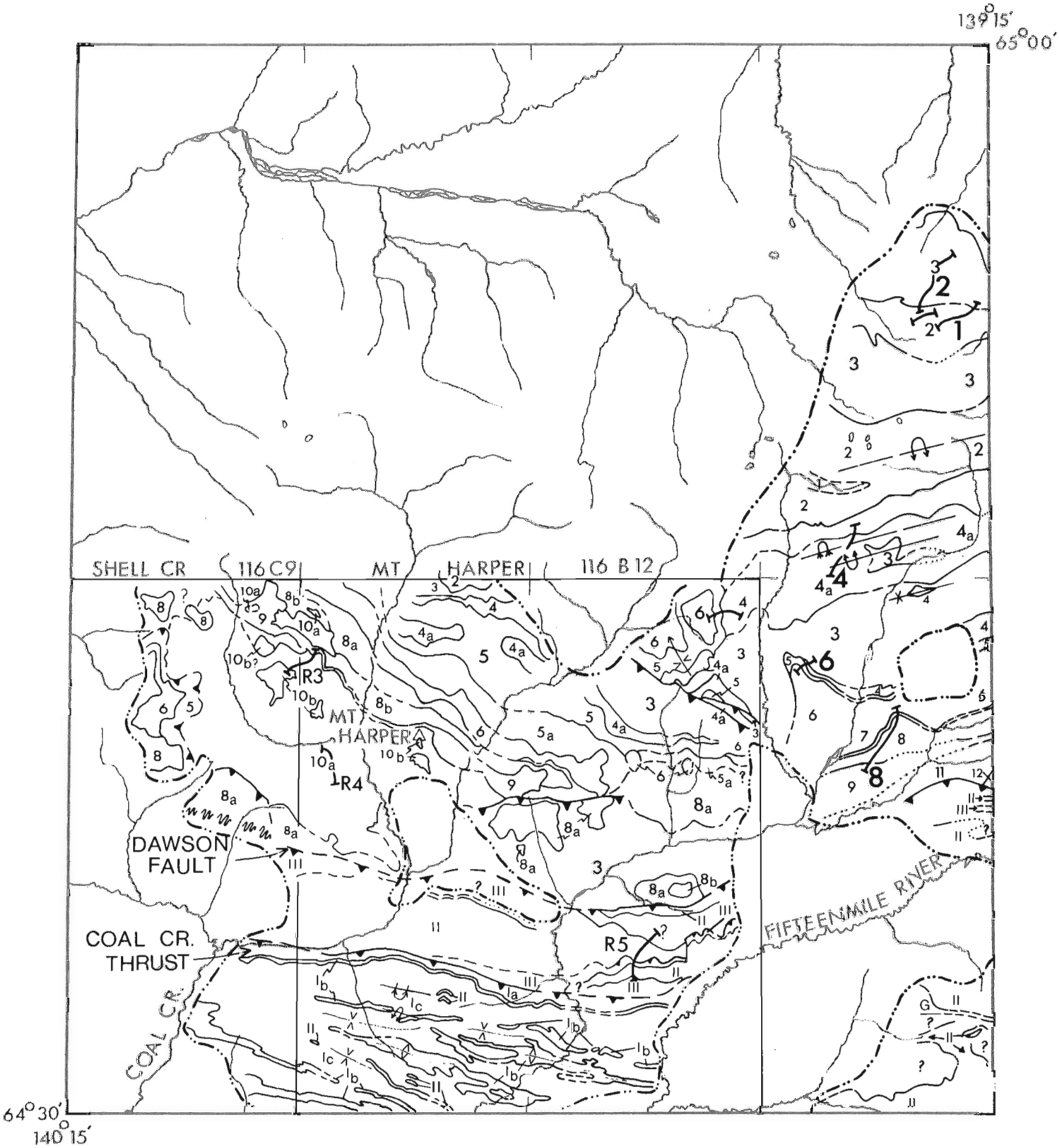

Figure 3. *Geological map of north-central Dawson map area.*

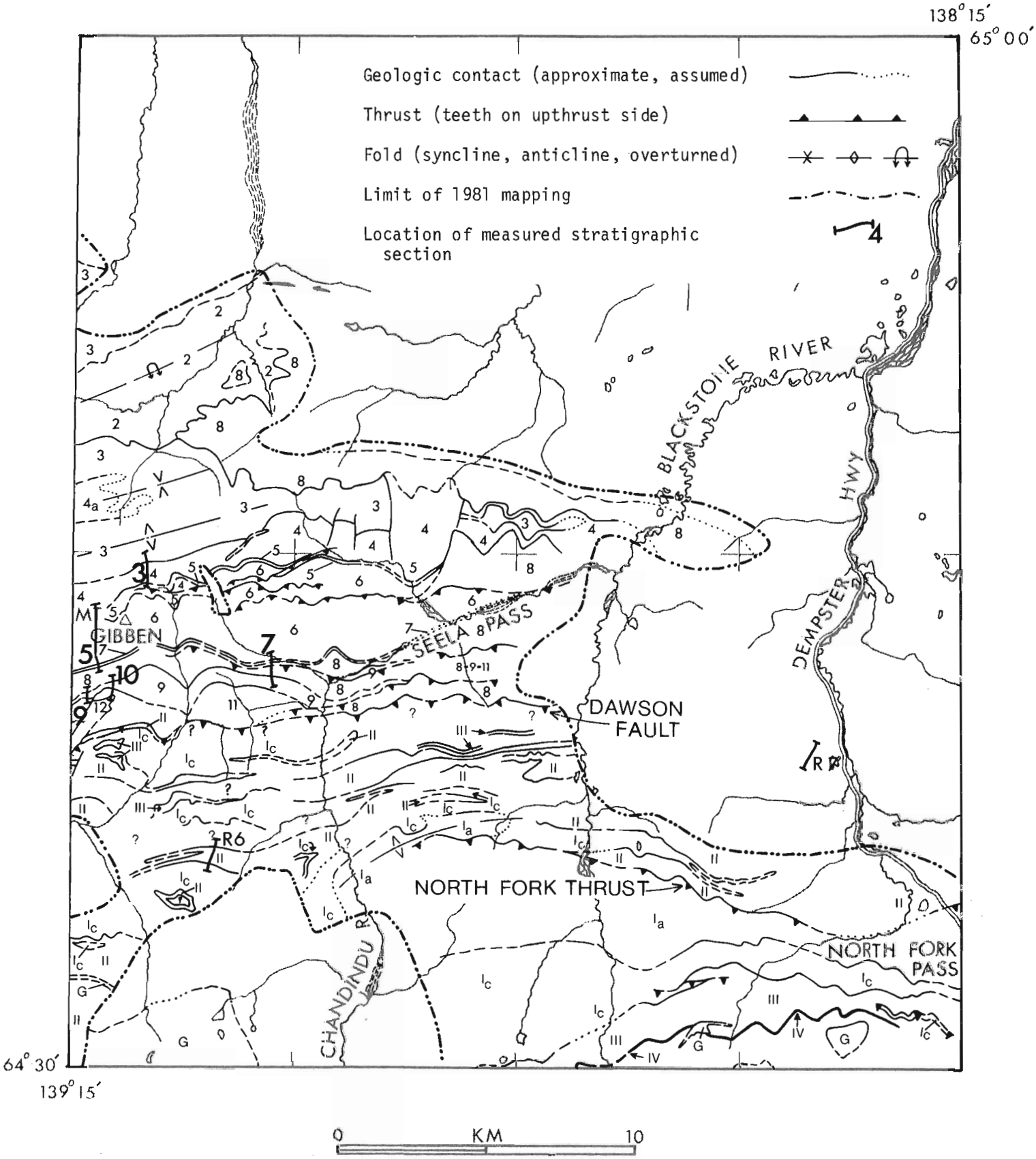
138° 15′
65° 00′
Geologic contact (approximate, assumed)
Thrust (teeth on upthrust side)
Fold (syncline, anticline, overturned)
Limit of 1981 mapping
Location of measured stratigraphic section
BLACKSTONE RIVER
DEMPSTER HWY
MT GIBBEN
SEELA PASS
DAWSON FAULT
NORTH FORK THRUST
NORTH FORK PASS
CHANDINDU R.
64° 30′
139° 15′
0 KM 10

MAP UNITS – FIGURE 3

SHELF ASSEMBLAGE

12	Silty dolomite, tan weathering; dolomitic siltstone; massive light grey dolomite
11	Dolomite, fine crystalline, oolitic, massive, light grey
10	Mt. Harper volcanic rocks
9	(9b) Conglomerate, pebble to cobble (dolomite quartzite, chert) (9a) Shale, siltstone, maroon; sandstone; conglomerate
8	(8b) Carbonaceous dolomite, dark grey, thick bedded (8a) Dolomite, light grey, fine crystalline, laminated
7	Shale, black; fine quartzite
6	Dolomite, light grey, massive, "craggy"
5	Shale, maroon, black; diamictite, thin beds; conglomerate; siltstone, quartzite
4a	Dolomite, laminated, light to medium grey; massive dolomite reefs; edgwise conglomerate stromatolites
4	Dolomite, shale interbeds, orange weathering; dolomite, light grey, massive, forms base and top
3	Phyllitic shale; fine quartzite; intrusive breccia
2	Limestone, wavy banded; dolomite; silty dolomite; cherty shale; intrusive breccia
1	Dolomite, dark grey, carbonaceous; siltstone, carbonaceous

BASIN ASSEMBLAGE

IV	Chert pebble conglomerate, black, argillaceous matrix
III	"Cherty" shale, siltstone; black chert
II	Volcanic rocks
Ic	Shale, maroon and green; siltstone; sandstone
Ib	Limestone, light grey, fine crystalline, discontinuous
Ia	Grit; sandstone; shale; bedded chert at top
G	Granitoid rock; unspecified

The basal contact is gradational, the upper contact sharp and probably unconformable.

Unit 4a: Unit 4a is interpreted as a lateral facies equivalent of unit 4. It rests on unit 3, is 810 m thick (at stratigraphic section 4) and consists of medium to thick bedded grey crystalline dolomite. It is overlain by a shale succession of undetermined thickness. The basal contact with unit 3 is a mixed gradation of argillite and breccias composed of tan weathering dolomite clasts in an argillaceous matrix (slope deposits?). Distinguishing features of unit 4a include grey colour banding caused by 100 m intervals of more recessive thin bedded carbonaceous dolomite, abundant intraformational flat pebble conglomerates near the base, conspicuous birdseye fabric in the upper third, presence of a massive discontinuous dolomite reef that weathers light grey to white, and a 35 m stromatolitic succession at the top.

The overlying shale unit contains orange weathering silty dolomite and limestone beds, but none of the coarser clastic rocks found near the base of unit 5 to the southeast. Correlation of the shale is uncertain.

Unit 5: Unit 5 is a conspicuous maroon and/or black shale marker that may contain pebble conglomerate, coarse gritty sandstones and thin diamictites.

East of Mount Gibben it is a conspicuous maroon marker, to the west it is black with tan and rusty brown weathering ribs of siltstone and mudstone. The conglomerate beds occur near the base and consist of quartzite, chert and jasper pebbles in a shale matrix; the diamictites occur as metre-thick beds and consist of quartzite pebbles and cobbles in shale; the gritty sandstones and quartzite occur throughout the succession. Thickness of the unit varies. At section 5 it is 144 m thick and consists mostly of maroon shale; at section 6 it is 294 m thick and consists of tan- and orange-weathering siltstones and quartzose sandstones and occasional thin laminated silty dolomite (and one 2 m bed of columnar stromatolites).

The basal contact is sharp and probably an unconformity; the upper contact is gradational into dolomite in some places and abrupt in others; map relations suggest that it is also an unconformity.

Unit 6: Unit 6 is a massive light grey dolomite succession that forms craggy cliffs along the southern flank of the Coal Creek Dome. It is monotonous, consisting of sugary textured crystalline dolomite, often without visible layering or other internal sedimentary features; some beds are cryptalgal laminated, stromatolites may be present, and intraformational breccias, some that appear to be the product of intense fracturing, are also present. Its overall massive homogeneous character, numerous zones and patches of light coloured silicification (especially near the top), and resistant craggy weathering nature distinguish it from older carbonate units, but it can be easily confused with younger units which exhibit many of the same features.

At section 5, near Mount Gibben, it totals 624 m. A thin recessive orange-tan weathering shale-silty dolomite interval 30 m thick allows the unit to be separated into two mappable members from Mount Gibben eastward to the Blackstone River. From Mount Gibben west to the headwaters of the Fifteenmile River this distinction is not possible, but farther west there is, again, a distinctive lower member that may represent a deeper water facies.

The upper contact with unit 7 is abrupt; the basal contact probably is unconformable, but it is uncertain whether or not the unconformity is at the depositional base or higher up within the basal 100 m of the section.

Unit 7: Unit 7 is only 50 to 60 m thick but it is an important marker separating the underlying craggy dolomite unit from younger light grey weathering dolomites of similar character. It can be traced along the south flank of the Coal Creek Dome and consists of black and brown recessive shale and mudstone with thin (5 cm) ribs of red weathering fine carbonaceous quartz sandstone. Lower and upper contacts are sharp.

Unit 8: Unit 8 is a regionally persistent dolomite succession along the flanks of the Coal Creek Dome. Along the southern limit of the Dome it is mainly a thick bedded to massive and texturally homogeneous dolostone, similar in most respects to Unit 6. But unlike the 'craggy dolomite', it forms ridges with smoother crests and gentle slopes. It is distinct because of subtle colour banding caused by thick (greater than 50 m) slightly darker grey intervals.

Internally it is complex. West of Seela Pass, it can be divided into two members: a lower member of dark grey carbonaceous dolomite with algal mounds and mud chip conglomerates; and an upper member of light grey massive cryptalgal laminated crystalline dolomite. Northeast and southeast of Seela Pass, the basal dark member is absent but dark intervals near the top contain beds, lenses and nodules of black chert and numerous layers of flat pebble conglomerate. On the northeast flank of the dome, unit 8 is a texturally homogeneous pelletal dolomite; a mottled light grey weathering rind is characteristic but black chert is lacking and silification is minor.

West of Mount Gibben, an obvious unconformity separates the lower dark member from the overlying light grey one. It is difficult to map laterally and we have not determined whether it truncates the lower member regionally to the east.

At section 7, southeast of Mount Gibben, unit 8 is 252 m thick; at section 8 the upper light grey member is 197 m thick and the lower member varies from 0 m up to (approximately) 100 m. Near Seela Pass thicknesses appear larger possibly because of duplication on unidentified thrusts.

Contacts are sharp, especially the upper one where there is an abrupt change to maroon and green quartzose siltstone and shale.

Unit 9a: Unit 9a is a maroon and green argillite-siltstone-sandstone-conglomerate succession that was traced from the headwaters of the Fifteenmile River eastward to Seela Pass. The dominant maroon siltstone is thin to medium bedded, ripple drift cross laminations are common; sandstone and conglomerate beds grade into each other and vary in thickness from less than a metre to more than 10 m. Clast proportion varies from less than 10 per cent to more than 70 per cent, usually in a sandy matrix. Chert, quartzite, dolomite and jasper are the dominant clast types; they are unsorted, generally angular, and poorly stratified.

Mudcracks in the shale indicate this is a shallow marine partly subaerial succession.

Unit 9a is only a few metres thick where it reaches the Fifteenmile River, but 10 km south of Mount Gibben, 237 m and 52 m were measured at sections 9 and 10 respectively; at section 6 it is 53 m thick and east of Seela Pass it is absent.

Unit 9b: Unit 9b is a massive pebble to boulder polymict conglomerate. It undergoes rapid lateral changes in thickness and facies, typical of a unit deposited near an uplifted terrane shedding coarse carbonate debris. Clast size varies from coarse grit to boulder; the most common clast types are quartzite (variety of colours), chert (variety of colours) and dolomite (variety of compositions). The clasts are generally subrounded to subangular, poorly sorted, and internal layering is poor to nonexistent. Unit 8 (and perhaps 6) may have been the source for much of the chert and dolomite, but a source for the quartzite is less obvious.

At stratigraphic sections 9 and 10, unit 9b is 36 m and 23 m thick, respectively; toward the west, in the Mount Harper region it is substantially thicker; and to the east along Seela Pass it thins to a few metres and changes facies to tan weathering quartz sandstone with floating chert pebbles and granules.

Both lower and upper contacts are gradational.

Unit 10 (Mt. Harper volcanics)[1]: A thick, layered succession of flows, pyroclastics and debris flows compose a deeply eroded complex, about 5 by 15 km long, around Mount Harper. The succession is at least 1000 m thick and its centre tapers toward the south and west to less than 100 m. It can be subdivided into three stratigraphic parts: a basal unit of submarine lavas, including pillow sequences up to 150 m thick; a middle unit dominated by debris and ash flows with lava blocks and pillow fragments in clay or ash matrix; and an upper unit near the centre of the complex consisting of silt and dolomitic mudstone with epiclastic volcanic cobbles and sparse dolomite clasts derived from units 6, 8 and 9. Along the southern and western sides of the complex the upper unit consists of silicified and oxidized lavas, locally vesicular and characterized by turquois coloured alteration patches and orange zeolites.

Prolonged volcanic activity at the centre of the pile produced the outward tapering geometry; accumulation of clastic rocks near the central part possibly reflects late stage collapse and local basin development by crustal relaxation during the waning stages of volcanic activity.

The Harper complex overlies unit 9 at its northern contact, and unit 8 farther to the south; overlying stratigraphy is not preserved. Westward along its southern margin units 3, 8 and 5 are thrust against it.

Unit 11: Unit 11 comprises 391 m of light grey homogeneous crystalline dolomite (stratigraphic section 9). It is massive to thick bedded, with a sugary texture that masks original sedimentary features such as laminations. The basal one third contains silty and sandy dolomite; beds several metres thick of silicified oolites and oncolites are common within the basal two thirds of the succession.

The most distinctive feature of this unit is a 'swallow's nest' weathering texture with smoothly weathering holes. These holes may be closely spaced, and are common within the upper third of the succession.

The lower contact of this unit was not observed but is likely gradational; the upper contact with unit 12 is abrupt.

Unit 12: Unit 12 is a thick bedded tan to light grey weathering sandy and silty dolomite succession. No thickness was measured but it is estimated to exceed 200 m. A basal unit of up to 5 m of fine orange-tan weathering dolomitic quartz sandstone separates it from unit 11. It is well bedded (with planar to undulating laminations), stromatolitic, burrowed and bioturbated.

Basin Assemblage

Unit I: Unit I can be subdivided into three mappable units: a lower gritty sandstone succession (unit Ia), a middle limestone (unit Ib) and an upper maroon and green shale succession (unit Ic).

[1] See Roots (1982) for detailed description.

Unit Ia: Unit Ia consists of sandstone, gritty sandstone, siltstone and shale with minor limestone and silty dolomite. The coarse lithologies dominate, typically as massive tan to rusty brown weathering ribs 10 or more metres thick separated by thin recessive intervals of argillaceous siltstone and shale. Most of the coarse granules are quartz (some of it opalescent blue). Feldspar and chert are minor constituents. Rarely, light grey limestone and/or tan weathering silty dolomite form discontinuous beds 10 to 50 cm thick.

The proportion of argillaceous rocks increases (exceeds 50%) within the upper 100 m of unit Ia. At the top is a distinctive marker of planar bedded, light grey weathering, greenish grey chert with argillaceous partings and interbeds. At North Fork Pass it is 71 m thick.

Internal sedimentary features such as grading, crossbedding and sole markings are rare; however rip-up clasts are common near the base of some sandstone units suggesting they are turbidites.

Thickness of unit Ia is not known, it probably exceeds 1000 m.

Unit Ib: Unit Ib consists of light grey to white microcrystalline limestone. At North Fork Pass beds 20 to 50 cm thick are interlayered with maroon shale. The entire unit is only 16 m thick. Throughout most of the region, it is thin and discontinuous, except in the southern parts of Harper and Shell map areas (116 B/12, C/9) where it is more than 100 m thick and serves as stratigraphic and structural marker (see Roots, 1982).

Unit Ib is tentatively correlated with the Keele Formation because it occupies the same relative stratigraphic position as in Nahanni map area and eastern Wernecke Mountains where a carbonate unit separates gritty sandstones below from maroon-green shales above (Gordey, 1978; Eisbacher, 1981, p. 18).

Unit Ic: Unit Ic consists of maroon and green shale, black shale, and thin intervals (0.5 m to 10 m) of fine grained tan weathering sandstone and siltstone. The lower contact with unit Ib may be sharp or a mixed gradation of thin limestone and shale beds; the upper contact is probably abrupt (a regional unconformity?). Mafic sills are present obscuring stratigraphic relationships. Volcanic flows of unit II may be intercalated with the upper maroon shales of unit Ic.

Several occurrences of the trace fossil **Oldhamia** have been found within the maroon argillite thereby conforming a latest Proterozoic age for this map unit.

Unit II: Unit II comprises a heterogeneous group of altered mafic lavas and debris flows. They exhibit a consistent style and composition despite their discontinuous lens-like geometry, scattered eruptive centres, and probable protracted time interval of emplacement. In the field they form prominent pinnacles 50 to 300 m thick and 5 to 20 km long; local thick accumulations, such as the 2000 m measured east of upper Blackstone River, mark volcanic centres. The abundance of flows increases northward, toward Dawson fault; south of the North Fork thrust, unit II is essentially absent, but immediately north it forms an integral component of basin assemblage stratigraphy concentrated between units Ic and III as well as being intercalated with each.

Breccia comprises more than 70 per cent of each accumulation in about equal proportions of debris flows and pyroclastic deposits; many of the pyroclastic accumulations are typical of basaltic cinder deposits in that they consist of vesicular lapilli lacking a primary matrix. The remaining 30 per cent consists of highly vesicular lava, including some pillow accumulations. Minor late stage felsic activity is suggested by white, cherty rocks within the top few metres of some accumulations, and a single occurrence of flowbanded lava.

Shallow submarine volcanism is indicated by the rock textures and minor structures, and the presence of limestone lenses interpreted as local patch reefs.

Unit III (Road River Formation): Unit III is a succession of black chert and siliceous shale (volcanic tuff?) equivalent in age to the Road River Formation. It is not always easy to differentiate between shales and cherts within the upper part of unit Ic and those belonging to the Road River.

There are two outcrop belts of this unit: a southern one that forms a broad northwest convex arc from North Fork Pass to the Chandindu River, and a northern belt adjacent to the Dawson fault.

The southern belt consists of massive to thick bedded black radiolarian(?) chert (near the base) overlain by green and grey orange-brown weathering siliceous (cherty) shale. Occasional beds of calcareous siltstone and limestone occur as well as more recessive carbonaceous shales. The basal contact is placed below the first thick black chert bed or greenish grey siliceous shale. The latter usually overlies the mafic sills intruding the contact zone between units Ic and III. At North Fork Pass, a massive black chert rib forms an obvious basal unit - there are no sills. The upper contact is sharp and, for the most part, easily recognized.

Within the northern outcrop belt we have not, as yet, determined a stratigraphic top or base for the Road River Formation.

Unit IV: Unit IV is a chert pebble conglomerate 10 to 30 m thick and is a convenient upper limit to unit III along the southern outcrop belt. The conglomerate is clast-supported and polymict (mainly black and green chert). The matrix of carbonaceous shale rarely exceeds 10 per cent. South of the area studied, unit IV was observed directly beneath the Tikandit Formation, a limestone unit of Permian age (Tempelman-Kluit, 1970). Therefore unit III is Permian or older and probably correlates with the 'Black Clastic' map unit of Late Devonian through Pennsylvanian age found in the Selwyn Basin and northern Rocky Mountains (Gordey, 1981; Gabrielse, 1976).

Unconformities

At least three (and possibly five) unconformities were recognized within the shelf assemblage (Fig. 2), each characterized by the rapid truncation of strata beneath it. Unit 8 rests successively on units 7, 6, 5, 4 and 3 directly north of Seela Pass (Fig. 3); unit 6 can be mapped on units 5, 4 and 3 near the headwaters of the Fifteenmile River; the thickness of unit 3 decreases from more than 1500 m on the northeast side of the Coal Creek Dome to less than 500 m at the headwaters of the Fifteenmile River; and unconformities within units 4 and 8 are also mappable but less obvious regionally.

Unconformities within the basin assemblage are probable. At North Fork Pass, basal black chert of the Road River Formation rests on maroon shales and pebble conglomerate of unit Ic. Cambrian strata were probably removed by erosion.

Structure

The prominent structures within Dawson map area are gently southdipping thrusts mapped along the southern flank of the Coal Creek Dome within the platform assemblage, and tight to isoclinal upright folds within the basin assemblage, especially within the southwestern part of the study area where unit Ib is a well exposed continuous marker. These structures formed early(?) in the Mesozoic adjacent to a then convergent continental margin (Tempelman-Kluit, 1979).

Even older structures appear to be present in the study area. North-trending high angle faults cut units 2, 3 and 4 but are overlapped by unit 8 (Fig. 3 north of Seela Pass). Unit II volcanic rocks are most abundant adjacent to the Dawson Fault suggesting it may have been the site of crustal extension long before its history as a thrust. A well developed and pervasive axial plane cleavage affects unit 3 but is not observed in younger clastic units.

References

Bell, R.T. and Delaney, G.D.
1977: Geology of some uranium occurrences in Yukon Territory; in Report of Activities, Part A, Geological Survey of Canada, Paper 77-1A, p. 33-37.

Eisbacher, G.H.
1981: Sedimentary tectonics and glacial record in the Windermere Supergroup, Mackenzie Mountains, Northwestern Canada; Geological Survey of Canada, Paper 80-27, 40 p.

Gabrielse, H.
1976: Environment of Canadian Cordilleran depositional basin; in Circum-Pacific Energy and Mineral Resources, American Association of Petroleum Geologists, Memoir 25, p. 492-502.

Gordey, S.P.
1978: Stratigraphy and structure of the Summit Lake area, Yukon and Northwest Territories; in Current Research, Part A, Geological Survey of Canada, Paper 78-1A, p. 43-48.

Green, L.H.
1972: Geology of Nash Creek, Larsen Creek, and Dawson map areas, Yukon Territory; Geological Survey of Canada, Memoir 364, 157 p.

Roots, C.F.
1982: Ogilvie Mountains Project: Part B. Volcanic rocks in north-central Dawson map area; in Current Research, Part A, Geological Survey of Canada, Paper 82-1A, note.

Tempelman-Kluit, D.J.
1970: Stratigraphy and structure of the "Keno Hill Quartzite" in Tombstone River – Upper Klondike River map-areas, Yukon Territory; Geological Survey of Canada, Bulletin 180, 102 p.

1979: Transported cataclasite, ophiolite and granodiorite in Yukon: evidence of arc-continent collision; Geological Survey of Canada, Paper 79-14, 27 p.

OGILVIE MOUNTAINS PROJECT, YUKON; PART B: VOLCANIC ROCKS IN NORTH-CENTRAL DAWSON MAP AREA

Project 800022

C.F. Roots[1]
Cordilleran Geology Division, Vancouver

Introduction

Volcanic rocks are an integral stratigraphic component of the Dawson map area (NTS 116 B, C) and provide an excellent opportunity to assess the role of volcanism during Late Proterozoic through Early Paleozoic evolution of the region. This is a preliminary account of the stratigraphic and structural setting of several volcanic complexes within the north-central part of the Dawson map area and serves as the framework for more detailed studies that will begin in 1982.

In the first systematic reconnaissance of the region Green (1972) outlined the widespread volcanic rocks, but essentials of style, composition, age and stratigraphic position remained obscure. Results from a field season of 1:50 000 scale mapping within Mount Harper (116 B/10) and Shell Creek (116 C/9) map areas combined with examinations of other portions of the volcanic belt farther east, demonstrated that there are two distinct types of volcanic deposits within contrasting sedimentary environments. Representative stratigraphic sections through both types of volcanic deposits are illustrated in Figure 1.

Unit II – Volcanic Rocks within the Basin Assemblage

Sericitized volcanic rocks consisting of vesicular mafic lava, ash and debris flows constitute Unit II (Fig. 1). They form discontinuous lens-shaped deposits that weather as prominent grey pinnacles towering above more recessive shales and mudstones of Units I and III.

Throughout the southern Ogilvie Mountains, volcanic breccia dominates Unit II. Because this lithology is poorly and discontinuously exposed, and almost wholly altered to clays, a nongenetic classification was used to describe them. Table I presents the diagnostic criteria used to determine mode of origin. Large scale features such as shape and stratigraphic association increased the interpretive accuracy.

The most abundant fragmental rocks are debris flows. All contain angular equidimensional clasts of all sizes, both vesicular and dense, varying slightly in mafic composition, but there is no internal organization in the deposits. They commonly form lenticular beds from 2 to 10 m thick, and hundreds of metres long.

Well stratified ash and lapilli form the base of volcanic piles as well as layers within most lava and debris flow successions. Lateral continuity of more than 150 m is not uncommon; one pyroclastic sequence 27 m thick was traced more than 5 km. Highly vesicular, cinder-like deposits are particularly common. They lack primary matrix, but infilling calcite has preserved the fragile clasts and uncompacted nature. Their texture resembles peperite breccia (J. Souther, personal communication), a term for tephra deposited within lime mudstone (Hoadley, 1953). Near the top of some piles are beds of light grey, rough-textured clay, formerly ash, containing rare limestone and sandstone pebbles, that are interpreted as tuffs.

Vesicular lava forms some massive flows, 0.5 to 2.5 m thick with related flow top breccias, but mostly discontinuous pillow accumulations. In general, pillows near the base are small (20-50 cm) bun-shaped and separated by thick selvages or ash; higher pillows are usually larger (40-150 cm), closely

[1]Carleton University, Ottawa, Ontario

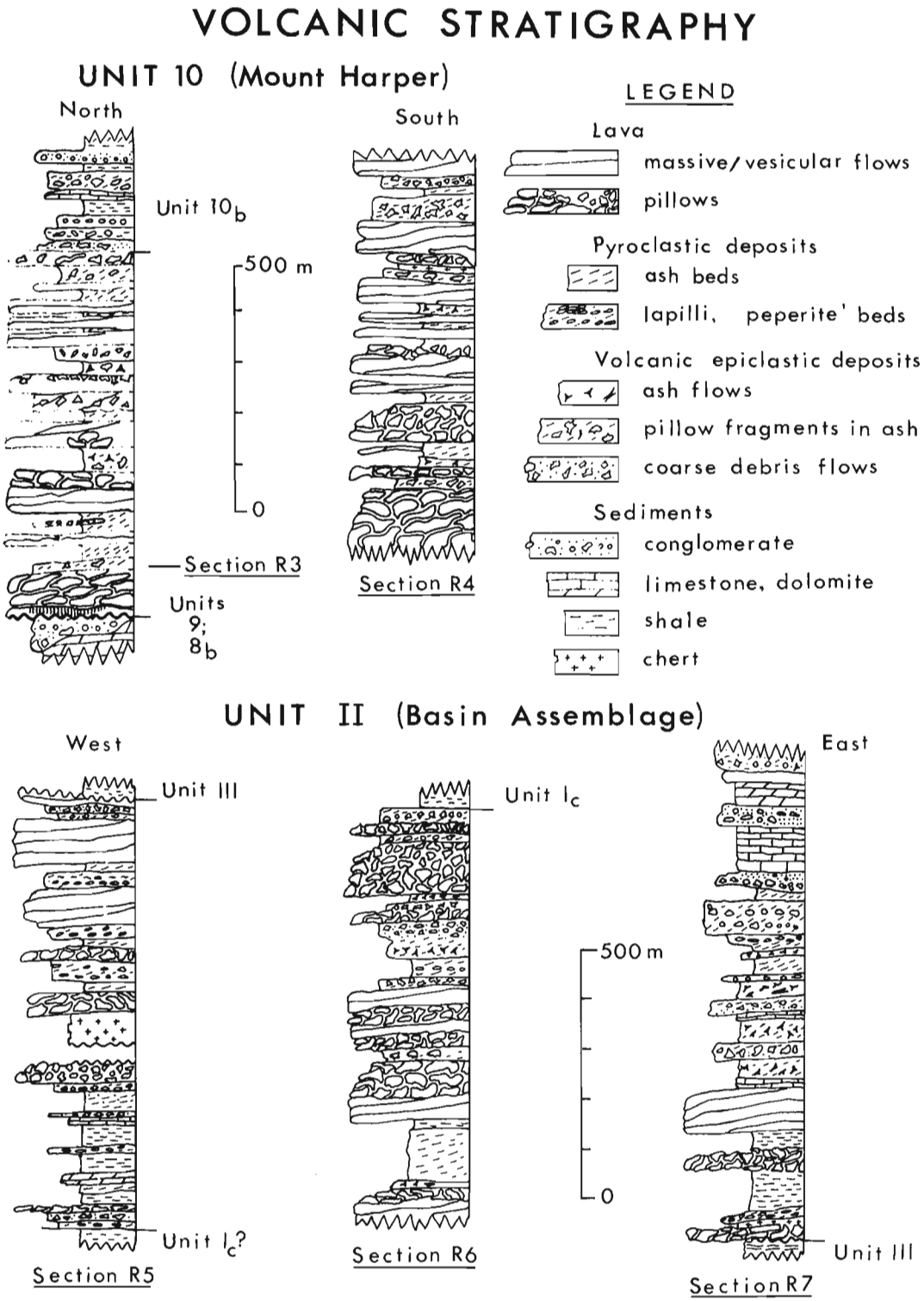

Figure 1. *Representative sections through volcanic piles in shelf and basin assemblages. Locations are shown on Figure 3 of Part A.*

fitted together and commonly tubular. Pillow fragment breccias are more abundant near the base, suggesting proximity above steeper terrain or more viscous brittle lava. The thickest pillow lava pile measured is 55 m having a lateral extent of only 150 m.

Unit II is interpreted as the product of episodic volcanism over a long period of time. The high density of vesicles and abundant chlorite alteration suggests deposition within a shallow marine environment. Areal distribution as elongate volcanic outcrops suggest narrow, fissure-like source areas, associated with deep seated crustal extension. The abundance of coarse, epiclastic flows attests to topographic relief and perhaps rapidly built volcanic piles. Subaqueous pyroclastic lapilli deposits would be proximal if solely from undersea eruptions; their greater extent near the top of the pile, together with elongated, more fluid pillow lavas suggest later, gently sloped edifices that may have reached the surface.

Unit 10 – Volcanic Rocks within the Shelf Assemblage

Volcanic rocks in a steep mountainous region 15 km by 5 km form an unique package that is here termed the Mount Harper volcanic complex. In most places it sits atop the carbonate stratigraphy of the south flank of the Coal Creek Dome. Total composite thickness is less than 100 m in the broad valley of the western part of the complex and up to 1100 m near the prominent peak of Mount Harper. Two representative sections are shown in Figure 2.

The volcanic rocks are distinguished from those of Unit II by their remarkable freshness; they lack pervasive clay alteration or calcite saturation. Like them, they are dominantly mafic, but are dark green to deep brown, rather than soft grey. Except for the uppermost lavas, vesicles are rare and tiny; a significant contrat to Unit II. From a distance, the Mount Harper rocks weather purplish grey, and reveal thick, subhorizontal layering within the complex.

The volcanic complex was partly explored during reconnaissance mapping in 1981. There are other localities of volcanic rocks with characteristics suggestive of Unit 10, but not as yet investigated. They include small deposits in valleys at the western edge of Shell Creek map sheet, and two possible centres east of the present study area. One of these shows prominent horizontal layering and probably overlies Unit II volcanic rocks; the other contains comparatively fresh-looking tuffs and lavas. If these volcanics are related to the Mount Harper Complex, they are significant because they span the Dawson Fault and may illustrate relations between the basin and shelf assemblages.

Unit 10 has been subdivided into two parts for descriptive purposes, unit 10a is dominantly volcanic rocks and unit 10b consists mainly of epiclastic rocks.

Unit 10a

The lava and breccias forming most of the complex, are undeformed, but the internal structure is complex. Three factors are known: a) the flows are discontinuous and irregularly scattered, b) original slopes were steep and uneven; and c) there was contemporaneous vertical faulting. In the extensive cliff exposures of the north side a lower, probably deeply eroded, volcanic structure lies beneath the main package, and both are overlain by epiclastic sediments (Unit 10_h). The volcanic succession, as exposed in the deeply incised centre of the complex, consists of: basal pillow lavas, debris flows with interbedded lava and ash, discontinuous pillow lava piles, scattered felsic tuffs and flows, and uppermost, oxidized lava flows. These general lithologic subdivisions are briefly described.

Lowermost pillow lava accumulations, common in several areas of the complex, are massive and 60 to 150 m thick. Tubular pillows 20 to 50 cm in diameter can be up to 4 m long. Rims are thick (1-2 cm), tightly interlocking and lack selvages. Dark green ash lenses and pillow fragments in ash become increasingly abundant upward.

The middle section is dominated by coarse and fine debris flows (see Table 1 criteria) which average 5 to 15 m thick and are composed of angular, equant lava blocks. Interbedded lavas, with minor pillow lava intervals, highlight the large scale layering visible from a distance. Debris flows predominate intervals up to 550 m thick.

Upper pillow lava piles were fed by dykes that are common in lower lithologies. A characteristic breccia consisting of "amoeboid-shaped" maroon clasts (5-150 cm) with epidotized rims supported in a coarse ash matrix is interpreted to be proximal to these submarine vents.

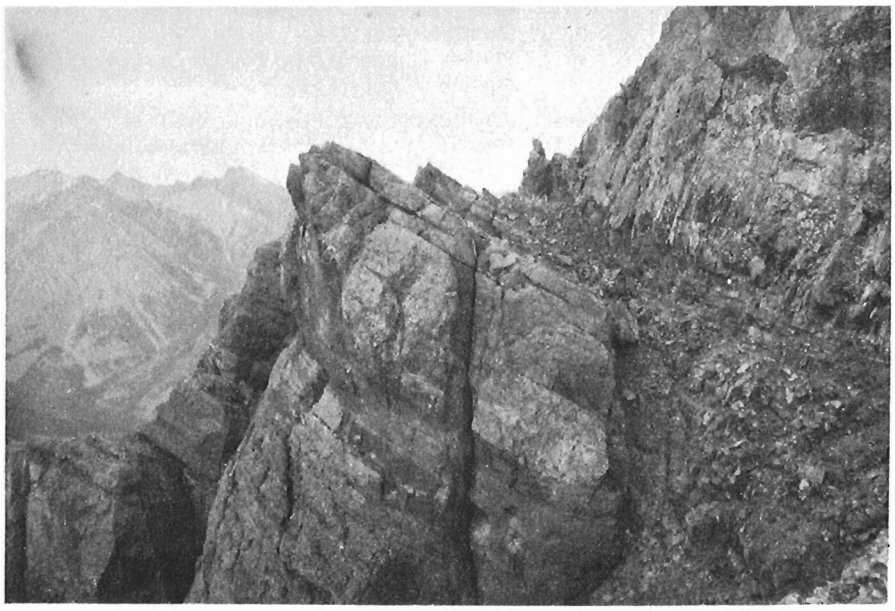

Figure 2

Lower contact of Unit 10, about 500 m northeast of Mount Harper. Basal columnar jointed lava disconformably overlies Unit 9, here silt and mudstone with suspended pebbles of dolomite, argillite and jasper. Staff in centre is 1.5 m long. In the background are shelf Units 6, 8b and 9 (from left), dipping southward.

Table 1

General criteria for interpretation of fragmental volcanic rocks

PYROCLASTIC DEPOSITS
preserved bombs, cored fragments
stratified fines (laminated ash suggests waterlain, but is similar to turbidite deposits)
primary matrix may be lacking in cinder, 'peperite' beds
VOLCANIC EPICLASTIC DEPOSITS (ash flows, debris flows)
high proportion of matrix
unsorted clasts; crude stratification of blocks
disconformable lower contacts
INTRUSION BRECCIAS
steep, crosscutting contacts
no stratification, but may be zoned inward
clasts are angular and closely packed; or well rounded and widely spaced in fine, unstratified ash

Central parts of the complex are overlain by Unit 10b, consisting of pyroclastic and epiclastic sediments. Flanking the south ridges of the complex, however, felsic and possibly subaerial volcanic lithlogies are found. They include isolated outcrops of bluish, flow-banded lava, and ash flow beds containing rhyolite chips. Purple and dark green vesicular lavas, with calcite and orange-pink chalcedony vugs cover much of the southern slopes. They are locally altered to striking turquoise hues. Individual lava flows 5 to 15 m thick form plateaus and scarps, particularly in the broad valley at the west end of the complex. They appear to be the uppermost volcanic lithology in the Mount Harper complex.

The basal pillow lavas of the complex overlie Unit 9 along its northern margin (Fig. 2). North of Mount Harper the uppermost conglomerate and mudstone horizons show disharmonic folds (20 cm scale) and the overlying lavas have spiracles along their base, suggesting that the early flows encountered soft, wet sediments. Along the south margin the lower contact is generally covered, but a canyon reveals vesicular lava, similar to the uppermost lithology of the complex, overlying north-dipping Unit 8a. The complex appears to have extended southward during its period of activity.

At present, only the southern part of the volcanic complex is preserved. Cliffs exposing a 300 m thickness of the complex along the northwest margin indicate the removal of a considerable portion to the north. Two elongate outcrops of volcanic breccia located north of the complex may be source areas, now exposed by deeper erosion. They have steep, crosscutting relations with enclosing units 8b and 9; in places envelopes of hydrothermal alteration and silicified dolomite are developed. Although most breccia within them are 'vent' or intrusion types, some 'pillow-like' shapes and ash layers do not appear to fit this interpretation. Their significance as feeder zones or separate volcanic complexes of perhaps an earlier age needs further investigation.

Volcanic activity indicated by Unit 10 could be related to the same tectonic event(s) that caused deposition of Unit 9. Only a brief time interval separates these units, because lowest lavas cover what were apparently unconsolidated sediments. As described in Thompson and Roots (1982), Unit 9 conglomerate reflects minimal transport, and is probably derived from rapidly uplifted terrain. The volcanic complex may have begun atop one of the steep boundary faults. At its south margin, lavas later in the history of the complex overlie Unit 8 dolomite where no conglomerate is present; perhaps the top of an uplifted block, overstepped by lava as the volcano built upon conglomerate in the adjacent depression. In any case, the nature of the volcanism here is different from the episodic fissure eruptions of Unit II; it consisted of several or numerous feeders in a single zone building a large volcanic pile that may have reached the surface in its late stages.

Unit 10b

This consists of a succession of volcanic pebble conglomerate, carbonate and locally derived clastic sediments more than 230 m thick that caps high ridges within the Mount Harper volcanic complex.

Maroon mudstone, with suspended, rounded cobbles is overlain by grey volcanic wacke and grit. Beds are well stratified but unsorted; the thickness of some tapers from metres to centimetres within 150 m. Dolomite cobbles are generally uncommon, but dominate some horizons in the northwest part of the complex. Orange, tan and grey weathering dolomite intervals up to 9 m thick occur in the succession and may be useful stratigraphic markers.

Unit 10b overlies several lithologies of Unit 10a with presumed unconformity. The upper contact is not preserved. Several exposures of the margins, which are vertical and unfaulted, suggest that the unit is a basin developed within the volcanic complex.

References

Green, L.H.
1972: Geology of Nash Creek, Larsen Creek and Dawson map-areas, Yukon Territory; Geological Survey of Canada, Memoir 364.

Hoadley, J.W.
1953: Geology and Mineral Deposits of the Zeballos – Nimpkish area, Vancouver Island, British Columbia; Geological Survey of Canada, Memoir 272.

Thompson, R.I. and Roots, C.F.
1982: Ogilvie Mountain Project, Yukon; part A: a new regional mapping program; in Current Research, Part A; Geological Survey of Canada, Paper 82-1A, note.

LAPIDARY MATERIAL ON GRAHAM ISLAND, QUEEN CHARLOTTE ISLANDS GROUP, BRITISH COLUMBIA

Project 490038

S. Leaming
Cordilleran Geology Division, Vancouver

Introduction

Graham Island (NTS 103 F, G, J, K) is the most northerly of the two largest islands in the Queen Charlotte Islands group. Long isolated with only access by air or tug-drawn barge, a rapidly improving ferry service from Prince Rupert will inevitably mean more visitors, a good number of whom will be mineral collectors or "rockhounds" attracted by reports of agates, petrified wood and other lapidary materials. It is the purpose of this brief report to mention some of the localities and the kinds of material which may be collected on Graham Island.

While the time and expense required to reach the island would scarcely be justified by the lapidary material per se, the natural beauty of the island, abundance of wildlife, and the relatively uncrowded life is attractive to all.

Some parts of the island are accessible only via logging roads restricted to weekend travel. Much of the island is inaccessible except along the coast by boat. A paved public highway from Queen Charlotte to Masset gives access to part of the coast, a few lakes and sheltered inlets.

The accompanying map is based largely on the work of Sutherland Brown (1968) with some personal observations made on a short visit to the island in 1981. Mr. Magnus Olsen at the Little Rock Shop in Port Clements was most helpful in pointing out collecting areas and his collection of agate, wood and fossils included some fine specimens of what could be found.

Collecting Areas

The easiest method of collecting is simply to walk the many miles of beaches on the receding tide when the clean wet pebbles, cobble and boulders may be rapidly inspected and agate, petrified wood, porphyry, jasper, epidote-altered volcanics, may be quickly spotted among the more abundant clasts of sedimentary rocks, granite, basalt, etc.

For beachcombing no knowledge of the geology is necessary. But all the material has come from the erosion of exposed formations and some collectors may prefer to search in the source rock. The map (Fig. 1) outlines four of the principal formations which probably account for most of the lapidary material on Graham Island. For more detail on the geology of the islands the work of Sutherland Brown should be consulted.

Skohun Formation

This Tertiary formation consists of sandstone, shale and conglomerate with minor lignite. Outcrops are scarce; the best exposure is east of Masset on the coast. Fossil shells and plants may be collected but little of lapidary value.

The olivine basalt forming Tow Hill intrudes this formation and contains some chalcedony and agate in vugs and fractures. The basalt probably contributes most of the beach agates from Masset to Rose Spit.

Masset Formation

The Masset Formation is largely basaltic and rhyolitic volcanic rock, in the form of flows, breccias and tuffs, with a few intrusive porphyries.

Many of the rocks contain amygdules and fracture-fillings of agate, opal and zeolites. Some of the banded rhyolites are useful lapidary materials for book ends or penstands. In places near intrusive bodies of granitic rocks, some epidotization of the basic volcanics produce green rocks of lapidary interest. Feldspar porphyry in the Masset Formation yields the "flower-stone", also of interest to "rockhounds".

Haida Formation

The Cretaceous Haida Formation consists of sandstone, siltstone and argillite. It contains some fossil shells, including ammonites, and carbonized wood, but little of lapidary value.

The argillite used by the Haida carvers may come from this formation, but most of it is not a collectable material. The unique properties of this rock apparently do not extend beyond the boundaries of the quarry owned by the Haidas and rather zealously guarded against trespass. This argillite is essentially a claystone, easily worked, homogeneous and fine grained, with little or no hard mineral components. One might find argillite approaching this quality outside the Haida claim but it is unlikely to be equalled.

Yakoun Formation

This is mainly a volcanic formation with much pyroclastic rocks but there are some wood-bearing sedimentary members. Sutherland Brown reports mesolite, heulandite and chabazite as the main zeolites. Most of the amygdaloidal rocks contain chlorite. Probably much of the agate found on the beaches of Masset Sound come from this formation.

Other Formations

Most of the few other formations present on Graham Island are sedimentary and contain some fossils but little of lapidary interest. The Triassic Karmutsen Formation is of some interest for its pillow breccia, jasper and zeolites but is rare on Graham Island. There are exposures in Rennel Sound and one might expect some pillow breccia or "Dallasite" on the beaches.

Reference

Sutherland, Brown, A.
1968: Geology of the Queen Charlotte Islands, British Columbia; British Columbia Department of Mines and Petroleum Resources, Bulletin No. 54.

From: Scientific and Technical Notes in Current Research, Part A; Geol. Surv. Can., Paper 82-1A.

Figure 1. *Lapidary material on Graham Island, Queen Charlotte Islands Group, British Columbia.*

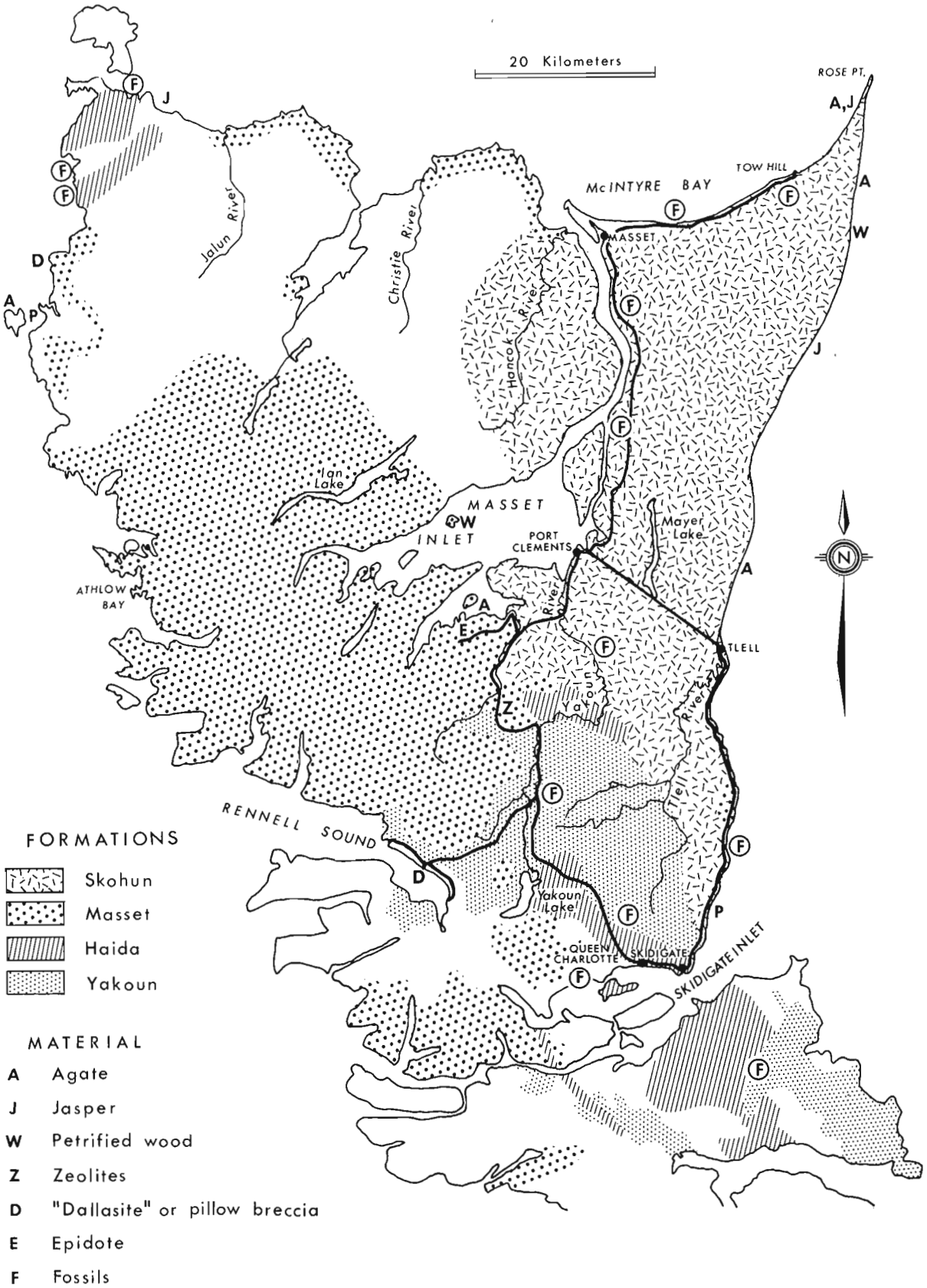

ULTRAMAFIC AND RELATED ROCKS IN CASSIAR DISTRICT, BRITISH COLUMBIA

Project 490038

S. Leaming
Cordilleran Geology Division, Vancouver

Introduction

The ultramafic and related rocks in Cassiar district (NTS 104 N, O, J) of northwestern British Columbia are disposed in two separate belts (Fig. 1). They follow the general northwesterly regional structural trend and are separated by intrusive rocks of the Cassiar batholith, and volcanic and sedimentary rocks of Precambrian to Triassic age. The southern belt is part of the Cache Creek Group which runs from southern British Columbia to the Yukon and beyond. The northerly belt comprises the Sylvester Group which also extends into Yukon Territory.

These belts have much in common being rocks of oceanic affinity consisting of serpentinized ultramafics, gabbro, basic volcanics, chert, pelite and limestone. They are in fact ophiolites. The ultramafic rocks of both belts contain at least one major asbestos deposit, numerous rodingite dykes, nephrite lodes, and minor amounts of copper minerals.

The ultramafic rocks have been pervasively serpentinized. They are light green weathering, black to dark green rocks which are highly sheared and slickensided along major fault zones, but massive and competent where they have escaped deformation.

Although some pure-olivine rocks (i.e., dunite) are present, most are pyroxene-bearing peridotites and therefore originally were harzburgite and wehrlite. Generally pyroxenes are more resistant to serpentinization and may still be present; commonly, however, the pyroxenes are now represented by bastite (serpentine pseudomorph after pyroxene). Pyroxenite forms a minor part of the lithology. Clinopyroxene appears to be more common than orthopyroxene. Gabbro is abundant and may form large masses especially in the Cache Creek Group. Most of the rocks are fine- to medium-grained, with rare pegmatitic phases. Low grade metamorphism has converted the pyroxene to amphibole and feldspars to albite. Epidote and carbonate has also developed.

Basic volcanic rocks are found in both groups, but as they commonly lack structures such as pillows, amygdules or flow criteria, they are difficult to recognize in the field.

In thin section these rocks are fine grained aggregates of epidote-group minerals, chlorite, carbonate and saussuritized plagioclase. Where the plagioclase can be determined it is commonly near albite-oligoclase.

The general similarity of rocks mapped as gabbro and greenstone suggest a consanguinity. Most of the pelitic rocks are mapped as phyllites. In places they contain much vein quartz of presumed metamorphic origin. Outcrops of black slate with the Cache Creek Group may be highly foliated pelites, but also may be rocks of the Jurassic Inklin Formation caught up in fault slices within the Cache Creek Group.

Although called limestone, the carbonate rocks are highly crystalline and would best be called marble. Few megafossils have been preserved. Microfossils, mainly

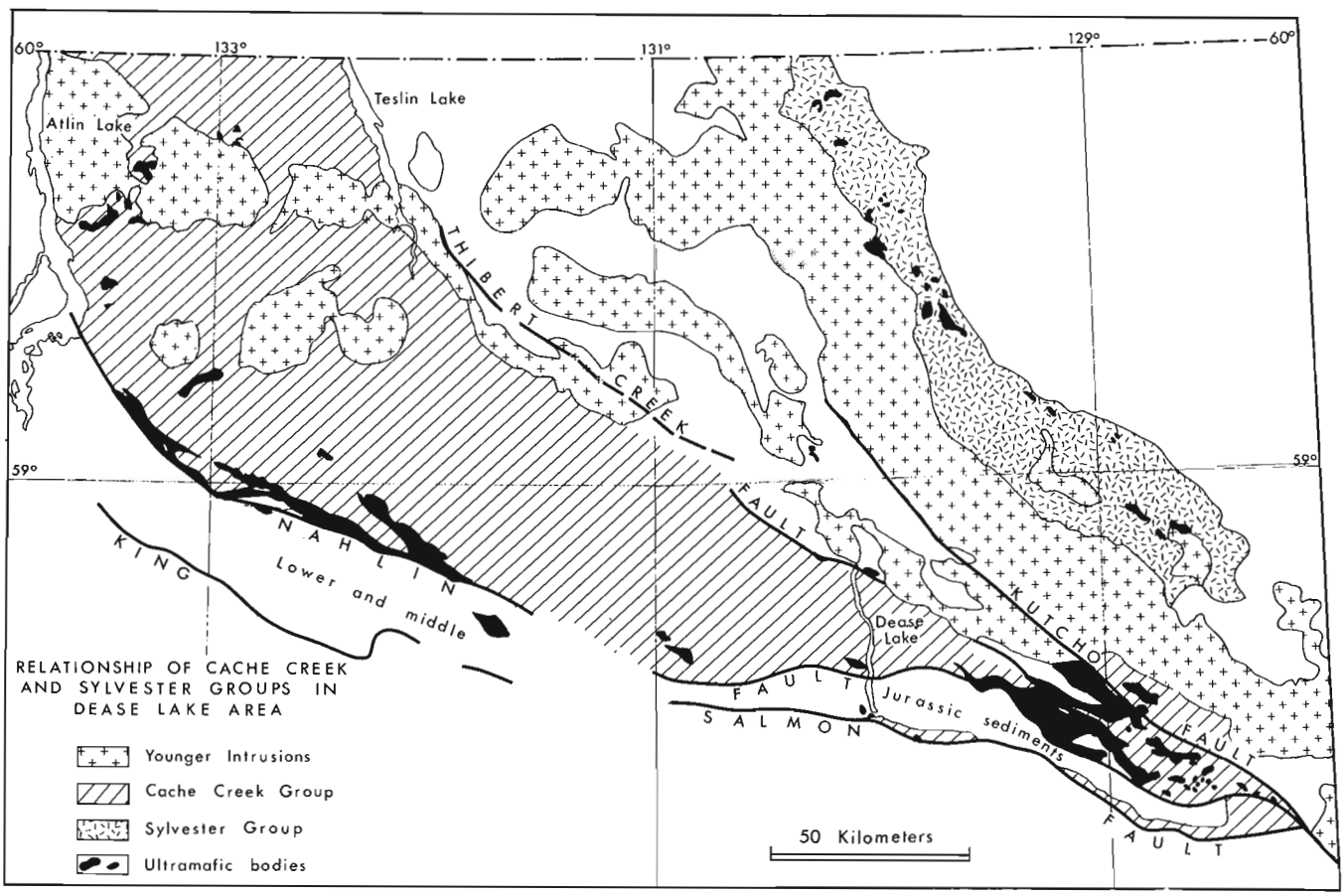

From: Scientific and Technical Notes in Current Research, Part A; Geol. Surv. Can., Paper 82-1A.

radiolaria, conodonts and fusulinids are the main paleontological evidence of the age of the carbonates which ranges from Mississippian through Permian.

The Cache Creek Group is much more of a tectonic mélange than is the Sylvester Group. It is characterized by blocks of chert, pelite, limestone and volcanics included in the ultramafic masses to a remarkable extent. The Sylvester Group contains much red jasper and green chert, whereas most of the Cache Creek chert is grey. There is red chert in the Cache Creek but the occurrences are small and discontinuous.

Listwanite (quartz-carbonate-mariposite) is much more abundant in the ultramafic rocks of the Cache Creek Group.

A significant difference in the two groups is found in the fusulinid fauna. The Cache Creek contains fusulinids of Tethyan affinity whereas the Sylvester contains typical Franklinian-Uralian types.

The differences in the two groups supports the theory (Monger, 1977) that they represent terranes added to the North American craton from different locations on the circum-Pacific tectonic belt.

Reference

Monger, J.W.H.
1977: Upper Paleozoic rocks of the western Canadian Cordillera and their bearing on Cordilleran evolution; Canadian Journal of Earth Sciences, v. 14, p. 1832-1859.

GEOLOGY OF THE FORT SMITH MAP AREA (EAST HALF), DISTRICT OF MACKENZIE

Project 800009

Hewitt H. Bostock,
Precambrian Geology Division

Geological reconnaissance of the Fort Smith map area (75 D) was completed during the summer of 1981 with mapping of the part between the 110th and 111th meridians. The geology within this area is closely related to that described for the western half of the sheet (Bostock, 1981) and the data described here are presented as an extension of the initial report on the west half of the sheet. A more comprehensive preliminary report and map covering the whole sheet are in preparation.

The east half of the Fort Smith area is approximately bisected by a major north-trending fault zone characterized by belts of mylonite and mylonitic gneisses. West of this zone are plutonic rocks of presumed Archean age, chiefly of quartz monzonitic to granodioritic composition. Within these rocks are remnants of Tsu Lake gneiss similar to that in the west half of the sheet (Bostock, 1981) containing upper amphibolite or granulite facies mineral assemblages. These rocks are intruded at their western margin by a megacrystic granitic diapir of probable Hudsonian age. Numerous zones of sharply to gradationally bounded augen gneiss to megacrystic granite also intrude these Archean rocks. Zones of syntectonic mafic dykes, amphibolites with variable biotite content, occur in the Archean basement and are most numerous in the east near the central zone of faulting.

East of the central fault zone the terrane is predominantly biotite gneiss within which persist severely deformed remnants of high grade pelitic gneiss, quartzite, and local calcsilicate gneiss, all of which resemble the Tsu Lake gneiss (Bostock, 1981). Syntectonic amphibolite dykes are widespread and show widely varied degrees of deformation and potash metasomatism. Variable assimilation of these dykes has so obscured the original nature of the biotite gneiss that it is not known to what extent it may represent modified and remobilized Archean plutonic rocks on the one hand, or biotite-bearing paragneiss, possibly related to the Tsu gneiss, on the other.

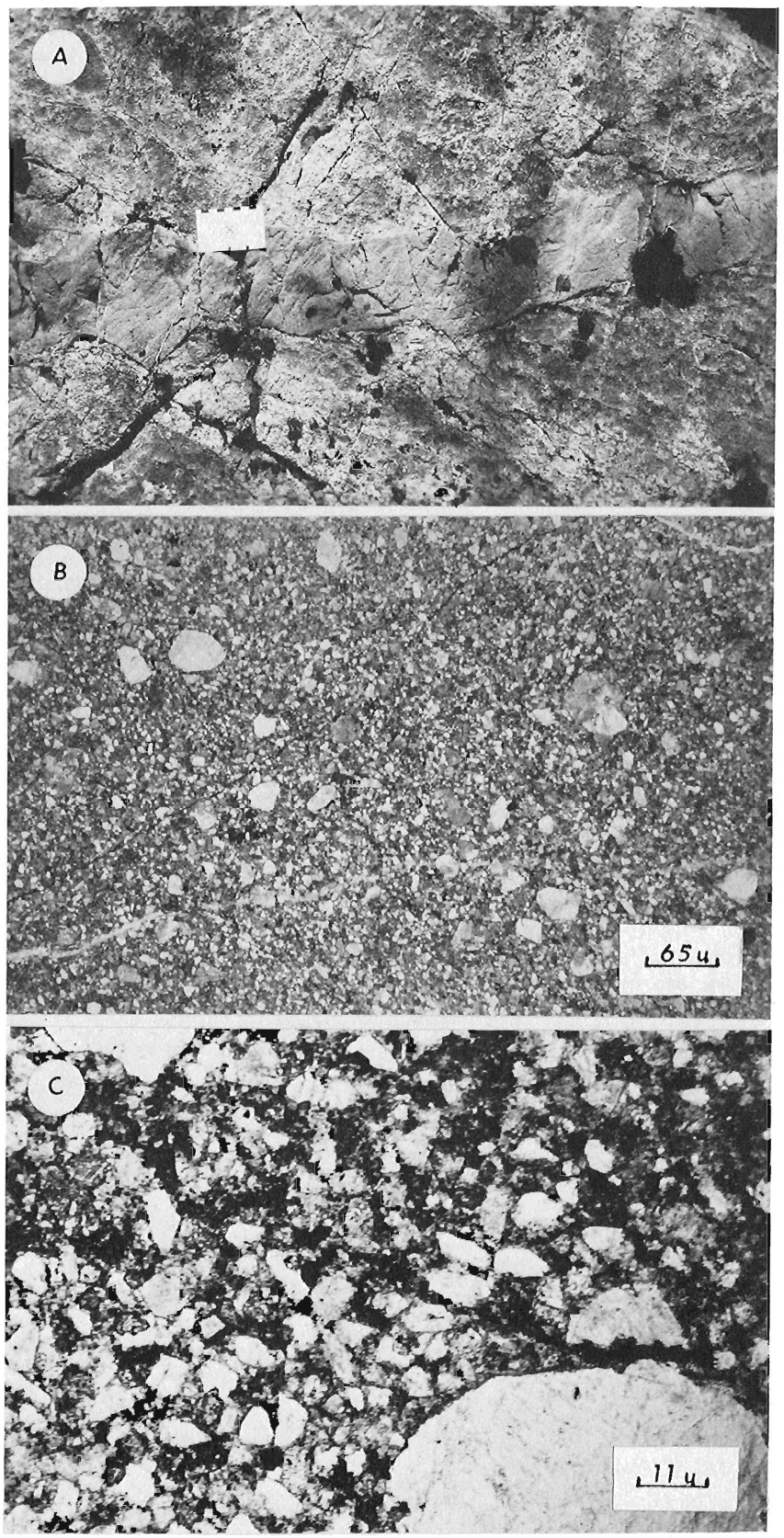

Figure 1. *Sandstone dyke*

A. Sandstone dyke cutting mylonitic breccia in Archean basement. GSC 202507-J

B. Photomicrograph (plain light) showing scattered subrounded phenoclasts of quartz, feldspar and rock fragments in finer partly calcareous matrix. GSC 202231-O

C. Photomicrograph (plain light) showing matrix of tiny angular quartz and weathered feldspar within the partly calcareous matrix between phenoclasts. GSC 202231-M

From: Scientific and Technical Notes in Current Research, Part A; Geol. Surv. Can., Paper 82-1A.

Between Natael Bay at the northwest end of Hill Island Lake and the junction of the central fault zone with the north border of the map area, the gneisses are transected by a possibly older zone of mylonites that appears to be truncated at its northern end by the central fault zone. Along and within this older zone of mylonites is a large remnant of granite-boulder conglomerate similar to conglomerate in the Nonacho Group which occurs in the northeast corner of the area. The conglomerate remnant, up to 2 km across, is highly folded with east-northeastward vergence. Also, within the mylonite zone but farther south, a second remnant of low grade metaturbidites occurs that is extensively intruded by a white muscovite granite not found elsewhere in the area. The metaturbidite remnant is complexly folded, and for the most part contains small biotite porphyroblasts, but locally large poikilitic cordierite porphyroblasts are present. It closely resembles similar turbidites exposed along Hill Island Lake with which it is nearly contiguous. Similar beds, which also occur at King Lake, north of the map area, have been mapped as part of the Nonacho Group by Henderson (1939).

A coarse grained pink granite stock intrudes the gneisses, mylonite and low grade clastic sediments (possibly correlative to the Nonacho Group) at Thekulthili Lake near the northeast corner of the map area. This granite is compositionally similar to the megacrystic granite west of the central fault zone and has been dated at 1900 Ma by the zircon concordia method. Bodies of intensely lineated to near massive augen gneiss and megacrystic granite occur within the biotite gneiss farther south and may be of about the same age as the granite stock. All of these rocks are intruded by undeformed basaltic dykes of the 1700 Ma Sparrow Dyke Swarm (McGlynn et al., 1974).

It has been suggested that deposition of the Nonacho Group occurred in response to crustal instability that developed in conjunction with emplacement of the Hudsonian megacrystic diapir farther west (Bostock, 1981). Latteral spreading of the diapir may be responsible for the east-northeastward vergence of folds within the large conglomerate remnant along the subsidiary mylonite zone. Still farther northeast, near the northeast corner of the map area, a case can be made for basement gneiss having been thrust against and possibly eastward over southwestward dipping Nonacho beds and is based on the following argument.

Mylonitic breccia south of the exposed limit of the Nonacho, and near the southwest shore of the lake which extends along a southeast-trending Nonacho-basement fault, has been penetrated by a fine grained, gritty, purple-red, sandstone dyke about 20 cm thick and at least 5 m long (Fig. 1A). The dyke has a zig-zag outcrop pattern unlike the Sparrow basalt dykes which, though their borders may be jagged, commonly have distinct west-northwestward trends. No alteration of the country rock is evident at the dyke contacts, and no flow banding is suggested within it (Fig. 1A). In thin section the dyke consists mainly of angular quartz, some weathered feldspar grains, and a few larger well rounded quartz and rock fragments in a partly calcareous matrix (Fig. 1B, C). The texture closely resembles that of an immature fine grained clastic sediment such as occurs within the Nonacho Group. It is possible that the dyke may have formed by simple infilling of fractures in the basement of Nonacho sediment from above; however, no Nonacho is exposed on this west side of the fault south of Thekulthili Lake. On the other hand, inasmuch as the dyke cuts mylonitic basement breccia that lies along a fault that follows the west border of the exposed Nonacho a few kilometres farther north, the dyke may well be slightly younger than the Nonacho Group. It may have formed as a result of upward movement of fine sand into fractures following thrusting of the basement northeastward over unconsolidated Nonacho sediments. Such an interpretation is consistent with northeastward vergence of folded Nonacho conglomerate farther southwest, and supports the view that this deformation was closely associated in time with Nonacho deposition. Because of the current interest in uranium exploration in this immediate area the structure along this fault deserves further investigation.

References

Bostock, H.H.
1981: A granitic diapir of batholithic dimensions at the west margin of the Churchill Province; in Current Research, Part B, Geological Survey of Canada, Paper 81-1B, p. 73-82.

Henderson, J.F.
1939: Taltson Lake, District of Mackenzie; Geological Survey of Canada, Map 525A with marginal notes.

McGlynn, J.C., Hanson, G.N., Irvine, E., and Park, J.K.
1974: Paleomagnetism and age of Nonacho Group sandstones and associated Sparrow dykes, District of Mackenzie; Canadian Journal of Earth Sciences, v. 11, p. 30-42.

GIAPP: IMAGE ANALYSIS PROGRAM AND APPLICATIONS, 1977-1981

Project 720089

A.G. Fabbri
Economic Geology Division

Introduction

The desire to simplify and expedite quantification and integration of geoscience data from maps and from descriptions of mineral occurrences has been the primary reason for studying the applicability of image processing to assessment of resources by statistical methods. Prior to 1977, several studies undertaken (Agterberg et al., 1972; Fabbri, 1975) required manual point counting of maps after their subdivision into arrays of 10 km x 10 km square cells.

GIAPP, a Geological Image Analysis Program Package, was programmed for the digitization and analysis of geological spatial data for the estimation of geometrical probabilities (Fabbri, 1980b). The development of the package was initiated in 1977 as a collaboration between the Geological Survey of Canada and the National Research Council of Canada. The activity on GIAPP was made possible via a "guest worker" agreement between the author and the Electrical Engineering Division of the National Research Council. In addition to the qualification of regional geoscience data from maps, several applications to quantitative microscopy of crystalline fabrics have been made.

Philosophy of the approach

GIAPP was started as a small set of existing routines for the management and processing of image data. The digitization of maps and line drawings, and various geological applications, required the preparation of new programs. Additional routines for specific applications were added to the package as the need arose.

Well known image processing techniques were used in programming, and, in particular, binary (black and white) images compressed to one bit per pixel were found convenient to process for the following three reasons:

1. Reduction of input/output requirements;
2. Reduction of processing time; and
3. Possibility to use bit shift and logical operators.

To simulate the performance of a real time image analyzer, the operators in 3., which are available in most general purpose computers, permit computations with the degree of parallellism implied by the word length of the computer, i.e., as many bits as there are in one word are processed simultaneously.

The present capabilities of GIAPP are summarized in Table 1. The terminology generally used in image processing is also used in Table 1. The programs have been developed first on a small computer dedicated to general image processing: a Modcomp II computer with 64 000 memory of 16 bit words, two tape drives and two disks. Initially the computer was interfaced with a flying spot scanner, a

Table 1

General description of the capabilities of GIAPP

General Features	Processing of Non-Compressed Images	Processing of Binary Compressed Images
-file searching, copying, erasing and reviewing	-smoothing, filtering, thresholding and graphical displays	-logical operations on or between binary images
-expansion and compression of binary data	-component labeling of binary images	-Minkowski operations by means of programmable structuring elements of any shape
-handling of commentaries added to image data sets by each processing routine	-line thinning	-two-dimensional auto- and cross-correlations
-processing of binary, labeled and grey level images for both square and hexagonal rasters	-phase labeling	-point and vector displays of binary images
-output of image data on magnetic tape for data transfer	-junction detection	-editing of binary images
-creation of binary compressed images of boundaries from a graphic tablet	-extraction of binary data from labeled images	-creation of binary images from data on cards or computed from interactive commands (masks, grids, (tests)
-scanning by means of a flying spot scanner	-digital displays	
	-other special purpose algorithms	
	-false colour displays	

From: Scientific and Technical Notes in Current Research, Part A; Geol. Surv. Can., Paper 82-1A.

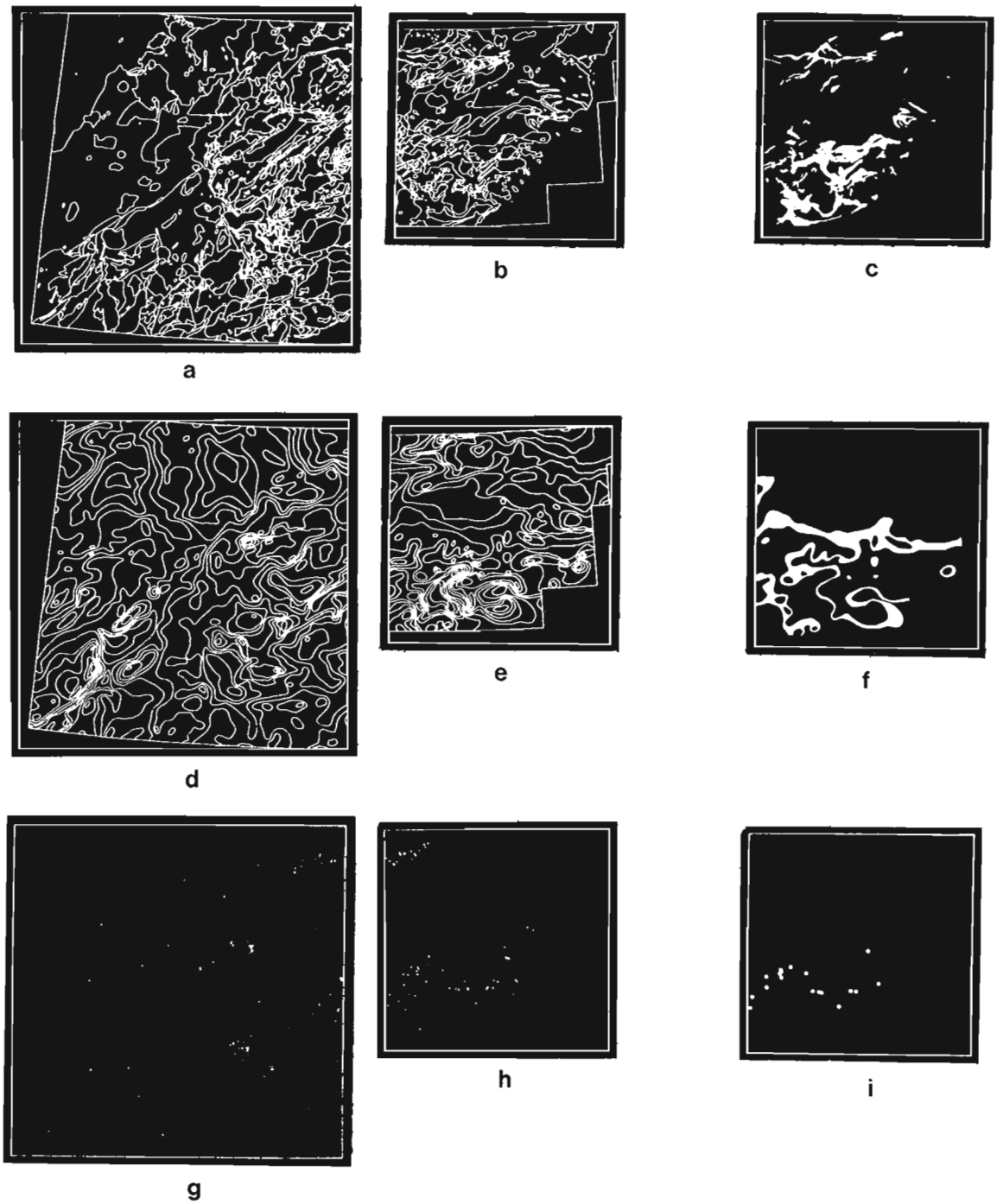

(a) *Binary image of the geological boundaries, west side of study area of size 915 pixels x 915 pixels.*

(b) *Same as in (a) for east side of size 610 pixels x 610 pixels.*

(c) *The binary image of Archean mafic volcanic rocks extracted from (b): there are 29 865 white pixels in the image (7466 km^2)*

(d) *Binary image of the contours of equal Bouguer anomaly for contour intervals of 5 milligals: west side, in registration with the image in (a)*

(e) *Same as in (d) for east side, in registration with the image in (b)*

(f) *Binary image of gravity interval -50/-55 milligals extracted from (e): there are 37 365 white pixels in this image (9341 km^2)*

(g) *Binary image of the location in west side, in registration with (a)*

(h) *Same as in (g) for 67 occurrences in east side, in registration with (b)*

(i) *Binary neighborhood transformation of a pattern with 19 white pixels extracted from (h), the base-metal occurrences in east side*

Figure 1. *Binary images of geological boundaries, gravity anomaly contours, and mineral occurrence locations in part of the District of Keewatin, Northwest Territories, Canada. Each pixel in the images corresponds to a square of 500 m x 500 m. Each pixel indicating the presence of a mineral occurrence has been expanded in size in the form of an octagon (approximating the circle) of 9 pixels in diameter. There are 1215 white pixels in this image (304 km^2). This transformation is called a dilation by an octagonal structuring element which is 9 pixels (4500 m) wide.*

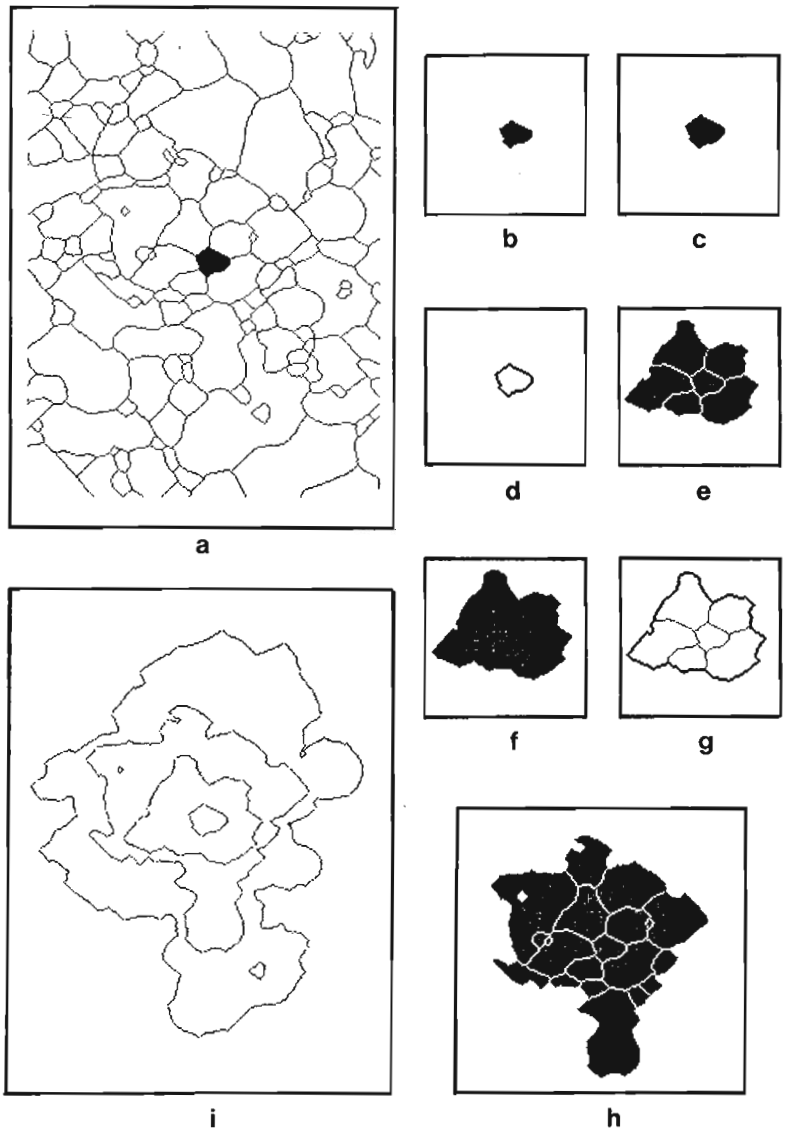

(a) Logical union of the image of the selected apatite profile and the image of the thinned boundaries

(b) The initial profile, +"seed"

(c) The dilatated seed

(d) The black pixels "added" by the dilation of the seed

(e) A first cluster of profiles

(f) The dilatated first cluster

(g) The black pixels "added" by the dilatation of the first cluster of profiles

(h) Image of the logical union of four "shells" of pixels, pointers to one-step to four-step adjacent profiles: each shell is a set of thin-line segments, interrupted in coincidence with junction-boundary pixels

Figure 2. *Example of iterative processing of the binary image of one profile of apatite extracted from the image of a granulite (of approximately 1300 grains, and 1000 pixels x 595 pixels), for coputing one-step to four-step adjacency relationships. From each shell the probability of adjacency can be estimated.*

Tektronix 611 video display unit, a Versatec dot matrix printer, a card reader and a graphic tablet digitizer. Later a Norpak image buffer and a Conrac colour television were added to the system. A major part of the package has been converted to a CDC Cyber 74 computer, (Fabbri et al., 1978) which allows 70 000 (octal) memory of 60 bit words for interactive processing and the access to several disks. In this second version a Tektronix 4014/1 video graphic terminal and a hard copy unit connected to it are the only communication and display devices available.

Applications

GIAPP was programmed to allow a geologist/user to digitize and analyze by himself images of a geological nature, and to develop applications to many different kinds of materials. The validity of the package as a laboratory tool for continued routine usage has been documented in the following fields:

a. digitization of maps and line drawings (Kasvand, 1981),

b. geoscience data integration and processing (Fabbri, 1980a, in press; Fabbri and Kasvand, 1978; Fabbri et al., 1978),

c. thematic mapping (Fabbri, 1981b),

d. stereology (Fabbri and Kasvand, 1980, 1981b; Fabbri and Masounave, 1980),

e. texture analysis by mathematical morphology (Fabbri, 1980b, 1981a),

f. pattern recognition (Fabbri and Kasvand, 1981a; Kasvand, 1981; Kasvand and Fabbri, 1978),

g. statistical analysis (Agterberg et al., 1981; Agterberg and Fabbri, 1978a, b).

Figure 1 illustrates an example of data base, produced by digitizing geological maps, gravity anomaly contour maps, and the locations of mineral occurrences in a large area of the District of Keewatin, Northwest Territories, Canada.

Figure 2 describes as application to a stereological problem in which adjacency relationships are measured to characterize the texture in a crystalline fabric.

The two examples of applications shown, illustrate the generality of the approach offered by GIAPP: from macroscopic (regional maps) to microscopic scale (crystalline fabrics from thin or polished sections.

Concluding remarks

GIAPP has so far had only relatively few users, consisting of the author and some of his colleagues. However, it has the potential for more intensive usage and applications. This was evident during a three-day workshop on computer graphics and image processing programs which preceded the 10th Geochautauqua on Computer Applications in the Earth Sciences held at the Geological Survey of Canada, Ottawa, October 23-24, 1981.

Geoscientists seem to have many different ideas on future applications of GIAPP because it simulates what a geologist does when he superimposes (stacks) tracings of different maps to compile a new map for special purposes. In addition, quantitative aspects are added by the capability of emasuring the areas and various other geometrical characteristics of each set of features in the overlays.

The quantitative microscopic analysis performed for characterizing particles or grains (from profiles or silhouettes from thin sections) in the plane of the microscope or in special instruments called "image analyzers" can also be simulated by GIAPP. All this is accomplished by using general purpose computing equipment.

References

Agterberg, F.P. and Fabbri, A.G.
1978a: Spatial correlation of stratigraphic units quantified from geological maps; Computers and Geosciences, v. 4, p. 285-294.

1978b: Statistical treatment of tectonic and mineral deposit data; Global Tectonics and Metallogeny, v. 1, p. 16-28.

Agterberg, F.P., Chung, C.F., Divi, S.R., Eade, K.E., and Fabbri, A.G.
1981: Preliminary geomathematical analysis of geological, mineral occurrence, and geophysical data, Southern District of Keewatin, Northwest Territories; Geological Survey of Canada, Open File 718.

Agterberg, F.P., Chung, C.F., Fabbri, A.G., Kelly, A.M., and Springer, J.S.
1972: Geomathematical evaluation of copper and zinc potential of the Abitibi area, Ontario and Quebec; Geological Survey of Canada, Paper 71-41, 55 p.

Fabbri, A.G.
1975: Design and structure of geological data banks for regional mineral potential evaluation. Canadian Institute of Mining and Metallurgy Bulletin, Aug. 1975, v. 68, no. 760, p. 91-98.

1980a: Digitization and processing by minicomputer of large regional geological maps and ancillary data on mineral resources; Proceedings of Internatinal Symposium. Machine Processing of Remotely Sensed Data and Soil Information Systems and Remote Sensing and Soil Survey, June 3-6, 1980, Purdue University, West Lafayette, Indiana, (Abstract), IEEE Catalog no. 80 CH 1533-9 MPRSD, p. 340.

1980b: GIAPP: geological image analysis program package for estimating geometrical probabilities; Computers and Geosciences, v. 6, p. 153-161.

1981a: Image Processing of Geological data; unpublished Ph.D. Thesis, University of Ottawa, Ottawa, Canada, 367 p.

1981b: Image processing of coincident binary patterns from geological and geophysical maps of mineralized areas, Proceedings of Canadian Man-Computer Communications Society, 7th Conference June 10-12, 1981, Waterloo, Ontario, p. 323-331.

Fabbri, A.G. (cont.)
Source listings for the geological image analysis program package GIAPP, operational on a Modcomp II computer; National Research Council Canada, Electrical Engineering Division, ERB Report. (in press)

Fabbri, A.G. and Kasvand, T.
1978: Picture processing of geological images; in Current Research, Part B, Geological Survey of Canada, Paper 78-1B, p. 169-174.

1980: A picture processing approach to stereological problems; Proceedings of 5th International Congress for Stereology, Salzburg, Austria, Sept. 4-8, 1979, Mikroskopie, v. 37, p. 431-436.

1981a: Applications at the interface between pattern recognition and geology; Sciences de la Terre, Serie Informatique Geologique, no. 15, p. 87-111.

1981b: Image processing for the detection of two-dimensional Markovian properties as function of distances from crystal profiles; Proceedings, 3rd European Symposium for Stereology, Ljubljana, Yugoslavia, June 22-26, 1981, p. 153-163.

Fabbri, A.G. and Masounave, J.
1980: Experiments on the characterization of metamorphic texures from a microphotographic of an amphibolite; 5th International Congress for Stereology, Slazburg, Austria, Sept. 4-8, 1979, Journal of Microscopy, v. 121, p. 111-17; also Mikroskopie, v. 37, p. 339-344.

Fabbri, A.G., Kasvand, T., and Stray, J.H.
1978: Implementation of an interactive system for computer processing of geological images; in Current Research, Part C, Geological Survey of Canada, Paper 78-1C, p. 123-124.

Kasvand, T.
1981: Computerized vision for the geologist; 10th Geochautauqua, Ottawa, Canada, Oct. 23-24, 1981, abstracts, p. 21.

Kasvand, T. and Fabbri, A.G.
1978: Automatic counting of alpha-particle tracks from autoradiographs of radioactive minerals; Proceedings. Eighth Annual Automatic Imagery Pattern Recognition Symposium, April 3-4, 1978, National Bureau of Standards, Gaithersburg, Maryland, R.A. Kirsch, and R.N. Nagel, ed., p. 11-26.

Kasvand, T., Fabbri, A.G., and Nel, L.D.
1981: Digitization and processing of large regional geological maps; National Research Council Canada, Electrical Engineering Division, Report ERB-938, 91 p.

Rosenfeld, A. and Kak, A.C.
1976: Digital Picture Processing; New York, Academic Press, 457 p.

APPLICATION OF A SPOT-TEST FOR FIELD IDENTIFICATION OF PHOSPHATIC SEDIMENTARY ROCKS IN YUKON

Projects 740081 and 790033

I.R. Jonasson and W.D. Goodfellow
Resource Geophysics and Geochemistry Division

Introduction

During the course of our geochemical studies in the Howards Pass area of Yukon, as part of the Nahanni I.M.P. Project, we investigated some carbonaceous cherts of Silurian age for their phosphorus content. Morganti (1979) had previously noted that these same units, present at the XY deposit, Howards Pass, overlie the orezone of Pb and Zn sulphides. He had also recorded some unusually high phosphorus levels. Subsequently the mineral fluorapatite was identified at the Geological Survey by X-ray diffraction as the source of this anomaly. The cherts in question commonly carry 5 to 15 per cent organic carbon which pervades the thin wavy bands of fluorapatite, which are usually not visible in hand specimens but can be seen in specimens cut across bedding. The nature of these rocks and their position in the stratigraphic succession at Howards Pass is not discussed here, but will form the subject matter of some forthcoming publications on Nahanni I.M.P.P.

The purpose of this short paper is to present a description of a modified field spot-test used to identify these phosphatic rocks on site when mapping or logging drill core. It will prove to be useful to exploration geologists in defining such marker units within what are otherwise featureless sequences of black chert.

The Method

The basic test is not new – it was described by Oakes (1938) for use in Oklahoma. The reagent we use is very similar to that described by Oakes; ours is more dilute to avoid some precipitation problems from saturated solution.

Mix 30 g molybdenum trioxide into 125 mL water and 25 mL concentrated ammonia solution. The slurry so formed is stirred slowly and carefully into 325 mL of 6M nitric acid. The slurry is added in small batches to avoid over-heating and the formation of hydrolyzate precipitates. Dilute to 500 mL, stand the solution in a dark place for about 24 hours and filter if necessary. It is best to store the reagent, an acid solution of ammonium molybdate, in an opaque plastic bottle since it is unstable in bright, direct light. Dropper bottles for field use should be similarly masked.

When freshly exposed rock surfaces are treated with the reagent, the presence of phosphate is indicated by the immediate formation of a bright yellow ammonium phosphomolybdate precipitate. The presence of carbonate may slow the colour development because nitric acid is consumed in dissolving the rock. The appearance of a cream rather than a yellow precipitate is a signal to add more spot reagent. The cream precipitate is molybdenum trioxide produced by base hydrolysis and should not be confused with a positive test response.

Pieces of phosphatic chert treated and not treated with the reagent are shown in Plate 1. Phosphate bands which would show a yellow stain are highlighted by stippling; other bands are of carbonate only. With careful application, the reagent can be used to stain phosphate grains and define texture sufficiently to enhance colour photography.

Table 1 presents a data set, for a short section of drill core, comparing actual P_2O_5 levels measured by colorimetric techniques with colour responses noted in the field. The latter are indicated only as strong, weak, or zero responses. We have found that in our samples the limit of detection is around 0.5% P_2O_5 when apatite minerals are the source of supply.

Table 1 also includes some data on CaO and F contents – other major constituents of fluorapatite. Plots of these against P_2O_5 content (not shown here) produce strong linear relationships, as expected, for the chert samples. CaO was determined by XRF, F was determined by ion selective electrode.

Table 1

Response of test reagent against P_2O_5 content of some diamond drill core samples

Metres from d.d.h. collar	Rock type	CaO(%)	F(%)	P_2O_5(%)	Colour response
4.57	chert	9.04	0.79	4.37	strong
7.62	chert	11.18	0.70	5.47	strong
10.67	chert	7.04	0.32	2.11	strong
13.72	chert	5.75	0.50	2.94	strong
17.07	chert	16.0	0.96	7.51	strong
19.81	chert	9.30	0.49	3.48	strong
22.86	chert	5.25	0.42	2.68	strong
25.81	chert	9.73	0.49	3.73	strong
29.26	chert	10.62	0.50	6.15	strong
31.39	carbonate	51.8	0.03	0.12	zero
35.36	chert	1.17	0.14	0.72	weak
38.40	chert	3.36	0.16	0.87	weak
43.89	chert	3.80	0.27	2.09	strong
47.55	carbonate	50.2	0.04	0.04	zero
50.29	chert	3.35	0.36	1.83	strong
53.64	chert	0.73	0.06	0.06	zero
55.17	chert	0.34	0.07	0.10	zero
58.21	carbonate	7.13	0.07	0.34	zero
59.13	carbonate	24.2	0.02	0.04	zero
61.57	carbonate	10.3	0.02	0.05	zero

From: Scientific and Technical Notes in Current Research, Part A; Geol. Surv. Can., Paper 82-1A.

Plate 1. Phosphatic chert: stained and unstained (top) yellow colour represented by stipple is not reproduced in black and white photograph. GSC 203759-B

Conclusion

The test for phosphate is quick and easy to perform on rock samples of all types. It could also be applied to soils or powdered rock samples following nitric acid leaching and treatment with the reagent on a porcelain spot test plate. Sensitivity, normally around 0.5% P_2O_5 in the solid sample, would probably be enhanced by this treatment.

References

Oakes, M.C.
1938: A field test for phosphates; Economic Geology, v. 33, p. 454-457.

Morganti, J.M.
1979: The geology and ore deposits of the Howards Pass area, Yukon and Northwest Territories; the origin of basinal sedimentary stratiform sulphide deposits; unpublished Ph.D. thesis, University of British Columbia, 317 p.

TRACE ELEMENT CONCENTRATIONS FROM OVERBURDEN SAMPLES IN NORTHEASTERN MANITOBA

Project 750072

L.A. Dredge
Terrain Sciences Division

Introduction

Samples of sandy till and stony pelite were collected in 1977 during the course of a helicopter-supported regional surficial mapping survey in Caribou River map area (54 M), northern Manitoba (Fig. 1; Dredge and Nixon, in press). Because of interest in the economic mineral potential of this area, trace element concentrations of copper, lead, zinc, cobalt, nickel, chromium, molybdenum, manganese, iron, and uranium were determined for each of 43 samples.

This paper presents the statistical and areal distributions of the results and indicates areas where elevated background values and anomalies are clustered.

Methods

Samples selected for trace element analysis were collected from till and stony pelite, over an area of about 8200 km^2. Sampling points were chosen so as to be representative of the region; sites were spaced roughly 10 km apart.

Samples were collected from sandy till and from stony marine pelite which mantles the till or has been incorporated into the upper part of the till by frost churning. Samples were collected from the sides of hand-dug pits below depths where oxidation was apparent. Most samples were taken from a depth of about 50 cm. At sites where more than one sample was taken, both samples appear on Figure 2 and have been shown in order of their stratigraphic position.

Analytical procedures follow the manner and rationale of previous till geochemistry studies at the Geological Study of Canada (see Klassen and Shilts, 1977). Trace element values were determined on the clay-sized fraction of overburden samples. Analyses were performed by Bondar-Clegg and Company Ltd., Ottawa, using atomic absorption techniques after La Force reverse aqua regia extraction for base metals and fluorimetric analysis after nitric acid extraction for uranium. Of the 43 samples submitted for analysis, 13 contained insufficient material for the uranium analyses.

Regional Geology

The terrain of the study area consists of a bedrock plain overlain generally by 1 to 6 m of glacial overburden. (One PolarGas borehole log shows 12 m of overburden; Shilts, 1980, Table 2). The regional slope of the terrain is very low, and rises inland from sea level to about 150 m at the western boundary of the map area at a rate of 2 m/km. Initial reconnaissance geological mapping was carried out by Davison (1966), and the area has been remapped in much greater detail by Schledewitz (1977a, b) and Schledewitz and Cameron (1977). Bedrock outcrops over 1 to 4% of the area and generally occurs as low isolated knolls. The Precambrian rock, generally Aphebian(?) in age, consists of intrusives and metasediments. Bedrock north of Little Seal River consists primarily of foliated quartz monzonite and south of the river, quartz diorite and granodiorite.

Bedrock is mantled by till and marine deposits, which constitute the material sampled and reported on in this paper. Surficial deposits have been mapped by Dredge and Nixon (in press), and generalized distributions of deposits, with sampling sites, are shown in Figure 1. The till is bouldery, with a sandy matrix, and forms extensive areas of ribbed moraine. The surface till was emplaced by ice flowing towards the south and southeast, although older buried till

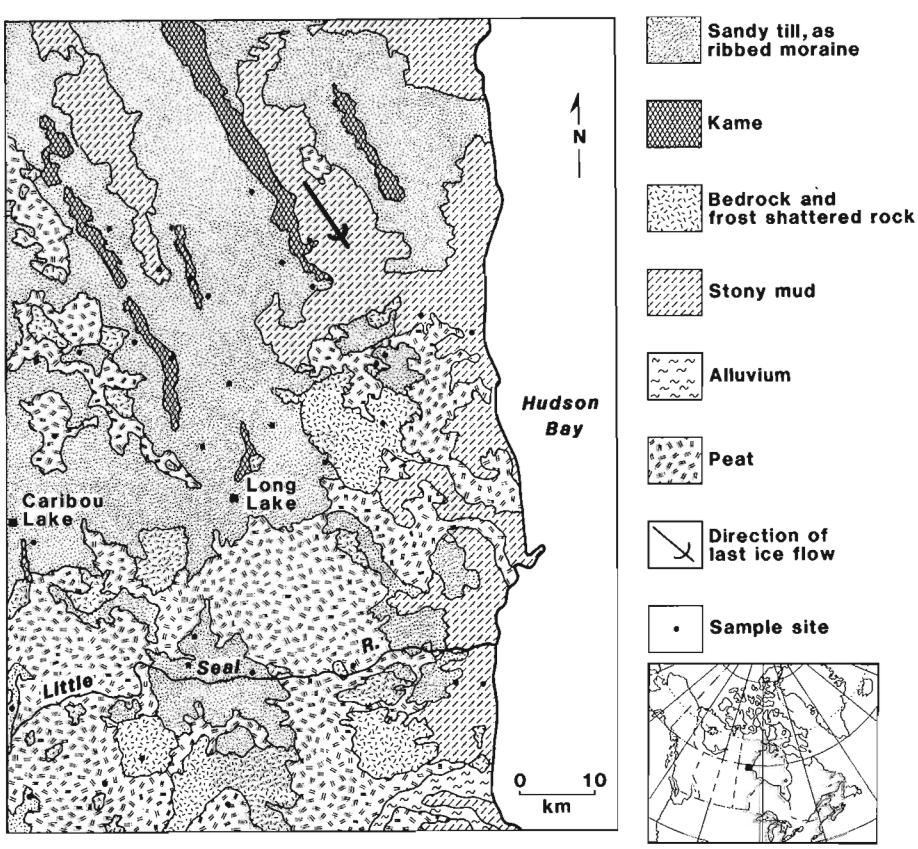

Figure 1

Generalized surficial geology of Caribou Lake map area showing sample sites.

From: Scientific and Technical Notes in Current Research, Part A; Geol. Surv. Can., Paper 82-1A.

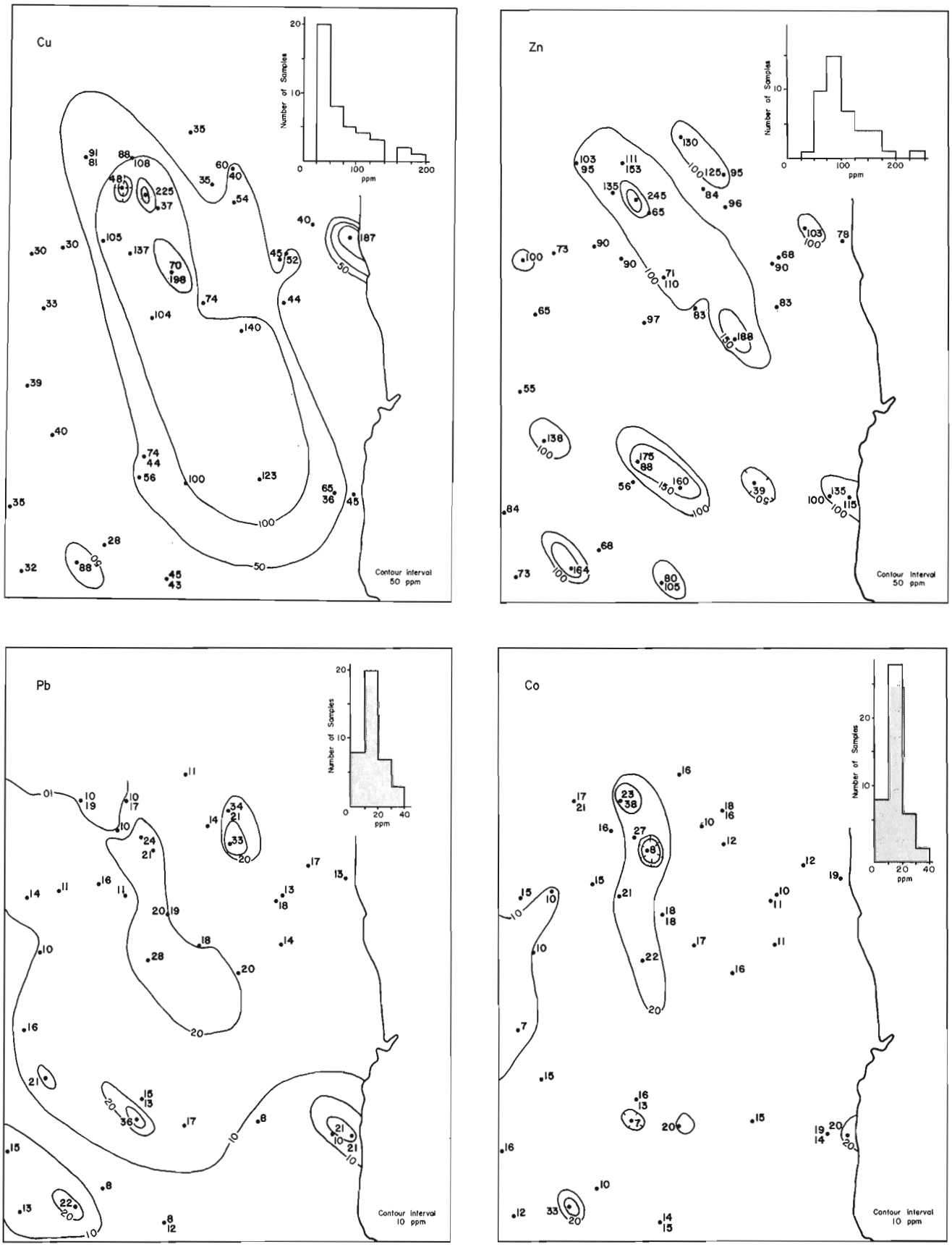

Figure 2. *Maps and histograms of trace element concentrations; abnormally high values are shown as shaded areas.*

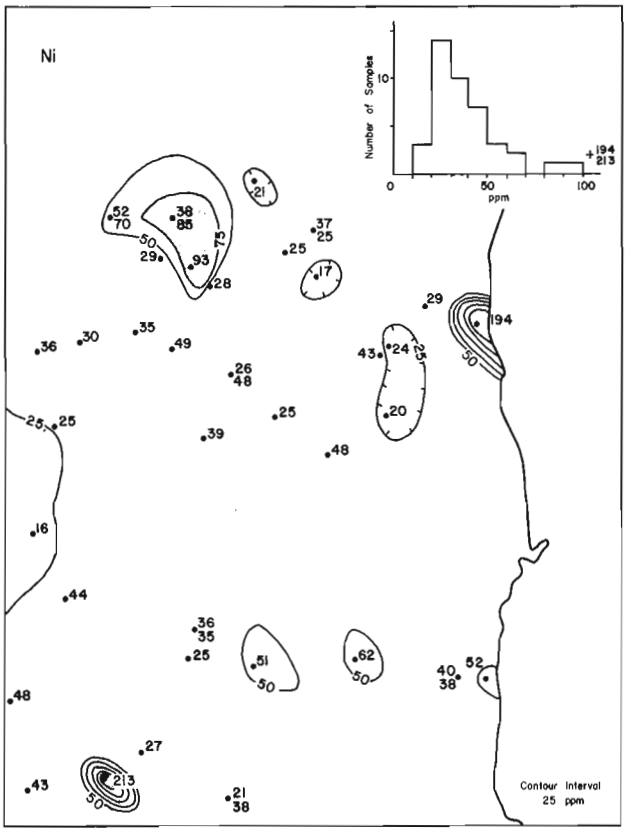

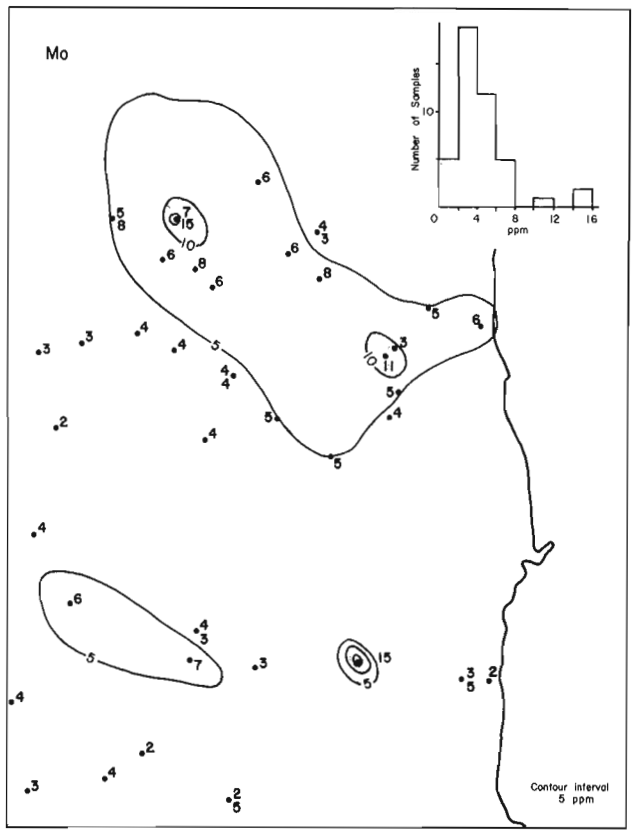

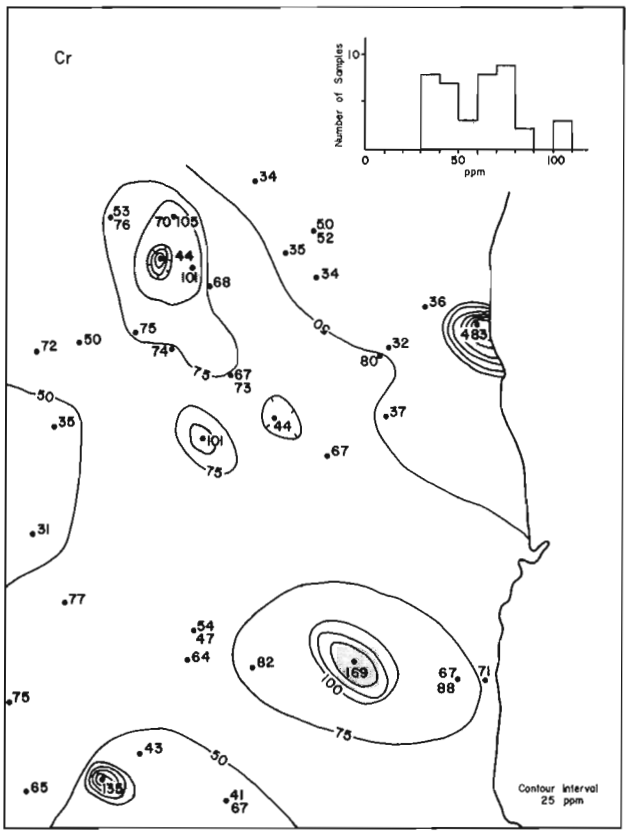

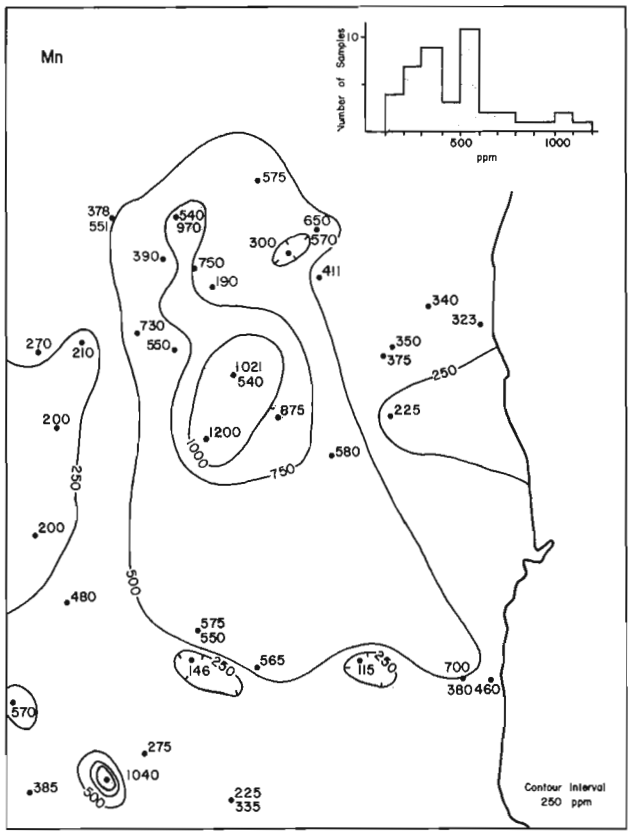

Figure 2 (cont.)

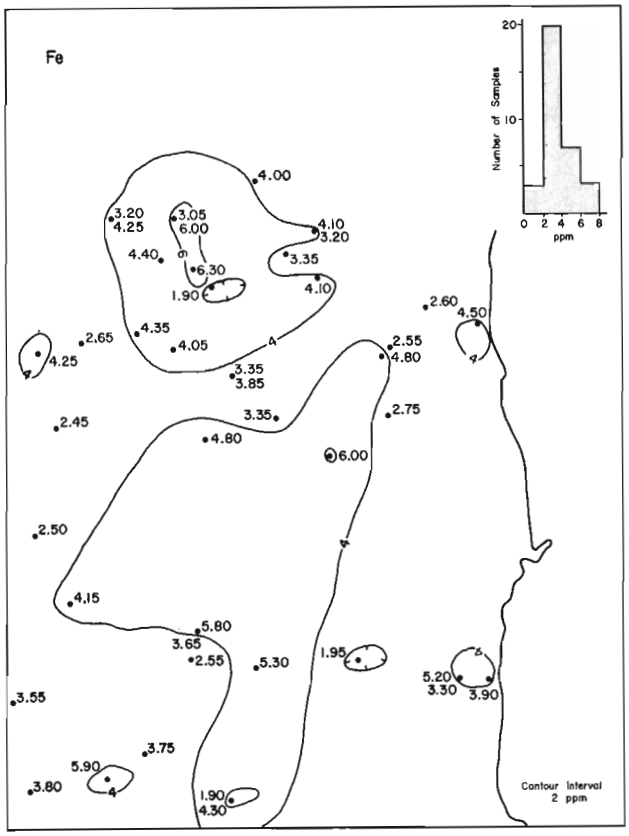

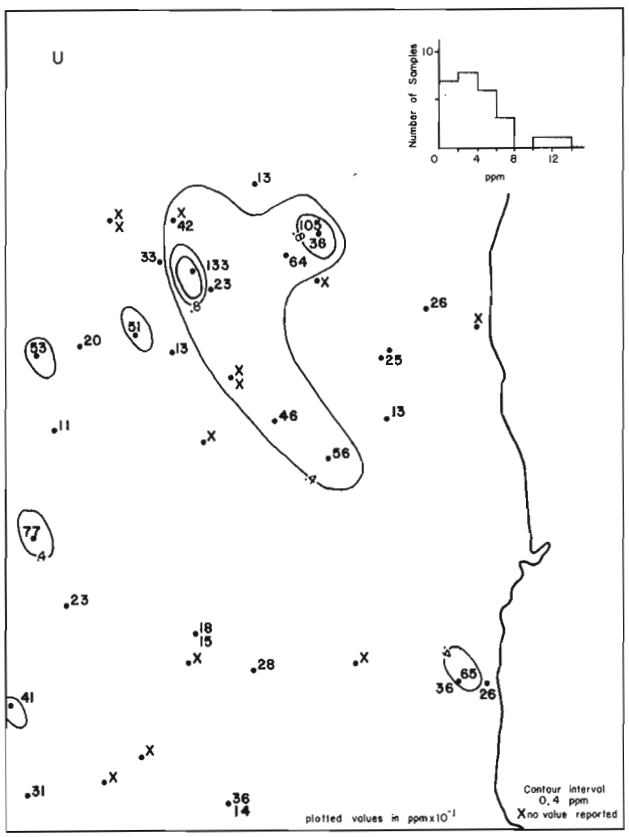

Figure 2 (cont.)

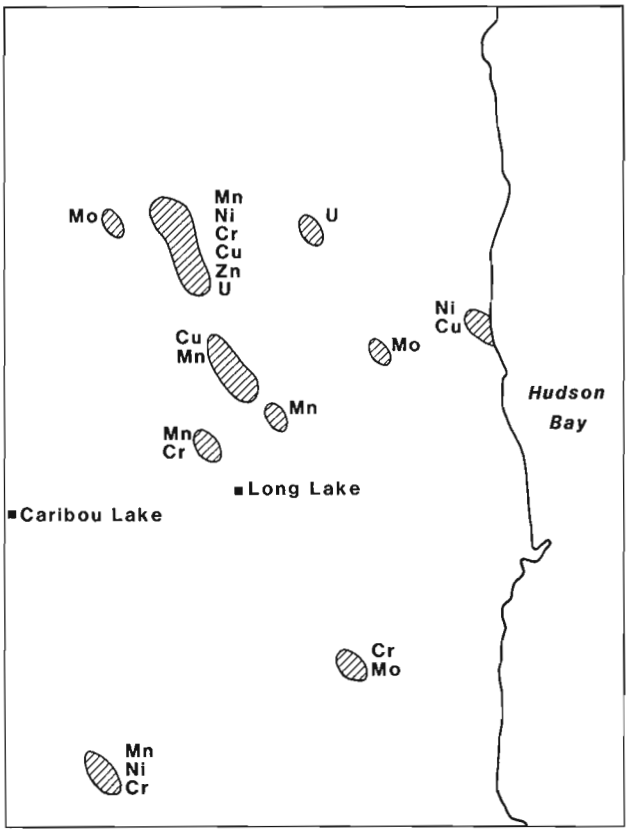

Figure 3. *Areas of high concentrations of the various trace elements.*

found in the northern part of the area does not necessarily have the same provenance. Much of the till debris has not travelled far from its bedrock source. Within the till areas are linear zones of reticulated kames, associated with break-up and disintegration of the ice mass. Poorly sorted stony marine sediments and ice-rafted debris deposited during the postglacial marine regression occupy areas near the coast and in places form a veneer over the sandy till. The remaining material of note is frost-heaved and frost-shattered bedrock which occupies extensive areas in the south (Fig. 1). Thin deposits of tundra peat are found over low wet areas.

The study area lies within the zone of continuous permafrost. Active layer depths vary from 0.3 m (in peat) to 2 m (sandy substrate).

Geochemistry

Frequency histograms of trace element values and their areal distributions are shown in Figure 2. The isopleth maps illustrate areal patterns; however, because of the wide spacing of samples, the isopleths should be regarded only as stylized trends. Most resultant patterns are irregular, but a trend parallel to ice flow direction is apparent in a few cases.

Most data shown relate to background levels of the elements analyzed, but a few anomalously high values of copper, zinc, nickel, chromium, molybdenum, and uranium are present. Because the samples are widely spaced, these locations do not necessarily reflect where the highest occurrences of these elements are to be found. They do, however, indicate areas that may merit further ground work. Both background and elevated values reported here are similar to

results derived from overburden samples from PolarGas cores (Shilts, 1980) from the same general area. No overburden samples were taken from east of Caribou Lake where high radioactivity levels were previously detected (Schledewitz and Cameron, 1977).

Sites with anomalously high trace element values have been plotted on Figure 3. Anomalous values of several elements are clustered together along a zone in sandy till through the middle part of the map area, but scattered anomalies are present elsewhere.

References

Davison, W.L.
1966: Caribou River map-area, Manitoba; Geological Survey of Canada, Paper 65-25, 6 p.

Dredge, L.A. and Nixon, M.F.
Surficial geology, Caribou River, Manitoba; Geological Survey of Canada, Map 5-1980, scale 1:250 000. (in press).

Klassen R.A. and Shilts, W.W.
1977: Glacial dispersal of uranium in the District of Keewatin, Canada; in Prospecting in Areas of Glacial Terrain; Institution of Mining and Metallurgy, London, p. 80-88.

Schledewitz, D.C.P.
1977a: The Seal River area; Manitoba Resources Division, Open File Report 77-3.

1977b: GS-1 Nejanilini-Caribou Lakes project; Manitoba Mineral Resources Division, Report of Activities, p. 5-12.

Schledewitz, D.C.P. and Cameron, H.D.M.
1977: Caribou River; Manitoba Resources Division, Preliminary Map 1977 S-3.

Shilts, W.W.
1980: Geochemical profile of till from Longlac, Ontario to Somerset Island; Canadian Institute of Mining and Metallurgy, Bulletin, v. 9, no. 822, p. 85-94.

RECOGNITION OF FROST-HEAVED OUTCROPS, ATHABASCA BASIN, SASKATCHEWAN

Project 780016

R.N.W. DiLabio
Terrain Sciences Division

Introduction

During field work in 1980 in the eastern part of the Athabasca basin, Saskatchewan, attention was given to the widespread occurrence of angular striated slabs of Athabasca Formation sandstone in many of the boulder fields in the region. The harder beds of quartz sandstone have retained striae and polish well, and such slabs are so numerous in places that they can be pieced together to form a continuous cover (R.H. Wallis, personal communication, 1980). Identification of boulder fields that are in fact heaved outcrops could aid boulder tracing, bedrock mapping, and overburden and diamond drilling in this area of rare outcrop. An experiment was performed to find a method to determine which boulder fields are heaved outcrops, and to determine if striae on fragments of heaved outcrops could still be used to infer ice movement direction.

Results

A small boulder field adjacent to an outcrop of flat-lying sandstone was examined at "Midwest Lake" (Map sheet 74I/8, UTM grid zone 13V, 553400, 6461900). Within a cluster of boulders occupying an area of about 3 m^2, the positions and sizes of 12 angular, striated (striae on top surface only) slabs of sandstone were determined. In addition, the strike and dip of the striated top surface of each slab (Fig. 1a) and the orientation of its striae (Fig. 1b) were measured. The slabs are 5 to 15 cm thick and from 35 by 20 to 140 by 80 cm in size on their striated surface. Many additional striated slabs were observed within 10 m of the cluster, but only 19 of them were measured. A small number of glacial erratics of striated sandstone, which could confuse recognition of heaved bedrock, were identified by better rounding and the presence of more than one striated surface; they were excluded from the study.

The high number (4/m^2) of angular, striated slabs of sandstone in the sampled area (Fig. 1a) is convincing evidence that the slabs represent an outcrop that has been heaved. The total area of the striated top surfaces of the slabs is estimated to be between 1.5 and 3.0 m^2, which corresponds well with the size of the sampled area.

The slabs are distributed in a circular pattern and most of them have low dips into or away from the circle (Fig. 1a). The absence of striated slabs from the centre of the circle may mean that slabs that once occupied the centre have been heaved to the margin. Lateral displacement of about 50 cm from the centre of the circle is indicated.

In general, striae on the slabs (Fig. 1b) are oriented parallel with drumlinoid ridges near the site and a prominent dispersal train of uraniferous till about 100 m southwest of the site. Most of the other 19 slabs that were examined conform to this trend. Striae that deviate strongly were found most commonly on slabs that are small, have steep dips, or are in close contact with other slabs. Rotation may have occurred in response to interference with other slabs, displacement by sliding from the centre of the circle, and tilting to high dips. Therefore, striae measurements may be reliable in boulder fields developed from the underlying bedrock if several of the larger, gently dipping slabs are examined.

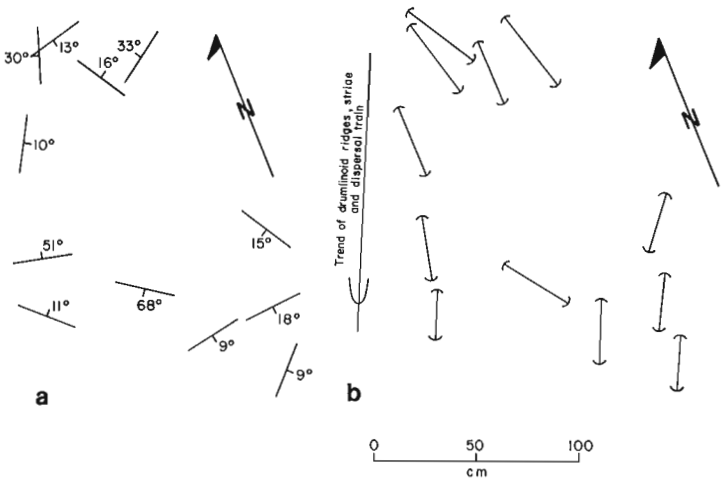

Figure 1. Maps of (a) attitude and (b) striae from the top surfaces of a cluster of frost-heaved slabs of sandstone.

Conclusions

1. In the Athabasca basin, boulder fields containing high numbers of angular, striated (striae on top surface only) slabs of Athabasca Formation sandstone can be assumed to be heaved outcrops (felsenmeer).
2. The circular distribution and attitude of striated slabs is consistent with an origin that involves a conical heave of bedded or sheeted bedrock over an ice lens as described by Kerr (1977), DiLabio (1978), Payette (1978), Thom (1978), and Dyke (1979). The fact that the original bedrock surface is preserved as the striated surface of the slabs means that rates and directions of heave could be estimated for the whole of the postglacial, which would complement present-day heave measurements (Dyke, 1979).
3. In the Athabasca basin, where directions of ice movement are required at a detailed scale for interpretation of dispersal trains of mineralized boulders and till, striae measurements may be made on large, gently dipping slabs of sandstone heaved in clusters from the bedrock.

References

DiLabio, R.N.W.
1978: Occurrences of disrupted bedrock on the Goulburn Group, eastern District of Mackenzie; in Current Research, Part A; Geological Survey of Canada, Paper 78-1A, p. 499-500.

Dyke, L.D.
1979: Bedrock heave in the central Canadian Arctic; in Current Research, Part A; Geological Survey of Canada, Paper 79-1A, p. 241-246.

Kerr, J. Wm.
1977: Frost and glacially deformed bedrock on Somerset Island, Northwest Territories; in Report of Activities, Part C; Geological Survey of Canada, Paper 77-1C, p. 75-77.

Payette, S.
1978: Les buttes rocheuses d'origine périglaciaire au Nouveau-Québec; Géographie physique et quaternaire, vol. 32, p. 369-374.

Thom, G.
1978: Disruption of bedrock by the growth and collapse of ice lenses; Journal of Glaciology, v. 20, p. 571-575.

From: Scientific and Technical Notes in Current Research, Part A; Geol. Surv. Can., Paper 82-1A.

WOOD IN QUATERNARY SEDIMENTS NEAR TIMMINS, ONTARIO

Project 780016

R.N.W. DiLabio
Terrain Sciences Division

Since the adoption of the reverse circulation drilling technique for deep till sampling in mineral exploration, hundreds of borings through Quaternary sediments have been made in the Timmins camp, initially in the search for base metal deposits and more recently in the search for gold deposits (Skinner, 1972; Averill, 1978; Brereton and Elson, 1979). At many drill sites, large numbers of wood chips have been noticed in the returning slurry, but these are not normally preserved. This report describes the areal distribution and stratigraphic positions of the known wood occurrences in Quaternary sediments near Timmins, Ontario, so that more data will be available on the stratigraphy of the region.

The scanty literature on buried wood near Timmins, i.e., a paper on work by Brereton and Elson (1979) in Currie Township and a radiocarbon date on wood from Kidd Township (Lowdon and Blake, 1979), suggests that buried wood is rare in the area, but such is not the case. Buried wood has been found in 12 townships extending in a broad arc north of Timmins from Robb Township to Currie Township (Fig. 1). Most of the sites were identified in the unpublished records of the overburden drilling program conducted by Skinner (1972), and a few samples have been sent to the Geological Survey by exploration companies. Undoubtedly, many more sites have not been sampled but have been noted in drill records in the assessment files of the Ontario Ministry of Natural Resources.

By far the most common and areally persistent stratigraphic position of wood is near or at the top of the silts, sands, or gravels that underlie Cochrane Till (Hughes, 1965) or underlie the fine grained sediments that were deposited in glacial Lake Barlow-Ojibway. One sample in this group, from Kidd Township, has a radiocarbon age of >28 000 years (GSC-1633; Lowdon and Blake, 1979). At no sites where wood has been found in this stratigraphic position is there evidence in the wood itself or in the enclosing sediments that the wood is in situ, so all these samples are classed as detrital (Fig. 1). Assuming that the wood is not a drilling contaminant from the surface, it may have been recycled in varying amounts from older beds such as the interglacial Missinaibi Formation (Skinner, 1973), the Mesozoic rocks of the Moose River basin, or presently unknown Quaternary organic beds. Because many of these sites are near the southern margin of Cochrane Till, it is possible that the wood was recycled during a Cochrane readvance, but the details of Cochrane events are still under study (J. Richard, personal communication, 1981).

Less commonly, detrital wood occurs in till or stratified sediments deep in the Quaternary sequence, underlying one or more tills. These are classed as detrital-subtill sites. One sample which has been examined, from Macklem Township, consists of pyritic, lignified wood and fresher wood. This suggests that the sample is a recycled mixture of Mesozoic and Quaternary wood fragments (unpublished GSC Wood Identification Report No. 80-37 by R.J. Mott).

At two sites, wood underlies till(s) at depth and overlies or is contained within oxidized sediments (paleosols?); these occurrences are classed as in situ (Fig. 1). At the site in Currie Township, moss associated with wood and oxidized clay has a radiocarbon age of >37 000 years (GSC-2148, Brereton and Elson, 1979); the clay and sand unit that contains the moss may be correlative with the Missinaibi Formation or may be an unknown Quaternary organic bed.

The drill record from hole FH-51 (unpublished data from Skinner, 1972) (Fig. 2) is unusual in that it illustrates both the detrital-subtill and in situ types of wood occurrences. Detrital wood was found in and under till at depths of 32.3, 33.9, and 35.3 m. In situ wood was found in oxidized silty clay at 37.5 m. The detrital wood probably was recycled from the lateral equivalent of the bed containing in situ wood. Unfortunately, none of the wood was preserved for dating.

Discussion

Knowledge of the local and regional stratigraphic framework (tills and nonglacial sediments) is essential for sample control in regional provenance studies and in drift

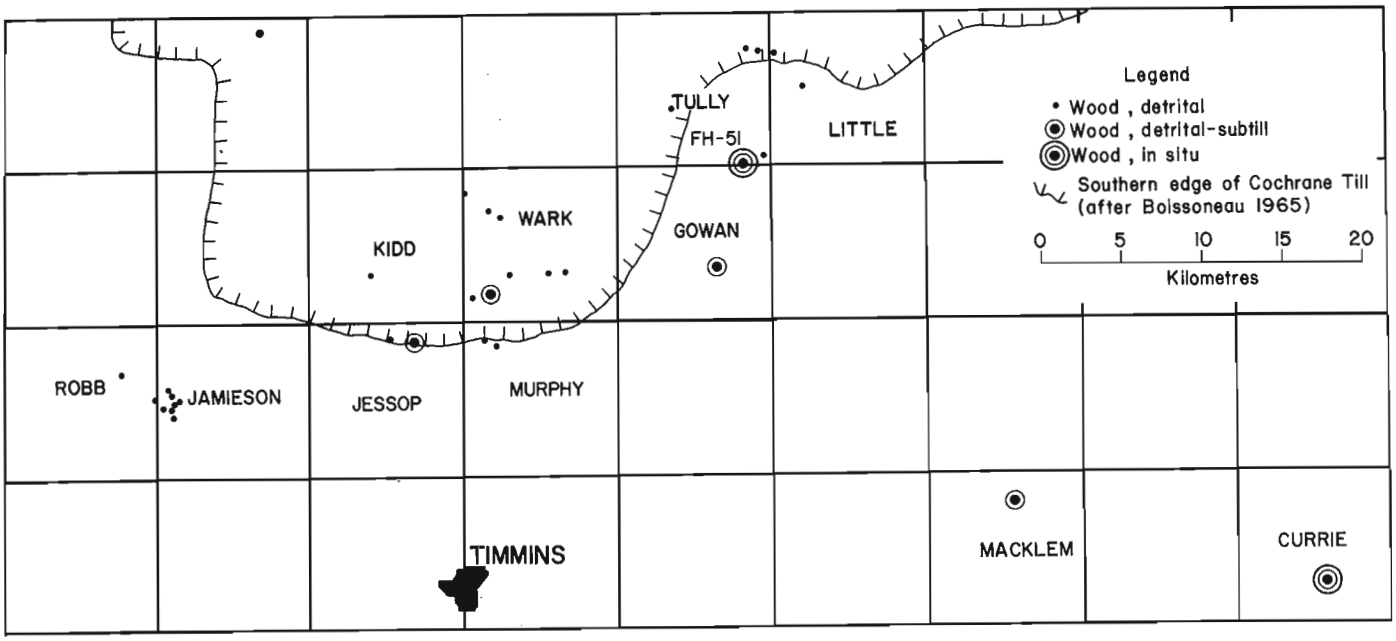

Figure 1. *Location map of occurrences of buried wood in the Timmins area. Grid shows township boundaries.*

From: Scientific and Technical Notes in Current Research, Part A; Geol. Surv. Can., Paper 82-1A.

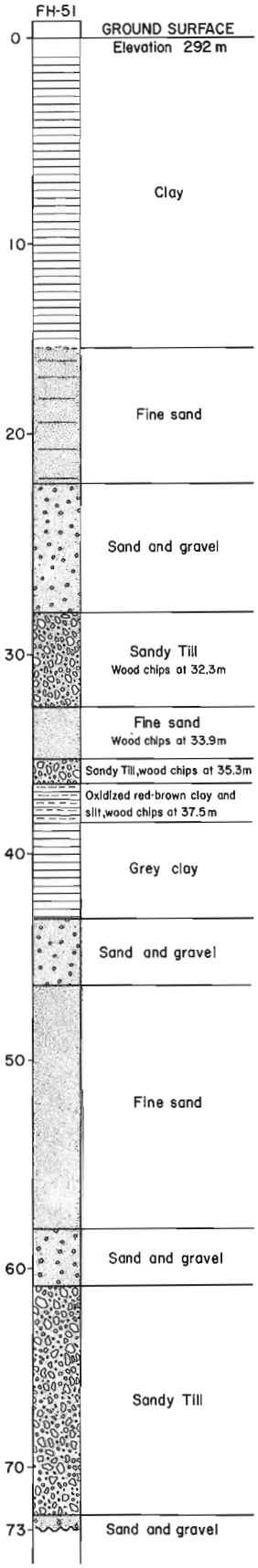

Figure 2.

Stratigraphy of overburden drillhole FH-51 (unpublished data from Skinner, 1972). See Figure 1 for location of drillhole.

prospecting. In this regard, the in situ wood is considered to represent one or more nonglacial intervals of at least interstadial rank and may be a regional stratigraphic marker horizon. It may be incorrect, however, to assume that in situ organic materials near Timmins are correlative with the Missinaibi Formation (last interglacial), in the light of recent research on the history of the Laurentide Ice Sheet in the Hudson Bay basin (Shilts et al., 1981; Shilts, in press). This research indicated that southern Hudson Bay may have been inundated by marine water (deglaciated) at about 76 000 and 35 000 years ago – previously unknown nonglacial events that may have had terrestrial equivalents in northern Ontario. Therefore, every occurrence of organic materials in the Quaternary sequence of northern Ontario should be described and sampled so that the stratigraphy of this region may be clarified further and related to that represented by marine deposits in the Hudson Bay Lowland.

The provenance of "old" tills, especially those underlying in situ organic deposits, must be considered as unknown. Therefore, ice-flow directions deduced from surface geomorphology and striae cannot be used with confidence to interpret the transport directions of the older tills sampled by reverse circulation drilling in this region. Mapping the abundances of distinctive local rocks and erratics present in such tills may provide evidence of provenance and ice-flow directions, as has been done by Shilts (in press) to map the flow paths of ice which originated in Nouveau Quebec and traversed the Hudson Bay Lowland during the last glaciation.

References

Averill, S.A.
1978: Overburden exploration and the glacial history of northern Canada; Canadian Mining Journal, v. 99, no. 4, p. 58-64.

Boissoneau, A.N.
1965: Algoma-Cochrane, surficial geology; Ontario Department of Lands and Forests, Map S365.

Brereton, W.E. and Elson, J.A.
1979: A late Pleistocene plant-bearing deposit in Currie Township, near Matheson, Ontario; Canadian Journal of Earth Sciences, v. 16, p. 1130-1136.

Hughes, O.L.
1965: Surficial geology of part of the Cochrane District, Ontario, Canada; in International Studies on the Quaternary, ed. H.E. Wright Jr. and D.G. Frey, Geological Society of America, Special Paper 84, p. 535-565.

Lowdon, J.A. and Blake, W., Jr.
1979: Geological Survey of Canada radiocarbon dates XIX; Geological Survey of Canada, Paper 79-7, 58 p.

Shilts, W.W.
Quaternary evolution of the Hudson/James Bay region; Le Naturaliste Canadien. (in press)

Shilts, W.W., Miller, G.H., and Andrews, J.J.
1981: Glacial flow indicators and Wisconsin glacial chronology, Hudson Bay/James Bay Lowlands: evidence against a Hudson Bay ice divide; Geological Society of America, Abstracts with Program, v. 13, p. 553.

Skinner, R.G.
1972: Drift prospecting in the Abitibi Clay Belt: Overburden drilling programme – methods and costs; Geological Survey of Canada, Open File 116.

1973: Quaternary stratigraphy of the Moose River basin, Ontario; Geological Survey of Canada, Bulletin 225, 77 p.

MINERALOGY AND PETROLOGY OF FOUR "STANDARD" SAMPLES OF IRON FORMATION

Projects 570029 and 690089

C.R. McLeod, Wan Liang-guo[1], and S. Abbey[2]
Economic Geology Division

Introduction

In conjunction with study of the geochemistry of iron formations (Gross and McLeod, 1980), within the scope of the Geological Survey of Canada project on the geology of iron deposits, and as a collaborative undertaking with the Analytical Chemistry Section, six bulk samples of Algoma type iron formation were collected from which four have been selected for use as "standard" samples.

A wide variety of reference samples of rocks is known to be available from geological institutions throughout the world. Our laboratories have participated in the collaborative analytical evaluation of many of them. Their compositions have ranged from granites and syenites through andesites, basalts, gabbros, etc., through serpentinites, peridotites and dunites, but none are available for iron formation rocks. One reference sample of iron formation rock, collected by the Geological Survey of Greenland (Appel, 1980) is known to be in preparation in France. However, a single sample is severely limited in application to a wide range of compositions, in minimizing the effects of uncertainties and possible interelement interferences and in detecting interlaboratory bias in collaborative analysis.

Many reference samples or iron ores are also available, but they have been evaluated only for constituents of direct interest to the iron and steel industry. Relatively little is known of their contents of components of geological interest – e.g. trace elements.

The availability of these samples as reference standards will be beneficial to other laboratories involved in the analysis of iron formations, as well as to project studies that are in progress at the Geological Survey.

It was decided that only oxide facies of iron formation would be used; selection of samples sites was based on the chemical composition of hand specimens previously collected and analyzed for project studies, and on the logistics of collection and availability of suitable material. Each bulk sample consisted of about 250 kg of iron formation that was broken in the field into pieces of less than fist-size to facilitate subsequent crushing of the material with batch-scale equipment. In addition, large pieces were collected to provide material for petrographic and mineralogical study and for pilot analytical work to determine which bulk samples might be most appropriate as reference materials. Where possible, bulk samples were taken from a well-defined bed or layer, using hand specimens of known composition as a guide. However, two of the six samples consisted of pieces of loose material collected where it was not practical to obtain the desired type of material in place. Channel samples were sliced from the representative pieces that were reserved for study purposes; these were crushed, ground and subsequently analyzed.

Ideally, the set of four "standard samples" should contain a gradation in concentration of as many elements as possible, although realistically these conditions would be difficult to attain, even if a much larger population of samples was available. Based on the composition as determined by analyses of the pilot samples for 24 constituents, four of the six bulk samples were selected for additional treatment as reference samples. Brief descriptions of these follow.

The Analytical Chemistry Section of the Geological Survey of Canada will collaborate with the Mineral Science Laboratories of Canada Centre for Mineral and Energy Technology (CANMET) in the processing and investigation of these samples, and their eventual establishment as reference materials. CANMET will undertake crushing, grinding, blending, sampling for homogeneity testing, and bottling of the samples. The GSC laboratories contribution will include analyses by various techniques to confirm homogeneity and to attempt to approach "true" composition, the organization and co-ordination of a collaborative analytical program with other laboratories, and the processing and publication of the resulting data.

Description of Samples

FeR-1 Location: Austin Brook, 27 km south-southwest of Bathurst, New Brunswick

The iron formation at Austin Brook, within the Tetagouche Group of Middle Ordovician age, is underlain by quartz-feldspar augen schist and overlain by rhyolite and rhyolite tuff (Skinner, 1974). Gross (1965) considered it to be of Algoma type. Selection of this sample locality, for high iron, manganese, phosphorous, barium and base metals, was based on the analyses of individual samples that were incorporated in a study by Saif (1980) of iron formation of the Bathurst district. The sample was obtained from a massive bed of magnetite-quartz iron formation about 15 cm thick consisting of magnetite bands with jasper laminae and lenses commonly 3 mm or less in thickness (Fig. 1). Thin, conformable laminae and crosslaminations of iron-poor material are evident in a polished slab of the sampled bed.

Figure 1. Polished slab representative of bed sampled for FeR-1, Austin Brook, N.B. Dark laminae are jasper. GSC 203779-D

From: Scientific and Technical Notes in Current Research, Part A; Geol. Surv. Can., Paper 82-1A.

[1]Geological Bureau of Inner Mongolia, People's Republic of China
[2]Central Laboratories and Technical Services Division

Magnetite and quartz are the main minerals present, constituting 55 and 30 per cent respectively of the total volume. Magnetite grains vary in size from 0.1 mm in diameter in the iron-rich bands to 0.2 mm in the iron-poor laminae. Minor oxidation of magnetite to martite and goethite is evident. Quartz grains are finer, averaging 0.04 mm in diameter. Apatite, siderite, daphnite and clinochlore are minor constituents and occur in laminae with magnetite and quartz; light green clinoclore has replaced some iron-bearing daphnite that exhibits a brownish tint in thin sections. Apatite crystals are 0.03 to 0.15 mm in length and constitute nearly 5 per cent of the sample by volume. The hematite content is about 3 per cent; the grains are very fine blades (0.005 mm in length) and are arranged in a subparallel pattern. Trace constituents include pyrite, galena, sphalerite, chalcopyrite and bornite, commonly occurring as dis-seminated grains but with galena showing an affinity for the jasper laminae.

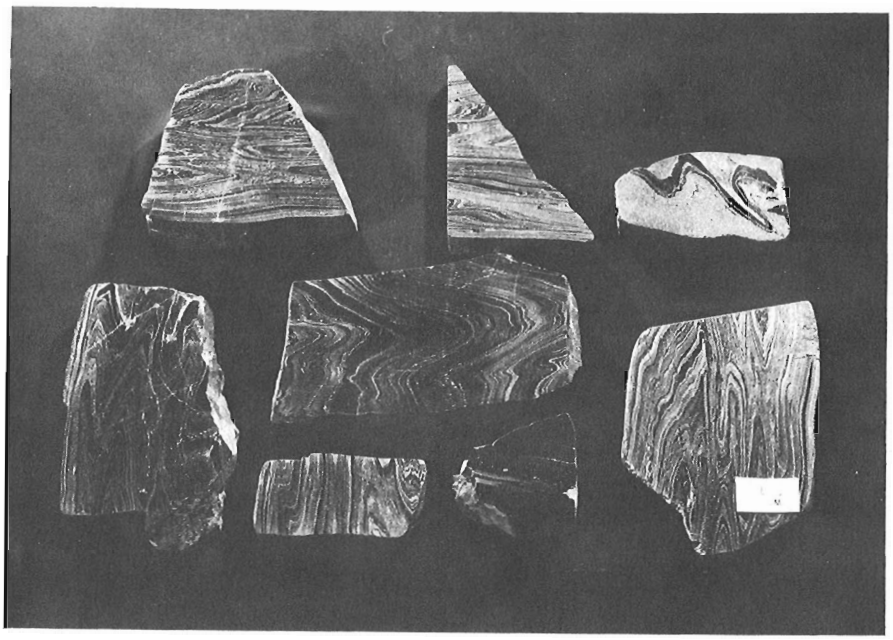

Figure 2. Folded magnetite-quartz iron formation representative of FeR-2, Griffith Mine. GSC 203779-A

Figure 3. Banded magnetite-chert iron formation from FeR-3, West Pit, Sherman Mine. GSC 203779

FeR-2 Location: North end of north pit, Griffith Mine, Bruce Lake, Ontario

Magnetite-quartz iron formation occurring within greywacke of Archean age has been mined at this property since 1968. The geology of the deposits and area has been described by Shklanka (1970). The geological environment is typical of many metasediment-hosted Archean iron formation deposits, and should be reflected in the aluminum, magnesium, potassium and titanium content of the bulk sample, which was acquired from a 40 cm bed of intensely folded, fine grained laminated iron formation containing intercalated amphibolite and metagreywacke. It was not possible to obtain a single representative sample across the width of the 40 cm bed because of the relatively strong cleavage present; eight specimens of varying size were selected from which material was cut for study and analysis (Fig. 2).

Magnetite makes up about 25 per cent of the sample by volume and occurs as subhedral to euhedral grains ranging in size from 0.03 to 0.15 mm and averaging 0.07 mm. It is concentrated in laminae that are commonly less than 1 mm thick, but which tend to thicken at the crests of folds. Amphibole and quartz are the major gangue minerals, with both green hornblende and bluish green amphibole present as prismatic crystals up to 2 mm in length that in many places enclose fine grained magnetite and quartz. Parallel blades of biotite occur with almandine in magnetite-poor layers. Irregular almandine crystals intergrown with biotite, and chlorite pseudomorphs in biotite were observed. Accessory minerals present include apatite, hematite, pyrite, marcasite, pyrrhotite and chalcopyrite; no titanium-bearing minerals were identified in the thin or polished sections from the representative samples.

FeR-3, FeR-4 Location: Sherman Mine, Temagami, Ontario

The Sherman Mine property encompasses deposits on the north and south limbs of the Tetapaga syncline in a sequence containing metavolcanic and pyroclastic rocks. Bennett (1978) has described the geology of the area and the main mineral deposits. Sample FeR-3 was taken from the west pit in the north limb of the syncline and consisted of several large blocks of loose material obtained from the floor of the pit from which representative pieces were broken (Fig. 3). An attempt was made to select pieces of similar appearance composed chiefly of quartz and magnetite with a minimum of intercalated material. The chert bands in the bulk sample ranges in colour from dark grey to maroon to the bright red jasper variety for which this mine is noted.

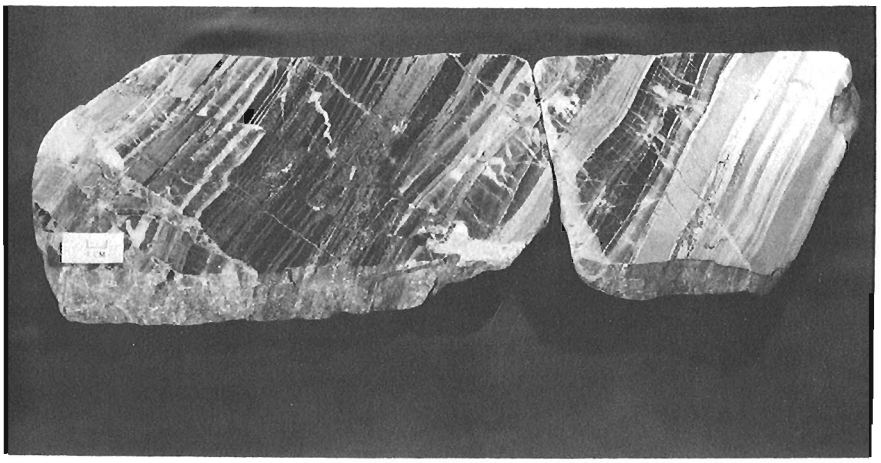

Figure 4

Magnetite-quartz iron formation with intercalated chloritic tuff, representative of bed sampled for FeR-4, South Pit, Sherman Mine. GSC 203779-B

Quartz is the most abundant mineral present and occurs as microcrystalline grains of 0.02 to 0.08 mm diameter with 120° triple-point junctions. Subhedral to euhedral magnetite grains averaging 0.04 mm are concentrated in laminae or bands up to 2 cm in thickness with associated carbonate, stilpnomelane, chlorite and sericite. Stilpnomelane shows strong green pleochroism in thin section and in some places has micaceous habit with sheets to 0.02 mm in length. Chlorite and sericite are disseminated or form irregular aggregates. Bladed hematite grains less than 0.01 mm in length occur as dusty inclusions, particularly in quartz; in jasper layers they tend to be oriented and form microlaminae. Trace amounts of apatite, pyrite and ilmenite were observed.

To provide variation in composition, sample FeR-4 was taken in the south pit from a 44 cm thick bed of cherty magnetite iron formation that contained interbanded chloritic tuff. The polished slabs (Fig. 4) represent about 39 cm of the material sampled and show the effects of minor movement and brecciation on the bed. Carbonate fracture fillings are apparently late and the distribution of much of the pyrite present seems to be related to them.

The mineral assemblage in this sample is similar to that in FeR-3, but the proportions of the minerals differ, and the texture is generally coarser. Grain size in the quartz bands ranges from 0.05 to 0.3 mm with veinlets containing crystals up to 2 mm in diameter. Magnetite is concentrated in laminae and bands to 2 cm in thickness. It is commonly subhedral to euhedral with grains varying in size from 0.02 to 0.1 mm. The tuffaceous bands contain quartz, chlorite and carbonate. Siderite is present as thin layers on either side of magnetite bands with chlorite and sericite occurring within them. Minor amounts of pyrite, apatite and chalcopyrite were observed but hematite is rare.

Acknowledgments

We thank G.A. Gross for suggestions and support and Lyn Anglin for capable and willing assistance in the field. We gratefully acknowledge the co-operation of R.N. Smith, Brunswick Mining and Smelting Corporation, J.D. Jeffries and F. Facca, The Griffith Mine, R.A. Rouleau, Cliffs of Canada Limited, and R. Garrett, Sherman Mine, National Steel Corportation and the watchman at Moose Mountain Mine, Capreol in obtaining the samples. We also thank S.I. Saif, University of Petroleum and Minerals, Dhahran, Saudi Arabia, for his contributions to project studies that were particularly useful in determining the location from which the Austin Brook sample should be taken.

References

Appel, P.W.U.
1980: Need for an iron-formation reference sample; Geostandards Newsletter, v. 4, No. 1, p. 19.

Bennett, G.
1978: Geology of the northeast Temagami area, Ontario; Ontario Geological Survey, Report 163, 128 p.

Gross, G.A.
1965: Geology of iron deposits in Canada: V. I, General geology and evaluation of iron deposits; Geological Survey of Canada, Economic Geology Report No. 22, 181 p.

Gross, G.A. and McLeod, C.R.
1980: A preliminary assessment of the chemical composition of iron formations in Canada; Canadian Mineralogist, v. 18, p. 223-229.

Saif, S.I.
1980: Petrographic and geochemical investigation of iron formation and other iron-rich rocks in Bathurst District; in Current Research, Part A, Geological Survey of Canada, Paper 80-1A, p. 309-317.

Shklanka, R.
1970: Geology of the Bruce Lake area; Ontario Division of Mines, Geological Report 82, 27 p.

Skinner, R.
1974: Geology of Tetagouche Lakes, Bathurst, and Nepisiguit Falls map-areas, New Brunswick; Geological Survey of Canada, Memoir 371, 133 p.

NOTES ON URANIUM INVESTIGATIONS IN THE CANADIAN CORDILLERA, 1981

Project 750069

R.T. Bell
Economic Geology Division

Field investigations for the purpose of uranium resource evaluation continued in northern British Columbia and in southern Yukon Territory. Observations and interpretations of general stratigraphic interest, based on field investigations during the summer of 1981, are included below.

Sustut and Sloko groups

As indicated last year (Bell, 1981) uranium mineralization and anomalously high radioactivity accompanies tuffs and tuffaceous sediments in the lower third of Brothers Peak[1] Formation of the Sustut Group near Brothers Peaks[1] and Edozadelly Mountain (NTS 94E). Similar indications of uranium were found farther north around Laslui Lake, Cold Fish Lake and Hyland Post (NTS 104H), with one occurrence north of Laslui Lake having 335 ppm U. In general the tuffaceous rocks contain between 4 and 10 ppm U, but anomalous zones contain between 10 and 30 ppm U with occasional centimetres thick pinkish altered zones having values greater than 60 ppm.

The author supports Eisbacher's view (1974) that the most likely source for the tuffs and tuffaceous rocks was the Sloko volcanoes to the northwest. Therefore the southern exposures of Sloko were investigated at Mount Helveker (NTS 104G) and in the southeast corner of Tulsequah map area (NTS 104K) as well as small outliers of possible Sloko and/or Sustut rocks.

Mount Helveker (NTS 104G)

Detailed field studies of Mount Helveker in Telegraph Creek map area (Souther, 1972) were completed. Preliminary observations and conclusions are summarized below.

(a) Minor contemporaneous volcanism occurred sporadically during deposition of the conglomerate-dominated sedimentary sequence below the Sloko flows, breccias and tuffs capping the mountain. These sediments are probably all correlative with the Brothers Peak Formation of the Sustut Group.

(b) The sedimentary sequence, about 400 m thick on the south side of the mountain, is about 200 m thicker on the north side. The sequence dips fairly uniformly northerly about 10 degrees. Local dip reversals and steepening are caused by faults rather than by regional general folds, or are only apparent because of crossbeds.

(c) Rapid facies changes in the sedimentary sequence reflect deposition in a rugged terrain, likely accompanied by contemporaneous faulting. Faulting also occurred during initial emplacement of the overlying Sloko volcanics, which together with the thick swarm of trachytic dykes suggests close proximity to a volcanic centre.

(d) The larger boulders and cobbles in the sedimentary sequence are dominantly biotite ± hornblende granodiorite and tonalite, and fine- to coarse-grained quartz monzonite of units 17 and 19 of Souther (1972). There appears to be a relative increase in boulders of the younger quartz monzonite in the higher parts of the sequence. Maximum boulder size is 67 cm.

(e) The sedimentary sequence is roughly divisible into a lower part that contains varicoloured sediments with a reddish cast to the conglomerates and an upper part that is entirely a drab greenish grey. On the north side of the mountain this transition occurs about 30 m beneath the volcanics whereas on the south and east side this transition occurs at about 100 m beneath them.

(f) Most uranium occurrences (Bell, 1981) were found only in the upper drab conglomeratic clastics, and only on the south side of the mountain. Uranium occurs as saléeite and torbernite, and is also associated with limonite and clays, with organic material and probably in opalescent coatings of pebbles and fractures. Bulk samplings over 2 m strike length and about 20 cm thickness of two zones yielded 789 and 843 ppm U. The exception to the above generalization is a tuffaceous unit with plant fragments lower in the south section which was not found to be radioactive in the field but nevertheless yielded 149 ppm U. All other tuffaceous units at Mount Helveker contained less than 10 ppm U.

Pitman and Tucho Rivers (NTS 104I)

A unit at 58°05'N, 128°18'W was recently reinterpreted as Middle Jurassic (Gabrielse, 1979) rather than correlative with Sustut Group (Gabrielse, 1962). The author agrees that it is not Sustut.

The northern part of this unit comprises a sequence of grey and green chert- and volcanic-pebble and breccia conglomerate interbedded with greywacke, siltstone and shale and intermediate volcanic tuffs, dipping monoclinally about 15 to 30 degrees southerly. This unconformably overlies a red and maroon volcanic breccia and redbed and mafic volcaniclastic sequence of the shallow water sediments dipping monoclinally about 10 to 20 degrees easterly. The former resembles some of the Bowser Assemblage and it is possible the latter may be as old as Late Triassic although no fossils have been found as yet.

No radioactive anomalies were detected in either sequence and both appear unlikely hosts for significant uranium mineralization.

Tuya River (NTS 104J)

Sedimentary rocks at the confluence of the Tuya and Little Tuya rivers have been considered to be possible correlatives of the Sustut Group (Gabrielse, 1980). Close investigation shows they are in fact interbedded with olivine basalt flows and contain abundant clasts of similar mafic rocks. They most likely represent distal, fluvial facies of the Level Mountain volcanics (Hamilton and Scarfe, 1977). Recent slumping has strongly affected these sediments just north of the confluence. One slumped tuffaceous mudstone has slightly higher radioactive response (1½ times background) which is interpreted as normal for rock of felsic composition.

These sediments contrast sharply with Sustut Group nearby in the Grand Canyon of the Stikine and with Sloko Group in the Tulsequah map area by being only weakly consolidated. They compare favourably in this respect with those described below on the Nahlin River.

Sheslay (NTS 104J)

The sequence of rocks immediately beneath the flat-lying olivine basalt north of Egnell Creek at Sheslay comprises varicoloured, vesicular and porphyritic flows, varicoloured, weakly consolidated tephra and very minor greenish grey volcaniclastic sandstones. They resemble more closely the Heart Peaks Formation (Souther, 1971) than Sloko Group (Hamilton and Scarfe, 1977; Gabrielse, 1980).

[1] The formally approved name "Brothers Peak Formation" does not include the plural form of the nearby Brothers Peaks.

From: Scientific and Technical Notes in Current Research, Part A; Geol. Surv. Can., Paper 82-1A.

White, partly glassy rhyolitic tuff and rusty conglomeratic sands occur immediately beneath the olivine basalt approximately 7 km north of Sheslay. These too may be part of the Heart Peaks sequence, but may represent an early, local, minor, felsic phase of the Level Mountain volcanics. They resemble both sands and sandy gravel at Tuya River and at Nahlin River.

No significant radioactive anomalies were detected.

Nahlin River (NTS 104J)

Weakly consolidated, brown weathering sandstone, siltstone and pebble conglomerate are interbedded with olivine basalt and breccia on Nahlin River about 3 km east of the confluence with Koshin River. No radioactive anomalies were detected.

Weakly consolidated, white weathering, felsic, lapilli tuff grading upwards to interbedded ash tuff and tuffaceous mudstones occurs just to the west, at the confluence with Koshin River. These are conformably overlain by olivine basalt. The tuff is weakly radioactive (twice background, 6.6 ppm U), interpreted as normal for rocks of this composition. A couple of small rusty spots, two or three centimetres in diameter yielded very slightly enhanced radioactivity (7.5 ppm U).

The rocks at these two localities have generally been interpreted as Cretaceous-Paleocene and possibly younger (unit KT of Gabrielse, 1980). The author proposes that they are indeed younger and that they are northwesterly, distal, sediment-dominated phases of the Level Mountain Group (unit MP of Gabrielse, 1980).

Sloko Group (NTS 104K/SE)

Investigations of Sloko Group in Cheja and Chechidla ranges provide the following observations and preliminary conclusions.

(a) No lithologies similar to the sequences examined near Sheslay, Nahlin River and Tuya River were observed.

(b) No strong radioactive anomalies in bedrock or in moraine boulders were detected. Enhanced radioactivity is entirely due to the felsic composition of these rocks, the most radioactive containing only 6 to 7.5 ppm U.

(c) Rusty alteration zones, after pyrite, pyrrhotite and/or siderite, are common.

One Ace Mountain (NTS 104P)

About 5 km northeast of One Ace Mountain is a belt of fine chert- and shale-pebble conglomerate with subordinate fine grained greywacke and siltstone. No contacts were observed but this sequence is probably fault bounded.

It is open for two interpretations (Gabrielse, 1963), namely that it is late Mesozoic to Early Tertiary (i.e. Sustut equivalent) or much earlier, perhaps even Late Paleozoic. The strongly lithified character of the unit, as well as the presence of a penetrative cleavage in the finer rocks suggest to the author that it is older than Late Mesozoic and unlikely to be Sustut equivalent.

No radioactive anomalies were detected.

Tsikhini Creek – Glenora (NTS 104G)

A thick sequence of vesicular and amygdular columnar basalt flows, agglomerates and breccias comprise a westerly dipping sequence at the mouth of Tsikhini Creek. Alteration zones within the breccias and agglomerates contain fairly massive, bright green aphanitic celadonite both as replacement of the breccia and as intraclast, banded claystone. Unfractured pieces of this celadonite (>30 cm diameter) are common and might be useful as artistic stone.

Lavas like these were not encountered within the Sloko sequence. Perhaps this sequence is younger, i.e. unit 25 rather than unit 24 of the Telegraph Creek map area (Souther, 1972).

No radioactive anomalies were detected and the environment appears unlikely to host significant uranium mineralization.

Cabin Creek (NTS 105B)

Pink coarsely porphyritic biotite-quartz monzonite and granite in the stock at Cabin Creek (Poole et al., 1960) displays four to six times radioactivity (6000 to 9000 cpm on T1 scale of TV1 McPhar scintillometer) relative to the country rocks. Quartz is generally smoky to black. Orthoclase phenocrysts usually range from 2-10 cm in length. At one locality (occurrence A of Table 1) near the centre of the stock is a pegmatitic phase with micrographic and myrmekitic intergrowths. The entire northern rim of the stock appears to be grey, medium grained biotite-quartz monzonite with sparse or no phenocrysts, and yields weaker radioactivity, less than 4000 cpm.

Uranium contents and strongly radioactive occurrences are noted in Table 1. These occurrences are in three rock types: dark smoky porphyritic biotite-quartz monzonite (the most common), xenoliths of biotite-magnetite-bearing fine grained gneiss, and pegmatite. Radioactivity is largely derived from opalescent coatings of fractures, and from euxenite-polycrase and monazite. Magnetite, ilmenite and apatite are present in some xenoliths and monzonite.

Other features in the area include scheelite-pyrrhotite-bearing quartz-biotite schists in the eastern contact zone accompanied by steeply dipping white quartz veins bearing black tourmaline and, in one occurrence, rutile. Pink quartz and skarn fragments occur in float.

Two other granitic intrusions were investigated in the area. One, southeast of Stoneaxe Lake, is lithologically similar to the Cabin Creek stock, and another, the Marker Lake Batholith, consists of granodiorite and contains much gneiss. No strong radioactive anomalies were detected in either body. A porphyritic (quartz, sanadine) felsite dyke cutting the Marker Lake Batholith yielded 3 times background radioactive response; however, two analyses gave 8.4 and 11.8 ppm U.

Table 1

Cabin Creek occurrences

Occurrences	Location	Type	Sample	U content ppm
A	60°37'20"N, 129°24'35"W	Pegmatite	outcrop	235
B	60°37'10"N, 129°25'12"W	Qtz. Monz.	float	1700 and >5000
C	60°39'26"N, 129°23'40"W	Qtz. Monz.	float	27.4
D	60°36'50"N, 129°27'30"W	Qtz. Monz.	outcrop	402
E	60°36'42"N, 129°27'10"W	Qtz. Monz.	outcrop	158
F	60°36'42"N, 129°28'10"W	Xenolith	talus	40.2
G	60°36'30"N, 129°28'55"W	Qtz. Monz.	float	not analyzed

Acknowledgments

Mineral determinations were made by A.L. Littlejohn and A.C. Roberts of the Central Laboratories and Technical Services Division. Uranium analyses by the neutron activation method were made by Atomic Energy of Canada, Limited. B. Downing, T. England, H. Gabrielse, J. Hobart, P. Newman, M. Stammers, P. Tegart and H.W. Tipper provided advice while in the field. J.-F. Marier provided exemplary field assistance.

References

Bell, R.T.
1981: Preliminary evaluation of uranium in Sustut and Bowser successor basins, British Columbia; in Current Research, Part A, Geological Survey of Canada, Paper 81-1A, p. 241-246.

Eisbacher, G.H.
1974: Sedimentary history and tectonic evolution of the Sustut and Sifton basins, north-central British Columbia; Geological Survey of Canada, Paper 73-71, 57 p.

Gabrielse, H.
1962: Geology, Cry Lake, British Columbia; Geological Survey of Canada, Map 29-1962.

Gabrielse, H. (cont.)
1963: McDame map-area, Cassiar District, British Columbia; Geological Survey of Canada, Memoir 319, 138 p.

1979: Geology, Cry Lake, British Columbia; Geological Survey of Canada, Open File 610.

1980: Geology, Dease Lake, British Columbia; Geological Survey of Canada, Open File 707.

Hamilton, T.S. and Scarfe, C.M.
1977: Preliminary report on the petrology of the Level Mountain Volcanic Centre, northwest British Columbia; in Report of Activities, Part A, Geological Survey of Canada, Paper 77-1A, p. 429-434.

Poole, W.H., Roddick, J.A., and Green, L.H.
1960: Geology, Wolf Lake, Yukon Territory; Geological Survey of Canada, Map 10-1960.

Souther, J.G.
1971: Geology and mineral deposits of Tulsequah map-area, British Columbia; Geological Survey of Canada, Memoir 362, 84 p.

1972: Telegraph Creek map-area, British Columbia; Geological Survey of Canada, Paper 71-44, 38 p.

STRATIGRAPHIC AND STRUCTURAL STUDIES, SOUTHERN ELLESMERE ISLAND, DISTRICT OF FRANKLIN

Projects 790042 and 810016

Andrew V. Okulitch and Ulrich Mayr
Institute of Sedimentary and Petroleum Geology, Calgary

Objectives

Detailed and systematic regional studies of Paleozoic stratigraphy, sedimentology, structure and tectonics were initiated in southern Ellesmere Island in 1980. The primary purposes of this operation are: refinement of stratigraphic data, resolution of correlation problems, interpretation of facies relationships, delineation of structural features, construction of cross-sections and modelling of tectonic processes and evolution of the Central Ellesmere Fold Belt and adjacent Arctic Platform. Such clarification of the geological history and present configuration of strata will lead to more precise estimates of the region's economic potential, particularly that of hydrocarbons.

Location

The project area (Fig. 1) embraces the outcrop belt of Paleozoic strata extending from southwestern Ellesmere Island eastward and northward, limited by exposures of the Precambrian Shield on the southeast and east and by overlying Mesozoic strata to the northwest. Extension of mapping may be undertaken in the future to examine largely unmapped regions of westernmost Ellesmere Island and northern Devon Island and to delineate structures in Mesozoic and Tertiary rocks to complete the tectonic study.

Project Responsibilities

A.V. Okulitch and U. Mayr share joint responsibility for all aspects of operations, research and publication. Okulitch has begun and will continue regional mapping over the entire project area with emphasis on structure. Mayr is responsible for all stratigraphic studies. R. Thorsteinsson is attached to the project in a consultative role but is also responsible for regional mapping, primarily in the Vendom Fiord map area (NTS 49 D), and related stratigraphic and paleontological research.

For studies in the Arctic Platform, where stratigraphic problems predominate, Mayr will be senior author and co-ordinator of future publications. Maps and reports dealing with the Central Ellesmere Fold Belt will be co-ordinated by Okulitch. Contributions to some or all publications will be made by students engaged in post-graduate research.

Previous Geological Investigations

The history of early exploration of southern Ellesmere Island was given by Blackadar (1963). Numerous scattered localities were studied during Operation Franklin in 1955 (Fortier et al., 1963) and systematic regional reconnaissance was carried out by Christie (1962), Kerr (1968), Thorsteinsson and others (published as Geological Survey of Canada Maps 1300A-1304A, 1307A, 1308A, 1312A, 1357A, 1358A), and Frisch et al. (1978; see Fig. 1). Kerr and Christie mapped parts of the Vendom Fiord (49 D) and Craig Harbour (49 A) map areas but the results were not published. The Paleozoic stratigraphy of the region was described in some detail by Kerr (1967a, b, 1976). Additional data were provided by Trettin (1978) and Nassichuk and Wilde (1977). More detailed studies within the project area include Mossop (1973), Mayr (1974), McGill (1974), Embry and Klovan (1976), Roblesky (1979) and Smith and Stearn (1981). During 1973 and 1974, two wells were drilled on southern Bjorne Peninsula with Silurian-Devonian carbonates as targets. Stratigraphy in these wells has been discussed by Mayr et al. (1978).

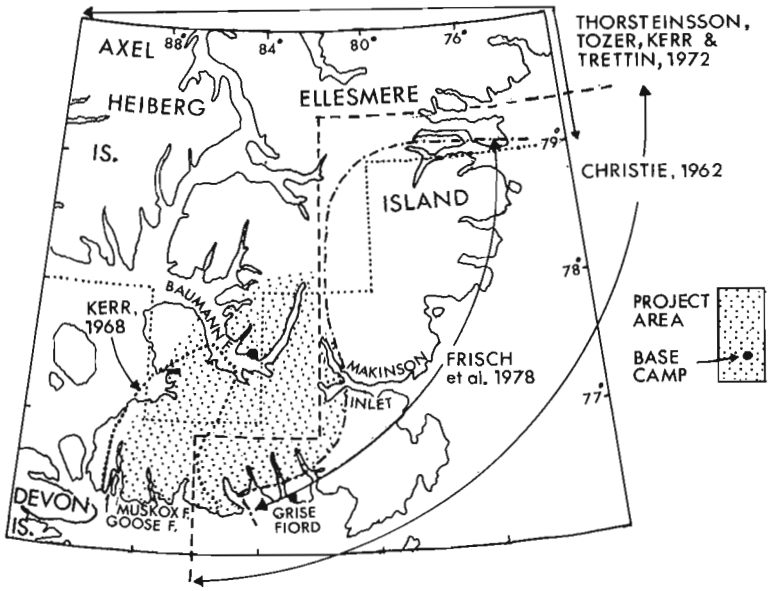

Figure 1. Index map.

Figure 2. Areal view to the east-northeast of the base camp at Baumann Fiord on alluvium mantled, recessive Eids Formation (Devonian). Beyond the creek are outcrops of the Ordovician Cornwallis Group carbonates exposed in the east-dipping limb of a fault-breached anticline. ISPG Photo 1697-7.

From: Scientific and Technical Notes in Current Research, Part A; Geol. Surv. Can., Paper 82-1A.

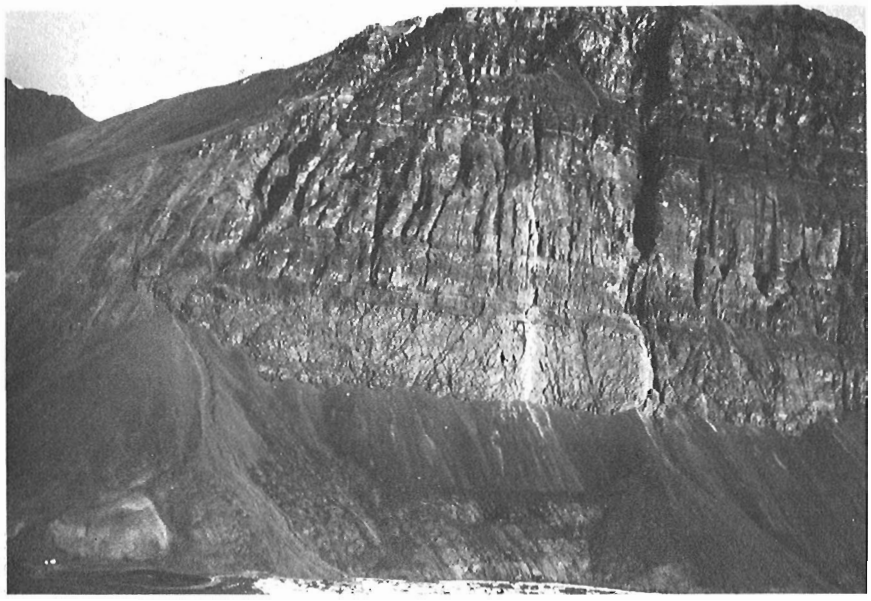

Figure 3. *Fly camp (lower left) at the base of a cliff of gently south-dipping Ordovician Allen Bay Formation carbonates at the head of Grise Fiord. ISPG Photo 1697-4*

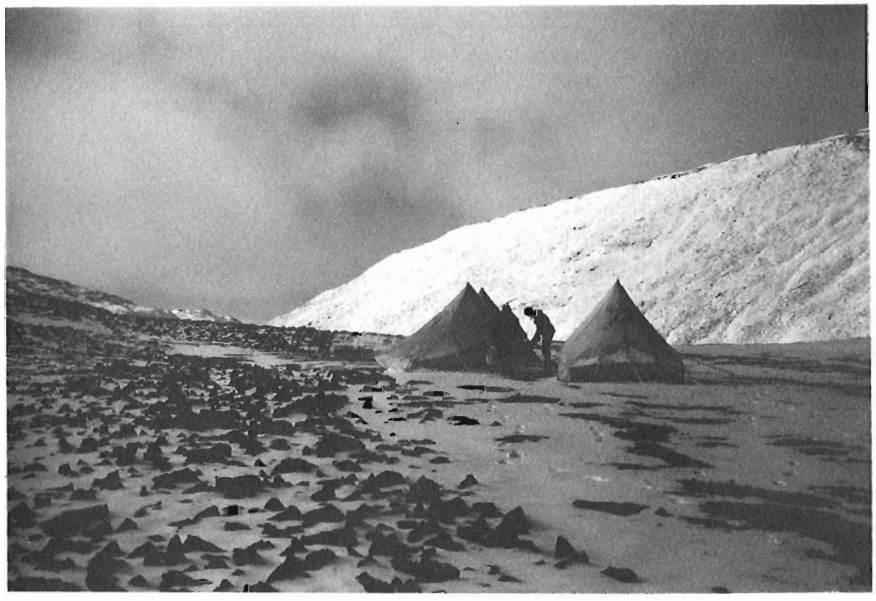

Figure 4. *Aftermath of July blizzard at flycamp on the Devonian Okse Bay Group clastic wedge near Bird Fiord. ISPG Photo 1697-2.*

Project Field Work

Reconnaissance and familiarization traverses in the project area were begun by Okulitch in 1980 during a 7 week period while attached to A.F. Embry's field party which occupied a base camp site also used in 1981. After initial regional examination of major stratigraphic units, work was concentrated along east-west fiords and valleys north of the camp that provided data for preliminary structure sections and appreciation of structural styles. During the summer of 1981 (20 June to 22 August) systematic mapping of the Baad Fiord (49 B) and Craig Harbour (49 A) map areas and adjacent parts of the Baumann Fiord (49 C) and Vendom Fiord (49 D) areas was undertaken. Work was done from the base camp at Baumann Fiord and from several fly camps along Makinson Inlet and in the southern fiord terrain.

Emphasis of the stratigraphic studies was on establishing the stratigraphic sequence in the southeastern part of the project area. J.J. Packard (senior field assistant) worked within the Cambrian-Ordovician sequence and U. Mayr examined Ordovician to Devonian rocks. The Devonian clastic wedge was studied for a doctoral thesis by R. Rice. J.L. Poey commenced a detailed study for a master's thesis of the Silurian carbonate-shale facies transition in the Baumann Fiord area.

Mapping was supported by a helicopter leased for two months from Midwest Helicopters, piloted by M. Aldersea and L. Ross and maintained by R. Cameron and J. Rabul. A second helicopter was intermittently available under lease from the Polar Continental Shelf Project, which also allotted 40 hours of Twin Otter aircraft time for movement of personnel, equipment and visitors to and from Resolute. Another 40 hours was obtained by lease from PCSP. Expediting services were provided by F. Alt of the PCSP. Aircraft fuel had been cached at the base camp airstrip by the Coast Guard vessel 'Franklin' during fall breakup of the previous year. E. Wolter provided excellent meals throughout both field seasons. W. Christiansen managed the camp cheerfully and efficiently. L. Ferguson, G. Perkins, S. Smith and D. Sylvestre fulfilled the duties of field assistants most satisfactorily.

Geological results of field operations are summarized in Mayr (1982), Okulitch (1982), Packard and Mayr (1982), Poey (1982) and Rice (1982).

References

Blackadar, R.G.
1963: History of Exploration, southern Ellesmere Island in Fortier, Y.O. et al.: Geology of the north-central part of the Arctic Archipelago, Northwest Territories (Operation Franklin); Geological Survey of Canada, Memoir 320, p. 264-266.

Christie, R.L.
1962: Geology, Alexandra Fiord, Ellesmere Island, District of Franklin; Geological Survey of Canada, Map 9-1962.

Embry, A.F. and Klovan, J.E.
1976: The Middle-Upper Devonian clastic wedge of the Franklinian Geosyncline; Bulletin of Canadian Petroleum Geology, v. 24, p. 485-639.

Fortier, Y.O., Blackadar, R.G., Glenister, B.F., Greiner, H.R., McLaren, D.J., McMillan, N.J., Norris, A.W., Roots, E.F., Souther, J.G., Thorsteinsson, R., and Tozer, E.T.
1963: Geology of the north-central part of the Arctic Archipelago, Northwest Territories (Operation Franklin); Geological Survey of Canada, Memoir 320.

Frisch, T., Morgan, W.C., and Dunning, G.R.
1978: Reconnaissance geology of the Precambrian Shield on Ellesmere and Coburg islands, Canadian Arctic Archipelago; in Current Research, Part A, Geological Survey of Canada, Paper 78-1A, p. 135-138.

Jones, Brian and Smith, G.P.
1980: Lower Devonian brachiopods from the Eids Formation, southwest Ellesmere Island, Arctic Canada; Journal of Paleontology, v. 54, no. 4, p. 675-695.

Kerr, J.W.
1967a: Vendom Fiord Formation – a new red-bed unit of probable early Middle Devonian (Eifelian) age, Ellesmere Island, Arctic Canada; Geological Survey of Canada, Paper 67-43.

1967b: Stratigraphy of central and eastern Ellesmere Island, Arctic Canada, Parts I and II; Geological Survey of Canada, Paper 67-27.

1968: Geology, southwestern Ellesmere Island, District of Franklin; Geological Survey of Canada, Map 10-1968.

1976: Stratigraphy of central and eastern Ellesmere Island, Part III, Upper Ordovician (Richmondian), Silurian and Devonian; Geological Survey of Canada, Bulletin 260.

Mayr, U.
1974: Lithologies and depositional environments of the Allen Bay-Read Bay formations (Ordovician-Silurian) on Svendsen Peninsula, central Ellesmere Island in Proceedings of the Symposium on the Geology of the Canadian Arctic, ed. J.D. Aitken and D.F. Glass; Geological Association of Canada and Canadian Society of Petroleum Geologists, p. 143-157.

1982: Lithostratigraphy (Ordovician to Devonian) of the Grise Fiord area, Ellesmere Island, N.W.T.; in Current Research Part A, Geological Survey of Canada, Paper 82-1A, report 10.

Mayr, U., Uyeno, T.T., and Barnes, C.R.
1978: Subsurface stratigraphy, conodont zonation and organic metamorphism of the lower Paleozoic succession, Bjorne Peninsula, Ellesmere Island, District of Franklin; in Current Research, Part A, Geological Survey of Canada, Paper 78-1A, p. 393-398.

McGill, P.C.
1974: The stratigraphy and structure of the Vendom Fiord area; Bulletin of Canadian Petroleum Geologists, v. 22, p. 361-386.

Mossop, G.D.
1973: Anhydrite-carbonate cycles of the Ordovician Baumann Fiord Formation, Ellesmere Island, Arctic Canada: a geological history; unpublished Ph.D. thesis, University of London, London, England.

Nassichuk, W.W. and Wilde, G.L.
1977: Permian fusulinaceans and stratigraphy at Blind Fiord, southwestern Ellesmere Island; Geological Survey of Canada, Bulletin 268.

Okulitch, A.V.
1982: Preliminary structure sections, southern Ellesmere Island, N.W.T.; in Current Research Part A, Geological Survey of Canada Paper 82-1A, report 9.

Packard, J. and Mayr, U.
1982: Cambrian and Ordovician stratigraphy of southern Ellesmere Island, District of Franklin; in Current Research Part A, Geological Survey of Canada Paper 82-1A, report 11.

Poey, J.-L.
1982: Preliminary report on Upper Ordovician to Upper Silurian carbonates, Baumann Fiord area, southwestern Ellesmere Island, District of Franklin; in Current Research Part A, Geological Survey of Canada, Paper 82-1A, report 12.

Rice, R.J.
1982: Sedimentology of the Late Middle and Upper Devonian Okse Bay Group, southwestern Ellesmere Island: a progress report; in Current Research Part A, Geological Survey of Canada, Paper 82-1A, report 13.

Roblesky, R.F.
1979: Upper Silurian (late Ludlovian) to Upper Devonian (Frasnian?) stratigraphy and depositional history of the Vendom Fiord region, Ellesmere Island, Canadian Arctic; unpublished M.Sc. thesis, University of Calgary.

Smith, G.P. and Stearn, C.W.
1981: The Devonian carbonate-clastic sequence on southwest Ellesmere Island, Arctic Canada: an example of progradation; in Program and Abstracts, Third International Symposium on Arctic Geology; Calgary, Alberta, p. 118.

Trettin, H.P.
1978: Devonian stratigraphy, west-central Ellesmere Island, Arctic Archipelago; Geological Survey of Canada, Bulletin 302.

INVESTIGATIONS OF BAFFIN ISLAND SHELF FROM SURFACE SHIP AND RESEARCH SUBMERSIBLE IN 1981

Brian MacLean,
Atlantic Geoscience Centre, Dartmouth

Introduction

Between September 9 and October 13, 1981, Atlantic Geoscience Centre (AGC) and Atlantic Oceanographic Laboratory (AOL), Bedford Institute of Oceanography, carried out a geological/chemical cruise (81-055) on the Baffin Island shelf using the surface ship **M.V. Pandora II** and the research submersible **Pisces IV.** This cruise was a follow-up to previous AGC bedrock and reconnaissance surficial geological investigations and to AGC and AOL oil seep studies in this area (e.g. MacLean and Falconer, 1979; MacLean et al., 1981a, b; Levy and MacLean, 1981). This report outlines the nature of the investigations and the preliminary results.

The cruise program was divided into two phases, objectives of which were as follows: Phase I (September 9-26) (a) to selectively sample the unconsolidated seabed sediments on the southeastern Baffin Island shelf to establish the physical composition and regional distribution of these units and, where possible, their significance in relation to Quaternary history of the region; (b) collection and analysis of subsamples of the samples from "a" and water surface and water column samples for baseline AOL chemical oceanography petroleum residue studies in the region. Phase II (September 26-October 13) was mainly concerned with various investigations with **Pisces IV** primarily in the area offshore from Scott Inlet on the northeastern Baffin Island shelf as a follow-up to previous surface ship investigations: (a) to examine the oil seep area off Scott Inlet to observe the source of seepage and manner of escape from the seabed and, if possible, to sample both the material seeping from the seafloor and the sediments from which seepage was occurring; (b) to examine and attempt to sample strata in the walls of Scott trough to more fully define the stratigraphy of the area; (c) to examine iceberg scours to obtain information on their physical size and character and subsequent deformation, if any; (d) to examine a few bedrock and/or surficial sediment features on the southeastern Baffin shelf en route southward from Scott Inlet to Nain, Labrador, the cruise termination point.

Results

The scientific program proceeded very well despite unfavourable sea conditions throughout most of Phase I. Fortunately good sea and weather conditions prevailed during most of Phase II when it was most needed for **Pisces** operations. Consequently, most of the cruise objectives were achieved.

Phase I

Sediment samples were collected at 123 stations mainly located on the southeastern Baffin shelf between Hudson Strait and Cape Dyer (Fig. 1). These comprised 117 Van Veen grab sample stations and 6 gravity core stations. Locations for these were determined on the basis of previously acquired acoustic data from which six tentative surficial units were interpreted. Subsamples of the sediment grab samples and gravity cores and samples of surface water at these stations, as well as 9 water column (bottle cast) stations, were collected for chemical analysis to determine the petroleum residues and concentrations of volatile hydrocarbons. Eleven surface water samples were also collected on the Labrador shelf en route to the Baffin program area. Only seven of the projected sediment sample stations were not occupied; the result of weather and ice conditions. The sediment sampling program also included 10 stations on the shelf between Cape Dyer and Broughton Island to assess the significance of terrace like features as possible indicators of former sea level stands.

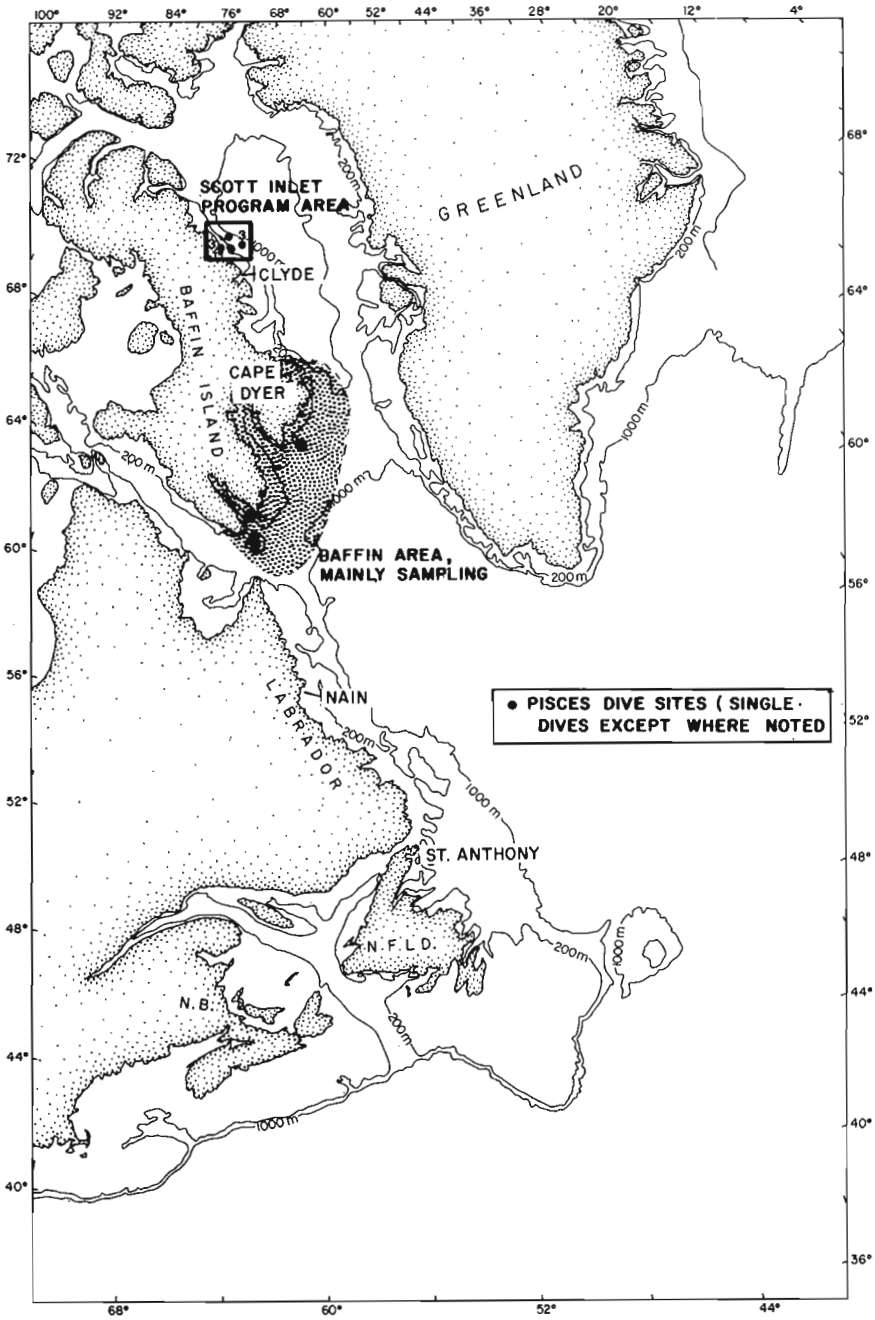

Figure 1. Index map showing program areas on the Baffin Island shelf.

From: Scientific and Technical Notes in Current Research, Part A; Geol. Surv. Can., Paper 82-1A.

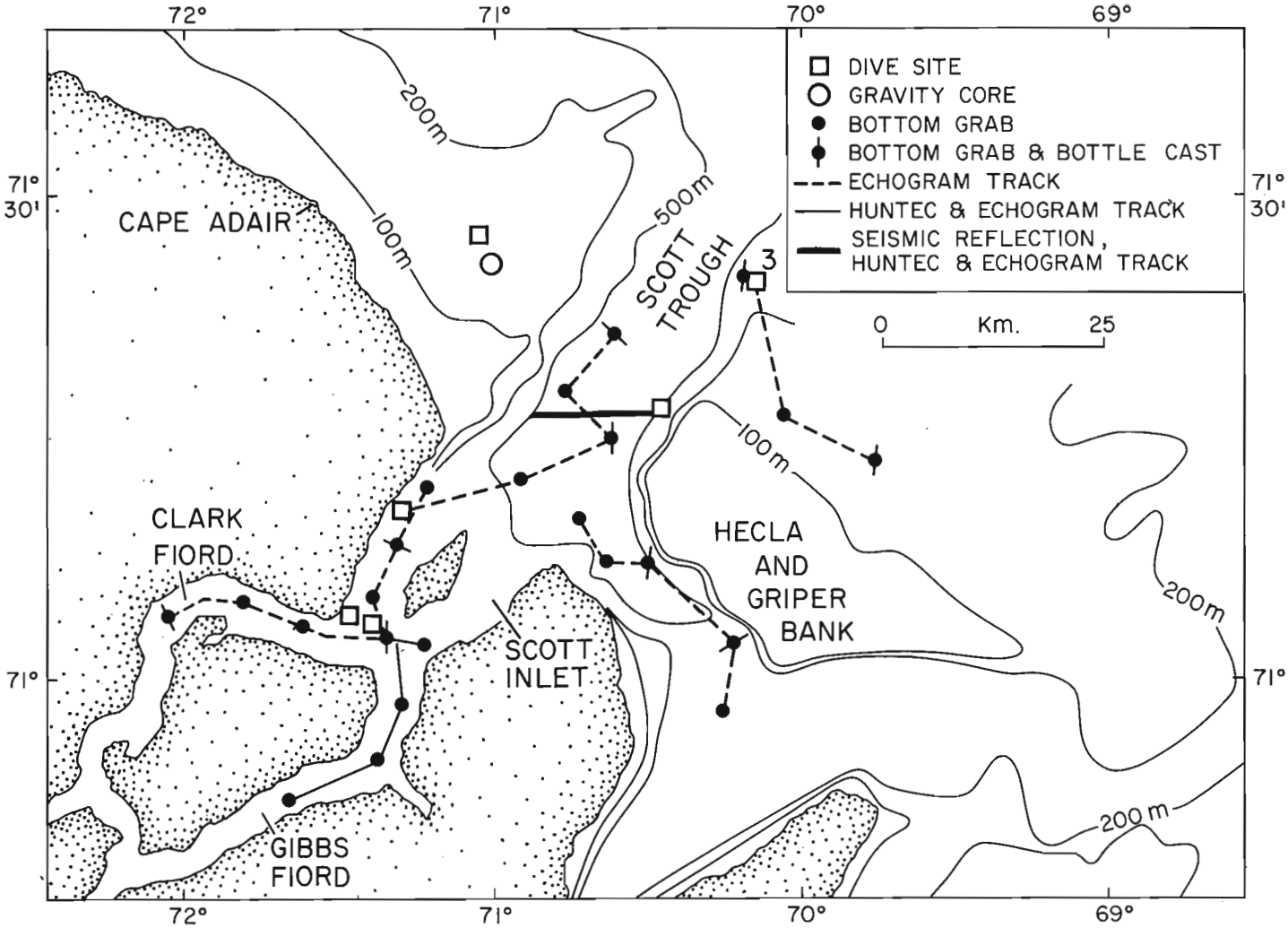

Figure 2. *Map showing* ***Pisces*** *dive, sample and acoustic profile locations in the vicinity of Scott Inlet, northeastern Baffin Island shelf.*

Phase II

Investigations during this phase were carried out mainly with **Pisces IV.** Ten dives were undertaken, 8 in the general Scott Inlet area, and 2 on the southeastern Baffin Island shelf (Fig. 1, 2).

The areal extent of the oil slick from the seep on the shelf off Scott Inlet as limited by winds and droplet eruption at the sea surface was similar to that observed in 1980 (Levy and MacLean, 1981). The seabed in the immediate slick area was traversed extensively during 3 dives with **Pisces** (totalling 14 hours) using a moored pinger as a reference point. No droplets or particles were observed escaping from the seafloor, but anomalous patches found in the sediments are believed to mark areas where seepage does occur, probably on a sporadic basis. These patches, circular to elongate in shape, ranged from single occurrences a few centimetres in diameter to groups within larger areas 2-3 m in diameter. These were characterized by a whitish "growth" and coloration of the surface sediment particles, absence of the fine sediment dusting frequently present on the seabed elsewhere, and the presence of dark grey to black discoloration of the underlying sediment. Preliminary analysis of samples of the underlying sediments indicated the presence of methane and traces of other petroleum gasses. Outcrops of metamorphic rocks on the adjacent Precambrian ridge (MacLean and Falconer, 1979; MacLean et al., 1981a) were also observed and sampled.

The southeast wall of Scott trough adjoining Hecla and Griper Bank was traversed with **Pisces** from 618-375 m depth and found to be virtually covered by unconsolidated sediments in the area traversed.

Examination of the seafloor with **Pisces** in an area north of Scott trough confirmed the presence of numerous large iceberg scours (up to approximately 30 m wide and 6 m deep) as previously indicated by sidescan sonar data. None of those encountered appear to be of immediately recent origin.

Three dives with **Pisces** were made on geological features inside Scott Inlet when visibility/sea conditions were unsuitable for launching and recovery of **Pisces** outside on the shelf. These were on the sill behind Scott Island, the small river delta to the north of Scott Island, and the west wall of the fiord 7.5 km west of Scott Island near the entrance to Clark Fiord.

Samples from twenty-three sediment and surface water stations, 9 water column stations and several acoustic profiles were acquired from Pandora on an opportunity basis including several in Scott Inlet, Clark and Gibbs fiords. Failure of navigational systems and discrepancies in radar positioning on the outer shelf caused abandonment of sampling in that area.

En route from Scott Inlet to Nain, investigations were made with **Pisces** of iceberg scours on the shelf seaward from Cumberland Sound, where they were found to be much more

subdued than farther north in the Scott Inlet offshore area, and of bedrock occurrences in the floor of Frobisher Bay where outcrops of strata of presumed Ordovician age were found.

Salient features observed during the various seabed investigations with **Pisces IV** were recorded photographically and on videotape.

Samples from the various localities examined during Phases I and II of cruise 81-055 will be subjected to sedimentological and chemical analyses and paleontological studies as appropriate. A generalized sediment distribution chart of the southeastern Baffin Island shelf, and detailed reports on specific seabed investigations undertaken with **Pisces** on the Baffin Island shelf will be prepared when analytical data are available.

Acknowledgments

The co-operation and assistance provided by Captains R.A. Jones and S. Gulati, officers, crew, scientific staff, and **Pisces IV** personnel headed by Mr. Frank Chambers, were excellent and their contribution to the success of the program is acknowledged with sincere thanks.

Thanks are also extended to E.M. Levy and R.T. Haworth for helpful comments and review of the manuscript.

References

Levy, E.M. and MacLean, B.
1981: Natural hydrocarbon seepage at Scott Inlet and Buchan Gulf, Baffin Island shelf: 1980 Update; in Current Research, Part A, Geological Survey of Canada, Paper 81-1A, p. 401-403.

MacLean, B. and Falconer, R.K.H.
1979: Baffin Island Shelf: results from marine geophysical and geological studies; in Canadian Society Petroleum Geologists – Canadian Society Exploration Geophysicists, Program and Abstracts, Calgary, 1979, p. 72.

MacLean, B., Falconer, R.K.H., and Levy, E.M.
1981a: Geological, geophysical, and chemical evidence for natural seepage of petroleum off the northeast coast of Baffin Island; Bulletin of Canadian Petroleum Geology, v. 29, no. 1, p. 75-95.

MacLean, B., Srivastava, S.P., and Haworth, R.T.
1981b: Bedrock structures off Cumberland Sound, Baffin Island shelf: core sample and geophysical data; in Third International Symposium on Arctic Geology, Calgary, June 28-July 1, 1981, Program and Abstracts, p. 83.

AUTHOR INDEX

*Numbers refer to Scientific and Technical Reports

NOTE TO CONTRIBUTORS

Submissions to the *Discussion* section of *Current Research* are welcome from both the staff of the Geological Survey and from the public. Discussions are limited to 6 double-spasced typewritten pages (about 1500 words) and are subject to review by the Chief Scientific Editor. Discussions are restricted to the scientific content of Geological Survey reports. General discussions concerning branch or government policy will not be accepted. Illustrations will be accepted only if, in the opinion of the editor, they are considered essential. In any case no redrafting will be undertaken and reproducible copy must accompany the original submissions. Discussion is limited to recent reports (not more than 2 years old) and may be in either English or French. Every effort is made to include both *Discussion* and *Reply* in the same issue. *Current Research* is published in January, June and November. Submissions for these issues should be received not later than November 1, April 1, and September 1 respectively. Submissions should be sent to the Chief Scientific Editor, Geological Survey of Canada, 601 Booth Street, Ottawa, Canada, K1A 0E8.

AVIS AUX AUTEURS D'ARTICLES

Nous encourageons tant le personnel de la Commission géologique que le grand public à nous faire parvenir des articles destinés à la section discussion *de la publication* Recherches en cours. *Le texte doit comprendre au plus six pages dactylographiées à double interligne (environ 1500 mots), texte qui peut faire l'objet d'un réexamen par le rédacteur en chef scientifique. Les discussions doivent se limiter au contenu scientifique des rapports de la Commission géologique. Les discussions générales sur la Direction ou les politiques gouvernementales ne seront pas acceptées. Les illustrations ne seront acceptées que dans la mesure où, selon l'opinion du rédacteur, elles seront considérées comme essentielles. Aucune retouche ne sera faite aux textes et dans tous les cas, une copie qui puisse être reproduite doit accompagner les textes originaux. Les discussions en français ou en anglais doivent se limiter aux rapports récents (au plus de 2 ans). On s'efforcera de faire coincider les articles destinés aux rubriques* discussions *et* réponses *dans le même numéro. La publication* Recherches en cours *paraît en janvier, en juin et en novembre. Les articles pour ces numéros doivent être reçus au plus tard le 1er novembre, le 1er avril et le 1er septembre respectivement. Les articles doivent être renvoyés au rédacteur en chef scientifique: Commission géologique du Canada, 601, rue Booth, Ottawa, Canada, K1A 0E8.*

Energy, Mines and Resources Canada
Énergie, Mines et Ressources Canada